PROCEEDINGS OF THE UNITED NATIONS CONFERENCE ON NEW SOURCES OF ENERGY

SOLAR ENERGY, WIND POWER AND GEOTHERMAL ENERGY
Rome, 21-31 August 1961

VOLUME 4. SOLAR ENERGY: I

ACTES OFFICIELS DE LA CONFÉRENCE DES NATIONS UNIES SUR LES SOURCES NOUVELLES D'ÉNERGIE

ÉNERGIE SOLAIRE, ÉNERGIE ÉOLIENNE ET ÉNERGIE GÉOTHERMIQUE
Rome, 21-31 août 1961

VOLUME 4. ÉNERGIE SOLAIRE : I

UNITED NATIONS / NATIONS UNIES
New York, 1964

E/CONF.35/5

UNITED NATIONS PUBLICATION

Sales No.: 63. I. 38

Price : $ U.S. 7.50
(or equivalent in other currencies)

PUBLICATION DES NATIONS UNIES

Numéro de vente : 63. I. 38

Prix : 7 dollars 50 (USA)
(ou l'équivalent en monnaie du pays)

INTRODUCTION

The United Nations Conference on New Sources of Energy was held in Rome from 21 to 31 August 1961. A brief review of the proceedings, of the papers submitted to the Conference and of the related discussions has been printed in *New Sources of Energy and Energy Development: Report on the United Nations Conference on New Sources of Energy.*[1] The same publication also contains the agenda and the lists of participants and conference officers, as well as lists of all the papers and reports.

The Proceedings of the Conference comprise seven volumes as follows:

Volume 1. General sessions.

Volume 2. Geothermal energy: I.

Volume 3. Geothermal energy: II.

Volume 4. Solar energy: I.

Volume 5. Solar energy: II.

Volume 6. Solar energy: III.

Volume 7. Wind power.

The present volume, "Solar energy: I", contains the papers and reports relating to the following agenda items: II.C.1. Use of solar energy for mechanical power and electricity production: (*a*) by means of piston engines and turbines; (*b*) by direct conversion to electricity: (*i*) by means of thermo-electric converters; (*ii*) by means of photo-electric cells; III.A. Solar energy availability and instruments for measurement; III.B. New materials in solar energy utilization.

The rapporteurs' general reports and their summations of the proceedings in connexion with each agenda item or sub-item are given in full in both English and French, as are those individual papers that were submitted to the Conference in both languages. With a few exceptions, all the papers are summarized in both English and French.

Within each agenda item or sub-item, the papers are printed in the alphabetical order of the authors' names. References supplied by the authors are listed after the text. As a rule, they are numbered consecutively throughout each paper and are indicated by Arabic figures in parentheses.

The reports and papers are printed in the form in which they were presented to the Conference, and the affiliations of the participants are those in effect at the time. Corrections to the papers have been incorporated; some of the figures have been rearranged; and minor editorial changes have been made.

The views and opinions expressed are those of the individual authors and do not imply the expression of any opinion on the part of the Secretariat of the United Nations.

The symbols appearing after the titles of the papers and reports, and in reference to them in the text, correspond to the symbols under which they were presented at the Conference. They have been abbreviated by the elimination of the prefix "E/CONF.35/", which should be included in all full references.

[1] United Nations publication, Sales No.: 62.I.21.

INTRODUCTION

La Conférence des Nations Unies sur les sources nouvelles d'énergie s'est tenue à Rome du 21 au 31 août 1961. Le document intitulé *Sources nouvelles d'énergie et production d'énergie : Rapport sur les travaux de la Conférence des Nations Unies sur les sources nouvelles d'énergie*[1] donne un aperçu des travaux, des mémoires soumis à la Conférence et des débats dont ceux-ci ont fait l'objet. Il contient en outre l'ordre du jour, la liste des membres du Bureau et des autres personnes ayant pris part à la Conférence, ainsi qu'une liste de tous les mémoires et rapports présentés.

Les Actes officiels de la Conférence comprennent les sept volumes suivants :

Volume 1. Sessions générales.
Volume 2. Énergie géothermique : I.
Volume 3. Énergie géothermique : II.
Volume 4. Énergie solaire : I.
Volume 5. Énergie solaire : II.
Volume 6. Énergie solaire : III.
Volume 7. Énergie éolienne.

Le présent volume, « Énergie solaire : I », groupe les mémoires et rapports ayant trait aux points suivants de l'ordre du jour : II.C.1. Utilisation de l'énergie solaire pour la production d'énergie mécanique et d'électricité : *a*) Au moyen de moteurs alternatifs et de turbines; *b*) Par conversion directe en électricité : *i*) au moyen de convertisseurs thermo-électriques; *ii*) au moyen de cellules photo-électriques; III.A. Énergie solaire disponible et instruments de mesure; III.B. Matières nouvelles employées dans l'utilisation de l'énergie solaire.

Les rapports généraux des rapporteurs et le résumé des débats sur chaque point ou subdivision de l'ordre du jour qui a été établi par le rapporteur intéressé sont donnés intégralement, en anglais et en français, ainsi que les mémoires qui ont été soumis à la Conférence dans les deux langues. Sauf quelques exceptions, ils sont tous résumés en anglais et en français.

Pour chaque point ou subdivision de l'ordre du jour, les mémoires sont classés dans l'ordre alphabétique des noms d'auteurs. La liste des références fournies par les auteurs figure à la suite du texte. D'une façon générale elles sont numérotées consécutivement pour chaque mémoire, et sont indiquées par des chiffres arabes entre parenthèses.

En règle générale, les rapports et mémoires sont publiés sous la forme dans laquelle ils ont été présentés à la Conférence, et les fonctions indiquées pour chaque participant sont celles qu'il occupait à cette époque. Toutefois, les corrections nécessaires ont été apportées et certaines figures ont été remaniées; des modifications de rédaction mineures ont de même été faites.

Les vues exprimées n'engagent que leur auteur et n'impliquent aucune prise de position de la part du Secrétariat de l'Organisation des Nations Unies.

Les cotes indiquées après les titres des mémoires et des rapports, ainsi que dans les renvois qui y sont faits dans le texte, correspondent aux cotes utilisées pour la Conférence. On les a cependant abrégées en éliminant « E/CONF.35 », qui doit être maintenu dans les cas où la référence complète est donnée

[1] Publication des Nations Unies, numéro de vente: 62.I.21.

TABLE OF CONTENTS* — TABLE DES MATIÈRES*

Agenda item II.C.1

USE OF SOLAR ENERGY FOR MECHANICAL POWER AND ELECTRICITY PRODUCTION:

(*a*) By means of piston engines and turbines ;

(*b*) By direct conversion to electricity :

(i) By means of thermoelectric converters ;

(ii) By means of photo-electric cells

Point II.C.1 de l'ordre du jour

UTILISATION DE L'ÉNERGIE SOLAIRE POUR LA PRODUCTION D'ÉNERGIE MÉCANIQUE ET D'ÉLECTRICITÉ

a) Au moyen de moteurs alternatifs et de turbines ;

b) Par conversion directe en électricité :

i) au moyen de convertisseurs thermo-électriques ;

ii) au moyen de cellules photo-électriques

II.C.1 (*a*)

General report — Rapport général

			Page
GR/9 (S)	Use of solar energy for mechanical power and electricity production by means of piston engines and turbines.	Tabor	3
	Utilisation de l'énergie solaire pour la production d'énergie mécanique et d'électricité au moyen de moteurs alternatifs et de turbines.		9
Rapporteur's summation		Tabor	16
Résumé du rapporteur			18

Individual papers — Mémoires

S/99	Thermal machines for the conversion of solar energy into mechanical power	D'Amelio	20
	Machines thermiques pour la conversion de l'énergie solaire en énergie mécanique (résumé)		25
S/15	Power as a by-product of competitive solar distillation . . .	Hummel	27
	L'énergie, sous-produit des installations économiques de distillation solaire (résumé)		36

* The first title refers to the original language; in most cases, it is followed by the translation in italics.

* Le premier titre est celui de la version originale; il est suivi, dans la plupart des cas, de sa traduction en caractères italiques.

			Page
S/27	The development of a 15-kW (el) solar mechanical engine for space application and its relationship to the fabrication of similar engines for terrestrial usage	Macauley	38
	Mise au point d'un moteur héliomécanique de 15 kW (mesures en électricité) destiné aux applications interplanétaires. Ses rapports avec la construction de moteurs analogues destinés à des applications terrestres (résumé)		57
S/47	Large-area solar collectors (solar ponds) for power production	Tabor	59
	Collecteurs solaires à grande surface (piscines solaires) pour la production d'énergie (résumé)		67
S/54	Small turbine for solar energy power package	Tabor, Bronicki	68
	Petite turbine pour centrale autonome à énergie solaire (résumé)		79
S/45	Étude économique du fonctionnement au Sahara des insolateurs à air	Touchais	82
	Economic study of the operation of atmospheric solar collectors in the Sahara (summary)		98

II.C.1 (b)

General report — Rapport général

GR/10 (S)	Use of solar energy for electricity production by direct conversion by means of thermoelectric converters and photo-electric cells	Baum	115
	Utilisation de l'énergie solaire pour la production d'électricité par conversion directe au moyen de convertisseurs thermo-électriques et de cellules photo-électriques		123
	Rapporteur's summation	Baum	132
	Résumé du rapporteur		133

Individual papers — Mémoires

S/118	Semiconductor converters of solar energy	Baum, Borovikova, Okhotin	134

II.C.1 (b) (*i*)

S/103	Preliminary tests of a solar heated thermoelectric converter	Daniels, Duffie, Löf, Breihan	145
	Essais préliminaires d'un convertisseur thermo-électrique à chauffage solaire (résumé)		147
S/78	Solar heated thermionic converter	Hatsopoulos, Brosens	148
	Convertisseur thermo-ionique à chauffage solaire (résumé)		152
S/12	Thermoelectric generators for the conversion of solar energy to produce electrical and mechanical power	Katz	153
	Générateurs thermo-électriques pour la conversion de l'énergie solaire en vue de la production d'énergie électrique et mécanique (résumé)		167
S/10	Athermoelectric generator	Kobayashi	168
	Un générateur thermo-électrique (résumé)		172
S/55	Nouveaux générateurs solaires thermo-électriques	Michel	173
	New solar thermoelectric generators—description, results and future prospects		179

			Page
S/84	Orientation des recherches techniques de l'I.E.S.U.A. pour la production d'énergie à partir du rayonnement solaire *(résumé)*.	Perrot, Touchais	185
	Technical research trends at I.E.S.U.A. for energy production from solar radiation		204
S/90	The conversion of solar energy to electricity by means of the thermionic converter	Wilson	223
	Conversion de l'énergie solaire en électricité au moyen d'une cellule thermo-ionique (résumé)		228

E.C.1 (*b*) (*ii*)

S/11	Utilization of silicon solar batteries	Kobayashi	229
	Emploi des batteries solaires au silicium (résumé)		235
S/19	Applications of photovoltaic cells in communications	Pearson	236
	Application des cellules photovoltaïques dans le domaine des télécommunications (résumé)		241
S/75	Latest developments in the field of photovoltaic conversion of solar energy	Prince	242
	Derniers progrès réalisés dans le domaine de la conversion photovoltaïque de l'énergie solaire (résumé)		253
S/106	Low-cost photovoltaic conversion of solar energy	Rappaport, Moss	254
	Conversion photovoltaïque de l'énergie solaire à prix modique (résumé)		257
S/56	Thin film photovoltaic devices for solar energy conversion . . .	Ravich	258
	Dispositifs photovoltaïques à pellicule mince pour la conversion de l'énergie solaire (résumé)		273
S/74	Developments in photovoltaic solar energy conversion for earth surface applications	Wolf	275
	Nouveaux progrès dans la conversion photovoltaïque de l'énergie solaire en vue d'applications à la surface de la terre (résumé) .		284

TABLE OF CONTENTS * — TABLE DES MATIÈRES *

Agenda item III.A

SOLAR ENERGY AVAILABILITY AND INSTRUMENTS FOR MEASUREMENT

Point III.A de l'ordre du jour

ÉNERGIE SOLAIRE DISPONIBLE ET INSTRUMENTS DE MESURE

General report — Rapport général

			Page
GR/11 (S)	Solar energy availability and instruments for measurement . . .	Blanco	289
	Énergie solaire disponible et instruments de mesure		293
Rapporteur's summation		Blanco	298
Résumé du rapporteur			301

Individual papers — Mémoires

S/20	Solar energy in Canada	Allcut, Hooper	304
	L'énergie solaire au Canada (résumé)		310
S/13	Some aspects of the climatology of solar radiation	Black	311
	Quelques aspects de la climatologie du rayonnement (résumé) .		317
S/59	Données météorologiques concernant l'ensoleillement et l'éclairement énergétique en vue des applications pratiques . . .	Dogniaux	319
	Meteorological data on sunshine duration and insolation for practical applications (summary)		334
S/117	Instrumentation for the measurement of solar radiation — a survey of modern techniques and recent developments . . .	Drummond	335
	Instruments de mesure du rayonnement solaire : aperçu des méthodes nouvelles et des progrès récents réalisés (résumé)		341
S/62	Solar radiation availability in the United Arab Republic . . .	Elnesr, Khalil	342
	Mesures du rayonnement solaire en République arabe unie (résumé)		347
S/74	Aspects of radiation climatology for the utilization of applied solar energy	Flach, Mörikofer	348
	Aspects de la climatologie du rayonnement pour l'application de l'énergie solaire (résumé)		354
S/95	Dispositifs de mesure du coefficient de rayonnement nocturne de matériaux divers, dans leurs conditions locales d'emploi . .	Gondet	355
	Devices for measuring the coefficient of nocturnal radiation of various materials under local conditions of use (summary) . .		358

* The first title refers to the original language; in most cases, it is followed by the translation in italics.

* Le premier titre est celui de la version originale; il est suivi, dans la plupart des cas, de sa traduction en caractères italiques.

			Page
S/61	Measurements of total radiation in networks	Gräfe	359
	Mesures du rayonnement global dans des réseaux de stations (résumé)		367
S/9	Simple instruments for the assessment of daily solar radiation intensity	Heywood	369
	Instruments simples pour l'évaluation de l'intensité du rayonnement solaire quotidien (résumé)		375
S/98	The estimation of monthly mean values of daily total short wave radiation on vertical and inclined surfaces from sunshine records for latitudes 40° N-40° S	Page	378
	Évaluation des valeurs moyennes mensuelles du rayonnement total à ondes courtes sur les surfaces verticales et inclinées, d'après les relevés d'ensoleillement pour les latitudes 40° N et 40° S (résumé)		389
S/80	Énergie solaire : les réseaux et les instruments actinométriques	de Brichambaut	391
	Solar energy — actinometric networks and instruments (summary)		394
S/41	Utilisation pratique des diagrammes de radiation solaire en vue de la détermination des rendements, des frais d'exploitation et des charges d'amortissement des insolateurs	Perrot, Touchais	395
	Practical use of solar radiation diagrams to determine the efficiency, operating costs and depreciation charges of solar power plants (summary)		409
S/69	La mesure absolue de l'énergie solaire	Peyturaux	412
	The absolute measurement of solar energy (summary)		421
S/105	Solar radiation and its measurement at a network of stations, with special reference to India	Ramdas	423
S/32	Solar radiation records in Australia and their presentation	Sapsford	433
	Relevés du rayonnement solaire en Australie (résumé)		442
S/92	Instrumentation for solar radiation measurements	Schoffer, Kuhn, Sapsford	444
	Instruments de mesure du rayonnement solaire (résumé)		454
S/2	The amount and properties of solar radiation in Japan and the instruments for its measurement	Sekihara	456
	Intensité et propriétés du rayonnement solaire au Japon et instruments utilisés pour sa mesure (résumé)		466
S/18	Solar radiation measurements in Canada	Truhlar, Latimer, Mateer, Godson	467
	Mesures du rayonnement solaire au Canada (résumé)		472
S/60	Distribution of solar energy over India	Venkiteshwaran	474
	Répartition de l'énergie solaire en Inde (résumé)		480
S/34	Nocturnal heat loss from horizontal surfaces in arid regions	Yellott, Kokoropoulos	481
	Pertes nocturnes de chaleur des surfaces horizontales dans les régions arides (résumé)		489

TABLE OF CONTENTS* — TABLE DES MATIÈRES*

Agenda item III.B

NEW MATERIALS IN SOLAR ENERGY UTILIZATION

Point III.B de l'ordre du jour

MATIÈRES NOUVELLES EMPLOYÉES DANS L'UTILISATION DE L'ÉNERGIE SOLAIRE

General report — Rapport général

			Page
GR/12 (S)	New materials in solar energy utilization	Duffie	493
	Matières nouvelles employées dans l'utilisation de l'énergie solaire		502
Rapporteur's summation		Duffie	512
Résumé du rapporteur			514

Individual papers — Mémoires

S/104	Solar focusing collectors of plastics	Daniels, Breihan	516
	Collecteurs de concentration solaire en composition plastique (résumé)		518
S/33	Plastic films for solar energy applications	Edlin, Willauer	519
	Pellicules en composition plastique pour les applications dans le domaine de l'énergie solaire (résumé)		535
S/43	Spectral and directional thermal radiation characteristics of selective surfaces for solar collectors	Edwards, Gier, Nelson, Roddick	536
	Caractéristiques spectrales et thermodirectionnelles de surfaces sélectives pour les collecteurs solaires (résumé)		552
S/71	Un nouveau collecteur de l'énergie rayonnante solaire — théorie et vérifications expérimentales	Francia	554
	A new collector of solar radiant energy — theory and experimental verification		572
S/42	The spectrum of materials available for the utilization and control of solar energy	Gaumer	589
	Choix de matériaux disponibles pour l'utilisation et le réglage de l'énergie solaire (résumé)		596
S/22	Step lenses and step prisms for utilization of solar energy	Oshida	598
	Lentilles et prismes à échelons pour l'utilisation de l'énergie solaire (résumé)		603

* The first title refers to the original language; in most cases, it is followed by the translation in italics.

* Le premier titre est celui de la version originale; il est suivi, dans la plupart des cas, de sa traduction en caractères italiques.

			Page
S/91	Verres et montages spéciaux pour l'utilisation de l'énergie solaire	Peyches	604
	Special glasses and mountings for the utilization of solar energy .		611
S/46	Further studies on selective black coatings	Tabor, Harris, Weinberger, Doron	618
	Études supplémentaires sur les revêtements noirs sélectifs (résumé)		623
S/6	Recherches sur les surfaces sélectives utilisables pour la climatisation des habitations	Trombe, Foëx, Lê Phat Vinh	625
	Studies on selective surfaces for air conditioning dwellings . . .		638
S/8	Emploi de certains alliages d'aluminium pour l'utilisation de l'énergie solaire	Vachet, Mercier	650
	Use of certain aluminium alloys in the utilization of solar energy .		658

EXPLANATORY NOTE

The following symbols have been used in this volume :

A full stop (.) is used to indicate decimals; spaces are inserted to distinguish thousands and millions.

In most cases abbreviations used by the authors have been retained.

For conversion factors to be used in obtaining metric equivalents of British units, or British equivalents of metric units, see *World Weights and Measures*, prepared by the Statistical Office of the United Nations in collaboration with the Food and Agriculture Organization of the United Nations *(Statistical Papers : Series M, No. 21;* United Nations publication, Sales No. : 55.XVII.2).

NOTE EXPLICATIVE

Les signes suivants ont été employés dans ce volume :

La virgule (,) indique les décimales; les espaces entre les chiffres distinguent les milliers et les millions.

Dans la plupart des cas, les abréviations utilisées par les auteurs ont été retenues.

Pour la conversion des mesures métriques en mesures anglaises et pour l'opération inverse, consulter la brochure *World Weights and Measures*, que le Bureau de statistique des Nations Unies a établi avec le concours de l'Organisation des Nations Unies pour l'alimentation et l'agriculture *(Études statistiques :* série M, nº 21; publication des Nations Unies, nº de vente : 55.XVII.2).

Agenda item II.C.1

Use of solar energy for mechanical power and electricity production:

(*a*) By means of piston engines and turbines;

(*b*) By direct conversion to electricity:

(i) By means of thermoelectric converters;

(iii) By means of photo-electric cells

Point II.C.1 de l'ordre du jour

Utilisation de l'énergie solaire pour la production d'énergie mécanique et d'électricité :

a) Au moyen de moteurs alternatifs et de turbines;

b) Par conversion directe en électricité :

i) au moyen de convertisseurs thermo-électriques;

ii) au moyen de cellules photo-électriques

Chairman — Président

Henri MASSON

Rapporteurs

II.C.1 (*a*) : Harry TABOR

II.C.1 (*b*) : Valentin A. BAUM

Agenda item II.C:1 (*a*)

USE OF SOLAR ENERGY FOR MECHANICAL POWER AND ELECTRICITY PRODUCTION BY MEANS OF PISTON ENGINES AND TURBINES

*Harry Tabor**

Of all the goals in solar energy utilisation, it appears that the most sought after has been mechanical and electrical power. It is, of course, necessary to add that the power produced must be reasonably priced. A number of technically successful solar power installations have been reported in the last hundred years, but none of them would be considered satisfactory today from the economic point of view. Admittedly the cost of solar power need not be as low as the cost of conventional power produced in high efficiency central power stations in industrial areas, for the solar power may be required in remote areas where a large central supply is neither available nor practical. But even in such areas there is a limit to what the consumer is prepared to pay for solar power. If the price is too high he may prefer to go without, or to utilise some other source such as batteries, windmills, steam engines burning waste products, small gasoline or diesel engines.

We will thus consider the present state of the art with special reference to the likely cost of solar power.

Three ranges of size

Solar power units may be roughly divided into three classes: the midget, the small and the large, the first representing power supplies of a few watts, the second being in the kilowatt range, i.e. from a fraction of a kW to several kW, and the third in the megawatt range.

Watt range

For a few watts of power it is almost certain that a mechanical heat engine would not be considered and only "static" systems (i.e. with no moving parts) would come into question. These include photo-electric cells and thermoelectric and thermionic generators, and as such are dealt with elsewhere in this conference and will not be considered further in this section.

Kilowatt and megawatt units

These have certain common problems as well as some rather fundamental differences.

The differences

(*a*) Megawatt units mean central power production and a power distribution network. This contradicts the philosophical principle that as power distribution has to be paid for whereas solar energy distribution is free, then solar energy should be collected and transformed *at the point of use.*

(*b*) Megawatt units involve very large areas of solar collection, so that if any conventional collector is considered, the maintenance problem may be insuperable.

(*c*) Because the megawatt unit involves a distribution system, the cost of power at the bus-bars must be considerably lower than for a kilowatt unit that may be located in any remote place. Also megawatt units imply advanced and probably industrialised communities which still further lowers the price that can be charged for power.

(*d*) Storage, to provide a firm supply, is a virtual necessity for a megawatt unit (except in the rare case of it being coupled to a grid also fed from conventional power stations) whereas the kilowatt unit may be used in many cases without storage, as, for example, when used for water pumping.

Because of these differences, most proposals for solar power units have been in the kilowatt class with only a very few suggestions in the megawatt sizes. In some of the latter, the differences enumerated above have not always been fully appreciated. For example, paper S/15 describes a power system involving a horizontal collector of one square mile in size covered with a plastic cover in one piece. There is no indication of how the plastic would be cleaned (except by rain) whilst, if damaged, repair could be very difficult.

The similarities

We now consider some of the problems and approaches common to both the kilowatt and megawatt sizes. These include maintenance and lifetime of the components, the operating temperature, efficiency and cost, the kind of heat engine, and the kind of collector.

(a) *Maintenance and life-time of the components*

As solar plants have no fuel costs, the entire power cost is made up of fixed charges (interest and

* Director, National Physical Laboratory of Israel, Jerusalem.

amortisation) and running costs. It follows therefore that much attention has to be paid to the longevity of the component parts (in relation to their cost) and to the maintenance expenses as part of the running costs.

(b) *The operating temperature*

The engine and collector are interconnected primarily through the choice of operating temperature. The following guide lines give an approximate view of the present state of the art.

For operating temperatures below 100°C it is possible to consider stationary non-focusing collectors. Apart from the advantages of being stationary and having no mirror surfaces that might distort or deteriorate, these collectors exploit diffuse (sky) radiation as well as the direct solar radiation.

For operating temperatures between about 100-200°C, stationary focusing collectors of low concentration power are required. Such collectors require their tilt to be varied to suit the seasons, but this is far less of a complication than a sun-tracking mechanism.

For operating temperatures above 200°C, focusing collectors which track the sun are required and at temperatures much above 200°C the mirror must be paraboloidal rather than cylindrical parabolic (more generally, it must be a double curvature surface, not a single curvature surface). Tracking collectors have the advantage that they "see" more sunshine than a fixed collector (about 40 per cent more) but the tracking mechanism for a large-area collector is extremely expensive because of the wind forces. Double curvature mirrors are so expensive that this writer does not believe they will ever be practical for terrestrial power application except in the midget sizes.

(c) *Efficiency and cost*

The interconnection between engine and collector is further related to a fundamental policy question, i.e., whether to have a high efficiency system with expensive engine and collectors or a low efficiency system with low-cost components.[1]

The policy question is brought out in two of the papers dealing with kilowatt plants. In paper S/54, the authors recognise that the collector is likely to be the most expensive item. They therefore concentrate on making the heat engine as efficient as possible with a moderate operating temperature, in order to keep the size of the collector down. A stationary cylindrical parabolic collector is envisaged and the operating temperature is 150-200°C. On the other hand, in paper S/99, the author expresses the view that the cheapest possible collector should be considered, i.e., one without cover glass or insulation and therefore operating at a low temperature (say 40-50°C). It is not possible to make a proper comparison between these different viewpoints as the latter paper has insufficient cost data, but it is clear that the collector must be extremely cheap (per unit area) in the latter case as the heat engine is likely to be only one-third as efficient as that quoted in the former paper.

At the other end of the scale, paper S/27 deals with a very efficient system (accurate paraboloidal sun-tracking mirror producing high temperatures for liquid-metal turbine), but as this is a power supply for space vehicles the cost is high—about an order of magnitude higher than that considered in the other papers—and it is by no means clear how, by relaxing for terrestrial application some of the special requirements of power supplies in space, this cost could be reduced substantially.[2]

In the final analysis the correct policy is that which leads to the lowest power costs, and these can be determined only by following through complete designs first on paper and subsequently on prototypes.

In the megawatt range the policy question has virtually been settled. The only exponent of high efficiency collectors and high temperature engines has been the Russian research group (1), and their proposal led to costs of about $2 000 per kW installed (2) so that it has not been further pursued. Other papers dealing with megawatt units consider extensive low cost non-focusing collectors with operating temperatures below 100°C.

(d) *The heat engine*

This is almost the only item where the kilowatt unit is at a serious disadvantage vis-à-vis the megawatt unit. For the latter, turbines—usually steam turbines—can be built that reach 60 per cent of the Carnot efficiency or better, whatever temperature range is considered. But small steam engines and turbines in the kilowatt size are notoriously inefficient. This matter has been studied in paper S/54 where it is shown that, if high molecular weight fluids having certain specific characteristics are employed instead of steam, there is every chance of producing kilowatt turbines with almost the same efficiency as megawatt units. With operating temperatures of 150-200°C, turbine efficiencies of 15-20 per cent—for a 2-10 kW unit—are anticipated.[3] Assuming a cylindrical parabolic collector to be 40 per cent efficient and to cost $20 per sq m leads to power costs of under 5 U.S. cents per kWh taking 6 per cent interest charges and a collector life of only six years.

[1] For space applications there is almost no choice; the high-efficiency system is needed to reduce dimension, weight and heat-sink requirements.

[2] The capital cost is over U.S.$7 000 per kW installed for a 15 kW unit. If the components are amortised at 6 per cent interest and 6 per cent sinking fund for their various estimated lifetimes and the plant works at full output for 8 640 hours per year, the capital cost component in the price of each kWh is over 14 cents.

[3] This relatively high efficiency permits the turbine to be fuel-operated economically during the cloudy season; where low temperature, low efficiency engines or turbines have been proposed, their operation by fuel during cloudy weather or collector breakdown is very inefficient and a second fuel-operated prime-mover may be necessary.

This development of an efficient small prime-mover operating at moderate temperatures may represent a major step forward in the realisation of practical kilowatt solar energy power packages.

(e) *The collector*

On the subject of solar collectors for kilowatt units, not too much progress is reported. Most studies on the conventional flat plate collector have been concerned with their use as heating devices. For power applications the proposals have nearly all been for focusing collectors with, in many cases, a recognition that it would be highly desirable to avoid sun tracking mountings. In this latter field of endeavour there have, unfortunately, been some errors in concept, optical systems having been proposed which cannot possibly do what their protagonists claim.[4]

The present writer demonstrated theoretically (3) that a stationary mirror system, with periodic seasonal tilt adjustment, could give an optical concentration of about three times whilst if completely fixed, i.e., with no seasonal tilt adjustments, no useful optical concentration is possible. Experience with practical collectors would appear to confirm these theoretical conclusions. An improvement in optical concentration can be obtained by the principle of the "part-time" mirror, i.e., a mirror constructed so that at different times of the day different parts contribute to the image formation (whilst the remainder of the mirror is "inactive"). Where the percentage of inactive mirrors is large the economics will generally prove to be unattractive. The principle of the "part-time" mirror can be used, but only to a small extent, by extending the area of a 100 per cent active mirror (the extensions being less than 100 per cent active). It is relatively easy to compute whether the extended areas of mirror pay for themselves by the extra sunshine, averaged over a year, that they deliver at the focus.

Suggestions for solar collectors for the megawatt units have been, and for understandable reasons, almost all concerned with horizontal non-focusing systems. Two papers in this section deal with this aspect. A third (unpublished) paper proposed conventional flat plate collectors floating on the sea and providing hot water as the heat source for a low temperature turbine, the sea providing the cold sink. The proximity of the hot and cold water supplies reduces the pumping problems that were encountered in the Claude-Boucherot proposals for obtaining power from the oceans. If one takes into account present day costs for flat plate collectors, the net cost of power from such a system would appear to be of an order of magnitude greater than the cost of power from conventional power plants.

Paper S/15 proposes a shallow water surface of the order of 1 sq mile in area, covered with plastic covers, and the author proposes an ingenious system whereby the top cover will be fitted as a single piece. The system is intended to produce distilled water as well as power, and this is a characteristic of most of the megawatt low-temperature water-operated solar power units. In such double-purpose units, the cost of power depends on the price charged for the distilled water; where fresh water is scarce and therefore permits sufficiently high price, the power can be reckoned as free. This is not an economically sound method of calculation or of comparison between alternative systems, and the water-pricing policy must therefore be very carefully examined. In truth, if the water is reasonably priced, it will have only a small effect on the price of the power. For example, a combined steam power unit with single effect condensation of steam to provide fresh water, operating at 90°C upper temperature and condensing at 30°C will yield about 14 litres of water for each kWhr of power produced,[5] or say a ton of water (c. 250 US gals) for 70 kWh. The water is only worth a few cents whereas the power is worth around 70 cents. It is therefore probably sounder, at least as a first approximation in comparing systems, to compute the price of the power from the costs of the system, treating the water as a free bonus, rather than the other way round. From the figures given in the paper, the cost of power should be about 3.5 cents and the matter is open to discussion today as to whether the system as proposed is feasible and practical. One point already mentioned is that the design of such a large area without subdividing walls would pose serious problems in keeping the plastic cover clean and in good repair.

The other paper in this group (S/47) starts with the hypothesis that one should try to avoid plastics, glass and metal for megawatt collector units and that therefore only a large body of water (either an ocean or an artificial lake) can be considered for large-area collectors. The "solar pond", as proposed, is black-bottomed, about a metre or so deep, and convection is suppressed by maintaining a density gradient in the pond by means of dissolved salt, having high concentration at the bottom and low at the top. Under such circumstances a metre of water is quite a good thermal insulator and temperatures in excess of 90°C are reported. The author points out three technical problems now under study: the maintenance of the density gradient, i.e., that it shall not be disturbed by waves or by the heat extraction process, the extraction of heat from the bottom of the pond and the removal of dirt falling into the pond. These three problems have not yet been solved in an entirely satisfactory manner, but are of the type that human ingenuity ought to be able to solve without unduly complicating the construction of the pond. Under such circumstances, power could be produced for around 1 US cent per

[4] This discrepancy, in some cases, has been due to using a crude two-dimensional diagram to represent a three-dimensional optical problem.

[5] This yield is for 60°C temperature difference. At higher temperature differences the water yield is proportionately lower and vice versa.

kWh and there is sufficient built-in storage to ensure a supply of power for a number of consecutive sunless days. Because of the salt requirements and the need for large flat areas, the solar pond would seem to be limited in application to seaboard or salt-lake areas of which, however, there are many in the under-developed areas of the world.

Basic economics

For most solar energy installations the maintenance and running cost must be low, for if this is not so, and we remember the large areas of collector involved, the over-all cost becomes unbearable. For units in the kilowatt sizes the areas are manageable and, provided there are no serious mechanical breakdowns, the routine maintenance will usually not be charged to the cost of power. The vital factor in cost is, therefore, the annual charges on capital investment.

The calculation of this cost is indicated in paper S/54 and a condensed treatment is given here because it highlights the extreme difficulty in getting a low unit power cost for any thermal solar energy power device.

If Q = total annual solar incidence on unit area of collector, kWh/m²;

A_c = area of collector, m²;

E_c = mean weighted efficiency of collector;

E_t = mean weighted efficiency of turbine or engine;

C = cost of unit area of collector, $ per m² (this includes all other costs that are proportional to collector area such as ground preparation, plumbing, etc.);

T = Cost of turbine and other fixed costs, $ per m² (this includes all costs of items whose size is scarcely dependent upon collector area but only on power rating of unit);

J = Annual charges on capital, expressed as a fraction. J_c applies to collector item, J_T applies to turbine item;

X = Utilisation factor.

Then power produced per year $= QE_cE_TA_c$ (kWh)

Power utilised per year $= XQE_cE_TA_c$ (kWh)

Capital cost $= CA_c + T$ ($)

Annual charges on capital $= CA_cJ_c + TJ_T$ ($)

$$\therefore \text{Cost per kWh} = \frac{CA_cJ_c + TJ_T}{XQE_cE_TA_c}$$

$$= \frac{1}{XQ} \cdot J_c \left[\frac{C}{E_cE_T} + \frac{T}{A_cE_cE_T} \times \frac{J_T}{J_c} \right]$$

In almost every case mentioned in the literature the second term in the square bracket is small compared with the first,[6] i.e., the collector is the major capital item of cost and we will thus pay particular attention to it.

When the manner in which all the variables C, E_c, E_t, J_T, J_c, A_c vary with temperature of operation and type of collector construction is known, it is possible to optimise the cost equation on a computer. But it is more instructive to the layman to treat the matter more simply by a few initial assumptions.

We assume that the turbine cost item is small and can be omitted at this stage. We assume that the operating temperature for a given-type collector and turbine has been chosen to give the highest over-all efficiency E_tE_c. It may be shown that, in the temperature ranges considered, the optimum operation temperature is that at which nearly half the energy reaching the receiver is lost by heat losses,[7] so that the collection efficiency will be about 0.4 for collectors in which 70-80 per cent of the incident radiation reaches the receiver. E_c can therefore be taken, at the optimum operating point, as about 0.4 for all real collectors of good design, with the exception of the solar pond where less than half the sunshine reaches the bottom (the "receiver") and E_c will be 0.15-0.20.

For a given site Q is fixed.[8] X depends upon the skill of the owner of the plant and every effort must be made to get X to approach unity.

We now see that the key item in determining power cost is $J_c \frac{C}{E_t}$.

The value of J_c depends upon the current rate of interest charged on capital and the expected lifetime of the collector. Values of J are given in appendix 2 of paper S/54. For example, at 6 per cent interest and a sinking fund carrying 6 per cent interest, the value of J is 0.203 for a six-year life and 0.103 for fifteen years. Where plastics are used in collector constructions to get prices down, a six-year life is probably the best that can be expected in the present state of the art. Collectors employing more durable materials (metal, glass, etc.) could probably be amortised over fifteen years whilst some collectors suggested for solar stills which involve only concrete, glass and asphalt could be amortised over much longer periods.

We now consider some typical values:

X = 1 (ideal!);

Q = 2 000 kWh per m², a value corresponding to a very sunny area and a stationary collector;

E_c = 0.4 as indicated above;

E_t = 0.15, corresponding to a heavy vapour turbine operating at 150°C. This value is several times greater than those given for low temperature engines in the literature;

[6] In megawatt units the items must be about equal if they are to compete with conventional power units since in the latter case the fuel component is of the order of half the power cost (see paper S/54).

[7] This is analogous to the internal losses in a battery coupled to the optimum load for maximum energy yield.

[8] This is related to the type of collector; a sun-tracking collector will "see" more sunshine than a fixed one.

C = \$20 per m² (stationary focusing collector). This appears to be about as low a price as anyone has dared to suggest in the kilowatt range of power units and almost certainly involves the use of plastics. Complicated mirrors or special materials can easily raise this price several times;

J_c = 0.203— i.e., assumes six-year life for the collector and 6 per cent interest charges.

Then the collector component in the power cost is:

$$\frac{1}{XQ} \cdot J_c \cdot \frac{C}{E_c E_t} = \left[\frac{1}{XQE_c}\right]\left(\frac{J_c C}{E_t}\right) = 3.4 \text{ US cents per kWh}$$

As the items in the square brackets are invariable (unless we go from a fixed to a sun-tracking collector) the only hopes for getting a lower price lie in the terms J_c, C and E_t. Clearly a large increase in E_t is not to be expected since even a high temperature plant will have a value of less than 0.3. Also as J_c is decreased by having a longer lifetime for the collector, C will tend to rise.

From this it becomes patently clear that for solar power units using conventional collectors, the chances of getting power much below about 5 cents per kWh is small. Some breakthrough in really cheap long-lived collectors is needed before the situation will be radically altered. Some clues in this direction appear in the megawatt collectors. For the solar pond (paper S/47) a cost C of \$1 per m² is postulated, and putting $E_c = 0.15$, $E_t = 0.10$, $J_c = 0.0872$ (20 years) the collector component of power cost is 0.29 cents per kWh. For the plastic-covered pond (paper S/15), the annual charges on the collector are given as \$885 178 (per sq mile) and the annual power yield as 29 055 840 kWh. This gives the collector component of the power price as approximate. This high value is because the author has given a J_c value of 0.313 to the plastic parts of the collector, i.e., a realistic 3-4 year life.[9]

The representative example given above which assumes $E_t = 0.15$ shows that any move to simplify the collector with consequent operation at lower temperature and leading to lower turbine efficiencies must be accompanied by a radical reduction in collector cost. Thus for E_t of the order of 0.05 due to low operating temperature (paper S/99), the collectors would have to fall to a third,[10] the price given in the above example to result in the same collector component in the power price.

Conclusions

For sizes in the range of a few kilowatts, there are good prospects of getting solar power in the near future at around 5 US cents per kWh in a sunny climate, using realistic interest and amortisation charges but omitting maintenance and operating costs. This implies the use of high efficiency heavy vapour turbines and collectors operating at about 150-200°C, with collector costs around \$20 per m² or collectors operating at lower temperatures but costing correspondingly less. Lower power costs can only come if the longevity of the collectors can be increased without a corresponding increase in their capital cost. If, for example, the collectors amortised over six years could be amortised over fifteen years the power cost would fall by nearly 2 cents per kWh.

Many consumers would consider 5 cents per kWh a reasonable price to pay for power in isolated communities, so the prospects for kilowatt power packages are quite good.

For large central power units in the megawatt class, a lower power price is essential and completely different types of collector, of an order of magnitude cheaper per unit area, must be evolved. Two suggestions have been forthcoming: one using plastic covers and hence having a high amortisation rate and one, the solar pond, using no plastics and amortised over a longer period. The solar pond still requires the solution of some serious problems. An extensive research programme is being actively pursued in Israel on this project and if successful could result in power costs of the order of 1 cent per kWh.

Topics proposed for discussion

(*a*) The papers as published. Validity of the authors' assumptions. Practicality of the proposals. New suggestions to correct errors in concept by the authors;

(*b*) Contributions (ideas, methods, concepts) to power production so far not proposed in the printed papers on collectors, on prime-movers, on energy exploitation (to match energy supply);

(*c*) Needs of under-developed countries. Kind of power supplies, for what purposes, in what sizes. Is continuous power essential in certain cases? What would be night load compared to day load? Should plant be suitable also for operation with fuel (during cloudy seasons) and what kind of fuels are available locally? In what cases will mechanical power suffice? When is electricity required? If only electricity is provided (so that mechanical power is obtained from electric motors) how much does this impede use of solar machines?

[9] Since this report was written, R. L. Hummel, author of paper S/15, has pointed out an error in determining the power yield of his 1 sq mile collector. He assumes an average daily heat yield of 400 BTU per sq ft which, fed into a turbine as proposed by the General Electric Company taking 44 000 BTU per kWh (full load) would yield 92×10^6 kWh per year and not the 29×10^6 given in his paper S/15, and quoted in this report. [Note that this corrected yield is now much closer to that estimated for a 1 sq km "solar pond" — in paper S/47 — of 30×10^6 kWh : 1 sq mile = 2.59 sq km.]

With this correction, the collector component of capital cost for the system proposed by R. L. Hummel becomes 1 cent and not 3 cents as stated above.

[10] This is not quite true : the low temperature collectors are non-focusing, so the Q value is higher.

Is cooling water available—i.e., what condensing temperatures?

(*d*) Maintenance and longevity of plant. Ability of local populations to maintain a solar plant. Cleaning of collectors, maintenance of engines, initial erection. Effect of climate, wind, storms, rain, erosion, corrosion. Effect of interference by wild animals, termites, etc.;

(*e*) Possibilities of local manufacture in part or in whole. Problems of transportation from point of manufacture to point of use.

References

1. Baum, V. A., Aparasi, R. R., and Garf, B. A., High Power Solar Installations, *Solar Energy I*, No. 1, pp. 6-12, Jan. 1957.
2. Tabor, H., Solar Energy, *Symposium Paper No. 12, UNESCO Symposium on Arid Zones*, May 1960.
3. Tabor, H., Stationary Mirror Systems for Solar Collectors, *Solar Energy II*, No. 3-4, July-Oct. 1958.

UTILISATION DE L'ÉNERGIE SOLAIRE POUR LA PRODUCTION D'ÉNERGIE MÉCANIQUE ET D'ÉLECTRICITÉ AU MOYEN DE MOTEURS ALTERNATIFS ET DE TURBINES

(Traduction du rapport précédent)

*Harry Tabor**

Parmi tous les buts de l'utilisation de l'énergie solaire, il semble que le plus recherché ait été la production d'énergie mécanique et électrique. Il est évidemment nécessaire d'ajouter que l'énergie produite doit l'être à un prix raisonnable. Un certain nombre d'installations d'énergie solaire réussies du point de vue technique ont été signalées dans des rapports au cours du dernier siècle, mais aucune d'elles ne serait considérée satisfaisante aujourd'hui du point de vue économique. Il faut admettre que le prix de revient de l'énergie solaire n'a pas besoin d'être aussi bas que celui de l'énergie classique produite dans des centrales à haut rendement dans des régions industrielles, car l'énergie solaire peut être nécessaire dans des régions éloignées où une alimentation centrale importante n'est ni disponible ni pratique. Mais, même dans de telles régions, le prix auquel le consommateur est prêt à payer l'énergie solaire ne peut dépasser certaines limites. Si le prix est trop élevé, il peut préférer s'en passer ou utiliser quelque autre source (bœufs, éoliennes, moteurs à vapeur brûlant des déchets, petits moteurs à essence ou diesel, etc.).

Nous examinerons par conséquent l'état actuel de la question en nous référant spécialement au prix de revient probable de l'énergie solaire.

Trois gammes de puissance

Les groupes solaires (groupes générateurs d'énergie mécanique à partir de l'énergie solaire) peuvent être grosso modo divisés en trois classes : les miniatures, les petits et les gros; les premiers représentant une production de puissance de quelques watts, les seconds étant de l'ordre des kilowatts, c'est-à-dire d'une fraction de kilowatt à plusieurs kilowatts, et les troisièmes de l'ordre du mégawatt.

Groupes solaires de l'ordre du watt

Pour quelques watts, il est à peu près certain qu'on n'envisagera pas de moteur thermique, mais uniquement des systèmes « statiques » (c'est-à-dire sans pièce en mouvement). Ceux-ci comprennent les cellules photoélectriques et les générateurs thermoélectriques et thermo-ioniques. Comme ils sont traités dans d'autres rapports de cette Conférence, nous ne les étudierons pas dans cette section.

Groupes de l'ordre du kilowatt et du mégawatt

Ils ont certains problèmes communs, mais présentent par ailleurs des différences fondamentales.

Différences

a) Les générateurs de l'ordre du mégawatt correspondent à une production d'énergie centralisée et à un réseau de distribution. Cela est en contradiction avec le principe selon lequel, puisqu'une distribution d'énergie doit en général être payée, alors que la distribution d'énergie solaire est libre, l'énergie solaire doit par conséquent être captée et transformée *au point d'utilisation.*

b) Les groupes de l'ordre du mégawatt exigent une très grande zone de captage d'énergie solaire, de sorte que, pour tout collecteur classique, le problème de l'entretien peut devenir insurmontable.

c) Étant donné que les groupes de l'ordre du mégawatt impliquent un réseau de distribution, le prix de revient de l'énergie aux barres omnibus doit être considérablement inférieur à celui d'un groupe de l'ordre du kilowatt qui peut être situé en n'importe quel point éloigné. Par conséquent, les groupes de l'ordre du mégawatt impliquent l'existence de collectivités évoluées et probablement industrialisées, ce qui abaisse encore davantage le prix qui peut être facturé pour l'énergie.

d) L'accumulation en vue d'assurer une alimentation régulière est une nécessité pour les groupes de l'ordre du mégawatt (sauf dans les rares cas où ils sont couplés à un réseau alimenté également par des centrales classiques), alors que les groupes de l'ordre du kilowatt peuvent être utilisés dans de nombreux cas sans accumulation, comme par exemple pour le pompage de l'eau.

C'est à cause de ces différences que de très nombreuses propositions ont été faites pour des groupes solaires de la classe du kilowatt, alors que de très rares suggestions ont été faites pour la classe du mégawatt. Dans certaines de ces suggestions, les différences énumérées ci-dessus n'ont pas toujours

* Directeur, Laboratoire national de physique d'Israël, Jérusalem.

été pleinement appréciées. Par exemple, le mémoire S/15 décrit un système comprenant un collecteur horizontal d'un mille carré (2,6 km²) recouvert d'une couverture plastique d'une seule pièce. On n'indique pas comment le plastique serait nettoyé (sauf par la pluie), et en cas d'avarie les réparations pourraient être très difficiles.

Similitudes

Nous allons maintenant examiner quelques-uns des problèmes et des solutions qui sont communs tant aux groupes de l'ordre du kilowatt qu'à ceux de l'ordre du mégawatt. Citons l'entretien et la durée de vie des éléments constituants, la température de fonctionnement, le rendement et le prix de revient, la nature du moteur thermique, la nature du collecteur.

a) *Entretien et durée de vie des éléments constituants*

Une centrale solaire n'entraîne pas de frais de combustible; le prix de revient de l'énergie est constitué entièrement des frais fixes (intérêt et amortissement) et des frais d'exploitation. Il s'ensuit qu'il faut accorder une très grande attention à la longévité des éléments constituants (en relation avec leur coût) et aux frais d'entretien, qui font partie des frais d'exploitation.

b) *Température de fonctionnement*

Le moteur et le collecteur sont liés principalement par le choix de la température de fonctionnement. Les principes suivants donneront une idée approximative de l'état actuel de la question.

Pour les températures de fonctionnement inférieures à 100 °C, il est possible d'envisager des collecteurs stationnaires non convergents. A part les avantages d'être stationnaires et de ne pas avoir de surfaces réfléchissantes susceptibles de se déformer ou de se détériorer, ces collecteurs exploitent le rayonnement diffus (ciel) aussi bien que le rayonnement solaire direct.

Pour les températures de fonctionnement comprises entre environ 100 et 200 °C, les collecteurs convergents stationnaires à faible concentration s'imposent. De tels collecteurs doivent pouvoir être inclinés à des angles différents selon les saisons, mais cela est une complication beaucoup moins grande que les mécanismes d'orientation destinés à suivre le cours du soleil.

Pour les températures de fonctionnement supérieures à 200 °C, des collecteurs orientables, qui suivent le cours du soleil, sont nécessaires, et pour les températures nettement au-dessus de 200 °C le miroir doit être un paraboloïde plutôt qu'un cylindre parabolique (d'une manière plus générale, il doit être une surfacce à double courbure, et non une surface à simple courbure). Les « collecteurs orientables » présentent l'avantage de « voir » plus de soleil qu'un collecteur fixe (environ 40 p. 100 de plus), mais le mécanisme d'orientation d'un collecteur de grande surface est extrêmement coûteux, par suite des sollicitations dues au vent. Les miroirs à double courbure sont si coûteux que nous ne pensons pas qu'ils soient jamais rentables pour des applications à la production d'énergie terrestre, sauf dans le cas des générateurs miniatures.

c) *Rendement et prix de revient*

L'interconnexion entre le moteur et le collecteur est en outre liée à une question de principe, à savoir au désir de réaliser soit un système à grand rendement avec un moteur et des collecteurs coûteux, soit un système à faible rendement avec des éléments constituants peu coûteux [1].

Cette question de principe est étudiée dans deux des mémoires qui traitent des groupes de l'ordre du kilowatt. Dans le mémoire S/54, les auteurs reconnaissent que le collecteur sera probablement le poste le plus coûteux : ils s'efforcent en conséquence de réaliser un moteur thermique de rendement aussi élevé que possible fonctionnant à une température modérée, en vue de limiter la dimension du collecteur : ils envisagent comme collecteur un cylindre parabolique, la température de fonctionnement étant de 150 à 200 °C. D'autre part, dans le mémoire S/99, l'auteur estime qu'il faut envisager le collecteur le moins cher possible, c'est-à-dire sans couverture de verre ou isolant, et par conséquent fonctionnant à basse température (de 40 à 50 °C par exemple). Il n'est pas possible d'établir une véritable comparaison entre ces différents points de vue, car le dernier mémoire ne fournit pas suffisamment de données sur les prix de revient; mais il est clair que le collecteur doit être extrêmement bon marché (par unité de surface) dans le dernier cas, car le moteur thermique n'aura probablement qu'un rendement du tiers de celui indiqué dans le mémoire précédent.

A l'autre bout de l'échelle, le mémoire S/27 traite d'un système à très haut rendement (miroir en paraboloïde précis, orienté pour suivre le soleil, produisant de hautes températures pour une turbine à métal liquide), mais, comme il s'agit d'une alimentation en énergie pour véhicules interplanétaires, le prix en est élevé (supérieur d'un ordre de grandeur environ à celui considéré dans les autres rapports), et il n'est pas du tout sûr qu'en assouplissant pour les applications terrestres certains des impératifs spéciaux de l'alimentation en énergie dans l'espace interplanétaire, ce prix de revient puisse être beaucoup réduit [2].

En dernière analyse, la politique correcte est celle qui conduit au prix de revient de l'énergie le plus faible, et cela ne peut être déterminé qu'en étudiant

---

[1] Pour les applications aux engins interplanétaires, il n'y a pour ainsi dire pas de choix : le système à fort rendement est nécessaire pour réduire les exigences de dimensions, de poids et de puits à chaleur.

[2] Le prix de revient dépasse 7 000 dollars par kilowatt installé pour un groupe de 15 kilowatts. Si ces éléments constituants sont amortis à 6 p. 100 d'intérêt et 6 p. 100 d'amortissement proprement dit pour leurs différentes longévités estimées, et si l'installation fonctionne à pleine charge 8 640 heures par an, l'élément frais de capital du prix de chaque kilowattheure dépasse 14 cents U.S.

les projets dans le détail, d'abord sur plan, puis sur prototype. Le seul partisan des collecteurs à rendement élevé et des moteurs à haute température a été le groupe de recherche russe (1), et sa proposition implique des prix de revient d'environ 2 000 dollars par kilowatt installé (2), de sorte que ce projet n'a pas été poursuivi. D'autres mémoires traitant de groupes de l'ordre du mégawatt envisagent des collecteurs de grande taille non convergents, peu coûteux et ayant des températures de fonctionnement inférieures à 100 °C.

d) *Le moteur thermique*

C'est à peu près le seul poste où le groupe de l'ordre du kilowatt est sérieusement désavantagé vis-à-vis du groupe de l'ordre du mégawatt. Pour ce dernier, les turbines (généralement des turbines à vapeur) peuvent atteindre 60 p. 100 du rendement de Carnot, ou même davantage, quelle que soit la gamme de température considérée. Par contre, on sait que les petits moteurs et turbines à vapeur de l'ordre du kilowatt ont un mauvais rendement. Cette question a été étudiée dans le mémoire S/54, où l'auteur montre que si l'on emploie, au lieu de vapeur, des fluides de fort poids moléculaire, ayant certaines caractéristiques spéciales, on a toutes chances de fabriquer des turbines de l'ordre du kilowatt ayant à peu près le même rendement que celles de l'ordre du mégawatt. Avec des températures de fonctionnement de 150 à 200 °C, on pense obtenir des rendements de l'ordre de 15 à 20 p. 100 des groupes de l'ordre de 2 à 10 kilowatts [3]. Si l'on suppose que le collecteur est un cylindre parabolique ayant un rendement de 40 p. 100 et coûtant 20 dollars par mètre carré, on obtient un prix d'énergie inférieur à 3 cents par kilowattheure, en admettant un taux d'intérêt de 6 p. 100 et une durée de vie du collecteur de six ans seulement. Cette mise au point d'un petit moteur à grand rendement fonctionnant à des températures modérées peut faire grandement progresser la réalisation de groupes préfabriqués pratiques produisant de l'énergie à base d'énergie solaire, de l'ordre du kilowatt.

e) *Le collecteur*

En ce qui concerne les collecteurs solaires pour groupes de l'ordre du kilowatt, les mémoires ne font pas état de grands progrès. La majorité des études sur le collecteur plan classique portent sur son utilisation en tant que dispositif de chauffage. Pour les applications en vue de la production d'énergie, presque toutes les propositions envisagent des collecteurs convergents, et dans de nombreux cas on a reconnu qu'il serait très souhaitable d'éviter les dispositifs d'orientation destinés à suivre le soleil. Dans ce dernier domaine de recherche, il y a eu malheureusement quelques erreurs de conception, car on a proposé des systèmes optiques qui sont dans l'impossibilité de faire ce que proclament leurs protagonistes [4].

L'auteur du présent rapport a démontré théoriquement (3) qu'un système de miroir stationnaire avec un ajustement saisonnier périodique par basculement peut donner une concentration optique d'environ trois fois, alors que lorsqu'il est complètement fixe, c'est-à-dire sans ajustement saisonnier par basculement, il ne peut donner aucune concentration optique utile. L'expérience des collecteurs pratiques semble confirmer ces conclusions théoriques. On peut obtenir une amélioration de la concentration optique par le principe du miroir à « temps partiel », c'est-à-dire d'un miroir construit de manière qu'aux différentes heures de la journée des parties différentes contribuent à la formation de l'image (pendant que le reste du miroir reste « inactif »). Lorsque le pourcentage de miroir inactif est important, les considérations économiques prouvent généralement que ce système ne présente pas d'intérêt. Le principe du miroir à « temps partiel » peut être utilisé, mais seulement dans une faible mesure, en étendant la surface d'un miroir actif à 100 p. 100 (cette extension étant inférieure à 100 p. 100 de la partie active), et il est relativement aisé de calculer si la partie étendue du miroir se trouve remboursée par le rayonnement solaire supplémentaire (moyenne sur un an) qu'elle fournit au foyer.

Les suggestions visant les collecteurs solaires pour groupes de l'ordre du mégawatt ont (pour des raisons compréhensibles) porté presque toutes sur les systèmes horizontaux non convergents. Deux mémoires de cette section traitent de cet aspect. Un troisième mémoire (non publié) a proposé des collecteurs classiques plans flottant sur la mer et fournissant de l'eau chaude à la source chaude pour une turbine à faible température, la mer constituant la source froide. La proximité de la source froide et de la source chaude réduit les problèmes de pompage auxquels s'est heurté le projet Claude-Boucherot pour extraire de l'énergie des océans. Si l'on applique les prix de revient actuels des collecteurs à plaques planes, le prix net de l'énergie fournie par un tel système semble être supérieur d'environ un ordre de grandeur au prix de l'énergie fournie par les centrales classiques.

Le mémoire S/15 propose un plan d'eau peu profond d'une surface de l'ordre d'un mille carré (2,6 km^2) couvert d'une couverture en plastique, et l'auteur propose un système ingénieux permettant d'adapter cette couverture, d'une seule pièce. Ce système a pour but de produire de l'eau distillée ainsi que de l'énergie, et cela est la caractéristique de la majorité des groupes solaires fonctionnant avec de l'eau à basse température. Dans de tels groupes à double fin, le coût de l'énergie dépend du prix auquel on fait payer l'eau distillée : lorsque

[3] Ce rendement relativement élevé permet d'exploiter économiquement la turbine avec des combustibles classiques pendant la saison nuageuse : lorsqu'on a proposé des moteurs ou turbines à faible température et faible rendement, leur exploitation au combustible pendant les saisons nuageuses ou pendant les pannes de collecteur a un mauvais rendement, et un second moteur fonctionnant au combustible traditionnel peut être nécessaire.

[4] Dans certains cas, ce désaccord est dû à l'utilisation de simples diagrammes à deux dimensions pour représenter un problème optique à trois dimensions.

l'eau douce est rare et permet par conséquent des prix suffisamment élevés, l'énergie peut être considérée comme gratuite. Cela n'est cependant pas une méthode économiquement saine de calcul ou de comparaison des différentes variantes, et la politique de fixation des prix de l'eau doit par conséquent être examinée très soigneusement. En vérité, si le prix de l'eau est fixé raisonnablement, il n'aura qu'un faible effet sur le prix de l'énergie. Par exemple, un générateur combiné d'énergie et de vapeur avec une condensation à simple effet de la vapeur pour fournir de l'eau douce, fonctionnant à une température de source chaude de 90 °C et condensant à 30 °C, rapportera environ 14 litres d'eau par kilowattheure d'énergie produite [5], soit une tonne d'eau (environ 250 gallons des États-Unis) pour 70 kWh. L'eau ne vaut que quelques cents, alors que l'énergie vaut environ 70 cents. Il est donc probablement plus juste (tout au moins en première approximation lorsqu'on compare les systèmes) de calculer le prix de l'énergie d'après le prix de revient du système, en traitant l'eau comme une prime gratuite, plutôt que de faire l'inverse. D'après les chiffres donnés dans ce mémoire, le prix de revient de l'énergie pourrait être d'environ 3,5 cents, et la question est de savoir si le système tel qu'il est envisagé est applicable et pratique. Autre point déjà mentionné : la conception d'une surface aussi grande sans murs de subdivision poserait de graves problèmes pour ce qui est du maintien de la couverture plastique propre et en bon état.

L'autre mémoire de ce groupe (S/47) commence par l'hypothèse que l'on doit s'efforcer d'éviter les plastiques, le verre et le métal pour les collecteurs de l'ordre du mégawatt, et que, par conséquent, seuls des grands plans d'eau (un océan ou un lac artificiel) peuvent être envisagés comme collecteurs de grande surface. La « piscine solaire » telle qu'il la propose a un fond noir, une profondeur de l'ordre du mètre, et la convexion y est supprimée en maintenant un gradient de densité dans la piscine au moyen de sel dissous ayant une concentration forte au fond et faible à la surface. Dans de telles conditions, un mètre d'eau constitue un bon isolant thermique, et le rapport indique des températures dépassant 90 °C. L'auteur signale trois problèmes techniques actuellement en cours d'étude : le maintien du gradient de densité, c'est-à-dire que celui-ci ne doit pas être troublé par les vagues ou par la méthode d'extraction de chaleur; l'extraction de chaleur du fond de la piscine; et l'évacuation des saletés tombant dans la piscine. Ces trois problèmes n'ont pas encore été résolus d'une manière entièrement satisfaisante, mais sont du type que l'ingéniosité humaine est capable de résoudre sans compliquer d'une façon extrême la construction de la piscine. Dans de telles conditions, l'énergie pourrait être produite à environ 1 cent des États-Unis par kilowattheure, et la capacité d'accumulation intrinsèque est suffisante pour assurer la fourniture d'énergie pendant un certain nombre de jours consécutifs sans ensoleillement. Étant donné les besoins en sel et ceux de grandes surfaces planes, la piscine solaire semble devoir se limiter dans ses applications aux régions des bords de la mer ou des lacs salés ou salines, dont il existe du reste un grand nombre dans les régions sous-développées du monde.

[5] Ce chiffre s'applique pour des différences de température de 60° C. Pour des différences supérieures, la production d'eau est proportionnellement basse et vice versa.

Considérations économiques fondamentales

Pour la majorité des installations à énergie solaire, les frais d'entretien et d'exploitation doivent être faibles car si tel n'est pas le cas, et nous nous rappelons les grandes surfaces de collecteur mises en jeu, le total des frais devient inadmissible. Pour les groupes de l'ordre du kilowatt, les surfaces sont maniables et, pourvu qu'il n'y ait pas de fâcheuses pannes mécaniques, l'entretien méthodique ne sera généralement pas imputé au prix de revient de l'énergie. Le facteur vital des frais est, par conséquent, constitué par les charges annuelles du capital investi.

Le calcul de ces frais est indiqué dans le mémoire S/54, et un calcul résumé est donné ci-dessous, car il met en relief la difficulté extrême que l'on éprouve à obtenir un faible prix de revient de l'énergie pour n'importe quel générateur d'énergie thermique à base d'énergie solaire.

Si Q = l'ensoleillement annuel total sur l'unité de surface du collecteur, exprimé en kWh par m²,
A_c = la surface du collecteur en m²,
E_c = le rendement moyen pondéré du collecteur,
E_t = le rendement moyen pondéré de la turbine ou du moteur,
C = le prix de revient de l'unité de surface du collecteur en dollars par m² (celui-ci comprend tous les autres prix qui sont proportionnels à la surface du collecteur, tels que la préparation du sol, la tuyauterie, etc.),
T = le prix de la turbine et les autres frais fixes en dollars par m² (celui-ci comprend tous les frais des postes dont l'importance ne dépend pas de la surface du collecteur, mais exclusivement de la puissance nominale du générateur),
J = charges annuelles de capital, exprimées sous forme d'une fraction (J_c s'applique aux collecteurs, et J_t à la turbine),
X = coefficient d'utilisation,

alors l'énergie produite par an $= QE_cE_tA_c$ (kWh)
l'énergie utilisée par an $= XQE_cE_tA_c$ (kWh)
les frais de capital $= CA_c + T$ (dollars)
les charges annuelles de capital $= CA_cJ_c + TJ_t$ (dollars)
∴ le prix de revient du kWh

$$= \frac{CA_cJ_c + TJ_t}{XQE_cE_tA_c}$$

$$= \frac{1}{XQ} \cdot J_c \left[\frac{C}{E_cE_t} + \frac{T}{A_cE_cE_t} \cdot \frac{J_t}{J_c} \right]$$

Dans presque tous les cas mentionnés dans les mémoires, le second terme entre crochets est faible comparé au premier[6], c'est-à-dire que le collecteur constitue le poste principal de capital du prix de revient, et nous lui accordons en conséquence une attention particulière.

Lorsqu'on connaît la manière dont varient toutes les variables C, E_c, E_t, J_t, J_c, A_c, en fonction de la température de fonctionnement et du type de construction du collecteur, il est possible d'optimiser l'équation des frais sur une calculatrice. Mais il est plus instructif pour le profane de traiter la question plus simplement à l'aide de quelques hypothèses initiales.

Nous supposerons que le poste prix de la turbine est faible et peut être négligé à ce stade. Nous supposerons que pour un type donné de collecteur et de turbine la température de fonctionnement a été choisie pour donner le rendement total E_tE_c le plus élevé. On peut montrer que, dans les gammes de température considérées, la température optimale de fonctionnement est celle pour laquelle à peu près la moitié de l'énergie incidente sur le récepteur est perdue par les pertes de chaleur[7], de sorte que le rendement du collecteur sera d'environ 0,4 pour les collecteurs dans lesquels 70 à 80 p. 100 du rayonnement incident atteignent le récepteur. Au point de fonctionnement optimal, on peut admettre en conséquence, pour E_c, une valeur d'environ 0,4 pour tous les collecteurs réels bien conçus, à l'exception de la piscine solaire, où moins de la moitié du rayonnement solaire atteint le fond (le « récepteur »), et E_c sera de 0,15 à 0,20.

Pour un site donné, Q est fixe[8], X dépend de la compétence de l'exploitant du groupe solaire, et tous les efforts doivent tendre à obtenir un X se rapprochant de l'unité.

Nous voyons maintenant que le poste clé déterminant le prix de revient de l'énergie est $J_c \frac{C}{E_t}$.

La valeur de J_c dépend du taux des intérêts grevant le capital et la durée de vie probable du collecteur. Les valeurs de J sont données dans l'annexe 2 du mémoire S/54. Pour un taux d'intérêt de 6 p. 100 et un fonds d'amortissement portant intérêt à 6 p. 100, par exemple, la valeur de J est de 0,203 pour une durée de vie de six ans et de 0,103 pour 15 ans. Lorsqu'on utilise des matières plastiques dans la construction des collecteurs pour réduire les prix, une durée de vie de six ans est probablement la meilleure que l'on puisse attendre dans l'état actuel de la technologie. Les collecteurs employant des matériaux plus durables (métal, verre, etc.) peuvent probablement être amortis sur 15 ans, alors que certains collecteurs proposés pour des alambics solaires, qui sont composés uniquement de béton, de verre et d'asphalte, peuvent être amortis sur des périodes beaucoup plus longues.

Considérons maintenant quelques valeurs typiques :

X = 1 (idéal!);

Q = 2 000 kWh par m², valeur correspondant à une région très ensoleillée et à un collecteur stationnaire;

E_c = 0,4, comme indiqué ci-dessus;

E_t = 0,15, correspondant à une turbine à vapeur lourde fonctionnant à 150 °C. Cette valeur est plusieurs fois plus élevée que celle donnée dans les mémoires pour les moteurs à basse température;

C = 20 dollars par m² (collecteur stationnaire convergent). Cela semble être le prix le plus bas qu'on ait osé suggérer pour les groupes solaires de l'ordre du kilowatt, et il suppose certainement l'utilisation de matières plastiques. Les miroirs compliqués ou les matériaux spéciaux peuvent facilement multiplier plusieurs fois ce prix;

J_c = 0,203, c'est-à-dire suppose une durée de vie de six ans pour le collecteur et des charges de 6 p. 100 d'intérêt.

Le poste collecteur du prix de revient de l'énergie devient alors :

$$\frac{1}{XQ} \cdot J_c \cdot \frac{C}{E_cE_t} = \left[\frac{1}{XQE_c}\right]\left(\frac{J_cC}{E_t}\right) = 3{,}4 \text{ cents E.-U. par kWh}$$

Comme les postes compris dans les crochets sont invariables (à moins que nous ne passions d'un collecteur fixe à un collecteur orientable suivant le soleil), le seul espoir d'obtenir un faible prix réside dans les termes J_c, C et E_t. Il est clair qu'il n'y a pas à attendre une forte augmentation de E_t, car même les installations à température élevée auront une valeur inférieure à 30 p. 100. Ainsi, lorsque J_c est réduit par suite de l'augmentation de la durée de vie du collecteur, C tend à augmenter.

On en déduit clairement que pour les groupes solaires utilisant des collecteurs traditionnels on a peu de chance de produire de l'énergie bien en dessous de 5 cents par kilowattheure. Une réduction très importante du prix des collecteurs à longue durée de vie est nécessaire avant que la situation se modifie radicalement. Quelques indices dans ce sens apparaissent dans le domaine des collecteurs de l'ordre du mégawatt. Pour la piscine solaire (mémoire S/47), on envisage un prix C de 1 dollar par

[6] Dans les groupes de l'ordre du mégawatt, ces termes doivent être sensiblement égaux pour permettre la concurrence avec les générateurs d'énergie classique, car, dans ce dernier cas, le poste « combustible » est de l'ordre de la moitié du prix de revient de l'énergie (voir mémoire S/54).

[7] Cela est analogue aux pertes internes dans une batterie couplée à la charge optimale pour la production d'énergie maximale.

[8] Celui-ci est fonction du type de collecteur : un collecteur orientable suivant le soleil « verra » plus de rayonnement solaire qu'un collecteur fixe.

mètre carré, et en posant $E_c = 0{,}15$, $E_t = 0{,}10$, $J_c = 0{,}0872$ (20 ans), le poste « collecteur » du prix de revient de l'énergie représente environ 0,29 cent par kilowattheure. Pour la piscine couverte de plastique (mémoire S/15), on indique des charges annuelles de collecteur de 885 178 dollars (par mille carré) et une production annuelle d'énergie de 29 055 840 kWh. Cela donne un poste « collecteur » du prix de l'énergie d'environ 3 cents. Cette valeur élevée provient du fait que l'auteur a donné une valeur J_c de 0,313 à la partie « matière plastique » du collecteur, c'est-à-dire une vie réelle de trois à quatre ans [9].

L'exemple typique donné ci-dessus et qui supposait $E_t = 0{,}15$ montre que toute modification en vue de simplifier le collecteur, entraînant une exploitation à de faibles températures et réduisant le rendement de la turbine, doit être accompagnée d'une réduction radicale du prix du collecteur. Ainsi pour E_t de l'ordre de 0,05, dû à la faible température de fonctionnement (mémoire S/99), il faudrait réduire le prix des collecteurs au tiers [10] des valeurs indiquées dans l'exemple ci-dessus pour obtenir le même poste « collecteur » dans le prix de l'énergie.

Conclusions

Pour les groupes solaires de l'ordre de quelques kilowatts, on a de bonnes perspectives d'obtenir de l'énergie d'origine solaire dans le proche avenir à environ 5 cents E.-U. par kilowattheure, dans un climat ensoleillé, en utilisant des charges d'intérêt et d'amortissement raisonnables, mais sans tenir compte de l'entretien et des frais d'exploitation. Cela implique l'utilisation de turbines à vapeur et collecteurs lourds à haut rendement fonctionnant à environ 150-200 °C, avec des prix de collecteur de l'ordre de 20 dollars par mètre carré ou des collecteurs fonctionnant à des températures plus basses, mais coûtant en conséquence moins cher. On ne pourra obtenir des prix de revient inférieurs de l'énergie que si l'on peut accroître la longévité des collecteurs sans augmenter en conséquence leur prix d'installation. Si, par exemple, les collecteurs amortis sur six ans pouvaient être amortis sur 15 ans, le prix de l'énergie baisserait d'environ 2 cents par kilowattheure.

De nombreux consommateurs considéreraient que 5 cents par kilowattheure constituent un prix raisonnable pour l'énergie dans les collectivités isolées, de sorte que les perspectives sont assez bonnes pour les centrales autonomes préfabriquées de l'ordre du kilowatt.

Pour les grandes centrales de la classe du mégawatt, un prix inférieur de l'énergie est essentiel, et l'on doit mettre au point des types complètement différents de collecteurs moins chers d'un ordre de grandeur par unité de surface. Deux suggestions ont été faites, l'une utilisant des couvertures en matières plastique, et ayant par conséquent un taux élevé d'amortissement, et l'autre (la piscine solaire) n'utilisant pas de plastique et amortie sur une période plus longue. La piscine solaire ne peut être réalisée que si l'on résout certains problèmes sérieux : les chercheurs israéliens ont lancé un programme de recherche à cette fin, et, s'il réussit, cela pourrait permettre d'obtenir des prix d'énergie de l'ordre de 1 cent par kilowattheure.

Sujets de discussion proposés

a) Examen des mémoires publiés : les hypothèses des auteurs sont-elles valables ? Leurs propositions sont-elles pratiques ? De nouvelles suggestions permettent-elles de corriger des erreurs de conception des auteurs ?

b) Contributions (idées, méthodes, conceptions) à la production de l'énergie qui n'ont pas été proposées jusqu'ici dans les mémoires imprimés : sur les collecteurs, sur les moteurs, sur l'exploitation de l'énergie (venant compléter la fourniture d'énergie).

c) Besoins des pays sous-développés : quelle sorte de fourniture d'énergie, à quelles fins, de quelles puissances ? Une fourniture continuelle d'énergie est-elle indispensable dans certains cas ? Quelle serait la charge de nuit comparée à la charge de jour ? Les installations devraient-elles pouvoir également être actionnées au combustible traditionnel (pendant les saisons nuageuses), et de quelle sorte de combustible dispose-t-on localement ? Quand l'électricité serait-elle nécessaire ? Dans quels cas l'énergie mécanique suffirait-elle ? Si l'on ne fournit que de l'électricité (de sorte que l'énergie mécanique devrait être obtenue à partir de moteurs électriques), dans quelle mesure cela fait-il obstacle à l'utilisation des machines solaires ?

Dispose-t-on d'eau de refroidissement (c'est-à-dire quelles sont les températures de condensation ?).

d) Entretien et longévité de l'installation : les populations locales peuvent-elles entretenir une installation solaire (nettoyage des collecteurs, entretien des moteurs, montage initial) ? Effet du climat (vent, tempêtes, pluie, érosion, corrosion) ; effet des animaux sauvages, termites, etc.

e) Possibilités de fabrication locale partielle ou totale : problèmes de transport du point de fabrication au point d'utilisation.

---

[9] Depuis la rédaction de ce rapport, R. L. Hummel, auteur du mémoire S/15, a relevé une erreur dans la détermination de l'énergie produite par son collecteur de 1 mille carré. Il suppose un apport journalier moyen de chaleur de 400 Btu par pied carré (1 080 Kcal par m²) qui, envoyé dans une turbine comme proposé par la General Electric Company en comptant 44 000 Btu par kilowattheure (11 000 Kcal par kWh) à pleine charge produirait 92×10^6 kWh par an, et non les 29×10^6 donnés dans son mémoire et rappelés dans le présent rapport.

Il faut noter que cette production corrigée est maintenant beaucoup plus proche de celle estimée pour une « piscine solaire » de 1 mille carré dans le mémoire S/47, de 30×10^6 kilowattheure (1 mille carré = 2,59 kilomètres carrés).

Avec cette correction, le poste « collecteur » des frais de capital du système proposé par R. L. Hummel devient de 1 cent et non 3 cents comme indiqué plus haut dans ce rapport.

[10] Cela n'est pas tout à fait exact ; les collecteurs à basse température n'étant pas convergents, la valeur Q est plus élevée.

Références

1. Baum, V. A., Aparasi, R. R., et Garf, B. A., High Power Solar Installations, *Solar Energy I*, n° 1, p. 6-12, janvier 1957.

2. Tabor, H., L'énergie solaire, *Document n° 12 du cycle d'études de l'UNESCO sur les zones arides*, mai 1960.

3. Tabor, H., Stationary Mirror Systems for Solar Collectors, *Solar Energy II*, n° 3-4, juillet-octobre 1958.

USE OF SOLAR ENERGY FOR MECHANICAL POWER AND ELECTRICITY PRODUCTION BY MEANS OF PISTON ENGINES AND TURBINES

Rapporteur's summation

The conversion of heat to power is such an old technology, and so much has been done in this field, that new breakthroughs are hardly to be expected. This is in contrast with the direct conversion systems covered in agenda item II.C.1 (*b*) that follows.

In the discussion of agenda item II.C.1 (*a*), it appeared that all we can hope to do is to chose optimum conditions for the operation of machines by sunshine, using known principles, such as hot air engines, vapour turbines, and the like. Clearly the question arises: With what does the solar power machine have to compete? Is there local timber or other fuel; can fuel oil be brought in at a reasonable price; is there an electricity network? One of the good features of the discussion in the technical session was that these questions were discussed in relation to under-developed countries, and the vital necessity of assessing the power needs of small communities was stressed. A delegate from Burma said that power in his country — in the remote areas — costs 15 cents per kWh, and this price could, in my view, easily be matched by a solar machine even with what is known today. As mentioned in earlier discussions, it depends on what the power is wanted for.

The discussion, and the papers submitted, divided power units into small units of, say, one to 10 kW, and larger units in the megawatt class. In the latter case these would almost certainly have to compete with conventional power units; the electric power cost would therefore have to be low (below one cent per kWh), and two papers discussed the interesting possibilities of large-area collectors. Probably neither of these authors would undertake to build such a plant at this time, but the ideas expressed were certainly interesting, both from a scientific and from a technological point of view.

The emphasis in the discussion was clearly on small units for the supply of limited amounts of power to areas generally not connected to an electric grid, where conventional fuels were either non-existent or extremely expensive. The thought seemed to be that units were needed in the range of one (or possibly 0.5) kW to about 10 kW, with somewhat larger units (25-50 kW) for larger communities.[1]

The question, "What would these units be used for?" is important in deciding what to construct. Water pumping seemed an obvious use, with electric light not far behind. No one seemed too worried about long-term storage guaranteeing a continuous supply, particularly in areas of under-employment, so that looms or other machines for local industry would work when there was sunshine; but a degree of storage able to give, say, five hours of electric lighting in the evening seemed desirable for the social progress of many communities.

From the technical point of view, there were the traditional arguments: whether to have a high-efficiency system operating at elevated temperatures and using an expensive collector system, or a low-temperature, lower efficiency device using simpler collectors. The final answers may come only when we have built the prototypes of various kinds and tried them out; paper studies are often deceptive.

In determining the size of a unit, not only are local needs to be studied but also the problems of transport and geographical location. One delegate pointed out that in his country there were very poor roads between villages — indeed they were not roads but tracks — so that a solar plant needed to be easily transportable. In hilly country, it should be designed in small units, since there might not be a large enough area to accommodate a large collector.

There was not much discussion of solar collectors for power since this subject had been discussed in other sessions on collectors, and the problems are the same after working temperature has been decided. There was considerable discussion, however, of new engine development; it included two demonstrations.

Hot air engines were discussed, and an extremely interesting small power model was exhibited. The efficiency can be very high, and the only difficulty appears to be that it operates best at high temperatures, using solar energy concentrated directly into the piston head. This would tend to limit the size of device of this kind that can be solar operated.

A vapour turbine operating at moderate temperatures was also described and demonstrated. This turbine shows satisfactory efficiency (in relation to the temperature of operation) and requires a relatively simple collector. This appeared to be the only proposal for which even an approximate guess at costs could be made, and the picture is quite encouraging.[2]

---

[1] One delegate thought 25 kW would supply the needs of up to 1 000 persons.

[2] This particular exhibit was an experimental model, designed to show the lines of thinking and working; it is still quite a long way from a prototype commercial installation.

In the session on solar cooling, some sociological difficulties were presented in attempts to get acceptance of solar devices, such as solar cookers, that may interfere with the individual habits of the household or housewife, or of solar refrigerators and air conditioners, which represent a new concept in many cases. It seems unlikely, however, that the solar power unit would meet with this kind of resistance; everyone is familiar with other sources of power, such as the ubiquitous gasolene engine. In this respect, the task of introduction is much easier.

The usefulness of a power source in any community — particularly if it does not require imported fuel — can be recognized by almost any community leadership and certainly by governments. Thus, if the price is right and financing is possible, solar power units, if technically satisfactory — a point stressed by G. O. G. Löf — constitute an area of solar energy utilization having a future.

What are the prospects of practical solar power? For large units: to produce centralized power at a price competitive with large thermal or hydroelectric stations, we can say that there are some ideas, but a great deal of work still has to be done before there is any certainty of the economic and technical viability of the proposed schemes. For small units: the future appears bright; there is a range of power prices with which the solar machine has to compete, so that it is probably possible to get into the top end of the range, i.e., a small area of the potential market, even with what is known today.

As research proceeds and the capital cost can be reduced, we can hope for an increase in the area where solar power units are competitive. It is not clear that we will progress to the point of satisfying everyone's needs, but my personal feeling is that a considerable and widening area of justifiable applicability is in view if the present research programmes are continued and expanded.

UTILISATION DE L'ÉNERGIE SOLAIRE POUR LA PRODUCTION D'ÉNERGIE MÉCANIQUE ET D'ÉLECTRICITÉ AU MOYEN DE MOTEURS ALTERNATIFS ET DE TURBINES

Résumé du Rapporteur

La conversion de la chaleur en énergie est une technique si ancienne et qui a fait l'objet de tant de travaux qu'on ne doit guère s'attendre à de grandes découvertes nouvelles; la situation est inverse en ce qui concerne les systèmes de conversion directe de l'énergie dont traite le point II.C.1, *b*, de l'ordre du jour.

Au cours de l'examen du point II.C.1, *a*, de l'ordre du jour, il est apparu que tout ce que l'on peut espérer est de choisir les conditions optimales de fonctionnement d'appareils solaires dont le principe est déjà connu : moteurs à air chaud, turbines à vapeur, etc. Manifestement, la question se pose de savoir avec quoi la machine solaire devra entrer en compétition. Trouve-t-on sur place du bois ou un autre combustible ? Le pétrole peut-il être amené à un prix raisonnable ? Existe-t-il un réseau de distribution d'électricité ? Un des avantages de la discussion en séance technique est que l'on a examiné ces questions du point de vue des pays sous-développés et souligné la nécessité vitale d'évaluer les besoins énergétiques des petites collectivités. Un participant birman a dit que dans son pays — tout au moins dans les régions isolées — l'énergie coûte 15 cents le kilowattheure, tarif qui pourrait, à mon avis, être facilement concurrencé par celui de l'électricité solaire, même en l'état actuel des connaissances. Comme on l'a dit précédemment, cela dépend de l'emploi que l'on veut faire de l'électricité.

Au cours de la discussion, et dans les mémoires présentés à la Conférence, on a distingué parmi les installations énergétiques les petites installations d'une puissance de 1 à 10 kW environ et les grandes installations d'une puissance de l'ordre du mégawatt. Ces dernières devraient presque à coup sûr entrer en compétition avec les centrales classiques; il faudrait donc que le coût de l'électricité soit peu élevé (inférieur à 1 cent par kilowattheure), et deux mémoires ont examiné les possibilités intéressantes qu'offrent les collecteurs de grande superficie. Sans doute ni l'un ni l'autre auteur ne voudrait-il entreprendre la construction d'une pareille installation à l'heure actuelle, mais les idées qu'ils ont avancées présentent un intérêt certain, aussi bien du point de vue scientifique que du point de vue technique.

Au cours de la discussion, on a mis très nettement au premier plan les petites installations capables de produire des quantités limitées d'électricité dans des régions qui ne sont généralement pas reliées à un réseau de distribution et où les combustibles classiques sont introuvables ou extrêmement chers. Il semble, de l'avis général, qu'il faille construire des installations ayant une puissance de l'ordre de 1 (ou peut-être 0,5) jusqu'à environ 10 kW, ainsi que des installations un peu plus importantes (25 à 50 kW) pour les grandes collectivités [1].

Il y a lieu de se demander, quand il s'agit de décider ce que l'on va construire, à quoi serviront les installations. Le pompage de l'eau est apparu comme une utilisation évidente de l'énergie solaire, la production d'électricité venant ensuite. Nul n'a semblé s'inquiéter outre mesure de la conservation de l'énergie pendant une longue période, ce qui assurerait la continuité de l'approvisionnement, notamment dans les régions de sous-emploi, de sorte que les métiers ou autres machines utilisés par l'industrie locale continueraient à fonctionner même en l'absence de soleil; mais il a semblé souhaitable pour le progrès social de nombreuses collectivités de pouvoir accumuler l'énergie solaire de manière à fournir, par exemple, cinq heures de courant pour l'éclairage pendant la soirée.

Du point de vue technique, on a procédé à la discussion classique, en se demandant si un système de grand rendement fonctionnant à des températures élevées et utilisant un collecteur coûteux est préférable à une installation de moindre rendement fonctionnant à basse température et utilisant un collecteur plus simple. On ne pourra donner une réponse définitive qu'après avoir construit et expérimenté divers prototypes, car les études théoriques sont souvent trompeuses.

Quand on détermine les dimensions d'une installation, il faut étudier non seulement les besoins locaux, mais encore les problèmes de transport et la situation géographique. Un participant a fait observer que dans son pays les villages n'étaient reliés entre eux que par des routes très mauvaises — ou plutôt des pistes —, de sorte qu'il fallait qu'une installation solaire soit facilement transportable. En pays accidenté, les installations doivent être conçues sous forme de petites unités, car il se pourrait qu'on n'y trouve pas une surface assez étendue pour implanter un grand collecteur.

La question des collecteurs d'énergie solaire n'a pas été étudiée longuement : elle l'avait été au cours d'autres séances spéciales, et les problèmes sont les

[1] Un participant a estimé qu'une puissance de 25 kW couvrirait les besoins d'un millier de personnes.

mêmes une fois qu'on a pris une décision quant à la température de fonctionnement. Mais on a longuement parlé, en revanche, de progrès concernant de nouveaux moteurs, et deux démonstrations ont été faites.

Les moteurs à air chaud ont fait l'objet d'un débat, et un modèle de petite puissance extrêmement intéressant a été exposé. Le rendement de ces moteurs peut être très élevé; leur seul inconvénient, semble-t-il, est qu'ils fonctionnent le mieux aux températures élevées si on concentre l'énergie solaire directement sur la tête du piston. Cet inconvénient aurait pour effet de limiter les dimensions d'un appareil de ce genre mû par l'énergie solaire.

Une turbine à vapeur fonctionnant à des températures moyennes a été également décrite et exposée. Elle a un rendement satisfaisant (compte tenu de la température de fonctionnement) et ne nécessite qu'un collecteur relativement simple. Cet appareil est, semble-t-il, le seul pour lequel on a donné ne fût-ce qu'une idée approximative du prix éventuel, et les perspectives sont très encourageantes [2].

Au cours de la séance consacrée à la production de froid par l'énergie solaire, on a signalé les difficultés d'ordre sociologique auxquelles on s'est heurté lorsqu'on a voulu faire accepter l'utilisation d'appareils solaires, tels que des cuisinières, propres à modifier les habitudes d'un ménage ou d'une ménagère, ou des réfrigérateurs et climatiseurs qui sont dans bien des cas des innovations. Mais il paraît très vraisemblable que l'installation d'appareils de production d'électricité solaire rencontre ce genre de résistance, car tout le monde connaît d'autres générateurs d'électricité, comme le moteur à essence que l'on trouve partout. A cet égard, le travail de présentation devient bien plus aisé.

L'utilité d'une source d'énergie dans une collectivité — notamment si cette source ne nécessite pas l'importation de combustible — peut être admise par presque tous les chefs de collectivité, et à coup sûr par les gouvernements. Ainsi donc, si le prix est raisonnable et le financement possible, les générateurs solaires, à condition d'être satisfaisants du point de vue technique — aspect sur lequel G. O. G. Löf a insisté —, sont une catégorie d'appareils qui donnent à l'utilisation de l'énergie solaire un avenir certain.

Quelles sont les perspectives d'utilisation de l'énergie solaire ? Pour les grandes installations, il s'agit de produire de l'électricité à un prix qui permette la concurrence avec les grandes centrales thermiques ou hydro-électriques; on peut dire que les idées sont là, mais il reste fort à faire avant de garantir avec certitude la rentabilité économique et technique des projets proposés. Pour les petites installations, l'avenir apparaît brillant : l'éventail des prix de l'électricité est très ouvert et les générateurs solaires doivent pouvoir fournir de l'électricité à un prix compétitif, probablement au haut de l'échelle des tarifs, c'est-à-dire dans un petit secteur du marché futur, même en l'état actuel des connaissances.

Au fur et à mesure que les recherches se poursuivent et que les frais d'équipement diminuent, on peut espérer élargir le secteur dans lequel les installations solaire sont compétitives. Nul ne sait si les progrès seront tels qu'ils permettront de satisfaire les besoins de chacun, mais, à mon avis, il est possible d'envisager un secteur considérable et qui ira s'élargissant, dans lequel il est justifié de mettre en œuvre des techniques d'exploitation de l'énergie solaire, à condition de poursuivre et d'intensifier les programmes actuels de recherche.

[2] L'appareil exposé n'était qu'un modèle expérimental destiné à faire la démonstration de la conception et du fonctionnement; ce n'est pas, loin s'en faut, un prototype d'installation commerciale.

THERMAL MACHINES FOR THE CONVERSION OF SOLAR ENERGY INTO MECHANICAL POWER

*Luigi D'Amelio**

While methods for the direct conversion of solar energy arriving on the earth into electric energy are being developed, or even better, while methods presently in use for such conversion are brought to acceptable economical levels, the old solar machine, i.e., the steam or hot-air thermal machine fed by solar heat collected either by concentration of solar radiation on surfaces of limited extension or by direct insolation of flat surfaces exposed to sun-rays, may still prove useful, especially in areas where lack of widespread distribution of traditional type energies, electric or fuel-born, makes energy procurement difficult and expensive, and where solar energy is available at a convenient intensity and with suitable presence diagram (Arizona, California, India, North Africa, etc.).

Objectively, any conception that a solar machine, specifically a thermal machine driven by solar heat, may economically compete with traditional type energies wherever they are available at normal costs, would prove illusory inasmuch as solar energy presents conspicuous disadvantages with respect to the former, such as intermittence in its present diagram and storage problems, over and above the economical factors which, independently of the specific type of energy considered, burden all self-producers of small quantities of energy.

The solar machine may therefore be beneficially employed, especially when no operational continuity is required, i.e., for irrigational purposes in areas where water is to be raised from limited depth. Solar energy, however, together with wind energy, offers a great advantage as compared with traditional type energies: it is available at no cost and neither requires a distribution system nor necessitates transportation from source. In other words, it can effectively substitute for other forms of energy wherever distribution costs to the site of the latter become prohibitive.

However, it is imperative that solar machines become positively practical and the cost of the unit of energy produced, inclusive of all ordinary and emergency maintenance charges, settles at a level comparable with that of traditional type energies furnished on site and inclusive of all the aforesaid factors.

At this point, it would be advisable to remark that, as of today, a truly practical solar machine (as used hereafter, the expression "solar machine" indicates a steam or hot-air thermal machine) has not been constructed. It can also be safely stated that, with the very rare exception of machines having a limited power output (fractions of a horsepower), no specimen is at present in operation on an industrial basis, in the commonly accepted meaning of those words. It may be therefore worthwhile to investigate the cause of the failure in the development and adoption of solar machines.

Recent models of solar machines with concentration of solar radiation do not show any appreciable difference especially when examining the boiler section, from the model developed by Monchot (1886-1872) or the one developed by Frank Schuman (1913, Meady, Egypt) which succeeded in producing 63 bhp, though it had to be provided with 1 200 sq m of insolated surface with a concentration ratio of 4.5 to 1. Among the solar machines without concentration of solar radiation, one of the most interesting is still the model developed by Frank Schuman, which had a 3 hp output and an 80 sq m insolated surface. Shall we then be led to the conclusion that half a century of intense progress has had no influence in this field?

It may be stated that in some respects, progress itself has hindered solar machine development, inasmuch as it has contributed to an ever-increasing distribution of electric energy or energy produced by small internal combustion engines at ever-decreasing cost, thereby making competition extremely difficult.

However, though limiting the adoption of solar machines to the areas mentioned above and to comparable ones, it might be questioned whether solar machine design has fully utilized the progress that has been achieved today. In my opinion, solar machine design has failed to utilize the means that progress, from time to time, has made available to it.

If we study solar machines with concentration type collectors made of parabolic mirrors or parabolic troughs composed of several flat mirrors arranged on a parabolic framework, we notice that researchers have devoted their efforts to increase the thermodynamic efficiency of the machine by augmenting the concentration ratio and raising the collection temperature, trying at the same time to reduce heat losses in the boiler located in the focus of the concentrator. The brilliant and ingenious solutions

* Institute of Mechanics, University of Naples.

devised so far, while leading to even more efficient models, have resulted in the construction of machines that are more suitable for laboratory than for industrial utilization and that are complicated and have high ordinary and emergency maintenance costs, limited life and, above all, ever-increasing operational difficulties.

In order to spread the use of solar machines, the economical factor, i.e., the cost of ready-for-use energy inclusive of all economical burdens, should be given utmost consideration. In my opinion, this cost, as determined by the employment of concentrator-collector systems, cannot be brought down to acceptable levels, especially because of mirror wear—and glass mirrors wear rapidly—of mirror delicacy and maintenance and of the necessity for expensive orientation during insolation hours and because of the problems resulting from fully automatic operation.

The flat collector systems, utilizing flat, glass-top boxes directly exposed to sun-rays, appear to be free from many of the disadvantages listed for concentrator-collector systems, but on the other hand, because of the smaller temperature drop between hot and cold sources, they require, of necessity, a larger, although less expensive insolated surface.

It may be noted that the difference between the two systems lies in the following: with reference to the unit of energy produced, the first system requires smaller insolated surfaces at a higher unit cost, while the second requires larger insolated surfaces at smaller unit cost.

A comparison between the two final products is fundamentally important: in concentrator-collector systems, the insolated surface is progressively reduced while the concentration ratio is increased, thereby raising the initial temperature. The cost of the final product per unit of energy and under identical conditions of insolation, air transparency, temperature, etc., has definitely increased, while the solar machine has constantly drawn away from economical utilization and acceptable operating conditions. With respect to the flat collector system, it can be affirmed that the same end results have been attained during these past years. Attempts have been made to reduce heat losses from flat boxes directly exposed to sun-rays by encasing them in thermally insulated containers. Heat losses through the side facing the sun have also been reduced through the application of single or double glass tops. Furthermore, systems have been developed to have the boxes continuously orientated in such a manner as to keep the insolated side perpendicular to sun-rays. Finally, and this is, very likely, the most serious mistake that has been made, consideration has been given to the problem of making the unit mobile, thereby developing expensive steel-bearing structures. It may be safely stated that through the addition of these various features, the cost of one sq m of insolated surface doubles or triples the cost of an equal size surface of a simple, flat box, exposed to solar radiation, with no thermal insulation, no glass tops, no orientators, and fixed. Such an increase occurs without the "active" surface, intended to produce more energy under the conditions indicated above, being proportionally reduced. The installation cost per unit of energy has therefore increased while the economical convenience has, of necessity, decreased.

As a result of all the above, the effective utilization of solar machines has become more remote and industrial applications almost obliterated. It may be added that, in order to make a solar plant acceptable, or rather, to make its cost acceptable, the trend is towards small power output installations, i.e. fractions of a horsepower, sometimes down to hundredths of a horsepower. It is evident that on this scale, the cost of a power unit, though obtained from traditional fuels, becomes prohibitive and plant operation absurd, especially if it requires the services of one person.

We are now faced with the following question: is it at present possible to construct a 2 or 3 hp solar machine that, under the above-mentioned conditions and in areas of limited electric energy distribution, may produce energy at economically acceptable levels?

Whoever has lived in the countryside, on farms located away from electric power distribution lines, knows by direct experience how useful it may prove to have, even for a few hours a day, a small power capacity to employ for irrigation purposes, to produce limited quantities of electric energy to be stored for farm use, etc. To realize this fact, one may recall the several thousands of wind-driven motors installed in areas where the diagram of wind presence indicates fairly constant conditions. It should be noted that an economical size wind-driven motor, of current model, with a wind-speed of 5 to 7 metres per second, and with a 6-metre diameter propeller, furnishes for a few hours per day a power output of less than 1 hp. It should also be noted that the power output diagram of such a motor is highly irregular and that costly storage facilities have to be installed if energy is drawn at a constant rate. In addition to that, a wind-driven motor is very expensive and leads, especially in hurricane areas, to very high maintenance expenses.

As compared with wind-driven motors, solar machines, installed in suitable areas, offer the advantages of continuous reliable operation, though limited to four or five hours a day, and of not being endangered by energy paroxysms which often destroy complete installations. The field of application of solar machines is therefore considerably wide and it is worth studying the problems connected to them with the intent of finding solutions economically acceptable.

As a result of the foregoing, the solution, in my opinion, is to be found in a solar machine reduced to its most simple expression, with respect to installation costs, maintenance expenses and operational features.

Flat collector solar machine

It may be usefui to recall, at this point and in very general terms, the operation of a flat collector solar machine. The machine is made of several components which may be examined separately:

(*a*) A flat surface, exposed to solar radiation and oriented in such a manner as to remain as long as possible perpendicular to sun-rays. This surface absorbs the solar heat while its temperature rises to the value $T1$;

(*b*) A boiler, operating at temperatures slightly different from surrounding values. It receives the collected heat and utilizes it to evaporate a suitable type fluid at a temperature $T2$ and a pressure $p2$;

(*c*) A steam engine, normally of a reciprocating type, which utilizes the vapour produced in the boiler and discharges it at a temperature $T3$ and a pressure $p2$;

(*d*) A condenser, in which the vapour converts back into liquid form ready for re-use in the boiler. The condenser is fed by a cooling medium, air or water, at a temperature $T4$.

Collection

Flat surface

A flat surface, exposed to solar radiation, absorbs a certain quantity of heat which is determined by the value of the temperature attained and the heat losses. These losses, in turn, depend upon the thermal insulation of the surface considered, both from radiation and conduction-convection. The difference Q between the collected heat and the heat losses is the quantity of heat available for utilization in the machine.

Under equal values of insolation and thermal insulation, and under equal surrounding conditions, Q is determined by the temperature of the flat collector and decreases rapidly as the temperature rises. At a certain value Te of the temperature, the heat losses will balance the input. Under these conditions, Q becomes zero and therefore, notwithstanding the maximum temperature drop between the collector and the condenser which results in the maximum thermodynamic efficiency, the mechanical work attainable from the engine is zero, this being the value of the quantity of heat available for the cycle.

Similarly, if the collection is made at the same temperature of the condenser $T3$, the quantity Q of heat available for the cycle would be the maximum, but no mechanical work would result, the temperature drop being zero.

Between these two limits, the optimum temperature Tm may be placed, by experiment, depending upon the location and the type of machine used, and noting that the maximum theoretical work is

$$L = 427\ Q \times \frac{T2 - T3}{T2}$$

where Ts are absolute temperatures. The engine follows a Rankine rather than a Carnot cycle, but in the case of close temperature values, like those under consideration, differences between economical coefficients and the two cycles are negligible.

It should be noted that the engine operates between the isothermal lines $T2$ and $T1$ during evaporation, and $T3$ and $T4$ during condensation; its maximum theoretical efficiency is as indicated above. $T2$ should therefore be close to $T1$, and $T3$ to $T4$.

Boiler

The heat collected may be conveyed to the boiler in several ways. It may be conveyed directly, by welding on the back of the flat plate exposed to solar radiation a flat coil containing the fluid to evaporate; or it may be conveyed indirectly, by transferring the heat to a medium—water— which conveys the heat to the boiler where the heat is released to the fluid to evaporate through the boiler walls. In this case, the insolated flat plate constitutes the upper surface of a sealed box where water is circulated.

It should be noted that the advantages offered by the first system are only apparent; the coil welded to the flat plate acts like a finned tube which entails taking into account the efficiency of the fin, i.e., the fact that the heat collected by the fin cannot be transferred to the foot of the same—the welding—and hence to the coil, but by conduction along the fin itself. The average collector temperature must therefore be higher than that of the coil and of the liquid to evaporate. The resulting temperature drop cannot be neglected.

On the other hand, in the case of heat transfer through a water medium, because of the high wall-water thermal conductivity and the limited thickness of the wall, the water covers the entire insolated surface and its temperature becomes very close to the collector's temperature with no appreciable resulting temperature drop.

The water conveyed to the boiler will release its heat to the fluid through the boiler walls, thereby originating a temperature drop.

In properly designed machines, both systems, coil and water transfer, are, with respect to temperature drops, practically equivalent. This is not the case when air is used as a transfer medium. The low wall-air thermal conductivity determines a far greater temperature drop.

When considering that a solar machine of the type described requires approximately 40 sq m of exposed surface per horsepower during hours of optimum insolation, it can be easily imagined what complications will result in a plant whose boiler, though made of a simple finned coil, extends on a surface which, for a 3 hp output, would be approximately 100 sq m. Being, of necessity, made in sections, its installation would require numerous vapour-tight couplings and joints, with the impending threat of

possible leaks of an expensive and not readily available item.

The coupling of boxes containing water at a pressure close to surrounding values is easier and simpler.

As water boxes are more commonly used, it may be worth while examining their structure. As mentioned above, there are two trends in water-box construction. The first calls for a thermal insulation of the generally short and rectangularly shaped box, to be effected, on the five unexposed sides, by means of a wooden casing containing the thermal insulation, and on the insolated surface, by a double glass top with an air chamber which acts as a heat trap. The second trend, surprisingly almost ignored, calls for the simplification of all components, curtailing thermal insulation, and prescribing the laying of water boxes on straw beds or directly on soil, in still air areas or where suitable protection from wind is available.

It is evident that with the latter arrangement, the equilibrium temperature *Te*, the optimum temperature *Tm* and the available heat *Q* all decrease; in other words, the efficiency per square metre of insolated surface decreases. For example, with an assumed condenser temperature of 20°C, experiments made at Tripoli and Bengasi, in areas protected from wind action, indicated that a simple water box had a thermodynamic efficiency slightly over one-half that of a water box thermally insulated on five sides and covered by a double glass top on the insolated surface. Specifically, while under experimental conditions, 30 sq m of insulated water boxes were required for each hp output, 50 sq m were required when using simple boxes. However, it should be noted that the 50 sq m of simple water boxes were considerably less expensive than the 30 sq m of insulated boxes.

It is evident that, on account of the extensive insolated surface, the application of orientators to solar machines of this kind is not feasible, if no excessive installation costs are to be incurred. However, with a good orientation during hours of optimum insolation, the lack of continuous orientation has a limited importance.

Great advantages may be obtained through the use of plastic material in water-box manufacture. The low thermal conductivity of this material gives it, though partially, thermal insulating properties. Because of the workability of plastics, the manufacture of boxes with strengthening ribs constitutes no problem.

In plastic boxes the surface exposed to solar radiation is either made of a metal sheet suitably fitted to the box, or by a transparent plastic sheet similar to the one used in the Schuman plant at Philadelphia (1909).

The employment of plastics may constitute one of the most important innovations made possible by progress.

Selective surfaces may also be utilized as collectors, in accordance with more recent trends. At present neither the efficiency nor the cost of selective surfaces is fully known. These surfaces, however, have to be protected by glass.

It is my opinion that flat collector solar machines may undergo practical development when plastic water boxes and selective surfaces are made available. Selective paints should be also mentioned at this point; they offer the advantages of easy renovation and low cost, but they also have to be subjected to further development.

To conclude, a solar machine thus designed may be considered a warm water engine of the type developed and widely employed with good results in other fields (thermal waters, waste waters, etc.).

The delivery of heat from the collector to the boiler is effected by water. It should be noted that effective water circulation will result in a heat transfer at a higher average temperature. It is emphasized, however, that certain limits should not be exceeded on account of friction losses.

Heat transfer at the boiler is made through its walls. In order to reduce the temperature drop for a given quantity of transferred heat, the contact surface will have to be increased. This increase will result in a larger amount of evaporating fluid being required to cover the contact surface with a minimum thickness. The cost of the fluid charge may therefore become very high, if not prohibitive. Furthermore, because these machines will be employed mostly in the countryside, a possible breakdown may cause the entire charge to leak out. In thermal-water engines, which operate within the same temperature range, this inconvenience has been eliminated in a very simple manner whose adoption in solar machines is recommended.

The plant boiler, of necessity large in volume, instead of being filled with fluid, is filled with water, hereafter designated as "water support". The heat is therefore transferred from the water circulating in the collectors to the water support through the boiler walls. The water support may be utilized at high pressure values. Because of the extent of the contact surface, the heat transfer is effected with a small temperature drop.

The fluid is introduced as a spray jet into the water support inside the boiler. The fluid should not be mixable with water; because of its low boiling point, ethyl chloride may be used. On account of the vast contact surface, the heat exchange between the water support and the fluid drops takes place with no appreciable temperature drop. The evaporation of the fluid inside the water activates an intense circulation of the latter inside the boiler, thereby augmenting the thermal conductivity between the collector water and the water support.

The vapour thus obtained is a mixture of steam and ethyl chloride vapour, in quantities inversely proportional to their pressures. Because of the pressure values, the mixture contains almost exclusively ethyl chloride vapour, and acts practically as ethyl chloride vapour.

Engine

With respect to the reciprocating engine, the progress in the technique of small refrigerating plants has led to so many improvements and simplifications in the shaft egress seal that designers have been completely relieved of the worry of fluid leaks; the same applies to the fluid feed pump. Such an installation may operate with a fluid charge of a few kilogrammes only, while the machine requires several tens of kilograms per hour.

Condenser

The condenser is a common surface-type condenser; it should be noted however, that the cooling water comes from the well and is raised by the machine; it is thus not available when starting the machine. An auxiliary cold water storage tank is therefore required.

Conclusions

The above notes are not intended to furnish the solution of the difficult problem concerning the development of a solar machine acceptable on both an industrial and economical basis in areas particularly favoured by insolation. The purpose of these notes is to indicate that a possibility of such a development exists and to illustrate a line to follow.

Much remains to be done through studies and experiments prior to attaining practical results: the utilization of plastics to obtain economical, strong and heat-saving boxes; the manufacture of flat collectors consisting of selective surfaces truly efficient, economical and durable; the utilization of selective paints which can be easily applied to surfaces exposed to solar radiation; the reduction of temperature drops in heat exchanges; the fluid charge in connexion with the development of engines run by vapour admixtures of unmixable liquids; the employment of recent-type seals for steam engines.

Simple machines, easy to operate and maintain — this should be the fundamental trend. Research has still a long way to go, but economical solutions are feasible and can be achieved. It is hoped that this conference will constitute an incentive towards more efficient and productive research.

Summary

The direct conversion of solar energy into electric energy, successfully experimented with during the past years, is still very far from having economically acceptable applications on an industrial basis. While awaiting further developments which, we hope, will make such a conversion economically possible, the old solar machine, consisting of a thermal engine run by steam or hot air, may still be usefully employed in areas where a good insolation diagram can be obtained and where a widespread distribution of traditional-type energies, such as electric energy and energy produced by internal combustion engines, is not available.

Wind-driven motors can furnish limited amounts of energy in windy areas. However, their output diagram is very irregular. By contrast, solar machines present, during insolation period, very regular diagrams and, as compared with wind-driven motors, offer the advantage of not being damaged or destroyed when wind energy becomes abnormal, i.e., during hurricanes.

Solar machines, with or without concentration of solar radiation, have failed, so far, to reach a stage where true economical and industrial applications are possible. An investigation of the cause of this failure reveals that it has been determined by economical convenience, rather than by thermodynamic considerations.

Solar machines have been equipped with concentrating mirrors of ever-increasing cost or with flat collectors whose glass tops and accurate thermal insulation have greatly contributed to raise installation costs per unit of power and per unit of energy to exceptionally high levels which become definitely prohibitive when charges for ordinary and emergency type maintenance, operating personnel, etc., are added.

The problem should therefore be examined from a different angle, by investigating the possibility of simplifying solar machines and reducing their costs through the utilization of the new materials that progress has made available.

In view of the fact that concentrator-collector systems are not likely to fall within the established economic limitations, mainly because of mirror maintenance and wear and of expensive orientators, attention should be devoted to flat collector systems.

By proper utilization of plastics, it would be possible to obtain collectors which do not require thermal insulation—thereby eliminating the costly insulating casings—and which can be laid directly on the ground, with no orientators.

Similarly, by eliminating glass tops, it would be possible to obtain collectors which, though less efficient, would furnish a power unit which would entail a larger insolated surface but would be obtained at a lesser over-all installation cost as a result of the decreased unit cost of the insolated surface.

Insolated surfaces may consist of selective surfaces which greatly improve collector efficiency and reduce the area required per power unit.

Insolated surfaces may also be coated with selective type paints with improved economical results.

Unfortunately, both selective surfaces and paints are not at present available on open markets, nor

are their cost and efficiency known. It is hoped that both items may soon become available at reasonable costs, since the development of flat collector solar machines is dependent, to a great extent, on this factor.

Without taking into consideration systems whose boiler consists of a finned tube (i.e., one which contains the fluid to evaporate and is directly exposed to solar radiation and which, because of the extent of the coil, leads to large-size units requiring great quantities of expensive and not readily available fluid, which, should any leakage occur, as often happens in this size boiler, is lost), attention should be drawn to flat box collectors where circulating water conveys the collected heat to a compact and strong boiler and releases it to the fluid by conduction through the boiler walls.

To reduce the fluid charge and the possibility of costly leakages, the use of machines run by vapour mixtures of unmixable liquids is recommended. In this case, the boiler is filled with water, designated as "water support", to which heat is transferred by the water circulating through the collector. The fluid to evaporate is spray-injected into the water support and evaporates with no appreciable temperature drop. The fluid to be used should not be mixable with water and, at temperatures ranging from 40°C to 50°C, should present high-pressure values of saturated vapour. Ethyl chloride, for example, meets these requirements. If ethyl chloride is used, the vapour obtained, which is a mixture of steam and ethyl chloride vapour in quantities directly proportioned to their pressures, contains almost exclusively ethyl chloride vapour and acts practically as such. Under these conditions, a fluid charge of only a few kilogrammes may be sufficient to operate a machine which requires a few hundred kilogrammes of vapour per hour. In other words, with respect to ethyl chloride, the boiler may be considered an instant vaporization type unit. Many other fluids may be used in lieu of ethyl chloride.

The steam engine may be of the reciprocating type, and good use should be made of vapour seals recently developed for small refrigerating plants, which have now reached high performance standards.

The condenser should be of the surface type. Sizes of boiler and condenser heat transfer surfaces should be large enough to reduce temperature drops. It would be necessary to provide the condenser with an auxiliary cold-water storage tank to make starting operations possible. During normal operation, the condenser is fed by the water pumped from the well.

By adopting the recommendations outlined above, a strong solar machine offering sound economical prospects could be developed, though it would require rather large insolated surfaces (from 40 to 50 sq m per horse-power).

A machine manufactured in accordance with the above-mentioned criteria may prove useful in areas of good insolation (Arizona, India, Africa, etc.), especially with respect to irrigation problems. Power output should not exceed 2 or 3 hp. Unit costs of energy thus obtained may successfully compete with unit costs of traditional type energies which, of necessity, differ considerably from current values in areas with widespread power distribution.

MACHINES THERMIQUES POUR LA CONVERSION DE L'ÉNERGIE SOLAIRE EN ÉNERGIE MÉCANIQUE

Résumé

La conversion directe d'énergie solaire en énergie électrique, sur laquelle on a fait des expériences avec succès au cours de ces dernières années, est encore très loin d'en être à des applications économiquement acceptables sur une base industrielle. En attendant que de nouveaux progrès rendent une telle conversion économiquement possible, ainsi que nous l'espérons, la vieille machine solaire constituée par un moteur thermique, à vapeur ou à air chaud, peut encore être utilisée avec succès dans les régions où on peut réaliser un bon diagramme d'ensoleillement et où fait défaut une distribution généralisée des types d'énergie classiques, comme l'énergie électrique et la force motrice produite par les moteurs à combustion interne.

Les moteurs éoliens peuvent fournir des quantités limitées d'énergie dans les régions où il y a beaucoup de vent. Leur production est cependant très irrégulière. Par contre, les machines solaires présentent pendant la période d'insolation des diagrammes très réguliers si on les compare aux éoliennes; elles offrent l'avantage de ne pas être endommagées ou détruites quand l'énergie éolienne devient anormale, c'est-à-dire pendant les ouragans.

Les machines solaires, avec ou sans concentration du rayonnement, n'ont pas encore atteint jusqu'à présent le stade où des applications véritablement économiques et industrielles sont possibles. Une étude des causes de cet échec montre que ce sont des questions d'ordre économique plutôt que des considérations thermodynamiques qui l'expliquent.

Les machines solaires ont été dotées de miroirs de concentration, de plus en plus coûteux, ou de collecteurs plats dont les couvertures en verre et l'isolement thermique complet ont beaucoup contribué à augmenter le coût d'installation par unité de puissance

et par unité d'énergie, pour les porter à des niveaux exceptionnellement élevés qui deviennent franchement prohibitifs quand on y ajoute les frais d'entretien ordinaires et d'urgence, ceux qui sont afférents au personnel d'exploitation, etc.

Il convient donc d'examiner le problème sous un angle différent, en étudiant la possibilité de simplifier les machines solaires et d'en réduire les frais par l'utilisation de nouveaux matériaux que les progrès ont rendus disponibles.

Étant donné que les systèmes concentrateurs-collecteurs ne tomberont probablement pas dans le cadre des limites dictées par des considérations économiques, principalement en raison de l'entretien et de l'usure des miroirs et des dispositifs d'orientation, qui sont fort coûteux, on s'attachera à l'étude des collecteurs plats.

En faisant judicieusement appel aux matières plastiques, il serait possible de réaliser des collecteurs n'exigeant pas d'isolement thermique (ce qui éliminerait les cuvelages isolants coûteux) que l'on pourrait poser directement sur le sol sans dispositif d'orientation. De même, en éliminant les couvertures en verre, il serait possible de réaliser des collecteurs qui, tout en ayant un moindre rendement, fourniraient des unités de puissance comportant une plus grande surface ensoleillée, mais s'achèteraient à de moindres prix d'ensemble par suite de la diminution du prix unitaire de la surface ensoleillée.

Les aires ensoleillées peuvent être constituées par des surfaces sélectives qui augmentent beaucoup le rendement du collecteur et réduisent la surface nécessaire par unité de puissance.

Les surfaces ensoleillées peuvent également être recouvertes de peinture d'un type sélectif, avec une nette amélioration des résultats économiques.

Malheureusement, ni les surfaces sélectives ni les peintures sélectives ne sont actuellement disponibles sur le marché libre; d'autre part, leur prix et leur rendement sont inconnus. Il est à souhaiter que ces surfaces et peintures soient bientôt disponibles à des prix raisonnables, car la mise au point de machines solaires à collecteur plat en dépend dans une grande mesure.

Il convient de laisser de côté les systèmes dont le bouilleur est constitué par un tube à ailettes contenant le fluide à évaporer et exposé directement au rayonnement solaire. (En raison de la longueur du serpentin, cela entraîne l'établissement d'unités de grandes dimensions exigeant des quantités importantes d'un fluide cher et qui n'est pas disponible facilement, lequel est perdu s'il y a des fuites, comme cela arrive souvent dans des bouilleurs de cette taille.) Par contre, on attirera l'attention sur les collecteurs à boîte plate dans lesquels l'eau de circulation transporte la chaleur accumulée à un bouilleur de faibles dimensions et résistant, pour la dégager dans le fluide par la conduction des parois du bouilleur.

Pour réduire la charge de fluide et la possibilité de fuites coûteuses, l'emploi de machines utilisant des mélanges de vapeurs de liquides non miscibles est recommandé. Dans ce cas, on remplit le bouilleur d'eau, que l'on appelle le « support-eau », à laquelle la chaleur est transmise par l'eau circulant à travers le collecteur. Le fluide à évaporer est injecté dans le support-eau et s'évapore sans chute de température appréciable. Le fluide à employer ne doit pas être miscible avec l'eau et, à des températures allant de 40 °C à 50 °C, doit présenter de grandes tensions de vapeur saturée. Le chlorure d'éthyle, par exemple, satisfait ces exigences. Si on se sert de chlorure d'éthyle, la vapeur obtenue, qui est un mélange de vapeur d'eau et de chlorure d'éthyle en quantité directement proportionnelle à leurs tensions partielles, contient presque exclusivement de la vapeur de chlorure d'éthyle et agit pratiquement comme s'il en était ainsi. Dans ces conditions, une charge de fluide ne dépassant pas quelques kilogrammes peut suffire à faire fonctionner une machine qui exige quelques centaines de kg de vapeur à l'heure. En d'autres termes, en ce qui concerne le chlorure d'éthyle, le bouilleur peut être considéré comme une unité à vaporisation instantanée. Nombre d'autres fluides peuvent être employés à la place du chlorure d'éthyle.

Le moteur à vapeur peut être du type alternatif et on devra faire bon usage des garnitures d'étanchéité qui ont été mises au point récemment pour les petites usines de réfrigération, lesquelles donnent maintenant d'excellents résultats.

Le condenseur doit être du type à surface. Les dimensions des surfaces de transmission de la chaleur du bouilleur et du condenseur seront assez grandes pour réduire les chutes de température. Il sera nécessaire de fournir au condenseur un réservoir auxiliaire d'eau froide pour permettre le démarrage. Pendant le fonctionnement normal, le condenseur est alimenté par de l'eau pompée du puits.

En tenant compte des recommandations présentées ci-dessus, on pourrait mettre au point une puissante machine solaire avec de bonnes perspectives économiques. Mais elle exigerait des surfaces ensoleillées assez grandes (de 40 à 50 m² par CV).

Une machine fabriquée conformément aux critères mentionnés ci-dessus pourra s'avérer utile dans les régions de bon ensoleillement (Arizona, Inde, Afrique, etc.), particulièrement pour les problèmes d'irrigation. Le débit d'énergie ne doit pas dépasser 2 ou 3 CV. Les prix unitaires de l'énergie ainsi réalisée pourront faire concurrence avec succès aux prix unitaires des énergies classiques qui, nécessairement, s'écartent beaucoup des valeurs courantes dans les régions où l'énergie est amplement répartie.

POWER AS A BY-PRODUCT OF COMPETITIVE SOLAR DISTILLATION

*Richard L. Hummel**

Solar radiation is used as an energy source for the following reasons: (*a*) because it is the only energy source available (in space or on the beach); (*b*) because it is available at a high temperature (solar furnaces); (*c*) because it is the cheapest source of energy; and (*d*) because of novelty or misapplication. The third case has the greatest potential for application, but the dilute nature of the solar radiation and the very large areas required to collect commercial quantities of energy make it difficult to apply and keep it cheap.

For power use and, in particular, for generating electricity in commercial quantities, energy concentration is required. The possibilities include: (*a*) converting solar energy to electrical energy directly and over a large area and then collecting the electricity; (*b*) concentrating the radiation by means of reflectors covering a large area to a high flux at the point of conversion; and (*c*) collecting and concentrating the solar energy into a cheap fluid over a large area and moving the fluid and its collected energy to the point of conversion. Direct conversion to electricity offers the highest conversion efficiency and the greatest convenience, but it does not offer convenient energy storage and is prohibitively expensive. The concentration of the solar radiation by means of reflectors would allow high temperature steam to be produced and is the approach most investigators have felt to be the most promising. The experience in commercial power plants that the higher efficiency of high temperature, high pressure systems leads to greatest economy, supports this approach. As yet, however, the reflectors designed have been too expensive to make this approach competitive for commercial power. The third prospect, collecting heat in a cheap fluid and transporting this to a central location, is by far the least efficient. Either the heat must be collected in a fluid at relatively low temperatures which offer, at best, low reversible heat to work conversion efficiencies and much lower practical efficiencies, or the heat must be collected at slightly higher temperatures (possibly 212°F) at a greatly reduced collection efficiency. This is the approach that this paper will present as having prospects at present of producing power competitively, for efficiency is but part of the story when dealing with an energy source which costs nothing itself. That greater efficiency leads to greater economy in a coal heated generating system does not change the fact that such a system is a solar energy conversion system of microscopic efficiency using the light-collecting properties of Cambrian ferns and the baking conditions of the earth's interior in the collection and transport of the energy. For that matter, coal's chief competitor in electric generation, hydroelectric power, is also a solar process of higher but still minute over-all efficiency.

The key to the costs of the system lies in a multiple cover sea water distillation still capable of covering huge heat collection areas at a reasonable cost. Used on an arid seacoast or saline lake, it is planned to collect an average of 400 Btu/ft²/day into water at a temperature ranging from 160°F to 210°F. Considerably more heat will enter the basin, but the majority of this heat will be lost directly. This loss, however, will result in the production of a considerable quantity of water to be sold in conjunction with the power. For heat collection at 180°F, the over-all conversion efficiency should be 2.7 per cent, or roughly one-fifth of the reversible Carnot efficiency. A power system (1) developed in 1954 to operate on 200° liquid water by General Electric in a study for the Hanford Works was used as a guide in this design. A one square mile heat collecting basin would produce an average of 88 000 kWh/day with water storage provided to maintain output at this level over a

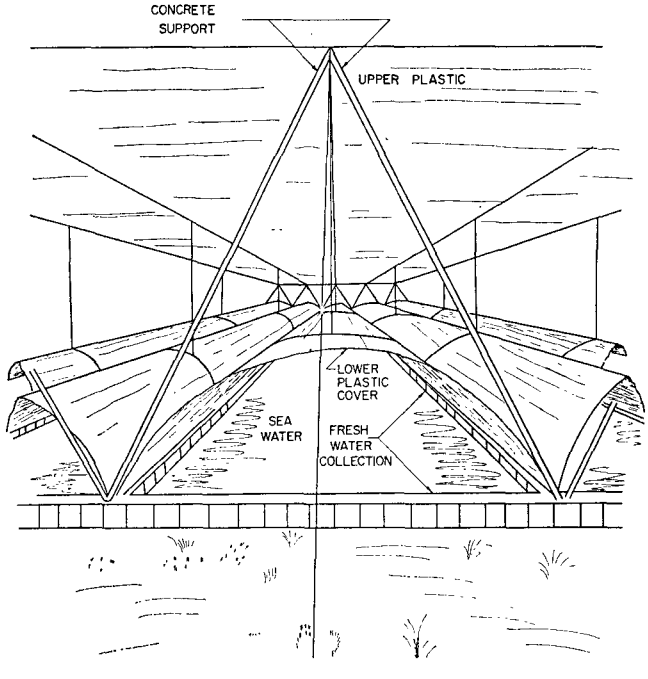


Figure 1. Heat-collecting basin

* Institute for Atomic Research, Iowa State University.

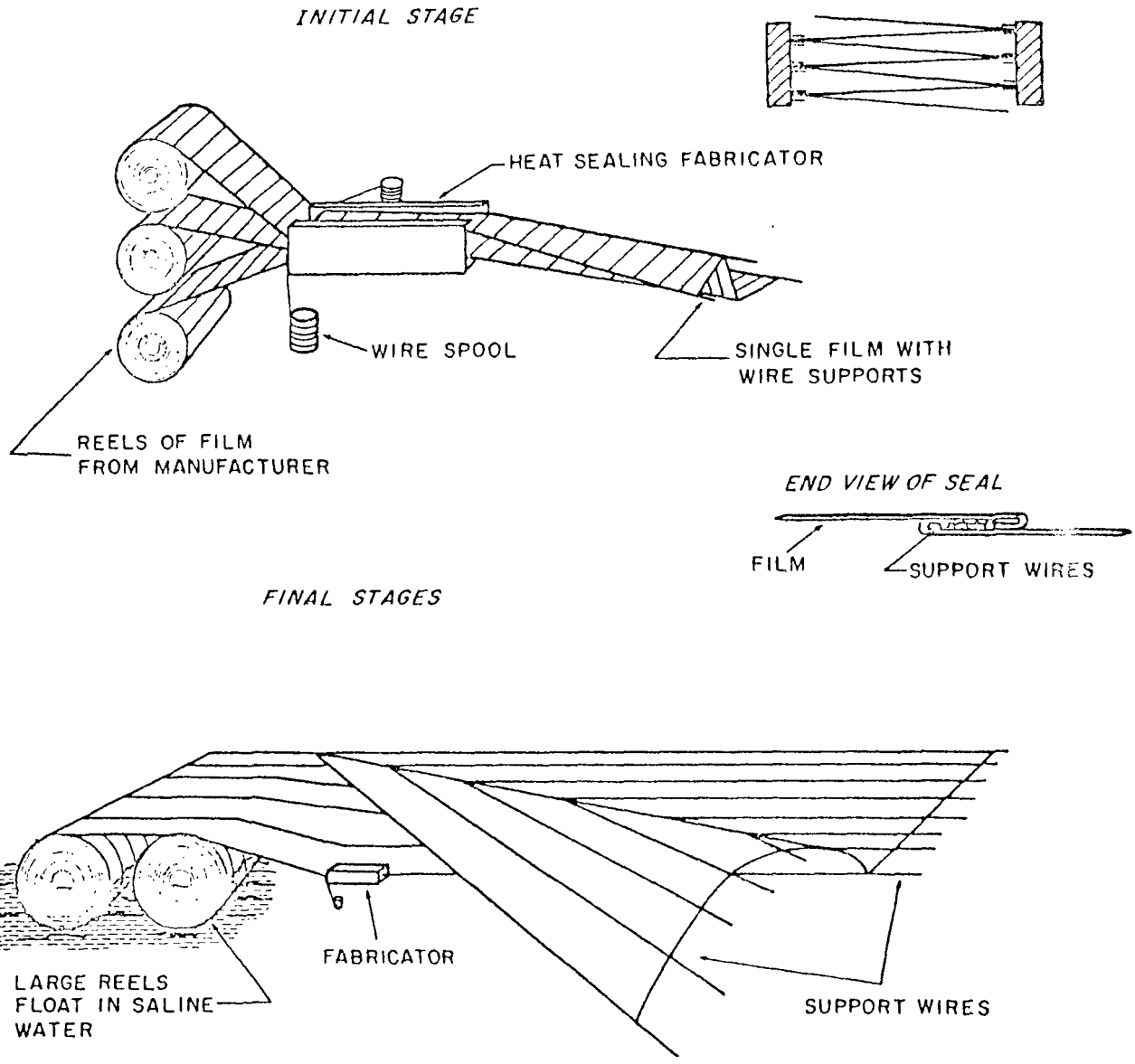


Figure 2. Plastic fabrication

four day period of bad weather if preceded by clear weather. Assuming a nonindustrial load having a peak hour, during the hottest days of the summer, of 2.7 × the average load, the generator and turbine were sized at 10 000 kWh. At present, the unit cost was calculated to be roughly 2.3/kWh, of which 0.48 was the cost of the conversion equipment and 1.7 was the cost of *not* producing 61 gal of water. Duffie and Lof indicate that 3/kWh would be competitive in the United States for a plant of this size (1). Improvements in plastic cost and/or plastic life expectancy will reduce this cost considerably.

The solar distillation still has been previously described by Hummel and Rudd (2), by Hummel (3, 4), and in another paper presented at this conference (5). It is shown in figure 1. The key to its reasonable cost lies to a large extent in the mechanical fabrication, on site, of the upper cover from standard long rolls of high-strength plastic into huge sheets requiring a minimum of labor for fabrication and erection. The cumulative strength of the surface comes primarily from steel wires fabricated into each seam between the strips from the original rolls. Handling of such huge sheets is possible only because of these wires and because the area of the basin can be flooded with sea water prior to fabrication and erection. The water will not only support the plastic and allow it to be moved easily without abrasion, but maintains it free of wind flutter. To lift a section of plastic an inch, the wind must statically support the greater weight of one inch of water plus overcoming the dynamic inertia of much greater masses of water. Fabrication is shown in figure 2, with a U.S. $250 000 fabricator overlapping and heat sealing a number of rolls of plastic at a time. For most of the basin cover, it is planned to use two strips of plastic in each panel, with the reinforcing wire also acting as a spacer. This will not slow down the fabrication

and will only slightly complicate the fabricator. Our sewing-machine companies provide us with an idea of the complex things that can be done in seams and insertions by means of simple guides.

The remainder of the basin below this upper surface resembles a conventional still, except that the semicylinder surfaces covering the evaporation basins directly are 50′ to 100′ wide. After all, there is no wind below the upper cover.

A program for the calculation of the dynamic behavior of an operating still has been written for an IBM-704 computer. Previous writers, Hottel and Woertz, have shown that theoretically valid calculations will be in excellent agreement with experiment (6). A calculation of the dynamic behavior is not only more informative as to still operation but is indeed simpler, for the temperatures of the water and of the ground depend only upon past heat accumulation and not at all upon present heat fluxes. This allows each mechanism of heat transport between surfaces to be evaluated independently by the best equation, regardless of complexity. A short trial and error loop is required to set the lowest cover temperature to the value giving the correct outside air temperature, but this converges simply and rapidly.[1] Conventional relationships were used for the radiant transfer of heat (7) and natural convection of heat (8) between dry surfaces, and heat transfer coefficients are chosen for forced convection to the wind. For convection transfer from the hot water surface, it was recognized that both heat and mass transfer contribute to the bouyancy causing the circulation of the air. The bouyancy effect between two elements of air at temperatures T and $T_H = T + \Delta t$ and mole fractions water vapor, y and $y_H = y + \Delta y$ is equal to

$$\frac{\rho - \rho_H}{\text{ave}} = \frac{(29 - 11y)\,\Delta t + 11\,T\,\Delta y}{\left(T + \frac{\Delta T}{2}\right)\left(\sum_{n=0}^{\infty}\left(\frac{t}{2T}\right)^n\right)\left(29 - 11\left(y + \frac{\Delta y}{2}\right)\right)} \qquad \frac{\Delta t}{T_{\text{ave}}} + \frac{\Delta M}{M_{\text{ave}}}$$

where ρ is the density at these temperatures given and M is the molecular weight of the gas mixture. For heat transfer alone, the equivalent term would be $\Delta t/T_{\text{ave}}$ which, due to the interrelationship of over-all temperature difference, ΔT, microscopic temperature difference, Δt, and $h/\rho C_p$, is replaced in the Grashof number by the term, $\Delta T/T = \Delta T\beta$. By means of the analogy between heat, mass and momentum transport, a similar replacement of the Δy by an over-all difference in equilibrium water mole fractions, ΔY, is possible, assuming only that $\Delta t \ll \Delta T$ and that $\Delta y \ll \Delta Y$. This permits correlations developed between heat transfer and Grashof number for flat plates to be used for combined heat and mass transfer, providing that an empirical constant is added to correct for the effect of goemetry other than flat plates upon the circulation and thus the coefficients. Further, since both the remainder of the Grashof number and the heat conductivity of the air changed markedly with temperature, it was convenient to use the relationship

$$h^3\left(\frac{\rho^2 g C_p}{T\mu k}\right) = 1.3392 \times 10^6/T^{1.9854}$$

which I found fitted the data given by McAdams (7) to less than 3 per cent over the range —300° F to 1 200°F and to less than 1 per cent over the range —300°F to 500°F. Incidentally, the relationship

$$\frac{\rho^2 g C_p}{T\mu k} = 6.5886 \times 10^{18}/T^{4.663}$$

is almost as good over a more limited temperature range.

In the heat transfer from surface to surface, it was important to distinguish between absorption and reflection of the sunlight, for the absorption in any layer at all will increase the Δt from that surface on out. It was found that the optical effects of the surfaces, including the bottom black surface, could be reduced algebraically to two or at most three coefficients per surface, of which only one varied from hour to hour with sun position. At present, adequate data are not available to fully handle the Mylar W1 and Mylar proposed for this still.

Heat transfer into the ground was calculated by the "Schmidt method" (7) (finite difference form of the time-dependent heat transfer equation in one dimension) for sufficient layers (107) as to give a $\frac{1}{2}$ response time of one year.

At the time of this writing, I have received from MURA a single set of nine calculations intended to give a rough picture of the geometric correction constant and upon operation of the solar still mentioned above (5). In a few weeks, I shall have more and, by August, an adequate amount. The calculations for a single cover and various constants have been compared with the limited data of Bloemer, Collins, and Eibling (9) and seem to indicate a constant between 1 and 2[2] but closer to 2 for the Lof still.

These preliminary calculations for the three cover still indicate an average daily operating temperature of roughly 145°F at low solar incidence of 1 300 Btu/h ft² day and of roughly 170°F at a solar incidence of 2 000 Btu/h ft² day with no heat being recovered. The temperatures would be lowered by heat recovery. How then can this still collect 400 Btu/day at temperatures from 160°F-210°F, as proposed for power generation? The simplest solution is to reduce the ruinous night-time heat losses by collecting the majority of the hottest water in a limited area at night, since the heat losses are proportional to area. The remaining water will drop to temperatures of

[1] Simple pre-estimation speeds this convergence.

[2] Unfortunately my vision is not good enough to read the data from the very small graph published with sufficient accuracy to fix the constant and a better fit will have to wait until more detailed data are received from them or other investigators.

low loss. Redistribution of the hot water in the morning will at least in part displace the cooled water, giving a gradient of water temperatures, including a large area of high temperature water to collect more heat. Trial calculations, supported by the machine calculations and previously based upon experimental and theoretical studies of flat plate collection (10) indicate that this step would be more than sufficient to attain the heat recovery and temperatures desired. Considerably more can be done, however, to increase the heat recovery or the temperatures.

Absorption and partial return of the radiant losses by IR absorbing gas between the upper and lower covers can offer an efficient way to reduce the radiation loss, which is the largest path of heat loss. It will not reflect or absorb solar radiation and offers a continuous thermal gradient and continuous absorption and partial return, and it can thus be more efficient than another layer of plastic. IR absorbing CO_2 and water vapor can be obtained at a nominal cost in huge quantities from the scrubbed and heat extracted exhaust of engines if diesel or natural gas motors are used to power the pumps and blowers. Additional organic materials, either in the exhaust or otherwise added, could help fill the windows in the CO_2, H_2O spectrum.

Additional plastic surfaces are another means of increasing the operating temperature by adding resistance to the heat loss, but this alone is not too effective, for the proportionate gain per surface becomes less and less while the cost rapidly mounts and increasing quantities of solar radiation are lost. Creating a smaller heat collecting basin with one or more covers of its own under the lower cover of a larger heat-collecting basin is, however, a different matter. A smaller area of plastic would be used and the temperature and heat recovery combination of the interior still with, let us say, two surfaces would be considerably higher than a similar area isolated but supplied with five covers. The reason is that the heat loss flux through the upper three surfaces will be greater than through the lower two surfaces if such a system is used, for the difference would be supplied from the heat recovered in the surrounding lower temperature basin. Another advantage is that part of the solar radiation loss from the covers of the hot basin can be used for evaporation in the surrounding basin.

A simpler and cheaper way to use the same idea is to have the basin under a lower cover partitioned into two sections, one of which is covered with a layer of oil to prevent its evaporation. Doing this in an unpartitioned basin would raise the temperature for power production, although preventing the use of the lost heat in water production; but doing it in a partitioned basin gives higher temperatures yet, and gives water production also. Additional plastic surfaces and an oil film can, of course, be combined.

The complete absence of wind under the upper surface makes possible an extremely inexpensive reflector to concentrate the solar radiation into certain of the channels. This can be done by hanging

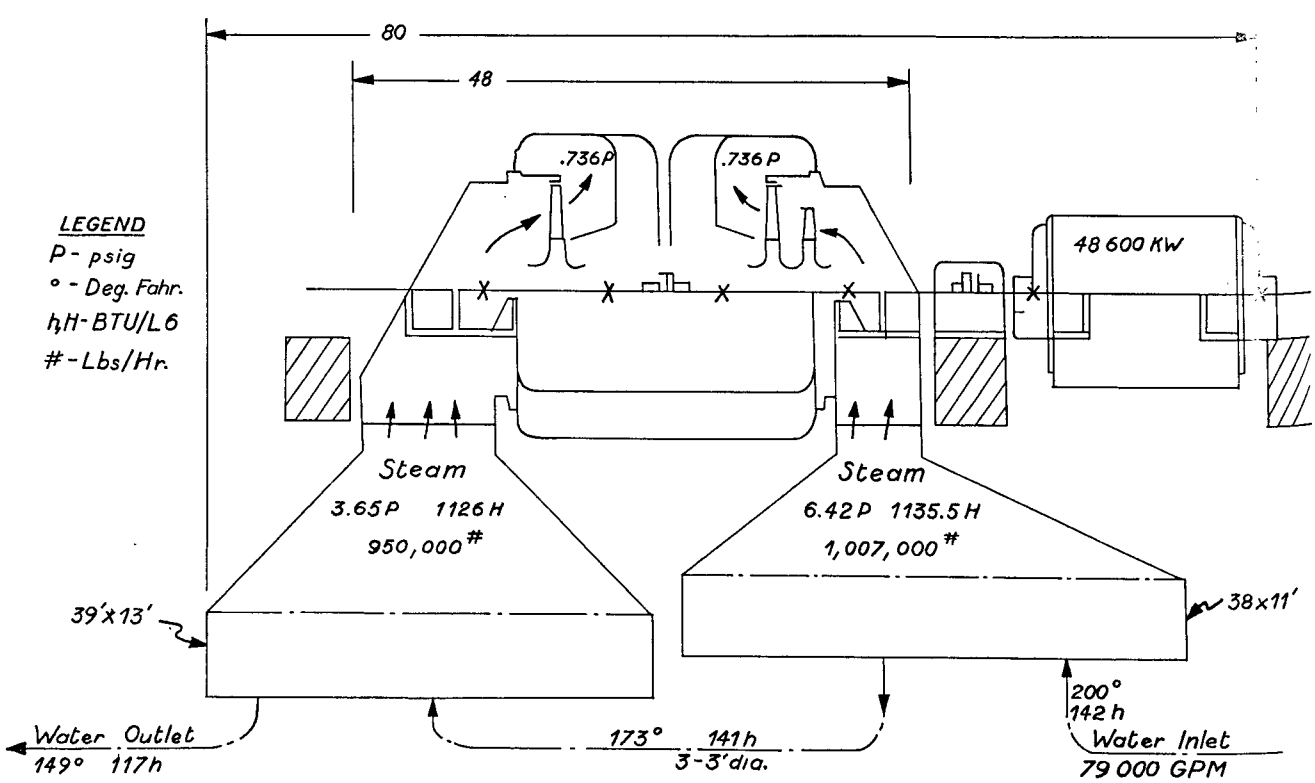


Figure 3. Turbine for solar distillation plant

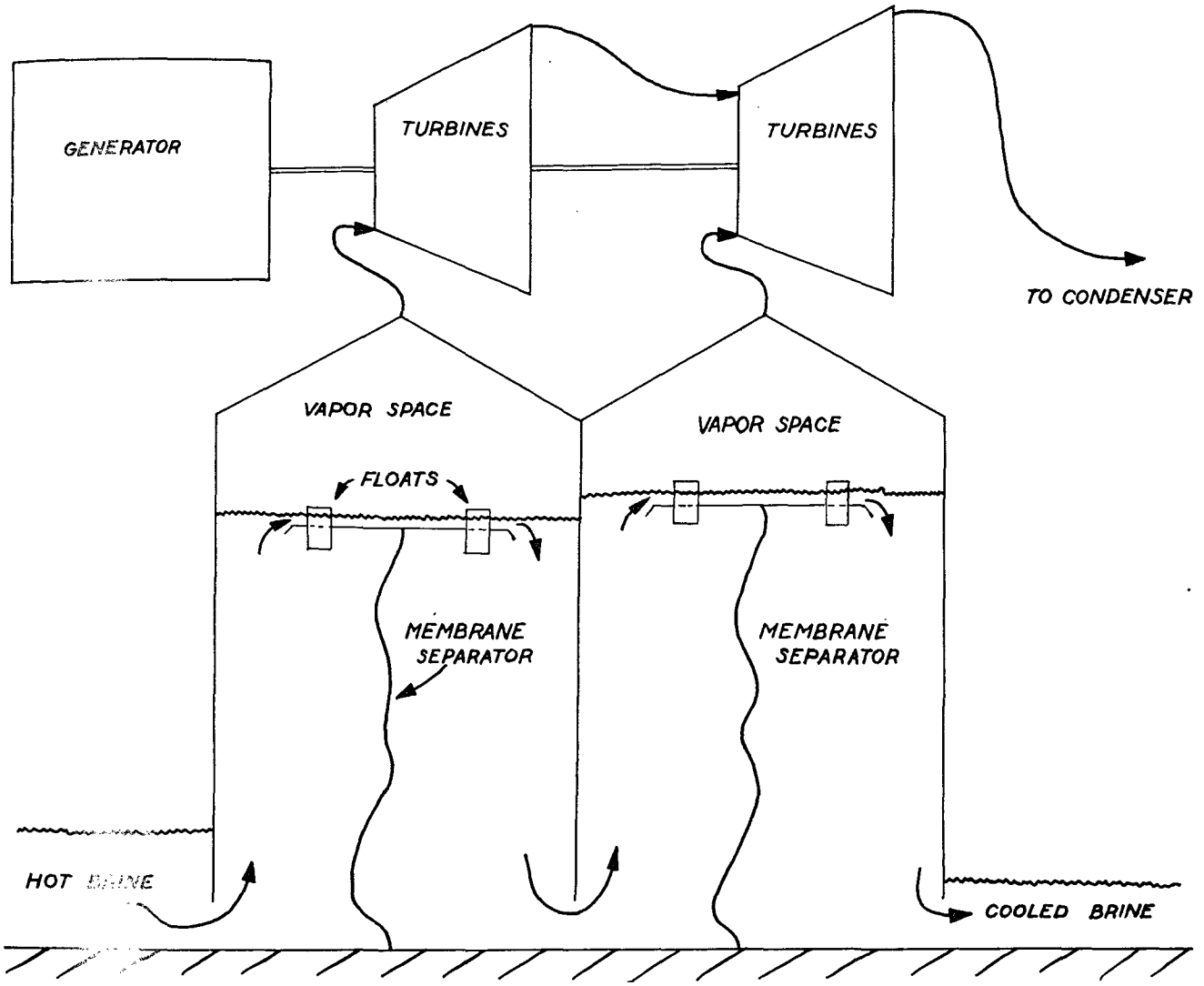


Figure 4. The floating syphons

a plastic sheet vertically just north of the channel from an east-west wire just under the cover. Ordinary plastic will reflect that half of the radiation of the correct polarization, and aluminized plastic will reflect all of it.

A better system yet, if the basin can naturally provide deep sections, is to employ Tabor's idea (11) and maintain a very hot concentrated, dense brine in the depths and a cooler sea water above it. Water production would supply all the hot concentrated brine that could be used in this scheme, and if a continuous concentration gradient were maintained, the temperatures in the depths could be considerable. Radiant heat transfer would have such a short mean free path as to be negligible with regard to water radiation itself, convection would be prevented by the density gradient, conduction would be low, and the hydrostatic head would permit temperatures above normal boiling to be developed. Also, all heat loss upward would be available for water distillation.

This effort for higher temperatures is justified by the higher efficiency to be gained, which increases more rapidly than the Carnot efficiency and is often worth a reasonable drop in total energy collected. This is especially true since heat in multiple-effect evaporation maintains efficiency better at reduced temperatures than power generation.

To convert the stored heat in the water to steam for turbine operation, General Electric proposed spraying the water into two staged flashing chambers. Their system is shown in figure 3. The disadvantage is that at least 20-30 feet of water head would be thrown away, requiring considerable pumps and pumping. I would propose to use the system shown in figure 4, where there is no spraying head loss and the flow head loss is kept low by large channels. The hot brine is forced to the top of the flashing chamber by a membrane barrier extending to the floor and to the walls and maintained at the proper height by floats. There will be a small irreversible Δt needed to nucleate the vaporization and flashing

from the shallow liquid that may not have been present in the spray towers with their high surface area, but this design permits the passage of much more brine for the same or less pumping work and thus less temperature loss between final vapor and entering liquid temperatures and improvement of over-all flashing efficiency. Flashing is a volumetric phenomenon, and apparently provides huge heat transfer coefficients. Dr. Othmer is studying the matter further.

The remainder of General Electric's suggestions are quite conventional, including a two-pass tube and shell heat exchanger operating on 60°F cooling water. It is unlikely that 60° water will be available, and a better condenser system is possible. A solution would be to spray sea water (to approach wet bulb temperatures) into a spray pond filled with high boiling hydrocarbon so as to cool the hydrocarbon by liquid-liquid extraction of heat. Woodward (12) studied liquid-liquid extraction of heat in a spray column and found coefficients of up to 8 000 to 11 000 Btu/ft³/°F/h, but he used the hydrocarbon as the dispersed phase. Coefficients should be higher with water as the dispersed phase. The cooled hydrocarbon would then be sprayed into the water vapor from the turbines to condense it. To reduce pumping work, it is likely that Bromley's string guides would be used rather than spray nozzles.

These changes should reduce the design costs slightly for the power generation segment of this design. The smaller size will increase it. For the present, however, G.E.'s figure of US $190 per installed kW will be used. For 10 000 kW maximum capacity, the cost would be $1 900 000, giving a twenty-year amortized annual cost of $210 600. Adding the annual cost of the heat collection basin as developed in table 1, the following is found to apply:

Annual cost = US $1 025 778
Power produced = 29 055 840 kWh/year
Water produced = 1 353 000 000 gal/year.

The following combination of prices could be used to pay the expenses (in U.S. dollars):

Power	*Water*
0.01/kWh	0.54/1 000 gal
0.02/kWh	0.32.8/1 000 gal
0.03/kWh	0.114/1 000 gal
0.0353/kWh	0.00/1 000 gal

Table 1. Cost estimate

Use and description	*Unit price (U.S. $)*	*Total cost (U.S. $)*	*Amortization (%)*	*Annual cost (U.S. $)*
Heat-collecting basins				
Land cost — 640 acres	100/acre	64 000	7.4	4 736
Land preparation — levelling, troughs, and blackening		2 000 000	7.4	148 000
Pumps and piping		200 000	7.4	14 800
Covers				
Mylar W1 — 28 000 000 ft², 201 000 lb	3.85/lb	773 850	31.3	242 235
Mylar — 28 000 000 ft², 201 000 lb	1.60/lb	321 600	31.3	100 661
Mylar — 42 000 000 ft², 302 000 lb	1.60/lb	483 200	31.3	151 242
Steel — 2 500 000 lb	0.12/lb	300 000	31.3	94 000
Concrete supports — 1 000 cu. yd.	80/cu yd	80 000	7.4	6 000
Fabrication unit			7.4	18 500
Labor (equipped) — 100 man-months		200 000	31.3	62 400
Total costs		4 673 450		885 678
Annual production (330 days/year)		1 353 000 000 gallons per year		
Unit water costs		$ 0.65 ger 1 000 gallons		

Addendum

POWER PLANT STUDY FOR SOLAR HEAT COLLECTING BASIN*

A January 24th letter from Mr. Richard L. Hummel, Iowa State University, Ames, Iowa, enclosed his paper dealing with the design and operation of a solar distillation plant. He has asked for assistance in appraising the power generation possibilities if the heat collecting basin was used to generate low pressure steam.

We were fortunate to find that in 1954 our Large Steam Turbine Department made complete power plant cost estimates for operating conditions very similar to those proposed by Mr. Hummel. This has permitted us to bring the cost data up to date and give a realistic picture of a power application that would apply within the range suggested.

The maximum rating of the turbine generator is 50 000 kW and the heat consumption is 2.3 billion Btu/hour, which is at the rate of 56 billion Btu per 24-hour day. This is roughly one half the maximum range of heat input specified, yet may be about the maximum size power plant that should be considered. We expect that consideration of capital investment would limit the power plant rating to near the seasonal average input, which we assume would be a fraction of that specified. Somewhat larger rated turbines are conceivable; however, cost data would not be readily available. Obviously, smaller plants are feasible, but the cost per kW would increase as rating is reduced and such plants are less likely to be economically practical.

Water from the heat-collecting basin is expected to range in temperature from 160° to 200°F. The one-mile-square basin is covered, suggesting the availability of vapor at these temperatures; however, we suspect that problems with noncondensable gases mixed with this vapor would make it impractical to maintain

* J. W. Mann.

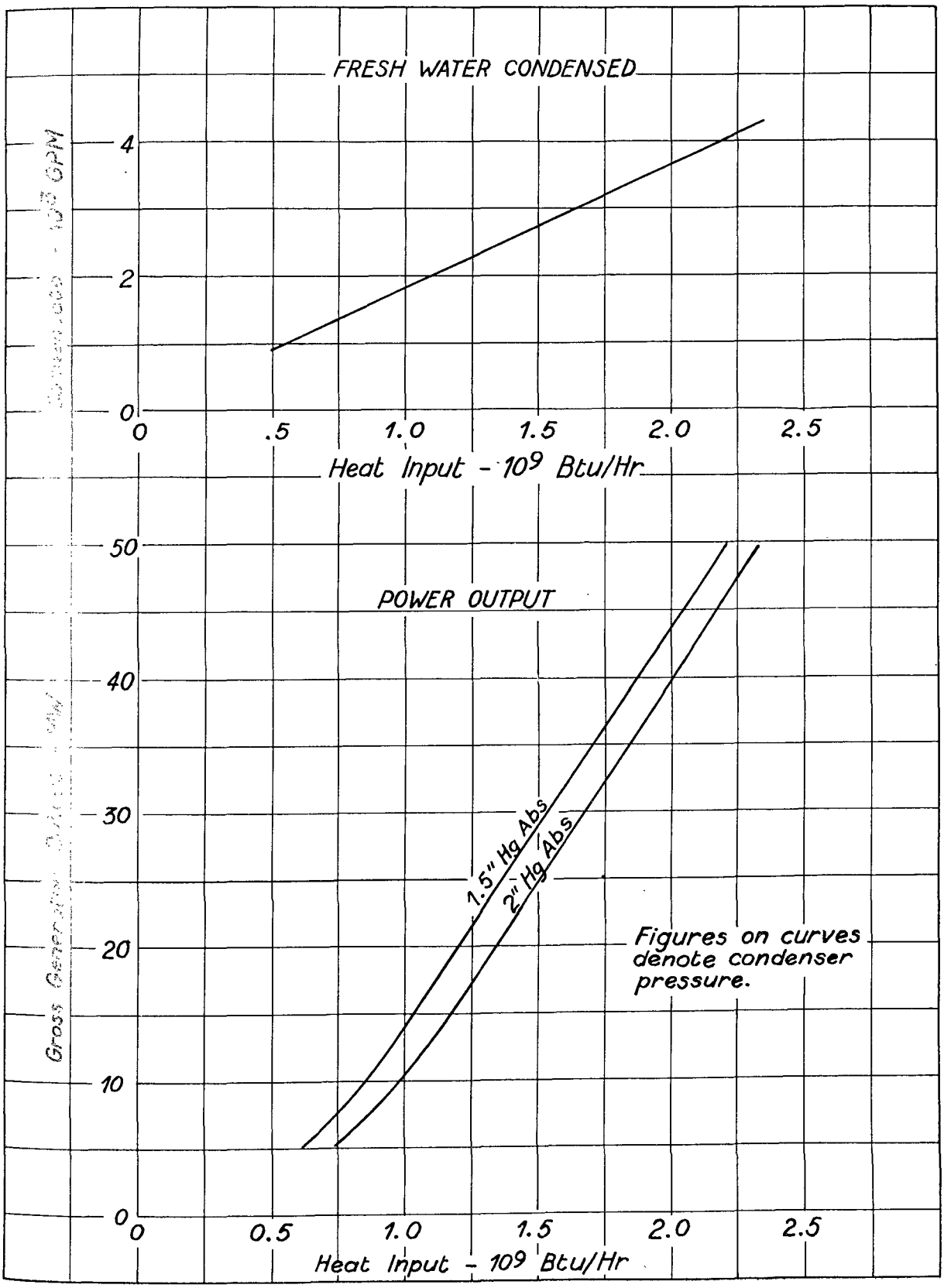

FRESH WATER CONDENSED
Gross Generator Output - 10^3 GPM
4
2
0
0
.5
1.0
1.5
2.0
2.5
Heat Input - 10^9 Btu/Hr
POWER OUTPUT
50
40
30
20
10
0
1.5" Hg Abs
2" Hg Abs
Figures on curves denote condenser pressure.
0
0.5
1.0
1.5
2.0
2.5
Heat Input - 10^9 Btu/Hr

Figure 5

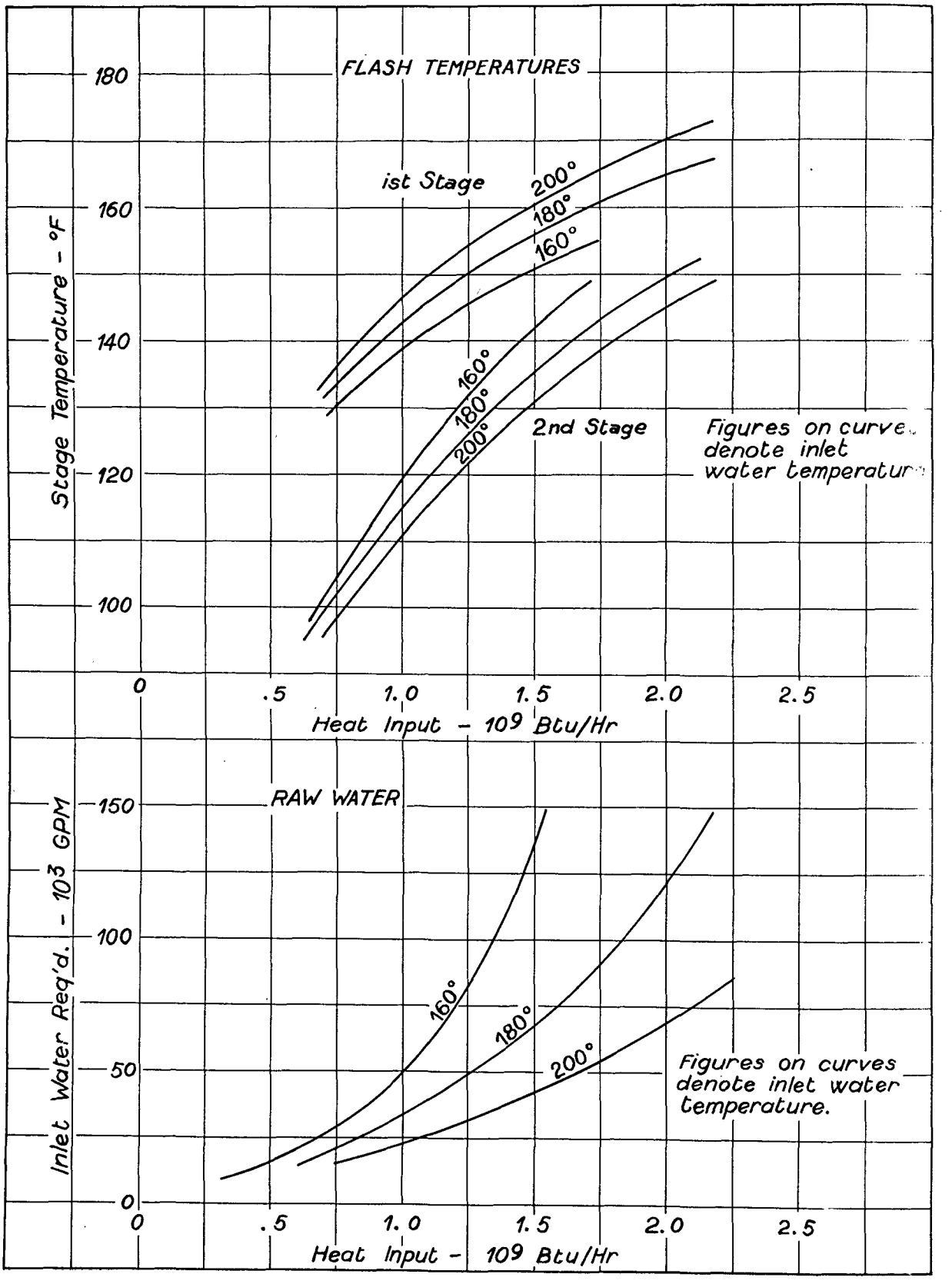

FLASH TEMPERATURES
ist Stage
200°
180°
160°
2nd Stage
160°
180°
200°
Figures on curves denote inlet water temperature
Stage Temperature - °F
180
160
140
120
100
0
.5
1.0
1.5
2.0
2.5
Heat Input - 10⁹ Btu/Hr
RAW WATER
160°
180°
200°
Figures on curves denote inlet water temperature.
Inlet Water Req'd. - 10³ GPM
150
100
50
0
0
.5
1.0
1.5
2.0
2.5
Heat Input - 10⁹ Btu/Hr

Figure 6

sufficient operation on vapor drawn directly from the basin. We are proposing that heated water be drawn from the basin and sprayed into a tank where it would be permitted to produce steam by flashing.

Figure 3 above is a cross-section view of the proposed turbine design. This ingenious design provides two stages of flashing which make possible a significant improvement in thermal efficiency relative to that obtainable with a single flash. Steam generated in the higher pressure flash stage passes through two stages of turbine blading, while steam from the low pressure flash tank passes through a single turbine stage. These parallel steam paths exhaust into a single condenser through side outlets in the exhaust hoods.

Figures 5 and 6 present curves describing the performance in terms of heat input and available basin water temperature. The following is a sample calculation for one point on these curves.

Inlet water temp., $T_o = 200°F$ $h_o = 168$ Btu/#

1st evaporation stage:

Flash temperature, $T_1 = 173°F$ (assumed)

$P_1 = 6.42$ psia $H_1 = 1\,135.5$ Btu/# $h_1 = 141$ Btu/#

$v_1 = 58.1$ cu.ft./#

$F_1 = 3.22 \times 10^6 (P_1/v_1)^{.5} = 3.22 \times 10^6 \left(\frac{6.42}{58.1}\right)^{.5} = 1.07 \times 10^6$ #/hr

$$\frac{F_1}{W} = \frac{h_o - h_1}{H_1 - h_1} = \frac{168 - 141}{1\,135.5 - 141} = 0.272$$

$$W = \frac{1.07 \times 10^6}{.0272 \times 500} = 79\,000 \text{ GPM}$$

Available energy to 1.5″ Hg abs. = 1 135.5 — 1 002 = 133.5

$$\text{Shaft input} = \frac{.73 \times 133.5 \times 1.07 \times 10^6}{3\,413} = 30\,600 \text{ kW}$$

2nd evaporation stage:

Flash temperature, $T_2 = 149°$ (trial)

$P_2 = 3.65$ psia $h_2 = 117$ Btu/# $H_2 = 1\,126$ Btu/#

$V_2 = 99$ cu.ft./#

$$F_2 = W\left(1 - \frac{F_1}{W}\right)\frac{h_1 - h_2}{H_2 - h_2} = 500 \times 79\,000 \times .973\,\frac{141 - 117}{1\,126 - 117} = .95 \times 10^6 \text{ \#/hr}$$

$F_2 = 4.95 \times 10^6 (P_2/v_2)^{.5}$

Check: $P_2 = \left(\frac{.95 \times 10^6}{4.95 \times 10^6}\right)^2 \times 99 = 3.65$ psia and $T_2 = 149°$

Available energy to 1.5″ Hg = 1 126 — 1 028 = 98 Btu/#

$$\text{Shaft input} = \frac{.72 \times 98 \times .95 \times 10^6}{3\,413} = 19\,600 \text{ kW}$$

Generator output = 97 (30 600 + 19 600) = 48 600 kW

Heat input = 2.02×10^6 (117 — 53) + 500 × 79 000 (168 — 117) = 2.15×10^9 Btu/hr

The costs estimated for this power plant, adjusted to present-day levels including freight and erection costs, are as follows:

	U.S. $
Turbine-generator (56 000 kVA, .85 PF)	3 160 000
Evaporator and piping	940 000
Condenser (150 000 sq. ft, 2 pass, 60°F)	1 200 000
Circulating water and supply works	1 800 000
Foundation, crane, buildings	675 000
Switchgear	740 000
Control board, instrumentation	135 000
	8 650 000

Assuming 5 000 kW pumping and auxiliary load, the net plant output would be 45 000 kW with installed cost at $190 per kW net. Conventional power plants of this net rating are usually reported to cost $150 to $175 per kW. Considering power generation as a by-product to fresh-water production, and no fuel costs, the estimated costs appear quite reasonable. Maintenance and operating costs for the power plant equipment are estimated at $100 000 and $165 000 per year respectively.

References

1. Duffie, J. A., and Lof, G. O. G., *The Canadian Journal of Chemical Engineering, 37:* 77 (April 1959).
2. Hummel, R. L., and Rudd, D. F., A Solar Distillation Design for the Economic Production of Fresh Water from Sea Water. Ames Lab. release, 1959.
3. Hummel, R. L., Four Methods for Possible Competitive Production of Fresh Water Through Solar Distillation. University of Michigan Industry Program release, July 1959.
4. Hummel, R. L., New Concepts in Solar Stills Leading to Low-Cost Fresh Water from Seawater. Paper presented at the St. Louis meeting of the ACS, March 1960.
5. Hummel, R. L., A Large-scale Low-cost Solar Heat Collector and Its Application to Sea Water Conversion, *Proceedings of the United Nations Conference on New Sources of Energy*, 1961; included in vol. IV [under agenda item III.E], paper S/28.
6. Hottel, H. C. and Woertz, B. B., *Trans. Am. Soc. Mech. Engrs., 64,* 91, 1942.
7. McAdams, W. H., *Heat Transmission,* McGraw Hill Book Company, Inc., 1954.
8. Jacob, M., *Heat Transfer,* 1st ed., vol. 1, Wiley, New York, 1949, 534 pp.
9. Bloemer, J. A., Collins, R. A., and Eibling, J. A., Progress Report on Field Evaluation of Solar Sea Water Stills. Paper presented at the Cleveland meeting of the ACS, April 1959.
10. Duffie, J. A., Lof, G. O. G., Salam, E. M. A., Solar Heat Exchangers, *Chem. Engr. Prog., 56,* 63, July 1960.
11. Tabor, H.
12. Woodward, T., Heat Transfer in a Spray Column, *Chem. Engr. Prog., 57,* 52, January 1961.

Summary

It has been recently proposed that a multiple-layer, transparent cover of steel-wire-reinforced plastic film can be mechanically fabricated and erected in very large sections and at an exceedingly low per area cost by the use of a flooded basin of large dimension to provide water support and control of the huge sheets during the fabrication and erection. The wind cannot pick up and whip to pieces a plastic surface that is resting upon and wetted by water. As a huge area capable of being flooded is a necessary prerequisite to large-scale solar distillation, it was then proposed that solar

stills could be constructed to convert sea water to fresh water at a competitive cost. Since such a solar still would operate with its heat collecting sea water at relatively high temperatures, the possibility that power could be obtained as a by-product to the water was explored in this paper.

The basic solar still, covering an area of 1 square mile, consists of black-bottomed basins 50′ to 100′ wide and probably on the order of 1 mile long, which are separated by condensate collecting troughs and immediately covered by a single flimsy condensing cover, referred to as the lower cover. The upper cover, separating the entire area from the outside and its winds, is dual-layered and is stretched taut and reasonably flat by the steel reinforcing wires every four feet, which also serve as a spacer between layers.

An IBM-704 program was written to calculate the hour-by-hour performance of a solar still from its operating parameters and from actual or simulated weather data. Combined mass and heat transfer were theoretically related to natural convection heat transfer alone, and a single correction factor per transfer region was used to allow for the difference in convection pattern between actual stills and flat horizontal surfaces. This factor is evaluated from experimental data. Solar radiation absorbed in each transparent layer is not only treated as a loss to the absorbing layer, but its contribution to the total Δt is included. Heat transfer into and out of the ground is also included.

Various means of raising the temperature at which heat for power generation is absorbed are considered. Storing a majority of the water at night or in bad weather within a restricted area—preferably an area covered by a radiation reflector—is quite effective. Dumping scrubbed motor exhaust gas into the huge space between upper and lower covers provides CO_2 to reduce radiation loss. An oil film over the water surface would raise the water temperature at the expense of water production by the "lost" heat. Additional layers of plastic covers raise temperature more, but at a much higher cost. Both of these measures separately or in combination are much more effective when applied to a portion of the basin under a single condensing cover, since then heat is recovered at fairly high temperature in the remainder of the basin and "sacrificed" on the condensing cover to reduce the heat loss from the hotter enclosed basin fraction. The wind-free volume under the upper cover makes possible the inexpensive hanging of large sheets of aluminized plastic in an east-west plane to concentrate the sun's radiation in some parts of the basin. If the anchor points of the wire supporting the plastic were moved at nightfall over the lower cover, the reflector would drape itself over the surface and reduce heat loss. The highest water temperatures can be produced by having deep basins containing concentrated brine in the depths and lighter sea water above, as suggested by Tabor.

The water, once heated, is flashed to yield steam either in a vacuum spray tower, as proposed by General Electric, or by a "floating syphon", as herein described. Maintaining vacuum is not a problem of the flashing chamber, but of the condensing chamber only. Conventional turbines, generators, switchgear equipment, controls, etc., are used as suggested by General Electric. For condensation, however, a three phase spray pond involving sea water, wind, and hydrocarbon is proposed to provide cooled hydrocarbon for spray condensing of the turbine condensate.

The total plant costs can be split arbitrarily between the power and the water. With 10 000 kW as maximum rated capacity, one such split would be powered at 2.2 cents per kW and water at 29 cents per 1 000 gallons.

L'ÉNERGIE, SOUS-PRODUIT DES INSTALLATIONS ÉCONOMIQUES DE DISTILLATION SOLAIRE

Résumé

On a récemment proposé la fabrication mécanique d'une pellicule en composition plastique transparente faite de plusieurs couches et renforcée par du fil métallique, que l'on pourrait alors monter en très grands panneaux à un coût extrêmement modique par unité de surface, en se servant d'un vaste bassin plein d'eau qui servirait de support à ces énormes feuilles et les tiendrait en place pendant leur fabrication et leur pose. Le vent ne peut pas enlever une feuille de composition plastique et la déchiqueter si elle repose sur de l'eau qui en même temps la mouille. Pour autant qu'une énorme aire susceptible d'être couverte d'eau est une condition préliminaire nécessaire à la distillation solaire à grande échelle, on a donc proposé que des bassins de distillation solaire soient construits pour convertir l'eau de mer en eau douce dans des conditions économiques permettant au procédé de faire utilement concurrence aux autres. Dans la mesure où une telle installation solaire de distillation fonctionnerait avec une masse d'eau de mer recueillant la chaleur à une température relativement élevée, la possibilité de récupérer de l'énergie comme sous-produit de l'eau fait l'objet d'un examen dans la présente communication.

L'installation de base, qui couvre une surface de 1 mille carré, est constituée par des bassins à fond noir d'une largeur de 50 à 100 pieds et d'une longueur

de l'ordre de 1 mille, séparés par des auges de récupération des produits de condensation et directement couverts par une couverture de condensation mince unique qui sera appelée la couverture inférieure. La couverture supérieure, qui sépare l'ensemble de l'aire de distillation de l'extérieur et la protège des vents, est à deux couches. Elle est tendue et maintenue assez plate par des fils de renfort en acier tous les quatre pieds, fils qui servent également d'entretoises pour séparer les deux couches.

On a mis au point un programme destiné à une machine à calculer IBM 704, dans le but de déterminer le fonctionnement d'un alambic solaire d'heure en heure à partir de ses paramètres et de données météorologiques réelles ou simulées. Un rapport théorique fut établi entre la masse et la transmission de chaleur combinées et la transmission de chaleur naturelle par convection seule; on fit usage d'un facteur de correction unique pour chaque région de transmission, pour tenir compte de la différence dans le régime de convection entre les alambics réels et des surfaces plates horizontales. On a évalué cet élément à partir de certaines données expérimentales. Le rayonnement solaire absorbé dans chaque couche transparente est traité non seulement comme étant une perte au profit de la couche absorbante, mais aussi en ce qui concerne la fraction du Δt global qu'il représente. Les transmissions de chaleur vers le sol et en provenance du sol sont également prises en considération.

L'auteur envisage plusieurs moyens d'élever la température à laquelle la chaleur destinée à la production d'énergie est absorbée. Le fait de mettre la majeure partie de l'eau en réserve la nuit ou par mauvais temps dans une zone limitée — de préférence couverte par un réflecteur de rayonnement — donne de très bons résultats. Le refoulement des gaz d'échappement de moteurs lavés dans l'immense espace disponible entre les couvertures supérieure et inférieure fournit du CO^2 qui vient réduire les pertes par rayonnement. Une pellicule d'huile sur l'eau fera monter sa température au détriment de la production d'eau par la chaleur « perdue ». L'emploi de couvertures en composition plastique supplémentaires fait monter la température davantage, mais à un prix très supérieur. Prises séparément ou en combinaison, ces deux mesures sont beaucoup plus efficaces quand on les applique à une fraction du bassin située sous une seule couverture de condensation, car la chaleur est alors récupérée à une température assez élevée, dans le reste du bassin, et « sacrifiée » à la couverture de condensation, pour réduire la perte de chaleur de la fraction plus chaude du bassin qui est enfermée. L'espace abrité du vent qui se trouve sous la couverture supérieure permet la suspension fort économique des grandes feuilles d'un composé plastique revêtu d'aluminium dans un plan est-ouest, de manière à concentrer le rayonnement solaire sur certaines zones du bassin. Si on déplaçait les points d'accrochage du fil qui soutient la composition plastique à la tombée de la nuit au-dessus de la couverture inférieure, le réflecteur se draperait sur la surface de cette dernière et réduirait les pertes de chaleur.

Les plus hautes températures de l'eau peuvent être produites en utilisant des bassins profonds qui contiennent de la saumure concentrée près du fond et de l'eau de mer plus légère au-dessus, ainsi que le suggère Tabor.

Une fois chauffée, l'eau est vaporisée très rapidement pour produire de la vapeur, soit dans une tour de pulvérisation à vide, ainsi que le préconise la General Electric, soit au moyen d'un « siphon flottant » ainsi que le décrit le présent mémoire. Le maintien du vide ne pose pas de problème pour l'enceinte de vaporisation rapide, mais seulement pour la chambre de condensation. On utilise des turbines, des générateurs, des tableaux de commutation, etc., du type classique, ainsi que le recommande la General Electric. Pour la condensation, cependant, on recommande l'emploi d'un bassin de pulvérisation à trois phases qui fait intervenir l'eau de mer, le vent et un hydrocarbure, de manière à fournir de l'hydrocarbure refroidi pour assurer la condensation par pulvérisation du produit de condensation en provenance de la turbine.

Les frais globaux peuvent être répartis arbitrairement entre l'énergie et l'eau. Avec une capacité nominale maxima de 10 000 kW, cette répartition pourrait être de 2,2 cents le kilowatt pour l'énergie et 29 cents les mille gallons pour l'eau.

THE DEVELOPMENT OF A 15-KW (el) SOLAR MECHANICAL ENGINE FOR SPACE APPLICATION AND ITS RELATIONSHIP TO THE FABRICATION OF SIMILAR ENGINES FOR TERRESTRIAL USAGE

*B. T. Macauley**

Much effort is presently being expended on the development of solar thermal-mechanical conversion systems designed to produce electrical power for space vehicle applications. Although these costly research and development programs are still in their early phases of progress, they are, nevertheless, attacking numerous difficult component and subsystem design problems whose successful solution will certainly assist those programs aimed at the practical use of solar energy for terrestrial mechanical power and electricity production.

The most obvious early economic contribution to terrestrial solar power generation applications which these ambitious space solar power system programs can make will be in the direction of advancing the state-of-the-art of solar technology along many broad lines of investigation. Much in the same manner that government-sponsored work on high-temperature materials research, advance design concepts, extensive component testing and development, etc., in support of mobile or flyable nuclear reactors, has immeasurably aided the progress of commercial nuclear power application programs, so will the extensive amount of investigations into developing highly accurate solar concentrators, highly efficient and reliable power conversion and generation components, new working fluids, new materials and fabrication techniques, etc., significantly bring closer the day when terrestrial solar power generation systems will be available in economic form.

To illustrate the design, development, and economic relationships between solar mechanical engines for space application and solar power generation systems for terrestrial uses, a specific research and development program, involving the design study of the largest known solar mechanical engine for use on space vehicles, has been chosen for discussion. The program to be described, called the 15 kW Solar Mechanical Engine Program, is an applied research and development effort aimed at providing for the growth and advancement in the state-of-the-art technology of dynamic solar conversion systems using high temperature working fluids and operating at relatively high power levels. Sundstrand Aviation, Denver, Division of the Sundstrand Corporation, is conducting for the government a research and development program aimed at the eventual production of a flyable, long duration solar thermal-mechanical power conversion system for use in space applications.[1]

General description of the 15-kW Solar Mechanical Engine Program

The specific objectives of the 15-kW Solar Mechanical Engine Program are to reveal and solve the critical component problems associated with advanced solar mechanical power concepts. In order to meet these objectives, since the development of a specific system is not yet called for, general preliminary design specifications of a dynamic solar conversion system were created by the government in order to permit an optimum system design to be established, hardware to be assembled for test, and research experiments to be defined and performed.

The major general preliminary system design specifications are as follows:

(*a*) Payload power: 15 kW of continuous electrical power at 3 200 cps, 120/208 volts, 3 Φ;

(*b*) System weight (max.): 1 000 lb (66.6 lb/kW);

(*c*) Operating life cycle: one year continuous operation during an orbit period having 60 minutes of sunlight and 40 minutes of shadow time;

(*d*) Launch and environmental conditions: maximum launch acceleration of 10 g along the longitudinal axis of the vehicle, 2 g along the lateral axis; zero gravity, vacuum, temperature, meteorite bombardment, cosmic radiation and Van Allen radiation as found at operational orbital altitudes.

To meet the above objectives, several areas can be immediately defined which require investigation in order to develop a light-weight dynamic solar conversion system having the capability to operate reliably and unattended for more than a year. These areas are as follows:

(*a*) Solar concentrator: configuration and fabrication concepts;

(*b*) Solar boiler-heat storage unit: configuration and materials for heat storage;

* Sundstrand Aviation, Denver Division of Sundstrand Corporation, Denver, Colorado.

[1] Work performed under Air Force Contract AF33(616)7128. Cognizant agency: Flight Accessories Laboratory, Wright Air Development Division, Ohio.

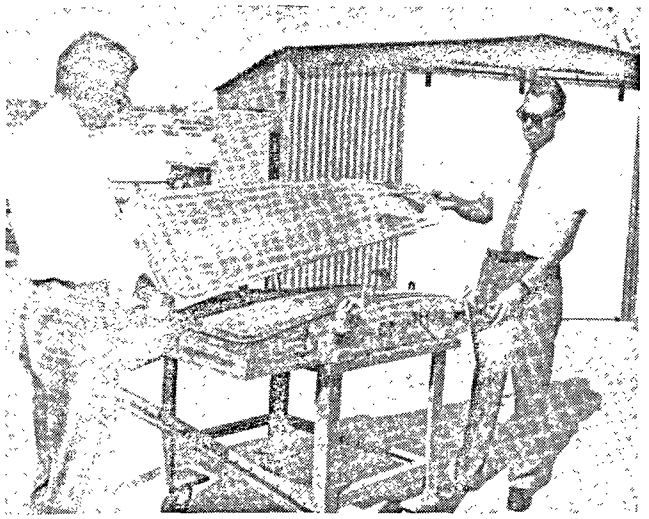


Figure 1. Mirror skin removed from die

(*c*) Cycle and working fluid: temperature levels for cycle operation, choice of working fluids, e.g. liquid metals, sulfur, bromides, etc.;

(*d*) Power conversion unit: turbine design, bearing selection, alternator type, etc.;

(*e*) Radiator-condenser: configuration and materials of construction;

(*f*) Payload-power system integration: storage of concentrator, relative location of major components, etc.

Each of the above areas will be briefly discussed.

SOLAR CONCENTRATOR SUB-SYSTEM

The magnitude of the problem of fabricating solar concentrator shapes which lend themselves to reasonable compactness for storage and eventual deployment with acceptable resultant accuracy was established by an extensive survey which showed that, while no limit existed with regard to the number of concepts for the design of storable, deployable, light-weight solar concentrators, little or no demonstrated state-of-the-art knowledge existed with respect to the actual fabrication of such devices having good optical accuracy. Hence, it was decided that two general approaches to the design and fabrication of large, ultra-light-weight, storable, deployable and optically accurate solar concentrators would be investigated in considerable detail.

The two fabrication concepts in question were (*a*) light-weight rigid shapes (plastic or metal skins) fabricated into segments suitable for storage and deployment and (*b*) inflatable shapes (made of mylar-type materials) which could be compactly stored and subsequently inflated and rigidized (by foam-in-place processes) to maintain contour accuracy in space for long periods of time.

Two firms were chosen from industry as having demonstrated fabrication ability in ultra-light-weight structures, and each was assigned the task of demonstrating the feasibility and practicality of building a flight prototype solar concentrator, constructing 10-foot demonstration models of a selected prototype configuration. A competition was established between the two subcontractors with each being given the following design objectives:

(*a*) Concentrator shape: paraboloid;

(*b*) Test concentrator diameter: 10 feet;

(*c*) Concentrator rim angle (θ_m): 60 degrees;

(*d*) Concentrator system specific weight (including mirror surface, backing structure, deployment and sun-orientation sub-system): 0.30 lb/ft^2 of mirror projected area;

(*e*) Surface reflectivity: 0.93 or better;

(*f*) Surface optical accuracy (following deployment): 98 per cent of the mirror's surface to reflect light rays corresponding to a tangential surface error (relative to a perfect paraboloid) of not more than $\pm \frac{3}{4}°$.

Ryan Aerospace, a division of Ryan Aeronautical Company, San Diego, California, was assigned the task of fabricating a 10-foot experimental concentrator made of aluminum. Figures 1, 2, 3 and 4 show various steps in the Ryan fabrication process for a petal-type concentrator.

Goodyear Aircraft, Akron, Ohio, was assigned the task of fabricating a 10-foot experimental concentrator made of flexible materials (mylar, teslar, etc.) which could be inflated to shape and subsequently foam rigidized to hold contour. Figures 5, 6, 7 and 8 show the general steps involved in the fabrication of inflatable devices.

Following nine months of effort, during which the two types of mirror were fabricated and delivered to Sundstrand for optical testing, the inflatable design concept developed by Goodyear Aircraft was finally chosen for further development in larger sizes



Figure 2. Welding lattice details into a blanket

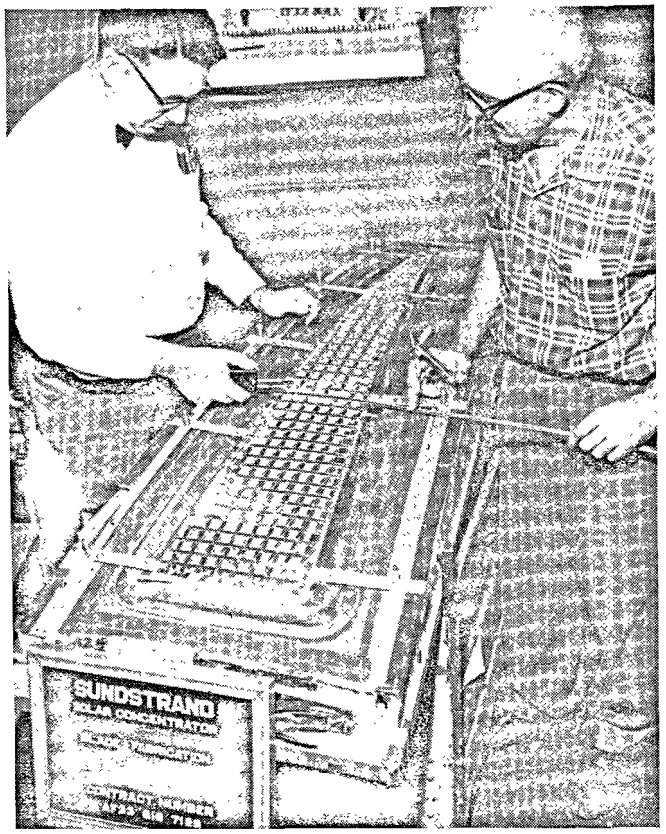


Figure 3. Locating blade details

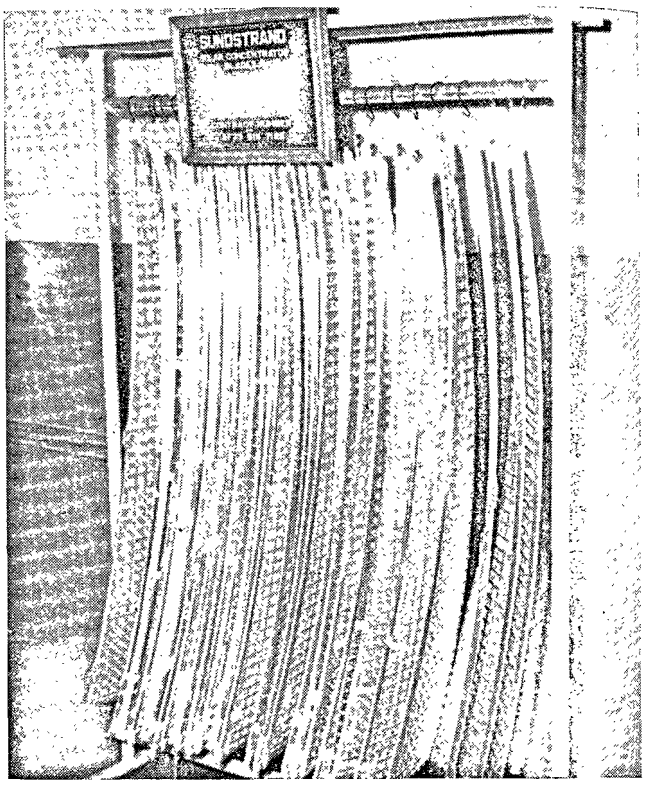


Figure 4. Completed blades

(up to 50 feet in diameter). Figure 9 shows the flux pattern determined from optical measurement for the Ryan 10-foot concentrator, and figure 10 shows the flux pattern obtained from optical measurements for the Goodyear inflatable-rigidized experimental mirror.[2]

In order to achieve the concentration efficiency which was felt to be necessary for a practical flight prototype solar dynamic power conversion system, an optical device called a Flux Trap[3] was developed, from basic studies, which has the property of being able to shrink the "fringe circle" in the mirror's focal plane into a smaller area (an area in size equivalent to the "solar spot" of an imperfect mirror). Its chief practical advantage is the fact that, for high temperature systems where re-radiated energy from a solar radiation receiver is an important system loss consideration, the size of the solar radiation receiver can be reduced appreciably. Without a Flux Trap device, inaccurate concentrators, having generalized focal plane fluxes similar to those shown in figure 11, would have to be inordinately large in diameter when used with high temperature solar energy receivers since, to minimize the re-radiation losses from high temperature receivers, the solar energy receivers would have to be kept small and, by being reduced in size, would fail to absorb all of the power reflected into the focal plane. (For further Flux Trap details, see references 1 and 2.)

Figure 12 is a picture of an experimental Flux Trap specifically designed for use with a 10-foot concentrator having a 60-degree rim angle and having no surface tangential error greater than $\pm \frac{3}{4}°$. This particular Flux Trap is commonly called a "back-to-back" configuration since it uses two reflecting sides of the developed configuration to re-direct "error" rays coming from the mirror. This configuration requires a double cavity to receive all of the focal plane flux. Other configurations have also been investigated. Figure 13 shows an early configuration developed for a mirror having a rim angle of 45° and a surface accuracy such that no point of the mirror has a tangential error greater than $\pm \frac{3}{4}$ of a degree. This configuration is commonly called a "forward facing" Flux Trap, since one compound curved surface is required and it "sees" all of the primary mirror's surface.[4]

By way of illustrating the fringe circle reduction available from, say, a 44.5-foot mirror (flight prototype size) with a rim angle of (*a*) 60 degrees and (*b*) 45 degrees and having no surface tangential

[2] Over 12 000 light ray measurements were taken on the two delivered test mirrors, five zones per mirror at every ½ degree interval and at three positions of mirror attitude to check gravity effects on contour.

[3] Trade mark of Sundstrand. Patent applied for.

[4] While the Flux Trap was initially developed around a paraboloid shape, its principles will also apply to parabolic-cylindrical shaped concentrators.

error greater than $\pm \frac{3}{4}$ of a degree, consider the following:

Case I. 44.5-foot mirror, $\theta_m = 60°$, $\delta_n = \pm \frac{3}{4}°$

The diameter of the fringe circle, d_{fc} is calculable from:

$$d_{fc} = D_m \left\{ \frac{\sin \varphi}{\sin \theta \cos (\theta + \varphi)} \right\}$$

where $\varphi = 2\,\delta_n + \alpha/2$ ($\alpha = .0093$ radians).

For this case, $d_{fc} = 3.348$ feet and the corresponding area, $A_{fc} = 8.806$ ft². For this large rim angle, a back-to-back Flux Trap configuration must be used. The total receiver (double cavity) areas, A_{FT} for this Flux Trap configuration, can be shown to be 2.594 ft², or *only* 29.4 per cent *of the original fringe circle area.*

Case II. 44.5-foot mirror, $\theta_m = 43°$, $\delta_n = \pm \frac{3}{4}°$

For this case, the area of the fringe circle can be calculated in the same manner as for case I and is equal to 6.3036 ft². However, for this example, a forward-facing Flux Trap would be used. Its diameter, hence cavity area, can be calculated from:

$$d_{FT} = \frac{D_m}{2} \left\{ \frac{\tan \varphi}{\tan \theta/2} \right\}$$

The inner cavity area is found to be equal to 2.383 ft² or only 37.8 per cent of the fringe circle area.

In both of the above cases, each of the cavity areas required with a Flux Trap is much less than the area of the mirror fringe circles, regardless of whether or not a relatively long or short focal length is chosen. The only major difference between case I and II is in the size and contour of the Flux Trap required. To date, experimental work is underway for making both radiometer measurements of resultant focal plane (cavity) fluxes and calorimeter measurements of mirror-Flux Trap concentration efficiencies.

Solar boiler-heat storage unit

Working in conjunction with the power conversion system cycle analysis, concentrator-Flux Trap evaluation, turbine design studies, etc., a somewhat unique solar energy receiver design configuration was evolved. This configuration, commonly referred to as a double boiler, permits enlarging the opening of a cavity-type energy receiver without the attendant increase in cavity re-radiation losses normally encountered in designing large-size, single-cavity configurations. This double boiler system, demonstrated by actual test, when combined with the Flux Trap device, permits the attainment of very high concentrator system efficiencies which are not possible to obtain in practice by conventional design methods. Figure 14 shows a layout drawing of the double-cavity energy receiver configuration chosen for development.

Based upon design and test programs, a near-optimum design of an integrated solar boiler-heat storage unit has been established. Two features of the developed design are worthy of special mention. First, the heat storage unit is a two-zone system (see figure 14). That is, the first portion of the power cycle, in which the low temperature cycle fluid is boiled, is accomplished using lithium hydride (LiH) as the heat storage material, while the latter stages of the heat input to the cycle, i.e., superheat and reheat stages, are accomplished using sodium fluoride (NaF). Cycle optimization studies have shown that this approach permits the attainment of the lightest possible component weight in comparison to using only one heat storage material for the general component design.

The second design feature of the heat storage unit consists of a mixture of lithium hydride, approximately 95 per cent by weight, and lithium metal, approximately 5 per cent by weight, as the low-temperature heat storage material. This approach makes a significant improvement in component weight reduction since the addition of lithium metal to the hydride compound increases substantially the thermal conductivity of the heat storage material and, hence, allows a reduction in component size through an increase in heat transfer performance. A further advantage is obtained by the Li-LiH material approach to heat storage design: the mixture prevents the occurrence of a difficult design situation in which the working fluid passages could be warped,

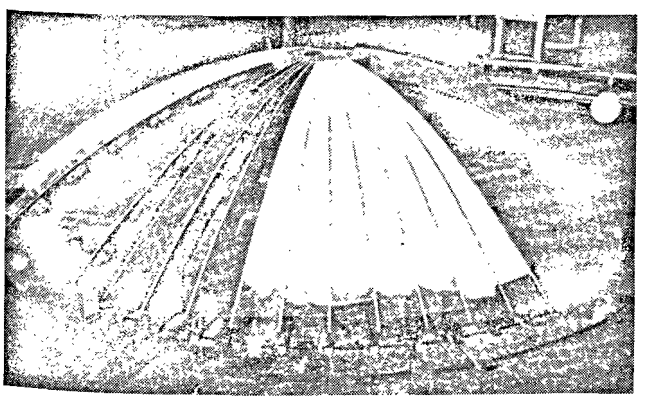


Figure 5. Details of construction of the 10-foot mold showing lay-up of plaster foam

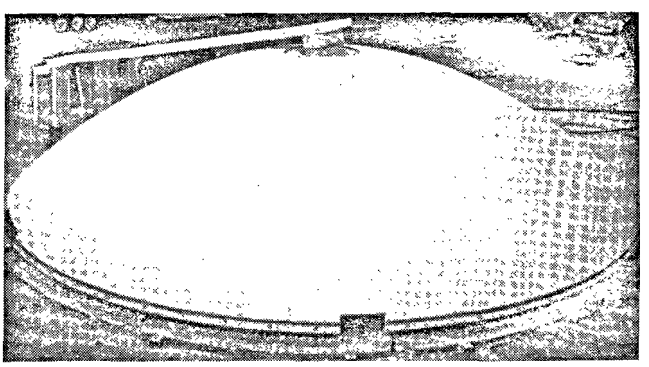


Figure 6. Finished 10-foot plaster mold ready for lay-up of milar gores

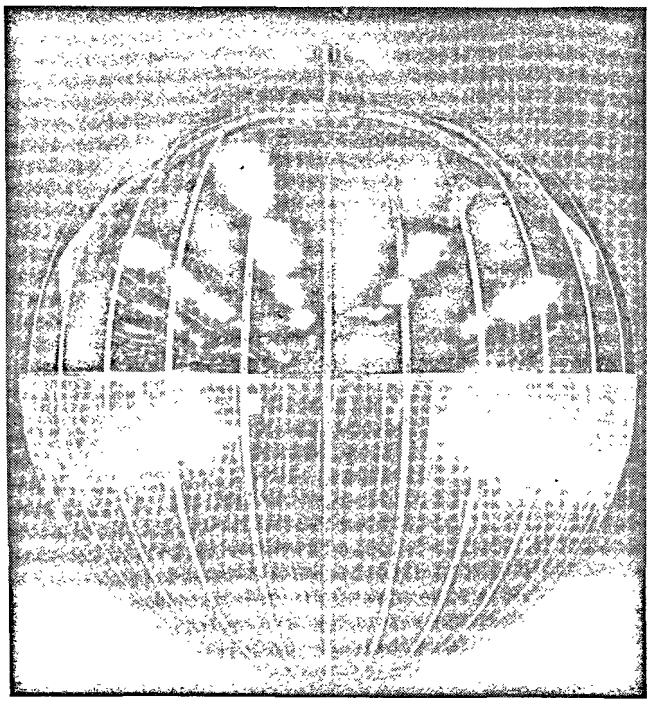


Figure 7. Inflated spherical balloon with parabolic end cap ready for rigidization

or even crushed to destruction, by use of only the single material, LiH, as it solidifies and melts during system operation between sunlight and darkness cycles of the orbit period.

A similar advantage is expected to be gained by using a mixture of NaF and Na for the high temperature portion of the heat storage cycle, and tests are being conducted to determine the feasibility of this approach.

Cycle and working fluid solution

At the outset of the program, a closed Rankine cycle was specified by the government for use with the 15-kW Solar Mechanical Engine. Thus, only the choice of working fluid and cycle states remained to be established. Taking into account all of the aforementioned design considerations, rubidium was chosen for the cycle working fluid, over potassium, mercury, aluminum bromide, sodium, and sulfur. The cycle conditions selected for the chosen working fluid are as follows :

Boil at 1 200°F; superheat to 1 750°F; expand to zero per cent moisture; reheat to 1 600°F; expand to 1.50 per cent moisture; reheat to 1 450°F; expand to 0.1 psi back pressure in a 25 per cent reaction turbine.

This cycle, which utilizes a nearly constant degree of superheat and reheat, is slightly less efficient than one using constant superheat and reheat temperature. However, it is superior from a solar boiler-heat storage unit design standpoint. The chosen cycle is 26.5 per cent efficient.

Figure 15 shows the temperature entropy diagram for the chosen cycle, and figure 16 shows the cycle schematic, including the temperatures and pressures of the fluid at each point in the cycle.

Power conversion unit

The power conversion unit, commonly referred to as the combined power unit, consists of a three-stage turbine, a homopolar inductor alternator, liquid metal hydrodynamic bearings, and a boiler feed pump, all assembled on a single shaft. All turbines are axial and full admission. The first and second stages are impulse turbines and the third a reaction turbine.

Figure 17 is an inboard profile of the combined power unit (CPU) showing the relative location of the aforementioned components. Figure 18 shows a cutaway isometric layout of the combined power unit.

Radiator-condenser

For space applications, since the only available means of rejecting cycle waste heat is by surface radiation to space, a special radiator condenser design must be considered. The design selected is an advanced concept, yet simple to fabricate and assemble.

The entire radiator-condenser is located at the circular end area of the available 10-foot diameter payload-cylinder, as shown in figure 19. Figure 20 shows how the 360-degree turbine diffuser at a 20-inch diameter is used as the vapor manifold, with the flow direction essentially radially outward to a liquid collector at the circumference on an $8\frac{1}{4}$-foot circle. This symmetrical configuration has no unbalanced torques. Figure 20 also shows the cross-sectional variation along any radial channel from the turbine diffuser exit to the manifold. The turbine diffuser reduces the vapor velocity to a value of 253 ft/sec at the entry to the condenser channels.

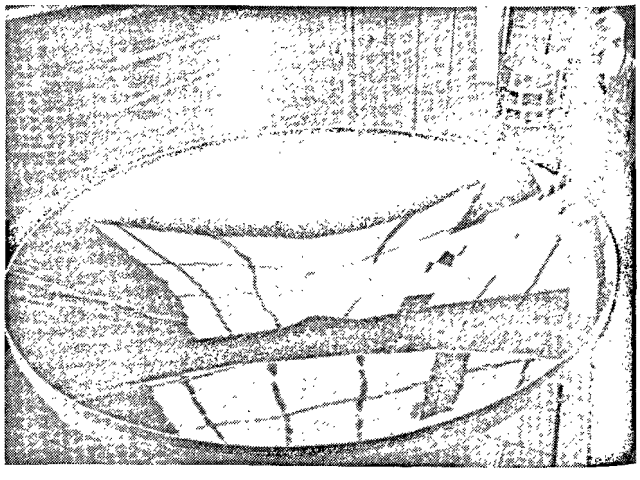
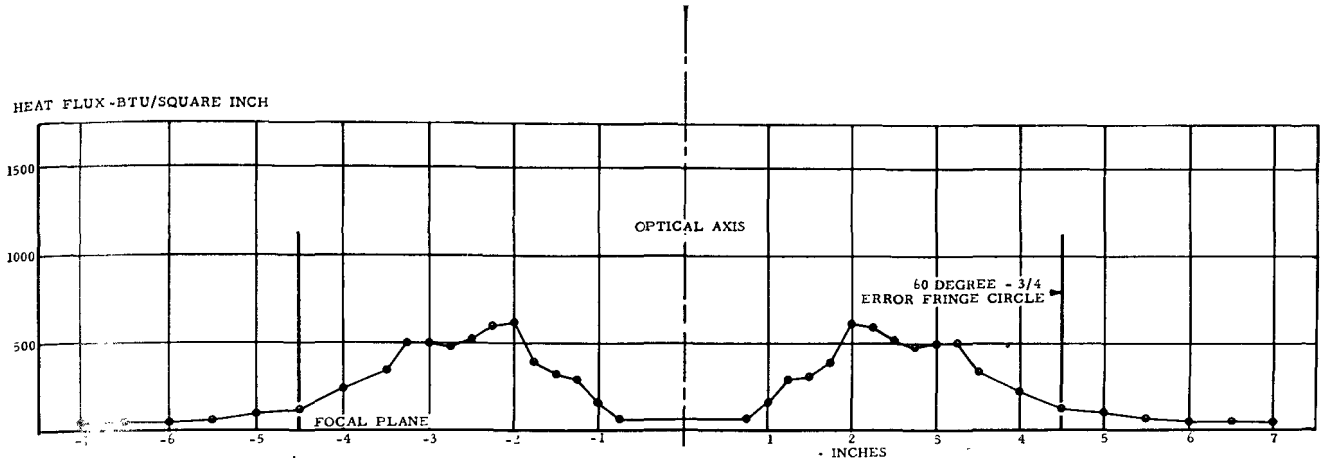
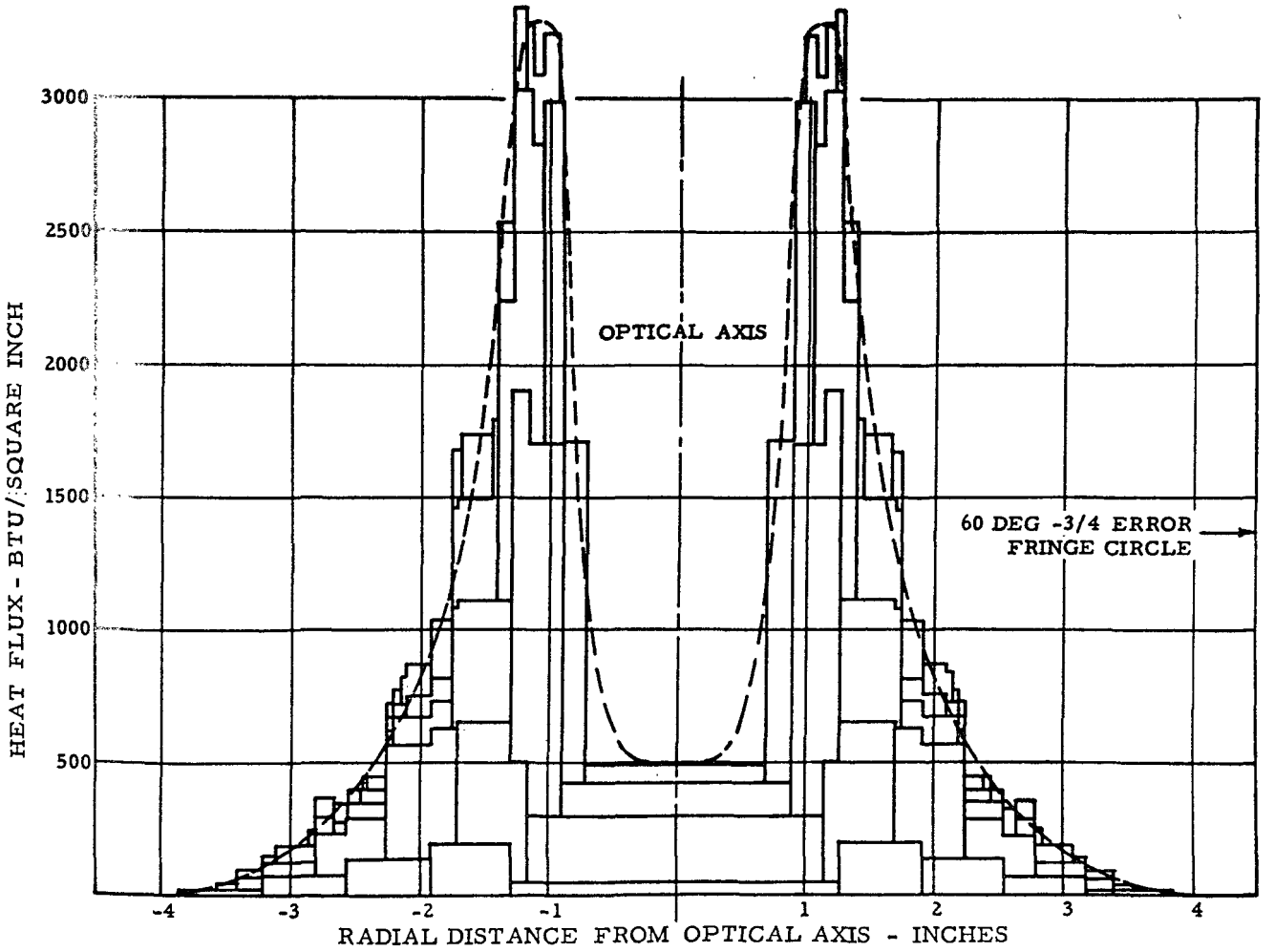


Figure 8. Finished experimental 10-foot mirror with foam backing following removal from form



SOLAR FLUX DISTRIBUTION - 10 FOOT 60 DEGREE
FABRICATED METAL MIRROR

Figure 9. Measured flux distribution for a petal-type deployable concentrator



FLUX DISTRIBUTION IN FOCAL PLANE 10' DIAMETER
RIGIDIZED PLASTIC MIRROR FINITE INTEGRATION OF
OPTICAL TEST DATA

Figure 10. Measured flux distribution for an inflated-rigidized-type concentrator

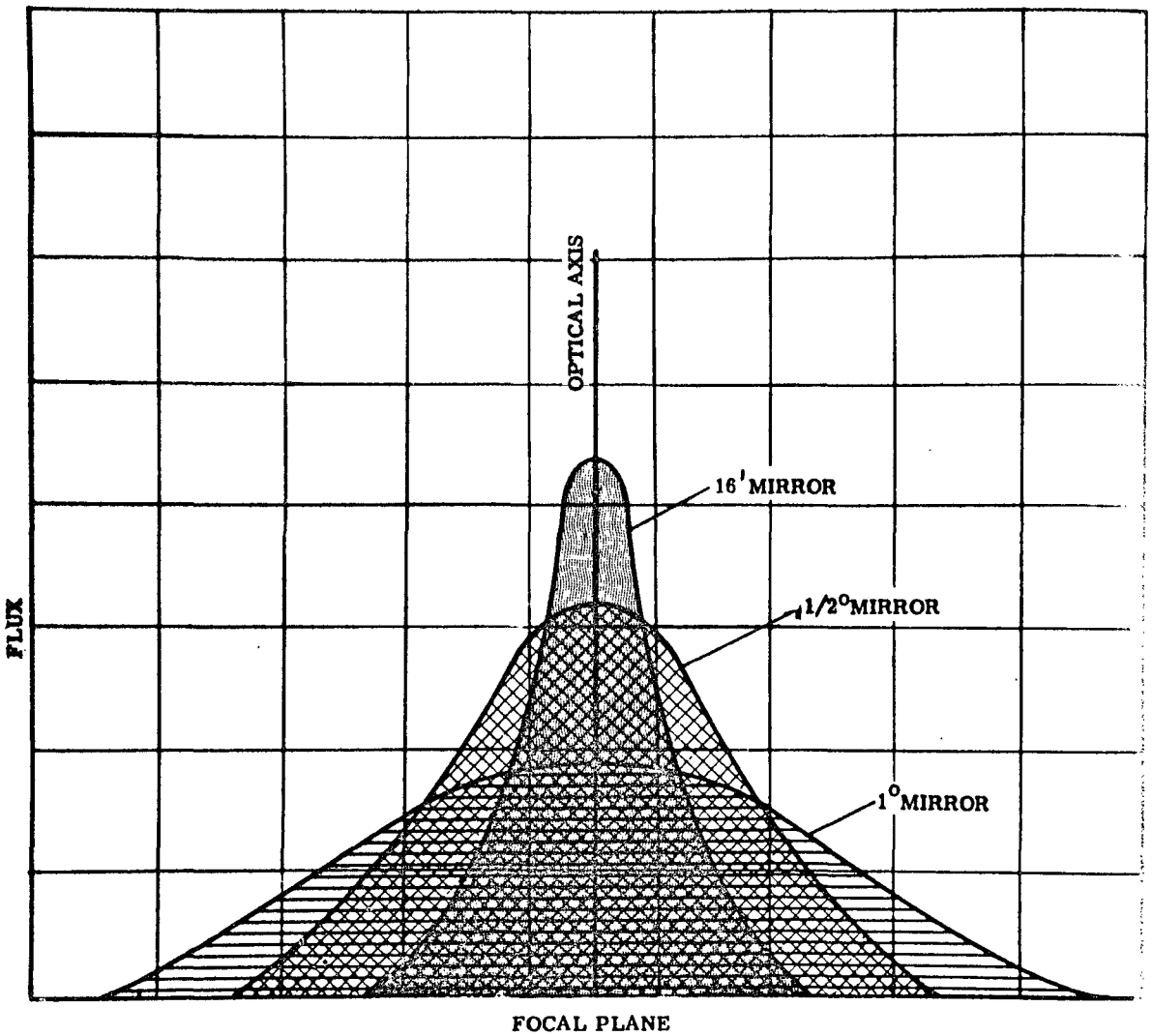


Figure 11. Plane profile of flux distribution for various-quality parabolic mirrors

Table 1. 15-kW Solar Mechanical Engine design characteristics

(a) *General parameters*

Working fluid	rubidium
Cycle efficiency	26.5
Sunlight-shadow ratio	60 min/40 min
Furnace factor	77 359
Mirror rim angle	60°

(b) *Component size and weights*

	Dimensions	*Weight*
1. Solar concentrator sub-system	Dia. = 43.838 ft; f = 18.982 ft	402.00 lb
2. Boiler-heat storage unit.	Dia. = 26.0 in; length = 27.5 in	406.93 lb
3. Combined power unit (24 000 rpm-32 000 cycle output)	1st wheel = 6.87 in; 2nd wheel = 7.34 in; 3rd wheel = 11.20 in	Total weight = 110.00 lb
4. Condenser	Dia. = 8.25 ft	64.20 lb
5. Controls		13.50 lb
6. Plumbing		7.00 lb
7. Fluid hold-up		5.00 lb
	TOTAL SYSTEM WEIGHT	1 008.63 lb

These channels in the plane of the 8¼-foot circle are curved, resembling an assembly of centrifugal blower vanes. The cross-sectional area of each identical channel decreases in the ratio of approximately 4.5 : 1 from turbine to liquid collector. This is achieved by decreasing the height parallel to the turbine axis at a rate exceeding the increase of channel width due to the increase in radius. The annular face remote from the turbine is plane and is exposed to the sun, while the other side is pointed at the solar mirror. Radiating surfaces, therefore, consist of two annuli (2 to 8¼ feet in diameter), having a total geometrical area of 92½ square feet, counting both surfaces. The radiating surfaces consist of beryllium sheets, 0.1077 inches thick for the outer and 0.020 inches for the inner annulus. Condenser tubes and radiator are thus combined into one structure. The dividers are made up of honeycomb-type material. This is a framework entirely surrounded by a skin, so that each curved portion represents a monocoque structure and serves to spread the two radiator surfaces apart in an axial direction. The condensation takes place during the chiefly radial, but curved flow. Before the liquid enters the circular collector, it passes through flow-equalizing, accurately sized orifices. At four points, high pressure liquid rubidium, after being used for alternator cooling, enters a jet pump where it accelerates to low pressure condensate by ejector action. The combined liquid streams then flow through four lines to the centrifugal pump inlet. The collector, having a wall thickness of 0.020 and 0.1077 inches, is constructed of beryllium, as are the distribution lines to the pump, which have an equivalent total flow area of about ¼ square inch.

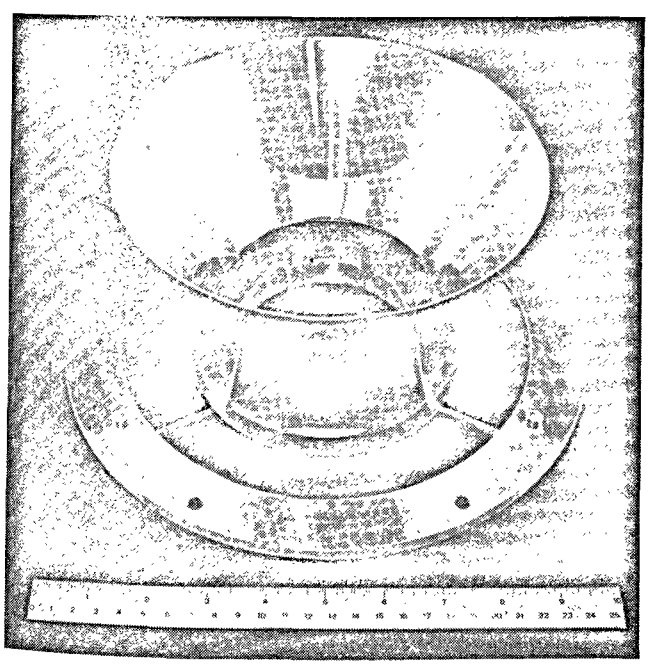


Figure 12. Solar mechanical engine flux trap. Back-to-back flux trap configuration for a 60° rim angle mirror

The entire external radiating surfaces, including the liquid fuel collector, jet pumps and distribution lines, are coated with 0.001 inch thickness of zinc oxide.

Integrated system summary

Based upon configuration studies of means of integrating the 15-kW solar dynamic power generation system with various payload bodies, an optimum configuration, shown in figures 21 and 22, was selected. As shown here, the inflatable mirror is folded and stored in a container in front of the rear plane-face of the radiator-condenser. The mirror is deployed by, first, the removal of the storage container by "blow away" action, second, the inflation of the balloon-paraboloid as shown in figure 22, and third, the foam rigidizing of the back side of the paraboloid after which time the balloon is separated from the mirror and allowed to float away, free in space.

The concentrator and power package are aligned by moving the mirror on extension support struts back over the power package as indicated by the phantom lines in figure 22. Following these steps, the power plant is ready for operation and will have a final configuration similar to that shown in the artist's drawing (figure 23). Table 1 lists a summary of the major design parameters for the 15-kW Solar Mechanical Engine.

State-of-the-art interrelationship between space and terrestrial solar engine programs

Owing to the fact that space solar engines must be designed to be ultra-light-weight, capable of maintenance free operation, ultra-reliable, and capable of operating under severe environmental conditions, their design objectives are, more often than not, considerably much more difficult, technically speak-

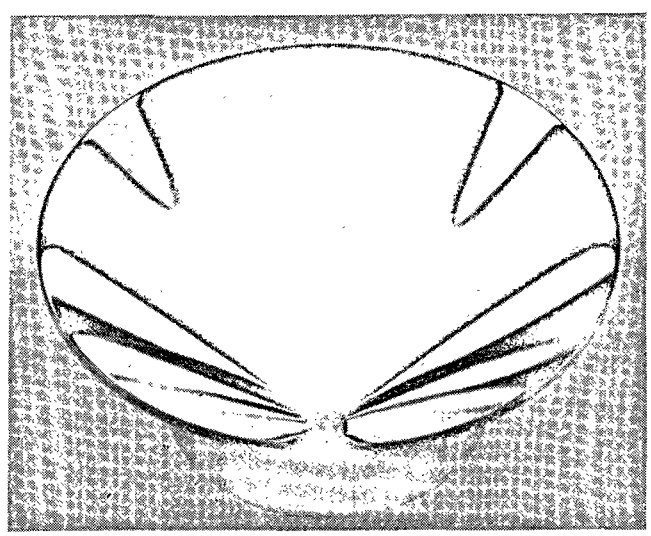


Figure 13. Forward facing flux trap for a 45° rim angle mirror

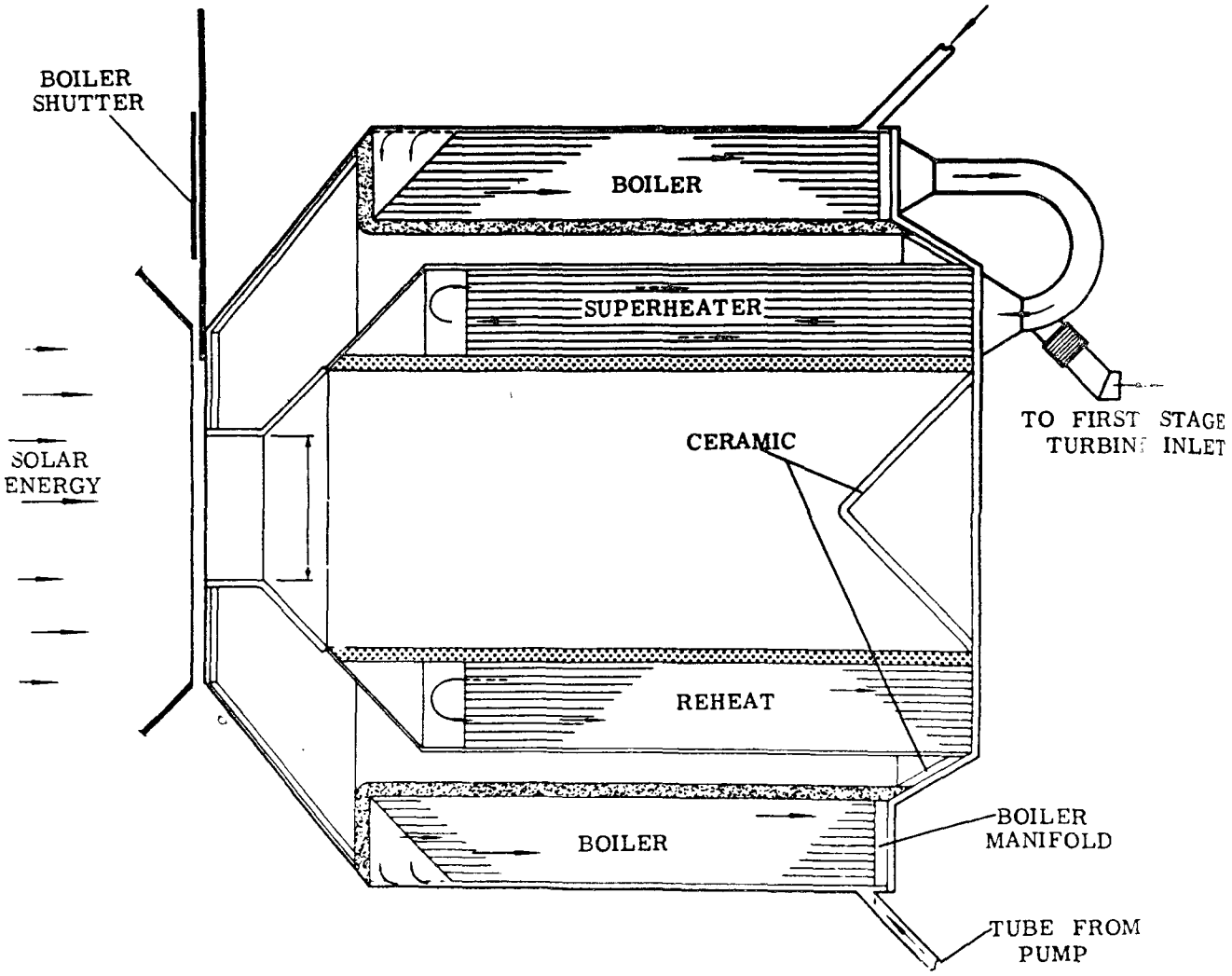


Figure 14. Boiler, super-heater and heat storage (cross-section)

ing, than are those normally established for terrestrial systems. However, it is just for this reason that space solar engine programs can make such significant contributions to developing a state-of-the-art technology for terrestrial engine programs. As was pointed out in the introduction, there are numerous examples of a program within one technological field having design objectives for one type of application which are much more stringent than those required for a different application within the same field of technology. Also, as progress in the more ambitious program is made, the goals of the less difficult program are oftentimes achieved, in a sense, almost automatically.

It is believed that the numerous space solar engine programs (the 15-kW Solar Mechanical Engine being one special case) will, in their research and development investigations, solve many of the problems which developers of terrestrial solar engines will face. Probably the strongest support of this viewpoint, to date, stems from the state-of-the-art progress currently being made in the areas of (*a*) solar concentrator development; (*b*) Flux Trap development; (*c*) low specific speed turbomachinery development; and (*d*) orientation and control systems development.

Terrestrial solar engines aimed at commercial applications naturally necessitate the consideration of economic factors in all component and sub-system design approaches. Thus, the over-all system configuration for terrestrial solar engines will probably not closely duplicate those configurations developed for space solar dynamic systems in which compactness and light weight are important design criteria. In many other aspects, however, there may exist close similarity between the components utilized by both of the solar engine applications. One example of this would be the solar concentrator.

Doubt has been expressed concerning the relative economic competitiveness of sun-tracking collectors when compared with semi-orientated fixed-positioned collector installations. This writer believes, however, that the lowest total system cost can only be achieved by designing into the system the highest efficiency possible, much in the same manner that present-day conventional fueled central station

power plants are designed. To achieve this objective, high working fluid temperatures are needed, which, for solar power plants, require that focusing collectors be used and that they be continuously sun oriented, to keep their size and hence cost to a minimum. Thus, solar collectors for terrestrial solar power plants could very well be much the same as those developed for space power plants.

From a system cost viewpoint, the solar collector concept being developed by Goodyear Aircraft for the Sundstrand 15-kW Solar Mechanical Engine Program has much to offer. First, the cost of the materials used—coated mylar, foams, etc.—are minimal, even for collectors 60 feet or more in diameter. For this type of collector, the main cost is in the labor required to lay up the gores. Once the basic tooling has been fabricated for large diameter configurations (which the 15-kW Solar Mechanical Engine Project will very shortly provide), any desired collector size, up to the limits of the tooling (50-60 feet), can be fabricated at reasonable cost.

A second cost advantage stems from the fact that the Goodyear type of collector can be mass-produced at a plant site, folded and packaged in a small shipping container (either vacuum sealed or containing an inert atmosphere), and easily and economically shipped to any remote part of the world along with the liquids required for foam rigidizing the mirror at the power plant site. Once at the site, the mirror can be positioned on the tracking rig, inflated and subsequently rigidized to hold its shape. This is an obvious advantage over solid plastic or metal-formed mirror segments which would have to be carefully packaged and handled during shipment. Experience gained to date with the latter type of concentrator proved the extreme handling care which this type must be given at all times in order to avoid surface damage.

In discussion with Goodyear Aircraft, it appears reasonable to believe that following the development and test of three or more flight-prototype-size solar collectors for space power system use, and by establishing production procedures for the manufacture of a large number of gore panels, foam mixes, etc., the cost of mirrors in the size range of 60 feet in diameter could be held to approximately U.S. $20 000, or may be less, if 800-1 000 units are to be produced.

If a nominal 30 000 hour life is assumed for ground type mirrors, then for a 15-kW ground solar power plant, the prorated installed cost would approximate 4.44 U.S. cents/kWh.

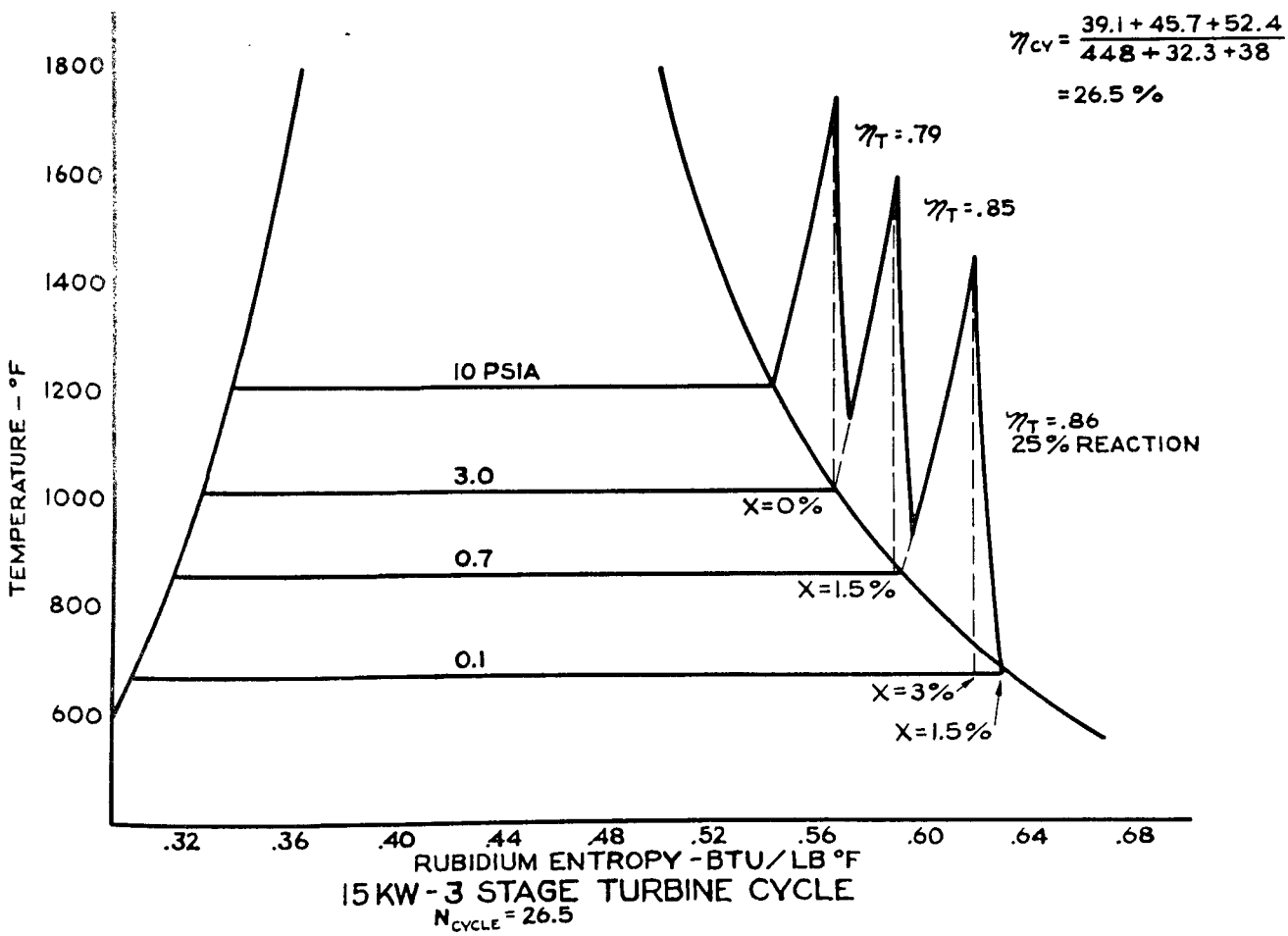


Figure 15

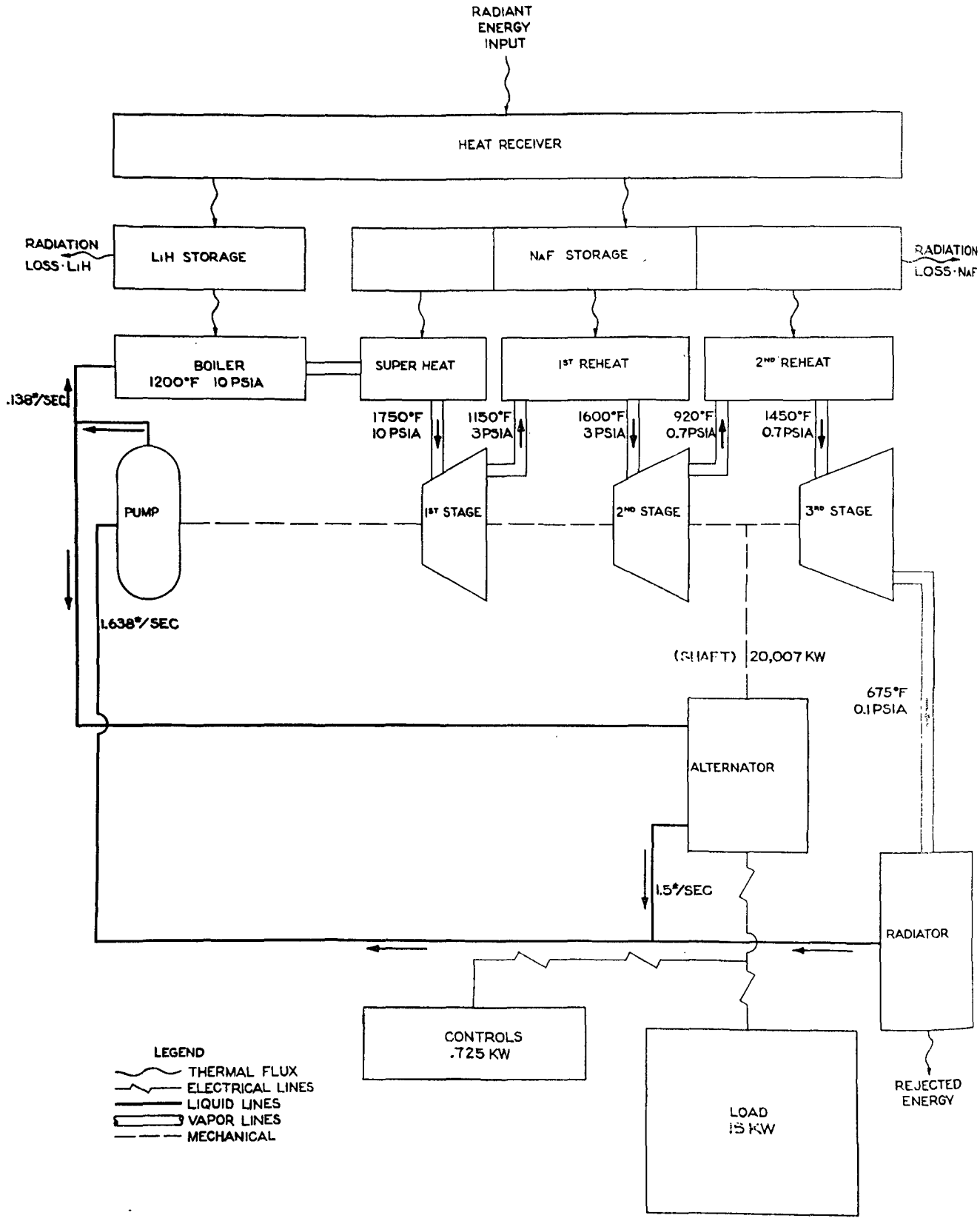


Figure 16. 15-kW cycle schematic diagram

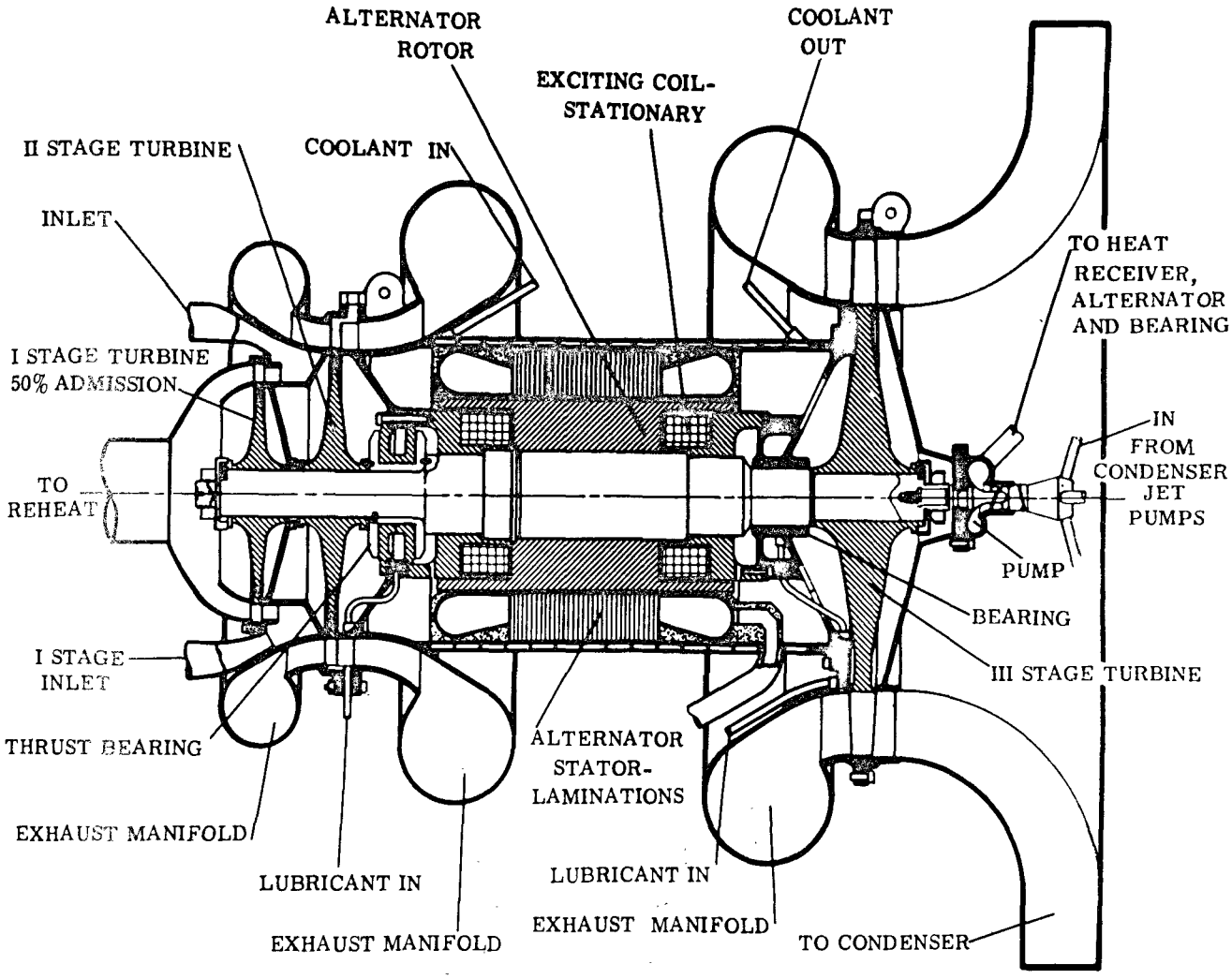


Figure 17. 15-kW solar power supply turbine alternator pump assembly

Today an automatic tracking rig which is capable of handling concentrators up to 34 feet in diameter can be bought for U.S. $36 000 (see figure 24). This price is for one-of-a-kind delivery and would be considerably reduced by production of large quantities. Under mass production, it is believed that tracking rigs capable of handling 60-70-foot-diameter mirrors could be obtained for $70 000-75 000. If, before a major overhaul is performed, a ten-year life is assumed for a tracking rig, its prorated installed cost for a 15-kW power plant would be about 5.71 cents/kWh.

Under similar production conditions, high-speed rotating assemblies (turbine, bearings and boiler feed pump) could be marketed for approximately U.S. $8 500 if either a closed Rankine or a closed Brayton cycle, using somewhat conventional working fluids (water, argon, Dowtherm-A, freon, etc.) is assumed. With non-corrosive media used, the rotating assembly which would be developed from the 10 000-hour life, 15-kW Solar Mechanical Engine Program, could be made reliable for a life of approximately 30 000 hours, since some routine maintenance is possible under terrestrial operating conditions. For some time now, gas turbines have been used in oil field applications which have run more than 17 000 hours between overhaul periods. These units encounter life problems due to the corrosiveness of their products of combustion, whereas closed cycle systems for terrestrial power applications would not necessarily encounter any severe corrosion problems. For the assumed lifetime, mentioned earlier, and for a 15 kW power plant, the prorated installed cost of the rotating assembly could be as low as 1.89 cents/kWh.

Since, for terrestrial applications, either low frequency A. C. or D. C. power will probably be required, conventional industrial generators with gearboxes to permit their being driven by high-speed turbomachinery will more than likely be used. Hence, in this respect, the configuration of the terrestrial solar power plant will differ from its parent system, the space solar power plant. Under quantity production conditions, 60-cycle alternators

could probably be purchased for no more than U.S. $1 100 and their associated gearboxes (24 000-3 600 rpm speed reduction) could be sold for approximately $450. Assuming their life span to be the same as that used for the previously described rotating assembly, the summed prorated installed costs for these two units would be about 0.344 cents/kWh.

The radiator and/or condenser for the terrestrial power plant will be significantly different from its space counterpart. Since cycle waste heat can be rejected by either natural of forced convection means, the terrestrial radiator-condenser can be compact and simple in its design. Under production conditions, quantities of these units can be obtained for U.S. $500-$700 apiece. Little or no corrosion problems are expected for this component; therefore, it should be good for at least five years before having to be replaced. Hence, for a 15-kW power plant, the prorated installed cost of one of these units would come to about 0.11 cents/kWh.

The control system for a terrestrial solar power plant can easily be built around the control system technology developed for long duration space solar power plants. There is an advantage to be accrued from doing this if a terrestrial solar power plant is to be used in remote or underdeveloped countries. First, a completely automatic control system of the type used in a space solar power plant will be developed as a fully integrated system, i.e., one in which sun tracking operations, temperature and speed control operations are completely interwoven, and hence will require a minimum of operating personnel to monitor and run the solar power plant. Likewise, the number of highly trained specialists required to run the ground solar power plant will be minimized, if not omitted altogether.

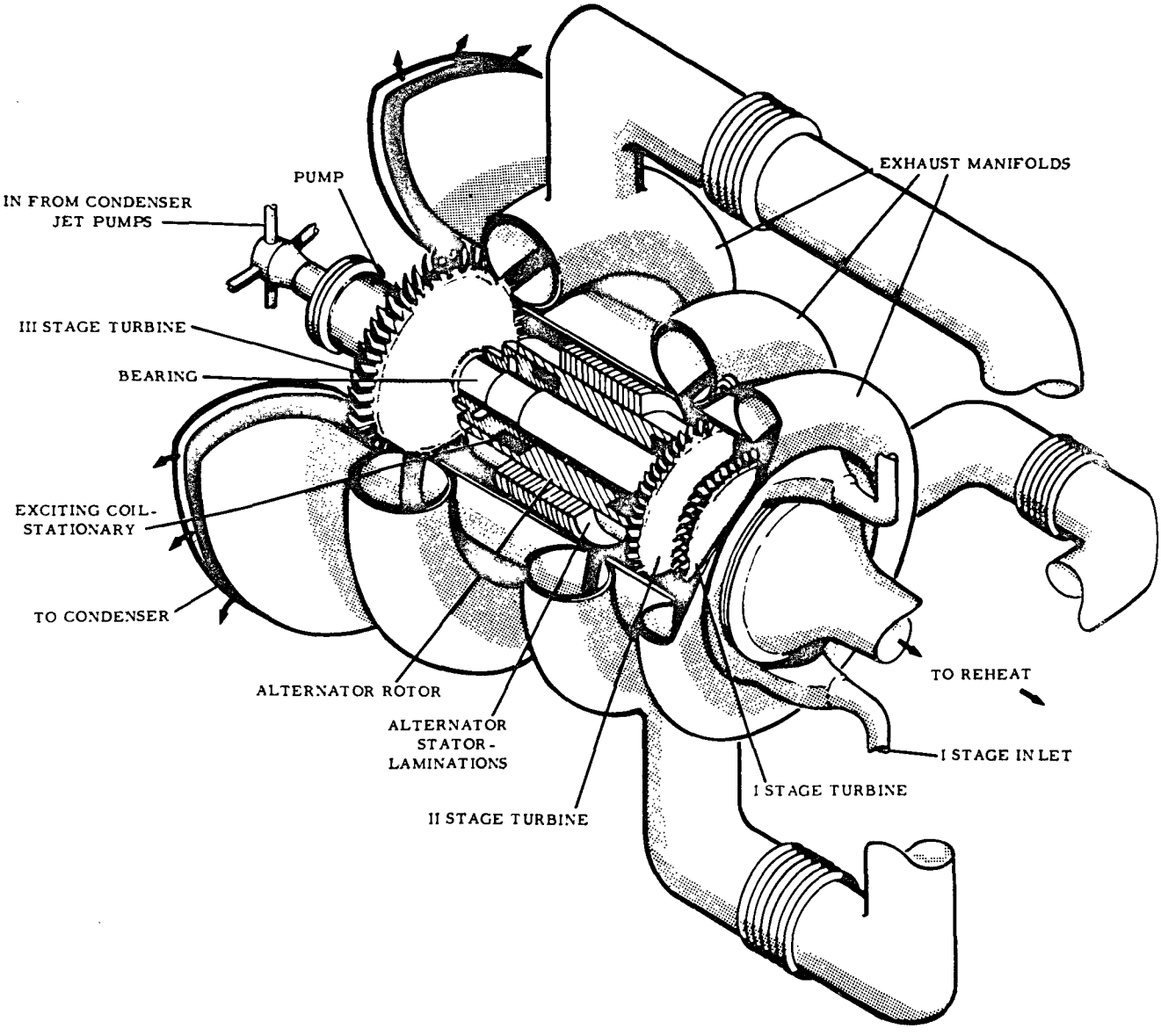


Figure 18. Isometric layout of the assembled combined power unit

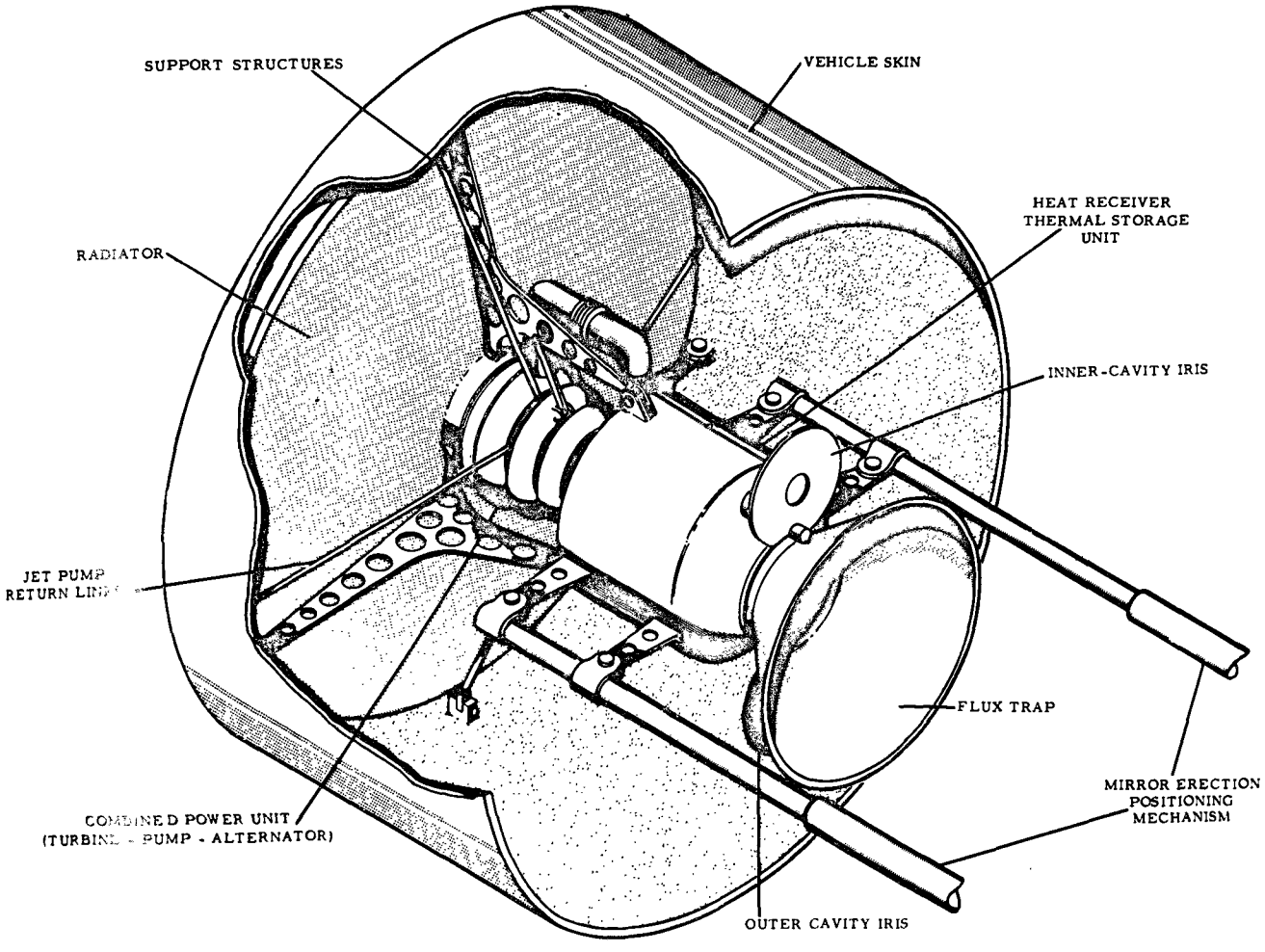


Figure 19. Installation of the circular radiator condenser in the payload vehicle

Based upon the rapid price reductions already accruing today for solid state devices planned for use on control loops, it is estimated that the necessary controls to orient the collector, maintain design point temperature levels and control component speeds can be obtained, in production quantities, for approximately U.S. $1 000, and hence, for an assumed mean time to failure (mtf) of 30 000 hours, their prorated installed cost would be around 0.22 cents/kWh.

Not yet discussed is the heat receiver unit. For a terrestrial solar power plant whenever high temperature heat storage is desired to be incorporated into the system design, the solar radiation receiver will more than likely be separated, component-wise, from the boiling and heat storage phase of system operation. In other words, the solar radiation receiver would have its thermal energy transferred, by a heat transfer loop, into a separate component which would integrate both the energy storage phase and cycle working fluid boiling and/or heating phases. Due to the large weights involved with the high temperature heat storage materials for ground

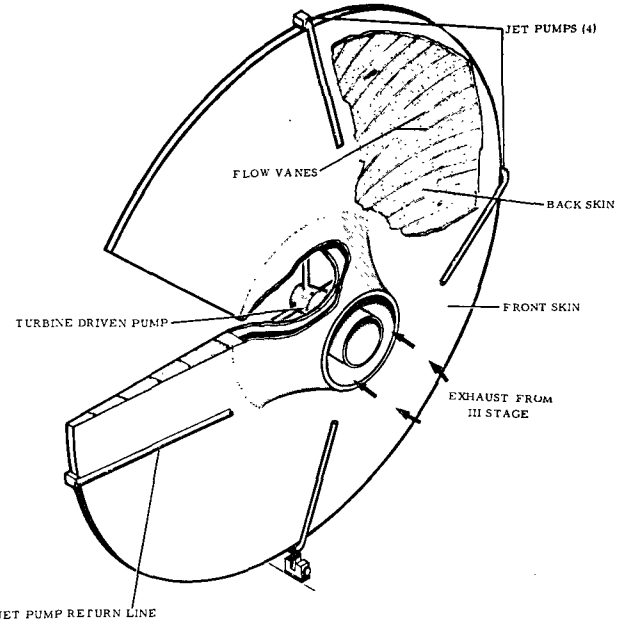


Figure 20. Isometric layout of the radiator condenser

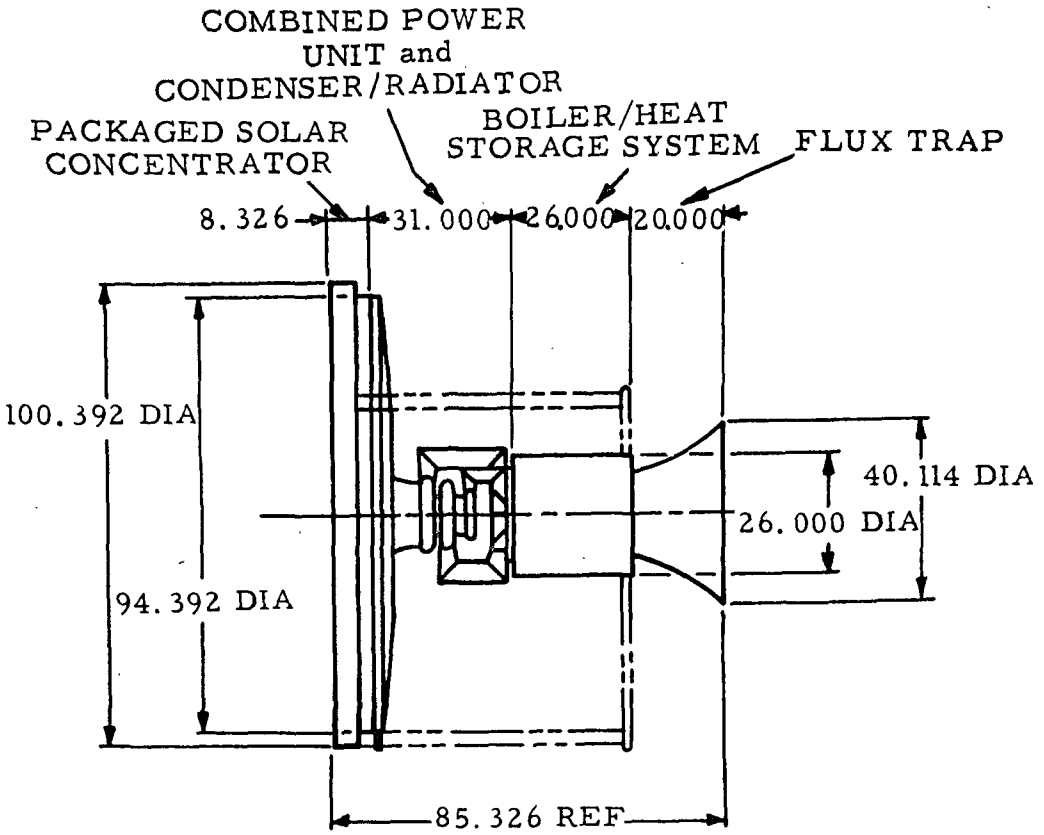


Figure 21. Packaging of Goodyear prototype solar concentrator

systems, it would not be feasible to fully integrate the boiling and heat storage process into one functional component, i.e. heat receiver-boiler-heat storage unit. However, the solar heat receiver for the terrestrial application would still look much like the component designed for space use (see figure 14). For high-temperature system operation, it would still be a double cavity design and its inner configuration would closely resemble that previously described in figure 14, except that no heat storage material would be installed and the flow passages would contain a non-boiling heat transfer fluid (Hg, NaK, etc.). Experi-

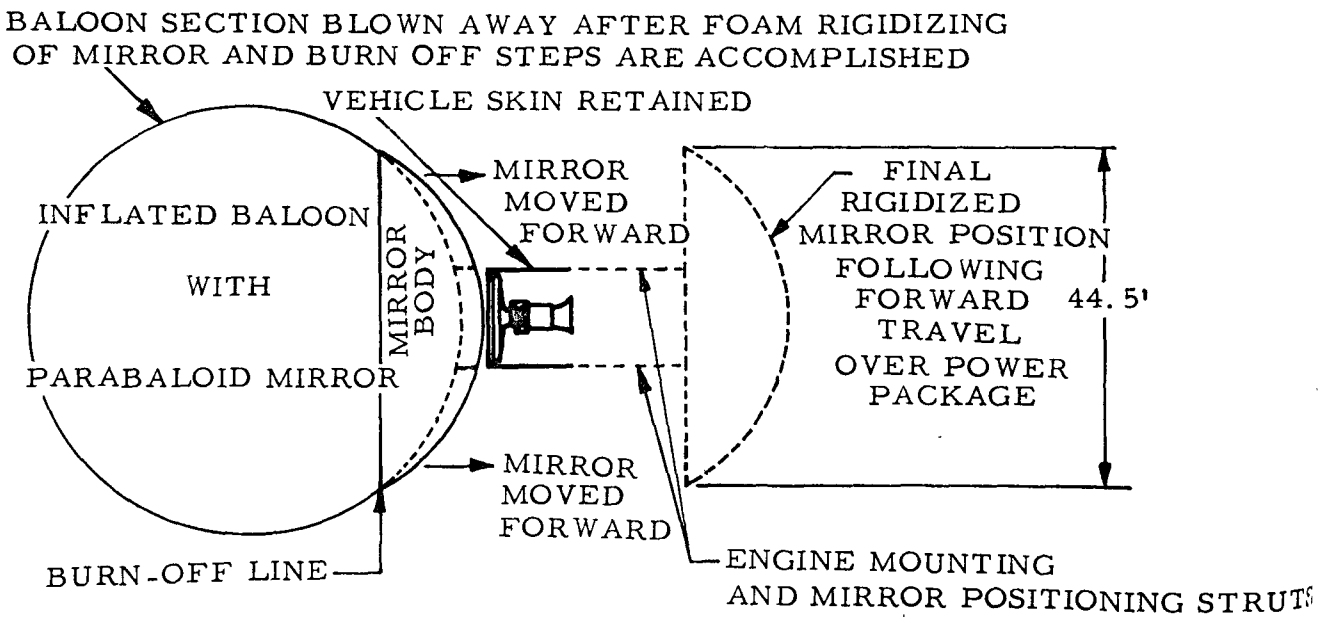


Figure 22. Deployment sequence of Goodyear inflatable solar concentrator

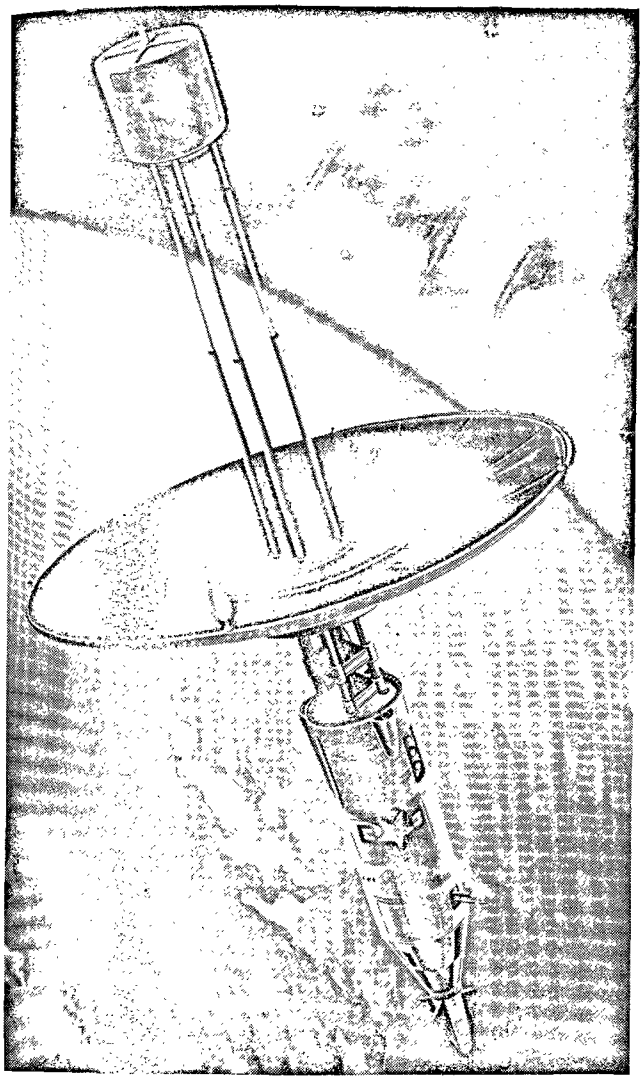


Figure 23. Artist's concept of operational 15-kW Solar Mechanical Engine

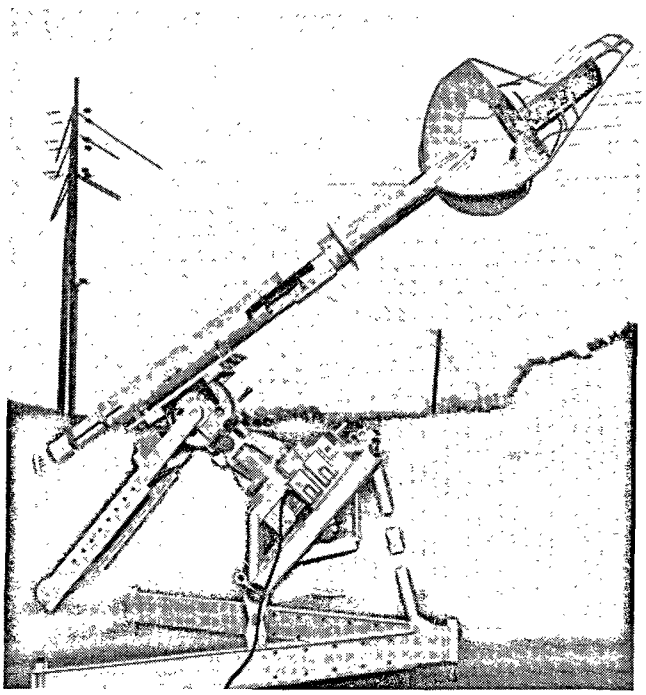


Figure 24. Automatic tracking rig

mental double cavity radiation-receiver-heat transfer sub-systems of the type described have been built for very little cost (approximately U.S. $3 500) and have been tested. In production quantities, these radiation receiver-loop sub-systems could be obtained for approximately $1 500 and should be good for five years of useful life. Thus, their prorated installed cost would be of the order of 0.23 cents/kWh.

The cost to affect high temperature thermal storage is difficult to assess without some detailed knowledge of the load profile dictated by consumer

Table 2. Estimated prorated operating cost of a 15-kW terrestrial solar power plant
(U.S. cents/kWh)

Component/Sub-system	*No energy storage capability*	*1200 kWh of energy storage*	*2400 kWh of energy storage*
Solar concentrator sub-system	4.4	4.4	4.4
Tracking rig	5.7	5.7	5.7
Turbo machinery	1.9	1.9	1.9
Alternator-gearbox	0.34	0.34	0.34
Controls (seeker, temp., and speed)	0.22	0.30	0.30
Radiator (-condenser)	0.1	0.1	0.1
Heat receiver loop	0.23	0.23	0.23
Thermal storage - boiler unit	—	0.0094(*a*)	0.017 (*b*)
TOTAL COSTS	12.89	13.83	14.59

NOTE: Heat storage material costs based on a latent heat of fusion value of 1075 Btu/lb for lithium hydride.
(*a*) Based upon 2 031 pounds of LiH used and 5-year life for the heat storage-boiler unit.
(*b*) Based upon 4 062 pounds of LiH used and 5-year life for the heat storage-boiler unit.

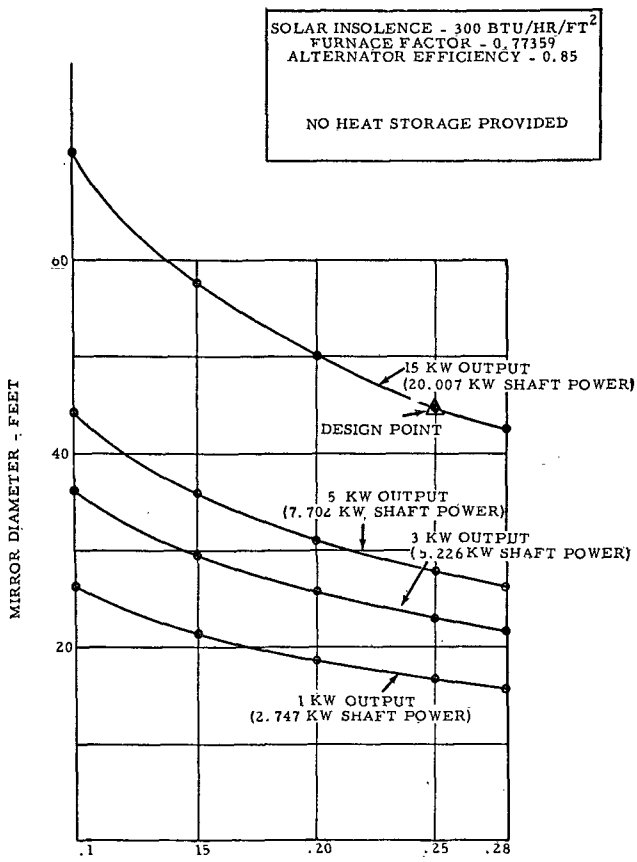


Figure 25. Cycle efficiency (η_{cy}) mirror diameter *vs* cycle efficiency

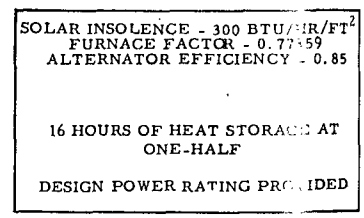
living patterns. In other words, the amount of thermal energy to be stored at high temperature for later use at night-time or during low quality sunlight periods will be closely tied to the high and low periods of power requirements associated with a given community. Optimization studies may well show that the lowest system cost could be achieved by a split between thermal energy storage and electrical energy storage. Such an anlysis is beyond the scope of this paper.

To give some feeling for final prorate dinstalled costs of a 15-kW terrestrial solar power plant designed around the technology available from a space system, table 1 has been prepared, which summarizes cost estimates in cents/kWh, for a solar plant with (*a*) no energy storage capability, (*b*) 15 kW output in daylight periods and 7.5 kW output from stored thermal energy during night-time operation, and (*c*) 15 kW output in both daylight and night-time periods. For cases (*b*) and (*c*) two assumptions were made, namely, that thermal energy was stored at a fairly high temperature (1 250°F) by using lithium hydride as the storage material, and that, within the next few years, the price of LiH would be approximately U.S. $1/lb in large-quantity orders (today the price of LiH in small pound lots is about $10/lb).

Conclusion

As can be seen from table 2, the prorated installed cost estimates of terrestrial solar power plants are rather high by comparison to conventional-fueled or nuclear-fueled control station power plant costs (3-10 mills/kWh), and these cost figures do not include nominal amortization charges, land, building, etc. Until prototype terrestrial plants of the type discussed in this paper are built and tested to gain operational and cost experience, there is no way, at this time, to affect great reductions in the cost picture presented herein.

If the cost figures presented are reasonable, the terrestrial solar power systems discussed will have to be considered for use in those parts of the world where more conventional fuel resources are either unavailable for power generation or where the remoteness of the region is such that other forms of power production present logistic problems either too costly or too inconvenient to be overcome. Certainly, the ease of packaging a solar power plant for shipment to practically any part of the world (where adequate sunlight is available for conversion into useful power) is an attractive feature for such systems. Furthermore, the ability of the solar power



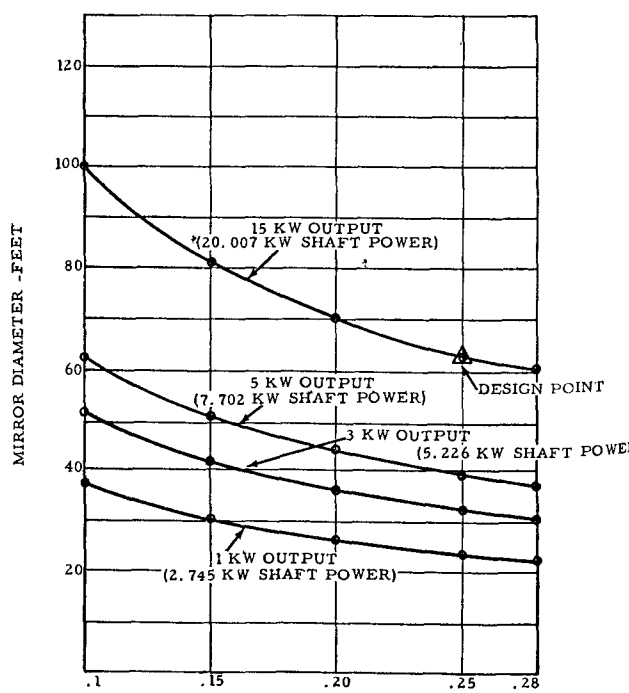


Figure 26. Cycle efficiency (η_{cy}) mirror diameter *vs* cycle efficiency

plant to be essentially a self-contained system lends it to being, relatively speaking, quick to assemble for operation and, if designed along the same operational lines as the space power system discussed earlier, would be simple to operate or maintain over long periods of time.

The ability of industry to bring the operational costs of terrestrial solar power lower than presently estimated will not only depend upon the advances made in the state-of-the-art technology via the numerous space solar power plant programs, but also very much upon the market potential for such systems. Clearly then, an extensive world-wide survey is needed to develop a market picture relative to terrestrial solar power plants so that developers of these systems can more fully exploit the advances being made in solar technology as it is developed by the current space power programs.

Acknowledgement

The writer gratefully acknowledges the assistance of Messrs. R. Weakley, H. D. Linhardt, G. Chesnut and R. Anderson in obtaining the data used in this paper.

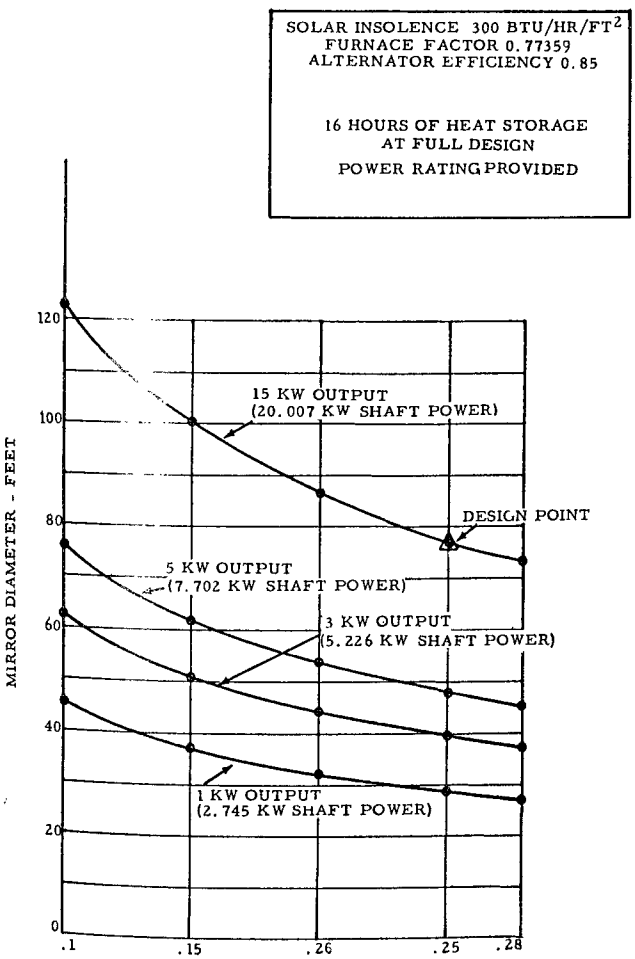


Figure 27. Cycle efficiency (η_{cy}) mirror diameter *vs* cycle efficiency

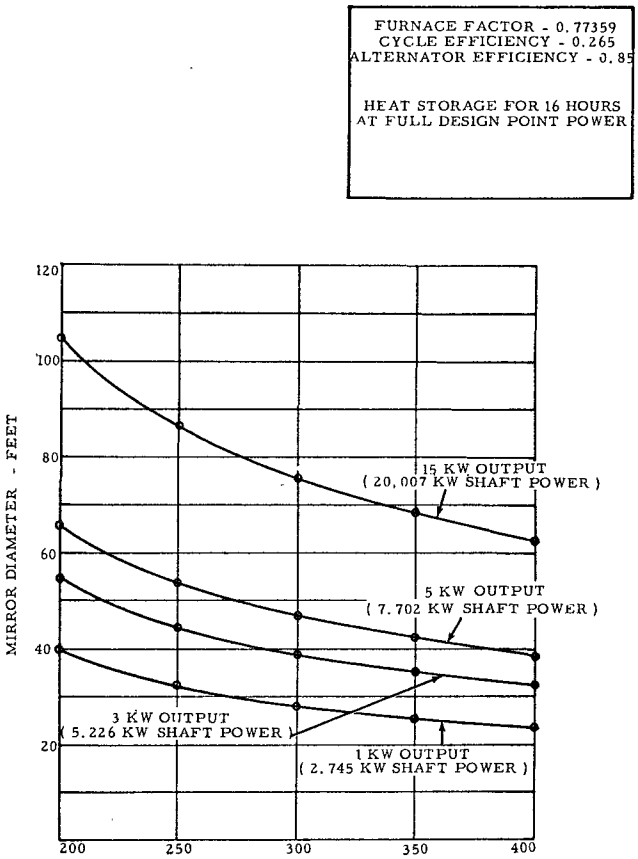


Figure 28. Direct solar insolence — Btu/hr/ft² mirror efficiency *vs* direct solar insolence (η_{cy})

Appendix

In order to assess the operational costs of a terrestrial solar dynamic power generation system which is based upon the developed (or soon to be developed) state-of-the-art technology of space-type solar dynamic engines, a study was made of the size required for mirrors, tracking rigs, heat storage-boiler units, etc., under varying conditions of solar insolence and system cycle efficiency. Figures 25-28 show the typical plots developed from IBM computer analysis upon which component sizing and eventually cost estimates were based.

The general design parameters finally chosen as a basis of evaluating the most probable component design trends and hence operational costs were as follows:

(*a*)	Cycle efficiency (including turbine stage efficiencies)	0.252
(*b*)	Turbine (and pump for Rankine systems) speed	24 000 rpm
(*c*)	Generator efficiency	0.85
(*d*)	Mechanical losses (bearings, pump, etc.)	1.50 kW
(*e*)	Power required for tracker drive, controls, instrumentation, etc.	0.725 kW
(*f*)	Direct solar insolence (taken as representing good sun climates, e.g., the south-western United States)	300 Btu/h/ft²

References

1. Macauley, B. T., Development of a high-powered solar mechanical engine. ASME paper presented at the ASME Aviation Conference, 12-15 March 1961, Los Angeles, California.
2. Macauley, B. T., Integrated low thrust solar propulsion-power generation system for communication satellites. SAE paper presented at the 1961 SAE National Aeronautical meeting, April 1961.
3. Linhardt, H. D., Research on Turbomachinery. (Unpublished.)
4. Acosta, A. J. and Linhardt, H. D., Note on the Application of Cascade Theory to Design Axial Flow Pumps. (ONR memorandum, unpublished.)
5. Silvern, D. H. and Linhardt, H. D., Analysis of Partial Admission Axial Impulse Turbines. ARS paper presented at the ARS semi-annual meeting, Los Angeles, California, 9-12 May 1960.

Summary

Much effort is presently being expended on the development of solar thermal-mechanical conversion systems designed to produce electrical power for space vehicle applications. Although these costly research and development programs are still in their early phases of progress, they are, nevertheless, attacking numerous difficult component and subsystem design problems whose successful solution will certainly assist those programs aimed at the practical use of solar energy for terrestrial mechanical power and electricity production.

The most obvious early economic contribution to terrestrial solar power generation applications which these ambitious space solar power system programs can make will be in the direction of advancing the state-of-the-art of solar technology along many broad lines of investigation. Much in the same manner that government-sponsored work on high-temperature materials research, advance design concepts, extensive component testing and development, etc., in support of mobile or flyable nuclear reactors, has immeasurably aided the progress of commercial nuclear power application programs, so will the extensive amount of investigations into developing highly accurate solar concentrators, highly efficient and reliable power conversion and generation components, new working fluids, new materials and fabrication techniques, etc., significantly bring closer the day when terrestrial solar power generation systems will be available in economic form.

To illustrate the design, development and economic relationships between solar mechanical engines for space application and solar power generation systems for terrestrial uses, a specific research and development program, involving the design study of the largest known solar mechanical engine for use on space vehicles, has been chosen for discussion. The program to be described, called the 15-kW Solar Mechanical Engine Program, is an applied research and development effort aimed at providing for the growth and advancement in the state-of-the-art technology of dynamic solar conversion systems using high-temperature working fluid and operating at relatively high power levels. Sundstrand Aviation—Denver, Division of the Sundstrand Corporation, is conducting for the government a research and development program aimed at the eventual production of a flyable, long duration solar thermal-mechanical power conversion system for use in space applications.

The specific objectives of the 15-kW Solar Mechanical Engine Program are to reveal and solve the critical component problems associated with advanced solar mechanical power concepts. In order to meet these objectives, since the development of a specific system is not yet called for, general preliminary design specifications of a dynamic solar conversion system were created by the government in order to permit an optimum system design to be established, hardware to be assembled for test and research experiments to be defined and performed.

The major, general preliminary system design specifications are as follows:

(*a*) Payload power: 15 kW of continuous electrical power at 3 200 cps, 120/208 volts, 3Φ;

(*b*) System weight (max.): 1 000 lb (66.6 lb/kW);

(*c*) Operating life cycle: One year continuous operation during an orbit period having 60 minutes of sunlight and 40 minutes of shadow time;

(*d*) Launch and environmental conditions: Maximum launch acceleration of 10 g along the longitudinal axis of the vehicle, 2 g along the lateral axis; zero gravity, vacuum, temperature, meteorite bombardment, cosmic radiation, and Van Allen radiation as found at operational orbital altitudes.

To meet the above objectives, a system design was established which has the following general component or sub-system features:

(*a*) Solar concentrator: 44.5-foot diameter paraboloid concentrator fabricated from plyable materials. The concentrator is inflated to shape and subsequently foam rigidized to hold its contour;

(*b*) Solar boiler-heat storage unit: a double cavity type boiler is used which has both rubidium boiling, superheat and reheat passages and provision for LiH heat storage material for low temperature (1 257°F) energy storage and NaF for high temperature (1 875°F) energy storage;

(*c*) Cycle and working fluid: a Rankine cycle with rubidium as the working fluid has been selected;

(*d*) Power conversion unit: A three-stage turbine rotating at 24 000 rpm which drives a homopolar inductor-type alternator. All rotating parts are integrated with liquid metal lubricated bearings, and all sub-assemblies are mounted on a single rotating shaft. No gears or seals are required.

(*e*) Radiator-condenser: A disc-shaped radiator-condenser has been chosen. This unit will be made of beryllium and, under zero-g conditions, will condense the Rb vapor, which discharges from the last turbine stage.

The component sizes, efficiencies and weights, as presently developed during the design phase of the 15-kW Solar Mechanical Engine Program, are summarized in table 1.

Using the general state-of-the-art currently developed, or soon to be achieved, by the 15-kW Solar Mechanical Engine Program which has been established to serve space-vehicle power needs, a study of the most probable cost of converting space solar engine technology into terrestrial solar engine applications was made. Table 2 lists a summary of the economic analysis performed for a 15-kW terrestrial solar power plant wherein (*a*) no provision for heat storage was made, (*b*) provision was made for 15 kW electrical output for an eight-hour period and 7.5 kW electrical output for a sixteen-hour period, by the use of high-temperature heat-storage materials, and (*c*) continuous operation over a twenty-four-hour period at a rated electrical output of 15 kW was provided through the use of a high-temperature heat-storage material (LiH).

MISE AU POINT D'UN MOTEUR HÉLIOMÉCANIQUE DE 15 KW (MESURES EN ÉLECTRICITÉ) DESTINÉ AUX APPLICATIONS INTERPLANÉTAIRES. SES RAPPORTS AVEC LA CONSTRUCTION DE MOTEURS ANALOGUES DESTINÉS A DES APPLICATIONS TERRESTRES

Résumé

On consacre actuellement des efforts considérables à la mise au point de systèmes de conversion thermo-mécanique de l'énergie solaire, destinés à subvenir aux besoins en électricité des véhicules interplanétaires de l'avenir. Bien que ces programmes onéreux de recherches et de mise en œuvre de dispositifs inédits en soient encore aux premières phases de leur développement, il n'en reste pas moins vrai qu'ils s'attaquent à la résolution de nombre de problèmes ardus ayant trait à la conception de certains des éléments et des groupes d'éléments constitutifs de ces dispositifs. Leur succès ne saurait manquer d'apporter une aide appréciable aux programmes qui s'efforcent de donner des applications terrestres pratiques à l'énergie solaire pour la production d'énergie mécanique et électrique.

L'apport économique presque immédiat le plus évident de ces programmes visant à la réalisation de systèmes de production de force motrice alimentés par l'énergie solaire en plein espace interplanétaire peut faire orienter la technologie solaire actuelle vers plusieurs domaines de recherches générales. Les travaux financés par le gouvernement sur le plan des recherches relatives au comportement des matériaux aux températures élevées, des conceptions ultra modernes, des essais et de la mise au point de divers groupes destinés à être utilisés dans des réacteurs nucléaires mobiles ou susceptibles d'être installés à bord d'un engin, ont joué un rôle dont on ne saurait trop souligner l'importance quant à la réalisation des programmes visant à l'application commerciale de l'énergie nucléaire. C'est d'une manière entièrement analogue que les nombreuses recherches menées sur la mise au point de concentrateurs d'énergie solaire éminemment précis, les groupes à très haut rendement et d'un fonctionnement sûr pour la conversion et la production de force motrice, les nouveaux fluides de travail, les matériaux inédits et les techniques de fabrication originales rapprocheront beaucoup le jour où les systèmes terrestres de production de force motrice, à partir de l'énergie solaire, seront disponibles dans des conditions économiques acceptables.

Pour illustrer la conception et la mise au point des moteurs héliomécaniques destinés à des applications interplanétaires et celles des systèmes terrestres de production de force motrice actionnés par l'énergie solaire, ainsi que leurs rapports économiques, on a choisi, aux fins de démonstration, un programme particulier de ce genre (recherches et mises au point) qui comporte les études préliminaires à la réalisation du plus puissant moteur héliomécanique connu, destiné à être utilisé à bord de véhicules interplanétaires. Le programme qui sera décrit, appelé programme du moteur héliomécanique de 15 kW, est constitué par des travaux de recherches et de science appliquée, visant à assurer le développement et le perfectionnement de la technologie des systèmes dynamiques de conversion de l'énergie solaire qui utilisent un fluide de travail à haute température et fonctionnent à des niveaux de puissance relativement élevés. La Sundstrand Aviation, Division de Denver de la Sundstrand Corporation, exécute actuellement pour le gouvernement un programme de ce genre, dont l'objectif est, en fin de compte, la production d'un système de conversion thermo-mécanique de l'énergie solaire à longue durée de fonctionnement capable d'être installé à bord d'un engin et destiné à recevoir des applications interplanétaires.

Les objectifs spécifiques du programme de mise au point d'un moteur héliomécanique de 15 kW s'attachent à mettre en lumière et à résoudre les problèmes critiques qui se posent dans la réalisation des pièces et des groupes des dispositifs destinés à la mise en œuvre pratique des points de vue les plus modernes sur les machines héliomécaniques. Pour réaliser de tels objectifs, dans la mesure où le moment n'est pas encore venu de mettre un système donné au point, le gouvernement a présenté les cahiers des charges préliminaires applicables à un système dynamique de conversion de l'énergie solaire, pour permettre l'établissement d'une conception optimale et de procéder au montage des pièces et groupes nécessaires aux fins des essais et expériences de recherches à décrire et à exécuter.

Les spécifications préliminaires principales sont les suivantes :

a) Puissance à fournir, dans les limites imposées par la charge payante : 15 kW d'énergie électrique en marche continue à 3 200 pps, sous 120/208 v. en triphasé;

b) Poids du système (maximum) 1 000 livres (66,6 livres par kW);

c) Cycle pendant la durée de fonctionnement utile : un an de fonctionnement continu sur une période qui, le long de l'orbite, comporte 60 minutes au soleil et 40 à l'ombre;

d) Conditions au lancement et caractéristiques du milieu : accélération maximum au lancement, 10 g suivant l'axe longitudinal du véhicule et 2 g suivant son axe transversal; annulation de la pesanteur; degré de vide, température, bombardement par météorites, radiations cosmiques et de Van Allen tels qu'on les rencontre aux altitudes prévues pour l'orbite.

Pour remplir les objectifs énumérés ci-dessus, il a été mis au point une formule, pour le système, qui se caractérise par les points généraux suivants quant aux éléments constitutifs et aux groupes :

a) Concentrateur d'énergie solaire : groupe paraboloïde de 44,5 pieds de diamètre fabriqué avec des matériaux souples. Il se gonfle pour prendre la forme voulue puis est rendu rigide par une mousse appropriée de manière à maintenir sa forme;

b) Bouilleur solaire — Accumulateur : on fera usage d'un bouilleur à double cavité doté de passages pour l'ébullition du rubidium, sa surchauffe et son réchauffage, avec les moyens de faire usage d'un matériau accumulateur de chaleur à l'hydrure de lithium pour les températures relativement basses (1 257 °F) et au fluorure de sodium pour l'accumulation d'énergie aux températures élevées (1 875 °F);

c) Cycle, fluide de travail : on a choisi le cycle de Rankine et le rubidium comme fluide de travail;

d) Groupe de conversion de l'énergie : une turbine à trois étages tournant à 24 000 t/m entraîne un alternateur du type à inducteurs homopolaires. Toutes les pièces tournantes sont reliées à des paliers lubrifiés au métal liquide de manière à faire bloc avec eux. Tous les sous-groupes sont montés sur un seul arbre tournant. Pas de roues dentées ou de joints d'étanchéité;

e) Radiateur-condenseur : on a choisi un radiateur-condenseur en forme de disque. Ce groupe sera en béryllium et, dans des conditions où la pesanteur est nulle, il assurera la condensation de la vapeur de rubidium s'échappant du dernier étage de la turbine.

Le tableau 1 donne un résumé des cotes des pièces et groupes, des rendements envisagés et de la recette des poids, tels qu'ils ont été arrêtés pendant la phase de mise au point des plans dans le cadre du programme d'exécution du projet de moteur héliomécanique de 15 kW.

Dans l'état de la technologie tel qu'il se présente actuellement ou tel qu'il sera avant peu pour les fins de ce projet, établi pour faire face aux besoins énergétiques d'un véhicule interplanétaire, on a procédé à une étude des frais les plus probables de conversion de la technologie applicable au moteur ainsi conçu aux besoins des applications à des moteurs solaires terrestres. Le tableau 2 représente un résumé de l'analyse économique ainsi faite pour une centrale de 15 kW à énergie solaire installée à terre dans laquelle : a) il n'est pas prévu de dispositif d'emmagasinage de la chaleur; b) on envisage un débit d'énergie électrique de 15 kW pour une période de huit heures et de 7,5 kW pour seize heures, en se servant de matériaux d'accumulation de l'énergie à haute température; c) le fonctionnement continu sur une période de 24 heures au débit électrique nominal de 15 kW a été assuré par l'emploi d'un matériau d'accumulation de la chaleur à haute température (LiH).

LARGE-AREA SOLAR COLLECTORS (SOLAR PONDS) FOR POWER PRODUCTION

*H. Tabor**

A very short description of the solar pond project was given in May 1959 (1) when the experiments were just commencing. A further account was presented at the Rehovot Conference on "Science for the Advancement of New States" in August 1960.

The present paper is an amplification of the latter account and provides a more detailed picture of the problems involved, and the economic prospects.

Background

The classical problem. "Intensive" collectors

The possibility of building large central solar power stations, in the megawatt class, using solar collectors of conventional type, seems very remote.

Four examples will illustrate the extreme difficulty in trying to produce power from solar energy at the world price of less than 1 US cent per kWh, not to mention the formidable maintenance problems.

Consider a heliostatically mounted paraboloidal mirror collector, the most efficient type known. If we assume a collector efficiency of 70 per cent, a turbogenerator efficiency of 35 per cent, and a sunny climate (3 000 kWh per sq m per year), the annual yield will be 735 kWh per sq m. For power at 0.6-0.8 cents per kWh, the fuel contribution is about 0.3 cents. This makes the annual value of the collector as a fuel saver about \$2.2 per sq m or say \$2, allowing 20 cents a year for maintenance. Taking capital charges as 13.6 per cent (6 per cent interest and ten-year sinking fund) the collector plus accessories (but without power plant) must cost less than \$15 per sq m, which is almost one order of magnitude less than the present cost of a fully automatic heliostatic paraboloidal collector of reasonable size.

For the second example we consider a simpler collector, such as a very good flat plate collector or a simple stationary cylindrical parabolic mirror type, working at a moderate temperature in the region of 150°C. Under optimum conditions, the over-all conversion efficiency will be at best 8 per cent, i.e., a third of that in the first example, and the sunshine "seen" will be only about $\frac{2}{3}$ of that for a heliostatic collector. Thus the collector system must cost less than $\frac{2}{9}$ of the cost in the first example, i.e., less than \$3.3 per m². This is about $\frac{1}{6}$ of the lowest cost, \$20/m², so far considered feasible for this type of collector.

Baum has presented the only detailed scheme for a large solar power installation (2). He has described a station to produce 11-13 tons of steam an hour or 20 000 tons per year at 400°C capable of producing 1 200 kW with a back pressure turbine or 2 200 kW with a condensing turbine, using 1 293 mirrors 15 sq m mounted on carriages rotating about a central boiler. At the Mont Louis symposium (1958) Baum gave the estimated cost as 18 000 000 rubles, i.e., about \$4 500 000. This makes a cost of over \$2 000 per kW installed, for the condensing unit, and the load factor is only 26 per cent.[1] The cost of the collector system is seen to be over \$200 per sq m. Taking annual charges on capital as 10 per cent, the cost per kWh produced is 9 cents excluding running costs.

A final example is the photoelectric solar cell. Assuming a conversion efficiency of 10 per cent and 2 400 kWh of sunshine per year per sq m and some new and cheap system of electrical energy storage and allowing some costs for the electrical equipment, the annual worth of the collector, for power at 0.6-0.8 cents per kWh, will be about \$1.2-1.5 per sq m. With capital charges at 7.8 per cent (25 years, 6 per cent) the permitted investment is about \$20 per m². Present-day costs are about 200 times this figure.

The above examples have been given to accentuate the extreme difficulty in getting cheap (competitive) electric power on a large scale using conventional solar collector systems. If this goal is ever to be achieved, the collectors must be at least an order of magnitude cheaper than any known present-day collectors and the maintenance cost of vast collector areas must be virtually zero.

The "extensive" approach

Claude (3) and his French colleagues recognised the ocean as the cheapest form of solar collector. Temperature differences between surface and deep waters of 20°C were noted (4). Whilst such temperatures are adequate to operate special turbines built for the purpose, the amount of energy consumed by the auxiliaries is very large. To improve the situation, French scientists suggested running the surface waters into shallow black-bottomed pans where the water would be further heated by the sun. A rise of only a few degrees was obtained even when

* National Physical Laboratory of Israel.

[1] Assumes 250 kWh produced per ton of steam : 5 000 000 kWh per year.

a heavy oil (mazoute) was used on the surface to reduce losses by evaporation (5).

The reason for the small rise in temperature in the pans is that the heated water at the bottom rises to the top by convection and the heat is quite rapidly dissipated to the surroundings.

In 1948, Rudolph Bloch suggested that an effective solar collector could be created by avoiding convection in a stratified salt solution, i.e., by creating a density gradient in a pond, as it had been observed (6) that in a certain saline lake in Hungary an increase in temperature with depth occurred (together with an increase in density) opposite to what is observed in the oceans. Because *stationary* water is a good insulator, a non-convecting black-bottomed pond should act as an efficient solar trap.

It was not until 1958 that this laboratory had the funds to inaugurate a research project on this idea. The initial experiments were not successful — our understanding of the problems was too naïve — but subsequent field experiments gave temperatures exceeding 90°C. This led to a much closer study of the physics of the problem and the possible economic viability.

Basic problems of the solar pond[2]

(*a*) Some of the major problems are as follows:

1. How much of the solar energy reaches the bottom and what happens to energy absorbed on the way down to the bottom.

2. How, and with what time variations, does energy enter the ground under the pond. To what extent does the ground provide heat storage in addition to the storage provided by the water.

3. What are the conditions for stability (i.e., no convection) in the pond.

4. What is the rate of diffusion of salt from the bottom (high concentration) to the top (low concentration) of the pond and what measures are to be taken to maintain a density gradient once achieved. How is the gradient achieved initially.

5. How is the heat to be extracted from the bottom of the pond without causing convection which would destroy the stability of the pond.

6. What is the effect of wind-induced waves on the surface of the pond. Will this cause "mixing".

7. What is the effect of evaporation from the surface. Can this cause local density gradients which might cause mixing.

8. What is the effect of dirt and dust falling into the pond. What measures are needed to keep the pond clean.

9. What are the optimum operating conditions for the pond as a source of heat or for producing mechanical power, i.e., temperature of operating and time-table of heat extraction. What is the expected annual yield per unit area.

[2] Detailed mathematical analyses will not be given here but will be published elsewhere.

(*b*) Answers, as far as they are known to date, are as follows:

1. The salt solutions used to date (mainly magnesium chloride), if clean, behave very much like pure water as far as optical absorption is concerned. However, if they are slightly dirty or contain suspended matter, the transmissivity can be much lower. Treating the solution as water, we know that about half the solar spectrum (that part above about 0.7 microns), is absorbed in the first few cm, after which the absorption is very slight. The greater the depth the less energy will reach the bottom but the greater the insulating effect of the upper water upon the heated lower portions. The optimum depth depends very much upon the cleanliness and whether the pond is suitable for supplying heat or power. For power applications it is estimated that the optimum depth will be between 1 and 2 metres, but it will be some time before the exact optimum can be computed. The effect of the heat absorbed on the way down is to change the temperature gradient so that the pond behaves, as far as heat loss from the bottom is concerned, as if it were slightly deeper than its actual depth.

2. For a small pond, the heat losses from the boundaries are excessive. As the pond is made larger, the effect of the peripheral losses decreases and the heat loss from the bottom vanishes completely if the pond is given enough time to heat up (a year or more). H. Weinberger has shown that a small pond gives a lower ultimate temperature rise than an infinite pond by a factor approximately $\left(1 - \frac{2h}{d}\right)$ where h is the depth and d is the diameter. This means that, for a pond 1 m deep if it is more than 20 m diameter it will approach within 90 per cent of an infinite pond.

Figure 1 shows, by calculations, how the bottom of an infinite pond will warm up if started in the spring or in the autumn, assuming that the ground under the pond has a thermal diffusivity equal to that of water, the pond is 1 m deep and the solution has properties similar to water. (Clear sunshine conditions at 32° latitude). No heat is extracted and it is assumed that — by some means — the solution does not boil. The curves show the effect of annual variation of solar intensity superimposed on an exponential type "soaking" curve for the ground. Calculations now in progress show that the ground provides a considerable storage effect. It cannot provide a constant power output for the whole year (except by running so hot in the summer that a great deal of energy is wasted), but periods of no sunshine for many days will pass almost unnoticed. This "built-in" storage is one of the attractions of the solar pond.

3. When a homogeneous horizontal layer of fluid is heated from below, convection will occur if the Grasshof-Prandtl product exceeds about 2 000. For liquids, this means that even a temperature difference of a fraction of a degree will cause convection.

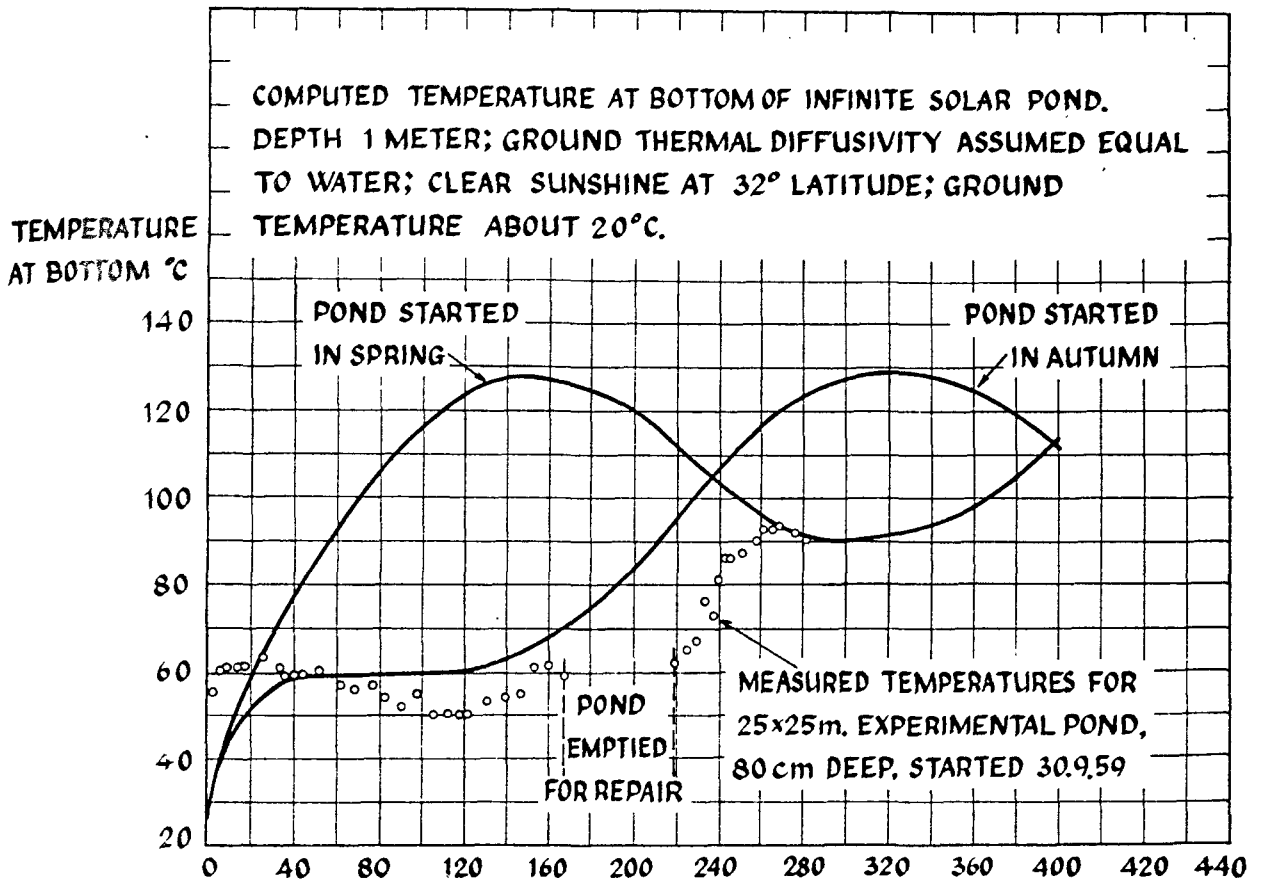


Figure 1. Days after completion of filling

If a density gradient dp/dh exists in the fluid before heating such that $\frac{dp}{dh} > 0$ (h measured from the top downwards) and after heating this gradient is not reversed at any time or place, no convection will occur. If the heating at the lower face of the layer is very rapid, then a high local temperature gradient is possible because of the low thermal diffusivity of stationary liquids and this temperature gradient causes a high change in local density gradient which can reverse the original gradient and cause convection. Thus the original density gradient required is a function not only of the depth and temperature differences expected but also of the rate of heat input at the bottom. If, as is shown later, a convecting or "mixing" zone exists at the bottom of the pond, rapid local changes of temperature are not possible and a lower dp/dh is adequate.

4. The rate of molecular salt diffusion is remarkably small and experimental ponds have been operated for months with no action being taken to correct for the diffusion. Thus for a magnesium chloride pond with a density of 1.0 at the top and 300 gm/litre $MgCl_2$ at the bottom (depth 1.3 m), with a temperature difference of 50°C and the concentration gradient such that the diffusion rate is the same at each level in the pond, the rate is about 50 gm per sq m per day. To maintain the gradient, a concentrated solution is injected into the bottom of the pond from time to time. The top of the pond is washed with fresh water or weak solution (sea water) with some overflow. Whatever the rate of overflow an equilibrium concentration will be created at the top such that the salt carried away in the overflow equals the salt diffusing upwards through the pond. Methods of setting up the density gradient initially are described in section 4.

5. The extraction of heat is one of the most interesting (and difficult) aspects of the solar pond. The obvious solution — to lay an array of pipes in the bottom through which a heat exchange fluid (probably water) is pumped — is not very practical for large ponds. (We are thinking in terms of ponds of 1 sq km.) Apart from the cost of the pipes and the pumping, it is an *a priori* condition for a heat exchanger that convection, either natural or forced, shall take place outside the pipes, yet convection is to be avoided in the pond. Thus, if there is no convection, the heat extraction will be very poor. If convection occurs, however, will it be limited to a layer at the bottom of the pond (and a little thicker than the diameter of the pipes) or will it gradually permeate the whole pond, thereby destroying the stability?

A more logical method is to "decant" a layer of liquid from the bottom of the pond, pass it over

an external heat exchanger and then return the liquid to the pond. Because of the density gradient it is, in fact, known that a layer can be removed without causing mixing of the pond, but the situation is complicated in the present application by the need to return the extracted fluid which will then be well mixed. This yields a pond with a density gradient in the upper portions and a homogeneous (convecting) zone at the bottom. There will be a tendency for this zone to grow in height, and the matter is now being studied with the help of glass tanks.

6. We have, at present, no answer to this question and both theoretical and experimental studies are in progress. That the effect of waves can be reduced to negligible proportions is almost certain, but if this means providing wind breaks at every few cm the cost and the loss in solar transmission may be prohibitive.

7. Evaporation at the surface can cause a local concentration of salt and possibly local reversal of the density gradient. (Upper layer mixing in an experimental pond was believed to be caused by evaporation.) If the pond surface is "washed" as indicated above it is thought that evaporation will not cause any difficulties.

8. The problem of keeping the pond clean is a serious one, though probably far simpler than trying to keep equally vast areas of glass or mirror clean. Dirt will be of four types :

(*a*) Particles that float on the surface. These may be blown to one side by the wind or possibly removed in the surface washing process.

(*b*) Particles that sink to the bottom. These cause no problem (if they sink fairly quickly) except that they may reduce the effective blackness of the bottom.

(*c*) Particles that remain suspended in the pond because of their small size or because their density corresponds to that of a certain level in the pond. This problem has not been solved and two approaches are being studied : a periodic horizontal "sweeping" of the pond with a vertical filter, and a slow movement of the entire pond involving passage through filters.

(*d*) Biological growth. It is believed that this can be adequately suppressed by chemical means.

9. Calculation of the optimum operating conditions is an extremely complex matter, as the number of variables is considerable : depth of pond, transparency, extraction temperature, thermal properties of the ground, latitude and solar insulation, timetable of energy extraction, etc. The possibilities of using an analogue computer (resistance-capacity simulator) are now being studied so that a high speed model of the pond can be set up.

Figure 2 shows a computation of the yield of the pond in terms of depth, transparency, temperature of extraction, based upon *mean* conditions, i.e., ignoring the cyclic variations of most of the variables and ignoring the slight benefit from heat absorbed in the upper portions of the pond. (The temperature rise of the pond above ambient is assumed to be the same as the temperature difference across the turbine; for each degree C that the former is greater than the latter there is a loss of output of 1-2 per cent of the output. As a first approximation we take a 20 per cent loss due to unavoidable temperature drops in the system.)

For pure water the mean transmission B will be slightly over 0.4 for the depths considered; a real pond will have a lower transmission. If we assume $B \sim 0.32$ then a pond 1 m deep has an optimum temperature rise of 50°C and the over-all conversion efficiency is $2\frac{1}{2}\ \% \times C$ where C is the factor by which a real turbine departs from a Carnot machine. For C 0.67 the over-all efficiency is 1.67 per cent or 1.33 per cent allowing for temperature losses. If the pond were increased in depth to 1.6 metres and the transmission dropped, say, to 0.3[2], then the over-all efficiency is 3.250 per cent, i.e., about 2.2 per cent or 1.76 per cent with temperature losses, with the optimum temperature rise of about 72°C. A deeper pond is more expensive to construct and maintain and this has to be taken into account in deciding the optimum depth.[3]

The example given in figure 2 is for the case of a mean solar insolation of 4,650 Kcals/m² per day, i.e., 1.97×10^9 kWh of heat per sq km per year.[4] If about $1\frac{1}{2}$ per cent of this is converted to electric power the annual yield is 30×10^6 kWh per sq km. (This is gross yield from which the power for auxiliaries has to be deducted.) For a 58 per cent annual load factor (i.e., 5 000 hours) the installed capacity is thus 6 000 kW per sq km.

Experimental results and techniques

The first experiments with solar ponds were conducted with sodium chloride solutions and the results were negative. It was subsequently shown mathematically that, due to the low solubility of common salt even at elevated temperatures, it is difficult to maintain stability for a pond with a bottom subject to variable heat fluxes. If a mixing zone exists at the bottom — which was not the case in the early experiments — stability is improved.

Subsequent experiments were conducted with magnesium chloride, carnalite or the end-brines from potash production at the Dead Sea (predominantly magnesium chloride). The end brines of any plant producing salt by solar evaporation could be used.

Outdoor experiments on small ponds — of the order of 1 × 1 m or 2 × 2 m — confirmed that no convection occurred despite the hotter fluid at the bottom. A check on the migration of salt from the

[3] The depths referred to here apply to the non-convecting layer. If there are mixing zones at the top or bottom of the pond, these call for a physically deeper pond which subtracts from rather than adds to the efficiency.

[4] Measured value for Jerusalem is about 10 per cent greater than this.

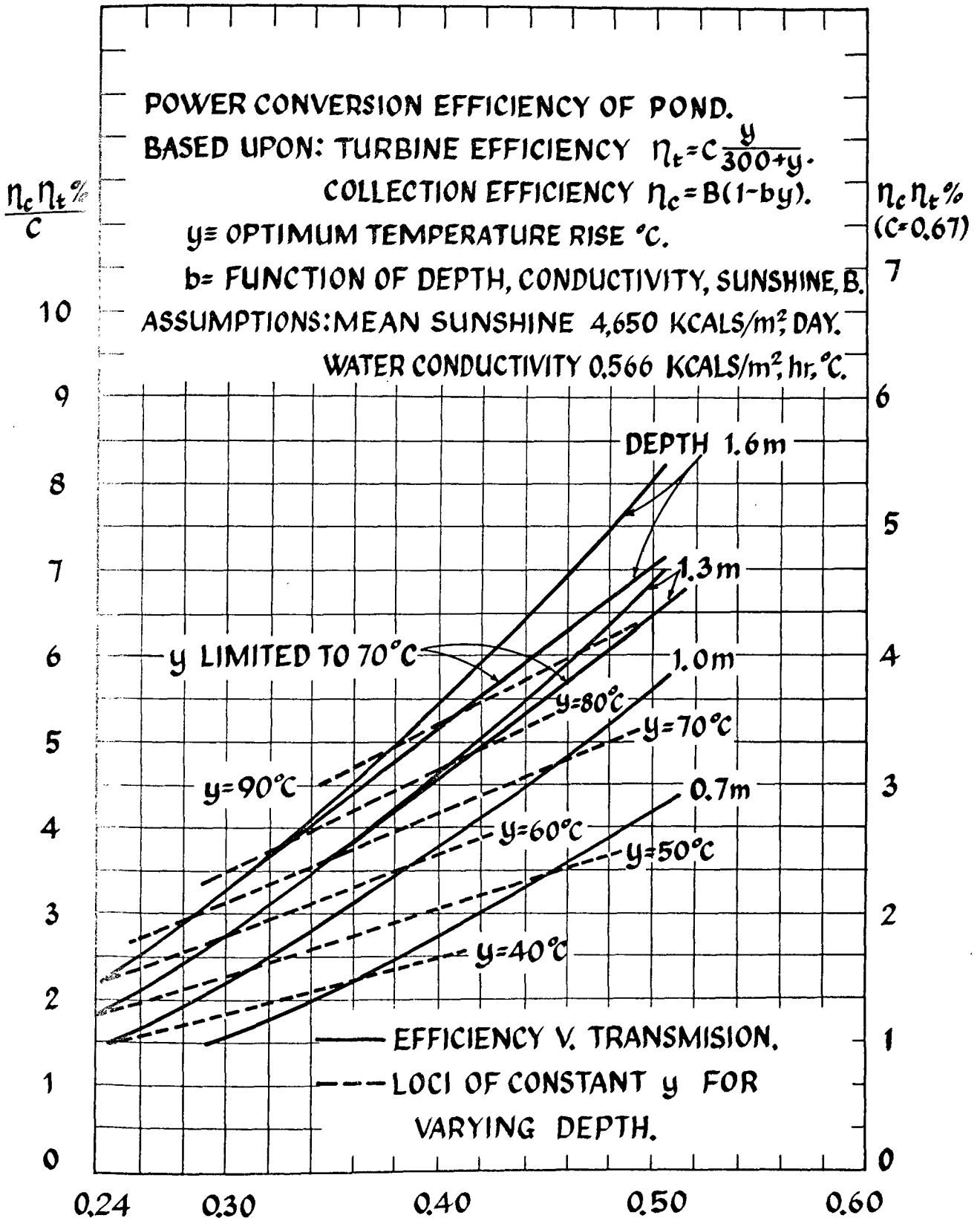


Figure 2. Mean transmission B

bottom to the top (by titrating the overflow) showed this to be fairly close to the computed value for molecular diffusion, i.e., no macromolecular motion could be occurring. The best temperature rise recorded was 35°C (from 25°C at the top to 60°C at the bottom). Small ponds have large edge losses even when some attempt is made to insulate the side walls. Furthermore, the incoming radiation is reduced due to the shadow of the walls at all but very high solar altitudes.

In September 1959, a 25 × 25-metre pond was put into commission. This was an old experimental evaporation pond at the Dead Sea Works Ltd. built some 25 years ago. The depth was 1 metre and was thus filled to only 80 cm. This pond was chosen because it existed and because, being at the Dead Sea, all the salt solutions needed were at hand. (As it turned out, it might have been better to have started with a new pond, but the cost would have been considerable.)

The pond was filled as follows : a mixing tank of 1 cu metre was mounted at the side of the pond so that water from a supply line and concentrated brine from another line could be mixed together before discharging into the pond. Flow meters in the lines indicated the amount of water and brine added. At four points in the pond, slightly in from the four corners, four wooden boards 1 m × 1 m were floated and held in position by cables which allowed them to rise and fall but to remain approximately in place. On the boards were 1" plastic tubes so arranged that solution coming out of the tube was dispersed horizontally over the board. The four tubes were connected together (in parallel formation) to the exit of the mixing tank. In this way the gradient could be built up, starting from the bottom with the highest concentration, and gradually reducing the concentration, the added solution floating on the heavier. The concentration was changed 8 times and the filling of 500 cu metres of solution was completed in 12 days. By the end of the filling, the steps in the density gradient had virtually vanished.

Because of technical difficulties, no washing of the surface was carried out, but about once a week water was added to make up for loss by evaporation. It was subsequently observed that the density gradient at the top of the pond was being lost at the rate of about 1 cm per week, i.e., a "mixing" or convecting zone appeared at the top. It was realised too late that failure to wash the surface was a serious error and it is possible that had this been done the upper layer mixing zone would not have appeared, or would have been much slower. It is believed that this zone is caused by evaporation or wind-induced waves, or a combination of both. Experiments are now planned to try to establish the share of each of these causes.

In April 1960, the walls of the pond sprang a leak and the pond was emptied for a few days whilst the walls were repaired and later refilled. The experiment was terminated in August 1960 when the upper zone mixing exceeded half the depth of the pond.

The temperature measured at the bottom of the pond is shown superimposed on figure 1 to show the similarity to the theoretical curve. That the temperature reached only 92°C is attributed to the reduced static depth of the pond and the fact that the solution became dirty owing to disintegration of the old wooden walls of the pond. A series of samples of solution taken from various depths at the end of the experiment showed that almost no sunshine was reaching the bottom.

Despite the faults and disappointments of this experiment, the results are very encouraging. That thermal stability with a bottom temperature of 92°C (which is about the temperature at which a full-size pond should be operated) and a surface temperature of 28-32°C can be obtained in practice, is inspiring.

Engineering aspects

It is too early to discuss the over-all engineering design of a solar pond used to create power. Points of study include:

(*a*) Surface condensers — which will provide fresh water as a by-product to the power (about 500 000 tons per sq km per year) — as an alternative to the cheaper jet condensers.

(*b*) Flash evaporation from the pond brines.

(*c*) Low-temperature turbines designed for variable input temperature.

The solar pond may be used to produce low temperature heat, i.e., below 100°C, for the chemical industry and other purposes. As seen in the next section, the pond should provide low-temperature calories at a price far below that obtained from fuel.

Economic perspectives

If a solar pond were a simple pond constructed on flat ground, with a suitable embankment, a free source of concentrated brine available, it is estimated that the cost, under local conditions, would be about $250 000 for a one sq km size, i.e. 25 cents per sq m, or two orders of magnitude lower than the cheapest present-day solar collectors. It may readily be shown that under these conditions the power produced would be the cheapest in the world and, if used as a source of low-temperature calories, the pond would pay for itself twice over in the first year [5] (after the initial heating-up period).

We know, of course, that a real solar pond will be more complicated than this because of the three major technological problems : the extraction of heat without disturbing the density gradient, the prevention of upper layer mixing due to waves and the maintenance of cleanliness in the pond.

[5] Because of heat losses, the useful energy extracted is only about half that reaching the bottom, at the operating temperature of 80-90°C. The collection efficiency is thus 15-20 per cent or the yield about 30 × 10^{10} Kcals per year per sq km. This is equivalent to 36 000 tons of fuel burnt at 85 per cent efficiency.

We do not know the measures that have to be taken, but clearly there is a very great incentive to find reasonable solutions to these problems. The following calculation indicates the orders of magnitude involved.

The production cost of power in the local fuel-fired station is approximately 1 cent per kWh. Of this, the fuel component is 48 per cent, the capital charges 32 per cent and the operating and maintenance costs 20 per cent. A comparison of the cost of the power generating equipment (for a 10 mW unit) shows that the solar plant will cost about the same as the fuel-fired plant. This is because whilst the solar plant has no boiler it has larger condensers and the low-temperature, low-pressure turbine will be physically larger than the fuel-fired unit. Not included are all the machinery, pumps, filters, etc. associated with the pond.

A 1 sq km pond operating at 1½ per cent over-all conversion efficiency will, under local conditions, produce 30 million kWh of electricity. At 1 cent per kWh the annual value is $300 000. Of this, 52 per cent is required to cover the capital charges and the operating costs of the station. This leaves $144 000 net value. A generous allowance for the cost of maintaining the pond and its machinery is $50 000 per year. The net value is reduced to $94 000. This is the return of the pond investment if the power cost is to be the same as that for a fuel-fired station.

If the pond is amortised over 20 years at 6 per cent interest and 6 per cent sinking fund the annual charges on capital are 8.72 per cent and the pond can cost up to $1 080 000.

This calculation shows that even if the pond and its associated equipment cost up to four times the cost of a "bare" pond, the cost of power produced will still be competitive with power produced from fuel. This is very encouraging. If fresh water is at a premium, the situation is even better. About 500 000 cu metres per year (125 million US gallons) of water are obtained for the difference in cost between surface condensers and jet condensers. This difference may be of the order of $80-100 000 extra investment or under $10 000 per year capital charges. If the water can be sold for more than 2 cents per ton (8 cents per 1 000 US gallons) this provides an additional source of income. At 40 cents per 1 000 US gallons, the lowest price at present considered possible for desalinated water, the net annual value of the pond is raised from $94 000 to $134 000.

If the solar station is situated in an area where fuel is expensive, the competitive cost of power is greater than 1 cent.

Production cost of power (cents) . . .	1	2	3
Permissible cost of pond of 1 sq km in millions of U.S. dollars	1.08	4.5	8.0

If the pond is used to provide low-grade heat, the net annual worth is $540 000, taking the cost of fuel at the site as $15 a ton.[6]

Conclusions

The solar pond holds out promise for being the cheapest known method of exploiting solar energy and is particularly suitable for large installations. It incorporates a considerable degree of built-in storage. A square km in a sunny climate should yield 30×10^6 kWh of power, equivalent to 6 000 kW installed and a 58 per cent load factor, or alternatively about 30×10^{10} Kcals of heat at temperatures around 80-90°C, equivalent to 36 000 tons of fuel burnt at 85 per cent efficiency. Three major problems require to be solved in a reasonable manner to make the solar pond practical and economic. These are: the extraction of heat from the bottom without disturbing the density gradient, the suppression of upper zone mixing due to the wind and methods for keeping the pond clean. An intense effort is being made to solve these problems.

Acknowledgements

More than a dozen staff scientists have contributed to our present knowledge on this subject. Special acknowledgement is made to the following:

R. M. Bloch, Director of Research, Dead Sea Works Ltd., who first proposed a stratified salt solution as a large-scale solar collector.

M. Goldstein, physical chemist, who was in charge of the project in its first year.

H. Weinberger, mathematical physicist who has made major contributions to the understanding of the physics of the problem.

A. Pinkus, chemical engineer, who overcame many practical problems in setting up the first experimental ponds.

[6] This is a low sea-board price. In under-developed areas it is not unusual to find the price delivered to the site to be $80-100 per ton.

References

1. Tabor, H., Solar Developments in Israel, *Solar Energy III*, No. 3, p. 9, Oct. 1959.
2. Baum, V. A., Aparasi, R. R. and Garf, B. A., High Power Solar Installations, *Solar Energy I*, No. 1, pp. 6-12, Jan. 1957.
3. Claude, Georges, Power from the Tropical Seas, *Mech. Eng. 52*: 1039-44, Dec. 1930.
4. Beau, C., Nizery, M., Industrial Utilisation of the Differences of Temperature between the deep and surface waters of the Seas, *Trans. 4th World Power Conference*. London. Lund Humphries Section K, Paper 3, pp. 2494-5, 1950.
5. Masson, Henri, Les Insolateurs à bas potentiel (étude théorique et expérimentale), *Trans. Conf. Use of Solar Energy — the Scientific Basis*, Tucson, vol. 3, p. 47-66, 1955.
6. Kalecsinski, V. A., Über die ungarischen wärmen und heissen Kochsalzseen als natürliche Wärmaccumulatoren, sowie über die Herstellung von Wärmen Salzseen und Wärmeaccumulatoren, *Ann. d. Physik (4)*, v. 7, pp. 408-416.

Summary

Four examples of classical "intensive" collectors (three thermal and one photoelectric) show that costs must be reduced by at least one order of magnitude in order to be able to produce power on a large scale at a competitive price of 1 U.S. cent per kWh at the bus-bars. Maintenance costs must also be reduced to a negligible figure.

This calls for collectors of a different type such as open bodies of water. As originally suggested by Claude, oceans can be used but the temperature differences available are small, and the use of black-bottomed solar heating pans to augment the temperature difference adds only a few degrees.

Stationary water is a good (and cheap) insulator, so that if convection can be suppressed a possibility for a large-area cheap solar collector exists.

The "solar pond" is an artificial black-bottomed pond or lake about 1-2 m deep in which convection is prevented by having a strong density gradient from the bottom to the top. The gradient is obtained by having a high concentration of suitable salts, such as magnesium chloride, at the bottom of the pond and a negligible concentration at the top. Molecular diffusion is extremely slow. Extra salt is added periodically at the bottom and the surface of the pond is washed to keep the top density low.

Small ponds have serious peripheral losses but in large ponds these are negligible, though it may take six months or more for the ground under the pond to soak up sufficient water to maintain the operating temperature.

The water, and particularly the ground under the pond, provides considerable built-in storage. Whilst the pond cannot store efficiently from summer to winter, normal interruptions of sunshine, even of many consecutive days, will scarcely affect the performance.

An experimental pond, 25 × 25 m, which reached temperatures of over 90°C at the bottom, is described. Because of infra-red absorption, less than half the incident solar energy can reach the bottom and, for power production purposes, the heat losses at the optimum operating temperature brings the collector efficiency down to 15-20 per cent. The optimum temperature rise (which depends on many factors) is 50-70°C and leads to a computed over-all conversion efficiency with a real turbine of about 1½ per cent. For a sunny climate with an annual incidence of 2 000 kWh per sq m a pond of 1 sq km should yield 30×10^6 kWh equivalent to 6 000 kW installed at 58 per cent load factor. If the pond can be built for about \$1 000 000,[7] the power produced will cost less than 1 cent per kWh. At a power cost of 2 cents, the pond may cost up to \$4 500 000. A limited amount of distilled water (about 500 000 tons per year per sq km) can be produced as a by-product for about 2 cents per ton, or the initial investment in the pond may be increased if the water is sold at more than 2 cents.

The physical problems associated with the pond are discussed. Three major scientific and technological problems have to be solved, and at a reasonable cost, before the solar pond becomes practical. These are: the extraction of heat without disturbing the density gradient, the prevention of mixing by wind-induced waves, and the maintenance of a clean pond. These are not easy matters, but the economic prospects are so attractive that an all-out effort is called for in seeking to solve them.

Because of the salt and flat land area requirements, the solar pond concept appears, at present, to be limited to areas that are, or could be, salt producing.

[7] If there were no technological problems as discussed later, the pond could be built at suitable site for about \$250 000. Interest charges are taken as 6 per cent and sinking fund calculated for 20 years.

COLLECTEURS SOLAIRES A GRANDE SURFACE (PISCINES SOLAIRES) POUR LA PRODUCTION D'ÉNERGIE

Résumé

Quatre exemples de collecteurs classiques « intensifs » (trois thermiques et un photo-électrique) permettent de démontrer qu'il faut réduire les prix d'un ordre de grandeur au moins pour pouvoir produire de grosses quantités d'énergie à des prix capables de faire concurrence à ceux des autres sources à raison de 1 cent de dollar E.U. par kWh aux barres omnibus. Les frais d'entretien doivent également être ramenés à un chiffre négligeable.

Ceci exige des collecteurs d'un type différent de celui qui est d'emploi courant, tels que des masses d'eau. Ainsi que Claude l'avait suggéré il y a longtemps, on peut utiliser les océans, mais les différences de températures qu'ils offrent sont faibles et l'utilisation de bassins de chauffage solaire à fond noirci pour augmenter la différence de température n'y ajoute que quelques degrés.

Les masses d'eaux stagnantes constituent un isolant satisfaisant et peu coûteux. Il est donc possible de disposer ainsi de collecteurs solaires de grande surface et à bon marché si l'on parvient à éliminer la convection.

La « piscine solaire » est une piscine artificielle ou un lac à fond noirci d'une profondeur d'un mètre ou deux, dans laquelle la convection est évitée par le moyen d'une forte variation de densité en allant du fond vers la surface. Cette variation se réalise en établissant une concentration élevée de sels appropriés, tels que le chlorure de magnésium, au fond de la piscine et une concentration négligeable près de la surface. La diffusion moléculaire est très lente : on ajoute périodiquement du sel au fond et on fait couler de l'eau en surface pour maintenir la faible densité superficielle.

Les petites piscines ont d'importantes pertes périphériques, mais ces mêmes pertes sont négligeables dans les grandes piscines; pourtant, il se peut que six mois ou plus s'écoulent avant que le sol situé au-dessous de la piscine soit porté à la température de fonctionnement.

L'eau — avec, plus particulièrement, le terrain qui est au-dessous de la piscine — constituent d'importants moyens naturels de mise d'énergie en réserve. Bien que la piscine ne puisse servir d'accumulateur de manière satisfaisante de l'été à l'hiver, les interruptions normales de l'ensoleillement — même pendant plusieurs jours consécutifs — ne se répercutent pour ainsi dire pas sur son rendement.

L'auteur décrit une piscine expérimentale de 25 × 25 m qui atteint des températures de plus de 90 °C près de son fond. En raison de l'absorption de l'infra-rouge, c'est moins de la moitié de l'énergie solaire incidente qui parvient jusqu'à ce fond de piscine et, pour les besoins de la production d'énergie, les pertes de chaleur à la température de fonctionnement optimale réduisent le rendement du collecteur à un chiffre compris entre 15 et 20 p. 100. La montée optimale de température (conditionnée par nombre d'éléments) est de 50 à 70 °C, donnant un rendement global de conversion, calculé au moyen d'une turbine réelle, d'environ 1½ p. 100. Pour un climat ensoleillé ayant une incidence annuelle de 2 000 kWh/m², une piscine de 1 km² doit donner 30 × 10^6 kWh correspondant à 6 000 kW installés avec un facteur de charge de 58 p. 100. Si on peut construire la piscine pour environ 1 000 000 de dollars [8], l'énergie produite coûtera moins d'un cent par kWh. Si on porte le prix de l'énergie à 2 cents, la piscine peut coûter jusqu'à 4 500 000 dollars. Une quantité limitée d'eau distillée (environ 500 000 tonnes par an et par km²) peut être fournie comme sous-produit à raison d'environ 2 cents par tonne; ce qui veut dire que si l'eau peut être vendue à plus de 2 cents, il n'y a aucun inconvénient à augmenter les sommes investies au début.

L'auteur passe en revue les problèmes physiques relatifs à la piscine. On doit résoudre trois principaux problèmes scientifiques et technologiques, et ceci à un prix raisonnable avant que la piscine solaire devienne utilisable. Ce sont l'extraction de la chaleur sans nuire à la variation de la densité, le moyen d'éviter les mélanges dûs aux vagues provoquées par le vent, et le maintien de la propreté de la piscine. Ces questions ne sont pas simples, mais les perspectives économiques en sont si attrayantes qu'il faut tout mettre en œuvre pour tenter de les résoudre.

Compte tenu des exigences quant aux sels et à la surface plate de terrain nécessaire, le concept de la piscine solaire semble actuellement être limité à des régions qui produisent, ou pourraient produire du sel.

[8] En l'absence de problèmes technologiques tels que ceux qui seront passés en revue plus bas, on pourrait construire la piscine, en un lieu approprié, pour environ 250 000 dollars. On calcule les intérêts à 6 p. 100 et le fond d'amortissement comme devant se répartir sur vingt ans.

SMALL TURBINE FOR SOLAR ENERGY POWER PACKAGE

*H. Tabor and L. Bronicki**

Part 1. The turbine

Basis of present research and development programme

The history of solar energy utilisation research and development work has shown that a most interesting and attractive goal is the small solar power package of a few horsepower capacity. Whilst large solar power stations are not attractive because of the very large collector areas involved, small units could have wide applicability if they were efficient.

Over the years many attempts have been made to build solar power plants in small sizes, from a fraction of a horsepower to a maximum of one hundred horsepower. In all cases of practical importance the prime-mover has been a reciprocating engine operated either from steam or from some lower boiling-point fluid. The use of engines rather than turbines stemmed from the recognition that turbines are generally considered superior to engines only in larger sizes (i.e., from 500 hp upwards).

For reasons enumerated below it was thought that, for the specific case of solar operated prime-movers where only very moderate boiler temperatures are available, a turbine might be more suitable than a reciprocating engine.

Turbine versus engine

Dealing in the main with steam prime-movers, since this is the field in which most experience has been accumulated, the advantages of the turbine over the reciprocating engine are:

1. Low maintenance and high reliability.
2. Easy regulation.
3. No internal lubrication other than the main bearings.
4. Possibility of large expansion to the condenser pressure and temperature.
5. High efficiency in large sizes.

The major disadvantages are:

1. In small sizes the efficiency is very low if a single wheel type is used, as in the De Laval type.
2. Multiple wheel or re-entry types are more efficient than the De Laval type but are relatively expensive owing to the high precision required in small sizes.
3. Unless superheating is employed, there is the risk of too high a moisture content in the expanded vapour, resulting in blade erosion and low efficiency.

With the rather low temperatures likely to be obtained from solar collectors, the prime-mover will be of the condensing type. Under condensing conditions a reciprocating engine operating with low-pressure steam must be of very large dimensions, so that if the disadvantages of the small turbine could be overcome, this would be a further factor favouring the turbine. As will be shown, by using a carefully selected working fluid other than water, a small turbine can be made nearly as efficient as a large unit working under the same conditions.

Turbine characteristics

When steam, even at comparatively low temperature, is expanded through a single nozzle to a condenser at ambient temperature, the velocity of efflux is over 1 000 metres per second, which calls for a bucket speed of 500 metres per second in a single wheel. Such speeds are about two to three times the practical limit, so that all single wheel type condensing turbines work with a poor bucket velocity ratio, resulting in poor efficiency. The introduction of additional wheels overcomes this difficulty but results in high costs for small turbines. Furthermore, the disc friction of a small turbine can consume a considerable fraction of the total power.

However, as pointed out by D'Amelio,[1] when a "heavy" vapour is used in a turbine in place of steam, the velocity of efflux is reduced approximately as the square root of the molecular weight increases, so that a vapour some 5-10 times as heavy as steam would make possible a single wheel turbine with a proper bucket velocity ratio. Furthermore, because the enthalpy per kgm is less for the heavy vapours than for steam (approximately in inverse proportion to the molecular weight) more vapour must be passed through the turbine for the same power output. Whilst this would be disadvantageous in large turbines, it is a great advantage in small turbines since it allows the blades to be larger and would bring the nozzles nearer to full admission. The larger Reynold's numbers resulting from the

* National Physical Laboratory of Israel.

[1] L. D'Amelio. A steam engine using a mixture of vapours from non-miscible fluids as a solar engine with flat plate collectors. *Contribution to the Conference on Solar Energy—The Scientific Basis*. Tucson, Arizona, November 1955.

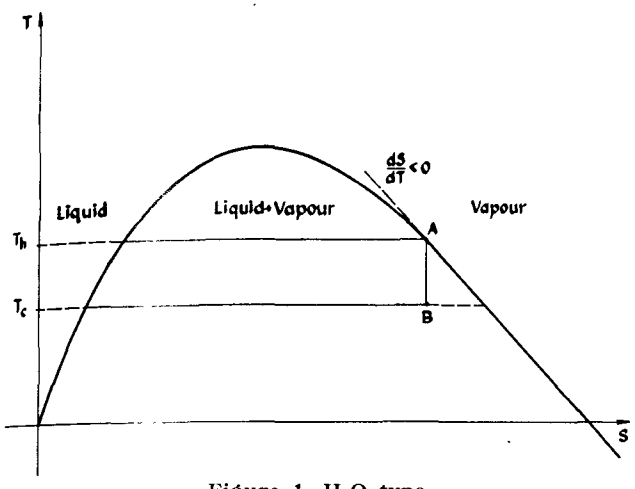


Figure 1. H_4O type

greater mass flow and large dimensions mean that nozzle and bucket efficiencies will be better than one might expect in a small turbine. The vapour may be chosen so that the pressure in the condenser results in a disc loss lower than that occurring with steam.

As regards the problem of excess moisture in the expanded vapour, it is interesting to note that many organic compounds [2] have a saturation curve (temperature-entropy) of positive slope (on the mixture-vapour side), whereas steam has a negative slope. As a consequence, isentropic expansion of saturated vapour results in slight superheating rather than in slight precipitation, so that the problem of liquid droplets eroding the bucket blades does not exist.

Scientific and engineering aspects [3]

The working fluid

1. *Molecular weight.* It may be shown that, to a first approximation, the velocity of efflux of a vapour after expansion in nozzles is inversely proportional to the square root of the molecular weight. This leads to the requirement that, for a single wheel turbine, the molecular weight should be over a hundred, preferably several hundred.

2. *Temperature entropy diagram.* The T-S diagram for water shows that the slope of the boundary between the liquid plus vapour phase and the pure vapour phase (which we shall call the vapour-mixture boundary) is negative, i.e.:

$$\frac{dS}{dT} < 0$$

This means that when saturated steam expands isentropically from point A to point B (figure 1) the steam becomes wet. If this wetness exceeds a certain amount it can cause erosion of the turbine blades.[4]

The T-S diagram for CCl_4 (figure 2) shows the vapour-mixture boundary almost vertical so that saturated vapour at A remains saturated (but not wet) after expansion to B.

The T-S diagram for many hydrocarbons—such as pentane, heptane, octane, shows a positive slope for the vapour-mixture boundary (figure 3). Thus when saturated vapour is expanded from the pressure corresponding to T_h (upper temperature) to the pressure corresponding to T_c (condenser temperature) the final condition of the vapour is superheated. This is good as far as the turbine blades are concerned, but bad for the cycle efficiency, for it can readily be demonstrated that the useful enthalpy drop is considerably less in figure 3 than in figure 2.

Consequently fluids were sought which had a nearly vertical vapour-mixture boundary. Yet as higher molecular weight fluids were examined, the $\frac{dS}{Td}$ slope seemed to get more positive, which was to be avoided.

A theoretical study by Dr. M. Goldstein then showed the very interesting fact that the slope of the vapour-mixture boundary is, to a first approximation, a function only of the number of atoms in the molecule, not of their weight or character, so that molecules with a small number of atoms would have T-S diagrams similar in shape to that of water (figure 1), whereas molecules with a large number of atoms would have a shape like that for C_8H_{18} (figure 3). A shape like figure 2 would call for a rather small number of atoms, say 5-10.

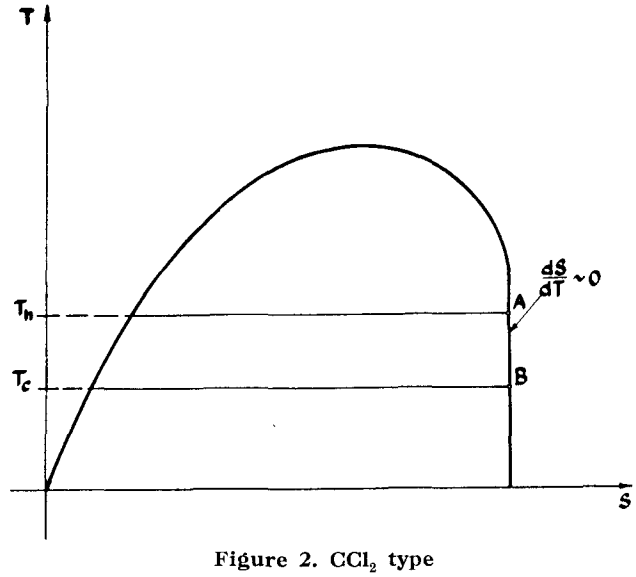


Figure 2. CCl_2 type

[2] Hexane, pentane, isobutane, etc.

[3] In view of the accent of this conference on practical matters this section is condensed and will be given in full elsewhere.

[4] In practical steam turbines the steam supply is always superheated and care is taken that point B represents not more than a small per cent of wetness. In solar installations, superheating presents serious difficulties and is usually impracticable.

A small number of atoms for a high molecular weight requires molecules with heavy atoms such as chlorine and bromine, and such fluids have been considered despite the possibilities of trouble due to decomposition and corrosion.

3. *Boiling point (bp).* The boiling point of the working fluid has a considerable influence on its performance in a turbine. The most important influence is the disc and blade friction of the wheel.

For a single wheel condensing impulse turbine, with all expansion taking place in the nozzles, the wheel rotates in an environment of vapour at condenser pressure, i.e., at approximately the vapour pressure of the working fluid at ambient temperatures.

It may be shown that the disc friction Nr will be given approximately by:

$$Nr = B \frac{P^{0.8}}{M^{1.5}\, n^{1.8}}$$

where B = a constant
P = condenser pressure in mm Hg
M = molecular weight
n = revolutions per minute

The disc friction can therefore be reduced by having a low vapour pressure, i.e., a high bp. However, there are limits to this because a very low vapour pressure means an abnormally large expansion ratio in the nozzles and, even more important, practical difficulties in maintaining the vacuum in the condenser. Where the molecular weight is high, a higher vapour pressure can be tolerated. Note that n cannot be increased indefinitely (by using a smaller disc diameter) because of increased bearing losses (proportional to n^3) and gear box troubles.

In the turbine we are considering, calculation gives the disc loss as 0.1 hp for monochlorobenzene (M = 112.5, bp = 132°C) and 0.22 hp for iso-octane (M = 114, bp = 100°C). For a 10 hp turbine these losses are small, but for a 1 hp unit they are large, in fact unacceptable in the case of the iso-octane,

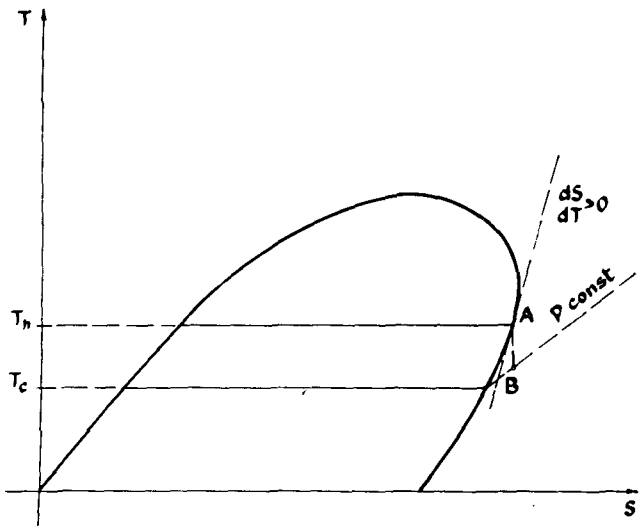


Figure 3. C_8H_{18} type

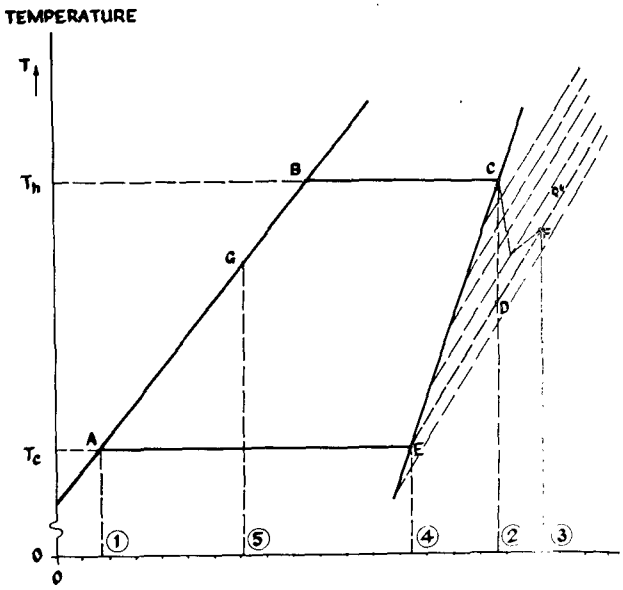


Figure 4. Entropy S

particularly as blade friction from partial admission must be added.

It thus appears that, as a rough guide, the bp should be above 100°C to keep the friction losser down and below 150°C to avoid very low condensef pressure.

4. *Stability and corrosivity.* A practical working fluid must be stable against decomposition and corrosion effects under prolonged heating in contact with conventional constructional materials. Some sixteen fluids (appendix 1) selected for their molecular weight and boiling point were subject to corrosion tests at 250°C (as against an expected working temperature of 150°C) in contact with steel, copper, aluminium, and mineral oils. Of these, nine were satisfactory. Of these only monochlorobenzene and 1,2,dichlorobenzene were considered suitable because of the shape of the T-S diagram, which is nearly vertical on the vapour-mixture boundary. The dichlorobenzene has a very low vapour pressure (bp = 180) and is intended only for smaller size turbines with air-cooled condensers. Monochlorobenzene has been taken as the material for general use.

Minor requirements of the fluids are that they shall not be too inflammable nor very toxic, but as the system is always out of doors and (supposedly) sealed these requirements are less rigid.

Summarising, we see that the ideal fluid should be chemically stable, have a high molecular weight, well over a hundred and preferably several hundred, a boiling point in the range of 100-150°C and a small number of atoms in the molecule. These four simultaneous conditions greatly limit the choice and, indeed, only one fluid (C_6H_5Cl) has been found to satisfy these requirements. As shown in the next section, the last requirement—a small number of atoms in the molecule—can be discarded, thus widening the choice of working fluids.

New cycle

In the previous section it was shown that a high molecular weight fluid was desirable, but that, in general, this led to a bad T-S diagram unless the number of atoms in the molecule could be kept low. In the course of the work it was found that a bad T-S diagram of the type of figure 3 could be "corrected" by a modification of the Rankine cycle.

Consider a Rankine cycle for the fluid in figure 4 (the abscissa is at $T = 0°K$). Liquid at temperature T_o, point A, is heated to T_h, point B, evaporated to point C and then allowed to expand and do work in a turbine. If the turbine were ideal the end-point would be at D (constant entropy) but in a real turbine the end point would be F, D and F being on the condenser pressure isobar. The vapour then passes into the condenser where it is desuperheated to point E and condensed to point A.

We have: heat supplied to fluid H_i = area 1ABC2
heat delivered as power output H_{oo} for ideal case = area ABCDE
heat delivered as power output for real case H_o = area ABCDE
= area DF23
= $H_{oo} \cdot \eta_s$

where η_s is the stage efficiency.

The turbine efficiency η_t is then

$$\eta_t = \frac{H_o}{H_i} = \eta_s \times \frac{H_{oo}}{H_i} = \eta_s \cdot \eta_{to}$$

where η_{to} is the ideal turbine efficiency.

Now it is observed that, because of the positive $\frac{dS}{dT}$ slope on the vapour-mixture boundary and the position of the isobars, the end points D and F represent superheated vapour, i.e., the temperature of the emergent vapour is above the condenser temperature. It follows therefore that the rejected super-heat can be used to preheat the liquid on its path from point A to point B.

Thus by means of a counterflow heat exchanger, referred to as a feedback heat exchanger, the heat that the boiler has to supply to reach the point C can be reduced by the amount fed back. For an ideal exchanger, the whole energy in the area 4EF3 can be fed back to provide the equal area 1AG5, provided G is at a lower temperature than F, which is found to be the case because of the slopes of the isobars.

The heat input from the boiler HiB becomes

H_{ib} = H_i — area 4EF3
= H_i — area 2DF3 — area 4ED2
= $H_i - H_{oo}(1 - \eta_s) - H_s$

where Hs is the area 4ED2 resulting from the positive $\frac{dS}{dT}$.

The turbine efficiency with feedback η_{tf} becomes

$$\eta_{tf} = \frac{H_o}{H_{ib}} = \frac{\eta_s \cdot H_{oo}}{H_i - H_{oo}(1 - \eta_s) - H_s}$$

$$= \eta_s \eta_{to} \left[\frac{1}{1 - \eta_{to}(1 - \eta_s) - \frac{H_s}{H_i}} \right]$$

The bracket shows that the efficiency is improved by two effects: the re-use of the heat H_s and the re-use of part of the internal stage losses in η_s.

It is found that the feedback improves the cycle in such a manner that the result is very nearly the same whatever fluid is used, whereas without the feedback the T-S shape has a large effect on Rankine cycle efficiency. (This point stands out when working near the critical point.)

It is thus possible, by use of the feedback heat exchanger, largely to ignore the shape of the T-S diagram and to select a fluid only on the basis of chemical stability, high molecular weight and boiling point in the correct range. Thus recently a new fluorine compound has been announced with a molecular weight over 400 and a bp of 100°C. The T-S diagram shows that 50 per cent of the input energy can be provided by the feedback and the resulting efficiency is almost identical to that for monochlorobenzene where only 5 per cent to 6 per cent is provided by feedback. (The high molecular weight would permit much lower speeds, thus greatly simplifying the mechanical design problems.)

This energy feedback should not be confused with the regenerative feed heating used in large steam turbines. In these systems steam is bled off the turbine at various points during the expansion and used to preheat the feed water. In that case the steam bled off does not continue through the turbine so that it does not do all the mechanical work it could.

In the present system only exhaust vapour is used, i.e., vapour which has already done all the mechanical work possible.

It will be noted that, in addition to improving the cycle shape because of the H_s/H_i term, some of the internal losses are recouped. In a single stage turbine (where there is no reheat factor) this can be important. For example, in a case where $\eta_{to} = 0.15$: $\eta_s = 0.7$ and $H_s/H_i = 0.40$ the square bracket

$$\frac{1}{1 - \eta_{to}(1 - \eta_s) - \frac{H_s}{H_i}} = \frac{1}{1 - .05 - .40} = \frac{1}{0.60 - .05}$$

or the recuperation of part of the internal losses increases over-all efficiency by 8 per cent.

Design considerations

Choice of fluid

As already indicated, some sixteen fluids were considered, but only one, monochlorobenzene (mcb) was found to satisfy the four conditions of high

stability, good Rankine efficiency even without the feedback heat exchanger described above (with the possibility of using the exchanger if the stage efficiency is low), reasonable molecular weight, and suitable condenser pressure. In addition, mcb is not too inflammable (comparable to kerosene), is available in high commercial purity and is low in price.

The use of some new fluorinated compounds of very high molecular weight, but relatively low boiling point, is being studied and their T-S diagrams have been prepared. They are very attractive, but the present costs are very high (about twenty times that of mcb) so that special low volume condensers, boilers and feedback heat exchangers must be designed. This work has been postponed and the present programme has been confined to mcb.

Operating temperature

The optimum temperature of operation of a solar turbine is that at which the product of the collector efficiency and turbine efficiency is a maximum. For heliostatically mounted collectors with a high concentration ratio the collection efficiency decreases only slowly with increasing temperature so that the optimum temperature is high and usually limited by other factors. However, it was assumed *a priori* that the present turbine would be operated from a stationary low concentration type collector since rotating collectors are very expensive. Under these circumstances the optimum temperature of operation is between about 140-200°C, dependent upon the detailed performance of the collector. Preliminary designs were based upon 150°C.

Size of unit

The first model has been designed to cover the range 2-10 kW with a single turbine, fewer nozzles being used for the smaller sizes than for the larger. Below about 2 kW the internal losses become a very serious fraction of the total power delivered. (There is no difficulty whatever in making larger units up to several hundred kW with a single disc, and even larger sizes with multiple discs.)

Engineering design

All the usual engineering features have had to be studied. As a compromise for a number of factors the disc diameter was chosen as 22 cm and the speed of rotation as approximately 18 000 rpm. A 6 : 1 gear box reduces the speed to 3 000 rpm. Studies were made on such questions as vibrations in shaft and blades, flow in blades, and high Mach numbers. It turns out that the Mach number is of the order of 3, considerably higher than for steam turbines, bearings, seals, ejector for maintaining the vacuum, etc.

The first model has been constructed with all the parts separated out to facilitate detailed studies and design improvements. A dual purpose boiler has been constructed that can be heated by steam from a solar collector (it was not considered advisable or practical to have mcb in the collector) or by electrical heating elements which make possible the determination of turbine thermodynamic efficiencies. No controls are fitted to this model, the control being exerted by the electrical dynemometer used to measure and absorb the power output.

At the time of writing, a second model is being designed as a complete and compact unit including an experimental heat storage unit.

Performance

Efficiencies have been computed for the case of a 10 kW unit with ten nozzles and 100 per cent admission, and the same unit used as a 2 kW turbine with two nozzles and 20 per cent admission. The fluid used is mcb and the nozzle-blade stage efficiency is taken as 0.77. The condenser temperature is taken as 30°C.

The losses other than the nozzle and blade losses are approximately:

	10 kW unit	*2 kW unit*
Disc-friction	74 W	74 W
Windage loss	0	6
Bearings [5] high speed shaft	150	150
low speed shaft (including seal)	20	20
Gears	200	40
TOTAL	444	345
Per cent of full power output	4.5 per cent	17.25 per cent
Per cent of half load (half number of nozzles)	9.8 per cent	35.2 per cent

[5] This is with oil lubrication, the oil being necessary to lubricate the internal gear box. If the gear box is eliminated or made external, mbc will be used for lubrication of the high speed bearing, and these losses will be reduced to less than half.

We obtain the following table for over-all turbine efficiency (generator losses not included):

Temperature range	*10 kW*		*2 kW*	
	Full load	*Half load*	*Full load*	*Half load*
140°C-30°C	.165	.158	.147	.128
160°C-30°C	.181	.173	.162	.141
180°C-30°C	.196	.187	.175	.152
200°C-30°C	.215	.205	.192	.166

Thus in the 160-180°C range, the efficiencies are of the order of 15-20 per cent with somewhat higher values at 200°C and lower values at 140°C.

At the time of writing, practical tests on the experimental turbine mounted on a dynamometer bench have just been started. Complete figures are not yet available, but it appears that in practice efficiencies close to the computed values are obtained.

Costs

No attempt has been made at this stage to make an accurate estimate of the cost of the turbine, but some indications are available.

The experimental model, with the disc made from a solid Hiduminium (aluminium alloy) forging with the blades milled from the solid, cost $900 including precision ground gears (which were several times oversized) and the housing and bearings. (Feed and lubrication pumps were not included.) Discussion with the manufacturer showed that on batch production the cost would be expected to fall to about $200. (For large scale mass production, as in gasoline engines, still lower prices would result.) To this must be added the cost of pumps, air ejector and controls. In part 2 the complete turbine is assumed to cost $500, which should be a safe upper figure.

Conclusions to part 1

It is seen that, by using a heavy fluid instead of steam, a single wheel condensing turbine in the 2-10 kW range can be built for operation at temperatures of 150-200°C, with efficiencies of the order of 15-20 per cent. This is very encouraging since such efficiencies are several times better than those of other engines of small size, thus reducing the size of the solar collectors needed. As shown in part 2, such efficiencies make small solar power packages economically attractive.

Appendix 1

Corrosion tests

Tests were conducted at 250°C for 100 hours first in dehydrated and evacuated vessels, then in presence of air and humidity, in contact with steel, copper, aluminium and mineral oils. Fluids tested were :

No.	*Name*		*M.W.*	*B.P.°C*
1.	Carbon tetrachloride	CCl_4	153.8	76.8
2.	Tetrachloroethylene	CCl_2CCl_2	165.9	121.2
3.	1-2 Dibromoethylene	CHBr-CHBr	185.9	110
4.	Diethyl cellosolve	$C_2H_5OCH_2CM_2OC_2H_5$	118.4	121.4
5.	Butyl propionate	$CH_3CH_2COOC_4H_9$	130.2	145.4
6.	Diacetone alcohol	$CH_3COCH_2C(OH)(CH_3)_2$	116.2	165
7.	Ethyleneglycol monomethyl ether acetate	$CH_3COOCH_2CH_2OCH_3$	118.1	143
8.	Butyl ether	$CH_3(CH_2)_3O(CH_2)CH_3$	102.2	91.4
9.	Orthoxylene	C_8H_{10}	106.2	144.4
10.	Diethyl carbonate	$(C_2H_5)_2CO_3$	118.1	125.8
11.	Methyl amyl alcohol	$(CH_3)_2CHCH_2CH(OH)CH_3$	102.2	149.5
12.	2,2,4, trimethyl pentane (iso-octane)	C_8H_{18}	114.2	99.3
13.	(Mono) chlorobenzene (MCB)	C_6H_5Cl	112.6	132
14.	Dichlorobenzene	$C_6H_4Cl_2$	147.0	180.0
15.	Butyl acetate	$CH_3COOC_4H_9$	116.2	126.5
16.	Ethyl benzene	$C_6H_5C_2H_5$	106.2	136.1

The first seven fluids were decomposed or attacked the metals. The last nine passed the tests satisfactorily. (Monobromobenzene was also found to be satisfactory, but was rejected because it has almost the same physical properties as dichlorobenzene, but is much more expensive.)

Part 2. Economic aspects of the small power package

The prospects for producing solar power at a price competitive with that of power produced at large central fuel-fired or nuclear power stations, where the power costs are under one U.S. cent per kWh, are very poor. However, the price paid for electricity on farms and other non-industrialised regions is much higher and it is with this figure that the small local solar energy power package has to compete.

Lof and Duffie have shown that the price paid for electricity in remote areas varies from 2-17 cents. The lower end of this range is for centrally produced power delivered to the consumer. For locally produced power the price is higher up the range.

We will now show that a solar energy power package should produce power at a price near the

lower end of this 2-17 cents price-range. Seven factors contribute to this price: the amount of sunshine available, the collector efficiency, the turbine efficiency, the load factor (dependent upon storage capacity), costs of the components and the interest and depreciation charges thereon, and running costs. A final factor is the exploitation factor x, i.e., the degree to which all the power produced is consumed. It is an *a priori* condition of solar devices that the exploitation factor shall be as near unity as possible, and we assume this to be the case.

Sunshine availability

Measurements in Jerusalem show that about 2 180 kWh of heat fall on each square metre of ground per year, from which it can be estimated that about 2 400 kWh fall on a square metre facing south and tilted at 32° to the horizontal, and about 2 600 kWh if the tilt is adjusted to suit the seasons.

These values include diffuse (sky) radiation. For focusing collectors (mirrors) the diffuse radiation is not collected and an approximate estimate of this (for Jerusalem) is about 15 per cent of the total. This reduces the total insolation from 2 600 to 2 200 kWh heat per year. To be on the safe side we take 2 000 kWh heat per m² per year, and this value is used in the present calculations.

The solar insolation value for Jerusalem is fairly representative of other sunny dry regions, though tropical areas with more cloud will have lower values.

As will be seen later, the results given below for Jerusalem sunshine can be used for any other site if, for the actual collector cost C (dollars per m²) we substitute $C \cdot Q_j/Q_s$ in the various formulas, where Q_j is the annual solar insolation on an adjustably tilted plate in Jerusalem (taken as 2 000 kWh heat per m²) and Q_s is the corresponding solar insolation at the given site.

Conversion efficiencies

As seen in part 1, turbine efficiencies of the order of 15-20 per cent can readily be achieved with turbines in the 2-10 kW range. The smaller sizes will show a considerable drop in efficiency at partial load due to the disc, blade and bearing friction, whereas this drop is small in the larger sizes. For the purpose of the present discussion, we assume mean efficiencies of 18 per cent for the 10 kW unit and 14 per cent for the 2 kW unit.

The efficiency of the collector cannot be known until its construction has been defined and to a slight extent its average efficiency is a function of the sunshine pattern. A good collector will have an efficiency of collection of 40-45 per cent at the optimum working temperature,[6] but it is not necessary, at this stage, to know the efficiency. This is because, as will be seen, the efficiency E_c only appears together with the cost C per square metre so that it is the ratio C/E_c which has to be known for a real collector.

Computation

Let Q = annual insolation on 1 m² of collector, kWh
E_c = efficiency of collection (weighted mean)
E_b = efficiency of turbine or turbine-generator
A = area of collector, square metres
K = rated power of unit in kW
Y = the number of hours per year of equivalent 100 per cent operation, i.e., KY = total kWh produced per year. $\frac{Y}{8\,640}$ = load factor
D = Cost of condenser per 1 000 Kcal/hr of heat condensed
B = Cost of heat storage system per 1 000 Kcal of heat stored
H = Number of hours of heat storage capacity required
i.e., BH = cost of heat storage system per 1 000 H Kcal stored
G = cost of electric generator per kW capacity
J = charges on capital, interest plus depreciation
T = cost of turbine
C = cost of collector, per sq m (of effective aperture)
p = cost of kWh produced (capital component)

Then power produced per year $= QAE_cE_t = KY$ . . . (1)

Capital cost of system = cost of turbine
plus condenser, plus heat storage
plus electric generator (if used)
plus collector.[7]

i.e., Capital cost $= T + 0.86\,\frac{(1 - E_t)}{E_t}\,KD$[8]
$+ \frac{0.86}{E_t}\,K\,BH + GK + CA$ . . . (2)

Using equation (1) for A and remembering that the total number of kWh per year is KY, we get, for investment costs only,

[6] It can be proved that the optimum operating temperature for a collector connected to a turbine is that at which the "retention" efficiency is about 0.55-0.6. To obtain the collection efficiency, this value is multiplied by the absorption-transmission coefficient, which may have a value about 0.7.

[7] Cost of preparing the ground is omitted. It can be incorporated in the unit cost C of the collector.

[8] A 1 kW turbine of efficiency E_t requires $\frac{1}{E_t}$ kW of heat input of which 1 kW is converted to power t and $\frac{1 - E_t}{E_t}$ is rejected in the condenser. Other losses such as the generator are ignored or can be lumped in E_t. Factor 0.86 represents 860 Kcal per kWh. (D and B are for 1 000 Kcal.)

Cost per kWh produced, $p = \frac{J}{YK}$ (capital cost) i.e.:

$$p = \frac{J}{YK}\left[T + 0.86\,\frac{(1-E_t)\,D + BH}{E_t}\,K + GK + \frac{CYK}{QE_tE_c}\right]$$

$$= J\left[\frac{T}{YK} + 0.86\,\frac{(1-E_t)\,D + BH}{YE_t} + \frac{C}{Y} + \frac{C}{QE_tE_c}\right] \quad . \quad . \quad . \quad (3)$$

We consider two sizes, 10 kW and 2 kW and two load factors:

(1) when $Y = 5\,000$ hours per year (57 per cent load factor) which means that the heat storage should be for about 18 hours ($H = 18$), i.e., to "stretch" the sunshine over the full 24-hour period;

(2) when $Y = 2\,500$ hours, i.e., no operation at night, with a few hours' storage capacity to flatten the daily sunshine curve to a reasonable degree ($H \sim 6$ hours).

We assume the following values:

Q = 2 000 kWh heat per year
E_t = 0.18 for 10 kW : 0.14 for 2 kW
D = \$10 per 1 000 Kcal condensed per hour
B = \$2 per 1 000 Kcal stored [9]
G = \$20 per kW
T = \$500

Equation (3) then gives for the four examples:

Case 1 10 kW, 5 000 hours

$$p^{10} = J\left(0.0565 + \frac{C}{360\,E_c}\right) \quad . \quad . \quad . \quad (4)$$

Case 2 10 kW, 2 500 hours

$$p = J\left(0.0663 + \frac{C}{360\,E_c}\right) \quad . \quad . \quad . \quad (5)$$

Case 3 2 kW, 5 000 hours

$$p = J\left(0.109 + \frac{C}{280\,E_c}\right) \quad . \quad . \quad . \quad (6)$$

Case 4 2 kW, 2 500 hours

$$p = J\left(0.159 + \frac{C}{280\,E_c}\right) \quad . \quad . \quad . \quad (7)$$

In the form of the equation given above, the amortisation and interest charges J are the same for the whole plant. In practice it can be assumed that the life of the collector will be far less than that of the turbine, condenser, etc. This requires a separate calculation for every case. However, an approximation permits generalized curves to be used. We assume a useful life for the collector of six years whereas for the turbine and other parts 15 years or more is readily achieved. From the table of appendix 2 we see that, whatever the rate of interest r, the value of J for 14-16 years is approximately half that for 6 years.

If we assume J_c to represent the annual charges on capital for the *collector*, and reckon the annual charges on the rest of the plant as $0.5\,J_c$, the equations (4)-(7) become:

Case 1 10 kW, 5 000 hours

$$p = J_c\left(0.0282 + \frac{C}{360\,E_c}\right) \quad . \quad . \quad . \quad (4')$$

Case 2 10 kW, 2 500 hours

$$p = J_c\left(0.0331 + \frac{C}{360\,E_c}\right) \quad . \quad . \quad . \quad (5')$$

Case 3 2 kW, 5 000 hours

$$p = J_c\left(0.0545 + \frac{C}{280\,E_c}\right) \quad . \quad . \quad . \quad (6')$$

Case 4 2 kW, 2 500 hours

$$p = J_c\left(0.0795 + \frac{C}{280\,E_c}\right) \quad . \quad . \quad . \quad (7')$$

The values of p/J_c (multiplied by 100 to convert p from dollars to cents) have been plotted against $\frac{C}{E_c}$ in fig. 5. (This form of presentation makes a single graph suitable whatever values of J_c, C or E_c are

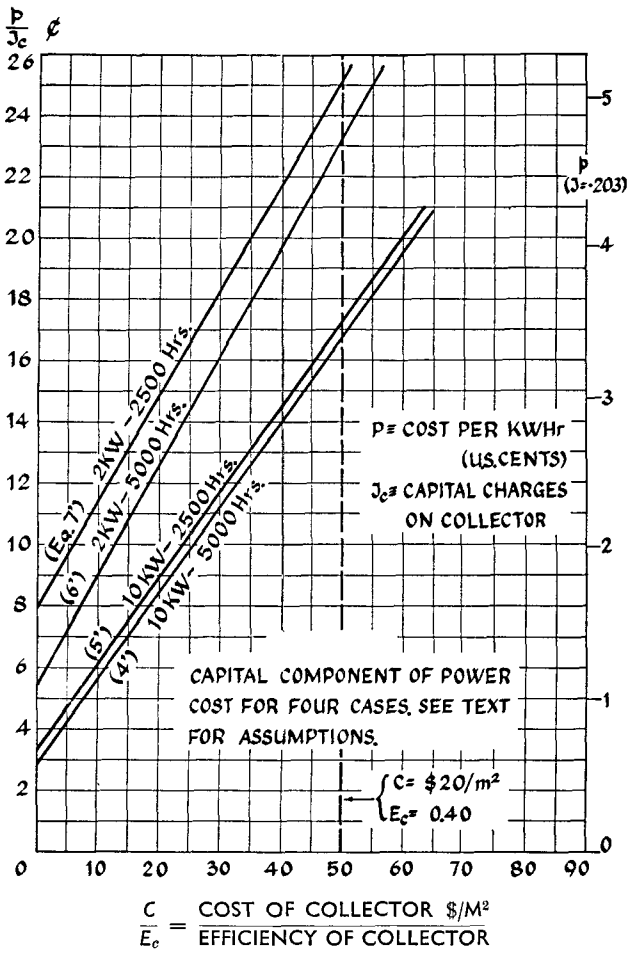


Figure 5

[9] Hypothesis: heat storage system not fully established at time of writing.

[10] p is in \$ per kWh.

taken and even a different solar intensity Q_s than that used in the calculations can be accounted for by substituting for the actual C the value $\frac{2\,000.C}{Q_s}$. The graphs clearly show that the collector cost, unless extremely low, is the dominant cost item.

In the work on solar collectors in this laboratory, we have set ourselves a target price of about $20 per square metre for the collector, a figure which seems achievable with rational modern design and materials.

Taking the collector efficiency E_c as 0.40 and the collector cost C = $20 per sq m, we obtain, for the four cases treated, p/J_c = 16.77, 17.22, 23.25 and 25.73 cents. Or taking J_c = 0.203, corresponding to 6 per cent annual interest plus six years sinking fund bearing the same interest (appendix 2), we obtain for the cost per kWh the values p = 3.4, 3.5, 4.7 and 5.2 cents. These values are extremely encouraging since, for small units on farms, the running costs — cleaning and maintenance — are unlikely to be reckoned at all. Mechanical breakdowns and parts replacement costs should be negligible for the turbine considered here because of the low temperatures and the absence of reciprocating parts. By comparison, maintenance on small diesel and gasolene engines is one of the main items in the cost of power produced from such units.

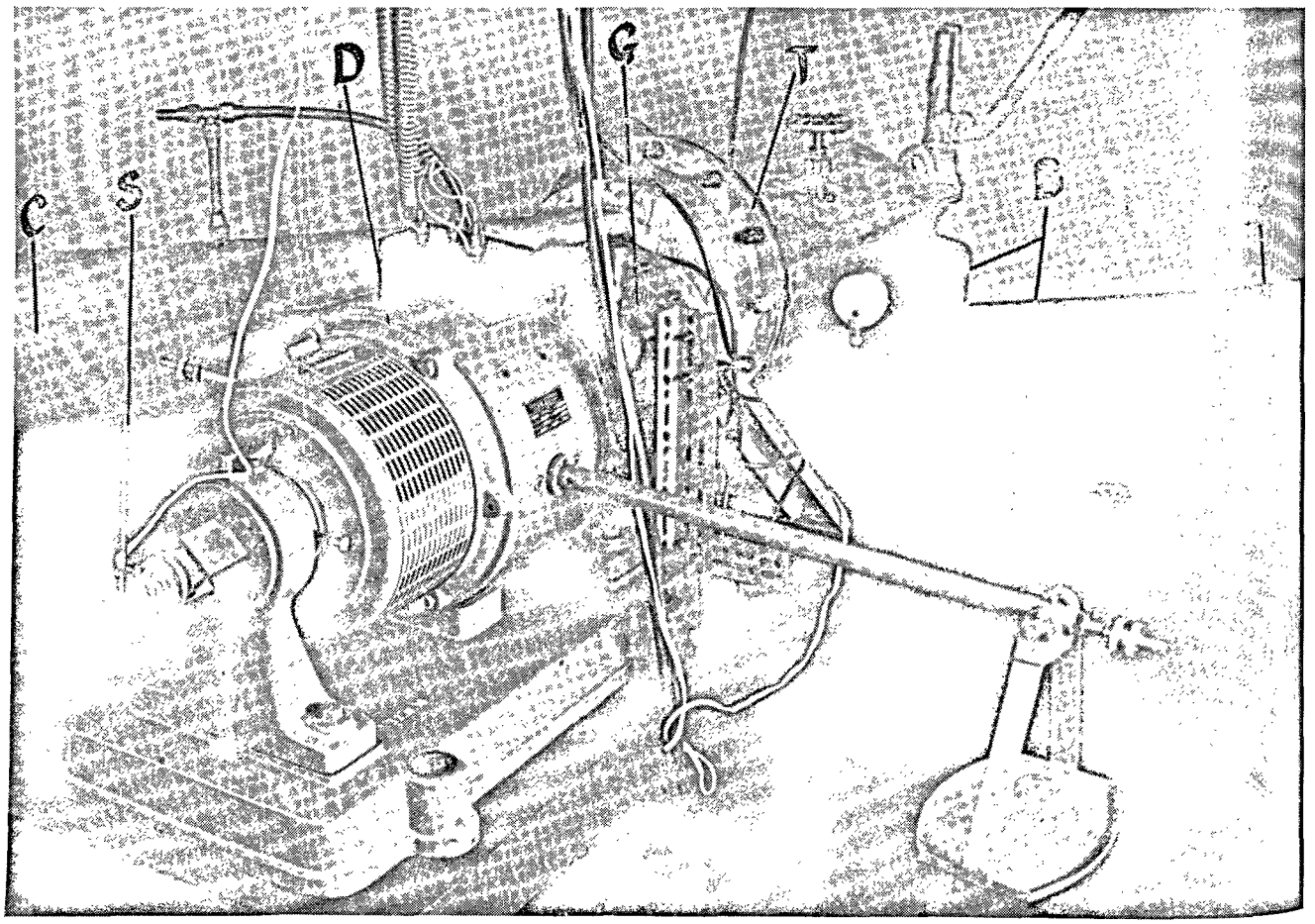
For the purpose of seeing what effect various items of cost exert on the final price of the power, table 1 shows the percentage of total power cost in equations (4')-(7'). The following points emerge from this table and an examination of equation (3).

(1) Except for the collector, whose size is proportional to the total annual collection, all the other items become, relatively, less expensive as Y, the number of equivalent hours of operation, is increased.

(2) As the turbine cost T has been taken as the same whether used for 2 kW or 10 kW (only the number of nozzles is changed), the turbine component of the cost is less for the larger units.

(3) Where the collector is the dominant cost item, as in the examples given, the price per kWh produced is scarcely dependent upon the number of hours of use Y, i.e., on the amount of heat storage unless the cost of storage B is excessive.

(4) Because of the dominant cost of the collector large errors in estimating the other items will have only a slight effect on the price of power. Only the



B = boiler; C = diffuser to condenser; D = dynamometer; F = line from feedpumps; G = gearbox; T = turbine; S = tachometer

Figure 6. Experimental turbine set-up

Table 1. Cost of power showing contribution of components

	Case 1 10 kW. 5 000 hr.	*Case 2 10 kW. 2 500 hr.*	*Case 3 2 kW. 5 000 hr.*	*Case 4 2 kW. 2 500 hr.*
p, cost per kWh, cents [a]	3.4	3.5	4.7	5.2
Per cent of power cost [b]				
Turbine	3.0	5.8	10.7	19.4
Condenser	2.4	4.5	2.3	4.1
Storage	10.3	6.6	9.5	5.7
Generator	1.2	2.3	0.9	1.6
Sub-total	16.9	19.2	23.4	30.8
Collector [c]	83.1	80.8	76.4	69.2
TOTAL	100	100	100	100
Installed cost per kW ($)	980	513	1 435	842

[a] Based upon $J_c = 0.203$, i.e., six years collector life and 6 per cent interest. If a different value of J_c is taken the other rows are unaffected. If the interest rate were 8 per cent the costs are increased by the factor 1 064.

[b] Capital charges on first four items taken as half those on the collector. See text.

[c] Based upon a collector with $C/E_c = \$50$ or $C = \$20$, $E_c = 0.40$. If a different collector cost or efficiency is taken the ratio between the sub-total row and the collector row will be altered. The relative costs of the turbine, condenser, storage and generator are unaffected.

turbine, in case 4, has much effect on the cost (19.4 per cent). The price of $500 is an upper value; a mass-produced unit would be far cheaper.

(5) The installed cost per kW is higher than for other prime movers, a result characteristic of solar installations. For the 2 kW unit the assumed price of $500, i.e., $250 per kW for the turbine, is a considerable fraction of the whole.

It should be noted that the prices of 3.4-5.2 cents per kWh given do not include the effect of the exploitation factor X. This can be serious if the owner of the plant is not skilful in using all the power that the sun supplies, for the cost is increased by the factor $1/X$. For example, if he uses only 80 per cent, the cost per kWh is increased by 25 per cent.

The costs of solar power as determined in this report are comparable with costs from other small prime-movers such as gasolene and diesel engines. This encouraging result is primarily due to the relatively high turbine efficiency; the efficiencies of other heat engines of small size proposed for solar energy have been much lower. Four very simple units tested in Wisconsin gave efficiencies of 1-2 per cent; the 100 hp engine (used at 50-50 hp) of the Shuman solar plant in Egypt in 1913 gave 10 per cent efficiency; the Italian Somor solar engine of 1-5 hp has an estimated cycle efficiency of about 6 per cent and an actual efficiency of perhaps half this; a thermoelectric engine operating at 400°C was expected to give 7 per cent, but actually gave 4 per cent (reported by Professor Baum of the USSR at the Mont Louis Solar Energy Conference in 1958).

The costs given do not include selling and erection costs.

CONCLUSIONS TO PART 2

For turbine units of 10 kW and 2 kW with storage arranged to give either 5 000 hours or 2 500 hours of full output per year, and operating in a climate similar to that of Jerusalem, the fixed charges component of the price of power produced is from 3.4-5.2 cents per kWh. This assumes a life of six years for the collector (and about 15 years for the other components) and interest rates of 6 per cent. The collector is assumed to be 40 per cent efficient and to cost $20 per sq m. About 70-80 per cent of this power cost is due to the collector and the price of the power is correspondingly affected by changes in the cost or efficiency of the collector. Maintenance and running costs are assumed to be very low. These power costs compare very favourably with power produced by other small-size prime-movers.

Appendix 2

Capital charges. In installations of the type considered the capital charges may be put as interest on the initial cost plus a sinking fund which will provide the replacement capital when the equipment becomes valueless. It is reasonable to assume that the sinking fund can bear the same interest rate as that paid on the capital (i.e., the current local interest rate). The following table gives the value J for the capital charges as

$$J = \frac{r}{100} + \frac{r}{100} \div \left[\left(1 + \frac{r}{100}\right)^n - 1\right]$$

where r is the interest rate in per cent
n is the number of years for the sinking fund.

	r =	4	5	6	7	8 %
n =	6	.191	.197	.203	.210	.216
	8	.149	.155	.161	.167	.174
	10	.123	.130	.136	.142	.149
	12	.107	.113	.119	.126	.133
	14	.095	.101	.108	.114	.121
	16	.086	.092	.099	.106	.111

Summary

Part 1. The turbine

A small power unit, of a few horsepower capacity, operated by sunshine, is a highly desirable goal. Steam engines and turbines in these sizes are all of very low efficiency, usually less than 5 per cent, resulting in the need for very large collectors. Small steam turbines are inefficient because of small dimensions and high disc losses, whilst small engines cannot exploit the full expansion of the steam.

Following D'Amelio, who pointed out the advantages of using a high molecular weight fluid in place of steam, the question of efficiency has been given special study.

It is shown that whilst with steam at moderate temperature, say 150-200°C, it is not possible to make a small turbine efficient as the use of heavy fluids makes high efficiency possible. The reasons for choosing a turbine rather than an engine are given. It is shown that the turbine can be a simple single wheel impulse type.

The working fluid should satisfy four conditions:

(1) The molecular weight should be over a hundred and preferably several hundred.

(2) The boiling point should be between 100-150°C. This is largely a consequence of the need to keep the disc friction low whilst avoiding too high a vacuum in the condenser.

(3) The fluid should be chemically stable and non-corrosive.

(4) The temperature-entropy diagram should be the correct shape. In this respect it is shown that whereas water shows a negative slope on the boundary between the liquid plus vapour phase and the pure vapour phase, hydrocarbons show a positive slope that seems to increase with increased molecular weight. This results in a low cycle efficiency. An ideal fluid should have an almost zero slope. A few liquids such as carbon tetrachloride and monochlorobenzene approach the ideal shape. It appears that the shape is predominantly a function of the *number* of atoms in the molecule (not of their *kind*) and that this should be about 5-10.

Of sixteen fluids studied as possibilities, only one satisfies all the above conditions, i.e., monochlorobenzene—which is also cheap. (Dichlorbenzene is preferable for very small turbines because its higher boiling point (180°C) gives lower disc losses.)

The fourth condition can be discarded by use of a new cycle, a modification of the Rankine cycle. Expansion in nozzles of saturated vapour of a fluid with a positive slope results in excessive superheating. The superheat can be used to preheat the feed to the boiler by means of a feed-back counter-flow heat exchanger. It is shown that the resultant cycle is largely independent of the fluid so that fluids with very bad T-S diagrams can be used. In some cases as much as 50 per cent of the feed heat is supplied from the feed-back. In addition to "correcting" the shape of the T-S diagram, the feed-back also recoups part of the internal heat losses.

A turbine in the 2-10 kW[11] range has been designed, in the first instance for monochlorbenzene where the feedback heat exchanger adds only 5 per cent to the efficiency and has therefore been omitted. Disc speed is 18 000 rpm with a 6 : 1 reduction gear. Design temperature 150°C. (The use of a much heavier fluid, with the feedback heat exchanger, which will result in lower speeds and possibly eliminate the gear-box will be studied later.)

Calculated losses, other than nozzle and blade losses, are 4.5 per cent for the 10 kW unit and 17 per cent for the 2 kW unit, both at full load. Taking the nozzle-blade efficiency as 0.77, the following computed efficiencies are obtained:

Temperature range	10 kW		2 kW	
	Full load	Half load	Full load	Half load
140°C-30°C . .	.165	.158	.147	.128
160°C-30°C . .	.181	.173	.162	.141
180°C-30°C . .	.196	.187	.175	.152
200°C-30°C . .	.215	.205	.192	.166

Thus efficiencies of the order of 15-20 per cent are obtained in the middle temperature range. Inital tests just commenced on the first experimental model show that efficiencies close to the computed values are to be expected. (A second model, as part of a complete power package including heat storage, is now in design.)

These efficiencies, with the moderate input temperature of 150°C, are several times better than those

[11] The 10 kW unit has 10 nozzles and 100 per cent admission. The 2 kW unit is identical but has only 2 nozzles.

of other small heat engines. As shown in part 2, such efficiencies make small solar power packages economically attractive.

Part 2. Economic aspects of the small power package

Seven factors contribute to the cost of power from a solar power package, i.e., amount of sunshine, collector efficiency, turbine efficiency, load factor, capital charges on the cost of the components, maintenance costs and the exploitation factor X, i.e., the fraction all the power produced that is consumed. The last is assumed to be unity; for any other value the cost of solar power is increased by the factor $\frac{1}{X}$. Maintenance costs are omitted from the calculations, as are selling and erection costs.

Formulae are set up for computing the cost of the power due to the first five factors and assuming that the capital charges on the turbine and other mechanical parts are half those on the collector. For example the collector life is taken as six years with 14-16 years for the other components.

A linear relationship exists between $\frac{P}{J_c}$ and $\frac{C}{E_c}$ where p is the cost of power, J_c is the annual capital charges rate, C is the cost of the collector per sq m and E_c is the collector efficiency. This form of presentation makes a single graph suitable whatever values of J_c, C or E_c are taken. Only if the cost of some component, such as the storage unit, or the turbine efficiency is changed is a new graph required. Allowance for annual solar insolation Q_s other than the assumed value of 2 000 kWh per sq m is made by substituting for the actual cost of the collector C the quantity $2\,000\ C/Q_s$.

Four examples are considered: 10 kW and 2 kW units with heat storage facilities for 5 000 hours per year of equivalent 100 per cent output, i.e., 58 per cent annual load factor and 2 500 hours. From part 1 the turbine efficiencies are taken as 18 per cent for the 10 kW unit and 14 per cent for the 2 kW unit.

Making reasonable assumptions for the cost of the components and allowing an arbitrary \$2 per 1 000 Kcal for heat storage, the costs of power for the four cases 10 kW, 5 000 hours, 10 kW, 2 500 hours; 2 kW, 5 000 hours, and 2 kW, 2 500 hours are: 3.4, 3.5, 4.7 and 5.2 U.S. cents per kWh, assuming a collector cost of \$20 per sq m and 40 per cent collector efficiency. The costs per kW installed are \$980, \$513, \$1 435 and \$842 respectively. The collector component of the power cost is 83 per cent, 81 per cent, 76 per cent and 69 per cent respectively showing the importance of high turbine efficiency. For the 5 000-hour units the heat storage contributes 10 per cent to the power cost, so if the heat storage unit were six times as expensive as assumed, the power cost would increase 50 per cent. These costs assume a six-year life for the collectors and 6 per cent interest charges. (For 8 per cent interest charges the costs are 6.4 per cent higher.)

The power costs given compare very favourably with power produced by other small size prime movers.

PETITE TURBINE POUR CENTRALE AUTONOME A ÉNERGIE SOLAIRE

Résumé

La turbine

Un petit groupe ayant une capacité de quelques chevaux et dont l'énergie est fournie par le soleil est d'une réalisation éminemment souhaitable. Tous les moteurs et toutes les turbines à vapeur de ces dimensions ont un bien faible rendement, habituellement moins de 5 p. 100, ce qui exige l'emploi de collecteurs de très grandes dimensions. Les petites turbines à vapeur doivent ce mauvais rendement à leurs faibles dimensions et aux pertes considérables au rotor, tandis que les petits moteurs ne peuvent pas pleinement exploiter la détente de la vapeur.

Après d'Amelio, qui a souligné les avantages de l'emploi d'un liquide à poids moléculaire élevé à la place de la vapeur d'eau, on a particulièrement étudié la question du rendement.

L'auteur montre que, lorsque l'on travaille avec de la vapeur d'eau à des températures modérées (entre 150 et 200 °C), il est impossible de tirer un grand rendement d'une petite turbine, tandis que l'emploi de fluides lourds permet d'augmenter ce rendement. L'auteur examine les raisons qui militent en faveur d'une turbine, plutôt que d'un moteur à piston. Il montre que la turbine peut être du type simple, à impulsion et à un seul rotor.

Le fluide de travail doit remplir quatre conditions :

1) Son poids moléculaire doit dépasser une centaine d'unités et, de préférence, atteindre plusieurs centaines d'unités;

2) Son point d'ébullition doit être compris entre 100 et 150 °C. Ceci, dans une large mesure, est une conséquence du besoin de maintenir au minimum le frottement du rotor tout en évitant d'avoir un vide trop poussé dans le condenseur;

3) Le fluide employé doit être chimiquement stable et non corrosif;

4) Le diagramme qui donne l'entropie en fonction de la température doit avoir la forme appropriée. A cet égard, l'auteur montre que, tandis que l'eau fait apparaître une pente négative sur la ligne qui sépare la phase liquide plus vapeur de la phase

vapeur pure, les hydrocarbures donnent une pente positive, qui semble augmenter avec le poids moléculaire. Ceci donne un faible rendement pour le cycle. Un fluide idéal doit avoir une pente presque nulle; rares sont les liquides qui, à l'instar du tétrachlorure de carbone et du monochlorobenzène, s'approchent de la forme idéale. Il semble que la forme du diagramme soit essentiellement fonction du *nombre* des atomes qui en constituent la molécule (et non pas de leur *nature*), nombre qui doit être de l'ordre de 5 à 10.

Sur un total de seize fluides étudiés quant à leurs possibilités, un seul remplit toutes les conditions mentionnées ci-dessus, à savoir le monochlorobenzène, lequel est également bon marché. (Le dichlorobenzène est à préférer pour les très petites turbines, étant donné que son point d'ébullition plus élevé, 180 °C, permet de réduire les pertes dans le rotor.)

La quatrième condition peut être éliminée en se servant d'un cycle nouveau ou modifié de Rankine. La détente d'une vapeur saturée d'un liquide à pente positive par des tuyères provoque une surchauffe excessive. On peut l'exploiter pour le réchauffage du liquide d'alimentation à la chaudière au moyen d'un échangeur de chaleur à contre courant et à retour. On démontre que le cycle qui en résulte est dans une large mesure indépendant du fluide, permettant l'emploi de ceux dont le diagramme T-S est très mauvais. Dans certains cas, la fraction de chaleur fournie par retour atteint 50 p. 100. Ne se limitant pas à corriger la forme du diagramme T-S, l'opération permet de récupérer également une partie de la chaleur perdue à l'intérieur du système.

On a réalisé une turbine dans la gamme allant de 2 à 10 kW [10], d'abord pour du monochlorobenzène, cas où l'échangeur de chaleur à retour n'ajoute que 5 p. 100 au rendement et a donc été laissé de côté. La vitesse du rotor est de 18 000 t/m, avec un train réducteur 6 : 1. La température nominale de fonctionnement est de 150 °C. (L'emploi d'un fluide beaucoup plus lourd, avec l'échangeur de chaleur à retour, qui donnera de moindres vitesses et éliminera peut-être le train réducteur, sera étudié par la suite.)

Les pertes calculées, autres que celles dans les tuyères et l'aubage, atteignent 4,5 p. 100 pour le groupe de 10 kW et 17 p. 100 pour le groupe de 2 kW, l'un et l'autre à pleine charge. Si l'on admet que le rendement du système tuyères-aubes est de 0,77, le calcul donne les rendements globaux suivants :

Gamme de températures	*10 kW*		*2 kW*	
	Pleine charge	*Demi-charge*	*Pleine charge*	*Demi-charge*
140 °C-30 °C .	0,165	0,158	0,147	0,128
160 °C-30 °C .	0,181	0,173	0,162	0,141
180 °C-30 °C .	0,196	0,187	0,175	0,152
200 °C-30 °C .	0,215	0,205	0,192	0,166

[10] Le groupe de 10 kW a 10 tuyères et 100 p. 100 d'admission; le groupe de 2 kW est identique, mais n'a que deux tuyères.

On réalise donc ainsi des rendements de l'ordre de 15 à 20 p. 100 dans la gamme des températures moyennes. Les premiers essais ont juste été commencés sur le premier modèle expérimental et révèlent que des rendements voisins de ceux qui ont été calculés peuvent être prévus. (Un deuxième modèle, qui fait partie d'une installation complète, avec accumulation de chaleur, est actuellement à l'étude.)

Ces rendements, pour une température d'admission modérée de 150 °C, sont de plusieurs fois supérieurs à ceux d'autres petits moteurs thermiques.

Comme l'auteur l'indique plus bas, ces rendements donnent un caractère économiquement attrayant aux petits groupes à énergie solaire.

Aspect économique de l'installation

Sept facteurs interviennent dans l'établissement du prix de revient de l'énergie fournie par un système solaire : la quantité de soleil, le rendement du collecteur, celui de la turbine, le facteur de charge, les investissements en capital représentés par le prix des éléments constitutifs du système, les frais d'entretien et le facteur d'exploitation X, c'est-à-dire la fraction de l'énergie produite qui est consommée. Cette dernière est supposée égale à l'unité : pour toute autre valeur, on multiplie le coût de l'énergie solaire par un facteur $\frac{1}{X}$. Les frais d'entretien sont laissés de côté dans les calculs, ainsi que les frais de vente et de construction.

On établit des formules pour le calcul du prix de revient de l'énergie dans la mesure où il est déterminé par les cinq premiers facteurs et en admettant que les investissements de capitaux au titre de la turbine et des autres pièces mécaniques sont moitié de ceux qui correspondent au collecteur. Par exemple, la durée de service de ce dernier est supposée être de six ans, et celle des autres éléments de 14 à 16 ans.

Il existe un rapport linéaire entre $\frac{P}{J_c}$ et $\frac{C}{E_c}$, expressions dans lesquelles p est le prix de l'énergie, J_c représente les frais annuels qui grèvent les capitaux, C le prix du collecteur par mètre carré et E_c le rendement du collecteur. Cette forme de présentation permet l'emploi d'un graphique unique, quelles que soient les valeurs de J_c, C ou E_c. Ce n'est que si le prix d'un élément quelconque, tel que celui qui correspond à l'accumulation, ou le rendement de la turbine, est modifié, qu'il faut un nouveau graphique. On peut envisager une insolation annuelle Q_s différente de la valeur supposée de 2 000 kWh/m² en substituant la quantité 2 000 C/Q_s au prix réel du collecteur C.

On envisage quatre exemples : des groupes de 10 kW et 2 kW avec des moyens d'emmagasiner la chaleur pendant 5 000 heures par an d'un débit équivalant à 100 p. 100 c'est-à-dire, un facteur annuel de charge de 58 p. 100, et 2 500 heures. On

prend (voir plus haut), des rendements de turbine de 18 p. 100 pour le groupe de 10 kW et de 14 p. 100 pour le groupe de 2 kW.

En faisant des hypothèses raisonnables pour le prix des éléments constitutifs et en prévoyant arbitrairement 2 dollars par 1 000 k cal pour l'emmagasinage de la chaleur, le coût de l'énergie pour les quatre cas (10 kW 5 000 heures; 10 kW 2 500 heures; 2 kW 5 000 heures; et 2 kW 2 500 heures) s'établit à 3,4, 3,5, 4,7 et 5,2 cents des États-Unis par kWh, en admettant que le collecteur revienne à 20 dollars par m^2 et que le rendement de ce collecteur soit de 40 p. 100. Les frais par kW installé sont de 980, 513, 1 435 et 842 dollars respectivement. Le collecteur représente 83, 81, 76 et 69 p. 100 des frais respectivement, ce qui souligne l'importance d'un fort rendement pour la turbine. Pour les groupes à 5 000 heures, l'emmagasinage de la chaleur représente 10 p. 100 des frais d'énergie, de sorte que, si le groupe d'emmagasinage de la chaleur coûtait six fois plus cher qu'il n'a été supposé, les frais de production d'énergie augmenteraient de 50 p. 100. Ces frais supposent une durée de service utile de 6 ans pour les collecteurs et des intérêts annuels de 6 p. 100. (Pour un intérêt de 8 p. 100, les frais monteraient de 6,4 p. 100).

Les prix donnés pour cette énergie peuvent soutenir une comparaison très favorable avec celles que produisent d'autres petits groupes.

ÉTUDE ÉCONOMIQUE DU FONCTIONNEMENT AU SAHARA DES INSOLATEURS A AIR

*M. Touchais**

Le rayonnement solaire est une énergie non dégradée; sa transformation en chaleur en vue de la convertir ensuite en d'autres formes d'énergie doit évidemment se faire à la plus haute température possible. Mais l'obtention de températures élevées suppose la concentration préalable du rayonnement, mettant en œuvre des miroirs et des mécanismes d'orientation dont le coût peut apparaître, à priori, comme devant être assez élevé.

Mais on sait qu'il est possible de trouver des besoins thermiques importants à assez faible température. La transformation du rayonnement solaire en chaleur peut alors s'opérer dans de simples insolateurs plats, de position invariable, que l'on s'efforce de réaliser le plus économiquement possible.

En ce qui concerne l'Institut de l'énergie solaire, qui se préoccupe plus particulièrement du Sahara, le chauffage de fluides, d'eau ou d'air, pour des usages divers dont le but essentiel est de modifier les conditions de vie du désert, lui apparaît être un problème important dont il convient de chercher une solution au moyen de la transformation de la radiation solaire, qui est très abondante dans les régions subtropicales.

De nombreuses réalisations de chauffage d'eau ou d'air existent de par le monde, et de nombreux chercheurs ou expérimentateurs se sont penchés sur la question. Nous n'avons pas l'intention d'innover en la matière. Mais ces réalisations ont généralement été conçues à relativement petite échelle. Or nous pensons que l'utilisation de l'énergie solaire ne peut présenter d'intérêt que si l'on envisage les transformations de quantités très importantes de rayonnement ou, ce qui revient exactement au même, que si l'on envisage l'implantation de surfaces insolées très étendues. Nous nous proposons en conséquence de travailler, non pas à l'échelle du mètre carré, mais de l'hectare. Les problèmes technologiques se posent alors d'une toute autre façon.

Nous limiterons volontairement le problème à la seule production d'air chaud. Tout d'abord, parce que l'utilisation de l'air chaud est immédiate pour :

Le chauffage d'hiver des locaux;

La circulation d'air rafraîchi par humidification l'été;

La constitution de la source froide au moyen d'une circulation d'air pour d'éventuelles machines thermiques (machines à combustion ou générateurs thermo-électriques).

C'est même cette dernière utilisation qui est à l'origine des travaux que nous désirons exposer aujourd'hui. Mais nous nous sommes rapidement aperçu que ce problème particulier nous amenait à traiter le problème général.

Pour être complet, on peut ajouter que la transformation du rayonnement solaire en énergie cinétique de l'air peut donner lieu à une transformation secondaire en énergie mécanique dont il peut être intéressant de connaître la valeur et les limites.

Nous nous sommes limités ensuite à la seule production d'air chaud, parce que, l'inertie thermique des insolateurs à air étant relativement faible, l'expérimentation, soit directe, soit par analogie électrique, est simple et rapide.

Il faut noter d'autre part que les résultats obtenus pour les insolateurs à air peuvent servir de base, dans l'étude des réchauffeurs d'eau et des évaporateurs à basse température.

Nous nous sommes décidés à conduire notre étude de la manière suivante. Les résultats déjà obtenus par d'autres chercheurs peuvent nous orienter immédiatement vers un type particulier d'insolateur de performances moyennes, avec un prix de construction pas trop élevé. Il nous suffira donc d'étudier dans le détail le fonctionnement technique et économique de grands insolateurs de ce type, et de comparer les caractéristiques de cet insolateur avec celles d'autres types, sans pour autant être obligés de reprendre une étude économique pour chacun d'eux. Notre travail comporte donc deux parties presque indépendantes : 1) Étude d'une installation complète à grande surface d'insolateurs à air, d'un type déterminé; 2) Étude expérimentale comparative de divers types d'insolateur à air.

Afin d'éliminer, dans la première partie, les paramètres qui n'intéressent pas directement le sujet, mais dont l'intervention au point de vue économique peut néanmoins être importante, nous avons convenu de soumettre notre étude aux exigences d'une implantation bien définie mais entièrement arbitraire, à savoir (figure 1) l'installation en un point situé au Sahara sur le plateau du Tademaït à 670 m d'altitude, par 28° 48′ de latitude Nord et 2° 32′ de longitude Est, sur la piste d'Alger à In-Salah, à distance à peu près égale d'El Goléa, Timimoun et In Salah. C'est un point situé en plein désert à une distance moyenne d'Alger, d'un accès relativement facile, présentant

* Ingénieur chargé de recherches, Institut de l'énergie solaire de l'Université d'Alger.

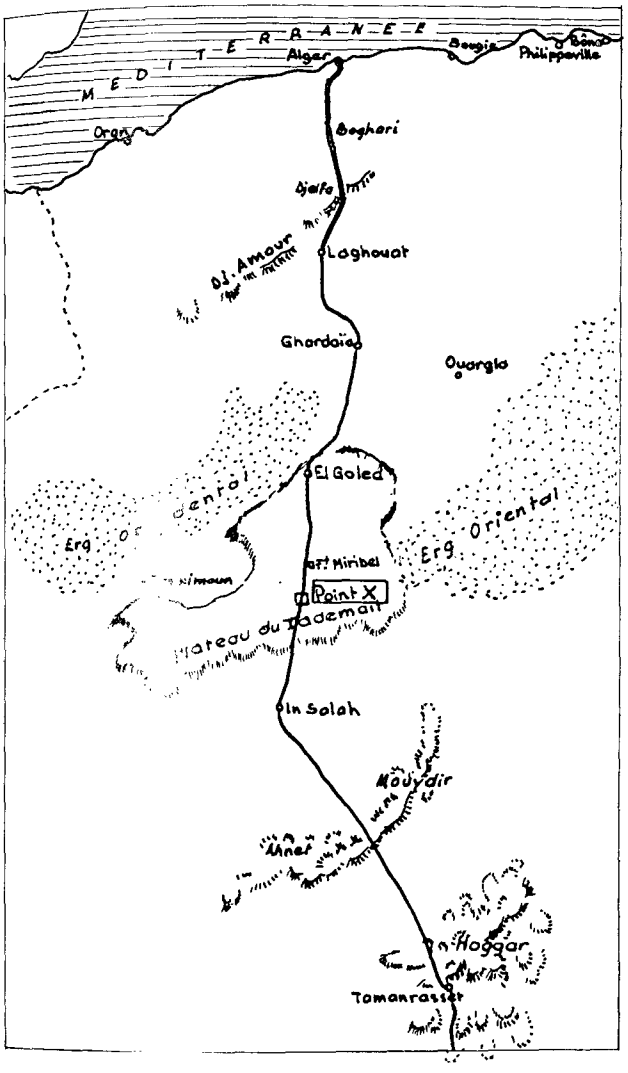


Figure 1

un bon ensoleillement, et entouré de stations météorologiques assez proches qui permettent d'interpoler facilement les caractéristiques climatologiques à utiliser.

Ces caractéristiques sont :

1) *Températures °C :*

	Max.	*Min.*	*Moy.*	*Amplitude journalière*	*Moyenne annuelle*
Janvier .	16	2,3	9,5	14,5	22,1
Juillet . .	40	24,5	32	16	

2) *Humidité :* La tension partielle moyenne de la vapeur d'eau est $t = 3$ mm, en hauteur de mercure.

3) *Facteur d'ensoleillement moyen :* $\sigma = 0{,}843$.

Pour la facilité de l'exposé, nous appellerons désormais ce point arbitraire, le point X.

Nous avons admis, d'autre part, que les surfaces insolées pouvaient servir à deux fins : a) Insolation proprement dite génératrice d'air chaud; b) Protection contre le soleil et les intempéries qu'offre un insolateur utilisé en couverture.

Pour nous exprimer autrement, la fonction de l'insolateur étant inséparable de l'utilisation, laquelle requiert la présence de bâtiments, nous supposons que les frais réels d'installation des insolateurs ont à être diminués du coût réel des bâtiments couvrant la même surface et couverts par les moyens habituels.

Ce point de vue est évidemment spécifique du climat saharien, et il eût été inexact de n'en pas tenir compte dans l'évaluation des frais. Un premier avantage de cette façon de voir est d'éliminer l'incidence sur le prix de la nécessité de construire les insolateurs en élévation pour éviter l'effet néfaste des vents de sable décapants. A 3 mètres en effet au-dessus du sol, les appareils n'ont à subir que des vents de poussière. Nous avons admis en conséquence que les entraits de la charpente support des insolateurs étaient à 3 mètres au-dessus du sol. Toute hauteur différente serait imputable au bâtiment en soi, et non au champ d'insolateurs.

Nous avons encore admis que les insolateurs devaient être placés face au Sud et inclinés sur le plan horizontal d'un angle sensiblement égal à la latitude du lieu, qui est l'angle optimum dans le site choisi, où la nébulosité et l'absorption atmosphérique sont relativement faibles.

L'insolation est en moyenne plus importante pour les insolateurs inclinés, et la pente facilite le nettoyage des surfaces. Ce problème du maintien des surfaces en bon état de propreté est d'ailleurs l'une des plus grosses difficultés de l'emploi des insolateurs au Sahara. Il en résulte des frais d'exploitation relativement importants dont nous tiendrons compte.

En ce qui concerne l'utilisation de l'air, on peut envisager trois possibilités :

1) Utilisation de l'air chauffé au conditionnement des locaux abrités par les insolateurs. Chauffage l'hiver et refroidissement par humidification l'été sans intervention d'aucun système accessoire (chaudières, groupes de compression, etc.).

2) Utilisation du mouvement de l'air provoqué par le tirage d'une cheminée pour le refroidissement de machines thermiques et plus spécialement pour le refroidissement des générateurs thermo-électriques.

3) Accessoirement, utilisation de l'énergie cinétique de l'air ainsi mis en mouvement.

Diagramme de fonctionnement des insolateurs à air

Notations :

l, largeur du canal : m.

L, longueur insolée du canal : m. L peut varier avec la saison suivant les dispositions adoptées. La surface insolée est $L\,l$: m².

h, hauteur du canal : m, supposée constante.
La section du canal est $l\,h$: m².

x, abcisse de la section étudiée à partir du début de la partie insolée; x varie de 0 à L.

Δx, élément d'insolateur de largeur 1 m, à l'abcisse x.

T_x, température de l'air à l'entrée de la section à l'abcisse x; $(T_x + \Delta T_x)$ est la température à la sortie de l'élément. T_x varie de T_e à T_s de l'entrée à la sortie.

T_a, température de l'atmosphère ambiante au-dessus de la couverture.

T_i, température de l'atmosphère intérieure au-dessous du fond isolé.

T_{v_c}, température de la voûte céleste. On prendra ici systématiquement $T_{v_c} = 0$ °C.

q_{i_Θ}, radiation incidente : W/m².

q_a, radiation absorbée par les surfaces qui transforment le rayonnement en chaleur : W/m²

$$q_a = \alpha_s \tau_v Q_{i_\Theta} \tag{1}$$

(α_s est le facteur d'absorption des surfaces réceptrices, τ_v est le facteur de transmission de la couverture, que l'on supposera à peu près indépendant de la hauteur du soleil.)

q_{p_c}, puissance calorifique perdue par la couverture : W/m².

q_{p_f}, puissance calorifique perdue par le fond de l'insolateur : W/m².

q_p, puissance calorifique perdue par l'insolateur.

$$q_p = q_{p_c} + q_{p_f} \tag{2}$$

q_u, échauffement de l'air : W/m²

$$q_u = q_a - q_p \tag{3}$$

v, vitesse de l'air à l'entrée de la partie isolée : m/s; le débit en volume est $v\,l\,h$: m³/s.

V, vitesse du vent : m/s.

e, état hygrométrique de l'air.

ρ, masse spécifique de l'air à l'entrée : kg/m³; on a pour l'air sec

$$\rho = 0{,}4645 \frac{P_a}{T_e + 273} \tag{4}$$

P_a étant la pression atmosphérique, soit au lieu choisi $P_a = 706$ mm de Hg.

C_p, chaleur spécifique de l'air : J/kg °C.

m, débit masse de l'air : kg/s; on a à l'entrée de la partie insolée

$$m = \rho\, l\, h\, v \tag{5}$$

et

$$q_u \Delta x = m\, C_p\, \Delta T_x \tag{6}$$

ou encore

$$\frac{dT_x}{dx} = \frac{q_u}{m\, C_p} \tag{7}$$

Q_a, radiation totale reçue par la surface réceptrice

$$Q_a = q_a\, L\, l. \tag{8}$$

Q_p, radiation totale perdue

$$Q_p = \int_o^L q_p\, dx \tag{9}$$

Q_u, échauffement total de l'air à la sortie

$$Q_u = \int_o^L q_u\, dx = m\, C_p\, (T_s - T_e) \tag{10}$$

S, surface occupée totale sur le terrain.

N, nombre d'insolateurs. La surface totale insolée est $N\,l\,L$.

L'insolateur est supposé en régime permanent.

L'étude analytique du fonctionnement de l'insolateur est rendue difficile par la présence de coefficients de transfert de chaleur non linéaires. Il faut soit expérimenter directement, ce qui présente de sérieuses difficultés, soit utiliser une méthode analogique en admettant que les lois de transfert de chaleur sont linéaires pour les intervalles de température qu'il y a à considérer [1].

Le fonctionnement en régime permanent de l'élément Δx peut être représenté électriquement par le schéma de la figure 2.

De (6) on tire

$$q_u = \frac{\Delta T_x}{\Delta R_x} \tag{11}$$

en posant

$$\Delta R_x = \frac{\Delta x}{m\, C_p} \tag{12}$$

La méthode consiste à soutirer un courant représentant q_u au nœud qui représente la masse d'air chauffé. On y arrive en introduisant entre le nœud et la masse représentant le milieu ambiant : 1) la résistance ΔR_x; 2) un générateur auxiliaire qui sert à régler le potentiel devant représenter la température T_x.

On divise l'insolateur en un nombre n de fractions $\Delta x_1, \Delta x_2, \ldots \Delta x_n$, qui ne sont pas nécessairement égales. On choisit une valeur de la radiation incidente $q_{i\Theta}$, un débit m à l'entrée de l'insolateur. On commence par la fraction d'entrée de longueur Δx_1, pour laquelle on a $T_1 = T_e$, avec la résistance

$$\Delta R_1 = \frac{\Delta x_1}{m\, C_p}$$

et on détermine expérimentalement ΔT_1.

On recommence avec la fraction suivante, en partant de $T_2 = T_1 + \Delta T_1$, etc... On relève les températures, ainsi que les différents flux thermiques, et l'on obtient des courbes de la forme

$$y = f_m\, Q_{i\Theta}\,(x), \tag{13}$$

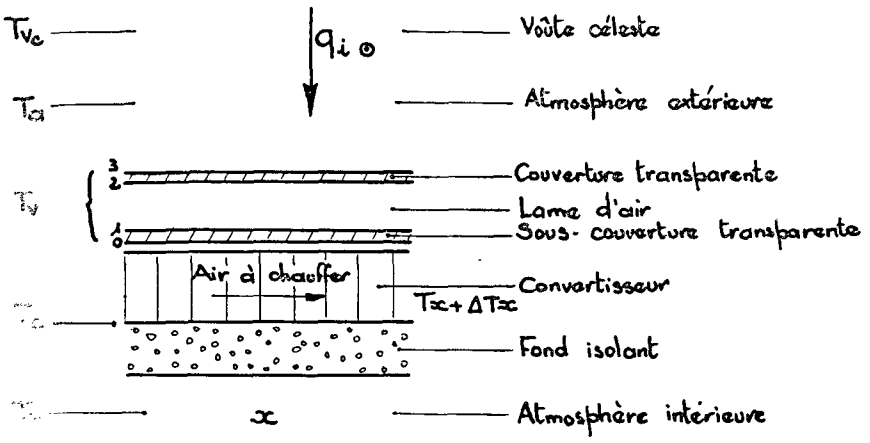
ou plus exactement des lignes polygonales qui se rapprochent d'autant plus des courbes réelles que l'on prend des Δx plus petits. Mais le nombre de fractions, et par suite la durée des mesures, s'accroissent en proportion inverse.

Le régime de fonctionnement au point d'abscisse x où la température de l'air est T_x correspond à $\Delta x = 0$ et $\Delta R_x = 0$. Il suffit, pour l'obtenir sur le circuit analogique, de remplacer ΔR_x par un court circuit, et de régler la tension du nœud au moyen du générateur auxiliaire à la valeur T_x. Ainsi qu'on le voit, le régime de fonctionnement dans la section d'abscisse x ne dépend que de la température T_x de cette section. En particulier, on a à l'entrée $T_1 = T_e$. Les ordonnées à l'origine des courbes $y = f_m Q_{i\Theta}\,(x)$ sont indépendantes de m.

Résultats des mesures effectuées sur l'insolateur expérimental choisi

L'insolateur expérimenté répond aux caractéristiques suivantes, légèrement différentes toutefois de celles de l'insolateur qui a été définitivement choisi : $l = 1$ m, $L = 5$ m, $h = 0{,}05$ m. D'où $lh = 0{,}05$ m².

[1] Voir Bulletin 3, Institut de l'énergie solaire, Université d'Alger.


Tvc
qi ⊙
Voûte céleste
Ta
Atmosphère extérieure
Tv
3
2
1
0
Couverture transparente
Lame d'air
Sous-couverture transparente
Air à chauffer
Convertisseur
Tc
Tsc + ΔTsc
Fond isolant
Ti
x
Atmosphère intérieure

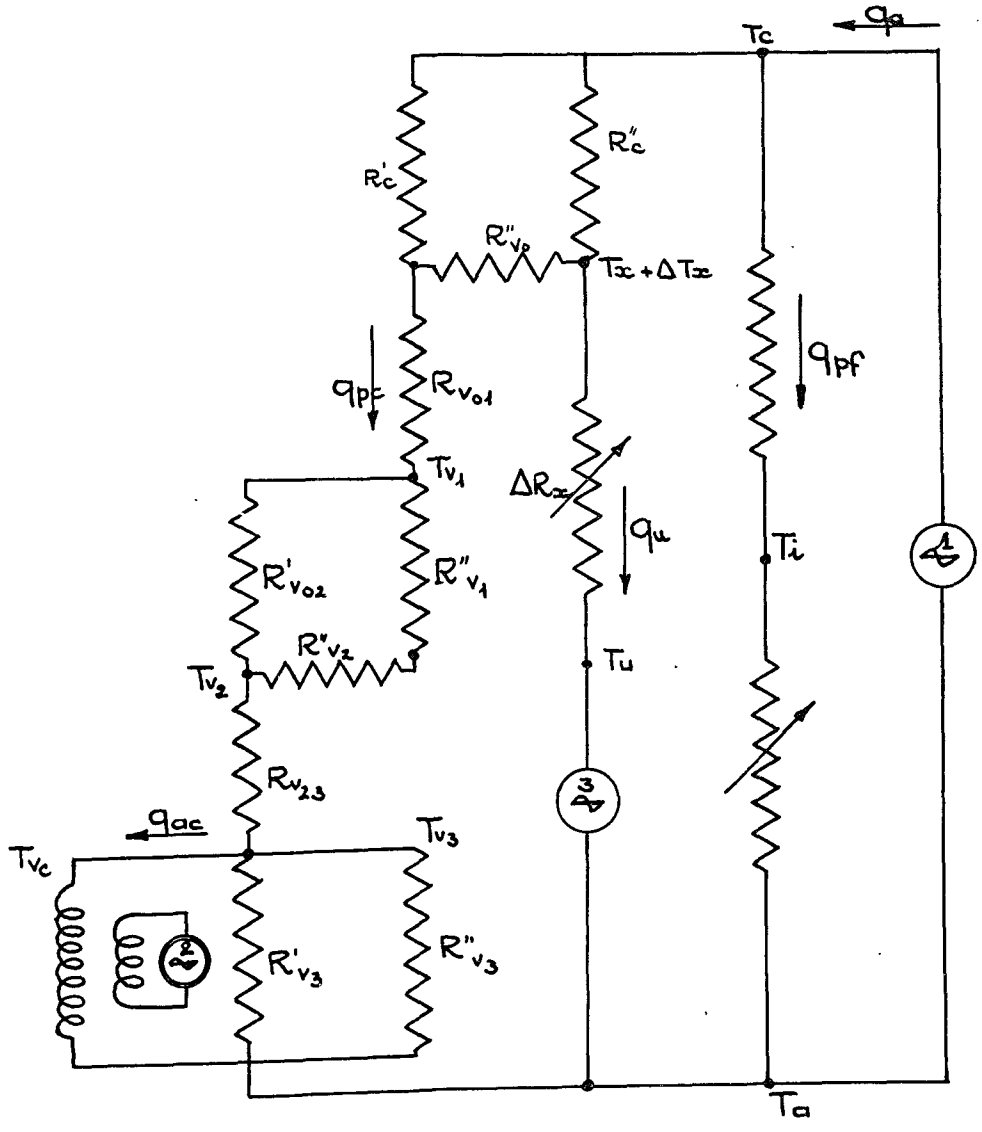

Tc
qa
R'c
R"c
R"vo
Tsc + ΔTsc
qpc
Rvo1
qpf
Tv1
ΔRx
qu
R'v02
R"v1
Ti
R"v2
Tv2
Tu
Rv23
qac
Tv3
Tvc
R'v3
R"v3
Ta

Figure 2

Couverture formée d'un verre double et d'un verre simple, avec lame d'air interposée de 5 mm. $\tau_v = 0{,}79$. Fond isolé; résistance thermique : 1 °C/W.m².

Coefficient de transfert par convection entre parois et air

$$A = 2{,}55\ \Delta T^{0{,}25}\ \text{W/m}^2.\text{°C}. \qquad (14)$$

Facteur d'émission de la surface réceptrice : $\varepsilon = 1$; le facteur d'absorption a cependant été pris égal à $\alpha_s = 0{,}95$.

Les mesures ont été effectuées en adoptant des Δx de 0,10 m pour les premières fractions et de 1 m pour les dernières. On a relevé les courbes

$$T = f(x),\ q_p = \varphi(x),\ q_u = \psi(x),$$

pour des vitesses de l'ordre de 0,20 m et 1 m par seconde, pour $q_a = 800$ W/m², et enfin pour $T_e = T_a$. Il a été relevé en outre, pour différentes valeurs de q_a, les ordonnées à l'origine des courbes précédentes et la courbe des températures statiques, c'est-à-dire pour $v = 0$.

Dans le cas où l'on a $T_e \neq T_a$, on est ramené au cas précédent par une translation des abcisses : l'origine de l'insolateur vient à l'abcisse x_e de l'insolateur primitif, pour laquelle la température de l'air est $T_x = T_e$.

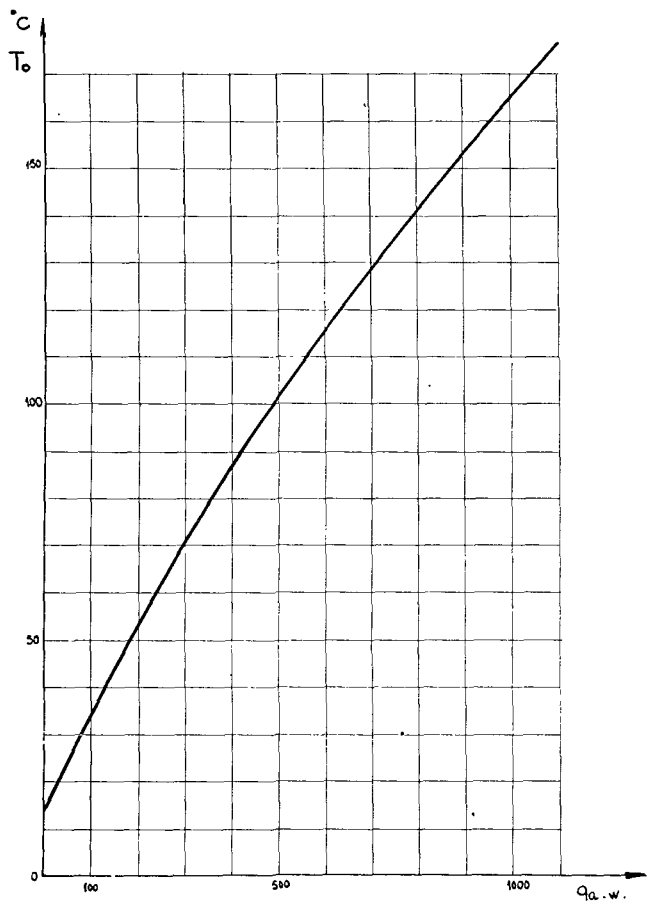


Figure 3

Il s'agit d'établir la *fonction caractéristique* de l'insolateur :

$$F = (Q_u, Q_{i\Theta}, T_s, T_e, T_a, T_i, T_{v_c}, m, e, P_a, L, V) = 0 \qquad (15)$$

qui permet d'étudier toutes les particularités de fonctionnement, mais nous en réduirons la complexité en nous limitant au cas défini par les conditions $P_a = 706$ mm, $h = 0$ p. 100, $V = 0$ m/s, $T_{v_c} = 0$ °C, $T_e = T_a = T_i = 22{,}1$ °C.

On a alors :

$\rho = 1{,}111$, $C_p = 1\,006\ J/\text{kg °C}$ (soit 0,2408 kcal/kg °C), $mC_p = 1\,118\ \rho hv = 55{,}9\ v$ W/°C

et nous posons

$$\theta = T_s - T_e \qquad (16)$$

avec

$$\theta_0 = T_0 - T_e \qquad (17)$$

$$M = \frac{m C_p}{L} \qquad (18)$$

$$Q_{u\ \text{moy}} = \frac{Q_u}{L} \qquad (19)$$

Les mesures étant assez longues, nous avons cherché à établir une forme analytique pouvant représenter les expériences avec une assez bonne approximation, nous permettant ainsi d'en réduire le nombre, ce qui nous a conduit à adopter la relation

$$\frac{\theta}{\theta_0} = 1 - e^{-kx} \qquad (20)$$

où k est défini par le fonctionnement de l'élément origine. On a

$$\frac{d\theta}{dx} = \theta_0\ k e^{-kx} \qquad (21)$$

et pour $x = 0$

$$\left[\frac{d\theta}{dx}\right]_0 = \frac{q_{u_0}}{LM} = \theta_0 k \qquad (22)$$

D'où

$$KLM = \frac{q_{u_0}}{\theta_0} \qquad (23)$$

Les relevés expérimentaux sur le circuit analogique montrent que q_{u_0} est à très peu près une fonction linéaire de q_a :

$$q_{u_0} = 0{,}71\ q_a - 39{,}62 \qquad (24)$$

d'où finalement la relation cherchée

$$Q_{u\ \text{moy}} = M\theta_0 \left[1 - e^{-\frac{0{,}71\ q_a - 39{,}62}{M\theta_0}}\right] = M\theta \qquad (25)$$

La fonction caractéristique peut alors se mettre sous la forme plus simple

$$F(Q_{u\ \text{moy}}, q_a, \theta, M) = 0 \qquad (26)$$

La figure 3 donne la courbe représentative de la température statique T_0 en fonction de q_a. Cette courbe et le système (25) permettent d'établir le diagramme de la figure 4, qui donne $Q_{u\ \text{moy}}$ en fonction de la radiation absorbée q_a pour $M = \text{Cte}$ et pour $\theta = \text{Cte}$. Le diagramme comporte également

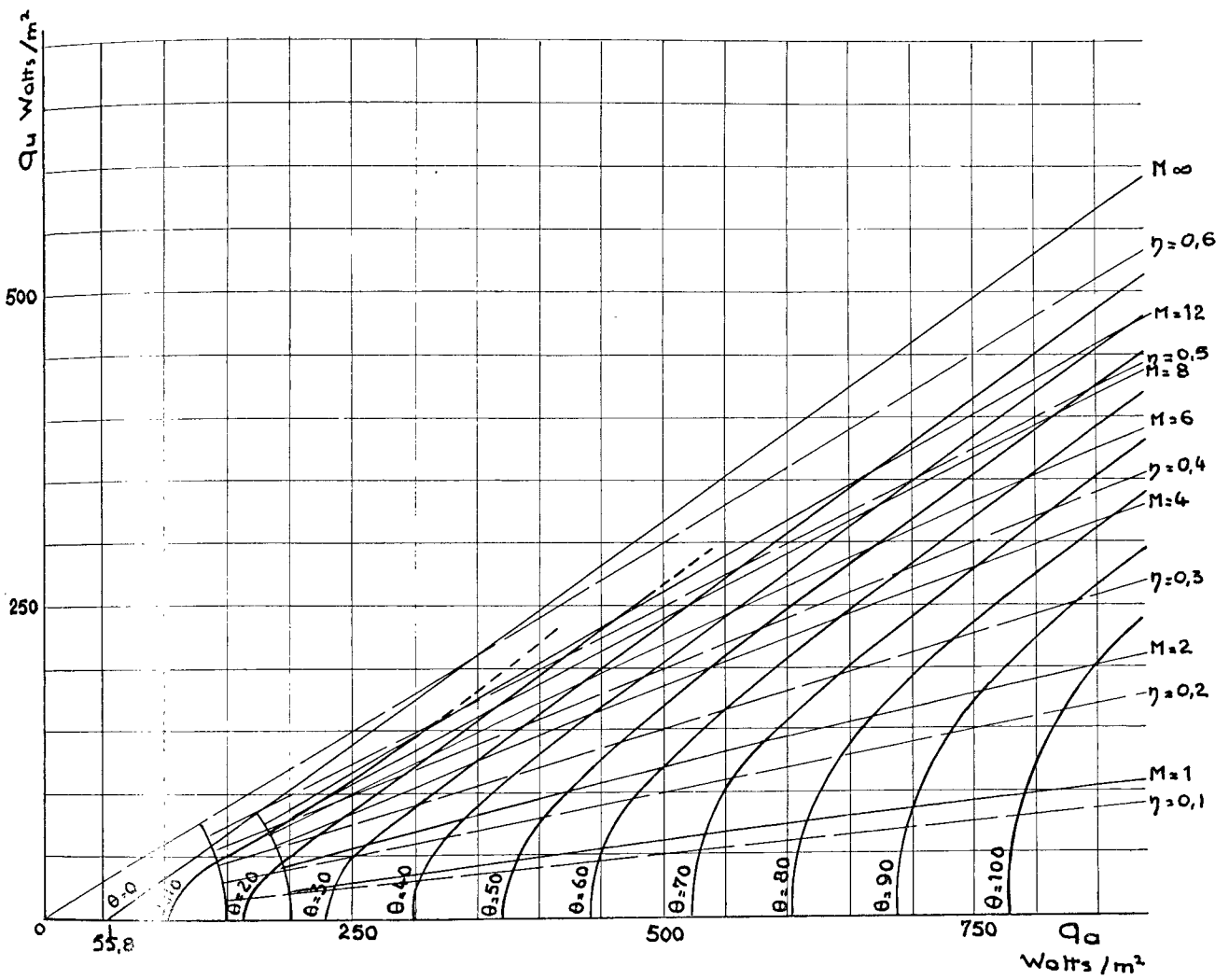


Figure 4

les lignes d'égal rendement qui sont des droites issues de l'origine.

Une observation importante peut être faite à l'examen de ce diagramme : le gain relatif de la chaleur extraite de l'insolateur décroît rapidement avec M. C'est-à-dire avec la vitesse à l'entrée. On voit qu'il n'y a pas intérêt à dépasser une valeur de M de l'ordre de 15 W/m°C et par suite des vitesses d'entrée de l'ordre du m/s.

Il résulte de cette observation que les pertes de charge à l'intérieur de l'insolateur sont généralement négligeables.

Selon l'utilisation que l'on a en vue, on peut désirer fonctionner, soit à T_s = Cte, soit à θ = Cte, soit à M = Cte, soit plus généralement de façon à satisfaire une certaine condition

$$f(\theta, M) = 0 \qquad (27)$$

Nous nous bornerons, dans ce qui suit, à étudier le fonctionnement de l'insolateur à θ = Cte.

Étude de la production d'air chaud à θ = Cte

La détermination de la quantité totale de chaleur extraite de l'insolateur pendant une période donnée, exige en général les opérations suivantes :

1) Établir pour toutes les journées $j = 1, 2, \ldots n$ de la période considérée, les diagrammes types de la radiation absorbée q_a. On peut ne pas tenir compte, dans une première approximation, de la radiation diffuse. Il faut alors déterminer la projection $q_{i\Theta}$ de la radiation directe sur la normale au plan de l'insolateur. On a

$$q_{i\Theta} = q_n \cos\delta \cos H \qquad (28)$$

q_a est alors donné par (1).

Le plus souvent, le diagramme de la radiation est inconnu. On pourra alors partir d'un diagramme type obtenu en extrapolant, pour la station choisie, les données climatologiques des stations météorologiques environnantes, en particulier en déterminant la tension moyenne de la vapeur d'eau et le facteur

moyen d'ensoleillement, ce qui permet d'établir les diagrammes types de la radiation directe pour le point choisi.

2) Sur le diagramme de fonctionnement de l'insolateur établi pour les températures T_a et T_{v_c} données, et sur la courbe θ = Cte choisie, déterminer pour chaque valeur de q_a la valeur correspondante de $Q_{u\ \text{moy}}$ et établir le diagramme journalier des chaleurs moyennes extraites.

Ce diagramme définit des limites inférieures et supérieures T_1 et T_2 de l'angle horaire, hors desquelles l'insolateur ne peut plus fonctionner à l'écart de températures θ imposé.

3) Déterminer pour chacune des journées de la période la longueur insolée L. La production journalière de chaleur de 1 m de largeur de l'insolateur est

$$L \int_{t_1}^{t_2} Q_{u\ \text{moy}}\, dt \qquad (29)$$

4) Calculer la production totale de chaleur dans la période donnée et pour la surface insolée $N\ell L$

$$N\ell \sum_{j=1}^{j=n} L \int_{t_1}^{t_2} Q_{u\ \text{moy}}\, dt \qquad (30)$$

Un tel calcul est très long et ne convient guère pour un avant-projet. Force est donc d'admettre certaines simplifications pour diminuer les calculs. Nous avons admis qu'une valeur approchée de la *production annuelle* pouvait être obtenue en se plaçant dans les conditions définies plus haut, dans la section intitulée « Diagramme de fonctionnement des insolateurs à air », et en adoptant des diagrammes journaliers moyens, soit par décades, soit par mois..., etc. Il suffit alors d'établir le diagramme journalier équivalent de la radiation absorbée q_a dans la période donnée, d'en déduire le diagramme correspondant $Q_{u\ \text{moy}}$. La production totale de chaleur est alors

$$365\, N\ell L_{\ \text{moy}} \int_{t_1}^{t_2} Q_{u\ \text{moy}}\, dt$$

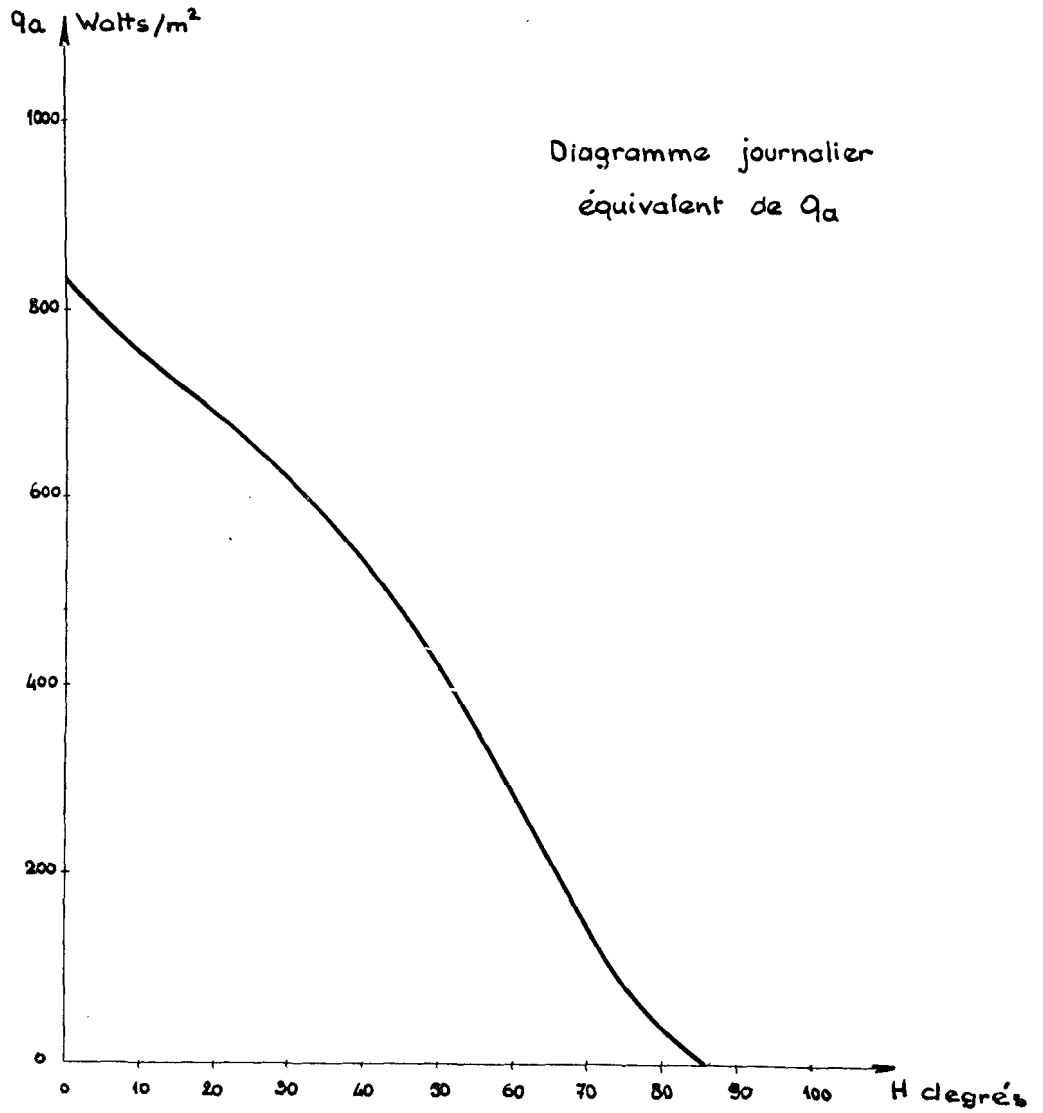


Figure 5

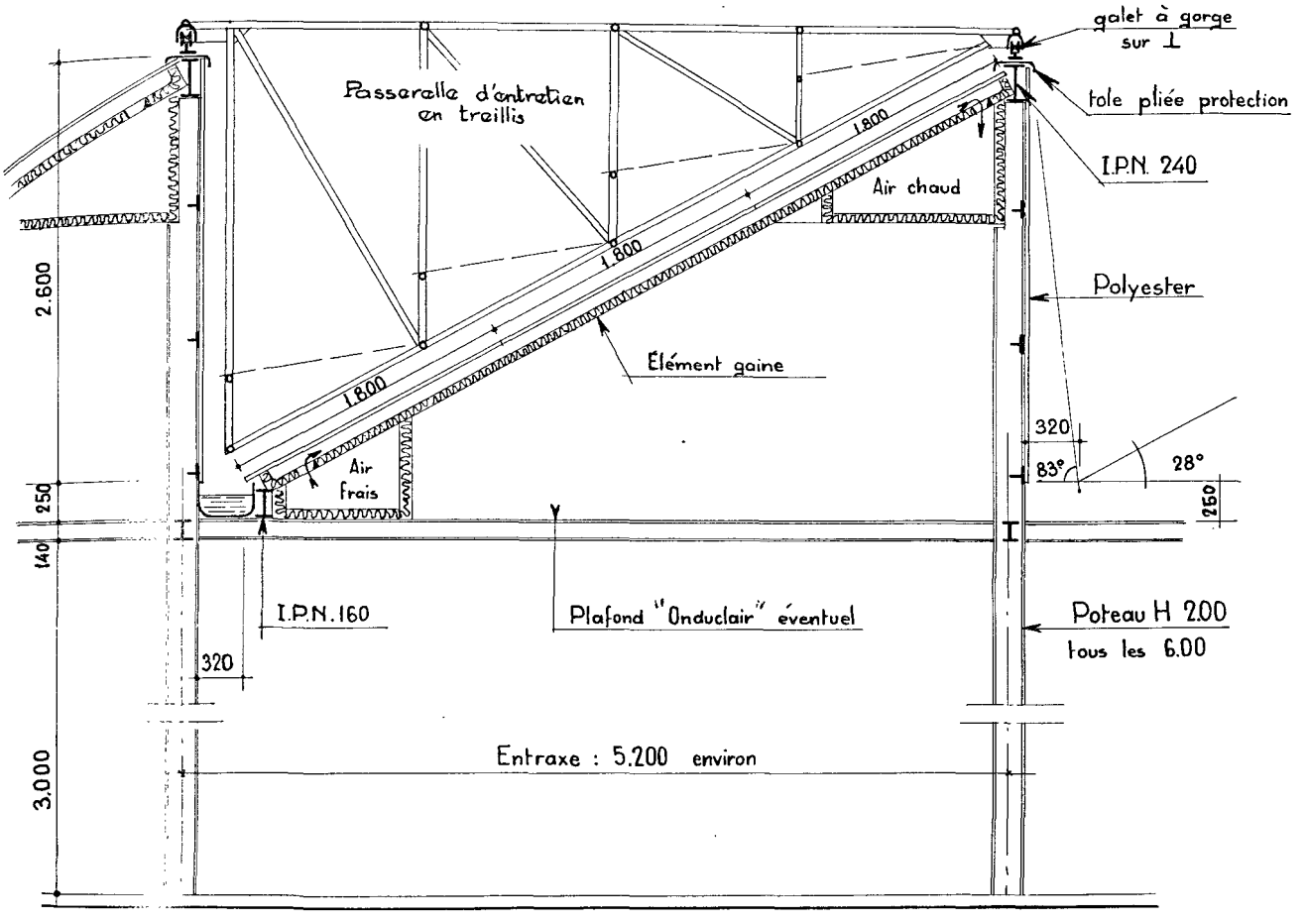


Figure 6

Nous avons effectué ce calcul pour $\theta = 40$ °C, qui est une valeur industriellement assez basse, et $\theta = 70$ °C, qui correspond à une température $T_s = 92$ °C, un peu inférieure à celle de l'ébullition de l'eau à l'altitude considérée. Nous avons adopté les valeurs suivantes :

$\ell = 0{,}545$ m,
$L_{min} = 3{,}25$ m, $L_{moy} = 4{,}31$ m, $L_{max} = 5{,}37$ m, et

pour 1 hectare, nous avons pris

$N = 3\,420$, soit 40 sheds de 50 m de long,
$S = 11\,400$ m². (Voir figures 6 et 7)

La figure 5 donne le diagramme monotone journalier équivalent de la radiation absorbée q_a en W/m² pour le lieu choisi et l'inclinaison donnée des insolateurs. L'énergie annuelle absorbée, calculée en planimétrant le diagramme, est de $16{,}4 \times 10^3$ M kcal, ce qui correspond à une énergie annuelle incidente de $21{,}8 \times 10^3$ M kcal.

En utilisant le diagramme de la figure 4, on obtient :

pour $\theta = 40$ °C $Q_{u\ an} = 5{,}62 \times 10^3$ M kcal,
$m_{max} = 101$ kg/s;

pour $\theta = 70$ °C $Q_{u\ an} = 3{,}24 \times 10^3$ M kcal,
$m_{max} = 44{,}5$ kg/s

Si la même quantité de chaleur avait été produite par combustion d'un fuel industriel (fuel n° 2 par exemple, de pouvoir calorifique inférieur, supposé égal à 10 500 kcal/kg), la consommation annuelle de combustible et les frais d'achat et d'acheminement à raison de 283 NF par tonne [2], seraient respectivement de

669 T pour $\theta = 40$ °C, soit 189 327 NF,
386 T pour $\theta = 70$ °C, soit 109 238 NF.

en supposant un rendement global de la combustion et des échanges de 80 p. 100 (rendement défavorable à la solution solaire).

Il est à noter que l'installation complète de chauffage utilisant le fuel comme combustible coûterait, pour un matériel monté en ordre de marche au point choisi, 350 000 NF.

Cette installation comporterait trois générateurs d'air chaud, d'un type commercial monobloc, de puissance moyenne unitaire 700 000 kcal/H, avec brûleurs, ventilateurs de soufflage et cheminées de 15 mètres, et accessoires d'installation : filtres, appareillage électrique et raccordements, appareils

[2] Ce prix s'entend pour une livraison en grande quantité. En petite quantité, le prix du fuel peut s'élever jusqu'à 440 NF par tonne.

de conduite et de contrôle automatique, trois cuves de stockage de 30 m³, nourrice de 500 litres, pompes de transvasement, vannes et tuyauteries, ainsi que les travaux de génie civil. La puissance électrique nécessaire serait de l'ordre de 55 cv.

Il faut bien entendu ne considérer le prix de cette installation que comme un ordre de grandeur, car il est susceptible de varier avec l'application exacte que l'on aura en vue.

Étude en avant-projet d'une installation complète

Le point X choisi pour édifier les insolateurs est situé à 230 km environ d'El Goléa, sur une piste qui, bien que non revêtue, est accessible aux transports lourds. El Goléa est une oasis assez importante qui possède un aérodrome. On dispose d'autre part d'eau potable à Fort Miribel, qui est à 100 km environ au nord du point X.

Le sol, qui est celui du plateau du Tademaït, est dur, ce qui permet d'envisager des fondations peu volumineuses.

Les travaux étant assez éloignés des grands centres (1 130 km environ d'Alger, les problèmes de transport et de main-d'œuvre sont prépondérents. Le coût d'un transport de 20 tonnes (ou 25 m³) approche 6 000 NF, toutes charges comprises.

Par ailleurs, il faut prévoir indépendamment des salaires et des périodes de repos par roulement, une dépense de l'ordre de 80 NF par homme-jour, avec en outre un voyage aérien de 500 NF par homme.

Il résulte de l'examen de ces différents postes de dépenses, qu'il y a lieu de prévoir l'emploi :

1) De matériaux légers et résistants;

2) De matériaux aussi peu encombrants que possible, car le chargement des camions doit s'effectuer au maximum de leur charge utile;

3) D'un personnel réduit et de qualité pour le montage des éléments sur place.

Ces conditions conduisent aux solutions suivantes.

Charpente

La charpente métallique apparaît avec évidence comme la solution la plus rationnelle au Sahara. Le métal est en effet relativement léger pour une même résistance; de plus, la tenue à l'oxydation est excellente dans ces climats très secs.

Cependant la solution traditionnelle de ferme en treillis est à rejeter parce qu'onéreuse de transport et de montage. Il faut donc s'en tenir à des éléments porteurs rectilignes tels que profilés à froid, tôles pliées ou profilés courants assemblés et boulonnés sur poteaux H et poutres de contreventement en IPN.

Les nécessités de l'exposition optimum des insolateurs conduisent à adopter une toiture en shed dont la pente est tournée vers le sud.

L'air est amené par une gaine isolée inférieure; il circule de bas en haut dans les insolateurs et est recueilli chaud, dans une gaine isolée supérieure. Les figures 6 et 7 donnent tous les détails de construction. A remarquer les dispositions prévues pour

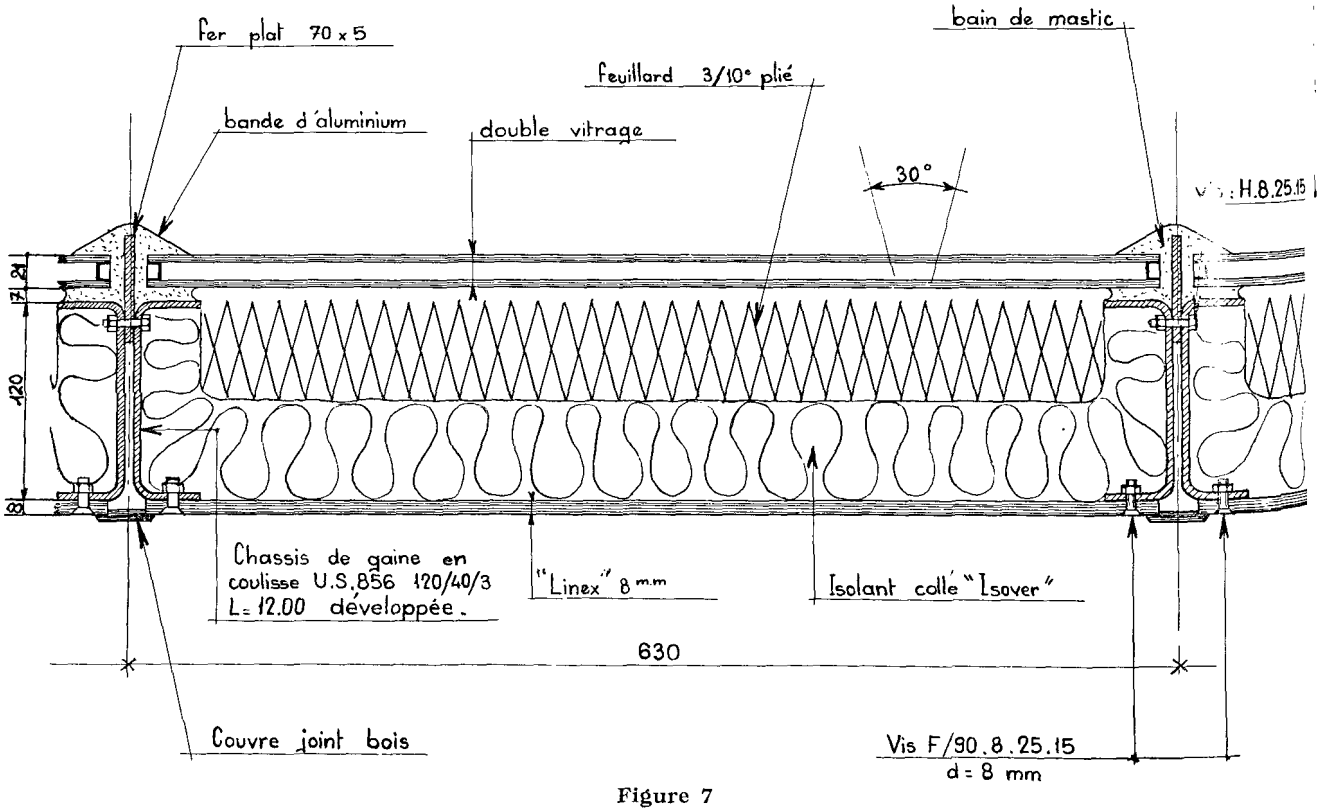


Figure 7

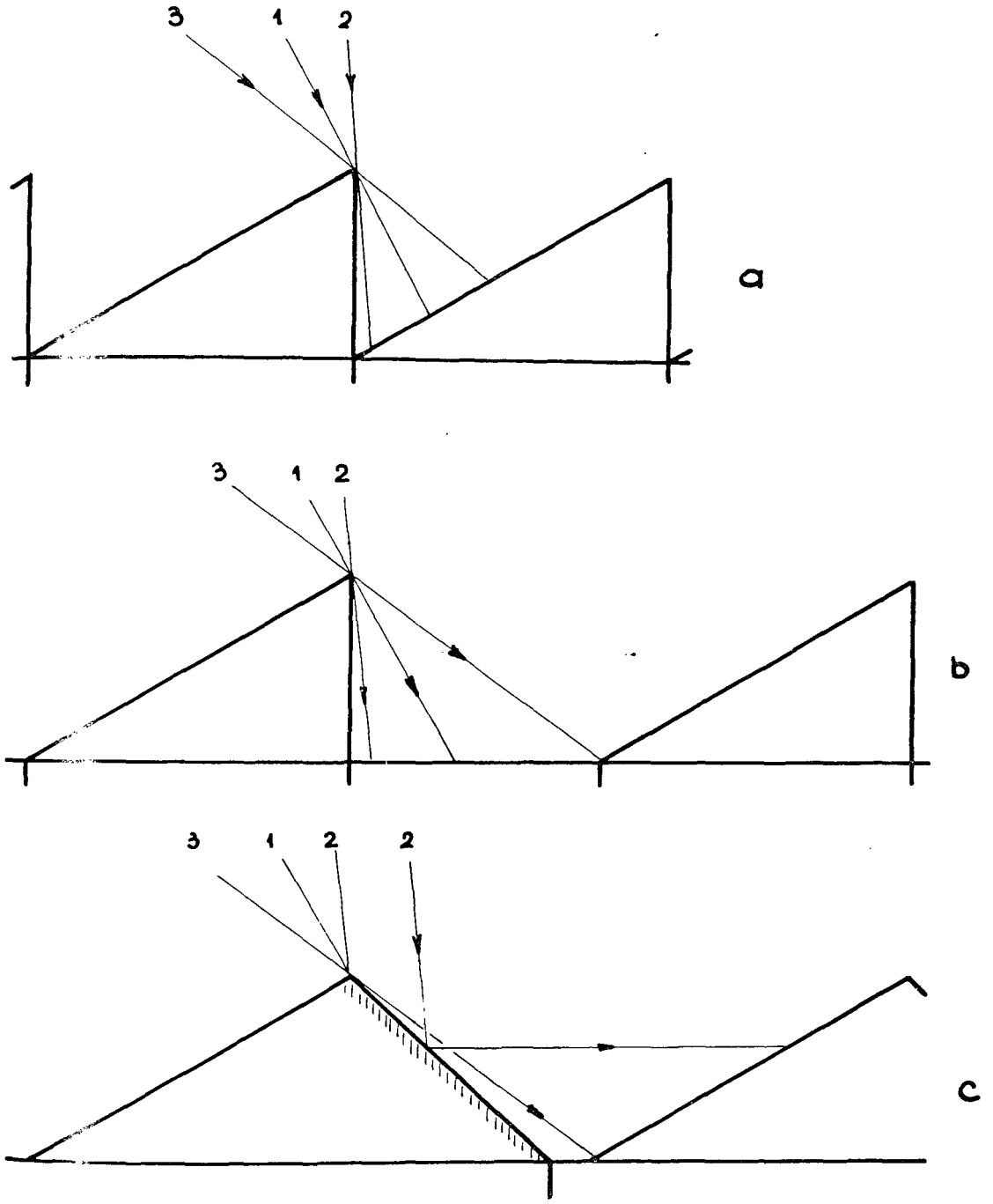


Figure 8

éviter de constituer des ponts thermiques entre les différentes parties de l'insolateur et de la charpente. L'été, l'insolation est totale; l'hiver, seule la partie supérieure de la couverture est insolée. Cela tient à l'ombre que chaque shed porte sur le shed suivant. Si l'on désirait avoir une insolation totale toute l'année, il y aurait lieu de séparer les bâtiments par un intervalle suffisant, mais cette disposition créerait des difficultés de contreventement et des suppléments de murs.

Les sheds peuvent avoir les dispositions représentées sur la figure 8. La forme (*a*), qui est la plus économique, est celle qui a été adoptée dans le présent travail. La forme (*b*) occupe davantage

de surface, mais les insolateurs sont constamment ensoleillés. La forme (*c*) occupe un peu moins de surface que la précédente, et permet, pendant la période estivale, le renforcement du rayonnement sur l'insolateur. La face nord des sheds peut en effet, dans ce cas, être recouverte d'éléments réfléchissants en aluminium, ou plus économiquement en plastique aluminé.

Il est évident que, pratiquement, les insolateurs n'occuperont jamais toute la surface couverte. Mais ces surfaces perdues pour la transformation en chaleur du rayonnement solaire sont à prendre en compte dans les frais imputables au bâtiment lui-même. Nos calculs du prix de revient seront donc pessima. La mise en place des diverses parties des insolateurs, l'entretien et le nettoyage, sont facilités par des passerelles d'entretien, roulant sur les lignes faîtières de deux sheds voisins.

Une distance de 5 à 6 mètres entre sheds paraît convenable pour avoir une bonne rigidité des supports rectilignes et une bonne tenue des vitrages, dont il faut éviter le bris sous les effets alternés du vent. Cette dimension permet en outre de limiter les hauteurs de sheds à 3 mètres environ.

En ce qui concerne les sheds, il paraît avantageux de les réaliser verticaux, afin d'obtenir des poutres de grande hauteur, d'assurer un contreventement efficace entre poteaux, et d'avoir éventuellement des travées plus longues que pourrait exiger la destination industrielle de certains bâtiments. Le bardage de la partie verticale des sheds peut être réalisé au moyen de plaques ondulées de polyester armé de fibres de verre.

Une évaluation approchée du prix de revient a montré que les transports intervenaient pour environ 10 p. 100 du total, et les frais d'hébergement de la main-d'œuvre pour 20 p. 100. Il y a donc intérêt à constituer des éléments entiers de couverture préfabriqués, groupant pannes et gaines chauffantes, mais vitrages bien entendu exclus. Le prix du transport s'en trouvera légèrement augmenté, mais la main-d'œuvre de montage sera notablement réduite, car il n'y aura plus qu'un assemblage rapide par boulons à faire sur place.

Insolateurs

Les insolateurs formant à la fois éléments de charpente, sont constitués de gaines préfabriquées comportant (voir figure 7) :

Deux longerons profilés en U à froid, entretoisés aux extrémités;

Un élément de plafond en « linex » (matériau isolant à base de fibre de lin et de résine synthétique), épaisseur 8 mm, vissé sous les ailes inférieures;

Des ouvertures aux extrémités pour l'arrivée et le départ de l'air;

Une isolation du fond et une isolation latérale, en feutre de fibre de verre (Isover), épaisseur 75 mm.

Les surfaces réceptrices de rayonnement sont formées de bandes de tôle mince noircie, pliées en accordéon aux angles de 30°, et maintenues en place par des fils métalliques. Ce système présente de nombreux avantages. Tout d'abord, la surface d'échange est multipliée par 2/cos 15° = 7,74. L'écart entre la température de l'air et celle de la surface réceptrice est moins grand. Ensuite, le fond isolant est à une température inférieure à celle de la surface réceptrice, diminuant ainsi les pertes par l'arrière; de plus, le facteur d'absorption de la surface réceptrice est augmenté. Cette surface peut être noircie, mais si l'on ne craint pas l'encrassement par les poussières, elle peut être aussi rendue sélective; enfin, les bandes étant d'une assez faible largeur (5 cm), les ondulations sont décalées d'un demi pas d'une bande à sa voisine, et le coefficient de transfert par convection s'en trouve notablement accru.

La couverture transparente est formée d'un double vitrage du type « Thermopane » ou similaire. Les éléments, de 0,60 m par 1,80 m, d'épaisseur totale 21 mm, présentent un encadrement métallique étanche, enfermant une lame d'air desséché de 12 mm; les dimensions adoptées sont les plus économiques, mais elles exigent l'emploi de trois longueurs par insolateur; l'assemblage est réalisé au moyen de joints plastiques; le poids de ces couvertures est de 20 kg/m².

La mise en place des couvertures se fait par masticage, un fer plat est, à cet effet, inséré entre deux longerons voisins, pour former té à vitrage. La qualité du mastic a une grosse importance, car il doit conserver son élasticité dans des conditions climatiques très dures. D'autre part, il faut observer que la toiture est soumise à des dépressions pouvant atteindre 90 kg/m², c'est-à-dire supérieures au poids des couvertures. Il est prévu d'utiliser soit le mastic « Stop Stora », qui a déjà fait ses preuves au Sahara, soit un ciment élastique à base de thiokol (PRC série 250). Une protection supplémentaire du mastic doit être réalisée par le collage d'une bande mince d'aluminium.

Les longerons ainsi que le masticage des couvertures font perdre environ 9 cm d'ensoleillement par insolateur, soit un peu moins de 15 p. 100 de la surface totale.

Évaluation

Frais de premier établissement

Nous donnons ci-après les résultats de l'étude détaillée des prix de la fourniture et de la main-d'œuvre, toutes charges et taxes comprises, ramenés au mètre carré. Ne sont pas compris, les murs de façades et leurs fondations, les peintures et les aménagements qui dépendent de la destination définitive des bâtiments, qui sont indépendants du mode de production de l'air chaud, et qui, en tout état de cause, appartiennent au bâtiment lui-même.

Évaluation des sheds avec insolateurs : prix au m²

	NF/m²
Fondations	8
Dallage	55
Charpente	140
Vitrages	125
Isolation des gaines	90
Bardage sheds	16,5
Plafond	26
Gaines de raccordement	60
Chéneaux	12,3
Descentes d'eau	1,7
Regards	4,2
Buses égouts	16
Total	554,70 couvert

soit pour la surface totale prise comme exemple :

$s = 11\,400$ m² Prix : 6 323 580 NF.

Dans le cas de l'édification des mêmes bâtiments en couverture traditionnelle aluminium ondulé, et isolation en laine de fibre de verre, les modifications de prix seraient :

		NF/m²	NF/m²
En déduction	Charpente : 140-100	40	
	Vitrages	125	
	Isolation	90	
	Gaines de raccordement	60	
			315
En supplément	Toiture aluminium	60	
	Isolation Isover + linex montés sur place y compris feutres spéciaux pour condensations	55	
			115
soit une plus-value de pour la solution insolateur.			200

Ainsi le supplément de dépenses occasionné par l'installation d'insolateurs pour produire de l'air chaud, serait pour la surface totale de . . . . . 2 280 000 NF

Il faut :

1) Ajouter à cette somme le prix des passerelles d'entretien et accessoires de nettoyage que nous avons évalués à . . . 5 000 NF

2) Déduire le coût de l'installation du chauffage-fuel précédemment évaluée . . . . . 350 000 NF

soit une moins-value de . . . . . 345 000 NF

Le supplément de dépenses ressort finalement à 1 935 000 NF

Des économies substantielles pourraient probablement être apportées si l'on pouvait remplacer la couverture de verre qui est assez lourde (20 kg/m²) par une couverture en film plastique. Reprenons l'évaluation dans cette hypothèse.

	NF/m²
Fondations	8
Dallage	55
Charpente	125
Couverture	35
Isolation des gaines	80
Bardage sheds	16,5
Plafond	26
Gaines de raccordement	60
Chéneaux	12,3
Descentes d'eau	1,7
Regards	4,2
Buses égouts	16
	439,7

soit pour la surface totale : 5 012 580 NF.

Dans le cas de la couverture traditionnelle, on aurait :

		NF/m²
En déduction :	Charpente	15 NF
	Couverture	35 NF
	Isolation	80 NF
	Gaines de raccordement	60 NF
		190
En supplément		115
soit une plus-value de		75 NF

et pour la surface totale : 855 000 NF.

Dans ce cas, le supplément de dépenses occasionné par l'installation d'insolateurs ne serait, pour la surface totale, que de

$$855\,000 - 355\,000 = 500\,000 \text{ NF}.$$

Frais d'exploitation

On peut admettre en première approximation que les frais de main-d'œuvre pour le nettoyage et l'entretien des insolateurs sont à peu près équivalents aux frais occasionnés par la conduite et l'entretien de l'installation de chauffe au mazout. Il est prudent toutefois de compter sur le remplacement de 1 p. 100 environ des couvertures de verre, brisées pour des raisons diverses. Là aussi, on peut admettre que ces frais de remplacement sont du même ordre de grandeur que les frais de réparation et de rechange du matériel de chauffage par combustible. L'économie annuelle est donc en définitive constituée par la valeur du combustible que l'on aurait dû brûler pour la même production de chaleur. Cette économie varie de 110 000 à 190 000 NF environ, suivant les caractéristiques de la production, ainsi que nous l'avons indiqué plus haut.

Nous n'ignorons pas combien doivent être nuancées les conclusions que l'on peut tirer de ces évaluations. Nous nous contenterons de faire observer qu'il apparaît avantageux d'utiliser l'énergie solaire lorsqu'il s'agit d'un chauffage d'air ne nécessitant pas de températures élevées. Une expérimentation à grande échelle paraît, dans ce cas, devoir être tout à

fait légitime. D'autant plus que nous avons volontairement conduit nos calculs dans les hypothèses les plus défavorables pour l'utilisation du rayonnement solaire.

L'intérêt de l'analyse à laquelle nous nous sommes livrés se trouve dans les valeurs relatives des différents postes de dépenses. Des améliorations importantes, on l'a vu, peuvent sans doute être apportées au projet tel que nous venons de l'exposer. Ainsi, la suppression de la couverture en verre et son remplacement par une couverture en film plastique, ainsi que l'allègement des surfaces d'échange, peuvent avoir une incidence directe sur les prix des postes correspondants, mais apporter également une réduction sensible du poids de la charpente.

D'autre part, le rendement thermique des insolateurs du type adopté sera très certainement, dans la pratique, notablement supérieur à celui que nous avons supposé pour rester pessimistes.

Étude comparative de divers types d'insolateurs

Les insolateurs à air peuvent se classer en deux grands groupes selon qu'ils fonctionnent avec ou sans effet de serre.

Insolateurs avec effet de serre

La couverture transparente peut être de verre et comporter une ou plusieurs lames d'air. L'expérience montre qu'il n'y a pas intérêt, sauf dans des cas particuliers, à dépasser deux lames d'air, soit une couverture transparente et deux sous-couvertures. La couverture doit pouvoir résister aux efforts du vent, qui souffle d'une manière particulièrement violente au Sahara. On est conduit à adopter pour la couverture le verre double (3,6 mm d'épaisseur) de 0,50 m à 0,60 m de large, et pour les sous-couvertures, des verres simples (1,8 mm d'épaisseur). Si la manutention est organisée mécaniquement, il y a intérêt à utiliser des panneaux préfabriqués tels que le « Thermopane » de St-Gobain ce qui réduit le risque de casse. La couverture de verre est assez lourde et constitue la partie la plus onéreuse de l'insolateur. D'autre part, elle se salit facilement et exige des travaux de nettoyage fréquents.

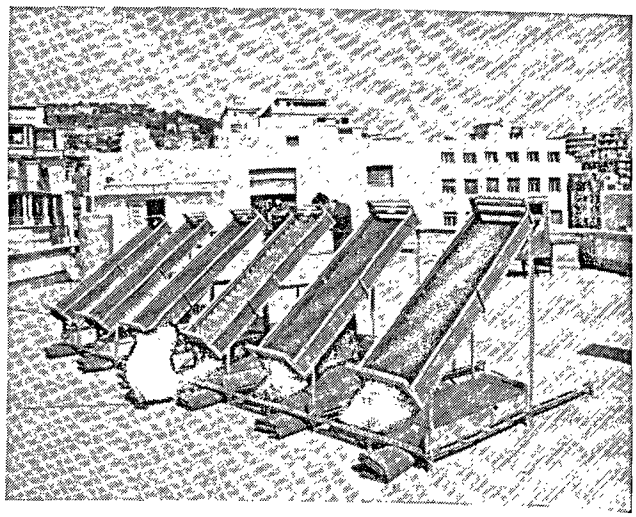


Figure 9

Des couvertures en plastique transparent peuvent être envisagées. Leurs propriétés optiques dans l'infra-rouge sont moins bonnes que le verre, mais elles sont incomparablement plus légères et présentent moins de risques de détérioration.

L'Institut de l'énergie solaire étudie actuellement une couverture utilisant le « Terphane », qui est le Mylar français. Cette couverture est en principe formée d'un cylindre de plastique de 0,06 mm d'épaisseur à bords collés suivant une génératrice. Ce cylindre s'enfile sur un cadre léger formé de deux tubes d'aluminium de 1 cm de diamètre, entretoisés par des tiges minces élastiques. On obtient ainsi une couverture toujours tendue emprisonnant une lame d'air.

La surface réceptrice du rayonnement solaire peut être pleine ou poreuse, en métal ou en matériau isolant, noircie ou recouverte d'un enduit à émission sélective. Elle peut être plane et offrir à la convection la même surface que l'insolateur, ou au contraire ondulée, pliée, plissée ou comportant des ailettes.

Les parois poreuses, c'est-à-dire les parois qui tout en étant opaques à la lumière, se laissent facilement traverser par l'air, sont d'une très grande diversité. Les expérimentateurs américains ont utilisé le grillage métallique, qui est excellent, mais lourd et cher; ils ont utilisé aussi un feuilletage de lames de verre partiellement noircies. Ce procédé est également lourd et onéreux. Nous avons ajouté à ces surfaces classiques des surfaces lamellaires ou en forme d'aubes, en métal ou en plastique, ainsi que des grilles en textile, en paille de riz ou en roseau.

Nous nous sommes arrêtés, pour le projet concernant l'insolateur précédemment exposé, aux surfaces en tôle mince, pliées en accordéon, aux angles de 30°. D'autres surfaces plus complexes, et dont la fabrication nécessiterait une mise au point industrielle pour les obtenir à bas prix, sont également en cours d'essais ou de projets.

La circulation de l'air se fait soit sur la surface isolée, soit au-dessous d'elle, soit au travers des surfaces; les coefficients de convection sont nettement plus élevés dans ce dernier cas.

Il est à signaler que les surfaces métalliques continues ont l'inconvénient de régulariser la température par conduction; les températures obtenues par ces surfaces sont moins élevées qu'avec les surfaces isolantes. Par contre, à égalité de température finale, elles sont d'un meilleur rendement.

Insolateurs sans effet de serre

Ces insolateurs sont d'une plus grande rusticité que les précédents, et le nettoyage des surfaces exposées aux intempéries présente moins d'impor-

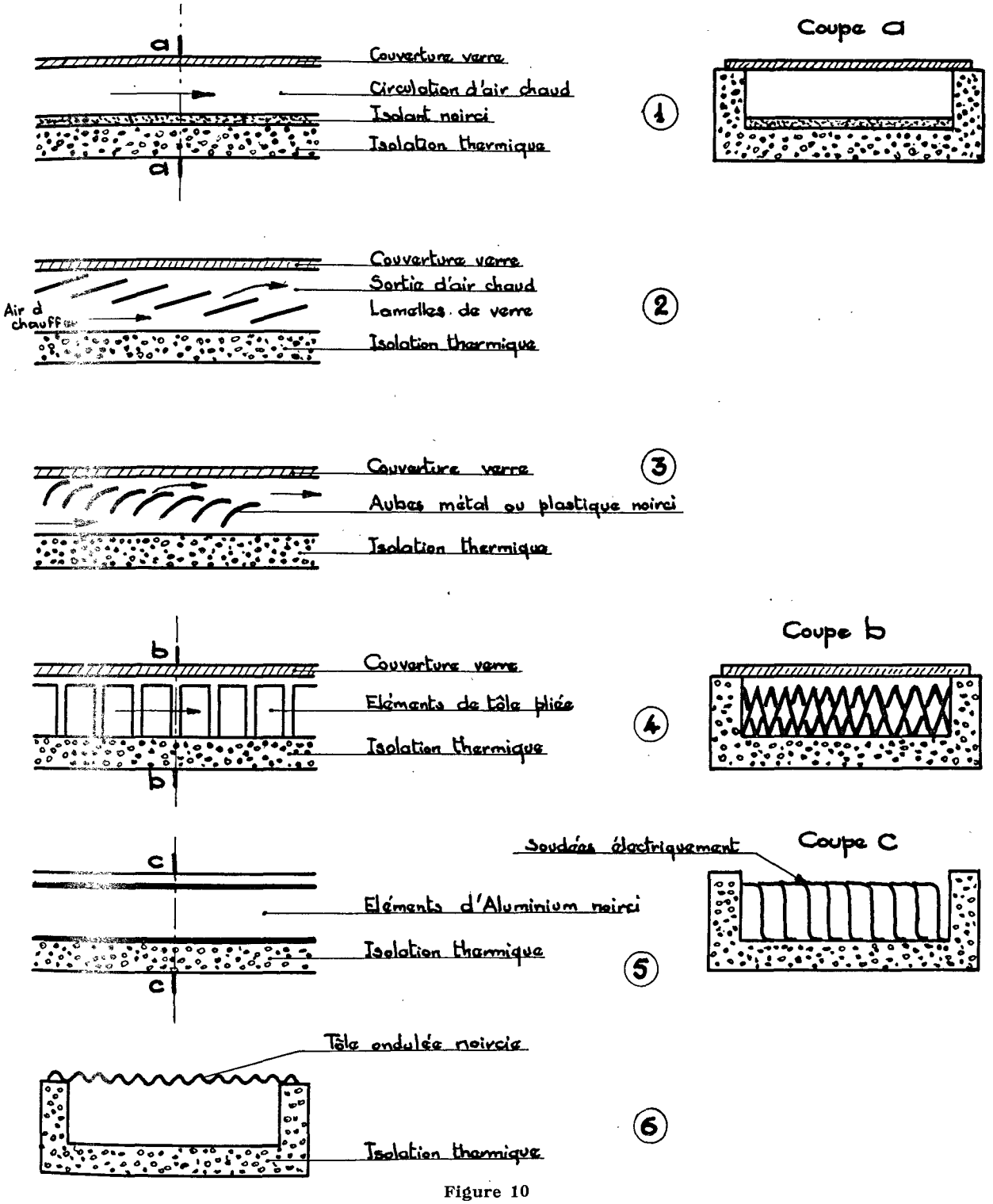


Figure 10

tance. On ne peut guère envisager que des surfaces réceptrices non sélectives, l'encrassement ayant pour effet de rendre la sélectivité inopérante; d'autre part, les surfaces sélectives sont toujours délicates et demandent à être protégées.

Le rendement des insolateurs sans effet de serre est nécessairement beaucoup plus faible que celui de ceux qui sont munis d'une couverture opaque au rayonnement infra-rouge; d'autre part, il est nécessaire que la chaleur traverse par conduction la surface réceptrice, afin de pouvoir chauffer l'air qui circule sur l'autre face. Cela exige que les surfaces réceptrices soient métalliques. La face inférieure en contact avec l'air peut être munie d'ailettes pour faciliter les transferts de chaleur par convection. La surface réceptrice doit en principe être plane,

fait légitime. D'autant plus que nous avons volontairement conduit nos calculs dans les hypothèses les plus défavorables pour l'utilisation du rayonnement solaire.

L'intérêt de l'analyse à laquelle nous nous sommes livrés se trouve dans les valeurs relatives des différents postes de dépenses. Des améliorations importantes, on l'a vu, peuvent sans doute être apportées au projet tel que nous venons de l'exposer. Ainsi, la suppression de la couverture en verre et son remplacement par une couverture en film plastique, ainsi que l'allègement des surfaces d'échange, peuvent avoir une incidence directe sur les prix des postes correspondants, mais apporter également une réduction sensible du poids de la charpente.

D'autre part, le rendement thermique des insolateurs du type adopté sera très certainement, dans la pratique, notablement supérieur à celui que nous avons supposé pour rester pessimistes.

Étude comparative de divers types d'insolateurs

Les insolateurs à air peuvent se classer en deux grands groupes selon qu'ils fonctionnent avec ou sans effet de serre.

Insolateurs avec effet de serre

La couverture transparente peut être de verre et comporter une ou plusieurs lames d'air. L'expérience montre qu'il n'y a pas intérêt, sauf dans des cas particuliers, à dépasser deux lames d'air, soit une couverture transparente et deux sous-couvertures. La couverture doit pouvoir résister aux efforts du vent, qui souffle d'une manière particulièrement violente au Sahara. On est conduit à adopter pour la couverture le verre double (3,6 mm d'épaisseur) de 0,50 m à 0,60 m de large, et pour les sous-couvertures, des verres simples (1,8 mm d'épaisseur). Si la manutention est organisée mécaniquement, il y a intérêt à utiliser des panneaux préfabriqués tels que le « Thermopane » de St-Gobain ce qui réduit le risque de casse. La couverture de verre est assez lourde et constitue la partie la plus onéreuse de l'insolateur. D'autre part, elle se salit facilement et exige des travaux de nettoyage fréquents.

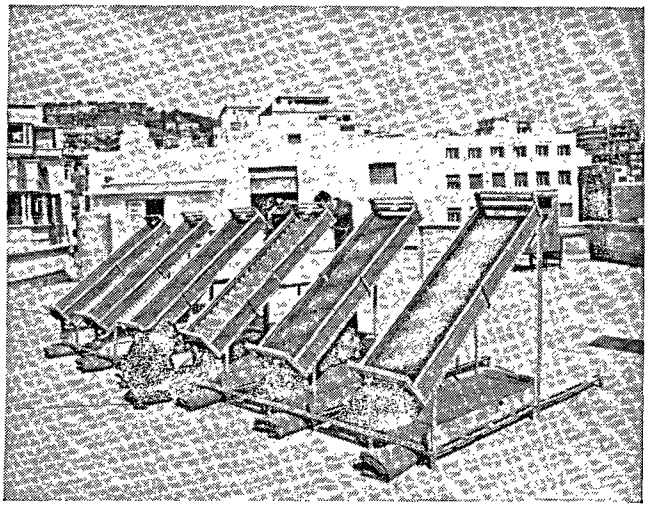


Figure 9

Des couvertures en plastique transparent peuvent être envisagées. Leurs propriétés optiques dans l'infra-rouge sont moins bonnes que le verre, mais elles sont incomparablement plus légères et présentent moins de risques de détérioration.

L'Institut de l'énergie solaire étudie actuellement une couverture utilisant le « Terphane », qui est le Mylar français. Cette couverture est en principe formée d'un cylindre de plastique de 0,06 mm d'épaisseur à bords collés suivant une génératrice. Ce cylindre s'enfile sur un cadre léger formé de deux tubes d'aluminium de 1 cm de diamètre, entretoisés par des tiges minces élastiques. On obtient ainsi une couverture toujours tendue emprisonnant une lame d'air.

La surface réceptrice du rayonnement solaire peut être pleine ou poreuse, en métal ou en matériau isolant, noircie ou recouverte d'un enduit à émission sélective. Elle peut être plane et offrir à la convection la même surface que l'insolateur, ou au contraire ondulée, pliée, plissée ou comportant des ailettes.

Les parois poreuses, c'est-à-dire les parois qui, tout en étant opaques à la lumière, se laissent facilement traverser par l'air, sont d'une très grande diversité. Les expérimentateurs américains ont utilisé le grillage métallique, qui est excellent, mais lourd et cher; ils ont utilisé aussi un feuilletage de lames de verre partiellement noircies. Ce procédé est également lourd et onéreux. Nous avons ajouté à ces surfaces classiques des surfaces lamellaires ou en forme d'aubes, en métal ou en plastique, ainsi que des grilles en textile, en paille de riz ou en roseau.

Nous nous sommes arrêtés, pour le projet concernant l'insolateur précédemment exposé, aux surfaces en tôle mince, pliées en accordéon, aux angles de 30°. D'autres surfaces plus complexes, et dont la fabrication nécessiterait une mise au point industrielle pour les obtenir à bas prix, sont également en cours d'essais ou de projets.

La circulation de l'air se fait soit sur la surface isolée, soit au-dessous d'elle, soit au travers des surfaces; les coefficients de convection sont nettement plus élevés dans ce dernier cas.

Il est à signaler que les surfaces métalliques continues ont l'inconvénient de régulariser la température par conduction; les températures obtenues par ces surfaces sont moins élevées qu'avec les surfaces isolantes. Par contre, à égalité de température finale, elles sont d'un meilleur rendement.

Insolateurs sans effet de serre

Ces insolateurs sont d'une plus grande rusticité que les précédents, et le nettoyage des surfaces exposées aux intempéries présente moins d'impor-

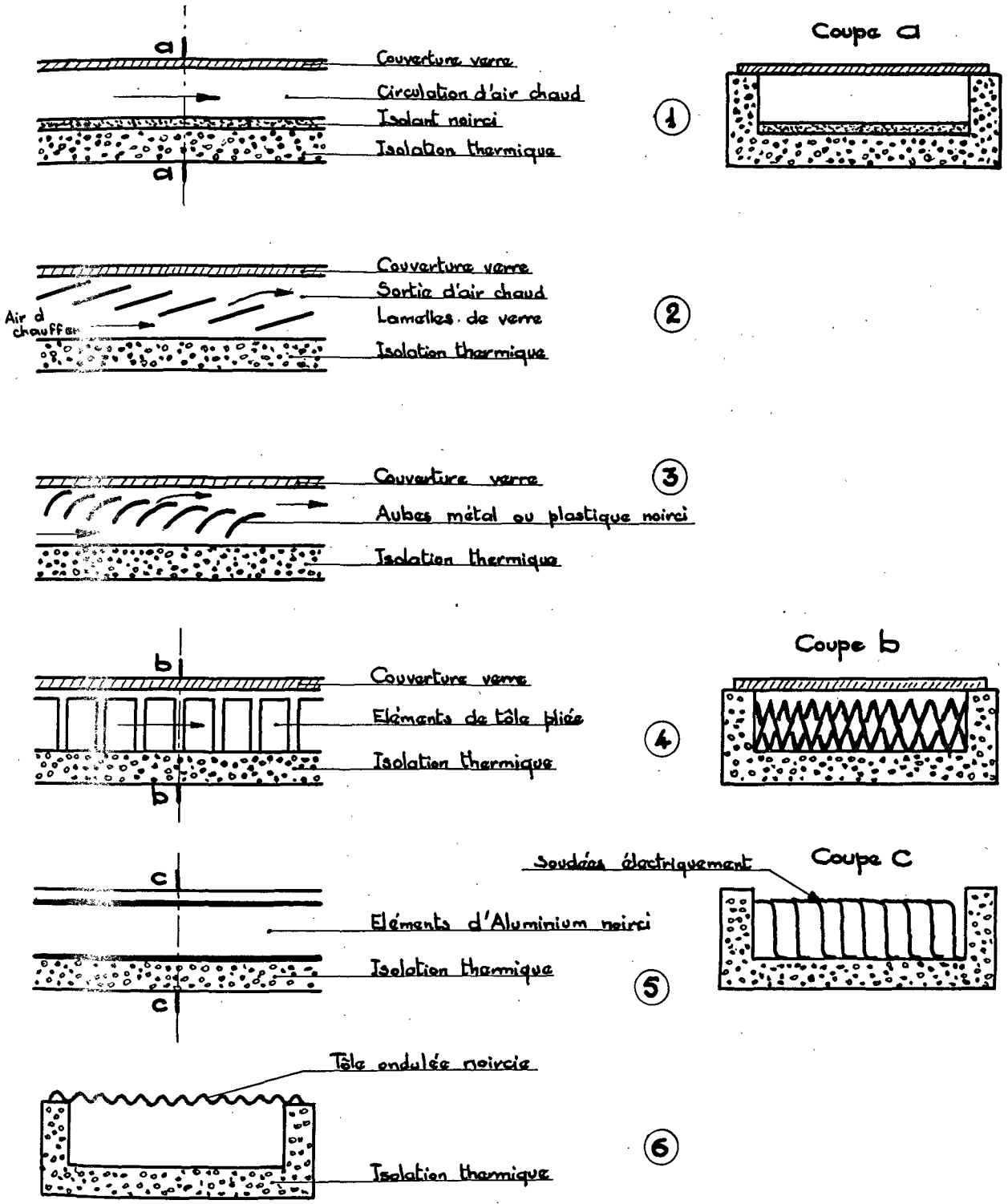


Figure 10

tance. On ne peut guère envisager que des surfaces réceptrices non sélectives, l'encrassement ayant pour effet de rendre la sélectivité inopérante; d'autre part, les surfaces sélectives sont toujours délicates et demandent à être protégées.

Le rendement des insolateurs sans effet de serre est nécessairement beaucoup plus faible que celui de ceux qui sont munis d'une couverture opaque au rayonnement infra-rouge; d'autre part, il est nécessaire que la chaleur traverse par conduction la surface réceptrice, afin de pouvoir chauffer l'air qui circule sur l'autre face. Cela exige que les surfaces réceptrices soient métalliques. La face inférieure en contact avec l'air peut être munie d'ailettes pour faciliter les transferts de chaleur par convection. La surface réceptrice doit en principe être plane,

pour présenter à sa partie supérieure le minimum de pertes par convection naturelle. Cependant, certains expérimentateurs ont utilisé la tôle ondulée ou la tôle pliée.

Les essais qui sont actuellement en cours, se développent de la manière suivante.

Les surfaces à étudier, groupées par six, sont exposées simultanément et dans des conditions aussi identiques que possible au rayonnement solaire. Les perturbations apportées par les variations de la radiation solaire, et de la température ambiante, de l'humidité atmosphérique et du vent, sont de cette manière pratiquement éliminées.

On mesure alors les températures et les débits d'air. Les résultats n'ont qu'une valeur relative, mais permettent de classer les surfaces, en comparant leur rendement, leurs pertes de charge et leur prix de revient.

Nous espérons ainsi, à l'issue des essais, pouvoir retenir un petit nombre de surfaces présentant un maximum d'avantages et susceptibles d'être industriellement utilisées.

La figure 9 donne une vue d'ensemble de l'installation qui a été montée sur la terrasse du bâtiment de Physique de l'Université d'Alger. La figure 10 donne les schémas de quelques-unes des surfaces en essais.

L'expérimentation est faite par le personnel du laboratoire de Physique P.C.B. de l'Université d'Alger, que nous remercions ici, et plus particulièrement A. Zerouki, qui s'est chargé des mesures et des calculs comparatifs.

Conclusion

L'intérêt pratique des insolateurs à exposition directe est assez limité; cependant, pour certaines applications qui n'exigent que des températures tout au plus égales à 100 °C, le travail d'avant-projet auquel nous nous sommes livrés montre que ces sortes d'appareils ne sont pas à rejeter, à priori.

L'Institut de l'énergie solaire de l'Université d'Alger s'intéresse plus spécialement à l'utilisation des insolateurs comme organes statiques permettant de faire circuler des masses importantes d'air pouvant être utilisées au refroidissement des générateurs thermo-électriques. Les études qui concernent cette application particulière sont actuellement en cours.

Résumé

La transformation du rayonnement solaire en chaleur à température relativement basse peut s'effectuer dans des appareils de construction simple et de position fixe, les insolateurs plats. Leur simplicité et leur faible prix de revient permettent de les implanter sur de grandes surfaces, donc de recueillir de grandes quantités de chaleur.

L'Institut de l'énergie solaire a envisagé la production à grande échelle d'air chaud qui pourrait servir à des usages divers : conditionnement de locaux, production d'énergie, constitution d'une source froide par circulation d'air pour des générateurs thermo-électriques.

Dans cet ordre d'idées, l'auteur s'est attaché à deux problèmes : 1) Étude d'une installation complète à grande surface d'insolateurs à air, d'un type déterminé; 2) Étude expérimentale comparative de divers types d'insolateurs.

Dans la première étude, on a supposé l'installation des insolateurs en un point déterminé, mais arbitraire, du plateau du Tadémaït, au Sahara. Ce point a pour principales caractéristiques climatologiques :

Température moyenne annuelle : 22,1 °C;

Tension partielle moyenne de vapeur d'eau : $t = 3$ mm de mercure;

Facteur d'ensoleillement moyen : $\sigma = 0{,}843$.

Le champ d'insolateurs a été considéré de deux points de vue, en tant que générateur d'air chaud, et en tant que couverture des bâtiments où serait utilisé cet air chaud.

De ce fait, le prix de revient de l'installation de chauffage d'air est la différence entre le prix de revient de l'ensemble et celui d'une charpente et d'une couverture classiques couvrant la même surface.

De l'étude climatologique de la station, il ressort que, pour obtenir un rendement optimum des surfaces absorbantes, les insolateurs doivent être inclinés sur l'horizontale d'un angle sensiblement égal à la latitude du lieu.

Étude de la production d'air chaud

Pour étudier le fonctionnement d'un insolateur, l'auteur a utilisé une méthode d'analogie électrique. L'expérimentation analogique a permis de tracer les courbes de la puissance utile en fonction de la puissance absorbée :

A θ constant, θ étant l'écart entre la température ambiante et la température de l'air à sa sortie de l'insolateur;

A débit d'air constant.

On a étudié plus spécialement la production d'air chaud à θ = Cte.

Les relevés climatologiques au point considéré donnent les diagrammes journaliers de la radiation solaire directe. On en déduit les diagrammes de la radiation normale au plan de l'insolateur, et, connaissant les caractéristiques de la surface absorbante, les diagrammes de la puissance absorbée, abstraction faite de la radiation diffuse, ce qui est une hypothèse pessimiste.

Ces diagrammes, joints à celui de la puissance utile en fonction de la puissance absorbée, à θ constant, permettent de tracer les diagrammes journaliers de la puissance utile pour deux valeurs arbitraires de θ, soit $\theta = 40$ °C et $\theta = 70$ °C.

Il est possible alors de calculer la production annuelle de chaleur d'une installation d'insolateurs couvrant une superficie assez étendue, un hectare par exemple.

Pour $\theta = 40$ °C, la production annuelle est de $5{,}62 \times 10^3 M$ kcal,

pour $\theta = 70$ °C, la production annuelle est de $3{,}24 \times 10^2 M$ kcal.

Si l'on avait utilisé du fuel industriel pour produire les mêmes quantités de chaleur, on aurait dépensé

669 T, soit 189 327 NF dans le premier cas,
386 T, soit 109 238 NF dans le second.

L'installation de chauffage au fuel montée au point choisi, coûterait environ 350 000 NF.

Étude de l'installation

Du fait de l'éloignement et de la difficulté d'accès, les problèmes de transport et de main-d'œuvre sont prépondérants. On a donc envisagé l'usage de matériaux légers et peu encombrants, et l'emploi d'un personnel réduit et de qualité, pour le montage.

La charpente a été conçue en éléments métalliques rectilignes avec toiture en shed à pente dirigée vers le sud. Chaque shed portant une ombre sur le suivant, la longueur insolée varie selon les saisons.

L'air froid arrive par une gaine à la base du shed et l'air chaud est collecté dans une autre gaine au sommet.

Les insolateurs proprement dits sont en éléments préfabriqués : la surface absorbante est constituée par des bandes de tôle noircie pliées en accordéon. Elle est isolée au fond et sur les côtés par un feutre de fibre de verre, et recouverte d'un double vitrage. La surface occupée au sol pour un hectare utile, est de 11 400 m².

La comparaison des prix d'une installation traditionnelle et d'une couverture à insolateurs fait ressortir une plus-value de 1 935 000 NF pour cette dernière. Si la couverture de verre pouvait être remplacée par une couverture en film plastique, cette plus-value pourrait être ramenée aux environs de 500 000 NF.

Quant aux frais d'exploitation, on peut considérer en première approximation qu'ils sont équivalents à ceux d'une installation de chauffe au mazout, tant pour les frais de main-d'œuvre, que pour les frais d'entretien et réparation du matériel.

En définitive, l'économie annuelle est constituée par la valeur du combustible qui aurait dû être brûlé pour la même production de chaleur, soit 110 000 à 190 000 NF.

En fait, l'auteur s'est toujours placé dans les conditions les plus défavorables. Les résultats réels seraient certainement supérieurs à ceux qui viennent d'être indiqués.

Étude comparative de divers types d'insolateurs

Insolateurs avec effet de serre. — La couverture transparente peut être constituée de lames de verre emprisonnant des lames d'air (deux au maximum). Il y a intérêt à utiliser des panneaux préfabriqués pour faciliter la manutention.

Mais le verre est lourd et se salit facilement. L'Institut de l'énergie solaire étudie une couverture en « Terphane », double film plastique de 0,06 mm d'épaisseur.

Les surfaces absorbantes sont de genres très divers : métalliques ou isolantes, pleines ou poreuses, planes ou ondulées. Plusieurs types de surfaces poreuses sont expérimentés par l'Institut de l'énergie solaire.

Insolateurs sans effet de serre. — Ces insolateurs sont de construction plus simple que les précédents, et le problème du salissement a moins d'importance, mais il rend impossible l'emploi de surfaces sélectives.

Le rendement est beaucoup plus faible en raison des pertes par rayonnement infra-rouge, conduction et convection.

Les essais se font par exposition simultanée de six surfaces différentes au rayonnement solaire. Il est alors possible de classer ces surfaces par comparaison des rendements, pertes de charge et prix de revient.

De cette expérimentation, l'auteur espère pouvoir retenir un petit nombre de surfaces susceptibles d'être utilisées industriellement.

Conclusion

L'intérêt pratique des insolateurs à exposition directe est assez limité, cependant pour certaines applications qui n'exigent que des températures tout au plus égales à 100 °C, le travail d'avant-projet auquel l'auteur s'est livré montre que ces sortes d'appareils ne sont pas à rejeter, *a priori*.

L'Institut de l'énergie solaire de l'Université d'Alger s'intéresse plus spécialement à l'utilisation des insolateurs comme organes statiques permettant de faire circuler des masses importantes d'air pouvant être utilisées au refroidissement des générateurs thermo-électriques. Les études qui concernent cette application particulière sont actuellement en cours.

ECONOMIC STUDY OF THE OPERATION OF ATMOSPHERIC SOLAR COLLECTORS IN THE SAHARA

(Translation of the foregoing paper)

*M. Touchais**

Solar radiation is an undergraded form of energy. Its conversion into heat for subsequent conversion into other forms of energy should obviously be accomplished at the highest possible temperature. But to obtain high temperatures means that the radiation must first be concentrated, using mirrors and orientation mechanisms at a cost that may *a priori* appear necessarily very high.

It is known, however, that important uses for thermal energy can be found even at fairly low temperatures. The conversion of solar radiation into heat may in that case be accomplished by simple flat fixed-position plate collectors. Efforts are being made to develop such collectors in the most economic versions possible.

The heating of fluids, air or water, for various uses essentially directed towards modifying the living conditions in the desert, is viewed as an important problem by the Institute of Solar Energy. This organization is concerned primarily with the Sahara, and believes that the solution towards making it habitable should be sought in the conversion of solar radiation, very abundant in subtropical regions.

Numerous methods of solar heating of water or air have been developed, and many investigators or experimenters are occupied with this problem. We do not claim to be innovators. But these methods have usually been conceived on a relatively small scale. We do believe, however, that the utilization of solar energy could not be of interest unless it involved the conversion of very large amounts of radiation, or, what amounts to exactly the same thing, unless it envisaged the installation of very large irradiated surfaces. Therefore we propose to work, not on the scale of the square metre, but on that of the hectare. In that case the technological problems assume an entirely different aspect.

We shall deliberately confine ourselves to the problem of hot-air production, first of all because hot air is used directly for: winter space-heating; summer circulation of air cooled by humidification; producing a heat sink by means of air circulation for possible thermal machines such as combustion engines or thermoelectric generators.

This latter use, surprisingly enough, was the starting point of the work we shall report here. We rapidly realized, however, that this specialized problem would bring us to the treatment of the general problem.

For the sake of completeness, we may add that the conversion of solar radiation into kinetic energy of the air can give rise to a secondary conversion into mechanical energy, whose value and limits might be of interest.

We confined ourselves to hot-air production alone for the further reason that the thermal inertia of solar collectors in air is relatively small, and experimentation, whether direct or by electrical simulation, is simple and rapid.

It should be noted, on the other hand, that the results obtained for solar collectors in air may serve as a base for studying water heaters and low-temperature evaporators.

We decided to conduct our study in the following way. The results of earlier investigators could orient us directly toward a particular type of medium-performance collector with not too high construction costs. It would then be sufficient to make a detailed study of the technological and economic operation of large-scale collectors of this type, and to compare their characteristics with those of other types, without being compelled to make an economic study for each of them. The work thus comprises two almost independent parts : 1. Study of a complete plant with a large atmospheric collector surface, of a specified type; 2. Comparative experimental study of various types of atmospheric solar collectors.

Desiring to eliminate, in part 1, the parameters which are not of direct interest, though they might be of economic importance, we decided to base our study on a very definite but entirely arbitrary site location, at the point on the Tademait plateau in the Sahara (figure 1), at altitude 670 m, at 28°48′ N. lato, 2°32′ E. long., on the trail from Algiers to In-Salah, approximately equidistant from El Golea, Timimoun and In Salah. This point is located in the middle of the desert, reasonably close to Algiers and relatively accessible. Its sunshine fraction is high, and there are fairly close meteorological stations on several sides, so that the climatological characteristics to be used can be easily interpolated.

* Engineer in charge of research, Institut de l'énergie solaire, Université d'Alger, Algéria.

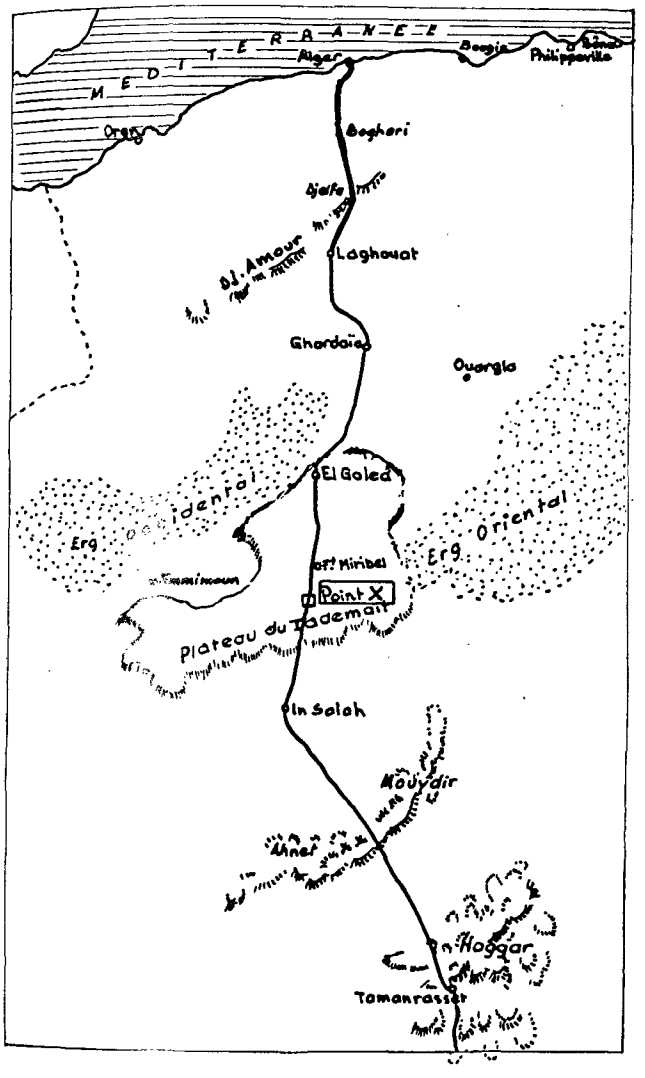


Figure 1

These characteristics are :

(1) *Temperatures, °C :*

	Max.	*Min.*	*Mean*	*Daily range*	*Annual mean*
January .	16	2.3	9.5	14.5	22.1
July . .	40	24.5	32	16	

(2) *Humidity :* The mean partial vapor pressure of water vapor is 3 mm Hg.

(3) *Mean sunshine factor :* $\sigma = 0.843$.

To facilitate the discussion, this arbitrary point will hereafter be termed point X.

We assumed that the insolated surfaces could serve two purposes :

(*a*) Hot-air generating insolation proper;

(*b*) Protection against the sun and weather afforded by a collector used at the same time as a sheltering cover.

In other words, since the function of the collector is inseparable from its utilization, which demands the existence of buildings, we assume the actual cost of collector installation to have been diminished by the cost of hypothetical buildings covering the same area but roofed by conventional methods.

This viewpoint is obviously peculiar to the Sahara climate, and it would have been a mistake to ignore it in estimating the costs. Its first advantage is that it eliminates the effect of collector height on construction costs. (It will be recalled that the collectors must be installed above the ground to avoid damage from the scouring action of sandstorms.) At 3 metres above the ground, the equipment will be exposed only to dust storms. We assumed, consequently, that the girders of the framework support the collectors 3 metres above the ground. Any other height would be attributable to the building itself, not to the collector field.

We also assumed that the collectors should face the south and be inclined to the horizon at an angle substantially equal to the latitude of the place, which is the optimum angle at the site selected, where the cloudiness and atmospheric absorption are relatively low.

The mean exposure is longer for inclined collectors, and the slope makes it easier to clean the surfaces. This problem of keeping the collector surfaces clean is one of the greatest difficulties in the use of collectors in the Sahara and is responsible for relatively important operating costs, which we shall take into account.

Three possibilities for utilizing the hot air may be envisaged :

(1) Use of the hot air for air conditioning the buildings covered by the collectors. Winter heating and summer refrigeration by humidification without the need for any accessory system such as boilers, compressor groups, etc.

(2) Use of the air motion due to the draft of a chimney for cooling thermal machines, especially for cooling thermoelectric generators.

(3) Incidental utilization of the kinetic energy of the air so put into motion.

Operating graph for atmospheric solar collectors

Notation

l, width of channel, m.

L, irradiated length of channel, m. L may vary with the season, according to the arrangements adopted. The irradiated surface is $L\,l$, m².

h, height of channel, m, taken as constant.
the cross-sectional area of the channel is $l\,h$, m².

x, abscissa of section studied from the beginning of the irradiated part; x varies from 0 to L.

Δx, element of collector 1 m wide, of abscissa x.

T_x, temperature of air at entrance to section of abscissa x; $T_x + \Delta T_x$ is the temperature on leaving that element. T_x varies from T_e to T_s from entrance to exit.

T_a, temperature of the ambient atmosphere above the cover.

T_i, temperature of the interior atmosphere below the insulated bottom.

T_{v_e}, temperature of the celestial vault, here taken systematically as 0°C.

q_{i_Θ}, incident radiation, W/m².

q_a, radiation absorbed by the surfaces converting it into heat, W/m².

$$q_a = \alpha_s \tau_v Q_{i_\Theta} \quad (1)$$

where α_s is the absorption factor of the receiving surfaces, and τ_v is the transmission factor of the cover, which is assumed to be almost independent of the altitude of the sun.

q_{p_c}, calorific power lost through the cover, W/m².

q_{p_f}, calorific power lost through the floor of the collector.

q_p, calorific power lost by the collector

$$q_p = q_{p_c} q_{p_f} \quad (2)$$

q_u, heating of the air, W/m²

$$q_u = q_a - q_p \quad (3)$$

v, velocity of the air on entering the irradiated part, m/s. The volume discharge is $v\, l\, h$, m³/s.

V, wind speed, m/s.

e, relative humidity of the air.

ρ, specific mass of the air at the entrance, kg/m³. For dry air

$$\rho = 0.4645 \frac{P_a}{Te\ 273} \quad (4)$$

where P_a is the atmospheric pressure, which at the site selected is 706 mm Hg.

C_p, specific heat of the air, J/kg°C.

m, mass discharge of air, kg/s; at the entrance to the irradiated part,

$$m = \rho\, l\, \mathrm{hv} \quad (5)$$

and

$$q_u \Delta x = m\, C_p\, \Delta T_x \quad (6)$$

or

$$\frac{dT_x}{dx} = \frac{q_u}{m\, C_p}. \quad (7)$$

Q_a, total radiation received by the receiving surface

$$Q_a = q_a\, L\, l \quad (8)$$

Q_p, total radiation lost

$$Q_p = \int_o^L q_p\, dx \quad (9)$$

Q_u, total heating of the air at exit

$$Q_u = \int_o^L q_u\, dx = m\, C_p\, (T_s - T_e) \quad (10)$$

S, total area occupied on the ground.

N, number of collectors. The total irradiated area is $N\, l\, L$.

The collector is assumed to operate under steady conditions.

The analytic study of the collector operation is made difficult by the presence of nonlinear heat transfer coefficients. One must either apply direct experiment, in spite of the serious difficulties, or use an analogous method, assuming the heat transfer laws to be linear for the temperature intervals under consideration.[1]

Operation of the element Δ_x under steady conditions may be electrically represented by the circuit of figure 2.

[1] See IESNA Bulletin No. 3.

From (6) we derive

$$q_u = \frac{\Delta T_x}{\Delta R_x} \quad (11)$$

setting

$$\Delta R_x = \frac{\Delta x}{m\, C_p} \quad (12)$$

The method consists in drawing a current representing q_u from the node representing the layer of heated air. This is accomplished by introducing, between the node and the mass representing the ambient, 1, the resistance ΔR_x, and 2, an auxiliary generator to regulate the voltage representing the temperature T_x.

The collector is divided into n sections, Δ_{x_1}, Δ_{x_2}, Δ_{x_n}, which are not necessarily equal. We select a value of the incident radiation q_{i_Θ} and a discharge m at the entrance to the collector. We begin with the fraction of the entrance of length Δ_{x_1}, for which $T_1 = T_e$, with the resistance

$$R_1 = \frac{x_1}{m\, C_p}$$

and determine ΔT_1 by experiment.

We start again with the following section, starting out from $T_2 = T_1 + T_1$, etc. The temperatures and the various heat fluxes are plotted, giving curves of the form

$$y = f_m\, Q_{i_\Theta}\, (x), \quad (13)$$

or, more precisely, polygonal lines which more nearly approach the real curves, the smaller the values of Δ_x that are taken. But the number of sections, and consequently also the time taken by the measurements, increase in inverse proportion.

The operating regime at the point of abscissa x, where the temperature of the air is T_x, corresponds to $\Delta_x = 0$ and $\Delta R_x = 0$. To obtain it on the analogous circuit, it is sufficient to replace ΔR_x by a short circuit, and to adjust the voltage of the node to the value T_x by using the auxiliary generator. It will be seen that the operating regime in the section of abscissa x depends only on the temperature T_x of that section. In particular, we have at the entrance $T_1 = T_e$. The ordinates at the origin of the curves $y = f_m\, Q_{i_\Theta}\, (x)$ are independent of m.

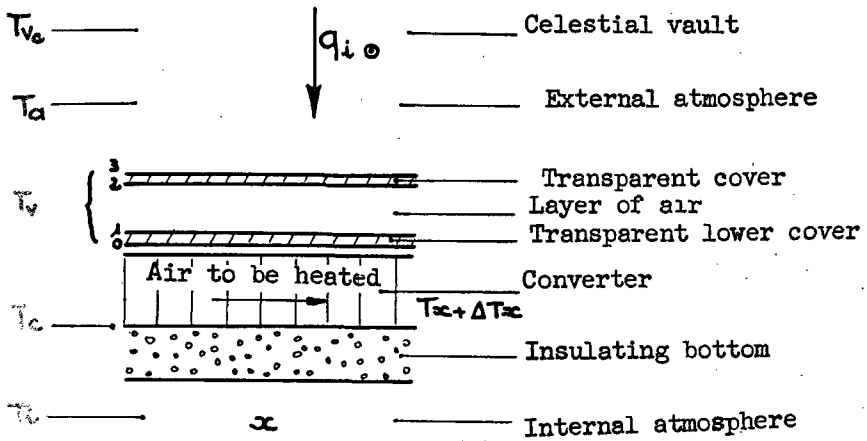
Results of measurements on the experimental solar collector selected

The test solar collector had the following characteristics, which differed slightly from those of the collector finally chosen :

$l = 1\ m$, $L = 5\ m$, $h = 0.05\ m$, whence $lh = 0.05$ m². The cover was made of a double glass and a single glass, with a 5 mm layer of air between them. $\tau_x = 0.79$. Insulated bottom; thermal resistance : $1°C/W$ m².

Coefficient of convective heat transfer between wall and air :

$$A = 2.55\, \Delta T^{0.25} \quad W/m^2.°C. \quad (14)$$


Celestial vault
External atmosphere
Transparent cover
Layer of air
Transparent lower cover
Air to be heated
Converter
Insulating bottom
Internal atmosphere

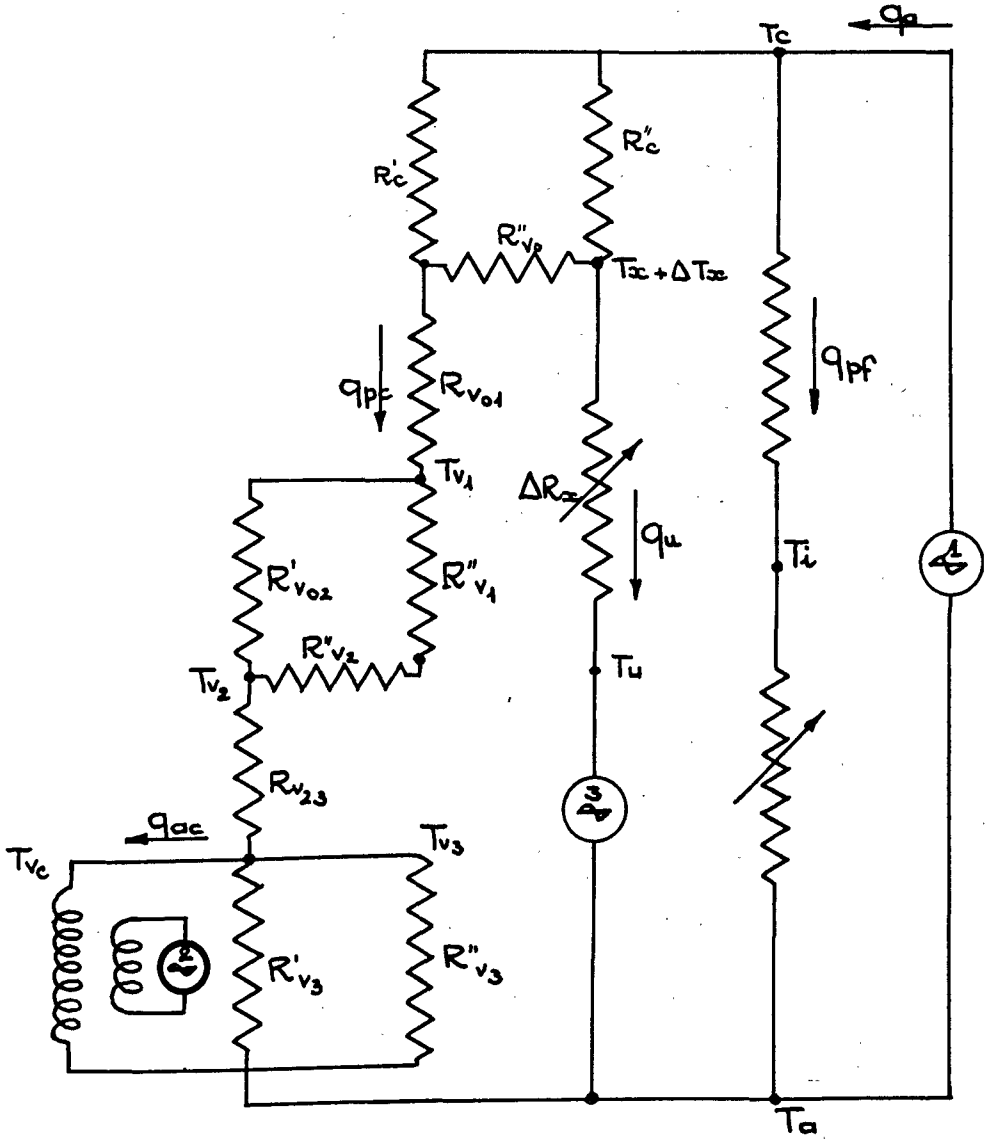

Tc
qa
R'c
R"c
R"v0
Tx + ΔTx
qpf
Rv01
Tv1
ΔRx
qu
Ti
R'v02
R"v1
R"v2
Tv2
Tu
Rv23
qac
Tv3
Tvc
R'v3
R"v3
Ta

Figure 2

Emission factor of the receiving surface $\varepsilon = 1$. The absorption factor, however, was taken as $\alpha_x = 0.95$.

The measurements were made at intervals Δ_x of 0.10 m for the first sections and of 1 m for the last ones. The curves :

$$T = f(x),\ q_p = \varphi(x),\ q_u = \psi(x),$$

were plotted for speeds of the order of 0.20 m and 1 m per sec. for $q_a = 800\ W/m^2$, and finally for $T_e \neq T_a$. In addition, the ordinates at the origin of these curves and the curve of static temperatures, that is, for $v = 0$, were noted.

In the case where $T_e \neq T_a$, we are brought back to the preceding case by a shift in abscissas : the origin of the collector is now at the abscissas : the origin of the collector is now at the abscissa x_e of the original collector, for which the air temperature is $T_x = T_e$.

The purpose is to establish the *characteristic function* of the collector :

$$F = (Q_u,\ Q_{i\Theta},\ T_s,\ T_e,\ T_a,\ T_i,\ T_{v_c},\ m,\ e,\ P_a,\ L,\ V) = 0, \quad (15)$$

which will allow us to study all the peculiarities of operation, but we shall reduce the complexity by limiting ourselves to the case defined by the conditions

$$P_a = 706 \text{ mm},\ h = 0 \text{ per cent},\ V = 0\ m/s,$$
$$T_{v_c} = 0°C,\ T_e = T_a = T_i = 22.1°C,$$

Then we have

$$\rho = 1.111,\ C_p = 1\,006\ j/\text{kg °C (or 0.2408 kcal/kg °C)},$$
$$m\,C_p = 1118\,\ell\,hv$$
$$= 55.9\,v\ W/°C$$

and we put

$$\theta = T_s - T_e, \quad (16)$$

with

$$\theta_o = T_o - T_e, \quad (17)$$

$$M = \frac{m\,C_p}{L} \quad (18)$$

$$Q_{u\ \text{mean}} = \frac{Q_u}{L} \quad (19)$$

Since the measurements were rather prolonged, we sought to establish an analytic form that could represent the experiments in rather good approximation, thus allowing to reduce their number. This led us to adopt the relation :

$$\frac{\theta}{\theta_o} = 1 - e^{-Kx} \quad (20)$$

where k is defined by the operation of the element of origin. We have

$$\frac{d\theta}{dx} = \theta_o\,k\,e^{-kx} \quad (21)$$

and for $x = 0$

$$\left(\frac{d\theta}{dx}\right)_o = \frac{q_{u_o}}{LM} = \theta_o\,k \quad (22)$$

whence

$$KLM = \frac{q_{u_o}}{\theta_o} \quad (23)$$

The experimental data on the analogous circuit show q_{u_o} to be a very nearly linear function of q_a :

$$q_{u_o} = 0.71\ q_a - 39.62, \quad (24)$$

whence, finally, we obtain the relation sought :

$$Q_{u\ \text{mean}} = M\,\theta_o\,1 - e - \frac{0.71\,q_a - 39.62}{M\,\theta_o} = M\,\theta \quad (25)$$

The characteristic function may now be put into the simpler form :

$$F\ (Q_{u\ \text{mean}},\ q_a,\ \theta,\ M) = 0. \quad (26)$$

Figure 3 gives the curve representing the static temperature T_o as a function of q_a. This curve and the system (25) permit us to draw figure 4, giving $Q_{u\ \text{mean}}$ as a function of the radiation absorbed, q_a, for $M = \text{Cte}$ and for $\theta = \text{Cte}$. The graph also includes lines of equal output, which are straight lines drawn from the origin.

Examination of this graph yields an important fact : the relative gain of the heat taken from the collector decreases rapidly with M, i.e., with the speed at entrance. It will be clear that there is no point in exceeding a value of M of the order of

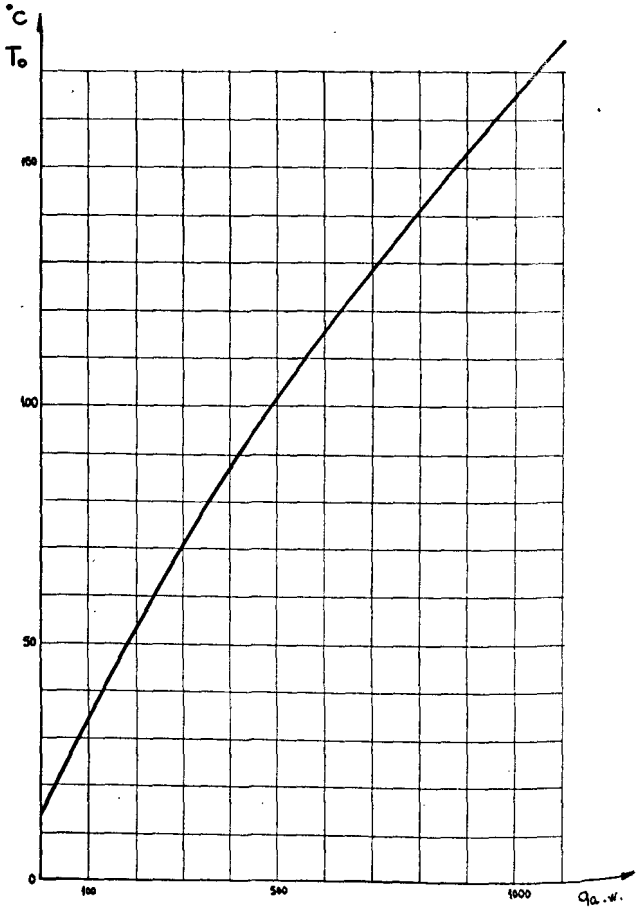


Figure 3

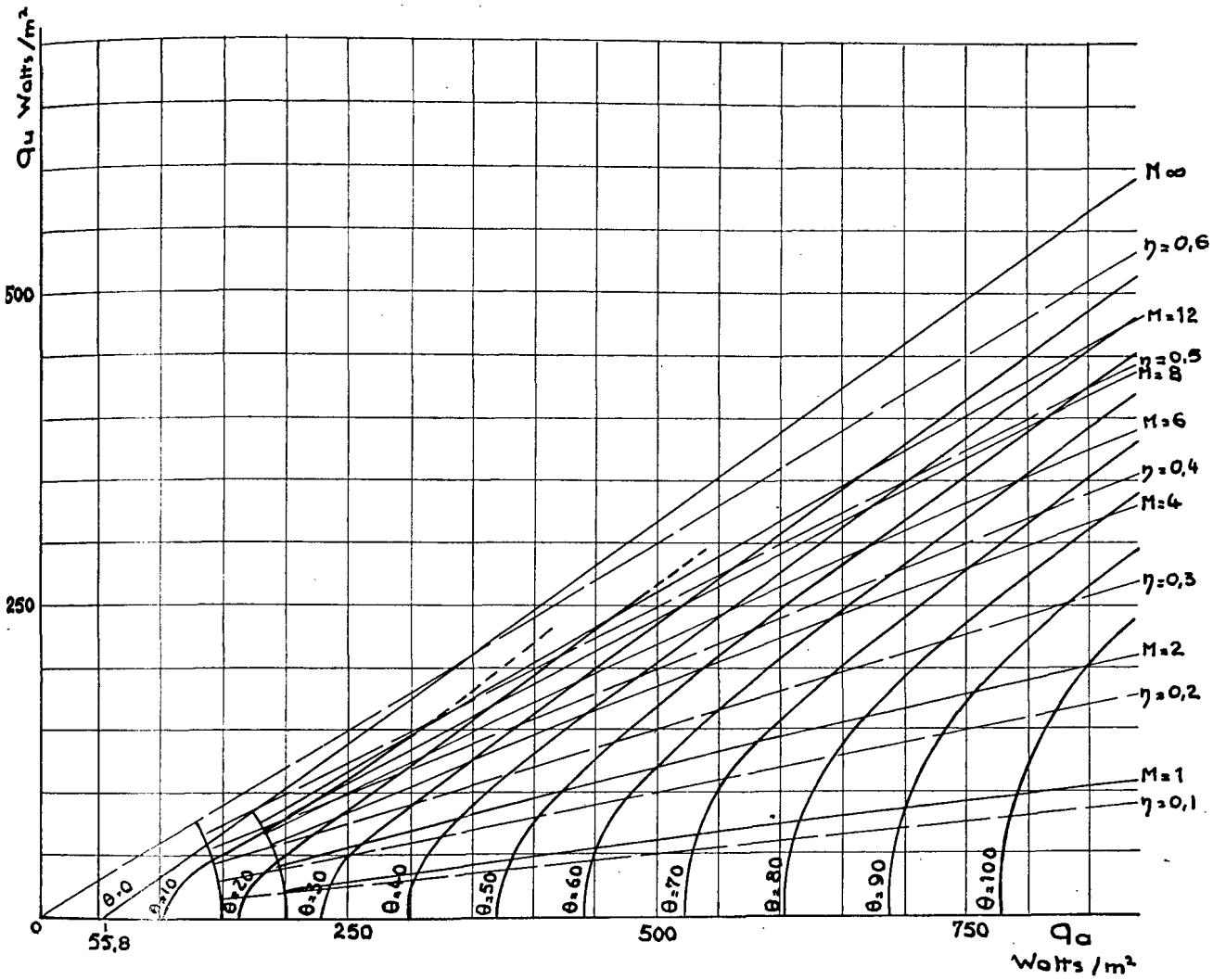


Figure 4

15 W/m °C, or, consequently, entrance speeds of the order of m/s.

It follows that the heat losses in the interior of the collector are in general negligible.

According to the use that is planned, one might desire to operate at T_s = Cte, at θ = Cte, or at M = Cte, or, more generally, in a manner satisfying a certain condition :

$$f(\theta, M) = 0. \tag{27}$$

We shall confine ourselves in what follows to studying the operation of a collector at θ = Cte.

Study of hot-air production at θ = Cte

The determination of the total quantity of heat extracted from the collector during a given period demands, in general, the following operations.

1. Draw typical graphs of the absorbed radiation q_a for all the days $j = 1, 2, \ldots n$ of the period under consideration. In first approximation the sky radiation may be neglected. The projection $q_{i\Theta}$ of the direct radiation on the normal to the plane of the collector must now be found.

We have

$$q_{i\Theta} = q_n \cos \delta \cos H. \tag{28}$$

q_a is then given by (1).

Most often the radiation diagram is unknown. In that case we may start out from a typical diagram obtained by extrapolating the climatological data of neighbouring meteorological stations to the station selected, and, in particular, by determining the average water vapour pressure and the mean sunshine factor, which will allow drawing the typical diagrams of direct radiation for the point selected.

2. On the operating graph of the collector, drawn for the given temperatures T_a and T_{v_c}, and on the curve θ = Cte selected, determine for each value of q_a the corresponding value of Q_u mean and draw the daily graph of mean heat extraction.

This graph defines the lower and upper limits T_1 and T_2 of the hour angle outside which the collector

cannot operate at the temperature difference θ assumed.

3. Determine the length irradiated L for each day of the period. The daily heat output of 1 m collector width is

$$L \int_{t_1}^{t_2} Q_{u\ \text{mean}}\, dt \qquad (29)$$

4. Calculate the total heat output in the given period for the irradiated area $N \ell L$:

$$N \ell \sum_{j=1}^{j=n} L \int_{t_1}^{t_2} Q_{u\ \text{mean}}\, dt \qquad (30)$$

Such a calculation is very long and is not at all suitable for a preliminary study. Certain simplifications must therefore necessarily be adopted to reduce the amount of calculation. We have assumed that a value close to the *annual output* could be obtained by adopting the conditions defined above and adopting mean daily diagrams, whether for 10-day periods, for months, etc. Thus, it will be sufficient to draw the equivalent daily diagram of the absorbed radiation in order to derive the corresponding diagram $Q_{u\ \text{mean}}$. The total heat output will then be

$$365\ N \ell L_{\text{mean}}\, dt \int_{t_1}^{t_2} Q_{u\ \text{mean}}\, dt$$

We have performed this calculation for $\theta = 40°C$, which is rather low from the industrial point of view, and for $\theta = 70°C$, which corresponds to a temperature $T_s = 92°C$, slightly below the boiling point of water at the altitude in question. We adopted the following values:

$\ell = 0.545$ m.

$L_{\min} = 3.25$ m, $L_{\text{mean}} = 4.31$ m, $L_{\max} = 5.37$ m,

and for 1 hectare, we took

$N = 3\,420$, or 40 sheds each 50 m long,

$S = 11\,400$ m². See figures 6 and 7.

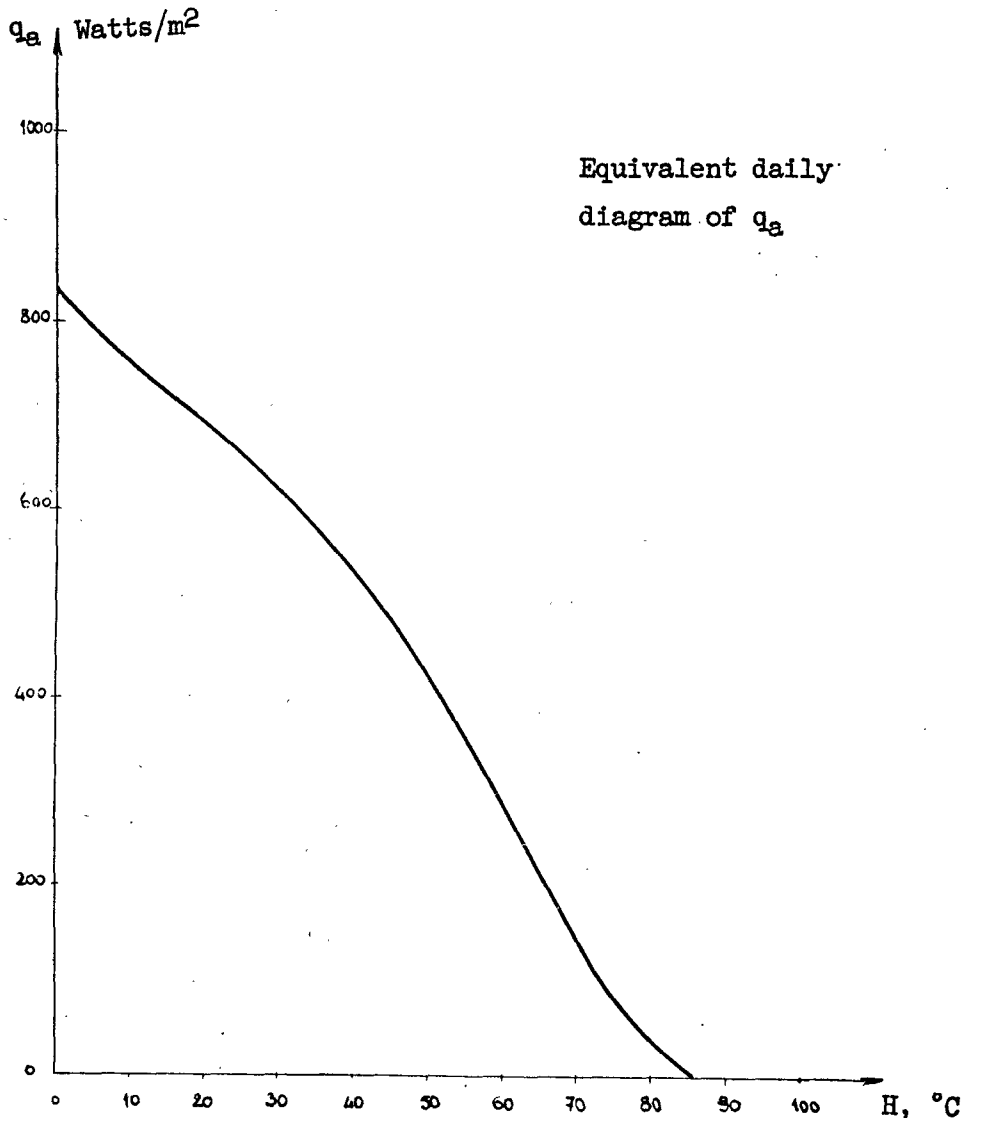


Figure 5

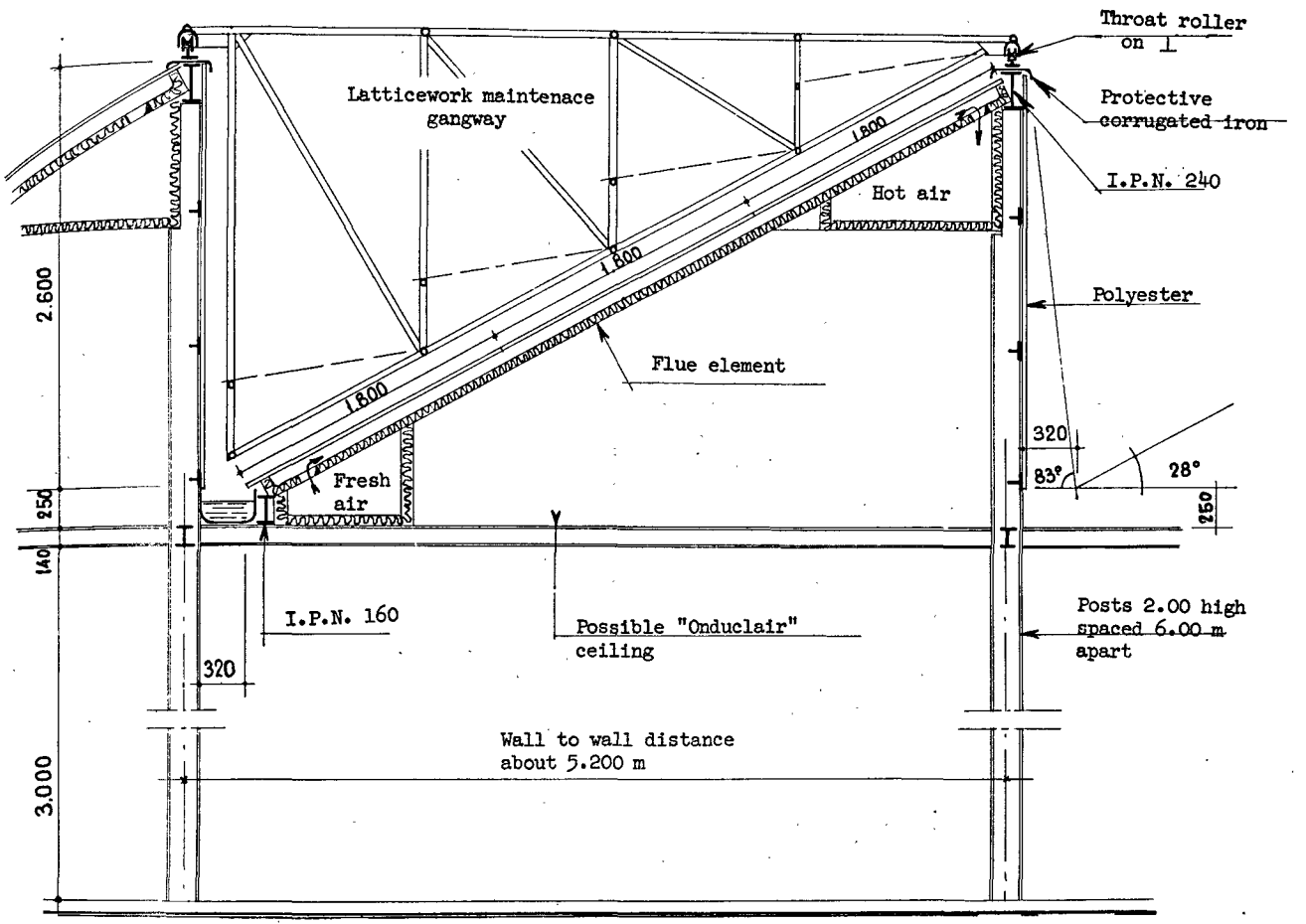


Figure 6

Figure 5 gives the equivalent daily monotonic diagram for the radiation absorbed q_a in W/m^2 for the site selected and the given inclination of the collectors. The annual energy absorbed, calculated by using a planimeter on the diagram, is 16.4×10^3 Mkcal, corresponding to an annual incident energy of 21.8×10^3 Mkcal.

Making use of the diagram of figure 4, we get

for $\Theta = 40°C$ $Q_{u\ an} = 5.62 \times 10^3$ Mkcal,
$m_{max} = 101$ kg/s;

for $\Theta = 70°C$ $Q_{u\ an} = 3.24 \times 10^3$ Mkcal,
$m_{max} = 44.5$ kg/s.

If the same quantity of heat had been produced by burning an industrial fuel (for instance, No. 2 fuel oil, of inferior heating value, assumed equal to 10 500 kcal/kg), the annual fuel consumption and the cost of fuel and transportation, at the rate of 283 NF per metric ton,[2] would be respectively

669 metric tons for $\Phi = 40°C$, or 189,327 NF,
386 metric tons for $\Phi = 70°C$, or 109,328 NF,

assuming that the global yield of the combustion and heat exchange was 80 per cent (a yield unfavourable to the solar solution).

It should be noted that a complete fuel-burning heating plant, for material installed and placed in operating condition at the point selected, would cost 350 000 NF.

Such a plant would comprise three hot-air generators, of an integral commercial type, with a mean unit capacity of 700 000 kcal/h, with burners, blowers, 15-meter smokestacks, fittings and accessories: filters, electrical equipment, connections, automatic feed and control apparatus, three 30 cu m storage tanks, 500 litre service tanks, transfer pumps, valves and piping, together with the civil engineering work. The electric power needed would be of the order of 55.

The cost of such a plant should, of course, be considered only as indicating the order of magnitude, for it may vary according to the exact application for which it is intended.

Preliminary study for a complete plant

The point X selected for erecting the solar collectors is located about 230 km from El Golea, on a

[2] This price would be for large-scale deliveries. In small quantities the price of fuel might be as much as 440 NF per metric ton.

trail that is unsurfaced but can be negotiated by heavy trucks. El Golea is a fairly important oasis and has an airfield. There is drinking water at Fort Miribel, about 100 km north of point X.

The soil of Tademait plateau is hard, so that the foundations required will not occupy a great volume.

The site is rather far away about 1,130 km from Algiers, and the problems of transportation and labour will be of major importance.

The cost of transporting 20 metric tons (or 25 cu m) is almost 6 000 NF, all charges included.

Independent provision must be made for wages and rest periods under way, an expense of the order of 80 NF per man-day, plus air fare of 500 NF per man.

Examination of these expense items indicates the advisability of using :

1. Light and strong materials;

2. Materials with the smallest possible bulk, since the trucks should carry their maximum useful load;

3. A small but highly qualified crew for installation of the components on the site.

These conditions lead to the following solutions.

Framework

A metal framework is obviously the most rational solution for the Sahara. Metal is relatively light for equal strength, and in these very dry climates its resistance to oxidation is excellent.

The traditional trussed girder solution, however, should be rejected on account of the high cost of transportation and erection. Rectilinear bearing members should therefore be used instead, such as cold-worked sections, folded or profiled sheet metal, assembled and bolted on *H* posts and *IPN* wind-bracing girders.

The need for optimum exposure of the solar collectors leads to the adoption of a shed roof sloping *S*.

The air is delivered by an insulated lower duct; it circulates upwards through the collectors and is collected hot in an upper insulated duct. Figures 6 and 7 show all the structural details. The measures to avoid thermal bridges between the various parts of the solar collector and the framework should be noted. In summer irradiation is total; in winter, only the upper part of the cover is exposed to direct sun. This is due to the shadow cast by each shed on the next one. If total year-round solar irradiation is desired, the buildings would have to be spaced sufficiently, but this arrangement would cause trouble in wind bracing and in providing supplementary walls.

The sheds might be arranged as shown in figure 8. Form *a* is the most economical, and has been adopted in this work.

Form *b* takes up more space, but the collectors are exposed to direct sun at all times during the day.

Form *c* takes slightly less space than form *b*, and allows reinforcement of the summer radiation

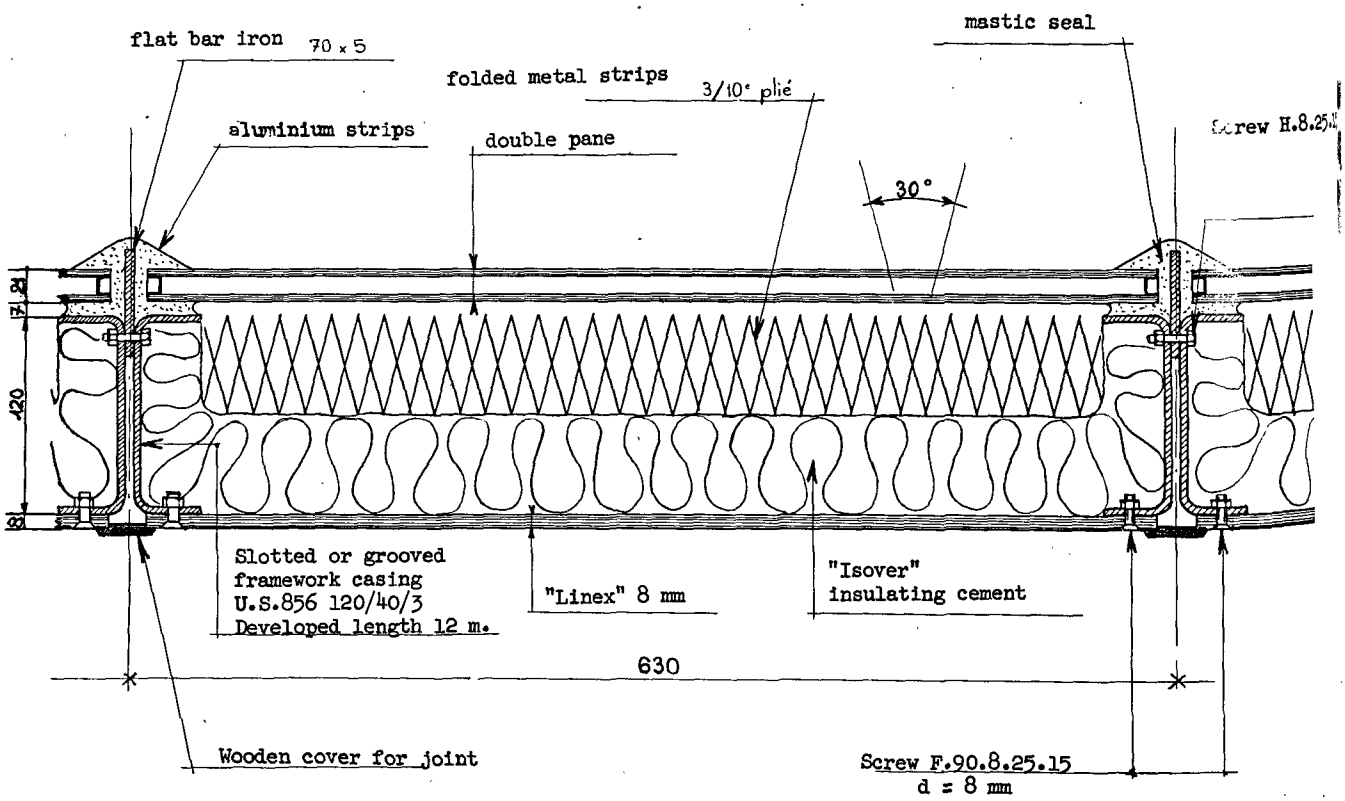
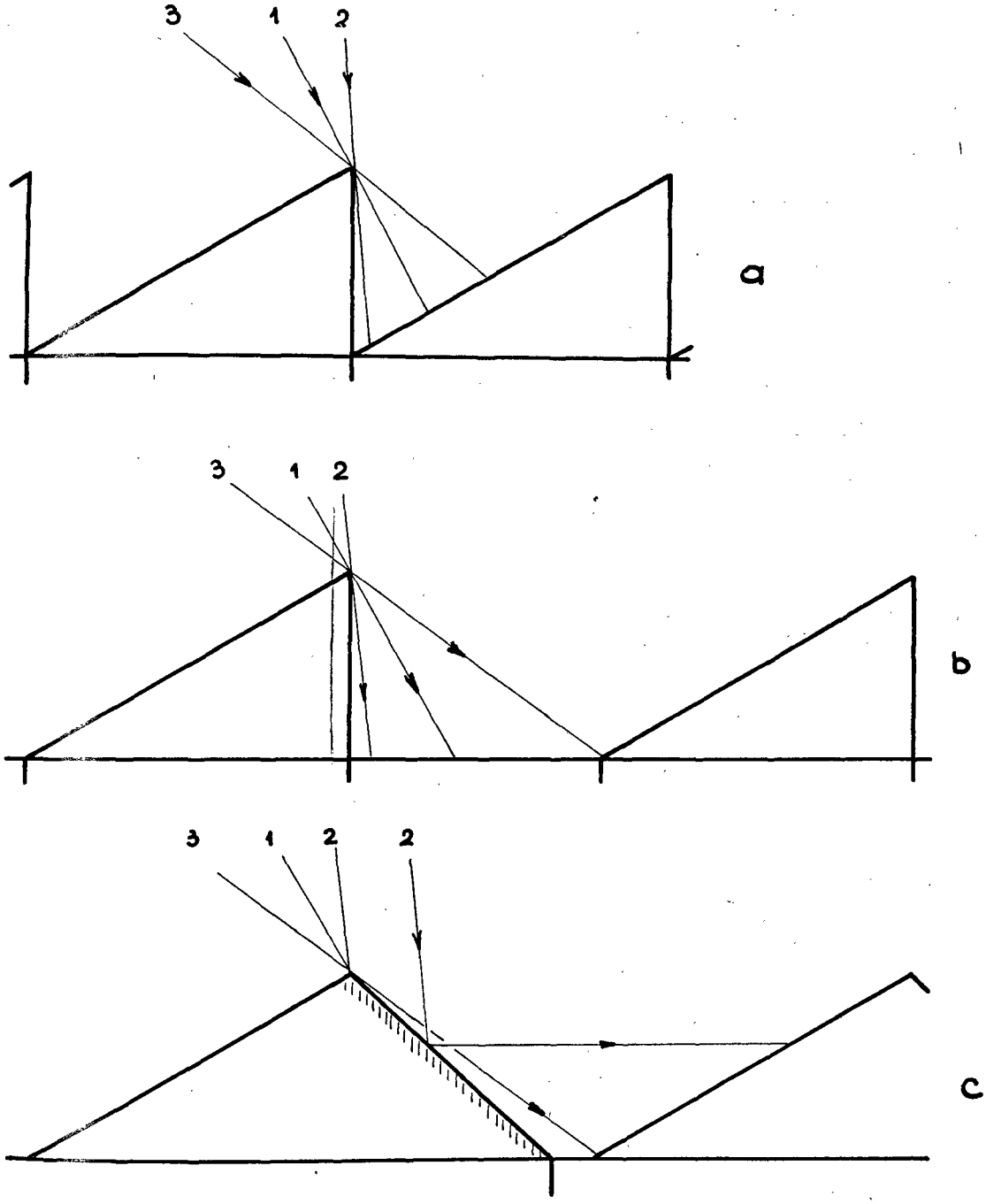


Figure 7



1. Equatorial plan
2. Incident radiation at the Summer solstice
3. Incident radiation at the Winter solstice

Figure 8

on the collector. In this case the N face of the sheds could be covered with reflecting elements of aluminium or, more economically, of aluminized plastic.

In practice, obviously, the collectors will never occupy the entire surface covered by the plant. But these areas, which are lost for the conversion of the solar radiation into heat, should be taken into account in the costs attributable to the building itself. Our calculations of the energy cost will thus be based on the most unfavourable assumptions. The installation of the various parts of the collectors, as well as their maintenance and cleaning, are facilitated by maintenance gangways sliding on the ridge lines of two adjoining sheds.

A distance of 5 or 6 m between sheds appears to be appropriate to ensure satisfactory rigidity of the rectilinear supports and good resistance of the glass, whose breakage under alternating action of the wind must be avoided. This spacing also permits limiting the shed height to about 3 m.

It seems advantageous to have the sheds vertical, in order to obtain very high girders, to provide effective wind-bracing between the posts, and, if desired, to have longer bays, which might be required by the industrial uses of certain buildings. The vertical part of the sheds may be shifted by means of corrugated polyester plates reinforced with fibreglass.

An approximate estimate of the construction cost has shown that transportation will be responsible for about 10 per cent of the total, and the cost of lodging the labour force for another 20 per cent. It would therefore be of interest to have entire members of the cover prefabricated, grouping the purlins and heating ducts in a single assembly, with the natural exception of the glass panes. This would slightly increase the cost of transportation, but would considerably reduce the erection labour time, for only a rapid assembly with bolts would have to be done on the site.

Solar collectors

The collectors, which also serve as structural members, are built of prefabricated ducts comprising (see figure 7) :

Two girders made of cold-rolled sections, tied at the ends;

A ceiling member of "linex" (an insulating material with a hemp fibre and synthetic resin base), 8 mm thick, screwed in under the lower flanges;

Apertures at both ends for admission and discharge of air;

Insulation at the bottom and on the sides, made of fibreglass felt (Isover, thickness 75 mm).

The radiation-receiving surfaces are made of bands of thin blackened sheet metal, accordion-pleated at angles of 30°, and held in place by metal wires. This system has many advantages. In the first place, the exchange surface is multiplied by $2/\cos 15° = 7.74$. The temperature difference between the air and the receiving surface is smaller. Then, the insulating bottom is at a lower temperature than the receiving surface, thus decreasing the losses behind. Moreover, the absorption factor of the receiving surface is increased. This surface may be blackened, but if there is no fear of soiling by dust, it may also be made selective. Finally, the bands are rather narrow — only 5 cm — and the undulations in each are half a step out of phase with those of the adjacent band, so that the convection transfer coefficient is markedly improved.

The transparent cover is made of a double pane of the "Thermopane" or similar type. The elements, each 0.60 m by 1.80 m, with a total thickness of 21 mm, present an impervious metallic framing, enclosing a layer of dehydrated air 12 mm thick. These dimensions are the most economic, but they demand the use of three different dimensions for each collector. Assembly is by means of plastic joints. These covers weigh 20 kg/m².

The covers are installed by puttying in. For this purpose a flat iron bar is inserted between two adjacent girders to form the T for glazing. The quality of the putty is very important, for it must maintain its elasticity under very severe climatic conditions. On the other hand, it should be noted that the roofing is subjected to depressions that may reach 90 kg/m², which is more than the weight of the cover. It is planned to use either "Stop Stora" putty, which has already given a good account of itself in the Sahara, or a thiokol-base elastic cement (P R C series 250). The putty should be additionally protected by glueing on a thin aluminium band.

The girders together with the puttying of the covers cause a loss of about 9 cm of exposed area per collector, or a little less than 15 per cent of the total surface.

Estimates

Initial expense

We present below the results of a detailed study of the cost of materials and labour, including all charges and taxes, in terms of new francs per sq m.

We have not included the front walls and their foundations, nor the painting and appointments, which depend on the ultimate purpose of the buildings, are independent of the mode of hot-air production, and, in any case, belong to the building itself rather than to the plant.

Estimate of sheds with collectors—costs per sq m

	NF/m²
Foundations	8
Pavement	55
Framework	150
Glazing	125
Insulation of ducts	90
Shifting mechanisms of sheds	16.5
Ceiling	26
Connecting ducts	60
Channels	12.3
Drains	1.7
Inspection holes	4.2
Sewer pipes	16
Total	554.70 of cover

or, for the total area taken as an example :

$A = 11\,400$ m² Cost: 6 323 580 NF

If the same buildings are erected with a conventional corrugated aluminium cover, and insulated with fibreglass felt, the changes in the costs will be:

		NF/m²	NF/m²
Deductions:	Framework : 140-100	40	
	Glass	125	
	Insulation	90	
	Connecting ducts	60	
			315
Additions:	Aluminium roofing	60	
	Isover linex insulation installed at the site, including special felts to ensure an airtight seal	55	
			115
Or an additional cost for the solar-collector solution of			200
Thus, the additional expense due to the installation of solar collectors for hot-air generation would be, for the total surface			2 280 000 NF
We must:			
(1) add the cost of the maintenance passageways and the cleaning accessories, estimated by us at		5 000 NF	
(2) subtract the cost of the fuel-burning heating plant, estimated above at		350 000 NF	
or a cost-reduction of			345 000 NF
The additional cost thus amounts finally to			1 935 000 NF

Substantial economies could probably be realized if the covering of glass, which is rather heavy (20 kg/m²), could be replaced by a covering of plastic film. Let us revise our estimate on this hypothesis.

	NF/m²
Foundations	8
Pavement	55
Framework	145
Covering	35
Insulation of ducts	80
Shifting mechanisms of sheds	16.5
Ceiling	26
Connecting ducts	60
Channels	12.3
Drains	1.7
Inspection holes	4.2
Sewer pipes	16
	439.7

or, for the total area : 5 012 580 NF.

In the case of a conventional covering, we would have :

		NF/m²
To subtract:	Framework	15
	Covering	35
	Insulation	80
	Connecting ducts	60
		190
To add		115
Or an additional cost of		75 NF

And, for the total area: 855 000 NF.

In this case, the additional cost due to the installation of the solar collectors would be, for the total surface, only

$$855\,000 - 355\,000 = 500\,000 \text{ NF}$$

Operating costs

We may assume, in first approximation, that the labour cost for the cleaning and maintenance of the solar collectors is roughly equivalent to the cost of operating and maintaining the fuel oil heating plant. It would, however, be prudent to count on the replacement of about 1 per cent of the glass covers which might be broken for various causes. Here as well we may assume that these replacement costs are of the same order of magnitude as the costs of repairing and replacing the material of a fuel heating plant. The annual saving, then, is definitively constituted by the cost of the fuel that would have been burned to generate the same quantity of heat. This saving ranges from about 110 000 to about 190 000 NF, according to the production characteristics, as indicated above.

We do not disregard the adjustments and reservations that must be applied to any conclusions drawn from these estimates. We confine ourselves to remarking that it would seem advantageous to utilize solar energy in cases of air heating not requiring high temperatures. Large-scale experimentation would then seem entirely legitimate, all the more since we have deliberately based our calculations on the hypotheses that are the most unfavourable for the utilization of solar radiation.

The interesting features of the analysis in which we have been engaged reside in the relative size of the various expense items. Such a project can without doubt be substantially improved, as we have just seen. Thus, the elimination of the glass covering and its replacement by a plastic film, like the reduction in the weight of the exchange surfaces, may have a direct effect on the corresponding cost items, and may also significantly decrease the weight of the framework.

On the other hand, the heat output of collectors of the type adopted will very certainly be substantially greater in practice than the output we assumed, to take a pessimistic position.

Comparative study of various types of collectors

Atmospheric solar collectors may be classified into two major groups, those operating with the hothouse effect, and those operating without it.

Collectors with the hothouse effect

The transparent cover may be of glass and enclose one or several layers of air. Experience shows that, except in special cases, there is no reason to go beyond two layers of air, that is, one transparent cover and two sub-covers. The cover must be able to resist the attack of the wind, which is particularly

violent in the Sahara. Double glasses (3.6 mm thick) from 0.50 to 0.60 m wide have been adopted for the covers, and single glasses (1.8 mm thick) for the sub-covers. If the maintenance department has a machine shop, prefabricated panes, like the "Thermopane" of St. Gobain, will be of interest, for there is less risk of breakage. The glass cover is rather heavy and is the most troublesome part of the collector. Then, too, it easily becomes dirty and requires frequent cleaning.

Transparent plastic covers can be envisaged. Their optical properties in the infrared are poorer than those of glass, but they are incomparably lighter and the risk of deterioration is less.

The Institute of Solar Energy is now studying a cover using "Therphane", which is the French Mylar. This cover is, in principle, made of a cylinder of plastic 0.06 mm thick with the edges glued together following a generatrix. The cylinder is stretched on a light frame made of two aluminium tubes 1 cm in diameter tied with thin elastic rods. This gives a cover that is always stretched and imprisons a lamina of air.

The surface receiving the solar radiation may be continuous or porous, of metal or insulating material, blackened or covered with a selectively emitting coating. It may be plane and offer the same surface for convection as the collector, or it may be corrugated, folded, creased, or ribbed.

Porous walls, that is, walls which, while opaque to light, do permit the ready passage of air, are very diverse. American experimenters have used a metal grating, which is excellent, though heavy and expensive. They have also used a leaf system of partially blackened glass layers. This is likewise heavy and troublesome. To these classic surfaces we have added lamellar surfaces or surfaces in the form of paddle-boards made of metal or plastic, as well as gratings made of textiles, rice straw or reed-grass.

For the project on the solar collector we have been discussing, we decided on surfaces of thin sheet metal, with accordion pleats, at 30° angles. Other more complex surfaces which will require industrial development to reduce their cost are also in the test or project stage.

The air circulates either on the insulated surface or below it. In the latter case the convection coefficients are markedly higher.

It should be pointed out that continuous metallic surfaces have the inconvenient feature of equalizing the temperature by conduction; the temperatures obtained with these surfaces are lower than with insulating surfaces. On the other hand, at equal final temperatures, their heat output is better.

Collectors without the hothouse effect

These collectors are more unsophisticated than those just discussed, and the cleaning of their surfaces exposed to the weather is less important. Only non-selective receiving surfaces of this type can be thought of, since dirt makes the selectivity inoperative. On the other hand, selective surfaces are always delicate and require protection.

The heat output of collectors without the hothouse effect is necessarily far lower than of those having a covering opaque to infrared radiation. On the other hand, the heat must traverse the receiving surface by conduction in order to be able to heat the air circulating on the other face. This requires the receiving surfaces to be metallic. The lower face, in contact with the air, may be ribbed to facilitate convective heat transfer. The receiving surface should, in principle, be plane, to minimize the natural convection losses from its upper surface. Some experimenters, however, have used corrugated or pleated sheet metal.

The tests now in progress are developing as follows.

The surfaces being studied are exposed simultaneously in groups of six, and under conditions as nearly identical as possible, to solar radiation. In this way we practically eliminate the disturbances due to the variations of solar radiation, ambient temperature, atmospheric humidity, and wind.

The temperatures and rates of air discharge are then measured. The results are only of relative value, but they do permit classification of the surfaces by comparing their heat output, heat losses and manufacturing cost.

We hope in this way, as a result of these tests, to be able to retain a small number of surfaces offering maximum advantages and suitable for industrial development.

Figure 9 is a general view of the plant installed on the terrace of the Physics Building at the University of Algiers. Figure 10 shows schematic diagrams of a few of the surfaces now being tested.

The experimental work has been done by the personnel of the P.C.B. Physics Laboratory, University of Algiers, to whom we here express our thanks,

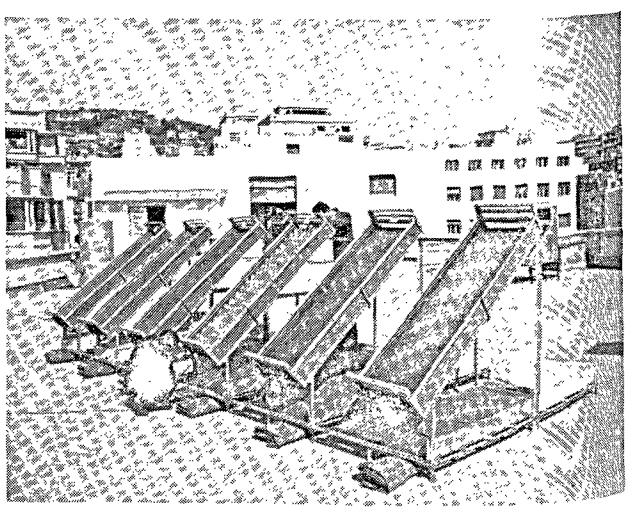


Figure 9

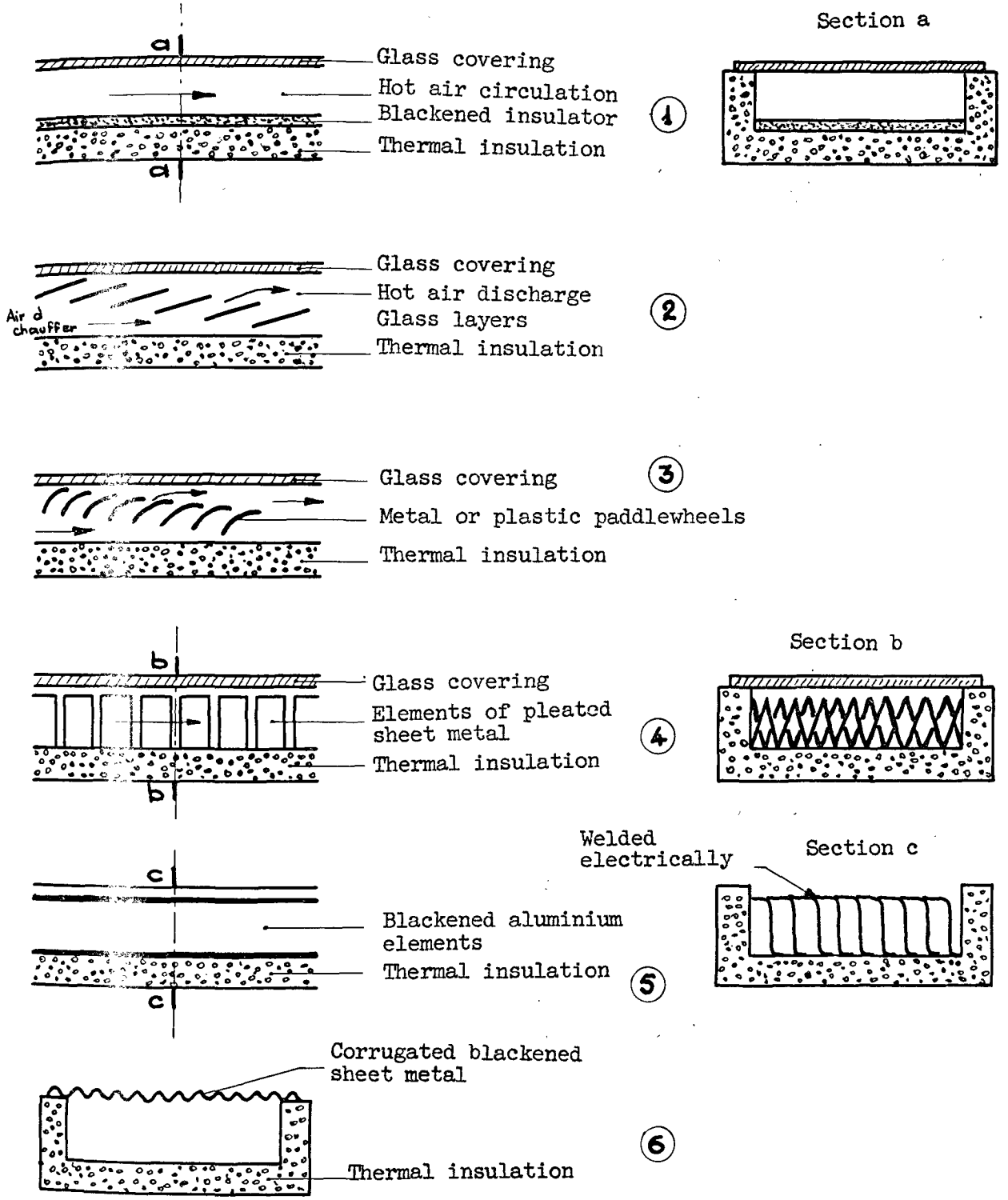


Figure 10

especially to A. Zerouki, who handled the measurements and the comparative calculations.

Conclusion

The practical interest of direct-exposure solar collectors is rather restricted, but for certain applications requiring temperatures of at most 100°C, the present preliinary study shomws that all these types should not be rejected *a priori*.

The Institute of Solar Energy of the University of Algiers is more particularly interested in the utilization of solar collectors as static elements for circulating large masses of air which could be used to cool thermoelectric generators. Studies on this particular application are now in progress.

Summary

Solar radiation may be converted into relatively low-temperature heat in devices of simple design and fixed position — flat solar energy collectors. Their simplicity and low fabrication cost permits their installation on large areas, and thus allows the production of large quantities of heat.

The Institute of Solar Energy has envisaged the large-scale generation of hot air, which might be used for various purposes, such as air conditioning, power generation, or as a heat sink to circulate air for cooling thermoelectric generators.

Against this background, the author has taken up two problems: 1. Study of a complete large-area plant using atmospheric solar collectors of a specified type, and 2. Comparative experimental study of various collector types.

In the first study, we assume the collectors to be installed at a specified but arbitrary point on the plateau of Tademait, in the Sahara. The principal climatological features of this point are as follows:

Mean annual temperature: 22.1°C.

Mean partial pressure of water vapour: 3 mm Hg.

Mean sunshine factor: $\sigma = 0.843$.

The collector field is considered from two points of view: as a hot-air generator, and as the cover for the buildings where this hot air will be utilized.

The capital costs of the air-heating system are thus the difference between the cost of the entire structure and the cost of a conventional framework and a conventional cover for the same area.

The climatological study of the station indicates that to optimize the heat production of the absorbing surfaces, the collectors must be inclined to the horizon at an angle substantially equal to the latitude of the place.

Study of hot-air production

The author used an electric analogous method to study collector operation. Simulation yielded curves of useful power against absorbed power, at constant θ, where θ is the difference between the atmospheric temperature and the temperature of the air leaving the collector and at constant air discharge.

In particular, we studied hot-air production at θ = Cte.

The climatological readings at the point in question gave daily curves of the direct solar radiation. From these we derived curves of the radiation normal to the collector plane. Knowing the characteristics of the absorbing surface as well as the curves of the absorbed power, after subtracting the sky radiation we drew up a pessimistic hypothesis.

These curves, in conjunction with the plot of useful power against absorbed power, at constant θ, allowed us to plot daily useful-power curves for two arbitrary values of θ 40°C.

We could then calculate the annual heat output from a collector plant covering a fairly large surface, a hectare for instance.

For θ = 40°C, the annual output is 5.62×10^3 Mkcal;

For θ = 70°C, the annual output is 3.24×10^3 Mkcal.

If industrial fuel had been burned to generate the same quantities of heat, it would have taken 669 metric tons, costing 189 327 NF in the first case; 366 metric tons, costing 109 238 NF in the second.

A fuel-burning heating plant installed at the point selected would cost about 350 000 NF.

Study of the construction job

The distance and difficult access make transportation and labour the major problems. Consequently we envisaged the use of light but not bulky materials and the employment of a small but highly qualified labour force for the erection.

The framework consisted of rectilinear metal members with a shed roof sloping south. Since each shed cast its shadow on the next, the irradiated length varied seasonally.

The cold air is delivered by a duct to the base of the shed, and the hot air is collected in another duct at the top.

The collectors themselves were made of prefabricated elements, with an absorbing surface of accordion-pleated bands of blackened sheet metal. It was insulated at the bottom and on the sides with fiberglass felt, and covered with double panes. The ground area occupied by a useful hectare was 11 400 m².

Comparison of the cost of a conventional installation and a solar-collector covering indicates that the latter would cost 1 935 000 NF more. If the glass cover could be replaced by one of plastic film, this difference could be brought down to about 500 000 NF.

The operating costs for labour, maintenance and repairs may all be considered in first approximation to be equivalent to those of a fuel-oil heating plant.

The annual saving results from eliminating the cost of the fuel that would have to be burned to generate the same amount of heat.

We show that this would range from 110 000 to 190 000 NF.

The most unfavourable assumptions have been made throughout the paper. The actual results would certainly be better than those we have found.

Comparative study of various collector types

Collectors with hothouse effect. The transparent cover may consist of glass sheets enclosing layers of air (two at most). The use of prefabricated panels to facilitate handling would be of interest.

But glass is heavy and soils easily. The Institute of Solar Energy is studying a cover made of "Terphane", a double plastic film 0.06 mm thick.

There are many different kinds of absorbing surfaces. They may be metal or insulating, continuous or porous, flat or corrugated. A number of types of porous surfaces are being tested by the Institute of Solar Energy.

Collectors without the hothouse effect. These collectors are simpler in design than the above types, and the problem of soiling is less important, but selective surfaces cannot be used.

Their heat output is much less, owing to losses by infrared radiation, conduction and convection.

The tests are made by simultaneous exposure of six different surfaces to solar radiation. The surfaces may then be classified by comparing heat output, heat losses and manufacturing cost.

The author hopes that this work will indicate a small number of surfaces suitable for industrial use.

Conclusion

Direct-exposure collectors are of rather limited practical interest, but for certain applications requiring top temperatures not over 100°C at most, this preliminary study does show that this type should not be rejected out of hand.

The Institute of Solar Energy of the University of Algiers is more particularly concerned with the use of solar collectors as static elements for circulating large masses of air that could be employed to cool thermoelectric generators. Studies on this application are in progress.

Agenda item II.C.1 (*b*)

USE OF SOLAR ENERGY FOR ELECTRICITY PRODUCTION BY DIRECT CONVERSION BY MEANS OF THERMOELECTRIC CONVERTERS AND PHOTO-ELECTRIC CELLS

*Valentin A. Baum**

Solar radiation began to be regarded as one of the possible additional sources of energy many years ago. At first a very modest role was relegated to it: it was believed that it would be used for obtaining low-potential heat (for heating water, hot-houses and so on).

At present, however, the consumption of energy has increased sharply and is continuing to increase. This is due to the growing population, its growing requirements, and the need to reclaim new territories for it. The reclamation of these new territories usually demands great effort and large amounts of energy to make them habitable. In view of the immense expenditure of fuel, which today forms the basis of the power industry, its supply is quickly being used up; the economics of the power industry is consequently changing in favour of those sources of energy which in the past could not compete with fuel.

In recent years, investigations carried out in a number of countries have already shown the possibility of utilising solar energy in the near future much more widely and in a more varied way, even at the present stage of technical possibilities open to us.

One of the most important practical tasks is the conversion of solar energy into electricity. This task has already been solved by using the conventional mechanical steam power cycle. It can also be solved, however, by using new methods based on the latest achievements in the physics of solid bodies and the production of new materials with special physical properties, as for instance semi-conductors.

Converters of solar energy into electricity which are already of practical interest and seem to have a very promising future are: (*a*) thermoelectric generators, (*b*) photoelectric batteries, and (*c*) thermionic converters.

These devices have a number of advantages over the conventional steam power installations, the principal one being the absence of moving parts. They are also comparatively simple to operate. It is expected that some of them may prove economically acceptable in the next few years for obtaining capacities ranging from several watts to one or more kilowatts; they could be used as a power supply for means of communication, for setting into motion small-capacity water-hauling machines, for lighting small houses and so on.

The term "new methods of converting energy" is somewhat ambiguous. The physical phenomena on which they are founded have been known for a very long time. Thus the phenomenon of thermoelectricity was discovered about 140 years ago, the photo-effect of the barrier layer was discovered some 175 years ago. The first solar thermogenerators, however, were made only at the end of the nineteenth century, and the first ventil photo-cells in 1930. The considerable attention devoted in a number of countries to thermocells and photo-cells made it possible to improve their technical characteristics radically. Though twenty years ago the efficiency of the conversion of solar energy into electricity by means of photo-cells and thermocells was only a few tenths of one per cent, it now equals about 10 per cent. A large number of papers on the theory of these devices and on the search for various semiconductors shows that it is possible to raise the efficiency of solar electric generators much more and to improve their other technical and economic characteristics.

It is impossible in this paper even to make reference to all the most important papers of different authors and organisations working on these problems, in view of their very large number. Reference will be made only to the papers submitted to the United Nations Conference on New Sources of Energy and to some of the articles which examine converters of solar energy exclusively.

Thermoelectric generators

General information

Thermoelectric generators (TEG) are devices that convert thermal energy directly into electricity. Their action is founded on the phenomenon discovered about 140 years ago, of the formation of an electric current in a circuit made of two different metals or semi-conductors when their points of contact or junction are kept at different temperatures.

* Deputy Director, Krzhizhanovski Power Institute, Head of Heliolaboratory, Moscow.

A TEG consists of a number of thermocells joined in series. It can be regarded as a thermal machine without moving parts which converts part of the heat brought to the hot junction into electricity. In accordance with the second law of thermodynamics, there are inevitable losses of energy in this converter, because of the transfer of heat by conductivity from the hot to the cold junction. In addition, part of the electricity generated in the cells is transformed into heat when the current passes through the circuit formed by the thermocells, which have a certain resistance, and part of this heat is lost. Depending on the design there can also be losses in devices for concentrating solar rays : losses due to the partial reflection of the rays from the surface of the battery, and losses by convection and radiation from the hot junction.

The efficiency of the conversion of heat passing through the thermocell into electricity depends on the physical properties of the materials of which it is made and on the temperature of the hot T_1 and cold T_2 junctions.

The materials is considered better the higher the value of

$$Z = \frac{\alpha^2 \sigma}{\lambda}$$

where α is the specific thermoelectromotive force,
σ is the electro conductivity, and
λ is the heat conductivity of the material.

For metals the correlation between α, σ and λ is very unfavourable, and the value of Z very small; consequently they are unsuitable as materials for power thermocells. Semi-conductors have a much higher value for Z. By using for one section of the thermocell a semi-conductor of the electronic type (type "n") and for the other a "p" type, it is possible to obtain thermocells having a sufficiently high efficiency.

The theory of the working of a thermocell, as a device converting the heat passing through it into electricity, gives the following formula for calculating the efficiency of the device :

$$[1] \qquad \eta = \frac{T_1 - T_0}{T_1} \frac{\sqrt{1 + \frac{1}{2} Z (T_1 + T_0)} - 1}{\sqrt{1 + \frac{1}{2} Z (T_1 + T_0)} + \frac{T_0}{T_1}}$$

If the efficiency is determined with respect to the flow of radial energy falling on the mirror of the solar thermoelectric generator, then one must also take into consideration the losses of energy due to the imperfect reflection of the rays from the mirror and to the incomplete absorption of the rays by the surface of the thermobattery, the convection losses and the radiation losses by the hot surfaces of the battery. In this case the general efficiency of a solar thermoelectric generator can be determined from the following formula :

$$[2] \qquad \eta_{gen} = RA \frac{T_1 - T_0}{T_1} \frac{\sqrt{1 + \frac{1}{2} Z (T_1 + T_0)} - 1}{\sqrt{1 + \frac{1}{2} Z (T_1 + T_0)} + \frac{T_0}{T_1}} \left[1 - \frac{F_b}{F_m} \frac{\sigma (T_1^4 - T_0^4) + k (T_1 - T_0)}{RAI} \right]$$

where σ is the coefficient of radiation of the material of the battery ($\sigma \simeq 4.2 \cdot 10^{-8}$)

T_1, T_2, T_0 are the temperatures of the hot and cold junctions of the battery and of the ambient air,

F_m is the effective surface of the mirror

F_b is the heated surface of the battery

α is the coefficient of heat losses by convection from the surface of the battery into the ambient air $\alpha = \frac{\text{(10-20 kgcal)}}{\text{m}^2/\text{hour}/^0\text{C}}$

R is the reflectivity of the mirror (0.75-0.85)

A is the absorptivity of the heated surface of the battery (0.85-0.9)

I is the direct solar radiation $\frac{\text{kgcal}}{\text{m}^2/\text{hour}}$

The quantity $\eta k = \frac{T_1 - T_2}{T_1}$ represents the efficiency of an ideal converter (the efficiency of the Carnot cycle); its value, depending on T_1, is given in table 1 for a case in which the cold junctions have a temperature $T_2 = 300°K$.

Table 1

T_1 . .	350	400	450	500	550	600	650	700	800	900	1 000	1 100	1 200
ηk . .	0.14	0.25	0.33	0.40	0.46	0.50	0.54	0.57	0.63	0.67	0.70	0.73	0.75

The formula $\eta_m = \frac{\sqrt{1 + \frac{1}{2} Z (T_1 + T_0)} - 1}{\sqrt{1 + \frac{1}{2} Z (T_1 + T_0)} + \frac{T_0}{T_1}}$ shows the relation between the quantity of heat converted by the material into electricity and the quantity

of heat which could have been converted if the properties of the material had been ideal.

Table 2 gives the values of η_m for certain materials having different Zs when $T_1 = 1000°K$ and $T_o = 300°K$.

Table 2

$Z \cdot 10^3$.	0.5	0.7	1.0	1.5	2	3	5	10	45
η_m . . .	0.1	0.14	0.18	0.24	0.29	0.36	0.45	0.58	0.78

It should be borne in mind that the values of α, σ and λ depend on the temperature at which the material works; consequently the choice of material for thermocells should be founded on the values of Z determined for working temperatures. For instance, the thermo-electromotive force for some materials changes with the temperature not only in value, but also in sign. Unfortunately it has not yet been possible to determine theoretically what materials would prove effective from the point of view of their use for thermocells. For the main part the search for suitable materials has been conducted experimentally. This research is now being conducted on a very large scale in many countries. As a result, it is possible to create thermocells having an efficiency of up to 10 per cent, and, if using multicascade schemes, up to 15 per cent.

In the Union of Soviet Socialist Republics, the Krzhizhanovski Power Institute has conducted research work on intermetallic compounds prepared from the usual commercial materials Bi_2Te_3, Sb_2Te_3, PbTe, PbSe, ZnSb, $CoSb_3$ and solid solutions based on them. The thermoelectrical properties of thirteen binary alloys of tellurium were investigated. In addition to the materials named, Ag_2Te, SnTe and GeTe have a high Z. Investigations of PbTe (p and n types), Bi_2Te_3, Sb_2Te_3 and, particularly, GeTe and its compounds with other systems have been carried out widely in the United States by Westinghouse, General Electric and the Radio Corporation of America. Many other compounds have also been investigated, for instance InPAs, AgSbTe and others. The firms Mercury and Co. and Minnesota Mining and Manufacturing Company in the United States have introduced industrial production of PbTe, Bi_2Te_3, PbSe. Similar work is also being done in France, the Federal Republic of Germany, Japan, the United Kingdom and other countries.

The investigations of silicides, of transition metals, carbides, borides and so on open up possibilities of using thermocells at high temperatures. Work in this field is being conducted in the Soviet Union, the United States (General Electric and others) and Japan (Electric Company). Silicides of transition materials having a $Z = 0.4 \cdot 10^{-3}$ $I/°C$, working at temperatures of 1 000°C at the hot junction of the thermocell, have been obtained. There are good prospects of obtaining materials with $Z = 1 \cdot 10^{-3}$ $I/°C$ and higher.

There are reports (6) that in the United States a gadolinium selenide (GdSe) has been obtained; it was used for a thermoelectric battery and achieved an efficiency of 55 per cent. This indicates the very great possibilities in the search for materials for thermocells.

Investigations of metal oxides and compounds with a mixed valency are still in the initial stages; however, they hold the promise of revealing interesting materials, such as NiO, TiO, NiOLi and CuOLi. The possibilities of obtaining materials for thermocells on the basis of rare earth metals is likewise promising.

It is at present inpossible to forecast theoretically what materials or compounds will be the most advantageous for creating thermogenerators. Only certain qualitative tendencies are being noted, and they demand experimental confirmation. It is even more necessary to conduct extensive investigations to obtain quantitative data on their thermoelectrical properties.

Table 3 gives data on the properties of thermoelectric materials at working temperatures.

Table 3

Material	*$Z \cdot 10^3$ $I/°C$ at working temperature*	*Working temperature (°C)*
ZnSb	0.5	400
$CoSb_3$. . . .	0.3-0.4	500
PbSe	0.8	700
PbTe	1.1	700
Bi_2Te_3 . . .	0.7	300
Sb_2Te_3 . . .	0.8	300
Bi_2Te_3-Sb_2Te_3	1.0	350
Ag_2Te. . . .	1.3	100
SnTe	0.9	500
GeTe	0.9	700

Paper S/118 shows the properties of certain materials as they vary with the temperature.

In formula 2 above, the part in square brackets can be regarded as the coefficient η_0 which takes into account the optical and thermal properties of the structure. It is easy to see that at large values of the coefficient of the geometrical concentration of rays $\frac{F_b}{F_m}$ it comes close to one. At small concentra-

tions it can greatly reduce the general efficiency of the device η_{gen}.

Calculations have shown that presumably in all cases solar thermoelectric generators should have mirrors concentrating the solar rays since (*a*) this makes it possible to raise the temperature of the hot junctions of the thermocell (T_1) and thus increase their efficiency, and (*b*) reduce the size and, consequently, the cost of the thermobattery.

The question of which kind of mirror should be used — parabolocylindrical or paraboloid — should be decided on the basis of calculations. It should be borne in mind, however, that paraboloid mirrors provide the opportunity of obtaining a coefficient of geometrical concentration of rays, even if they are imperfectly manufactured. K = 200 to 1 000, while for parabolocylindrical mirrors K = 10 to 30.

It is probably not feasible to make thermoelectric generators in which the hot junctions are enclosed in a device of the hot-box type, since they have a very low efficiency and will probably prove considerably more expensive, although simpler in operation since they do not necessitate following the sun (E. Weston, 3).

Some data on existing solar thermoelectric generators

The first attempts to use thermocells as converters of solar energy into electricity were made at the end of the nineteenth and the beginning of the twentieth century. Thus in 1888 E. Weston applied for a patent for a solar thermoelectric generator (3). In 1908 W. Zerassky (4) developed and tested a solar thermoelectric battery whose hot surface was enclosed in a glass box. The material used for the thermocell was an alloy of zinc and antimony and silver-plated wire. In 1913 W. Coblentz (5) made a generator out of copper-constantan thermocouples. In 1954 M. Telkes (2) tested solar thermoelectric generators with thermocells made of different semi-conductors. The best results were obtained with cells in which the positive electrode was made of ZnPb with admixtures, and the negative electrode of an alloy containing 91 per cent Bi and 9 per cent Sb. A thermoelectric generator made on the principle of the hot-box had an efficiency of 0.63 per cent, while one with a lens had an efficiency of 3.35 per cent. The power equalled 0.156 watts.

In 1955 the Krzhizhanovski Power Institute made a solar thermoelectric generator consisting of 840 ZnSb-constatan thermocells. The hot junctions were heated by rays reflected from a paraboloid mirror 2 m in diameter, while the opposite junctions were cooled by running water. The efficiency of the thermocells equalled 3.45 per cent, and that of the entire installation η_{gen} = 0.8 per cent. The useful power of the installation was 18.9 W with I = 0.9 A and U = 21 V.

In 1960 the same institute made several solar thermoelectric generators in which the materials used were alloys of tellurium. Their power was about 10 W. The thermobatteries were heated by rays focused by means of aluminium paraboloid mirrors having a surface of about 1.2 m². The efficiency of the device as a whole was about 1.5 per cent.

Michel, in his paper (S/55), described a solar thermoelectric generator of the hot-box type, built and tested in France. It had two glass sheets with a total heated surface of 17 sq m. The power of the battery amounted to 5.5 W/m² when the solar radiation I = 680 kgcal/m² hour, and 7 W/m² when I = 860 kgcal/m²h. The useful power of the installation amounted to 120 W.

The material used for the thermocells was a bismuth telluride. At the hot junctions a temperature of 140°C was maintained and the temperature of the cold junctions was 20-25°C higher than that of the ambient air. The installation used selective films for reducing radiation losses at the hot junctions of the cells. The author believes that it is possible to raise the efficiency of this installation. He considers that from one sq m of his installation 50 watt-hours a day can be received. Thus, to obtain a power of one kW it would be necessary to have surface area of not less than 100 sq m.

K. Katz, in his paper (S/12), reports on a number of different thermoelectric generators working on fuel, atomic energy and solar energy. One of the thermoelectric generators has a power up to 5 kW. The paper describes a solar thermoelectric generator having a power of 100 watts which could drive an electric motor connected with a pump. The author estimates the efficiency of the thermoelectric generator at 5 per cent and believes that in future it could be brought up to 8 per cent. The author also calculates the possible cost of the electricity produced by this installation on the assumption that the thermoelectric generator could work for several years. He believes solar thermoelectric generators to be of considerable interest, since they could be used for driving irrigation pumps. In this paper the efficiency of the thermogenerator and its life are estimated to be unusually great compared with the estimates of other investigators.

In the paper (S/103) by R. Breihan, F. Daniels, J. Duffie and G. Löf, the results are given of tests of the thermoelectric generator described in S/12. This generator was placed near the focal point of a paraboloid reflector, 6 feet in diameter, made of plastics. The surface of the paraboloid was covered by a thin aluminised mylar polyester film. The paraboloid gave a concentration of the sun's rays 264 times greater than that of natural solar radiation. The power of the thermoelectric generator was from 22 to 40 W.

The authors note that more than 50 per cent of the energy of the sun's rays is lost because of the imperfection of the mirror. The remaining energy, however, is focused sufficiently well on a comparatively small surface. The distribution of energy in the focal region was investigated. The authors consider these investigations to be preliminary, and they will continue them in the near future.

M. Perrot and M. Touchais in their paper (S/84) give calculations for solar thermoelectric generators. They come to the conclusion (one which is probably acknowledged by most research workers in this field) that the direct heating of the hot junctions of thermoelectric generators by the sun's rays is not feasible, and it is necessary to give up this idea. Only installations using concentrated solar rays should be considered. They built and tested a solar thermoelectric generator, however, without a concentration of rays — adapted for use in the Sahara. The difficulty in this case was the cooling of the thermocells. The authors believe that since the air is very dry in the Sahara, the temperature could possibly be effectively reduced by moistening.

M. Kobayashi (S/10) examined the use of silicides of transitory materials — n-type CoSi, p-type CrSi and p-type $MnSi_2$ — as materials for thermoelectric generators. At temperatures of about 1 000°C they had fairly high $Z = \frac{\alpha^2\sigma}{\lambda}$ and could be used to make thermocells with an efficiency of from 6 to 12 per cent. These materials were used to make a thermoelectric generator 15 × 15 × 6 cm in size with a power of 10 W. The author notes that difficulties arose because of the fragility of the materials. Sintering was used to protect the hot junctions of the generator from oxidation. The author believes that generators of the type he proposes could be of great practical interest.

Problems in improving technical characteristics of solar thermoelectric generators

The theory of solar thermoelectric generators and experience in building and testing them makes it possible to establish the principal structural and technological criteria determining the optimal types.

Some general conclusions can be drawn. Thus, for instance, most investigators consider that solar thermoelectric generators should always be supplied with a device for concentrating rays, since the increased concentration of radiation not only makes it possible to raise the temperature of the hot junctions, and consequently the efficiency, but it also sharply reduces the size of the thermobatteries and the expenditure of material. There are contrary opinions, however.

The most complicated problems in building solar thermoelectric generators are those of commutation, the permissible maximum temperature of the hot junctions, protection of the hot junctions from oxidation and deformation. In hot climates another difficult problem is that of drawing the heat away from the cold junctions of the generator. If the solar thermoelectric generator is used for hauling water, the junctions can be cooled by the water. Should there be insufficient supplies of water, however, then the method of cooling by evaporation should be considered and compared with the method of raising the temperature at the cold end of the thermogenerator.

Although attempts have been made to determine the economic characteristics of solar thermoelectric generators, it is, however, too early to conclude anything definite. Further experimental data have still to be accumulated. A very important problem is that of levelling the radial energy falling from the concentrating mirror to the battery. This is examined in paper S/118.

Thermoelectronic and thermionic converters

The question of the practical significance of the conversion of thermal energy into electricity was probably first raised clearly in 1949 by A. F. Ioffe (1, 7). However, Webster (9) reported on the work done by Schlichter, who had examined the question of thermoelectronic converters as far back as 1915.

The main losses of energy in the thermocells described above are connected with the transition of heat from the hot junction to the cold as a result of heat conduction. Although thermoelectric generators made of semi-conductors have a smaller ratio σ/λ than those made of metals, in this case, too, the drifting of electrons inside the semi-conductor, together with transfer of heat energy by photons creates an unfavourable ratio of mobility to heat conductivity. From this point of view, thermocells without heat conduction are of great interest—a thermoelectronic converter of energy based on thermoelectronic emission in a vacuum.

When the cathode is heated in a vacuum thermoelectronic tube joint in a circuit with a resistance R, a certain difference in potentials arises between the cathode and anode which produces a stationary electric current in the circuit. Consequently, in this case the thermoelectronic tube can be regarded as a thermoelectronic vacuum thermocell—a converter of thermal energy into electricity. In principle this converter is very simple, and the calculations made by a number of authors show that under certain conditions it can have a high efficiency rate. A very important feature is that the temperature of the cathode can be very high—2 000°-2 500°C, and the cooling of the anode, which has a temperature of 600-700°C, can be much simpler than in the case of a thermoelectric generator. Research workers in many countries have lately been engaged in attempting to create such a source of energy.

In 1958 Hatsopoulus and Kay made and tested a thermovacuum cell in the United States; this worked at a cathode temperature of 1 200°C. The efficiency of the cell, according to the authors, amounted to 13 per cent, and the power to 0.8 W/cm².

The main difficulty in building thermoelectronic generators is that of reducing the space charge which arises in the space between the electrodes. One way of solving this problem is by lessening the distance between the cathode and electrode to a few microns. This method is simple in principle, but is very difficult to accomplish technically.

Most investigators have chosen a different way: that of neutralising the charge by introducing vapours of cesium into the space between the electrodes. By correctly choosing the cesium vapour tension and the ratio between the length of the free electrons and atoms and the geometric sizes of the path instrument, the characteristics of the thermocell can be improved considerably. The same direction was taken by the work on thermoelements with gas plasms. Houston's estimates (8) have shown that in this case an efficiency of more than 30 per cent can be obtained.

Cesium thermocells were made in the United States by Hernquist and Kanevski in 1957 (efficiency 10.4 per cent and power 12 W/cm²), by Wilson in 1959 (efficiency 9.2 per cent), Grover, in the United States in 1958, created an interesting design for a converter placed in a reactor, converting atomic energy directly into electricity. The efficiency was 5 per cent and the temperature of the cathode 2 700°K.

A thermoelectronic generator filled with cesium was investigated at the Krzhizhanovski Power Institute of the USSR Academy of Sciences in 1959. At a cathode temperature of 2 900°K, the efficiency was 4 per cent and the specific power 11 W/cm².

A Red Bank, New Jersey, laboratory developed a cesium thermoelectronic converter of solar energy into electricity. The capacity of the generator was 5W.

G. Hatsopoulos and P. Brosens (S/78) examined the work of thermionic converters, materials for making them and their technical characteristics. They note that since it is difficult to bring the cathode and anode closer than 10 microns, the maximum current which could be obtained from vacuum cells is equal to about one A/cm². Such a current can be achieved when the temperature on the cathode equals about 1 200°C. The power in this case equals about one W/cm², and the efficiency 10 per cent. In practice a power of 0.6 W/cm² is achieved with an efficiency of 6 per cent.

If the charge in the space between electrodes is decreased by introducing positive ions it is possible to increase the distance between the electrodes to one which can easily be established in practice. In cesium thermionic converters the ionisation of atoms of cesium when colliding with the cathode is used. The temperature of the cathode is about 2 200°C. From these cells a power of 20 W/cm² with an efficiency of 15 per cent can be obtained. The authors believe that because the construction of thermionic converters is simple, they can be used to transform solar energy. Pure metals, such as molybdenum, copper and tantalum, are used for their construction. About 0.1 gr of the reflecting metal and 5 gr of such inexpensive metals as copper are used per unit of power. Their length of service is estimated at 10 000-50 000 hours.

V. Wilson in his paper (S/90) describes the work of various types of thermionic converters and examines the possibility of their use for obtaining electricity from the sun by inexpensive methods.

In order to be able to utilise on earth the devices developed for artificial space bodies, it is essential to protect them from oxidation. Two methods are examined: (*a*) placing several converters from the cathode side into a large vacuum enclosure and (*b*) building a converter with ceramic parts which can withstand the oxidising effect of the air at high temperatures. The author believes the first method to be far too expensive and complicated. The second method, although less effective so far as efficiency is concerned, can still prove to be cheaper.

As a result of an examination of the work conducted until now on thermionic and thermoelectronic converters, it can be concluded that these devices are in a certain respect easier to use in outer space, without atmosphere, than on earth. The difficulties for use on earth consist of the need (*a*) to create and maintain a vacuum in the inter-electrode space, for vacuum elements, (*b*) to protect the cathode which has a very high temperature from the oxidising influence of the atmosphere, (*c*) to create cheap but accurate mirrors for concentrating the rays (since only then is it possible to obtain a sufficiently high temperature at the cathode). The economic feasibility of using these devices will depend on how successfully these difficulties are overcome.

Photo-cells as converters of solar energy into electricity

In recent years the work done by investigators in a number of countries has made it possible to build various photo-cells which can be regarded as converters of the radiant energy of the sun into electricity. The range of use of photo-electric devices is spreading each year. Though a few years ago photo-cells were used only as registering devices, lately they are coming to assume more and more significance as sources of power for apparatus converting sunlight into electricity with an efficiency of 13 per cent. This progress was made in the space of a few years. The most important achievements were scored in making photo-cells out of monocrystallic silicon.

Until 1953 it was believed that the efficiency of photo-cells could not be more than 0.6 per cent. In 1954, however, Chapin, Fuller and Pearson reported that their silicon photo-cell could have an efficiency of 6 per cent (10), and at the world symposium on applications of solar energy in Arizona in 1955, Pearson (12) announced that photo-cells with an efficiency of 11 per cent had been made in the laboratories of the Bell Telephone Company.

At present these devices are being produced on an industrial scale in a number of countries for special consumers of energy: for man-made space bodies, for communication purposes when the cost of the consumed power is not important.

The ordinary consumers of power cannot use these photo-cells, however, because of the high cost.

A kilowatt of power from photo-cells, for instance, now costs about 100 times more than that generated by conventional fuel power stations. M. Prince (S/65) notes that the cost of silicon photo-batteries at present is $175 per watt; a year ago it was $275 per watt; and three years ago, $500. It can be expected that in the near future the cost will be $100 per watt. L. Ravich (S/56) estimates the cost of photo-batteries at present at $250 a watt.

The main reason for the high cost of photo-cells lies in the fact that they are made of super-pure silicon, the production of which is very expensive. At present many investigations are being carried out into the problem of lowering the cost of photo-cells.

M. Wolf in his paper (S/44) examines the question of what should be done to enable photo-cells to be used widely. He names three main trends: using concentrators, improving efficiency and reducing costs by simplifying technological processes.

One of the possible ways of reducing the cost of photo-cells is by using polycrystallic silicon instead of monocrystallic. The cost of photo-cells made in this way in the Soviet Union (11) was one-half or one-third of the cost of photo-cells made with monocrystals. Their efficiency was 4-6 per cent (at normal solar illumination they give 5-6 W/cm²), and the ratio between the output parameters and the temperatures was similar to that of photo-cells made from monocrystallic silicon.

P. Rappoport and H. Moss in their paper (S/106) describe an interesting type of photo-cell made of cadmium sulfide (CdS) deposited on a copper layer. Such a photo-cell has an efficiency of 3.5 per cent. Its construction is comparatively simple, and the cost should not be high. The authors believe that the efficiency of the photo-cell could be increased to 6 per cent; if other materials, such as silicon, are used for deposition, it could be raised to 10 per cent.

The experiments in making photo-cells with two separate energy gaps (electro-optical systems) are directed towards the use of a wider section of the solar spectrum by photo-cells, and consequently towards increasing efficiency. The same aim is served by covering the working surface of the photo-cell with a thin film which converts the ultra-violet section of the spectrum into visible light used by the photo-cell (Technical Operations, Inc.).

One of the ways of improving silicon photo-cells is by finding a compromise correlation between the thickness of the alloy layer and its resistance. Series resistance can be lowered by putting contacts on the surface of the photo-cell in the form of a grid. These contacts make it possible to build photo-cells with a greater working surface.

A reduction in the weight of photo-cells and in the expenditure of material on them can be achieved by making photo-cells with a large surface out of thin layers of silicon (S/56). These layers can be prepared either by the deformation of silicon (rolling, stamping) or by the decomposition of silicon tetrachloride by hydrogen. The cost of photo-cells obtained by these methods, however, still remains high.

The use of photo-cells with concentrators of solar energy is being investigated both in the Soviet Union and in the United States. At the Krzhizhanovski Power Institute, experiments have been carried out to determine the influence of illumination on the voltamperic characteristics of photo-cells. For ideal photo-cells, theory suggests an almost linear dependence between the power of the photo-cells and the illumination (13). But in actual photo-cells an increase in the illumination increases the power only up to a certain value, which depends on a number of factors. Any further increase in the illumination leaves it almost unchanged. Such a non-linear dependence is due to the dispersion of a considerable part of the power on the series resistance of the photo-cell. Nevertheless, use of concentrators of solar energy can give (if there is sufficient cooling) a considerable increase in the power—about 20-30 times (S/118).

The use of intensified illumination without compulsory cooling is worth while only up to a fourfold to fivefold concentration of natural solar radiation, since the temperature of the photo-cells at greater concentrations increases sharply. In some cases it was possible to obtain a seventyfold increase in the power of the photo-cell by increasing the falling light 100 times (14).

Under certain conditions the use of concentrated rays is profitable since the cost of a unit of surface of photo-cells is several hundred times higher than that of mirrors. Possibly, by using concentrating mirrors and cooling the photo-cells and by improving the tapping of the current, it will be possible to solve the problem of creating economically acceptable devices for obtaining electricity from the sun.

At the Krzhizhanovski Power Institute several experimental photo-electric generators of this kind were built. The photo-electric generator consisted of photo-batteries with a surface of 100 cm², which was illuminated by concentrated solar rays reflected from an aluminium mirror with an effective surface of 1.2 m². The reflection coefficient of the mirror was about 0.7. The photo-battery was placed in an enclosure with a glass top. Water was passed through the chamber to cool the outside surface of the photo-battery. The useful power of the installation at a radiation of $I = 700$ kgcal/m² hour was about 10 W. The same photo-battery without a mirror gave a useful power of 0.5 W, that is, twenty times less.

From the point of view of working with concentrators of solar energy, photo-batteries made of materials other than silicon seem to be promising. Theory shows that photo-cells from materials having a greater width of the barrier layer than silicon should work better at higher temperatures (S/56). These materials include indium phosphide, gallium arsenide, cadmium telluride, aluminium antimony and cadmium

sulphide. Many research workers are at present building photo-cells out of these materials. In the Soviet Union in 1959 a photo-cell with an efficiency of 3 per cent was made of cadmium telluride (15). In the United States the physics department at Itek Laboratories is making multilayer photo-cells sprayed with cadmium sulphide (S/56). The efficiency of these photo-cells is 4-6 per cent. The maximum of the spectral characteristic is at the wave-length of 8 000Å.

The Radio Corporation of America has made a photo-cell of gallium arsenide capable of working at temperatures of 400°C without a noticeable reduction in efficiency. If it proves possible to introduce the mass production of such photo-cells, this would greatly widen their range of application.

Even at the existing high cost of solar photo-cells, their use at times proves profitable in solving some problems of supplying electricity to consumers. Papers have been submitted to this conference which note some fields of application of photo-cells.

G. Pearson (S/40) reports commercial tests of a telephone fed by solar batteries (Bell Telephone Company). The tests were made over a period of six months. In Japan solar batteries were successfully used, together with accumulators, to feed the apparatus of lighthouses; these are described in a paper by M. Kobayashi (S/11).

An examination of the existing literature on solar photo-cells leads to the conclusion that costly, highly effective, silicon photo-cells can have wide application only by using the method of increasing the concentration of the falling rays. At the same time, however, it is necessary to improve the tapping of the current in order to lessen the internal resistance of the photo-cell. It is essential, of course, to have artificial cooling of the surface of the cell.

It is likewise necessary to design a photo-cell with a sprayed layer. This could prove very effective, since the cost of such photo-cells might be economically feasible. Such methods as finding the most advantageous geometry for photo-cells, simplifying technology in making the material and the photo-cells, increasing the scale of production and so on can also have a noticeable effect in perfecting and reducing the costs of photo-cells.

Suggested topics for discussion

1. Thermoelectric generators:
   (*a*) Choice of materials;
   (*b*) Methods of increasing longevity;
   (*c*) Heat removal from cold junctions.
2. Thermionic convertors:
   (*a*) Materials and coating for cathode and anode;
   (*b*) Preservation of cathode from oxidation;
   (*c*) Methods of lessening space charge.
3. Photo-cells:
   (*a*) Materials;
   (*b*) Methods of extension of useful spectral band;
   (*c*) Reduction of photo-cell temperature;
   (*d*) Removal of current and lessening of internal electrical resistance;
   (*e*) Use of intensive radiant flow.
4. General subjects:
   (*a*) Influence of energy flow unevenness on efficiency;
   (*b*) Methods of flow and temperature levelling;
   (*c*) Prospects of reduction in initial cost and cost of power from direct conversion and their effect on possible applications in less developed countries.

References

1. Ioffe, A., *Poluprovodniki v sovremennoi fisike* (Semi-conductors in modern physics), USSR Acad. Sc., 1954.
2. Telkes, M., *Journ. Appl. Phys.*, No. 6, 1954.
3. Weston, E. U.S. patent No. 389, 124, 1888.
4. Zerassky, W. *Russkij astronomicheskij calendar*, 1909.
5. Coblentz, W., U.S. patent No. 1 077 219, 1913.
6. *Electronics*, No. 51, Dec. 1960.
7. Dobretsov, L., Termoelectronnye preobrazovatelin, *Jonrnal technicheskoi phisiki, VXXX*, No. 4, 1960.
8. Houston, *Journ. Appl. Phys., 30*, No. 4, 1959.
9. Webster, *Journ. Appl. Phys., 30*, No. 4, 488, 1959.
10. Chapin, D., Fuller, C., Perason, G., *Journ. Appl. Phys., 25*, 676, 1954.
11. Gliberman, A., Zaitseva, A., Landsman, A., *Phisika tverdogo tela, 11*, No. 8, 1960.
12. Pearson, G., Electricity from the sun, *Proceedings World Sympos. Appl. Sol. En.*, Arizona, 1955.
13. Prince, M., *Journal. Appl. Phys., 26* (59), 534, 1955.
14. Baum, V., Borovikova, R., Okhotin, A., *Ingenerno-Physichesky Journal, 3*, No. 3, Minsk, 1960.
15. Maslakovetz, *Physiko-technichesky Journal, 2*, Moscow, 1960.

UTILISATION DE L'ÉNERGIE SOLAIRE POUR LA PRODUCTION D'ÉLECTRICITÉ PAR CONVERSION DIRECTE, AU MOYEN DE CONVERTISSEURS THERMO-ÉLECTRIQUES ET DE CELLULES PHOTO-ÉLECTRIQUES

(Traduction du rapport précédent)

*Valentin A. Baum**

Il y a déjà longtemps que l'on a commencé à considérer le rayonnement solaire comme une des sources complémentaires éventuelles d'énergie. Au début, on ne lui assignait qu'un rôle très modeste : on supposait qu'il serait utilisé pour obtenir une chaleur à faible potentiel (pour le chauffage de l'eau, des serres, et pour d'autres buts analogues).

Aujourd'hui, la consommation d'énergie s'est brusquement accrue et continue de s'accroître constamment. Ce phénomène s'explique par l'augmentation de la population et l'accroissement de ses besoins, la nécessité d'assimiler de nouveaux territoires pour y installer ce surcroît de population. Pour adapter ces nouveaux territoires aux nécessités vitales, il faut habituellement déployer de grands efforts et dépenser de grandes quantités d'énergie. Étant donné les énormes dépenses de combustible sur quoi est fondée l'énergétique contemporaine, les réserves de combustibles diminuent rapidement; aussi l'économie de l'industrie énergétique se transforme-t-elle en ayant recours à des ressources énergétiques qui, jadis, ne pouvaient pas concurrencer le combustible.

Ces dernières années, les recherches effectuées dans nombre de pays ont montré la possibilité d'utiliser de manière beaucoup plus large et diversifiée l'énergie solaire, cela dans des délais très courts, même étant donné le niveau actuel des possibilités techniques.

Au point de vue pratique, l'un des problèmes majeurs est la conversion de l'énergie du rayonnement solaire en énergie électrique.

La solution de ce problème avait déjà été abordée en employant le cycle de vapeur classique. Cependant on peut aussi réaliser cette solution par de nouvelles méthodes fondées sur les progrès réalisés dans le domaine de la physique du corps solide et dans celui de la technique de fabrication de nouveaux matériaux à propriétés physiques spéciales, notamment ceux dits semi-conducteurs.

Pratiquement, les installations dès maintenant intéressantes et pleines de promesses pour un prochain avenir comme convertisseurs de l'énergie solaire rayonnante sont : 1) les générateurs thermo-électriques, 2) les générateurs photo-électriques, 3) les dispositifs thermo-électroniques et thermo-ioniques.

Ces dispositifs présentent sur les machines à vapeur ordinaires beaucoup d'avantages, dont le principal est l'absence d'organes mobiles. Ils seront aussi relativement simples à exploiter. On suppose que, dans les toutes prochaines années, certains d'entre-eux pourront économiquement être adoptés pour fournir des puissances allant de quelques watts jusqu'à un kilowatt et davantage; on pourra les employer pour l'alimentation de pompes d'eau de faible puissance, pour l'éclairage de petits immeubles, etc.

Le terme « méthodes nouvelles de conversion de l'énergie » est quelque peu ambigu. Les phénomènes physiques sur lesquels ces méthodes reposent sont connus depuis longtemps. C'est ainsi que le phénomène de la thermo-électricité a été découvert il y a 140 ans; l'effet photo-électrique de la couche d'arrêt a été révélé il y a environ 175 ans. Par contre, les premiers thermo-générateurs solaires n'ont été construits qu'à la fin du dix-neuvième siècle, et la première cellule photo-électrique à soupape date de 1930. L'attention considérable accordée dans nombre de pays aux éléments thermo-électriques et aux cellules photo-électriques a permis d'augmenter brusquement leurs caractéristiques techniques, et si, il y a vingt ans, le rendement global de la conversion de l'énergie solaire en énergie électrique au moyen de cellules photo-électriques et d'éléments thermo-électriques pouvait être d'environ quelques dixièmes pour cent, il est actuellement de l'ordre de 10 p. 100. Un grand nombre de travaux sur la théorie de ces appareils et sur la recherche de divers matériaux semi-conducteurs démontre qu'il est possible d'améliorer encore notablement le rendement global des électro-générateurs solaires, et aussi certaines autres de leurs caractéristiques techniques et économiques.

Dans le présent rapport, il n'est même pas possible de citer tous les travaux les plus importants des divers auteurs et organismes qui se sont mis à l'étude de ces problèmes, tant est grand le nombre de ces travaux. Nous ne citerons que les mémoires soumis à la Conférence des Nations Unies sur les sources nouvelles d'énergie et quelques articles où l'on étudie les convertisseurs de l'énergie solaire.

* Directeur adjoint de l'Institut Krjijanovski de l'énergie, chef du Laboratoire solaire, Moscou.

Thermo-électrogénérateurs

Renseignements généraux

Le thermo-électrogénérateur (TEG) est une installation qui convertit l'énergie thermique directement en énergie électrique. Son fonctionnement est basé sur le phénomène, découvert il y a environ 140 ans, de la naissance d'un courant électrique dans une chaîne formée par deux métaux ou semi-conducteurs lorsque leurs jonctions (contacts, soudures) sont maintenues à des températures différentes.

Un TEG se compose d'un certain nombre de ces éléments thermo-électriques montés en série. On peut le considérer comme une machine thermique sans organes mobiles, laquelle convertit en électricité une partie de la chaleur amenée sur les jonctions chaudes. Conformément à la deuxième loi de la thermodynamique, il se produit inévitablement dans ce convertisseur des pertes irréversibles d'énergie, étant donné le transport de chaleur, par conductibilité thermique, des jonctions chaudes aux jonctions froides. En outre, une partie de l'énergie électrique produite dans les éléments est convertie en chaleur par le passage du courant dans la chaîne formée par les éléments thermo-électriques ayant une résistance électrique déterminée, et une partie de cette chaleur se disperse sans être utilisée. Suivant le mode de construction, il y a aussi des pertes dans les installations qui concentrent les rayons solaires, des pertes par réflexion partielle des rayons solaires sur la surface des batteries, des pertes par convection et par rayonnement à partir des jonctions chaudes.

Le rendement global de la conversion en énergie électrique de la chaleur passant à travers l'élément thermo-électrique est fonction des propriétés physiques des matériaux qui constituent ce dernier et des températures respectives des jonctions chaudes (T_1) et des jonctions froides (T_2).

On considère le matériau comme meilleur plus est grande la valeur de la quantité

$$Z = \frac{\alpha^2 \sigma}{\lambda}$$

où α = la force thermo-électromotrice spécifique,
σ = la conductance
et λ = le coefficient de conductibilité thermique du matériau.

Pour les métaux, les rapports entre α, σ et λ étant très défavorables (les valeurs de Z sont alors faibles), ils ne conviennent pas comme matériaux pour les éléments thermo-électriques énergétiques. Pour les semi-conducteurs, les valeurs de Z sont bien plus grandes. En employant pour une chaîne d'éléments thermo-électriques un semi-conducteur du type électronique (type N) et pour l'autre chaîne un autre type perforé (type P), on réussit à obtenir des éléments thermo-électriques ayant un rendement global suffisamment élevé.

La théorie du travail d'un élément thermo-électrique, en tant que dispositif convertissant la chaleur qui le traverse en énergie électrique, fournit l'expression suivante pour le calcul du rendement global :

$$\eta = \frac{T_1 - T_0}{T_1} \frac{\sqrt{1 + \frac{1}{2} Z (T_1 + T_0)} - 1}{\sqrt{1 + \frac{1}{2} Z (T_1 + T_0)} + \frac{T_0}{T_1}} \quad (1)$$

Si l'on définit le rendement global par rapport au flux d'énergie de rayonnement incident sur le miroir du générateur thermo-électrique solaire, il faut tenir compte aussi des pertes d'énergie dues à la réflexion partielle des rayons à partir des miroirs qui concentrent les rayons et à l'absorption incomplète du rayonnement par la surface des batteries thermiques, des pertes par convection, et enfin des pertes par rayonnement des surfaces chaudes des batteries. Dans ce cas, le rendement global du générateur thermo-électrique peut être défini par la relation suivante :

$$[2]\ \eta_{gen} = RA \frac{T_1 - T_0}{T_1} \frac{\sqrt{1 + \frac{1}{2} Z (T_1 + T_0)} - 1}{\sqrt{1 + \frac{1}{2} Z (T_1 + T_0)} + \frac{T_0}{T_1}} \left[1 - \frac{F_b}{F_m} \frac{\sigma (T_1^4 - T_0^4) + k (T_1 - T_0)}{RAI} \right]$$

Ici σ = coefficient de rayonnement du matériau de la batterie ($\sigma \cong 4{,}2 \cdot 10^{-8}$),

T_1, T_2, T_0 = températures de jonction chaudes et froides de la batterie et du milieu ambiant,

F_m = aire efficace du miroir,

F_b = aire de la surface chauffée de la batterie,

α = coefficient d'émission thermique par convection, à partir de la surface de la batterie, dans l'air ambiant $\left(\alpha = 10\text{-}20 \frac{\text{Kcal}}{\text{m}^2/\text{h}/°\text{C}}\right)$,

R = coefficient de réflexion du miroir (0,75-0,85),

A = capacité d'absorption du rayonnement solaire par la surface chauffable de la batterie (0,85-0,9),

I = rayonnement solaire direct $\frac{\text{Kcal}}{\text{m}^2/\text{h}}$.

La quantité $\eta_k = \frac{T_1 - T_2}{T_1}$ représente le rendement global idéal du convertisseur (rendement global du cycle de Carnot); ses valeurs en fonction de T_1 figurent dans le tableau 1 pour le cas où les jonctions froides ont une température $T_2 = 300$ °K.

Tableau 1

T_1 . .	350	400	450	500	550	600	650	700	800	900	1 000	1 100	1 200
η_k . .	0,14	0,25	0,33	0,40	0,46	0,50	0,54	0,57	0,63	0,67	0,70	0,73	0,75

La quantité $\eta_m = \dfrac{\sqrt{1 + \frac{1}{2} Z (T_1 + T_0)} - 1}{\sqrt{1 + \frac{1}{2} Z (T_1 + T_0)} + \frac{T_0}{T_1}}$ indique le rapport entre la quantité de chaleur convertie par le matériau en énergie électrique et la quantité de chaleur qui pourrait être convertie si le matériau avait des propriétés idéales.

Le tableau 2 donne les valeurs de cette quantité pour quelques matériaux classiques ayant une valeur Z différente pour $T_1 = 1\,000$ °K et $T_0 = 300$ °K.

Tableau 2

$Z.10^3$.	0,5	0,7	1,0	1,5	2	3	5	10	45
η_m . . .	0,1	0,14	0,18	0,24	0,29	0,36	0,45	0,58	0,78

Il ne faut pas perdre de vue que les valeurs α, σ et λ sont fonction de la température à laquelle travaille le matériau et, par conséquent, le choix des matériaux pour les éléments thermo-électriques doit se baser sur les valeurs de Z, déterminées pour les températures de régime. Par exemple, la force thermo-électromotrice α pour quelques matériaux varie avec les changements de température, non seulement en valeur absolue, mais aussi en signe. Malheureusement, il n'est pas encore possible de déterminer par la théorie quels matériaux peuvent être efficaces au point de vue de leur emploi pour les éléments thermo-électriques. En règle générale, les travaux sur la recherche de matériaux adéquats se poursuivent expérimentalement. De vastes recherches de cette nature sont effectuées dans beaucoup de pays. Le résultat en est qu'il est possible de constituer des éléments thermo-électriques dont le rendement global va jusqu'à 10 p. 100, et par l'emploi de modèles à cascades multiples, jusqu'à 15 p. 100.

En Union soviétique, à l'Institut Krjijanovsky de l'énergie, on a fait des recherches sur les combinaisons intermétalliques (préparées avec des matériaux de type commercial) Bi_2Te_3, Sb_2Te_3, PbTe, PbSe, ZnSb, $CoSb_3$ et de solutions solides qui les contiennent. On a étudié les propriétés caractéristiques de 13 alliages binaires du tellure. Tout comme pour les matériaux déjà mentionnés, des facteurs Z élevés se retrouvent dans Ag_2Te, SnTe et GeTe. Aux États-Unis, la firme Westinghouse, la General Electric et la Radio Corporation of America ont effectué d'amples travaux de recherche sur PbTe (N et P) Bi_2Te_3, Sb_2Te_3 et surtout GeTe et ses composés avec d'autres systèmes.

Beaucoup d'autres combinaisons ont été étudiées, par exemple InPAs, AgSbTe, etc. Les firmes Mercury and Co. et Minnesota Mining and Manufacturing Company aux États-Unis ont mis au point la production industrielle de PbTe, Bi_2Te_3, PbSe. Des travaux du même genre se poursuivent au Japon, en France, en Angleterre, en République fédérale d'Allemagne et dans d'autres pays.

L'étude des siliciures des métaux de transition, des carbures, des borures, etc. laisse entrevoir des possibilités d'utilisation des éléments thermo-électriques à hautes températures. Des travaux dans ce domaine sont en train en URSS, aux États-Unis (General Electric et autres), au Japon (Electric Company). On a obtenu des siliciures de métaux de transition avec $Z = 0{,}4.10^{-3} I/°C$, employés à des températures allant jusqu'à 1 000 °C à la jonction chaude de l'élément thermo-électrique. On s'attend à obtenir des matériaux avec $Z = 1 . 10^{-3}\ I/°C$ et davantage.

On annonce (6) qu'aux États-Unis il a été obtenu un séléniure de gadolinium, dont l'emploi dans des batteries thermo-électriques permet d'atteindre un rendement global de 55 p. 100. Cela indique les grandes possibilités que l'on peut rencontrer sur la voie de la recherche des matériaux pour éléments thermo-électriques.

L'étude des oxydes métalliques et des composés à valence mixte en est encore au stade initial; on signale toutefois des matériaux intéressants tels que NiO, TiO, NiOLi, CuOLi, etc.

On s'attend à trouver des matériaux pour éléments thermo-électriques en partant des éléments de terres rares.

Il n'est pas possible actuellement de prédire théoriquement les matériaux ou leurs composés qui présentent le plus d'avantages pour la construction de thermo-générateurs. Nous n'indiquons ici que certaines tendances qualitatives, qui exigent une vérification expérimentale. De vastes recherches sont *a fortiori* nécessaires pour obtenir des données quantitatives sur les propriétés thermo-électriques.

Le tableau 3 fournit des renseignements sur les propriétés de quelques matériaux thermo-électriques aux températures de régime.

Tableau 3

Matériau	$Z \cdot 10^3$ *1/°C à la température de régime*	*Température de régime*
ZnSb	0,5	400
$CoSb_3$	0,3-0,4	500
PbSe	0,8	700
PbTe	1,1	700
Bi_2Te_3	0,7	300
Sb_2Te_3	0,8	300
Bi_2Te_3-Sb_2Te_3	1,0	350
Ag_2Te	1,3	100
SnTe	0,9	500
GeTe	0,9	700

Le mémoire S/118 fait voir les propriétés de quelques matériaux en fonction de la température.

Dans la formule (2), on peut considérer l'expression entre crochets comme le coefficient η_0, tenant compte des propriétés optiques et thermo-techniques de la construction. On voit facilement que cette quantité, pour les valeurs élevées du coefficient de concentration géométrique des rayons $\frac{F_m}{F_b}$ reste proche de l'unité. Si la valeur de la concentration est faible, il peut se produire une baisse considérable du rendement global η_{gen} de l'installation.

Des calculs montrent que dans tous les cas les générateurs thermo-électriques devraient probablement comporter des miroirs qui concentrent les rayons du soleil; cela donne la possibilité (1) de relever la température T_1 des jonctions chaudes des éléments thermo-électriques et, ce faisant, d'augmenter leur rendement global, et (2) de diminuer les dimensions et par conséquent le coût des batteries thermiques.

Pour résoudre la question de savoir s'il faut employer des miroirs paraboliques ou cylindroparaboliques, on doit s'en rapporter au calcul. Il faut toutefois bien tenir compte du fait que les miroirs paraboliques permettent d'obtenir un coefficient de concentration géométrique des rayons $K = 200$ à 1 000, même si leur construction n'est pas précise, alors que pour les miroirs cylindroparaboliques $K = 10$ à 30.

Il ne serait sans doute pas indiqué de construire des générateurs thermo-électriques dans lesquels les jonctions chaudes sont enfermées dans un dispositif du genre serre chaude, étant donné que ces dispositifs ont un rendement global très bas et se révéleront vraisemblablement beaucoup plus dispendieux, bien qu'ils soient d'un fonctionnement plus simple, puisqu'ils n'ont pas besoin de suivre le mouvement apparent du soleil (3).

Quelques renseignements sur les thermo-électrogénérateurs solaires réalisés

Les premières tentatives d'utilisation des éléments thermo-électriques comme convertisseurs de l'énergie solaire en énergie électrique remontent à la fin du dix-neuvième siècle et au début du vingtième. C'est ainsi qu'en 1888 E. Weston prit un brevet pour un générateur thermo-électrique solaire (3). En 1908, W. Zerassky (4) élabora et expérimenta une batterie thermo-électrique solaire dont la surface chaude était enfermée dans un châssis vitré. Le matériau utilisé pour les éléments thermo-électriques était un alliage de zinc et d'antimoine et des fils de ruolz. En 1913 W. Coblentz (5) fit un générateur en assemblant des thermocouples de cuivre-constantan. En 1954, M. Telkes (2) fit des expériences sur des thermo-électrogénérateurs avec éléments thermo-électriques constitués par divers semi-conducteurs. Les meilleurs résultats furent obtenus avec des éléments dont l'électrode positive était en ZnPb avec alliages, et l'électrode négative était composée d'un alliage de 91 p. 100 de Bi avec 9 p. 100 de Sb. Le TEG construit sur le type serre chaude avait un rendement global de 0,63 p. 100 et le TEG muni d'une lentille concentrant les rayons du soleil avait un rendement global de 3,35 p. 100. La puissance de cette installation était de 0,156 watts.

En 1955, à l'Institut Krjijanovski on construisit un TEG solaire composé de 840 éléments thermo-électriques Zn Sb-constantan. Les jonctions chaudes étaient chauffées par des rayons reflétés par un miroir parabolique de 2 m de diamètre et les jonctions opposées étaient refroidies par de l'eau courante. Le rendement global des éléments thermo-électriques était de 3,45 p. 100 et le rendement global de l'installation entière ηgen était de 0,8 p. 100. La puissance utile de l'installation était de 18,9 watts avec une intensité de $I = 0,9$ ampères et une tension $U = 21$ volts.

En 1960, au même Institut on établit quelques petits TEG dont les matériaux étaient des alliages de tellure. Leur puissance était d'environ 10 watts. Les batteries thermiques étaient chauffées par des rayons focalisés au moyen de miroirs paraboliques aluminisés ayant une superficie de 1,2 m². Le rendement global de toute l'installation était d'environ 1,5 p. 100.

Michel (mémoire S/55) a décrit un TEG solaire construit et expérimenté en France du type serre chaude, avec deux vitres, dont la superficie chauffable était de 17 m². La puissance de la batterie était de 5,5 W /m² avec une intensité de radiation solaire $I = 680$ Kcal/m²/h et de 7 W/m² pour $I = 860$ Kcal/m²/h. La puissance totale de l'installation était de 120 watts.

Le matériau utilisé pour les éléments thermo-électriques était du tellurure de bismuth. Les jonctions chaudes étaient maintenues à une température de 140 °C et les jonctions froides à une température dépassant de 20 à 25 °C celle de l'air ambiant. Dans la construction, on avait utilisé des plaques collectrices sélectives pour abaisser la perte par rayonnement des jonctions chaudes des éléments. L'auteur croit possible d'élever le rendement global de cette installation. Il estime que, par m² de cette installation, on peut obtenir 50 Wh par jour. Ainsi, pour obtenir 1 kW de puissance, il faut une superficie d'au moins 100 m².

Katz (mémoire S/12) donne des précisions sur une série de divers TEG qui opèrent au moyen de combustible, d'énergie atomique ou d'énergie solaire. Un de ces TEG avait une puissance allant jusqu'à 5 kW. Ce mémoire décrit un TEG solaire de 100 W qui pouvait mettre en marche un moteur électrique relié à une pompe. Le rendement global du TEG est estimé par l'auteur à 5 p. 100, et pourrait être, d'après l'auteur, porté à 8 p. 100. Katz évalue aussi le coût éventuel de l'énergie électrique produite par cette installation, en supposant que ce TEG pourra fonctionner quelques années durant. L'auteur estime que les TEG peuvent présenter un certain intérêt, puisqu'ils pourront servir à mettre en marche des pompes pour l'irrigation.

Dans cet article, les valeurs du rendement global du thermo-générateur et sa durée de fonctionnement sont évaluées bien plus haut que les chiffres correspondants obtenus par quelques autres chercheurs.

Dans le mémoire S/103, R. Breihan, F. Daniels, J. Duffie et G. Löf donnent les résultats de l'essai du TEG décrit dans S/12. Ce générateur était logé près du foyer d'un réflecteur parabolique (ayant un diamètre de 1,8 m, soit 6 pieds) en matière plastique. La surface du paraboloïde était couverte d'une pellicule mince aluminisée du genre mylar (*aluminized mylar polyester film*). Le paraboloïde produisait une concentration du flux lumineux 264 fois plus forte que la radiation solaire naturelle. La puissance de ce TEG était de 22 à 40 W.

Les auteurs montrent que plus de 50 p. 100 de l'énergie des rayons solaires sont perdus par suite de l'imperfection du miroir. Toutefois, la fraction restante de l'énergie est suffisamment bien focalisée sur une surface relativement faible. On a étudié la répartition de l'énergie dans la région de la tache focale. Les auteurs estiment que ce sont là des expériences profitables et les poursuivront dans un très bref délai.

Dans le mémoire S/84, M. Perrot et M. Touchais exposent les calculs pour des TEG solaires. Les auteurs arrivent à la conclusion (admise, semble-t-il, par la plupart de ceux qui travaillent dans ce domaine) que l'échauffement direct des jonctions chaudes du TEG par les rayons solaires n'est pas réalisable et qu'il faut y renoncer. Il convient de n'étudier que les installations faisant appel à la concentration des rayons solaires. Toutefois ils ont construit et expérimenté un TEG sans concentration qu'ils ont adapté pour des travaux dans les conditions régnant au Sahara. Le problème difficile est ici le refroidissement des éléments thermo-électriques. Les auteurs estiment qu'étant donné la sécheresse de l'air au Sahara, on pourra abaisser efficacement la température par humidification.

M. Kobayashi (S/10) étudie l'emploi comme matériaux pour les TEG de siliciures de matériaux de transition : CoSi type N, CrSi type P, $MnSi_2$ type P. A une température d'environ 1 000 °C ils ont un facteur $Z = \frac{\alpha^2\sigma}{\lambda}$ assez élevé et on peut construire avec eux des éléments dont le rendement global va de 6 à 12 p. 100. De tels matériaux ont servi à construire un TEG dont les dimensions étaient 15 × 15 × 6 cm et la puissance 10 W. L'auteur estime que les difficultés survenues proviennent de la fragilité de ces matériaux.

Pour empêcher l'oxydation des jonctions chaudes du générateur, on a eu recours au frittage (*sintering*) des éléments. L'auteur pense que les générateurs du type qu'il propose présenteront un grand intérêt pratique.

Problèmes en matière d'amélioration des caractéristiques techniques des thermo-électrogénérateurs solaires

La théorie élaborée pour les TEG solaires, l'expérience acquise dans leur construction et les recherches déjà faites à leur sujet permettent dès maintenant de fixer, pour leur construction et leur technologie, des critères fondamentaux déterminant les types optimaux de ces installations.

Il est possible de tirer déjà certaines conclusions générales. Ainsi, la plupart des chercheurs estiment que les TEG solaires doivent toujours être dotés d'une installation pour la concentration des rayons; en effet, l'augmentation de la concentration de l'énergie rayonnante permet non seulement d'élever la température des jonctions chaudes et, par conséquent, la valeur du rendement global, mais aussi de diminuer les dimensions des batteries thermiques et la dépense des matériaux. Mais il existe également des points de vue opposés.

Les problèmes les plus compliqués soulevés par la création de TEG solaires sont les questions de commutation, de température maximale pour les jonctions chaudes, de protection des jonctions chaudes contre l'oxydation et la déformation. Lorsqu'on est sous un climat brûlant, une question compliquée consiste à refroidir les jonctions froides des TEG solaires. Dans le cas où le TEG solaire servira à pomper de l'eau, le refroidissement des jonctions pourra s'effectuer en utilisant l'eau pompée; mais là où il n'y a pas assez d'eau il faut envisager la méthode de refroidissement par évaporation, qu'on comparera à la méthode d'élévation de température sur le côté froid du thermo-générateur.

On a cherché à déterminer les caractéristiques économiques des TEG solaires; toutefois pour le moment il est difficile d'être catégorique à ce sujet. Il faut encore accumuler les données expérimentales.

Une question d'extrême importance consiste à égaliser le flux du rayonnement d'énergie qui tombe du miroir concentreur sur la batterie. Cette question est examinée dans le mémoire S/118.

Convertisseurs thermo-électriques et thermo-ioniques

Il semble que la question de la portée pratique de la conversion directe de l'énergie thermique en énergie électrique a été posée nettement pour la première fois par A. Ioffe en 1949 (1, 7). Cependant,

Webster (9) a rendu compte des travaux de Schlichter qui déjà, en 1915, avait étudié les convertisseurs thermo-ioniques.

La perte principale d'énergie dans les éléments thermo-électriques mentionnés plus haut tient au passage de chaleur de la jonction chaude à la jonction froide, par conduction thermique. Bien que dans les éléments thermo-électriques à semi-conducteurs le rapport σ/λ soit moindre que dans les thermo-électriques à métaux, ici par contre, la dispersion des électrons à l'intérieur du semi-conducteur et le transfert d'énergie thermique par les photons font que le rapport de la mobilité à la conductance thermique est défavorable. A ce point de vue, un grand intérêt s'attache à l'élément thermo-électrique sans conduction thermique comme convertisseur thermo-électronique d'énergie fondé sur l'émission thermo-électronique dans le vide.

Lorsqu'on porte à incandescence la cathode d'une lampe électronique à vide montée dans un circuit avec la résistance R, il se produit entre la cathode et l'anode une certaine différence de potentiel, laquelle crée dans le circuit un courant électrique fixe. Dans ce cas, la lampe thermo-électronique peut donc être considérée comme un thermo-élément thermo-électronique à vide, convertisseur de l'énergie thermique en énergie électrique. En théorie, un tel convertisseur est extrêmement simple et les calculs effectués par nombre d'auteurs ont montré qu'il peut posséder, dans certaines conditions, un rendement global élevé. Un fait aussi très important est qu'on peut avoir ainsi à la cathode une température élevée allant jusqu'à 2 000 ou 2 500 °C, et l'évacuation de chaleur de l'anode qui est à une température de 600 à 700 °C peut être bien plus simple à réaliser que dans le cas, par exemple, de l'utilisation d'un TEG. De nombreux savants du monde entier se sont récemment attachés à résoudre le problème de la construction d'une telle source d'énergie.

En 1958, aux États-Unis, Hatsopoulos et Kay ont réalisé et expérimenté un élément thermique à vide, fonctionnant à une température de 1 200 °C à la cathode. Le rendement global de cet élément, affirment les auteurs, est de 13 p. 100 et la puissance de 0,8 W/cm².

La difficulté fondamentale pour réaliser des générateurs thermo-électroniques consiste à réduire la charge d'espace qui se produit dans l'espace entre les électrodes. Un des moyens de résoudre ce problème est de réduire à quelques microns la distance entre la cathode et l'anode. C'est là un moyen théoriquement simple, mais difficile à réaliser en pratique.

La plupart des chercheurs se sont engagés dans une autre voie : la neutralisation de la charge d'espace par l'introduction dans l'espace entre les électrodes de vapeurs de césium. Il est possible d'améliorer considérablement les indices de l'élément thermo-électrique en sélectionnant convenablement la tension de la vapeur de césium et le rapport entre la longueur de libre parcours des électrons et atomes, d'une part, et la géométrie de l'appareil, d'autre part. Dans ce sens, des travaux ont porté sur un élément thermo-électrique plasmagazeux. Les calculs de Houston (8) ont prouvé que dans ce cas le rendement global peut dépasser 30 p. 100.

Des éléments thermo-électriques au césium ont été réalisés aux États-Unis par Hernquist et Kanevski en 1957 (rendement global 10,4 p. 100, puissance 12 W/cm²) par Wilson en 1959 (rendement global 9,2 p. 100). Grover (États-Unis), en 1958, a mis au point une conception intéressante pour un convertisseur logé dans un réacteur et convertissant directement l'énergie atomique en énergie électrique. Le rendement global de l'installation était de 5 p. 100. La température à la cathode était d'environ 2 700 °K.

En Union soviétique, l'Institut Krjijanovsky de l'Académie des sciences a étudié en 1959 un générateur thermo-électronique au césium. La température à la cathode étant de 2 900 °K, le rendement global a été de 4 p. 100 et la puissance spécifique de 11 W/cm².

Un laboratoire situé à Red Bank, dans le New Jersey, a réalisé un convertisseur thermo-électronique au césium de l'énergie solaire en énergie électrique. La puissance du générateur est de 5 W.

Dans le mémoire S/78, G. Hatsopoulos et P. Brosens étudient les conditions de fonctionnement de convertisseurs thermo-ioniques, les matériaux pour les construire, et leurs caractéristiques techniques. Ils font voir, étant donné la difficulté de ramener la distance entre la cathode et l'anode à moins de 10 microns, que le courant maximal que l'on puisse obtenir dans des éléments à vide est d'environ 1 ampère/cm². Cette intensité peut être atteinte avec une température à la cathode d'environ 1 200 °C, la puissance obtenue étant d'environ 1 W/cm² et le rendement global inférieur à 10 p. 100. En pratique, on atteint une puissance de 0,6 W/cm² avec un rendement global de 6 p. 100.

Si l'on réduit la charge dans l'espace entre les électrodes en introduisant des ions positifs, il est possible de ramener la distance entre les électrodes à des dimensions faciles à réaliser dans les installations pratiques. Dans les convertisseurs au césium, on utilise l'ionisation des atomes de césium frappant la cathode portée à une température d'environ 2 200 °C. Avec ces éléments, on a obtenu une puissance de 20 W/cm², le rendement global étant de 15 p. 100. Les auteurs estiment qu'étant donné la facilité de construction des convertisseurs thermo-ioniques, on peut les utiliser pour la conversion de l'énergie solaire. On y emploie des métaux purs comme le molybdène, le cuivre, le tantale. Pour une unité de puissance, il faut employer 0,1 g de métal réflecteur et 5 g de métaux bon marché comme le cuivre. Leur durée de service est évaluée à 10 000-50 000 heures.

Dans le mémoire S/90, V. Wilson décrit le fonctionnement de divers types de convertisseurs thermo-ioniques et examine la possibilité d'employer ces installations pour obtenir à bas prix de l'énergie électrique en utilisant le rayonnement solaire.

Pour adapter aux conditions terrestres les appareils conçus pour des satellites artificiels, il faut les protéger contre l'oxydation. L'auteur examine deux méthodes : 1) renfermer plusieurs convertisseurs du côté cathode dans un grand compartiment où l'on a fait le vide (large vacuum enclosure), 2) construire un convertisseur avec des parties en céramique, qui pourraient, à de hautes températures, résister à l'action oxydante de l'air. L'auteur pense que la première variante est coûteuse et compliquée; si la seconde variante est moins efficace quant au rendement, elle peut par contre se révéler moins coûteuse.

L'examen des travaux effectués jusqu'à maintenant au sujet des convertisseurs thermo-ioniques et thermo-électroniques permet de conclure que ces dispositifs peuvent être, sous un certain rapport, utilisés plus simplement dans les conditions de l'espace cosmique extra-atmosphérique que dans les conditions terrestres. Pour les conditions terrestres, les difficultés consistent dans la nécessité : 1) de créer et de maintenir le vide dans l'espace entre les électrodes (pour les éléments placés sous vide); 2) de protéger contre l'action oxydante de l'atmosphère la cathode qui se trouve à très haute température; 3) de construire des miroirs peu coûteux mais précis concentrant les rayons (ceci est indispensable pour obtenir des températures suffisamment hautes à la cathode). Un emploi économiquement rationnel de ces dispositifs dépendra du succès remporté pour surmonter ces difficultés.

Cellules photo-électriques comme convertisseurs de l'énergie du rayonnement solaire en énergie électrique

Au cours des dernières années, les travaux des savants de nombreux pays ont permis de créer diverses cellules photo-électriques que l'on peut considérer comme des convertisseurs de l'énergie du rayonnement solaire en énergie électrique. D'année en année, le champ d'application des dispositifs photo-électriques va en s'élargissant. Il y a quelques années, les cellules photo-électriques ne servaient que de dispositifs d'enregistrement. Mais depuis peu de temps, une importance toujours plus grande s'attache aux cellules photo-électriques comme source d'alimentation des appareils qui convertissent la lumière solaire en énergie électrique avec un rendement allant jusqu'à 13 p. 100. Ce progrès a été réalisé en quelques années.

Les plus grandes réussites ont été réalisées dans le domaine de la fabrication de cellules photo-électriques à partir du silicium mono-cristallin.

Jusqu'à 1953, on pensait que le rendement global des cellules photo-électriques ne pouvait pas dépasser 0,6 p. 100; pourtant, en 1954, Chapin, Fuller et Pearson annonçaient que leur cellule photo-électrique au siliucim pouvait avoir un rendement global de 6 p. 100 (10) et, en 1955, à la Conférence mondiale de l'utilisation de l'énergie solaire, en Arizona, Pearson (12) annonça qu'au laboratoire de la Bell Telephone Company on avait construit des cellules photo-électriques ayant un rendement global de 11 p. 100.

Actuellement des dispositifs de ce genre sont produits industriellement dans nombre de pays pour divers consommateurs spéciaux d'énergie — pour les satellites artificiels, pour les télécommunications, là où la question du coût ne joue pas un grand rôle. Par contre, les consommateurs ordinaires d'énergie ne peuvent employer les cellules photo-électriques, du fait de leur prix élevé. Une puissance établie de 1 kW provenant de cellules photo-électriques revient actuellement cent fois plus cher, par exemple, que dans les centrales thermo-électriques ordinaires. M. Prince (S/65) indique que le coût des batteries photo-électriques au silicium est actuellement de 175 dollars par watt; il y a un an le coût en était de 275 et il y a trois ans de 500 dollars. On peut à peu près compter que dans un proche avenir le watt reviendra à 100 dollars.

L. Ravich (S/56) estime que le coût actuel des batteries photo-électriques est de 250 dollars par watt.

La cause principale de cette cherté des cellules photo-électriques est qu'elles sont fabriquées à partir d'un silicium de très grande pureté dont la production est très coûteuse.

Actuellement on effectue de nombreuses recherches afin de résoudre le problème de la réduction du prix des cellules photo-électriques.

M. Wolf, dans le mémoire S/44, étudie la question de savoir quels perfectionnements il faut apporter pour que les cellules photo-électriques puissent être largement employées dans la pratique. Il indique trois tendances principales : emploi de concentrateurs, amélioration du rendement global, réduction du prix par application d'une technologie simplifiée.

Un des moyens éventuels de réduire le prix des cellules photo-électriques est d'employer du silicium polycristallin au lieu de silicium monocristallin. Le coût des cellules photo-électriques ainsi obtenues en URSS (11) est la moitié ou le tiers de celui des cellules à monocristaux. Leur rendement global est de 4 à 6 p. 100 (à une lumière solaire normale, ces cellules photo-électriques fournissent de 5 à 6 W/cm²) et le rapport entre les paramètres de sortie et les températures est analogue à celui des cellules photo-électriques constituées avec un silicium monocristallin.

P. Rappaport et H. Moss (S/106) décrivent dans leur étude une cellule photo-électrique au sulfure de cadmium CdS, intéressante quant au principe de sa construction, sous forme de précipité sur une couche de cuivre (*copper layer*). Cette cellule photo-électrique a un rendement global de 3,5 p. 100. Sa préparation est relativement simple et son coût doit être peu élevé. Les auteurs estiment que le rendement global de cette cellule photo-électrique peut être élevé jusqu'à 6 p. 100 et, par l'emploi d'autres matériaux précipités, par exemple le silicium, jusqu'à 10 p. 100.

C'est vers l'utilisation par les cellules photo-électriques d'une bande plus large du spectre solaire, le rendement global étant par conséquent plus élevé, que s'orientent les travaux en matière de réalisation de cellules photo-électriques avec deux zones interdites (*electro-optical systems*). Dans ce même but, la superficie active des cellules photo-électriques est recouverte d'une pellicule mince, convertissant les rayonnements de la région ultra-violette du spectre en lumière visible, utilisable par la cellule photo-électrique (Technical Operations, Inc.).

Un moyen d'améliorer les cellules photo-électriques à silicium consiste à établir un compromis entre l'épaisseur de la couche d'alliage et sa résistance. On peut abaisser la résistance en série en disposant à la surface de la cellule photo-électrique des contacts réticulaires. Ces contacts permettent de construire des cellules photo-électriques à grande surface active.

La réduction du poids des cellules photo-électriques et la diminution des dépenses en matériaux constituants peuvent être réalisées par la fabrication de cellules photo-électriques de grande surface en pellicules minces de silicium (S/56). Ces pellicules peuvent être préparées soit par déformation du silicium (laminage, estampage), soit par décomposition du tétrachlorure de silicium par l'hydrogène. Toutefois, les cellules photo-électriques préparées par ces méthodes reviennent très cher.

L'emploi de photo-batteries avec concentrateurs d'énergie solaire fait l'objet de recherches tant en URSS qu'aux États-Unis. A l'Institut Krjijanovski (URSS), il a été effectué des recherches sur l'importance de l'intensité d'éclairement sur les caractéristiques en volts-ampères des photo-éléments au silicium. Pour des cellules photo-électriques idéales au silicium, la théorie prévoit que la puissance à la sortie d'un élément est une fonction presque linéaire de l'intensité d'éclairement (13). Mais dans les cellules photo-électriques réelles, l'augmentation de la puissance incidente ne provoque un accroissement de la puissance sortante que jusqu'à une certaine quantité qui dépend de multiples facteurs. Une augmentation nouvelle de l'intensité d'éclairement ne fait pour ainsi dire pas varier cette quantité. Cette non-linéarité s'explique par la dispersion d'une fraction considérable de la puissance sur la résistance en série de la cellule photo-électrique. Malgré tout, l'usage de concentrateurs d'énergie solaire peut donner (si l'on dispose de refroidissement suffisant) une augmentation notable de la puissance, le facteur de multiplication variant de 20 à 30 (S/118). L'utilisation d'une plus grande intensité d'éclairage sans refroidissement forcé n'est rationnelle que si elle ne dépasse pas de quatre ou cinq fois la concentration du rayonnement solaire naturel, car la température des cellules photo-électriques s'élève fortement en présence de grandes concentrations.

Dans certains cas, en ayant recours au refroidissement, on a réussi à obtenir une augmentation de la puissance d'une cellule photo-électrique égale à 70 fois, alors que l'intensité du faisceau de lumière incidente augmente de 100 fois (14).

Dans certaines conditions, l'emploi de la concentration des rayons est avantageuse, puisque le coût de l'unité de surface des cellules photo-électriques est plusieurs centaines de fois plus élevé que pour les miroirs. Il se peut que, par l'emploi de miroirs concaves, en refroidissant les cellules photo-électriques et en améliorant les conditions de prise de courant, on puisse résoudre le problème de la création d'un dispositif économiquement acceptable pour l'obtention d'énergie électrique grâce au rayonnement solaire.

A l'Institut Krjijanovski, on a construit plusieurs exemplaires expérimentaux de photo-électrogénérateurs. Le photo-électrogénérateur consistait en une batterie photo-électrique d'une superficie de 100 cm², éclairée par les rayons solaires concentrés reflétés par un miroir en aluminium d'une superficie effective de 1,2 m². Le coefficient de réflexion du miroir atteignait environ 0,7. La batterie photo-électrique était placée dans un compartiment à couvercle vitré. Il y passait de l'eau qui refroidissait la surface extérieure de la batterie. La puissance utile fournie par cette installation était de 10 W environ, l'intensité de la radiation étant de $I = 700 \frac{\text{kcal}}{\text{m}^2/\text{h}}$. Cette même batterie, sans employer le miroir, aurait donné une puissance utile de 0,5 W, c'est-à-dire 20 fois moins.

Au point de vue du fonctionnement avec concentrateurs d'énergie solaire, ce qui paraît le plus prometteur, ce sont les batteries photo-électriques faites de matériaux autres que le silicium. La théorie montre que les cellules photo-électriques constituées de matériaux ayant une zone interdite plus large que celle pour le silicium doivent mieux fonctionner aux hautes températures (S/56). Parmi ces matériaux, citons le phosphure d'indium, l'arséniure de gallium, le tellurure de cadmium, l'aluminium antimonié, le sulfure de cadmium. Actuellement, de nombreux savants effectuent des travaux concernant la création de cellules photo-électriques avec ces matériaux. En URSS, en 1959, on a construit une cellule photo-électrique en tellurure de cadmium dont le rendement global (15) était de 3 p. 100. Aux États-Unis, la section de physique des Itek Laboratories, prépare des cellules photo-électriques à plusieurs couches par vaporisation de sulfure de cadmium (S/56) : Le rendement global en est de 4 à 6 p. 100. Le maximum de leurs caractéristiques spectrales est atteint sur la longueur d'ondes de 8 000 Å.

La Radio Corporation of America (États-Unis) a préparé une cellule photo-électrique en arséniure de gallium, capable de fonctionner sous une température de 400 °C sans diminution notable du rendement. Si l'on réussit à mettre au point la fabrication en série de ces cellules photo-électriques, le domaine de leur emploi sera grandement étendu.

Même vu le prix élevé à l'heure actuelle de ces cellules photo-électriques, ces dispositifs sont parfois

d'un emploi avantageux pour certains problèmes d'approvisionnement de consommateurs d'énergie électrique. C'est ainsi que sont présentés à la présente Conférence des mémoires où sont indiqués certains domaines d'emploi des cellules photo-électriques.

Dans son mémoire S/40, G. Pearson relate les expériences commerciales faites sur des installations téléphoniques alimentées par une batterie solaire (Bell Telephone Co.). Ces expériences ont duré six mois.

Au Japon, des batteries solaires de pair avec des accumulateurs, ont été employées avec succès pour alimenter les appareils des phares maritimes. La description en est faite par M. Kobayashi (S/11).

Cet examen de la documentation consacrée aux cellules photo-électriques permet de conclure que les cellules au silicium, à fort rendement mais coûteuses, ne peuvent se répandre largement que si l'on a recours à la méthode qui consiste à renforcer la concentration de la lumière incidente. Toutefois, il est en même temps nécessaire, par un des moyens possibles, d'améliorer le prélèvement de courant afin de réduire la résistance intérieure des cellules photo-électriques. En outre, il faut évidemment refroidir artificiellement la surface de la cellule.

Il est également nécessaire de réaliser une cellule photo-électrique à pellicule vaporisée. Ceci peut se révéler très efficace, car le coût de telles cellules photo-électriques peut apparaître comme économiquement acceptable. Les méthodes telles que la solution de problèmes relatifs à la géométrie la plus avantageuse des cellules photo-électriques, la simplification de la technologie de préparation des matériaux et des cellules photo-électriques, l'accroissement de l'échelle de production, etc., peuvent aussi influer notablement sur la réduction du coût des cellules photo-électriques.

Sujets de discussion proposés

1. Thermo-électrogénérateurs :
   a) Choix des matériaux;
   b) Procédés à appliquer pour accroître la longévité;
   c) Élimination de la chaleur des jonctions froides.
2. Convertisseurs thermo-ioniques :
   a) Matériaux et revêtements des cathodes et anodes;
   b) Protection des cathodes contre l'oxydation;
   c) Méthodes permettant de réduire les charges d'espace.
3. Cellules photo-électriques :
   a) Matériaux;
   b) Procédés permettant d'étendre la bande utile du spectre solaire;
   c) Réduction de la température des cellules photo-électriques;
   d) Prélèvement de courant et réducton de la résistance électrique interne;
   e) Emploi d'un faisceau de lumière intense.
4. Sujets généraux :
   a) Influence de l'inégalité du débit d'énergie sur le rendement;
   b) Méthodes permettant d'égaliser le débit et la température;
   c) Serait-il possible de réduire le coût initial et le coût de l'énergie par conversion directe, et quelles répercussions cette réduction aurait-elle sur les applications possibles dans les pays sous-développés?

Références

1. Ioffe, A., *Poluprovodniki v sovremennoi fisike*, URSS, Acad. Sc. 1954.
2. Telkes, M., *Journ. Appl. Phys.*, nº 6, 1954.
3. Weston, E., brevet des E.-U., nº 389 124, 1888.
4. Zerasskv, W., *Russkij astronomicheskij calendar*, 1909.
5. Coblentz, W., brevet des E.-U. nº 1 077 219, 1913.
6. *Electronics*, nº 51, décembre 1960.
7. Dobretsov, L., Termoelectronnye preobrazovatelin, *Journal technicheskoi phisiki*, VXXX, nº 4, 1960.
8. Houston, *Journ. Appl. Phys.*, 30, nº 4, 1959.
9. Webster, *Journ. Appl. Phys.*, 30, nº 4, 488, 1959.
10. Chapin, D., Fuller C., Pearson G., *Journ. Appl. Phys.*, 25, 676, 1954.
11. Gliberman, A., Zaitseva A., Landsman A., *Phisika tverdogo tela*, 11, nº 8, 1960.
12. Pearson, G., Electricity from the sun, *Proceedings World Sympos. Appl. Sol. En.*, Arizona, 1955.
13. Prince, M., *Journ. Appl. Phys.*, 26 (59), 534, 1955.
14. Baum, V., Borovikova R., Okhotin A., *Ingenerno-Physichesky Journal*, 3, nº 3, Minsk, 1960.
15. Maslakovetz, *Physiko-technichesky Journal*, 2, Moscow, 1960.

USE OF SOLAR ENERGY FOR ELECTRICITY PRODUCTION BY DIRECT CONVERSION BY MEANS OF THERMOELECTRIC CONVERTERS AND PHOTO-ELECTRIC CELLS

Rapporteur's summation

Eminent specialists in the field of the conversion of solar into electrical energy made supplementary statements of some interest during the discussion of agenda items II C.1 (*b*) (i) and (ii). Though time was limited, there was a very useful exchange of views and ideas, and a discussion of prospects for the future.

There was general agreement on some problems, but there were differences in other fields. Different scientists attempted to solve the same problem by employing various methods or, rather, they approached the same problem from different viewpoints. Three kinds of converter are described briefly below.

Thermoelectric generators

The opinion was expressed that solar thermoelectric generators should be built without solar ray concentrators. The arguments for this position mentioned favourable conditions for thermo elements, which would work in not-too-high temperatures and would therefore be more durable. In addition, the sun-tracking mechanism could be avoided. These are very serious considerations, but it should not be forgotten that with small differences in temperatures at the hot and cold joints of thermo elements, the thermodynamic efficiency of the device is comparatively low. A more important deficiency is that the waste of heat from the heated surfaces will be high because of the large dimensions. The total cost of a surface unit is always more than the cost of the surface unit of the concentrator. Concentrating rays a hundredfold allows reduction in the surfaces of solar batteries and a corresponding reduction in their cost. Relevant estimates of the benefit are necessary for comparison. On the basis of calculations, we consider the concentration of solar rays necessary.

What is most important at present in developing solar thermoelectro generators? New materials with perfected thermoelectric characteristics need to be investigated; attempts to increase the period of service of solar batteries are necessary.[1]

Thermionic converters

These were examined in less detail. There were very marked contradictions in opinion concerning the efficiency of such devices, as well as their prospects. There is need for techniques and designs for such devices, as well as plans for different approaches to prospective research.

Photo-electric converters

Their main deficiency is their high cost. Different ways proposed by various investigators to overcome this include the following:

(*a*) The use of polycrystal materials reduces the cost considerably, but also reduces the efficiency of the device.

(*b*) The use of "double-sided" photo-elements and a common optical system with poor concentration of solar rays permits a twofold to fourfold increase in the energy output of a unit of the photo-element surface.

(*c*) The use of high concentrations in artificial cooling of the photo-elements and reducing their internal resistance would allow a considerable increase in the energy output from a unit of the photo-element surface.

Though the cooling problem has been solved in some research attempts, there are no radical solutions for reducing internal resistance. It may be that these solutions will be found, in which case the problem of cheap energy production by solar radiation would be considered solved. It is obvious that research should proceed in many directions. The best solution of the problem will become clear in time. Exchange of scientific information will avoid parallel expensive research.

---

[1] Speakers at the Conference agreed that a statement in the press on the excellent qualities of selenite cadmium was incorrect. Investigations regarding this material have taken place in France, the Union of Soviet Socialist Republics, and other countries. These studies revealed its inferior qualities; it is not suitable for thermo elements.

UTILISATION DE L'ÉNERGIE SOLAIRE POUR LA PRODUCTION D'ÉLECTRICITÉ PAR CONVERSION DIRECTE AU MOYEN DE CONVERTISSEURS THERMO-ÉLECTRIQUES ET DE CELLULES PHOTO-ÉLECTRIQUES

Résumé du rapporteur

D'éminents spécialistes de la conversion de l'énergie solaire en électricité ont fait des déclarations intéressantes au cours de l'examen des points II.C.1 *b*) i) et ii) de l'ordre du jour. Bien que le temps fut limité, un très utile échange de vues et d'idées a eu lieu et les perspectives d'avenir ont pu être examinées. L'accord a été général sur quelques problèmes, mais des divergences d'opinion se sont manifestées dans d'autres domaines. Plusieurs savants ont essayé de résoudre le même problème par diverses méthodes ou, plus exactement, ont abordé le même problème à des points de vue différents. Nous décrivons ci-après trois types de convertisseurs.

Générateurs thermo-électriques

On a estimé qu'il fallait construire des générateurs thermo-électriques solaires qui ne soient pas équipés de collecteurs paraboliques. Les partisans de cette thèse ont fait état de la situation favorable en ce qui concerne les thermo-couples, qui fonctionneraient à des températures assez peu élevées et seraient donc plus durables. De plus, on pourrait se dispenser du mécanisme de pointage sur le soleil. Ce sont là des arguments très sérieux, mais il ne faut pas oublier que s'il n'y a pas une grande différence de température entre l'extrémité chaude et l'extrémité froide des thermo-couples, l'appareil n'a qu'un faible rendement thermodynamique. Un autre inconvénient, plus grave, est que la déperdition calorique des surfaces chauffées sera sensible en raison des grandes dimensions de l'appareil. Le coût total de l'unité de surface est toujours supérieur au coût de l'unité de surface du concentrateur. Une concentration des rayons au facteur 100 permet de réduire la surface des piles solaires, et de ce fait, leur coût. Il faut procéder à des estimations pertinentes de l'avantage de ces générateurs aux fins de comparaison. A notre avis, d'après les calculs effectués, la concentration des rayons solaires est indispensable.

Quel est actuellement l'aspect le plus important de la mise au point de générateurs solaires thermo-électriques? Il faut étudier des matériaux nouveaux présentant de meilleures caractéristiques thermo-électriques et s'efforcer d'allonger la durée d'utilisation des piles solaires [1].

Convertisseurs thermo-électroniques

La discussion sur ces appareils a été moins approfondie. Les avis ont différé très sensiblement quant à leur efficacité et à leurs perspectives d'emploi. Il faut mettre au point des techniques et des modèles nouveaux et élaborer des plans touchant les diverses manières d'aborder les recherches.

Convertisseurs photo-électriques

Le défaut principal de ces appareils est leur coût élevé. Plusieurs chercheurs ont proposé diverses solutions pour surmonter cet obstacle, et notamment :

a) L'utilisation de matériaux polycristallins qui réduit considérablement le coût, mais également l'efficacité de l'appareil;

b) L'utilisation de photo-éléments à double face et d'un système optique ordinaire de faible concentration qui permet de doubler ou quadrupler l'énergie obtenue par unité de surface du photo-élément;

c) L'utilisation de hautes concentrations lors du refroidissement artificiel des photo-éléments et de l'affaiblissement de leur résistance interne, qui permet d'accroître considérablement l'énergie produite par unité de surface du photo-élément.

Si quelques chercheurs ont résolu le problème du refroidissement, aucune solution définitive n'a été trouvée pour diminuer la résistance interne. Il se peut qu'on en trouve une; alors, le problème de la production d'énergie solaire à bon marché sera considéré comme résolu. Il est manifeste que la recherche doit se faire dans de nombreuses directions. La meilleure solution se dégagera en temps utile. En attendant, l'échange de renseignements scientifiques évitera le chevauchement de recherches coûteuses.

[1] Quelques orateurs ont reconnu qu'une information de presse sur les excellentes qualités du sélénite de cadmium était inexacte. Des études de ce matériau entreprises en France, en Union des Républiques socialistes soviétiques et dans d'autres pays, ont révélé ses qualités inférieures. Le cadmium ne convient pas à la fabrication de thermo-couples.

Agenda item II.C.1 (*b*)

SEMICONDUCTOR CONVERTERS OF SOLAR ENERGY

V. A. Baum, R. P. Borovikova and A. S. Okhotin *

During recent years, one of the most promising trends in heliotechnique has been the conversion of solar energy into electric energy by means of semiconductors. The progress that has been made in manufacturing techniques of semiconductors has made it possible to construct devices that efficiently convert the energy of the sun into electric energy. This conversion may be accomplished in two ways: radiant energy of the sun—electricity by thermoelements; radiant energy of the sun—electricity by photoelectric cells. It has been shown that the theoretically attainable efficiency of thermoelements is about 35 per cent (1), and that of photocells, 25 per cent (2). At present, there are thermoelements with efficiencies of 10 per cent, double-stage thermoelements with efficiencies of 13 per cent, and photo-cells with efficiencies of 10 per cent (up to 13 per cent in some cases).

The heliotechnical laboratory of the Power Institute of the USSR Academy of Sciences has been conducting research in this field during the past several years. The present paper is a summary of some of these investigations.

Thermoelectric converters of solar energy

I. The theory of solar thermal generators

The intrinsic efficiency of a thermoelement operating from any source of heat energy is of the form:

$$\eta = \frac{T_1 - T_2}{T_1} \frac{\sqrt{1 - T_1 Z} - 1}{\sqrt{1 - T_1 Z} + 1} \qquad [1]$$

where T_1 is the temperature of the hot end of the thermoelement, T_2 is the temperature of the cold end of the thermoelement, $Z = \frac{\alpha_2 \sigma}{\lambda}$ is a factor that accounts for the physical properties of the material of the thermoelement (α is the specific thermoelectromotive force, σ is the electric conductivity, and λ is the thermal conductivity).

From this equation, it is clear that high efficiencies of thermoelements may be obtained by creating considerable differences of temperature at the junctions. In the case of solar energy, this is possible only through the use of concentrators of radiant energy; concentrators reduce heat losses due to radiation and convection in proportion to the value of the coefficient of geometrical concentration K. The thermal scheme of a solar thermogenerator operating jointly with a concentrator is as follows: the solar energy Q_r incident on a concentrator of area F_m is reflected from it onto a thermobattery. In the process, the concentrator absorbs part of the energy Q_m, which is proportional to (1—R_m), where R_m is the reflectivity of the mirror $Q_m = Q_r\ (1-R_m)\ F_m$. The radiant flux incident on a thermobattery of area F_{tb} is reflected from it to an amount Q_{ref} that is proportional to (1—A), where A is the absorptivity of the surface of the thermogenerator:

$$Q_{ref} = (1 - A)\ Q_r\ R_m\ F_{tb} \qquad [2]$$

The remaining heat passes through the thermobattery to an amount Q_t and is converted into electric energy W watt. Owing to the passage of an electric current, there will be an additional generation of Peltier heat Q_p and Joule heat Q_j. Due to the established temperature difference, part of the heat will be lost by radiation Q_{rad} and by convection Q_{conv}. Consequently, the thermal balance of a solar thermogenerator will be:

$$Q_r F_{tb} = Q_m F_m + Q_{ref} F_m + Q_t F_{tb} + Q_p F_{tb} - \frac{1}{2} Q_j F_{tb} + Q_{rad} F_{tb} + Q_{conv} F_{tb} \qquad [3]$$

The equation of heat balance permits, in general form, a determination of the efficiency of a solar thermogenerator:

$$\eta = \frac{0.8\ W}{Q_r\ F_m} \qquad [4]$$

which consists of the product of the efficiencies of the thermoelement proper:

$$\eta_{te} = \frac{0.86\ W}{Q_t + Q_p - \frac{1}{2} Q_j} = \frac{0.5\ (T_1 - T_2)}{T_1 \frac{2}{Z} - 0.25\ (T_1 - T_2)}, \qquad [5]$$

and the coefficient of optical and heat losses:

$$\eta_{tl} = \left[1 - \frac{\sigma_r\ (T_1^4 - T_0^4) + \alpha_e\ (T_1 - T_0)}{R_m A Q_r K}\right] R_m A \qquad [6]$$

where σ_r is the reduced coefficient of radiation of the heated side of the thermobattery. α_c is the coefficient of heat transfer from the heated side of the thermobattery, T_o is the ambient temperature, and $K = \frac{F_m}{F_{tb}}$ is the coefficient of geometrical concentration of solar energy.

* Krzhizhanovski Power Institute, USSR Academy of Sciences, Moscow.

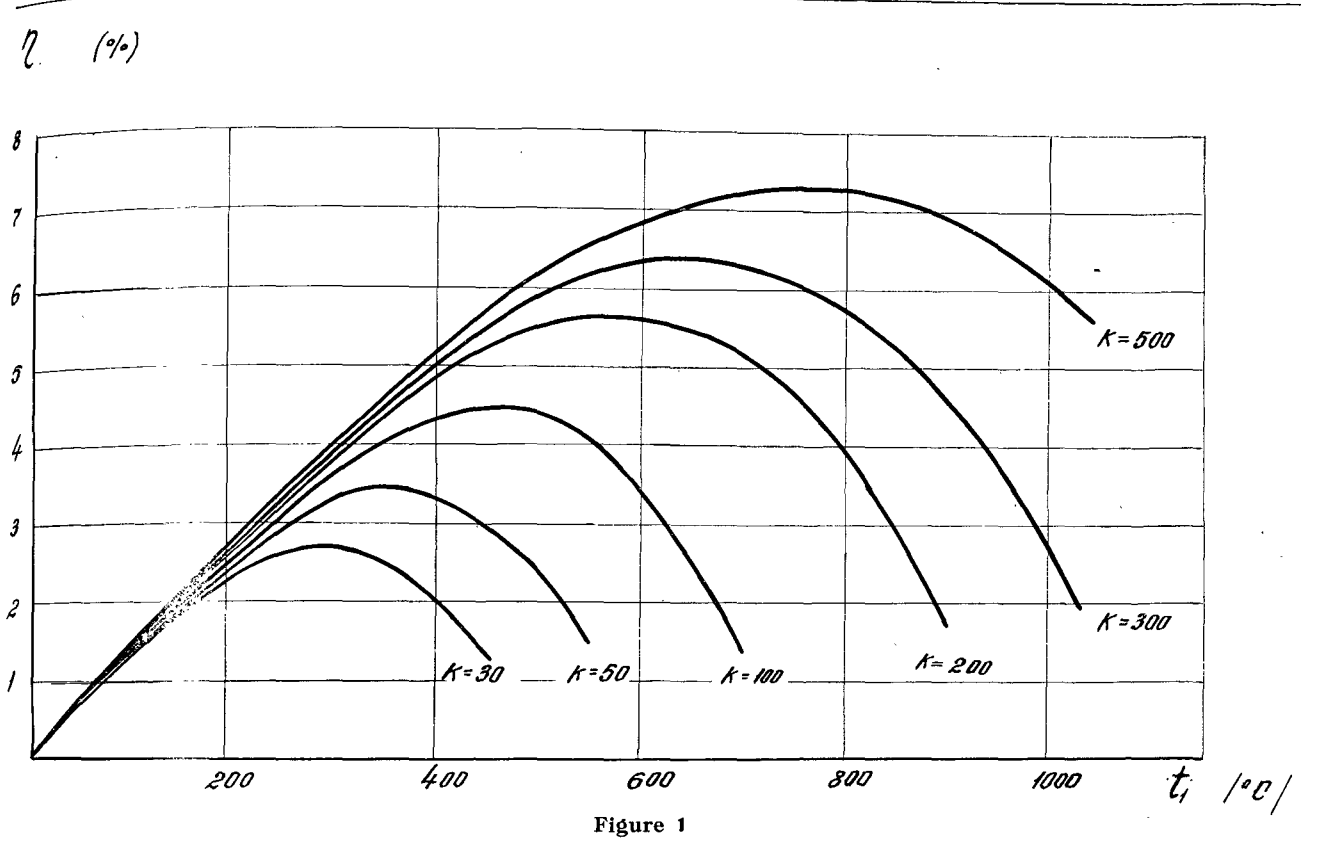


Figure 1

An analysis of equation [4] above for various K Z and ΔT shows that the efficiency of a solar thermogenerator increases with increasing $\overline{Z}$ and K, approaches a certain limit when the value of ΔT is constant. For given $\overline{Z}$ and K, the efficiency of a thermogenerator attains a maximum at a certain optimal value of ΔT. Figure 1 shows η as a function of ΔT and K for $Z = 1 \times 10^{-3}$ 1/°C; similar curves may be obtained for any Z.

Equation [4] permits determining the optimal temperature difference on thermoelements and the optimal degree of concentration at both of which the value of η will be a maximum for some selected material. In these computations, it was taken that α_c 5 Kcal/m² h°C, $A = 0.95$. Optimal temperature on the hot ends of a thermogenerator, given a constant temperature of the cold end and with all other conditions being equal, may be obtained by varying the height of the thermoelement ℓ. From the heat balance equation, it is easy to obtain an equation that permits determining T_i. Solving the equation of the heat balance for various values of ℓ, it is possible to obtain ℓ as a function of T.

The useful power of the thermogenerator may be determined as the product of the current I and the voltage V:

$$W = IV \text{ watts} \qquad [7]$$

Expressing the current and the voltage in terms of the parameters of an thermoelectrogenerator, we get

$$W = 1.16\, Z\, \psi\, \gamma\, \Delta\, T_q\, F_{tb} \text{ watts} \qquad [8]$$

where ψ is a factor that takes into account the effect of Peltier heat and Joule heat and is equal to

$$\left[1 + \frac{\overline{Z}}{8.32}\left(T_1 + \frac{\Delta T}{4}\right)\right]^{-1} \qquad [9]$$

γ is a factor that depends on the internal and external resistances (when they are equal, $\gamma = 0.25$)

$$\gamma = \sqrt{1 + T_1 \overline{Z}}\,(1 + \sqrt{1 + T_1 \overline{Z}})^{-2} \qquad [10]$$

q is the intensity of the heat flow passing through the thermobattery (Kcal/m²h).

However, when studying the operation of a solar thermogenerator, it is more important to proceed from the value of the solar radiation Q_r. Altering expression [8] above, we get:

$$W = Y\, \psi\, \gamma\, q^2\, v \qquad [11]$$

where

$$Y = \frac{\overline{Z}}{\lambda} = \frac{\alpha^2\, \sigma}{\lambda^2} \qquad [12]$$

v is the volume of the thermobattery,

$$2 = Q_r\, \eta \text{ Kcal/m²h} \qquad [13]$$

It should be pointed out that in all the foregoing reasoning, the thermoelectric parameters were taken to be average in a given temperature interval, while the heat flux was taken to be uniformly distributed over the area of the thermogenerator. Calculations have shown that the first condition introduces into the values obtained an error that does not exceed 5 per cent, while the second condition requires

corrections, because it is known that the intensity of radiation in a cone of rays reflected by concentrators varies according to a Gaussian curve. In particular, for paraboloidal mirrors

$$q = Ce^{-c_1 r_f^2} \qquad [14]$$

where C is the maximum heat flux in the centre of the focal spot, C_1 is a characteristic of the geometrical precision of the reflector, rf is the radius of the focal spot, and accordingly,

$$W = 1.16\,\bar{Z}\,\psi\,\gamma\,\frac{\ell}{\lambda}\left(\frac{C}{m^2}\right)^2\frac{\pi}{C_1}\left(1 - e^{-(2c_1/m^2)\,rm^2}\right) \qquad [15]$$

where r_m is the radius of the spot in any plane of the reflection cone, and $m = \frac{r_m}{r_f}$.

From this equation, it follows that a solar thermogenerator operating under uneven irradiation of the hot ends will be less effective.

From all that has been said, it follows that to build an efficient solar thermogenerator it is necessary to develop the following:

(*a*) Materials for thermoelements with as high $\bar{Z}$ as possible. Indeed, all other conditions being equal and given a concentration equal, say, to 100, η 4.48 per cent, for $\bar{Z} = 1 \times 10^{-3}$ 1/°C, and for $\bar{Z} = 5 \times 10^{-3}$ 1/°C $\eta = 10.28$ per cent;

(*b*) Materials functioning at high temperature, which permits working at higher concentration and obtaining higher efficiencies. Thus, at $\bar{Z} = 1 \times 10^{-3}$ 1/°C for $\varkappa = 30$. $T_{max} = 250$°C, $\eta = 2.7$ per cent, and for $\varkappa = 500$. $T_{max} = 750$°C, $\eta = 7.3$ per cent, at $Z = 5 \times 10^{-3}$ 1/°C $\varkappa = 30$. $T_{max} = 250$°C $\eta = 6.96$ per cent, $\varkappa = 500$, $T_{max} = 700$°C, η — 14.75 per cent.

II. Materials for solar thermogenerators

The choice of materials for thermoelements is very complicated at the present time, because it is impossible to define theoretically which compounds are most suitable. Here, we indicate only some qualitative tendencies that require extensive experimental verification.

Extensive, though disconnected, researches in this field that have been carried out in the Soviet Union, the United States and other countries have made it possible to select a number of materials with parameters Z that ensure the earlier mentioned high efficiencies. These include:

ZnSb ($Z = 0.8 \times 10^{-3}$ 1/°C), CoSb ($Z = 0.4 \times 10^{-3}$ 1/°C)
PbSb ($Z = 0.7 \times 10^{-3}$ 1/°C), PbSe ($Z = 1.1 \times 10^{-3}$ 1/°C)
BiSb ($Z = 1.95 \times 10^{-3}$ 1/°C), PbTe ($Z = 1.4 \times 10^{-3}$ 1/°C)
Bl_2Te_3 ($Z = 1.6 \times 10^{-3}$ 1/°C), Sb_2Te_3 ($Z = 0.19 \times 10^{-3}$ 1/°C);
the triple compounds BiTeSb ($Z = 2.8 \times 10^{-3}$ 1/°C)
BiTeSe ($Z = 2.4 \times 10^{-3}$ 1/°C), PbTeSe ($Z = 0.9 \times 10^{-3}$ 1/°C)
InAsP ($Z = 0.95 \times 10^{-3}$ 1/°C), GeTe ($Z = 0.9 \times 10^{-3}$ 1/°C).

In most cases here, the values of Z are given for room temperature, which does not permit us to judge properly the applicability of the material. Studies are necessary of the properties of materials in a broad temperature range. It is important to determine the temperature boundary of the applicability of a given compound.

The Helio-Laboratory of the Power Institute of the USSR Academy of Sciences has carried out an investigation of the properties of binary compounds of tellurium: FeTe, CoTe, GeTe, PdTe, AgTe, Ag_3Te_2, Ag_2Te. InTe, In_2Te, SuTe, Sb_2Te_3, PbTe and Bi_2Te_3. Room-temperature measurements determined compositions that corresponded to maximal values of $\alpha^2\sigma$ (at $\lambda e \gg \lambda e$ one can evaluate the effectiveness from $\alpha^2\sigma$ instead of from Z). Also investigated was the influence of various impurities on the properties of tellurides. The samples were manufactured by moulding, because the thermal batteries are mainly made out of moulded elements. In a broad interval of temperatures, measurements were made of the thermoelectromotive force α by a technique conventional for semiconductors, of the electric conductivity σ and the thermal conductivity λ by the Colrausch method, and the Hall effect by the method of direct current and constant magnetic field.

Investigations showed that nearly all of the tellurides considered are intermetallics in a nondegenerate or close to nondegenerate state. The thermoelectromotive force is sufficiently large and increases with the temperature, while the electrical conductivity diminishes. The compounds FeTe, CoTe, PdTe, and In_2Te had low values and they should be classified as degenerate semiconductors. As a rule, the introduction, into the compound, of small quantities of impurities does not alter the character of change α and σ with temperature, although their numerical values decrease somewhat. The thermal conductivity of the tellurides we have investigated varies with the temperature in different ways; in most cases, it falls with the temperature, but for some it increases. For the materials studied, the increase with temperature is possibly to be explained by the presence of a large number of defects in the crystal lattice of the material, that is, when the lattice is, essentially, absent. The numerical values of thermal conductivity are small. The introduction of impurities into the majority of tellurides decreases the thermal conductivity, which may be accounted for by the more intense scattering of phonons on the impurity atoms. In some of the tellurides that were studied, the increase in thermal conductivity with increase in impurity content may be due to the fact that the impurities fill the lattice defects. The lattice or phonon component, which diminishes with rise in temperature, is the principal component of the thermal conductivity of tellurides at room temperature. At high temperatures, the electronic thermal conductivity in most tellurides is nearly equal to the lattice thermal conductivity, and an additional thermal conductivity

appears in a number of other materials. An analysis of the data obtained has shown that for two- and five-atomic binary compounds of tellurium there is a correlation between their molecular weight M and the lattice thermal-conductivity λ_e, which is of the form:

$$\lambda_e = 3.2 \times 10^4 \, M^{-1.5} \text{ Kcal/m hr°C} \qquad [16]$$

It holds at room temperature.

On the basis of measurements of the Hall effect of the electrical conductivity and thermoelectromotive force, computations were made for the investigated tellurides, of the density values of the current carriers, their mobility, and the effective mass. An analysis of the electrical parameters has shown that for the majority of tellurides, scattering of the current carriers takes place on thermal oscillations of the lattice (the mobility decreases with rise in temperature). Scattering on impurity ions occurs only in FeTe and Ag_3Te_2. The effective mass m of all studied compounds does not vary with temperatures. A consideration of the dependence of the mobility of the carriers μ upon the molecular weight of the investigated tellurides at room temperature demonstrated that for two-atomic compounds,

$$\mu = 0.75 \, M^{2.5} \qquad [17]$$

and for five-atomic compounds,

$$\mu = 4.75 \, M^5 \qquad [18]$$

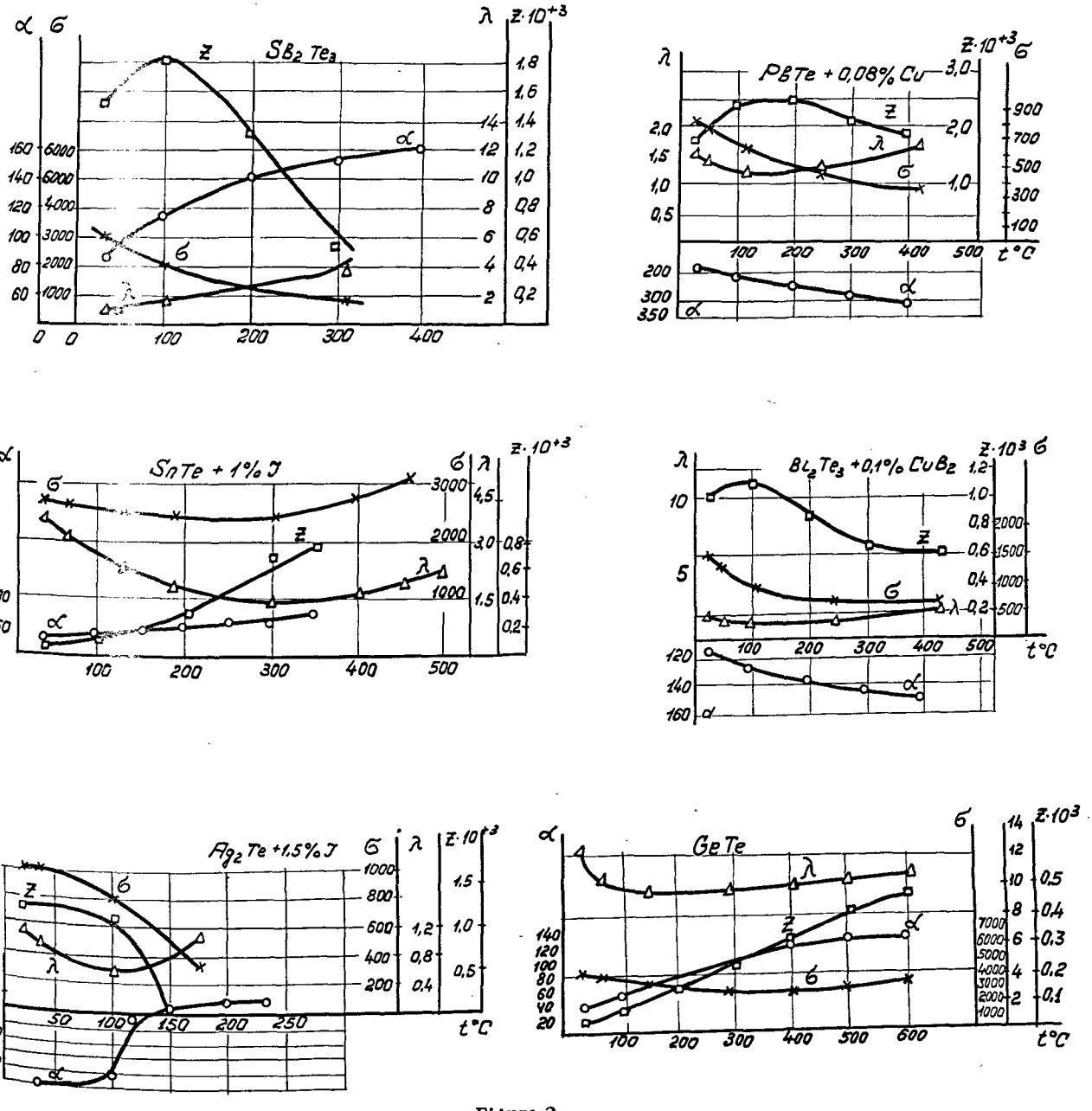


Figure 2

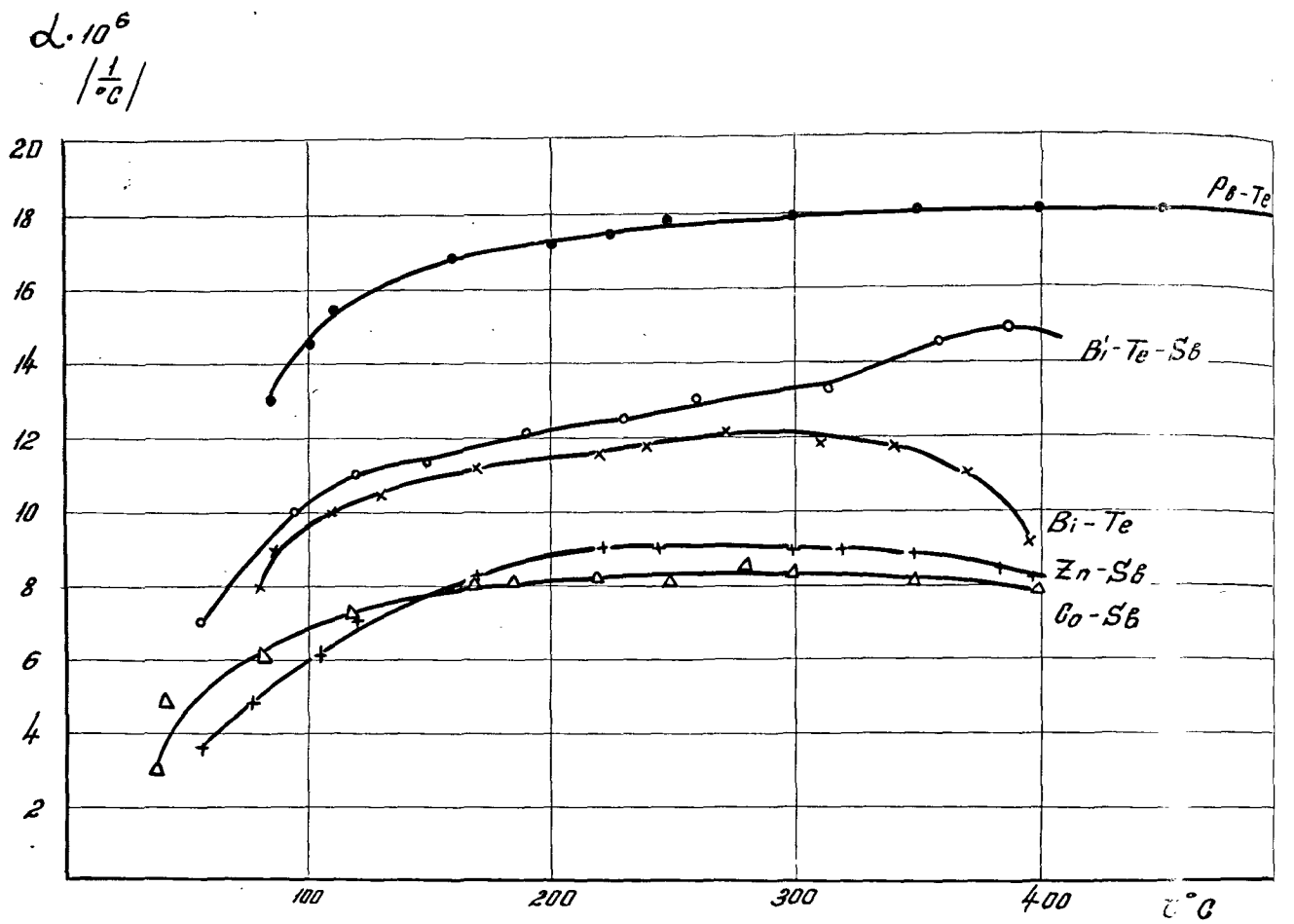


Figure 3

It is known (3) that the dependence of the factor of effectiveness $\bar{Z}$ upon the physical parameters of the material is of the form

$$Z = 1.2 \times 10^{-7} \frac{\mu}{\lambda e} \left(\frac{m}{m_0} \frac{T}{T_0}\right)^{\frac{3}{2}} e^2 \qquad [19]$$

where $m_0 = 9.1 \times 10^{28}$ gm, T_0 — 300°K and $\bar{Z}$ is a parameter that defines the scattering mechanism, and for the investigated tellurides it may, to a certain degree of accuracy, be taken equal to unity. Two assumptions are made in the derivation of this formula : first $\lambda_e > e$, and second the materials are in a nondegenerate state, i.e., classical statistics are applicable to them. These assumptions correspond to the properties of the binary compounds of tellurium.

Substituting into equation [19] above the values μ and λ_e, we find that at room temperature ($T =$ 300°K) for two-atomic compounds of tellurium we have

$$Z = 8.5 \times 10^{25} M^4 (m^x)^{\frac{3}{2}} \qquad [20]$$

and for five-atomic compounds,

$$Z = 5.55 \times 10^{26} M^{6.5} (m^x)^{\frac{3}{2}} \qquad [21]$$

On the basis of the equations obtained, we may draw the conclusion that the thermoelectric effectiveness of compounds increases with their molecular weight. Indeed, the values of Z computed on the basis of measured thermoelectric properties have shown that the best materials for thermoelements are tellurides with high molecular weights: GeTe, S_2Te, Ag_2Te, PbTe, Sb_3Te_2 and Bi_2Te_3. The triple alloy Sb_2Te_3 — Bi_2Te_3 possesses good properties. The introduction of impurities into some of them improved their properties still more.

It is impossible to consider the relations [20] and [21] above over the entire operating interval of temperatures due to different variations of λ_e and μ with temperature. Inasmuch as quantitative regularities have not been detected here, it is necessary to know the factor $\bar{Z}$ in a broad range of temperatures for the materials under study. Figure 2 gives the temperature relations of the thermoelectric properties of materials for thermogenerators for the best alloys of tellurium. It will be seen that for the majority of compounds the factor varies differently with temperature, which leads to a quantitative variation of the relations obtained.

When evaluating the applicability of materials for thermogenerators, one must know their maximal operating temperature. This may be done by measuring the coefficient of linear expansion of the materials.

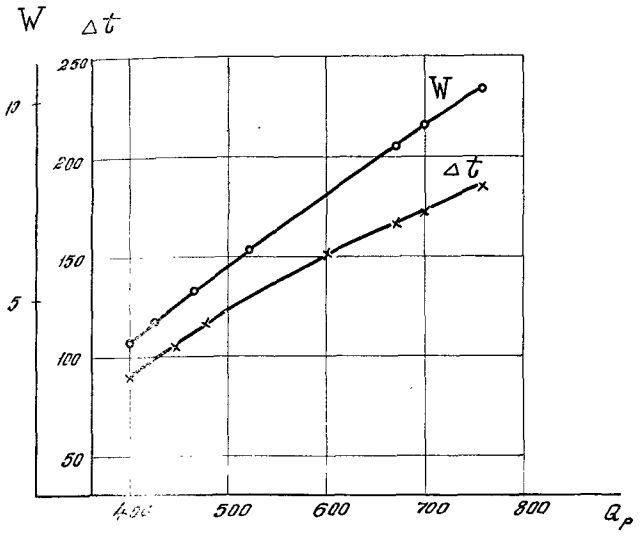


Figure 4

It must likewise be found for the choice of thermoelectric couples (it is better to manufacture a thermoelement from materials with the equal coefficients of linear expansion).

Figure 3 gives the coefficients of linear expansion for the alloys PbTe, $BiTe_3$, BiTeSb, SnTe, ZnSb and CoSb. At temperatures above 400°C, the alloys Bi_2Te_3 and BiTeSb can no longer be effectively utilized in thermogenerators. The close values of their coefficients of linear expansion permit manufacturing out of them thermo-elements of sufficiently strong construction.

The alloy PbTe may be used at still higher temperatures, but the values of its coefficient of linear expansion are higher than those of the preceding alloys. ZnSb and CoSb have close values of coefficients of linear expansion, and what is more, they can be used at still higher temperatures.

It should be stressed that to manufacture alloys with good thermoelectric properties requires extreme care, because their properties are highly dependent upon the purity of the initial materials and the technological procedures. The materials obtained made it possible to construct a number of solar thermogenerators.

III. The principles of constructing solar thermogenerators

The calculations of efficiency and power given in section I above and the determination of Z for a number of materials given in section II referred to the ideal case. In real designs of solar thermogenerators, there are other numerous losses that reduce the effectiveness of their action. The principal task of the designer is to reduce these losses to a minimum. Firstly, an important problem in constructing the thermo-element proper is its commutation. The commutation must be able to withstand a high temperature, have a small resistance and ensure extended operation of the thermobattery. Taking into account the resistance of commutation (ohm-cm²), the factor Z will be of the form (3):

$$\overline{Z} = \frac{\alpha^2}{\lambda\left(\rho + \frac{\bar{\rho}}{\ell}\right)} \qquad [22]$$

whence it is seen that the greater the quantity $\bar{\rho}$, the less the value of $\overline{Z}$ and, consequently, the efficiency. For the materials given above, $\bar{\rho}$ must be less than 10^{-5} ohm-cm². There are various ways of creating such commutation: moulding the commutation bars, welding them, joining by the diffusion method, baking, soldering, etc.

In addition to the commutation of the separate cells, it is necessary to join them into a battery so as not to increase the internal resistance, not to give rise to destructive mechanical forces due to thermal stresses, and to have a high (as ligh as possible) filling factor of the area of the thermal battery by the cells.

It was pointed out above that a solar thermogenerator will function effectively if the temperature on the hot ends of all cells of the battery is the same and if there is reliable cooling of the opposite ends. The first requirement can be met in the following different ways.

(*a*) A concentrator can be produced that yields, in the focal plane, a more uniform distribution of the radiant flux intensity than that distribution which is obtained in the case of a paraboloidal concentrator. G. I. Markov has proposed and made a facet concentrator, in which the central facets are larger than the peripheral facets, and they all produce (in the focal plane) roughly the same sized light spots, which overlap. R. R. Aparisi and B. A. Garf designed a concentrator which, in the central part, has a smaller curvature than that of a paraboloid and thus obtained a more uniform distribu-

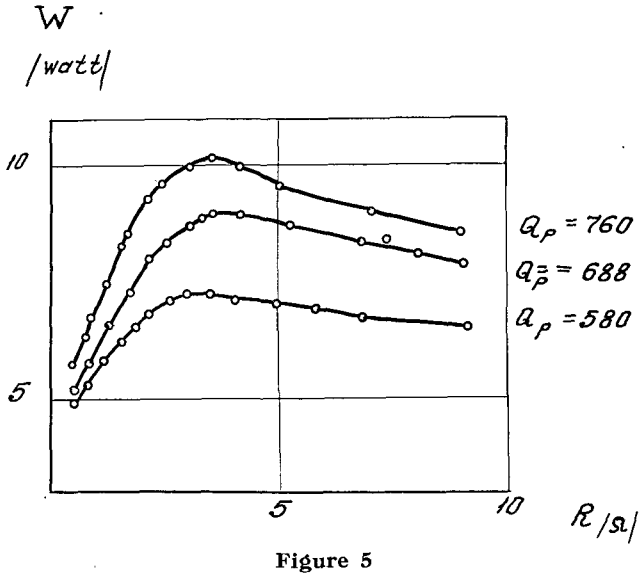


Figure 5

tion of the radiant flux in the focal plane. The equation of the generating element of this concentrator in the polar co-ordinate system is of the form:

$$\rho' = C_0 \frac{1 - k' - \varphi \tan \frac{\theta}{2}}{1 + k' + \varphi \tan \frac{\theta}{2}} \frac{1}{\varphi + \sin \theta} \qquad [23]$$

where φ is the aperture angle,

$$k' = \sqrt{1 + \tan^2 \varphi}$$

θ is determined from the equation for the focal length,

$$f = \rho' \cos \theta$$

C_0 is determined from the condition $\theta = 0$, $\rho' = \rho'_0$.

(*b*) A battery of thermoelements of various length can be made, if we know the law of distribution of the incident flux. The length of the element turns out to be inversely proportional to the intensity of the radiant at the given point. In the foregoing cases, the hot ends will be heated directly by the solar radiation.

(*c*) On the hot end, one can put a plate with high thermal conductivity that equalizes the heat flux, or use may be made of a high-boiling-point heat-transfer agent. However, in this method there will be heat losses associated with the thermal resistance of the plate or heat-transfer agent, and also of the insulation layer.

IV. Some operating characteristics of solar thermogenerators

The reasoning and calculations of the preceding section were verified in an experimental solar thermogenerator produced at the Power Institute of the Academy of Sciences. Investigations of solar thermogenerators made it possible to obtain their power characteristics as a function of external parameters. The principal parameter is solar radiation, which varies throughout the day. Figure 4 gives, as a function of the variation of solar radiation, the temperature difference on thermoelements and the power output of one of the solar thermogenerators with a small-size facet mirror that ensures a sufficiently uniform thermal flux. The different heating of the thermobattery affects the variation

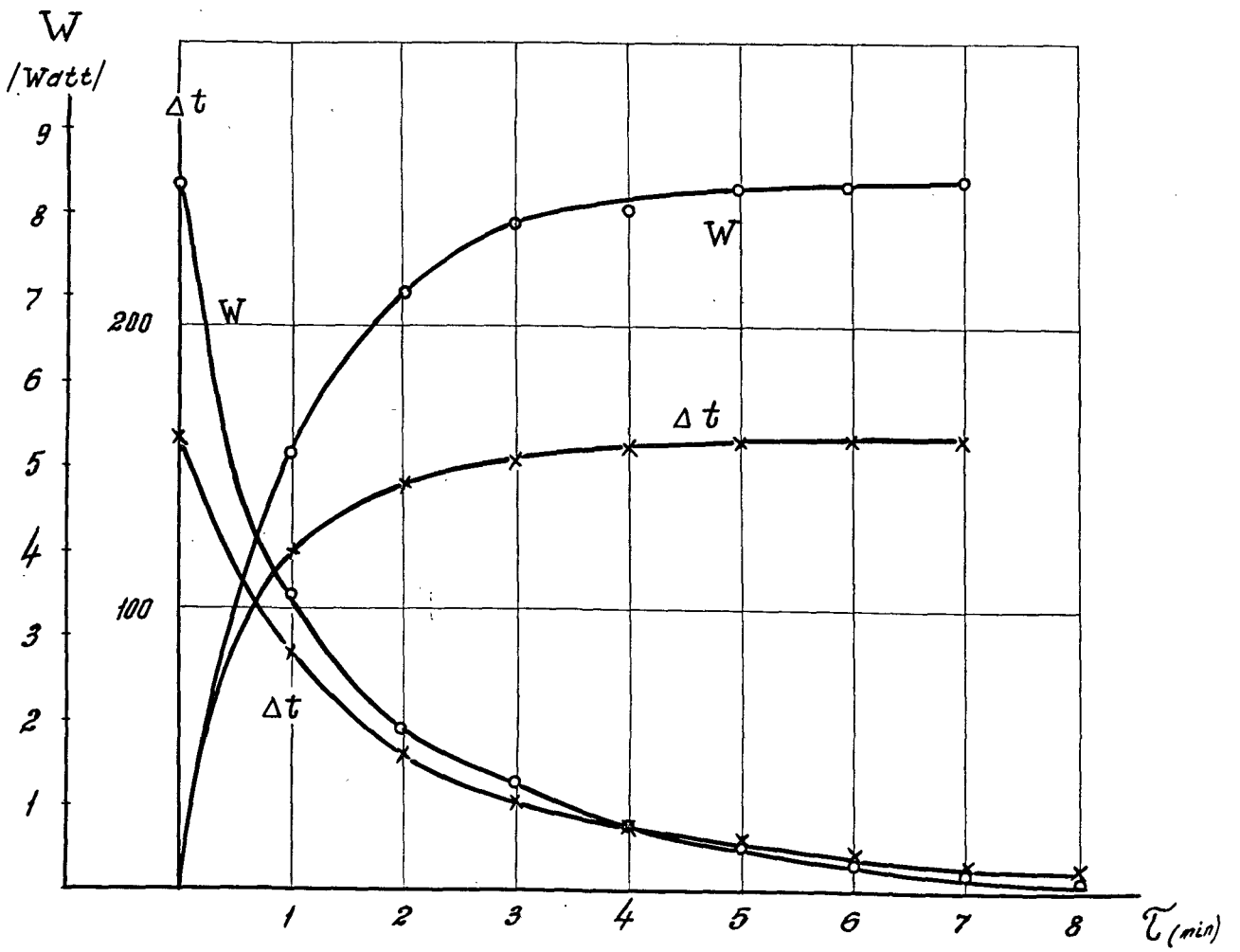


Figure 6

of its internal resistance, and since it is known that maximum power output occurs when the internal resistance of the thermogenerator is equal to the external load resistance, relations were obtained of power as a function of the external resistance for various Q_r (figure 5). As is seen, the maximum power for smaller Q_r is displaced towards smaller resistances but this displacement is slight. On the basis of these curves, the conclusion may be drawn that one should take the external resistance greater than the internal resistance of the thermobattery, because in this mode of operation, the power of the thermogenerator varies but slightly. A load resistance equal to or less than the resistance of the thermogenerator can cause a sharp decrease in the power output in the case of slight variations in the radiation conditions.

A solar thermogenerator can function in conditions of variable cloudiness. This was confirmed by investigations of solar thermogenerators in non-steady conditions. As may be seen from figure 6, when the thermogenerator is heated from the cold state, its power reaches almost maximum in a mere 3 minutes after the start of heating, although complete maximum power output is attained only in 6 minutes. Initially, cooling takes place very rapidly, but then it becomes smoother, and in 8 minutes the power output of the generator is nearly zero. This indicates that solar thermogenerators are almost inert, and the heating and cooling time should be disregarded when computing their economical effectiveness. Investigation into the energy characteristics of solar thermogenerators and the elaboration of statistical relations connecting the power output and climatic factors made it possible to obtain a

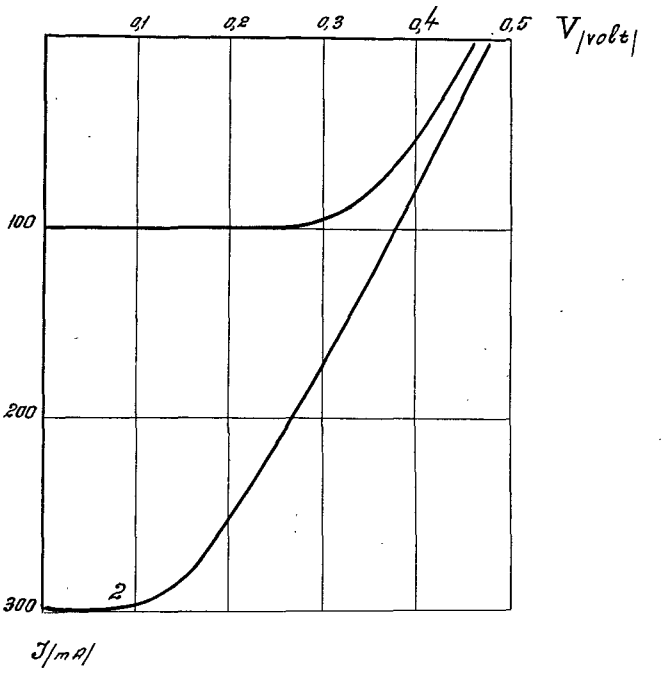


Figure 7

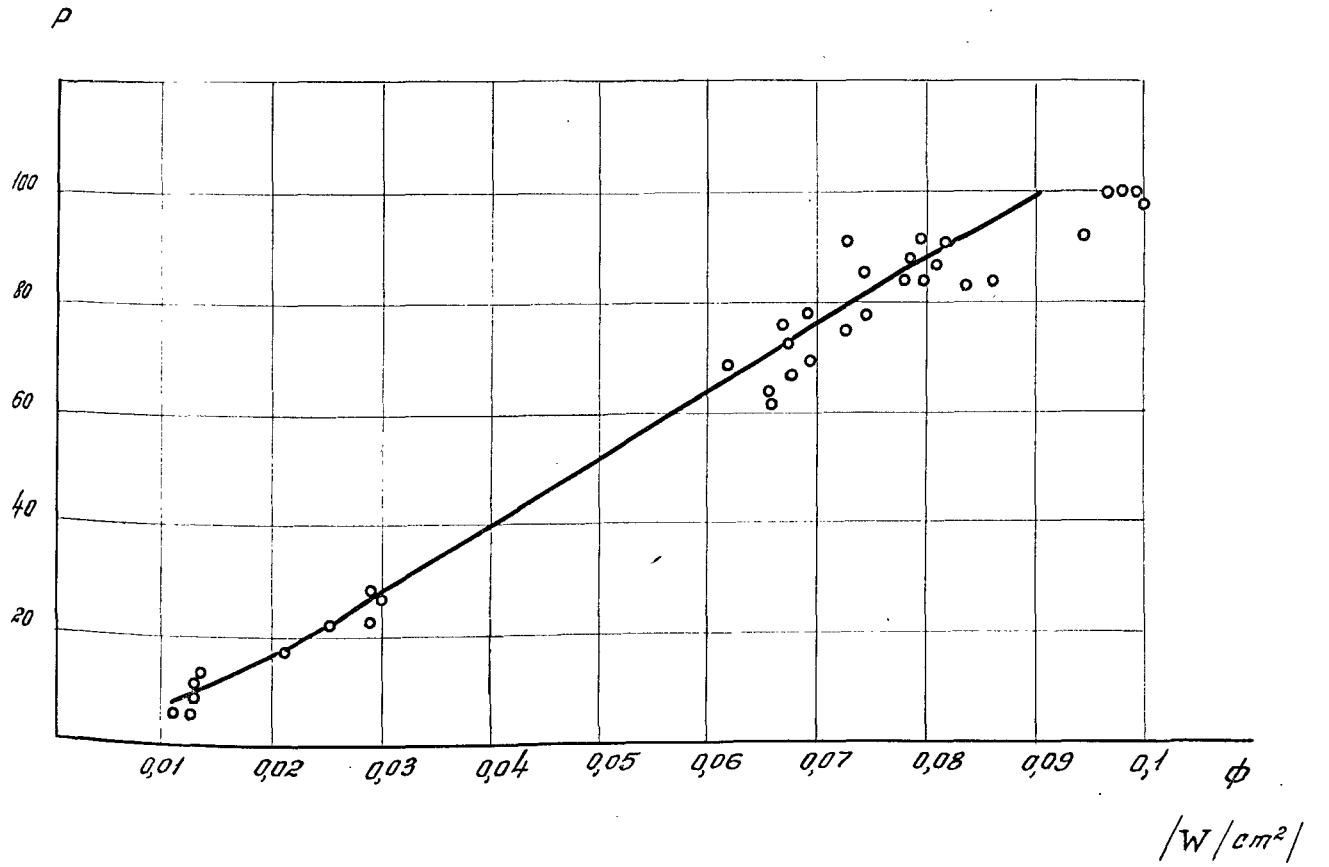


Figure 8

relationship for the monthly power output of a solar thermogenerator in kilowatt-hours per square metre of reflector:

$$W = (0.0117\,\tau = 0.104)\,\eta \qquad [24]$$

where τ is the number of hours of sunshine per month.

This relation holds for solar thermogenerators in the southern latitudes of the USSR between 35° and 47° N.L.

Photoelectric converters of solar energy

Silicon photocells used in the Soviet Union have efficiencies of 10 to 12 per cent. Since they are rather expensive, it is important to study ways of reducing their cost and to find methods of increasing the power output taken from the unit operating area of the photocell. One of the ways of reducing the cost of photocells is by using polycrystalline silicon in place of single crystals as the initial material. Presently developed photocells made of polycrystalline silicon (4) are two to three times cheaper than photocells made from single crystals. At the same time, given normal solar illumination, these photocells yield 5 to 6 W/cm². Their parameters vary with temperature and illumination, just the same as the parameters of single-crystal photocells. The deleterious effect of intercrystalline junctions was eliminated by depositing, on the working surface of the photocell, a network of current taps.

Also of interest is raising the output power of a photocell by the use of mirrors to concentrate the light flux on the surface of the photocell. An examination of the volt-ampere characteristics of photocells leads to the following conclusions.

For the ideal photocell, in which the series resistance R_s is zero, theory (5) gives the dependences, upon illumination Q_r of the optimal current and optimal voltage of a photocell in the form $I_{opt} \sim Q_r$, $V_{opt} \sim ln\ Q_r$.

Consequently, the output power of a photocell is equal to the product of the current and voltage and must increase almost linearly with increasing illumination:

$$P_{out} \sim Q_r\, ln\, Q_r \qquad [25]$$

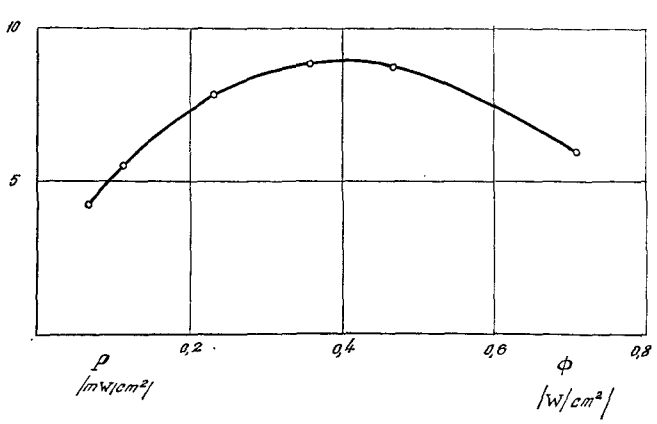


Figure 9

Thus, by increasing the illumination of a photocell, it is possible to increase appreciably its useful power.

However, in real photocells, there are factors that upset the derived relation [25] above and reduce the output power of photocells, particularly in the case of high light fluxes. One is the series resistance of the photocell. For real photocells (on the condition that the shunt resistance is sufficiently large), the volt-ampere characteristic is of the form:

$$ln\left(\frac{I + I_f}{I_o} + 1\right) = \frac{q}{\varkappa T}\,V - IR_s) \qquad [26]$$

where I_f is the short-circuit current of the photocell, I_o is the reverse saturation current, q is the electron charge, $\varkappa$ is Boltzmann's constant, and T is the temperature in degrees Kelvin.

It is obvious that the voltage drop on the resistance should reduce the operating voltage of the photocell and make its characteristic more sloping. Since increasing the illumination causes, primarily, an increase in the current of the photocell, it follows that more and more of the output power of the photocell will be lost in the series resistance:

$$P_{out} = -IV = -I\frac{\varkappa T}{q}\,ln\left(\frac{I + I_f}{I_o} + 1\right) - I^2R_s \qquad [27]$$

Figure 7 gives two-volt-ampere characteristics of a photocell that are computed for two levels of illumination (for $I_o = 10^{-9}$ Å, $R_s = 1$ ohm). Since the short-circuit current is a linear function of Q_r (6) for not too high illumination, it may be roughly considered that curve 2 corresponds to an illumination three times that of curve 1. Here, the optimal power is equal to 28.8 mW and 53.5 mW, respectively, i.e., shows an increase by a factor of 1.85 and not 3. To summarize, in real photocells the relationship of output power of a photocell as a function of the illumination will be nonlinear due to scattering or a considerable portion of the power on R_s. Besides, in the case of large illuminations, nonlinearity in the relationship of the current of the photocell as a function of the quantity of energy incident on its surface (6) should be evident.

We carried out experimental investigations to determine the effect of illumination on the volt-ampere characteristics of silicon photocells with efficiencies of from 3 to 10 per cent. The power of the photocells was computed at optimal load resistance. All measurements were carried out in sunlight. During measurements in the region of Q_r = 0.013-0.1 W/cm², the photocells were not thermostated and had a temperature of 35-40°C. The temperature of the photocells was measured by soldered thermocouples. The results of the measurements in the region of small illuminations are given in figure 8. The spread of experimental dots relative to the theoretical curve (continuous line) is slight. Therefore, in this case, the relation $P_{out} \sim Q_r\, ln\, Q_r$ holds.

At higher levels of illumination (up to 15-20 W/cm²), the photocells were studied both without cooling

and with cooling. In the case without cooling, the temperature of the photocells rose sharply: up to 110°C for $Q_r = 0.4$ W/cm² and higher. For this reason, the power of photocells increases only up to a fourfold to fivefold concentration of the light flux (i.e. up to $Q_r = 0.3$-0.5 W/cm²), and then falls (figure 9). For the majority of the studied photocells, the output power increases roughly by a factor of two, as compared to the power at $Q_r = 0.06$ W/cm², and fourfold to fivefold only for several photocells.

To eliminate heating of the photocells, they were placed in a heat-exchanger with a transparent bottom. Water heated to 20°C was passed through the heat-exchanger. In this case, the temperature of the photocells did not exceed 55°C, even at an illumination of 15 W/cm².

Losses of the light flux in the reflector and the bottom of the refrigerator came to 30 per cent of the total power incident on the reflector and were taken into account in the calculations.

When the illumination is increased, there is observed, along with a slight increase in the no-load voltage, a sharp rise in the current of the photocells, particularly in the region of small-load resistance. The optimal load resistance then diminishes several-fold. There is likewise a drop in the optimal voltage of the photocell, and the shape of the volt-ampere characteristic approaches that of a triangle (figure 10).

This deterioration in the change of the volt-ampere characteristic naturally brings about a fall in the degree of increase of the power of the photocell.

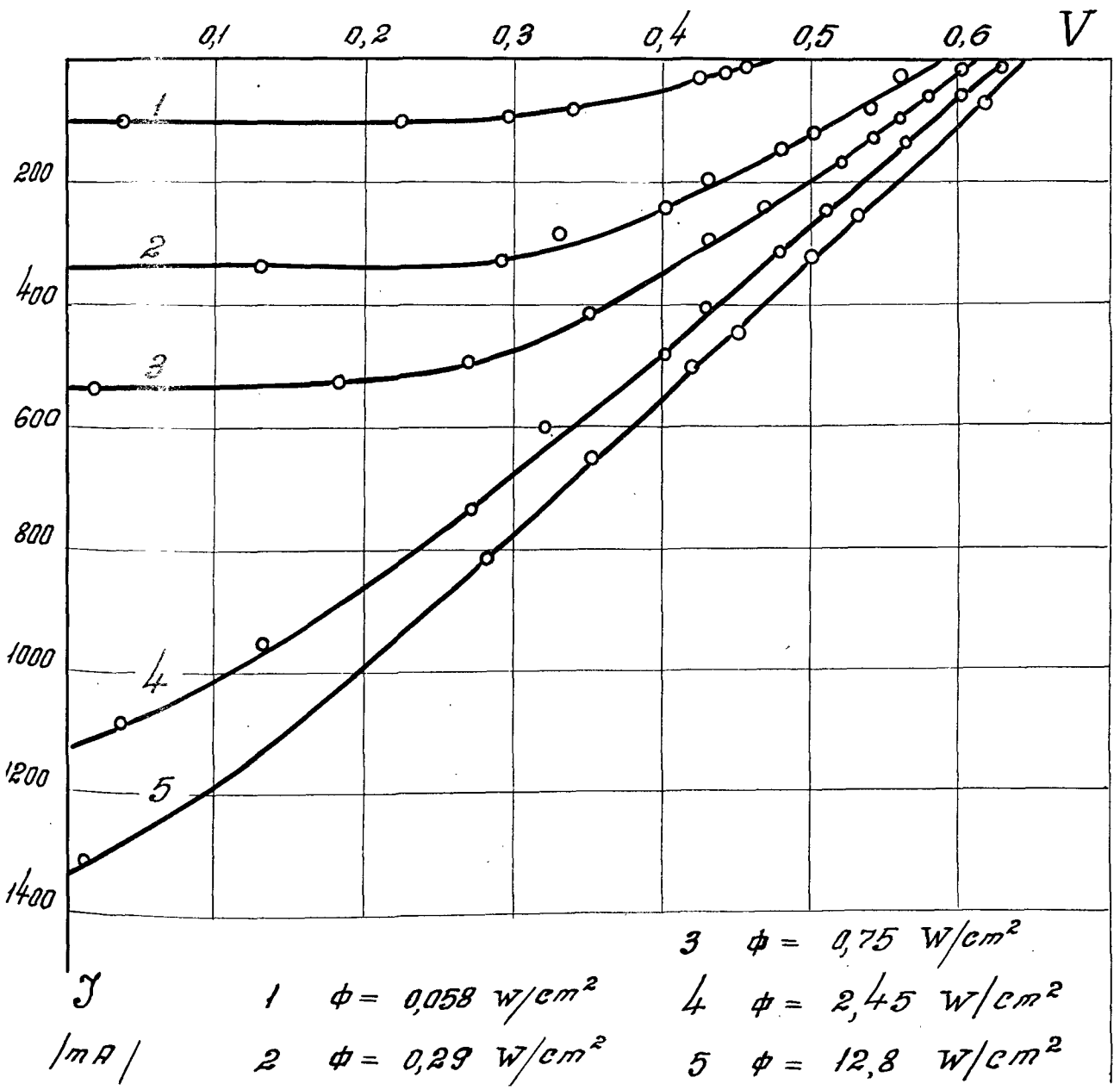


Figure 10

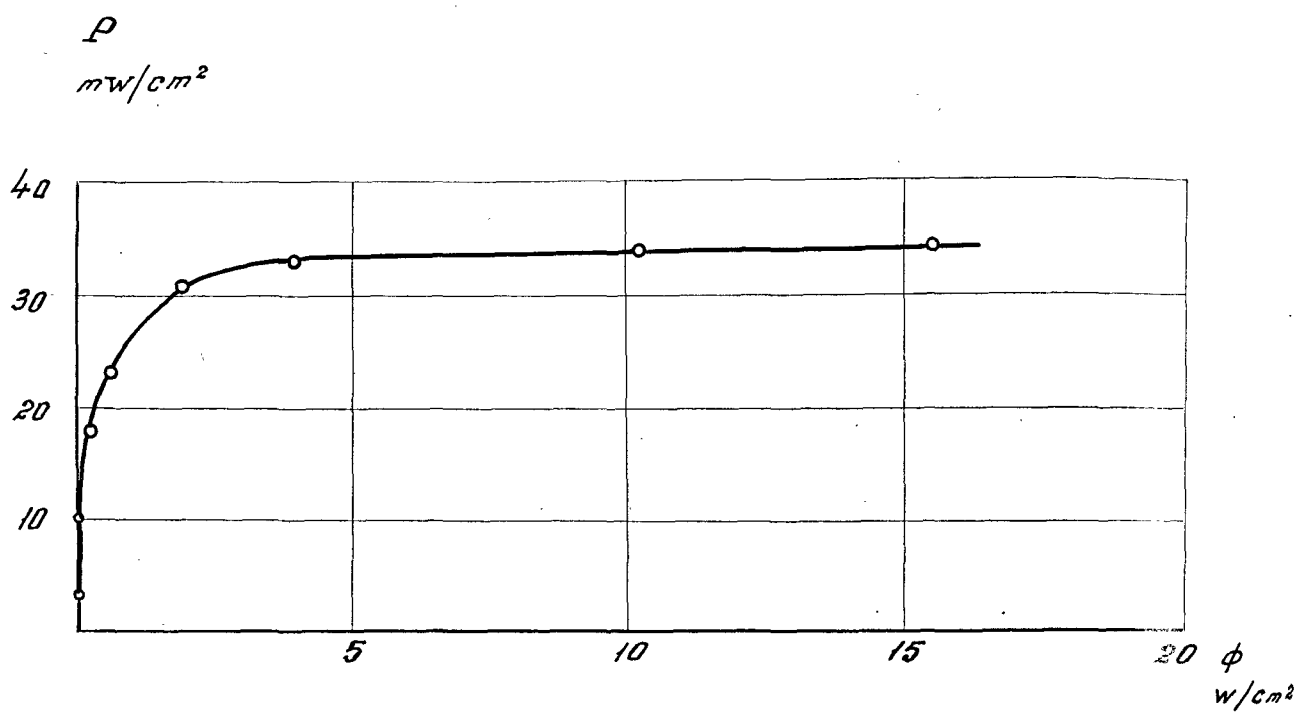


Figure 11

A large number of photocells were studied at various levels of illumination. The results of the measurements show (figure 11) that the output power of photocells rises rapidly with increase in Q_r roughly up to 2-3 W/cm², and then remains practically constant within a rather broad range of illumination : up to 20 W/cm². The maximal increase in power (with respect to the power of the photocell under normal illumination) came out to 10-30 times for a 60 to 70-fold concentration of the light flux. In individual cases, the power of the photocell increased by a factor of 70 for a 150-fold concentration. In most cases, the increase in power of photocells with low efficiency is greater than that of photocells with an efficiency of 5 to 10 per cent.

Conclusion

To summarize, on the basis of these measurements, we can draw the following conclusion : despite the fact that the increase in power of a photocell is nonlinearly dependent on the increase in illumination the use of devices that concentrate the light flux on the surface of the photocells (when this surface is cooled) produces a considerable increase in the output power.

References

1. Ioffe, A. F., *Semiconductor Thermoelements*, 1960.
2. Loferski, J. J., *J. Appl. Phys.*, 27 (7), 777 (1956).
3. Stilbans, L. S. and Kolenko, *Semiconductors in Science and Technology*, vol. 2, 1959.
4. Gliberman, A. Ya., Zaitseva, A. K., Landsman, A. P., *FTT*, vol. II, issue 8 (1960).
5. Prince, M. B., *J. Appl. Phys.*, 26 (5), 534 (1955).
6. Subashiev, V. K. and Sominsky, M. S., *Semiconductors in science and technology*, vol. II (1959).

Bibliography

Baum, V., Research on the use of solar energy made in the USSR. Paper for the Symposium on Solar Energy, held in Washington, 24 March 1961.

Baum, V. and Okhotin, A., *Ingenerno-phys. Journ.*, No. 11 (1959), Minsk.

Tepliakov, D., *Ingenerno-phys. Journ.*, No. 4 (1958), Minsk.

Vavilov, V., Malovetskaja, Galkin, *Atomic Energy*, No. 5 (1958), Moscow.

Baum, V., Borovikova, R. and Okhotin, A., *Ingenerno-phys. Journ.*, No. 8 (1960), Minsk.

PRELIMINARY TESTS OF A SOLAR-HEATED THERMOELECTRIC CONVERTER

Farrington Daniels, John A. Duffie, George O. G. Löf and Roger R. Breihan *

Thermoelectric converters such as those described by Kurt Katz at this conference (1) have been operated with a focusing solar collector. Although the system has not been optimized, the preliminary experimental results are presented here with discussions of the magnitude of possible improvements.

Two thermoelectric units built at the laboratories of the Westinghouse Corporation have been used in these experiments. One is provided with a receiving block of stainless steel, 5 inches square, the other with a $\frac{1}{4}$ inch copper square, clad in stainless steel, to spread the absorbed heat and give a more uniform distribution of temperature across the hot junctions. A small hole in the edge of the plate permitted the insertion of thermocouples to determine the temperature of the radiation-receiving plate. The units weighed about 9 pounds.

The thermoelectric converter was placed in a square frame attached to the rim of a 6-foot parabolic plastic collector covered with aluminized mylar polyester film as shown in figure 1. The reflectors were 5-foot and 6-foot aperture paraboloids fabricated of plastics as described in another paper presented at this conference (2) and having focal lengths of 2 to 3 feet.

Part of the radiation was reflected from the aluminized mylar onto the 5-inch square target (the face of the generator). In the center of the focal area the intensity of radiation of one of these reflectors was 264 times the incident beam radiation. The pattern of the 6-foot plastic parabola is shown in figure 2 and was obtained by photographic techniques using moonlight. The contour lines give the relative intensity of reflected radiation, i.e., the ratio of intensity to the intensity of the incident beam. The intensification factors are taken as the same for solar radiation.

The total radiation hitting the 5-inch square target was determined calorimetrically as described in the above-mentioned paper (2). A square of copper, 5 inches square and $\frac{3}{8}$ inch thick, was painted with Dupont flat black paint and held in front of the thermoelectric unit for 15 or 30 seconds and then quickly immersed in a deep, narrow square calorimeter can of copper holding 500 ml of water. The temperature rise permitted a calculation of the number of calories of radiation taken up by the copper block.

It is important to have a black highly absorptive surface on the plate which receives the solar radiation and one which gives a reduced emissivity in the infrared. Black paint cannot be used because of the high operating temperature.

A satisfactory selective radiation surface 3 was prepared by nickel plating the stainless steel and then plating copper 5×10^{-5} cm thick. When the sun's radiation is focused on it, the copper is oxidized in a few minutes to give a black adhering film of copper oxide. If the copper plate is too thick the copper oxide eventually peels off and becomes permanent. Copper oxide coatings of this type prepared from copper-plated surfaces have been shown to have absorptivity of solar radiation of about 85 per cent and emissivity in the infrared of about 25 per cent, and they appear to be permanent in air.

Results

Measurements were carried out only in clear skies and usually between 9 a.m. and 3 p.m. The solar

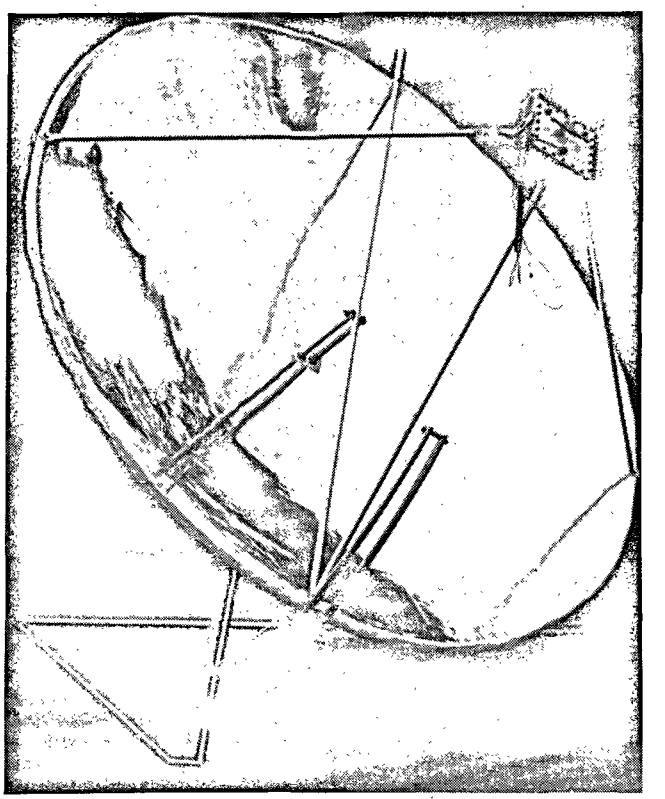


Figure 1. Six-foot plaster parabolic collector focusing on thermoelectric converter 5 inches square

* Solar Energy Laboratory, University of Wisconsin.

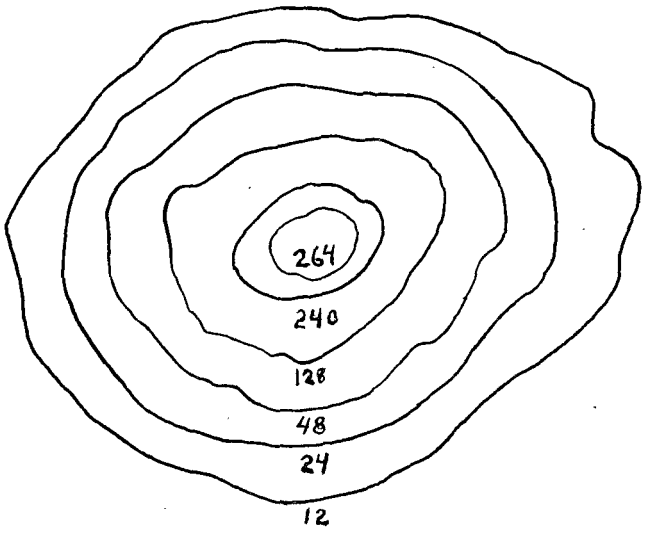


Figure 2. Pattern of focused radiation on a 5-inch square, showing areas of intensification of solar radiation

radiation was measured with an Eppley pyroheliometer mounted in a long tube and aimed directly at the sun, or with a collimated silicon photovoltaic cell which had been calibrated against an Eppley pyroheliometer. When the experiments were carried out, the incident radiation was 1.25 to 1.45 langleys. The solar radiation intercepted by the focusing collector was calculated from the effective area of the collector (27 sq. ft.) and the langleys of solar radiation.

The radiation hitting the thermoelectric generator (5 inches square) was determined calorimetrically. The heat lost in the water was determined by measuring the temperature of the inlet water (15°C) and that of the water (26°C) after passing through the thermoelectric unit, and determining the rate of flow of the water (1 liter per 54 sec.).

The open circuit voltage of the thermoelectric unit was determined with a potentiometer and the short-circuit amperage was determined with very large copper leads connected to an ammeter with an internal resistance of 5 milliohms. The product of these two divided by four gave the wattage.

Experiments were carried on for more than forty hours and water was pumped continuously with an inefficient motor and pump for several hours.

It is clear that these preliminary results are unsatisfactory, but the measurements show where significant improvements can be made.

The loss of focused radiation between interception by the 6-foot diameter collector and delivery to the 5-inch square target is about 50 per cent. Most of this is due to poor reflectivity from the aluminized mylar. Direct reflectivity tests on similar material showed that only about 65 per cent of the incident light is reflected as specular reflection.

The data given in table 1 are representative of the performance in these first tests.

Table 1. Preliminary data for thermoelectric conversion of solar radiation

Radiation intercepted by the 6-foot-diameter collector		34 800 cal per min.
Radiation focused onto the 5-inch-square target	Photography : 14 300	Calorimetry: 16 000 cal per min.
Temperature of receiving target	485°C	
Heat removed in flowing water		12 000 cal per min.
Open circuit voltage	4.0 volts	
Closed circuit amperage	22-40 amperes	
Electrical energy produced	22-40 watts	308-560 cal per min.
Per cent of radiation focused on target	Photography: 41	Calorimetry: 46
Per cent of heat hitting target converted into electricity	2.2-3.9	2.0-3.5
Ratio of electricity produced to heat taken up by water	0.026-0.046	

The difference of 4 000 calories per minute between the heat hitting the target 16 000 calories per minute, and the heat collected by the cooling water, 12 000 calories per minute, is due to radiation losses, convection losses, conduction losses and reflectivity losses from the black copper oxide surface. Rough but conservative calculations of these losses give an estimated value of 4 500 calories.

The difference between the 34 800 calories per minute of incident radiation and the 16 000 calories per minute focused on the target is due to poor specular reflectivity and macroscopic imperfections and some deviation from pure parabolic form. Of these, the greatest losses are due to the poor reflectivity of the aluminized mylar. Experimental tests indicated a reflectivity of only about 65 per cent.

Conclusions

These preliminary results are being followed by more extensive measurements which will be reported later. It is particularly important to improve the

reflecting surface of the aluminized mylar. Experiments indicate that this can be done and that the attachment of the mylar to the plastic form leads to a loss in reflectivity.

Some improvement is possible in the shape and rigidity of the focusing collector. It is planned to try out new thermoelectric units of higher voltage and wattage and to construct a plastic collector 8 feet in diameter instead of 6 feet.

The low voltage of these thermoelectric units is a handicap for operating small direct-current motors. The closed-circuit voltage of the motors needs to be considerably higher than that of the units described here. It was found, however, that the solar-operated thermoelectric converter was very effective in charging lead-acid electric storage batteries. In one experiment, a bank of six small 2-volt cells was charged in parallel for several hours and then discharged in series to provide a higher voltage for more efficient operation of a motor.

It has been shown that it is practical to heat thermoelectric units with solar energy up to about 500°C, which is a suitable temperature for long-lived thermoelements. Improvements both in the focusing collectors and in the thermoelectric converter can be expected. Further tests on durability over longer time intervals will be reported.

It is hoped that within the next few months sufficient data will have been collected to give some cost data and economic estimates.

Acknowledgements

The authors wish to express their appreciation to the Rockefeller Foundation for the support of this research.

References

1. Katz, K., Thermoelectric generators for the conversion of solar energy to produce electrical and mechanical power, *Proceedings of the United Nations Conference on New Sources of Energy*, 1961, included below, paper S/12.

2. Daniels, F. and Breihan, R. R., Solar focusing collectors of plastics, *Proceedings of the United Nations Conference on New Sources of Energy*, 1961; included below [under agenda item III.B], paper S/104.

3. Kokoropoulos, P., Salam, E. and Daniels, F., Selective Radiation Coatings. Preparation and High Temperature Stability, *Solar Energy* 3 (4), p. 19 (1959).

Summary

Preliminary data are reported on the production of electric currents by focused sunlight on a thermoelectric converter made at the laboratories of the Westinghouse Corporation.

The collector with aluminized mylar on a plastic parabolic reflector 6 feet in diameter focused less than 50 per cent of the intercepted solar radiation on the converter, which was 5 inches square.

The converter received 16 kilocalories of heat and gave up 12 kilocalories of heat to the cooling water while producing a maximum of 40 watts of electricity at low voltage. Some of the ways in which improvements can be made are pointed out.

ESSAIS PRÉLIMINAIRES D'UN CONVERTISSEUR THERMO-ÉLECTRIQUE A CHAUFFAGE SOLAIRE

Résumé

Ce mémoire présente des données préliminaires sur la production de courant électrique par la concentration de la lumière solaire sur un convertisseur thermo-électrique fabriqué au laboratoire de la Westinghouse Company.

Le collecteur, constitué par du Mylar aluminisé sur un réflecteur parabolique en composition plastique de 6 pieds de diamètre (1,82 m) a concentré moins de 50 p. 100 du rayonnement solaire intercepté sur le convertisseur carré de 5 pouces de côté (13 cm).

Le convertisseur a reçu 16 grandes calories de chaleur et en a donné 12 à l'eau de refroidissement, tout en produisant un maximum de 40 W d'électricité à faible tension. Les auteurs indiquent certaines méthodes grâce auxquelles on pourra réaliser des améliorations.

SOLAR HEATED THERMIONIC CONVERTER

George N. Hatsopoulos and Pierre J. Brosens ***

The direct conversion of heat into electrical energy offers many advantages over the more customary approach which involves an intermediate conversion of heat into mechanical energy. Direct conversion devices do not involve moving mechanical parts and so are silent. They do not require lubrication and can operate for long periods of time with practically no supervision. In addition, they offer the prospect of higher efficiency in the small power field; smaller weight and size, and a more compact design requiring relatively little maintenance. They can be easily scaled up or down in size to practically any source of heat ranging from solar energy to nuclear reactors.

In recent years, direct conversion of heat into electricity has attracted considerable attention which has resulted in a large research and development effort by both commercial and military agencies.

The devices for direct conversion being developed today can be classified in two categories: thermionic engines and thermoelectric generators.

The purpose of the present paper is to describe the principle of operation of thermionic engines, their advantages and uses in the direct generation of electricity from solar energy.

Principles of operation of thermionic engines

The principle of operation of thermionic devices is based on the phenomenon of electron emission from metals at high temperatures, known as the Edison effect. The use of this effect for converting heat into electricity was first suggested by Schlichter (1) in 1915. Subsequently, Champeix (2) in 1951 gave a qualitative discussion of this method and concluded that it was impractical. The first detailed thermionic and thermodynamic study of the subject was given by one of the authors (3) in 1956, who analyzed the use of close spacings and of a crossed electric and magnetic field for controlling the effects of space charge. Subsequently, Moss (4), Hatsopoulos and Kaye (5), Wilson (6), Houston (7), Hernqvist et al (8), Grover et al (9), and Nottingham (10) published studies describing analytic and experimental results on various thermionic devices.

A thermionic converter is a device which accepts heat at a high temperature, rejects heat at a lower temperature and generates a driving potential difference which causes an electric current to flow through an external load. It consists of an electron emitter which receives heat and delivers electrons that are transported through an intervening space to an electron collector. (The collector is kept at a temperature lower than the emitter by means of appropriate cooling.)

The current flowing through a thermionic converter is predominantly controlled by the properties of the emitter and the transport mechanism. The output voltage also depends on the transport mechanism and, in addition, on the work function of the collector. It is desirable that the emitter be operated at a high temperature and yet have a low work function. Composite surfaces consisting of mixtures of oxides, such as barium oxide, strontium oxide, etc., may be operated stably at temperatures of about 1 200°C and have sufficiently low work functions at this temperature to emit currents of the order of 5 amp/cm^2. Pure refractory metals, on the other hand, such as tungsten, tantalum and molybdenum, can be operated at temperatures in excess of 2 000°C but have a work function too high to yield a satisfactory current density. In the presence of sufficiently high concentration of cesium vapor, however, these metals are subjected to a lowering of their work function and can be made to emit currents in excess of 100 amp/cm^2.

Due to their low work function, the materials mentioned above are also used for the collector. The work functions obtained here are smaller than those of the emitter, since the work function is an increasing function of temperature.

The electrons are emitted through the interelectrode space onto the collector. These electrodes, being negatively charged, result in a negative potential barrier which is called a space charge barrier. This phenomenon may cause a decrease in the output current by many orders of magnitude. In order to prevent the formation of a space charge barrier in the interelectrode space of a thermionic converter, two methods have been used in practice. The first method consists of reducing the interelectrode spacing to a few microns and the second of introducing positive ions. The former method has resulted in the development of the close-spaced vacuum thermionic converter, while the latter has resulted in the development of the cesium thermionic converter.

* Associate Professor, Massachusetts Institute of Technology, Cambridge, and President, Thermo Electron Engineering Corporation, Waltham, Massachusetts.

** Director of Development, Thermo Electron Engineering Corporation, Waltham, Massachusetts.

In a vacuum thermionic converter, the smaller the spacing the larger the current that can flow between the electrodes before space charge effects appear. Since practical considerations limit the interelectrode spacing to values greater than 10 microns, it can be shown analytically that the maximum current that can be obtained from a vacuum thermionic converter is of the order of 1 amp/cm². Such current is easily obtainable from an emitter operating at a temperature of about 1 200°C and, therefore, an increase of the emitter temperature of such a converter above that value would produce little gain. With these limitations in mind, it can be shown that the output power of these converters is below 1 watt/cm² at efficiencies of less than 10 per cent. Practical converters built to date have yielded power densities of about 0.6 watt/cm² and efficiencies of about 6 per cent.

Cesium converters rely on the phenomenon of ionization of cesium atoms when striking a hot surface. In order for the mechanism of surface ionization to produce a substantial yield of ions, the emitter must be kept at relatively high temperatures of the order of 2 200°C. Cesium converters operating at these high emitter temperatures have been tested in various laboratories throughout the country and have yielded power outputs as high as 20 watt/cm² at efficiencies of over 15 per cent.

The spectacular performance of the earliest design of cesium converters was tempered by the fact that the temperature limitation of most available heat sources, including gas, was thought to be lower than the operating temperature of the emitters of cesium converters and, therefore, the applicability of these converters was considered extremely limited. However, in recent developments the use of close spacing in cesium converters has permitted their operation at temperatures of the order of 1 500°C. Such close-spaced cesium converters have been very recently constructed and tested at Thermo Electron Engineering Corporation and have yielded power densities in excess of 12 watt/cm² and efficiencies in excess of 15 per cent. The spacing required for these converters is of the order of 0.04 inch, which is about 10 times larger than the spacing used in vacuum converters.

Applications

Thermionic converters are very simple in their construction. Cesium converters in particular do not require an extreme accuracy in their construction. The materials used are readily available pure metals such as molybdenum, copper and tantalum. Due to their high power density, the amount of material used per unit of output power is relatively small. For example, a typical converter will require $\frac{1}{10}$ gram of refractory metals per watt of output and 5 grams of lower-priced materials such as copper and ceramics. As a result, it is expected that the manufacturing cost of thermionic engines in mass production quantities will be considerably lower than the cost of manufacturing rotating machinery in the power range of several kilowatts.

When coupled with a clean source of heat, such as solar energy, the life of these engines is expected to be of the order of 10 000 to 50 000 hours, which is one order higher than the life of conventional electric generators. Furthermore, the maintenance and repairs during the life of the converter are expected to be practically nil.

Owing to the simplicity of their design, thermionic engines contructed to date have proved extremely rugged and have withstood accelerations up to 30 gs without failure. Such a characteristic, in addition to light weight, makes them very suitable for applications requiring portable generators.

Thermionic generators operate silently, which makes then very advantageous for military as well as home use.

It is expected that presently thermionic generators will be used in a large variety of applications requiring power from 100 watts to 100 kilowatts. In this power range, conventional rotating electrical generators, coupled with an internal combustion engine, have an overall system efficiency of about 10 per cent. The efficiencies obtained to date in thermionic systems have compared favorably.

Taking into consideration the advantages mentioned above, it becomes evident that thermionic generators can find many and varied uses in homes and industry. The most promising of these in the near future are those which involve solar energy as a source of heat. This is primarily due to the fact that solar energy does not present the problems associated with the use of oxidizing heat sources such as the combustion of fossil fuels and the material compatibility problems associated with nuclear applications.

Solar energy coupled with a thermionic engine could be used today for powering relay stations for communications. It can also be used for irrigation systems, in which case the generator is particularly advantageous in that no electric storage system is required. Its useful function can be performed during the hours of available sunlight. Moreover, the fact that thermionic units can operate very effectively and economically in producing little power makes them very useful in powering small and remotely located farms.

State of the Art and the Development of Thermionic Engines for Space Applications

Much of the effort in the development of thermionic engines has been directed towards studies of the practicability of solar thermionic space power systems. This seems to be one of the areas where thermionic devices will be put to practical use first.

In space applications, it is necessary to construct devices which incorporate provisions for the collection of solar heat and have long life characteristics. The requirement to collect solar heat specifies the

type of device geometry that can be used. The long life requirement implies that only cathode materials with low evaporation rates and structural materials with high resistance to cesium corrosion should be used.

Although much progress can still be made in this field of materials technology, the development programs presently in progress have advanced enough for long life thermionic devices to be constructed. Figure 1 shows one of the more recent units where solar heating is simulated by electron bombardment. In test, the device has given an output of 200 amperes, one volt and an overall efficiency of 12.6 per cent. As the figure shows, the device requires a vacuum envelope. This is not only because the electron bombardment unit requires a vacuum, but also because the materials used in the construction of this unit could not stand the oxidizing effects of the earth's atmosphere. This is not a shortcoming since the particular unit shown is intended for space applications. However, in the case of thermionic devices to operate on the earth, these should be provided with protective features to prevent oxidizing.

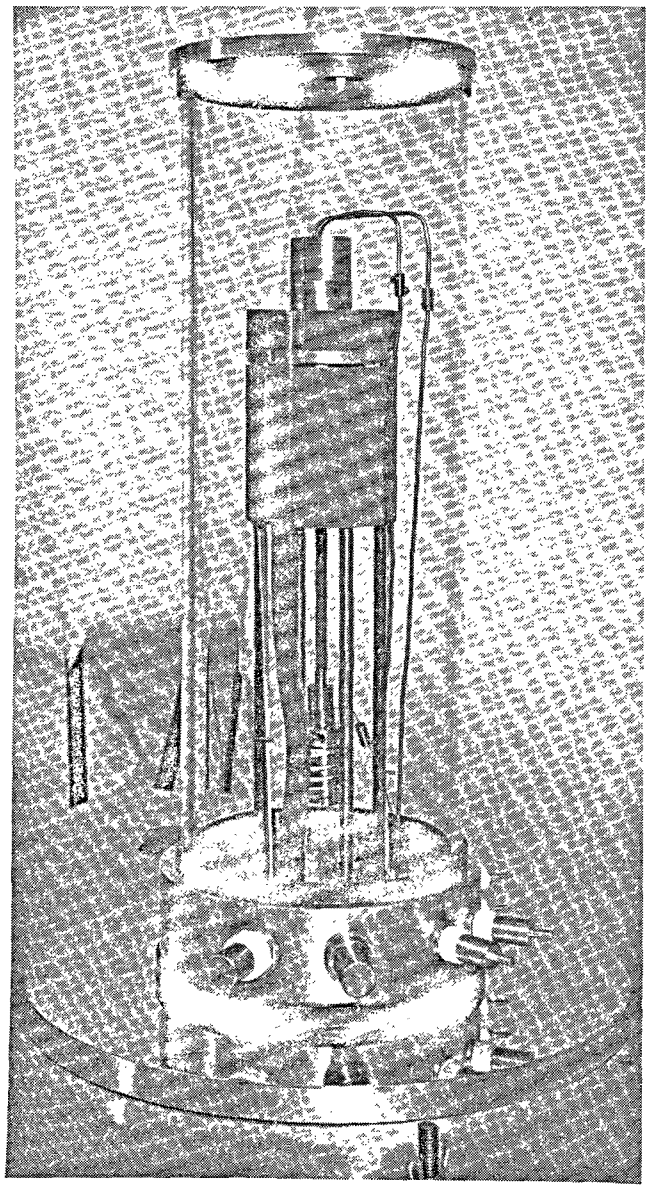


Figure 1

At present, new development programs are under way which aim at the construction of modular devices where a solar cavity is surrounded by several units. In such configurations, it becomes possible to achieve output voltages of the order of six volts and the construction of the individual modules is considerably simpler. It is believed that overall efficiency in excess of 20 per cent can be attained.

Earthbound solar thermionic systems

An earthbound solar thermionic system will consist essentially of a solar concentrator in the form of a parabolic mirror, a cavity-type thermionic engine, and a tracking device to follow the sun. Preliminary optimization studies have indicated that the aperture of the parabolic concentrator should be about 45°. The best materials to use for efficient reflection of the sun's light is silver, which would have an overall reflectivity in excess of 92 per cent. It is, however, difficult to protect this material against tarnishing and for the present, at least, aluminium with silicon monoxide coating seems to be a more adequater eflective material. Its overall reflectivity would be of the order of 89 per cent.

The solar concentrator should be a very precise structure with surface errors having variance of no more than $\frac{1}{10}$ of a degree. Although this represents an extreme accuracy of fabrication, it appears that development work presently in progress for space applications will lead to inexpensive means of constructing such shapes with even higher accuracy.

A similar accuracy requirement exists for the tracking mechanism which would have to maintain the orientation of the solar concentration axis aligned with the sun's direction within $\frac{1}{10}$ of a degree. Calculations indicate that if the tracking mechanism and the solar concentrator satisfy these requirements, an overall efficiency of solar flux absorption of 83 per cent can be achieved when heating thermionic diodes in a cavity at 1 700°C and when the solar concentrator axis is lined up with the sun's direction. In the case of a $\frac{1}{10}$ degree misalignment of the solar concentrator, this efficiency would be 74 per cent. Thus, a solar concentrator five feet in diameter would be capable of providing a cluster of thermionic diodes with a minimum heat input of about 1 500 watts.

Figure 2 shows schematically the configuration of a multi-module thermionic engine that can be used in the earth's atmosphere. In this arrangement, the high temperature cavity and most of the diodes' structures are protected from oxidation by a bell jar which keeps the cavity evacuated. The rest of the device is built with materials that operate at a suf-

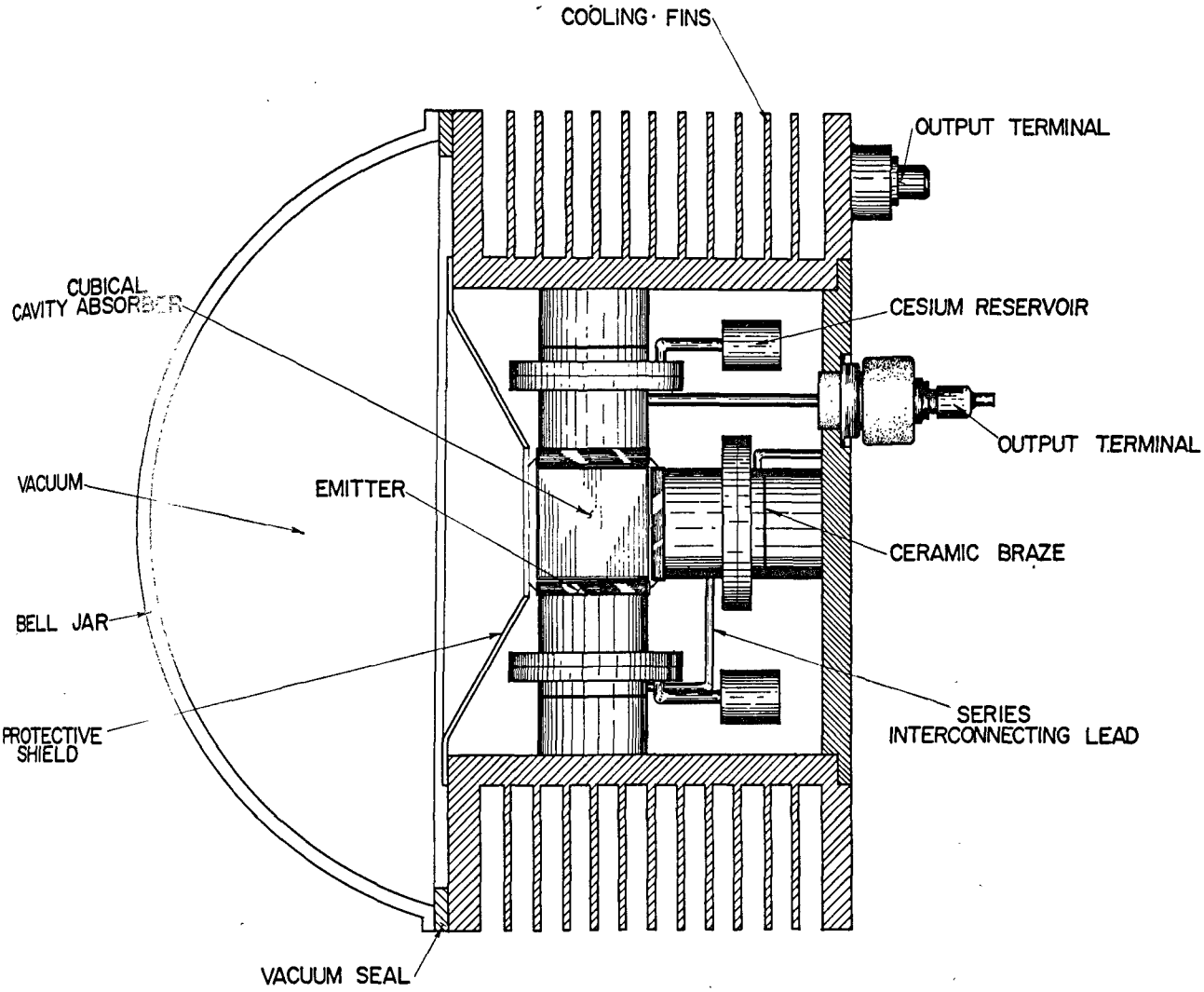


Figure 2. Earthbound solar thermionic engine

ficiently low temperature to avoid deterioration in the earth's atmosphere. Each diode is essentially a cylindrical structure topped by a flat square emitter surface which faces the solar cavity. Five such diodes would be used to form five faces of a cube, the sixth face being left open to admit the oncoming concentrator flux. The cubic cavity would be slightly smaller than a cube two centimeters on a side. At a thermionic engine efficiency of 20 per cent, a system using a five foot solar concentrator would deliver 300 watts of electrical power and would have an overall efficiency of 17 per cent.

In addition, such systems requiring a minimum of maintenance would be reasonably rugged and, in the case of a system with a concentrator of the order of five feet in diameter, it could be transported with relative ease. The weight of a five foot system could be as low as 30 pounds.

Conclusion

From the foregoing, it appears that earthbound solar thermionic systems might find many applications in those areas of the world where solar energy is abundant and where the locations of utilization of electrical energy are too remote to make the distribution of electrical power from centralized stations economical. Probably, the solar thermionic power systems are the most promising means for converting solar energy into electricity on earth, both from a point of view of conversion efficiency and of cost of installation involved.

References

1. W. Schlichter, Die Spontane Elektronenemission von Glühender Metalle und das Glunelektrische Element, Dissertation, Göttingen, 1915.
2. Champeix, M. R., Transformation of Heat into Electrical Energy in Thermionic Phenomena, *Le Vide*, vol. 6, pp. 936-940, January 1951.
3. Hatsopoulos, G. N., The Thermoelectron Engine, *Sc. D. Dissertation*, M. I. T., Cambridge, Mass, May 1956.
4. Moss, H., Thermionic Diodes as Energy Converters, *J. of Electronics*, January 1957, 2, 305.
5. Hatsopoulos, G. N., Kaye, J., Analysis and Experimental Results of a Diode Configuration of a Novel Thermoelectron Engine, *Proc. I.R.E.*, September 1958, 46, 1574.
6. Wilson, V. C., Conversion of Heat to Electricity by Thermionic Emission, *J.A.P.*, 1959, 30, 475-481.
7. Houston, J. M., Theoretical Efficiency of Thermionic Energy Converters, J.M., *J.A.P.*, 1959, 30, 481-487.
8. Hernqvist, K. G., Kanefsky, J., Norman, F. H., Thermionic Energy Converter, *R.C.A. Rev.*, June 1958, 244.
9. Grover, G. M., Rochling, D. J., Salmi, E. W., Properties of a Thermoelectric Cell, *J.A.P.*, November 1958, 29, 1611.
10. Nottingham, W. B., Thermionic Diode as a Heat-to-Electrical Power Transducer, *J.A.P.*, 1959, 30, 413-417.

Summary

After a brief historic review of the development of thermionic conversion, a description of the principles of operation of thermionic engines is given. A discussion of the potential advantages of thermionic engines to be used in converting solar energy into electric power is also given. Experimental results on recently tested engines for use in space applications show that these systems can also be used in the near future for ground applications. A brief description of a ground solar thermionic conversion system follows.

In conclusion, thermionic engines coupled with solar concentrators promise inexpensive, lightweight, maintenance-free generators of power in the range of 100 watts to 100 kilowatts having an over-all efficiency of about 17 per cent for an operation life of up to 50 000 hours.

CONVERTISSEUR THERMO-IONIQUE A CHAUFFAGE SOLAIRE

Résumé

Après une brève revue historique de l'évolution de la conversion thermo-ionique, les auteurs donnent une description des principes de fonctionnement des moteurs thermo-ioniques. Ils examinent les avantages possibles de ces moteurs quand il s'agit de convertir l'énergie solaire en énergie électrique. Ce mémoire donne les résultats expérimentaux réalisés avec des moteurs soumis à de récents essais, en vue de leur utilisation pour des applications à bord de véhicules interplanétaires, qui démontrent que ces systèmes pourraient également recevoir avant peu des applications terrestres. Les auteurs donnent une brève description d'un système de conversion thermo-ionique de l'énergie solaire à terre.

En conclusion, les moteurs thermo-ioniques, en liaison avec des concentrateurs solaires, promettent de fournir des générateurs d'énergie légers et peu coûteux dans la gamme allant de 100 W à 100 kW, avec un rendement global de l'ordre de 17 p. 100, pour une durée utile de service pouvant atteindre 50 000 heures.

THERMOELECTRIC GENERATORS FOR THE CONVERSION OF SOLAR ENERGY TO PRODUCE ELECTRICAL AND MECHANICAL POWER

Kurt Katz *

While the discovery of the thermoelectric effect dates to the early part of the nineteenth century, the practical utilization thereof, for purposes other than temperature sensing, is only now achieving feasibility for providing less limited power requirements. It was in 1822 that the German physicist Seebeck discovered that a voltage was developed in a loop containing two dissimilar metals, provided that the two junctions were maintained at different temperatures. Twelve years thereafter, the French physicist, Peltier, discovered that the junction between two dissimilar metals acted as a heat source or heat sink, depending upon the direction of electric current flow. Furthermore, he found the strength of the heat source or sink to be proportional to the current itself. It was in 1845 that Lord Kelvin elucidated the fundamentals of this effect and developed his basic relations. The lack of practical applications of thermoelectricity over the past century was due to the low efficiency of known materials.

The recent reactivation and advancements in thermoelectric power generation were to a large extent nurtured by advances in solid state theory which have led to the development of "tailored" semiconductor materials for various ranges of temperature.

The potential applications of this mode of energy conversion are many, as some of the recently built thermoelectric devices will testify (1), (2), (3). This paper will restrict itself to the utilization of solar energy as the heat source. Solar energy utilization in tropic zone areas of the world, that have not yet achieved any extensive degree of mechanization, offers the hope of an improved standard of living. Since the pumping of water can be achieved without any provision for energy storage to compensate for the intermittency of the sun, the pumping of water for irrigation and household uses appears as a logical initial application of solar-thermoelectric power generation. As Daniels points out, the next step may be electric lighting for homes and villages, followed by some village industries such as weaving, carpentry, etc. (4) These second stage applications require some provisions for energy storage in addition to the basic solar thermoelectric generator system.

A solar-thermoelectric generating system offers a static, high reliability, maintenance free system that is independent of any transportation supply problem, once installed. The maintenance free aspects of this system make possible the widespread application thereof in nations where technically skilled individuals are at a premium. Several solar thermoelectric devices have been operated and some of the results, with particular emphasis on the solar collector requirements for this type of system, appear in a complementary paper (5).

The design and performance capability of thermoelectric generators for the conversion of solar energy and relative system economics are the scope of this paper. A brief review of the equations and parameters of importance in predicting performance of a thermoelectric generator, along with the status of materials for this mode of energy conversion, will be presented, with the aim of providing overall clarity.

Thermoelectric power generation

Device efficiency

Figure 1 shows a simple thermoelectric circuit with the letters P and N designating the two different materials that comprise the basic couple.[1] The terminology of materials identification is identical with that employed in the semiconductor field. One of the junctions of this couple is maintained in contact with the heat source, at a temperature level T_1, and the other with the heat sink at a temper-

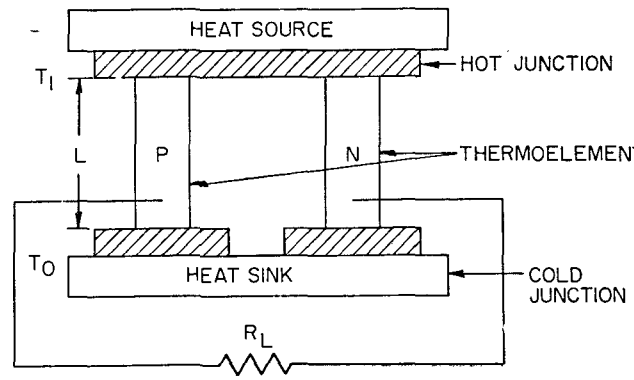


Figure 1. Basic thermoelectric couple

* Central Research Laboratories, Westinghouse Electric Corporation, Pittsburgh, Pennsylvania.

[1] These symbols have been used throughout. See end of paper for complete list.

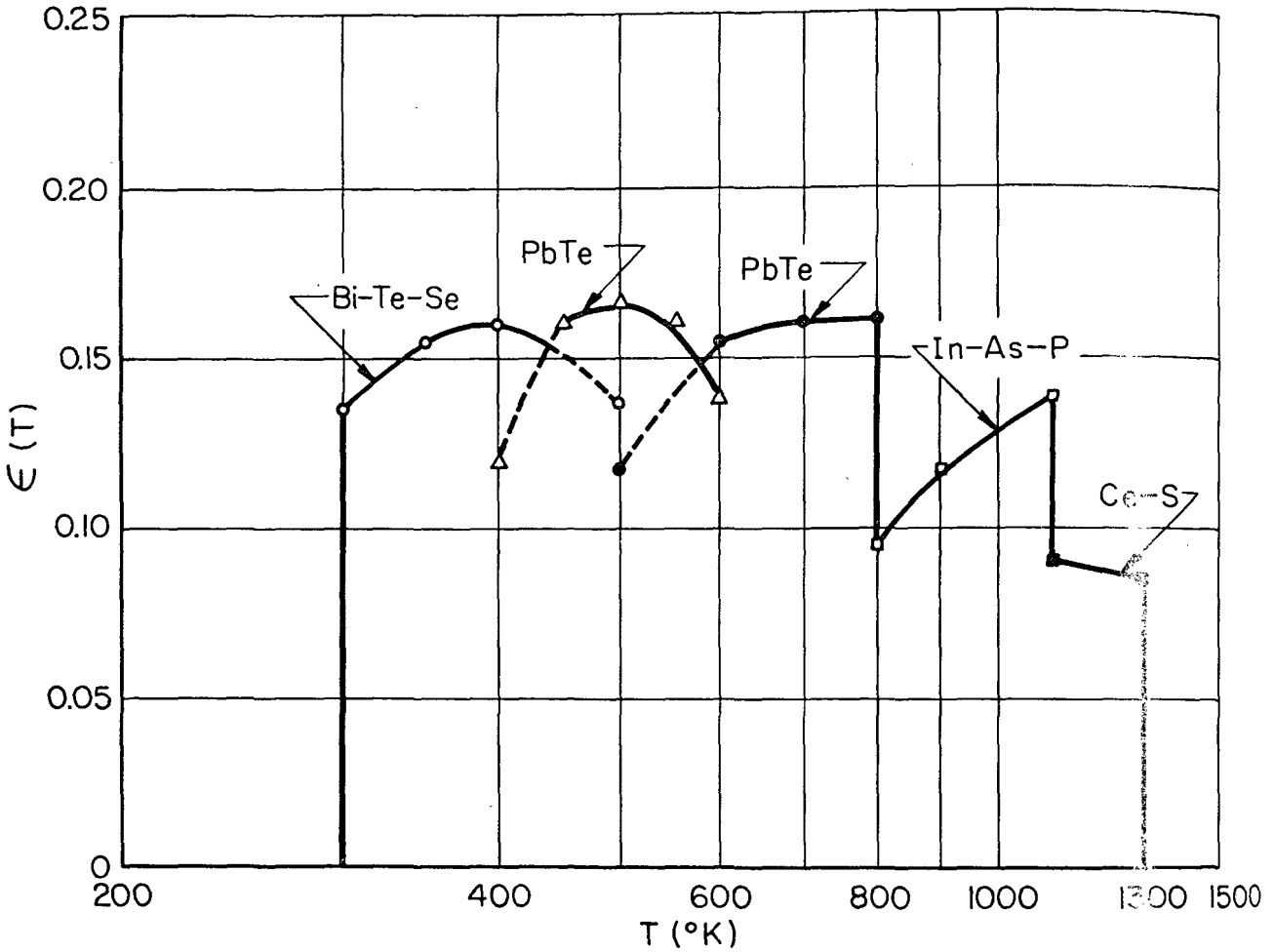


Figure 2. N-type thermoelectric materials

ature level of T_0. The overall thermoelectric conversion efficiency will be defined as:

"The ratio of useful electrical energy delivered to the external circuit to the energy absorbed at the hot junction."

The rigorous development of the equations that govern device efficiency and the phenomenology of the thermoelectric effect appears in several texts and papers and so will not be repeated (6) (7) (8). The heat removed at the hot junction consists of:

1. Peltier heat, Q_P
2. Conduction transport to the cold junction Q_c
3. One half of the Joule heat that is generated within the thermoelements, Q_j, and returned to the heat source.

The Thomson effect is small in comparison with the other terms and as Ioffe points out is accounted for when an average Seebeck coefficient is used. Therefore, the heat removed at the hot junction is:

$$Q = Q_P + Q_c - Q_j \tag{1}$$

where

$$Q_P = \pi I \tag{2}$$

$$Q_c = \frac{KA\Delta T}{L} \tag{3}$$

$$Q_j = \tfrac{1}{2} I^2 R_i \tag{4}$$

Letting P_L equal the energy delivered to the external circuit the efficiency based on the above definition is:

$$\eta = \frac{P_L}{\frac{KA\Delta T}{L} + \pi I - \tfrac{1}{2} I^2 R_i} \tag{5}$$

The Peltier coefficient π can be evaluated from the experimentally measured Seebeck coefficient α, by the Kelvin relation,

$$\pi = \alpha T \tag{6}$$

Furthermore,

$$\frac{KA\Delta T}{L} = \left[\frac{K_P A_P}{L_P} + \frac{K_N A_N}{L_N}\right] \Delta T \tag{7}$$

and assuming the cross-sectional area and length of the P and N thermoelements to be the same, which in practice is generally the case, then expression (7) can be rewritten in terms of an effective thermal conductivity — K:

$$\overline{K} = (K_P + K_N)\frac{A}{L} \tag{8}$$

By the same token,

$$R_j = \frac{\rho_P L_P}{A_P} + \frac{\rho_N L_P}{A_N} \tag{9}$$

can be related to an effective internal resistance $\overline{R}_i$, namely:

$$\overline{R}_i = [\rho_P + \rho_N] \frac{A}{L} \tag{10}$$

The useful energy delivered to the load is

$$P_L = IE_L \tag{11}$$

and since

$$E_G = E_i + E_L \tag{12}$$

the current can be equated as:

$$I = \frac{E_G}{R_i + bR_i} = \frac{E_i}{R_i} = \frac{E_L}{bR_i} \tag{13}$$

The generated voltage E_G is determined by the Seebeck coefficient of the P and N thermoelements and the thermal differential maintained across the element. Thus

$$E_G = (\alpha_P + \alpha_N)\,\Delta T \tag{14}$$

also letting $\bar{\alpha}$ be the effective Seebeck coefficient for the couple

$$\bar{\alpha} = \alpha_P + \alpha_N \tag{15}$$

equation (5) can be rewritten in terms of measurable quantities,

$$\eta = \left(\frac{\Delta T}{T_1}\right) \left[\frac{\dfrac{b}{b+1}}{1 + \left(\dfrac{\overline{KR}_i}{\bar{a}^2}\right)\left(\dfrac{b+1}{T_1}\right) - \left(\dfrac{\Delta T}{2T_1}\right)\left(\dfrac{1}{b+1}\right)}\right] \tag{16}$$

Equation (16) shows the efficiency of a thermoelectric generating device is a function of:

1. The temperature difference between the hot and cold junction;

2. The term $\overline{KR}/\bar{\alpha}^2$, which is strictly a materials parameter and denoted, generally, as $1/Z$. Therefore, equation (16) may be abbreviated as:

$$\eta = \eta_c \times \eta_{T.C.} \tag{17}$$

i.e., the product of the Carnot efficiency and a materials efficiency, defined as $\eta_{T.C.}$ The condition for maximum power to the load imposes the require-

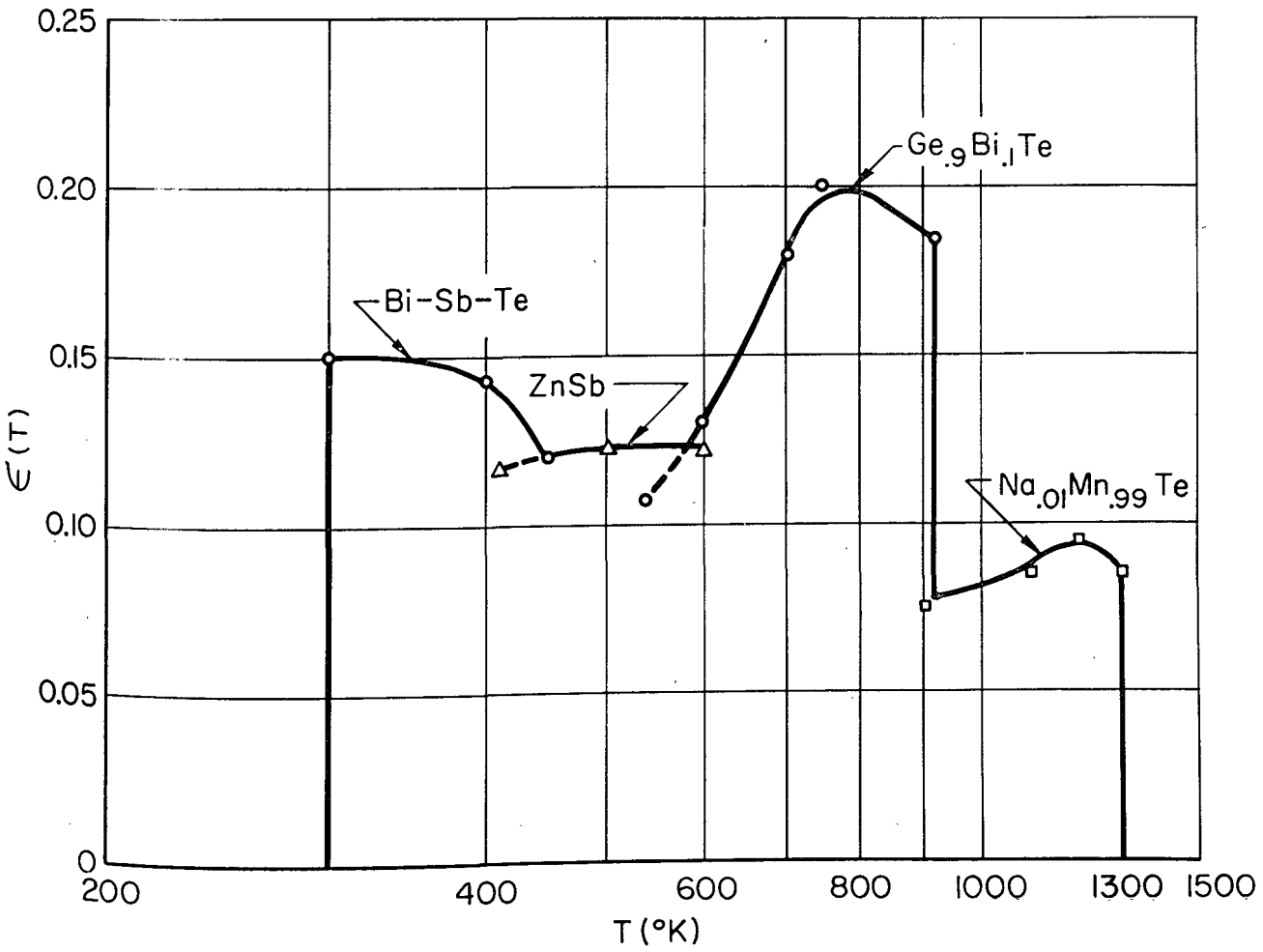


Figure 3. P-type thermoelectric materials

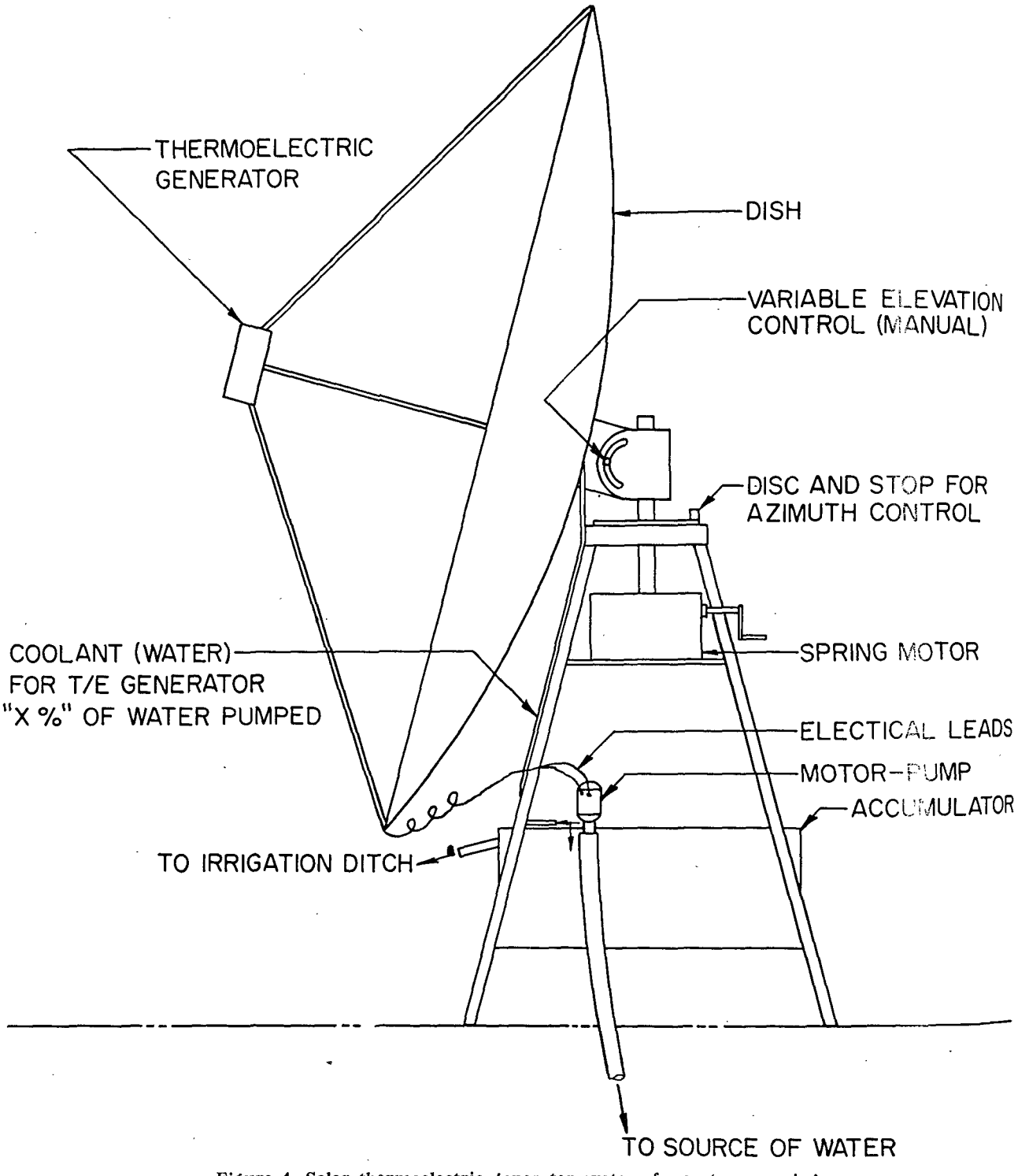


Figure 4. Solar thermoelectric generator system for water pumping

ment that $b = 1$ in which case equation (16) reduces to :

$$\eta = \frac{T_1 - T_0}{2\left[T_1 + \frac{2}{Z} - \frac{1}{4}(T_1 - T_0)\right]} = \frac{\Delta T}{2\left[T_1 + \frac{2}{Z} - \frac{\Delta T}{4}\right]} \quad [18]$$

Thermoelectric materials

As noted in the previous section, the equations which describe thermoelectric conversion efficiency contain three material characteristics and these can be grouped together to give a material figure of merit. This figure of merit serves as a basis for thermoelectric materials evaluation.

In the past few years the thermoelectric materials

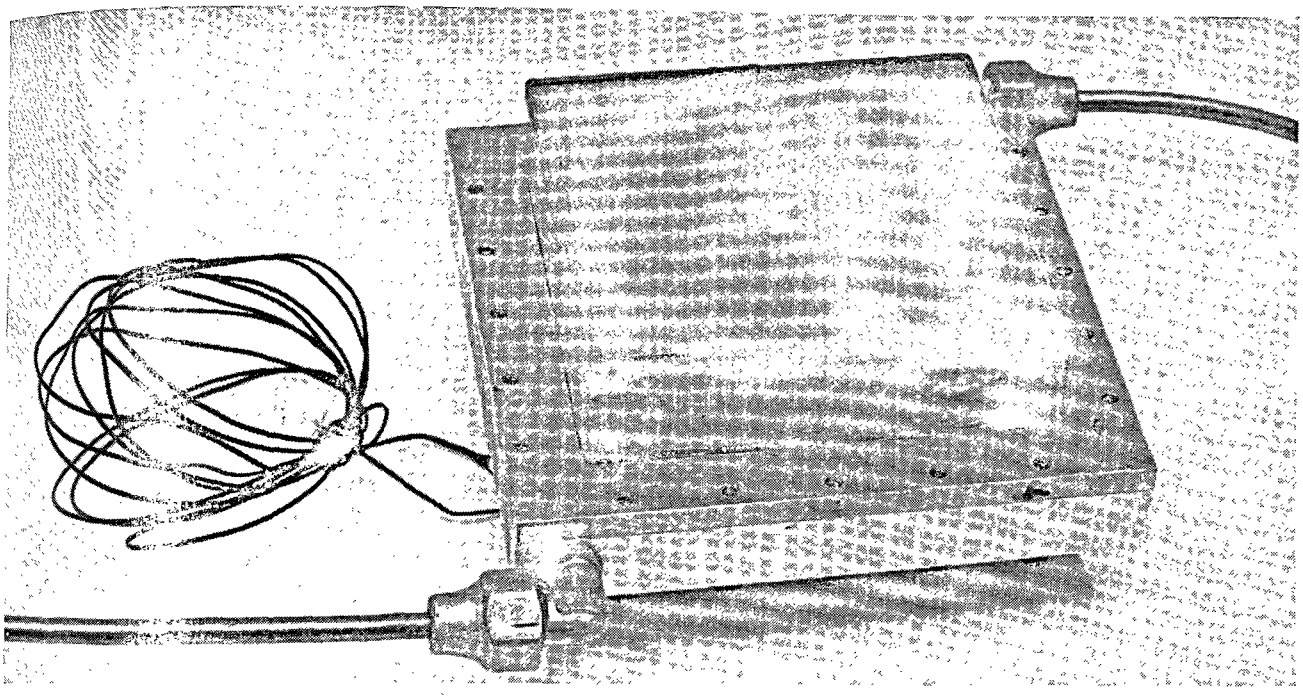


Figure 5. Target view of solar thermoelectric generator

development effort has been concentrated on two classes of materials which to date have shown the most promise for efficient power generation. These two classes of materials may in a somewhat general sense be classified as semiconductors and mixed valence materials.

Semiconductors

The semiconducting elements are the *A* sub-group elements in a number of columns of the periodic table. These elements are outlined in the following array.

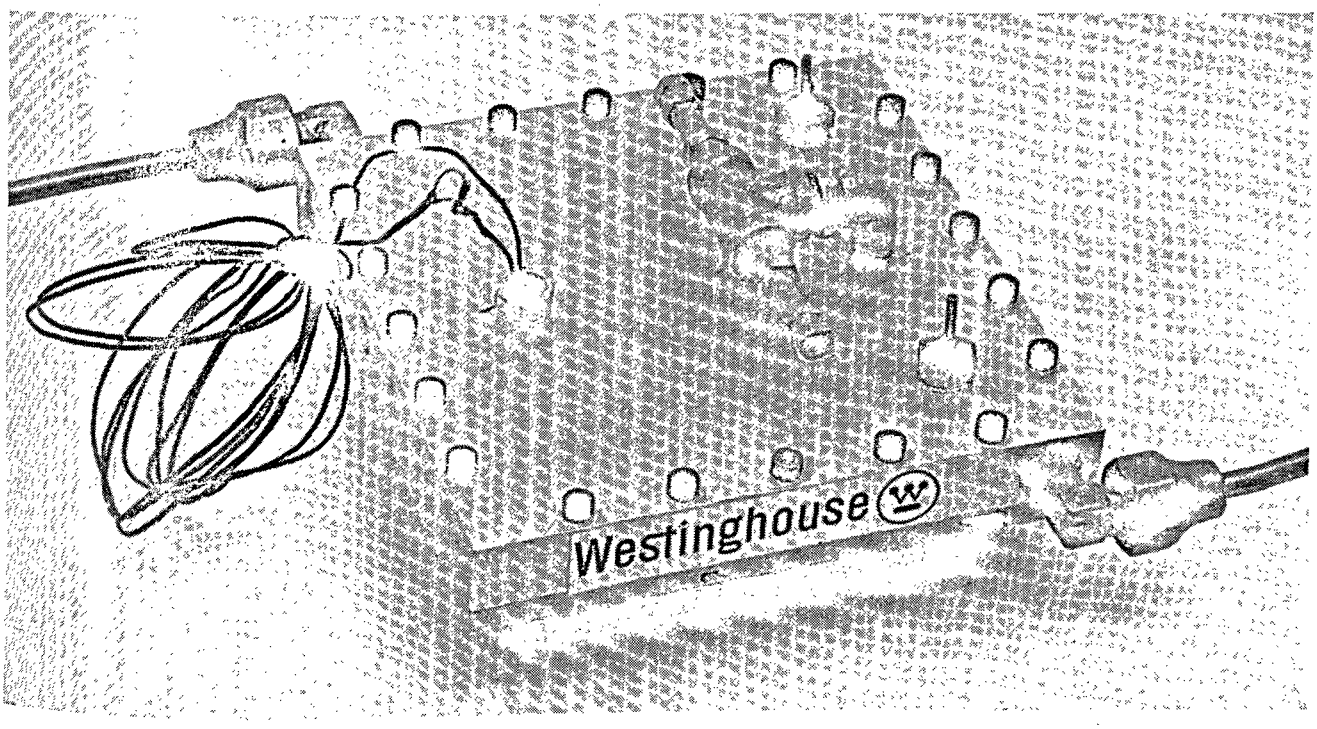


Figure 6. Solar thermoelectric generator

III	IV	V	VI	VII
B	C	N	O	F
Al	Si	P	S	Cl
Ga	Ge	As	Se	Br
In	Sn	Sb	Te	I
Tl	Pb	Bi	Po	At

Of the above elements, silicon and germanium have received a great deal of attention because of their technical importance in the field of crystal diodes and transistors.

The thermoelectric characteristics of many semiconductor materials have been investigated. Some of these materials are cuprous oxide, selenium sulfide, lead telluride, germanium telluride, bismuth telluride, and lead sulfide (9).

The thermoelectric parameters of the semiconductor materials can be altered to achieve favorable thermoelectric characteristics by "tailoring". Two ways of altering semiconductor properties are "doping," which means the introduction of foreign materials into the lattice and by creating lattice defects.

Figures 2 and 3 represent a plot of ε versus temperature for several of the better performing, presently available, P and N type thermoelectric materials.

The $\varepsilon(T)$ is an alternate way of defining the materials efficiency and is defined as:

$$\varepsilon(T) = \frac{\sqrt{TZ+1}-1}{\sqrt{TZ+1}+1}$$

$\varepsilon(T)$ represents an idealized situation since the Joule effect is neglected.

Mixed valence material

A mixed valence material may be defined as a compound containing an ion in two different valence states. The mixed valence materials are compounds, mainly, of the transition elements. Mixed valency may be produced either by substitution of an

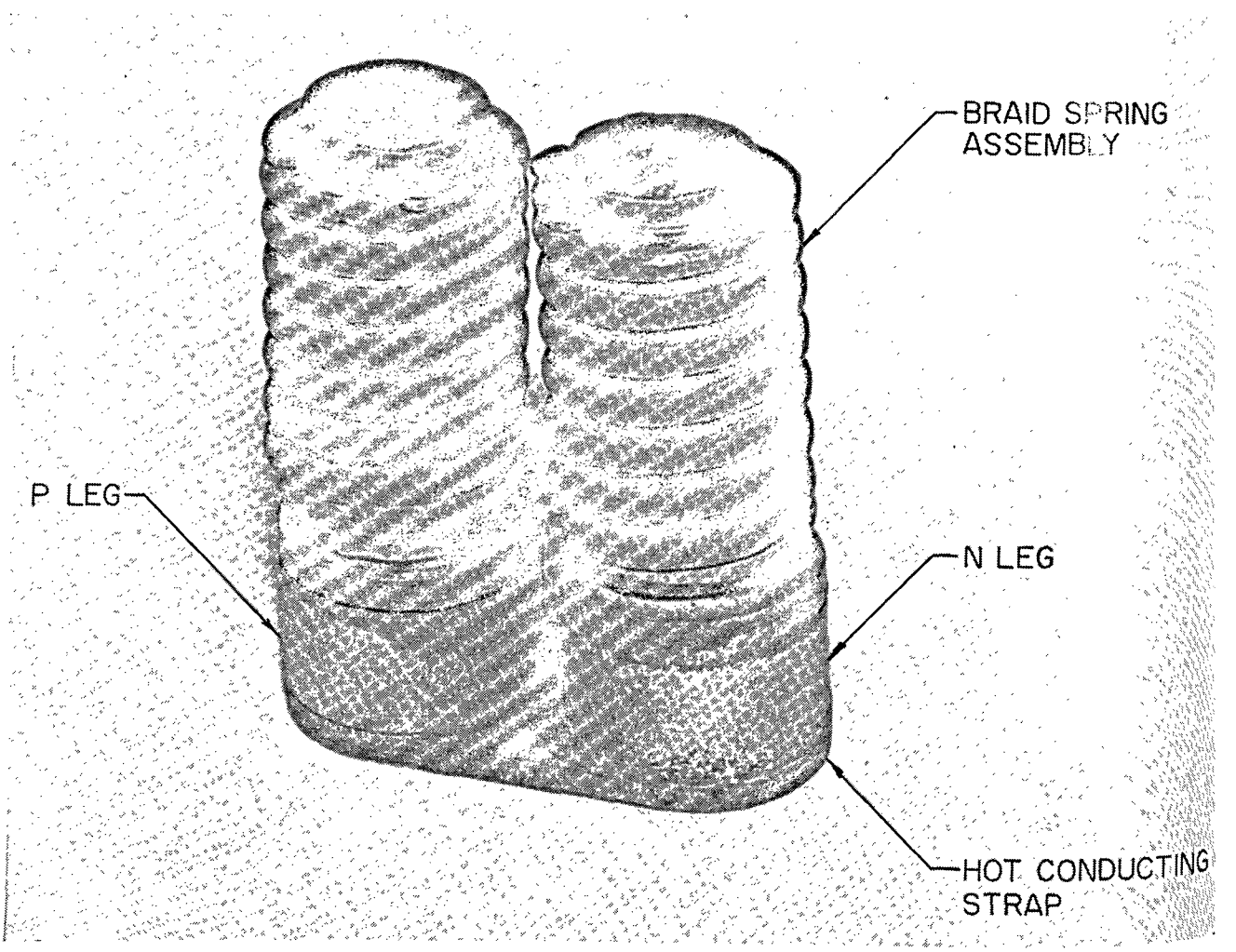


Figure 7. Thermocouple design used in generator construction

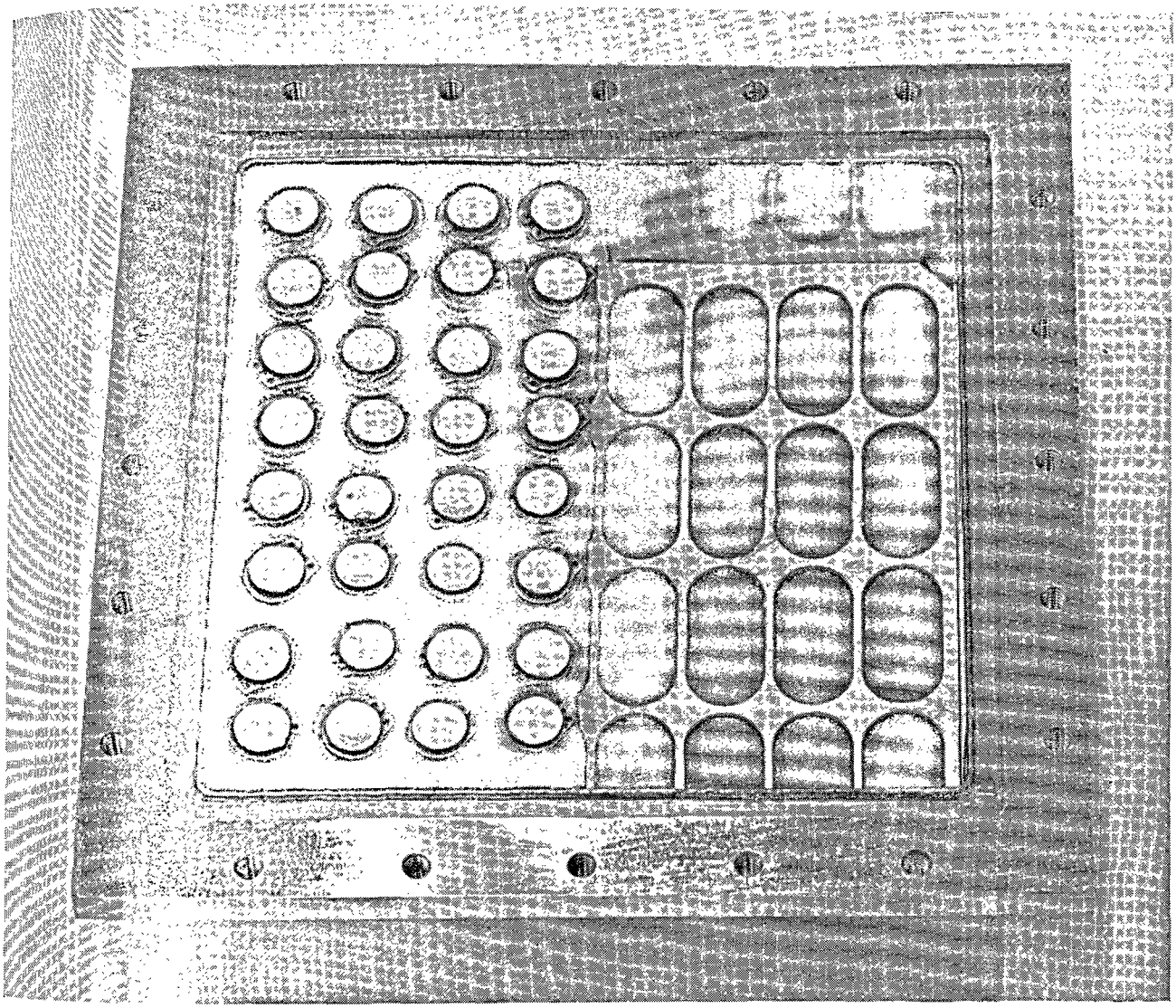


Figure 8. Assembly of thermoelectric generator

appropriate foreign ion or by having an excess in one of the constituents of the material.

To illustrate foreign ion substitution, suppose that in a nickel oxide lattice, NiO, a fraction x of the Ni ions is replaced by Li ions. Since the lithium ion, Li, can have only a single plus charge, the resulting material can be written as:

$$Li_x^{+} \; Ni_x^{+++} \; Ni_{(1-2x)}^{++} \; O^{=}$$

The case of excess in one of the elements can also be illustrated with NiO. Assume excess oxygen is added in the preparation of this material; then in order to maintain electrical neutrality, the Ni ion again assumes the plus two and plus three states in order to balance the fixed minus two charge of the excess oxygen. The equation which represents this situation is:

$$Ni_{(1-2x)}^{++} \; Ni_{2x}^{+++} \; O_{1+x}^{=}$$

The major experimental work with mixed valence material is in progress at the Westinghouse Research Laboratories under a Navy Department Bureau of Ships contract (10). Several mixed valence thermoelectric materials have been reported.

	Temp. range (°C)	$\eta_{T.C.}$
NiO-Li doped	400-1 100	0.02
CuO-Li doped	200- 700	0.003
MnTe-As doped	25- 550	0.040

On the basis of present theory and limited experimental investigation, it appears that below 800°C the most efficient thermoelectric materials are intermetallic semiconductors. The mixed valence materials have comparably low efficiencies below 800°C but become attractive at higher temperatures.

Solar thermoelectric generators

In this section the design of one of the experimental solar thermoelectric generators will be described.

Figure 4 shows a system for the harnessing of the sun's rays and the conversion of the energy contained therein to useful work by means of a thermoelectric generator. Figures 5 and 6 show the target surface (area on which the solar energy is focused) and a cold side view of the solar thermoelectric generator that has been operating.

Thermocouples and insulation

The basic power generating thermocouple used in this particular generator, together with its spring-braid assembly, is shown in figure 7. A total of 32 thermocouples were used in this unit. The *P*-leg and *N*-leg were metallurgically bonded to the hot strap and braids. The flexible braid-spring assembly conducts heat and electricity between the thermoelectric material and the copper conducting straps at the cold side of the generator. The hot and cold conducting straps provide series electrical connections between adjacent thermocouple legs and provide contact surfaces for heat transfer to the electrical insulations at the generator walls.

To allow adequate thermal contact between the straps and the generator wall insulations, the spring of the braid-spring assembly is used to force the straps against the insulations. The spring also keeps the thermoelectric material under compression, thereby reducing tensile stresses caused by bending. A snap ring at the end of each braid causes the springs to push the braid ends against the cold straps upon assembly of the generator.

The electrical insulation between the thermocouple ladders and the generator wall is 2 to 3 mil thick, natural mica sheet. A matrix of mica composition material is used to keep the couples separated in the generator. Figure 8 shows half of the 32 couples arranged in the module prior to connecting the cold side straps.

Generator structure

The cold side of the generator is made of $\frac{3}{4}$" aluminium that has a series of coolant passages bored in both directions to obtain cross flow. The generator side wall is made of 12 mil type 316

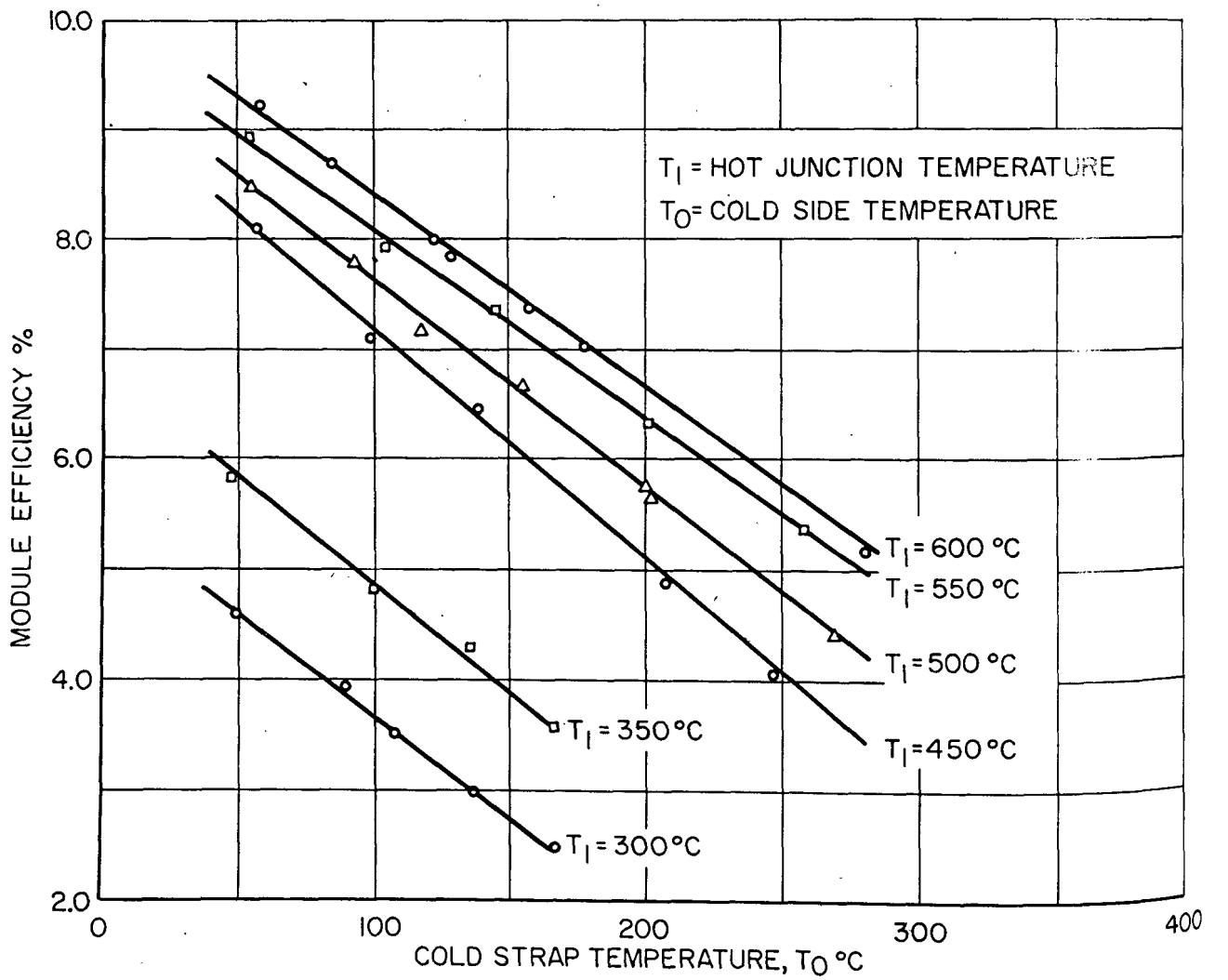


Figure 9. Module efficiency *vs.* cold side temperature

stainless that is welded to the base plate. The generator side walls are made this thin to minimize heat conduction along the frame. At the cold end there is welded a collar to which the heat exchanger is attached. The groove seen in figure 8 is for the insertion of a rubber gasket prior to sealing the generator.

The electrical leads and two thermocouples, one attached on the couple hot strap and the other on the cold, come through the cover plate. The tee connection on the cover plate was installed for inert atmosphere operation, which is desirable when the generator operates at 600°C for extended periods. The unit described here has been operating at 450°C hot side, at which conditions no inert atmosphere is required.

Performance

The generator shown in figure 6 weighs 9.2 lb. If weight is a problem, and no attempt was made to minimize this parameter in the generator under discussion, a water-cooled unit with present state of technology should be capable of 20 watts/lb.

The following tabulation gives the maximum power ($R_i = R_L$) obtained at different thermal gradients.

Table 1

T_1 °C	T_0 °C	E_G volts	Power (watts)
265	48	1.45	13.6
400	68	2.85	36.1
408	69	3.0	39.8
416	68	3.25	41.7
452	70	4.9	50.0

If this generator were operated at 600°C hot side its capability at this condition, based on the data of table 1, is 100 watts.

The efficiency characteristics for the type of couple employed in this generator are plotted in figure 9.

Since thermoelectric power generation may be viewed as a modular concept, its efficiency is not affected by generator size. In the ensuing section various parameters effecting size, economics, etc. will be discussed.

Parametric evaluation of thermoelectric generators

The aim of this section will be to describe the various parameters that effect the thermoelectric generator design with particular emphasis on the application cited in figure 4.

Heat transfer

Most of the present-day thermoelectric materials exhibit an average thermal conductivity of approximately 1 Btu/hr-ft-°F (0.0173 watts/cm); in the

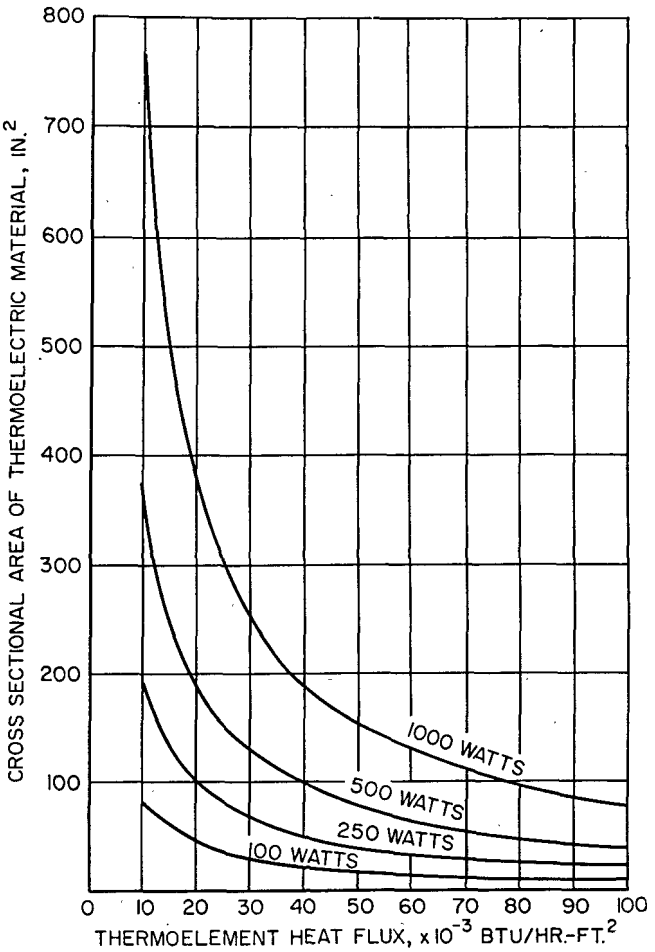


Figure 10. Thermoelectric material heat transfer area required *vs.* heat flux and generator rating

subsequent data this value is used. The generator hot junction will in the following analysis be maintained at 842°F (450°C) as this appears to be a good compromise value for long-life thermoelectric generators, and the type of solar collector precision attainable at minimum cost. The generator cold side will be maintained at 158°F (70°C) by means of water cooling. The thermoelectric conversion efficiency for this temperature range is about 6.5 per cent and this value will be used in the following analysis. It should be noted that this is somewhat lower than the value predicted in figure 9; however, the data there are obtained under more controlled conditions and thus various practical factors are taken into account in using the 6.5 per cent figure. The solar energy focused by a parabolic collector on the target will be taken as 210 Btu/hr.-ft^2 (570 kg-cal/hr-m^2) of collector. Thus, the collector size, target size, and couple heat flux desired are interrelated. The cross sectional area of the thermoelements (P and N materials) occupies about 55 per cent of the total target area.

Figure 10 relates the thermoelectric material heat transfer area required as a function of heat flux and generator rating. Since the thermoelement is to operate with a fixed ΔT, a given heat flux also

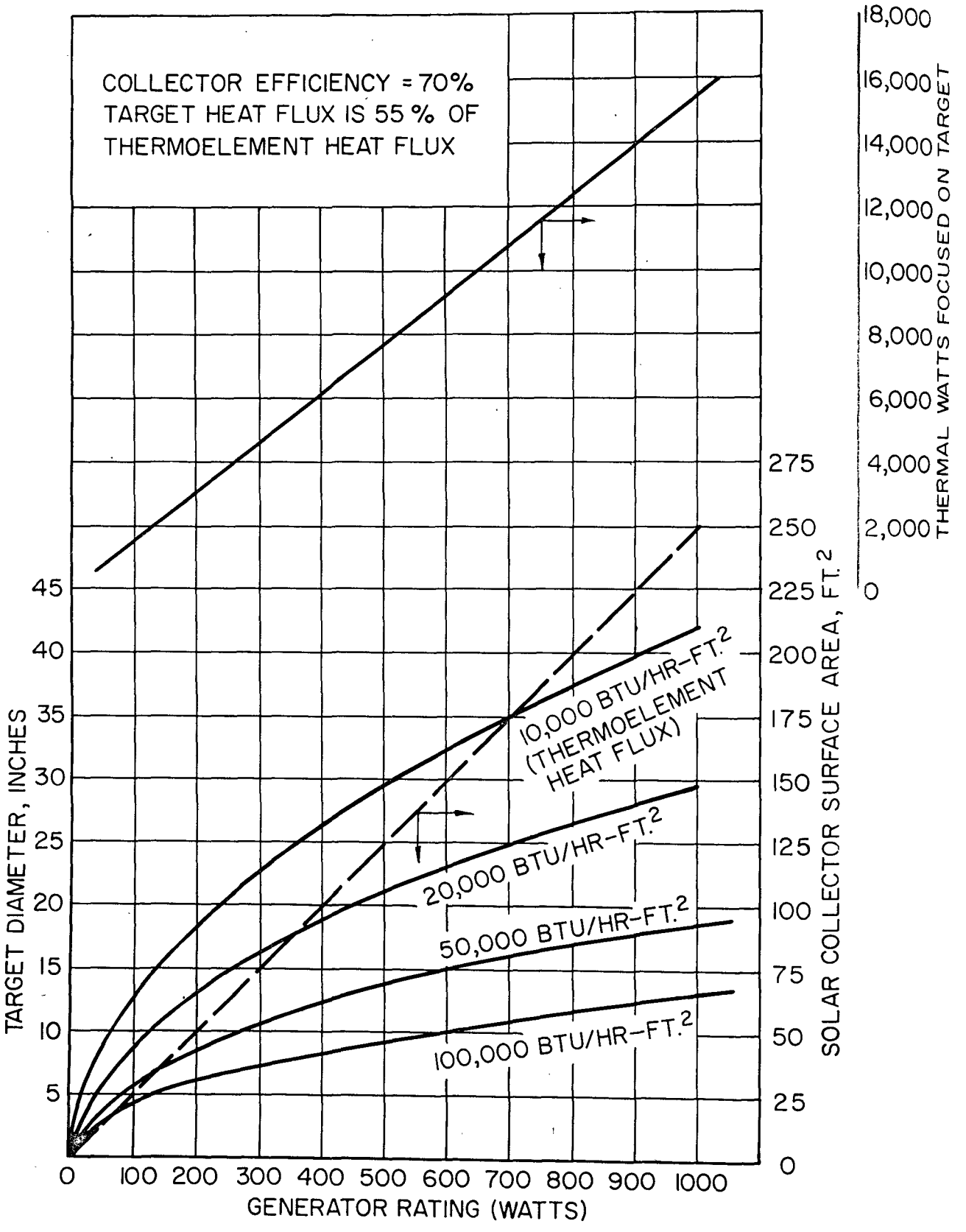


Figure 11. Solar system parameters as a function of generator electrical rating

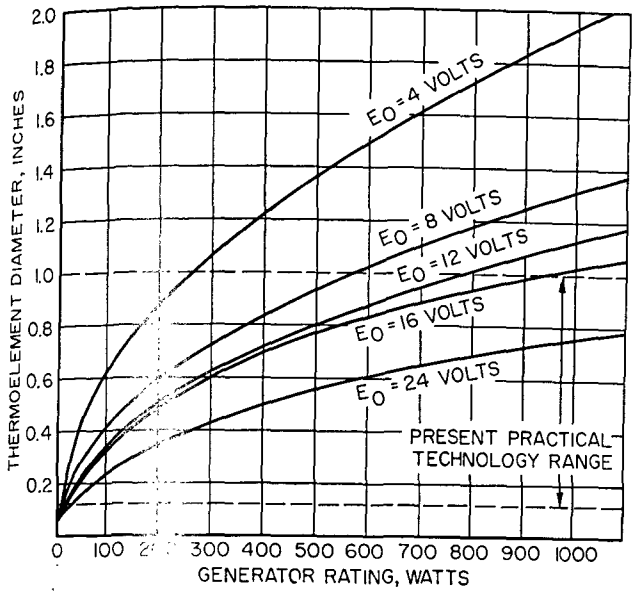


Figure 12. Thermoelement diameter *vs.* generator rating and open circuit voltage

establishes the element length. Table 2 gives the thermoelement length required for various heat fluxes.

Table 2

Heat flux $\frac{Btu}{Hr\text{-}Ft^2}$	Thermoelement length (L) in
10 000	0.83
20 000	0.42
50 000	0.17
100 000	0.083

The generator target diameter and target heat flux required, based on the 55 per cent space utilization factor, are shown in figure 11. Thus, with the data contained in figures 10 and 11 the selection of any two variables such as generator rating and heat flux fixes the target area and solar collector area.

Voltage

Heat transfer and the thermoelectric conversion efficiency establish the amount of surface area and length of thermoelement required for a specific generator rating. However, it is the voltage desired that dictates the number of couples into which the required quantity of thermoelectric material is divided. As previously mentioned the generated voltage, per couple, is:

$$E_G = \bar{\alpha}\Delta T$$

and thus, for any voltage XE_G, X couples must be connected in series. For most of the present thermoelectric couples $\bar{\alpha}$ is in the order of 400×10^{-6} volts/°C. Thus, at a $\Delta T = 380$°C, $E_G = .152$ volts/couple. Table 3 relates the number of couples, and this is independent of generator size and power density required for a specific voltage.

Table 3

Open circuit voltage (E_0)	4	6	10	12	18	24
Number of couples (N).	26	39	66	78	117	156

Combining the data in table 4 with the data in figure 11 establishes the individual thermoelement diameter (there is a P and N type thermoelement per couple) required for various open circuit voltages and generator sizes. These data are plotted in figure 12. Superimposed on figure 12 is the present practical range of the technology for making these thermoelements. Thus, for any generator rating and open circuit voltage, the couple dimensions are fixed. In quantity production it is envisioned that

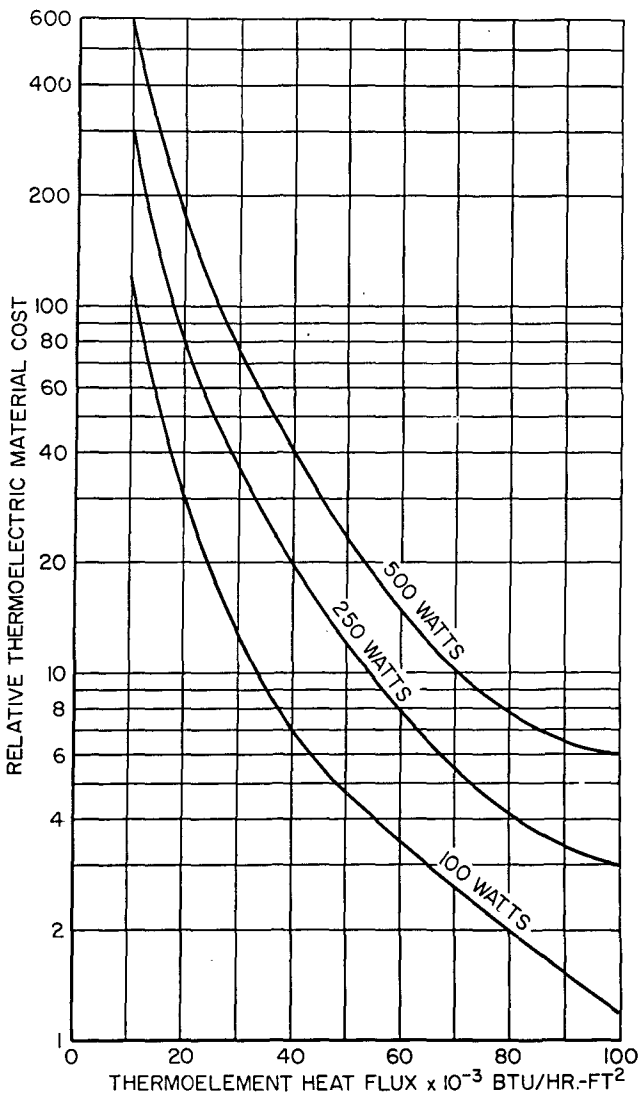


Figure 13. Relative thermoelectric material cost as a function of heat flux

several standard size couples would be available and the generator is then designed and fabricated on this basis.

Cost analysis

Device cost and utility are the two most important variables in determining usages and market potential. In this section the various factors that constitute the cost of the thermoelectric generator and their interrelationship will be discussed. First, there is the quantity of thermoelectric material required; as shown in figure 10 and table 2 this is strictly a function of the heat flux for any generator rating. In figure 13, there is plotted relative material cost, and it is obvious that high heat fluxes are desirable. Present technology is capable of sustaining a thermal heat flux of about 50 000 Btu/hr-ft^2 (15.8 watts/cm^2) through the thermoelements.

In addition to the basic materials cost, there is the cost of translating a given amount of material, fixed by heat transfer considerations and generator size, into "X" couples, established by the desired voltage. As a first order approximation, it can be assumed that the amount of labor in making the couple is the same for the range of pellet diameters

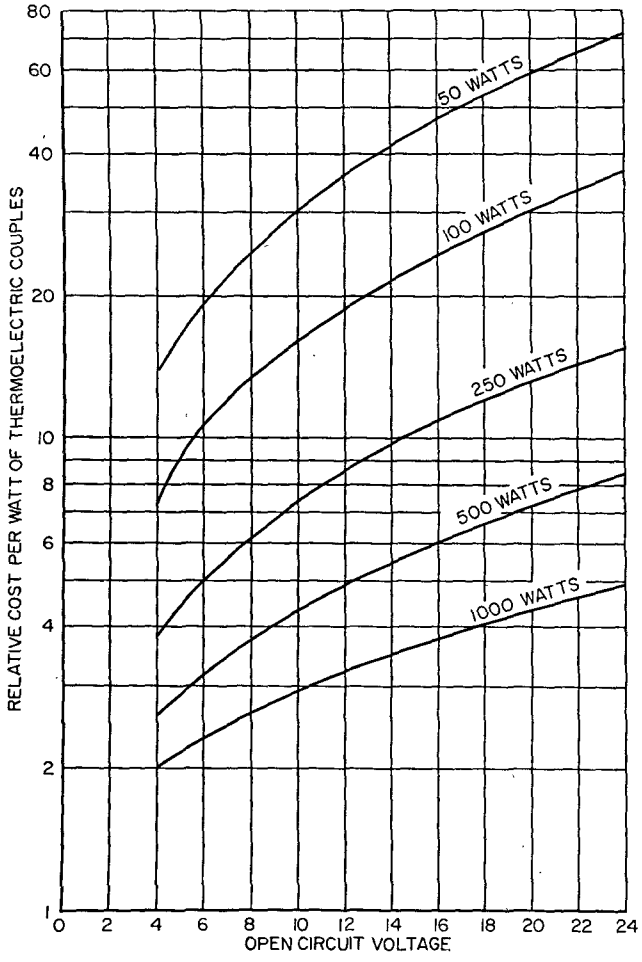


Figure 14. Relative cost per watt of electric power as a function of voltage and generator rating

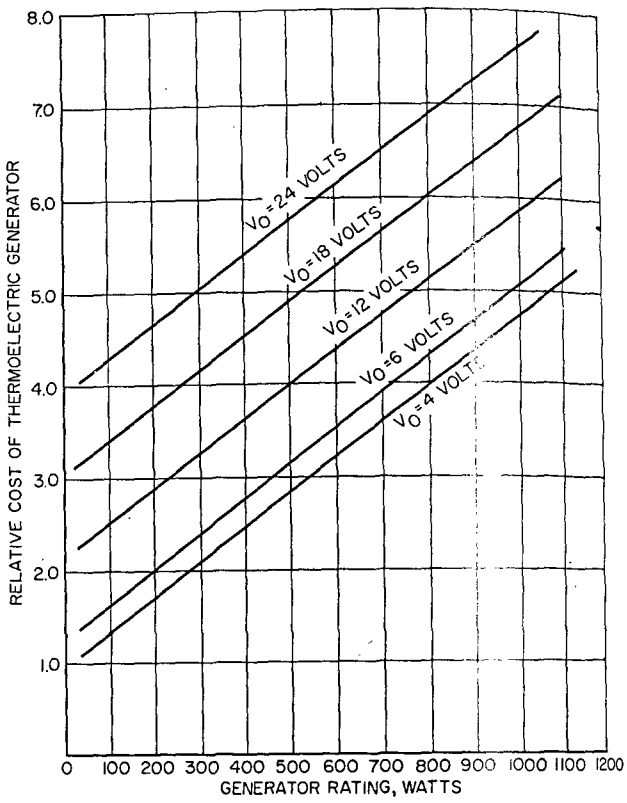


Figure 15. Relative thermoelectric generator cost as a function of size and voltage

shown in figure 12, as being practical. Thus, coupling the data of figure 13 with table 3, we can also plot relative cost per watt (el) as a function of open circuit voltage for various generator sizes. Figure 14 is such a plot.

Based on the data of figure 14, the generator voltage should be the lowest that the designated system can employ, assuming no counter cost is incurred. When the generator output is fed to a motor, the improved efficiency attained with higher voltage must be balanced off against initial investment. In addition to the couple cost there is the fabrication of the couple housing and assembly thereof. The cost of this phase is nearly independent of voltage for a fixed generator rating. With respect to generator size, the cost of construction materials is proportional to the size, while the cost of labor, based on a cursory analysis, should increase by about 25 per cent of the rating increase. Figure 15 is a plot of relative costs for a thermoelectric generator that converts solar energy as a function of size and voltage.

A more thorough comprehension of the potential that this mode of energy conversion, utilizing solar energy, has to offer the underdeveloped nations can be obtained by the following irrigation application illustration. Assuming the following conditions:

Solar collector — 8′ dia.
Thermoelectric generator 125 watts at $V_0 = 4$ volts
Annual water requirement = 12″
Annual operating hours = 2 500

Pumping head = 20′
Pump efficiency = 50 per cent
Motor efficiency

V_0	η per cent	V_0	η per cent
4	35	16	65
8	50	20	70
12	60	24	75

we can analyze the effect of combining solar-thermoelectric system modules to one motor pump. Figure 16 shows the effect of combining these modules on acres that can be irrigated and the relative cost for irrigation.

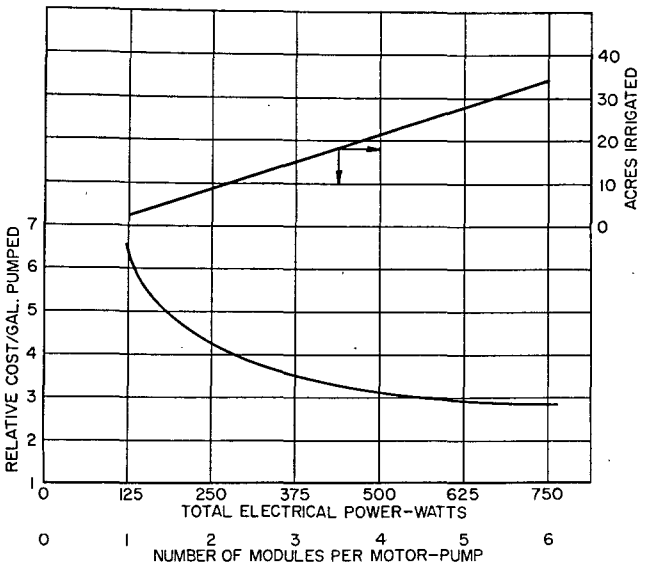


Figure 16. Modular solar thermoelectric system for irrigation (basis 125 watts 4 volt modules)

Conclusions

The aims of this paper were to relate the design features of a working model of a solar thermoelectric generator and, secondly, to discuss the relative design and economic parameters for this mode of energy conversion. The reason for relative costing rather than an absolute value is because the units, to date, were built on a research and development basis.

Only recently has the fabrication of thermoelectric generators progressed to the point where it has been transferred from the research and development section to one of the manufacturing divisions. A best estimate at this time is 7-10 cents kWh for the cost of the electrical energy from a solar-thermoelectric generator in the size range discussed. In the future, with continued research and development, it should be possible to improve the efficiency and extend generator life. Coupling this with mass production techniques should, in all probability, reduce the cost of electric power per kWh. However, even at the present cost estimate, and it should be recognized that this is only the best estimate we can make at this time, solar thermoelectric power generation appears attractive for many areas of the world.

Nomenclature

The following symbols have been used throughout the paper:

Q — Heat rate Btu/hr
I — Current—amperes
K — Thermal conductivity—Btu/hr-ft-°F
R — Electrical resistance—ohms
A — Cross-sectional area perpendicular to heat transfer — ft²
L — Length in direction of thermal gradient—ft
T — Temperature—°F
π — Peltier coefficient—volts
α — Seebeck coefficient—volts/°C
Δ — Electrical resistivity—ohm-ft
P — Power—watts
E — Voltage
b — Constant ratio—R_L/R_i
η — Efficiency

Subscripts

O — Cold junction
1 — Hot junction
G — Generator
L — Load
i — Internal
c — Carnot cycle
$T.C.$ — Thermoelectric material
P — P-type material
N — N-type material
oc — Open circuit

References

1. Corry, T. M., Moreland, W. C., and Strickland, E. L., Design of 100 Watt Thermoelectric Generator, *Elec. Eng.*, June 1960.
2. Merrill, P. S., Forejt, D. A., Pityk, P. E., Spira, G., and Kuesar, P. E., SNAP-10 Experimental Thermoelectric Generator, presented at Thermoelectric Conference, Dallas, Texas, 8-12 Jan. 1961.
3. Fisher, M. D., Kastovich, J. C., Moreland, W. C., and Corry, T. M., Experimental 5 kW Thermoelectric Generator, Dallas, Texas, 8-12 Jan. 1961.
4. Daniels, F., The Sun's Energy, *Scientific Monthly*, 82: 247-54, 1956.
5. Daniels, F., Duffie, J. A., Löf, G. O. G., and Breihan, R. R., Tests of Solar Thermoelectric Generator System, *Proceedings of the United Nations Conference on New Sources of Energy, 1961*, included above, paper S/103.
6. Ioffe, A. F., Semiconductor Thermoelements and Thermoelectric Cooling, *Infosearch Limited*, London, 1957 (translated from Russian).
7. Jaumot, F. E., Jr., Thermoelectric Effects, *Proc. of I. R. E.*, 46: 538-54, 1958.
8. Ure, R. W., and Heikes, R. R., Science and Engineering of Thermoelectricity, *Interscience*, New York, 1961.
9. Westinghouse Research Laboratories, *Thermoelectric Quarterly Progress Report*, Pittsburgh 35, Pa, W.G.O. No. W6-79 150-CE.
10. United States Navy, Bu Ships Contract Nobs-84 317.

Summary

The potential applications of thermoelectric power generation are numerous, as the spectrum of devices and systems built or planned to date testify. This paper, however, is restricted to the utilization of solar energy as the heat source, and the conversion thereof to electrical energy by means of thermoelectric conversion (Seebeck-Peltier effect). Solar energy utilization in tropic zone areas of the world that have not yet achieved any extensive degree of mechanization offers the hope of an improved standard of living. The pumping of water for irrigation and household uses appears as a logical first generation application of solar thermoelectric power generation.

A solar-thermoelectric generating system offers a static, high reliability, maintenance-free system, that is independent of any transported supplies once installed. The maintenance-free aspect of this system makes possible the widespread application thereof in nations where technically skilled individuals are at a premium.

The design and performance capability of thermoelectric generators for the conversion of solar energy and relative system economics are the scope of this paper. A brief review of the equations and parameters of importance in predicting performance of a thermoelectric generator, and the status of materials for this mode of energy conversion, are presented.

From equation (16) it can be seen that the efficiency of a thermoelectric generating device is the product of the Carnot efficiency as well as a materials efficiency. Figures 2 and 3 represent a plot of this materials efficiency versus temperature for some of the better performing, presently available *P* and *N* type thermoelectric materials. The classes of materials—namely, conductor and mixed valency materials—which to date have shown the greatest promise for efficient thermoelectric conversion are also discussed.

Two specific facets of the thermoelectric generator *per se* are presented. These are the mechanics of construction and a detailed analysis of the parameters that effect the system economics. Figures 5 and 6 show a thermoelectric generator that has been operating from focused solar energy. Generators of this type are capable of 20 watts/lb and a power density of approximately 1 watt/inch^3. The performance of this specific generator with respect to power output as a function of temperature differential is cited in table 1, while the conversion efficiency is presented in figure 9.

With respect to thermoelectric generator economics, the parameters of importance are the heat transfer aspects of the system, since these establish the amount of thermoelectric materials required, the desired voltage (which in turn defines the number of thermoelectric couples or basic units that must be connected in series), and the generator size. Figure 13 shows how the relative cost of the thermoelectric material varies as a function of the heat flux through the thermoelements. Figure 14 depicts the relative cost per watt of the thermoelectric couples (figure 14) as a function of open circuit voltage and generator rating.

Viewing these results, which are based on present semi-continuous production technologies and thus assume a fixed manufacturing cost per couple, the generator voltage should be the lowest that the designated system can use, assuming no counter cost is incurred. In the case where the electric energy is fed to a d.c. motor, the improved efficiency attained with higher voltage must be balanced off against initial investment. In addition to the basic couple cost there is also the cost of fabrication of the couple housing and its associated cold side heat exchanger that must be considered in the total cost picture. Figure 15 represents the relative cost of the generator as a function of size, at various voltages.

Figure 16 shows the effect of coupling solar thermoelectric modules to one motor and pump for irrigation in terms of relative water cost per gallon and acres that can be irrigated per unit.

As a best estimate at this time 7-10 cents/kWh for the cost of electrical energy from a solar-thermoelectric generator appears plausible in the size ranges discussed (50-1 000 watts). With time, the efficiency of thermoelectric materials should improve and this plus mass production techniques will in all probability further reduce the cost of electric power per kWh. However, even at the present cost range, solar-thermoelectric power generation appears attractive for many areas of the world.

GÉNÉRATEURS THERMO-ÉLECTRIQUES POUR LA CONVERSION DE L'ÉNERGIE SOLAIRE EN VUE DE LA PRODUCTION D'ÉNERGIE ÉLECTRIQUE ET MÉCANIQUE

Résumé

Les applications possibles de la production d'énergie thermo-électrique sont nombreuses, ainsi qu'il ressort de la variété des systèmes ou dispositifs déjà réalisés ou projetés à cette fin. On s'en tiendra toutefois, dans le présent mémoire, à l'utilisation de l'énergie solaire comme source de chaleur et à sa conversion en énergie électrique par un procédé thermo-électrique (effet de Seebeck-Peltier). L'utilisation de l'énergie électrique dans les régions tropicales du globe qui n'ont pas encore réalisé un degré de mécanisation avancé vient offrir l'espoir d'un relèvement du niveau de vie des populations. Le pompage de l'eau d'irrigation et certains emplois ménagers semblent devoir constituer la première série logique d'applications de la production thermo-électrique de l'énergie.

Le système thermo-électrique producteur d'énergie solaire est un dispositif statique au fonctionnement éminemment sûr, qui n'exige pas d'entretien et reste indépendant de toutes fournitures à transporter une fois qu'il est installé. Cette absence d'entretien permet l'application généralisée du système dans les nations où les techniciens bien entraînés sont rares.

L'auteur étudie, dans le présent mémoire, la conception et les possibilités des générateurs thermo-électriques pour la conversion de l'énergie solaire, puis les aspects économiques des systèmes qui en font usage. Il passe rapidement en revue les équations et les paramètres importants pour les prévisions de fonctionnement d'un générateur thermo-électrique, ainsi que l'état actuel des fournitures de matériaux pour ce genre de conversion de l'énergie.

L'équation (5) montre que le rendement d'une installation thermo-électrique de production de courant est le produit du rendement de Carnot par celui des matériaux employés. Les figures 2 et 3 présentent un tracé de ce rendement des matériaux en fonction de la température, pour quelques-uns des matériaux thermo-électriques, des types *P* et *N*, qui donnent de bons résultats et dont on dispose actuellement. L'auteur examine également les catégories de matériaux, à savoir les semi-conducteurs et les matériaux à valences mixtes qui, jusqu'à présent, semblent promettre le plus comme convertisseurs thermo-électriques.

Ce mémoire cite deux aspects spécifiques propres au générateur thermo-électrique : les détails mécaniques de la construction et l'analyse détaillée des paramètres déterminent l'économie du système. Les figures 5 et 6 portent sur un générateur thermo-électrique utilisant pour son fonctionnement l'énergie solaire concentrée. Les générateurs de ce modèle sont capables de livrer 44 watts par kilogramme, avec une densité de puissance de l'ordre du watt par pouce cube. La manière de fonctionner de ce générateur quant à son débit d'énergie en fonction de la différence de température est résumée par la figure 9.

En ce qui concerne les questions économiques relatives au générateur thermo-électrique, les paramètres importants sont les aspects des transmissions de chaleur dans l'installation, car ce sont eux qui déterminent les quantités de matériaux à propriétés thermo-électriques nécessaires, la tension cherchée (qui, à son tour, détermine le nombre de couples thermo-électriques ou d'unités de base qu'il faut monter en série), et enfin les dimensions du générateur. La figure 13 indique comment les prix relatifs des matériaux à propriétés thermo-électriques varient en fonction du flux de chaleur dans les thermo-éléments. La figure 14 montre le coût relatif par watt des couples thermo-électriques (figure 7) en fonction de la tension à circuit ouvert et de la capacité nominale du générateur.

Quand on examine ces résultats, qui reposent sur les technologies actuelles de production semi-continue et présupposent donc un prix de fabrication fixe par couple, la tension du générateur s'avère comme devant être la plus faible que le système en cause puisse utiliser, en admettant qu'il n'intervienne pas de frais spéciaux pour réduire ou annuler ces économies. Dans le cas où l'énergie électrique est fournie à un moteur à courant continu, l'amélioration de rendement qu'autorise la plus forte tension doit être rapprochée des frais de premier établissement. Outre le coût de base du thermo-couple, il convient de songer également aux frais de fabrication de son boîtier et de l'échangeur de chaleur à paroi froide qu'on y associe, pour se faire une idée d'ensemble de l'investissement requis. La figure 15 représente le coût relatif du générateur en fonction de sa taille et pour diverses tensions.

La figure 16 indique l'effet du couplage de modules thermo-électriques sur un moteur et une pompe d'irrigation en fonction du coût relatif de l'eau par gallon et de l'étendue de terrain (en acres) qui peut être irriguée avec chaque unité.

La meilleure évaluation que l'on puisse faire actuellement est de 7 à 10 cents par kWh pour le prix de l'énergie électrique fournie par un générateur thermo-électrique solaire, valeur qui semble acceptable dans la gamme de puissances passée en revue (de 50 à 1 000 watts). Le rendement des matériaux thermo-électriques doit normalement s'améliorer avec le temps et ceci, avec l'emploi des techniques de la production en grande série, viendra très probablement apporter une nouvelle réduction au prix de l'énergie électrique par kWh. Néanmoins, même avec les prix actuels, la production solaire d'énergie thermo-électrique semble attrayante pour nombre de régions du monde.

A THERMOELECTRIC GENERATOR

Masatsugu Kobayashi *

Direct conversion of heat to electricity by means of the Seebeck effect is presently being developed for the generation of electric power ranging from several to several hundred watts. This renewal of interest is based on recent advances[1] in the development of special semiconducting materials having low electric resistivity, low lattice thermal conductivity and a high Seebeck coefficient.

Recently we constructed thermoelectric generators utilizing a combination of sintered silicides of transition metals (p-n junction). These materials have high melting points and can be operated above 900°C. The conversion efficiencies of the sintered materials decrease a little, compared with pulled crystals; however, the cost reduction and the simplicity of construction of the p-n junction by this process are remarkable. In this paper, the properties of the materials, the method of preparation of p-n junction and the characteristics of the generators are reported briefly. Owing to the high working temperature of the junction the conversion efficiency of the generator is relatively high.

Basic problems of thermoelectricity

As is well known, the Seebeck effect discovered in 1821 makes possible the direct conversion of heat to electricity without the use of intermediate machines. Conversion efficiency is very important, because a practical use of the Seebeck effect depends heavily upon the efficiency. This is determined both by two temperatures T_1 and T_0, which are the temperatures at the hot and cold junctions, respectively, and by physical properties of materials of the thermoelements. As can be shown by an elementary energy calculation, the properties of the materials of the thermocouple are included in one quantity, Z, which determines the usefulness of the thermoelements

$$[1] \qquad Z = \frac{(\alpha_n - \alpha_p)^2}{(\sqrt{\varkappa_n \rho_n} + \sqrt{\varkappa_p \rho_p})^2}$$

where α_n and α_p are the Seebeck coefficients of the n- and p-type materials, $\varkappa_n$ and $\varkappa_p$ are their thermal conductivities, and ρ_p and ρ_n are their electrical resistivities. The maximum efficiency, η, can be written in terms of Z, T_1 and T_0 as

$$[2] \qquad \eta = \frac{T_1 - T_0}{T_1} \times \frac{[1 + \tfrac{1}{2}(T_0 + T_1) Z]^{\frac{1}{2}} - 1}{[1 + \tfrac{1}{2}(T_0 + T_1) Z]^{\frac{1}{2}} + \frac{T_0}{T_1}}$$

It is most important for the construction of a thermoelectric generator to use materials in which the figure of merit, Z, is large up to very high temperatures, resulting in a large value of the conversion efficiency.

From semiconductor physics it is well known that Seebeck coefficient and resistivity both decrease with increasing carrier density in the component semiconductor. Low carrier densities, such as those found in insulators, result in the Seebeck coefficient of millivolts per degree; however, the resistivity is very high. In case of metals, though the resistivity is in the range of $10^{-5} \sim 10^{-6}$ ohm-cm, the Seebeck coefficient is very small ($\sim$ microvolts per degree). Thus both materials result in low values of Z. It is necessary to control the carrier density to get an optimum value. This is the reason why semiconductors are commonly used.

Ordinary semiconductors, however, have the general disadvantages of a temperature limitation

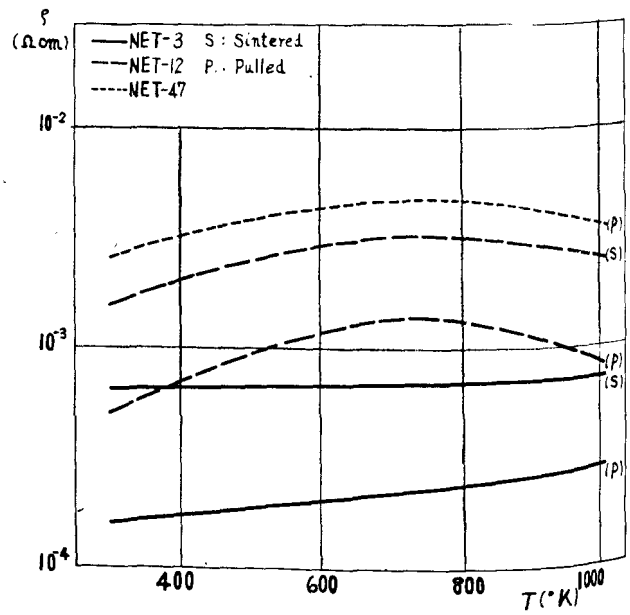


Figure 1. Resistivity versus absolute temperature for NET-3, NET-12 and NET-47

* Director, Research Laboratory, Nippon Electric Company, Ltd., Japan.

[1] Kaye, J. and Welsh, J. A., *Direct Conversion of Heat to Electricity*, John Wiley and Sons, Inc., New York, London, 1960.

due to intrinsic conduction. At temperatures above the onset of intrinsic conduction, the value of the Seebeck coefficient tends to zero, resulting in a low value of the figure of merit. This property eliminates many semiconductors from operation at temperature above about 600°C. It is clear that for high temperature operation of thermoelectric materials, a non-intrinsic semiconductor type is needed. In connexion with the high melting point and stability in oxidizing atmosphere, it is interesting to investigate the thermoelectrical properties of transition metal silicides.

Preparation and characteristics of thermoelements

Silicides of transition metals are characterized in general by hard, brittle interstitial compounds which have very high melting points. Great varieties of crystal structure are encountered in these compounds, and their electrical resistivities range from 10^{-4} to 10^{-2} ohm-cm.

The compounds were prepared by melting the component materials together in a quartz crucible by means of an h.f. generator. Specimens were obtained either by pulling or by pressing and sintering the compounds once prepared. An ordinary d.c. method was used in measuring the resistivity and Seebeck coefficient. The thermal conductivity was measured by an absolute method in a vacuum of about 10^{-3} mm Hg with use of copper-constantan thermocouples.

Some of the transition metal silicides exhibited interesting properties for the purpose of thermoelectric generation. In figures 1 and 2 are shown, respectively, the observed electrical resistivity, ρ, and the Seebeck coefficient, α, reduced to the value

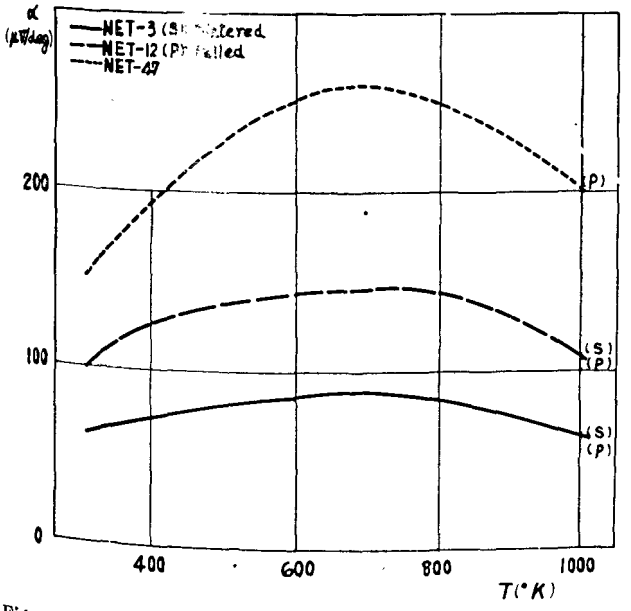


Figure 2. Seebeck coefficient versus absolute temperature for NET-3, NET-12 and NET-47

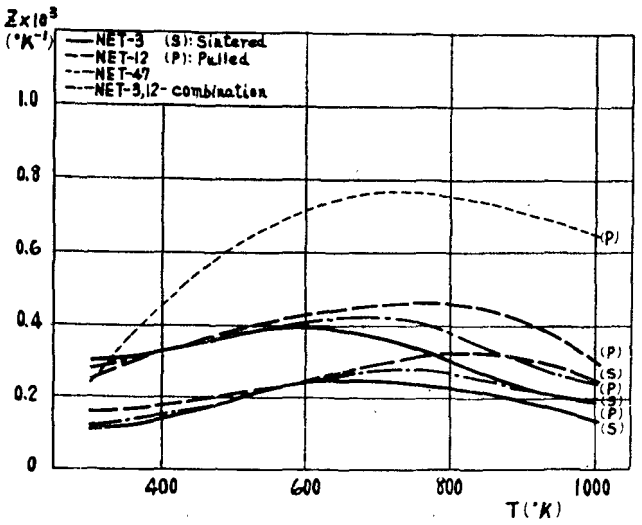


Figure 3. Figure of merit versus absolute temperature for NET-3, NET-12, NET-47 and their combinations

against platinum. Figures 3 and 4 show the figure of merit, Z, and conversion efficiency, η, respectively, calculated from the equations [1] and [2]. The value of the thermal conductivity at various temperatures were calculated by the resistivity data and the thermal conductivity at room temperature, assuming that the lattice part of the thermal conductivity is inversely proportional to the absolute temperature and the electronic part obeys the Wiedemann-Franz law. In the figures the results are shown for three kinds of the compounds: solid lines for NET-3, broken lines for NET-12 and dotted lines for NET-47. Symbols (S) and (P) marked on the curves designate the method of preparation of the specimens: (S) for sintering and (P) for pulling.

The most difficult problem in the construction of the thermoelectric generator pertains to the method of bonding the hot junction. At temperature above 700°C, the conventional brazing or pressure contact method seems to be undesirable from the points of oxidation, contact resistance and cracks due to thermal stress, etc. Since the carrier mobility is proved to be as small as 1 cm²/volt./sec. from the Hall data, the sintering method is promising. The originally small mobility is expected to be decreased to a smaller extent. Here, we constructed a sintered U-shaped bar in which NET-3 and NET-12 arms were joined together through the intermediate layer composed of a mixture of the component materials. The calculated values of Z and η for the sintered bar are also shown in figures 3 and 4 by the chained lines. Although the conversion efficiency is considerably decreased because of the increase of the resistivities, the sintering method is rather attractive from the point of view of cost reduction and simplification in manufacturing. Using this method, the superior characteristics of a *p-n* junction free from oxidation, contact resistance and thermal stress are readily obtained, and no matter how brittle, the mechanical intensity of the material is greatly increased.

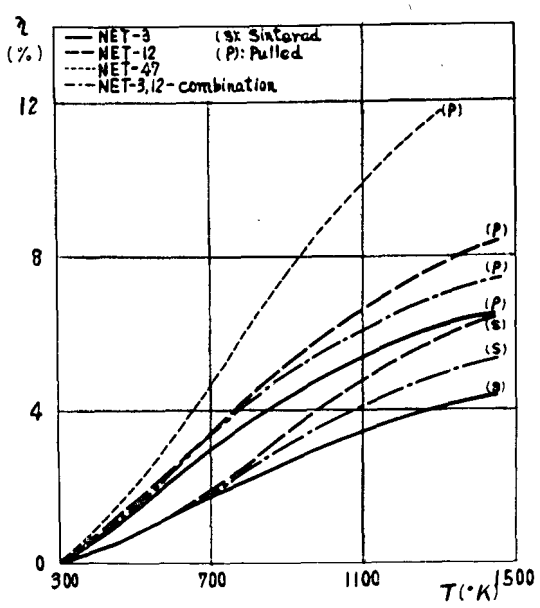


Figure 4. Conversion efficiency versus absolute temperature for NET-3, NET-12, NET-47 and their combinations

Effects of doped impurity metals and of deviation from stoichiometry on the thermoelectric properties of the silicides were studied. The former was found to be relatively insensitive. When the content of impurity metals, which were usually contained in the component metals and/or silicon, was less than 0.5 per cent, no appreciable effects were observed. The latter was more sensitive than the former. The deviation of about 0.3 per cent gave rise to appreciable changes in the properties. Several modifications of NET-12 were found to have α in the range 200 $\sim$ 300 μV/deg. and ρ in the range 2 $\sim$ 4 $\times$ 10^{-3} ohm-cm.

Construction of the generator

The silicides of transition metals are refractory materials. Layers of silica formed on the surface of the silicides at high temperatures prohibit further oxidation of the silicides. Because of the fact that the silicides have high Seebeck coefficients over the wide temperature range, they are inherently suitable to the generator for high temperature use.

The cross section of the n_2-branch (NET-3) is 3 $\times$ 7 mm^2 and that of the p-branch (NET-12) is 7.5 $\times$ 7 mm^2 with the length of 50 mm. The cold ends of the element are nickel plated and soldered to fins which are cooled by water or by natural convection of air. The contact resistance at the cold ends is negligible. This element produces 0.2 volt (open circuit voltage) and about 3 amperes (short circuit current) at a temperature difference of 900°C. The calculated efficiency at ΔT = 900°C is about 4.5 per cent.

A schematic diagram of a prototype five watt generator is shown in figure 5. Propane gas is used as a heat source. Efficiency obtained was about 2 per cent at average ΔT =700°C. One of the most difficult problems in designing the generator is to keep the temperature of hot junctions of all elements at a nearly equal temperature. If this is done, an efficiency of over 3 per cent may be expected.

So far the most convenient heat source is propane gas, because the gas is liquefied at about seven atmospheric pressures. Utilization of condensed solar energy by means of a rectangular cone-shaped mirror or by means of a combination of concave and plane mirrors will also be designed.

Application

Use of the thermoelectric generator should be considered from several points of view, viz., cost, durability and convenience of operation and maintenance. The generator is rugged, light in weight and small in size. It may be one of the simplest and most convenient devices to convert heat into electricity. It has no moving parts, and a very long life can be expected if overheating is avoided by suitable control of heat input.

Its application may be classified as follows: (i) Thermoelectric generators for special applications; (ii) Thermoelectric generators for entertainment use;

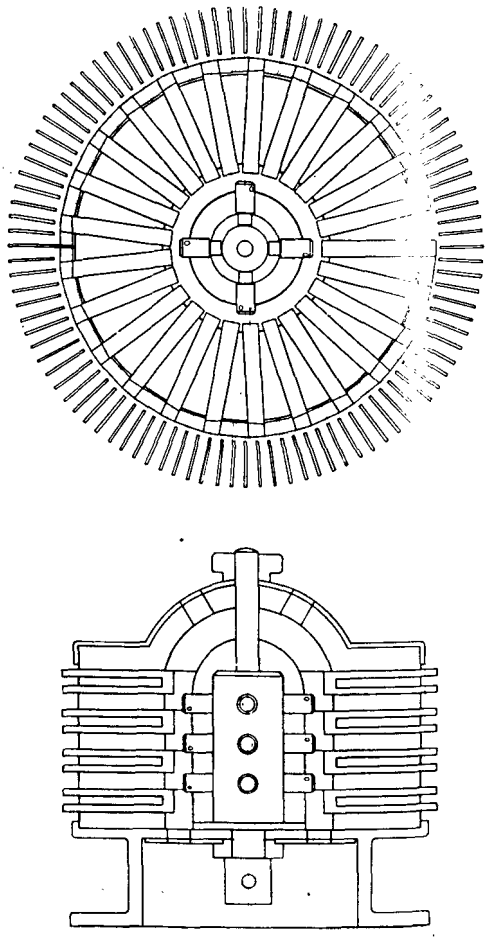


Figure 5. Schematic diagram of a five-watt prototype thermoelectric generator

and (iii) Thermoelectric generators for central-station power.

In the case of the second and third classifications, cost is the primary consideration. At the present stage of development of the thermoelectric generator, its initial cost is still high, and its conversion efficiency is low. Thus the application may be limited to the first category, where convenience is the primary consideration, and cost is secondary.

Special applications are numerous and diverse; space vehicle, automobiles, lighthouses and communication stations are only a few of many uses. An illustrated comparison of cost between a solar battery (curve A), heat engine generator (curve B) and the thermoelectric generator (curve C) is shown in figure 6 as a function of output power in the case of lighthouses. A life of twenty years is assumed for each generator. The costs include initial costs of the generators, controls, secondary batteries and fuel and repair costs required during their lives. Convention efficiencies of 10 per cent and 2 per cent are assumed for the heat engine and the thermoelectric generator, respectively. The solar battery may be the most convenient power source because of its simplicity in performance and its external and independent source of energy the sun. However, its initial cost is relatively high for large power sources. The heat engine is, at present, limited to relatively large power sources, and its maintenance is not so simple as that of a thermoelectric generator. As is seen in figure 6, the thermoelectric generator may be most economical for a power source in the range between one watt and one hundred watts. Several kinds of generator have been constructed in the laboratory. Prototype thermoelectric generators of five watts and of one hundred watts are now being constructed for a lighted buoy and a lighthouse, respectively, for aid to navigation.

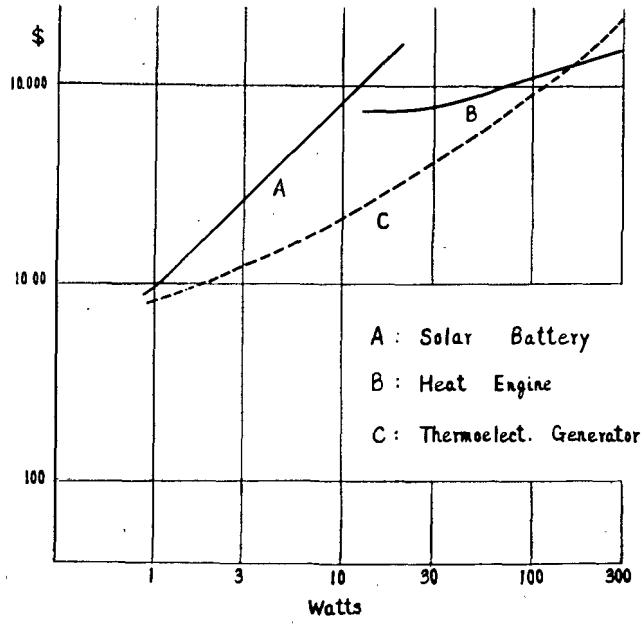


Figure 6. Comparison of costs of solar battery, heat engine generator and thermoelectric generator as a function of output power

Conclusions

The merits of the utilization of the silicides of transition metals are as follows : (i) The raw materials are abundant on earth, and no such high purities of the materials are needed as in the case of transistor technology. (ii) They are inherently refractory and suitable to a thermoelectric generator for high temperature use, resulting in a relatively high conversion efficiency. (iii) Construction of the U-shaped *p-n* junction by sintering process is possible owing to the low mobilities of current carriers in the silicides. Although the conversion efficiency of the sintered junction is reduced a little, compared with that of the junction constructed with the pulled crystals, cost reduction and simplicity in construction of *p-n* junction free from contact resistance and cracks are remarkable. The generator constructed by the sintered elements may be one of the most economical power sources in the power range of one to 100 watts.

Bibliography

Ioffe, A. F., *Semiconductor Thermoelements and Thermoelectric Cooling*, Infosearch, Ltd., London, 1957.

Irving, B. C. and Miller, E., *Thermoelectric Materials and Devices*, Reinhold Publishing Corp., New York, 1960.

Summary

Utilization of some silicides of transition metals for the purpose of the thermoelectric generator is reported in this paper. The raw materials of the silicides are abundant on earth, and no such high purities of the materials are required as in the case of semiconductor technology. The silicides are inherently refractory materials and have relatively large values for the figure of merit up to 1 000°C. Thus they are suitable for thermoelements for high temperature use, resulting in high conversion efficiencies, ranging from 6 per cent up to 12 per cent.

The U-shaped *p-n* junction is constructed by pressing and sintering the powder of the component materials. Owing to the high densities and low

mobilities of current carriers in the silicides, the resistivities of the sintered materials are not increased seriously. Although the conversion efficiency of the sintered junction is reduced a little, compared with that of the junction constructed with the pulled crystals, the cost reduction and simplicity in the construction of a *p-n* junction free from contact resistance and cracks are remarkable.

Thermoelectric properties of the silicides are given in the temperature range between room temperature and 1 000°C. Calculated efficiencies of the junctions constructed by the sintering method and by combination of the pulled crystals are about 4.5 per cent and 6.5 per cent at $\Delta T = 900$°C, respectively. Efficiency of 2 per cent was observed for a prototype 5-watt generator at average $\Delta T = 700$°C. A comparison of costs of solar batteries, heat engine generators and thermoelectric generators is also given. The last may be most economical in the power range from one to 100 watts.

UN GÉNÉRATEUR THERMO-ÉLECTRIQUE

Résumé

L'auteur décrit l'utilisation de certains siliciures des métaux de transition pour les besoins d'un générateur thermo-électrique. Les matières premières qui constituent les siliciures sont abondantes de par tout le globe et on peut se contenter de produits n'ayant pas les puretés extrêmement élevées qu'exige, par exemple, la technologie des semi-conducteurs. Les siliciures sont intrinsèquement des matériaux réfractaires et leurs coefficients de résistance sont relativement élevés jusqu'à 1 000 °C. Ils se prêtent donc bien à une utilisation comme thermo-éléments pour applications aux températures élevées, donnant de gros rendements de conversion qui s'échelonnent entre 6 et 12 p. 100.

On réalise une jonction *P-N* en forme d'U en comprimant et en frittant les matériaux pulvérisés. Compte tenu des densités élevées et de la faible mobilité des porteurs de courants dans les siliciures, la résistivité des matériaux frittés n'est pas indûment accrue. Bien que le rendement de conversion de la jonction frittée ne soit réduit que dans une faible mesure par rapport à celle que l'on réaliserait avec les cristaux étirés, la réduction des frais de réalisation et la simplicité de fabrication de jonctions *P-N* exemptes de résistance de contact et de fêlures est remarquable.

L'auteur donne les propriétés thermo-électriques des siliciures sur une gamme s'étendant de la température ambiante à 1 000 °C. Les rendements calculés des jonctions réalisées par la méthode du frittage et la combinaison de cristaux étirés sont de l'ordre de 4,5 et 6,5 p. 100 pour $\Delta T = 900$ °C respectivement. Un rendement de 2 p. 100 fut observé pour un générateur prototype de 5 watts avec un ΔT moyen de 700 °C. L'auteur présente également une comparaison des frais entre les batteries solaires, les générateurs à moteurs thermiques et les générateurs thermo-électriques. Ces derniers sont peut-être les plus économiques dans la gamme de puissances allant de 1 à 100 watts environ.

NOUVEAUX GÉNÉRATEURS SOLAIRES THERMO-ÉLECTRIQUES

R. Michel *

Les études effectuées par la Compagnie générale de T.S.F., tant pour le compte de la Sté d'études et d'applications industrielles de l'énergie solaire que pour celui du B.I.A. (Bureau d'investissement en Afrique), se sont concrétisées par la réalisation de générateurs solaires de dimensions et de puissances de plus en plus grandes, expérimentés à Colomb Béchar et à Toulon.

Nous nous proposons, après un rapide rappel des principes théoriques qui sont à la base de ces appareils, de décrire ces réalisations, de tirer les leçons qui en ont découlé et de présenter les espoirs qu'elles autorisent. Il est un trait à noter, c'est un décalage constant entre le niveau de la technique et les caractéristiques des générateurs; ces derniers, de par les grandes surfaces qu'ils commencent à couvrir, exigent de très nombreuses pièces détachées, et sont des œuvres de longue haleine; cependant, les recherches de laboratoire se poursuivent, et leurs conclusions sont généralement formulées lors du montage d'un appareil selon une technique donc déjà dépassée.

Principe de fonctionnement

Le cœur du générateur étant constitué par des thermo-couples en semi-conducteurs, tous les dispositifs associés ont pour but de les faire traverser sous la plus grande différence de température possible par le plus grand flux de chaleur possible, et, les matériaux utilisés ayant leurs performances généralement en décroissance quand la température s'élève, d'évacuer la chaleur aux jonctions froides sous la plus faible température possible. Or, la différence de température utile varie en raison inverse de la puissance calorifique transmise dans les couples, quand la dimension de ceux-ci varie en même temps que leur conductance thermique; de ce fait, le produit des deux premières grandeurs passe par un maximum, et il existe une dimension optimale de couples, corollaire d'un écart de température utile optimum pour une valeur donnée de la puissance du rayonnement solaire.

Le rayonnement solaire est capté par des plaques collectrices d'un bon coefficient d'absorption dans le spectre visible. Ces plaques sont recouvertes de feuilles transparentes, dont le nombre n'est pas indifférent. En effet, plus il est grand, plus faible est la part de rayonnement transmise, mais meilleur est l'isolement thermique de la face avant, car ce cloisonnement coupe la convection gazeuse, et arrête le rayonnement infra-rouge des collecteurs, chaque plaque rayonnant elle-même en avant et en arrière selon sa température propre. Les collecteurs peuvent être de deux types, soit simplement noircis — leur émissivité infra-rouge est alors élevée et le nombre des feuilles transparentes doit être grand (3 ou 4) — soit sélectifs, c'est-à-dire offrant, en même temps qu'un bon facteur de captation de la lumière visible, une faible émissivité infra-rouge — le nombre de séparateurs doit être alors plus faible (2 ou 3) pour améliorer le facteur de transmission, alors que celui de captation est un peu réduit.

Le flux calorifique qui a traversé les couples et le flux de déperdition qui est passé en dehors sont évacués par le fond du générateur. Ce flux de déperdition est réduit par un calorifugeage, généralement à la laine de verre.

Historique des réalisations

Si la théorie complète du fonctionnement des générateurs solaires n'a été établie que tout récemment, pour être un guide sûr du dimensionnement de leurs paramètres tout en fournissant les valeurs limites de leurs performances possibles, les premières maquettes réalisées l'ont été un peu empiriquement et, par suite du décalage déjà mentionné entre les acquis théoriques et techniques et la mise en œuvre des connaissances, seul le générateur qui sera mis en œuvre dans le courant de cette année, et dont une petite maquette « éclatée » est présentée à l'occasion de cette Conférence, peut se targuer d'un décalage minime avec les conceptions actuelles de nos laboratoires et de nos bureaux d'études.

Jusqu'au printemps 1960, la taille des maquettes n'avait guère dépassé le mètre carré d'aire utile, limite des appareils essayés en 1959 en France métropolitaine à Manosque, et en 1960 au Sahara à Colomb Béchar. L'année 1959 avait vu le premier progrès décisif dans la substitution aux thermo-couples groupés en piles collées sous les collecteurs, de thermo-couples individuels soudés chacun sous leur collecteur, ce qui éliminait une résistance thermique très gênante. Cependant, alors même que ces essais se poursuivaient, les éléments d'un générateur de 17,4 m² étaient en préparation et furent assemblés en France près de Toulon pour être expérimentés dès la fin de l'été 1960. Le générateur le plus récent, de concep-

* Président de la Société d'études et d'applications industrielles de l'énergie solaire, Paris.

tion et de réalisation, objet de la maquette présentée, pourra se compter vraisemblablement au nombre des plus importantes réalisations en ce domaine, avec ses neuf éléments de 8 m², soit en tout 72 m²; c'est un appareil de type industriel à modules préfabriqués, à assembler en place avec des pièces standardisées.

Générateur de 17,4 m²

Notons au préalable que la valeur insolite de cette aire utile n'est pas le fait du hasard, mais représente celle de deux éléments de 8,7 m², soit 1 m × 8,7 m, la longueur étant conditionnée par celle de cornières perforées de type standard qui constituent les châssis.

Structure

L'unité d'aire normalisée est le décimètre, c'est l'aire du collecteur individuel. La C.S.F. ayant commencé par équiper les prototypes de collecteurs sélectifs en aluminium sous deux plaques de verre distantes de 1 cm, et ayant relevé des performances identiques avec des collecteurs noircis, toutes autres choses demeurant inchangées, a utilisé pour cet appareil des collecteurs en aluminium déjà approvisionnés, mais noircis.

Chaque collecteur est soudé sur un couple en tellurure de bismuth fritté d'une conductance voisine de 2×10^{-2} W °K^{-1}, valeur nettement inférieure à l'optimum, déterminé bien après la conception de cet appareil. Chaque barreau de couple est lui-même soudé sur un pied de couple en aluminium étamé en forme de L faisant office de conducteur électrique et thermique. Un système de plaques porte-ailettes en aluminium étamé supporte les L et assure, en même temps que la continuité électrique de la chaîne, l'évacuation de la chaleur. Une bande est formée de 10 cellules élémentaires de 1 dm² ou 10 couples et mesure 1 mètre. Les bandes sont assemblées côte à côte sur des profilés en alliage léger porteurs avec interposition d'un isolant. Des morceaux de câbles serrés aux extrémités des bandes les mettent en série. Du matelas de laine de verre hyperfine est bourré entre collecteurs et plaques porte-ailettes. L'orientation des bandes et des ailettes est selon le méridien.

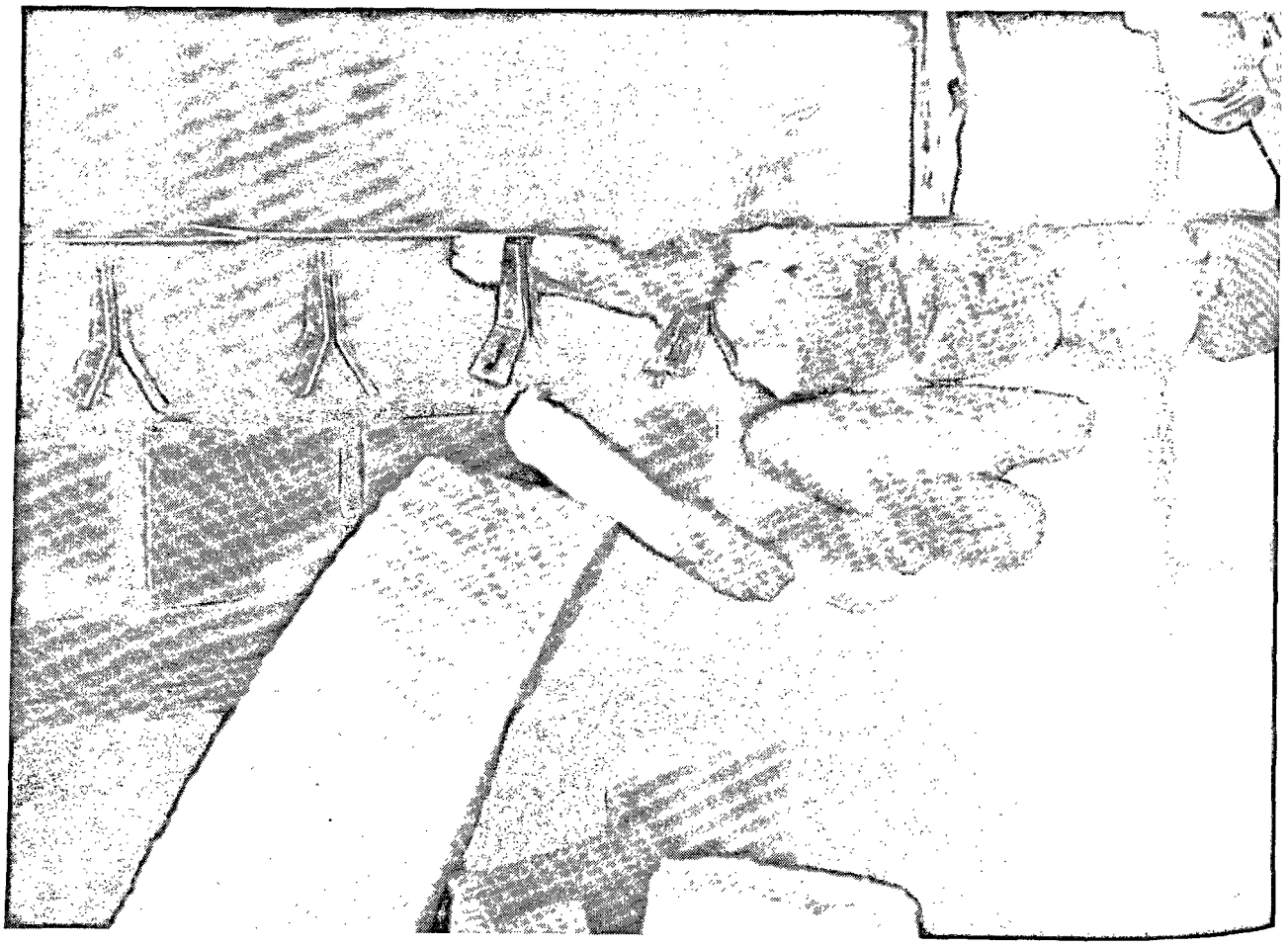


Figure 1. Générateur de 17 m². Détail de la structure; le garnissage à la laine de verre est en cours et progresse de gauche à droite

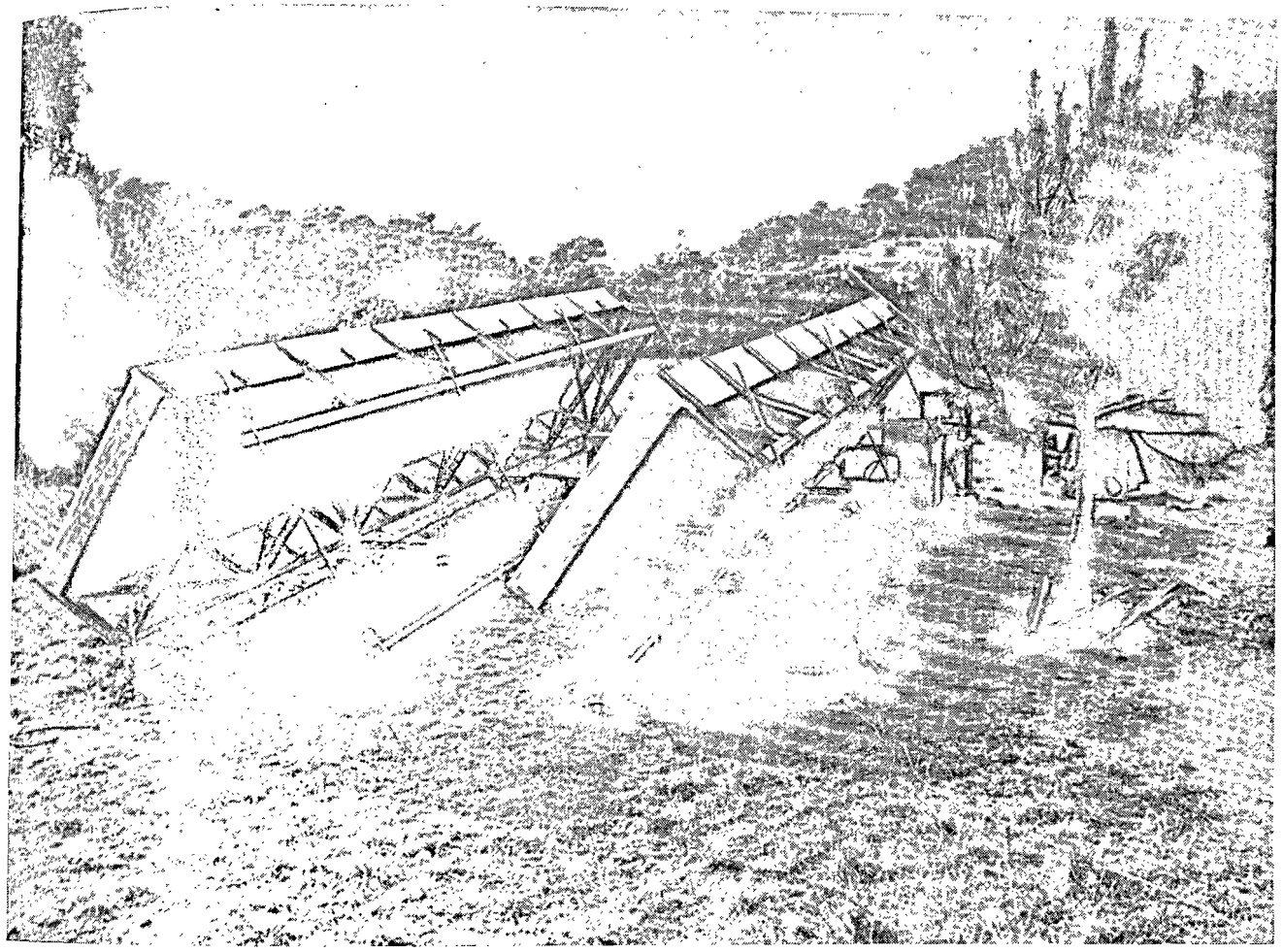


Figure 2. Générateur de 17 m². Vue arrière d'est en ouest en position hivernale

La mosaïque des collecteurs est recouverte de trois plaques de verre double distantes de 25 à 30 mm reposant sur des cornières en alliage léger. Les côtés sont soigneusement calorifugés à la laine de verre.

L'échauffement considérable des vitres et les gradients thermiques régnant près des bords sont une cause de casse; pour l'éviter, les deux premières couches de vitres doivent reposer sur des supports isolants et leur aire doit épouser exactement celle de l'ensemble des collecteurs. L'influence néfaste du vent doit être combattue par un calfeutrage soigné de l'ensemble, pour lui conférer une certaine étanchéité.

Performances

Les deux éléments de 8,7 m² diffèrent entre eux essentiellement par la qualité du calfeutrage et du calorifugeage; ils ont été chacun scindés en deux sections mesurées séparément; une fois éliminés les couples à jonctions défectueuses, on a la répartition suivante des unités de 1 dm² :

Section	A 1	A 2	B 1	B 2
Nombre d'unités	416	409	424	402

Pour une puissance globale sur charge adaptée de 77 watts sous un rayonnement de 850 W m^{-2}, la puissance se répartit ainsi selon les sections (en watts au mètre carré) :

A 1	*A 2*	*B 1*	*B 2*
3,7	$4,4_5$	$5,5_5$	5,0

Comparativement, des éléments analogues essayés à Colomb Béchar avaient fourni 7 W m^{-2} sous un rayonnement de 1 kW m^{-2}.

Le diagramme de la figure 5 représente, tracé avec une moyenne de relevés, la variation avec le rayonnement de la puissance globale fournie à une batterie de 16 éléments alcalins de 15 Ah.

Il est à noter que, sur la base de la meilleure section, la puissance maximale sous un rayonnement de 850 W m^{-2} serait de :

$$5,5_5 \times 17,4 = 97 \text{ watts}$$

Pour 7 W m^{-2}, on aurait :

$$7 \times 17,4 = 121 \text{ watts}$$

Du point de vue des énergies journalières intégrées, en charge sur les 16 éléments alcalins, le générateur

global a fourni en moyenne 200 Wh par kWh m^{-2} de rayonnement solaire au-dessus du seuil de charge, ce qui correspond à 9,5 Wh m^{-2} pour la section la moins bonne et à 14,5 Wh m^{-2} pour la meilleure. A titre indicatif, l'énergie du rayonnement solaire au-dessus du seuil 450 W m^{-2} peut atteindre 3 kWh m^{-2} par un jour particulièrement ensoleillé au Sahara, ce qui aurait pour corollaire une énergie utile globale voisine de 600 Wh; mais on peut trouver aussi des jours où l'énergie du rayonnement n'est voisine que de 1 kWh m^{-2}.

Enseignements tirés

En dehors du dimensionnement des couples, le défaut principal de cet appareil réside dans les jonctions entre pièces d'aluminium, fragiles mécaniquement et exagérément résistantes au point de vue électrique; si, de ce dernier fait, les performances sont notablement détériorées, la fragilité impose des servitudes de transport — sous forme de cellules élémentaires — et un montage complet et long sur place.

Le principe structural, bien que satisfaisant techniquement, s'allie à un prix de revient assez élevé. D'ailleurs, même sur le plan technique, on a observé au bout de quelques mois de service, sous l'action supposée de l'humidité, des défauts d'isolement par rapport à la masse.

Enfin, le châssis et toutes les parties auxiliaires n'ont pas été étudiés aussi complètement que la cellule de base pour être fonctionnels.

GÉNÉRATEUR DE 72 M^2

Structure

Il y a encore un couple par collecteur carré de 1 dm^2, la cellule élémentaire est plutôt la bande de 1 m de long, essentiellement constituée par un profilé en aluminium-silicium, ailettage auto-porteur, oxydé anodiquement, sur lequel sont fixés des pieds de couple en aluminium en forme de U, qui assurent les conductions électrique et thermique; la base plate du U présente une aire assez grande pour transmettre à travers un collage au silicone la chaleur des jonctions froides à l'ailettage. Les collec-

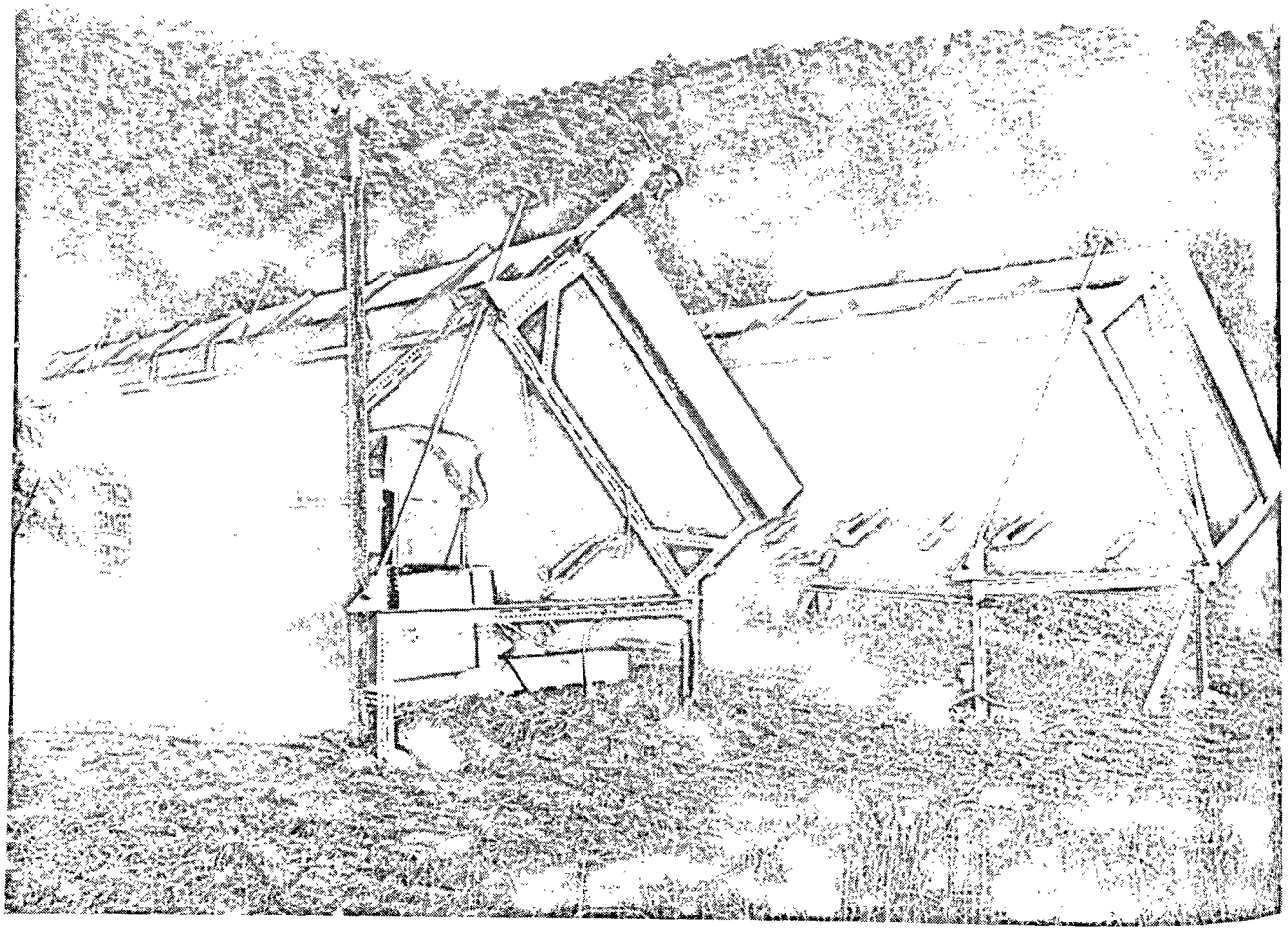


Figure 3. Générateur de 17 m^2. Vue arrière d'ouest en est en position hivernale. Au premier plan la circuiterie de charge et de mesure, l'anémomètre et l'actinomètre

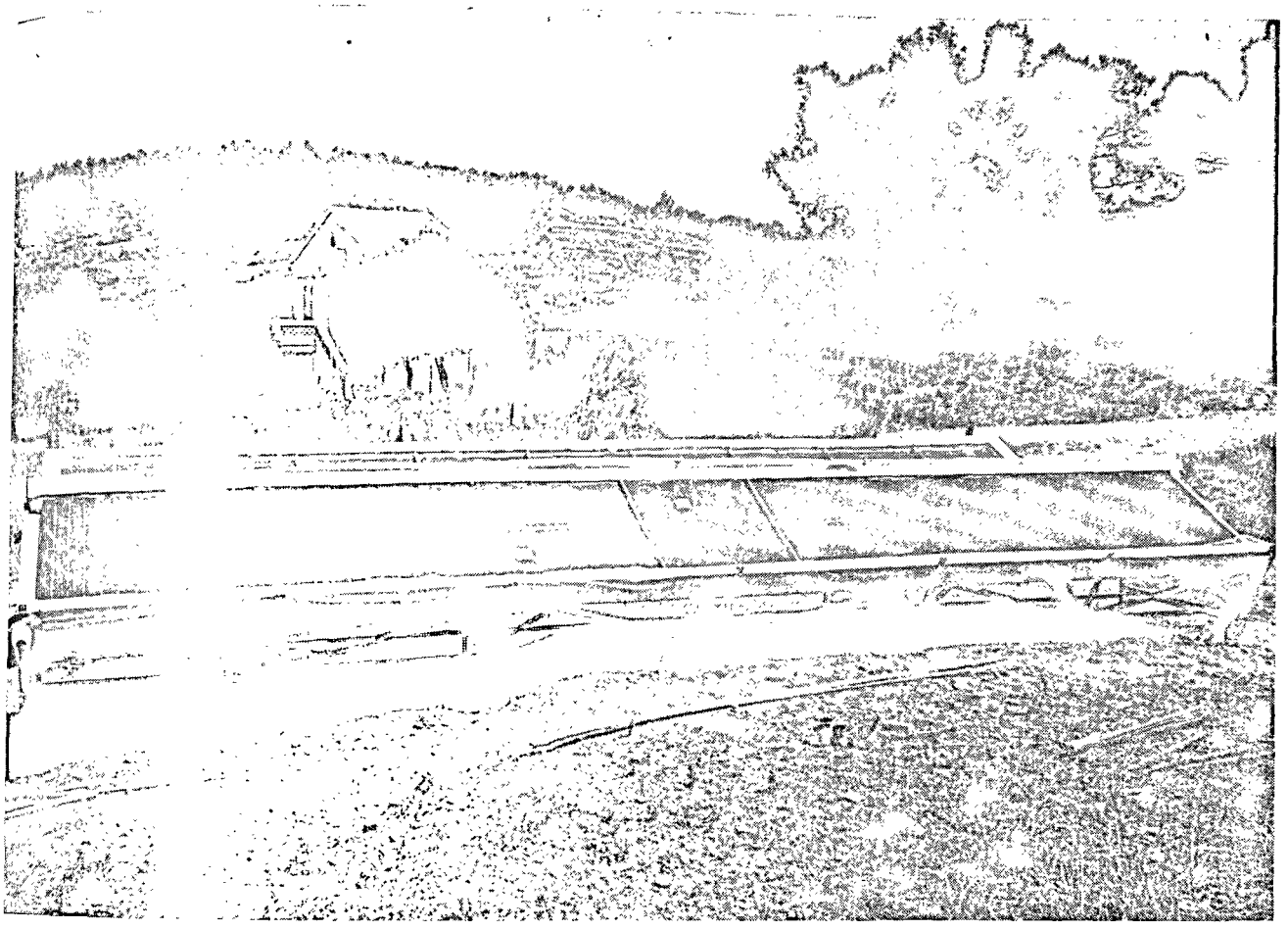


Figure 4. Générateur de 17 m². Vue générale de face en position estivale, avant l'achèvement de l'isolement supérieur

teurs sont en cuivre noirci et les couples, métallisés, sont soudés à l'étain d'une part sur le collecteur, et d'autre part sur le haut des pieds, avec un intermédiaire en cuivre. Les jonctions obtenues présentent une grande solidité, du fait que le matériau semi-conducteur n'est pas soumis aux tensions mécaniques provenant de coefficients de dilatation très différents. Les branches des U offrent une certaine élasticité, gage de faibles contraintes sur les soudures.

Les bandes, isolées électriquement du circuit des couples par leur anodisation, sont montées sur des barres de bakélite pour constituer des modules de cinq unités (0,5 m²), dont la solidité des jonctions autorise le transport sous cette forme dans un emballage adéquat.

Les modules préfabriqués sont prévus pour être assemblés par six en unités de 3 m². Nous présentons ici une petite unité de deux modules. L'appareil en cours d'installation a des éléments de trois unités, soit 18 modules. Le châssis est en tube d'acier galvanisé sur lequel sont fixées les pièces de maintien en tôle et profilés en T d'acier zingué. L'isolant thermique est encore du matelas de laine de verre comprimée, et l'isolant de la face avant est réalisé par trois feuilles en fluorure de polyvinyle et une vitre de verre double.

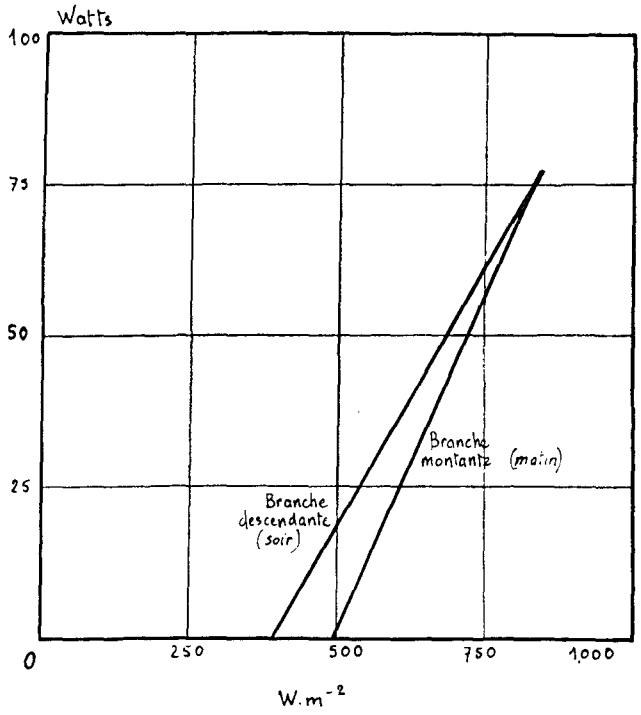


Figure 5. Générateur de 17 m², puissance utile globale en fonction du rayonnement solaire

La tension en charge est à prendre entre 1 et 1,5 volt par mètre carré. Pratiquement, les trois unités d'un élément sont montées en parallèle, travaillant ainsi entre 3 et 4,5 volts, et les huit éléments sont montés en série en vue de charger une batterie alcaline étanche de 24 volts, 160 Ah à travers un jeu de diodes au silicium, destinées à éviter la décharge de la batterie dans le générateur la nuit; un dispositif auxiliaire à mano-contacts et relais règle la charge.

Perspectives

Il est encore trop tôt pour tirer des enseignements du nouveau générateur solaire de grande puissance. Pour la première fois, un générateur bénéficiant des derniers acquis techniques des laboratoires de la C.S.F., notamment au point de vue de la qualité des jonctions et de la rationalisation des éléments préfabriqués, va pouvoir être soumis à une expérimentation longue et suivie au Sahara.

Certainement, des retouches minimes s'avèreront nécessaires, mais, à ce détail près, on peut dire qu'un générateur opérationnel, dont le transport en éléments normalisés et le montage relativement rapide en place sont possibles, est présenté sur le marché.

Sur ces mêmes bases, des couples en matériaux à base de tellurure de bismuth à cristaux orientés pourraient être substitués à ceux en matériaux frittés, avec un notable accroissement des performances. Si de tels couples ont déjà été préparés, leur développement industriel est du domaine du proche avenir.

Les efforts vont se poursuivre en deux grandes voies distinctes :

Le perfectionnement des générateurs de ce type — dont la théorie a pu déjà fixer les performances asymptotes — c'est-à-dire chercher de nouveau à accroître le rendement surfacique par l'utilisation de collecteurs sélectifs améliorés, et à abaisser le prix de revient surfacique tout en conservant un rendement acceptable. Dans les deux cas, les études en cours sur le vieillissement des jonctions conduiront à une très longue prolongation des performances sans détérioration.

L'étude et la réalisation des générateurs à rendement accru utilisant des couples en semi-conducteurs admettant des températures de jonctions chaudes élevées, avec concentration de la lumière par miroirs cylindro-paraboliques à orientation manuelle ou automatique.

Résumé

Les études effectuées par la Compagnie générale de T.S.F., tant pour le compte de la Société d'études et d'applications industrielles de l'énergie solaire que pour celui du B.I.A. (Bureau d'investissement en Afrique), se sont poursuivies ces dernières années dans le domaine de la théorie et des recherches de laboratoire.

Après l'expérimentation en France, à Manosque, et en Afrique, à Colomb Béchar, de générateurs solaires plans de petites dimensions, des essais à plus grande échelle ont eu lieu en 1960 en France, près de Toulon, sur un appareil de 17 m², et cette année voit la mise en œuvre d'un générateur vraiment opérationnel, à éléments préfabriqués normalisés, de 72 m², dont une petite maquette est présentée.

Sous des surfaces transparentes en verre ou fluorure de polyvinyle qui cloisonnent l'espace et s'opposent à la déperdition thermique, des plaques collectrices s'échauffent sous l'action du rayonnement solaire; elles ont pour but de faire traverser par un flux calorifique des thermo-couples en semi-conducteurs, dont la conductance doit être optimisée; ce flux est évacué par un ailettage garnissant le fond de l'appareil. Avec des collecteurs uniformément noirs dans le spectre visible et infra-rouge, il est bon d'utiliser quatre nappes transparentes; avec des collecteurs dits « sélectifs » à faible émissivité infra-rouge, ce nombre se ramène à deux.

Le générateur de 17 m², dont les différentes sections étaient de valeurs inégales, a pu produire, selon les sections, des puissances électriques utiles comprises entre 3,7 et 5,5 watts au mètre carré sous un rayonnement de 850 watts au mètre carré, ce qui correspond pour la meilleure section à 7 W m^{-2} sous un rayonnement de 1 kW m^{-2}. En chargeant une batterie de 16 éléments alcalins, l'appareil, qui travaillait en fait au-dessus d'un seuil de rayonnement de 450 W m^{-2}, fournissait une énergie électrique proportionnelle à l'énergie du rayonnement intégrée au-dessous du seuil, soit environ globalement 200 Wh par kWh m^{-2}.

Cet appareil, à couples non optimisés, présentait l'inconvénient de jonctions imparfaites, d'une structure de châssis et parties auxiliaires trop peu fonctionnelle, et d'un prix de revient de fabrication, de transport et de montage trop élevé.

Le nouveau générateur comprend huit éléments de 9 m² utiles, chacun monté sur châssis métallique à l'épreuve des intempéries. Ses éléments actifs sont des modules de 50 dm², soit 50 couples solidement soudés sous 50 collecteurs, montés sur profilés à ailettes auto-porteurs. Il doit maintenir en charge une batterie de 20 éléments alcalins de 160 Ah. Cet appareil, bien que prévu pour être installé à demeure, est cependant facilement montable, démontable et transportable en pièces détachées et modules.

Les buts visés sont l'emploi de thermo-couples à performances et jonctions améliorées. Si les collecteurs sélectifs en aluminium traité n'ont pas encore justifié leur emploi de préférence à celui des collecteurs noircis, de nouveaux collecteurs hautement sélectifs sont à l'étude. En ce genre d'appareils, le point ultime à considérer est essentiellement le rapport de l'investissement consenti à la puissance utile, et toute ligne de conduite lui est subordonnée.

NEW SOLAR THERMOELECTRIC GENERATORS — DESCRIPTION, RESULTS AND FUTURE PROSPECTS

(Translation of the foregoing paper)

R. Michel *

The studies conducted by the Compagnie générale de T.S.F. on behalf of the Société d'études et d'applications industrielles de l'énergie solaire, and of the B.I.A. (Bureau d'investissement en Afrique) have now been embodied in the development of solar generators of greater and greater size and power that have been tested at Colomb Bechar and Toulon.

After rapidly reviewing the theoretical principles on which these devices are based, we propose to describe these embodiments, to draw lessons from them, and to point out the prospects they offer. The constant lag between the level of the technology and the characteristics of these generators must be noted. On account of the extensive areas they are commencing to cover, they demand very numerous details, and are long and exacting projects. But the laboratory research continues, and its conclusions

* Président, Société d'études et d'applications industrielles de l'énergie solaire, Paris.

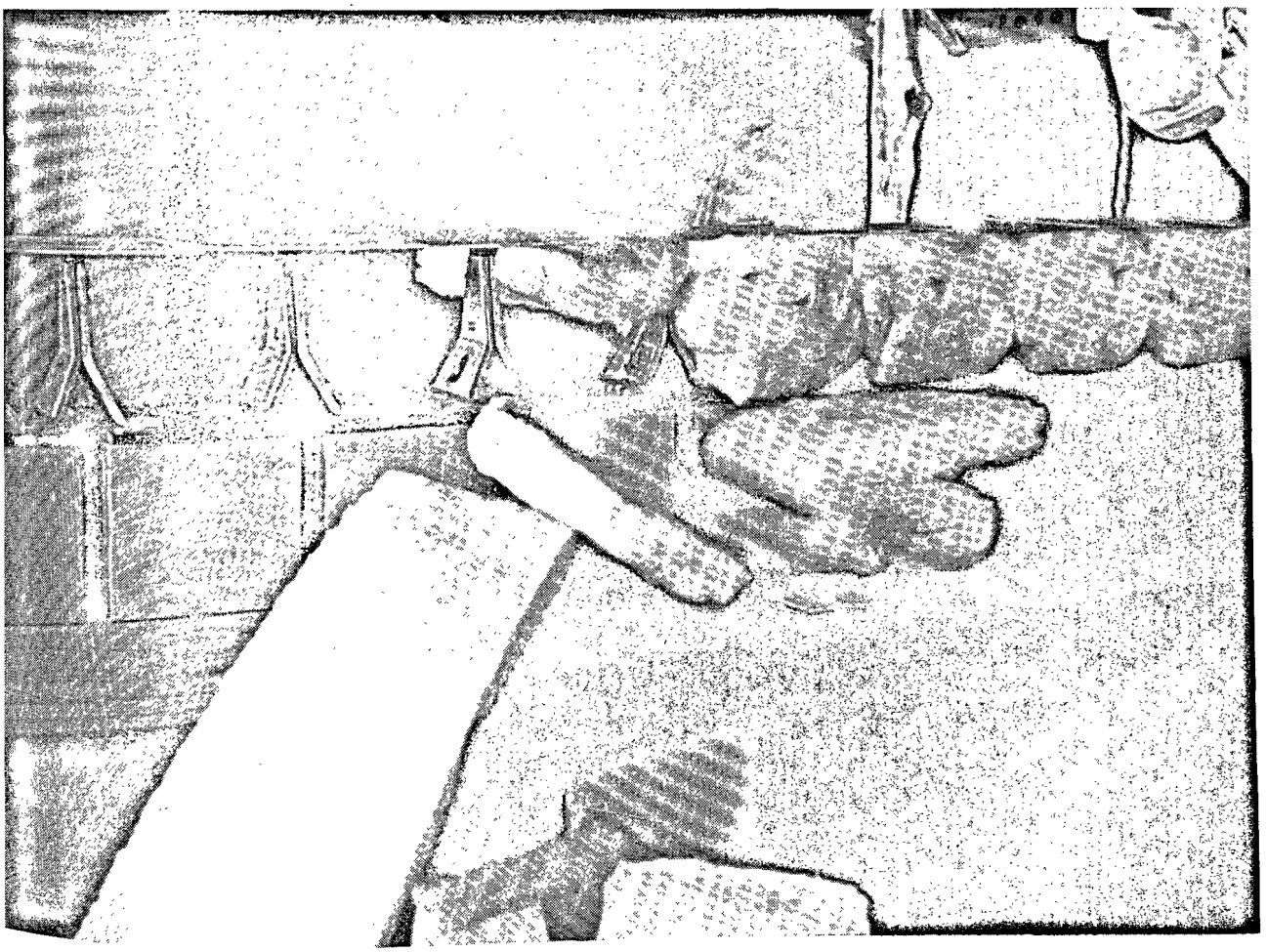


Figure 1. 17 - m² generator. Detail of the structure; the glass wool lining is being applied. The work is in progress from left to right

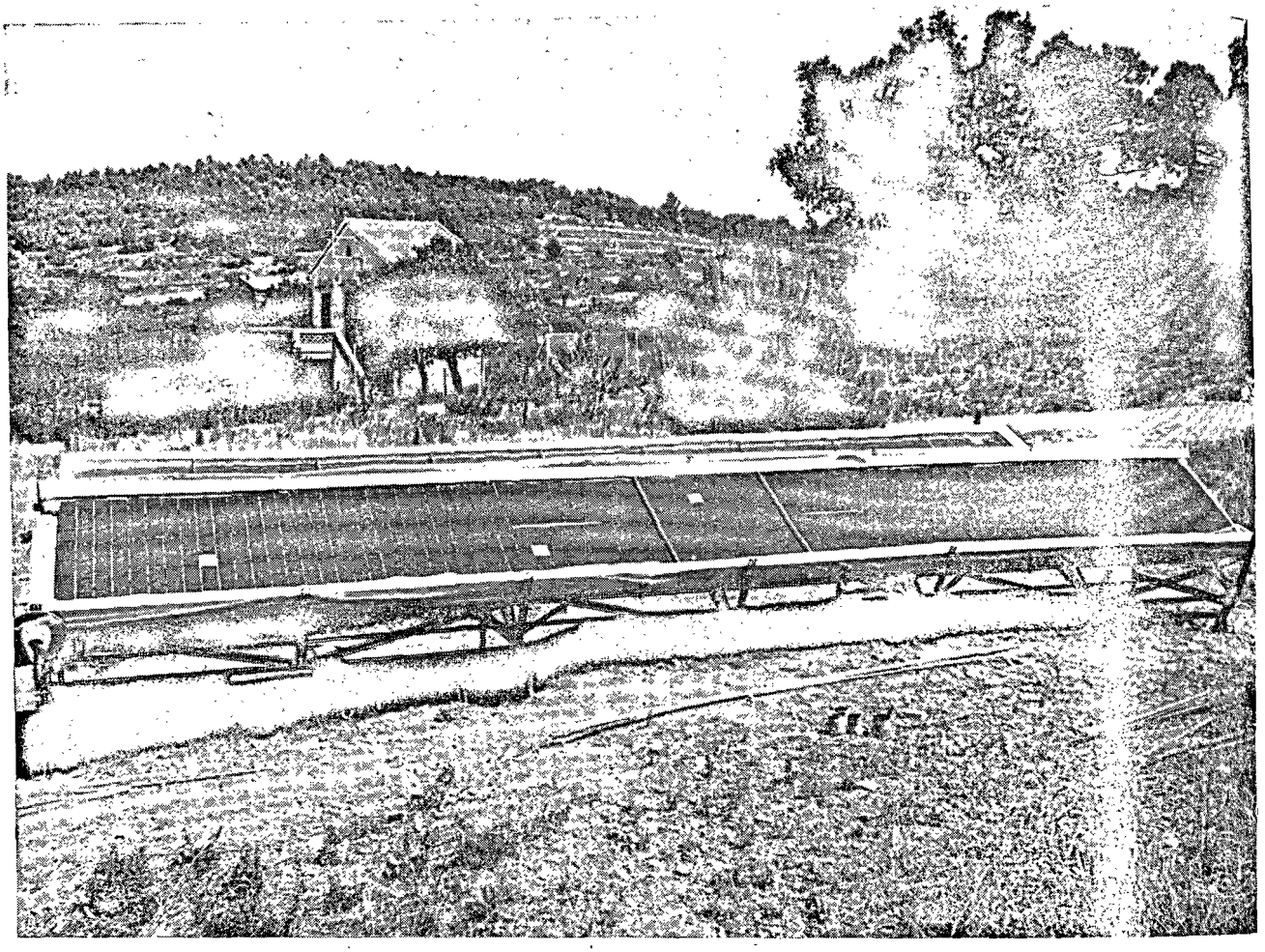


Figure 2. 17 - m² generator. Rear view from east to west in winter position

have generally been formulated by the time a device has been designed and built by a technique already outstripped.

Principle of operation

Semiconductor thermocouples are the heart of the generator, and the object of all the accessory arrangements is to pass the greatest possible flux through them at the greatest possible temperature difference. Since the performance of the materials utilised generally falls off with rising temperatures, it is necessary to remove the heat from the cold junctions at the lowest possible temperature. But the useful temperature difference varies inversely as the thermal power transmitted by the couples, while the size of the thermocouples varies with their thermal conduction. The product of the first two quantities therefore passes through a maximum, and there exists an optimum size of the couples, associated with an optimum useful temperature-difference for a given level of solar-radiation power.

The solar radiation is captured by collector plates with a good absorption coefficient in the visible spectrum. These plates are covered by transparent sheets. The number of these sheets is not unimportant. For the greater the number, the smaller the fraction of radiation transmitted, but the better the thermal insulation of the front face, for these partitions cut off the gas convection and stop the infrared radiation of the collectors, each plate itself radiating in front and rear according to its own temperature. The collectors may be of two types, either simply blackened, in which case their infrared emissivity is elevated and the number of transparent sheets must be great (three or four); or they may be selective, that is, having both a good absorption factor for visible light and a low infrared emissivity. In that case the number of separators should be smaller (two or three) to improve the transmission factor, while the absorption is a little reduced.

The calorific heat flux that has passed through the thermocouples and the waste heat flux that has missed them are both removed through the generator bottom. This waste flux is reduced by thermal insulation, usually with glass wool.

History of development

While the complete theory of the operation of solar generators has been only very recently established, as a reliable guide to the dimensioning of

their parameters and a source of limiting values for their possible performance, the development of first models was somewhat empirical. Owing to the lag we have mentioned between the building up of theory and techniques and the actual realization of the newly acquired knowledge, only the generator that will be put into operation in the course of the present year (1960), a small "exploded" model of which is being presented to this conference, can boast a minimum development lag between the present ideas of our laboratories and the work of our design offices.

Up to spring 1960, the size of the models never exceeded the square metre of useful area that was the limit of the devices tested in 1959 in metropolitan France, at Manosque and in 1960 in the Sahara, at Colomb Bechar. The year 1959 saw the first decisive progress in the replacement of thermocouples grouped in piles cemented under the collectors by individual thermocouples, each soldered under its own collector, thus eliminating a very troublesome thermal resistance. However, even while these tests were going on, the elements of a 17.4 sq m generator were being prepared, and were assembled in France near Toulon for testing at the end of summer 1960. The generator of most recent conception and execution, the original of the model we are presenting, can probably be numbered among the most important developments in this field, with its 9 elements, each 8 sq m, or a total surface of 72 sq m. It is an industrial-type device using prefabricated modules for on-site assembly with standardized parts.

The 17.4-sq m generator

First of all we note that the unusual useful area was not the result of chance, but represents that of two elements each of 8.7 sq m—that is, 1 × 8.7 m, the length being taken on account of the standard perforated angles forming the chassis.

Structure

The standardized unit of area is the square decimetre. This is the area of the individual collector.

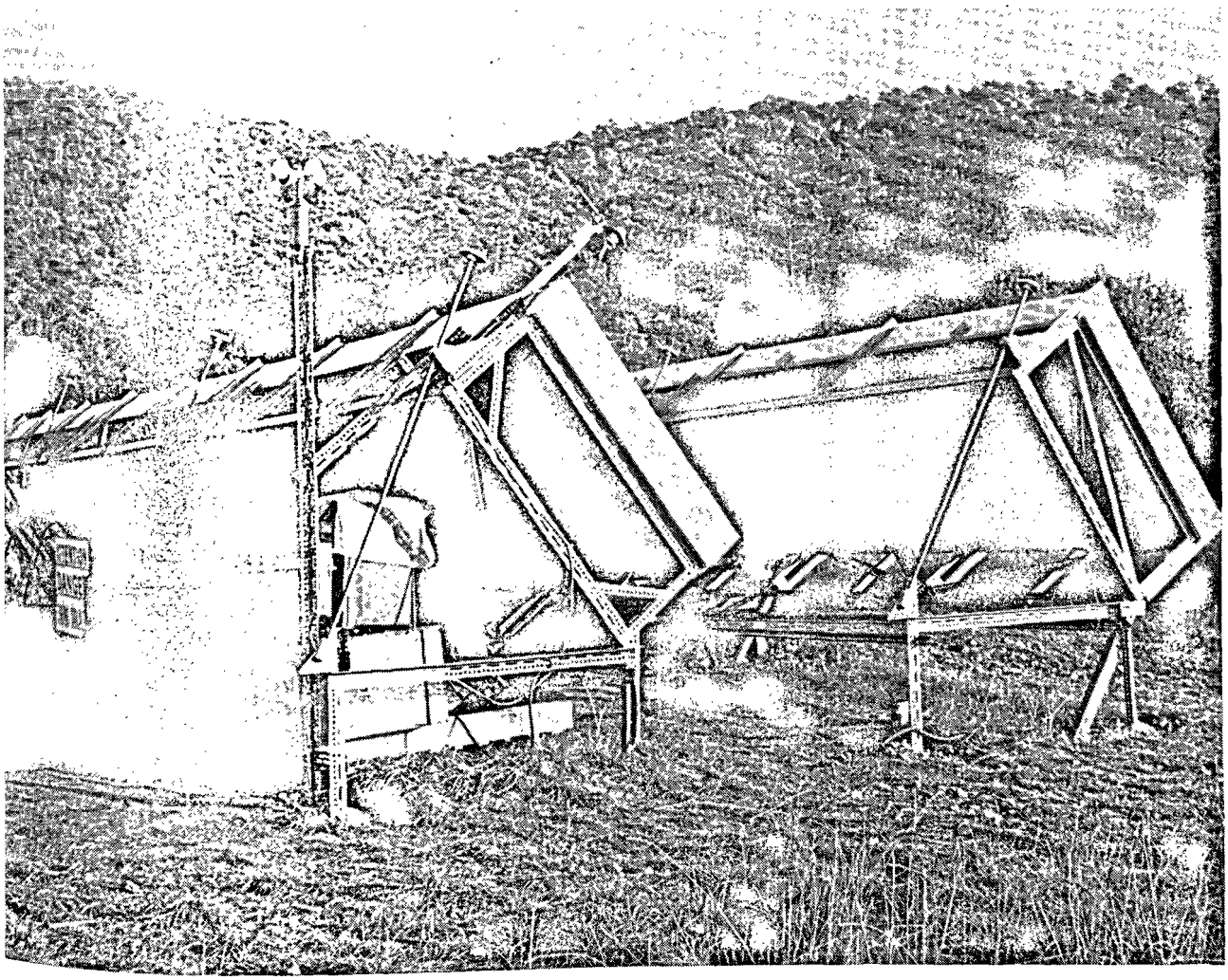


Figure 3. 17-m² generator. Rear view from west to east in winter position. In the foreground the charging and measurement circuitry, the anemometer and actinometer

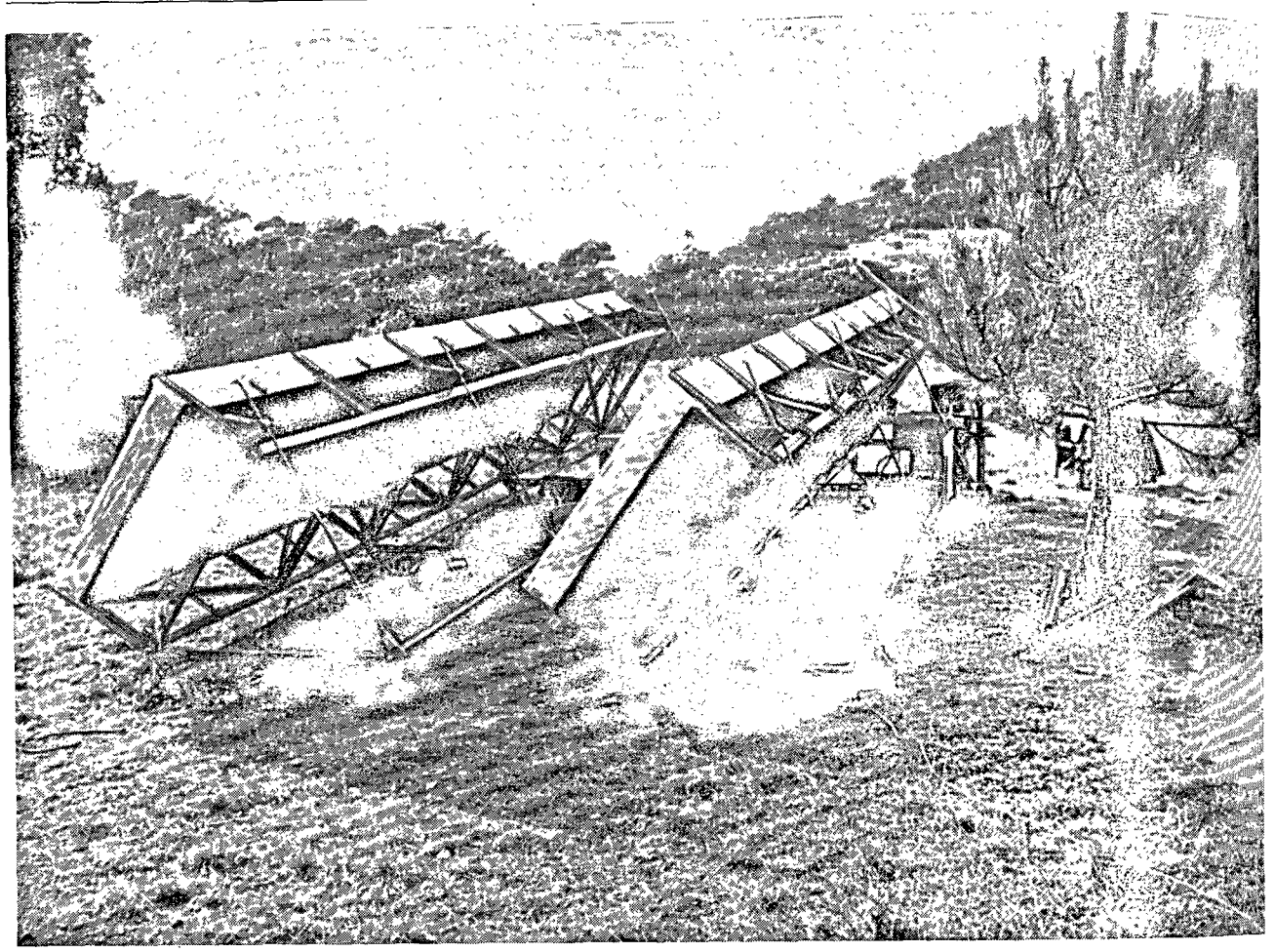


Figure 4. 17-m² generator. General view of front in summer position, before finishing the upper insulation

The C.S.F. (Radio Corporation) had commenced by placing the prototypes of the aluminium selective collectors beneath two glass plates spaced 1 cm apart, having found their performance to be identical with that of the blackened collectors, other things being equal. Aluminium collectors already in stock, but blackened, were therefore used in this generator.

Each collector is soldered over a fritted bismuth telluride thermocouple with a conductance close to 2×10^{-2} W°K^{-1}, a value definitely below the optimum, which was determined only well after the designing of this device had been completed. Each bar of the couple is itself soldered to a tin-plated aluminium leg of the couple, L shaped and serving as electrical and thermal conductor. A system of finned plates of tinplated aluminium supports the Ls and ensures the electrical continuity of the chain as well as heat removal. A band is made of 10 elementary 1-sq m cells or 10 couples and is 1 m in size. The bands are assembled side by side on light-alloy supporting profiles separated by insulating material. Pieces of cable clamped to the ends of the bands connect them in series. Hyperfine glass wool is packed between the collectors and the finned plates. The bands and fins are oriented meridianally.

The mosaic of collectors is covered with three double glass plates 25 to 30 mm apart resting on light-alloy angle pieces. The sides are carefully heat-insulated with glass wool.

The substantial heating of the glass and the heat gradients near the edges are a cause of breakage. To prevent this, the first two layers of glass rest on insulating supports, and their areas must exactly match that of the whole collector group. The harmful effect of the wind should be combated by carefully stopping up any crevices to give the assembly a certain degree of tightness.

Performance

The two 8.7-sq m elements differ essentially in the quality of their hermetization and thermal insulation. Each of them were divided into two sections measured separately. After the thermocouples with defective junctions had been removed, the following was the distribution of the 1-sq dm units :

Section	A 1	A 2	B 1	B 2
Number of units . .	416	409	424	402

For a total power of 77 watts under a radiation of 850 W m^{-2}, at the load adopted, the power was distributed as follows among the sections (in watts per sq m)

A1	*A2*	*B1*	*B2*
3.7	4.4_5	5.5_5	5.0

By comparison, the similar elements tested at Colomb Bechar yielded 7 W m^{-2} under a radiation of 1 kW m^{-2}.

Figure 5, plotted from the mean readings, represents the variation of the total power delivered to a battery of 16 alkaline cells of 15 amp h.

It should be noted that, based on the best section, the maximum power under a radiation of 850 W m^{-2} would be :

$$5.6_5 \times 17.4 = 97 \text{ watts}$$

For 7 W m^{-2}, we would have :

$$7 \times 17.4 = 121 \text{ watts}$$

As for the integrated daily energies charging the 16 alkaline cells, the total generator delivered an average of 200 Wh per kWh m^{-2} of solar radiation, above the charging threshold, corresponding to 9.5 Wh m^{-2} for the poorest section, and to 14.5 Wh m^{-2} for the best one. For guidance, we may state that the energy of solar radiation above the threshold of 450 W m^{-2} may reach 3 kWh m^{-2} on a particularly sunny day in the Sahara, from which it would follow that the total useful energy would be close to 600 Wh. But there are also days when the radiation energy is only about 1 kWh m^{-2}.

Information derived

In addition to the dimensioning of the thermocouples, the principal shortcoming of this device resides in the junctions between the aluminium parts, which are mechanically fragile and have an excessive electrical resistance. While this latter fact results in markedly poorer performance, their fragility makes it necessary to transport them in the form of elementary cells and to have the complete and time-consuming assembly done on the site.

The structural principle is technically satisfactory, but involves a rather high first cost. Moreover, even from the technical point of view, defects in the insulation of the mass have been observed after several months of service, presumably due to the humidity.

Finally, neither the chassis nor the auxiliary parts have been studied as completely as the basic cell with a view to rendering them functional.

The 72-sq m generator

Structure

This also has one thermocouple to a square collector 1 dm on a side. The elementary cell here is the band 1 m long, essentially formed of a profile of an aluminium-silicon alloy, with self-supporting ribs, anodized, on which the U-shaped aluminium legs of the thermocouple are attached, providing electrical and thermal conduction. The base plate of the U has an area sufficiently great to transmit the heat from the cold junctions across a silicone adhesive to the rib system. The collectors are made of blackened copper. The metallized thermocouples are soldered to the tin, on the one hand on the collector, and on the other at the upper parts of the legs, with a copper connection. The junctions are very sturdy, since the semiconductor material is not subjected to mechanical stresses due to very different coefficients of expansion. The branches of the U have a certain elasticity, so that the constraints on the soldered sites are small.

The bands, electrically insulated by their anodisation from the thermocouple circuit, are mounted on bakelite bars in modules of 5 units (0.5 sq m) which can be transported in this form if properly packed, in view of the ruggedness of the junctions.

The prefabricated modules are designed for assembly in groups of six into units of 3 sq m. We present here a small 2-module unit. The device being installed has elements of three units, or 18 modules. The chassis is a tube of galvanised steel to which handles of sheet metal and T profiles of galvanised steel are attached. Here again the thermal insulator is of compressed glass wool, and the insulator of the front face is formed of three polyvinyl fluoride sheets and one pane of double glass.

The charging voltage should be from 1 to 1.5 volts per sq m. In practice, the three units of an element are connected in parallel, thus operating between

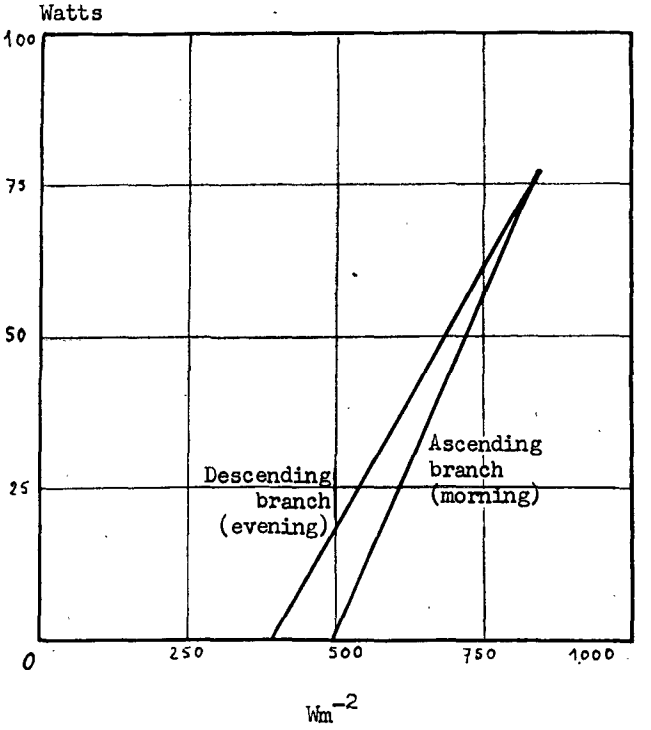


Figure 5. 17-m² generator. Total useful power as a function of solar radiation

3 and 4.5 volts, and the 8 elements are connected in series to charge an airtight 24-volt, 160-amp h alkaline battery across a set of silicon diodes designed to prevent the discharge of the battery through the generator at night. The charging is regulated by an auxiliary arrangement with manual contacts and relays.

Prospects

It is still too early to draw conclusions about the new high-power solar generator. For the first time a generator with the latest technical developments of the radio corporation, manifested especially in the quality of the junctions and the rationalisation of the prefabricated elements, will be subjected to long and continued experimentation in the Sahara.

Minor refinements will of course prove necessary, but except for such details, it may be said that an operational generator, which can be transported in the form of standardised components and assembled relatively rapidly on site, has now been placed on the market.

On these same bases, thermocouples of materials based on bismuth telluride, with oriented crystals, could be substituted for thermocouples of fritted materials, with a marked improvement in performance. Such couples have already been built, and their industrial development will follow in the near future.

The work will proceed in two different main directions :

1. Perfecting generators of this type, for which theory has already fixed the asymptotes; that is, seeking further improvement of the output per unit area by using improved selective collectors, and a reduction of the manufacturing cost per unit area while maintaining satisfactory output. In both cases, the research now in progress on the ageing of junctions will lead to a very great prolongation of undeteriorated performance.

2. Study and realization of generators with increased output using semiconductor thermocouples permitting high temperatures of the hot junctions, with manually or automatically oriented cylindro parabolic mirrors employed to concentrate the light.

Summary

Studies by the Cie Générale de T.S.F. (General Radio Corporation) for the account of the Society for the study and industrial applications of solar energy and of the B.I.A. (Bureau d'Investissement en Afrique (African Investment Bureau)), have been conducted during the last few years in the fields of theory and laboratory research.

After small flat solar generators had been tested at Manosque, France, and Colomb Bechar, Africa, tests on a larger scale were conducted in 1960 near Toulon, France, on a generator 17 sq m in area, and in the same year a genuinely operational 72-sq m generator built of prefabricated standardized components will also be put into service. A small model of it is presented.

Under transparent surfaces of glass or polyvinyl fluoride, which partition the space and oppose heat losses, collector plates are heated by solar radiation, with the object of causing a heat flux to pass through semiconductor thermocouples, which should be of optimum conductance. This heat flux is then removed by a system of fins at the bottom of the generator. With collectors of uniform blackness throughout the visible and infrared spectrum, it is well to use four transparent sheets. With what are called "selective" collectors, having a low infrared emissivity, this number is reduced to two.

The sections of the 17-sq m generator differ in output, and according to the section, the generator produced useful electric power of 3.7 to 5.5 watts/sq m under a radiation of 850 watts/sq m, corresponding for the best section to 7 watts/sq m under a radiation of 1 kW/sq m. In charging a battery of 16 alkaline cells the generator, which was in fact operating at over the radiation threshold of 450 watts/sq m, yielded a quantity of electric energy proportional to the radiation energy integrated above the threshold, or a total yield of about 200 watt-hours per kWh m².

This apparatus, with non-optimised couples, had the disadvantages of imperfect junctions, of insufficiently functional structure of chassis and auxiliary parts, and of excessive fabrication, transportation and assembly costs.

The new generator comprises 8 cells, each of 9 sq m useful area, mounted on a weatherproof metal chassis. Its active elements are 50 sq dm modules, or 50 couples integrally welded under 50 collectors, mounted on ribbed self-supporting profiles. A battery of 20 alkaline cells of 160 amp h should be kept charged by it. While this generator was designed for home installation, it can nevertheless be easily assembled, disassembled and transported in separate modules.

The object envisaged is the employment of thermocouples with improved performance and improved junctions. While selective collectors of treated aluminium have not yet justified their use in preference to blackened collectors, new highly selective collectors are now under study. In this type of device, the ultimate point to be considered is essentially the relation between investment and useful power, and all lines of conduct are subordinate to it.

ORIENTATION DES RECHERCHES TECHNIQUES DE L'I.E.S.U.A. POUR LA PRODUCTION D'ÉNERGIE A PARTIR DU RAYONNEMENT SOLAIRE

M. Perrot * *et M. Touchais* **

L'Institut de l'énergie solaire de l'Université d'Alger s'intéresse organiquement à tous les aspects de l'utilisation pratique de cette énergie considérable qui nous est dispensée par le soleil. Cependant ses efforts actuels s'orientent tout spécialement vers les applications qui, d'une part ont un caractère immédiatement industriel, et d'autre part apparaissent comme susceptibles d'être utilisées au Sahara, que l'on doit considérer comme la grande réserve française d'énergie solaire.

Dans l'état actuel de la technique, seules les transformations thermiques à températures plus ou moins élevées peuvent donner lieu à des applications immédiates; il s'agit de les rendre compétitives avec l'emploi des autres formes d'énergie. Il n'y a d'ailleurs pas lieu de se préoccuper outre mesure des applications elles-mêmes; en effet, dès que l'on pourra mettre à la disposition des industriels des quantités suffisantes d'énergie aux températures voulues et à des prix raisonnables, les divers spécialistes se chargeront de l'utiliser selon leurs techniques propres.

Mais bien que le problème doive être examiné dans toute sa généralité, ce serait une grossière erreur de méthode que de ne pas se référer à priori à une application bien déterminée. En effet, dans les dispositifs à mettre au point, il y a des détails souvent étrangers à l'objet principal qui interviennent d'une manière prépondérante dans le choix des matériaux, des performances, dans les procédés de fabrication ou les méthodes d'exploitation.

Ne pas vouloir en tenir compte, c'est se vouer à des recherches qui risquent de rester stériles. L'objectif que s'est donc proposé l'I.E.S.U.A. a été la réalisation d'une centrale solaire thermo-électrique; projet ambitieux, certes, dans l'état actuel de la technique des semi-conducteurs, mais extrêmement instructif, car les processus thermiques ont une très grande importance dans les générateurs thermo-électriques. L'adaptation des moyens de concentration du rayonnement solaire aux piles thermo-électriques paraît susceptible de révéler des problèmes déjà connus, mais qui se présentent sous un aspect nouveau.

Cependant, les activités de l'I.E.S.U.A. ne se bornent pas à l'étude de ce problème particulier; l'I.E.S. se doit d'examiner systématiquement toutes les applications possibles. Outre les applications thermo-électriques, l'I.E.S. s'intéresse également aux problèmes de conversion thermo-mécanique, ainsi qu'aux problèmes de conversion thermo-ionique et photo-ionique de l'énergie solaire.

Le développement de ces diverses applications dépend étroitement de la possibilité de capter et concentrer de grandes quantités d'énergie.

La présente communication va traiter en conséquence assez succinctement d'abord des moyens de captation et de concentration du rayonnement solaire en vue d'alimenter la source chaude du générateur thermo-électrique, et d'une manière plus développée ensuite, des considérations sur les générateurs thermo-électriques eux-mêmes.

Mais auparavant, il paraît intéressant d'exposer quelques principes directeurs de nos recherches. Certains d'entre eux sont connus, mais il n'est pas inutile de les rappeler. D'autres risquent d'être sujets à controverse, et nous devons essayer de les bien expliciter.

Tout d'abord, il faut s'élever contre le leurre de la quasi-gratuité de l'énergie solaire. Le rayonnement solaire, dans son état actuel, est une énergie encore très chère, et les systèmes de transformation de l'énergie solaire ne peuvent donc pas se permettre de fonctionner avec de mauvais rendements, sauf peut-être pour les petites installations.

D'autre part, ce n'est qu'en apparence que l'énergie solaire paraît être très répandue, nous sous-entendons, bien entendu, avec possibilité de transformation industrielle. Les régions où l'on peut la considérer comme se présentant avec abondance sont malheureusement parmi les plus déshéritées du globe. Il semble donc que l'utilisation de notables quantités d'énergie solaire doive s'accompagner d'une mise en exploitation concomittante des zones arides. Le problème de l'énergie solaire paraît être, en ce qui concerne l'I.E.S.U.A., un problème spécifiquement saharien.

Du fait de sa très grande variabilité, de sa nature aléatoire, on a souvent tendance à confondre les deux problèmes de la transformation du rayonnement solaire en une énergie directement utilisable et celui de son stockage. Lorsqu'il s'agit de petites puissances, ou encore de températures relativement basses, on peut songer au stockage de l'énergie transformée, mais dans la perspective de la fabrication

* Directeur de l'Institut de l'énergie solaire de l'Université d'Alger, Algérie.

** Ingénieur chargé de recherches, Institut de l'énergie solaire de l'Université d'Alger, Algérie.

de grandes quantités d'énergie, le problème se modifie. Ce n'est plus un problème de stockage qui se présente, mais d'énergie de complément. Or il se trouve que, par un heureux hasard, le Sahara, source immense d'énergie solaire, est également un réservoir important de combustibles fossiles. Une centrale solaire apparaît donc nécessairement comme une centrale mixte, soleil et gaz naturel, ou soleil et pétrole.

D'ailleurs, cettte relation qui existe entre le rayonnement solaire et les combustibles fossiles est plus profonde qu'il ne paraît de prime abord. Il semble bien que l'existence véritablement industrielle de l'énergie solaire aura pour conséquence immédiate une certaine limitation dans la consommation des énergies d'origine classiques. Lorsque la transformation industrielle de l'énergie solaire aura une existence effective, le problème de la distribution rationnelle générale des sources d'énergie se posera dans le monde, et il faudra distinguer les énergies qui peuvent s'emmagasiner, se transporter sans gros frais, comme les combustibles liquides, de celles qui doivent être dépensées sur place, dans le voisinage le plus immédiat, comme l'énergie solaire et l'énergie éolienne, ou dont le transport est onéreux, comme l'énergie électrique. Le rendement des installations de transformation de l'énergie solaire se posera alors avec beaucoup plus d'acuité, ce qui vient corroborer les conséquences du premier principe précédemment énoncé. Ainsi, contrairement à ce que l'on pense, la présence de pétrole et de gaz combustibles au Sahara ne diminue pas, bien au contraire, l'intérêt que l'on peut attacher à l'utilisation de l'énergie solaire.

Il ne faut pas oublier, pour termilner, que a transformation de l'énergie solaire par voie thermique en une autre forme d'énergie (énergie mécanique, énergie électrique) exige la présence d'une source froide. Cette source froide ne peut guère se trouver au Sahara que dans l'atmosphère, or la température de l'air ambiant, pour les couches basses de l'atmosphère, peut atteindre de 40 à 50 °C. Deux conséquences importantes en résultent : d'abord la nécessité de fonctionner à la source chaude avec des températures relativement élevées, d'où l'obligation d'une certaine concentration du rayonnement solaire; ensuite l'intérêt des systèmes susceptibles de faire mouvoir une grande masse d'air sans intervention notable d'énergie extérieure. L'Institut de l'énergie solaire était donc tout naturellement amené à étudier, d'une part des systèmes de miroirs, d'autre part les insolateurs à air. Le programme de ses travaux se comprend dès lors aisément :

Étude de la radiation solaire;

Étude des insolateurs, et plus particulièrement des cheminées solaires;

Étude des générateurs thermo-électriques, tout d'abord des générateurs à exposition directe, c'est-à-dire des insolateurs thermo-électriques, ensuite à circulation de fluide, ce qui entraîne l'étude des systèmes de miroirs et de chaudières.

Nous allons examiner ici plus particulièrement, les systèmes de captation et de concentration du rayonnement solaire et les générateurs thermo-électriques.

La captation avec concentration du rayonnement solaire

Il s'agit bien entendu de la captation sur de grandes surfaces, mais envisagée dans une application particulière à la thermo-électricité. On peut envisager pour cela l'extension des grands miroirs qui ont été construits en divers points du globe : l'héliodyne de la station solaire de la Bouzareah, le four solaire de Mont-Louis et celui en cours de projet d'Odeillo, le four solaire de Natike, enfin celui actuellement en construction à Tokyo. Ces fours sont surtout des appareils d'expérimentation, et sont beaucoup trop onéreux pour devenir des appareils industriels. L'héliodyne, par exemple, qui a été conçue pour une réalisation industrielle, puisque les surfaces réfléchissantes sont fabriquées par emboutissage, revenait à l'époque de sa construction à environ 20 000 NF le mètre carré de surface de captation. L'appareil de Tokyo revient, d'après les renseignements que nous avons pu avoir, à environ 7 500 NF le mètre carré de surface de captation, mais ce prix ne comprend pas de nombreux postes, les études en particulier, dont il a été tenu compte dans le prix précédent de l'héliodyne.

La façon de concevoir le mode de captation du rayonnement solaire dépend des températures que l'on désire obtenir. Pour des températures inférieures à 300 °C, ce qui est à peu près la température d'évaporation de certains liquides thermophores comme le « Gilotherm » ou le « Fluitherm » on peut s'adresser aux systèmes à foyers multiples que nous appellerons des *collecteurs* [1] par opposition aux *insolateurs*. Il y a là une question de terminologie qu'il y aurait lieu de clarifier. Nous préférons pour notre part appeler insolateurs les appareils qui opèrent la transformation en chaleur à l'endroit même qui reçoit le rayonnement. Les collecteurs introduisent une opération supplémentaire, qui est le changement de direction du rayonnement avec effet directif, afin de produire la concentration. Cela n'exclut pas, pour les insolateurs, la possibilité d'un certain renforcement du rayonnement solaire, qui ne va pas au-delà de quelques unités et qui peut être produit, soit par des miroirs, soit par les surfaces diffusantes, soit par des couvertures réfractrices. Cela n'exclut pas non plus, pour les insolateurs, une certaine concentration par conduction thermique longitudinale, ainsi que nous l'expliquerons plus loin en détail. Pour nous, les collecteurs sont, en définitive, des systèmes à focalisations multiples. Ils peuvent, comme les insolateurs, être protégés par une couverture qui a un double but, celui de protéger les surfaces réfléchissantes (le nettoyage d'une couverture transparente étant plus aisé que celui d'un miroir, dont la surface est toujours délicate), et celui de séparer ensuite l'atmosphère

[1] On les appelle aussi des *insolateurs par focalisation*.

intérieure, qui s'échauffe en raison des diverses pertes, parmi lesquelles il faut compter l'absorption propre des miroirs, pour permettre dans une certaine mesure la récupération de ces pertes. Le gros avantage des systèmes à foyers multiples est de ne pas nécessiter une très grande précision dans l'orientation de ces surfaces. Il peut donc être fait usage de mécanismes relativement rustiques; or, c'est ce problème d'orientation des surfaces réfléchissantes qui est le gros problème de la concentration du rayonnement solaire. On peut être tenté, d'ailleurs, de simplifier ce problème en ne se bornant qu'aux modifications saisonnières de l'orientation, et il faut alors utiliser des réflecteurs cylindro-paraboliques. Nous pensons qu'en la matière il n'est pas opportun d'être pour les demi-mesures; nous nous tournons résolument vers les éléments de surfaces paraboloïdes et devrons porter tous nos efforts vers la réalisation économique des supports orientables. Il faut remarquer que, dans le cas des surfaces étendues, une certaine simplification dans le mécanisme d'orientation peut être apportée, en observant que le mouvement des collecteurs se fait de manière que les surfaces de captation sont toutes parallèles.

Les collecteurs que nous avons en vue, établis selon des procédés mis au point par des firmes locales, sont conçus de manière à chauffer un liquide thermophore qui soit en même temps isolant électrique. C'est la circulation de ce liquide sur les armatures chaudes des piles thermo-électriques qui apporte par convection la chaleur à transformer en énergie électrique. L'utilisation de ce fluide serait mixte. Une première chute de température se ferait dans les piles thermo-électriques, et une autre dans les appareils de chauffage destinés, soit à la circulation de l'air de refroidissement, soit pour tout autre usage. Les surfaces réfléchissantes sont en tôles très minces d'aluminium brillantées et aluminées, ou en plastique tel que la « Lumaline » collé sur des formes spéciales en stuc ou en polyester armé de fibres de verre.

Pour des températures supérieures à 300 °C, notre projet se résume dans l'utilisation de deux procédés nouveaux[2]. C'est un système assez complexe à foyer unique qui utilise une multitude de miroirs indépendants, répartis sur le terrain exploité. Chaque miroir, à un instant donné, est orienté de manière à concentrer le rayonnement reçu dans l'ouverture du foyer, placé en élévation et à une certaine distance au-dessus du sol. Ainsi que l'on peut s'en rendre compte immédiatement, un tel système exige la réalisation précise de deux conditions :

Une orientation exacte et indépendante des vicissitudes atmosphériques;

Une forme exacte amenant le faisceau réfléchi à se concentrer très précisément dans l'ouverture du foyer. Chaque élément de miroir représente à chaque instant un élément de paraboloïde dont les paramètres varient avec le temps.

[2] Brevets français 1 238 883 et PV 830 443.

Il s'agissait donc, en étude préliminaire, de s'assurer :

1) Des conditions imposées par la distribution de tels éléments de miroirs sur le terrain;

2) D'examiner les différentes possibilités de mécanismes d'orientation et la télécommande précise de ces mécanismes;

3) De vérifier la possibilité de réaliser simplement des surfaces paraboloïdales de formes variables.

Des travaux assez importants ont été entrepris en ce qui concerne les deux premiers points. Il paraît encore prématuré d'en donner les résultats. Quant au troisième point, nous avons cherché à réaliser les éléments paraboloïdes réfléchissants avec de simples tôles d'aluminium brillantées et aluminées. Les premières expériences ont été encourageantes, puisque nous avons réussi à focaliser sur une distance de 9 m avec des aberrations inférieures à 5 millièmes, en utilisant une tôle d'aluminium de 16-10 mm d'épaisseur en rectangles de 1 mètre sur 0,5 m.

La concentration de grandes quantités de rayonnement solaire conduit à prévoir la focalisation sur des distances plus grandes que celles expérimentées, ce qui nécessite à fortiori des rayons de courbure plus grands, ce qui entraîne une plus grande facilité de déformation des tôles réfléchissantes.

En première étape, avec ce système de captation, nous avons l'intention d'utiliser l'air comme fluide intermédiaire pour le chauffage des armatures chaudes des piles thermo-électriques. La raison en est que pour avoir de très grandes quantités d'énergie, nous nous heurterions à de très grandes difficultés si nous voulions réaliser un foyer fermé. Le foyer ouvert est beaucoup plus simple, mais il entraîne la nécessité de chauffer l'air, même si ce n'était pas le but poursuivi et la fonction principale du foyer.

Tandis que les collecteurs du rayonnement solaire paraissent être une solution immédiate, susceptible de résoudre sans trop de difficultés le problème du générateur thermo-électrique fonctionnant avec un rendement acceptable, les systèmes à champs de miroirs déformables paraissent devoir être une solution d'avenir, non seulement pour la conversion thermo-électrique, mais surtout pour les conversions thermo et photo-ioniques du rayonnement solaire. L'I.E.S. se doit de ne pas négliger cette solution. Elle pose toutefois, pour l'instant, des problèmes techniques extrêmement complexes et que nous aborderons l'un après l'autre.

Nous allons exposer maintenant, d'une manière un peu plus détaillée, nos travaux et nos projets concernant les générateurs thermo-électriques proprement dits.

Conversion du rayonnement solaire par voie thermo-électrique

Un générateur thermo-électrique est essentiellement constitué d'un ensemble de thermo-éléments disposés entre deux armatures : une armature chaude et une armature froide.

La chaleur peut être amenée à l'armature chaude soit par un fluide (liquide ou gaz) circulant sans changer de phase le long de surfaces en contact direct avec l'armature chaude, soit par condensation d'une vapeur sur ces surfaces, soit enfin par conversion directe du rayonnement solaire en énergie thermique.

La chaleur, après avoir traversé les thermo-éléments, peut être évacuée, soit comme précédemment par circulation d'un fluide sans changement de phase, soit par vaporisation d'un liquide, soit enfin par rayonnement dans l'espace.

Lorsque le générateur est directement insolé, il peut être *fixe* ou *orientable*. Dans le premier cas, la surface réceptrice du rayonnement ne doit en principe pas être directive, sauf peut-être pour les positions basses du soleil; le rayonnement peut être *renforcé* par des miroirs fixes ou des diffuseurs. Dans le deuxième cas, la surface peut être directive; c'est le cas des surfaces formées de cônes creux à petit angle au sommet, ou des surfaces fonctionnant par réflexion ou réfraction.

Les surfaces réceptrices peuvent être sélectives, c'est-à-dire absorber convenablement dans le spectre visible et émettre peu dans l'infra-rouge éloigné. Cette sélectivité peut être obtenue par un traitement approprié de la surface, ou encore par l'interposition sur le rayonnement à l'arrivée d'une couverture transparente fonctionnant par « effet de serre », enfin par les deux procédés simultanément.

Lorsque l'exposition du générateur est fixe, il existe une inclinaison optima qui dépend de la latitude, de l'absorption moyenne atmosphérique et des caractéristiques statistiques de la nébulosité.

Lorsqu'il y a circulation d'un fluide, le mouvement peut être *naturel* (thermo-siphon, principe de la paroi froide) ou bien *forcé*. Dans ce cas, le générateur comporte des parties supplémentaires pour les services auxiliaires (ventilateurs ou pompes).

Lorsque le générateur thermo-électrique est destiné à la conversion de l'énergie solaire en énergie électrique, il est nécessaire de tenir compte de la grande variabilité du rayonnement solaire : variation diurne régulière ou accidentelle. Deux modes d'exploitation sont alors possibles : ou bien le chauffage des armatures chaudes se fait à l'aide d'un fluide intermédiaire, ou bien il est procédé à l'insolation directe.

Dans le premier cas, on s'arrange bien entendu pour fonctionner à températures constantes, et ces températures sont choisies aussi voisines que possible de celles de meilleur rendement du matériau thermo-électrique mis en œuvre. C'est évidemment alors le débit du fluide qui varie, et il en résulte une variation du nombre de piles élémentaires en service. Pratiquement, le générateur est divisé en un certain nombre de groupes de piles qui sont introduits dans le circuit électrique ou éliminés pour maintenir constante la tension aux bornes, à la tolérance admise près.

Dans le deuxième cas, il faut interposer entre le générateur et l'utilisation un convertisseur continu-continu qui permette l'adaptation de la résistance du circuit de charge à la résistance interne du générateur et qui soit également régulateur de tension. Mais le rendement moyen du générateur est bien plus bas dans ce deuxième cas.

De toutes façons, quel que soit le mode d'exploitation, il existe une température maximum des armatures chaudes à ne pas dépasser sous peine de dégradation irréversible du générateur. L'installation du générateur doit alors être complétée par des organes de sécurité.

A ces considérations techniques très générales, il faut ajouter les sujétions climatologiques. L'I.E.S.-U.A. s'intéresse tout particulièrement aux applications sahariennes de l'énergie solaire. C'est donc dans le cadre d'une utilisation possible au Sahara qu'il convient d'étudier la construction des générateurs thermo-électriques. Trois observations importantes sont à faire :

1) Il est loisible au Sahara de choisir des sites où l'ensoleillement est élevé.

2) On ne peut guère compter que sur l'air ambiant pour le refroidissement des générateurs. Toutefois la grande siccité de l'air permet d'envisager un complément de refroidissement par humidification.

3) Les vents de sable ou de poussière sont assez fréquents. Le talus naturel du sable sec provenant de l'érosion est de 22° sur l'horizontale, mais les poussières extrêmement fines, dont les dimensions peuvent atteindre quelques microns, s'accrochent très facilement. Par vent de sable, les grains les plus gros, dont on peut craindre l'accumulation ou l'effet de décapage, ne s'élèvent guère au-dessus de 2 m.

Il résulte de ces observations :

a) Que les générateurs thermo-électriques doivent être organisés pour être refroidis par circulation d'air. Or cet air peut atteindre en certaines circonstances des températures relativement élevées (40 ou 45 °C).

b) Que le salissement des systèmes de captation ou des couvertures transparentes des insolateurs peut amener d'importantes réductions de l'énergie incidente et des frais élevés d'exploitation pour le nettoyage. Les surfaces traitées pour être sélectives perdent leurs propriétés lorsqu'elles sont recouvertes de poussière.

Les questions financières ont également leur incidence. Le matériau thermo-électrique est relativement cher. On peut trouver en France du tellurure de bismuth des types N et P à environ 7 000 NF le kg. Ce prix est plus que doublé pour les matériaux de provenance américaine. D'autre part, la mise en œuvre des matériaux est délicate, les armatures sont assez ouvragées, surtout lorsqu'elles comportent des radiateurs à air. Les coefficients de transfert par convection de l'air sont en effet généralement faibles, ce qui oblige à des surfaces développées. Il apparaît donc indispensable de faire fonctionner les thermo-éléments dans les meilleures conditions de rendement, c'est-à-dire à la température la plus favorable. Cela suppose, si la chaleur est fournie par le soleil, l'emploi

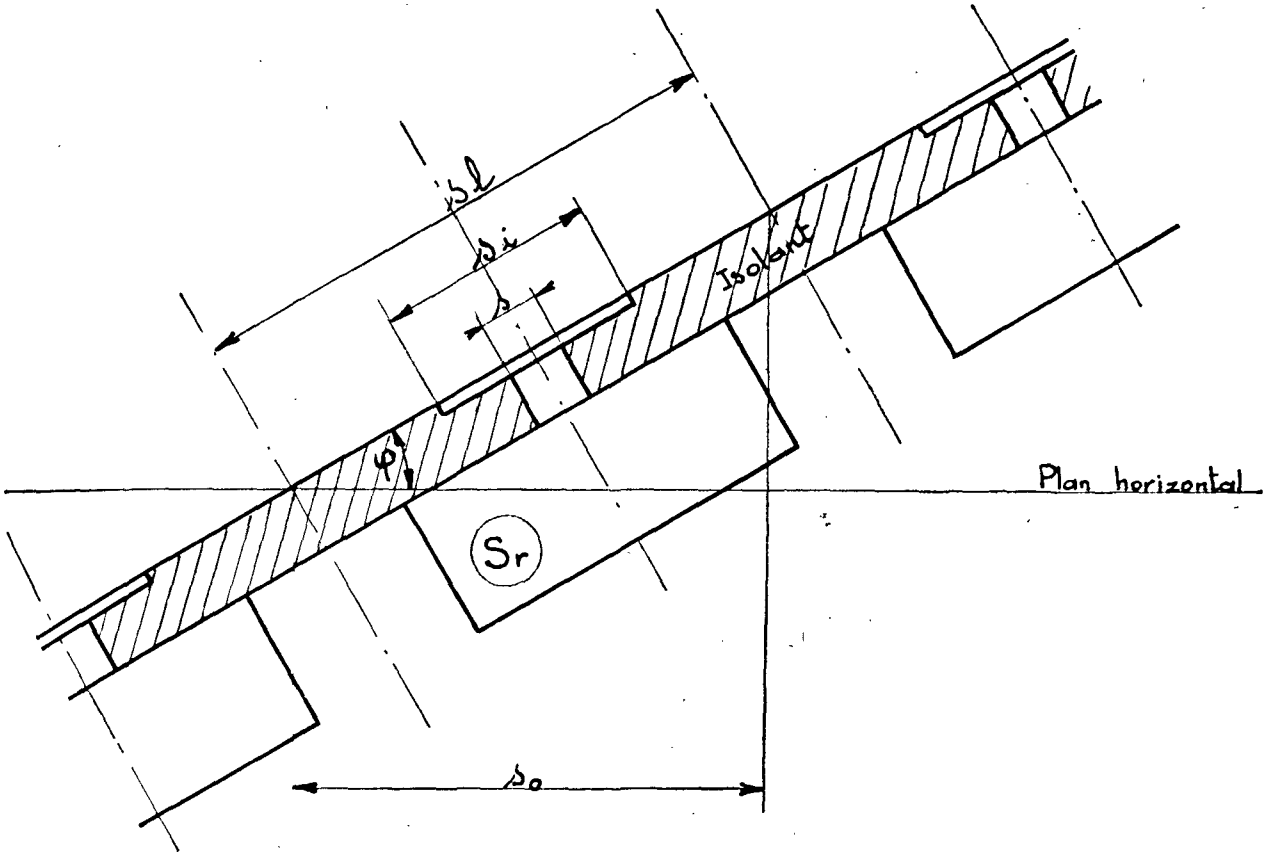


Figure 1

d'un fluide intermédiaire et d'un système de captation et de concentration du rayonnement au foyer d'une chaudière.

La circulation de l'air de refroidissement, d'autre part, doit autant que possible être provoquée par le chauffage solaire lui-même, afin d'éviter de prélever sur un organe de transformation, dont le prix est nécessairement élevé, une partie de l'énergie nécessaire au mouvement de l'air.

On voit qu'une telle installation met en œuvre des éléments techniques très divers, qu'il convient d'étudier chacun séparément en eux-mêmes, d'abord.

Les insolateurs à air font l'objet d'une communication séparée (mémoire S/45). Leur étude est facilitée par un procédé d'analogie électrique qui est très utile également dans l'étude des insolateurs thermo-électriques. Ce procédé sera décrit dans la présente communication, qui traitera plus spécialement du générateur thermo-électrique lui-même, et décrira le prototype en cours d'expérimentation à l'Institut de l'énergie solaire de l'Université d'Alger.

Le problème du matériau le plus convenable à employer, de son usinage et de son montage sur les armatures a été laissé complètement de côté. Des laboratoires très importants, tant en France qu'à l'étranger, étudient avec soin ces questions. L'.I.E.S. s'est donc borné, dans une phase préliminaire, à examiner les problèmes que pouvait soulever la construction d'un insolateur thermo-électrique fixe, à exposition directe, de petite puissance, destiné à être utilisé au Sahara en vue d'alimenter, soit des systèmes de télétransmissions (télémesures ou télécontrôles), soit de très petites machines (ventilateurs de conditionnement, petites pompes de service d'eau, etc). Il importait en effet de savoir si, pour de petites applications, il était possible de réaliser un générateur assez rustique, et dont le prix de revient ne soit pas prohibitif.

Les surfaces de réception sélectives ayant été abandonnées pour des raisons de salissement, il importait d'étudier plus particulièrement la surface absorbante de l'armature chaude. D'autre part, subsistait toujours le problème de l'évacuation de la chaleur ayant traversé les éléments thermo-électriques. Une observation d'ordre économique a permis d'orienter les solutions :

Il faut commencer par bien s'entendre sur l'exacte signification qu'il convient de donner à la *surface du générateur*. Dans l'étude analytique de la question, plusieurs surfaces se présentent (figure 1) :

Tout d'abord la *section* s de l'élément thermo-électrique (s_n pour l'élément du type n, s_p du type p) qui intervient dans la définition du *rapport de forme* $\gamma = h/s$, h étant la hauteur du barreau thermo-électrique. Si le générateur comporte n éléments (soit $n/2$ couples), la section totale ou surface des éléments thermo-électriques est $n/2$ $(s_n + s_p)$.

L'armature chaude présente généralement une *surface insolée* s_i qui est constante si elle est plane, mais qui peut varier avec la position du soleil si elle présente des creux ou des saillies; s_i est alors la surface insolée à midi vrai, lorsque le soleil est dans le plan équatorial.

L'insolateur lui-même réserve pour chaque élément une surface s_1 ou *surface illuminée* dont la projection sur le plan horizontal est $s_o = s_1/\cos\varphi$, en désignant par φ l'inclinaison (généralement voisine de la latitude du lieu) de la surface réceptrice de l'insolateur sur le plan horizontal.

s_o est la *surface d'occupation* du terrain associé à l'élément. On voit aisément que seules des considérations économiques peuvent empêcher que s_1 soit beaucoup plus grand que s_i. Mais si le prix de l'élément thermo-électrique est relativement élevé, rapporté à sa surface insolée, le prix de l'excédent de surface illuminée peut être très faible. Il suffit en effet à cette surface excédentaire de représenter une bonne isolation thermique entre la région des armatures chaudes et la région des armatures froides. Si cette surface excédentaire est absorbante, toute l'énergie solaire reçue alimente les pertes, sauf si un léger courant de convection s'établit entre la surface isolante chaude et les armatures voisines, qui sont nécessairement, du fait de l'écoulement de la chaleur, à une température moins élevée. Il peut donc être bénéfique d'avoir une surface illuminée supérieure à la surface insolée. D'autant plus que l'on fournit ainsi à l'armature froide plus de place pour développer ses surfaces radiatrices.

Dans ces conditions, rapporter la puissance électrique produite à la surface occupée sur le terrain n'a pas beaucoup de signification, surtout lorsque ce terrain est situé au Sahara. De même, inclure dans les pertes celles de la surface excédentaire n'a pas beaucoup plus de sens que si on voulait inclure également les pertes de toutes les surfaces désertiques ou inutilisées du globe.

Il existe dès lors deux moyens de réaliser le radiateur de l'armature froide : soit disposer des ailettes de refroidissement perpendiculairement à la surface réceptrice, soit, ce qui apparaît plus rationnel (car on peut développer plus facilement les surfaces de refroidissement), les disposer parallèlement.

La forme des surfaces illuminées n'est pas quelconque. Ces surfaces se disposent en effet comme les éléments d'un carrelage; elles doivent donc être carrées ou hexagonales. Cette dernière est la meilleure forme, comme étant la plus proche du cercle. C'est la forme à adopter pour les ailettes parallèles à la surface réceptrice.

L'Institut de l'énergie solaire, dans son prototype (figure 1), a adopté les ailettes normales, comme étant de construction plus facile. Les éléments sont alignés côte à côte, et les rangées ainsi réalisées sont séparées entre elles par une surface noircie simplement isolante.

Toutefois, pour régulariser un peu l'insolation des armatures chaudes, ces dernières sont munies d'ailettes basses, méridiennes, qui ne se portent pas ombre dès que le soleil dépasse une hauteur de 30°, hauteur admise pour le seuil de fonctionnement du générateur. Ces ailettes, ainsi que celles des armatures froides, servent également de connexions électriques entre les éléments.

Le mouvement de l'air est activé par le tirage d'une cheminée. Une chambre de détente à l'arrivée de l'air de refroidissement le dépoussière des grains les plus lourds; il traverse ensuite les surfaces d'évaporation d'un humidificateur qui peut abaisser sa température de près de 10 °C avant de circuler sur les ailettes de refroidissement.

Les grandes lignes du générateur désiré ayant été arrêtées, il fallait procéder au dimensionnement optimum des diverses parties.

Nous avons été amenés à établir pour cela une théorie simplifiée du fonctionnement des thermopiles, qui a pu recevoir une représentation électrique, ce qui a permis de vérifier, avant construction, les diverses particularités de fonctionnement, ce qui a permis également de modifier certains points de détail en raison de la connaissance plus précise des phénomènes. La méthode d'étude par analogie électrique a un second avantage, outre celui de préfigurer le fonctionnement d'un générateur projeté. Le générateur étant construit, en effet, il n'est guère possible de le démonter pour modifier certains éléments dont dépendent les dimensions définitives. On utilise alors la méthode analogique réglée d'abord de manière à représenter avec une assez bonne approximation les phénomènes tels qu'ils sont observés sur le générateur réel. Il est alors assez facile d'apporter les modifications désirées sur le modèle analogique et d'expérimenter sur lui, avec quelque chance de certitude.

Il n'est même pas nécessaire d'équiper le générateur en étude de tous ses éléments thermo-électriques. Le fonctionnement thermique étant le phénomène essentiel, les matériaux thermo-électriques peuvent être utilisés pour réaliser un petit nombre de couples, qui sont disposés au milieu des autres, équipés d'un matériau quelconque ayant même résistance thermique. Le fonctionnement électrique étudié sur ce petit nombre d'éléments réels peut sans aucune difficulté être extrapolé à l'ensemble des éléments. Tout ceci n'est valable, bien entendu, que dans l'hypothèse, malheureusement vérifiée, d'un assez faible rendement du générateur.

Quoi qu'il en soit, ces méthodes approchées peuvent être d'un précieux enseignement pour l'emploi de méthodes plus précises qui s'imposeraient pour des rendements supérieurs à 6 ou 7 p. 100.

Étude électrique et thermique simplifiée des générateurs hélio-thermo-électriques

Rendement interne

Dans l'étude du fonctionnement des piles thermo-électriques, on a coutume de partir du système

classique d'équations I, dont quatre seulement sont indépendantes :

$$
\begin{aligned}
q_c &= \frac{T_c - T_f}{R_t} - \frac{r_t I^2}{2} + I \alpha T_c \\
q_f &= \frac{T_c - T_f}{R_t} + \frac{r_t I^2}{2} + I \alpha T_f = \frac{T_f - T_a}{R_f} \\
P_u &= q_c - q_f = -r_t I^2 + I \alpha (T_c - T_f) = r_e I^2 \\
I &= \alpha \frac{T_c - T_f}{r_t + r_e}
\end{aligned}
\qquad (1)
$$

Dans ce système :

q_c est la quantité de chaleur fournie par la source chaude, dans l'unité de temps, à la température T_c, en °C;

q_f est la quantité de chaleur enlevée par la source froide, dans l'unité de temps, à la température T_f, en °C;

R_t est la résistance du couple thermo-électrique entre soudures (les barreaux du couple sont thermiquement en parallèle);

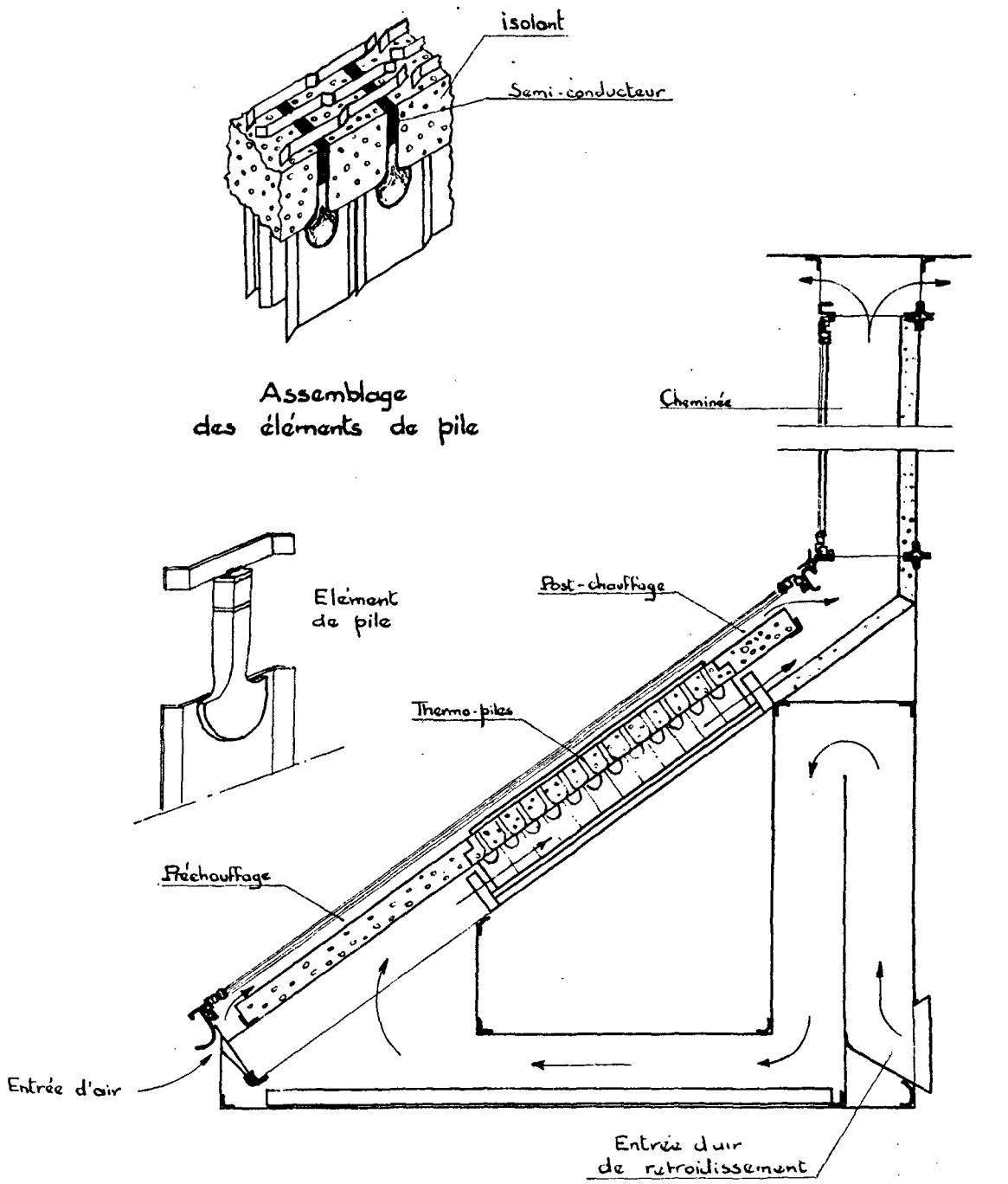


Figure 2. Thermogénérateur : coupe méridienne

R_f est la résistance thermique des radiateurs d'évacuation de la chaleur au milieu ambiant à la température T_a, en °C (les radiateurs du couple sont thermiquement en parallèle);

r_i est la résistance électrique du couple entre soudures, ou résistance interne (les barreaux du couple sont électriquement en série);

r_e est la résistance externe; elle comporte la résistance de charge r' disposée entre les bornes de la pile et la résistance électrique r des soudures et des connexions intérieures;

P_u est la puissance électrique utilisable; la puissance réellement utilisée est

$$P = r' I^2 = P_u - r I^2;$$

I est l'intensité dans le circuit électrique, en ampères;

α est le pouvoir thermo-électrique du couple, en V/°C.

On pose :

$$(1\text{-}1)\quad m = \frac{r_e}{r_i}, \qquad (1\text{-}2)\quad k = \frac{R_f}{R_i}, \qquad (1\text{-}3)\quad \gamma = \frac{h}{s}$$

h étant la hauteur du barreau thermo-électrique et s sa section; γ est le *rapport de forme*. Généralement, les deux barreaux d'un couple, de rapports de forme γ_1 et γ_2 ont des caractéristiques différentes : α_1, ρ_1, $\varkappa_1$, pour l'un, α_2, ρ_2, $\varkappa_2$, pour l'autre. On a :

$$(1\text{-}4)\quad r_i = \rho_1 \gamma_1 + \rho_2 \gamma_2, \qquad (1\text{-}5)\quad R_i = \frac{\gamma_1 \gamma_2}{\varkappa_1 \gamma_2 + \varkappa_2 \gamma_1}$$

ρ étant la résistivité électrique, et $\varkappa$ la conductibilité thermique.

Il est possible de définir un barreau fictif de rapport de forme $\gamma = \gamma_1$ et de caractéristiques :

$$\alpha = \frac{\alpha_1 + \alpha_2}{2}$$

$$\rho = \frac{1}{2}\left[\rho_1 + \sqrt{\rho_1 \rho_2 \frac{\varkappa_2}{\varkappa_1}}\right]$$

$$\varkappa = \frac{1}{2}\left[\varkappa_1 + \sqrt{\varkappa_1 \varkappa_2 \frac{\rho_2}{\rho_1}}\right]$$

On peut alors se permettre de ne considérer que l'un des éléments du couple.

r_i, R_i, R_f sont dès lors relatifs à ce seul élément et non, comme précédemment, au couple. On a dans ces conditions :

$$(1\text{-}4')\quad r_i = \rho \gamma, \qquad (1\text{-}5')\quad R_i = \frac{\gamma}{\varkappa} \text{ et } \qquad (1\text{-}6)\quad k \gamma = \varkappa R_f$$

Il y a lieu de noter ici que α est sensiblement indépendant de la température. Par contre ρ et $\varkappa$ dépendent généralement des températures extrêmes T_c et T_f, et k des températures extrêmes T_f et T_a.

S'il y a n éléments (soit $n/2$ couples), la résistance électrique interne du générateur est

$$(1\text{-}7)\qquad r_{i_t} = n r_i$$

sa résistance thermique interne est :

$$(1\text{-}8)\qquad R_{i_t} = \frac{R_i}{n}$$

la résistance thermique du radiateur est :

$$(1\text{-}9)\qquad R_{f_t} = \frac{R_f}{n}$$

Le *facteur de mérite*, défini par Joffe, de ce matériau fictif, est :

$$Z = \frac{\alpha^2}{\rho \varkappa}$$

Nous préférerons considérer le rapport inverse :

$$(1\text{-}10)\qquad \tau = \frac{\rho \varkappa}{\alpha^2}$$

qui est homogène à une température absolue, et que nous appellerons *température caractéristique* du matériau. τ dépend généralement lui aussi, des températures T_c et T_f.

On pose encore :

$$(1\text{-}11)\qquad q_u = \frac{T_c - T_f}{R_i} = \frac{\varkappa}{\lambda}(T_c - T_f)$$

Le *rendement interne* de la pile thermo-électrique est :

$$(1\text{-}12)\qquad \eta_i = \frac{P_u}{q_c}$$

On montre que le rendement η_i et la puissance P_u sont maxima lorsqu'on fait $m = 1$, à la condition, ce qui est le cas avec les matériaux actuellement connus, fonctionnant à des températures relativement peu élevées, que le rendement soit faible.

On a alors :

$$(1\text{-}13)\quad P_u = \frac{\alpha^2 (T_c - T_f)^2}{4 \rho \gamma} = \frac{(T_c - T_f)^2}{4 \tau} \frac{\varkappa}{\gamma}$$

et, pour n éléments :

$$(1\text{-}14)\qquad P_{u_t} = n P_u = \frac{(T_c - T_f)^2}{4 \tau} \frac{\varkappa s}{h}$$

Si s_i est la portion de surface insolée correspondant à l'élément considéré, nous appellerons *rapport de concentration* le rapport :

$$(1\text{-}14)\qquad C = \frac{s_i}{s}$$

Le volume du matériau thermo-électrique d'un élément est :

$$(1\text{-}15)\qquad v = h s$$

Rendement global

La surface insolée s_i, section du faisceau lumineux incident pour un miroir, qui est la surface réceptrice dans le cas d'un insolateur à exposition directe, absorbe la quantité de chaleur q_a.

Désignons par $Q_{i\Theta}$ la radiation incidente, qui est la radiation directe dans le cas des miroirs et l'éclairement énergétique total de la surface exposée dans le

cas d'un insolateur. $Q_{t\Theta}$ dépend de la position du soleil et des conditions météorologiques.

Si le chauffage a lieu par circulation d'un fluide, on s'arrange pour réaliser pendant la durée de fonctionnement les conditions de transformation optima. On admet en première analyse que la température ambiante reste constante, alors qu'en réalité, on le sait, elle varie avec $Q_{t\Theta}$ dans le même sens mais avec un décalage d'une heure ou deux; les conditions optima se traduisent par la permanence des diverses grandeurs en jeu. On a donc :

$$q_a = \eta s_t Q_{t\Theta} = \text{Cte} \qquad (2\text{-}1)$$

η étant le rendement de la transformation du rayonnement solaire en chaleur.

C'est la surface insolée s_t qui doit alors varier avec $Q_{t\Theta}$ pour maintenir permanentes les conditions de fonctionnement.

Si le chauffage a lieu par insolation directe, on a :

$$q_a = \alpha_s \tau_v Q_{t\Theta} s_t + q_e s_t \qquad (2\text{-}2)$$

en désignant par :

α_s le facteur moyen d'absorption de la surface insolée,

τ_v le facteur de transmission des milieux traversés par le rayonnement avant d'arriver à la surface réceptrice,

q_e la quantité de chaleur fournie à l'armature chaude, généralement par convection, par les surfaces illuminées excédentaires.

q_a est alors variable.

La puissance q_p perdue par le générateur en amont de l'armature chaude ne dépend alors que de la température T_c de cette armature, de la température ambiante T_a et éventuellement de celle T_{vc} de la voûte céleste, cette dernière pouvant atteindre par ciel très clair — 100 °C; q_p en aucun cas, ne dépend des caractéristiques strictement thermo-électriques de la pile.

q_p est le plus souvent nul lorsqu'on opère le chauffage par circulation d'un fluide. Il n'en est pas de même pour les insolateurs. Lorsque le générateur fonctionne comme insolateur, l'expérimentation montre que l'on peut écrire avec une assez bonne approximation, dans les zones de températures où l'on opère :

$$q_p = [a + b\,(T_c - T_a) + c\,(T_c - T_a)^2]\, s_t \qquad (2\text{-}3)$$

où a, b, c, sont des coefficients, rapportés à une surface insolée unitaire, qui sont positifs, et qui dépendent des conditions météorologiques et plus spécialement du vent. La valeur de c est d'ailleurs assez petite. Ainsi pour une surface noircie, avec une couverture formée de deux verres, on a, en air calme:

$a = 40$ W, $\quad b = 3{,}2$ W/°C, $\quad c = 0{,}023$ W/°C²

On a d'autre part :

$$q_c = q_a - q_p \qquad (2\text{-}4)$$

Le système (I) donne alors :

$$q_a - q_p = q_f - r_i I^2 + I\alpha\,(T_c - T_f = q_f + P_u$$

et finalement :

$$q_a = q_f + q_p + P_u \qquad (2\text{-}5)$$

Le *rendement global* du générateur est :

$$\eta_g = \frac{P_u}{q_a} \qquad (2\text{-}6)$$

Pour une énergie incidente donnée, ce rendement varie comme la puissance utilisable. Il y a donc lieu en définitive, de ne rechercher que les conditions de puissance utilisable maxima.

Théorie simplifiée

Dans la théorie élémentaire du système, on suppose que le rendement est assez petit pour que la puissance utilisable soit faible auprès des flux de chaleur en jeu. On peut alors admettre que tout se passe comme si la transformation de chaleur en énergie électrique se faisait au niveau de la jonction chaude et que les pertes par effet Joule n'apparaissaient qu'au niveau de cette jonction. Cette hypothèse n'est qu'un expédient mathématique et n'a bien entendu aucune signification physique [3]. Elle se traduit simplement par la relation :

$$q_u = q_f \qquad (3\text{-}1)$$

ou encore :

$$\frac{T_c - T_f}{R_t} = \frac{T_f - T_a}{R_f} \qquad (3\text{-}2)$$

d'où l'on tire :

$$T_c - T_f = \frac{T_c - T_a}{1 + k} \qquad (3\text{-}3)$$

et

$$T_f - T_a = (T_c - T_a)\,\frac{k}{1 + k} \qquad (3\text{-}4)$$

(2-5) devient :

$$q_a = q_u + q_p + P_u \qquad (3\text{-}5)$$

(1-11) s'écrit :

$$q_u = \frac{T_c - T_a}{1 + k}\,\frac{\varkappa}{\gamma} \qquad (3\text{-}6)$$

(1-12) s'écrit :

$$\eta_t = \frac{P_u}{q_a - q_p} \simeq \frac{P_u}{q_u} = \frac{T_c - T_a}{\tau}\,\frac{1}{4\,(1 + k)} \qquad (3\text{-}7)$$

(1-13) s'écrit

$$P_u = \frac{(T_c - T_a)^2\,\varkappa}{4\,\tau\,(1 + k)^2\,\gamma} = \frac{(T_c - T_a)^2}{4\,\tau}\,\frac{k}{R_f\,(1 + k)^2} = \frac{\alpha^2}{4\,\rho\,\gamma}\left[\frac{T_c - T_a}{1 + k}\right]^2 \qquad (3\text{-}8)$$

et, pour n éléments :

$$P_{u_t} = \frac{(T_c - T_a)^2\,\varkappa\, n\, s}{4\,\tau\,(1 + k)^2\,h} \qquad (3\text{-}9)$$

[3] On montre que l'erreur qui résulte de cette hypothèse sur le calcul du rendement interne est seulement $\Delta\eta_i = \eta_i^2/\theta$ en désignant par θ le rendement du cycle de Carnot évoluant entre les mêmes températures. Ainsi pour $\eta_i = 1$ p. 100, $\theta = 50$ p. 100, $\Delta\eta_i = 2 \cdot 10^{-4}$.

A l'aide des formules ainsi établies, nous allons étudier les deux cas qui nous intéressent plus spécialement :

1) Chauffage du générateur par convection : circulation d'un fluide ou condensation d'une vapeur.

2) Chauffage du générateur par insolation.

Dans le premier cas, on peut considérer que l'on a affaire à une source chaude quasi infinie, et l'on peut supposer que le générateur fonctionne à températures constantes, et plus particulièrement aux températures T_c et T_f optima pendant toute la durée de captation du rayonnement solaire.

Dans le deuxième cas, le flux de chaleur absorbé est limité au rayonnement solaire et varie avec lui. Le générateur fonctionne à températures variables. Il existe un seuil des températures qui est défini par les possibilités techniques d'utilisation de l'énergie produite.

Nous n'examinerons que le cas du refroidissement par circulation d'air à la température ambiante, en convection naturelle ou forcée. La résistance R_f est alors de la forme :

$$R_f = \frac{1}{A\, S_r\, (T_f - T_a)^{0,25}} \tag{3-10}$$

en désignant par S_r la surface d'échange du radiateur, A étant un coefficient qui dépend de la forme et des dimensions du radiateur, de la vitesse du fluide de refroidissement, de sa nature, et en particulier de son humidité, etc. On peut, dans une théorie qui n'a d'autre but que de rechercher la forme approximative des relations entre les différentes grandeurs, supposer A = Cte. On pose :

$$\sigma = \frac{S_r}{s} \tag{3-11}$$

σ est la *surface relative du radiateur*; il dépend de considérations économiques et varie selon le système de radiateur adopté; il est choisi à priori.

On a alors, avec (3-4) :

$$R_f = \frac{1}{A\, s\, \sigma\, (T_c - T_a)^{0,25}} \sqrt[4]{\frac{1+k}{k}} \tag{3-12}$$

et, avec (3-8) :

$$P_u = A\, s\, \sigma\, \frac{(T_c - T_a)^{2,25}}{4\tau} \sqrt[4]{\frac{k^5}{(1+k)^9}} \tag{3-13}$$

L'intensité est, d'après (I) et (3-3) :

$$I = \frac{\alpha}{2\rho} \frac{T_c - T_a}{\gamma\,(1+k)} \tag{3-14}$$

la tension est, d'après (1-1) :

$$u = r'\, I, \quad \text{avec (3-16)} \quad r' = \rho\,\gamma - r \tag{3-15}$$

S'il y a n éléments en série, la tension aux bornes du générateur est :

$$u_t - n\,(\rho\,\gamma - r)\, \frac{\alpha\,(T_c - T_a)}{2\,\rho\,\gamma\,(1+k)} \tag{3-17}$$

et la puissance fournie au circuit extérieur :

$$P_t = u_t\, I = n^2\,(\rho\,\gamma - r) \left[\frac{\alpha\,(T_c - T_a)}{2\,\rho\,\gamma\,(1+k)}\right]^2 \tag{3-18}$$

On peut admettre que la température varie linéairement à l'intérieur du barreau. Si x est la distance à la soudure chaude d'une section, à la température T, on a :

$$\frac{x}{h} = \frac{T_c - T}{T_c - T_f} = \frac{T_c - T}{T_c - T_a}\,(1+k) \tag{3-19}$$

Les valeurs de ρ et $\varkappa$ à utiliser correspondent à la température moyenne :

$$T_{moy} = \frac{T_c + T_f}{2} = T_c - \frac{T_c - T_a}{2\,(1+k)} \tag{3-20}$$

Dimensionnement des générateurs thermo-électriques

Premier cas : chauffage par convection

Pendant la durée de captation du rayonnement le générateur fonctionne aux valeurs optima des températures. Il y a donc lieu, d'après (3-18), de rechercher le minimum de l'expression :

$$y = \frac{(1+k)^9}{k^5} \tag{4-1}$$

qui a lieu pour :

$$k = \frac{5}{4} = 1{,}25 \tag{4-2}$$

On a :

$$\sqrt[4]{\frac{k^5}{(1+k)^9}} = 0{,}212$$

et, d'autre part :

(4-3) et (4-4)

$$\gamma = \frac{\varkappa}{k} \cdot R_f = \frac{\varkappa}{A\, s\, \sigma\, (T_c - T_a)^{0,25}} \sqrt[4]{\frac{1+k}{k^5}} = \frac{h}{s}$$

d'où :

$$h = 0{,}926\, \frac{\varkappa}{A\, \sigma\, (T_c - T_a)^{0,25}} \tag{4-5}$$

et

$$P_{u\,max} = 0{,}053\, \frac{A\, s\, \sigma\, (T_c - T_a)^{2,25}}{\tau} \tag{4-6}$$

La puissance utilisable maximum par unité de volume du barreau thermo-électrique est :

$$\omega = \frac{P_{u\,max}}{v} = 0{,}057\, \frac{A^2\, \sigma^2\, \alpha^2\, (T_c - T_a)^{2,5}}{\rho\, \varkappa^2} \tag{4-7}$$

elle est d'autant plus élevée que le coefficient de transfert A, la surface relative de radiation σ et l'expression

$$\frac{\alpha^2\, (T_c - T_a)^{2,5}}{\rho\, \varkappa^2} \tag{4-8}$$

sont plus grands. L'expression (4-8) croît avec T_c. Il y a donc intérêt à fonctionner aussi près que possible du maximum technique $T_{c\,max}$.

(3-19) devient :

$$T_{moy} = \frac{7}{9}\, T_c + \frac{2}{9}\, T_a \tag{4-9}$$

Pour dimensionner la pile, il faut choisir au préalable le matériau thermo-électrique, sa section s, la température ambiante T_a, la température T_c

de l'armature chaude, le type de radiateur et sa surface relative σ.

On peut alors calculer h avec (4-5) et par conséquent γ; $P_{u\ \max}$ avec (4-6); $i_{\max}$ avec (3-14). Si l'on se donne le nombre d'éléments n, on peut calculer u_t et P_t avec (3-17) et (3-18), la résistance r des soudures et des connexions intérieures étant définie par les exigences de la construction.

Application numérique

Adoptons pour $T_a = 30$ °C et $T_c = 200$ °C les caractéristiques suivantes d'un matériau d'origine américaine :

$\alpha = 204.10^{-6}$ V/°C
$\rho = (0{,}522 + 0{,}00474\ T)\ 10^{-5}\ \Omega.m$
$\varkappa = 3{,}59 - 0{,}0106\ T$

On a $T_{moy} = 162$ °C; d'où :

$\rho = 1{,}288.10^{-5}$, $\varkappa = 1{,}87$, $\tau = 578$ °K

Prenons :

$\sigma = 100$, $A = 2{,}55$ W/m², $s = 10^{-4}$ m²

on a :

$h = 1{,}9$ mm
$P_{u\ \max} = 0{,}24$ W
$T_c - T_f = 75{,}6$ °C
$T_f - T_a = 94{,}4$ °C
$T_f = 124{,}4$ °C
$\gamma = 18{,}7$
$R_t = 19$ °C/W
$r_t = 2{,}411 \cdot 10^{-4}\ \Omega$
$q_u = 7{,}56$ W
$q_a = 7{,}70$ W
$\eta_g = 3{,}2$ p. 100
$I = 31{,}1\ A$

Il ne faut pas se faire d'illusions sur la précision de ces calculs, du fait de l'incertitude sur les valeurs exactes de α, ρ, $\varkappa$, et surtout du coefficient de transfert A. D'autre part, il n'a pas été tenu compte de l'incidence de la résistance r des soudures et des connexions intérieures.

Deuxième cas : chauffage par insolation

La température T_c de l'armature chaude dépend ici de la radiation solaire.

(2-3), (3-5), (3-6) et (3-8) donnent :

$$(4\text{-}10)\quad \left[\frac{T_c - T_a}{1+k}\right]^2 \left[\frac{\varkappa}{4\tau h C} + c\,(1+k)^2\right] + \frac{T_c - T_a}{1+k}\left[\frac{\varkappa}{hC} + b\,(1+k)\right] + (a - \alpha_s \tau_v Q_{i\Theta}) = 0$$

relation indépendante de la section s du barreau.

Plaçons-nous dans le cas où le coefficient du terme du second degré est négligeable, c'est-à-dire dans le cas où la valeur de l'expression

$$(4\text{-}11)\quad Z = c + \frac{\varkappa}{4\tau h C\,(1+k)^2} = c + \frac{\alpha^2}{4 h C \rho\,(1+k)^2}$$

est petite auprès des autres coefficients. Cette hypothèse peut être faite d'autant plus facilement que les coefficients a, b, c et les paramètres α_s, τ_v, $Q_{i\Theta}$ et q_e résultent de relevés expérimentaux assez incertains.

Il vient :

$$(4\text{-}12)\quad \frac{T_c - T_a}{1+k} = \frac{\alpha_s \tau_v Q_{i\Theta} - a}{b\,(1+k) + \dfrac{\varkappa}{hC}}$$

ou encore :

$$(4\text{-}13)\quad T_c - T_a = \frac{\alpha_s \tau_v Q_{i\Theta} - a}{b + \dfrac{\varkappa}{hC\,(1+k)}}$$

et, avec (3-8) :

$$(4\text{-}14)\quad P_u = \frac{\alpha^2 (\alpha_s \tau_v Q_{i\Theta} - a)^2}{4\rho C h \left[b\,(1+k) + \dfrac{\varkappa}{hC}\right]^2} \cdot s_i$$

Pour une valeur déterminée de la radiation solaire, α étant pratiquement constant, le maximum de P_u correspond au minimum de l'expression

$$(4\text{-}15)\quad E = \rho C h \left[b\,(1+k) + \frac{\varkappa}{hC}\right]^2$$

On a d'autre part :

(4-16)

$$R_f = \frac{k\gamma}{\varkappa} = \frac{1}{A s \sigma (T_c - T_a)^{0,25}} \sqrt[4]{\frac{1+k}{k}} = \frac{1}{A s \sigma (\alpha_s \tau_v Q_{i\Theta} - a)^{0,25}} \sqrt[4]{\frac{b\,(1+k) + \dfrac{\varkappa}{Ch}}{k}}$$

d'où :

(4-17)

$$A\,\sigma\,(\alpha_s \tau_v Q_{i\Theta} - a)^{0,25} = \frac{\varkappa}{kh} \sqrt[4]{b\left(1 + \frac{1}{k} + \frac{\varkappa}{kCh}\right.}$$

qui donne une relation entre k et h, en fonction de l'ensoleillement et du rapport de concentration $C = s_i/s$.

Posons :

$$(4\text{-}18)\quad B = \sqrt[4]{b\left(1 + \frac{1}{k} + \frac{1}{C}\frac{\varkappa}{kh}\right.}$$

et

$$(4\text{-}19)\quad M = A\sigma\,(\alpha_s \tau_v Q_{i\Theta} - a)^{0,25}$$

B varie relativement peu, comme on peut le voir dans l'application numérique ci-après, avec les valeurs de k et de h qui satisfont à la relation (4-17); il peut être considéré, pour une valeur déterminée de C et une valeur moyenne de ρ et de $\varkappa$, comme constante. On a :

$$(4\text{-}20)\quad kh = \frac{\varkappa B}{M} = \text{Cte}$$

Comme on a, d'autre part :

$$(4\text{-}21)\quad kh = s\varkappa R_f$$

la constance approximative de $B = M\,s\,R_f$ se traduit par la constance approximative de la résistance thermique R_f du radiateur, ce qui est un résultat assez remarquable.

(4-15) devient :

$$(4\text{-}22)\quad E = \rho C h \left| b\left(1 + \frac{\varkappa B}{h M}\right) + \frac{\varkappa}{C h}\right|^2$$

$$= \rho C h \left| b + \frac{\varkappa}{h}\left(\frac{1}{C} + \frac{B b}{M}\right)\right|^2$$

$$= \rho C \left| h b^2 + 2 b \varkappa \left(\frac{1}{C} + \frac{B b}{M}\right) + \frac{\varkappa^2}{h}\left(\frac{1}{C} + \frac{B b}{M}\right)^2\right|$$

et l'on a :

$$(4\text{-}23)\quad \frac{dE}{dh} = \rho C \left| b^2 - \frac{\varkappa^2}{h^2}\left(\frac{1}{C} + \frac{B b}{M}\right)^2\right|$$

$$(4\text{-}24)\quad \frac{d^2E}{dh^2} = \frac{2\varkappa^2}{h^3}\left(\frac{1}{C} + \frac{B b}{M}\right)^2 > 0$$

Le minimum a lieu pour :

$$(4\text{-}25)\quad h = \varkappa \left|\frac{1}{b C} + \frac{B}{M}\right| = \varkappa \left|\frac{1}{b C} + s R_f\right|$$

et, par conséquent,

$$(4\text{-}26)\quad k = \frac{\dfrac{B}{M}}{\dfrac{1}{b C} + \dfrac{B}{M}}$$

d'où :

$$(4\text{-}27)\quad E_{min} = \rho C \varkappa \left(\frac{1}{b C} + \frac{B}{M}\right)\left[b + \frac{\dfrac{1}{C} + \dfrac{B b}{M}}{\dfrac{1}{b C} + \dfrac{B}{M}}\right]^2$$

$$= 4 \rho C \varkappa \left|\frac{1}{C} + \frac{B b}{M}\right|^2$$

$$= \frac{4 \rho \varkappa}{C}\left|1 + \frac{B b C}{M}\right|^2$$

On a :

$$(4\text{-}28)\quad h(1 + k) = \varkappa \left|\frac{1}{b C} + \frac{2B}{M}\right|$$

et

$$(4\text{-}29)\quad 1 + \frac{1}{k} = \frac{\dfrac{B}{M} + \left(\dfrac{1}{b C} + \dfrac{B}{M}\right)}{\dfrac{B}{M}} = 2 + \frac{M}{B b C}$$

d'après (4-18), B peut être défini par l'expression :

$$(4\text{-}30)\quad B^2 = \sqrt[2]{2\left(b + \frac{M}{B C}\right)}$$

dont le calcul graphique est facile.

Applications numériques

Pour dimensionner la pile, on se donne généralement le matériau thermo-électrique, c'est-à-dire α, ρ, $\varkappa$, dont on prend une valeur moyenne correspondant à 50 °C, par exemple; on se donne en outre la température ambiante T_a, la radiation incidente $\alpha_s \tau_r Q_{th}$, la section s du barreau, la surface relative σ du radiateur, et le type du radiateur qui définit A, la courbe des pertes q_p en fonction de l'écart de température $(T_c - T_a)$ des surfaces réceptrices du rayonnement avec l'ambiante, c'est-à-dire les coefficients a et b et le rapport de concentration $C = s_t/s$.

Premier procédé. On désire fonctionner à la puissance maximum. On tire de (4-30) une valeur approximative de B que l'on introduit dans (4-25) pour obtenir h et dans (4-20) pour obtenir τ.

Deuxième procédé. On se donne h encore γ. k est donné par (4-17). La puissance P de la pile n'est généralement pas dans ce cas la puissance maximum.

Posons, pour le même matériau que dans l'exemple précédent :

α	$= 204 \cdot 10^{-6}$ V/°C	
ρ_{moy}	$= 0{,}76 \cdot 10^{-5}\ \Omega$.m	
$\varkappa_{moy}$	$= 3{,}09$ W/°C.m	
τ_{moy}	$= 564{,}3$ °K	
T_a	$= 30$ °C	
s	$= 10^{-4}$ m²	
σ	$= 100$	
A	$= 2{,}55$ W/m²	
$\alpha_s \tau_r Q_{th}$	$= 500$ W/m²	
a	$= 39$ W	(Valeurs obtenues par linéarisation de la courbe des pertes).
b	$= 3{,}8$ W/°C	

On a :

$$M = 2{,}55 \cdot 10^2 \sqrt[4]{500 - 39} = 1\,813{,}2$$

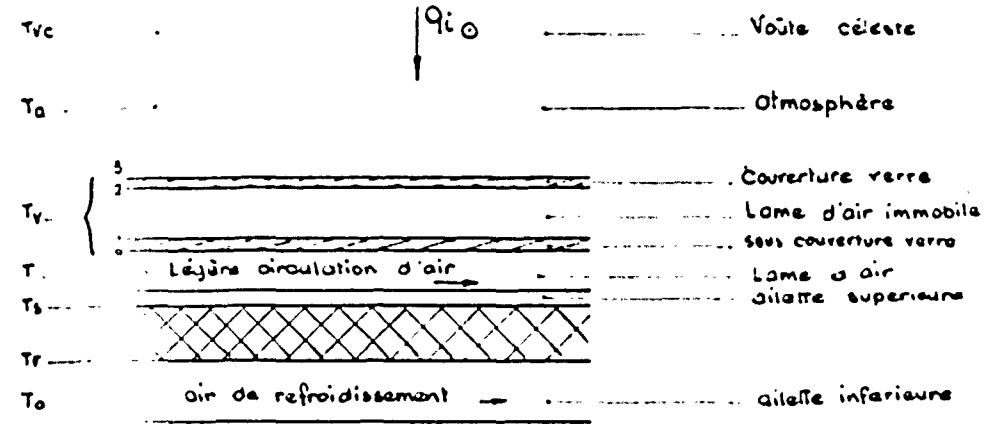
Premier procédé :

(4-30) donne :

$$B^2 = \sqrt[2]{7{,}6 + \frac{2\,364}{B C}}$$

dont les solutions en fonction de C sont données par le tableau ci-dessous, où l'on a fait figurer également les valeurs correspondantes de $k\,h$, h, k, $(T_c - T_a)$, $P_{u\,max}$, ainsi que les coefficients de l'équation (4-10). On peut vérifier que Z peut bien être négligé, ainsi qu'il avait été supposé.

C	1	2	10	100	1 000
B	4,75	4,14	3,04	2,09	1,67
$k\,h$	$12{,}42 \cdot 10^{-3}$	$10{,}82 \cdot 10^{-3}$	$7{,}95 \cdot 10^{-3}$	$5{,}46 \cdot 10^{-3}$	$4{,}36 \cdot 10^{-3}$
h	0,825	0,418	0,089	0,0136	0,00517
k	0,015	0,0258	0,089	0,147	0,843
$(T_c - T_a)$°C	61,6	62,2	65,98	85,4	111,8
$P_{u\,max}$ (W)	$0{,}61 \cdot 10^{-3}$	$1{,}2 \cdot 10^{-3}$	$5{,}53 \cdot 10^{-3}$	$48{,}6 \cdot 10^{-3}$	$97{,}5 \cdot 10^{-3}$
Z	0,0246	0,0245	0,0243	0,0237	0,02308
$b + \dfrac{\varkappa}{1 + k\,h\,C}$	7,49	7,39	6,98	5,78	4,12


Tvc
qi
Voûte céleste
Ta
Atmosphère
Tv
3
2
1
0
Couverture verre
Lame d'air immobile
sous couverture verre
T
Légère circulation d'air
Lame d air
Ts
ailette superieure
Tf
To
air de refroidissement
ailette inferieure

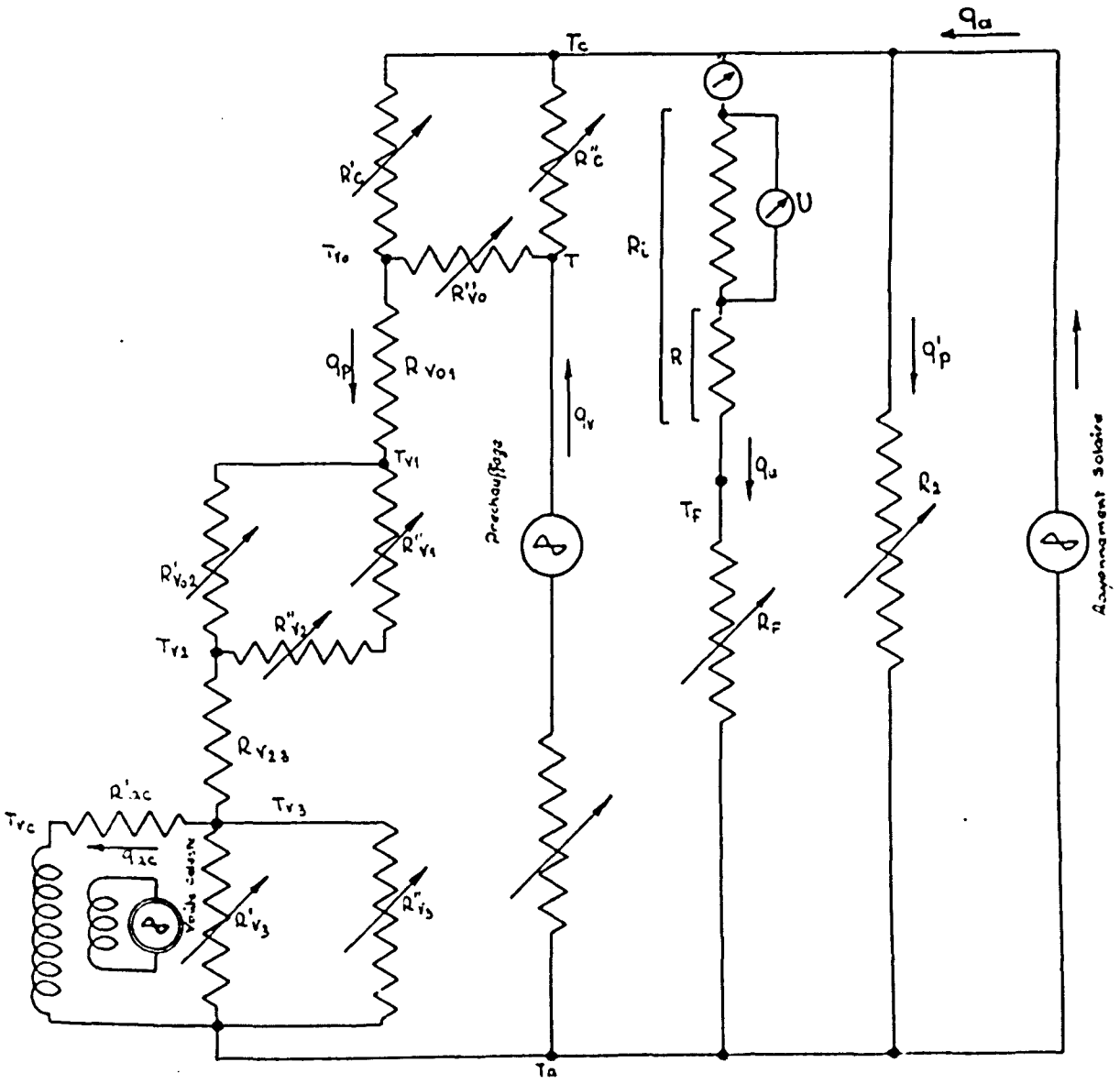

qa
Tc
R'c
R''c
Tvo
T
R''vo
Ri
U
qp
Rvo1
R
q'p
qv
Tv1
Préchauffage
qu
R2
R'v2
R''v1
TF
Tv2
R''v2
RF
Rv23
R'2c
Tv3
Tvc
q2c
Vers le capteur
R'v3
R''v3
Ta
Appoint solaire

Figure 3

Deuxième procédé :

Dans les mêmes conditions, posons $h = 10^{-2}$ m et prenons le cas où $C = 10$.

De (4-20) on tire :

$$k\,h = 7{,}5 \cdot 10^{-3}$$

On a :

$$k = \frac{7{,}5 \cdot 10^{-3}}{10^{-2}} = 0{,}75$$

avec (4-13) :

$$T_c - T_a = \frac{461}{21{,}45} = 21{,}5\ ^\circ\text{C}$$

$$P_u = 2{,}0610^{-3}\ \text{W}$$

soit moins de la moitié de la puissance maximum.

Comparaison entre les deux procédés de chauffage

Le moyen le plus simple est de comparer les puissances volumiques ω dans chacun des cas. On a, d'après (4-7) :

$$\frac{P_u}{v} = \omega = \frac{(T_c - T_a)^2}{4\,\rho\,h^2\,(1+k)^2} \tag{4-31}$$

d'où :

$$\frac{\omega_1}{\omega_2} = \left[\frac{\rho_2\,h_2^2\,(1+k_2)^2}{\rho_1\,h_1^2\,(1+k_1)^2}\right]\left[\frac{T_{c_1} - T_a}{T_{c_2} - T_a}\right]^2 \tag{4-32}$$

On a d'autre part, d'après (3-12) :

$$R_f = \frac{k\,h}{\varkappa_s} = \frac{1}{A\,s\,\sigma\,(T_c - T_a)^{0{,}25}}\sqrt[4]{\frac{1+k}{k}} \tag{4-33}$$

Dans les limites des valeurs possibles de k, le radical varie assez peu. On peut donc écrire généralement :

$$k\,h = P\,(T_c - T_a)^{-0{,}25} \tag{4-34}$$

où P est une constante.

Il vient :

$$h\,(1+k) = P\left(\frac{1+k}{k}\right)(T_c - T_a)^{-0{,}25} \tag{4-35}$$

et

$$\frac{\omega_1}{\omega_2} = \frac{\rho_2}{\rho_1}\left[\frac{k_1\,(1+k_2)}{k_2\,(1+k_1)}\right]^2\left[\frac{T_{c_1} - T_a}{T_{c_2} - T_a}\right]^{2{,}25} \tag{4-36}$$

ρ_1 et ρ_2 sont généralement voisins; il en est de même pour k_1 et k_2; le terme prépondérant est alors :

$$\left[\frac{T_{c_1} - T_a}{T_{c_2} - T_a}\right]^{2{,}25}$$

Or, non seulement T_{c_2} est notablement plus bas que T_{c_1}, mais il varie continuellement en cours de journée. Il en résulte que le procédé de chauffage par insolation est très nettement désavantagé par rapport à celui qui utilise un fluide intermédiaire.

L'unique avantage que l'on peut reconnaître aux générateurs directement insolés est une certaine simplicité de construction.

Étude d'un générateur thermo-électrique à exposition fixe directe par analogie électrique

Représentation analogique

La méthode d'analogie électrique dans l'étude du fonctionnement thermique des insolateurs n'est applicable que si l'on suppose la possibilité de linéariser les transferts de chaleur par rayonnement et par convection. C'est le cas des insolateurs et par conséquent des générateurs thermo-électriques à exposition directe. La figure 3 représente le schéma de principe du générateur étudié et le circuit électrique analogique correspondant.[4]

La correspondance entre les grandeurs thermiques et les grandeurs électriques analogues, ainsi que les rapports qui ont été choisis, sont donnés ci-dessous :

Grandeurs thermiques		*Grandeurs électriques correspondantes*		
T : température (°C)	**T**	volts. . . .	(1)	$T = K_v\,\mathbf{T}$ avec $K_v = 1$
q : flux calorifique (W/m²)	**q**	ampères . .	(2)	$q = K_p\,\mathbf{q}$ avec $K_q = 10^5$
R : résistance thermique (°C/W)	**R**	ohms . . .	(3)	$R = K_r\,\mathbf{R}$ avec $K_s = 10^{-5}$

Si l'on admet la théorie simplifiée précédemment exposée, il est possible de représenter, tout au moins approximativement, le circuit électrique réel du générateur thermo-électrique étudié par le circuit électrique qui représente le circuit thermique de ce même générateur.

Supposons en effet que l'on représente la résistance électrique r_t du générateur par la résistance électrique $\mathbf{R_i}$, qui représente la résistance thermique interne R_t, et le courant i par le courant $\mathbf{q_u}$ qui représente le flux calorifique q_u dans le barreau. Le rapport

$$\frac{\mathbf{R_i}}{r_t}$$

représente le facteur par lequel il faut multiplier une résistance électrique du générateur réel pour obtenir sa représentation dans le schéma analogique.

Ainsi, la résistance r sera représentée par une résistance électrique

$$\mathbf{R} = \frac{r}{r_t}\,\mathbf{R_i}$$

la résistance de charge $(r_t - r)$ sera représentée par $\mathbf{R_i} - \mathbf{R}$. Mais le circuit thermique ne comporte qu'une branche, alors que le circuit électrique réel en comporte deux. Si l'on désire utiliser la résistance électrique du schéma analogique qui représente le circuit thermique pour représenter l'une des branches du circuit électrique réel, il faut supposer qu'elle représente la branche externe.

La tension $\mathbf{u}$ mesurée aux bornes de $\mathbf{R_i} - \mathbf{R}$ est :

$$\mathbf{u} = [\mathbf{R_i} - \mathbf{R}]\,\mathbf{q_u}$$

[4] Pour le mode opératoire, voir le Bulletin 3 de l'I.E.S.U.A

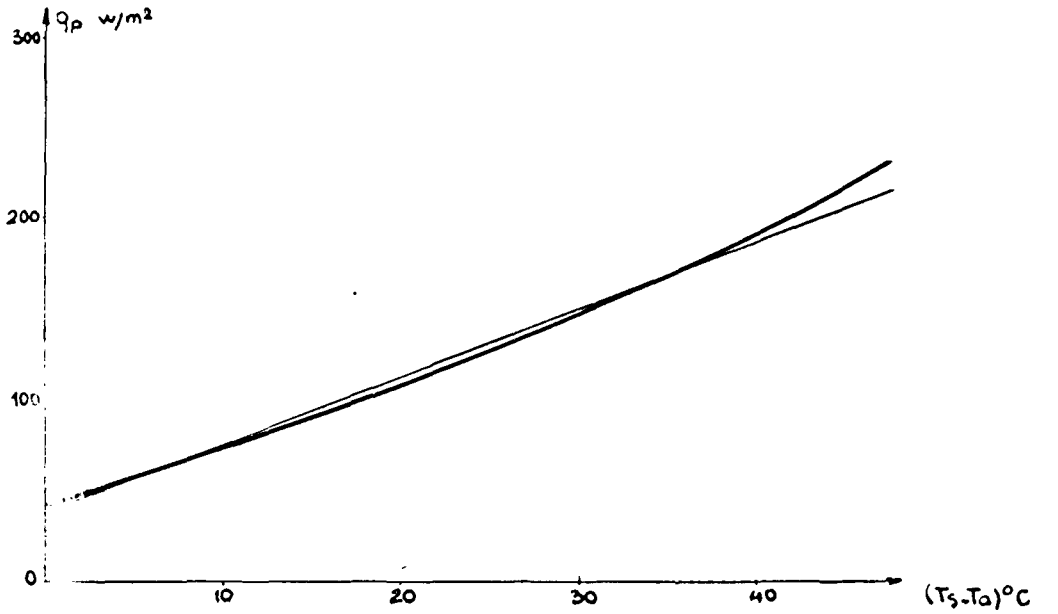


Figure 4

elle doit représenter la tension u aux bornes du générateur réel.

La puissance électrique produite par le générateur réel et utilisable est :

$$p = ui$$

elle est représentée par le produit $\mathbf{u}\ \mathbf{q_u}$. Il reste à déterminer les rapports

$$\frac{\mathbf{q_u}}{i} \qquad \text{et} \qquad \frac{\mathbf{u}}{u}$$

Les relations

$$r_i = \rho\,\gamma \qquad \text{et} \qquad R_i = \frac{\gamma}{\varkappa}$$

donnent :

$$r_i = R_i\,\rho\,\varkappa = K_r\,\mathbf{R_i}\,\rho\,\varkappa$$

d'où :

$$\frac{\mathbf{R_i}}{r_i} = \frac{1}{K_r\,\rho\,\varkappa} \tag{4}$$

Les relations

$$i = \frac{\alpha\,(T_s - T_f)}{2\,r_i} \qquad \text{et} \qquad q_u = \frac{T_s - T_f}{R_i}$$

donnent :

$$i = \frac{\alpha}{2\,\rho\,\varkappa}\,K_q\,\mathbf{q_u}$$

d'où :

$$\frac{\mathbf{q_u}}{i} = \frac{2\,\rho\,\varkappa}{\alpha\,K_q} \tag{5}$$

De (4) et (5) on tire :

$$\frac{\mathbf{u}}{u} = \frac{2}{\alpha\,K_r\,K_q} \tag{6}$$

De (5) et (6) :

$$\frac{\mathbf{u}\,\mathbf{q_u}}{P} = \frac{4\,\rho\,\varkappa}{K_r\,\alpha^2\,K_q^2} \tag{7}$$

Si N est le nombre d'éléments ($N/2$ couples) dans l'unité de surface insolée, on a :

$$R_i = \frac{R}{N} \tag{8} \qquad q_i = N_q \tag{9}$$

$$r_{i_i} = N\,r_i \tag{10} \qquad i_i = i \tag{11}$$

$$\frac{\mathbf{R_{i_i}}}{r_{i_i}} = \frac{1}{N^2\,K_r\,\rho\,\varkappa} \tag{12}$$

$$\frac{\mathbf{q_{u_i}}}{i_i} = \frac{2\,N\,\rho\,\varkappa}{\alpha\,K_q} \tag{13}$$

$$\frac{\mathbf{u_i}}{u_i} = \frac{2}{N\,\alpha\,K_r\,K_q} \tag{14}$$

$$\frac{\mathbf{u_i}\,\mathbf{q_{u_i}}}{P_i} = \frac{4\,\rho\,\varkappa}{\alpha^2\,K_r\,K_q^2} \tag{15}$$

Les formules (12) à (15) permettent de passer des mesures effectuées sur le schéma analogique aux grandeurs électriques réelles. Il faut bien noter que dans cette représentation on a fait abstraction des perturbations apportées au flux calorifique par l'effet Joule.

Description du prototype expérimental

Ainsi qu'on a pu le voir plus haut à propos des générateurs à exposition directe, il y a intérêt à augmenter le rapport de concentration C. Un moyen très simple et qui a été souvent utilisé consiste à réaliser l'armature chaude avec une plaque assez étendue disposée de manière à recevoir le rayonnement solaire. Lorsque l'on utilise des surfaces sélec-

tives, ce moyen est sans doute suffisant, mais pour nous qui ne pouvons utiliser de surfaces spécialement traitées à cause de l'effet néfaste de la poussière, nous avons cherché à utiliser la convection qui transporte la chaleur des surfaces que nous avons au début appelées excédentaires et dont le prix d'occupation du terrain est relativement faible, pour la transmettre à l'armature chaude.

Le premier type de générateur que nous avons construit et dont le détail est donné sur la figure 2 a justement pour objet de déterminer l'importance de ce transfert de chaleur et au besoin de l'améliorer. Si, comme nous l'espérons, les résultats sont favorables, nous pourrons utiliser concurremment les deux procédés : extension de la surface insolée et utilisation de la convection au moyen de petites ailettes dont cette surface serait munie.

Ce sont donc surtout des préoccupations constructives qui ont guidé le dimensionnement du prototype expérimental réalisé. Le générateur proprement dit est amovible, et peut être remplacé, s'il est besoin, par un autre générateur répondant à des exigences différentes; le châssis est prévu pour être facilement modifié et s'adapter à diverses latitudes. D'autre part, la cheminée peut être allongée au moyen d'éléments intermédiaires démontables.

L'expérimentation a pour but de déterminer les valeurs des résistances thermiques à introduire dans le circuit analogique pour obtenir une assez bonne concordance entre les résultats des mesures effectuées sur l'appareil lui-même au soleil et ceux effectués sur le circuit analogique, puis de rechercher par voie analogique les conditions de meilleur fonctionnement.

En fait, jusqu'ici, le prototype construit n'a servi qu'à préciser les grandeurs à introduire dans le circuit analogique, et une expérimentation préliminaire a été faite à l'aide de ce circuit. Ce qui a permis d'établir la courbe des pertes q_p de l'isolateur par mètre carré de surface insolée, en fonction de l'écart de températures $(T_c - T_a)$. Cette courbe (figure 4) peut être remplacée par une droite définie par les coefficients :

$$a = 39\ \mathrm{W/m^2} \qquad b = 3{,}8\ \mathrm{W/°C.m^2}$$

qui sont nécessaires dans l'étude du générateur optimum.

La figure 5 donne le diagramme monotone journalier équivalent que nous avons choisi pour l'étude théorique du fonctionnement de notre générateur prototype. Il correspond aux conditions climatologiques d'un point situé en plein Sahara, sous le 30e parallèle.

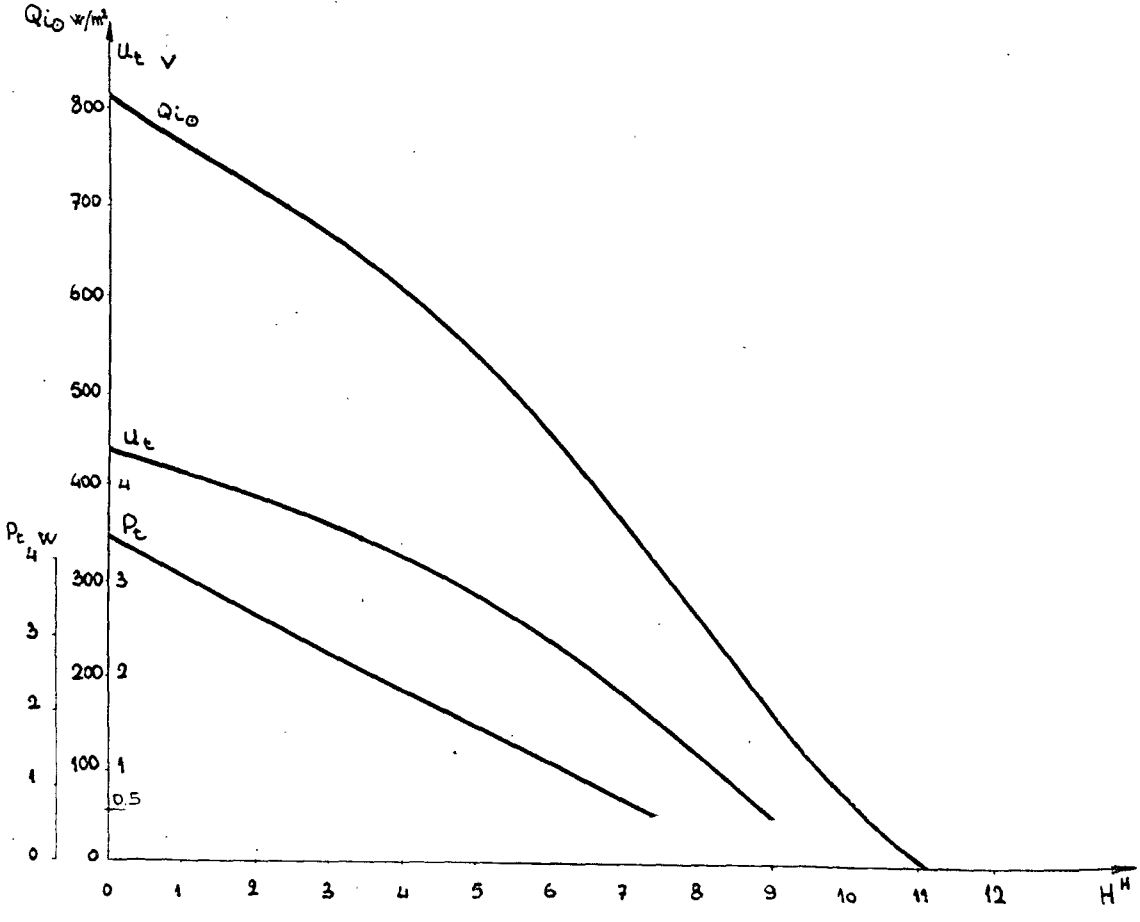


Figure 5

Sur la même figure ont été représentées les courbes monotones correspondantes de la puissance P_u et de la tension aux bornes d'un générateur formé de 1 000 éléments (500 couples), analogue à celui qui a fait l'objet d'une application numérique antérieure.

Conclusion

Il apparaît comme évident, à la suite de l'analyse faite au début de cet exposé, qu'il ne faut pas espérer tirer de très grandes puissances des générateurs hélio-thermo-électriques, avec les matériaux que l'on trouve actuellement sur le marché. Le prix élevé des semi-conducteurs nécessaires, exige que l'on utilise les moyens les meilleurs pour opérer la transformation. Il faut donc s'orienter vers les solutions qui séparent la captation et la transformation en chaleur du rayonnement solaire de la conversion thermo-électrique proprement dite.

Cependant, la grande rusticité des générateurs à exposition directe peut rendre des services dans des installations isolées et pour de très petites puissances, par exemple dans le cas d'une télécommande ou d'une télésignalisation. C'est d'ailleurs en vue de la réalisation de postes météorologiques automatiques que l'I.E.S.U.A. a entrepris des études sur cette sorte de générateur.

Le problème fondamental, ainsi qu'on l'a déjà dit, est celui du radiateur d'évacuation de la chaleur. L'I.E.S.U.A. étudie actuellement un système d'ailettes parallèles au plan de l'insolateur, ce qui permet un plus grand développement des surfaces, et de choisir ainsi des valeurs de σ plus élevées. L'I.E.S.U.A. étudie également un système d'ailettes à vaporisation interne fonctionnant suivant un principe proposé par Joffe, et qui permettrait de disposer de plus grandes valeurs de σ.

En ce qui concerne la surface réceptrice, si la sélectivité n'est pas recommandable pour les surfaces soumises aux vicissitudes atmosphériques, elle peut l'être si l'on réalise une protection suffisante : étanchéité, vide ou couverture réfractrice et isolante au contact des armatures chaudes. L'I.E.S.U.A. a l'intention de poursuivre des recherches dans ce sens.

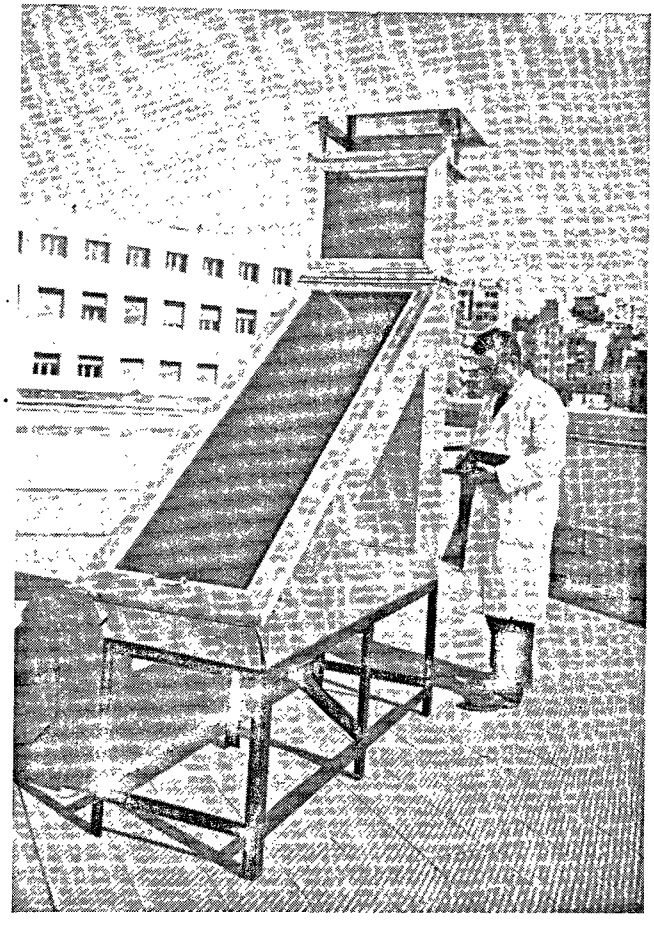


Figure 6. Aspect extérieur du thermogénérateur de la figure 2

Résumé

L'I.E.S.U.A. se propose d'étudier tous les procédés de production d'énergie à partir du rayonnement solaire, mais désire mettre l'accent sur les procédés immédiats de transformation industrielle. Dans l'état actuel de la technique, seuls les procédés thermiques peuvent être valablement envisagés. Il s'agit donc de collecter des quantités importantes d'énergie solaire et de les concentrer suffisamment pour obtenir des températures à caractère industriel.

Si un tel résultat peut être obtenu par des moyens compétitifs dans certaines conditions, les techniciens spécialistes (thermiciens, thermodynamiciens, ingénieurs chimistes, etc.) peuvent se charger de trouver, selon leurs méthodes propres, l'utilisation industrielle de l'énergie thermique ainsi mise à leur disposition.

Mais avant de se consacrer entièrement à ce problème majeur, l'I.E.S.U.A. croit nécessaire de procéder à une analyse systématique des phénomènes dont le concours pourra être requis ultérieurement.

Les auteurs exposent dans une première partie quelques principes directeurs de leurs recherches. Ils observent en particulier que, contrairement à ce que l'on croit communément, l'énergie solaire est une énergie très chère, qui est surtout abondante pour une transformation industrielle dans les zones arides, et plus spécialement au Sahara. Par ailleurs, les problèmes de stockage ne se posent vraiment que pour les petites puissances, ou encore lorsqu'on utilise des températures relativement basses; sinon, c'est un problème de puissance de complément qui

se pose, et qui peut être heureusement résolu au Sahara au moyen des énergies fossiles.

Les auteurs observent enfin que la source froide que requiert toute transformation thermodynamique de l'énergie solaire ne peut se trouver au Sahara que dans l'air ambiant; il en résulte le grand intérêt des systèmes qui peuvent faire mouvoir de grandes masses d'air sans intervention d'autre énergie que l'énergie solaire.

Le programme des travaux de l'Institut de l'énergie solaire se comprend dès lors aisément : étude de la radiation solaire, étude des insolateurs et plus particulièrement des cheminées solaires, étude des générateurs thermo-électriques, tout d'abord des générateurs à exposition directe, c'est-à-dire des insolateurs thermo-électriques, ensuite à circulation de fluides, ce qui entraîne l'étude du système des miroirs et des chaudières.

Dans une seconde partie, les auteurs examinent rapidement les procédés de captation avec concentration du rayonnement solaire qui sont à l'étude et qui comportent, pour des températures inférieures à 300 °C, des collecteurs orientables formés d'éléments de miroirs paraboloïdes et fonctionnant par focalisation multiple. Ces collecteurs sont destinés à chauffer des liquides thermophores.

Pour des températures supérieures à 300 °C, les projets se résument dans l'utilisation de deux procédés nouveaux qui envisagent l'emploi d'éléments de miroirs paraboloïdes déformables distribués sur de grandes surfaces.

Ces miroirs sont constitués de simples tôles planes d'aluminium brillantées et aluminées et convenablement déformées. Une bonne focalisation a été obtenue avec une tôle d'aluminium de 1,6 mm d'épaisseur, à une distance de 9 m.

Dans une troisième partie, les auteurs examinent les conditions techniques de réalisation des générateurs thermo-électriques destinés à fonctionner au Sahara. Deux conditions sont fondamentales.

a) Les générateurs thermo-électriques doivent être organisés pour être refroidis par circulation d'air. Or cet air peut atteindre en certaines circonstances des températures relativement élevées (40 ou 45 °C).

b) Le salissement des systèmes de captation ou des couvertures transparentes des insolateurs peut amener d'importantes réductions de l'énergie incidente et des frais élevés d'exploitation pour le nettoyage. Les surfaces qui ont été traitées pour être sélectives perdent leurs propriétés sous la poussière.

L'utilisation du système d'équations classiques pour étudier le fonctionnement théorique des générateurs thermo-électriques conduit à une assez grande complexité analytique, et les auteurs observent que dans le cas de l'emploi des matériaux thermo-électriques actuellement sur le marché, dont les rendements sont faibles, il est possible de négliger certains termes et de simplifier ainsi l'appareil mathématique. Ils observent d'autre part que les pertes d'un insolateur thermo-électrique par la couverture transparente peuvent être mis généralement sous forme parabolique en fonction de l'écart de températures entre l'armature chaude et le milieu ambiant. Ils font intervenir alors les rapports suivants :

Rapport de forme $\gamma = \frac{h}{s}$, h étant la hauteur du barreau de section s;

Rapport $k = \frac{R_f}{R_t}$ de la résistance thermique R_f du radiateur à celle R_t du barreau;

Rapport de concentration $C = \frac{s_t}{s}$ ou rapport de la surface insolée en contact thermique avec l'armature chaude à la section s du barreau;

Rapport $\sigma = \frac{S_r}{s}$ de la surface du radiateur à celle du barreau.

Dans ces conditions, la température de l'armature froide s'exprime simplement en fonction de celle de l'armature chaude et de la température ambiante. On a

$$T_c - T_f = \frac{T_c - T_a}{1 + k}$$

Les formules qui donnent la valeur des différentes grandeurs sont établies facilement, même dans le seul cas qui est examiné et qui correspond au refroidissement du radiateur par l'air. On a en particulier

$$P_u = A\, s\, \sigma \frac{(T_c - T_a)^{2,25}}{4\tau} \sqrt[4]{\frac{k^5}{(1+k)^9}}$$

formule dans laquelle :

P_u est la puissance utilisable,
A le coefficient de transfert de chaleur par convection,
T_c la température de l'armature chaude, en °C,
T_a la température ambiante, en °C,
$\tau = \frac{\alpha^2}{\rho\varkappa}$ la température caractéristique du matériau, en °K.

Le chauffage de l'armature chaude peut être réalisé, soit par circulation d'un fluide au préalable chauffé au moyen du soleil, soit par exposition directe au soleil.

Le chauffage par circulation d'un fluide est le plus rationnel, car il permet de faire fonctionner la pile thermo-électrique à températures constantes. On montre qu'il existe une valeur optima du rapport k, soit $k = 1{,}25$. Le dimensionnement de la pile se fait alors aisément en partant de cette condition, et on constate que son rendement global peut atteindre des valeurs relativement élevées. Ainsi, il a été calculé que le rendement global pouvait atteindre 3 p. 100 pour des barreaux en tellurure de bismuth d'origine américaine et fonctionnant à 200 °C. Le calcul montre que la hauteur du barreau est très faible, soit de l'ordre de 2 mm.

Dans le cas du chauffage par insolation directe, les calculs sont beaucoup moins faciles, et il faut faire intervenir des simplifications numériques. Des

conditions de puissance maxima sont alors établies, qui dépendent du rapport de concentration *C*. On constate que l'on est conduit à des hauteurs relativement grandes du barreau, à moins d'adopter des concentrations élevées, et à des puissances relativement faibles. Mais alors que dans le cas de la circulation d'un fluide chauffé au moyen du soleil les variations diurnes de la radiation ne se traduisent que par une variation du nombre des générateurs en parallèle, dans le cas du chauffage par insolation directe, les variations de l'énergie incidente se traduisent par des variations beaucoup plus grandes de la tension aux bornes et de la puissance fournie. Les conditions de rendement maximum ne peuvent être satisfaites que pour une valeur déterminée de la radiation. Il en résulte, en dernière analyse, que le mode de chauffage par insolation directe est actuellement onéreux et doit être abandonné.

Toutes les particularités de fonctionnement des générateurs thermo-électriques peuvent être étudiées commodément au moyen d'une analogie électrique moyennant certaines hypothèses simplificatrices que l'on est en droit de faire lorsqu'il s'agit de semi-conducteurs dont les rendements internes sont faibles, ce qui est le cas. Toutefois, il n'est pas possible de représenter avec assez de précision sur le circuit analogique les phénomènes réels de transfert de chaleur; aussi paraît-il intéressant d'étudier sur un prototype réel les véritables performances calculées par ailleurs. Bien que le générateur à exposition directe ne puisse être considéré comme la solution définitive des générateurs thermo-électriques, il a pour lui l'avantage d'être très rustique; aussi l'Institut de l'énergie solaire de l'Université d'Alger a construit un prototype qui tient compte des sujétions sahariennes rappelées plus haut. Les surfaces réceptrices du rayonnement solaire ne sont donc pas des surfaces sélectives. Le générateur est constitué par une surface de préchauffage relativement importante, avec une légère circulation d'air qui vient apporter de la chaleur à l'armature chaude concurremment au rayonnement solaire. Le générateur comporte également une surface de post-chauffage et une cheminée pour accélérer le tirage de l'air de refroidissement; ce dernier étant très sec, la possibilité est prévue de l'humidifier pour le refroidir.

Afin que la construction du prototype ne se confine pas dans la solution de problèmes gratuits, il a été conçu pour une destination précise à l'alimentation d'un poste météorologique automatique à émission radio-électrique. Il a été nécessaire alors, pour compenser les variations de tension dues aux variations du rayonnement solaire, d'interposer entre le générateur et l'utilisation un convertisseur continu-continu servant à la fois de régulateur de tension, d'adaptation d'indépendance et de stockage de l'énergie.

En conclusion, les auteurs attirent l'attention sur le problème fondamental de ces générateurs, qui réside dans le radiateur d'évacuation de la chaleur. Des essais sont actuellement en cours pour augmenter la surface relative σ du radiateur.

TECHNICAL RESEARCH TRENDS AT I.E.S.U.A. FOR ENERGY PRODUCTION FROM SOLAR RADIATION

(Translation of the foregoing paper)

*M. Perrot * and M. Touchais ***

The Institute of Solar Energy of the University of Algiers has a profound and integrated interest in all aspects of the practical utilization of the substantial amount of energy lavished on us by the sun. Its present efforts, however, are more particularly directed towards applications which, on the one hand, are of directly industrial nature, and, on the other hand, appear capable of use in the Sahara, which must be regarded as the great French reserve of solar energy.

In the present state of the science, only thermal transformations at temperatures more or less elevated can give rise to immediate applications; the question is whether such applications can be competitive with the use of other forms of energy. There is, however, no reason for undue preoccupation with the applications themselves, for as soon as sufficient quantities of energy can be placed at the disposition of industrialists at the desired temperatures, and at reasonable cost, the specialists concerned will themselves undertake to utilize it in their own fields.

But although the problem should be examined in all its generality, it would be a gross error of method not to have reference, *a priori*, to a very clear and definite application. The arrangements adopted for development and refinement of a basic principle frequently do contain details unrelated to the primary object — details which enter in dominating fashion into the choice of materials, performances, manufacturing processes or methods of operation.

Refusal to take this into account means to devote oneself to research that may remain sterile. The objective set for itself by the I.E.S.U.A. has thus been to build a solar thermoelectric power station — an ambitious project indeed, in the present state of semiconductor technology, but nevertheless extremely instructive, for thermal processes are of immense importance in thermoelectric generators. The adaptation of the means of concentrating solar radiation to thermoelectric piles appears capable of revealing problems which, while they may already be known, still present themselves in a new light.

The activities of I.E.S.U.A., however, are not confined to the study of this particular problem; it is equally its duty to examine systematically all the possible applications. Besides the thermoelectric applications, the Institute is interested in the problems of thermomechanical conversion of solar energy, such as the problems of its thermoionic and photoionic conversion.

The development of these varied applications depends primarily on the possibility of capturing and concentrating large amounts of energy.

This paper will therefore first discuss very briefly the means of capturing and concentrating solar radiation for feeding the heat source of a thermoelectric generator, and then, in greater detail, will consider thermoelectric generators themselves.

But first of all it will be of interest to state a few guiding principles of our research. Some of them are well known, but it will not be a waste of time to recall them. Others may be controversial, and we should attempt to clarify them.

First of all, we must speak out against the allurement that solar energy is practically free for the taking. Solar radiation, in the present state of the art, is a form of energy that is still very expensive, since the systems for its conversion cannot afford the luxury of operating at low efficiencies, except perhaps for small installations.

On the other hand—this is only seemingly true — solar energy does appear to be very widely distributed; we mean, of course, with possibilities of industrial conversion. The regions where it may be considered abundant are unfortunately among the most desolate and backward in the world. It would seem, then, that the harnessing of significant amounts of solar energy should be accompanied by a concomitant commencement of arid-region exploitation. The problem of solar energy, as far as the I.E.S.U.A. is concerned, is a specifically Saharan problem.

By reason of very high variability and the random nature of solar energy, there is often a tendency to confuse two distinct problems, that of the conversion of solar energy into directly useful energy, and that of its storage. In the case of low power installations, or of relatively low temperatures, one may dream of the storage of converted energy; but in the perspective of the production of large amounts of energy, the problem is modified. The problem is

* Director, Institut de l'énergie solaire de l'Université d'Alger, Algeria.

** Research Engineer, Institut de l'énergie solaire de l'Université d'Alger, Algeria.

no longer one of storage, but one of auxiliary energy. But it happens that, by a fortunate chance, the Sahara, which is an immense source of solar energy, is also an important reservoir of fossil fuel. A solar power station would thus necessarily take the form of a mixed power station, operating on sun and natural gas, or sun and oil.

This relation between solar radiation and fossil fuels is more profound than it appears at first glance. It would seem that the truly industrial existence of solar energy would have the immediate consequence of imposing a certain limitation on the consumption of the conventional forms of energy. When the industrial conversion of solar energy becomes effective, the problem of the rational general distribution of the sources of energy will be posed throughout the world, and a distinction will have to be drawn between those forms of energy that can be stored, and can be transported without great cost, like the liquid fuels, and those forms that must be consumed at the site of production, or in its immediate vicinity, like solar energy and windpower, or, again, those whose transportation is expensive, like electric energy. The efficiency of solar-energy conversion plants will then become a much more acute question, which will corroborate the consequences of the first principle enunciated above. Thus, contrary to common belief, the presence of oil and natural gas in the Sahara does not at all diminish the interest that might attach to the utilization of solar energy, but, quite the other way round, increases it.

In conclusion, it should not be forgotten that the conversion of solar energy by the thermal route into a different form of energy — mechanical or electrical energy — demands the presence of a heat sink. This heat sink can be found in the Sahara only in the atmosphere. But the ambient temperature in the lower levels of the atmosphere may attain 40° to 50°C. Two important consequences follow. First, one must operate with the heat source at relatively high temperatures, thus requiring a certain concentration of the solar radiation. Next, considerable interest attaches to systems that can move a large mass of air without marked intervention of external energy. The Institute of Solar Energy was thus very naturally led to study mirror systems, on the one hand, and atmospheric solar collectors, on the other. Its research programme will now be readily understood:

Study of solar radiation;

Study of solar collectors, with special reference to solar chimneys; and

Study of thermoelectric generators, first of all direct-exposure generators, and then fluid-circulation generators, which in turn involves the study of systems of mirrors and boilers.

We shall examine here, more particularly, the systems of capturing and concentrating solar energy, and thermoelectric generators. The solar radiation and atmospheric solar collectors will be the subjects of other communications.

The concentrated capture of solar energy

We are, of course, here concerned with capture on large surfaces, but envisaged in its particular application to thermoelectricity. For this purpose one might envisage the extension of the great mirrors which have been constructed at various points of the earth: the Heliodyne of the Bouzareah Solar Station, the solar furnace of Mont Louis and that in the design stage at Odeillo, the solar furnace at Natike, and, finally, the one now under construction at Tokyo. These furnaces are primarily experimental plants, and are far too costly and burdensome to become industrial plants. The Heliodyne, for example, which was conceived for an industrial development, since its reflecting surfaces are fabricated by stamping, cost when it was built about 20 000 NF per square metre of collecting surface. The Tokyo furnace, according to information received by us, costs about 7 500 NF per square metre of collecting surface, but this cost does not include numerous items, especially the research, which was included in the previous cost of the Heliodyne.

The manner of conceiving the method of energy collection depends on the desired temperatures. For temperatures under 300°C, which is close to the boiling point of certain liquid heat-transfer agents like "Gilotherm", "Fluitherm", etc., one may use the multiple-focus systems which we shall call *collectors*[1] in distinction from *insolators*.[2] This is a question of terminology, which should be clarified. For our part we prefer the term "insolators" as applied to devices that accomplish the conversion into heat at the same place where the radiation is received. The collectors introduce a supplementary operation, which is the change of direction of the radiation, with a directional effect, in order to produce the concentration. This does not include, for the insolators, the possibility of a certain reinforcement of the solar radiation, not going beyond a factor of several units, and which may be produced by mirrors, by diffusing surfaces, or by reflecting covers. This definition likewise does not exclude, for the insolators, a certain concentration by longitudinal thermal conduction, as we shall explain in detail later. For us, collectors are definitely multiple-focus systems.

They may be protected, as are insolators, by a cover which has a dual purpose — to protect the reflecting surfaces (the cleaning of a transparent cover being easier than that of a mirror, whose surface is always delicate) and that of separating the internal atmosphere, which becomes heated by reason of the various losses, including the absorption, strictly speaking, by the mirrors, to permit, to some extent, the recovery of these losses. The great advantage of multiple-focus systems is that they do not require very high precision in the orientation of these surfaces. Relatively crude mechanisms may thus be used. But it is this problem of the reflecting

[1] Also termed *focusing insolators*.

[2] These are usually termed *collectors* in the literature. They are likewise so termed in this translation.

surfaces that is the great problem of the concentration of solar radiation. One might be tempted to simplify this problem by confining oneself to seasonal changes of orientation. In that case, cylindro-parabolic reflectors should be used. We believe it is not advisable to favour half-measures; we therefore turn resolutely towards the elements of paraboloidal surfaces and must exert every effort towards the economic realization of orientable mountings. It should be noted that, in the case of extended surfaces, a certain modification may be made in the orienting mechanism, observing that the motion, in the case of collectors, takes place in such a way that the collecting surfaces are always parallel.

The collectors we have in mind, built according to procedures developed by local firms, are designed to heat a liquid heat-transfer agent which is also an electrical insulator. The circulation of this liquid over the hot armatures of the thermoelectric piles convectively transfers the heat to be converted into electrical energy. The utilization of this fluid serves two purposes. The first temperature drop takes place in the thermoelectric piles. There is another drop in the heaters designed to circulate the cooling air or for any other uses. The reflecting surfaces are very thin sheets of polished aluminium or aluminized sheet metal, or of plastic, such as "Lumaline", cemented on special shapes made of stucco or polyester reinforced by glass fibres. We shall probably be in a position to furnish more information on installations of this kind at the time of the conference.

For temperatures over 300°C, our project reduces down to the use of two new processes.[3] It is a rather complex, single-focus system, using a large number of independent mirrors distributed over the site. Each mirror, at any given time, is oriented so as to concentrate the radiation received in the aperture of the focus, elevated a certain distance above the ground. As will be seen at once, such a system demands the exact satisfaction of three conditions :

Exact orientation, independent of the atmospheric conditions.

An exact shape, causing the very precise concentration of the reflected beam in the aperture of the focus. Each mirror element represents, at each given instant, an element of a paraboloid whose parameters vary with time.

The task was thus in our preliminary study :

1. To assure ourselves of the conditions imposed by the distribution of such mirror elements over the site;

2. To examine the various possible mechanisms for orientation, and the precise remote control of such mechanism;

3. To verify the possibility of simple realization of paraboloidal surfaces of time-variable shape.

[3] French patents 1 238 883 and PV 830 443.

Rather important projects have been initiated on the first two of these points. It would as yet be premature to give the results. As for the third point, we have sought to realize the paraboloidal reflecting elements with simple electrobrightened aluminium and aluminized sheet metal. The first experiments have been encouraging, since we have succeeded in obtaining a focus at 9 m with aberrations below 5 thousandths, using aluminium sheet 16/10 mm thick in rectangles 1 × 0.5 m.

The concentration of large amounts of solar radiation leads to envisaging a focus at distances greater than those already tried, requiring, *a fortiori*, greater radii of curvature and consequently greater deformability of the reflecting metal sheets.

In the first stage we intend to use air as the heat-transfer agent with this energy capture system, for heating the hot armatures of the thermoelectric piles. The reason is that if we tried to realize a closed focal region we should encounter very great difficulties if the quantities of energy to be developed were very great. The open focus is far simpler, but it does involve heating the air, even if that were not the purpose and primary function of the focus.

While solar radiation collectors appear to be an immediate solution, capable of solving, without too much difficulty, the problem of a thermoelectric generator operating at acceptable efficiency, systems with fields of deformable mirrors would seem in all probability to be a solution of the future, not alone for thermoelectric conversion but, above all, for thermo-ionic and photo-ionic conversion. The Institute must not neglect this solution. It does, at the moment, pose extremely complex technical problems, which we shall take up one after the other.

We shall now discuss, in somewhat more detail, our work and our projects relating to thermoelectric generators proper.

Direct thermoelectric conversion of solar radiation

A thermoelectric generator consists essentially of a set of thermoelements arranged between two armatures, a hot armature and a cold one.

The heat may be delivered to the hot armature by a fluid — a liquid or gas circulating without change of phase along surfaces in direct contact with the hot armature; by condensation of a vapour on these surfaces; or, finally, by direct conversion of the solar radiation into thermal energy.

After having passed the thermoelements, the heat may be discharged, as above, by circulation of a fluid without change of phase; by vaporization of a liquid; or, finally, by radiation into space.

When the generator is directly insolated, it may be *fixed* or *orientable*. In the former case, the surface receiving the radiation must not, in principle, be directional, excepting perhaps at low solar altitudes; the radiation may be *reinforced* by fixed mirrors or by diffusers. In the latter case, the surface may

be directional, as in the case of surfaces formed by hollow cones with small vertex angles, or of surfaces operating by reflection or refraction.

The receiving surfaces may be selective, that is, they may absorb appropriately in the visible spectrum and emit little in the far infrared. Such selectivity may be obtained by appropriate treatment of the surface, or interposition above the incoming radiation of a transparent covering giving the "hothouse effect", or by both these methods.

When the generator exposure is fixed, there is an optimum angle of inclination which depends on the latitude, the mean atmospheric absorption, and the statistical characteristics of the cloudiness.

When there is fluid circulation, the movement may be *natural* (thermo-siphon, cold-wall principle) or *forced*. In this case, the generator includes additional parts for auxiliary services — fans or pumps.

When the thermoelectric generator is designed to convert solar energy into electrical energy, the high variability of solar radiation must be taken into account — both its regular diurnal march and its random variation. Two modes of operation are possible. Either the hot junctions are heated by the aid of an intermediate fluid, or by means of direct insolation.

In the former case, the device of course is to operate at constant temperatures, which are chosen as close as possible to those of optimum yield of the thermoelectric material involved. Obviously in this case it will be the mass flow rate of the fluid that will vary, and consequently the number of elementary piles in service will also vary. In practice the generator is divided into a certain number of groups of piles which are switched into the electric circuit, or switched off, to hold the voltage across the terminals constant within the tolerances adopted.

In the latter case a D.C.-D.C. converter must be interposed between generator and load, to match the resistance of the charging circuit to the internal resistance of the generator, and to operate at the same time as a voltage regulator. But the mean efficiency of the generator is considerably lower in the latter case.

In any case, whatever the mode of operation, there is a maximum temperature of the hot junctions which must not be exceeded, if irreversible degradation of the generator is to be avoided. The generator installation in that case must also include safety devices.

Controlling climatological factors must be added to these very general technological considerations. The I.E.S.U.A. is most particularly interested in the Saharan applications of solar energy. The design of the thermoelectric generator must thus be studied with special reference to its possible utilization in the Sahara. There are three important remarks to be made here :

1. The choice of sites of elevated insolation is permissible in the Sahara.

2. One can count only on the atmosphere for cooling the generators. However, the great dryness of the air permits us to envisage additional cooling by humidification.

3. Sandstorms and dust storms are very frequent. The natural slope of dry sand due to erosion has an inclination of 22° to the horizon, but extremely fine dust particles, running down to a few microns in diameter, adhere very easily. In a sandstorm, the coarsest grains, whose accumulation or grinding effect might be feared, do not rise at all above 2 m from the ground.

It follows from these remarks that:

(*a*) Thermoelectric generators must be designed for cooling by air circulation. However, under certain circumstances this air may reach the relatively elevated temperatures of 40 or 45°C.

(*b*) Dirt on the energy collection systems or the transparent covers of the solar collectors may cause important decreases in the incident energy and high operating costs for cleaning. Surfaces treated to make them selective lose their selectivity when coated with dust.

Financial questions are also relevant. The thermoelectric material is relatively expensive. Bismuth telluride of types n and p may be had in France at about 7 000 NF per kg. Material from the United States is more than twice as expensive. Moreover, the utilization of these materials is a delicate matter. The armatures are highly sophisticated, especially when they include air radiators. The convective transfer coefficients of air are usually low, requiring extensive and developed surfaces. It is thus essential to operate the thermoelements under optimum efficiency conditions, that is, at the most favourable temperatures. If the heat is provided by the sun, this implies the use of an intermediate fluid and a system of collecting and concentrating the radiation at the focus of a boiler.

On the other hand, the circulation of the cooling air should as far as possible be due to the solar heating itself, to avoid the need for a conversion unit, which would necessarily cost the high price of using part of the energy required for moving the air.

It will be seen that such a plant involves very varied techniques, and that each of them must at first be studied individually.

Atmospheric solar collectors are likewise discussed in a separate paper (S/45). Their study is facilitated by an electrical analogous method, which is also very useful in the study of thermoelectric solar collectors. This method will be described in the present paper, which will have special reference to the thermoelectric generator itself, and will describe the prototype now under test at the Institute of Solar Energy, University of Algiers.

The problem of the most suitable material, its machining and its installation on the armatures, has been entirely disregarded here. Very important laboratories in France and abroad are carefully studying these questions. The Institute of Solar Energy is thus confined, in the preliminary phase

to the examination of the problems that might arise in building a fixed-position thermoelectric solar collector, direct exposure, low power, designed for use in the Sahara to supply power for telemechanical systems (telemetering or remote control), or for very small machines (air-conditioning fans, small water pumps, etc.). It was, in fact, important to know whether a fairly unsophisticated generator of nonprohibitive cost could be developed for small applications.

Selective reception surfaces had been abandoned on account of the soiling, and it was important to study in more detail the absorbing surface of the hot armature. On the other hand, the problem of removing the heat that had passed the thermoelements still persisted. An economic observation permitted orientation of the solutions.

One must begin by making it very clear just what meaning was to be assigned to the term *generator surface*. Several surfaces are involved in the analytic study of the question (figure 1).

First of all there is the section s of the thermoelement (s_n for the n type element, s_p for the p-type) which enters into the *form factor* $\gamma = h/s$, where h is the height of the thermoelectric bar. If the generator has n elements (or $n/2$ couples), the total section, or surface, of the thermoelectric elements is $n/2\ (s_n + s_p)$.

The hot armature generally presents an insolated surface s_i which is constant if it is plane, but may vary with the position of the sun if it has hollows or ridges; s_i in that case is the surface insolated at true noon, when the sun is in the equatorial plane.

The collector itself reserves for each element a surface s_1 or *illuminated surface*, the projection of which on the horizontal plane is $s_o = s_1/\cos\varphi$, where φ is the inclination (usually close to the latitude of the place) of the receiving surface of the collector to the horizontal plane.

s_o is the *surface occupied* on the ground associated with the element. It will easily be seen that only economic conditions could prevent s_1 from being much greater than s_i. But if the cost of the thermoelectric element is relatively high, related to its insolated surface, the cost of the excess illuminated surface may be very low. It would, indeed, be sufficient if this excess surface represented a good thermal insulation between the region of the hot armatures and that of the cold armatures. If this excess surface is absorbing, all the solar energy received will feed the losses, unless a slight convection current were to flow between the hot insulating surface and the adjacent armatures which, owing to the heat flow, are at a lower temperature. It may thus be beneficial to have an illuminated surface greater than the insolated surface, all the

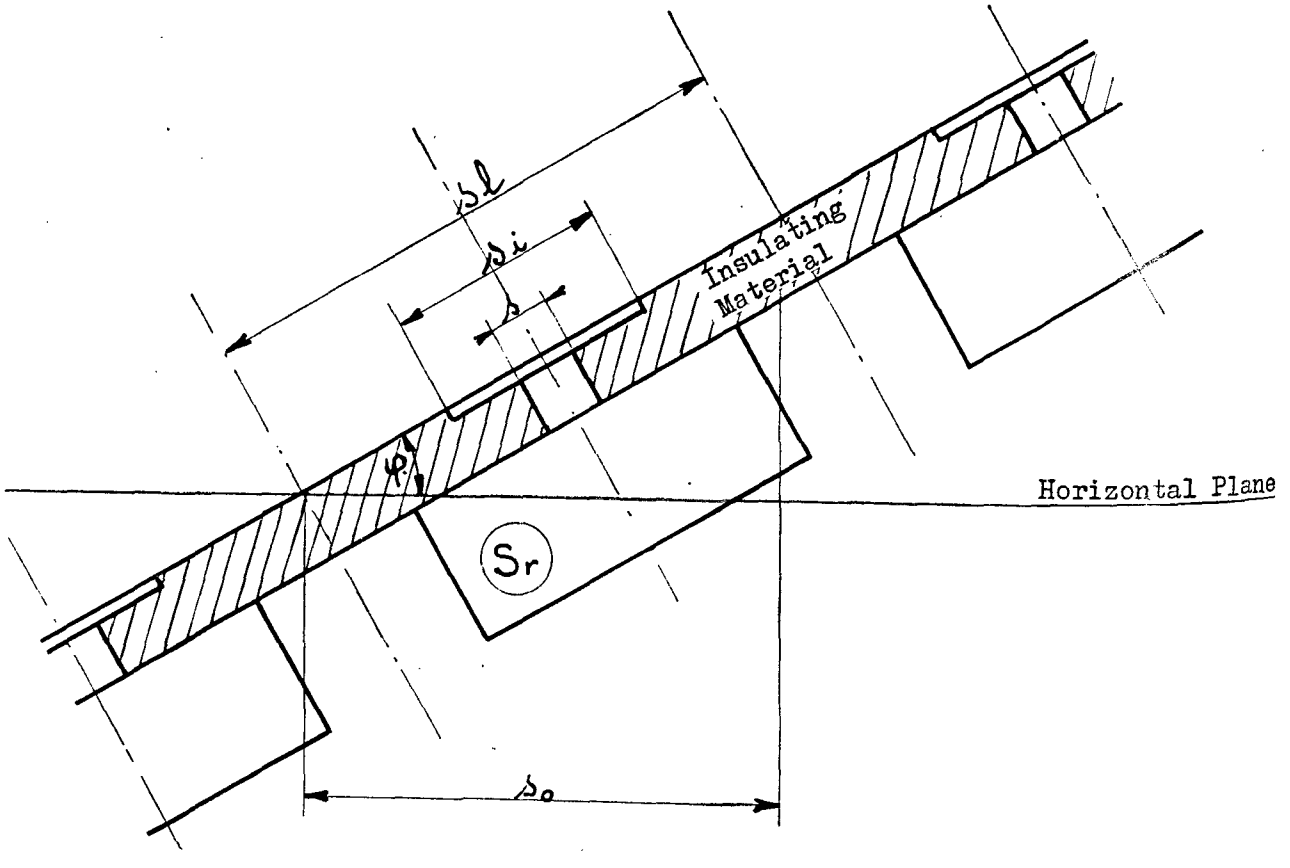


Figure 1.

more so since this will give the cold armature more room to develop its radiating surfaces.

Under these conditions, it no longer makes much sense to relate the electric power generated to the ground area occupied by the generator, especially when this ground is located in the Sahara. There is similarly not much more sense in including the losses of the excess surface among the losses of the generator than if one were equally to include the losses of all the desert or unutilized areas of the world.

There are thus two ways of designing the radiator of the cold armature, either to place the cooling fins perpendicular to the receiving surface, or what appears the more rational alternative, since the cooling surfaces could more easily be developed, to arrange them parallel to the receiving surface.

The shape of the illuminated surfaces may not be arbitrary. These surfaces are, indeed, arranged in checkerboard fashion, and must thus be square or hexagonal. Hexagonal would be the better shape, since it is closer to the circle, and should be adopted for the fins parallel to the receiving surface.

In its prototype (figure 1), the Institute of Solar Energy has adopted normal fins, since their construction is easier. The elements are aligned side by side, and the rows so formed are separated by a simply insulating blackened surface.

However, in order to make the insolation of the hot armatures a little more regular, the connectors are provided with low meridian fins which no longer cast a shadow after the sun has climbed to an altitude of 30°, which is assumed to be the threshold of generator operation. These fins, like those of the cold armatures, likewise serve as electrical connexions between the elements.

The motion of the air is activated by the draught from a chimney. An expansion chamber at the cooling-air inlet removes the heaviest grains of dust from the air, which then passes the evaporating surfaces of a humidifier and may drop about 10°C in temperature before circulating over the cooling fins.

Once the general features of the desired generator had been decided, the next step was the optimum dimensioning of the various parts.

This led us to establish a simplified theory of thermopile operation, which could be given an electrical representation, so that the various details of operation could be checked before construction and certain points in the detail design could be modified in the light of our more precise knowledge of the phenomena. The electrical analogous method has a second advantage, besides that of showing in advance the operation of a projected generator. Once the generator has been built, indeed, it can no longer be disassembled to modify certain elements which depend on the definitive dimensions. The analogous method is then used, at first so set as to represent in rather good approximation the phenomena observed on the actual generator. It will then be easy enough to make the desired modifications on the analogous model and to experiment on it, with some chance of reliability.

It is not even necessary to equip the generator under study with all of its thermoelectric elements. Since the thermal operation is the essential phenomenon, the thermoelectric materials may be utilized to realize a small number of couples located among others made of some material with the same thermal resistance. The electrical operation studied on this small number of real elements can be extrapolated without trouble to the entire set of elements. All this, of course, applies only under the hypothesis, which has unfortunately been verified, of a rather low generator efficiency.

However that may be, these approximate methods may provide precious instruction in the use of more precise methods which are essential if efficiencies higher than 6 to 7 per cent are to be obtained.

Simplified electrical and thermal study of solar thermoelectric generators

Internal efficiency

It is customary, in studying the operation of thermoelectric piles, to start out from the classical system of equations I, only four of which are independent :

$$q_c = \frac{T_c - T_f}{R_i} - \frac{r_i I^2}{2} - I \alpha T_c$$

$$q_f = \frac{T_c - T_f}{R_i} - \frac{r_i I^2}{2} - I \alpha T_f = \frac{T_f - T_a}{R_f}$$

$$P_u = q_c - q_f = r_i I^2 - I \alpha (T_c - T_f) = r_e I^2$$

$$I = \alpha \frac{T_c - T_f}{r_i - r_e}$$

where

q_c is the quantity of heat supplied by the heat source in unit time, at temperature T_c, in °C;

q_f is the quantity of heat removed by the heat sink in unit time, at temperature T_f, in °C;

R_i is the thermal resistance of the thermoelectric couple between junctions (the bars of the couple are thermally in parallel);

R_f is the thermal resistance of the radiators removing the heat into the ambient at temperature T_a, in °C (the radiators of the couple are thermally in parallel);

r_i is the electrical resistance of the couple between junctions, or the internal resistance (the bars of the couple are electrically in series);

r_e is the external resistance; it consists of the resistance of the charge r' between the terminals of the pile and the electrical resistance r of the junctions and the internal connexions;

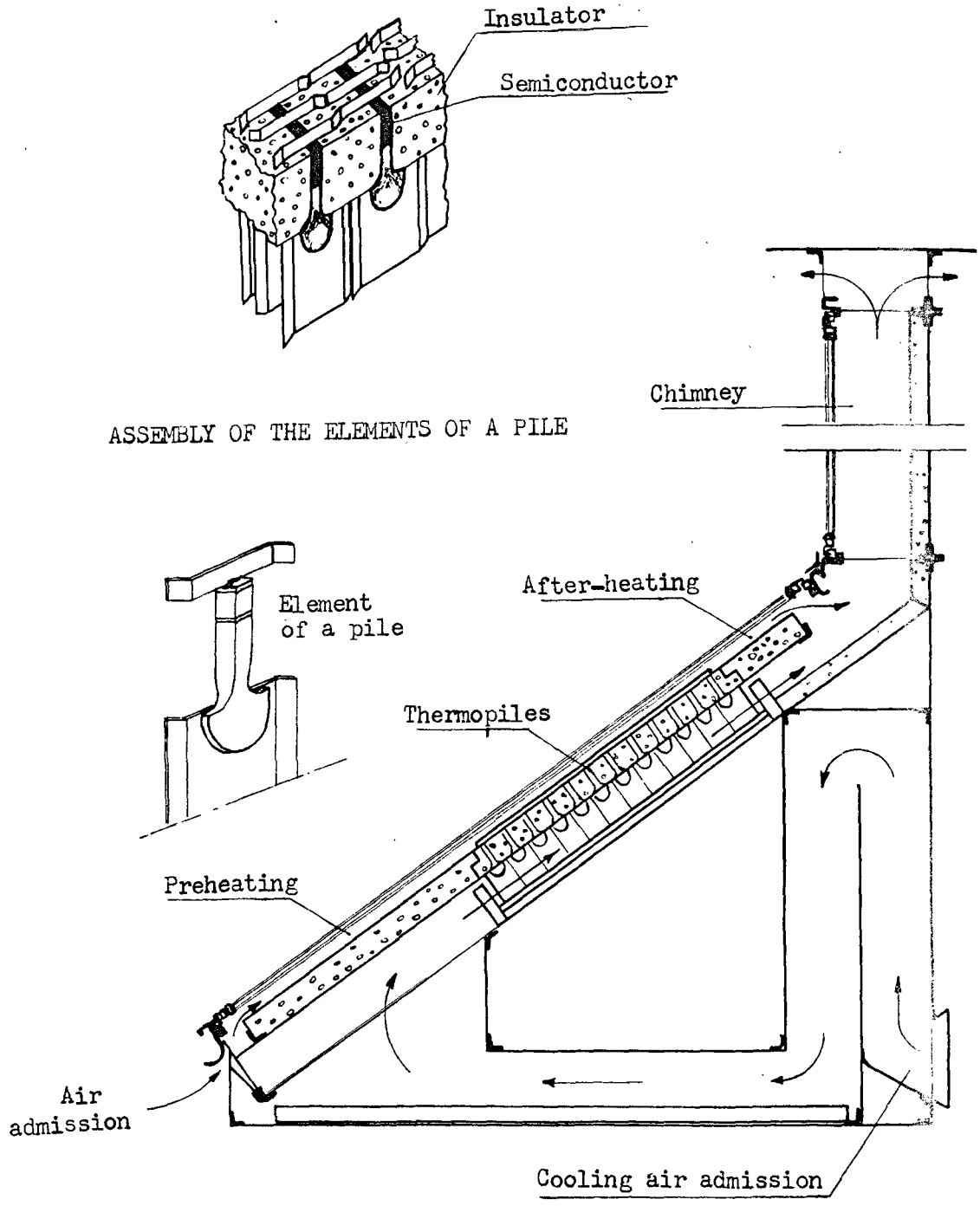


Figure 2. Thermogenerator (meridian section)

P_u is the useful electric power; the power actually used is

$$P = r' I^2 = P_u - r I^2$$

I is the current in the electrical circuit, in amp;

α is the thermoelectric power of the couple, in V/°C.

We set :

(1-1) $m = \frac{r_e}{r_i}$, (1-2) $k = \frac{R_f}{R_i}$, (1-3) $\gamma = \frac{h}{s}$

where h is the height of the thermoelectric bar and s its section; γ is the *form factor*. The two bars of a couple, with from factors γ_1 and γ_2 respectively, generally have different characteristics:

$\alpha_1 \rho_1 \varkappa_1$ for one, $\alpha_2 \rho_2 \varkappa_2$ for the others. We have

(1-4) $$r_i = \rho_1 \gamma_1 + \rho_2 \gamma_2,$$

(1-5) $$R_i = \frac{\gamma_1 \gamma_2}{\varkappa_1 \gamma_2 + \varkappa_2 \gamma_1}$$

ρ being the electrical resistivity and $\varkappa$ the thermal conductivity.

It is possible to define a fictitious bar of form factor $\gamma = \gamma_1$ and the characteristics :

$$\alpha = \frac{\alpha_1 + \alpha_2}{2}$$

$$\rho = \frac{1}{2}\left[\rho_1 + \sqrt{\rho_1 \rho_2 \frac{\varkappa_2}{\varkappa_1}}\right]$$

$$\varkappa = \frac{1}{2}\left[\varkappa_1 + \sqrt{\varkappa_1 \varkappa_2 \frac{\rho_2}{\rho_1}}\right]$$

We may now consider only one of the elements of the couple.

r_i, R_i, R_f are henceforth relative only to this one element, and not, as before, to the couple. Under these conditions, we have

(1-4') $r_i = \rho\,\gamma$, (1-5') $R_i = \frac{\gamma}{\varkappa}$ and (1-6) $k\,\gamma = \varkappa\,R_f$

It should be noted here that α is independent of the temperature. On the other hand, ρ and $\varkappa$ generally do depend on the extreme temperatures T_c and T_f, and k on the extreme temperatures T_f and T_a.

If there are n elements (or $n/2$ couples), the internal electrical resistance of the generator is

(1-7) $$r_{i_i} = n\,r_i$$

its internal thermal resistance is

(1-8) $$R_{i_i} = \frac{R_i}{n}$$

the thermal resistance of the radiator is

(1-9) $$R_{f_i} = \frac{R_f}{n}$$

The *factor of merit*, as defined by Joffe, of this fictitious material is

$$z = \frac{\alpha^2}{\rho\,\varkappa}$$

We prefer to consider the inverse ratio:

(1-10) $$\tau = \frac{\rho\,\varkappa}{\alpha^2}$$

which is homogeneous at a certain absolute temperature, which we shall term the *characteristic temperature* of the material. τ likewise depends generally on the temperatures T_c and T_f.

We now put

(1-11) $$q_u = \frac{T_c - T_f}{R_i} = \frac{\varkappa}{\gamma}(T_c - T_f)$$

The *internal efficiency* of the thermoelectric pile is

(1-12) $$\eta_i = \frac{P_u}{q_c}$$

We shall show that the efficiency η_i and the power P_u are maximum when m = 1, on condition —as is the case with the materials known today, which operate at relatively moderate temperatures— that the efficiency is low.

We now have

(1-13) $$P_u = \frac{\alpha^2 (T_c - T_f)^2}{4\rho\gamma} = \frac{(T_c - T_f)^2}{4\tau}\frac{\varkappa}{\gamma}$$

and for n elements

(1-14) $$P_{u_i} = n\,P_u = \frac{(T_c - T_f)^2}{4\tau}\varkappa\frac{ns}{h}$$

If s_i is the portion of the insolated surface corresponding to the element under consideration, we shall term *concentration ratio* the ratio

(1-14) $$C = \frac{s_i}{s}$$

The volume of the thermoelectric material of an element is

(1-15) $$v = h\,s$$

Global efficiency

The insolated surface s_i, which is the section of the light beam incident on a mirror, the receiving surface in the case of a direct-exposure solar collector, absorbs the quantity of heat q_a.

Let $Q_{i\Theta}$ be the incident radiation, which is the direct radiation in the case of a mirror and the total irradiance of the exposed surface in the case of a solar collector $Q_{i\Theta}$ depends on the position of the sun and on the meteorological conditions.

If the heating takes place by circulation of a fluid, the set-up will be such as to give the optimum conversion conditions during the period of operation. In our first analysis the ambient temperature will be assumed constant, while in reality, of course, it varies directly with $Q_{i\Theta}$ *in the same sense* but with a lag of an hour or two; the optimum conditions will be expressed by the constant values of the various quantities involved. Then we have

(2-1) $$q_a = \eta\,s_i\,Q_{i\Theta} = \text{Cte}$$

where η is the efficiency of the conversion of solar radiation into heat.

It is the insolated surface s_i that must in this case vary with $Q_{i\Theta}$ in order to maintain the operating conditions constant.

If the heating takes place by direct insolation, we have

(2-2) $$q_a = \alpha_s\,\tau_v\,Q_{i\Theta}\,s_i + q_e\,s_i,$$

where

α_s is the mean absorption factor of the insolated surface

τ_v is the transmission factor of the media traversed by the radiation before arrival at the receiving surface

q_e is the quantity of heat supplied to the hot armature, generally by convection, by the excess illuminated surfaces

q_a in this case is variable.

The power q_p lost by the generator before the hot armature depends in this case only on the

temperature T_c of that armature, on the ambient temperature T_a, and possibly also on the sky temperature T_{vc}, which can reach —100°C for a very clear sky. In no case will q_p depend on the strictly thermoelectric characteristics of the pile.

The value of q_p is usually zero when the heating is accomplished by the circulation of a fluid. This is not the case for solar collectors. When the generator operates as a solar collector, experiment shows that, for the temperature zones in which it operates, we may write, in rather good approximation:

$$q_p = [a + b\,(T_c - T_a) + c\,(T_c - T_a)^2]\,s_t \tag{2-3}$$

where a, b, c are coefficients relating to a unit insolated surface, and are positive and depend on the meteorological conditions, especially the wind. The value of c is rather low. Thus, for a blackened surface, with a cover formed by two panes of glass, we have, in calm air,

$$a = 40\ \text{W}, \qquad b = 3.2\ \text{W/°C}, \qquad c = 0.023\ \text{W/°C}^2$$

On the other hand, we have

$$q_c = q_a - q_p \tag{2-4}$$

System I then gives

$$q_a - q_p = q_f - r_i I^2 + I\,\alpha\,(T_c - T_f) = q_f + P_u$$

and, finally

$$q_a = q_f + q_p + P_u \tag{2-5}$$

The *global efficiency* of the generator is

$$\eta_g = \frac{P_u}{q_a} \tag{2-6}$$

At given incident energy, this efficiency varies as the useful power. Thus, definitively, only conditions of maximum useful power should be sought.

Simplified theory

The elementary theory of the system assumes the efficiency to be so low that the useful power is small by comparison to the energy fluxes involved. It may then be assumed that everything happens as though conversion of heat into electrical energy took place at the level of the hot junction, and that the Joule-effect losses appeared only at that level. This hypothesis is merely a mathematical expedient, and, of course, has no physical meaning.[4] It is represented simply by the relation

$$q_u = q_f \tag{3-1}$$

or

$$\frac{T_c - T_f}{R_i} = \frac{T_f - T_a}{R_f} \tag{3-2}$$

whence we derive

$$T_c - T_f = \frac{T_c - T_a}{1 + k} \tag{3-3}$$

and

$$T_f - T_a = (T_c - T_a)\,\frac{k}{1 + k} \tag{3-4}$$

(2-5) becomes

$$q_a = q_u + q_p + P_u \tag{3-5}$$

(1-11) is now written

$$q_u = \frac{T_c - T_a}{1 + k}\,\frac{\varkappa}{\gamma} \tag{3-6}$$

(1-12) is written

$$\eta_i = \frac{P_u}{q_a - q_p} \simeq \frac{P_u}{q_u} = \frac{T_c - T_a}{\tau}\,\frac{1}{4\,(1 + k)} \tag{3-7}$$

(1-13) is written

$$P_u = \frac{(T_c - T_a)^2}{4\,\tau\,(1 + k)^2}\,\frac{\varkappa}{\gamma} = \frac{(T_c - T_a)^2}{4\,\tau}\,\frac{k}{R_f\,(1 + k)^2} = \frac{\alpha^2}{4\,\rho\,\gamma}\left[\frac{T_c - T_a}{1 + k}\right]^2 \tag{3-8}$$

and for n elements

$$P_{u_t} = \frac{(T_c - T_a)^2\,\varkappa\,n\,s}{4\,\tau\,(1 + k)^2\,h} \tag{3-9}$$

By the aid of the formulae so established, we shall now study the two cases of more particular interest to us:

1. Heating of the generator by convection: circulation of a fluid or condensation of a vapour.

2. Heating of the generator by insolation.

In the former case, it may be considered that we are dealing with a quasi-infinite heat-source, and the generator may be assumed to operate at constant temperatures, and, more particularly, at optimum temperatures T_c and T_f during the entire period of collection of solar radiation

In the latter case, the best flux absorbed is confined to the solar radiation, and varies with it. The generator operates at variable temperatures. There is a temperature threshold, defined by the technical possibilities of utilizing the energy produced.

We shall discuss only the case of cooling by circulation of air at the ambient temperature, by natural or forced convection. The resistance R_f is then of the form

$$R_f = \frac{1}{A\,S_r\,(T_f - T_a)^{0.25}} \tag{3-10}$$

where S_r is the exchange surface of the radiator, while A is a coefficient depending on the shape and dimensions of the radiator, the velocity of the cooling fluid, its nature, and especially its humidity, etc. In a theory which has no other object than to seek the approximate form of the relations between the various quantities, we may assume that A = Cte. We put

$$\sigma = \frac{S_r}{s} \tag{3-11}$$

[4] We shall show that the error due to this hypothesis in the calculated internal efficiency is only $\Delta\eta_i = \frac{\eta\, i^2}{\theta}$ where θ denotes the efficiency of a Carnot cycle between the same temperatures. Thus, for $\eta_i = 1$ per cent, $\theta = 50$ per cent, $\Delta\eta_i = 2 \times 10^{-4}$.

σ is the *specific surface of the radiator*; it depends on economic considerations and varies according to the radiator system adopted. It is selected *a priori*.

Thus, by (3-4), we have

$$(3\text{-}12) \qquad R_f = \frac{1}{A\, s\, \sigma\, (T_c - T_a)^{0.25}} \sqrt[4]{\frac{1+k}{k}}$$

and by (3-8)

$$(3\text{-}13) \qquad P_u = A\, s\, \sigma\, \frac{(T_c - T_a)^{2.25}}{4\tau} \sqrt[4]{\frac{k^5}{(1+k)^9}}$$

The current is by system I and (3-3)

$$(3\text{-}14) \qquad I = \frac{\alpha}{2\rho\gamma} \frac{T_c - T_a}{(1+k)}$$

The voltage is by (1-1)

$$(3\text{-}15) \quad u = r' i \quad \text{with (3-16)} \quad r' = \rho\gamma - r$$

If there are n elements in series, the voltage across the generator terminals is

$$(3\text{-}17) \qquad u_t = n\,(\rho\gamma - r)\, \frac{\alpha\,(T_c - T_a)}{2\rho\gamma\,(1+k)}$$

and the power delivered to the external circuit is

$$(3\text{-}18) \quad P_t = u\, I = n^2\,(\rho\gamma - r) \left[\frac{\alpha\,(T_c - T_a)}{2\rho\gamma\,(1+k)}\right]^2$$

The temperature may be assumed to vary linearly in the interior of the bar. If x is the distance to the hot junction of a section, at temperature T, we have

$$(3\text{-}19) \qquad \frac{x}{h} = \frac{T_c - T}{T_c - T_f} = \frac{T_c - T}{T_c - T_a}\,(1+k)$$

The values of ρ and $\varkappa$ to be used correspond to the mean temperature

$$(3\text{-}20) \qquad T_{ave} = \frac{T_c + T_f}{2} = T_c - \frac{T_c - T_a}{2\,(1+k)}$$

Dimensioning of thermoelectric generators

Case 1. *Convection heating*

During the collection of solar energy the generator operates at the optimum temperatures. One should thus, by (3-13), seek the minimum of the expression

$$(4\text{-}1) \qquad y = \frac{(1+k)^9}{k^5}$$

which occurs at

$$(4\text{-}2) \qquad k = \frac{5}{4} = 1.25$$

We have

$$\sqrt[4]{\frac{k^5}{(1+k)^9}} = 0.212$$

and, on the other hand (4-3) and (4-4)

$$\gamma = \frac{\varkappa}{k} \cdot R_f = \frac{\varkappa}{A\, s\, \sigma\, (T_c - T_a)^{0.25}} \sqrt[4]{\frac{1+k}{k^5}} = \frac{h}{s}$$

whence

$$(4\text{-}5) \qquad h = 0.926\, \frac{\varkappa}{A\, \sigma\, (T_c - T_a)^{0.25}}$$

and

$$(4\text{-}6) \qquad P_{u\,max} = 0.053\, \frac{A\, s\, \sigma\, (T_c - T_a)^{2.25}}{\tau}$$

The maximum useful power per unit volume of the thermoelectric bar is

$$(4\text{-}7) \qquad \omega = \frac{P_{u\,max}}{v} = 0.057\, \frac{A^2\, \sigma^2\, \alpha^2\, (T_c - T_a)^{2.5}}{\rho\, \varkappa^2}$$

Its value is higher the higher the transfer coefficient A, the specific surface of radiation σ, and the expression.

$$(4\text{-}8) \qquad \frac{\alpha^2\, (T_c - T_a)^{2.5}}{\rho\, \varkappa^2}$$

The expression (4-8) increases with T_c. It is therefore well to operate as close as possible to the technical maximum T_c max.

(3-19) becomes

$$(4\text{-}9) \qquad T_{ave} = \frac{7}{9}\, T_c + \frac{2}{9}\, T_a$$

To take the dimensions of the pile, one must first select the thermoelectric material, its section s, the ambient temperature T_a, the temperature T_c of the hot armature, the type of the radiator, and its specific surface σ.

We may then calculate h by (4-5) and consequently also γ; P_u max by (4-6); i max by (3-14). If the number of elements n is assigned, u_t and P_t may be calculated by (3-17) and (3-18), the resistance r of the junctions and interior connexions being defined by the requirements of the design.

Numerical application

Let us adopt, for $T_a = 30°C$ and $T_c = 200°C$, the following characteristics of a material originating in the United States:

$$\alpha = 204 \cdot 10^{-6}\ V/°C$$
$$\rho = (0.522 + 0.00474\, T)\ 10^{-5}\ \Omega.m$$
$$\varkappa = 3.59 - 0.0106\, T.$$

We have $T_{mean} = 162°C$, whence

$$\rho = 1.288 \cdot 10^{-5}, \qquad \varkappa = 1.87, \qquad \tau = 578°K$$

Let us take

$$\sigma = 100, \qquad A = 2.55\ W/m^2, \qquad s = 10^{-4}\ m^2.$$

Then we have

$$h = 1.9\ mm$$
$$P_{u\,max} = 0.24\ W$$
$$T_c - T_f = 75.6°C$$
$$T_f - T_a = 94.4°C$$
$$T_f = 124.4°C$$

$\gamma = 18.7$
$R_i = 10°\text{C/W}$
$r_i = 2.411 \cdot 10^{-4}\ \Omega$
$q_u = 7.56\ \text{W}$
$q_a = 7.70\ \text{W}$
$\eta_g = 3.2$ per cent
$I = 31.1\ \text{A}$

We should cherish no illusions about the accuracy of the calculations, owing to the uncertainty of the exact values of α, ρ, $\varkappa$, and above all of the transfer coefficient A. On the other hand, the effect of the resistance r of the junctions and interior connexions has not been taken into account.

Case 2. *Heating by insolation*

The temperature T_c of the hot armature here depends on the solar radiation.

(2-3), (3-5), (3-6) and (3-8) give

$$(4\text{-}10)\quad \left[\frac{T_c - T_a}{1+k}\right]^2 \left[\frac{\varkappa}{4\tau h E} + c\,(1+k)^2\right] + \frac{T_c - T_a}{1+k}\left[\frac{\varkappa}{hC} + b\,(1+k)\right] + (a - \alpha_s \tau_v Q_{i\Theta}) = O,$$

which is a relation independent of the section s of the bar.

Let us take the case where the coefficient of the second-degree term is negligible, that is, where the value of the expression

$$(4\text{-}11)\quad Z = c + \frac{\varkappa}{4\tau h C (1+k)^2} = c + \frac{\alpha^2}{4 h C \rho (1+k)^2}$$

is small by comparison to the other coefficients. This hypothesis may be adopted all the more easily, since the coefficients a, b, c and the parameters α_s, τ_v, $Q_{i\Theta}$ and Q_e result from rather uncertain experimental data,

We have

$$(4\text{-}12)\quad \frac{T_c - T_a}{1+k} = \frac{\alpha_s \tau_v Q_{i\Theta} - a}{b\,(1+k) + \dfrac{\varkappa}{hC}}$$

or

$$(4\text{-}13)\quad T_c - T_a = \frac{\alpha_s \tau_v Q_{i\Theta} - a}{b + \dfrac{\varkappa}{hC\,(1+k)}}$$

and, by (3-8),

$$(4\text{-}14)\quad P_u = \frac{\alpha^2 (\alpha_s \tau_v Q_{i\Theta} - a)^2}{4 \rho C h \left[b\,(1+k) + \dfrac{\varkappa}{hC}\right]^2} \cdot s_i$$

For a given value of the solar radiation, α being practically constant, the maximum of P_u corresponds to the minimum of the expression

$$(4\text{-}15)\quad E = \rho C h \left[b\,(1+k) + \frac{\varkappa}{hC}\right]^2$$

On the other hand, we have

(4-16)

$$R_f = \frac{k\gamma}{\varkappa} = \frac{1}{A s \sigma (T_c - T_a)^{0.25}} \sqrt[4]{\frac{1+k}{k}} = \frac{1}{A s \sigma (\alpha_s \tau_v Q_{i\Theta} - a)^{0.25}} \sqrt[4]{\frac{b\,(1+k) + \dfrac{\varkappa}{Ch}}{k}}$$

whence

(4-17)

$$A \sigma (\alpha_s \tau_v Q_{i\Theta} - a)^{0.25} = \frac{\varkappa}{kh} \sqrt[4]{b\left(1 + \frac{1}{k}\right) + \frac{\varkappa}{kCh}}$$

which gives a relation between k and h as a function of the insolation and of the concentration ratio $C = s_i/s$.

Let

$$(4\text{-}18)\quad B = \sqrt[4]{b\left(1 + \frac{1}{k}\right) + \frac{1}{C}\frac{\varkappa}{kh}}$$

and

$$(4\text{-}19)\quad M = A \sigma (\alpha_s \tau_v Q_{i\Theta} - a)^{0.25}$$

B varies relatively little, as may be seen from the numerical application to follow, with the values of k and h that satisfy the relation (4-17); it may be considered a constant for a certain value of C and mean values of ρ and $\varkappa$. Then we have

$$(4\text{-}20)\quad kh = \frac{\varkappa B}{M} = \text{Cte}$$

Since, on the other hand, we have

$$(4\text{-}21)\quad kh = s \varkappa R_f,$$

the approximate constancy of $B = M s R_f$ is expressed in the approximate constancy of the thermal resistance R_f of the radiator, which is a rather noteworthy result.

(4-15) becomes

$$(4\text{-}22)\quad E = \rho C h \left[b\left(1 + \frac{\varkappa B}{hM}\right) + \frac{\varkappa}{Ch}\right]^2 = \rho C h \left[b + \frac{\varkappa}{b}\left(\frac{1}{C} + \frac{B b}{M}\right)\right]^2$$

$$= \rho C \left[h b^2 + 2 b \varkappa \left(\frac{1}{C} + \frac{B b}{M}\right) + \frac{\varkappa^2}{b}\left(\frac{1}{C} + \frac{B b}{M}\right)^2\right]$$

and we have

$$(4\text{-}23)\qquad \frac{d\,E}{d\,b} = \rho\, C \left[b^2 - \frac{\varkappa^2}{h^2}\left(\frac{1}{C} + \frac{B\,b}{M}\right)^2 \right]$$

$$(4\text{-}24)\qquad \frac{d^2\,E}{d\,h^2} = \frac{2\,\varkappa^2}{h^3}\left(\frac{1}{C} + \frac{B\,b}{M}\right)^2 > 0$$

The minimum occurs at

$$(4\text{-}25)\qquad h = \varkappa\left[\frac{1}{b\,C} + \frac{B}{M}\right] = \varkappa\left[\frac{1}{b\,C} + s\,R_f\right]$$

and consequently

$$(4\text{-}26)\qquad b = \frac{B}{M}\,\frac{1}{\dfrac{1}{b\,C} + \dfrac{B}{M}}$$

whence

$$(4\text{-}27)\qquad E_{\min} = \rho\, C\,\varkappa\left(\frac{1}{b\,C} + \frac{B}{M}\right)\left[b + \frac{\dfrac{1}{C} + \dfrac{B\,b}{M}}{\dfrac{1}{b\,C} + \dfrac{B}{M}} \right]^2$$

$$= 4\,\rho\, C\,\varkappa\left[\frac{1}{C} + \frac{B\,b}{M}\right]$$

$$= \frac{4\,\rho\,\varkappa}{C}\left[1 + \frac{B\,b\,C}{M}\right]^2$$

We have

$$(4\text{-}28)\qquad h\,(1 + k) = \varkappa\left[\frac{1}{b\,C} + \frac{2\,B}{M}\right]$$

and

$$(4\text{-}29)\qquad 1 + k = \frac{\dfrac{B}{M} + \left(\dfrac{1}{b\,C} + \dfrac{B}{M}\right)}{\dfrac{B}{M}} = 2 + \frac{M}{B\,b\,C}$$

by (4-18), B may be defined by the expression

$$(4\text{-}30)\qquad B^2 = \sqrt[2]{2\left(b + \frac{M}{B\,C}\right)}$$

which may be easily calculated graphically.

Numerical applications

To take the dimension of the pile, one usually takes the thermoelectric material, that is, α, ρ, $\varkappa$, for which mean values corresponding, for instance, to 50°C are taken. We also assign the ambient temperature T_a, the incident radiation $\alpha_s\ \tau_v\ Q_{i\Phi}$ the section s of the bar, the specific surface σ of the radiator, and the type of radiator which defines A, the curve of losses q_p plotted against the temperature difference $T_c - T_a$ between the radiation-receiving surfaces and the ambient, that is, the coefficients a and b and the concentration ratio $C = s_i/s$.

First heating method : Operation at maximum power is desired. From (4-30) an approximate value of B is derived and is substituted into (4-25) to find h, and into (4-20) to find k.

Second heating method : h or γ is assigned. k is given by (4-17). The power P_u of the pile is not generally the maximum power in this case.

Let us take, for the same material as in the last example

α	$= 204{,}10^{-6}$ V/°C	
ρ_{ave}	$= 0.76 \cdot 10^{-5}\ \Omega$.m	
$\varkappa_{ave}$	$= 3.09$ W/°C.m	
τ_{ave}	$= 564.3$°K	
T_a	$= 30$°C	
s	$= 10^{-4}$ m^2	
σ	$= 100$	
A	$= 2.55$ W/m^2	
$\alpha_s\,\tau_v\,Q_{i\Theta}$	$= 500$ W/m^2	
a	$= 39$ W	(Values obtained by linearization of the loss curve.)
b	$= 3.8$ W/°C	

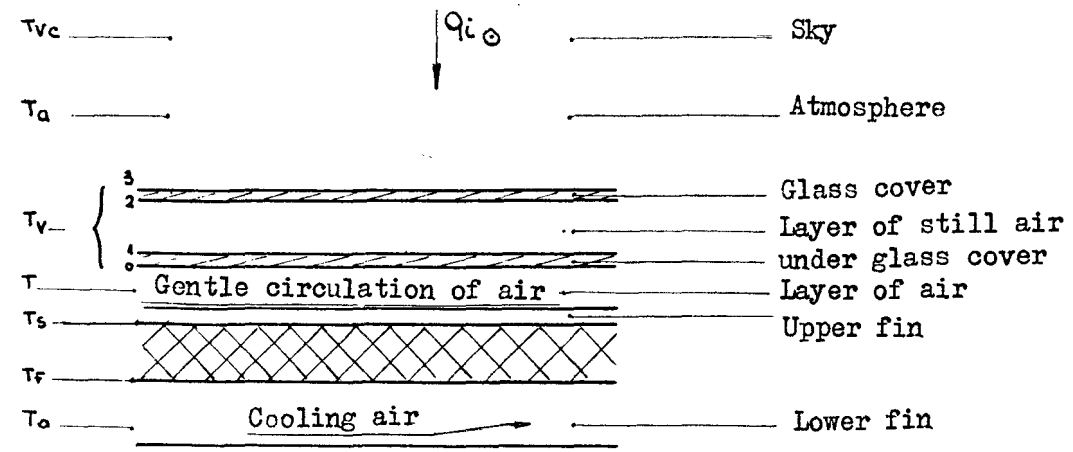
We have $M = 2.55 \cdot 10^2 \sqrt[4]{500 - 39} = 1\,182$

First method

(4-30) gives $\qquad B^2 = \sqrt[4]{7.6\,\dfrac{2\,364}{B\,C}}$

for which the following table gives the solutions as a function of C, as well as the corresponding values of kh, h, k $(T_c - T_a)$ and P_u max and the coefficients of the equation (4-10). We may verify the fact Z may really be neglected, as we assumed.

C	1	2	10	100	1 000
B	4.75	4.14	3.04	2.09	1.67
$k\,h$	$12.42 \cdot 10^{-3}$	$10.82 \cdot 10^{-3}$	$7.95 \cdot 10^{-3}$	$5.46 \cdot 10^{-3}$	$4.36 \cdot 10^{-3}$
h	0.825	0.418	0.089	0.0136	0.00517
k	0.015	0.0258	0.089	0.147	0.843
$(T_c - T_a)$°C	61.6	62.2	65.98	8.54	111.8
$P_{u\ \max}$ (W)	$0.61 \cdot 10^{-3}$	$1.2 \cdot 10^{-3}$	$5.53 \cdot 10^{-3}$	$48.6 \cdot 10^{-3}$	$97.5 \cdot 10^{-3}$
Z	0.0246	0.0245	0.0243	0.0237	0.02308
$b + \dfrac{1}{1+k}\,\dfrac{\varkappa}{hc}$	7.49	7.39	6.98	5.78	4.12


Tvc
Ta
Tv
T
Ts
Tf
To
Sky
Atmosphere
Glass cover
Layer of still air
under glass cover
Gentle circulation of air
Layer of air
Upper fin
Cooling air
Lower fin

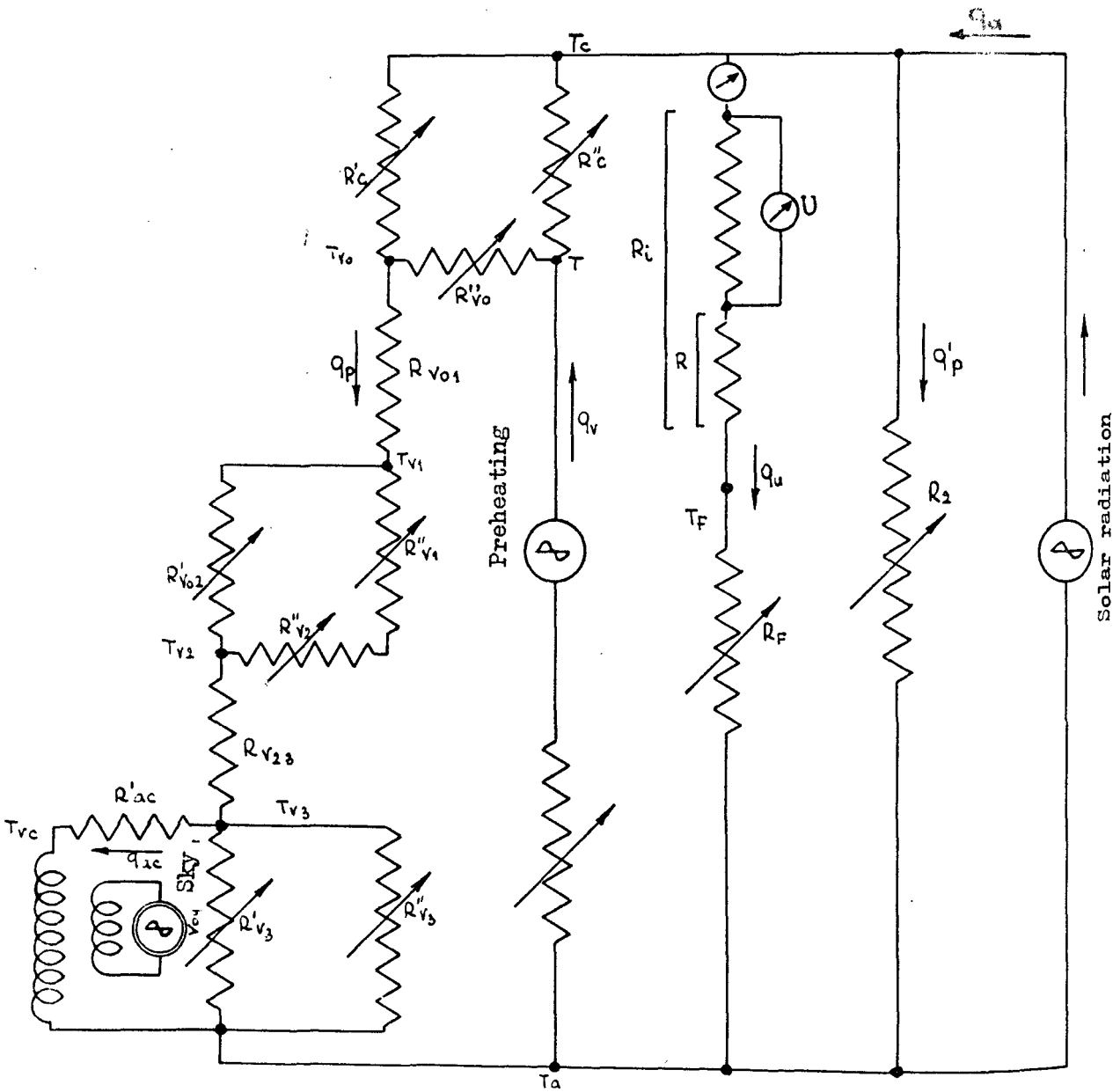

Tc
R'c
R"c
Tvo
R"vo
T
Ri
U
R
qp
Rvo1
qv
Preheating
Tv1
R'vo2
R"v1
R"v2
Tv2
Rv23
R'ac
Tvc
Tv3
qac
Sky
R'v3
R"v3
Ta
qu
TF
RF
q'p
R2
Solar radiation
qa

Figure 3

Second method

Under the same conditions, let us put $h = 10^{-2}$m, and let us take the case where $C = 10$. From (4-20) we get $kh = 7.5 \times 10^{-3}$.

We have

$$k = \frac{7.5\ 10^{-3}}{10^{-2}} = 0.75$$

by (4-13): $T_c - T_a = \frac{461}{21.45} = 21.5°C$

$$P_u = 2.0610^{-3}\ W$$

or less than half the maximum power.

Comparison between the two heating methods

The simplest way is to compare the value of ω, the power per unit volume, in each case. By (4-7) we have

$$(4\text{-}31) \qquad \frac{P_u}{v} = \omega = \frac{(T_c - T_a)^2}{4\,\rho\,h^2\,(1+k)^2}$$

whence

$$(4\text{-}32) \qquad \frac{\omega_1}{\omega_2} = \left[\frac{\rho_2\,h_2^2\,(1+k_2)^2}{\rho_1\,h_1^2\,(1+k_1)^2}\right]\left[\frac{T_{c_1} - T_a}{T_{c_2} - T_a}\right]^2$$

On the other hand we have (3-12)

$$(4\text{-}33) \qquad R_f = \frac{k\,h}{\lambda\,s} = \frac{1}{A\,s\,\sigma\,(T_c - T_a)^{0.25}}\sqrt[4]{\frac{1+k}{k}}$$

Within the range of possible values k, the variation of the radical is rather small, we may thus, in general, write

$$(4\text{-}34) \qquad k\,h = P\,(T_c - T_a)^{-0.25}$$

where P is a constant.

We now have

$$(4\text{-}35) \qquad h\,(1+k) = P\left(\frac{1+k}{k}\right)(T_c - T_a)^{-0.25}$$

and

$$(4\text{-}36) \qquad \frac{\omega_1}{\omega_2} = \frac{\rho_2}{\rho_1}\left[\frac{k_1\,(1+k_2)}{k_2\,(1+k_1)}\right]^2\left[\frac{T_{c_1} - T_a}{T_{c_2} - T_a}\right]^{-2.25}$$

ρ_1 and ρ_2 are usually close together, as k_1 and k_2 are; the preponderant term, then, is

$$\left[\frac{T_{c_1} - T_a}{T_{c_2} - T_a}\right]^{2.25}$$

But not only is T_{c_2} markedly lower than T_{c_1} but it varies continually during the course of the day. Consequently the method of heating by insolation is very appreciably less advantageous than the method that uses a heat-transfer medium.

The only advantage that can be attributed to direct-insolation generators is a certain simplicity of design.

Study of a fixed direct-exposure thermoelectric generator by the electrical analogous method

Analogous representation

The electrical analogous method is applicable to the study of the thermal operation of solar collectors only if we assume that linearization of the radiative and convective heat transfer is possible. This is the case with solar collectors, and, consequently, with direct-exposure thermoelectric generators as well. Figure 3 is a schematic diagram of the generator under study and of the corresponding electrical analogous circuit.[5]

The correspondence between the thermal quantities and the corresponding electrical analogous quantities, as well as the ratios selected, were as follows:

Thermal quantities		*Corresponding electrical quantities*
t : temperature, °C	**T** volts.	(1) $T = K_v\,\mathbf{T}$ where $K_v = 1$;
q : heat flux, w/m²	**q** amperes.	(2) $q = K_p\,\mathbf{q}$ where $K_q = 10^5$;
R : thermal resistance, °C/w	**R** ohms.	(3) $R = K_r\,\mathbf{R}$ where $K_r = 10^{-5}$.

If we adopt the simplified theory set forth above, the real electrical circuit of the thermoelectric generator study may be at least approximately represented by the electric circuit that acts as a thermal circuit of the same generator.

Let us assume that the electrical resistance r_i of the generator is represented by the electrical resistance $\mathbf{R_i}$ which represents the internal thermal resistance R_i; and the current i by the current $\mathbf{q_u}$ which represents the heat flux q_u in the bar. The ratio

$$\frac{\mathbf{R_i}}{r_i}$$

represents the factor which the electrical resistance of the real generator must be multiplied to obtain its representation in the analogue circuit. Thus the resistance r will be represented by an electrical resistance:

$$\mathbf{R} = \frac{r}{r_i}\,\mathbf{R_i}$$

and the internal resistance $(r_i - r)$ by $\mathbf{R_i} - \mathbf{R}$. But the thermal circuit will consist of only a single branch, while the electric circuit will have two. If we desire to use the electrical resistance of the analogous circuit which represents the thermal circuit to represent one of the branches of the real electric circuit, it must be assumed to represent the external branch.

[5] For the technique of the operation, the reader is referred to the indications given in I.E.S.U.A. Bulletin No. 3.

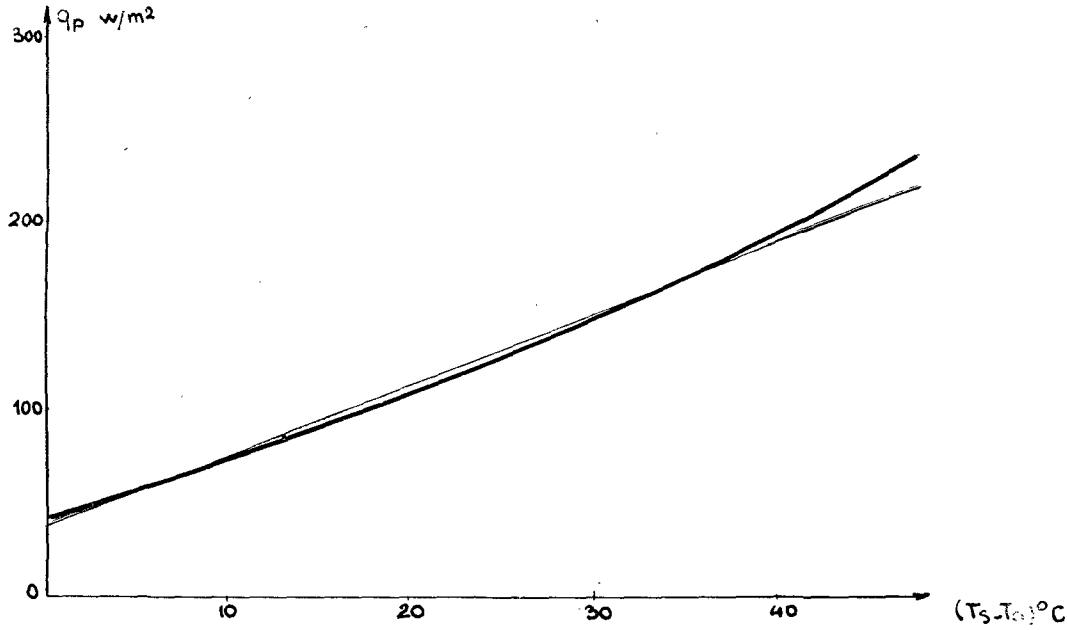


Figure 4

The voltage **u** measured across the terminals of $\mathbf{R_i} - \mathbf{R}$ is

$$\mathbf{u} = [\mathbf{R_i} - \mathbf{R}]\, \mathbf{q_u}$$

It should represent the voltage u across the terminals of the real generator.

The electric power produced by the actual working generator is

$$p = ui$$

It is represented by the product $\mathbf{u}\, \mathbf{q_u}$. It remains to determine the relations

$$\frac{\mathbf{q_u}}{i} \quad \text{and} \quad \frac{\mathbf{u}}{u}$$

The relations

$$r_i = \rho\, \gamma \quad \text{and} \quad R_i = \frac{\gamma}{\varkappa}$$

give

$$r_i = R_i\, \rho\, \varkappa = K_r\, \mathbf{R_i}\, \rho\, \varkappa$$

whence

$$\frac{\mathbf{R_i}}{r_i} = \frac{1}{K_r\, \rho\, \varkappa} \tag{4}$$

The relations

$$i = \frac{\alpha\,(T_s - T_f)}{2\, r_i} \quad \text{and} \quad q_u = \frac{T_s - T_f}{R_i}$$

give

$$i = \frac{\alpha}{2\, \rho\, \varkappa}\, K_q\, \mathbf{q_u}$$

whence

$$\frac{\mathbf{q_u}}{i} = \frac{2\, \rho\, \varkappa}{\alpha\, K_q} \tag{5}$$

From (4) and (5) we derive

$$\frac{\mathbf{u}}{u} = \frac{2}{\alpha\, K_r\, K_q} \tag{6}$$

From (5) and (6) :

$$\frac{\mathbf{u}\, \mathbf{q_u}}{P} = \frac{4\, \rho\, \varkappa}{K_r\, \alpha^2 K_q^2} \tag{7}$$

If N is the number of elements (N/ couples) in unit insolated surface, we have

$$R_t = \frac{R}{N} \tag{8}$$

$$q_t = N\, q \tag{9}$$

$$r_{i_t} = N_{r_i} \tag{10}$$

$$i_t = i \tag{11}$$

$$\frac{\mathbf{R_{i_t}}}{r_{i_t}} = \frac{1}{N^2\, K_r\, \rho\, \varkappa} \tag{12}$$

$$\frac{\mathbf{q_{u_t}}}{i_t} = \frac{2\, N\, \rho\, \varkappa}{\alpha\, K_q} \tag{13}$$

$$\frac{\mathbf{u_t}}{u_t} = \frac{2}{N\, \alpha\, K_r\, K_q} \tag{14}$$

$$\frac{\mathbf{u_t}\, \mathbf{q_{u_t}}}{P_t} = \frac{4\, \rho\, \varkappa}{\alpha^2\, K_r\, K_q^2} \tag{15}$$

Eqs. (12) to (15) allow us to pass from the measurements performed on the analogous circuit to the real electrical quantities. It should be clearly borne in mind that the disturbances in the heat flux due to the Joule effect are ignored in this representation.

Description of the experimental prototype

As we have seen in the last chapter, when discussing direct-exposure generators, it is desirable to

increase the concentration ratio C. A very simple method, which is often used, is to design the hot armature with a rather extensive plate in order to receive the solar radiation. When selective surfaces are used, this method is doubtless sufficient, but since we could not use specially treated surfaces on account of the harmful effect of the dust, we attempted to utilize the convection removing the heat from what we termed excess surfaces at the beginning of this paper (which involve only a relatively low cost for the ground area occupied) to transfer it to the hot armature.

The first type of generator constructed by us is shown in detail in figure 2. Its object was precisely to determine the importance of this heat transfer, and the need of improving it. If, as we hope, the results are favourable, we shall be able to use both methods concurrently—i.e., extension of the insolated surface and utilization of the convection by means of small fins to be placed in this surface.

Thus, design considerations were the primary factors that guided the dimensions of the experimental prototype that has been built. The generator proper is movable, and may be replaced if necessary by a different generator meeting different requirements. The frame is so built as to be easily modified and adapted to different latitudes. The chimney, too, may be lengthened by means of demountable intermediate elements.

The object of the experiments is to determine the values of the thermal resistances to be introduced into the analogous circuit to obtain sufficiently good agreement between the measurements made on the generator itself when exposed to the sun and those made on the analogous circuit, and then to seek the conditions for better operation by the analogous method.

Up to now, the prototype has been used only to refine the quantities to be incorporated in the analogous circuit, and preliminary experiments have been run by the aid of that circuit. This has allowed us to find the curve of the losses q_p of the solar collector per square metre of insolated surfaces, plotted against the temperature difference ($T_c = T_a$). This curve (figure 4) may be replaced by a straight line defined by the coefficients:

$$a = 39\ \mathrm{W/m^2}, \qquad b = 3.8\ \mathrm{W/^\circ C\ m^2}$$

which are required for the study of the optimum generator.

Figure 5 gives the equivalent monotonic daily graph selected by us for the theoretical study of the operation of our prototype generator. It corresponds

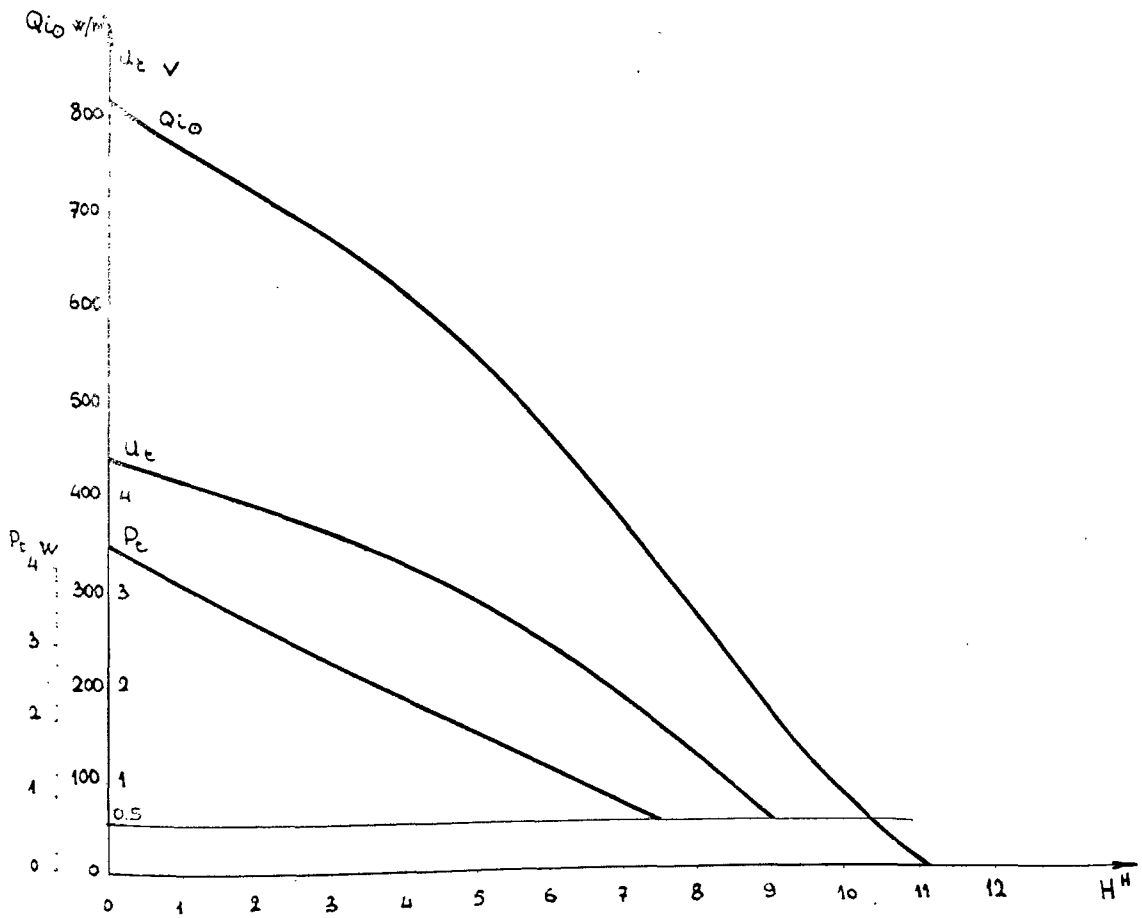


Figure 5

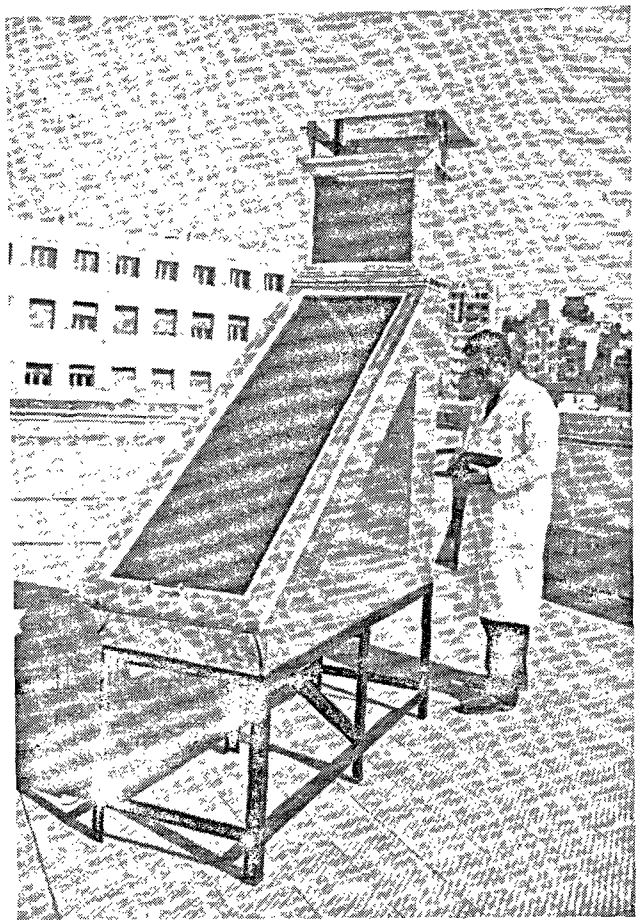


Figure 6

to the climatological conditions at a point located in the heart of the Sahara, on the 30th parallel.

The same figure also shows the monotonic curves corresponding to the power P_u and to the voltage across the terminals of a generator composed of 1 000 elements (500 couples) similar to the one used in the numerical example above.

Conclusion

It is evident from the analysis at the beginning of this paper that very great power cannot be expected from solar thermoelectric generators using the materials now on the market. The high cost of the required semiconductors demands the use of the best methods to accomplish the conversion. The line of attack should therefore be directed towards solutions that separate the collection of the solar radiation and its conversion into heat from the thermoelectric conversion proper.

The very lack of sophistication, however, of the direct-exposure generators may be of service in isolated installations and for very low power requirements, for instance in the case of telemetering or remote control. Incidentally, it was with the establishment of automatic meteorological stations that I.E.S.U.A. undertook its studies on this type of generator.

The fundamental problem, as has already been mentioned, is that of the heat-removal radiator. The I.E.S.U.A. is now studying a system of parallel fins on the plane of the collector, which allows greater development of the surfaces, and thus permits selection of higher values of σ. It is likewise studying a system of internal-vaporization fins operating on the principle proposed by Joffe, which would make higher values of σ available.

As for the receiving surface, while selectivity cannot be recommended for surfaces subject to the severity of weather conditions, it could be, provided adequate protection for such surfaces could be provided: impermeable, vacuum or refracting cover, and heat insulating in contact with the hot armatures. The I.E.S.U.A. intends to pursue research in this direction.

Summary

The I.E.S.U.A. proposes to study all methods of producing energy from solar radiation, but it desires to emphasize direct industrial conversion processes. In the present state of the art, only thermal processes may be validly envisaged. What is to be done, then, is to collect large amounts of solar energy and to concentrate them sufficiently to give industrial temperatures.

If such a result is attainable by competitive means under certain conditions, the specialized engineers, i.e., heat engineers, specialists in thermodynamics, chemical engineers, etc., may undertake to find, according to their own methods, the industrial utilization of the thermal energy thus placed at their disposal.

But before devoting itself completely to this major problem, the I.E.S.U.A. believes it essential to proceed to a systematic analysis of the phenomena that may later be used.

In the first part of this paper, the authors give several principles that have guided their research. They note, in particular, that, contrary to the general belief, solar energy is a very costly form of energy, which is abundant for industrial conversion primarily in arid regions, and more particularly in the Sahara. There are, however, really no storage problems, except for low-power applications, or when relatively low temperatures are employed; but there is a problem of auxiliary power, which can be satisfactorily solved with fossil fuels, in the Sahara.

The authors note, finally, that the heat sink required for every thermodynamic transformation of solar energy can be found in the Sahara only in the atmosphere. This fact is responsible for the great interest that attaches to systems capable of moving large masses of air without using any energy other than solar.

The research programme of the Institute of Solar Energy can thus be readily outlined: study of solar radiation, study of solar collectors with special reference to solar chimneys, study of thermoelectric generators, primarily of the direct-exposure type—that is, thermoelectric solar collectors to be followed by the study of fluid-circulation generators, which involves the study of systems of mirrors and boilers.

In the second part of the paper, the authors rapidly examine the systems of collecting and concentrating solar energy now under study, which consist, for temperatures under 300°C, of orientable collectors formed of paraboloidal mirror elements, and operate by multiple focusing. These collectors are designed to heat liquid heat-transfer agents.

For temperatures over 300°C, the projects boil down to the utilization of two new processes employing elements of deformable paraboloidal mirrors distributed over large surfaces.

These mirrors have been built of simple flat sheets of polished aluminium or aluminized sheet metal, appropriately deformed. A good focus at a distance of 9 m was obtained with aluminium sheet 1.6 mm thick.

In the third part, the authors discuss the technical conditions for the developments of thermoelectric generators to operate in the Sahara. Two conditions are fundamental:

(*a*) Thermoelectric generators must be designed to be cooled by air circulation. But this air may under certain circumstances reach the relatively high temperatures of 40 or 50°C.

(*b*) Dirt on the collector systems or transparent covers of solar collectors may cause large decreases in the incident energy and involve high operating expense.

The use of the system of classical equations for studying the theoretical operation of thermoelectric generators results in great analytic complexity, and the authors note that where the low-efficiency thermoelectric materials now on the market are used, certain terms may be neglected, thus simplifying the mathematical apparatus. They also note that the losses of a thermoelectric generator due to the transparent covering may in general be expressed in the parabolic form as a function of the temperature drop between the hot armature and the atmosphere. They now introduce the following ratios:

Form factor $\gamma = h/S$, h being the height of the bar of section s;

The ratio $k = R_f/R_t$ of the thermal resistance R_f of the radiator to R_t, that of the bar;

The concentration ratio $C = S_t/S$, or the ratio of the insolated surface in thermal contact with the hot armature to the section s of the bar;

Finally, the ratio $\sigma = S_r/s$ of the radiator surface to the bar surface.

Under these conditions, the temperature of the cold armature is expressed simply, as a function of the hot armature temperature and the ambient temperature. We have

$$T_c - T_f = \frac{T_c - T_a}{1\ k}$$

The formulae giving the values of the various quantities are easily established, even in the only case examined, which corresponds to air cooling of the radiator. We have, in particular:

$$P_u = A\, s\, \sigma\, \frac{(T_c - T_a)^{2.25}}{4\tau} \sqrt[4]{k^5/(1-k)^9}$$

where

P_u is the useful power;
A the convective heat-transfer coefficient;
T_c the hot-armature temperature, in °C;
T_a the ambient temperature, in °C;
$\tau = \frac{\alpha 2}{\rho \varkappa}$ the characteristic temperature of the material, in °k.

The hot armature may be heated either by circulation of a fluid itself first heated by the sun, or by direct exposure to the sun.

Fluid-circulation heating is more rational, since it permits operation of the thermoelectric pile at constant temperatures. The authors show that there is an optimum value of the ratio k, namely $k = 1.25$. The pile is then easily measured, starting out from this condition, and the authors find that its global efficiency may attain relatively high levels. Thus they calculate that the global efficiency may reach 3 per cent for bars of bismuth telluride from the United States operating at 200°C. Calculation shows the height of the bar to be very low, of the order of 2 mm.

In the case of heating by direct insolation, the calculations are much less easy and numerical simplifications must be applied. Conditions for maximum power are then established. They depend on the concentration ratio C. The authors note that a relatively high bar results, unless elevated concentrations are adopted; and that the power will be relatively low. But in the case of circulation of a fluid heated by the sun, the diurnal variations of the radiation will only cause changes equivalent to those due to varying the number of generators in parallel, while in the case of heating by direct insolation, the variations of the incident energy will lead to much greater fluctuations of the voltage across the terminals and of the power output. The conditions of maximum efficiency can be satisfied only by a certain value of the radiation. The result, in the last analysis, is that the method of heating by direct insolation is disadvantageous today, and should be abandoned.

All the details of operation of thermoelectric generators may be studied conveniently by means

of an electrical analogy, applying certain simplifying hypotheses which are justified in the case of semiconductors of low internal efficiency, as is, in fact, the case. But the real heat-transfer phenomena cannot be represented with sufficient precision on the analogous circuit, so that it is of interest to study on a real prototype the true performances already calculated. Although the direct-exposure generator cannot be considered the definitive solution for the thermoelectric generator, it does have the advantage of being very simple and unsophisticated. The Institute of Solar Energy of the University of Algiers has therefore built a prototype that takes account of the restrictive conditions of the Sahara mentioned above. The surfaces for receiving the solar radiation are thus nonselective. The generator consists of a relatively large preheating surface with a gentle circulation of air, which delivers heat to the hot armature concurrently with the solar radiation. The generator also has an after-heating surface and a chimney to accelerate the draught of cooling air. Since this air is very dry, the possibility of humidifying it to cool it is also envisaged.

To prevent the design of the prototype from being restricted to the solution of unmotivated problems, a precise destination was built to feed an automatic meteorological station with radio and line transmission of data. It was necessary in this case to compensate the voltage fluctuations due to the variations in solar radiation, and to interpose between the generator and the load a D.C.-D.C. converter serving at the time as a voltage regulator, an independent adapter, and an energy accumulator.

In conclusion, the authors call attention to the fundamental problem of these generators, which lies in the heat-removal radiator. Experiments are now in progress with a view to increasing the specific surface σ of the radiator.

THE CONVERSION OF SOLAR ENERGY TO ELECTRICITY BY MEANS OF THE THERMIONIC CONVERTER

Volney C. Wilson *

The thermionic converter is a static, high temperature heat engine that converts heat into low voltage direct current electricity (1). This paper briefly describes the operation of various types of thermionic converter and then considers the possibility of utilizing thermionic converters to generate inexpensive electricity from solar energy.

Description of the thermionic generator

Figure 1 illustrates a thermionic converter. It consists of a hot surface to emit electrons by thermionic emission and a cool surface to collect the electrons. The two surfaces must be electrically insulated, and the space between the surfaces must be evacuated or filled with an easily ionized vapor.

An electric generator must have a source of electric charge, must develop a voltage to drive the charge, and should have a low internal impedance. The electric charge is generated in a thermionic converter by thermionic emission from the hot electrode. Heat also develops the potential to drive the charge. This is illustrated in figure 2. In this diagram the electron potential (negative potential) is plotted increasing in the up direction on the ordinate, and separation between the electrodes is shown on the abscissa. An electron that has just left the cathode has kinetic energy because it has just left a hot surface, but the electron also has potential energy by virtue of its position relative to the electrons inside the metal.

If we think of the fermi level as representing the average potential of the electrons in the metal, then the electron which has just left the metal has been lifted by heat up a potential hill represented by the work function of the surface of the metal, Φ_c. If the surface has a $\Phi_c = 3$ volts and is at a temperature of 2 320°K, then the average kinetic energy of an emitted electron toward the anode is 0.2 electron volts and the potential energy is 3 electron volts. It is apparent that it is very important to collect the electrons in such a way that the potential energy is conserved as much as possible. Assuming for the moment that the electrons can be collected without a loss of potential in the region between the electrodes, as the electrons enter the collector they will lose an amount of potential represented by the work function of the collecting surface. Any remaining potential is available for the electrons to do work in an external circuit. This is the difference in potential of the fermi levels of the collector and emitter represented by V_o in figure 2. Although the real source of energy and potential is heat, the available driving potential is the difference between the work functions of the two surfaces Φ_c—Φ_A. It is apparent from what has been said that it is extremely important to have as low a Φ_A as possible. However, the lower the work function the higher the thermionic emission at a given temperature. Therefore, to prevent the anode from emitting much more than the cathode, the anode must be much cooler than the cathode. Thus we see that the device is a heat engine. In fact it is limited in maximum efficiency by Carnot's law.

Turning to the question of the internal impedance of the generator, that is the problem of getting the electrons to the collecting surface, if the two electrodes are 0.01 cm apart and the space between the electrodes is evacuated, then a negative space charge will be developed by the cloud of electrons over the surface of the emitter, and very few electrons will have sufficient energy to reach the collector. To overcome the space charge barrier, the electrodes

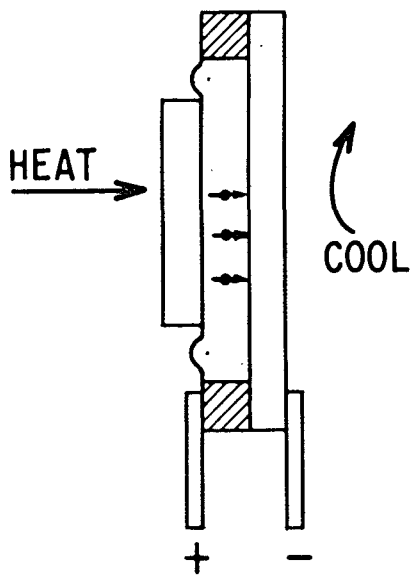


Figure 1. Schematic diagram of a thermionic converter

* General Electric Research Laboratory, Schenectady, New York.

must be spaced about 0.0005 cm apart. To obtain high electron emission from the cathode, it is usually heated to a temperature at which the cathode surface material evaporates sufficiently to deposit a layer of cathode emitter material quickly on the collecting or anode surface. Fortunately, the commonly used vacuum tube cathode materials, such as barium strontium oxide, have positive temperature coefficients of the work functions, so that the hotter emitting surface has a higher Φ than the collector. J. E. Beggs (2) has built many vacuum thermionic converters of about 3 cm² cross section with 0.0006 cm spacing. His best converter used a strontium calcium oxide cathode, and at 1 400°K developed 1.1 watts/cm² at an over-all efficiency of 4.5 per cent. These converters usually have had platinum outer surfaces to resist the oxidation of the atmosphere.

A second method of overcoming the space charge to enable the electrons to reach the anode is to introduce positive ions in the space between the electrodes. Cesium has the lowest ionization potential of the common elements. In fact, cesium can be ionized on a hot surface with a work function of 3 volts or more. One type of cesium converter uses a cathode such as uranium carbide ($\Phi \approx 3.4$) or thorium impregnated in tungsten ($\Phi \approx 3.2$). When the cathode is driven to about 2 200°K, a high electron emission is obtained, and sufficient positive ions are formed by surface ionization on the cathode to neutralize the negative space charge. In addition, a layer of cesium forms on the anode surface and produces a very low Φ_A. Houston (3) built a cylindrical converter of this type, using thorium impregnated in tungsten and produced 4.3 watts/cm² at 7.5 per cent efficiency.

The most promising converters are those in which the cesium is used to perform three functions. In addition to providing positive ions and a low work function anode, a partial atomic layer of cesium on the cathode can be used to adjust the work function of the cathode. Figure 4 shows such a device developed by Lawrence and Wilson (4) for use with solar energy in outer space. Tungsten was used as the base material for the partial layer of cesium on the cathode. This laboratory demonstration model was set up in a vacuum bell jar and heated by electron bombardment to simulate solar energy. The converter developed 7.5 watts/cm² at 15 per cent efficiency. Recently Rasor (5) has reported the results from a cylindrical converter of this type using molybdenum as the cathode base in which he obtained 8.2 watts/cm² at 17 per cent efficiency. A study of Rasor's data indicates that he had a loss of potential between the cathode and anode of about 0.2 volts. Houston and Wilson have observed that anodes covered with a monolayer of cesium have a work function of 1.4 volts.

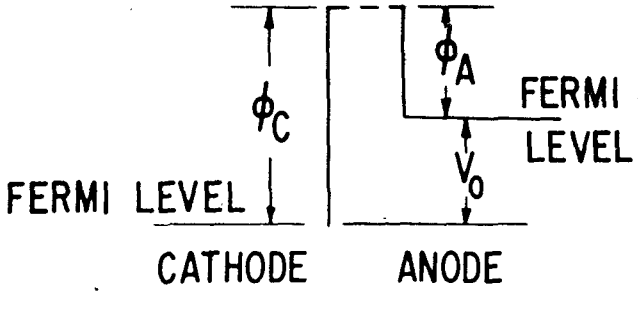


Figure 2. Energy diagram of a thermionic converter

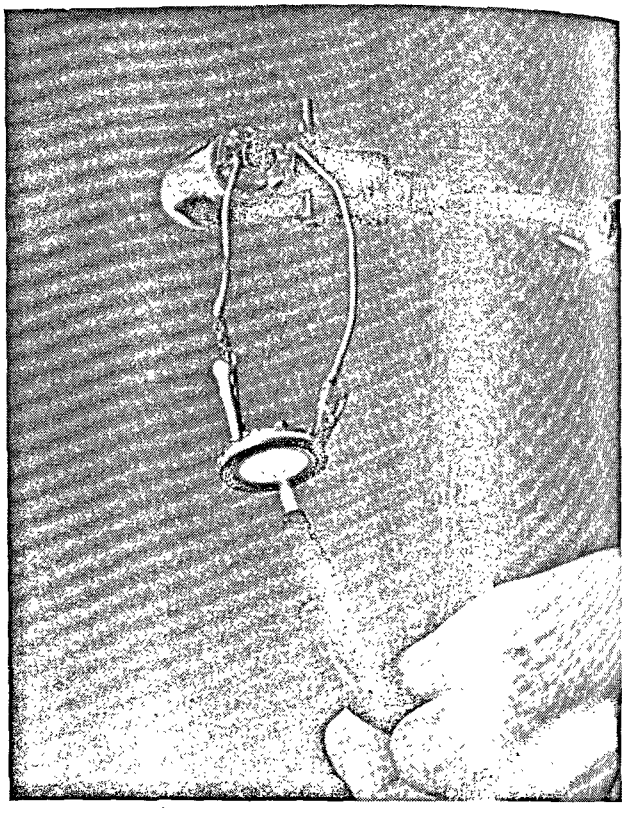


Figure 3. Demonstration of a vacuum converter operated by a gas flame

Figure 5 shows a set of calculations of the efficiencies as a function of cathode temperature. These are efficiencies that look reasonable to obtain with various work functions of the cathode. These calculations assumed the cathode emissivity of molybdenum and an anode emissivity of 0.5. It is difficult to keep the anode highly polished. Impurities from the cathode spoil the emissivity. The dashed curve is the author's estimate of the efficiencies to expect within the next year or two. It is doubtful if sufficient ions are produced by a 2.75 volt surface. Therefore the dashed line is drawn to the right of the 2.75 volt cathode line. Also included in figure 5 are the points represented by Beggs' vacuum converter and Rasor's cesium converter.

Coupling the thermionic converter to solar collectors

Solar collectors can be made quite efficient, however, as the object receiving the radiation becomes

hotter and hotter, more and more heat is radiated from the receiver; so the net efficiency falls off rapidly as the temperature of the receiver increases. McClelland has calculated the concentration efficiency as a function of absorber temperature. Figure 6 is a reproduction of one of McClelland's (6) curves for a low quality searchlight mirror. In particular, this curve assumes a cavity absorber; it assumes the mirror is a paraboloid of revolution with a diameter to focal length ratio of 2.3 (rim angle = 60°) and the geometric error of the mirror is expressed as $\sigma\ h/d = 1$, where σh is the standard deviation of the displacements from perfect focus and d is the theoretical solar image diameter. This curve shows the amount of the incident energy that passes into the cavity absorber minus the amount that re-radiates back out of the absorber opening. It would be ideal to have all of this energy that is trapped in the absorber pass through the thermionic converters; however, the walls of the cavity are not perfect heat insulators and part of the energy will therefore be lost by leakage radiation. This loss will increase

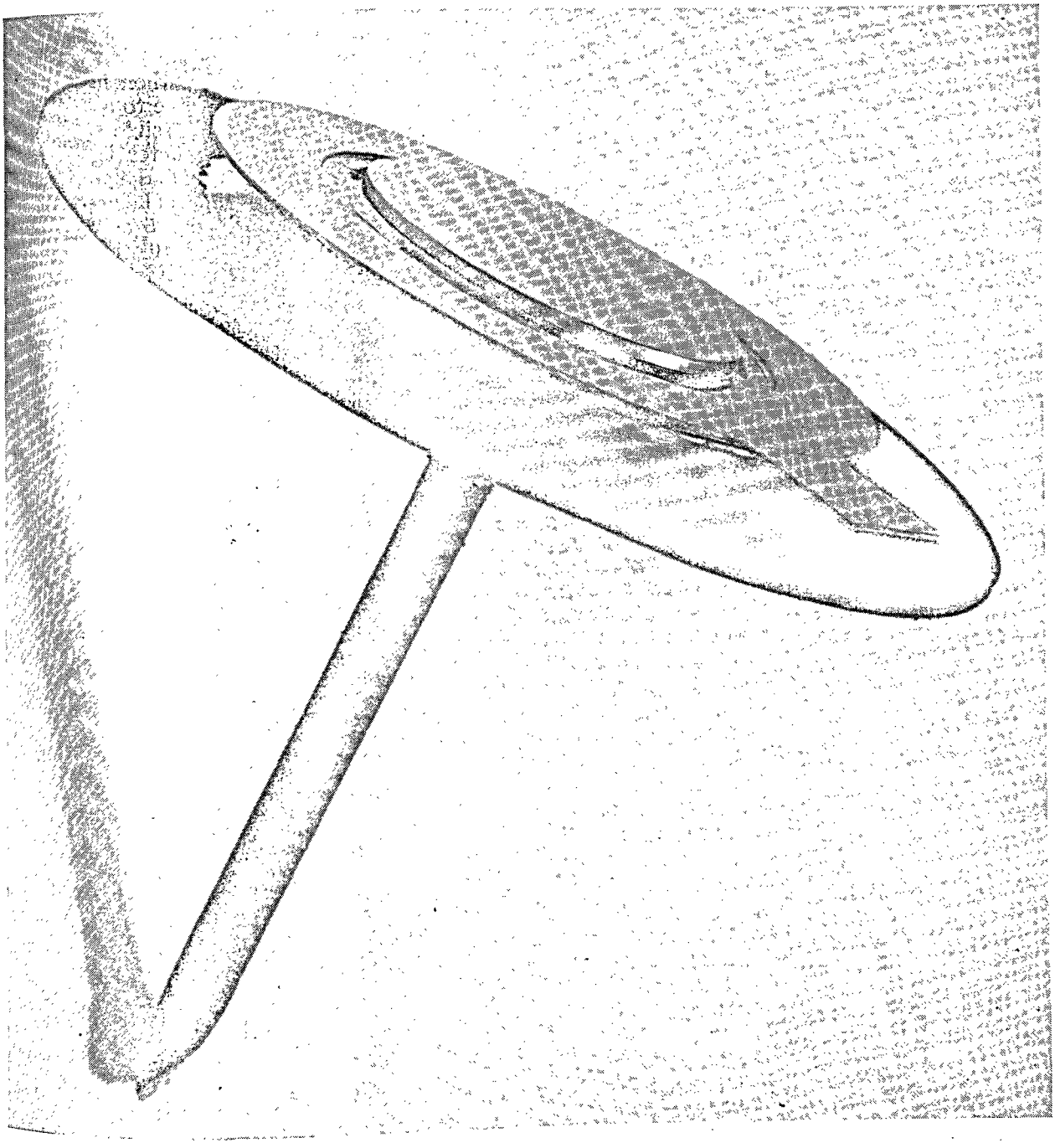


Figure 4. Cesium converter designed to use solar energy in outer space

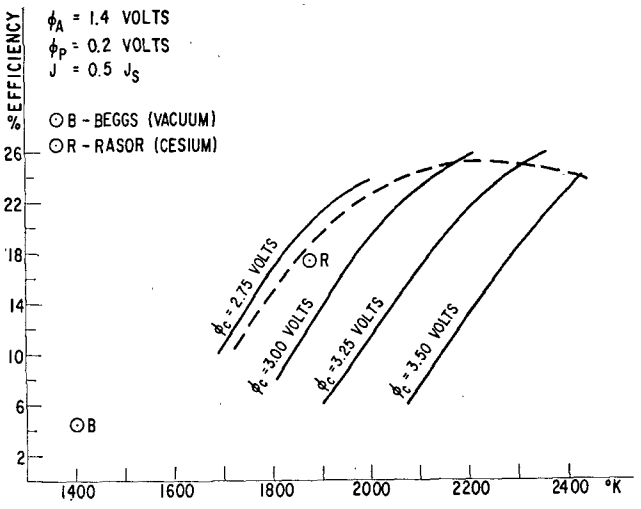


Figure 5. Cathode temperature

at higher temperatures. Efforts to reduce this loss will be discussed later. The dashed line of figure 6 represents an estimate of the per cent of the incident solar energy on the mirror that will flow through the converters. Multiplying this dashed line by the converter efficiency curve taken from figure 5, one obtains the lowest curve of figure 6, which is the anticipated over-all efficiency of a thermionic converter system as a function of the cavity and cathode temperature. At 1 900°K the over-all efficiency is 9.5 per cent. One may now estimate how large such a system must be to generate one horsepower of electricity. One horsepower is 746 watts. At 9.5 per cent efficiency, this will require a total incident energy of 7 850 watts. C. G. Abbot reports that in desert areas and low latitudes the incident radiation is 1.35 cal/cm²/min or 0.095 watts/cm².

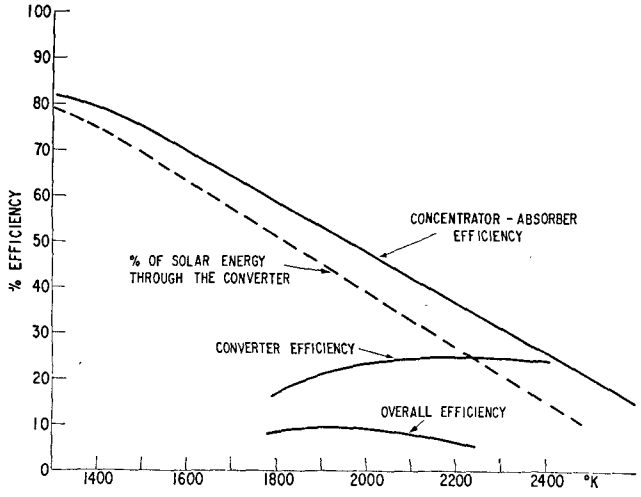


Figure 6. Cavity and cathode temperature: estimates of efficiencies of solar concentrators, cesium converters, and their combined efficiencies as a function of cathode and collector temperatures

Therefore 82 600 cm² of mirror are required; or a parabola 3.25 meters in diameter is required.

Figure 7 illustrates one possible configuration for a cavity absorber and thermionic converter assembly. Light from the parabolic mirror would pass through the glass dome, 1, into the black body cavity, 2. As mentioned above, it is desirable to insulate the cavity thermally and force the maximum heat to flow through the converters. Therefore the entire assembly would be in a vacuum enclosure, 3. Many thin, highly reflecting foils, 4, would be used as radiation shields. Figure 8 illustrates a practical thermionic converter developed by Jensen (7) that might be used in such an absorber. This device, which is capable of being produced in quantity, developed 5 watts/cm² at a calculated efficiency of 14 to 16 per cent when heated by an electron bombardment heat source to a temperature of 1 775°K. Figure 7 shows a possible configuration in which a converter in the center is surrounded by six converters in the first ring and eight converters in the next ring. This would make a total of 15 converters. If each converter has 5 cm² area of the cathode and anode and develops 10 watts per cm² at a cathode temperature of 1 900°K, the total power would be 750 watts. If each converter develops 1.25 volts at 40 amperes, the 15 in series would develop 18.75 volts at 40 amperes. The series connections would be made inside the vacuum enclosure and only two leads would be brought out through vacuum tight insulating bushings.

For this conference we were asked to estimate costs. When one studies the complexity of figure 7 it is difficult to imagine that even in fairly large

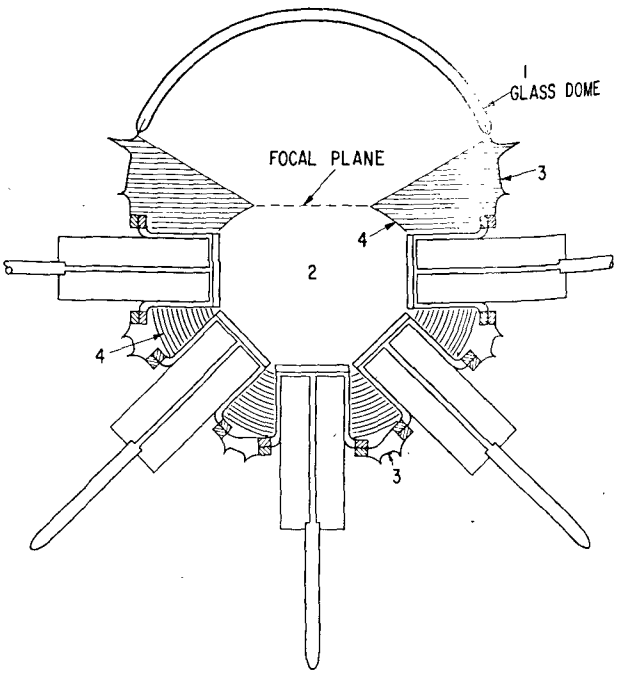


Figure 7. Schematic diagram of an assembly of fifteen cesium converters to develop one horsepower

quantities a one-horsepower electric generator could be built for less than $1 500. In addition to this, a high precision mirror, 3.25 meters in diameter, is required; and finally a mounting and mechanism for tracking the sun must be provided.

To try to make the generator less expensive to build, one is tempted to omit the vacuum enclosure. However, this enclosure appears necessary to protect the materials that are at the high temperatures and to provide thermal insulation. It is the author's opinion that the material problems and the assembly techniques are state-of-the-art in the large vacuum power tube industry. This approach represented by figure 7 looks feasible and would produce the best efficiency, but is very expensive.

There are other possible approaches. One would be to adapt Beggs' vacuum converter to heat it with solar energy. This would be straightforward. In fact, as a demonstration, Beggs has used an inexpensive plastic Fresnel lens to concentrate solar energy on one of his converters. In this case the receiver is not a black body cavity so the solar collection would not be as high as one would expect from figure 6 (79 per cent at 1 400°K). Also, the cathode would be operating in air so convection cooling would be quite great. One might expect with a 4.5 per cent efficient converter that 2.5 or 3 per cent over-all efficiency might be obtained.

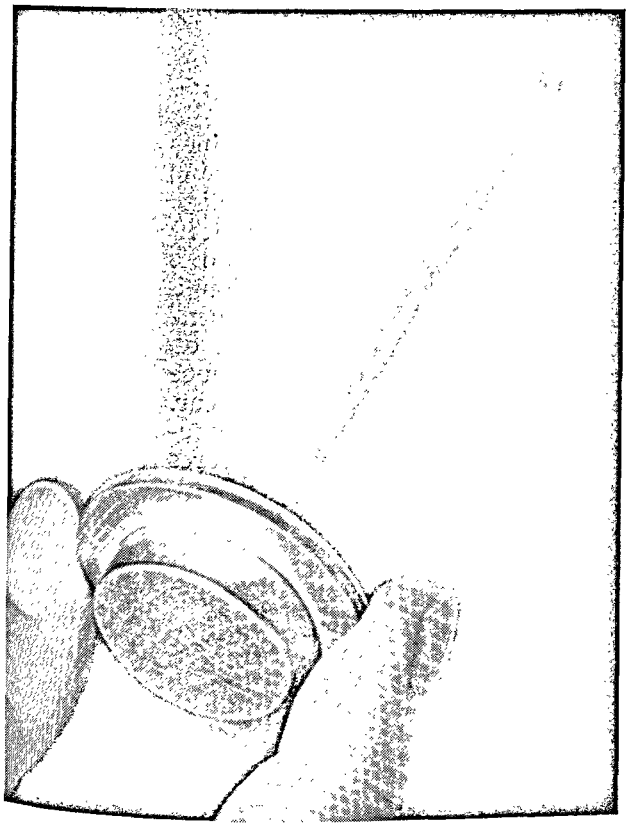


Figure 8. Type of thermionic converter that could be used inside a vacuum enclosure such as figure 7

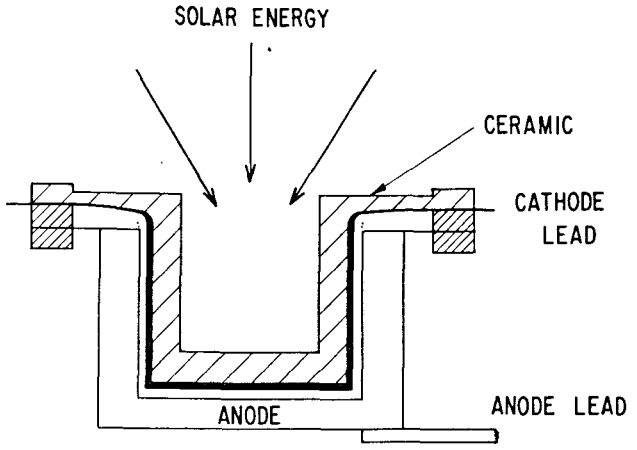


Figure 9. A proposed simplified cesium converter design

Long life vacuum converters at 1 400°K have not, however, been developed. To obtain a life of 1 000 hours or so the cathode temperature must be reduced, and the resulting output and efficiency are much lower, perhaps 0.2 watt/cm^2 and 1 per cent efficiency.

Another approach is to make individual cesium thermionic converters with ceramic surfaces exposed to air at high temperature. Figure 9 illustrates this concept. The solar radiation would be concentrated inside a ceramic cup. The cathode and electrical lead to the cathode would be a plating of a refractory metal on the outside of the cup. The rim of the cup would be thin to reduce heat flow to the seal. The anode and heat removal radiator would completely surround the cathode. Cooling of the ceramic rim by air convections would reduce the efficiency of the system. Each converter would be heated by a separate small collecting mirror; and, since smaller mirrors would be required than for an assembly like figure 7, probably the collecting system would be less expensive. One aiming system could be used to direct a number of collector-converter assemblies mechanically ganged together.

The development problems would include an investigation to see if a ceramic can be made really gas tight at 1 900°K; methods to develop oxidation resistant high temperature coatings with high solar absorption for the solar collecting surface; and investigations of solid state reactions between the hot ceramic and the refractory metal cathode. Essentially, the development problems are problems of high temperature materials.

Conclusions

Solar concentrators and thermionic converters could probably be developed to convert about 9.5 per cent of the solar energy to electricity. A system to obtain this efficiency would be extremely complicated to build and would be expensive. If solar converters having ceramic envelopes could be developed, they would be less efficient, but probably the system would be less expensive to produce.

References

1. Wilson, V. C., Conversion of Heat to Electricity by Thermionic Emission, *J. Appl. Phys. 30, 475*, 1959.
For a more complete bibliography, see Kaye, J. and Welsh, J. A., *Direct Conversion of Heat to Electricity*, John Wiley & Sons, Inc., New York City.
2. Beggs, J. E., Vacuum Thermionic Energy Converter, submitted to *J. Appl. Phys.*, 1961.
3. Houston, J. M., Massachusetts Institute of Technology, *Physical Electronics Conference Report*, March 1960.
4. Wilson, V. C., Cesium Converter Studies, American Rocket Society, *Paper 1282-60*, September 1960.
5. Rasor, N., Experimental Research on the Cesium Thermionic Converter, Institute of the Aeronautical Sciences, *Paper 61-72*, January 1961.
6. McClelland, D. H., Solar Concentration for High Temperature Space Power Systems — Fig. 9, American Rocket Society, *Paper 1314-60*, September 1960.
7. Jensen, A. O., Power Tube Department, General Electric Company, Schenectady, N.Y., private communication.

Summary

Currently, thermionic converters are being engineered for use in converting solar energy to electricity for space vehicles. To adapt this development for inexpensive electric power on the earth, the converters must be redesigned to make them resistant to oxidation by the atmosphere and to make them less expensive to build. Two quite different engineering approaches are presented. One approach is to build several converters inside a large vacuum enclosure, the outer surface of which does not operate at the converter cathode temperature. The other approach is to build individual converters with ceramic parts to withstand oxidation by air at the high temperatures.

CONVERSION DE L'ÉNERGIE SOLAIRE EN ÉLECTRICITÉ AU MOYEN D'UNE CELLULE THERMO-IONIQUE

Résumé

On met actuellement au point des convertisseurs thermo-ioniques destinés à transformer l'énergie solaire en électricité pour les besoins de certains véhicules interplanétaires. Pour adapter ces conceptions à la production économique de courant électrique dans des installations terrestres, il faut reprendre la construction des convertisseurs de manière à les rendre résistants à l'oxydation par l'atmosphère et à ramener leurs prix de construction à des proportions plus modiques. L'auteur présente deux techniques entièrement différentes pour attaquer le problème. L'une envisage la construction de plusieurs convertisseurs à l'intérieur d'une chambre à vide dont la surface extérieure ne fonctionne pas à la température de la cathode du convertisseur. L'autre consiste à construire des convertisseurs individuels en pièces de composition céramique pour qu'elles résistent à l'oxydation par l'air aux températures élevées.

UTILIZATION OF SILICON SOLAR BATTERIES

Masatsugu Kobayashi *

The utilization of inexhaustible energy from the sun is one of the most important scientific problems which mankind is facing. The conversion of solar energy into electrical energy by use of solar batteries is an excellent method, though there remain some problems concerning the economy and reliability of the solar battery as a power source.

The solar battery was invented and reported in 1954 by Chapin *et al.* of the Bell Telephone Laboratories (1). In Japan, the study of the silicon solar battery began in 1955 in our laboratory; an unattended VHF repeater station equipped with 70 watt solar batteries was installed on a mountain in 1958 for the first trial (2), and the unattended lighthouse with 14.5 watt batteries on shallows in Seto Sea in 1959 (3).

The information obtained from these installations suggests that the utilization of solar batteries is very promising in such remote places, from the standpoint of technology, reliability and economy. This conclusion prompted the erection of many repeater stations and lighthouses equipped with solar batteries in 1960.

This paper is concerned with the electrical characteristics, utilization, reliability and cost of silicon solar batteries.

* Director, Research Laboratory, Nippon Electric Company, Ltd., Japan.

Electrical characteristics of silicon solar cells

The shapes of the silicon solar cell are usually of circular type and of rectangular type. The cell used as a power source is circular, about 28 mm in diameter.

The change of power output from the solar cell, with the load resistance under full sunlight, is shown in figure 1. The maximum output power is about 40 mW, and the cell can produce 0.5 to 0.6 volts on open circuit and about 150 mA under short-circuit conditions.

The relations among output power, short-circuit current, open-circuit voltage, matching load resistance and light intensity are shown in figure 2. As the light intensity increases, output power and short-circuit current increase, open-circuit voltage does not change, and the value of the matching load resistance decreases.

The temperature dependence of the electrical characteristics of solar cells is shown in figure 3. As a result of the decreases of open-circuit voltage with the increase in temperature, output power decreases at the rate of about 0.7 per cent per degree C above room temperature.

The theoretical conversion efficiency of solar energy into electrical energy is about 22 per cent. The

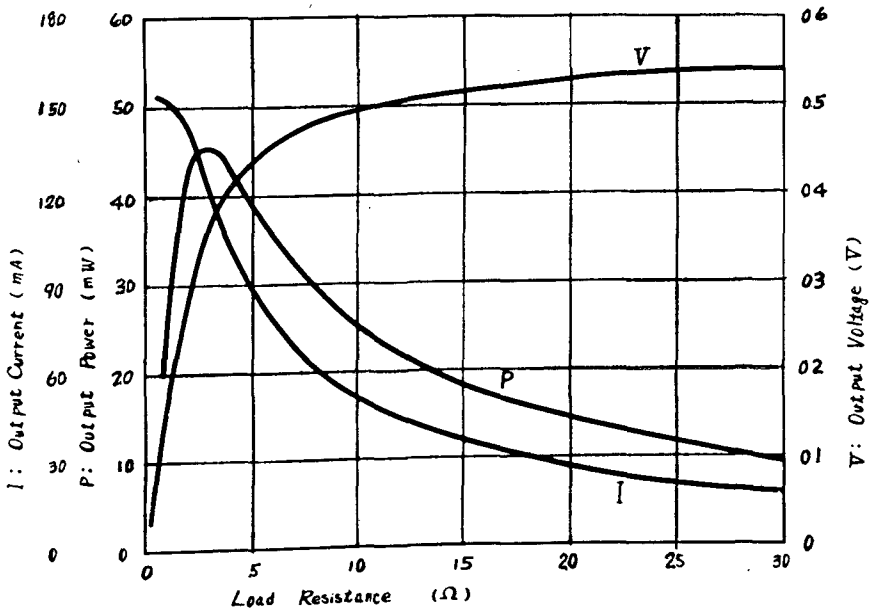


Figure 1. Output characteristics of one silicon cell

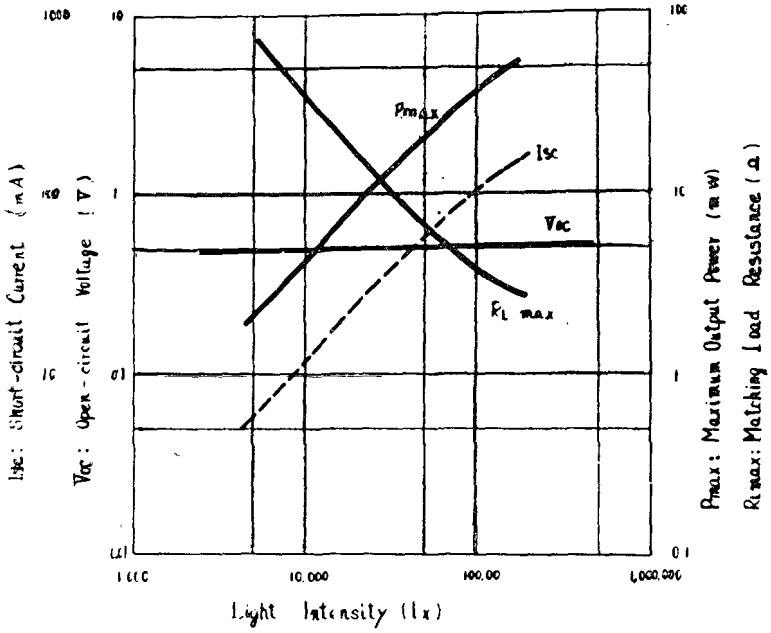


Figure 2. Relations between output characteristics and light intensity

batteries which were produced about 1958 had a conversion efficiency of 4 to 6 per cent. Lately, as a result of the reduction in loss, the efficiency has been raised from 8 per cent to 12 per cent, on the average. The maximum efficiency of 18 per cent was obtained in our company.

Utilization

The applications of silicon solar cells may be classified as follows: (*a*) Light detector, such as sunlight valve and automatic change of head-light beam, etc.; (*b*) Direct power source for electrical equipment. In this paper, the utilization of solar batteries of the second category is described.

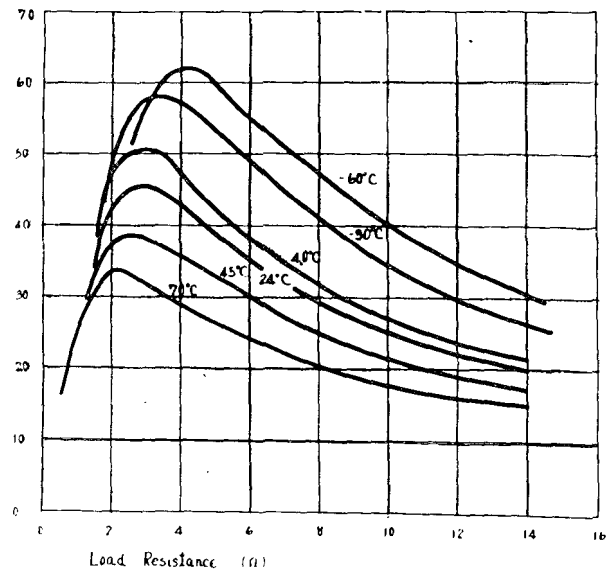


Figure 3. Temperature dependence of output power

Power supply system

The output power of the solar batteries is charged in Ni-Cd batteries through a germanium diode to be provided for use at night and during cloudy days. Germanium diode is used to prevent discharging current through the solar batteries. The circuit connecting the solar batteries, the Ni-Cd batteries and the load is shown in figure 4.

The determinations of the output power of the solar batteries and the capacity of the storage batteries is an important problem for the operation of electrical equipment. These factors are determined by weather conditions and the location where solar batteries are installed.

The necessary output power of the solar batteries and the capacity of the storage batteries are estimated as follows. In Japan, the working time of the solar batteries is six hours a day, on the average, when the weather is fine for one half a month and the other half of the month is cloudy. Therefore, the solar

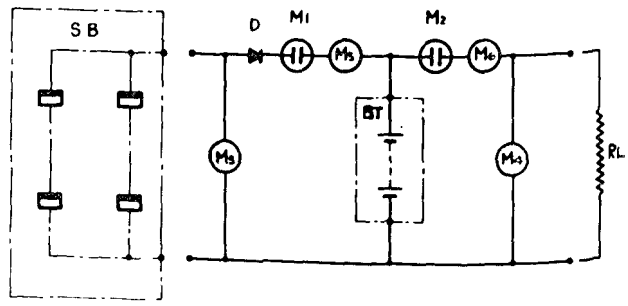


Figure 4. Power supply system

SB: Si solar batteries; D: diode; BT: Ni-Cd batteries; M_1, M_2: volta meter; M_3, M_4: voltage meter; M_5, M_6: ampere meter; R_L: Load.

Table 1. Utilization of silicon solar batteries in Japan

Use	*Location*	*Solar batteries*					*Date of erection*
		Voltage (volts)	*Power (watts)*	*Number of series connections*	*Number of parallel connections*	*Total*	
Tohoku Electric Power Co.:							
VHF (150 MC)			6.5	28	63		
repeater station	Mt. Shinobu	60	70	207	8	4 320	Nov. 1958
		130		450	2		
Maritime Safety Board:							
10 W lighthouse	Ikada Shallows	12	13.5	54	12	648	Nov. 1959
Electric Power Development Co.:							
VHF (150 MC)	Mt. Mitsuji	12	30	45	27	1 215	Mar. 1960
repeater station	Mt. Noki	12	30	45	30	1 350	Aug. 1960
Maritime Safety Board:							
10 W lighthouse	Katsuo Island	12	13.5	54	12	648	
10 W lighthouse	Hakan Island	12	13.5	54	12	648	
10 W lighthouse	Manaita Shallows	12	13.5	54	12	648	
10 W lighthouse	Saki Shallows	12	13.5	54	12	648	Dec. 1960
10 W lighthouse	Funa Beach	12	10	54	9	486	
25 W lighthouse	Tateme Point	12	15	54	13	702	
25 W lighthouse	Uoko Island	12	29.5	54	26	1 404	
NHK Broadcasting Corp.:							
VHF (60 MC)	Nakatsugawa	12	3	54	2	108	
repeater station	Gero	12	3	54	2	108	Oct. 1960
	Matsuame	12	3	54	2	108	

batteries work one-eighth of a day, on the average. The needed power of the solar batteries is therefore eight times greater than the average power consumption.

To lay up solar energy against a long series of rainy days, the capacity of the Ni-Cd batteries is designed to work for a month without charging. And it is also designed so as to keep its initial condition with a new supply of the electrolyte only once a year.

An array of solar batteries

The silicon solar cells are sealed in an acryl resin container, and these units are arranged on an iron panel. The iron panel is fixed out of doors, facing to the south, and its angle of elevation is adjusted to absorb solar energy most effectively at any season of the year. It has been shown theoretically and experimentally that this angle nearly coincides with the latitude of the place where solar batteries are installed.

Utilization of solar batteries in Japan

Many repeater stations and lighthouses have been installed since the unattended VHF repeater station

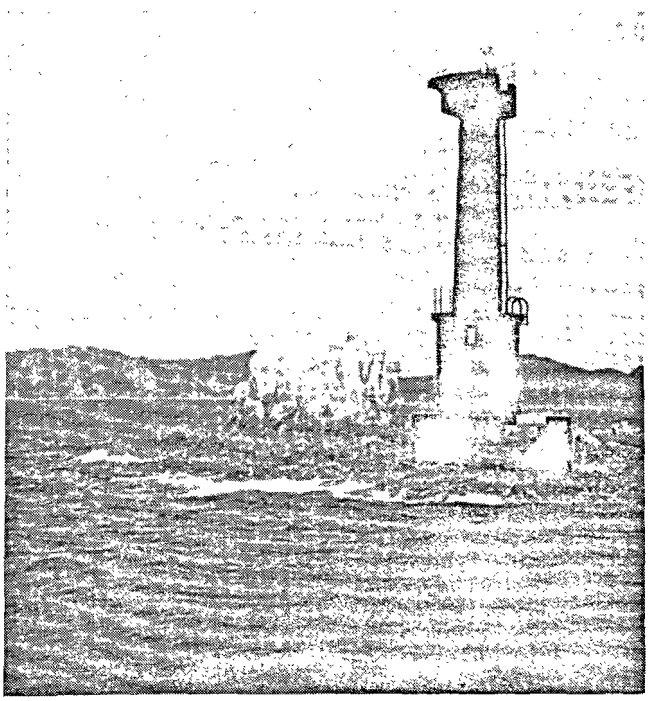


Figure 5. The lighthouse at Ikada Shallows

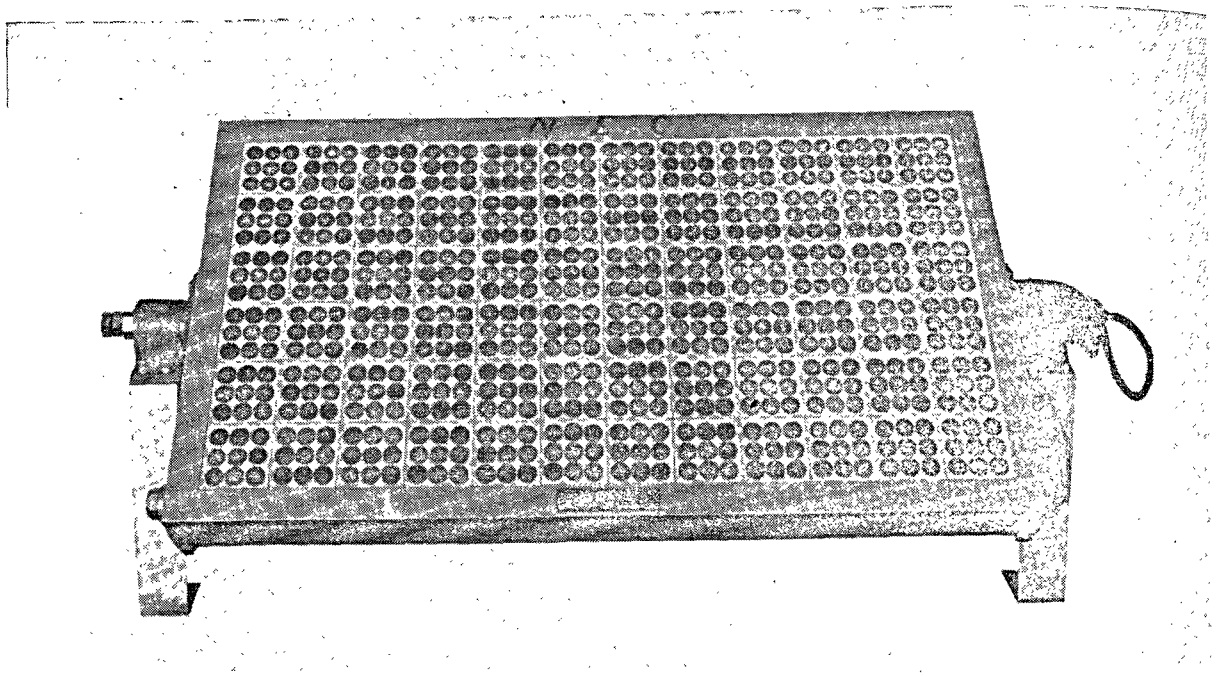


Figure 6. Solar batteries at Ikada Shallows

Table 2. Operating conditions, lighthouse at Ikada Shallows

Publication permitted by courtesy of the Maritime Safety Board

	Nov. 28 1959	*Dec. 9*	*19*	*30*	*Jan. 9 1960*	*18*	*29*	*Feb. 13*	*29*	*Mar. 12*	*19*	*Apr.*	*13*	*24*
	(Started)													
Time		09 : 30	10 : 00			10 : 00	14 : 30	14 : 20	13 : 00	09 : 30	09 : 20	10 [illegible]	10 : 00	10 : 00
Weather		Cloudy	Cloudy	Slightly cloudy	Clear	Clear	Clear	Fair	Cloudy	Cloudy	Clear	Cloudy	Rainy	Clear
Temperature (°C)		12.5	8.0	7.5	11.0	8.0	6.0	11.5	12.0	14.0	9.0	13.5	12.0	21.0
Direction of wind		NNE	N	NNW	W	N	W	SW	SSE	W	N	NE	WSW	N
Velocity of wind (m/sec)		6.0	2.0	3.0	1.0	4.0	13.0	2.0	5.0	4.0	3.0	4.0	4.0	2.0
Illumination (10^3 lx)		17	7	30	80	31	130	102	15	15	27	28	13	28
Surface temperature of solar batteries (°C)		13.0	10.0	10.0	15.2	10.0	12.0	16.5	15.0	15.0	18.0	15.9	12.5	22.0
Charging voltage (V)		14.0	14.0	14.2	14.5	14.1	16.5	16.5	14.5	14.0	14.6	14.4	14.0	14.5
Charging current (A)		0.2	0.03	0.4	0.7	0.5	0.72	0.7	0.19	0.188	0.48	0.23	0.17	0.28
TOTAL CHARGE (AH)	0	42	72	102	126	163	198	257	328	360	382	431	446.5	511.5

	May 9	*17*	*June 7*	*26*	*July 15*	*27*	*Aug. 6*	*26*	*Sept. 17*	*29*	*Oct. 20*	*Nov. 7*	*18*
Time	10 : 00	14 : 55	13 : 10	11 : 20	13 : 40	08 : 45	12 : 50	13 : 50	17 : 10	13 : 30	16 : 00	09 : 30	09 : 45
Weather	Cloudy rainy	Fair	Clear	Clear	Cloudy	Fair	Cloudy	Fair	Clear	Fair	Fair	Fair	Clear
Temperature (°C)	15.5	22.5	24.0	27.0	28.7	29	28.5	28.5	27.5	22.0	20.0	17	16
Direction of wind	E	—	SE	E	WNW	SW	SE	SW	N	N	N	N	N
Velocity of wind (m/sec)	7.0	0	3.0	2.0	7.0	4.0	6.0	3.0	2.0	7.5	6.0	7.0	2.0
Illumination (10^3 lx)	10	36	26	38	46	13	60	73	5	90	14	3	60
Surface temperature of solar batteries (°C)	18.0	37.0	32.0		37.0	33.5	34.0	45.0	32.0	30.5	22.0	23.0	24
Charging voltage (V)	14.5	14.5	14.5	14.9	14.5	13.4	14.2	14.7	14.2	15.0	14.9	13.8	14.5
Charging current (A)	0.1	0.5	0.22	0.33	0.65	0.35	0.38	0.4	0.14	0.7	0.1	0.1	0.7
TOTAL CHARGE (AH)	559	594	669	709	772	829	869	953	1 003	1 053	1 123	1 201	1 243

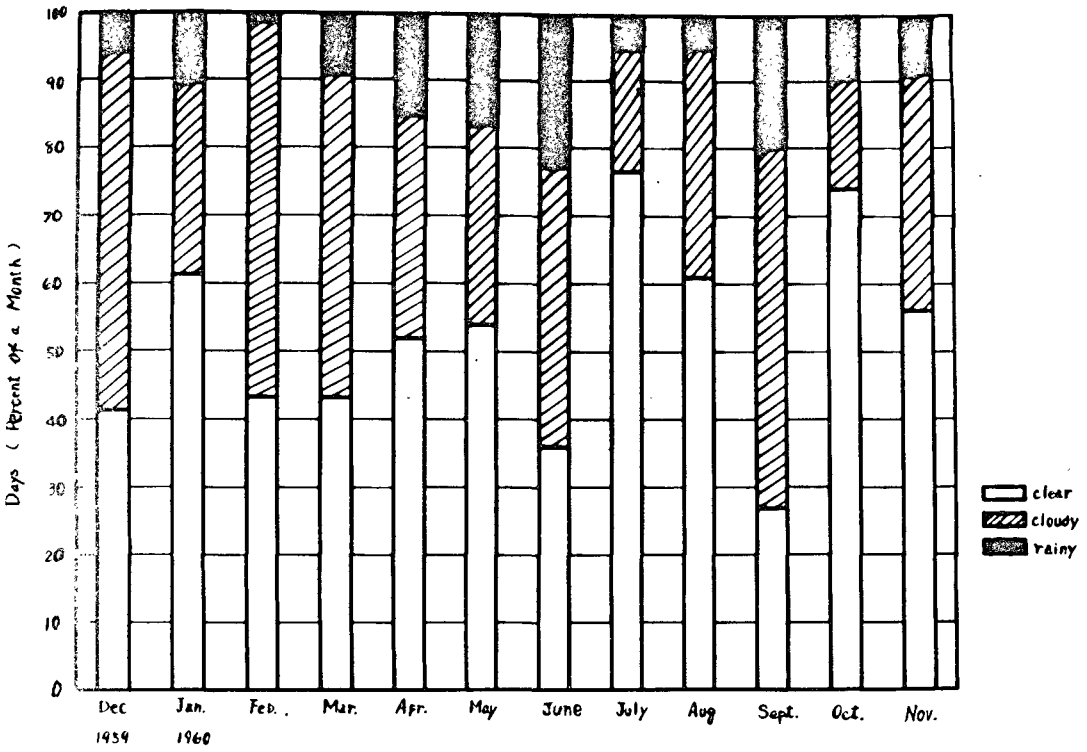


Figure 7. Weather conditions, lighthouse at Ikada Shallows

equipped with silicon solar batteries as a power source was erected in 1958. These installations are shown in table 1. The lighthouse and its solar batteries, installed at Ikada Shallows in 1959, are shown in figure 5 and figure 6. The further establishment of additional stations and lighthouses is planned in Japan.

Reliability

Repeater stations or lighthouses with solar batteries as the power source are usually installed in remote places or on isolated islands. The solar batteries are set outside and exposed to rain, various types of radiation and heat and cold. Therefore, durability

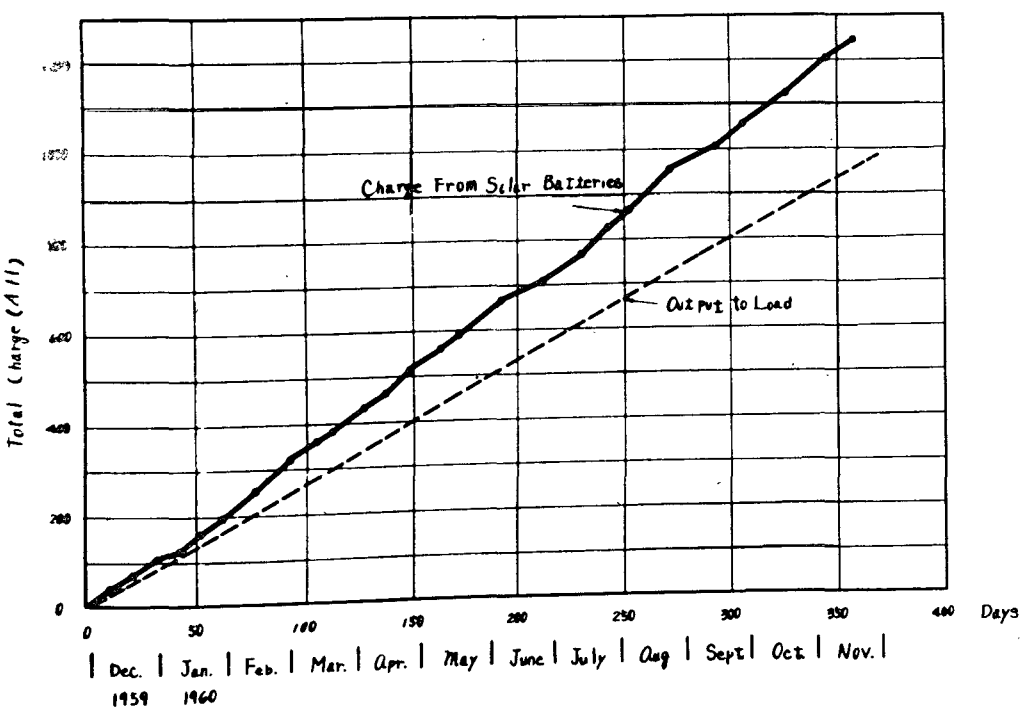


Figure 8. Charge from the solar batteries and output to the load, lighthouse at Ikada Shallows

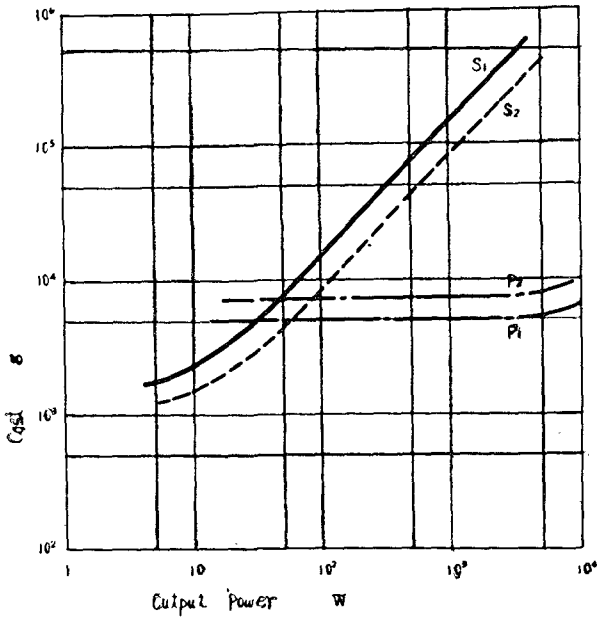


Figure 9. Comparative costs of construction

S_1: Cost of silicon solar batteries at present; S_2: Cost of silicon solar batteries in the near future; P_1: Construction cost of power line on level ground; P_2: Construction cost of power line among mountains.

and reliability are necessary for the design of solar batteries and other equipment. Many repeater stations and lighthouses have been operated in Japan without any trouble since they were erected.

The operating conditions of the unattended lighthouse which was installed at Ikada Shallows in Seto Sea in 1959 are shown in table 2, and figures 7 and 8. Publication of these data are permitted through the courtesy of the Japanese Maritime Safety Board.

The weather and operating conditions of the equipment are shown in table 2. Monthly weather conditions are shown in figure 7. The charge from the solar batteries and output to the load are shown in figure 8; the former was about 1.2 times greater than the latter. During the last year only 2 litres of electrolyte was supplied to the Ni-Cd batteries, and the surface of the silicon solar batteries was sometimes cleaned to remove dust. The electrical equipment with solar batteries as a power source could be operated non-intermittently for many years with trivial upkeep once or twice a year.

Cost of silicon solar batteries

It has been reported that the cost of solar batteries is higher than that of other power sources, and this high cost hinders their general use. The cost of solar batteries as a power source, including cells, containers, panel, diode, control box and Ni-Cd batteries, is about $130 per watt, as shown by the curve S_1 in figure 9. In the near future, however, it is expected to be reduced to about two-thirds of the present figure (curve S_2). On the other hand, the cost of the construction of a power line per kilometre on level ground and among mountains is about $5 000 to $7 000, shown by curve P_1 and curve P_2, respectively.

The construction of solar batteries is more economical than that of a power line one km long in such a case, since the required power supply is less than about 50 watts. The longer the power line, the higher the value of the power of the border line available for solar cells.

On the other hand, there are other power sources, such as diesel engine generators and thermoelectric generators; but they cannot operate without a fuel supply. Therefore, solar batteries may be a very excellent power source in remote places.

Conclusion

Since 1958, many repeater stations and lighthouses with solar batteries as the power source have been erected in Japan, and they have been operated without trouble. It is expected that electrical equipment with solar batteries as a power source may be non-intermittently operated for a long period with only trivial upkeep once or twice a year.

From the economic point of view, silicon solar batteries are a very excellent power source in remote places, isolated islands and space.

References

1. Chapin, D. M., Fuller, C. S. and Pearson, G. L., New Silicon p-n Junction Photocell for Converting Solar Radiation into Electrical Power, *J. Appl. Phys. 25:* 676, 1954.

2. Kobayashi, M., Ishikawa, Y. and Hayashi, K., Solar Batteries for Use as the Power Source of Unattended UHF Repeaters, International Conv. on Transistors and Associated Semiconductor Devices, London, May 1959.

3. Hirai, S., and Kobayashi, M., Unattended Lighthouse Using Solar Batteries as Power Source, Sixth International Technical Conference on Lighthouses and Other Aids to Navigation, Washington, D.C., Sept. 1960.

Summary

Conversion of solar energy into electrical energy by means of silicon solar batteries is one of the most convenient and excellent methods owing to their light weight, reliability and long life, though their initial costs are relatively high for large power sources.

Six repeater stations and eight lighthouses equipped with solar batteries as power sources were installed on several mountains, shallows, capes and beaches during 1958 to 1960 in Japan. No difficulties have been observed. The batteries are expected to be able to operate for many years with upkeep only once or twice a year.

In this paper, the electrical characteristics of the solar cells, their performance and the cost of solar batteries as a power source are discussed. The cost at present is about $130 per watt, and they are cheaper than a power line, if the required supply is less than about 50 watts, at a place one km distant from a power station. In the near future, it is expected that the initial cost may be reduced to about two-thirds of the present figure.

EMPLOI DES BATTERIES SOLAIRES AU SILICIUM

Résumé

La conversion de l'énergie solaire en énergie électrique au moyen de batteries au silicium est l'une des méthodes les plus commodes et les meilleures en raison de leur légèreté, de la régularité de leur fonctionnement et de leur grande durée de service, bien que les frais de premier établissement qu'elles entraînent soient relativement élevés aux puissances importantes.

On a procédé au Japon, entre 1958 et 1960, à l'installation de six stations de répétition et huit phares dont la source d'énergie est constituée par des batteries solaires. Ces installations se trouvent sur plusieurs montagnes, des hauts-fonds, des caps et des plages. On n'a pas observé de difficultés. On s'attend à ce que ces batteries continuent à fonctionner pendant de longues années, avec seulement une ou deux visites d'entretien par an.

L'auteur passe en revue, dans le présent mémoire, les caractéristiques électriques des cellules solaires, leur fonctionnement et leur coût en tant que sources d'énergie. Le prix actuel s'établit à 130 dollars par watt environ, et elles sont plus économiques que le réseau si les besoins sont inférieurs à une cinquantaine de watts en un lieu situé à un kilomètre d'une centrale. On s'attend, dans le proche avenir, à ce que les frais de premier établissement soient ramenés aux deux tiers de leur chiffre actuel, ou à peu près.

APPLICATIONS OF PHOTOVOLTAIC CELLS IN COMMUNICATIONS

Gerald L. Pearson *

The barrier-layer photovoltaic cell was first developed about 80 years ago, using selenium (1) as the light sensitive material. Modern selenium cells are widely used in present-day industry for such diverse purposes as photographic exposure meters, photoswitches and photoelectric eyes. They have an over-all conversion efficiency of about 0.6 per cent when operated in direct sunlight.

In 1954, workers at the Bell Telephone Laboratories (2) succeeded in improving the efficiency of photovoltaic cells to 6 per cent through the use of a thin boron diffused layer on the surface of single crystal n-type silicon. A great deal of development work has gone into such devices during the past few years, and they are now commercially available from a number of manufacturers at efficiencies of up to 14 per cent for converting the solar radiation incident upon them directly into electric power (3). This conversion efficiency compares favorably with other types of modern power plants, such as the gasolene engine and the steam generator. It is therefore technically feasible to use solar batteries as power supplies at locations remote from commercial power lines. This paper discusses communication applications of solar batteries in terrestrial telephone systems and in space vehicles. In addition, new configurations of light sensitive *p-n-p* silicon diodes are described; they promise to be useful in frequency modulated communication systems.

The accepted value of the solar radiation constant (energy falling on one square centimeter area at normal incidence outside the earth's atmosphere) is 1.94 calories per minute or 135 milliwatts per square centimeter. A portion of this energy is absorbed in passing through the earth's atmosphere but on a clear day up to 120 milliwatts may be incident on a square centimeter of the earth's surface. Taking conservative estimates of 10 per cent solar battery efficiency and 100 milliwatts/cm^2 of solar radiation at the earth's surface one may then calculate 100 watts and 135 watts, respectively, for the electric power output from one square meter of solar batteries located on the earth and in outer space.

When a solar battery power supply capable of furnishing electric power continuously, regardless of the position of the sun and the weather conditions, is required one must provide an accumulator to store excess energy for use when the solar radiation is weak or completely absent. The practical solution to this problem has been found in electrochemical storage batteries. For terrestrial use, these may be of the lead-acid variety but in space applications one must use sealed units such as nickel-cadmium cells.

A terrestrial solar power plant for telephone equipment

The first commercial application (3) of the silicon solar battery was its use as the primary power source for a Bell type P rural carrier system at Americus, Georgia, beginning on 4 October 1955. Figure 1 is a photograph of the light transducer used in this installation. An array of silicon cells, 432 in number, was interconnected to furnish a maximum of 10 watts of electric power at 22 volts when irradiated with bright sunlight. The transducer was mounted in a fixed position 55 degrees from the horizontal. A storage battery consisting of 96 sealed nickel-cadmium storage cells of 1¼ volts was mounted at the base of the pole and the transducer served as a trickle charger to keep these cells adequately charged at all times. The nickel-cadmium cells were interconnected to form a "storage module" rated at 22 volts and 15 amp-hours. This amounted to a reserve power sufficient to operate the system during ten days of inclement weather before complete discharge.

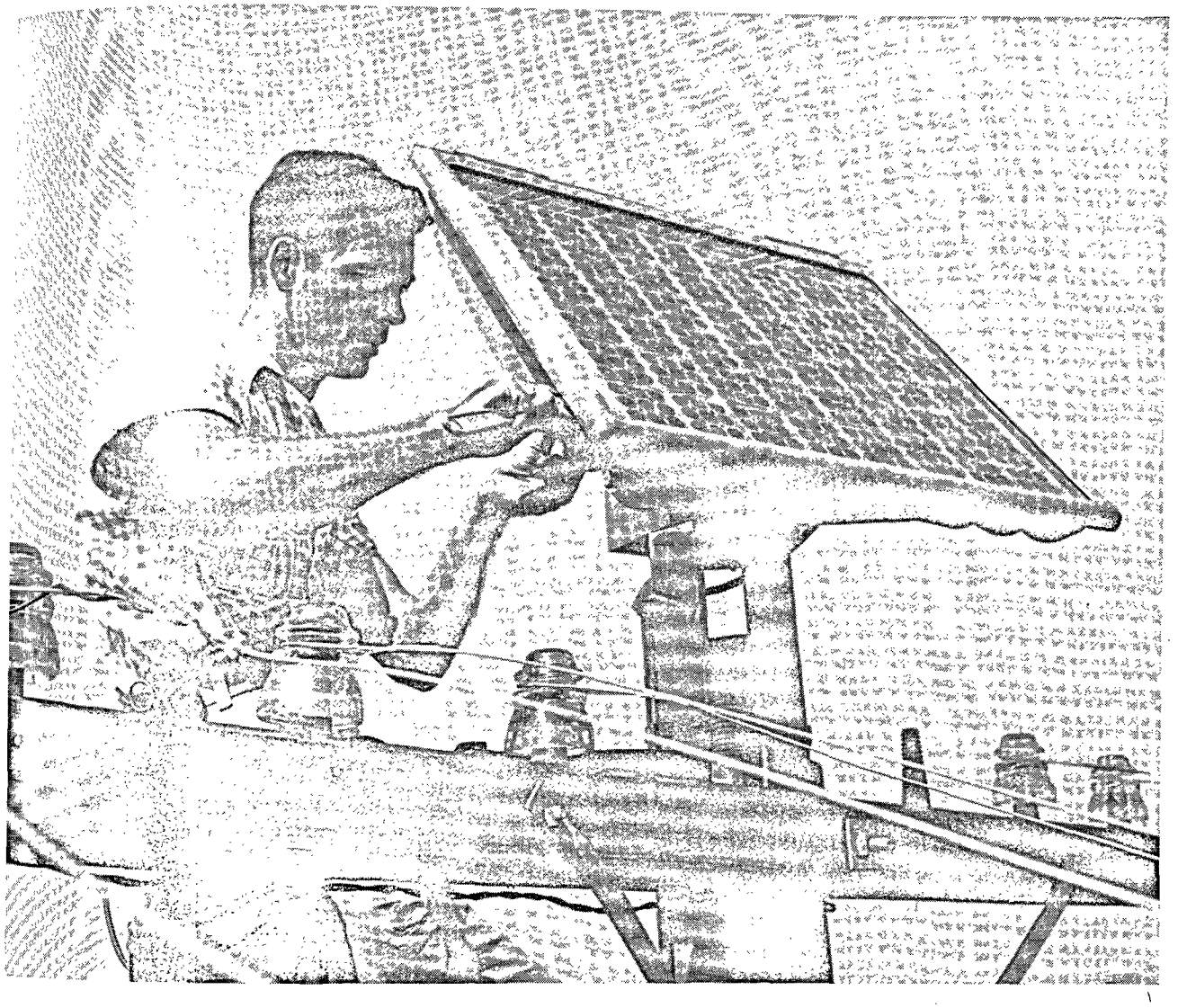
On 4 October 1955, the carrier terminal was connected to the solar power plant and for the next six months of commercial use all the power required by the terminal was supplied by the sun. The average current drain to the transmission circuits, carriers signaling circuits and alarm was about 0.3 amperes at 22 volts. At the end of this period the trial was ended and the carrier system was again supplied by a conventional power source.

On the basis of this test it was concluded that technical feasibility had been demonstrated for a solar power plant capable of furnishing about one watt. An analysis of costs, however, showed that it could not compete on an annual charge basis with conventional power supplies in the continental United States. In parts of the world where conventional power is either more expensive or not available, such a solar power supply might very well prove to be economic.

Space communications

Silicon photovoltaic cells have been used as power supplies for instruments and transmitters in a

* Electronics Research Laboratories, Stanford University, Stanford, California.



[Bell Telephone Laboratories photo]

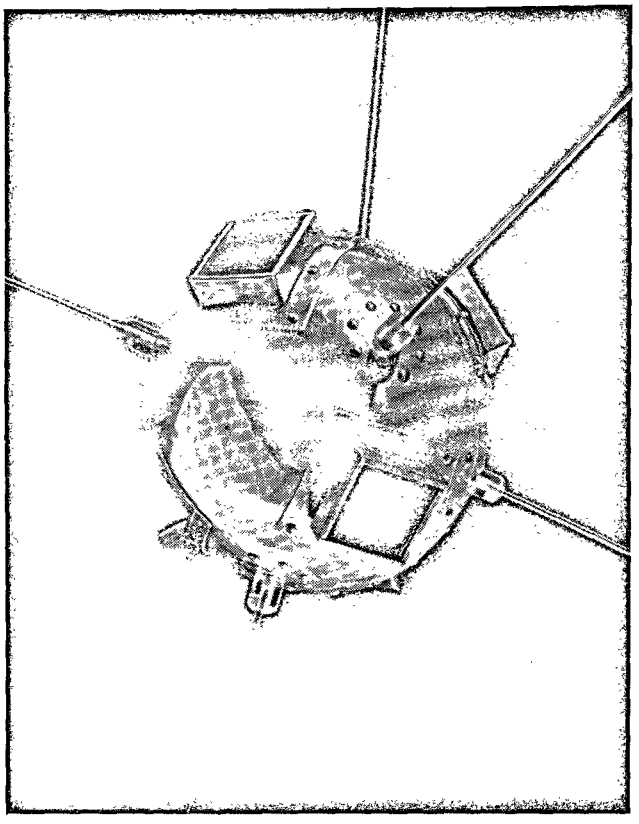
Figure 1. Silicon photocells used to power telecommunication system

number of space vehicles during the past three years. Whereas electrochemical batteries have proven satisfactory for short periods of time, the only proven long-lived power supply for space use, at the present time, consists of silicon photovoltaic cells.

The first use of solar batteries in an orbiting satellite was in Vanguard I, which was launched at Cape Canaveral, Florida, on 17 March 1958 (figure 2). This vehicle contained two transmitters (5); the one operating at 108.00 Mc ± 4 kc was powered by a mercury storage battery which failed after about three weeks, the other operating at 108.03 Mc ± 4 kc was powered by photovoltaic cells and is still operating satisfactorily after more than three years in space. In this installation the power from the solar transducer is fed directly to the transmitter without electrochemical storage so that no signal is transmitted when the vehicle is in the shadow of the earth.

The second successful use of silicon solar cells in an orbiting satellite was in Sputnik III, which was launched in Russia on 15 May 1958 (6). Since that time silicon solar cells have been successfully employed for the conversion of solar energy to electrical energy in a number of space vehicles, including Explorers VI and VII, Pioneer V, Tiros I and II, Transit I-B and II-A, and Courier IB. These later installations have included electrochemical storage batteries with the solar cells acting as trickle chargers so that continuous power is available.

Whereas cost per watt is a most important factor in the terrestrial uses of solar cells, the overriding factors for space use are watts per pound and reliability. With present day cells and mounting procedures it has been possible to design power packs for space use which furnish 3.5 watt/pound including storage batteries (7). This figure will undoubtedly be raised with the development of better non-



[*Bell Telephone Laboratories photo*]

Figure 2. Model of Vanguard I earth satellite showing silicon photocell mountings

reflecting surfaces, heat control, and methods for the mounting of cells. The reliability record of solar cells in space has been excellent since there are no moving parts which might contribute to failure. Contacts to the silicon wafers are an ever present source of trouble but these have proven to be quite permanent.

A major problem associated with the use of silicon photovoltaic cells in space probes is radiation damage resulting from bombardment by high energy electrons and protons in outer space. This is particularly serious in the inner (mainly protons) and the outer (mainly electrons) Van Allen radiation belts which center 3 600 km and 16 000 km above the equator (8). Damage from electrons can be minimized by a reasonable amount of shielding but the high energy protons are so penetrating that shielding seems impractical.

In order to obtain quantitative information on the degradation of solar cells under bombardment by high energy particles, a series of laboratory experiments was performed[1] in which boron diffused silicon cells (initial conversion efficiency of 9 per cent) were monitored during bombardment by electrons and protons of different energies. The energy ranges were chosen to match those expected in space and were between 0.17 and 1.5 Mev for electrons and between 45 and 155 Mev for protons. Short circuit current under fixed illumination was measured as a function integrated flux in particles per cm². The integrated flux required to degrade the short circuit current by 25 per cent is shown in figure 3. Subsequent experiments indicated that conversion efficiency into a matched load is nearly proportional to short circuit current. It can be seen from these curves that electron damage decreases with decrease in energy, with a threshold at about 0.25 Mev, while proton damage increases with decrease in energy. The proton relation is to be expected since the knockon cross section of a silicon atom to high speed protons increases with decreasing velocity. After quantitative data relating to density of charged particles versus energy is obtained in outer space, the measurements presented here will make it possible to calculate expected solar battery life. In general it can be said that for the energies used in these measurements an integrated flux of about 10^{13} electrons or 5×10^{10} protons degraded the cells by 25 per cent. A recent announcement (9) from the United States Army Signal Research and Development Laboratory describes a new type of radiation resistant solar cell in which phosphorus is diffused

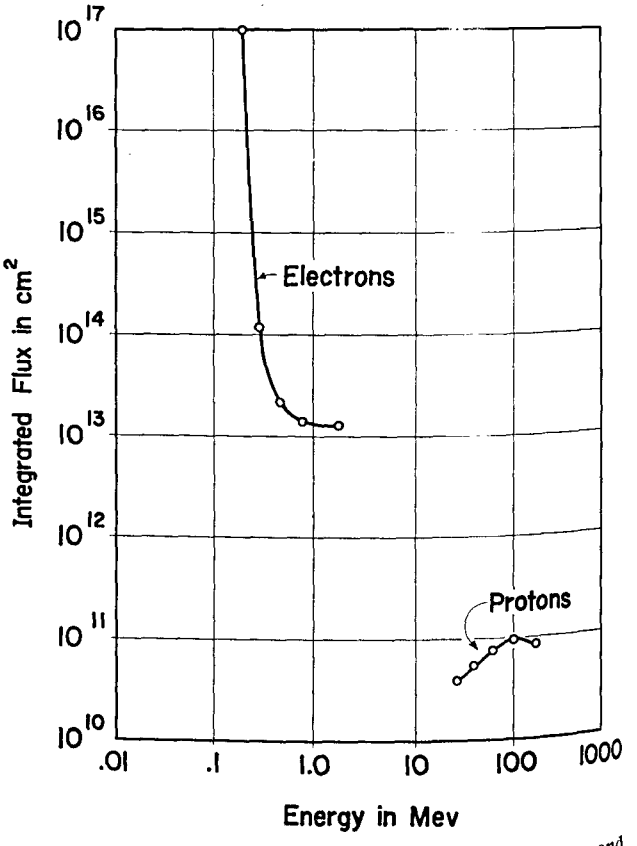


Figure 3. Integrated flux of high energy electrons and protons required to reduce conversion efficiency of silicon photocells by 25 per cent

[1] These measurements were made in conjunction with W. L. Brown of Bell Telephone Laboratories. We wish to thank R. Wilson for permitting us to use the Harvard University cyclotron for the proton experiments.

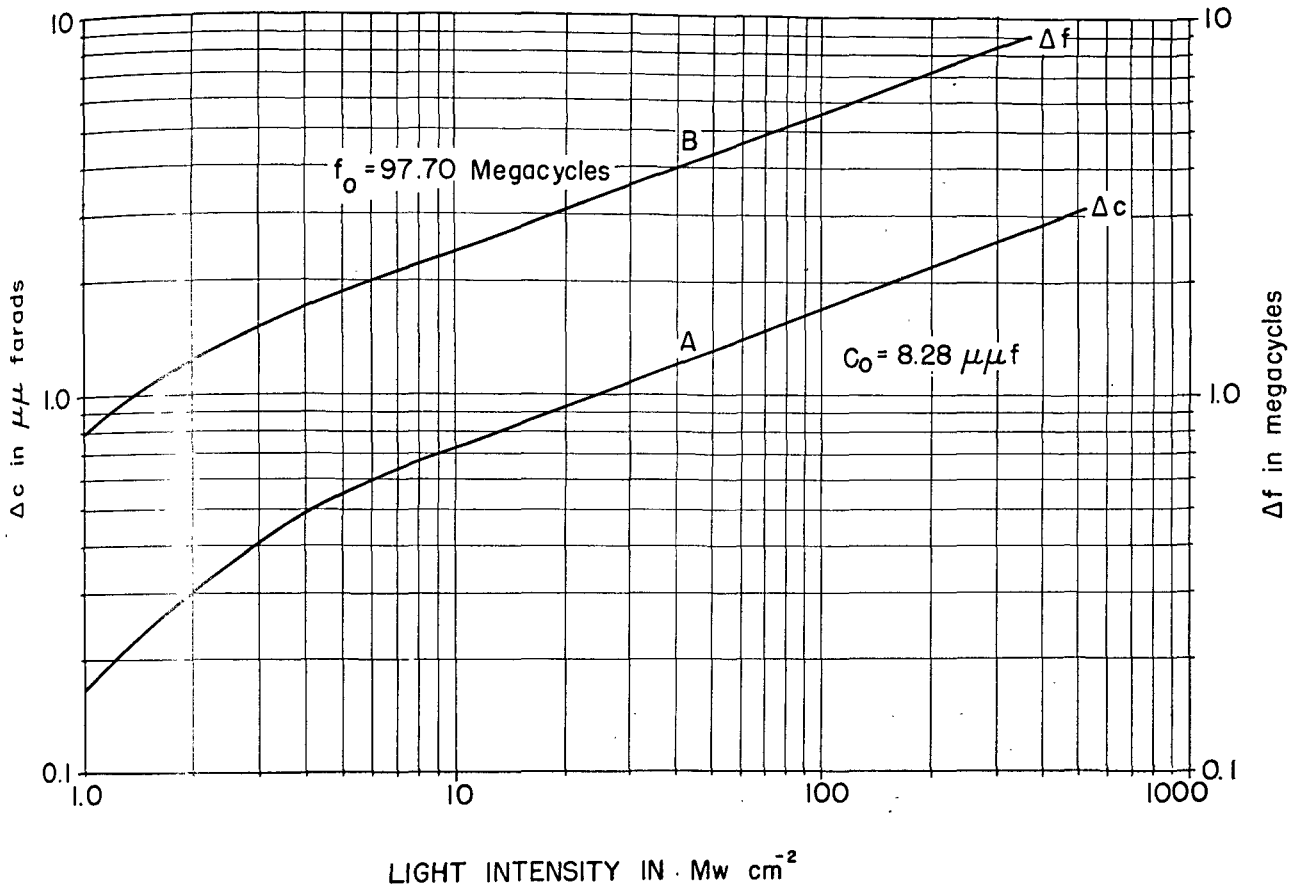


Figure 4. (A) Increase in capacity (ΔC) of p-n-p silicon photocell as a function of light intensity; (B) Decrease in frequency (Δf) of 100 megacycle oscillator as a function of light intensity

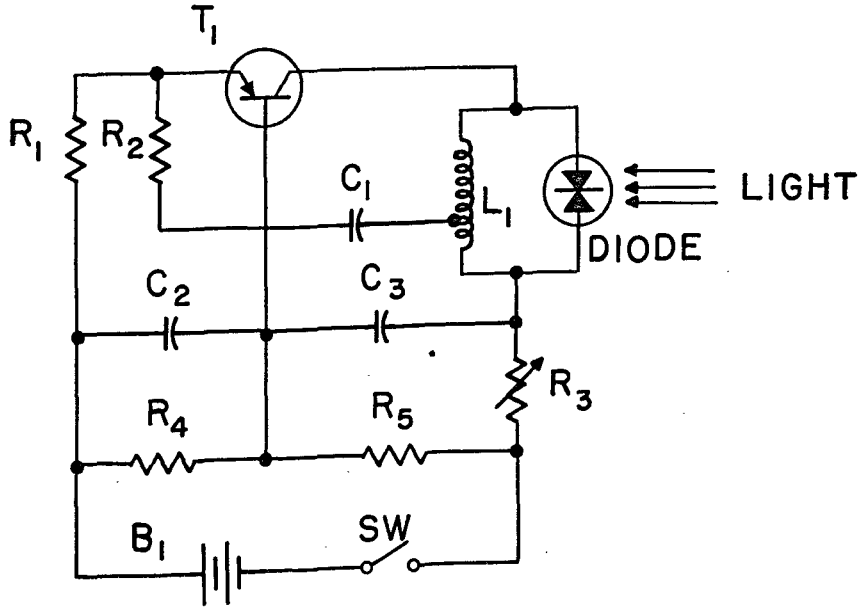


Figure 5. Circuit of transistor oscillator employing p-n-p photodiode in tank circuit

into p-type silicon. Preliminary measurements indicate that this type of cell may withstand flux of a greater order of magnitude before deterioration becomes serious.

Light communications system

The capacitance of a *p-n-p* diffused silicon diode is increased when light falls on the junction (10). This capacitance modulation comes about because the photons generate hole-electron pairs in and near the junctions. The holes are collected in the *p*-layer while the electrons drift to either *n*-layer, thus biasing the junctions in their forward direction and increasing their junction capacitances. A zero-bias capacitance versus light intensity plot[2] for such a diode having an area of approximately 0.01 cm² is shown in curve A of figure 4. In connection with this figure, it should be mentioned that the diode header was not designed for maximum light interception at the junctions; hence, the light energy actually falling on the junctions is somewhat less than the incident light flux plotted here.

The capacitance modulation property of the diode provides a simple means for varying the tank circuit capacitance of an oscillator and thereby producing an output frequency which is related to the incident light intensity. This effect has been used in a nominal 100 Mc transistorized FM transmitter (11) whose circuit diagram is shown in figure 5 to test the principles outlined above. The circuit components of this equipment are shown in the figures given below, and the measured decrease in frequency as a function of incident light intensity is shown as curve B in figure 4. Good agreement between theory and experiment is found through the tank circuit relation $\Delta f/f = -\Delta C/2\Delta C$.

Values of components shown in figure 5

C_1 — 15 μμf	R_2 — 240 Ω	R_5 — 12 kΩ
C_2, O_3 — 001 μf	R_3 — 5 kΩ	T_1 — 2N 499
R_1 — 350 Ω	R_4 — 2.4 kΩ	B_1 — 15 volts
L_1 — Six turns with feedback tap at one full turn		

It is significant that a frequency modulation of about 1 per cent is obtained at an incident light flux of only 1 milliwatt per square centimeter. The *p-n-p* diode together with a high frequency transmitter is thus a convenient and extremely sensitive means for signaling quantitative light flux data. In addition, tests have shown that the above system is a practical means for converting an amplitude modulated light signal directly into a high quality frequency modulated electrical signal.

[2] The measurements on this light modulated capacitor were made with the aid of J. M. Klein while the author was at Bell Telephone Laboratories.

References

1. Adams, W. G., and Day, R. E., The Action of Light on Selenium, *Proceedings of the Royal Society of London 25:* 113-7, 1876.
2. Chapin, D. M., Fuller, C. S. and Pearson, G. L., A New Silicon p-n Junction Photocell for Converting Solar Radiation into Electrical Power, *J. Appl. Phys. 25:* 676-7, 1954.
3. Prince, M. B., and Wolf, W., New Developments in Silicon Photovoltaic Devices, *J. Brit. IRE 18:* 583-95, 1958.
4. Smith, D. H., A One-Watt Solar Power Plant, *Comm. and Elect. 45:* 530-35, 1959.
5. Easton, R. L., and Votaw, M. J., Vanguard IGY Satellite (1958 Beta), *Rev. Sci. Instr. 30:* 70-5, 1959.
6. Mikhaylov, M., Information on Soviet Bloc International Geophysical Cooperation — 1959, United States Dept. of Commerce, *Bulletin P B 131632-70,* June 12, 1959.
7. Daniel, A. F., Solar Batteries, *Proc. IRE 48:* 636-41, 1960.
8. Van Allen, J. A., The Geomagnetically Trapped Corpuscular Radiation, *Geophys. Res. 64:* 1683-8, 1959.
9. *The Sun At Work, 5:* No. 3, 4-5, 1960.
10. Gibbons, J. F., and Pearson, G. L., P-N-P Variable Capacitance Diode, *Proc. IRE 48:* 253-5, 1960.
11. Thomas, D. E., A Point-Contact Transistor VHF FM Transmitter, *Trans. Inst. Radio Engrs: ED-1, No. 2,* 43-52, 1954.

Summary

Photoelectric cells which convert solar energy directly into electric energy are ideally suited for furnishing power to communication systems located at great distances from commercial power supplies. Although the solar flux density usually amounts to under 120 milliwatts per cm² at the earth's surface, this is sufficient to provide power for modern transistorized communication systems. These might include either wire or radio installations and land based as well as space applications.

The results of a commercial trial on a carrier telephone installation carried out by the Bell Telephone Company at Americus, Georgia, over a six-month period are described in this paper. These include engineering considerations and cost analysis data.

The applications of photoelectric cells to power communication equipment in artificial space satellites are considered. Practical experience obtained from a number of such installations is outlined. The problems discussed include: (*a*) power-to-weight

ratio, (*b*) storage of energy for use in dark periods, and (*c*) radiation damage from high energy particles in outer space.

A new use for *p-n-p* junction photovoltaic cells in frequency modulated systems is described. In this application a variation in the light intensity falling on the junctions alters the capacitance and thereby provides a simple means of producing an oscillator output frequency which is related to the incident light intensity. This effect has been used in an FM transmitter operating at 100 Mc to produce a frequency shift of 800 kc for an incident light intensity of 1 mw/cm². Inherent advantages in signal-to-noise properties of this system make it ideal for monitoring changes in various physical parameters at remote locations. The entire system can be powered by photoelectric cells, and servicing is seldom required.

APPLICATION DES CELLULES PHOTOVOLTAÏQUES DANS LE DOMAINE DES TÉLÉCOMMUNICATIONS

Résumé

Les cellules photo-électriques qui assurent la conversion directe de l'énergie solaire en énergie électrique s'adaptent idéalement à la fourniture de force motrice aux systèmes de télécommunications qui se trouvent à de grandes distances de sources commerciales d'énergie. Bien que la densité du flux solaire ne dépasse habituellement pas 120 milliwatts par cm² à la surface de la terre, ceci est suffisant pour faire face aux besoins d'énergie des systèmes de télécommunications modernes dotés de transistors. Ces installations peuvent comporter des systèmes de télécommunications par fil ou sans fil, basés sur terre ou même à bord d'astronefs.

Les résultats des essais commerciaux qui ont été exécutés pendant six mois sur une installation de téléphonie à ondes porteuses par la Bell Telephone Company à Americus, état de Géorgie, États-Unis, font l'objet d'une description dans le présent mémoire. Cette description comporte des considérations techniques et des données sur l'analyse des prix de revient.

L'auteur passe en revue les applications des cellules photo-électriques au matériel de télécommunications à bord des satellites artificiels. Il résume l'expérience pratique fournie par un grand nombre d'installations de cet ordre. Les problèmes examinés comprennent : *a*) le rapport puissance/poids; *b*) l'accumulation d'énergie pour les périodes d'obscurcissements; *c*) les dégâts dus au rayonnement par les particules à grande énergie dans l'espace interplanétaire.

L'auteur décrit une nouvelle application des cellules photovoltaïques à jonction *p-n-p*. Dans cette application, les variations de l'intensité lumineuse sur les jonctions modifient la capacité et fournissent donc un moyen simple de réaliser une fréquence de sortie d'oscillateur qui est en rapport avec l'intensité de la lumière incidente. Cet effet a été utilisé dans un émetteur à modulation en fréquence fonctionnant à 100 Mc pour obtenir des excursions de fréquence de 800 kc pour une intensité de lumière incidente de 1 mW/cm². Les avantages intrinsèques du rapport signal-bruit, dans ce système, le rendent idéal pour la télésurveillance des variations de divers paramètres physiques. On peut fournir l'énergie à la totalité du système au moyen de cellules photo-électriques et il est rarement nécessaire d'y faire des travaux d'entretien.

LATEST DEVELOPMENTS IN THE FIELD OF PHOTOVOLTAIC CONVERSION OF SOLAR ENERGY

M. B. Prince *

Since photovoltaic solar energy conversion is the mechanism for obtaining electrical power directly from solar radiation, which is abundantly available, it appears to be a timely task to summarize the present state of the art in this field. The major goals of the development work undertaken on devices based on this mechanism for terrestial applications were lower cost-to-power ratios and higher reliability. It is interesting to review, in the light of the experience gained, the difficulties encountered with these devices, and the corrective measures undertaken. This is followed in this paper by a discussion of the improvements introduced on the present standard device, namely the silicon solar cell. Attempts to develop methods for preparing large area and thin film silicon solar devices are reviewed. A survey is given of the progress made in the application of other semiconductor materials to solar photovoltaic energy conversion. Finally, costs are considered, and several applications are discussed.

Essential contributions to the analysis of the photovoltaic effect or of the device operation have not been made during the past year, with the exception of a new explanation for the operation of the cadmium sulfide solar cell (1). In view of the length of this paper, only references to previous publications will be given for the whole complex of the device analysis (2, 3, 4, 5, 6).

* Vice-President, Hoffman Electronics Corporation (Semiconductor Division), El Monte, California.

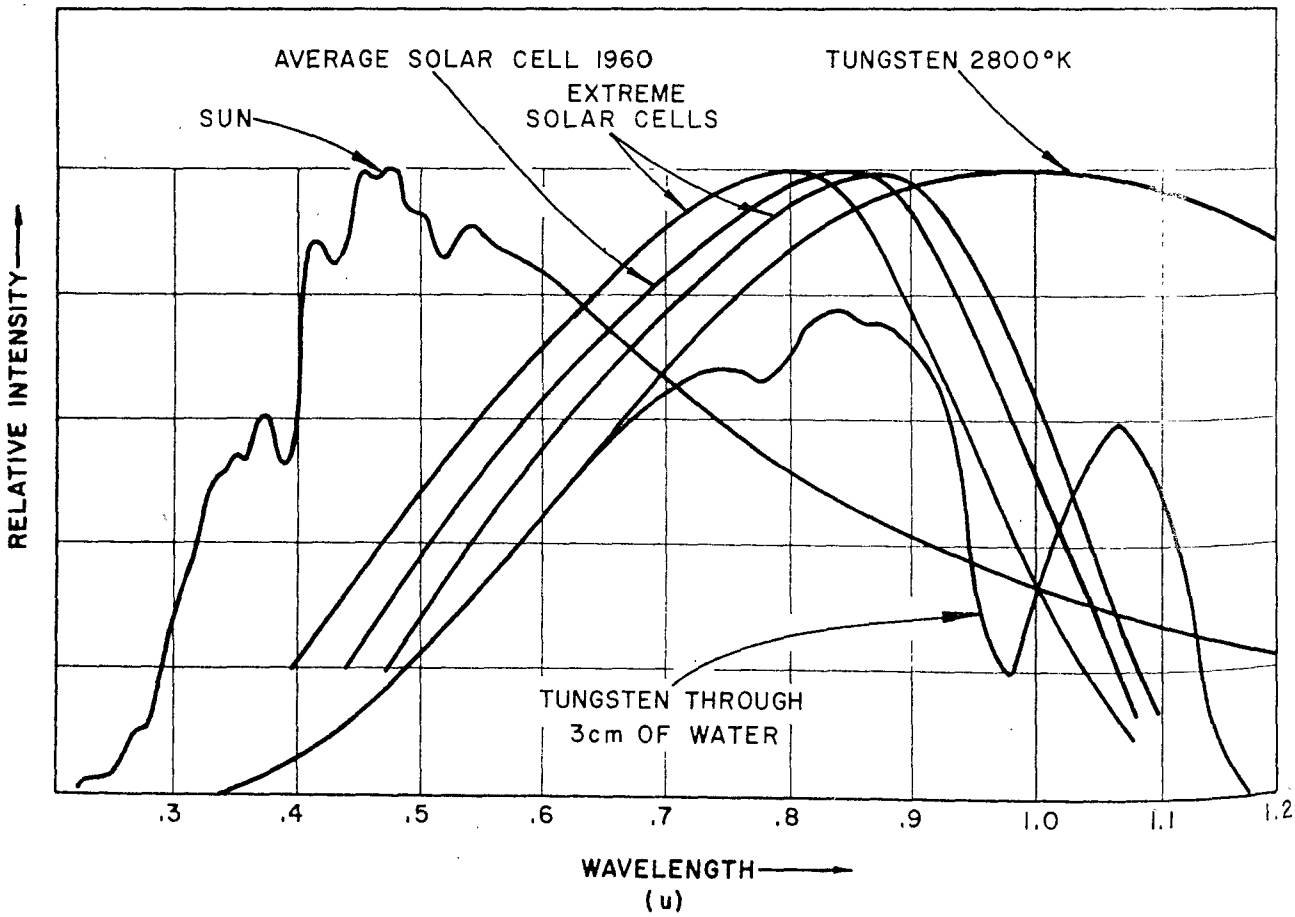


Figure 1

The major difficulty experienced with the silicon solar cells for terrestrial applications during the past year was the measurement problem, which was encountered because of the introduction of insufficient sunlight simulation for the performance determination of silicon solar cells, coupled with a variation in the spectral response of these devices.

The problem of performance measurements on solar cells

Since the prime objective of the solar cell is to convert solar energy into useful electrical energy, the basic performance measurement has to be connected with the solar radiation. The standard instrument used for the determination of the energy content in the solar radiation received is the pyrheliometer. The principle of the measurement is to obtain the electrical output of the solar cells in sunlight, using the pyrheliometer as the calibration instrument. Difficulties are encountered even at this point. The pyrheliometer measurement is dependent on the ambient temperature as well as on the tilt of the device. Besides variations found in the basic calibration of the instrument, a few other unknown variables also seem to affect the measurements. The result is an uncertainty in the pyrheliometer readings of several per cent for the 90 per cent confidence level. Another larger problem area is the variation of the spectral distribution of sunlight. Variations in the intensity of the sunlight as received on the earth's surface are due to various amounts of attenuation in the atmosphere. Since the atmosphere is not a neutral attenuator, the intensity variations are always connected with changes in the spectral distribution, and various spectral distributions are even found with the same integrated light intensity. Since the pyrheliometer is a relatively flat receiver, while the solar cell is a selective receiver, discrepancies in solar cell output measurements are normal. Such discrepancies have been observed to be a much as ± 10 per cent between different measurements on the same cell.

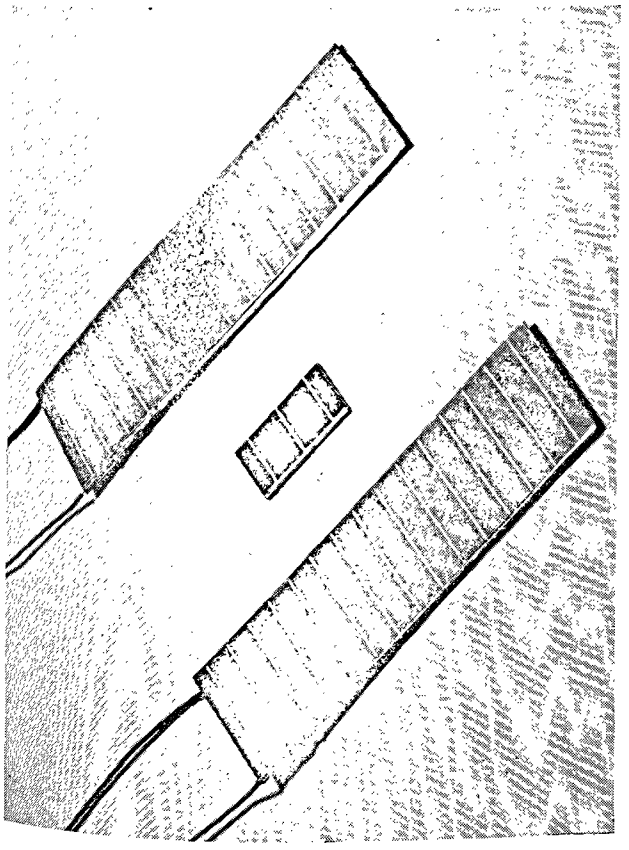


Figure 2

Since measurements as described above are too dependent on weather conditions to be useful for production and regular inspection purposes, a measurement method capable of being performed in the laboratory at all times was devised. Tungsten light sources have been found in the past to be the most suitable artificial sources because of their short term stability as well as their long term stability. The spectral distribution of this light source can be kept constant by measurement of the color temperature and by regulation of the input power. The desired light intensity is then obtained by varying the distance between the source and the object. Repeatability of solar cell measurements with such tungsten light sources within ± 1 per cent over periods of the order of a day and within ± 2 per cent for longer times for the 90 per cent confidence level have been achieved. The color temperature of these tungsten light sources is now normally set to $2\,800 \pm 50$°K, while the intensity is adjusted by means of so-called standard cells which have been calibrated in sunlight, as described above. The parameter used on the standard cells for this light intensity transfer is the short circuit current.

If all solar cells had exactly the same spectral response, then such a transfer from one source with a specific spectral distribution would be perfectly valid.

Figure 1 shows, for comparison purposes, a normalized spectral distribution of sunlight as it is received outside the earth's atmosphere (7) and the spectral distribution of a tungsten light source with a color temperature of 2 800°K. It also shows the spectral distribution of the same tungsten light after passage through a water layer of 3 cm thickness (8).

It has been found that a considerable spread exists in spectral response between various production cells. This spread causes some uncertainty in a measurement method involving a variation of the source spectrum. Figure 1 also shows the average spectral response of the typical silicon solar cell as produced throughout the year 1960. This average response curve was determined from a sample of 400 production cells, having conversion efficiencies between 9 and 13 per cent. Two other curves show the extremes of the spectral responses found in the same study. If one chooses cells having a spectral

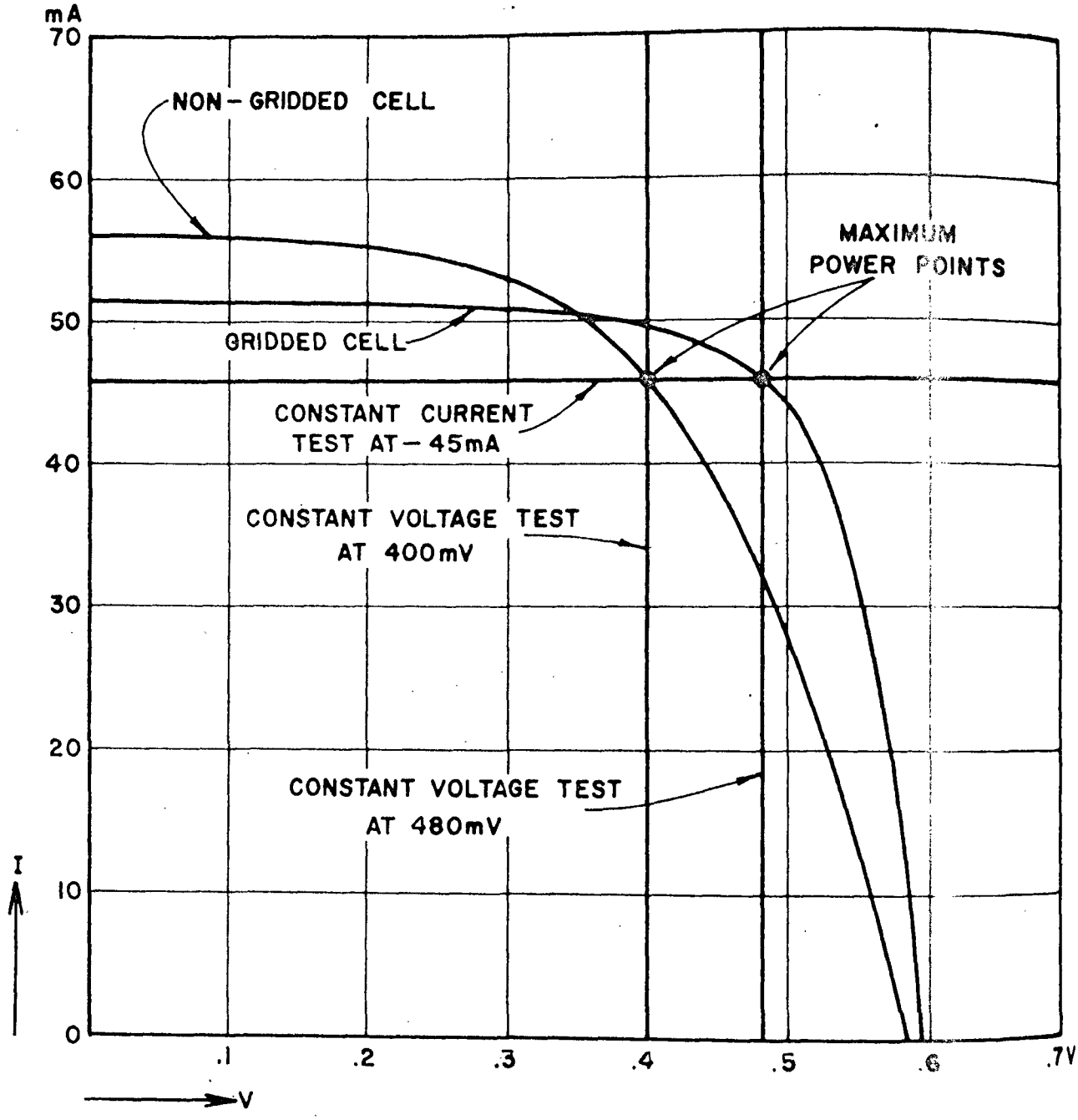


Figure 3. Constant voltage and constant current — test of solar cells type 120 C, at 25°C

response very close to the average of the production spread for the preparation of the standard cells, then the average measurement should be proper with a symmetrical deviation for the production spread.

Recently it has been found that the average spectral response of the production solar cells can fluctuate with time. This results in obtaining improper measurements at certain times for the whole production by use of the tungsten system. Such a problem has been experienced recently. Since the selection, preparation, and calibration of standard cells is a very tedious and time-consuming process, it appears impractical to prepare standard cells whenever a fluctuation of the production spectral distribution is experienced.

The ideal solution to this problem is the creation of a "sunlight simulator"; that is, a light source which exhibits the same spectral distribution and intensity as observed in the solar radiation. Such light sources which closely meet the spectral distribution of the solar radiation, and which are capable of very good short and long term stability, are under development at various organizations. The best candidates at the present time appear to be

carbon arcs, if efforts to obtain the needed stability are successful; a plasma jet system developed by Mt. Vernon Research Laboratories; and the application of xenon high pressure arc sources combined with filters, separately under development at the present time by General Electric Company, Spectrolaboratories and the Hoffman Semiconductor Division. Prototypes of some of these sources are already finding limited application.

These efforts to find the proper light source are paralleled by meetings between representatives of the interested industries, with the objective of standardizing methods and tolerances, and of resolving the problems encountered.

Improvements on the silicon solar cell during 1960-1961

Two significant improvements have been made on the silicon solar cell during the past year and a half. The first one, already available for production cells, was the introduction of the gridding method. The second one consists of a shift of the spectral response in order to obtain improved efficiency in sunlight. This shift was made possible only through the introduction of the gridding method.

Gridded cell

It has been found that in actual silicon solar cells the internal series resistance is large enough so that it causes a deviation of the current-voltage characteristic from its ideal curve. With the best methods presently known, the impurity concentration of the diffused p-layer cannot be made sufficiently high in order to keep the series resistance of the p-layer negligibly small for p-layer thickness as small as desirable for obtaining highest collection efficiency. In the present silicon solar cell a compromise is obtained between p-layer thickness and p-layer series resistance in order to obtain the highest possible over-all efficiency (2).

A substantial decrease in the total p-layer series resistance can be achieved by applying metallic grids over the p-layer. Figure 2 shows silicon solar cells of different sizes with such grids applied. These grids reduce the resistance of the p-layer by lowering the length of the current path through this layer to the next collecting metallic line having low resis-

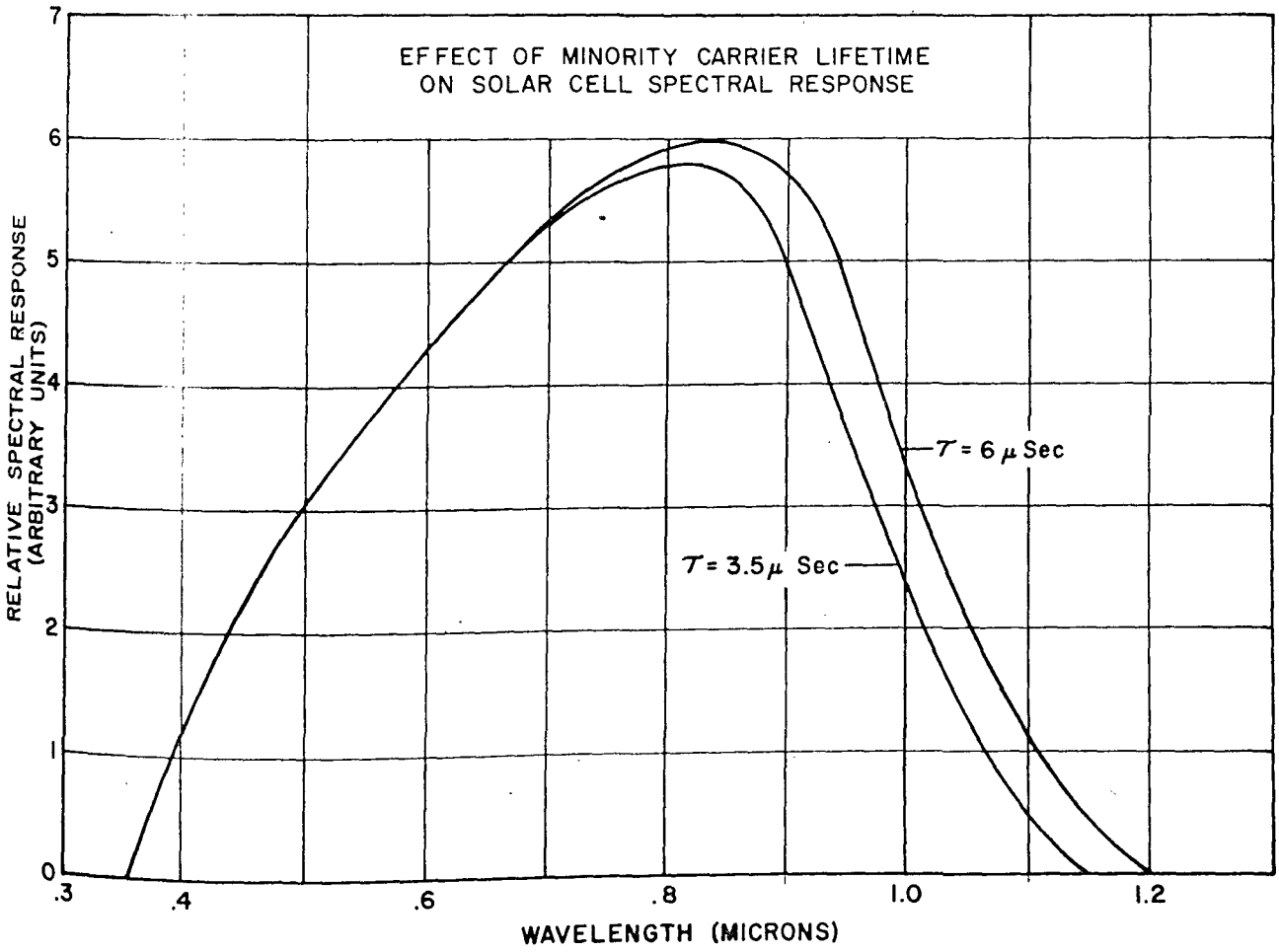


Figure 4 a

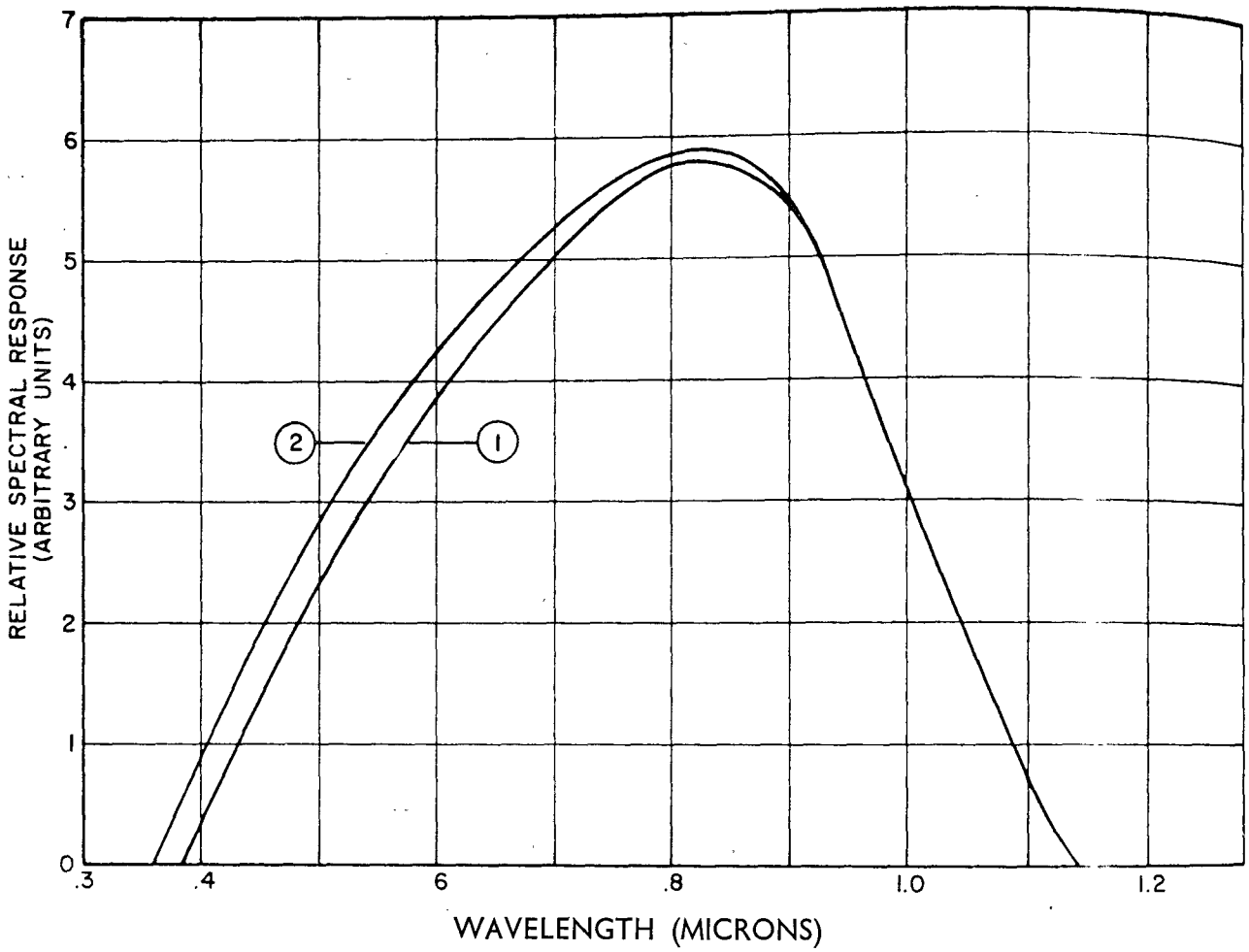


Figure 4 b

tance. This effect is so great that despite the loss of part of the active area due to coverage by these grid lines, the efficiency of gridded solar cells of 1 × 2 cm size has been found to be on the average 1.5 per cent higher than that of non-gridded, but otherwise identical, cells. This efficiency calculation is based on the total exposed area of the cell in a series shingle, counting the area covered by grid lines as exposed area. The introduction of such grids also permits freedom from such considerations of size and shape of solar cells as were previously necessary for optimum performance. Solar cells of 2 × 7.5 cm size with grids have now been made with better then 12 per cent efficiency. The two large cells shown in figure 2 are of this size.

The reduction of the series resistance causes a change in the current-voltage characteristic, as indicated in figure 3, for a gridded and a non-gridded cell. The open circuit voltage should be identical, and the difference in short circuit current due to the coverage of part of the active area by grid lines is also normally not as large as appears in this figure. The major feature is, however, clearly indicated: the characteristic is more "squared", resulting in a higher voltage forthe maximum power point, which occurs at the same current value so that a higher output power results. Consequently, on a power panel having to meet a certain load voltage, fewer cells can be connected in series in order to reach this voltage, which leads either to a reduction in the total panel area for equal power output, or to an increase in power output by adding additional series strings to fill the original panel area.

Spectral response modification for improved sunlight performance

It has been shown previously (4, 5, 6) that the long wavelength part of the spectral response curve of silicon solar cells is mainly affected by the minority carrier lifetime of the base material, which usually is an *n*-region, and that the short wavelength part of the spectral response is influenced by the minority carrier diffusion length and the thickness of the diffused layer, which normally is a *p*-type layer. These theoretical considerations have been verified by recent developments.

First, strides were made toward improved minority carrier lifetimes in the base region, which resulted in an increase of the spectral response toward the

long wavelength side as shown in figure 4 a. This improvement was accomplished during 1959, and it led to the difficulties with measurement methods explained in an earlier section. At that time, an increase in the base minority carrier lifetime was the only possible approach to an improvement, since before the advent of the gridding technique a change in the thickness or the minority carrier diffusion length of the p-layer could not lead to better efficiencies. This had its cause in the previous optimization of impurity concentration and the p-layer thickness so as to give the best compromise between short circuit current and series resistance. After the gridding method was introduced, efforts could be undertaken toward reaching a new compromise of p-layer thickness and minority carrier diffusion length by modification of the diffusion parameters. The interesting feature is that modifications of either the short wavelength or the long wavelength part of the spectral response curve can be achieved without affecting the other part.

Figure 4 b shows the spectral response curves of two silicon solar cells which were prepared with identical parameters except for some diffusion modification. The cell represented by curve 1 has been fabricated with the same diffusion parameters as were used before the introduction of the gridding technique. Curve 2 represents a cell with the modified diffusion parameters. Both cells have the same base material minority carrier lifetime, and therefore the same long wavelength response.

The short circuit current of a solar cell is proportional to the integral under a curve which is obtained by multiplying the cell spectral response curve, point for point, with the spectral distribution of the light source. Since tungsten light (2 800°K) contains only a small amount of energy in the short wevelength part of the spectrum, the modification of the spectral response curve as indicated in figure 4 b will result in a hardly noticeable difference in the short circuit current, if measurements are performed under tungsten light sources. This is indicated in figure 5 a, which shows curves for the two cells, 1 and 2, of figure 4 b. These curves, labeled 1 and 2 for the two cells, were obtained by the explained spectral response-spectral distribution multiplication

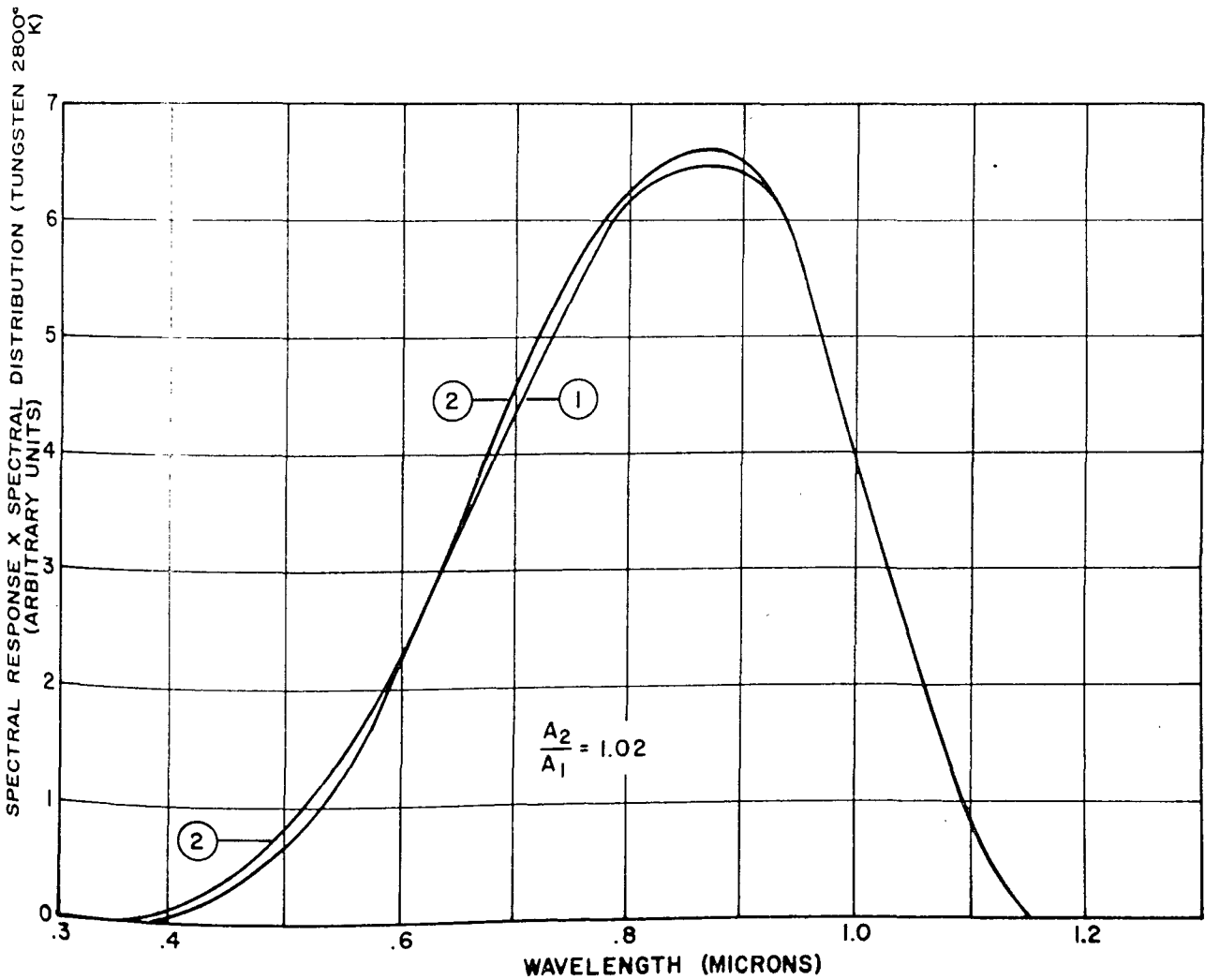


Figure 5 a

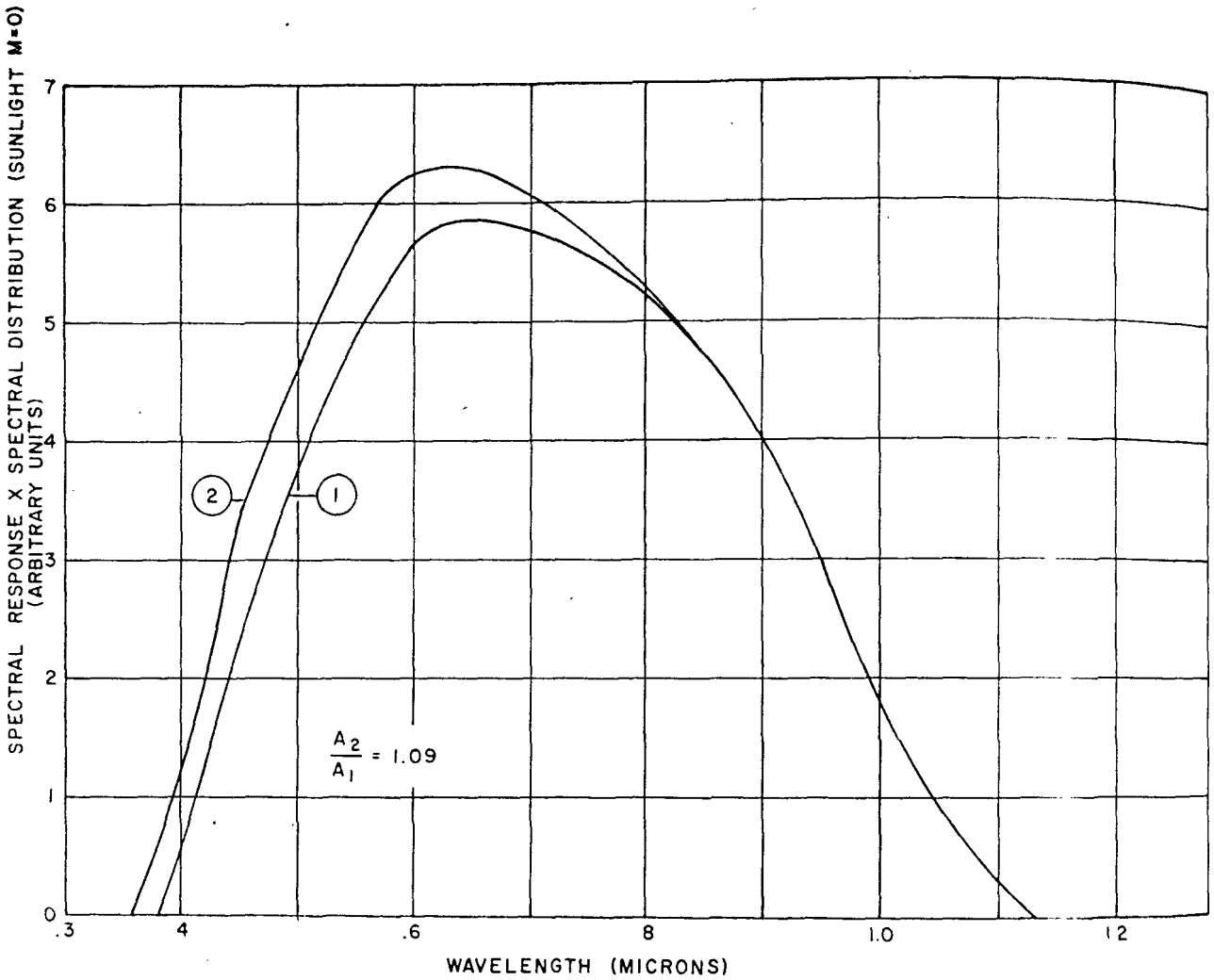


Figure 5 b

method. Figure 5 b shows a corresponding set of curves for the same cells, but this time by using the spectral distribution of sunlight as received outside the earth's atmosphere. Here the difference in spectral response between the two cells results in a marked difference in the two curves, leading to a ratio of the integrated areas under the curves of 1.09, as compared to a ratio of 1.02 for the two curves of figure 5 a. The interesting result of this modification is, therefore, that cells are obtained which show a performance under tungsten light comparable to that of the cells prepared with the previously used parameters, but that the same cells will produce higher short circuit current and correspondingly higher power output in sunlight than the older cells.

New configurations and approaches on silicon solar cells

Large area single crystal cells

The advent of the gridding technique permits complete freedom from geometrical considerations for the first time for the design of solar cells. Since diffusions can be controlled with sufficient uniformity, the size of the cells is determined only by limitations in crystal growing and cutting techniques. Future developments probably will retain the rectangular configuration owing to its advantage in better area utilization. Cells as large as $2 \times 7\frac{1}{2}$ cm have been prepared with efficiencies as high as those obtained in the smaller types. Preparation of these cells is possible since single crystals of silicon with over 5 cm diameter and more than 10 cm length, having good crystalline properties, are readily available now. Essential difficulties are not expected to be encountered by going to still larger sizes, and 10×2 cm is anticipated as the next step.

These larger area cells have the advantages of lower cost per unit power because of decreased handling time in preparation as well as in application of the cells, and of higher reliability because of reduction in the number of contacts to be made. Though this approach uses standard methods, it would be very desirable to obtain large area single crystalline wafers without the presently used cutting

process in which about 50 per cent of the valuable raw material is lost. A method successfully applied to germanium by Bösenberg (9) consists in casting the material in a mold and successive gradient cooling after attachment of a seed crystal. This method is, however, not applicable to silicon owing to the high reactivity of this element with every known material which can be used for a mold. Another approach with the same objective has recently been pursued by W. R. Grace and Co. on an ARPA contract.[1] Here molten silicon was floated on molten lead and then gradient cooled after attachment of a seed crystal. This method was expected to be workable since lead was supposed to have a very small solubility in silicon and not to act as an electrically active impurity. Experience showed, however, that these assumptions were not correct. Beyond this, difficulties were encountered in the preparation of thinner wafers since surface tension caused formation of a lens-shaped molten silicon mass rather than a flat thin layer.

Another approach, not resulting in large wafers but possibly in long strips of solar cells, is pursued by the Westinghouse Electric Corporation on a WADD contract.[2] This approach consists in the application of the dendritic growth method to silicon and the preparation of solar cells from these dendritic crystals. This growth method was very successfully used with germanium, and diodes and transistors were prepared from this material. Although not much information is available about the progress of this project, it appears that difficulties encountered earlier in the growing of the dendritic crystals or ribbons of silicon are being worked out. Some solar cells have been prepared from such dendritically grown crystals, and achievement of efficiencies as high as those obtained in solar cells prepared from single crystals grown by the Szochralski method have been reported.

Another line of attack is the preparation of thin film solar cells. The obvious advantages of such an approach are the most conservative use of the costly silicon raw material, the possibility of readily preparing large area devices, and the possibility of obtaining flexible cells which should be capable of relieving some of the storage, transportation, and deployment problems of extremely large area energy converters. There are, however, obvious difficulties connected with this approach, and it is questionable whether sufficiently large efficiencies can be obtained in order to make this approach competitive with the one pursued presently.

Thin film solar cells

A thin film solar cell has a basic physical performance limit given by its thickness. This is due to the magnitude of the absorption coefficient which in silicon varies strongly with wavelength over the range of interest for solar energy conversion, as shown in figure 6 of this paper. Since rather small absorption coefficients are found towards the longer wavelengths, only a small portion of the incident energy will be absorbed in thin films in these wavelength regions. Figure 7 shows that portion of the energy available in sunlight at wavelength up to 1.1 μ, which can be absorbed in films of different thicknesses. The calculations leading to this curve were based on the spectral distribution of sunlight as received in free space (10) and on figure 6 in this paper.

Appropriate factors obtained from figure 7 have to be applied to the limit conversion efficiency as well as to the actually obtainable conversion efficiencies for silicon solar cells, if these are to be made from thin films. These data therefore give valuable design information for the thin film solar cell development.

Another limitation is that of the crystallinity of the thin films. It is most improbable that any reasonable degree of conversion can be obtained in solar cells of the *p-n* junction type prepared from amorphous films or films of very small crystal size. It should however be possible to utilize so-called surface barriers or metal to semiconductor junctions in order to obtain a certain amount of conversion.

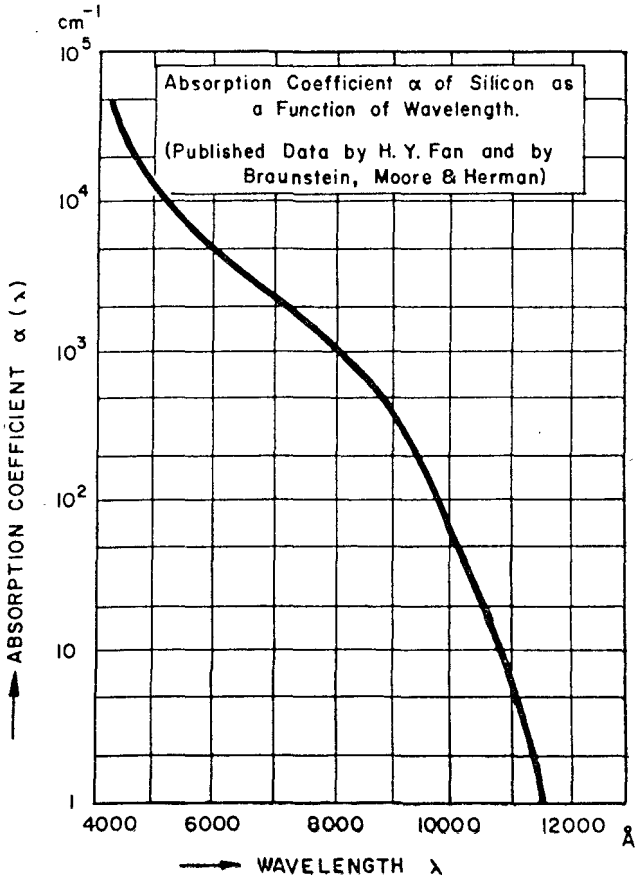


Figure 6

[1] Contract No. DA 36-039 SC-85242, dated 8-31-59, from the U.S. Army Signal Res. and Dev. Lab., Ft. Monmouth, New Jersey, to W. R. Grace and Co., Res. Div., Clarksville, Maryland.

[2] Contract No. AF 33(616)-6612 from Wright Air Dev. Div., Dayton, Ohio, to Westinghouse Electric Corporation, Pittsburgh, Pennsylvania.

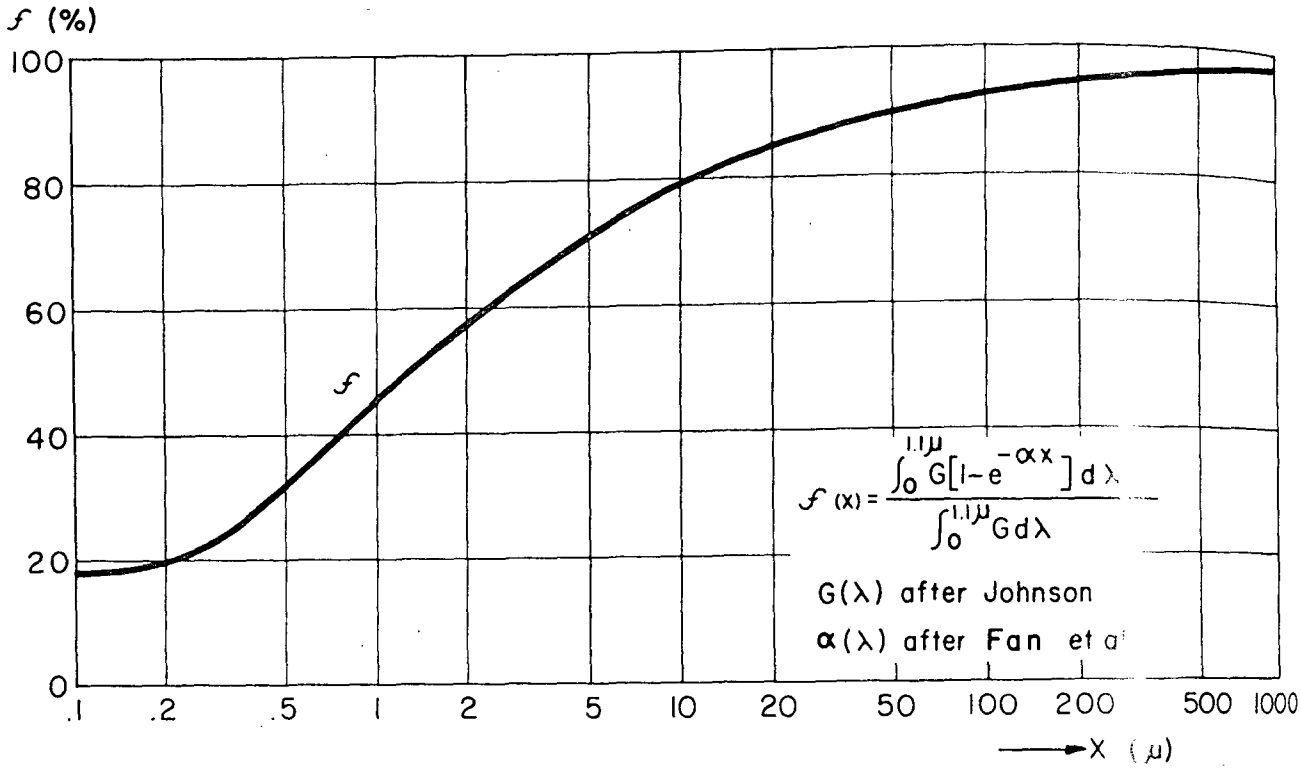


Figure 7

Another approach would be to obtain large crystal or even single crystalline thin films. Epitaxial growth and gradient cooling with seed attachment after melting or near melting of the film are two different approaches investigated for this purpose. Success has been met with certain epitaxial growth experiments using freshly etched silicon as a substrate.

Three different methods for the deposition of the silicon for the formation of the thin films have been or are presently under investigation. These three methods are : (*a*) vacuum deposition, (*b*) electrolytic plating, and (*c*) pyrolytic decomposition. Of these methods, only the last one has met with reasonable success in the past. One frequently used pyrolytic process consists of the decomposition of silane on heated substrates in a hydrogen atmosphere. Large crystallites could be deposited on various substrates, and single crystal films were grown on single crystal silicon substrates. *P-n* junctions exhibiting good

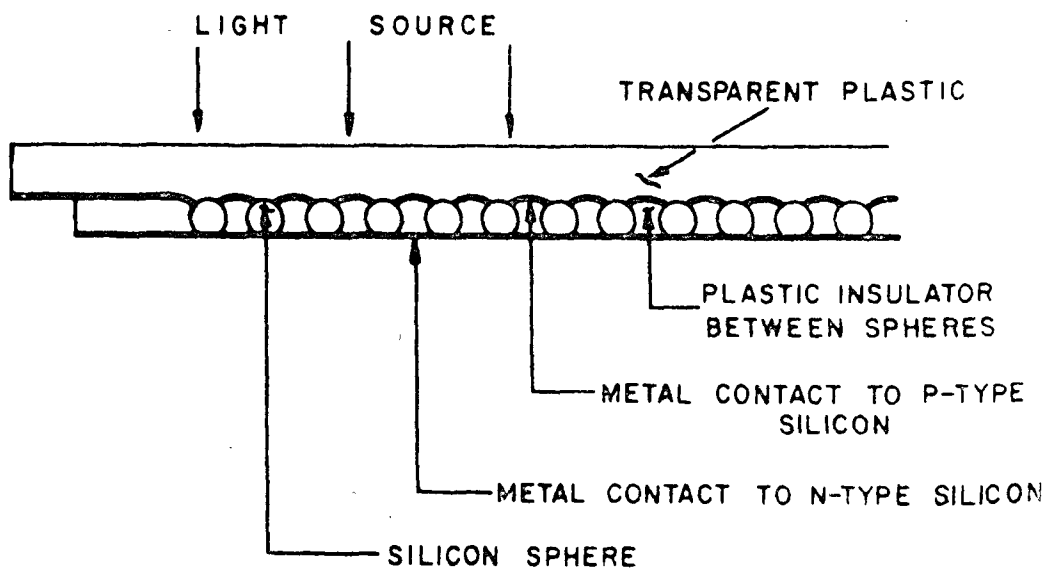


Figure 8. Cross-sectional view of large-area solar cell composed of silicon spheres

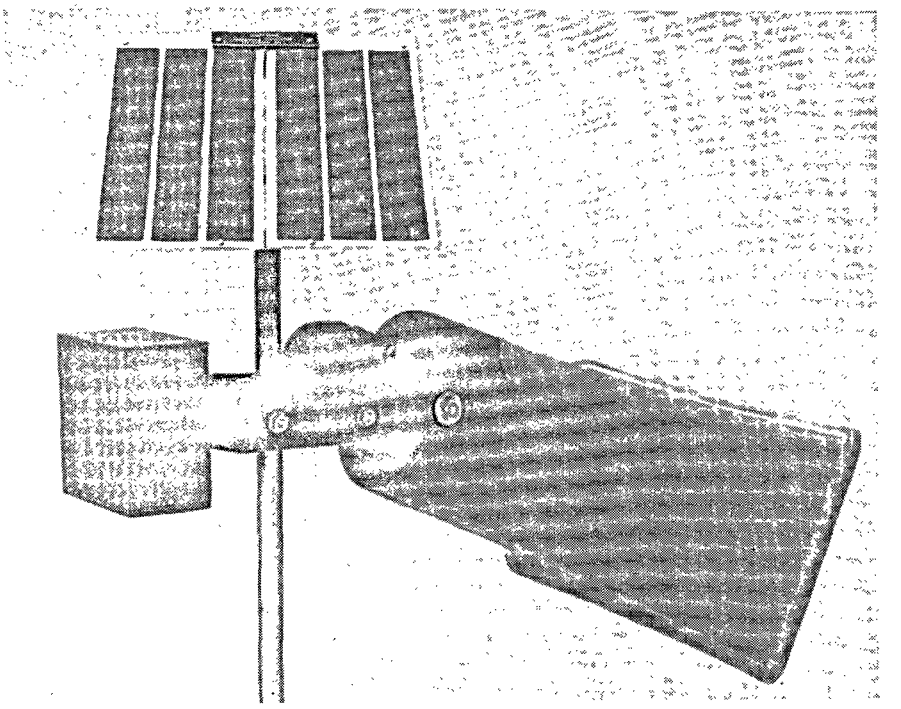


Figure 9

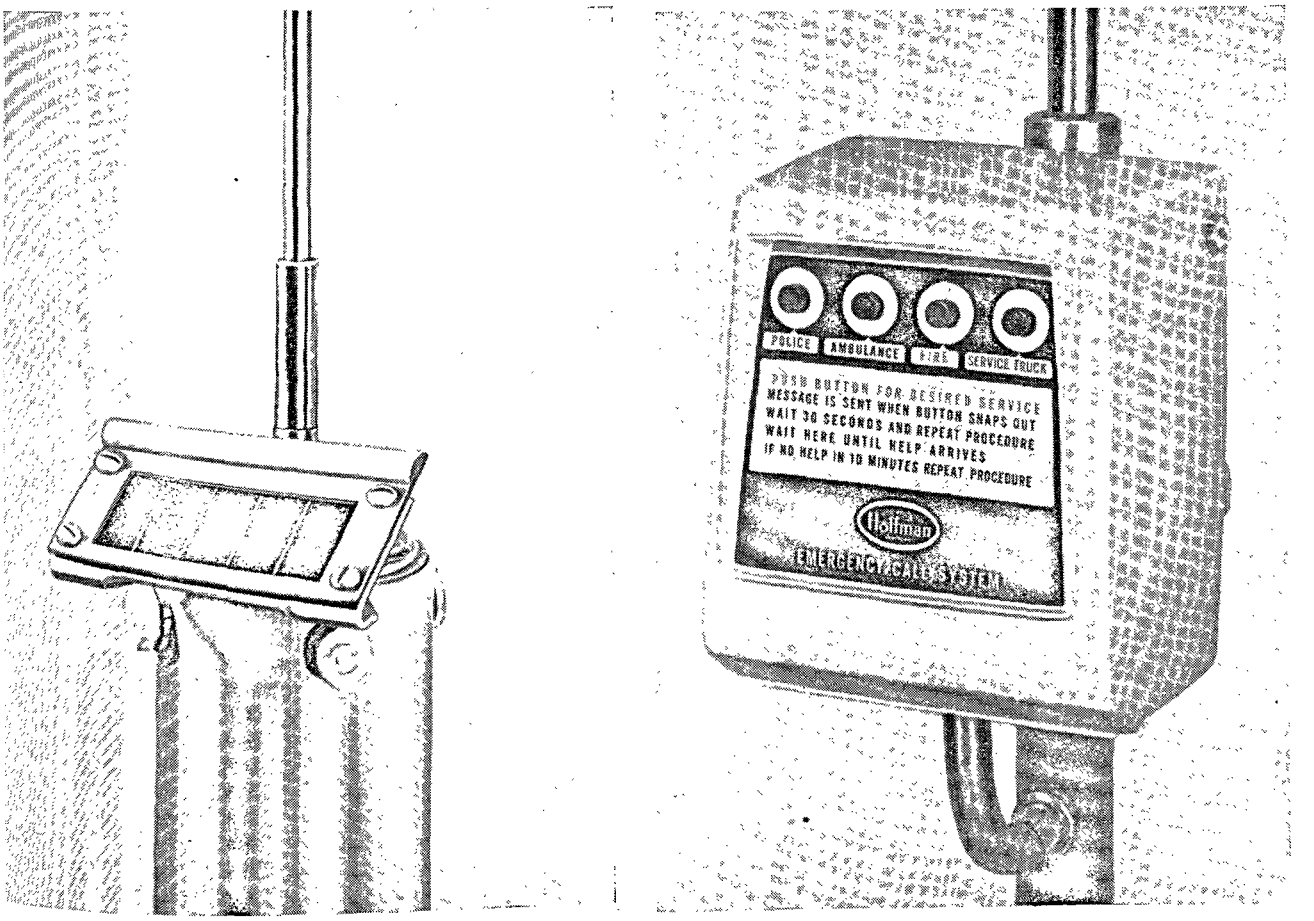


Figure 10

Figure 11

diode characteristics were formed by this method, and photovoltaic conversion was observed. This work is being pursued further.

Other approaches and materials

A quite different approach has been conceived and pursued at the Hoffman Electronics Corporation Semiconductor Division, and is to be continued. It consists of the preparation of an array of silicon spheres containing a *p-n* junction (figure 8). The major problem in this approach is the economical preparation of small silicon spheres.

Work on gallium arsenide solar cells, integrally composed variable solar cells, stacked variable energy gap solar cells, gallium telluride solar cells, and cadmium sulfide solar cells has been pursued, without promising results. The most promising of all of these approaches has been that of thin film cadmium sulfide solar cell activity, which is being pursued by the Harsham Chemical Company (11). Efficiencies as high as 4.5 per cent have been obtained in small areas of these films.

Developments in cost reduction

At the present time high efficiency silicon solar cells sell for approximately $175 per watt; that is, sufficient cells to produce one watt of electrical power on the earth's surface in bright sunlight are commercially sold for approximately $175. This figure compares with $275 per watt approximately one year ago and $500 per watt three years ago. It is estimated that these single crystal silicon solar cells could be produced in large quantities at a price of $100 per watt. It is for this reason that many organizations have directed considerable effort to developing lower efficiency, large area inexpensive solar cells. It has been estimated that for terrestrial use in areas that are inaccessible for electrical power, it will be necessary to reduce the cost per watt of electrical power from solar cells to approximately $20.

Applications

Finally, two applications that have shown considerable promise should be described briefly. These were both developed by the Hoffman Electronics Corporation. The first is entitled the Community Listening System. It consists of a panel (figure 9) of solar cells that maintain a charge on a battery which will operate a fixed station receiver with a large loudspeaker output. Such a system can be used in small villages, where electrical power is not available, for the purpose of educating the inhabitants. The second system is called the Safety Satellite System and can be used on highways for emergency calling. Figure 10 shows a small assembly of cells that again maintain a charge on a battery which will operate a transmitter. This transmitter is shown in figure 11 and can indicate to the receiver, which may be as far away as 25 kilometers, where one of four services are needed—police, ambulance, fire, or service truck.

Conclusion

A review of the work performed on photovoltaic solar energy conversion shows that certain problem areas have been encountered, but that efforts to overcome the difficulties are well under way. Beyond this, further improvements in the performance of the silicon solar cells have been achieved; these make better solar power panels feasible with up to 13 per cent conversion efficiency based on the total panel area. Work on other materials and on new approaches resulted in some interesting insights, but have not yet led to any improvement in performance or economy.

Acknowledgements

The author would like to acknowledge the assistance and work performed by others, both in his organization and in others. Much of the present paper has been taken from a paper presented by M. Wolf, Hoffman Electronics Corporation, 3 February 1961, at the Winter Convention of Military Electronics, Professional Group on Military Electronics, IRE, at Los Angeles, California. The grooded cell and spectral response improvements have been primarily the work of E. L. Ralph and Peter Iles.

Other major contributions in new ideas have been acknowledged in the references and footnotes. The two applications described at the end of the paper have been developed by Donald Bright of the Commercial Division of Hoffman Electronics Corporation.

References

1. Williams, R. and Bube, R. H., Photoemission in the Photovoltaic Effect in Cadmium Sulphide Crystals, *J. Appl. Phys.*, vol. 31, pp. 968-978, June 1960.
2. Prince, M. B., Silicon Solar Energy Converters, *Jour. Appl. Phys. 26*, 534-540, May 1955.
3. Loferski, J. J., Theoretical Considerations Governing the Choice of the Optimum Semiconductor for Photovoltaic Solar Energy Conversion, *Jour. Appl. Phys., 27*, pp. 777-784, July 1956.
4. Wolf, M. and Prince, M. B., New Developments in Silicon Photovoltaic Devices and Their Application in Electronics, published in *Solid State Physics in Electronics and Telecommunications*, Proceedings of an international conference held in Brussels, Belgium, 2-7 June 1958, vol. II, pp. 1180-1196, Academic Press, London and New York, 1960.
5. Prince, M. B. and Wolf, M., New Developments in Silicon Photovoltaic Devices, *Jour. of the British Inst. of Radio Eng., 18*, pp. 583-595, October 1958.

6. Wolf, M., Limitations and Possibilities for Improvement of Photovoltaic Solar Energy Converters, Part I, *Proc. IRE, 48,* pp. 1246-1263, July 1960.

7. Johnson, F. S., The Solar Constant, *J. of Meteorology, 11,* pp. 431-439, December 1954.

8. Rauschenbach, H., Understanding Solar Measurements, Part II, *Hoffman Semiconductor Product Application News,* May-June 1960, pp. 6-9, Hoffman Electronics Corporation, Semiconductor Division, El Monte, California.

9. Bosenberg, W., Kokillen Guss von duennen einkristallinen Germanium Platten, *Z.f. Angew. Phys. einschl. Nukleonik, 9,* pp. 347-349, No. 7, 1957.

10. Johnson, F. S., The Solar Constant, *Jour. Meteorology 11,* pp. 431-439, 1954.

11. Middleton, A. E., Gorski, D. A. and Shirland, F. A., Evaporated Cds Film Photovoltaic Cells for Solar Energy Conversion, *Paper 1291-60,* presented at the American Rocket Soc. Space Power System Conference, Santa Monica, California, 27-30 September 1960.

Summary

Silicon photovoltaic cells have been improved through basic scientific developments so that 12 to 14 per cent conversion efficiencies are obtained in production quantities of these devices. The major improvements have consisted in increasing the lifetime of bulk silicon, introducing gridding techniques for contacts, and reducing the thickness of the diffused layer.

Other developments for the purpose of reducing costs for photovoltaic conversion of solar energy include the investigation of thin film silicon cells, studies of other materials, and increasing the area of silicon solar cells. Comments are made concerning the cost of photovoltaic energy converters at present and in the near future, and two applications are described.

DERNIERS PROGRÈS RÉALISÉS DANS LE DOMAINE DE LA CONVERSION PHOTOVOLTAÏQUE DE L'ÉNERGIE SOLAIRE

Résumé

Les cellules photovoltaïques au silicium ont bénéficié de perfectionnements dus à diverses découvertes scientifiques théoriques, de telle sorte qu'on réalise des rendements de conversion compris entre 12 et 14 p. 100 lorsque ces dispositifs sont produits en quantités importantes. Les principales améliorations résident dans l'augmentation de la durée de vie utile du silicium en vrac, l'adoption de techniques de préparation de réseaux pour les contacts et la réduction de l'épaisseur de la couche diffusée.

Les autres progrès réalisés sur le plan de la réduction des frais pour la conversion photovoltaïque de l'énergie solaire comprennent des études sur les cellules au silicium à pellicule mince, des recherches sur d'autres matériaux et l'augmentation de la surface des cellules solaires au silicium. L'auteur examine la question du coût des convertisseurs d'énergie photovoltaïque dans le présent et pour le proche avenir, et donne la description de deux de leurs applications.

LOW-COST PHOTOVOLTAIC CONVERSION OF SOLAR ENERGY

P. Rappaport and H. I. Moss *

The purpose of this paper is to indicate how the photovoltaic effect (solar cells) can be used as an energy source in terrestrial applications especially for under-developed countries. Undoubtedly, the economists will be the final judges in this situation, and while the authors are not economic experts, it does seem to be an obvious fact that present-day devices are far too expensive for consideration as power sources in all but a few specialized applications. In the case of an artificial earth satellite, where the only long-term power source available is the silicon solar cell and where cost has not been of major importance, the solar cell has been eminently successful. For such applications it is estimated that the cost is about U.S. $1 000/watt.

Economics of solar cell power

Perhaps the ultimate in terrestrial use of solar energy is the production of power for ordinary home use. Consider a 1 000 square foot home in an area where 100 w/ft² of solar energy is available for an appreciable part of the year. If the sunlight striking such a roof were converted with 10 per cent efficiency, ten kW of electrical energy would be available. This, if suitably stored, would provide sufficient electricity for typical home use, including air conditioning when most needed. At present prices, the cost of silicon solar cells alone for such an installation would be over U.S. $1 000 000. This high cost is due to the requirement that the silicon be formed into single crystals before making the solar cells. If, on the other hand, solar cells could be made by evaporation, sputtering, settling or some other deposition technique not requiring the single crystal phase, there is no reason why the cell cost could not be reduced appreciably. Such techniques are used in many fabrication processes; they are quite inexpensive and have already yielded promising results for solar cells (1, 2).

If a large area deposited cell were made at the cost of U.S. $1-10 per square foot, the cost of the above-described roof might be as low as $1 000. Perhaps this would still be expensive for under-developed countries, but from the viewpoint of the house cost and the cost of electricity, it would be quite reasonable, even in parts of the United States. At the rate of $0.02/kWh and assuming a continuous average daily sunshine of 33 watts sq. ft., this unit would pay for itself in two years with a duty factor of 85 per cent and in ten years with a 15 per cent duty factor. The duty factor involves the number of sunless days and other losses that vary according to location on the earth. Certainly, in areas where sunshine is plentiful, such a device would be economically attractive. Other costs, such as electrical power storage and installation, are not included. Much work is going on in storage systems, and it is assumed here that advances will produce a suitably economic device (3).

State of the thin-film art

There have been a number of good review papers (4, 5, 6) on the subject of solar cells since the first

* RCA Laboratories, Princeton, New Jersey.

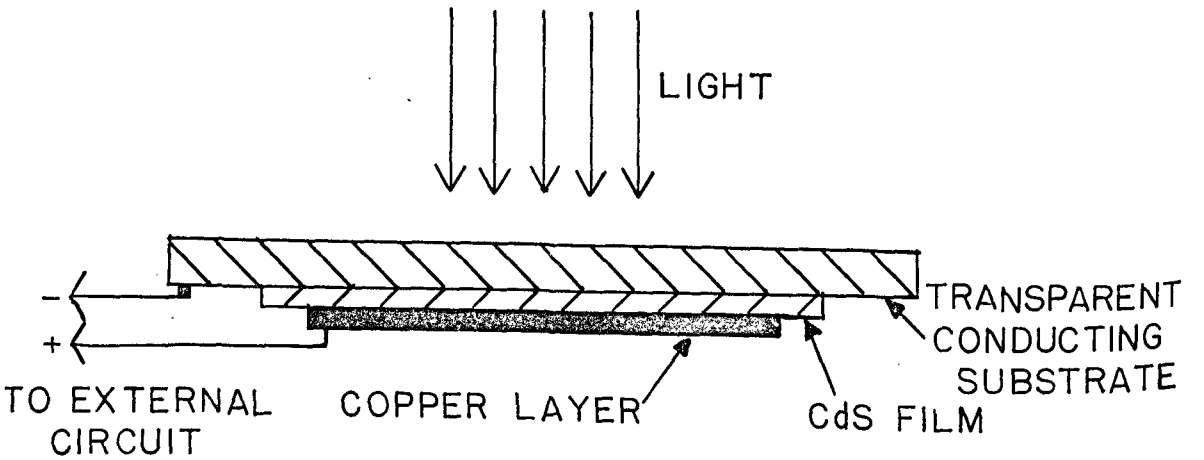


Figure 1. Geometry of CdS evaporated-layer photovoltaic cell

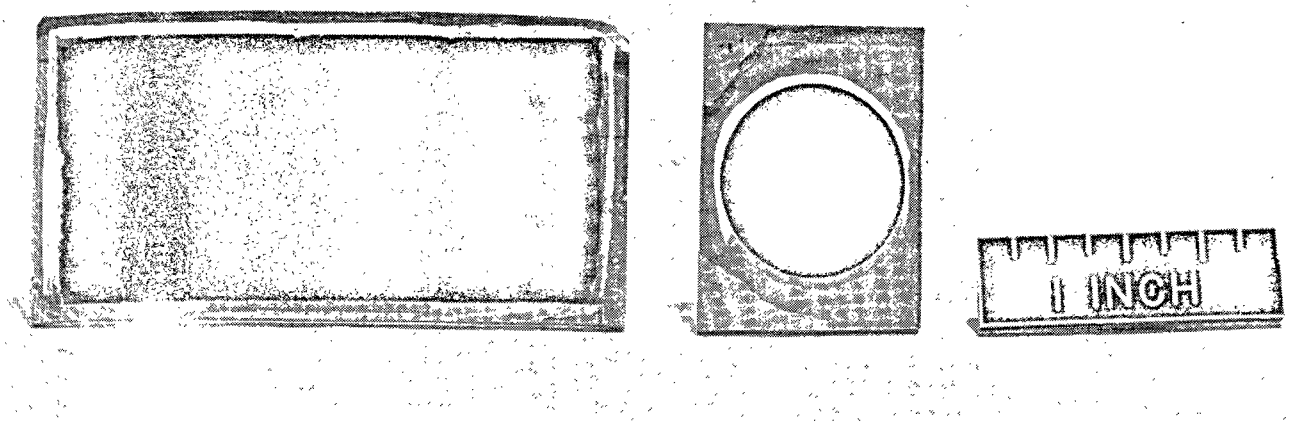


Figure 2. CdS thin-film photovoltaic cell

paper in 1954 by Chapin, Fuller and Pearson (7), and no attempt will be made here to further review the subject except as applicable to the present discussion. Table 1 shows a comparison of experimentally achieved solar energy conversion efficiencies of single crystal cells versus non-single crystal cells.

Table 1. Solar conversion efficiency for various semiconductors

Material	*Efficiency (%)*			
	Single crystal		*Non-single crystal*	
Silicon	14	(5)	10	(8)
Gallium arsenide . . .	10	(9)	—	
Cadmium sulfide . . .	8	(9)	3.5	(2)
Cadmium telluride . . .	4	(10)	< 1	(13)
Indium phosphide . . .	2	(4)	—	
Gallium phosphide . . .	1	(11)	—	
Selenium	—		1	(12)

It is seen that at the present time, the single crystal results are far superior. This is due to the fact that the great bulk of the work has been applied to single crystals because of the past emphasis on high efficiency. Although a small effort has been applied to polycrystalline films, some of the results achieved have been quite promising. Such film devices, besides being lower in cost, should also be lighter in weight (important for space applications) and more reliable because of the reduced number of connections inherent in large area panels as compared to 1 × 2 cm cells.

The work on single-crystal cells gives an upper limit to the efficiency that one might expect from a polycrystalline film. Thus it is reasonable to expect 10 per cent efficiency from a silicon deposition. The item in table 1 corresponding to the silicon non-single crystal cells was for a polycristalline cell made by Elliot *et al.* (8). In these cells, the grain size was about $\frac{1}{2}$ mm. This is larger than one would expect from a truly inexpensive deposition process like vacuum deposition or sputtering.

The essential properties that a thin film of a polycrystalline semi-conductor must possess to be applicable to photovoltaic-cell fabrication are as follows. In the case of a *p-n* junction cell, the thickness of the film must be great enough to absorb an appreciable amount of the photons having an energy greater than the band gap of the film material (8, 9, 14). Also, the carrier diffusion lengths must equal or exceed the film thickness. In the case of a polycrystalline layer, the minimum grain size must be at least equivalent to the film thickness. This insures that a carrier diffusing towards the junction will not be intercepted by a grain boundary and thus given an opportunity to recombine. In the case of a metal-semiconductor junction photovoltaic cell, the above requirements for a thin layer may not have to be as stringent as for a *p-n* junction device.

There have been a few reports in the literature before 1960 concerning the application of sintered or vacuum evaporated polycrystalline semiconductor films to photovoltaic cell fabrication. Some of the materials that have been investigated include cadmium sulfide (15), cadmium telluride (13), silicon (14), selenium (12), and certain organic semiconductors (16). The conversion efficiencies of these cells amounted to 1 per cent or less. Cast silicon cells have been made which are polycristalline with grain sizes of 5×10^{-2} cm and show efficiencies of about 10 per cent (8). An evaporated cadmium sulfide film photovoltaic cell exhibiting an efficiency of 3.5 per cent has been reported by Middleton, Gorski, and Shirland (2).

Experimental work on cadmium sulfide film cells

Cadmium sulfide layers were vacuum deposited onto heated conducting Pyrex substrates. The pres-

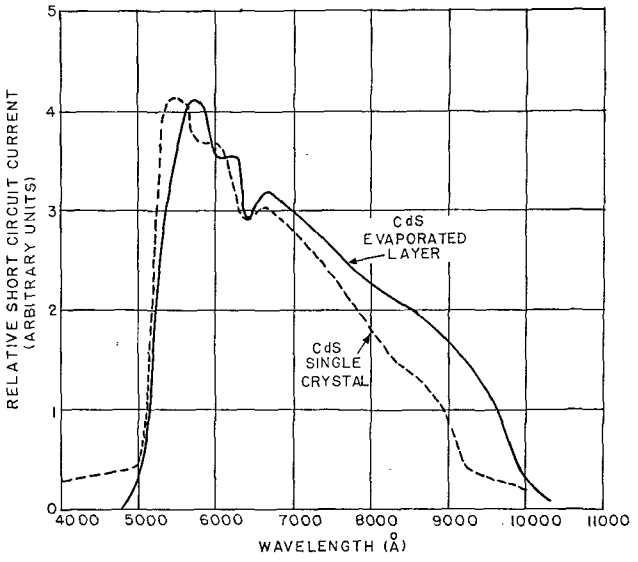


Figure 3. Spectral response of CdS-copper photovoltaic cells

sure during the evaporation was about 10^{-5} mm Hg. These layers were about 5-10 microns thick and were hard and adherent. Microscopic and x-ray diffraction studies revealed the layers to be microcrystalline and free from pin-holes. Their optical properties appeared to be very similar to cadmium sulfide single crystals. The evaporated layers without additional treatment are relatively conducting because of the presence of excess cadmium. The resistivity of these films could be as low as 1 to 10 ohm-cm.

Fabrication of the photovoltaic cell was completed by applying an opaque layer of copper to the exposed surface of the cadmium sulfide layer followed by a suitable heat treatment. The geometry of the finished cell is illustrated in figure 1. Electrical contacts to the cell were made on the copper layer and on the conducting substrate.

Back-wall illumination of these cells with an artificial light source equivalent to a sunlight radiation density of 92 milliwatts/cm^2 can produce open-circuit voltages up to 0.5 volt and short-circuit current densities up to 5 milliamperes/cm^2. Conversion efficiencies over 1 per cent are readily obtained. Cells with active areas up to 10 cm^2 have been fabricated; however, the highest efficiencies were obtained from cells with areas of about 1 cm^2.

Figure 2 shows a photograph of two typical experimental cadmium sulfide cells deposited on a glass substrate. Note that the glass is the top surface of the cell and that this provides protection and ease of cleaning.

Figure 3 shows the spectral response of a typical cell when illuminated with a Bausch and Lomb grating monochromator. The cell response has been normalized to take into consideration differences in the spectral intensity transmitted by the monochromator. This curve is similar to curves obtained from single-crystal cadmium sulfide-copper photovoltaic cells. The dashed curve in figure 3 is the spectral response of such a single-crystal cell, normalized so its maximum coincides with the maximum of the evaporated-layer cell.

References

1. Moss, H. I., Large-Area Thin-Film Photovoltaic Cells, *RCA Review, 22,* 29 (1961).
2. Middleton, A. E., Gorski, D. A. and Shirland, F. A., Evaporated CdS Film Photovoltaic Cells for Solar Energy Conversion. American Rocket Society Space Power Systems Conference, Santa Monica, California, 27-30 September, 1960, paper 1291-60.
3. Evans, G. E., Electrochemical Energy Storage for Intermittent Power Sources. *Proceedings of the United Nations Conference on New Sources of Energy,* 1961; included in vol. I [under agenda item II.D.2], paper GEN/3.
4. Rappaport, P., The Photovoltaic Effect and Its Utilization, *RCA Review, 20,* 373 (1959).
5. Wolf, M., Limitations and Possibilities for Improvements of Photovoltaic Solar Energy Converters, *Proc. IRE, 48,* 1246 (1960).
6. Pearson, G. L., Conversion of Solar to Electrical Energy, *Amer. Jour. Phys., 25,* 591 (1957).
7. Chapin, D. M., Fuller, C. S. and Pearson, G. L., A New Silicon P-N Junction Photocell for Converting Solar Radiation into Electrical Power, *Jour. Appl. Phys., 25,* 676 (1954).
8. Elliott, J. F., Meikleham, V. F. and Kolbe, C. L., Large Area Solar Cells. American Rocket Society Space Power Systems Conference, Santa Monica, California, 27-30 September 1960, paper 1290-60.
9. Cherry, W. R., Advanced Photovoltaic Devices. 14th Annual Power Sources Conference, Atlantic City, New Jersey, 17-19 May 1960.
10. Vodakov, Yu. A., Lomakina, G. A., Naumov, G. P. and Maslakovets, Yu. P., A P-N Junction Photocell made of CdTe, *Soviet Physics, Solid State,* vol. 2, No. 1, 1 (1960).
11. Wysocki, J. J., Loferski, J. J. and Rappaport, P., Research on Photovoltaic Converters. 14th Annual Power Sources Conference Proceedings, Atlantic City, New Jersey, 17-19 May 1960.
12. Zworykin, V. K. and Ramberg, E. G., *Photoelectricity* J. Wiley, New York, 1949.
13. Goldstein, B. and Pensak, L., High-Voltage Photovoltaic Effect, *Jour. Appl. Phys., 30,* 155 (1959).
14. Prince, M. B., Large Area Silicon Solar Cells. 14th Annual Power Sources Conference, Atlantic City, New Jersey, 17-19 May 1960.
15. Carlson, A., Shiozawa and Finegan. U.S. Patent No. 2 820 841.
16. Kearns, D. and Calvin, M., Photovoltaic Effect and Photoconductivity in Laminated Organic Systems, *Jour. Chem. Phys., 29,* 950 (1958).

Summary

Present-day solar cells are much too expensive to provide electrical power for everyday terrestrial applications. The major reason for this is the need to make single crystals. Solar cells that are made by a deposition technique from a suitable raw material would be inherently inexpensive. A cost of U.S. $1 to $10 per square foot of a 10 per cent efficient solar cell would probably bring the cost into the range of economic feasibility for home use. A practical and inexpensive cadmium sulfide solar cell that is 3.5 per cent efficient has been achieved. Such cells may be perfected to yield 6 per cent; however, with further research, other materials such as silicon may yield an inexpensive film-type cell with efficiencies approaching 10 per cent.

CONVERSION PHOTOVOLTAÏQUE DE L'ÉNERGIE SOLAIRE A PRIX MODIQUE

Résumé

Les cellules solaires modernes sont beaucoup trop coûteuses pour fournir de l'énergie électrique en vue des applications terrestres possibles de tous les jours. La principale raison de cet état de choses est le besoin de réaliser des cristaux isolés. Les cellules solaires construites au moyen d'une technique de dépôt appropriée, à partir d'une matière première également convenable, seraient intrinsèquement peu coûteuses. Un coût de 1 à 10 dollars des États-Unis par pied carré (10 à 100 dollars par m² ou à peu près) pour une cellule solaire ayant un rendement de 10 p. 100, ramènerait probablement son prix entre les limites de ce qui est économiquement faisable pour des applications ménagères. On a mis au point une technique permettant de réaliser des cellules solaires au sulfure de cadmium dont le rendement est de 3,5 p. 100. Il convient toutefois de noter qu'on peut les perfectionner pour arriver au rendement de 6 p. 100. Avec des recherches supplémentaires, d'autres matériaux tels que le silicium pourront donner des cellules peu coûteuses du genre à pellicule avec des rendements proches de 10 p. 100.

THIN FILM PHOTOVOLTAIC DEVICES FOR SOLAR ENERGY CONVERSION

Leonard E. Ravich *

While some interesting long-range possibilities exist for large-scale conversion of solar energy directly into electricity, most methods proposed for *low-cost* solar energy utilization by photovoltaic means have been limited by a series of complex, interdependent factors. The problem has been further compounded when the goal has been to provide useful energy conversion devices for under-developed countries. Large-area, low-cost photovoltaic cells and panels with high efficiency and reliability are required. Further, the devices must be simple to fabricate and maintain, must operate efficiently with unsophisticated solar concentrators and must maintain their characteristics even at relatively high temperatures. The purpose of this paper is to review briefly the theoretical and practical limitations of presently available solar cells and to describe a current research program whose objectives are to provide large-area, low-cost photovoltaic layers possessing the reliability and simplicity of fabrication and operation required for solar energy conversion devices designed for operation in less developed areas.

The large number of photovoltaic power sources that have been designed, constructed and used in space vehicles attest to their utility, efficiency and reliability. However, it is necessary to consider the economic factors involved in employing presently available solar cells in power conversion panels for use in less developed countries. Evans *et al.* (1) analyzed the economic factors in solar panel design and reported that the potential advantages of oriented systems lie in decreased panel weight, size and cost. As a rule of thumb, for intermediate and higher power ranges, randomly oriented systems will require four times as many solar cells as an oriented system and twice the panel weight. For a one kW power supply in earth orbit, this typically means the difference between 50 000 cells and 200 000 solar cells (1 × 2 cm), between a cost of U.S. $250 000 and $1 000 000 for cells, between 100 and 400 square feet of active mounting area and 200 lb or 400 lb panel and support weight. In the one kW case, an oriented system would therefore be considered essential. However, for a 100 watt power supply, the cell cost saving from orientation is reduced to about $60 000 and the weight saving to about 20 lb. Since the weight and cost of a reliable orientation system could easily exceed these bounds, the complexity and reduced reliability of the oriented system would dictate random orientation for small power systems and partial orientation for intermediate ones.

It would be ludicrous to suggest the use of such panels for power generation in under-developed areas. However, the need for economical, light-weight power sources ranging from a few milliwatts to a kilowatt or more is obvious. The problems of supplying large numbers of light weight single crystal solar cells (i.e., silicon) at low cost have reduced the possibility of substantial inroads into under-developed area markets where cost, weight and size are factors.

What characteristics should ideal solar cells have for use in low-cost solar energy conversion devices? They should be : (*a*) reliable, (*b*) simple to use and maintain, (*c*) made of inexpensive materials that do not require highly sophisticated purification techniques, (*d*) light-weight, and (*e*) flat or contoured as required. Further, the cells should be so simple to make that they could be fabricated with inexperienced help and low-cost equipment in the country in which they are to be used.

Large-area silicon cells

Various techniques for fabricating large area solar cells are under investigation. Elliot and Meikleham (2) reported on the fabrication of large area silicon solar cells. Because of the advanced state of development of silicon, this material was chosen as a basic material to be used in their investigations. They are investigating two techniques. One is large area thin film cells, and the other the mechanical deformation of silicon (i.e., rolling, extruding, forging, etc.) into large area thin sheets. Although they believe that the thin-film approach appears to be the most attractive as a long-range solution to the problem, the mechanical deformation of silicon is more straightforward and offers the possibility of a more immediate answer to the large area solar cell problem. The techniques for making the large area wrought silicon cells are still fairly complex and expensive. Either zone refined single crystal ingots or polycrystalline ingots are encased in a molybdenum jacket to provide a thermal mass and support material during the deformation process. The samples are heated to 1 300-1 350°C and then rolled. The molybdenum jacket is then removed by an oxidation process. After the sheet is cleaned, it is made into a cell using conventional techniques.

The fabrication of thin film silicon cells by other techniques has also been investigated. Teal *et al.* (3)

* Director, Physics and Chemistry Research Division, Itek Laboratories, Lexington, Massachusetts.

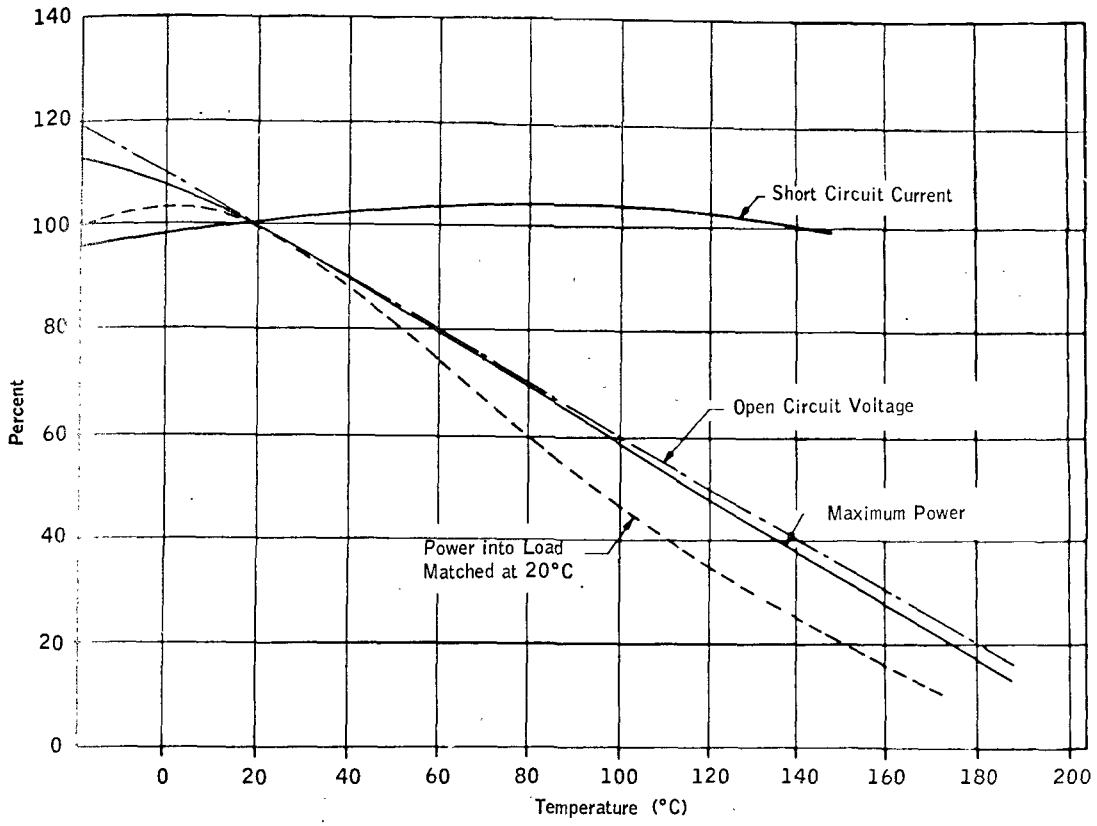


Figure 1. Relative thermal effects on open circuit voltage, short circuit current, maximum power, and power into a (roomtemperature) matched load for a typical silicon solar cell

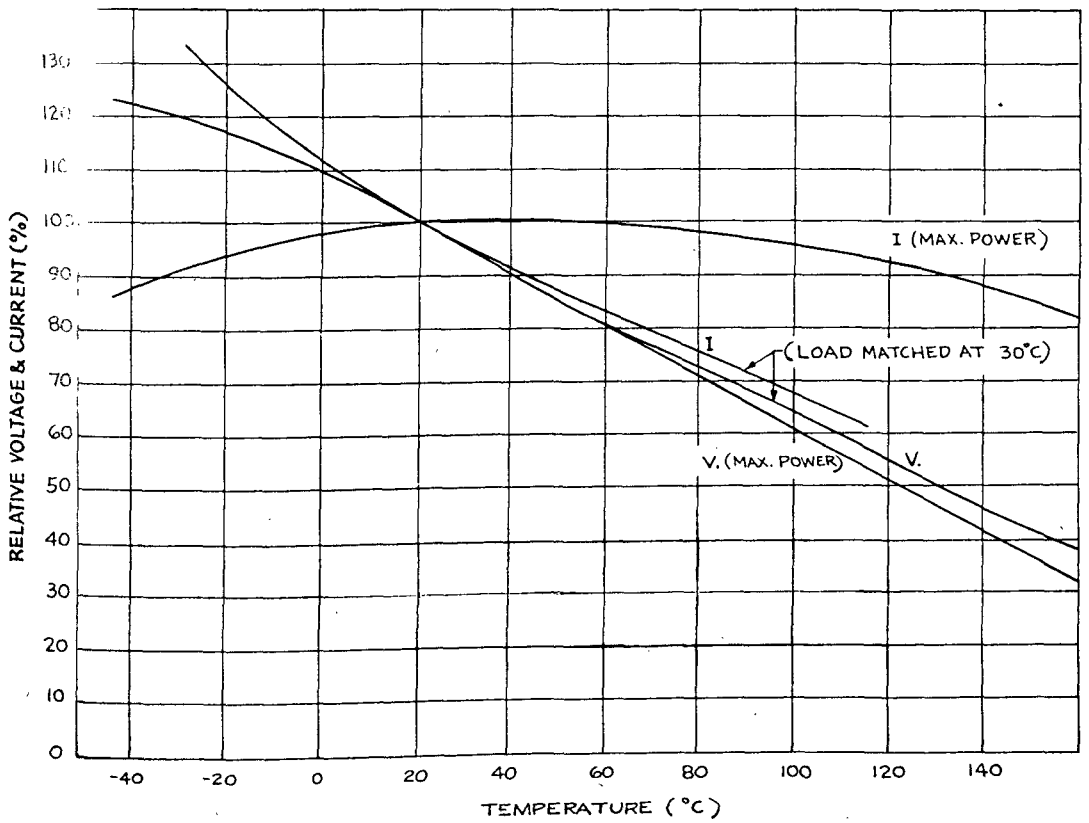


Figure 2. Relative thermal effects on voltage and current at maximum power and for load matched at 30°C

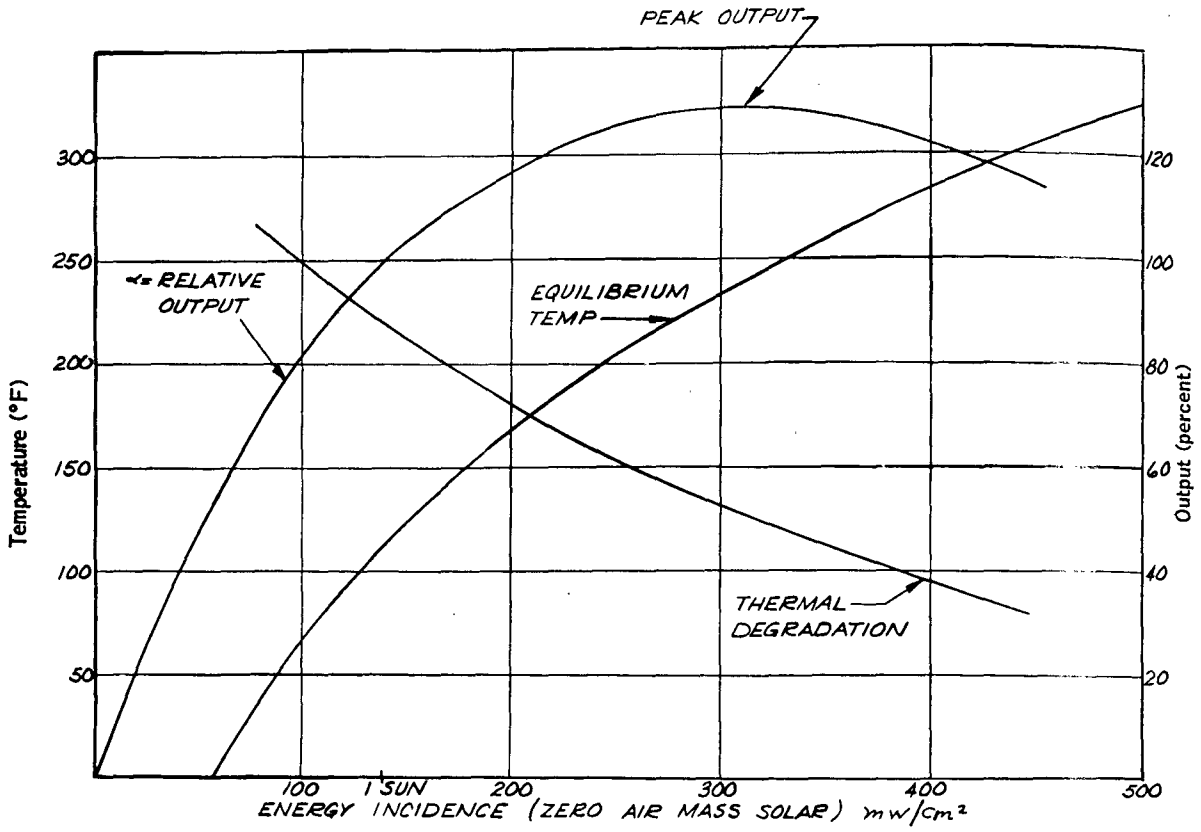


Figure 3. Equilibrium temperature, thermal degradation factor, and relative output of cell panel *vs.* energy incidence

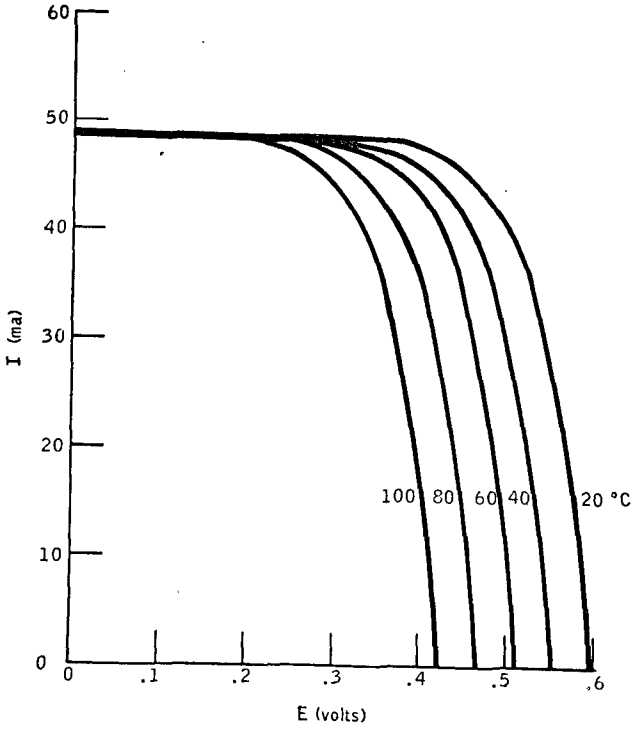


Figure 4. Temperature degradation of typical silicon solar cell

have reported on the deposition of silicon films by the reduction of silicon tetrachloride with hydrogen. The most satisfactory films were prepared on magnesium oxide substrates at 1 100°C.

Theoretically, there should be no limit to the size of a power supply that could be built with cells constructed as described above. However, assuming successful completion of present research programs, there will still be severe limitations imposed by the limited supply of silicon available and the specialized production capacity required to do the job.

Silicon solar cells may not be the most effective for solar energy conversion panels, even if the effective area could be substantially increased and the cost lowered to a favorable level. The concentration of incident solar energy onto large area photovoltaic cells will substantially increase the efficiency of the cells. At the same time, however, the concentration of solar energy onto the cells will also increase its temperature. The effect of temperature on silicon solar cells is dramatically illustrated by figures 1-4 (1). Figures 1 and 2 show the variation of specific cell parameters as a function of temperature. Although the effect of temperature on current is quite small, the rapid decrease of power, voltage and internal impedance with increasing temperature is significant. Figure 3 shows the thermal degradation effects

caused by solar radiation impinging on a silicon solar cell in zero air mass, and the effect of temperature on voltage and current characteristics of a typical p-n silicon cell is shown in figure 4. The temperature dependence of the material in the cells employed must, therefore, be an important consideration. A brief discussion of the mechanism of the photovoltaic effect may help in understanding the temperature problems associated with solar energy panels made up of photovoltaic cells and solar concentrators (4).

The photovoltaic effect

Upon irradiation of a photovoltaic layer, the electron minority carriers in the p-type portion of the layer move across the barrier, while the hole minority carriers in the n-type portion also move across the barrier. Together these comprise the current flow in a reverse direction of the barrier. If the junction is short circuited, the sum of these two currents is the observed short-circuit current i_s. With open circuit measurements, a voltage is built up across the junction just sufficient to counterbalance the current flow i_s. The difference between the location of the Fermi levels in the two portions of the material before contact V_{max} determines the maximum value which the open circuit voltage V_o can attain. Fan (5) reported that a p-n junction photo-voltage could be expressed by

$$V_o = \frac{kT}{e}\left[1n\left(\frac{n_p}{n_n}\right) - 1n\left(\frac{n_{po}}{n_{no}}\right)\right] \qquad [1]$$

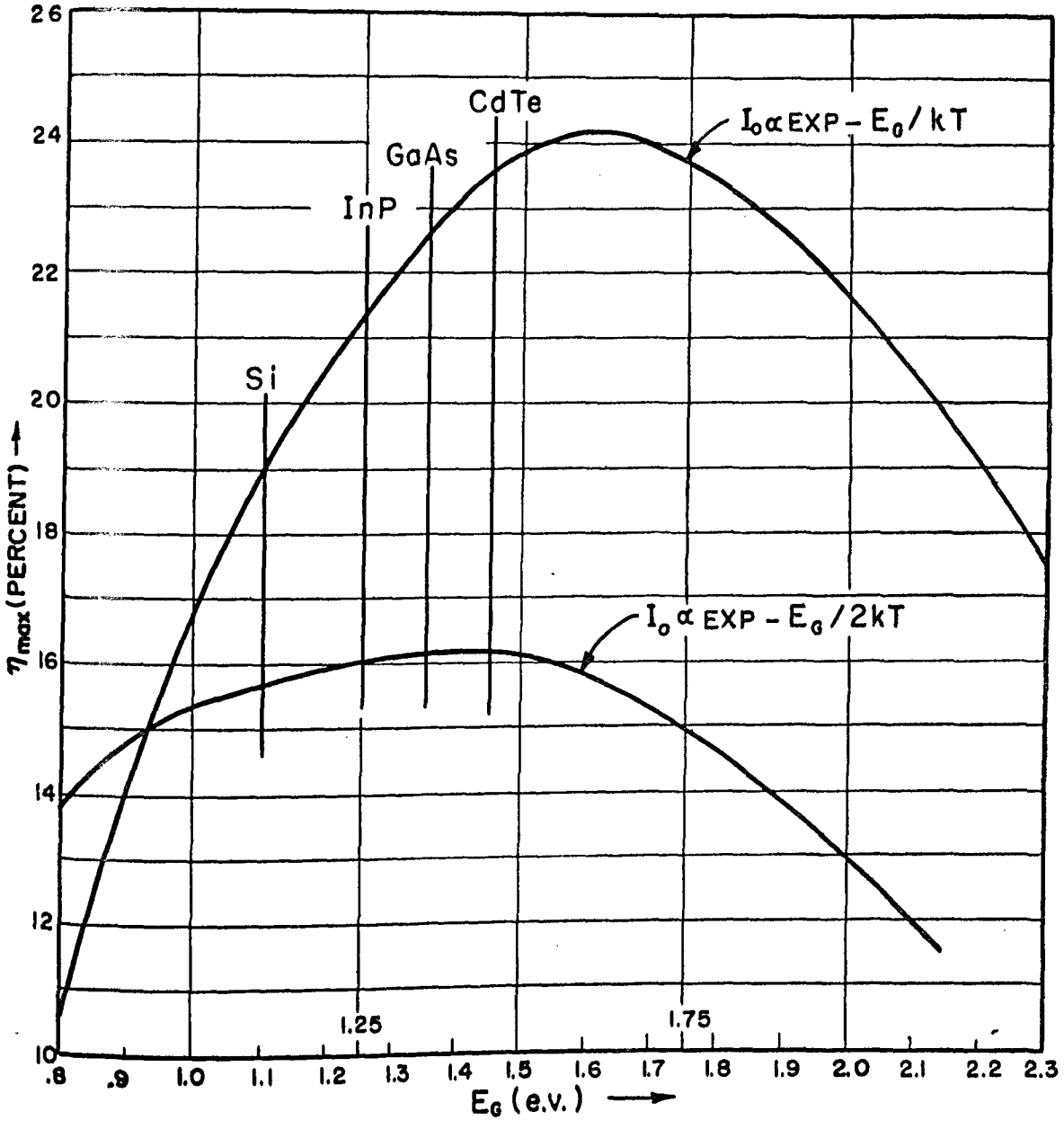


Figure 5. Theoretical efficiency *vs.* semiconductor band gap

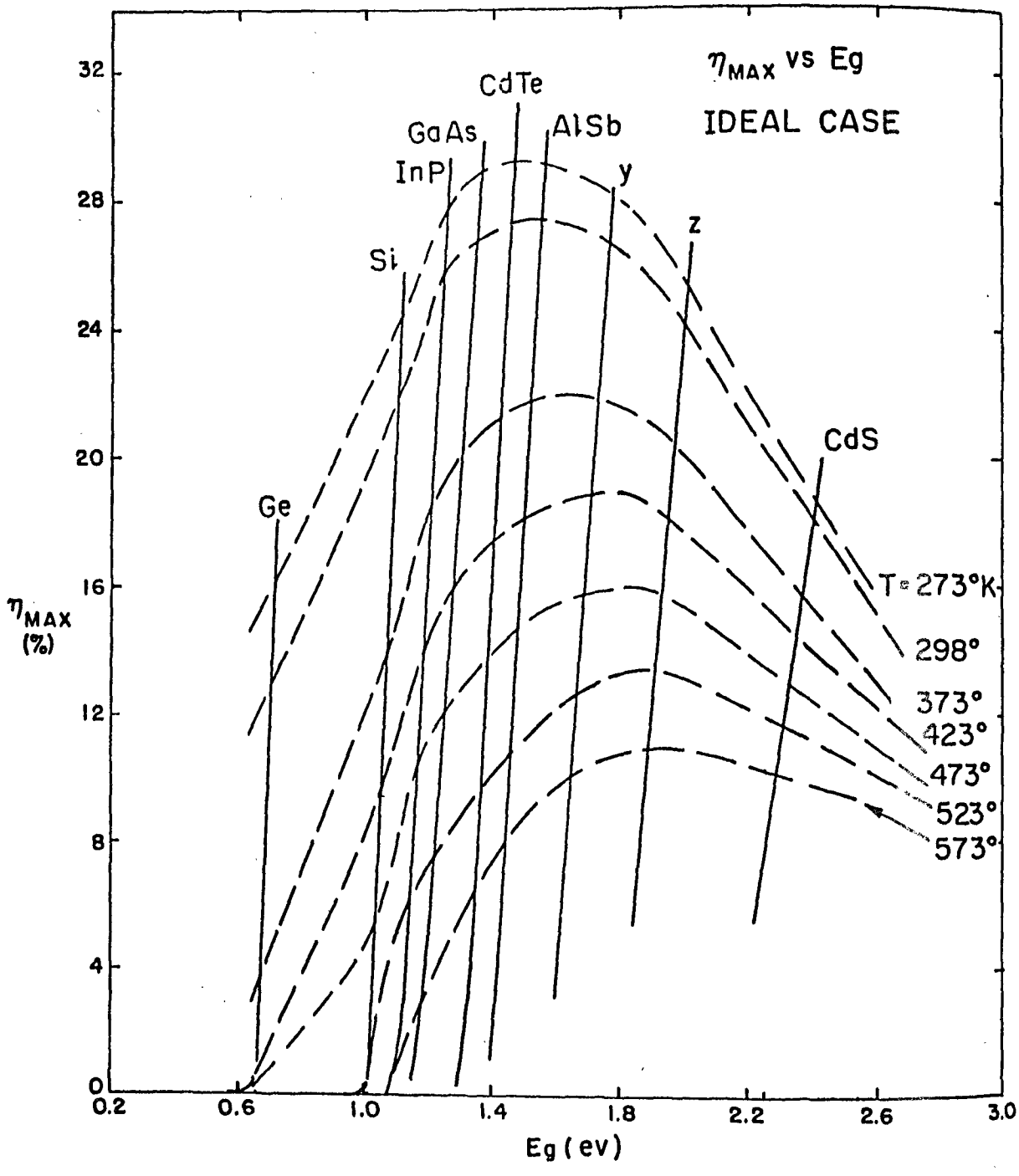


Figure 6. Efficiency *vs.* energy gap with temperature as a parameter

where :

n_{po} = concentration of minority carriers in the p-type material in the dark;

n_p = concentration of minority carriers in the p-type material under illumination;

n_{no} = concentration of minority carriers in the n-type material in the dark;

n_n = concentration of minority carriers in the n-type material under illumination.

For $n_{no} \approx n_n$, equation (1) above may be rewritten as:

$$V_o = \frac{kT}{e} 1n \left(1 + \frac{\Delta n_p}{n_{po}}\right) \qquad [2]$$

where :

$$\Delta n_p = n_p - n_{po}$$

This expression has been successfully applied to describe the photovoltaic effect in p-n junctions of germanium (6) and lead sulphide (7). If we let

$\lambda = e/kT$ and recognize that $\Delta n_p/n_{po} = i_s/i_o$, where i_o is the reverse saturation current in the absence of radiation, equation (2) above can be rewritten as :

$$\lambda V_o = 1 n \left(\frac{i_s}{i_o} + 1\right) \qquad [3]$$

This relationship is satisfied for p-n junctions in many materials, usually, however, the required value for λ to fit experimental data is less than e/kT. The photovoltaic effect for p-n junctions in CdS has been reported by Reynolds and Czyzak (8), Reynolds *et al.* (9), Nadyhakov and Andreichin (10) and Nadyhakov *et al.* (11).

The efficiency of the photovoltaic conversion of radiant energy to electricity is an important factor to consider in evaluating the optimum cell material for large area devices. Loferski and Rappaport (12) determine the maximum efficiency η_{max} with which this conversion can take place by :

$$\eta_{max} = (1 - R)(1 - T)\, e\, \frac{V_{mp}}{E_{avg}}\, \frac{n_{ph}(E_G)}{N_{ph}} \qquad [4]$$

where :

R = reflection coefficient;
T = transmission coefficient;
V_{mp} = voltage at maximum power;
E_{avg} = average energy of incident photons;
$n_{ph}(E_G)$ = the number of photons incident on the junction per unit time with sufficient energy to create hole-electron pairs;
N_{pn} = the total number of photons incident on the junction per unit time.

The value of λV_{mp} is given by :

$$e\lambda V_{mp}(1 + V_{mp}) = \frac{i_s}{i_o} + 1 \qquad [5]$$

Loferski (13), Rittner (14), Cummerow (15) and Pfann and van Roosbroeck (16) have all presented theoretical analyses of the materials most suited for the photovoltaic conversion of solar energy into electricity. They all agree that the optimum material must have as small a band gap as possible to utilize the major portion of the solar spectrum. Concurrently, the optimum material must also have as large a band gap as possible to minimize the magnitude of the reverse current i_o. Their calculations indicate that the optimum band gap lies between 1.2 and 1.6 ev. The possibility that $\lambda < e/kT$ broadens this range to about 1.2-2.0 ev. Figures 5 and 6 show curves derived by Loferski (17) indicating the materials showing most promise to date. According to the results of his analysis, semiconductors with energy-gap values larger than silicon (1.1 ev) and less than 2.0 ev should be able to achieve solar energy conversion efficiencies greater than silicon. Queisser (18) used thermodynamic principles to calculate the "ultimate efficiency" of solar cells. He postulates that the best possible energy conversion would result if every solar photon with energy higher than the gap created one hole-electron pair at gap voltage. Figure 7 shows

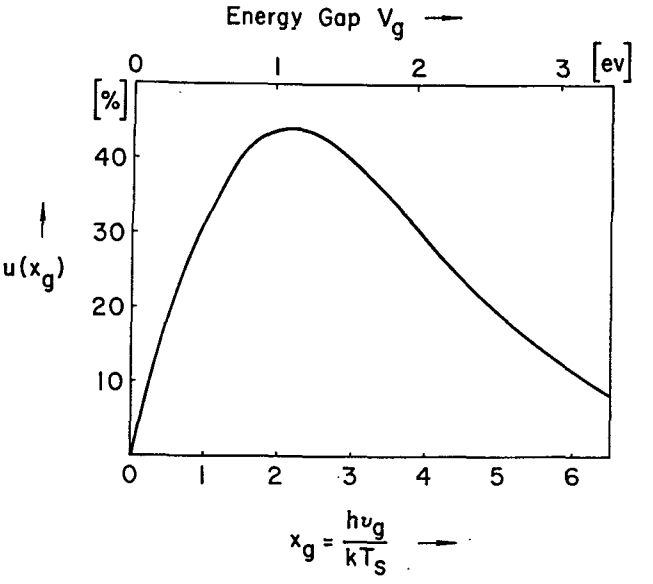


Figure 7. "Ultimate efficiency" of theoretical solar cell (cell at T = °K, irradiated by the sun, a black body of 6 000°K)

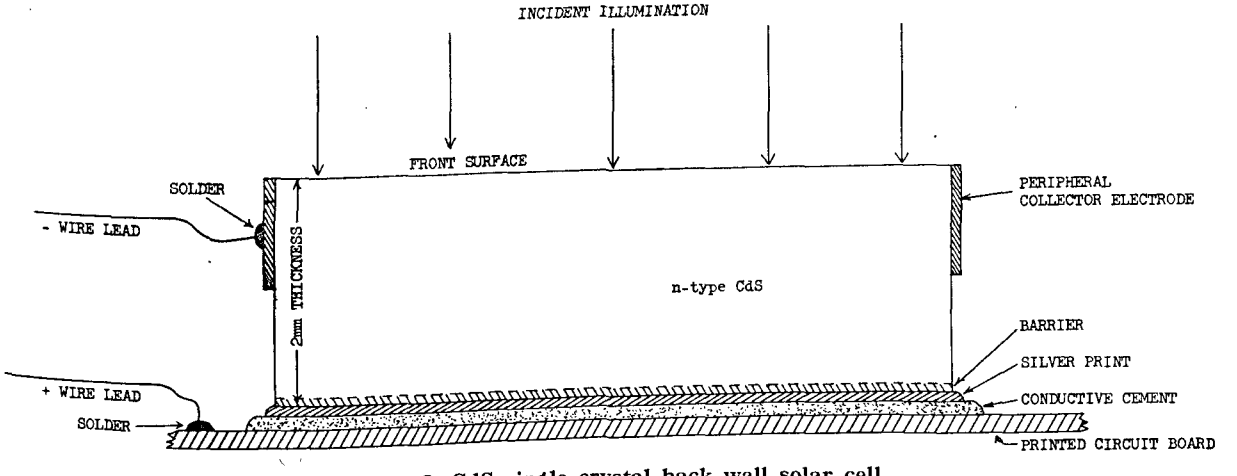


Figure 8. CdS single crystal back-wall solar cell

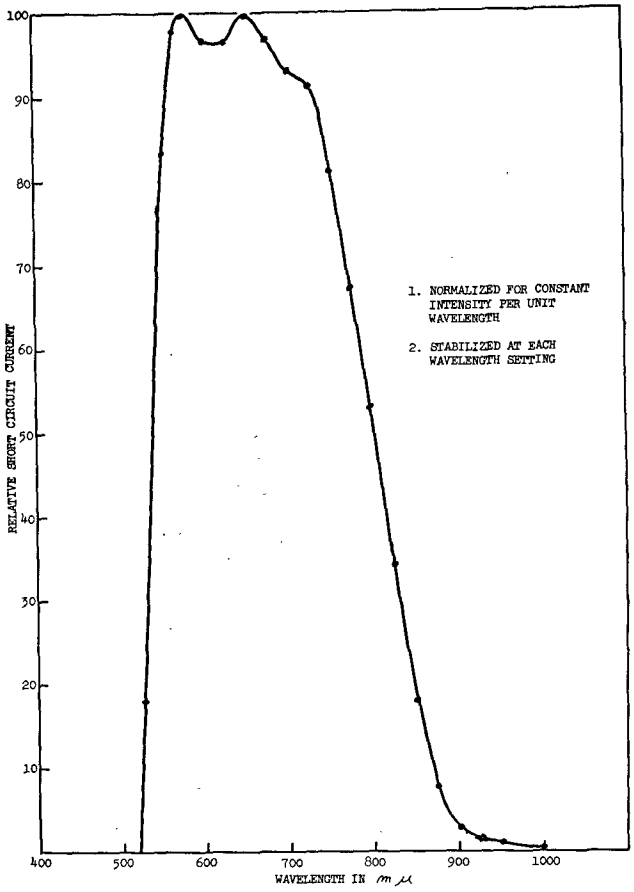


Figure 9. Photovoltaic response of CdS single-crystal cell

graphically this "ultimate efficiency" and its dependence upon the energy gap. However, please note that this case corresponds to a cell at $T = 0°K$, irradiated by the sun, thought to be a black body of 6 000°K. As soon as we have "non-zero temperatures", not all hole-electron pairs can be extracted from the load, even in principle. The higher the temperature, the lower the efficiency, particularly with small energy-gap semiconductors.

Thus, a most important factor in the choice of a semiconductor for solar energy conversion is its operating characteristic as a function of *temperature*. Loferski (17) concludes that GaAS, for example, would be superior to Si at elevated temperatures and that it could be used at temperatures above 150°C. In addition to the obvious advantage of high temperature operation, cells made from large energy-gap semiconductors should be used in systems where the solar radiation is concentrated onto large area photovoltaic cells. The increased radiant energy input would certainly increase the cell operating temperature.

Single crystal CdS photovoltaic cells

Table 1 (19) shows the energy-gaps of a few semiconductor materials that have been investigated for photovoltaic solar energy conversion. Cadmium sulfide, with an energy-gap of 2.4 ev and a reported maximum efficiency of 5-6 per cent should provide an ideal material for photovoltaic cells designed for high temperature operation. Reynolds *et al.* (20) discussed the possibility of using single CdS crystals for photovoltaic cells as early as 1954. Hammond and Shirland (21) described single crystal photovoltaic cells made with copper oxide barriers. In their technique, an opaque, black copper oxide barrier layer is applied to a slice of a single crystal cadmium sulfide ingot which is then suitably mounted to provide a photovoltaic cell (figure 8). Solar energy impinging on the cell is transmitted to the opaque barrier at the back side of the cell where it is absorbed and converted to electrical energy. These "back wall" cells (as opposed to "front wall" for the cell configuration providing the conversion of light into electrical energy by absorption near the incident surface followed by the diffusion of charge carriers to a barrier near this incident surface) were difficult to produce because of the many problems involved in: (*a*) large CdS single crystal ingot production; (*b*) cutting uniform thin wafers from the ingot; (*c*) making large area solar cells; and (*d*) producing functional cells with minimum weight and volume.

The photovoltaic response of a typical single-crystal "back wall" cell is shown in figure 9 (19). The authors conclude that the response indicated supports the muti-level transition and variable gap transition mechanisms as being responsible for the CdS cell's conversion of solar to electrical energy.

Thin film CdS "back wall" photovoltaic cells

Middleton *et al.* (19) reported that they could replace the CdS single crystal slab by an evaporated

Table 1. Comparison of some solar cells

Material	*Material form*	*Type of junction*	*Surface on which solar energy is incident*	*Reported max. eff.*	*Energy gap of the material*
Si	Single crystal	Diffused *p-n*	Front wall	14-15 %	1.1 ev
GaAs	Single crystal	Diffused *p-n*	Front wall	7 %	1.35 ev
CdS	Single crystal	Unknown, complex	Back wall	5-6 %	2.4 ev
Se	Polycrystal	Metal-insulator-semi-conductor	Front wall	1 %	2.2 ev
Cu_2O	Polycrystal	Semi-conductor-insulator-metal	Back wall	Approx. 0.5 %	2.1 ev

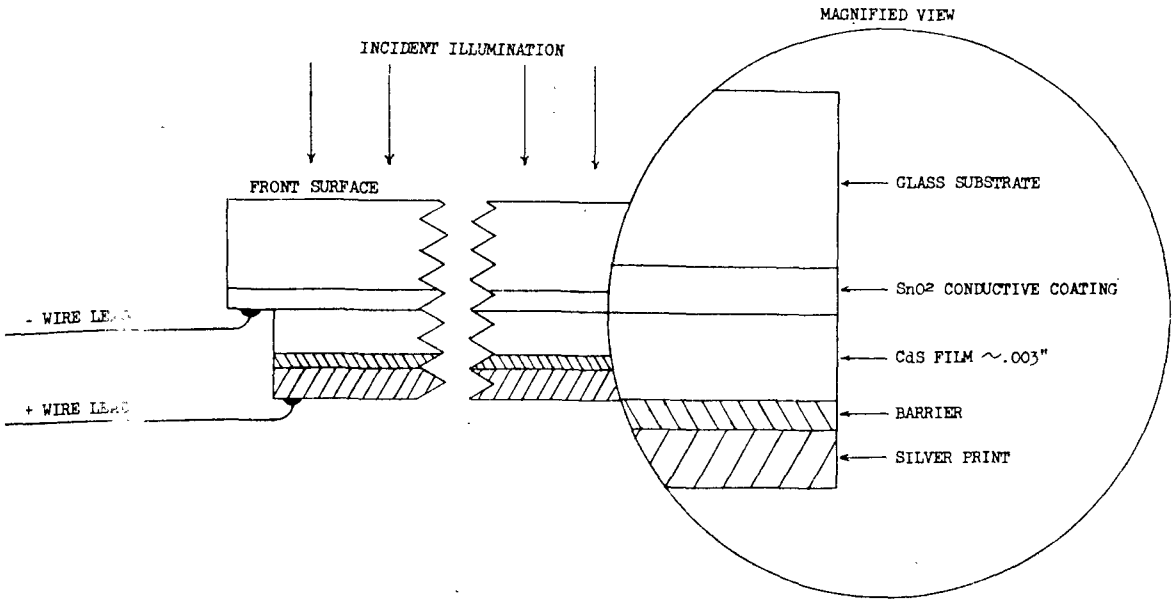


Figure 10. CdS film back-wall solar cell

CdS polycrystalline layer without changing the nature of the photovoltaic conversion. They evaporated indium chloride doped CdS crystal chips onto glass substrates at temperatures between 75°C and 350°C. They used lightly frosted glass substrates to improve adherence of the layer. A transparent conducting tin oxide film was deposited on the glass prior to CdS deposition. The barrier layer was prepared by electroplating copper at high current density on the top of the CdS polycrystalline layer to produce a black mossy-like plating. The finely divided copper was then oxidized by exposure to air at 275°C for about 10 seconds. After oxidation, conducting silver paint was applied to the copper-treated surface to complete the cell (figure 10). Figure 11 (19) shows the spectral response of the film cell compared to that for a single crystal. It is interesting to note that the response range (0.515 to 0.95 microns) and the shape of the two response curves are similar.

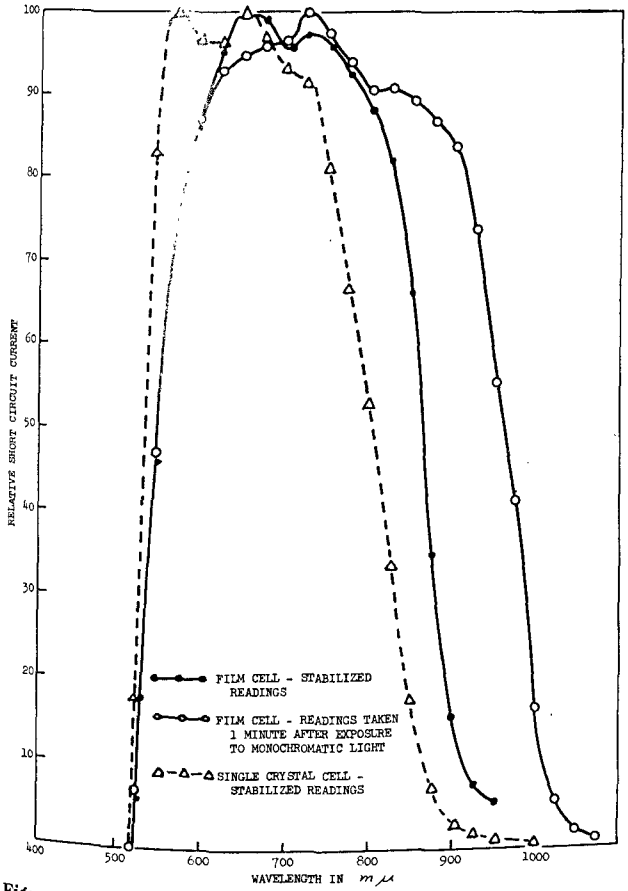


Figure 11. Comparison of photovoltaic spectral response of CdS film cells obtained with and without stabilization

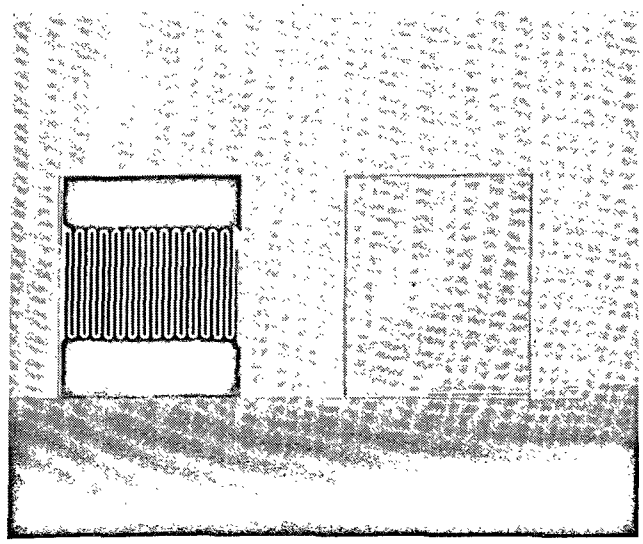


Figure 12. Conductive layers on Pyrex solar cell base plates; gold "comb" electrode (left) and transparent tin oxide-gold layer (right)

Thin film CdS "transparent" photovoltaic cells

Neither the photovoltaic cells available commercially nor the experimental photovoltaic cells disclosed in the numerous papers published to date have been notably suited for use in low-cost solar energy conversion devices of interest to underdeveloped areas. The physics group at Itek Laboratories set out to develop a cell that would meet the minimal requirements for a low-cost, rugged cell. The cell specifications included the following:

(*a*) The starting material had to be inexpensive and easy to obtain;

(*b*) The cell had to be fabricated with standard vacuum equipment and with techniques that could be taught to relatively unskilled persons;

(*c*) The cell had to operate effectively with no mechanical orientation system or optical collector or, at most, with a simple sheet metal or foil collector;

(*d*) The cell had to operate effectively over a wide temperature range and have a broad spectral response;

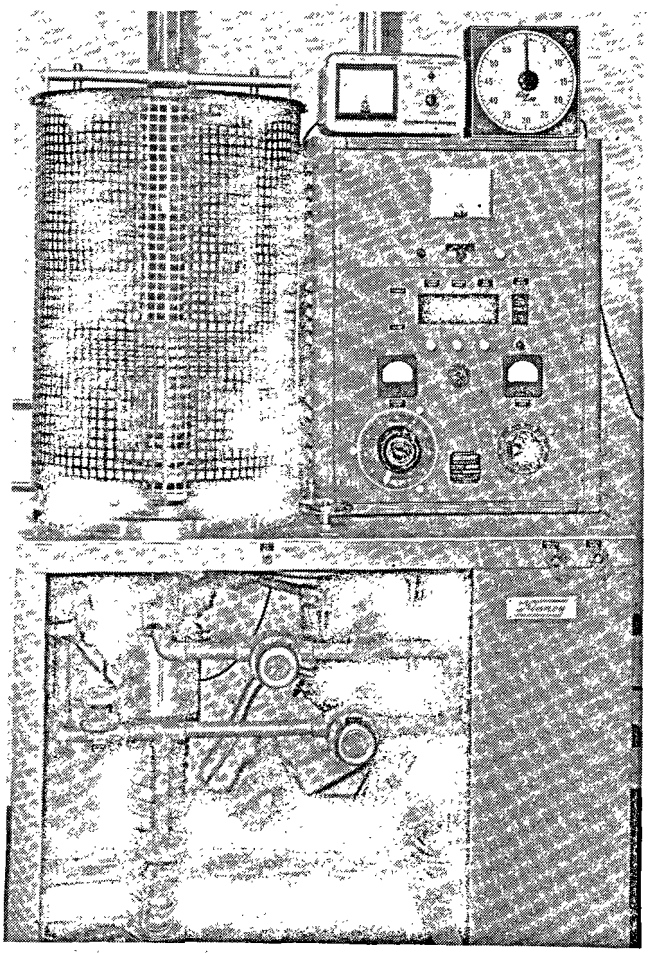


Figure 13. Vacuum apparatus used for preparing thin film photovoltaic layers showing pumps, bell jar and controls

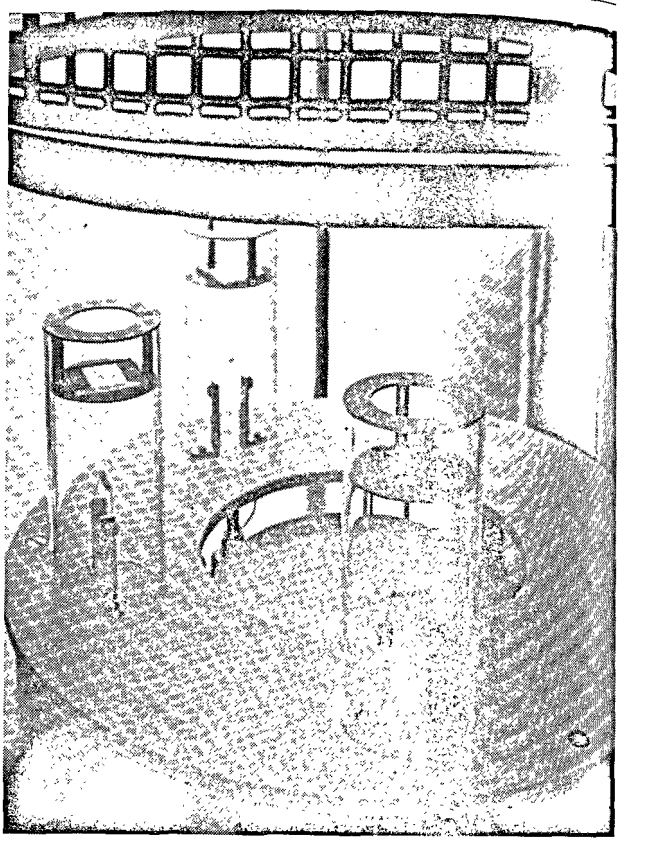


Figure 14. Close-up view of vacuum bell jar showing cell fabrication chambers with plate holders and molybdenum support coils

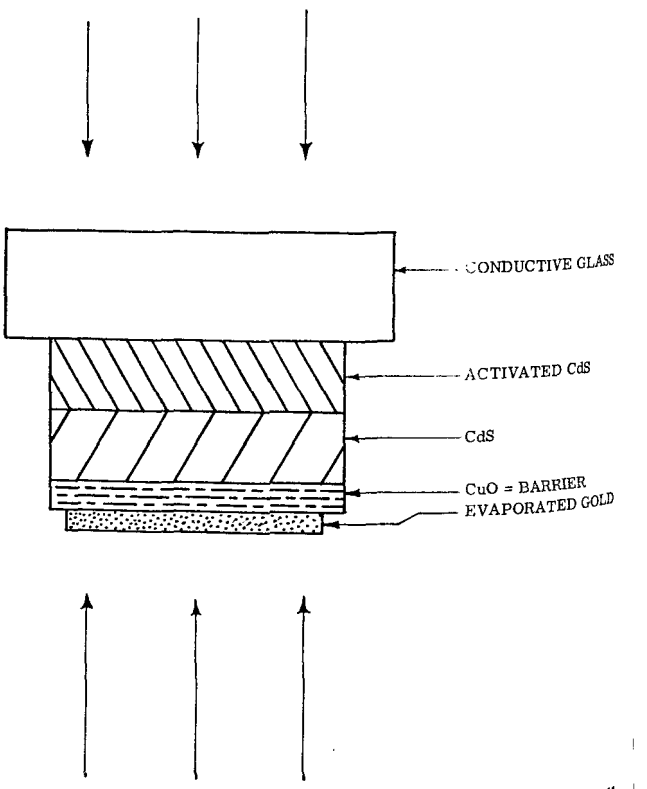


Figure 15. CdS-film back and front wall photo voltaic cell

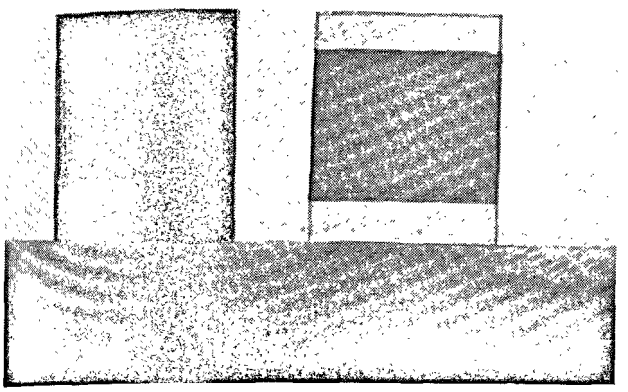


Figure 16. CdS thin film solar cells : gold "comb" electrode cell (left); transparent electrode cell (right)

(e) The cell had to be rugged, withstand a wide variety of environmental conditions with a minimum amount of protection.

Under the direction of Miss Ilse Abrahamsohn, the Thin Film Research Section at Itek Laboratories has developed new and novel evaporated CdS photocells having characteristics markedly different from those reported heretofore and meeting many of the specifications outlined above. The multilayer, transparent photovoltaic cells are relatively simple to make, have good efficiencies and exhibit spectral response characteristics not anticipated by theoretical mechanisms heretofore published.

CdS powder containing a donor impurity is evaporated from one or more molybdenum supports onto a smooth Pyrex glass plate. Two types of conductive substrates have been used : a tin oxide layer containing a small amount of gold is applied to the plate before the CdS evaporation or a metallic gold "comb" electrode is applied by photo-etching (figure 12). The tin oxide-gold layer is preferable for the Itek cells because it will transmit 90 per cent of incident radiation as compared with 50 per cent mission for the gold "comb" electrode. This high radiant energy transmission, coupled with the transparent photovoltaic layers made as described below, provides cells that approach optimum photovoltaic conversion efficiency.

The evaporation of the CdS film is carried out in a modified commercial diffusion pump bell-jar unit (figures 13 and 14) at a pressure of 5×10^{-6} mm. Hg for about 30 minutes. The coated plate is baked in air at 600°C for 45 minutes, cooled slowly to 200°C and returned to the bell-jar. A second and third (if desired) CdS film is deposited over the first one with an air bake as described above between each deposition. The number of layers applied is determined by the layer thickness desired. A small amount of acceptor impurity is incorporated into the CdS powder used for the final layer.

After the required number of doped CdS layers are applied to the glass substrate and the final baking has taken place, a thin copper layer is vacuum deposited onto CdS. The plate is then baked in air at 400°C for 15 minutes to form a *transparent* Cu-oxide barrier layer. The cell is completed by vacuum depositing a thin transparent gold film over the copper oxide layer as the top electrode (figures 15, 16 and 17).

The optimum thickness for the multilayer cell has been determined to be 10-20 μ. Thinner films have low sensitivity and it is difficult to control the diffusion of the copper oxide barrier layer. Further, thin layers often have "pin-holes" that cause shorting of the cell.

The donor and acceptor impurities introduced into the CdS film determine the spectral response

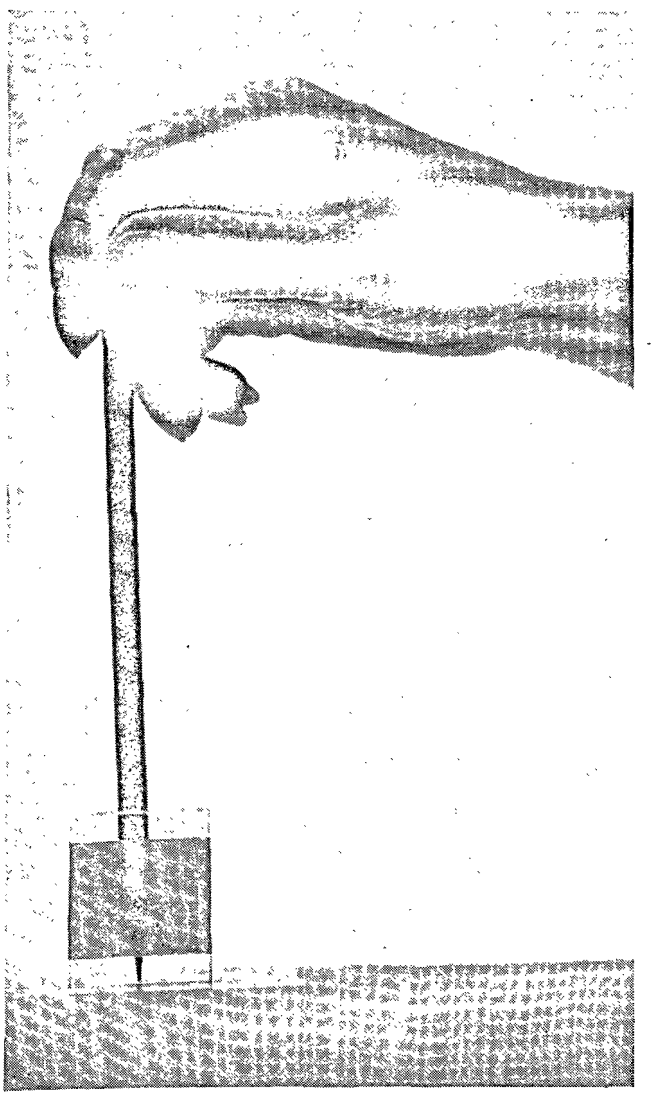


Figure 17. Close-up view of CdS solar cell showing relative light transmission

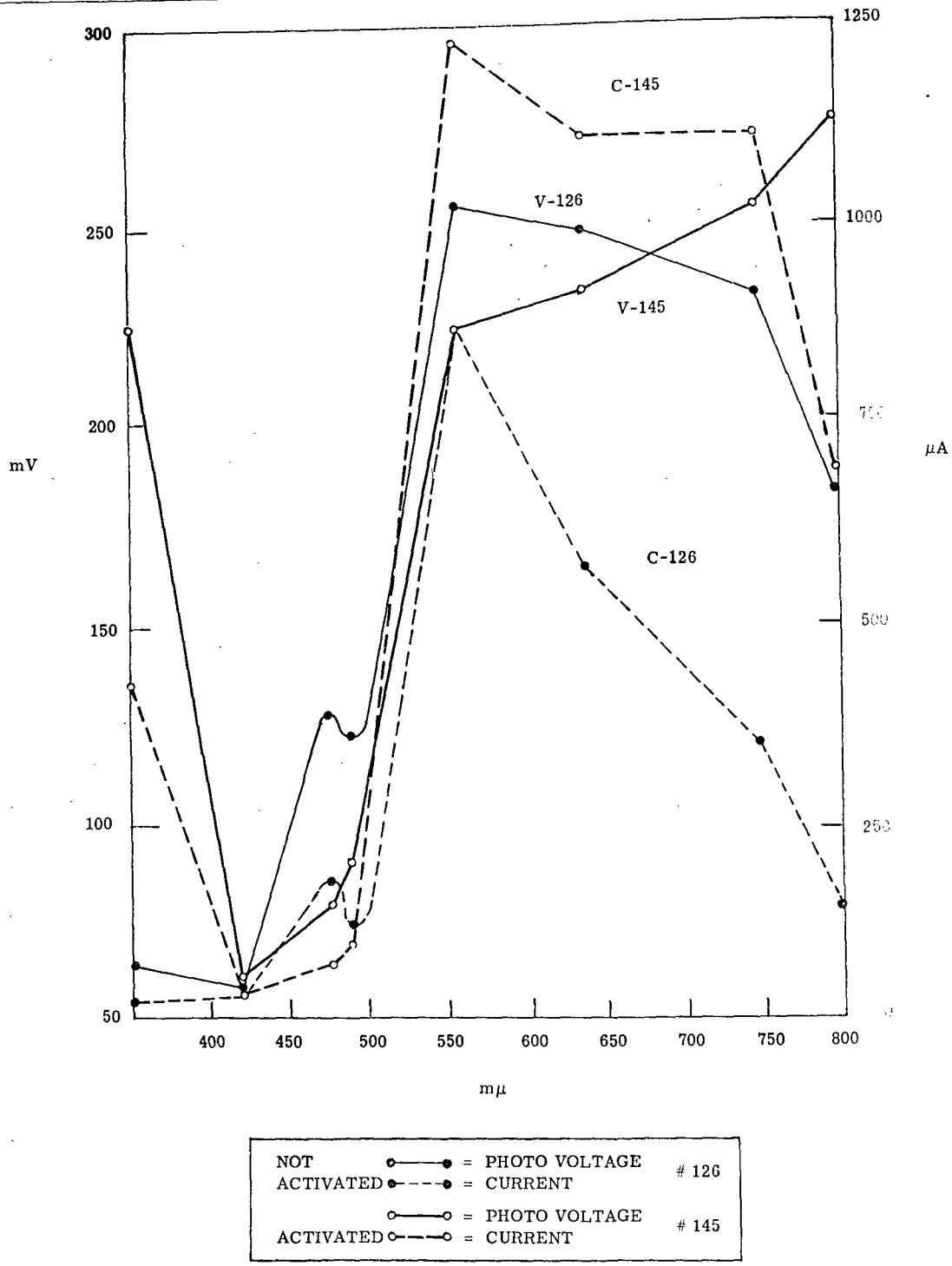


Figure 18. Spectral response for typical Itek cells with and without added acceptor impurities

and the Δ of the cell. Δ is defined as the ratio of

$$\frac{\text{light current—dark current}}{\text{dark current}}$$

The donor impurity increases the cell conductivity (light and dark current) and time constant by replacing a sulfide ion in the crystal lattice with a chloride ion. The acceptor impurity replaces cadmium in the lattice and shifts the spectral response towards the longer wavelength portion of the spectrum. However, the acceptor impurity also reduces light and dark current and time constant. Thus, it is necessary to provide a compromise ratio of doner impurity and acceptor impurity to obtain an optimum value for Δ. Figure 18 shows the spectral response for typical cells of identical thickness, one with and one without acceptor impurity added. The u.v.

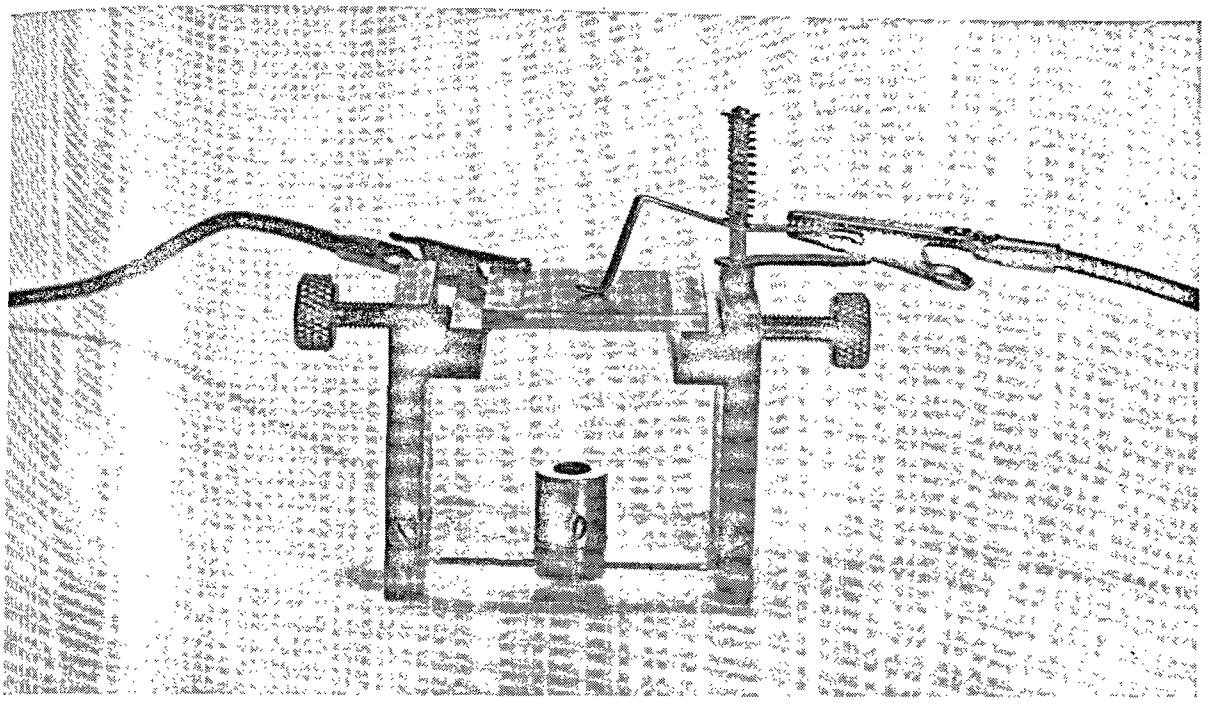


Figure 19. Close-up view of cell holder showing test arrangement for illumination incident on barrier surface

response is particularly interesting, and further studies are in progress on improving the cell efficiency at shorter wavelengths.

All measurements were made at room temperature with a monochrometer of a calibrated tungsten source with Corning filters through the cell. The cell can be illuminated from either side (figures 19, 20 and 21). Dark and light currents (photoconductivity) are measured by applying an external potential of 1.5 volts through the cell thickness. Photovoltages were measured with a Kintel Digital Voltmeter and short-circuit current with a Sylvania ammeter. The

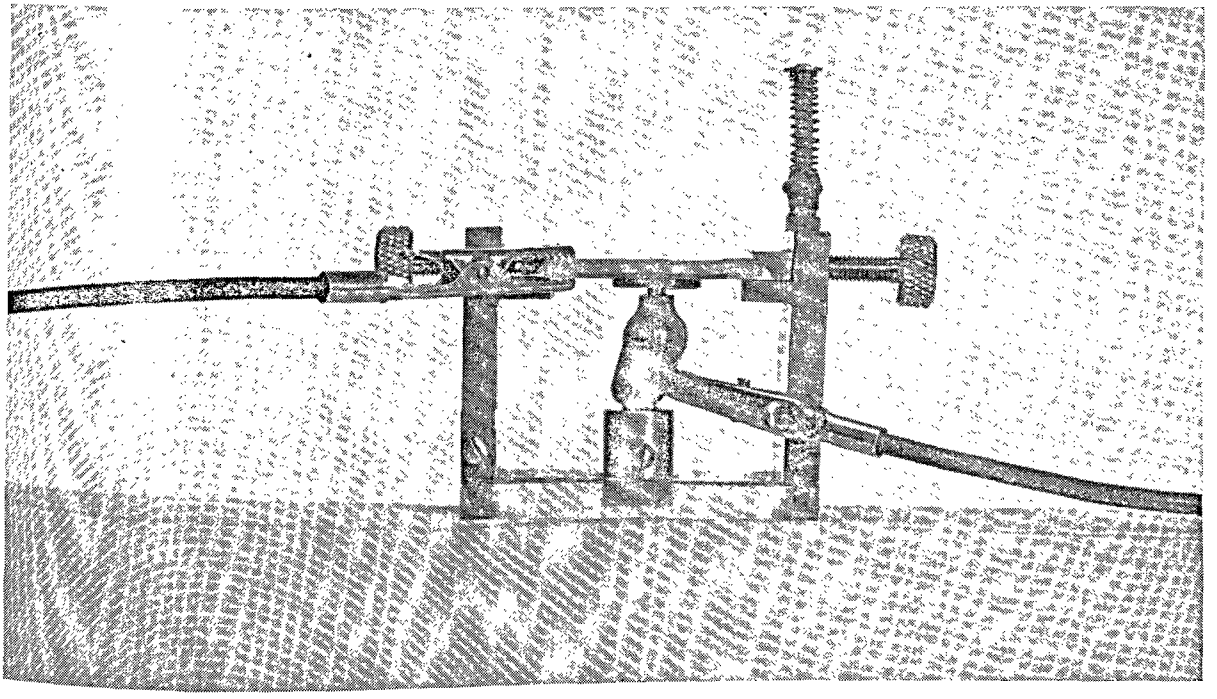


Figure 20. Close-up view of cell holder showing test arrangement for illumination incident on glass surface

following correlations between the photovoltaic and photoconductive characteristics of the cell were observed: cells with large dark current produced small photovoltages but provided high short-circuit photocurrents. On the other hand, cells with small dark currents and small photoconductivity produced high photovoltages and low short-circuit currents. In other words, Δ has to be as high as possible to provide cells with maximum power output.

Figure 22 shows that the photovoltage does not increase linearly with increasing light intensity but appears to level off at about 1 000 foot-candles. The short circuit current (when the cell is illuminated on the glass side) does appear to increase linearly with increasing light intensity.

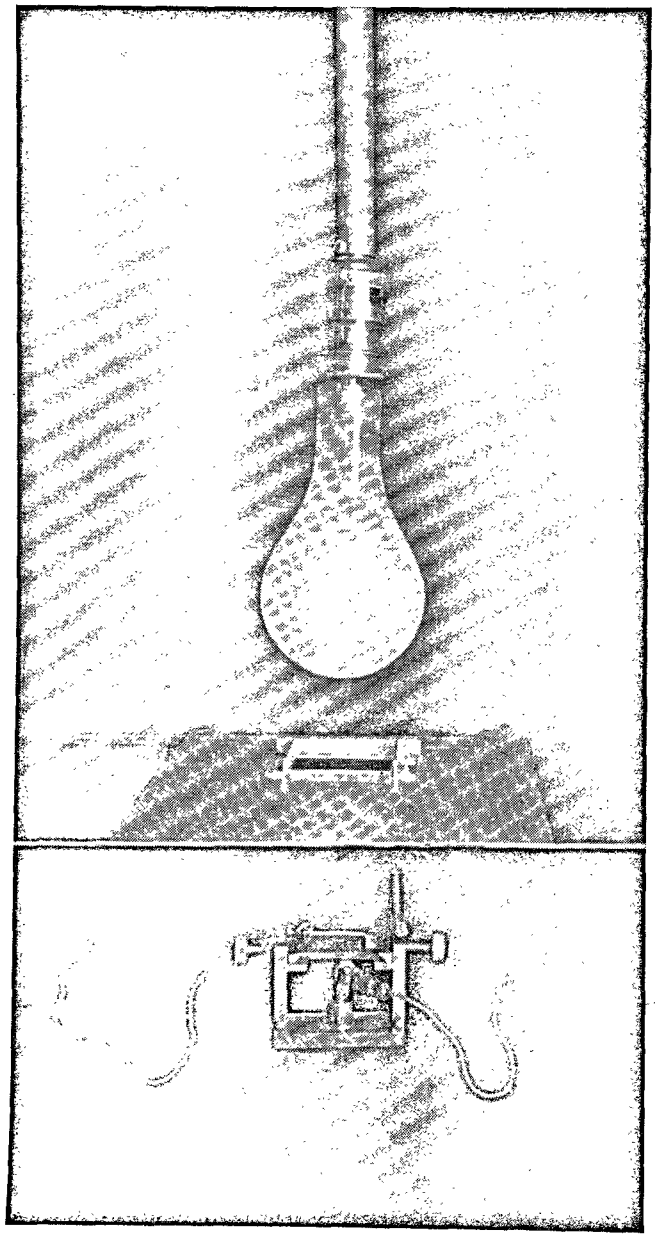


Figure 21. Test box showing calibrated lamp, filter holder and cell clamp

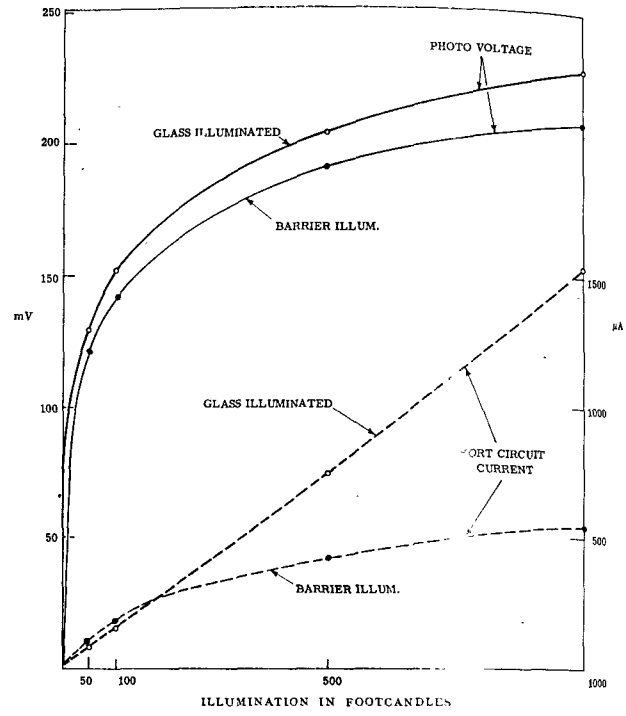


Figure 22. Photovoltage and photocurrent vs. light intensity for cell illuminated on glass side and on transparent barrier side

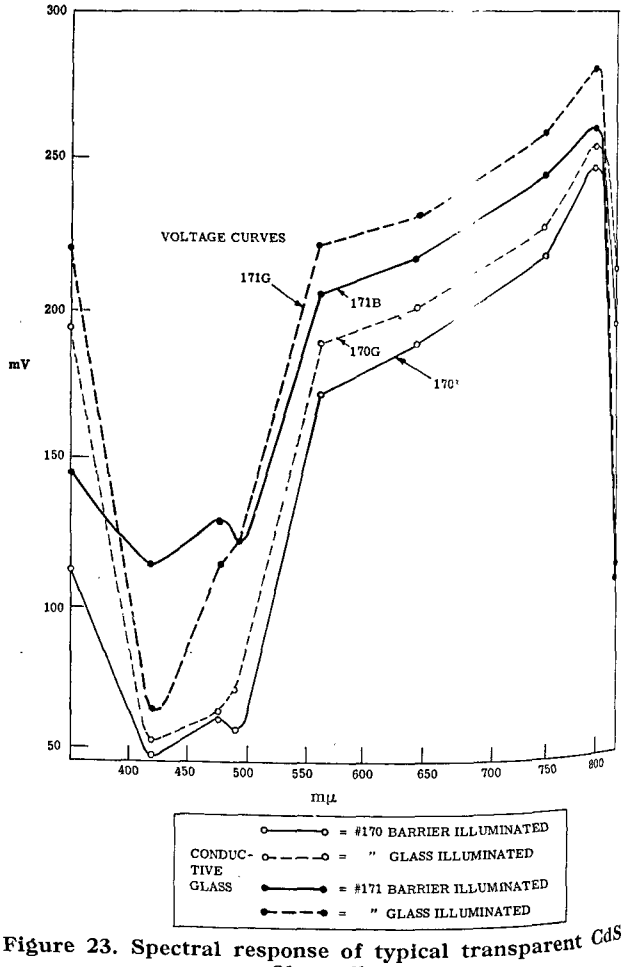


Figure 23. Spectral response of typical transparent CdS film cells

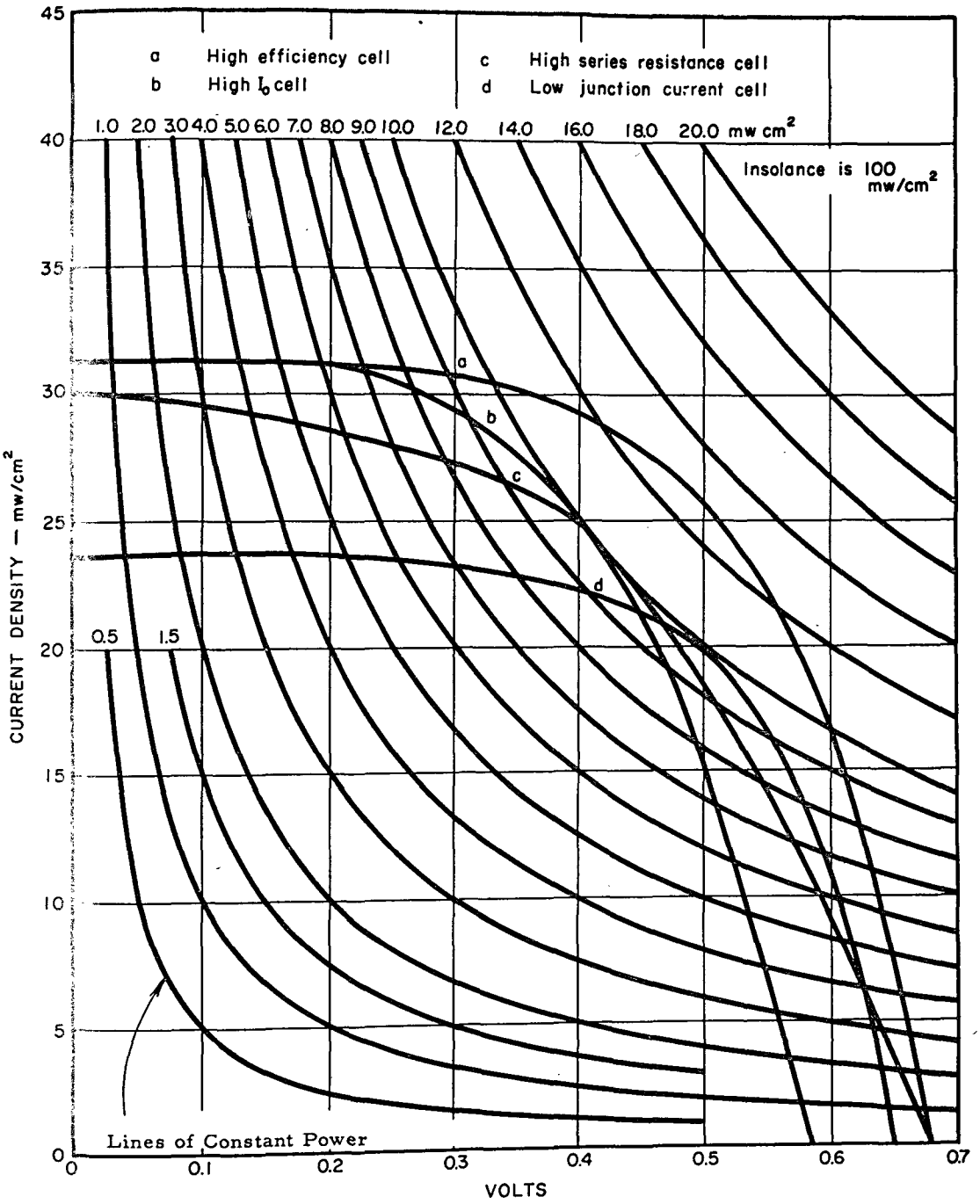


Figure 24. Typical variation of silicon solar cell characteristics

The stability of the cells has been quite remarkable. The characteristics of several unprotected layers prepared six months ago have remained constant.

Although the mechanism of these photovoltaic cells is not fully understood, we can make certain broad assumptions: the nature of the effect may be that of a *p-n* junction between *n*-type CdS and a *p*-type barrier or, because of the multilayer construction of the cell, photovoltages may occur at the interfaces of the several layers. It is interesting, however, to mention again the differences between the Itek cells and those reported in the literature.

(*a*) The use of powdered CdS with controlled impurity additions instead of single crystal chips provides a simple and inexpensive starting material for the preparation of Itek photovoltaic cells.

(*b*) The photovoltaic layer has excellent adhesion to the Pyrex glass plates. A roughened plate surface may increase layer adhesion but will certainly affect the optical and electrical properties of the cell.

(*c*) The use of transparent electrodes and barriers permits irradiation of the cell on either surface, thus avoiding the orientation problem that exists with "back wall" or "front wall" cells.

(*d*) The cell can be illuminated from both sides simultaneously or a reflective coating could be placed on one side of the cell. In either case, a greater utilization of available radiant energy is possible.

(*e*) Where strong light intensities are available, two or more cells can be "stacked" so that radiation passing through one cell could impinge on another directly below it, thus providing a means for greater utilization of impinging radiation.

(*f*) Our standard laboratory test cell has an active area of 1.8 cm × 2.6 cm. This is not a limiting dimension, and larger areas on contoured and flexible substrates have been made.

(*g*) Itek cells have sensitivity in the ultraviolet as well as in the far red portion of the spectrum. Published curves for other CdS cells show only a single peak at 6 000 Å with little or no sensitivity in the ultraviolet or far red.

(*h*) Itek CdS photovoltaic cells can be fabricated with predetermined and reproducible characteristics. This has not always been the case with silicon cells where deviation of cell characteristics are such that, although they can be matched in current and voltage at one point, there can be serious mismatches at other points. Figure 24 (1) shows typical variations of silicon cell characteristics.

References

1. Evans, W. H., Mann, A. E. and Wright, W. V. Jr., Solar Panel Design Considerations. Paper presented at the American Rocket Society Space Power Systems Conference, 1960.
2. Elliot, J. F. and Meikleham, V. F., Large Area Solar Cells. Presented at the American Rocket Society Space Power Systems Conference, 1960.
3. Teal, C. K., Fisher, J. R., and Treptow, A. W., A New Bridge Photocell Employing A Photoconducting Effect in Silicon, Some Properties of High-Purity Silicon, *J. App. Phys.* 17 : 879 (1946).
4. Bube, R. H., *Photoconductivity of Solids*. John Wiley and Sons, New York, 1960.
5. Fan, H. Y., *Phys Rev.* 75 : 163 (1949).
6. Becker, M. and Fan, H. Y., *Phys. Rev.* 78 : 301 (1950).
7. Backovsky, Malkovskas and Tauc, Cyech., *J. Phys.* 4 : 98 (1954).
8. Reynolds, D. C. and Czyzak, S. J., *Phys. Rev.* 96 : 1705 (1954).
9. Reynolds, Leies, Autes and Marburger, *Phys. Rev.* 96 : 533 (1954).
10. Nadyhakov, G. and Andreichin, R., *Compt. rend. acad. bulgare sci.* 7 : 13 (1954).
11. Nadyhakov, Andreichin and Borisov, *Compt. rend. acad. bulgare sci.* 7 : 17 (1954).
12. Loferski, J. J. and Rappaport, P., *Methods of Experimental Physics*, 6B : 365, Academic Press, New York, 1959.
13. Loferski, J. J., *J. App. Phys.* 27 : 777 (1956).
14. Rittner, E. S., *Phys. Rev.* 96 : 1708 (1954)
15. Cummerow, R. L., *Phys. Rev.*, 95 : 16 (1954).
16. Pfann, W. G. and van Roosbroeck, *J. Phys.* 25 : 1422 (1954).
17. Loferski, J. J., The Photovoltaic Effect and Solar Energy Conversion. Paper presented at the American Rocket Society Space Power Systems Conference, 1960
18. Queisser, Hans J. and Shockley, W. Some Theoretical Aspects of the Physics of Solar Cells. Paper presented at the American Rocket Society Space Power Systems Conference, 1960.
19. Middleton, A. E., Gorski, D. A. and Shirland, F. A., Evaporated CdS Film Photovoltaic Cells for Solar Energy Conversion. Paper presented at the American Rocket Society Space Power Systems Conference, 1960
20. Reynolds, Leies, Antes and Marburger, *Phys. Rev.* 96 : 533 (1954).
21. Hammond, D. A. and Shirland, F. A. Cadmium Sulfide Solar Energy Generator for Space Vehicles. *Proc. Electronic Components Conf.*, Philadelphia, 1958.

Summary

While interesting possibilities exist for large-scale conversion of solar energy directly into electricity, most methods proposed for low-cost solar energy utilization by photovoltaic means have been limited by a series of complex interdependent factors. Providing useful energy conversion devices for electrical power sources in under-developed countries further compounds the problem. Large area, low-cost photovoltaic cells, possessing the characteristics of high efficiency, good reliability, ease of operation and simple fabrication and maintenance, are required. Most importantly, the photovoltaic layer must have good efficiency at elevated temperatures. This is particularly critical if solar collectors are used. The paper briefly reviews the theoretical and practical limitations of currently available solar cells and describes a research program in progress designed to provide large area photovoltaic layers possessing the characteristics uniquely suited to low-cost energy conversion devices.

A one kilowatt power supply using silicon solar cells costs between U.S. $250 000 and $1 000 000 and weighs between 200 and 400 pounds, including the panel and supports. It would be ludicrous to suggest the use of such panels for power generation in under-developed areas. Several groups are investigating techniques for making large area photovoltaic cells. Silicon cells have been made by mechanical deformation of silicon (rolling, extruding, forging) into large area thin sheets. Thin-film silicon cells have been made by the reduction of silicon tetrachloride with hydrogen. Both techniques are

expensive, and severe limitations are imposed by the limited supply of silicon available and the specialized production capacity required to do the job. The paper shows that silicon cells may not be the most effective, even if the cell area could be substantially increased and the cost lowered to a favorable level. Concentration of incident solar energy onto a silicon layer will increase the effective radiation but will also increase the cell temperature and thus reduce cell efficiency to an unacceptable level. A theoretical discussion is included to emphasize the importance of choosing the optimum photoconductive material for high temperature solar cells. It is concluded that large energy gap materials are best for the fabrication of solar cells to be operated at elevated temperatures.

Cadmium sulfide with an energy gap of 2.4 ev (as opposed to silicon with an energy gap of 1.1. ev) is chosen as an optimum material. The fabrication techniques and characteristics of single-crystal CdS cells with opaque copper oxide barriers are described. "Back wall" evaporated CdS photovoltaic layers with opaque copper oxide barriers are also described and their characteristics discussed.

The Physics Department at Itek Laboratories has developed evaporated CdS photovoltaic cells having characteristics markedly different from those reported heretofore. The multilayer "transparent" photovoltaic cells are relatively simple to make, have good efficiencies (4-6 per cent) and exhibit spectral response characteristics not anticipated by theoretical mechanisms heretofore published (peaks at about 8 000 Å). The cell is made by evaporating CdS powder containing a donor impurity onto a conductive substrate applied to a Pyrex glass plate. The substrate may either be a gold "comb" electrode or a transparent tin oxide layer. The CdS film is prepared in a commercially available vacuum unit at a pressure of 5×10^{-6} mm Hg for about 30 minutes. The coated plate is then baked in air at 600°C for 45 minutes, cooled slowly to 200°C and returned to the bell-jar for the application of a second and third (if desired) CdS layer. The number of layers applied is determined by the layer thickness and the electrical characteristics desired. A small amount of acceptor impurity is added to the CdS powder used to prepare the top layer. A thin copper layer is then vacuum deposited onto the CdS. The plate is then baked in air at 400°C for 15 minutes to form a *transparent* copper oxide barrier layer. The cell is completed by vacuum depositing a thin transparent gold film over the copper oxide barrier as the top electrode. Layers have been deposited on both rigid and flexible substrates. The "transparent" cells can be illuminated from either side and can be "stacked" for maximum utilization of incident radiation.

DISPOSITIFS PHOTOVOLTAÏQUES A PELLICULE MINCE POUR LA CONVERSION DE L'ÉNERGIE SOLAIRE

Résumé

Bien qu'il existe des possibilités intéressantes pour la conversion directe de l'énergie solaire en électricité sur une grande échelle, la plupart des méthodes qui sont proposées pour la mise en œuvre de l'énergie solaire à bon compte par des moyens photovoltaïques se trouvent limitées par une série de facteurs complexes et mutuellement interdépendants. Le besoin de réaliser des dispostitifs utilisables de conversion d'énergie destinés à servir de sources d'énergie électrique dans les pays sous-développés complique encore le problème. Il leur faut des cellules photovoltaïques à grande surface et d'un prix modique, ayant des caractéristiques telles qu'un rendement élevé et une bonne régularité de fonctionnement, d'une exploitation facile, simplement construits et d'un entretien commode. Chose plus importante, la couche photovoltaïque doit avoir un bon rendement aux températures élevées. C'est là une exigence particulièrement difficile quand il s'agit de collecteurs solaires. L'auteur passe brièvement en revue, dans ce mémoire, les limitations théoriques et pratiques applicables aux cellules solaires dont on dispose actuellement, et décrit un programme de recherches actuellement en voie d'exécution, conçu pour réaliser des couches photovoltaïques à grande surface dotées de caractéristiques particulièrement indiquées pour leur intégration dans des dispositifs de conversion d'énergie à prix modique.

Une source d'énergie de 1 kW faisant usage de cellules solaires au silicium coûte entre 250 000 et 1 000 000 de dollars des États-Unis et pèse entre 200 et 400 livres (90 et 180 kg), y compris panneaux et supports. Il serait absurde de suggérer l'emploi de panneaux de ce genre pour produire de l'énergie dans les régions sous-développées. Plusieurs groupes procèdent à l'étude des techniques propres à la réalisation de cellules photovoltaïques à grande surface. On a réalisé des cellules au silicium par déformation mécanique de cet élément (laminage, travail à la presse, forage) aboutissant à la production de feuilles minces de grande surface. Des cellules au silicium à pellicule mince ont également été réalisées par la réduction du tétrachlorure de silicium par l'hydrogène. Les deux techniques sont coûteuses et le manque de silicium et des installations de production spécialisées dont on a besoin, en limite beaucoup le domaine d'application. Ce mémoire révèle que les cellules au silicium ne sont peut-être pas les plus efficaces dont on dispose, même en augmentant beaucoup la surface des cellules et en ramenant leur prix à un niveau favorable. La concentration de l'énergie solaire incidente sur une couche de silicium

augmente le rayonnement utile, mais fait également monter la température de la cellule et, de la sorte, ramène son rendement à un niveau qui cesse d'être acceptable. L'auteur présente un examen théorique de la question, en soulignant l'importance du choix du matériau photoconducteur optimum pour les cellules solaires à haute température. Il aboutit à la conclusion que les matériaux qui présentent une large discontinuité énergétique sont ceux qui se prêtent le mieux à la fabrication de cellules solaires destinées à fonctionner à des températures élevées.

On a choisi le sulfure de cadmium, dont la discontinuité énergétique est de 2,4 ev (alors que celle du silicium est de 1,1 ev) comme produit optimal. L'auteur décrit les techniques de fabrication et les caractéristiques des cellules monocristallines au sulfure de cadmium avec barrière opaque en oxyde de cuivre. Il examine également les couches photovoltaïques à sulfure de cadmium évaporé du type « Back wall », avec barrière opaque en oxyde de cuivre, et passe en revue leurs caractéristiques.

Le service de physique d'Itek Laboratories a mis au point des cellules photovoltaïques à sulfure de cadmium évaporé, dont les caractéristiques sont très différentes de celles qui ont retenu l'attention jusqu'à présent. Les cellules photovoltaïques « transparentes » à couches multiples sont d'une réalisation relativement simple, leur rendement est bon (4 à 6 p. 100) et elles ont des caractéristiques de réponse spectrale que les modèles théoriques publiés jusqu'à présent ne permettent pas de prévoir (maxima à environ 8 000 Å). On réalise la cellule en faisant évaporer de la poudre de sulfure de cadmium qui contient une impureté d'apport sur un support conducteur étalé à son tour sur une plaque en verre pyrex. Le support peut être soit une électrode « peigne » en or, soit une couche transparente d'oxyde d'étain. On prépare la pellicule de sulfure de cadmium au moyen d'un appareil à vide que l'on trouve dans le commerce, sous une pression de 5×10^{-6} mm Hg pendant 30 minutes environ. La plaque ainsi enduite est alors cuite à l'air à 600 °C pendant 45 minutes, refroidie lentement jusqu'à 200 °C et renvoyée à l'appareil à vide, en vue de l'application d'une deuxième et d'une troisième couche de sulfure de cadmium en cas de besoin. Le nombre des couches ainsi appliquées est déterminé par leur épaisseur et les caractéristiques électriques cherchées. On ajoute une certaine dose d'impuretés (d'un corps accepteur) à la poudre de sulfure de cadmium dont on se sert pour préparer la couche supérieure. On dépose alors une couche mince de cuivre (sous le vide) sur le sulfure de cadmium. On fait cuire la plaque à l'air à 400 °C pendant 15 minutes, pour réaliser une couche d'arrêt en oxyde de cuivre transparent. La cellule est complétée par le dépôt, toujours sous le vide, d'une pellicule transparente d'or mince sur la couche d'arrêt d'oxyde de cuivre comme électrode supérieure. De telles couches ont été déposées tant sur des supports rigides que sur des bases flexibles. Les cellules « transparentes » peuvent être éclairées d'un côté ou de l'autre, et on peut les empiler en vue de réaliser un maximum d'exploitation du rayonnement incident.

DEVELOPMENTS IN PHOTOVOLTAIC SOLAR ENERGY CONVERSION FOR EARTH SURFACE APPLICATIONS

M. Wolf *

Although photovoltaic solar energy conversion has been developed into the most suitable power source for space vehicles based on reliability, weight, and cost (1), and although it has been used in this application nearly exclusively and with great success in a large and steadily growing number of missions (2), it did not find its way to any appreciable extent into the circle of power systems for earth surface application. The reason for this is of an economical nature.

Rather sophisticated photovoltaic solar energy conversion systems have been developed for space vehicle applications. They have undergone very substantial ground testing and modification programs until the proper construction methods were found, resulting in the desired reliability under extreme environmental conditions. The final space missions then supplied the proof to the soundness of the development programs and to the extreme longevity and reliability of the systems thus evolved. Comparable efforts have not been undertaken for the development of suitable and reliable photovoltaic solar energy conversion systems for earth surface applications. A few attempts have been made to construct and test such systems in ground installations, but these efforts were mostly short-term approaches without necessary design, test, and modification programs, and were therefore doomed to failure.

A second and important reason for the lag in the introduction of photovoltaic solar energy conversion into earth surface power supplies lies in the strong competition from other power sources. This competition is mainly felt in the relatively large initial outlay necessary for the photovoltaic solar energy converter in comparison to other power sources. Moreover, proper economical evaluation of the competitive situation between an earth surface installation of a photovoltaic solar energy conversion system and other power sources is hindered by the lack of experience with the first, especially with respect to useful lifetimes and maintenance costs.

In the following paragraphs, an installation and maintenance cost analysis for the competing power sources is carried out in order to determine the conditions under which photovoltaic solar energy converters can be applied advantageously. A review of recent advancements in solar cell technology with ensuing cost reductions and a discussion of future developments complete the paper.

* Heliotek Corporation, Sylmar, California.

Present economical earth surface applications for photovoltaic solar energy converters

The introduction of photovoltaic solar energy conversion systems for earth surface applications is hindered mainly by the competition from other power sources. There are a number of applications, however, where the photovoltaic solar energy conversion system would have a place even in its present form, and at its present cost, except for some design modifications relative to specific application and environment.

Since electric power transmitted by conducting lines is the strongest competitor to photovoltaic solar energy conversion, any application to a system containing conducting transmission lines or located in the vicinity of such lines is to be ruled out from the start. This includes application to telephone repeater stations, since a pair of wires can readily be added to an existing pole line for the transmission of electric power or the information and the electric power can be transmitted over the same wires—i.e., by use of a carrier system.

Therefore, it must be concluded that a place for photovoltaic solar power systems presently appears to exist only in the field of wireless communications, and even there only for installations in remote areas, where access is difficult and where electric power distribution lines are distant. Such applications may involve a microwave relay station, a navigational beacon of the optical or radio type, an observation post, be it of forestry, weather observation, civilian police or military nature.

Most of these applications require continuous readiness. Therefore energy storage has to be provided, since the source—namely, solar radiation—is available on the earth surface only during part of the day. A system without provision for energy storage would involve about half the original installation cost, have a higher reliability and a longer lifetime, and require less maintenance. In the following cost analysis, a system incorporating energy storage is compared with competitive power sources at various power levels and as a function of distance from the load to the nearest power line or transportation facility.

For the purpose of evaluation, difficulty of access to the location has been postulated, possibly involving hand carrying of loads through mountain terrain or jungles, or clearing and reclearing of the access paths for every entry. Therefore, a transportation cost of U.S. $0.10 per pound-mile of load and distance from the nearest transportation facility site is used throughout, together with $5.00 per man-mile round trip for personnel transport. Since these assumptions are key factors in the evaluation, they should be carefully determined for every individual application, preceding a feasibility study according to the method outlined here. Figure 1 presents the original installation cost as a function of distance from the nearest existing power line or transportation facility, i.e., truckable road for the different power systems in competition. Power systems which are not commercially available, or are not thoroughly developed and proven at this time, like thermoelectric and thermionic generators, are not included in the analysis. Discussed are a power transmission line, a motor generator set, a system of electro-chemical primary cells, i.e., dry cells, and the photovoltaic solar energy converter system.

For the power line, an installation cost of U.S. $2.00 per foot has been applied. This figure is slightly below the one used in estimates by the Los Angeles City Department of Water and Power (3) for transmission lines having wooden poles and wooden crossbars, to be installed in readily accessible areas. The $2.00 figure has been applied in the analysis, realizing that much larger numbers may apply to difficult access areas. Also, the transportation cost factors have been neglected in this case.

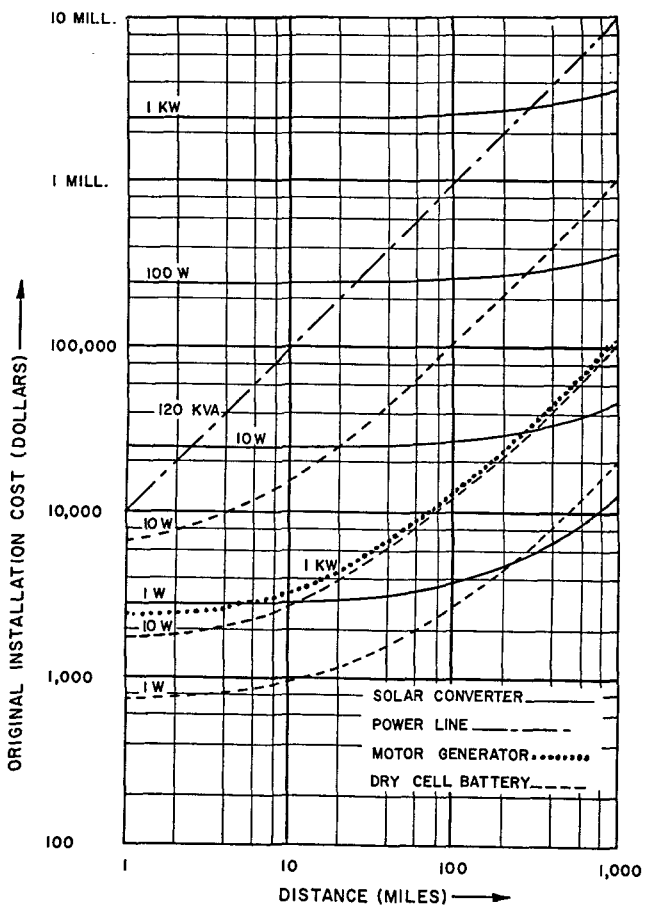


Figure 1

It should be noted that the power needs discussed here are mostly under 1 kW. No essential cost increase is, however, connected with the installation of a power line of larger capacity. Such a line could have 4 800 volts and a capacity of 120 kVA. It could fulfill additional requirements and may for this reason be sometimes preferred over lower priced systems.

The second system considered is a motor-generator set. The smallest practical size of a motor-generator for continuous duty has about 1 kW capacity. If it is to be used in a remote location with minimum maintenance, it would have to be of a special high reliability type. Its original cost, including control devices and gas tank, is estimated at U.S. $1 000, and its weight at 1 000 pounds, including gas for trial runs. Further allocated are 256 man-hours at $1 280 by two men (personnel transportation). These assumptions, together with the freight transportation charge, lead to the curve labeled "motor-generator" in figure 1.

The next system considered consists of dry cells, having a capacity of 20 watt-hours per pound. Therefore, in a year, about 450 pounds of batteries are needed to deliver 1 watt continuously. For the purpose of this analysis, ten battery replacements per year are considered, necessitating installation of 45 pounds of batteries. The present cost of good dry cells in quantities is about U.S. $0.50 per pound. The original installation involves about $25 for batteries, fixed gear estimated to cost about $400 and to weigh 55 pounds, plus an original installation of 64 man-hours at $320 by two men. These numbers result in the curve labeled "1 watt dry cell", in figure 1. By multiplications with 10 and 100, the "10 watt dry cell" and "100 watt dry cell" curves are obtained which refer to dry cell installations delivering continuously 10 watts and 100 watts, respectively, except that the fixed gear costs have been raised to only $750 and $2 000, respectively, and the installation outlay to $640 and $1,300 respectively.

For the photovoltaic solar energy conversion system, a figure of U.S. $250 per watt rated capacity is used for a flat solar converter panel. This number is doubled to include storage batteries and regulation devices for continuous power delivery. It is further assumed that a 1-watt flat collector will deliver 6 watt-hours per day, taking geographical location and weather conditions into account. Of these 6 watt-hours, 1.2 watt hours are delivered directly to the load, while 4.8 watt-hours are used for battery charging. With 67 per cent battery efficiency, 3.6 watt-hours are available from the battery, for a total of 4.8 watt-hours delivered to the load during 24 hours, corresponding to 0.2 watts supplied continuously. For a 1-watt continuous power require-

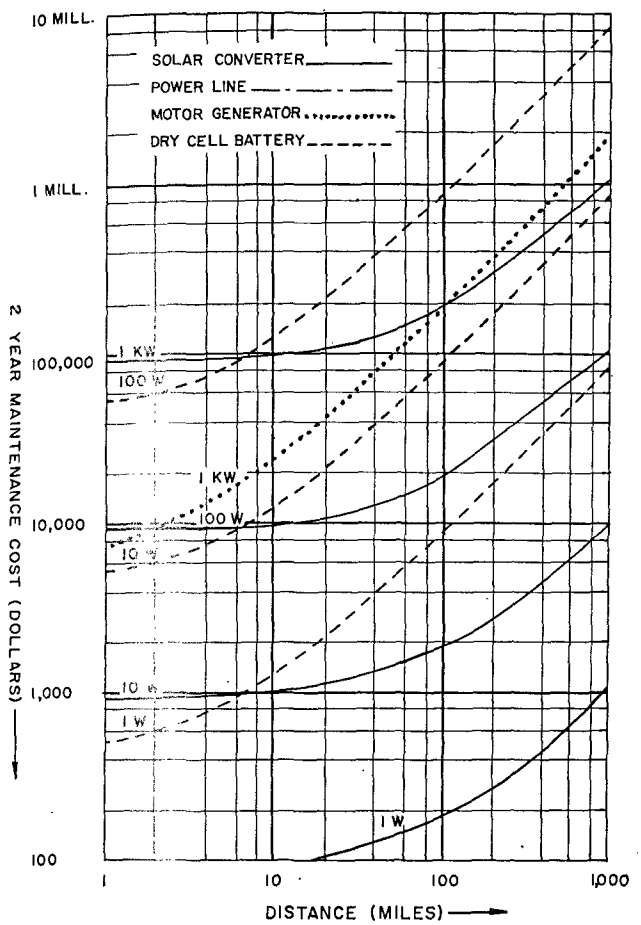


Figure 2

ment, a 5-watt photovoltaic solar energy converter has to be installed. Using thirty sealed nickel-cadmium cells size "D", with a total capacity of 111 watt-hours, a depth of discharge of 13 per cent is obtained, which is conducive for long battery life and high efficiency and for bridging several overcast days. The weight of these batteries is 10 pounds. Assuming the additional gear to weigh 10 pounds, including one pound for the solar panel, and installation time of 64 man-hours at $320 for two men, one arrives at the curve labeled "1-watt solar converter" in figure 1. Properly scaled-up numbers lead to curves for the 10-watt, 100-watt, and 1-kW photovoltaic solar energy conversion systems, labeled correspondingly in figure 1. For the 100-watt system, 128 man-hours at $640, and for the 1-kW system, 640 man-hours at $6 400 for four men have been applied for the installation.

Figure 2 shows the two-year maintenance costs for the various systems. The power line is assumed to require no maintenance. The motor-generator has to be periodically supplied with fuel. Assuming a 70 per cent over-all efficiency for this system, it will use 17 520 pounds in two years at a cost of U.S. $1 000 to deliver 1 kW continuously. Because of continuous duty in a remote location without repair facilities, the engine will have to be removed for overhaul and replaced once a year. The same base costs as in figure 1 are applied here, resulting in the curve labeled "1-kW motor generator" of figure 2.

For the dry cells, U.S. $430 have to be spent per watt in two years for replacement batteries, weighing 860 pounds. This leads to the curves in figure 2 labeled "1 W", "10 W", and "100 W dry cells", respectively.

The photovoltaic solar energy conversion system is expected to require no maintenance except for an occasional cleaning of the collector face by the person making a routine check of the remainder of the system, and except for replacement of the storage cells at the end of the two-year period. This involves the transport of batteries plus their original cost, resulting in the curves labeled "1 W", "10 W", "100 W", and "1 kW solar converters", respectively, in figure 2.

Adding the original installation costs and the two-year maintenance costs from figures 1 and 2, the total expenses connected with two-year operation of the systems are obtained and the curves of figure 3. Figure 3 shows that already after two years of operation, the total expense for a 10-watt system located farther than 20 miles from an access road or farther than $2\frac{1}{2}$ miles from a power line is lowest for the photovoltaic solar energy conversion system.

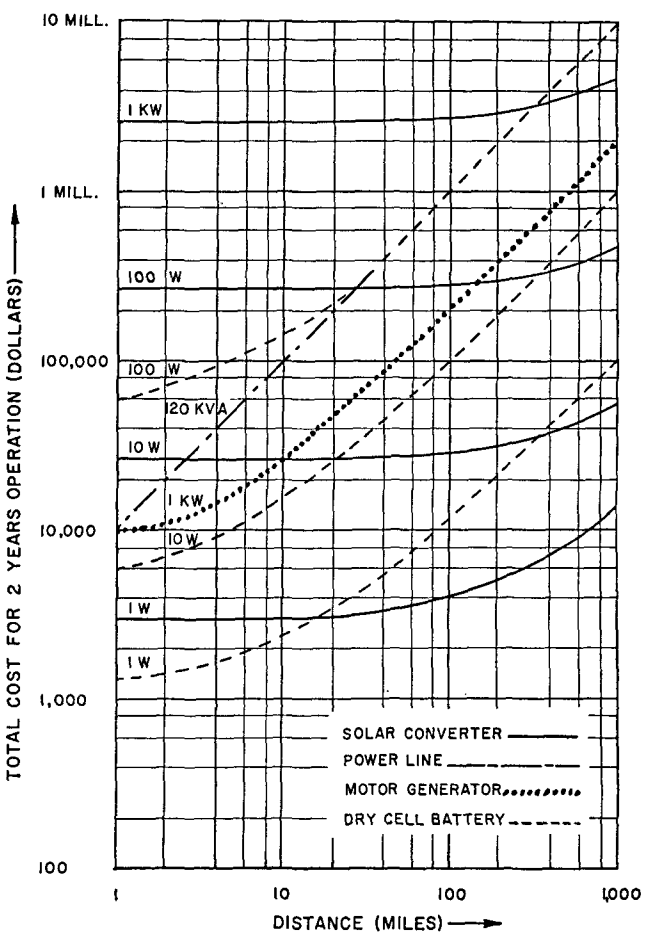


Figure 3

To consider the total accrued costs after twenty years, the two-year maintenance costs are multiplied by 10 and added to the original installation cost. The results are presented in figure 4. One exception has been made in assuming that the power line has to be replaced towards the end of the twenty-year term.

Figure 4 shows that for continuous power requirements up to 20 watts, the photovoltaic solar energy conversion system incurs, over twenty years, lower total outlays than any other system, except for a power line available at a distance of less than 3½ miles. Even at the 100-W level, the photovoltaic solar energy converter is competitive for distances over 18 miles, and at the 1-kW level, for distances over 33 miles.

The foregoing analysis shows that under certain conditions, a photovoltaic solar energy converter at present costs can well compete with other power sources. In some cases, new designs to meet certain requirements on the structure, i.e., incorporating cooling fins, may be desired, while in others structures very similar to those designed for space vehicles are advantageous because of their proven characteristics and their light weight, which can be of importance in remote applications.

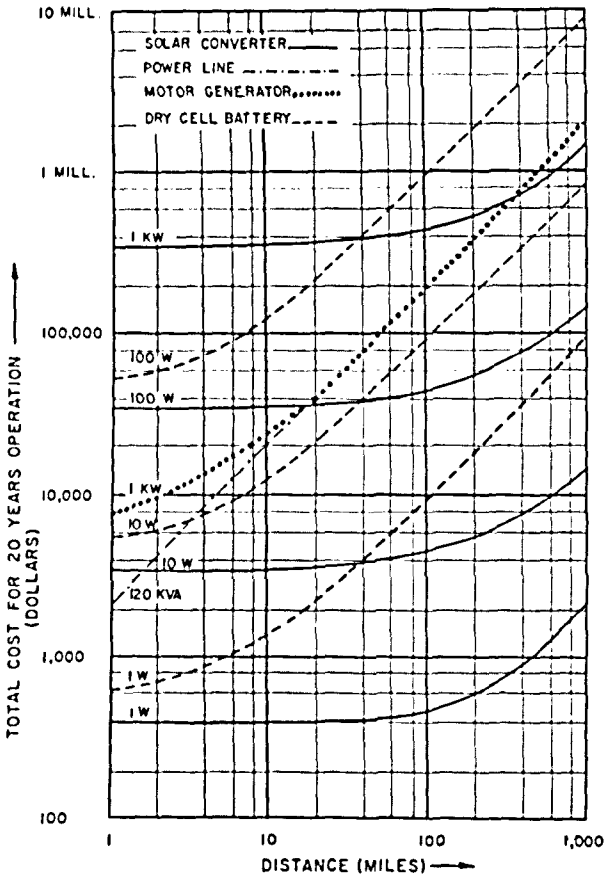


Figure 4

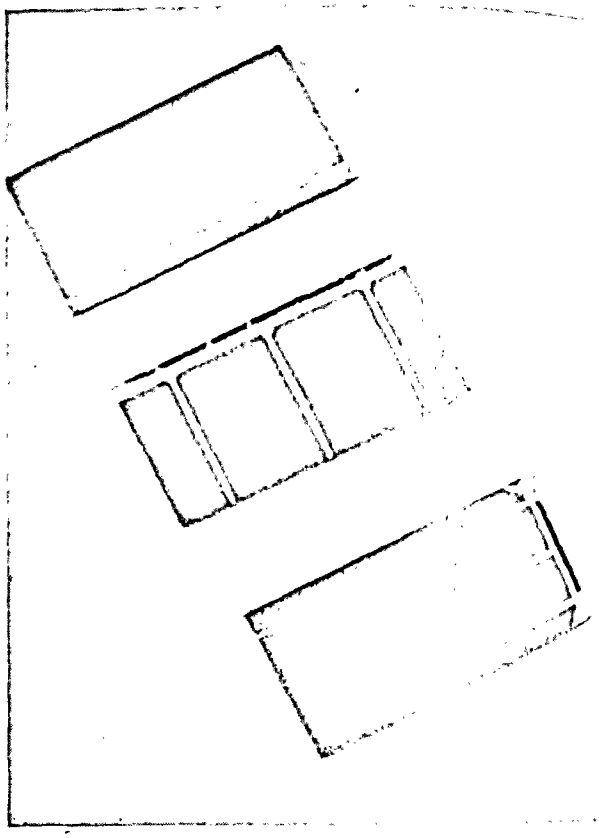


Figure 5. Developments in photovoltaic solar energy conversion for all surface applications

The cost significance of solar cell improvements

Cost reductions for photovoltaic solar energy converting systems can be obtained by two approaches:

(*a*) A direct reduction in the cost of the unit cell;

(*b*) An improvement of the unit cell performance without a price increase.

Both approaches are important, and with the present limited market and high material costs, approach (*b*) was easier realizable. A 35 per cent improvement as obtained recently (see below) reduces the number of cells needed to obtain a certain system output by 26 per cent. An identical percentage cost reduction is achieved for the complete panel, since the installation cost of solar cells to a converter panel is proportional to the number of cells used, independent of the panel power output. Conversely, a cost reduction connected with a decrease in cell performance can easily be annihilated by the higher cost of mounting a larger number of cells to an increased size converter panel.

The fulfillment of older estimates for potential solar cell price reductions by factors of 2 to 4, obtainable by introduction of mass production techniques and automation combined with a steady market, does not appear imminent in the very near future.

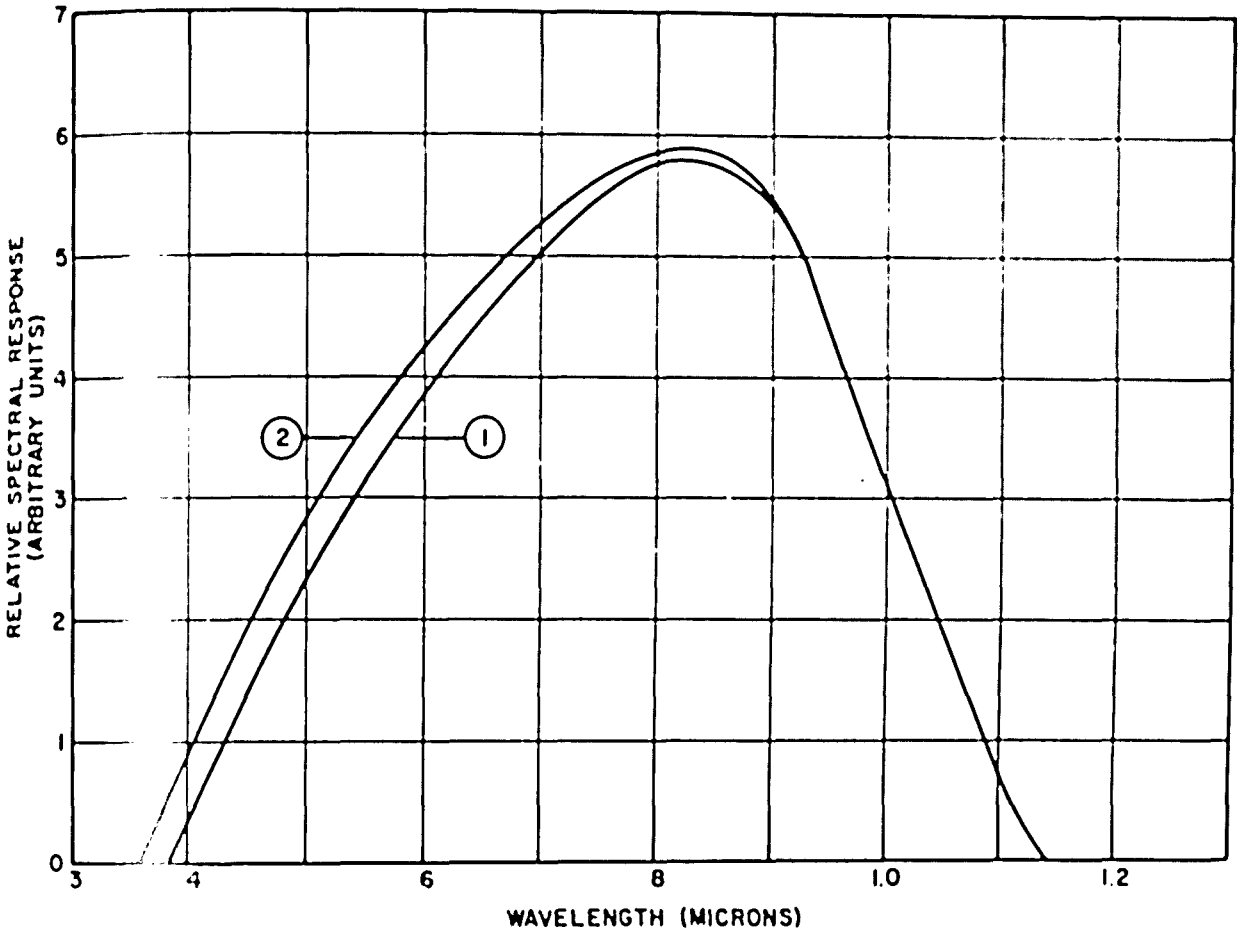


Figure 6

Other approaches which can lead to a substantial reduction of the cost of photovoltaic solar energy converter systems are discussed in later sections.

Recent improvements in silicon solar cells and in their application to power systems

Silicon solar cells have been commercially available for more than five years but are still continuously being perfected. The most recent advancements are the introduction of metallic grid lines for the reduction of series resistance and a shift of the spectral response for better sunlight performance (4).

The application of metallic grid lines over the diffused layer results in a decrease of its effective sheet resistance (5) and a 15 to 20 per cent increase of the power output over otherwise identical solar cells. (Figure 5 compares gridded cell in centre to other cell at left.) This improvement is achieved despite the coverage of a small portion of the active area. Other advantages obtained by the use of grid lines are: the possibility of decreasing the thickness of the diffused layer and improving the spectral response, the freedom of choice for solar cell size and geometry, and improved performance at high light levels as obtainable by use of concentrators. New fabrication techniques were developed for the application of the grid lines, which also provide more flexibility for the contact design.

One result of these developments is the emergence of a new solar cell equally suited for parallel and series connection. (Figure 5, cell at right.) This design does not change the efficiency based on the active area, but rather increases the active area per cell and with it the power output by 8 per cent, thus permitting use of a smaller number of cells for achievement of a certain power system design objective.

The second improvement is a result of the introduction of the grids. On past solar cells, the sheet resistance of the diffused layer was one of the important parameters in the determination of its optimum thickness, with collection efficiency as the other parameter (6). The compromise obtained in the competition between these two parameters resulted in a spectral response which was relatively unfavorable at the shorter wave-lengths, where the solar radiation has its peak intensities. Since the application of grids removed the strong relationship between the diffused layer thickness and its sheet resistance,

freedom for the variation of the short wave-length part of the spectral response was obtained. Decreases of the diffused layer thickness, leading to increased short wave-length response, are sought for. Figure 6, curve 2, shows the spectral response for a cell having smaller p-layer thickness than that producing curve 1, everything else being identical. Limitations to this development are found in material parameters and process difficulties. At this time, an average improvement of solar cell performance in earth surface sunlight by 8 per cent has been achieved through the reduction of the p^+ layer thickness. As a result of these improvements, solar cells converting 11.5 per cent of the incident radiant solar energy into electrical power at the earth surface are now available in quantities. This compares to the 8.5 per cent efficiency of production solar cells only a little more than a year ago. Although such progress can be reported for the silicon solar cells, a survey of the numerous efforts undertaken on other materials and methods does not show significant advances (4). The principle of multiple transitions with its potential for the largest efficiencies was not further investigated, partly because of lack of basic knowledge of the properties of trapping levels (5).

New concepts for lower-cost photovoltaic solar energy conversion systems

The cost of the photovoltaic solar energy converter itself can be reduced principally by two approaches: (*a*) by lowering the price of the photovoltaic elements, and (*b*) by decreasing their number used in the system. Further cost reductions may be effected by reduction of the converter temperature through improved thermal control, and through application of the most favorable energy storage devices.

Thin-film solar cells

After analyzing the cost factors for the various types of solar cells and different methods for their fabrication, a major possibility for drastic cost reduction appears to be the introduction of thin-film techniques for large area devices. Past research indicated that the photovoltaic *p-n* junction cells in general and the silicon material in particular are not conducive to the preparation of thin-film solar cells (7, 8). The *p-n* junction properties which determine the device characteristics are influenced by the crystal structure and require the film to be composed of large crystals. Also, the process of photon absorption and generation of carriers in the material dictates a minimum film thickness for reasonable efficiencies.

However, the recently discovered photoemissive mechanism in cadmium-sulfide cells (9) appears promising for the preparation of thin-film solar cells. The photon absorption and carrier generation appear to take place in or very near a boundary layer between the copper contact or an oxide film on it and the cadmium sulfide. The current-voltage characteristic is determined by the potential barrier formed by this boundary layer. Thus, independence is gained from the film thickness and the crystalline properties of the semiconducting material. Recently published early results of developmental work in progress at the Harshaw Chemical Company (10, 11) show that efficiencies of 2 to 2.5 per cent have been obtained on evaporated film cadmium sulfide solar cells of 20 cm^2 size. Efficiencies as high as 4.5 per cent have been obtained over small areas of these larger cells. This indicates that better efficiencies should be obtainable with improved process control. If it becomes possible to deposit these films at low cost directly on inexpensive support structures, then this approach may make photovoltaic solar energy conversion economically feasible for widespread earth surface applications.

Application of concentrators

One cause for the high cost of photovoltaic solar energy conversion is the low energy density of the solar radiation, which can reach, on the earth surface, 1 kW/m^2 under optimum conditions. Therefore, relatively large collectors have to be built and covered with solar cells. The application of concentrators permits covering part of the converter area with expensive photovoltaic cells, while filling the remainder with relatively inexpensive reflectors which direct the radiation onto the converting elements. From a multitude of concentrator configurations, integrated structures for reflectors and solar cell support appear most feasible because of their simplicity, low weight and easier heat control. Such structures are the "Modular Channel Concentrator" (figure 7) and the "Modular Truncated Pyramid

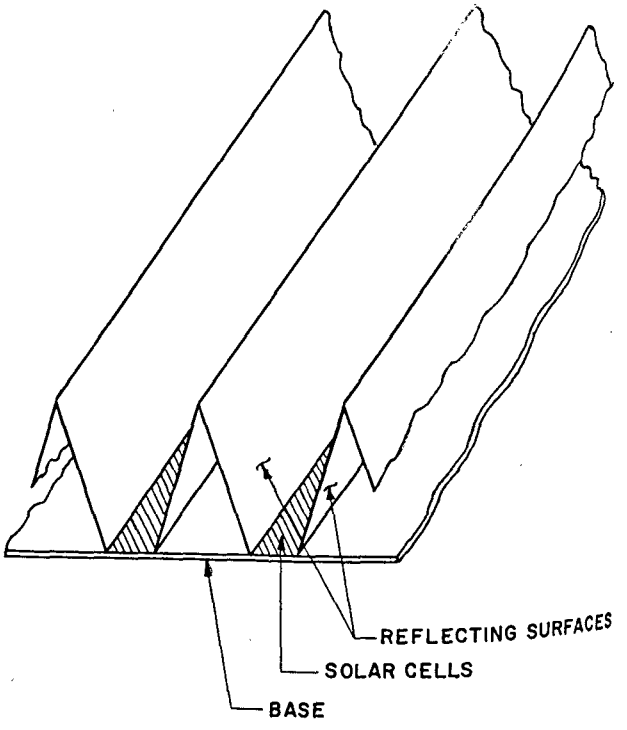


Figure 7. Modular channel concentrator

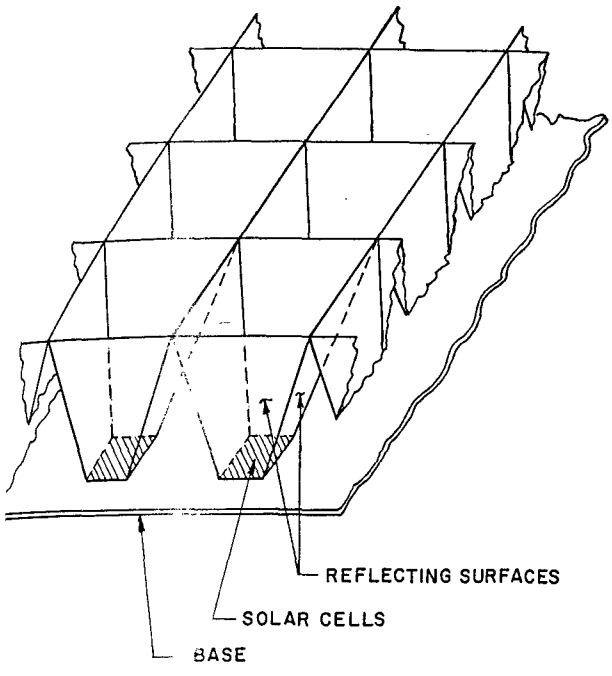


Figure 8. Modular truncated pyramid reflector

Reflector" (figure 8). The channel concentrator gives concentration ratios near 2.5, while concentration ratios of 5 to 7 may be obtained with truncated pyramid reflectors. Application of concentration ratios larger than 5 to 7 to photovoltaic converters does not appear favorable due to thermal control difficulties and increased series resistance losses at the ensuing high current densities in the solar cells.

The channel concentrator may be used with fixed orientation, if the longitudinal axis of the channel parallels the east-west direction, with the declination adjusted for best year-average performance. The truncated pyramid reflector, with its higher concentration ratio, needs tracking for good performance. For the choice between the channel and the truncated pyramid reflectors, a trade-off study between system complexity, reliability, and cost will have to be undertaken.

Thermal control

Thermal control is an important problem connected with photovoltaic solar energy conversion, but to a greater extent with the application of concentrators than with flat collectors. Contrary to thermal devices, photovoltaic converters exhibit reduced efficiencies at higher operating temperatures. Temperature control on the earth surface can be achieved through conduction, free or forced convection, and radiation. In the case of concentrator application, the solar cell covered area which needs cooling is smaller than the collector. Only channel, truncated pyramid, and double reflector concentrators permit extension of the irradiated area for cooling purposes. Either the reflectors or the backing structure may be used for this. An important point is to design these structures for sufficient heat conduction from the solar cells to the cooling surfaces. This can be achieved by increasing the structural cross-section and adding weight, which may in some cases be economically objectionable.

A better method for conduction enhancement lies in the modular design concept (figure 9). It can readily be shown that the temperature difference between the irradiated area and the coldest part of the cooling area is approximately proportional to the size of the irradiated area assuming uniform energy density F_o over all irradiated areas:

$$\Delta T \approx \frac{a^2 F_o}{2ct}\left[ln\left(1+\frac{2d}{a}-\frac{d}{a\left(1+\frac{2d}{a}\right)}\right]\right. \quad [1]$$

Here c = thermal conductivity, t = thickness of conducting sheet, and a and d as in figure 9.

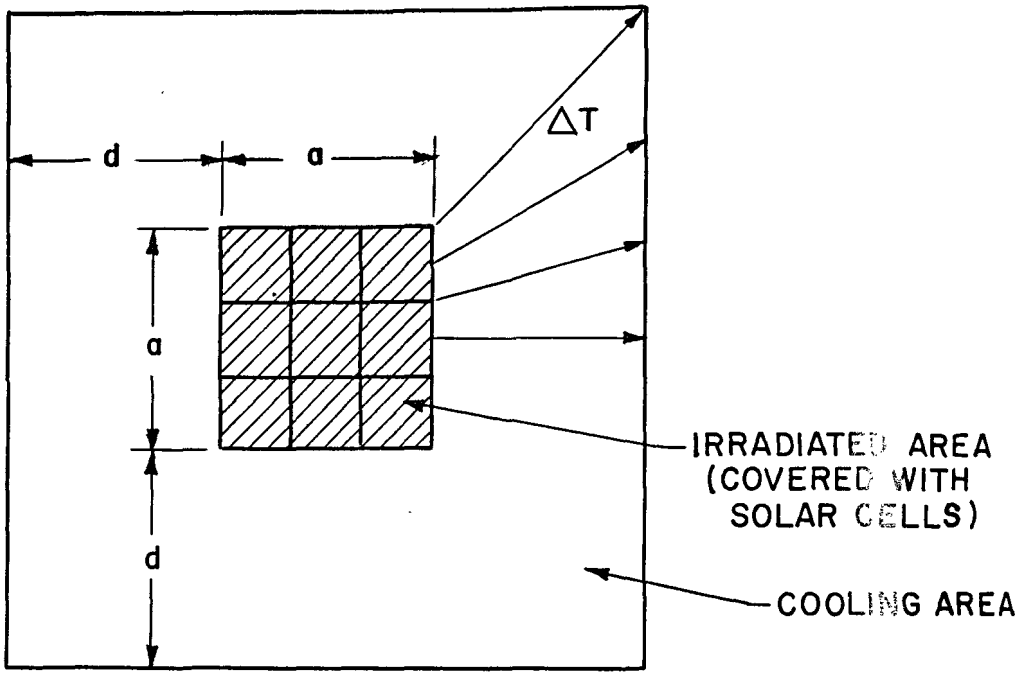
The only approximation in the derivation of equation [1] above was made by assuming the temperature difference to be small, so that the heat loss is uniform for all surface elements.

It is practical to utilize the whole collector area for cooling, thus obtaining similar conditions as for a flat converter. Even in this case, the operating temperature will be considerably above the ambient (by about 40-50°C), using free convection of air and radiation as heat transfer mechanisms. Application of additional cooling means is therefore indicated.

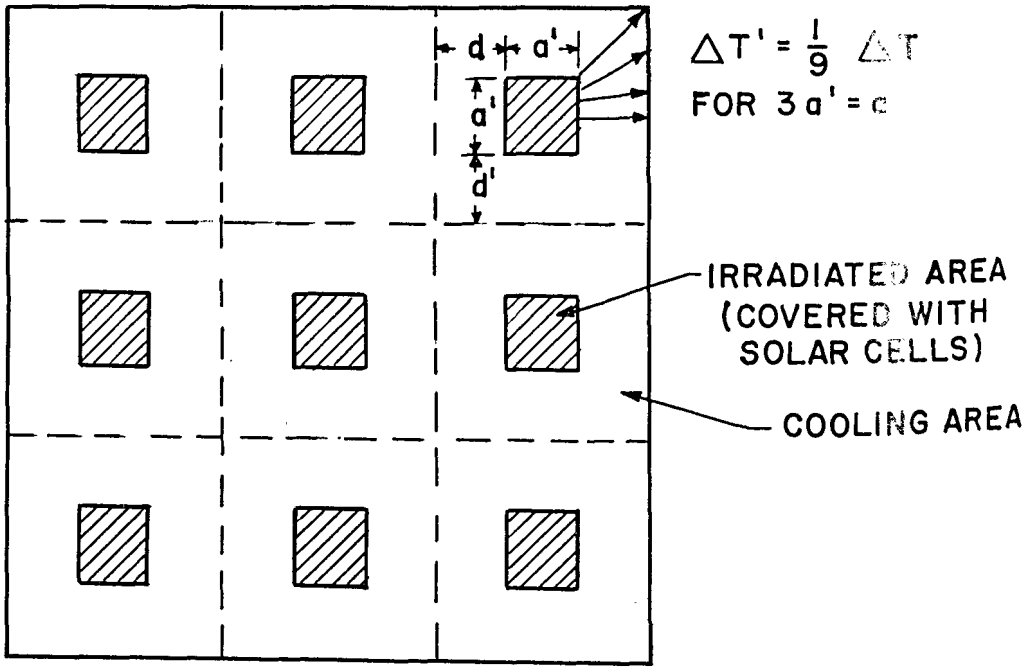
One method is forced convection, i.e., using a high heat capacity medium like water. Forced convection is, however, usually associated with energy consumption, i.e., in pumps, and is therefore undesirable for systems in which energy conservation is important. In some cases, free convection of the cooling liquid may be possible in closed or open cycle systems. Occasionally, a large reservoir functioning as heat sink may be available. In other cases, evaporative cooling may be applicable. One very practical method is the application of fins to increase the area for free convection. Increasing the cooling area twenty-fold reduces the temperature rise above the ambient to 17°C, without use of other control methods.

A method commonly used for temperature control on space vehicles consists in the application of optically selective coatings. Their use is indicated also for earth surface applications, independent of other temperature control methods applied. Some of these spectrally selective coatings filter the incident radiation by reflecting the photovoltaically ineffective radiation, thus reducing the temperature rise (12). Another coating is used to increase the emissivity of the solar cell active surfaces. Structural members exposed to the incident radiation are covered with a low absorptivity coating to reduce the energy absorption, but having high emissivity for black body radiation around 300°K.

Judicious selection of the most suitable combination of thermal control methods for the individual



a/STANDARD PANEL DESIGN WITH COOLING AREA



b/ MODULAR PANEL DESIGN WITH COOLING AREA

Figure 9

case will result in efficient application of the photovoltaic cells.

Energy storage methods

The most practical way of storing energy in a photovoltaic system is electrical storage. Due to its effect on over-all system size and cost, the most efficient storage method should be selected. At the present time, electrochemical batteries are indicated, although in the near future, reversible fuel cells are expected to become available and be preferred because of their higher efficiencies. In the meantime, the more expensive, but highly reliable sealed nickel cadmium storage cell may be preferred over the lead acid cell, which requires more control and frequent maintenance.

Conclusion

An analysis indicates that present photovoltaic solar energy converters are economically feasible for earth surface application in remote locations and at low power levels. Some design hints are given for such systems. The recent improvements for silicon solar cells are reviewed, and the direction towards lower cost photovoltaic converters is indicated.

References

1. Refer to vol. 3, *Energy Conversion for Space Power*, in the American Rocket Society series entitled *Progress in Astronautics and Aeronautics*, Academic Press, New York, 1961.
2. Snyder, N. W. and Karcher, R., Solar Cell-storage Battery Space Power System Review. Delivered at ARS Space Power Symposium, Santa Monica, California, September 27-30, 1960; published in vol. 3 of the ARS series entitled *Progress in Astronautics and Aeronautics*, Academic Press, New York, 1961.
3. Bennett, K. B., private communication.
4. Wolf, M., The Present State-of-the-Art of Photovoltaic Solar Energy Conversion. Presented at the 1961 Winter Convention on Military Electronics, February 1-3, 1961, Los Angeles, California; published in the June 1961 issue of *Solar Energy Journal*, Association for Applied Solar Energy, Tucson, Arizona.
5. Wolf, M., Limitations and Possibilities for Improvement of Photovoltaic Solar Energy Converters. Part 1 : Considerations for Earth's Surface Operation, *Proc. IRE, 48*, pp. 1246-1263, July 1959.
6. Wolf, M. and Prince, M. B., New Developments in Silicon Photovoltaic Devices and Their Applications to Electronics. Congress for Solid State Physics and its Applications in Electronics and Communications, Brussels, Belgium, June 2-7, 1958; Academic Press, Inc., New York, N.Y. (1960), Vol. 2.
7. Wolf, M., Advances in Silicon Solar Cell Development. The ARS Space Power Symposium, Santa Monica, California, September 27-30, 1960; published in vol. 3 of the ARS series entitled *Progress in Astronautics and Aeronautics*, Academic Press, New York, 1961.
8. Elliott, J. F., Meikleham, V. F. (Mrs.) and Kolbe, C. L., Thin Film Silicon Solar Cells. The Space Power Symposium of the American Rocket Society, Santa Monica, California, September 27-30, 1960; published in vol. 3 of the ARS Progress Series, Academic Press, New York, 1961.
9. Williams, R. and Bube, R. H., Photoemission in the Photovoltaic Effect in Cadmium Sulfide Crystals, *J. Appl. Phys.*, vol. 31, pp. 968-978 (June 1960).
10. Shirland, F. A., Photovoltaic Cadmium Sulfide, ARL Technical Report #62 93 (August 1960), Contract AF 33(616)-3466, Project No. 7116, Aeronautical Res. Lab., Air Force Res. Div., Air Res. and Dev. Command, Wright-Patterson AFB, Ohio.
11. Middleton, A. E., Gorski, D. A. and Shirland, F. A., Evaporated CdS Film Photovoltaic Cells for Solar Energy Conversion. Presented at the American Rocket Society Space Power Symposium, Santa Monica, California, September 27-30, 1960; published in vol. 3 of the ARS series entitled *Progress in Astronautics and Aeronautics*, Academic Press, New York, 1961.
12. Wright, W. V., Jr., Evans, W. H. and Mann, A. S., Solar Panel Design Considerations. The ARS Space Power Symposium, Santa Monica, California, September 27-30, 1960; published in vol. 3 of the ARS series entitled *Progress in Aeronautics and Astronautics*, Academic Press, New York, 1961.

Summary

Despite great strides made in the development of photovoltaic solar energy conversion for applications in space, little progress has been reported for earth surface applications. The reason for this lies in the severe competition from other energy sources, the exploitation of which frequently requires a lesser investment. The large investment needed for the utilization of solar energy is attributable to the low energy density of the radiation. The purpose of this paper is to investigate, first, under which conditions present silicon solar cells may be advantageously chosen for power supplies on the earth, and secondly, which new developments can lead to further solar energy utilization.

One present potential economical application is in remote, low-power, wireless communication stations. Such applications may involve a microwave relay station, a navigational beacon of the optical or radio type, or an observation post, be it of forestry, weather observation, civilian police or military nature. Applications without need for energy storage are more attractive due to simplicity, increased reliability and economy of the system. Usually, storage will be needed, however. Sealed nickel cadmium cells appear

to be the most suitable storage devices for remote locations. An analysis indicates that photovoltaic solar energy conversion systems at 20 W incur, during twenty years, lower total outlays than any other system, except for a power line available at a distance of less than 3½ miles. Even at the 100-W level, the photovoltaic solar energy converter is competitive for distances over 18 miles, and at the 1-kW level, for distances over 33 miles. Already on a two-year basis, small photovoltaic systems can well compete in remote locations with the other power sources, including power line, motor-generator, and dry cells.

The second part, treating new developments, deals with three approaches: improved efficiency of the converter cells, cost-reduction through new technologies and increased application of concentrators.

Efficiency improvements lead to reductions of size and cost of the over-all system. Recent developments on silicon solar cells increased the performance from about 8.5 per cent earth surface sunlight efficiency available on production line cells a little more than a year ago, to 11.5 per cent. Series resistance reduction through application of metallic grids over the diffused layer and a spectral response change were the major improvements. A survey of numerous efforts undertaken on other materials and methods does not show significant advances. The principle of multiple transitions, with its potential for the greatest efficiencies, was not further investigated, partly because of lack of basic knowledge of the properties of trapping levels.

Highest expectations for low cost and large area are attached to new technologies, especially to thin-film solar cells. Here, significant progress has been reported during the past year. The photoemissive properties of copper contacts on cadmium sulfide make this a natural candidate for a film device. Recently published early results of developmental work in progress at the Harshaw Chemical Company show that efficiencies of 2 to 2.5 per cent have been obtained on evaporated film cadmium sulfide solar cells of 20 cm² size. Efficiencies as high as 4.5 per cent have been obtained over small areas of these larger cells. This indicates that greater efficiencies should be obtainable with improved process control.

The application of concentrators permits covering part of the converter area with expensive photovoltaic cells, while filling the remainder with relatively inexpensive reflectors which direct the radiation onto the converting elements. Developments in progress on channel and truncated pyramid concentrators raise hopes for feasibility of larger-scale solar energy conversion. They provide concentration ratios of 2.5 and 5-7, respectively, while also permitting ready application of various thermal control methods.

Thermal control becomes most important with the application of concentrators. Methods for improved utilization of conduction and convection for solar cell cooling are discussed, with emphasis on modular design and use of fins.

The application of optically selective coatings to avoid absorption of photovoltaically ineffective radiation, and to obtain desired absorption and emission properties on solar cells and structural parts, as they have been developed and perfected for use on space vehicle solar converters, will be found most useful for thermal control on earth surface photovoltaic solar energy converters, especially if used in conjunction with other cooling methods.

NOUVEAUX PROGRÈS DANS LA CONVERSION PHOTOVOLTAÏQUE DE L'ÉNERGIE SOLAIRE EN VUE D'APPLICATIONS A LA SURFACE DE LA TERRE

Résumé

Malgré les grands progrès faits dans la mise au point de systèmes de conversion photovoltaïque de l'énergie solaire en vue de son utilisation dans l'espace interplanétaire, on ne signale que peu de progrès en ce qui concerne les applications à la surface de la terre. Cela peut être attribué à la concurrence intense que lui font d'autres sources d'énergie, et dont la mise en œuvre exige, le plus souvent, de moindres placements. Les gros investissements nécessaires en vue de l'utilisation de l'énergie solaire peuvent être attribués à la faible densité d'énergie du rayonnement. On se propose, dans le présent mémoire, de voir tout d'abord dans quelles conditions les cellules solaires actuelles, au silicium, peuvent être choisies de manière avantageuse aux fins de fournir de la force motrice sur terre et, deuxièmement, quels sont les nouveaux progrès qui pourraient mener à d'autres utilisations.

Une application économique possible s'adapte aux postes de télécommunication sans fils, se trouvant dans des lieux peu accessibles et exigeant peu d'énergie. Ces applications peuvent intéresser un relai en micro-ondes, une balise pour la navigation du type optique ou radio, ou encore un poste d'observation, qu'il s'agisse d'une forêt, d'un système météorologique, de la police, ou encore d'une installation militaire. Les applications dans lesquelles il n'est pas nécessaire de mettre l'énergie en réserve sont plus intéressantes, étant donné la simplicité du système, son économie et la meilleure régularité de fonctionnement. Mais il est généralement nécessaire de mettre de l'énergie en réserve. Les cellules hermétiques au nickel cadmium semblent constituer les dispositifs de mise en réserve les plus indiqués pour les lieux peu accessibles. Une analyse indique que des systèmes de conversion photovoltaïque de

l'énergie solaire à 20 Watts occasionnent, durant 20 ans, des dépenses totales inférieures à celles requises par tout autre système, sauf au cas où une ligne de transmission existe à une distance de moins de 5 km (3½ milles). Même au niveau de 100 W, le convertisseur d'énergie solaire photovoltaïque peut faire concurrence aux autres méthodes quand il s'agit de distances dépassant 18 milles (30 km) et au niveau de 1 kW pour des distances de plus de 33 milles (55 km). Sur une base de deux ans, de petits systèmes photovoltaïques peuvent dès maintenant faire concurrence aux autres sources d'énergie, dans les lieux peu accessibles, notamment aux lignes de transmission, aux groupes moteur-générateur et aux cellules sèches.

La deuxième partie du mémoire porte sur les nouveaux perfectionnements et s'intéresse à trois techniques : amélioration du rendement des cellules de conversion, réduction des frais par les nouvelles technologies, et application accrue des concentrateurs.

Les améliorations du rendement mènent à des réductions des dimensions et du coût de l'ensemble du système. Les progrès récents ayant trait au rendement des cellules solaires au silicium ont permis d'augmenter ce rendement disponible en surface pour la lumière solaire de 8,5 p. 100 environ, il y a un peu plus d'un an, à 11,5 p. 100 au moyen de leur fabrication en grande série. La réduction de la résistance en série par l'application de grilles métalliques sur la couche diffusée et des modifications dans la réponse spectrale, constituent les principales améliorations. Des études sur nombre d'efforts entrepris en ce qui concerne d'autres matériaux et d'autres méthodes, ne révèlent pas de progrès importants. Le principe des transitions multiples, avec la capacité de réaliser les plus grands rendements, n'a pas fait l'objet d'études plus poussées, partiellement en raison du manque de connaissances fondamentales sur les propriétés des niveaux dans lesquels les électrons sont capturés.

Les plus grands espoirs en ce qui concerne les grandes surfaces et les frais réduits sont orientés vers les nouvelles technologies, particulièrement celles des cellules solaires à pellicules minces. Ici on a signalé des progrès appréciables au cours de l'année écoulée. Les propriétés photo-émissives des contacts du cuivre sur le sulfure de cadmium en font un candidat tout naturel pour un système à pellicule. Les premiers résultats, récemment publiés, des travaux de développement en cours à la Harshaw Chemical Company révèlent que des rendements de 2 à 2,5 p. 100 ont été réalisés sur des cellules solaires au sulfure de cadmium à pellicule évaporée de 20 cm². Des rendements allant jusqu'à 4,5 p. 100 ont été réalisés sur des petites surfaces de ces plus grandes cellules.

Ceci indique que l'on pourrait réaliser de meilleurs rendements avec un meilleur contrôle des procédés de fabrication.

L'utilisation de concentrateurs permet de couvrir une partie de la surface du convertisseur par des cellules photovoltaïques coûteuses, tout en remplissant le reste avec des réflecteurs relativement peu coûteux; ceux-ci orientent le rayonnement vers les éléments de conversion. Les progrès faits sur les concentrateurs à cannelures et à pyramide tronquée permettent d'entrevoir la réalisation d'une conversion de l'énergie solaire à une plus grande échelle. Ils permettent de réaliser des rapports de concentration de 2,5 et 5 à 7 respectivement, tout en permettant une application facile de diverses méthodes de contrôle thermique.

Le contrôle thermique devient très important avec l'application des concentrateurs. Les méthodes d'amélioration de l'utilisation de la conduction et de la convection pour le refroidissement des cellules solaires sont passées en revue, en soulignant la technique modulaire et l'utilisation des ailettes.

Surtout s'il en est fait usage en liaison avec d'autres méthodes de refroidissement, il sera particulièrement utile, pour la commande thermique à la surface de la terre avec des convertisseurs d'énergie solaire, de procéder à l'application de couches optiquement sélectives pour éviter l'absorption d'un rayonnement inefficace du point de vue photovoltaïque, et pour obtenir les propriétés recherchées d'absorption et d'émission des cellules solaires et des pièces structurelles perfectionnées qui ont été mises au point pour leur utilisation dans des convertisseurs d'énergie solaire pour véhicules inter-planétaires.

Agenda item III.A

SOLAR ENERGY AVAILABILITY AND INSTRUMENTS FOR MEASUREMENT

Point III.A de l'ordre du jour

ÉNERGIE SOLAIRE DISPONIBLE ET INSTRUMENTS DE MESURE

Chairman — Président

Andrew J. DRUMMOND

Rapporteur

Pedro BLÁNCO

SOLAR ENERGY AVAILABILITY AND INSTRUMENTS FOR MEASUREMENT

Pedro Blanco *

The utilization of solar energy, like that of any other form of energy, must be based on the most exact possible knowledge of its characteristics, since the machines, apparatus and installations for such utilization must be designed having regard to the structure, concentration, variation, location, etc., of this energy, and the service that such installations are intended to provide. The problem of determining the availability and characteristics of solar energy is of basic importance. This is, of course, the reason for its inclusion in the programme of the United Nations Conference on New Forms of Energy. The number and quality of the papers on the theme "Solar energy availability and measurement instruments" are likewise an indication of the general interest in this problem and provide existing and proposed approximations and means for its satisfactory solution.

It must, on the other hand, be borne in mind that, from the point of view of this conference, the fundamental object of determining the availability and characteristics of solar energy is its utilization for human welfare. This is, of course, an object of clearly utilitarian nature, and the scientific and technical aspects of this problem must therefore be so oriented as to render the desired practical result attainable.

Available solar energy and networks for its measurement

Total quantity of energy

The assessment of the solar energy incident on a surface normal to the solar beams at the outer boundary of the earth's atmosphere leads us to what is termed the "solar constant". Its generally accepted value of 1.98 cal cm^{-2} min^{-1}, or 138 mw cm^{-2}, indicates that the solar energy incident on the entire surface of the earth, allowing for the part reflected, diffused and absorbed by the atmosphere, is expressed by the enormous figure of 2 300 Q/year (Q — 0.25 × 10^{18} kcal), which is more than the entire energy contained in all existing reserves of fossile fuel, together with the fission energy of all known uranium and thorium reserves (1). Part of this fabulous store of energy is indirectly utilized by man in the form of plant and animal products, i.e., rain, wind, etc. But the average radiation incident on the continents and islands is approximately 600 Q/year, and this is the part most easily utilized by man, whose activities for the most part take place on land. The direct utilization of as much of this immense amount of energy as possible is the object of the attempt to learn its properties on a world-wide scale, in the greatest practicable detail.

This quantity of 600 Q/year is not uniformly distributed over the land surface rising above the waters, and while it is easy to determine the influence of some of the factors responsible for its unequal distribution, such as the geographic location and the air mass, when the atmosphere is uncontaminated (2), there are also other factors, such as topography, meteorological elements, atmospheric dust and contamination, etc., whose theoretical estimation involves certain difficulties. Accordingly, to learn the distribution and availability of solar energy on the land surface, this energy must be measured in the greatest possible detail.

Solar measurement networks

This work of measuring solar energy is being performed in Australia (S/32), Canada (S/18 and S/20), France (S/69), India (S/60 and S/105), Japan (S/2), and many other countries interested in harnessing the new sources of energy, especially those of the flux type, in order to economize the natural deposits of fossil and nuclear fuels as much as possible. Recent statistics indicate that some 330 pyrheliometric stations in the various countries of the world are today engaged in recording total solar radiation. (2) The density of distribution of these stations, whether related to national area or to population, varies from country to country. Unfortunately, the countries with extensive arid zones, which in general are also under-developed, are the very countries with the smallest numbers of such stations per unit area, although the utilization of that energy would be of advantage to many of them, in view of the scarcity or high cost of conventional sources of energy in their territory.

A study of papers S/2, S/18, S/20, S/32, S/60, S/62, S/69, S/74 and S/105, and of the numerous available data on solar radiation, shows that most of the stations of the world solar measurement network belong to meteorological and geophysical networks which, for very understandable and appropriate reasons, are located on sites which, however suitable for meteorological and geophysical observations, are not, in many cases, the most suitable for solar energy utilization. The detection of the microclimates that may frequently occur in highly dissected areas demands a network of stations usually denser than the meteorological network,

* Director, Comisión Nacional de Energías Especiales, Madrid.

sited at locations unusual for meteorological work but demanding rational examination in advance, having regard to local topographic and meteorological conditions. In regions with faint topographic and hydrographic detail, lower densities may be permissible for solar energy networks, but in establishing them, one must always remember the possible variations in atmospheric humidity between the coast and interior of such regions.

Finally, there is the problem of setting up solar measurement networks in desert regions, which must be studied with reference not only to the local needs for service but also to the possible utilization of the energy available there. The low population of such zones limits the local demand for energy, but perhaps an appropriate reconstruction plan for these areas, together with the harnessing of solar energy, might encourage the settlement of the regions selected, just as the establishment of means of transportation, sewage systems, water, gas and electricity "direct" the development and growth of the great urban centres.

It is only by means of an adequate and rational network for solar energy measurement on a world-wide scale, with a view to the harnessing of solar energy, that the distribution and local characteristics of solar energy available on the earth's surface can be learned, on a global basis, with sufficient guarantee of accuracy. The fact that many of the countries in highly insolated areas are under-developed and possess extensive desert zones leads one to believe that this ideal network cannot be established without recourse to international co-operation. It would be desirable if an agreement on such co-operation could be reached through appropriate international agencies and/or associations, so that the improvement of the solar measurement networks of the more highly developed countries, taken together with those that might by agreement be established in the under-developed countries, would constitute a world network for this purpose. This would permit the completion, with a higher degree of precision, of a task as interesting as that accomplished by Black on the distribution of solar radiation over the earth's surface (3).

Instrumentation for measuring solar radiation

Solar radiation on the earth's surface

To understand the difficulty presented by the problem of recording the solar energy it should be remembered that, near the earth's surface, where it is easiest to locate machines for harnessing this energy, the components of solar radiation reduce down, in the simplest scheme, to direct radiation, diffuse radiation, and radiation reflected by the earth's surface. The energy spectrum of each of these components has well-known limits, although its maximum may vary with elevation above sea level, atmospheric transparency or turbidity, the nature and size of the particles responsible for such turbidity, the local character of the terrain, etc. The percentage share of each of these components in the total radiation received by a body likewise varies, primarily with the astronomical, geographical, and meteorological variables, and with the varying atmospheric contamination. In many cases the total flux of calorific radiation, whatever its composition, can be utilized. For certain special applications, however, such as those requiring the use of focal concentrators, the only radiation of basic utility is the direct radiation whose parallel beams may be utilized by appropriate orientation of the axis or plane of symmetry of the concentrators. While it may be sufficient, for most of these applications, to know the total radiation received, there are cases where the value of each of the above components must be known separately, sometimes also including the nocturnal radiation emitted by the earth itself, as a hot body.

It is therefore not surprising that the numerous and valuable papers presented to this section of the conference should include studies of the solar radiation and instrumentation for measuring it by Gräfe (S/61), Peyturaux (S/69), Perrin de Brichambaut (S/80), Schoffer, Kuhn and Sapsford (S/92) and Drummond (S/117); studies on insolation and natural illumination in its architectural applications, by Dogniaux (S/59); on mean levels of total radiation incident on vertical and inclined surfaces, based on solar data, by Page (S/98), and on certain aspects of solar radiation in relation to its energetic utilization, by Flach and Mörikofer (S/74). The nocturnal radiation from horizontal surfaces in arid zones has likewise been the subject of study and measurement by Yellott and Kokoropoulos (S/34), and by Gondet (S/95). On the other hand, the nocturnal radiation from various materials has also been studied and measured, for application to the problem of residential air-conditioning in desert areas.

The solar energy data required for planning apparatus utilizing such energy

For the purpose of planning apparatus and installations for utilizing solar energy, it is usually necessary to know, for the projected site of the machine, over the longest possible period—covering several successive years—at least the diurnal march of direct and diffuse solar radiation incident on a horizontal surface. The ideal would be to have a continuous daily record of the variation of intensity of each of these radiations, thus indicating the maximum values of the components of the solar radiation received in the locality, to enable engineers to predict the maximum possible production. Starting out from these data in the form of continuous records, the total and mean daily, monthly and annual values may be determined, if desired. Moreover, for the purpose of determining the size and cost of the energy storage installations, in those plants that require them, it will also be necessary to derive from these continuous records the curves indicating the frequency distribution of the number of days or hours which, over the course of the year,

reach specified values of intensity of energy. Black has done this for various localities (S/13). To give the greatest possible reliability to these curves of statistical distribution of energy throughout the year, data for a large number of years should be utilized, and these data, since they are strongly influenced by meteorological factors, should cover at least an elementary 11-year cycle. However, if a limit of error for the actual mean value is fixed for it (S/13), the number of years to be covered may be decreased or increased in accordance with the local meteorological characteristics. The ideal would be, for greater accuracy and speed in the processing of the results, to have the radiation records so arranged as to be easily processed by electronic computers.

Unfortunately there are many places today which might be of interest for the installation of plants for utilization of solar energy in which the records indicated in the preceding paragraph are not available. It will take an average of ten years to accumulate such records. Since it is reasonable to expect that the use of installations for harnessing solar energies will become wide-spread before this period of ten years has passed, Perrot and Touchais have developed a method which uses the sunshine duration data, recorded by means of simple sunshine recorders at most meteorological stations, for the purpose of planning solar energy installations (S/41). Use of such data is naturally an advantage. This is an important contribution to fill the need for solar data for designing solar installations, until sufficient statistical data of solar radiation records with the characteristics indicated above become available.

Apparatus employed for recording solar radiation

Solar energy data for planning solar installations are not at present recorded with Campbell-Stokes or Jordan sunshine recorders (4), nor with instruments like the Abbot water-flow pyrheliometer (5), the Abbot silver-disc pyrheliometer (6), or the Ångström compensation pyrheliometer (7), which are generally used for precision measurements and are reference instruments in primary meteorological stations, at which the calibration system prescribed by recommendation I of the 1956 International Radiation Conference must be maintained (8). Such instruments require qualified and very experienced personnel to operate them.

A sollar radiation record that can be used for planning purposes may be made with instruments which have been used for years by the meteorological services of many countries in their secondary stations. They are characterized primarily by the continuous recording of global solar radiation (direct and diffuse) or of the diffuse radiation alone. Almost always, however, they measure the sunshine on a horizontal plane, in order to simplify the instrument mechanically. They are based on two essentially different systems. One group includes bimetallic actinometers, such as the Fuess-Robitzsch actinometer (9) and similar instruments. The other group includes thermoelectric actinometers, such as the Eppley pyrheliometer (pyranometer), the Moll-Gorczynski solarimeter, and similar instruments. While the value of the direct solar radiation may be found by taking the difference, when these instruments are used, it may also be found directly with a pyrheliometer, such as the Abbot silver-disc instrument already mentioned, or similar types. For cases where a continuous record of solar radiation is not required, the well-known simple Bellani distillation pyranometer, or lucimeter, is ordinarily used (11).

The idea of having solar energy recorders that are inexpensive, resistant to atmospheric influences and simple to operate, for manufacture in large-scale series with prospects of possible expansion of the solar measurement networks, has been considered by various specialists, with the following interesting results :

(*a*) A solar calorimeter, described in S/9, has been designed and tested by Heywood. This calorimeter, like the Bellani lucimeter, gives the total number of calories received from the sun at its site taken from a single reading every 24 hours. Under certain conditions, these results show appreciable disagreement with those obtained by more precise instruments. The author estimates the cost of this calorimeter at about U.S. $18. It is now in the testing stage.

(*b*) The possible use of the solar cell as a pyranometer has been studied by MacDonald, who found the errors of spectral response, the apparent sturdiness and the rapid response tolerable by comparison with the fragility and slower response of thermopile pyranometers (11). Schoffer, Kuhn and Sapsford (S/92) have also done work in this direction with the silicon cell, and their results are very promising. The silicon-cell pyranometer readings show slight discrepancies ($< \pm$ 0.05 Ly/min) from those of the Eppley pyrheliometer (pyranometer), but they are practically compensated for in the total value for the daily radiation.

(*c*) A solar radiation integrator, based on the silicon cell, has also been developed by Schoffer, Kuhn and Sapsford (S/92), since it was found the solar radiation data are more useful for certain applications in the integrated form. Their tests on this integrator have given satisfactory results; the maximum error was 2 per cent.

(*d*) Schoffer, Kuhn and Sapsford (S/92) have developed an economical pyrheliometer (radiometer) based on the economical Suomi-Kuhn radiometer (12). The test results are promising; the error is of the order of 5 per cent. It will cost less than $50, since the basic radiometer is available commercially for about $10.

Required accuracy of solar radiation records

Several types of existing solar radiation recorders show an extraordinary dispersion between their mean readings, while others are well compensated

(S/117), with an error of the order of ± 1 per cent, which we regard as too small for engineering use. We consider that, for purposes of calculation, local solar radiation data may be acceptable if the error in the total daily reading does not exceed ± 4 - 5 per cent, since the other design data, such as mechanical resistance, thermal conductivity, etc., of the materials, and the very hypotheses of calculation, contain greater errors.

We consider that a maximum error of ± 5 per cent in the total daily readings and ± 10 per cent in instantaneous readings has already been attained, and that the manufacturers of solar radiation recorders could easily do better. If these limits were adopted, the makers could pay more attention to the other characteristics of these recorders. Drummond (S/117) gives an excellent list of the principal features desirable for solar radiation recorders. The following might well be added to this list, in view of the possible increase in the number of secondary stations located in under-developed countries:

(1) Ease of operation by non-specialized personnel.

(2) Difficulty of accidental decalibration during operation—that is, good long-term stability of calibration.

We consider that, in the present state of the art, the known ideas and systems could be improved to give an instrument that would continuously record the global solar radiation (direct and diffuse), with a satisfactory degree of compromise between the individual characteristics in the above group, and which could be series-produced at reasonable cost. An instrument of this kind could serve for "standard" use at the secondary stations, to record the solar radiation with a view to its utilization. It is to be hoped that the instrument makers, faced with this possibility, will intensify their interesting work of research and testing and will orient it to this end.

Conclusion

One of the practical objects of this United Nations Conference on New Sources of Energy is, of course, the utilization of solar energy for the welfare of mankind. For this purpose, a study of the valuable papers presented under section III.A of the agenda, and a general study of the theme of this section, permits us to draw the following conclusions:

(1) After rational study, the network of actinometric stations should be expanded to provide the most exact knowledge possible of the distribution of solar energy over the surface of the earth, to disclose the microclimates, and, in general, the zones where solar energy is at levels sufficient for utilization.

(2) The allowable errors of solar radiation records should be raised to limits permitted by conservative standards of design, to facilitate the manufacture of recording instruments and lower their cost.

(3) The great variety of instruments now in use at secondary stations for recording solar radiation should be reduced to a single type for each class of measurement. This type should possess characteristics suitable to combine the advantages of series production with those of more convenient comparison of the results, by combining the methods and scales of measurement.

(4) A "standard" system of presentation of the data of solar radiation measurements should be adopted for all places, to make them as useful as possible for planning apparatus to utilize solar energy.

Themes proposed for discussion

(1) Ways of attaining international co-operation to expand the network of actinometric stations into an efficient and integrated body.

(2) Maximum allowable limits of error of measurement of actinometric records for design purposes.

(3) Most appropriate characteristics to be possessed by possible "standard" solar radiation recorders for planning purposes, and the path towards their development.

(4) "Standardization" of data for planning purposes, derived from solar radiation recorders.

References

1. Azcarraga, L. de., Aprovechamiento de las energías solar y cólica. Tomo V, *Sección II C, Publicaciones de la Sesión Parcial de Madrid de la Conferencia Mundial de la Energía.* Junio 1960.
2. Ward, G. T., Possibilities for the utilization of solar energy in under-developed rural areas. FAO Farm Power and Machinery, *Informal Working Bulletin No. 16,* 1961.
3. Black, J. N., The Distribution of Solar Radiation over the Earth's Surface. *Arch. Met. Geophys. Bioklimatol.* Springer, Verlag, Vienna. Series B, 7 (2): 165-189, 1956.
4. Knowles, W. E. and Spilhaus, A. F., Meteorological Instruments, *University of Toronto Press,* 1953.
5. Abbot, C. G. and Aldrich, L. B., An improved water-flow pyrheliometer and the standard scale of solar radiation. *Smithsonian Miscellaneous Collections, 87 (15),* 1932.
6. Aldrich, L. B., The Abbot silver-disc pyrheliometer, *Smithsonian Miscellaneous Collections, III (14),* 1949.
7. Ϛngström, K., The absolute determination of the radiation of heat with the electric compensation pyrheliometer, with examples of the application of the instrument. *Astrophysic Journal,* University of Chicago Press, 9, 1899.
8. Conférence internationale du rayonnement, Recommandations I à VIII. Résolution I. *CIMO-II/Doc. 7,* Annexe III, 1956.
9. Robitzsch, M., Über den Bimetallaktinographen Fuss-Robitzsch, *Gerlands Beitr. Geophys.,* 35, 1932.
10. Ranzi, I., Una priorita italiana : l'attinometro a distillazione de Bellani. *Nuovo Cimento.* ann. V, no. 6, 1928.
11. MacDonald, T. H., The Solar Cell as a Pyranometer Receiver, Instruments-Automation Conference. Preprint number 12-NY60, 1960.
12. Suomi, V. E. and Kuhn, P. M., An Economical Net Radiometer, *Tellus, 10,* No. 1, 1958.

ÉNERGIE SOLAIRE DISPONIBLE ET INSTRUMENTS DE MESURE

(Traduction du rapport précédent)

Pedro Blanco *

L'utilisation de l'énergie solaire, comme celle de tout autre type d'énergie, doit être fondée sur la connaissance la plus précise possible des caractéristiques de cette énergie, puisque les machines, les dispositifs et les installations destinés à cette utilisation doivent être conçus en fonction de la structure, de la concentration, de la variation, de la localisation, etc. de l'énergie solaire; il en va de même des fonctions que doivent remplir ces installations. L'inscription du problème posé par l'acquisition de connaissances sur la disponibilité et les caractéristiques de l'énergie solaire à l'ordre du jour de cette Conférence des Nations Unies sur les sources nouvelles d'énergie est due, sans aucun doute, à son importance fondamentale. D'autres signes de l'intérêt général que suscite ce problème sont la quantité et la qualité des mémoires présentés sur le sujet « Énergie solaire disponible et instruments de mesure ». Ces mémoires montrent les approximations et les moyens utilisés ou proposés pour aboutir à une solution convenable.

Il convient de tenir compte d'autre part que, du point de vue de cette Conférence, le principal but à atteindre grâce à la connaissance de l'énergie solaire disponible et de ses caractéristiques est son utilisation pour le bien-être de l'homme. C'est un but, sans aucun doute, de caractère profondément utilitaire, et l'étude scientifique et technique de ce problème doit donc être orientée d'une façon qui permette d'atteindre le résultat pratique attendu.

Énergie solaire disponible et réseaux de prospection

Quantité globale d'énergie

L'évaluation de l'énergie solaire incidente sur une surface perpendiculaire aux rayons solaires à la limite extérieure de l'atmosphère terrestre conduit à ce que l'on appelle la « constante solaire » dont la valeur adoptée actuellement est de 1,98 cal cm^2 min^{-1}, soit 138 mW cm^{-2}. Ainsi, la quantité d'énergie solaire qui parvient à la surface du globe atteint, après soustraction de l'énergie réfléchie, diffusée et absorbée dans l'atmosphère, l'énorme valeur de 2 300 Q/an ($Q = 0{,}25 \times 10^{18}$ kcal), supérieure aux réserves actuelles de tous les gisements naturels de combustibles fossiles et aux réserves d'énergie de fission obtenue à partir de l'uranium et du thorium (1). L'homme profite indirectement d'une partie de cette quantité fabuleuse d'énergie sous forme de production végétale et animale, de pluie, de vent, etc. Mais la fraction qui peut parvenir en moyenne à la surface des continents et des îles et qui est plus facilement utilisable de façon directe par l'homme dont les activités se déroulent sur terre ferme, atteint environ 600 Q/an. L'utilisation directe de la fraction la plus accessible de cette importante quantité d'énergie justifie les tentatives faites à l'échelle mondiale pour acquérir les connaissances les plus détaillées possibles de ses propriétés.

La quantité de 600 Q/an, mentionnée plus haut, n'est pas distribuée de façon uniforme à la surface qui émerge des océans; l'influence de certains des facteurs qui provoquent cette irrégularité de distribution peut être déterminée facilement comme dans le cas de la situation géographique (2) et de la masse d'air lorsque l'atmosphère est pure, mais il en existe d'autres, par exemple, la configuration topographique, les variables météorologiques, les poussières et la pollution de l'atmosphère, etc., dont l'appréciation théorique se heurte à certaines difficultés. Pour cette raison, la connaissance de la distribution et de la disponibilité de l'énergie solaire à la surface de la terre exige des mesures directes, détaillées au maximum.

Réseaux de prospection

Ce travail de mesure de l'énergie solaire est effectué par l'Australie (S/32), par le Canada (S/18 et S/20), par la France (S/69), par l'Inde (S/60 et S/105), par le Japon (S/2) et par de nombreux autres pays qui s'intéressent à l'utilisation des sources nouvelles d'énergie, en particulier d'énergie à flux, afin d'économiser au maximum les réserves naturelles de combustibles fossiles et nucléaires. Il semble, d'après les statistiques récentes (2), qu'il existe dans les divers pays du monde près de 330 stations pyrhéliométriques qui accumulent des renseignements sur le rayonnement global. D'un pays à l'autre, la densité de ces stations varie considérablement tant du point de vue de la superficie qu'elles couvrent que de celui de la population. Malheureusement, les pays qui présentent de grandes étendues arides et qui sont, en général, peu développés, sont ceux qui possèdent, proportionnellement à leur surface, le plus petit

* Directeur de la Comisión Nacional de Energías Especiales, Madrid.

nombre de stations d'enregistrement de l'énergie solaire, alors que la plupart d'entre eux pourraient tirer un avantage notable de l'utilisation de cette énergie, étant donné la rareté ou le prix élevé, dans ces pays, de l'énergie provenant d'autres sources.

Il ressort de l'étude des mémoires S/2, S/18, S/20, S/32, S/60, S/62, S/69, S/74, S/105 et des nombreux renseignements disponibles sur le rayonnement solaire, que les stations du réseau mondial actinométrique correspondent, dans leur majorité, aux réseaux météorologiques et géophysiques, dont la distribution géographique convient pour des raisons évidentes aux fins météorologiques ou géophysiques, mais n'est pas toujours la plus propice aux études concernant l'utilisation de l'énergie solaire. La détection de microclimats, fréquents dans les régions caractérisées par une orographie accidentée, exige l'établissement en des points peu habituels pour les travaux météorologiques d'un réseau généralement plus dense que le réseau météorologique et fondé sur des études préliminaires judicieuses qui tiennent compte des conditions orographiques et météorologiques locales. Dans les régions à orographie ou à hydrographie peu détaillées, on pourra admettre un réseau de prospection solaire moins dense, mais il faudra considérer, lors de son établissement, les variations de l'humidité qui peuvent se présenter entre la côte et l'intérieur du pays. Finalement, le problème de l'établissement de réseaux de prospection solaire dans les zones désertiques doit être étudié sous ses deux aspects, à savoir : celui des besoins locaux et celui de l'utilisation éventuelle de l'énergie disponible. A cause de la faible densité de population de ces régions, les besoins en énergie y sont peu importants, mais il se pourrait qu'un programme convenable de développement, comprenant l'utilisation d'énergie solaire, favorise le peuplement des zones choisies, de la même façon que les voies de communication, les canalisations d'eau, de gaz et d'électricité « dirigent » l'accroissement et l'extension des grands centres urbains.

Seul un réseau actinométrique convenable et judicieux, établi à l'échelle mondiale en vue de l'utilisation de l'énergie solaire, peut permettre d'accumuler des connaissances suffisamment certaines de la distribution et des caractéristiques locales des quantités de cette énergie qui sont disponibles à la surface terrestre. Le fait qu'un grand nombre des pays situés dans des zones de fort ensoleillement soient insuffisamment développés et possèdent de grandes étendues désertiques, conduit à supposer que l'établissement d'un tel réseau idéal ne pourra pas être réalisé sans faire appel à la collaboration internationale. Il serait souhaitable qu'un accord soit conclu par l'intermédiaire des organisations et/ou des associations internationales compétentes au sujet d'une telle collaboration, de façon que les réseaux actinométriques perfectionnés des pays à niveau de développement élevé et ceux qu'il serait convenu d'établir dans les pays sous-développés s'intègrent au réseau mondial aux fins de cette prospection. Cela permettrait de réaliser avec une précision plus grande des travaux aussi intéressants que celui de Black (3) sur la distribution du rayonnement solaire à la surface de la terre.

Instruments de mesure de l'énergie solaire

Rayonnement solaire reçu par la surface du globe terrestre

Pour comprendre les difficultés du problème posé par l'enregistrement de l'énergie solaire, il convient de rappeler qu'au voisinage du sol, là où il est le plus aisé d'installer les dispositifs qui serviront à capter cette énergie, le schéma le plus simple du rayonnement solaire comprend trois composantes : le rayonnement direct, le rayonnement diffusé et le rayonnement réfléchi par la surface terrestre. Le spectre d'énergie de chacune de ces trois composantes comporte des limites bien connues, mais ses valeurs de pointe peuvent varier avec l'altitude du sol, la transparence ou la turbidité de l'atmosphère, la nature et les dimensions des particules qui la troublent, la nature locale de la surface terrestre, etc. D'autre part, le pourcentage du rayonnement total reçu par un corps, correspondant à chacune des composantes indiquées plus haut, varie également, surtout en fonction de variables astronomiques, géographiques, météorologiques et aussi en fonction des variables de la pollution atmosphérique. Très souvent, il est possible d'utiliser le flux total du rayonnement calorifique indépendamment de sa composition, mais pour certaines applications particulières, comme dans tous les cas où l'on fait appel aux récepteurs à focalisation, seule la composante directe, dont les rayons parallèles sont captés en orientant de façon convenable l'axe ou le plan de symétrie de ces récepteurs, présente une utilité véritable. C'est pourquoi, bien qu'il suffise pour la plupart des applications de connaître le rayonnement global reçu, il existe des cas où il est nécessaire de disposer des valeurs de chacune des composantes et parfois, également, de celle du rayonnement nocturne émis par la terre en tant que corps chaud.

Il n'est donc pas étonnant que parmi les nombreuses communications de grande valeur présentées à cette séance de la Conférence se trouvent les travaux de Gräfe (S/61), Peyturaux (S/69), Perrin de Brichambaut (S/80), Schöffer, Kuhn et Sapsford (S/92) et de Drummond (S/117) sur le rayonnement solaire et les instruments qui servent à le mesurer; les travaux de Dogniaux (S/59) sur l'ensoleillement et l'éclairage naturel tel qu'il s'applique en architecture; le mémoire de Page (S/98) sur les niveaux moyens du rayonnement total reçu par les surfaces : verticales et inclinées, basé sur les relevés du rayonnement solaire; et la communication de Flach et Mörikofer (S/74) sur certains aspects du rayonnement solaire relatifs à son utilisation énergétique. En outre, le rayonnement nocturne émis par les

surfaces horizontales dans les régions arides a été étudié et mesuré par Yellot et Kokoropoulos (S/34), de même que le rayonnement nocturne de divers matériaux en vue des applications aux problèmes de climatisation de l'habitation dans les zones désertiques, par Gondet (S/95).

Renseignements sur l'énergie solaire indispensables pour les projets de dispositifs d'utilisation

En général, l'élaboration des projets de dispositifs et d'installations d'utilisation de l'énergie solaire exige au moins la connaissance de la variation journalière, au lieu considéré pour leur établissement, des composantes directe et diffusée du rayonnement solaire reçu par une surface horizontale pendant une période aussi longue que possible, s'étendant sur plusieurs années consécutives. La solution idéale serait de pouvoir disposer d'enregistrements journaliers continus des variations de l'intensité de chacune de ces composantes, ce qui permettrait de connaître les valeurs maximales des composantes du rayonnement reçu au lieu considéré; ces valeurs sont indispensables aux ingénieurs pour prévoir la production maximum possible. A partir de ces données, obtenues sous forme d'enregistrements continus, il est possible de déterminer les valeurs totales et moyennes, journalières, mensuelles et annuelles qui sont également intéressantes. De plus, pour établir les dimensions et le coût des dispositifs d'emmagasinage de l'énergie dans les installations où ils sont nécessaires, il faudra déduire, à partir de ces enregistrements continus, les courbes qui montrent la distribution spectrale du nombre de jours ou d'heures correspondant, au cours de l'année par exemple, à des valeurs déterminées de l'intensité de l'énergie, comme cela a été fait par Black (S/13), pour certaines régions. Pour obtenir la certitude la plus grande possible pour ces courbes spectrales ou de distribution statistique de l'énergie pendant l'année, il convient d'utiliser des données qui correspondent à un grand nombre d'années consécutives; comme ces données sont fortement influencées par les facteurs météorologiques, elles devraient s'étendre au moins au cycle élémentaire de onze années. Toutefois, si on fixait à cette fin une limite de l'erreur relativement à la valeur moyenne réelle (S/13), ce nombre d'années pourrait être augmenté ou diminué selon les caractéristiques météorologiques locales. Les meilleures conditions pour une plus grande certitude et une plus grande rapidité d'élaboration des résultats, sont celles où l'on peut préparer facilement les chiffres du rayonnement de façon qu'ils puissent être traités par les calculatrices électroniques.

Malheureusement, il existe actuellement de nombreuses régions où il pourrait être intéressant d'installer des machines d'utilisation de l'énergie solaire et pour lesquelles on ne dispose pas de données semblables à celles qui sont indiquées au paragraphe précédent et dont l'accumulation exige en moyenne une dizaine d'années. Il est raisonnable de supposer que l'emploi des appareils d'utilisation de l'énergie solaire se répandra avant la fin de cette période, et Perrot et Touchais (S/41) ont élaboré une méthode dont l'avantage est de permettre l'utilisation aux fins des projets d'installations solaires des données sur l'ensoleillement recueillies jusqu'à présent par la plupart des stations météorologiques à l'aide d'héliographes simples; leur travail constitue une contribution importante au problème des besoins en renseignements sur le rayonnement solaire nécessaires pour l'étude des projets d'installations solaires jusqu'à ce que soient disponibles des statistiques suffisantes du rayonnement solaire avec les caractéristiques indiquées au paragraphe précédent.

Instruments utilisés pour l'enregistrement du rayonnement solaire

Actuellement, l'enregistrement des données de l'énergie solaire nécessaires aux études de projets d'installations solaires n'est effectué ni à l'aide d'héliographes du type Campbell-Stokes ou du type Jordan (4), ni avec des instruments tels que le pyrhéliomètre à eau d'Abbot (5), le pyrhéliomètre à disque d'argent d'Abbot (6) ou le pyrhéliomètre à compensation d'Ångström (7), qui sont les appareils utilisés d'ordinaire pour effectuer les mesures de précision ou comme étalons dans les stations météorologiques primaires et pour lesquels il convient d'appliquer les dispositions de la Recommendation I de la Conférence internationale du rayonnement de 1956 (8) concernant la correspondance des échelles, et qui sont en outre des appareils devant être manipulés par un personnel qualifié, possédant une grande expérience.

Les relevés du rayonnement solaire, utilisables pour l'établissement de projets, peuvent être obtenus à l'aide des appareils dont se servent depuis des années les stations secondaires des services météorologiques de nombreux pays et dont le caractère principal est d'enregistrer en continu le rayonnement solaire global (direct et diffusé) ou le rayonnement diffusé seul, en mesurant presque toujours l'insolation dans un plan horizontal, par souci de simplicité mécanique. Les deux systèmes d'enregistreurs qui diffèrent par leur principe sont les actinomètres bimétalliques, entre autres le solarimètre du type Füess-Robitzsch (9), et les actinomètres thermoélectriques tels que le pyrhéliomètre (pyranomètre) du type Eppley, le solarimètre du type Moll-Gerczynski, etc. Bien qu'il soit possible de déduire la valeur de la composante directe par soustraction des résultats donnés par ces appareils, on peut également l'obtenir de façon directe, à l'aide d'un instrument tel que le pyrhéliomètre à disque d'argent d'Abbot, mentionné plus haut, par exemple. Dans les cas où la continuité des relevés n'est pas indispensable, on utilise fréquemment le pyranomètre de Bellani, appareil simple et bien connu (10).

Étant donné les perspectives d'amplification des réseaux de prospection, divers spécialistes ont étudié la conception, pour une fabrication industrielle,

d'enregistreurs de l'énergie solaire, économiques, résistants aux agents atmosphériques et simples à manipuler; les résultats intéressants obtenus sont les suivants :

a) Un calorimètre solaire, décrit dans la communication S/9, conçu et essayé par Heywood. Ce calorimètre donne, en une seule lecture effectuée toutes les 24 heures, de même que le pyranomètre de Bellani, la quantité totale de calories reçues du soleil au lieu de son installation; dans certaines conditions, ces relevés présentent des écarts sensibles par rapport aux résultats obtenus avec des instruments de plus grande précision. L'auteur estime le prix de cet appareil à 18 dollars environ. Le calorimètre se trouve actuellement au stade expérimental;

b) La possibilité d'utiliser la cellule solaire comme pyranomètre a été étudiée par Mac Donald (11); cet auteur estime que les erreurs de réponse spectrale de la cellule sont admissibles et que sa robustesse et sa rapidité de réponse dépassent celles des pyranomètres à thermopile. Schöffer, Kuhn et Sapsford (S/92) ont également effectué des recherches dans ce sens avec des cellules au silicium. Les résultats de leurs expériences semblent très prometteurs : les faibles écarts (inférieurs à $\pm$ 0,05 Ly/min) entre les résultats du pyranomètre à cellule au silicium et ceux du pyrhéliomètre (pyranomètre) du type Eppley sont pratiquement compensés sur le total du rayonnement journalier;

c) Un intégrateur de rayonnement solaire, à cellule au silicium, élaboré par Schöffer, Kuhn et Sapsford (S/92), compte tenu de l'utilité plus grande pour certaines applications de données sur le rayonnement solaire obtenues sous forme intégrée; les expériences effectuées à l'aide de cet intégrateur de rayonnement solaire ont été satisfaisantes : l'erreur maximum est de 2 p. 100;

d) Le pyrhéliomètre (radiomètre) économique, élaboré par Schöffer, Kuhn et Sapsford (S/92) à partir du radiomètre à prix modique de Suomi et Kuhn (12), offre de bonnes perspectives; actuellement, l'erreur est de l'ordre de 5 p. 100. Son prix sera inférieur à 50 dollars, puisque le radiomètre de départ peut être obtenu dans le commerce pour 10 dollars environ.

Précision exigée des enregistrements du rayonnement solaire

Il existe actuellement, parmi les nombreux types d'appareils enregistreurs du rayonnement solaire, des instruments qui accusent une très grande dispersion entre leurs lectures moyennes, et d'autres, avec une bonne compensation (S/117), dont l'erreur — de l'ordre de $\pm$ 1 p. 100 — nous paraît beaucoup trop faible pour les mesures techniques. Il semble que l'on puisse admettre pour les calculs des données entachées d'une erreur qui ne dépasse pas $\pm$ 4 ou 5 p. 100 sur le total journalier, puisqu'en général les autres données des projets, telles que la résistance mécanique, la conductibilité thermique, etc. des matériaux, et les hypothèses mêmes des calculs comportent des erreurs plus grandes.

On peut considérer que la limite supérieure de $\pm$ 5 p. 100 sur le total journalier et celle de $\pm$ 10 p. 100 sur la lecture instantanée constituent un but qui est déjà atteint et qui peut être facilement dépassé par les fabricants d'instruments enregistreurs du rayonnement solaire, ce qui leur permettrait de rechercher l'amélioration d'autres caractéristiques de ces appareils. Drummond a donné (S/117) une indication excellente des caractéristiques que les enregistreurs de rayonnement solaire devraient réunir; compte tenu de l'augmentation possible du nombre des stations secondaires dans les pays sous-développés, il conviendrait d'y ajouter les suivantes :

1) Possibilité de manipulation facile par un personnel non spécialisé;

2) Difficulté de dérégler l'appareil par inadvertance pendant la manipulation; en d'autres termes, bonne conservation du calibrage dans le temps.

Il semble qu'au stade actuel du développement technique, il soit possible de perfectionner les idées et les systèmes déjà connus et d'aboutir à un appareil d'enregistrement continu du rayonnement solaire global (direct et diffusé) qui représente un compromis acceptable pour l'ensemble des caractéristiques mentionnées plus haut et qui puisse être produit industriellement à un prix raisonnable. Un tel instrument pourrait être l'objet d'une utilisation « type » dans les stations secondaires pour l'enregistrement du rayonnement solaire en vue de l'utilisation de cette énergie, et il faut espérer que, devant cette possibilité, les fabricants d'instruments intensifieront leurs recherches et leurs travaux expérimentaux en les orientant vers ce but.

Conclusion

Sans doute, l'un des buts pratiques que l'on cherche à atteindre au moyen de cette Conférence des Nations Unies sur les sources nouvelles d'énergie est l'application pratique de l'énergie solaire au profit de l'homme. L'étude des contributions de grande valeur, présentées au titre du point III.A de l'ordre du jour de cette Conférence et celle, plus générale, du sujet de cette session, permettent de tirer les conclusions suivantes :

1) Il convient d'amplifier d'une façon judicieuse les réseaux actinométriques afin de connaître avec la plus grande précision possible la distribution de l'énergie solaire à la surface terrestre et de pouvoir mettre en évidence les microclimats et, plus généralement, les zones caractéristiques par un niveau énergétique convenant à l'utilisation;

2) Il convient de fixer à un niveau convenable du point de vue de normes de projet prudentes, la valeur de l'erreur admissible pour les enregistrements du rayonnement solaire afin de rendre plus facile la fabrication des appareils d'enregistrement et de réduire leur prix;

3) Il convient de réduire, pour chaque catégorie de mesures, le grand nombre d'appareils de divers types utilisés dans les stations secondaires pour l'enregistrement du rayonnement solaire à un seul type avec les caractéristiques correspondantes, étant donné les avantages d'une production industrielle et ceux d'une comparaison plus facile des résultats apportés par l'uniformisation des méthodes et des échelles de mesure;

4) Il convient d'adopter un système « type » de présentation des résultats d'enregistrement du rayonnement solaire dans toutes les régions dans le but de leur conférer une utilité maximum pour les études des projets de dispositifs destinés à l'utilisation de l'énergie solaire.

Sujets de discussion proposés

1) Voies à suivre pour atteindre une collaboration internationale qui soit en mesure de réaliser une amplification du réseau actinométrique en un ensemble efficace.

2) Limites maximales admissibles de l'erreur de mesure des relevés actinométriques utilisés pour les études de projets.

3) Principales caractéristiques à exiger des appareils « types » possibles d'enregistrement du rayonnement solaire pour les projets et voies de développement.

4) « Normalisation » des données obtenues à partir des enregistrements du rayonnement solaire en vue de l'élaboration des projets.

Références

1. Azcarraga, L. de, Aprovechamiento de las energías solar y eólica, Tom. V, Seccion II C, *Publicaciones de la Sesión Parcial de Madrid de la Conferencia Mundial de la Energía*, Junio 1960.
2. Ward, G. T., Possibilities for the utilization of solar energy in under-developed rural areas, FAO Farm Power and Machinery, *Informal Working Bulletin No. 16*, 1961.
3. Black, J. N., The Distribution of Solar Radiation over the Earth's Surface, *Arch. Met. Geophys. Bioklimatol.*, Springer, Verlag, Vienna, Series B, 7 (2): 165-189, 1956.
4. Knowles, W. E. et Spilhaus, A. F., *Meteorological Instruments*, University of Toronto Press, 1953.
5. Abbot, C. G. et Aldrich, L. B., An improved water-flow pyrheliometer and the standard scale of solar radiation, *Smithsonian Miscellaneous Collections*, 87 (15), 1932.
6. Aldrich, L. B., The Abbot silver-disc pyrheliometer, *Smithsonian Miscellaneous Collections*, 111 (14), 1949.
7. Ångström, K., The absolute determination of the radiation of heat with the electric compensation pyrheliometer, with examples of the application of the instrument, *Astrophysic. Journal*, University of Chicago Press, 9, 1899.
8. Conférence internationale du rayonnement, Recommandations I à VIII, Résolution I. *CIMO-II/Doc. 7*, Annexe III, 1956.
9. Robitzsch, M., Über den Bimetallaktinographen Füess-Robitzsch, *Gerlands Beitr. Geophys.*, 35, 1932.
10. Ranzi, I., Una priorita italiana : l'attinometro a distillazione de Bellani, *Nuovo Cimento*, ann. V, nº 6, 1928.
11. MacDonald, T. H., The Solar Cell as a Pyranometer Receiver, Instruments-Automation Conference, Preprint Number 12-NY60, 1960.
12. Suomi, V. E. et Kuhn, P. M., An Economical Net Radiometer, *Tellus*, 10, nº 1, 1958.

SOLAR ENERGY AVAILABILITY AND INSTRUMENTS FOR MEASUREMENT

Rapporteur's summation

The deliberations with regard to agenda item III.A, entitled "Solar energy availability and instruments for measurement", made it amply clear that specialists are giving due attention to the general problems of determining the properties of solar radiation and ascertaining the distribution of solar radiation over the earth's surface.

There is obviously good reason for the interest shown in these problems, since a proper solution of them is essential for the utilization of solar energy.

Specialists in solar energy do not, of course, have the same worry that besets petroleum experts regarding how long their source of energy will last. Solar technicians know that their source is one which mankind can hardly exhaust.

Nevertheless, although solar radiation is constantly pouring down on half of the earth's surface, its intensity at each point depends not only on the geographical position and the time of day but also on other factors which make it impossible to predict the exact quantity of solar energy that will be received at every spot on earth.

Local measurement of solar radiation is therefore necessary to determine as accurately as possible the energy potential at each locality and also, with acceptable precision, the energy distribution over the face of the earth.

To put it briefly, it may be said that the following three basic problems must be tackled if we are to ascertain the distribution of solar radiation intensities for the purpose of utilizing the sun's energy:

(*a*) Solar measurement networks;

(*b*) Solar radiation recorders;

(*c*) Required accuracy of radiation records.

Another problem, though one of lesser importance than these three, is that of standardizing the presentation of the data which are required for the planning of solar energy installations and which must be derived from the radiation records.

These four problems actually constitute the essence of each of the topics proposed in the general report for discussion, and there now follows a summary of the position in each case in the light of the papers presented and of the discussion at the relevant technical session.

Solar measurement networks

Most solar technicians agree that the solar measurement networks which now exist in the different countries of the world do not offer a sufficient basis for the compilation of a world map from which the best sites for the utilization of solar radiation as a source of power could be accurately determined.

The main reason for this is that most stations in existing networks have been set up by the national meteorological services at places where facilities already exist for the reading and maintenance of the instruments and that this factor has prevailed over the need to find those places where the solar radiation reaches levels sufficient for utilization by solar installations.

In consequence, it is precisely the arid zones and the developing countries—which are generally situated in areas with low population densities—about which the sparsest information on solar radiation levels is available. This is particularly unfortunate because these are the very areas which should be most quickly helped to harness this form of energy as a means of promoting land recovery and rapid development.

It is possibly for this reason that in the discussion of the first topic—"Ways of attaining international co-operation to expand the network of actinometric stations into an efficient and integrated body"—no opposition was voiced to the suggestion that a project should be prepared for the rational and co-ordinated expansion of solar measurement networks in the arid zones and the developing countries. To ensure the proper development of this project, it is suggested that the advice of UNESCO should be sought and that an international fund should be set up for the provision of recording instruments and of technical assistance and training in matters of operation and maintenance. Dr. Langlo, the Chief of the World Meteorological Organization's Technical Division, agreed in his statement that this proposal for economic aid seemed appropriate, and he noted that the question might be dealt with at the closing session of the Conference.

Another suggestion for improving the solar measurement network was that the developed countries should expand their own networks with a view to the practical application of solar energy. The important work on radiation and radiation measurement instruments carried out during the past ten years by the World Meteorological Organization was recognized, and it was suggested, without any opposition being voiced, that the international character and the structure of that agency might make it a suitable instrument for ensuring that the rationally expanded networks were integrated in

an efficient world-wide system. To achieve this end, both members and non-members of WMO would have to follow the instructions issued by that organization in this regard. Both in the general project referred to earlier and in the projects of the individual countries, an effort should be made, in areas with irregular terrain, to find micro-climates where conditions are favourable for the utilization of solar energy. In any event, there should always be close co-operation with the various meteorological services, in view of their experience in this field.

Before concluding this point, it might be well to stress once again, as regards both the general project to expand the solar measurement network in arid zones and the projects of the developed countries, that in determining the location of the new stations, the main consideration should be to discover the sites best suited for the utilization of solar energy rather than to rely on existing sites that have facilities for solar radiation measurement. In this respect, one of the papers submitted makes it clear that even in areas with fairly level terrain, the quantities of solar radiation received at points relatively close to one another show appreciable differences.

Although the solar radiation data collected by the meteorological services in all countries have been and will continue to be most valuable for the rational planning of expanded actinometric networks, their use for the establishment of solar energy installations should be preceded by a process of careful selection. The WMO publication announced by Dr. Langle, which deals with meteorological data including solar radiation, will also be a valuable guide for solar technicians.

Radiation measurement instruments and permissible error

For the sake of brevity, the conclusions reached on the second and third discussion topics will be presented simultaneously. These topics are:

(*a*) Maximum allowable limits of error of measurement of actinometric records for design purposes;

(*b*) Most appropriate characteristics to be possessed by possible "standard" solar radiation recorders for planning purposes, and the path towards their development.

The first of these topics is actually implicit in the second, since accuracy of measurement is necessarily one of the characteristics of recording instruments.

It was generally agreed that efforts should be made to develop recording instruments which by and large would have the characteristics outlined in the paper (S/117) presented by Mr. Drummond, the chairman of technical session III.A. Since these instruments would have to be used in arid zones and developing countries and, even when used in other countries, would in most cases very likely have to be installed at points far from urban centres, they should possess the following additional characteristics:

(*a*) Ease of operation by non-specialized personnel;

(*b*) Difficulty of accidental decalibration during operation, that is, good long-term stability of calibration.

As regards the margin of error, the need to give more attention to other features of the instruments without raising their cost was the basis for the suggestion in the general report that a tolerance of ± 4 or possibly ± 5 per cent in both the instantaneous readings and the daily totals might be allowed. In the relevant technical session, stress was laid on the desirability of having inexpensive instruments, but it was felt that in no case should an error of more than 10 per cent be tolerated, either in the instantaneous readings or in the daily radiation totals. This point gave rise to considerable discussion. Some took the point of view of the scientist who demands extreme accuracy in the taking of measurements and who prefers instruments of high precision even if they are costly and limited in number. Others took the position of the solar technician who, to achieve the aforementioned expansion of networks, prefers to have many solar radiation recorders that are simple, sturdy and as inexpensive as possible even if they are not exceptional for their accuracy.

A maximum error of ± 3 per cent was suggested and generally accepted, but it should be noted that this represents no special sacrifice of accuracy to price or other features of the recording instruments since this margin of error is customary for most measurement purposes in engineering.

Another highly desirable feature of the recorders would be the ability to produce records that could be processed *directly* by electronic computers, for this would greatly facilitate the calculation of the data needed for the planning of solar installations.

We accordingly consider that solar energy recorders should, like any other practical device, represent a satisfactory compromise between the various features desired. The ideal would be achieved if the manufacturers of recording instruments were to find as neat a solution to the technical side of the problem as the WMO Commission for Instruments and Methods of Observation found for the formulation of its statement: "To give particular attention to the development and study of simple instruments combining acceptable accuracy with a modest price."[1]

Radiation data for planning purposes

The discussion topic was "'Standardization' of data for planning purposes, derived from solar radiation recorders".

[1] WMO. No. 64.RP.26, resolution 9 (CIMO-II), p. 35, abridged final report of the second session, Paris, 18 June-6 July 1957.

Compared with the three preceding topics, this one is of lesser importance and urgency since practice itself will gradually reveal the best forms in which to present for planning purposes the data derived from local radiation records.

It is interesting, however, that the data required by solar technicians have been set forth in an *ideal programme* worked out by Dr. Tabor on the basis of other programmes.[1]

The data that would be provided under this ideal programme are:

(*a*) Monthly means of the daily march of intensity of direct normal solar radiation or direct radiation on a horizontal plane;

(*b*) Monthly means of the daily march of diffuse radiation on a horizontal plane;

(*c*) Monthly means of daily totals corresponding to (*a*) and (*b*);

(*d*) Some indication of the interruption of sunshine, such as information on bright sunshine duration (monthly totals; monthly mean of daily march if possible);

(*e*) Statistical data on the frequency of sequences of days with values of total daily incidence (on a horizontal plane) below arbitrary fixed levels;

(*f*) Statistical data on the frequency of sequences of days with sunshine duration falling below arbitrary fixed levels. In both (*e*) and (*f*) the arbitrary fixed levels could be expressed as fractions of the long-term monthly means, or in absolute terms.

With a view to standardizing the recording instruments which are to provide the information for this ideal programme, it was suggested, and no opposition to the suggestion was voiced, that item (*a*) should be reworded so that direct solar radiation would refer only to a horizontal plane and not to normal incidence.

For the same purpose of standardizing the recording instruments, it is suggested that item (*f*) should be deleted and that item (*d*) of the ideal programme should be replaced by the following:

"(*d*) Statistical data on the frequency of sequences of days with values of direct daily radiation (on a horizontal plane) below arbitrary fixed levels."

In this way, the radiation records providing the data for the ideal programme could be furnished at any particular point by two basically identical recording instruments, one for total and the other for diffuse radiation.

To sum up, there was agreement on the need for the following:

(1) Rationally actinometric expanding networks, as indicated earlier, with a view to obtaining data for the utilization of solar energy;

(2) Developing solar radiation recording instruments which are both sturdy and simple and which combine acceptable accuracy with a reasonable cost;

(3) Securing the data, indicated earlier, which the solar engineer requires for the planning of solar installations.

In conclusion, I should like to thank Col. Alfred G. Katzin, the Executive Secretary of the Conference and his entire team, for their effective help in the conduct of the technical sessions of the Conference. I wish also to congratulate them on the extraordinary work they performed earlier in order to make this conference possible.

[1] Tabor, H., General Survey of Engineering Interest in Solar Radiation and the Radiation required by Engineers. International Symposium, Vienna, August 1961.

ÉNERGIE SOLAIRE DISPONIBLE ET INSTRUMENTS DE MESURE

Résumé du rapporteur

Les travaux relevant du point III.A. de l'ordre du jour de la Conférence, intitulé « Energie solaire disponible et instruments de mesure, » montrent bien que les spécialistes prêtent l'attention voulue aux problèmes généraux que pose la connaissance des caractéristiques du rayonnement solaire et de ses variations d'intensité sur la surface de la terre.

Il est évident que l'intérêt qu'ils portent à ces problèmes est justifié, car de leur solution correcte dépendra l'utilisation de l'énergie solaire.

Assurément, les spécialistes de l'énergie solaire n'ont pas les mêmes préoccupations que les techniciens du pétrole quant à la durée d'utilisation de leur source d'énergie : ils savent que l'énergie solaire est pratiquement inépuisable pour l'humanité.

Toutefois, bien que le rayonnement solaire baigne continuellement la moitié de la surface de la terre, son intensité en chaque lieu dépend non seulement de la position géographique de ce lieu et de l'heure du jour, mais aussi d'autres facteurs qui ne permettent pas de prévoir avec exactitude la quantité d'énergie solaire qui y sera reçue.

Il est donc indispensable de mesurer localement le rayonnement solaire, afin de connaître le plus exactement possible la quantité d'énergie disponible en chaque lieu et de savoir, avec une précision acceptable, comment cette énergie est répartie sur la surface de la terre.

En résumé, nous dirons que, pour arriver à connaître la répartition de l'intensité du rayonnement solaire afin d'en exploiter l'énergie, il faut aborder les problèmes fondamentaux suivants :

a) Réseaux pyrhéliométriques;

b) Appareils de mesure du rayonnement solaire;

c) Précision requise dans la mesure du rayonnement.

Un autre problème, moins important toutefois que les précédents, concerne la normalisation des données, élaborées à partir des mesures du rayonnement, dont on a besoin pour établir les plans des installations qui utiliseront l'énergie solaire.

Ces quatre problèmes constituaient, en fait, l'essence des quatre thèmes que le rapport général proposait à notre examen; nous allons faire le point de chacun d'eux, en fonction des rapports présentés et des interventions orales faites au cours des séances techniques correspondantes.

Réseaux pyrhéliométriques

La plupart des spécialistes de l'énergie solaire estiment que les réseaux pyrhéliométriques en service dans les divers pays du monde ne sont pas suffisants pour établir une carte mondiale permettant de déterminer avec exactitude les emplacements qui se prêteraient le mieux à l'utilisation énergétique du rayonnement solaire.

Cela tient principalement à ce que la plupart des stations des réseaux actuels ont été installées par les services météorologiques nationaux; ceux-ci tiennent compte généralement des facilités qu'offre tel ou tel endroit pour la lecture et l'entretien des appareils de météorologie, mais ne se soucient guère de rechercher les lieux où le rayonnement solaire est assez intense pour se prêter à l'utilisation par des installations spéciales.

Voilà pourquoi c'est précisément dans les zones arides et dans les pays en voie de développement, régions où la population est généralement peu dense, que l'on connaît le plus mal les variations de l'intensité du rayonnement solaire. Il y a là un handicap sérieux, car ce sont ces régions qu'il s'agit d'aider au plus tôt, en vue de leur relèvement et de leur développement accéléré, par l'utilisation de cette source d'énergie.

Ce fait explique sans doute pourquoi, au cours de la discussion du premier sujet, « Voies à suivre pour atteindre une collaboration internationale qui soit en mesure de réaliser une amplification du réseau actinométrique en un ensemble efficace », personne ne s'est opposé à la proposition tendant à élaborer un projet rationnel et coordonné pour l'extension des réseaux pyrhéliométriques dans les zones arides et les pays en voie de développement. Pour l'exécution de ce projet, le rapport proposait de demander le concours technique de l'UNESCO et de faire appel éventuellement à des fonds de caractère international pour la fourniture d'appareils enregistreurs, ainsi que pour l'assistance technique et la formation nécessaire au personnel chargé du fonctionnement et de l'entretien de ces appareils. Dans son intervention, le Chef de la section technique de l'OMM, M. Langlo, a admis l'intérêt de cette formule d'aide économique, et il a indiqué que cette question pourrait être traitée à la séance de clôture de la Conférence.

Pour compléter le réseau pyrhéliométrique, on a proposé également que les pays avancés développent leur propre réseau en tenant compte des applications pratiques de l'énergie solaire. On a noté les travaux importants que l'Organisation météorologique mondiale a consacrés au rayonnement et aux instruments destinés à le mesurer, pendant les dix dernières années, et on a estimé, sans qu'il y

ait eu d'objection, que le caractère international et la structure de cette Organisation pourraient lui permettre de centraliser les efforts destinés à obtenir l'intégration, en un ensemble efficace de portée mondiale, desdits réseaux pyrhéliométriques rationnellement développés. Pour cela, tant les États membres de l'OMM que les États non membres devront suivre les directives de l'Organisation à cette fin. Aussi bien dans le projet général mentionné plus haut que dans les projets particuliers de chaque pays, on devra s'attacher, pour ce qui est des régions de relief accidenté, à déceler des microclimats qui présentent des conditions favorables à l'exploitation de l'énergie solaire. On devra dans tous les cas procéder en liaison étroite avec les services météorologiques nationaux, en raison de leur expérience dans ce domaine.

Avant d'en terminer avec ce point, nous voudrions souligner à nouveau qu'il importe, tant dans le projet général d'extension du réseau pyrhéliométrique dans les zones arides que dans les projets concernant les réseaux des pays développés, de choisir, pour la mise en place des stations nouvelles, des lieux qui se prêtent à l'exploitation de l'énergie solaire, au lieu de s'en tenir aux stations existantes de mesure du rayonnement solaire. A cet égard, nous devons faire observer, d'après l'un des rapports présentés, que même dans les zones peu accidentées, des lieux relativement proches présentent des différences sensibles quant à l'intensité du rayonnement solaire qu'ils reçoivent.

Il n'en reste pas moins que les données sur le rayonnement solaire obtenues par les services météorologiques de tous les pays ont été et seront très utiles pour orienter la planification rationnelle de l'extension des réseaux actinométriques; toutefois, si l'on veut les utiliser pour créer des usines d'énergie solaire, il faudra bien les trier au préalable. La publication de l'OMM sur les données météorologiques, y compris le rayonnement solaire, annoncée par M. Langlo, constituera également un guide précieux pour les spécialistes de l'énergie solaire.

Instruments de mesure du rayonnement et erreur tolérée

Nous allons, pour abréger, exposer simultanément les conclusions des débats concernant les sujets proposés 2 et 3, à savoir :

Limites maximales admissibles de l'erreur de mesure des relevés actinométriques utilisés pour les études de projets, et

Principales caractéristiques à exiger des appareils 'types' possibles d'enregistrement du rayonnement solaire pour les projets et voies de développement.

En réalité, le premier point est contenu implicitement dans le second, puisque la précision de la mesure fait partie des caractéristiques des appareils enregistreurs.

La conclusion unanime a été qu'il fallait essayer d'obtenir des appareils enregistreurs qui possèdent, d'une manière générale, les caractéristiques indiquées par le président de la séance technique III.A, A. J. Drummond, dans son mémoire (S/117). Comme lesdits instruments devront être utilisés aussi bien dans les zones arides et dans les pays en voie de développement que dans les autres, mais que, dans la plupart des cas, il faudra les installer dans des lieux qui pourront être éloignés des centres urbains, ils devront avoir également les caractéristiques suivantes :

a) Pouvoir être maniés sans difficulté par un personnel non spécialisé;

b) Ne pas se dérégler facilement au cours du maniement, c'est-à-dire garder intact pendant longtemps le réglage effectué.

Quant à la question de l'erreur dans la mesure, on a proposé dans le rapport général, par souci de prêter plus d'attention aux autres caractéristiques sans élever le coût des appareils, d'admettre une marge d'erreur en plus ou en moins, de 4 à 5 p. 100, tant dans l'enregistrement instantané que dans l'enregistrement de l'insolation totale par jour. Au cours de la séance technique correspondante, on a insisté sur l'utilité de construire des appareils économiques, tout en soulignant qu'on ne devait en aucune manière tolérer une erreur supérieure à 10 p. 100 dans l'enregistrement instantané ni dans l'enregistrement du rayonnement total par jour. La discussion a été vive. On a exposé d'un côté le point de vue du savant qui exige des mesures extrêmement rigoureuses et qui préfère des instruments de grande précision même s'ils sont coûteux et peu nombreux. De l'autre côté il y avait le point de vue du technicien qui a besoin, pour l'extension des réseaux dont nous avons parlé, d'un grand nombre d'appareils enregistreurs du rayonnement solaire, qui soient simples et robustes et, si possible peu coûteux, même s'ils ne sont pas d'une précision extraordinaire.

On est convenu de tolérer une erreur maximale de 3 p. 100 en plus ou en moins, mais il faut reconnaître qu'il n'y a là aucune concession particulière en faveur du prix ou d'autres caractéristiques des appareils de mesure, car cette marge d'erreur est normale pour la plupart des grandeurs avec lesquelles opèrent les ingénieurs.

Il serait également très souhaitable que les enregistrements de mesures effectués par ces appareils puissent être utilisés *directement* par des machines électroniques de manière à faciliter le calcul des données nécessaires pour établir les plans d'usines solaires.

C'est pourquoi nous estimons que les instruments de mesure destinés à l'exploitation de l'énergie solaire doivent être, comme toute réalisation pratique, un compromis satisfaisant entre les diverses caractéristiques souhaitées; l'idéal serait que les fabricants d'instruments trouvent une formule qui soit aussi parfaite techniquement que l'est grammaticalement la résolution 9 de la CIMO [1] de l'Organi-

[1] OMM. n° 64.RP.26., 1957, page 38 du Rapport final abrégé de la deuxième session (Paris, 18 juin-6 juillet 1957).

sation météorologique mondiale, laquelle prévoit d'« accorder une attention particulière au développement et à l'étude d'instruments à la fois simples et pratiques, ayant une précision satisfaisante et un prix modéré ».

Données sur le rayonnement nécessaires à la conception des usines solaires

Le sujet de discussion correspondant s'intitule : « 'Normalisation' des données obtenues à partir des enregistrements du rayonnement solaire en vue de l'élaboration des projets. »

Cette question est moins importante et moins urgente que les trois précédentes, car c'est la pratique qui nous dira sous quelle forme il convient de présenter, en vue de la conception des usines solaires, les données élaborées à partir des mesures locales du rayonnement solaire.

Il n'en est pas moins intéressant de noter que les données nécessaires aux spécialistes de l'énergie solaire ont été précisées dans un *programme idéal* établi par H. Tabor [2] à partir d'autres programmes.

Les données envisagées dans ce programme idéal sont les suivantes :

a) Moyennes mensuelles de la variation journalière de l'intensité du rayonnement solaire direct à incidence normale ou du rayonnement direct sur un plan horizontal;

b) Moyennes mensuelles de la variation journalière du rayonnement diffus sur un plan horizontal;

c) Moyennes mensuelles des totaux journaliers correspondant à *a* et *b*;

d) Indication des interruptions de l'ensoleillement : renseignements sur la durée de l'ensoleillement (ensoleillement total mensuel, moyenne mensuelle de l'ensoleillement journalier, si possible);

e) Données statistiques sur la fréquence des séries de journées pendant lesquelles l'intensité de l'ensoleillement total par jour (sur un plan horizontal) est inférieure à une valeur fixée arbitrairement;

f) Données statistiques sur la fréquence des séries de journées pendant lesquelles la durée de l'ensoleillement est inférieure à un niveau fixé arbitrairement.

Pour *e* et *f*, les niveaux fixés arbitrairement pourraient s'exprimer en fraction de la moyenne mensuelle pour une longue période, ou en valeur absolue.

Cependant, en vue de la normalisation des appareils destinés à fournir les données de ce programme idéal, il a été proposé, sans qu'il y ait eu d'objections, de modifier ce programme (au point *a*) de manière qu'on ne mesure que le rayonnement solaire direct sur un plan horizontal et non le rayonnement direct à incidence normale.

Pour les mêmes raisons de normalisation des appareils de mesure, on propose de supprimer le point *f* et de modifier le point *d* du programme idéal susmentionné comme suit :

d) Données statistiques sur la fréquence des séries de journées pendant lesquelles l'intensité du rayonnement direct par jour (sur un plan horizontal) est inférieure à une valeur fixée arbitrairement.

De cette manière, les données du programme idéal pourraient être obtenues en tout lieu au moyen de deux instruments essentiellement identiques, l'un enregistrant le rayonnement total et l'autre le rayonnement diffus.

En résumé, l'accord s'est fait sur les points suivants :

1) Il convient d'étendre rationnellement, de la manière indiquée, les réseaux de stations actinométriques en vue de recueillir des données pour l'exploitation de l'énergie solaire;

2) Il convient de réaliser des instruments de mesure du rayonnement solaire qui, étant à la fois robustes et simples, aient une précision acceptable et un prix raisonnable;

3) Il y a lieu de recueillir, de la manière indiquée plus haut, les données dont les spécialistes de l'énergie solaire ont besoin pour établir les plans d'usines solaires.

Je tiens pour terminer à remercier le secrétaire exécutif de la Conférence, le Colonel Alfred G. Katzin, et toute son équipe, pour l'aide efficace qu'ils ont prêtée au déroulement de nos séances techniques. Je les félicite également du travail extraordinaire qu'ils ont accompli pour permettre la réunion même de la Conférence.

[2] Tabor, H., *General Survey of Engineering Interest in Solar Radiation and the Radiation Data required by Engineers*, Colloque international de Vienne, août 1961.

SOLAR ENERGY IN CANADA

E. A. Allcut and F. C. Hooper *

Several writers have indicated the relationship that exists between annual income *per capita* and the rate of energy consumption (1, 2). It has been stated by C. C. Furnas that "within the next half century, the world population will undoubtedly expand from the present two and three-quarter billion to five or six billion" (3). Similar predictions have been made by other authorities. In addition to the task of feeding these multitudes, it seems evident that the rising tide of nationalism in relatively undeveloped countries, accompanied by incessant demands for higher standards of living, will cause the drain on our fuel resources to increase in geometric progression. Also, in economic and political matters, all countries are interdependent to some degree, so that rising consumptions of capital energy resources in one part of the world inevitably result in smaller supplies elsewhere, combined with general increases of cost. This argument presupposes that all the energy used comes from a limited "capital" supply but, in each country, there are also available other resources, which are constantly being renewed and the use of which implies living, partly, on "income". To this extent, the depletion of energy capital may be diminished, but the final result will depend on the conditions that are peculiar to the country concerned. Thus, the problem has no single answer; its solution will depend on the local circumstances.

The controlling conditions as far as Canada is concerned are the facts that the Dominion is a large land mass, having an area of 3 845 000 square miles, situated mostly between latitudes 42 and 70 degrees North, and straddling nearly 90 degrees of longitude. In so large and diversified a country, it is evident that climatic conditions vary considerably, but, apart from scattered settlements in the north, most of the eighteen million people are settled in a relatively narrow band, south of latitude 55 degrees North and, therefore, the following remarks relate almost entirely to that area in which the maximum concentration of population and industry occurs. Moreover, the economy of Canada has recently been transformed from an agrarian to an industrial basis and the amount of energy used annually has increased 2.4 times during the past thirty years. It is anticipated that, during the next twenty years, the population will be about doubled and the energy consumption tripled.

During the past thirty years, the sources from which Canada's energy is obtained have changed radically. For instance, in 1926, about 69 per cent of the energy supply was derived from coal. The present proportion, however, is only about 28 per cent and is still falling. Simultaneously, the energy derived from petroleum has risen from 10 per cent to 52 per cent of the total. Natural gas now accounts for five per cent of the energy supply but, by 1980, it is expected to be about 20 per cent. These figures indicate the extent and rapidity with which Canada's energy resources are being exploited and, more particularly, those that are easily accessible.

Many of the existing and future difficulties in the economic use of these resources are occasioned by the fact that most of them are located in the extreme east and west, and thus are far away from the largest markets which are in the central provinces. The long hauls and lengthy transmission and pipe lines required add considerably to the cost of using Canadian fuels. This has created the anomalous situation in which mines are being closed in Nova Scotia and miners are unemployed, while Ontario, which accounts for some 50 per cent of Canada's coal consumption, is importing 12 million tons annually (97.4 per cent of the total) from the United States. The fundamental Canadian problem is neither an over-all surplus nor a shortage of fuel, but simply an uneconomic distribution in the geographical circumstances.

With regard to "income" energy, most of this is in the form of waterpower. In Ontario, the economically available hydraulic resources have already been harnessed, together with 70 per cent of those in the province of Quebec, so that, apart from the extreme eastern and western regions, little unusued water power is now readily accessible. The part played by wood in the production of energy is inconsiderable. The possibilities of wind and tidal power, particularly in the Bay of Fundy, have been studied, but there is little promise of relief from these sources.

Much has been said about the abundant promise of atomic fission, and experimental work has been done, as a result of which some rather extravagant claims have been made, mostly by interested parties. The "Gordon Commission" forecast that nuclear energy would supply five per cent of the nation's energy requirements within fifteen years and nearly thirteen per cent in twenty years (4). Still more optimistic predictions have been made by the Hydro Electric Power Commission of Ontario, but forecasts of a similar nature made in the past have not materialised and the present ones are of dubious validity.

* University of Toronto, Canada.

It is still true that the cost of power produced by nuclear fission is much higher than that produced from fuel or water power, and the inherent hazards of the former process are still formidable. Possibly, these problems may be solved in time but, in the meantime, it seems unwise to erect a national energy structure on so insecure a foundation.

It follows, therefore, that there is some real basis for concern about the future energy position in Canada, and that the possibilities of solar energy are worth investigating. As in other places, these possibilities depend on a combination of location and application. For instance, in the northern parts of Canada, there are many small and remote communities in which energy is required in limited quantities for supplying heat, power and water. Unfortunately, however, in these high latitudes, the mean annual hours of bright sunshine are about 1 400 to 1 600 and, in the month of December, fewer than 25 hours of sunshine may be experienced. The prospects of employing solar energy to solve the problems peculiar to the northern area are not very bright.

The more southerly part of Canada accounts for practically all of the country's energy consumption which, in 1926, was equivalent to about 49.4 million tons of coal and rose to 118.8 million in 1958. It is anticipated that, within the next twenty years, it will amount to the equivalent of 356 million tons (2). The proportions employed for industrial, mining and transportation purposes were 54 per cent in 1926, 63 per cent in 1958 and may be as high as 67 per cent in 1980. It is here assumed that there is little or no prospect of using solar energy for any of these purposes, but there still remains the relatively large field of residential and commercial space heating, which requires comparatively low temperatures and accounts for some 25 to 30 per cent of the total energy consumption. Indeed, in 1958, the heating load consumed the equivalent of 34.5 million tons of coal and it seems probable that, by 1980, this figure may rise to 81 million tons.

In Ontario, which is the most populous and most heavily industrialised of the provinces, less than 12 per cent of the energy consumed is derived from local sources and no less than 45 per cent is imported from other countries, principally from the United States (5). Thus, the combination of high costs of transportation, possible interruptions of supply, large local residential loads and comparatively low latitudes, probably renders the southern part of Ontario the most promising location for the investigation of the possibilities of using solar energy in Canada.

Assuming that the heating load follows the usual pattern of 30 per cent of the total, in 1959 the consumption for this purpose in Ontario amounted to 343 000 billion btu, which quantity was provided by natural gas, oil and coal. It is possible, also, that the consumption may increase to 800 000 billion Btu within the next twenty years.

If some part of these quantities can be met by energy received from the sun, the drain on our fuel resources will be reduced correspondingly and, with fewer imports, the internal financial situation will be improved.

In view of this situation, it is perhaps surprising how little attention has been devoted to research on solar energy in Canada. In the past decade only a few limited projects in this area have been undertaken in Canadian universities, perhaps the most extensive of which has been in the University of Toronto under the general direction of the authors. This work has been entirely directed toward the space heating application under the conditions prevailing in southern Ontario.

Initially some considerable attention was devoted to the design of flat plate collectors for use in temperatures which in winter not infrequently fall below zero degrees Fahrenheit, in which the proportion of diffuse to total solar radiation tends to be high, and which was throught to pose problems of icing and snow accumulation. It eventually appeared that the performance of flat plate collectors differed only in degree under these circumstances, that more than two plates of glass were not justified, and that at the high angles of slant required in any case by the latitude, snow did not long remain on the trap surface. Special precautions were necessary to avoid freezing in circulating water systems, but such provision can be made in several ways, although at some expense.

It did become apparent, however, that the southern Ontario region favoured long-term heat storage, and that a solar space heating system which would be entirely independent of auxiliary sources for this region would almost necessarily require a seasonal carry-over of stored heat, or annual heat storage. In Toronto during the heating season the monthly total of sunshine hours averages well below one hundred, less than one-third of the summer season values (6). Moreover, a solar trap of adequate capacity to meet the load on a short-term (ten-day) storage basis, would exceed in area the projected south-facing area of a normal house and require separate supporting structures, a consideration not always recognized by those making studies in this field.

While the choice of annual heat storage greatly reduces the required area of the solar heat trap, the capacity and efficiency of the heat storage and the minimum useful temperature level of the heating medium will govern the extent of the saving in heat trap size. After analyzing several designs, it was concluded that a solar heated house, fitted with a panel heating system which could effectively utilize heat at temperatures as low as 80°F, and which employed a high capacity but not necessarily well-insulated reservoir reaching a maximum temperature of heat storage of 145°F, came as close as economically feasible to a completely solar-heated building in the Toronto area.

Investigation of storage reservoirs led to consideration of several systems. The latent heat type of storage was examined and rejected for technical reasons (7). Heat pump combinations with low

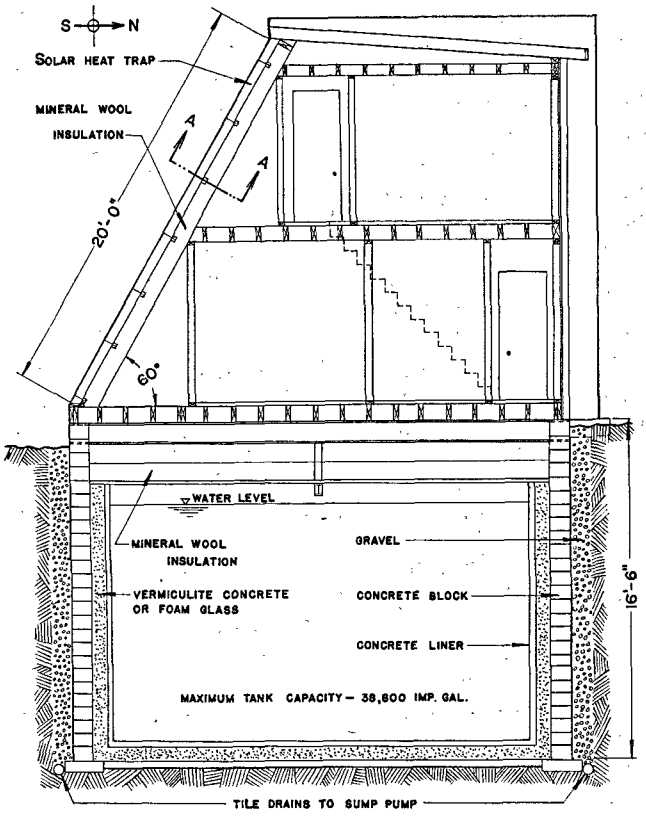


Figure 1. Cross-section of solar heated house

temperature storage did not appear feasible in the economic sense (8). Considerable experimental and analytical attention was devoted to the highly attractive possibility of using the ground for a heat reservoir in conjunction with buried pipe grids. This system might be made to work if sufficient control of ground water movement could be achieved, and if the installation were relatively large. It was, however, abandoned for practical use with small sized systems. The form of storage ultimately favoured was that of a waterproofed basement filled with water, such as shown in figure 1 (9). Since frost heave effects require deep foundation walls in Canadian houses, the additional cost of deepening and waterproofing this structure should not be too great, and certainly would be well below the cost of equivalent steel tanks. In such a storage, especially if uninsulated, the surrounding earth is a definite part of the thermal system and effectively increases the capacity of the storage in cyclical low-temperature storage applications.

The conditions under which a solar heating system using annual storage would become economically competitive with other systems on an absolute basis remain unclear. Several writers, including Speyer (10), have suggested that annual storage is unlikely to prove feasible, but the assumptions inherent in such appraisals are open to argument and the matter is dependent upon many factors, including the unit costs taken and the technical performance of the

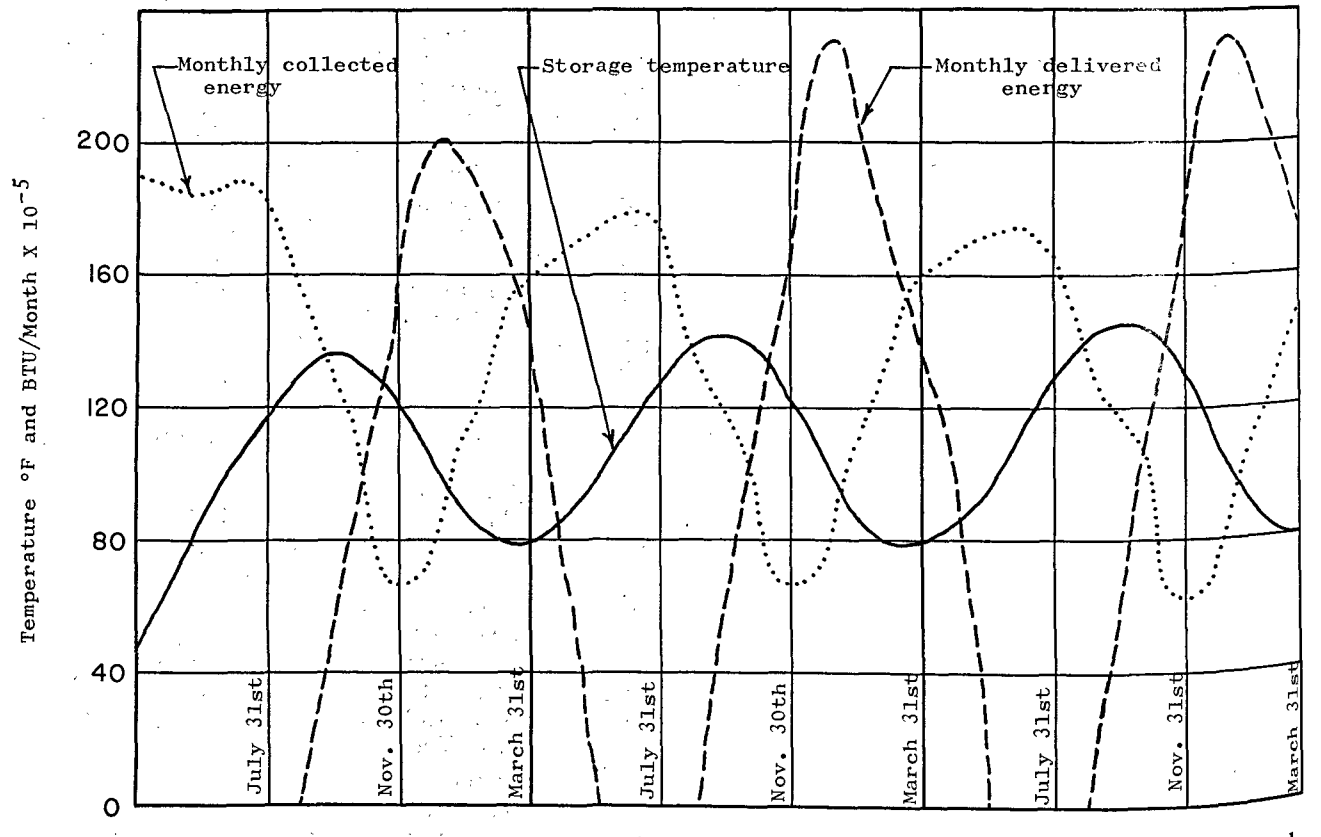


Figure 2. The performance during the first three years of operation of a solar house heating system with annual heat storage as evaluated from a thermal model test

two basic elements, the collector and the storage. In recent work at Toronto, a thermal model has been employed in assessing the technical performance which can be expected from solar house heating systems requiring no auxiliary heat source and employing large heat reservoirs for heat storage on an annual basis (11). Physically, the heat storages considered were of the water-filled basement type already described.

The model consists of a sand box in which a scale model of the basement tank is fitted. It can be show that, for equivalence, the Fourier numbers for the model and prototype must be equal, that is:

$$\frac{\alpha_M \theta_M}{L_M^2} = \frac{\alpha_p \theta_p}{L_p^2}$$

where the subscripts refer to the model and the prototype and θ is time, L linear dimension, and α thermal diffusivity of the surrounding solid.

If the tank is insulated, it may be necessary to consider the boundary resistance to heat flow, which would require that the Nusselt Numbers also be equal. In uninsulated basements this factor is negligible. The work has suggested that insulation may not be economically justified in such storages.

In figure 2 results are shown from one model evaluation of the performance of a solar house during the first three years of its operation, beginning with an initially cold (46°F) storage tank. For this test, a model scale of 12 inches equal to (0.05 inches)$^{\frac{1}{2}}$ was used. The thermal properties of the model sand were taken as equal to those of the soil surrounding the prototype. The time scale was such that one half minute in the model equalled one day in the prototype. This required a little over nine hours to simulate a three-year test period. The ratio of heat quantity in the prototype to that in the model was 154 440.

The house represented had a 50 000 Imperial gallon water storage tank, a heat load of 775 btu/°F.hr, a 600-square-foot collector tilted at 60° to the horizontal and having a known efficiency dependence upon the temperature difference between the storage water and the air, and the angle of solar incidence.

In operating the model, quantities of heat were added to or withdrawn from storage by exchanging the water in the model. The appropriate amount was recalculated every few minutes from the observed storage temperature and the known house heat load and collector performance which corresponded to the mean air temperature and solar incidence at the prototype time of the year.

This model was very flexible and could be made to simulate a very wide variety of prototype conditions, including various soil characteristics, complex trap performances and a variety of assumed heat demands.

One of the principal factors to be determined prior to an evaluation of the performance to be expected from a solar heating system is the solar energy incident upon the heat trap, based on a function of time, geometry and weather, and subdivided between direct and diffuse radiation. Methods are available for the prediction of the solar energy which would be available at any point on the world's surface. These calculations take into account the time of year, the latitude and other geometrical factors as well as cloud cover, atmospheric dust and moisture content, and other meteorological factors. In fact, however, they are crude and approximate for specific applications. The reason for this is that there are factors present which cause great local variations in the weather. Accurate assessments of the availability of solar energy in any particular area are necessarily a matter of local observation, although it is surprising how little use has been made of such observations up to the present time in solar energy analyses.

Recognizing this problem, a study has been conducted based upon the actual recorded data available for Toronto (12). These data consist of Eppley pyrheliometer readings at hourly intervals for total and diffuse radiation upon a horizontal surface, recorded by the meteorology branch of the Dominion government. Although at present such observations are recorded by relatively few of the weather observatories throughout the world, this is the probable form in which insolation readings would be made if and when this service is undertaken by more stations.

Unfortunately, such data are very bulky, and for practical purposes it proved advisable to reduce them to simpler terms for the purpose of calculating the radiation which would fall upon a flat plate collector oriented at various angles of tilt and in various directions. In thus reducing the data, it was necessary to introduce several arbitrary assumptions. It appears to the authors that others will find this approach useful and that they, too, will find it necessary to reduce the data in some arbitrary manner. In view of the fact that no other such re-

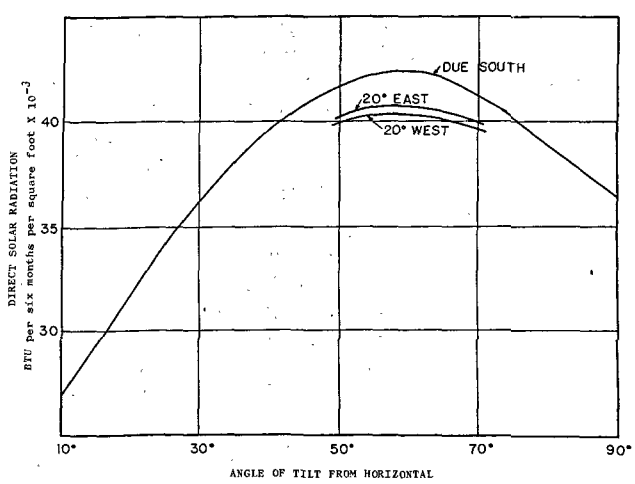


Figure 3. The results of an analysis based on observed weather data are plotted to show the effect of orientation on the direct solar radiation incident upon a flat plate collector

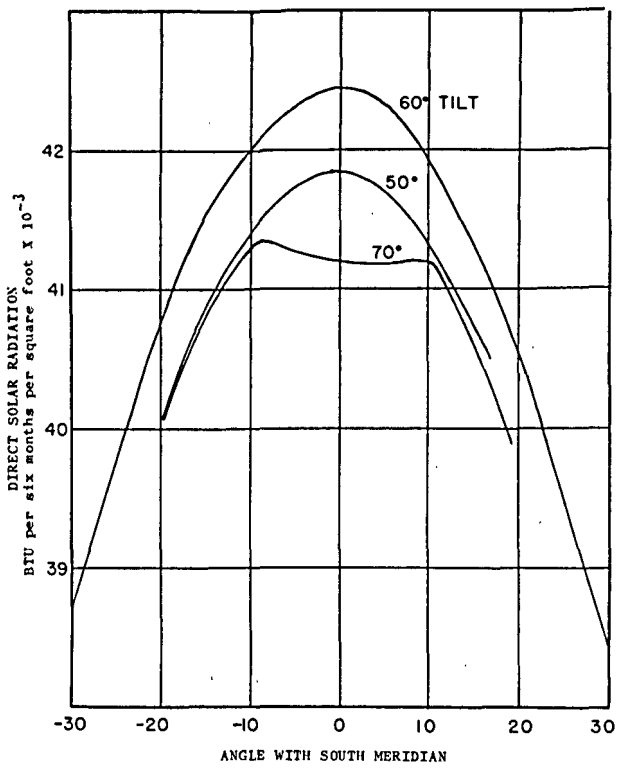


Figure 4. Variations in direct incidence due to eastward or westward orientation

commendation appears to exist, and of the obvious desirability of a standard procedure which would render the results of such analyses properly comparable with one another, the authors offer for consideration the following procedures which have been employed at Toronto:

(*a*) The errors in the Eppley pyrheliometer due to ambient temperature variation, cosine variation and other effects, should be considered to be either self-compensating or zero, and consequently the direct reading should be accepted as correct.

(*b*) The hourly radiation, for any given hour in the year, should be obtained by averaging the values observed at the identical hour on the designated day, the day preceding, and the day following, for each of three successive years. This average of nine values reduces both the amount of processed data to be handled and the random variations amongst them.

(*c*) The albedo, which influences the diffuse radiation received by a tilted surface, should be taken as 0.2 for all locations save in those places where snow cover is customarily encountered. In these locations the albedo shall be taken as 0.6 for the months in which snow normally lies on the ground.

(*d*) The local apparent hour angle, rather than the local hour angle, should be used in calculations, neglecting the small errors due to time zone and earth axis precession effects.

Even with the simplifications permitted by these assumptions, the quantity of data to be handled is considerable, amounting to thirteen values for direct radiation, thirteen values for diffuse radiation, and a declination angle for each day of the year. Since a considerable mathematical manipulation is required on each hourly item to convert the horizontal observations to the actual trap orientation under consideration, a digital computer was employed to handle the bulky data and extensive calculations involved. This procedure has proved to be convenient and powerful, permitting very rapid evaluation of all factors relating to solar incidence in the locality where the observations were taken.

The information which can thus be provided with ease includes the interrelationships between angle of tilt and incidence of direct, indirect and total radiation as instantaneous or integrated values over any time period, sequences of clear, partly cloudy or overcast hours, days or other time periods, statistical distribution of hours with various levels of solar intensity and computation of actual heat collected in any time period by a solar trap of predetermined characteristics.

Typical results obtained by such procedures are shown in figures 3 and 4. Clearly the optimum angle of tilt can be determined very accurately for a locality from data such as that shown in figure 3. In figure 4 the influence of a local weather characteristic, which tends to produce more early morning than late afternoon sunshine, can be seen. There are probably locations where such effects are much stronger and where a direction other than due south is indicated for a heat trap. Standard computer programmes to perform all such operations could easily be provided.

Acknowledgements

The authors gratefully acknowledge the contributions made to the solar energy research programme here reported by the following graduate students in the Department of Mechanical Engineering at the University of Toronto: E. Koczkur, J. L. Loth, F. K. Tsou, P. F. O'Rourke, G. H. West, and F. J. Gwodz.

Special thanks are due to C. L. Mateer of the Department of Transport for his extensive assistance in our solar incidence studies.

Financial assistance was given to this programme by the National Research Council of Canada and by the School of Engineering Research of the University of Toronto. To these organizations the authors' thanks are also extended.

References

1. Yellott, John I., Energy for Tomorrow . . . Inventory and Appraisal *Power Engineering*, December 1956.
2. Shotwell, John S. G., Canada's Energy Resources to 1989 . . . A Forecast, *Engineering Journal*, October 1960.
3. Furnas, C. C., There's always the sociological factor, *Mechanical Engineering*, February 1961.
4. *Report of Royal Commission on Canada's Economic Prospects*, The Queen's Printer, Ottawa, 1958.
5. *Report on the origin of Ontario's Energy Supply*, unpublished, Dept. of Energy Resources, Ontario, 1961.
6. *Sunshine and Insolations*, Joint publication of the Division of Building Research, National Research Council of Canada and the Meteorological Division, Department of Transport of Canada.
7. Hodgins, J. H. and Hoffman, T. W., The storage and transfer of low potential heat, *Canadian Journal of Technology 33*: 293-302, 1955.
8. Allcut, E. A. and Hooper, F. C., The possibilities of the heat pump in Canada. General discussion on Heat Transfer, *A.S.M.E. and I. Mech. E.*, London, England, September 1951.
9. Hooper, F. C., The Possibility of Complete Solar Heating of Canadian Buildings, *Engineering Journal*, November 1955.
10. Speyer, Edward, Optimum Storage of Heat with a Solar House, *Solar Energy, Vol. III, Number 4*, December 1959.
11. Loth, J. L., *A Model Analysis of Cyclic Heat Storage in Underground Reservoirs*, M.A.Sc. Thesis, U. of T., 1958.
12. Koczkur, E., *The Effect of Orientation on Solar Incidence in the Toronto Area*, M.A.Sc. Thesis, U. of T., 1960.

Summary

The fundamental Canadian energy problem at present is neither an over-all shortage nor a surplus of fuel, but an uneconomic geographical distribution of sources of supply in the extreme east and west of the country relative to the main concentration of industrial and domestic consumers in central Canada. This creates a situation in which, for the present, there is financial motivation for use of alternative energy sources in central Canada but no general feeling of urgency. In this circumstance, some investigation of the possibilities of local use of solar energy as a fossil fuel substitute for space heating purposes appears justified on economic grounds, and in the longer term as a provision against a possibly critical situation in the future. Solar heating does not appear to offer good prospects for the solution of the special energy problems of the remote communities of the vast Canadian north.

Research at the University of Toronto directed toward the identification and examination of those problems of solar space heating peculiar to the Canadian situation suggested that flat plate collector designs suitable in more southerly locations would, with slight modification, be equally suitable in Canada. It appears, however, that a solar heating system which would be independent of auxiliary heat sources and suitable for a house in southern Ontario would require long-term heat storage, to carry over for winter use heat collected during the warmer months.

The paper reports upon the use of scale models of water-filled basement heat storage reservoirs used to predict the behaviour of complete full-scale systems including house, solar collector, and storage characteristics, over periods of several years. The equipment essentially consists of a sand box in which is placed a small-scale model of the underground heat reservoir. The Fourier numbers for the model and prototype are held constant. A typical time scale is one minute in the model equal to two days of real time. By a running calculation during a test, heat supply or withdrawal rates are determined and the model continuously adjusted in accordance with the corresponding prototype solar collector performance and building heat demands. A typical result for a three-year period, showing storage temperature and heat supply and withdrawal rates, is given.

The paper also reports a study of the solar energy incident upon flat plate collectors with various orientations in the Toronto area. This is based upon the actual hourly recordings of direct and total incidence upon a horizontal surface as read at the Toronto weather station on an Eppley pyrheliometer. The data and computations, which would otherwise be impossibly bulky and onerous, were readily handled by a digital computer. The method used appears to offer clear advantages over methods based on analytical procedures in accounting for local weather variations and peculiarities. A standard set of assumptions would be necessary in handling data in this manner if similar studies made at different places are to be properly comparable. The assumptions made in this study are put forward for consideration in this respect.

L'ÉNERGIE SOLAIRE AU CANADA

Résumé

Le problème essentiel qui se pose actuellement au Canada en matière d'énergie n'est ni une insuffisance d'ensemble ni un excédent de combustible. Il tient à une répartition géographique anti-économique des sources d'approvisionnement d'énergie, à l'extrême est et à l'extrême ouest du pays, tandis que les consommateurs ménagers et industriels se trouvent concentrés au premier chef dans la région centrale. Ceci crée une situation dans laquelle il existe des raisons financières de s'intéresser aux sources nouvelles d'énergie dans le Canada central, sans toutefois que la question revête un aspect d'urgence. Dans ces conditions, certaines recherches sur les possibilités d'utilisation locale de l'énergie solaire pour le remplacement des combustibles fossiles pour le chauffage des locaux semblent justifiées du point de vue économique et, à long terme, pour se prémunir contre une situation qui, à l'avenir, pourrait devenir critique. Le chauffage solaire ne semble pas offrir de perspectives encourageantes quant à la solution des problèmes énergétiques spéciaux qui se posent pour les agglomérations isolées du grand nord canadien.

Les recherches menées à l'Université de Toronto dans le but de préciser et d'examiner les problèmes de chauffage solaire des locaux qui sont propres à la situation canadienne ont laissé entrevoir que les collecteurs à plaque plate qui se prêtent bien au fonctionnement sous des latitudes plus méridionales conviendraient également au Canada, avec de légères modifications. Il semblerait toutefois qu'une installation de chauffage solaire indépendante de sources auxiliaires de chaleur et indiquée pour une maison située dans la partie méridionale de l'Ontario exigerait la mise en réserve de la chaleur pendant longtemps pour conserver, en vue de leur utilisation en hiver, les calories récupérées pendant les mois plus chauds.

Ce mémoire signale l'emploi de modèles réduits de réservoirs ou d'accumulateurs remplis d'eau et installés en sous-sol pour prévoir le comportement de systèmes complets à l'échelle normale, notamment pour observer les caractéristiques de la maison, du collecteur et des accumulateurs pendant des périodes de plusieurs années. Le matériel est essentiellement constitué par une boîte à sable dans laquelle est placé un modèle à échelle réduite du réservoir de chaleur à installer en sous-sol. Les chiffres de Fourier sont tenus constants pour le modèle et le prototype. Une échelle type, pour le temps, est une minute avec le modèle pour deux jours de temps réel. En faisant les calculs voulus au cours d'un essai, on détermine les régimes de fourniture et de retrait de chaleur et on règle continuellement le modèle conformément au comportement du collecteur solaire prototype et aux exigences de chaleur de la maison. Les auteurs donnent un résultat type pour une période de trois ans, qui indique la température d'emmagasinage et le régime de fourniture et de retrait de la chaleur.

Ce mémoire signale également une étude de l'énergie solaire incidente sur des collecteurs à plaque plate avec diverses orientations, dans la région de Toronto. Ceci repose sur des enregistrements horaires effectifs de l'énergie incidente totale et directe sur une surface horizontale, telle qu'elle est lue au poste météorologique de Toronto avec un pyrhéliomètre d'Eppley. Les données et les calculs, qui seraient autrement longs et difficiles à manier au point d'être inutilisables, furent rapidement résolus par une machine à calculer du type numérique. La méthode utilisée semble présenter de nets avantages, par rapport à celles qui s'en remettent aux techniques analytiques, pour tenir compte des variations et des particularités locales du temps. Il serait nécessaire de se servir d'un jeu standard d'hypothèses pour exploiter les données de cette manière si des études similaires, à exécuter en divers lieux, doivent être véritablement comparables à celles-ci. C'est dans cet esprit que ce mémoire soumet à l'examen des membres de la Conférence les hypothèses sur lesquelles repose le présent travail.

SOME ASPECTS OF THE CLIMATOLOGY OF SOLAR RADIATION

J. N. Black *

The study of the climatology of global radiation has lagged far behind that of other meteorological elements; this is particularly apparent in the less developed parts of the world, where few radiation observations have been made. This is greatly to be regretted, since in these regions the utilization of solar energy has great possibilities, and a knowledge of the radiation climate is therefore very desirable. In this paper it is proposed to discuss in some detail three aspects of radiation climatology: first, the paucity of radiation records in the less developed countries and the ways in which estimates may be used to supplement observations; secondly, the number of years of observations required to establish reliable mean values of global radiation; and thirdly, the frequency of periods of low radiation.

A full understanding of the radiation climate is clearly necessary before efficient and economic apparatus can be designed for the utilization of solar energy. To take a very simple example, in the construction of a solar water heater, details of the radiation regime must be known before the capacity of the auxiliary water heater and the size of the storage tank can be calculated. To quote Morse (1): "In determining the amount of auxiliary heating necessary, allowance has been made for some heating in months where the mean daily solar output exceeds that required, since it is usually undesirable to install sufficient storage to cope with more than two successive days of low solar radiation." To the best of the present writer's knowledge, however, no studies of the frequency of occurrence of periods of successive days of low radiation have hitherto been published.

Radiation records and surveys

Although there are now published records of global radiation for well over 400 stations, these stations are concentrated principally in North America and Europe, relatively few networks being maintained in other continents. For Africa, for instance, the most recent issue of the *Quarterly Radiation Bulletin* lists data for some 25 stations south of or on the equator, while there are elsewhere published data for about 6 stations north of the equator, the whole continent thus being covered by about 30 records. In Australia, where utilization of solar power could be extremely valuable, data for about 10 stations only are being collected. This is in contrast with the United States of America, a land area of similar size to Australia, where over 80 recording stations are being maintained. The only records the author has seen for China and south-east Asia are for recently established stations in Singapore and Hong Kong, a long established station at Macao, and a short period of observations at Zi-ka-wei some years ago (2), though it is probable that other records exist.

In recent years, however, and particularly under the stimulus of the I.G.Y., a number of new networks have been established, for instance in Argentina, and it is hoped that the next decade will see a great advance in the understanding of global radiation.

At the present time, however, the necessary background information for the utilization of solar energy in the less developed countries is not directly available, but it is nevertheless possible to obtain estimates of radiation derived either on theoretical grounds or from a relationship with a known meteorological parameter such as the duration of sunshine or cloudiness. Such estimates have been used in the delineation of three sets of monthly charts for the world — Budyko (3), Black (4) and Bernhardt and Philipps (5), and for a number of regional surveys, the locations of which are given in figure 1. These cover Canada (Mateer (6), Jackson (7)); United States of America (Fritz and Macdonald (8)); Scandinavia (Auren (9)); Finland (Luneland (10)); the Soviet Union (Berliand and Efimova (11)) and New Zealand (Gabites (12)). These seven surveys give the data for each month, and there is another survey by Dubief (13) which gives December and June maps for North Africa. In addition, some areas have been charted directly from observed data: northern Europe by Black (14), extended to cover the United Kingdom by Day (see 15), Japan by Kawabata and Fujito (16) and "summer" and "winter" maps for southern Africa by Drummond and Vowinckel (17). The actinometric bulletins of Portugal (18) and Italy (19) include a chart for each month, and the United States Climatological Summaries print for each month a map of the departures of radiation from the mean.

It is reasonable to assume that surveys may be arrayed in order of decreasing precision as (*a*) regional surveys based directly on observed data, (*b*) regional surveys based on estimates and (*c*) global surveys. The accuracy of the three global surveys was compared by Black (14) for an area of northern Europe, and it was shown that in Budyko's survey, estimates

* Waite Agricultural Research Institute, University of Adelaide, South Australia.

L'ÉNERGIE SOLAIRE AU CANADA

Résumé

Le problème essentiel qui se pose actuellement au Canada en matière d'énergie n'est ni une insuffisance d'ensemble ni un excédent de combustible. Il tient à une répartition géographique anti-économique des sources d'approvisionnement d'énergie, à l'extrême est et à l'extrême ouest du pays, tandis que les consommateurs ménagers et industriels se trouvent concentrés au premier chef dans la région centrale. Ceci crée une situation dans laquelle il existe des raisons financières de s'intéresser aux sources nouvelles d'énergie dans le Canada central, sans toutefois que la question revête un aspect d'urgence. Dans ces conditions, certaines recherches sur les possibilités d'utilisation locale de l'énergie solaire pour le remplacement des combustibles fossiles pour le chauffage des locaux semblent justifiées du point de vue économique et, à long terme, pour se prémunir contre une situation qui, à l'avenir, pourrait devenir critique. Le chauffage solaire ne semble pas offrir de perspectives encourageantes quant à la solution des problèmes énergétiques spéciaux qui se posent pour les agglomérations isolées du grand nord canadien.

Les recherches menées à l'Université de Toronto dans le but de préciser et d'examiner les problèmes de chauffage solaire des locaux qui sont propres à la situation canadienne ont laissé entrevoir que les collecteurs à plaque plate qui se prêtent bien au fonctionnement sous des latitudes plus méridionales conviendraient également au Canada, avec de légères modifications. Il semblerait toutefois qu'une installation de chauffage solaire indépendante de sources auxiliaires de chaleur et indiquée pour une maison située dans la partie méridionale de l'Ontario exigerait la mise en réserve de la chaleur pendant longtemps pour conserver, en vue de leur utilisation en hiver, les calories récupérées pendant les mois plus chauds.

Ce mémoire signale l'emploi de modèles réduits de réservoirs ou d'accumulateurs remplis d'eau et installés en sous-sol pour prévoir le comportement de systèmes complets à l'échelle normale, notamment pour observer les caractéristiques de la maison, du collecteur et des accumulateurs pendant des périodes de plusieurs années. Le matériel est essentiellement constitué par une boîte à sable dans laquelle est placé un modèle à échelle réduite du réservoir de chaleur à installer en sous-sol. Les chiffres de Fourier sont tenus constants pour le modèle et le prototype. Une échelle type, pour le temps, est une minute avec le modèle pour deux jours de temps réel. En faisant les calculs voulus au cours d'un essai, on détermine les régimes de fourniture et de retrait de chaleur et on règle continuellement le modèle conformément au comportement du collecteur solaire prototype et aux exigences de chaleur de la maison. Les auteurs donnent un résultat type pour une période de trois ans, qui indique la température d'emmagasinage et le régime de fourniture et de retrait de la chaleur.

Ce mémoire signale également une étude de l'énergie solaire incidente sur des collecteurs à plaque plate avec diverses orientations, dans la région de Toronto. Ceci repose sur des enregistrements horaires effectifs de l'énergie incidente totale et directe sur une surface horizontale, telle qu'elle est lue au poste météorologique de Toronto avec un pyrhéliomètre d'Eppley. Les données et les calculs, qui seraient autrement longs et difficiles à manier au point d'être inutilisables, furent rapidement résolus par une machine à calculer du type numérique. La méthode utilisée semble présenter de nets avantages, par rapport à celles qui s'en remettent aux techniques analytiques, pour tenir compte des variations et des particularités locales du temps. Il serait nécessaire de se servir d'un jeu standard d'hypothèses pour exploiter les données de cette manière si des études similaires, à exécuter en divers lieux, doivent être véritablement comparables à celles-ci. C'est dans cet esprit que ce mémoire soumet à l'examen des membres de la Conférence les hypothèses sur lesquelles repose le présent travail.

SOME ASPECTS OF THE CLIMATOLOGY OF SOLAR RADIATION

J. N. Black *

The study of the climatology of global radiation has lagged far behind that of other meteorological elements; this is particularly apparent in the less developed parts of the world, where few radiation observations have been made. This is greatly to be regretted, since in these regions the utilization of solar energy has great possibilities, and a knowledge of the radiation climate is therefore very desirable. In this paper it is proposed to discuss in some detail three aspects of radiation climatology: first, the paucity of radiation records in the less developed countries and the ways in which estimates may be used to supplement observations; secondly, the number of years of observations required to establish reliable mean values of global radiation; and thirdly, the frequency of periods of low radiation.

A full understanding of the radiation climate is clearly necessary before efficient and economic apparatus can be designed for the utilization of solar energy. To take a very simple example, in the construction of a solar water heater, details of the radiation regime must be known before the capacity of the auxiliary water heater and the size of the storage tank can be calculated. To quote Morse (1): "In determining the amount of auxiliary heating necessary, allowance has been made for some heating in months where the mean daily solar output exceeds that required, since it is usually undesirable to install sufficient storage to cope with more than two successive days of low solar radiation." To the best of the present writer's knowledge, however, no studies of the frequency of occurrence of periods of successive days of low radiation have hitherto been published.

Radiation records and surveys

Although there are now published records of global radiation for well over 400 stations, these stations are concentrated principally in North America and Europe, relatively few networks being maintained in other continents. For Africa, for instance, the most recent issue of the *Quarterly Radiation Bulletin* lists data for some 25 stations south of or on the equator, while there are elsewhere published data for about 6 stations north of the equator, the whole continent thus being covered by about 30 records. In Australia, where utilization of solar power could be extremely valuable, data for about 10 stations only are being collected. This is in contrast with the United States of America, a land area of similar size to Australia, where over 80 recording stations are being maintained. The only records the author has seen for China and south-east Asia are for recently established stations in Singapore and Hong Kong, a long established station at Macao, and a short period of observations at Zi-ka-wei some years ago (2), though it is probable that other records exist.

In recent years, however, and particularly under the stimulus of the I.G.Y., a number of new networks have been established, for instance in Argentina, and it is hoped that the next decade will see a great advance in the understanding of global radiation.

At the present time, however, the necessary background information for the utilization of solar energy in the less developed countries is not directly available, but it is nevertheless possible to obtain estimates of radiation derived either on theoretical grounds or from a relationship with a known meteorological parameter such as the duration of sunshine or cloudiness. Such estimates have been used in the delineation of three sets of monthly charts for the world — Budyko (3), Black (4) and Bernhardt and Philipps (5), and for a number of regional surveys, the locations of which are given in figure 1. These cover Canada (Mateer (6), Jackson (7)); United States of America (Fritz and Macdonald (8)); Scandinavia (Auren (9)); Finland (Luneland (10)); the Soviet Union (Berliand and Efimova (11)) and New Zealand (Gabites (12)). These seven surveys give the data for each month, and there is another survey by Dubief (13) which gives December and June maps for North Africa. In addition, some areas have been charted directly from observed data: northern Europe by Black (14), extended to cover the United Kingdom by Day (see 15), Japan by Kawabata and Fujito (16) and "summer" and "winter" maps for southern Africa by Drummond and Vowinckel (17). The actinometric bulletins of Portugal (18) and Italy (19) include a chart for each month, and the United States Climatological Summaries print for each month a map of the departures of radiation from the mean.

It is reasonable to assume that surveys may be arrayed in order of decreasing precision as (*a*) regional surveys based directly on observed data, (*b*) regional surveys based on estimates and (*c*) global surveys. The accuracy of the three global surveys was compared by Black (14) for an area of northern Europe, and it was shown that in Budyko's survey, estimates

* Waite Agricultural Research Institute, University of Adelaide, South Australia.

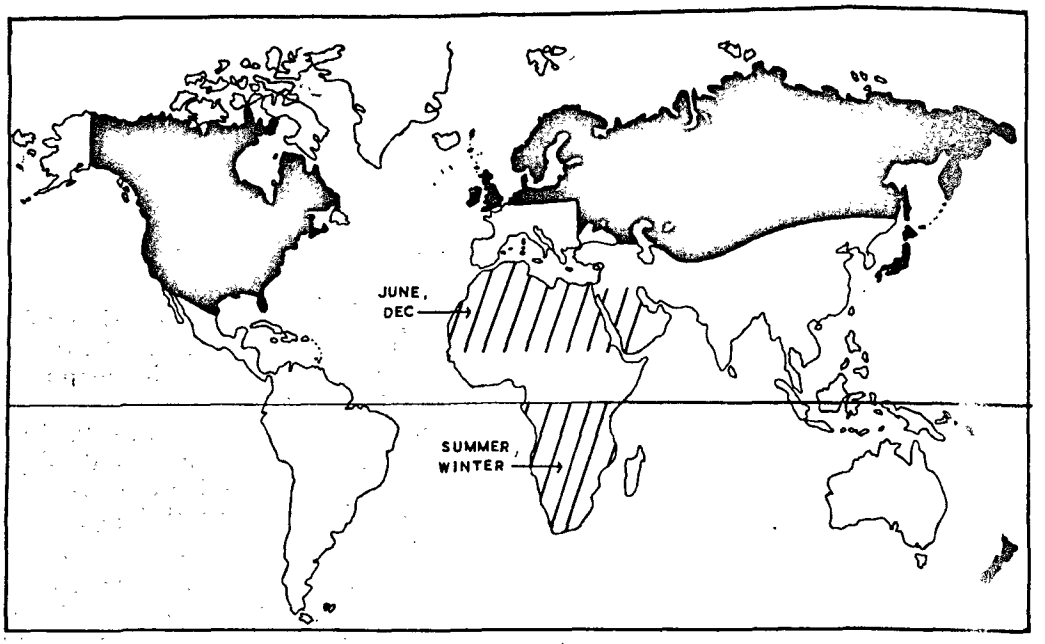


Figure 1. Regions of the world for which surveys of global radiation are available

departed from observed data from +17 to 2 —per cent; in Black's survey, from +17 to —7 per cent and in Bernhardt and Philipps' survey, from +31 to +6 per cent, while the averages of the twelve monthly departures were +3 per cent, +3 per cent and 10 per cent, respectively. An alternative approach to the assessment of the accuracy of surveys based on estimates is to attempt to join up surveys of two contiguous regions; when this was tried for the surveys of Fritz and Macdonald (United States) and Mateer (Canada), it was found that they matched well, except for the Great Lakes district. In fact, margins of surveys based on estimates are apt to be less accurate than the centre, since it is at the margins that the relationships between the meteorological parameters used are most likely to break down. The accuracy of different methods of obtaining estimates for individual stations can easily be assessed if records are already available as a basis for comparison (see Hinzpeter (20) or Kacvinská (21)), but it should be noted that a method satisfactory at the survey level may well be inappropriate at the individual station level. Also, a method satisfactory in one climate may be quite unsatisfactory in another; for instance, Dubief (13) found that values estimated by the method of Black (4) for Tamanrasset, in Algeria, were very close to the observed values, and he therefore used this method to chart radiation for the whole of North Africa and part of the Arabian peninsula. On the other hand, Wartena (22) found that the same method gave estimates for Baghdad that were too high in summer and far too low in cloudy weather.

Variability of radiation observations

In the examination of radiation data, it is often desirable to know the between-year variability of the observed values; it is, for instance, necessary to know the variability before the length of record required for an accurate estimate of the true mean of the daily radiation for each month can be deter-

Table 1. Calculated length of record (years) to establish true mean ± 5%, 0.05P

Station	*Jan.*	*Feb.*	*Mar.*	*Apr.*	*May*	*June*	*July*	*Aug.*	*Sept.*	*Oct.*	*Nov.*	*Dec.*	*Latitude*	*Length of record available (years)*	*Source of data*
Tacubaya (Mexico) . .	16	> 30	20	18	24	30	> 30	23	> 30	> 30	23	12	19.4°N	11	(23)
Tamanrasset (Algeria) .	5	9	10	18	5	7	6	9	11	12	4	17	22.8°N	12	(13)
Dry Creek (South Australia)	3	9	8	18	19	14	11	9	11	8	3	3	34.8°S	12	(24)
Albuquerque (New Mexico)	10	18	14	6	9	5	5	5	19	16	9	16	35.8°N	9	(25)
Fresno (California) . . .	> 30	> 30	23	9	8	6	7	7	9	24	17	> 30	36.7°N	24	(26)
Lisbon (Portugal) . . .	> 30	> 30	> 30	27	19	14	11	9	19	16	28	> 30	38.7°N	20	(25)
Sverdlovsk (USSR) . .	24	29	> 30	29	23	11	14	29	7	12	21	> 30	56.7°N	11	(27)

mined. The variability can be presented either as a statistic, such as the coefficient of the variability, or as the number of years for which it is necessary to continue observations before an estimate of the true mean within certain arbitrary limits, and at a given level of probability, can be obtained. The lengths of record needed for an estimate of the true mean ±5 per cent, at 0.05 probability, have been calculated for each month for a number of stations and are given in table 1. Unfortunately, there are few long-term records in desert and tropical climates, but the data suggest that there are marked differences in variability that would repay detailed study. There is a general trend for much higher variability in winter than in summer, particularly in the stations with a "Mediterranean" type climate (Dry Creek, Fresno and Lisbon). The data for Sverdlovsk have been added to provide a comparison with a station of higher latitude.

However, many of the climates of the less developed parts of the world are paralleled in the United States, and the accompanying map (figure 2) shows the length of record required for an accurate estimate of the mean monthly radiation in July for 32 stations in that part of the United States south of 40°N. It is clear that there is a marked trend across the continent, and this trend is not related to the radiation income for the month, to the precipitation or to the mean temperature. Although the month chosen is July, which, on the basis of table 1, should be one of the least variable, long periods are nevertheless necessary in some regions before reliable means can be established. It might be argued that to examine the data for one month only is unreasonable, since differing seasonal trends for different areas may obscure the pattern of variability; a number of stations, well distributed over the map, were taken and the variability of the January, April and October data was also calculated. These calculations confirmed the pattern for July, though there were a few individual differences: one station (Hatteras, North Carolina), with significantly lower variability in April than July, and one (Atlanta, Georgia) with lowest variability in January.

Since comparable extensive data are not available for other countries, it is suggested that this map of the Unites States might well be used as a guide in the establishment of radiation networks and in the examination of radiation data in regions of similar climates.

Periods of low radiation

The problem of periods of successive days of low radiation, and its bearing on the utilization of solar energy, has already been mentioned. With this in mind, a number of records of daily values of radiation have been examined; these records have been selected as far as possible to represent climates of or similar to those of the less developed parts of the world, but the paucity of daily records over a sufficiently long period left little room for choice. In the absence of specific critical levels of radiation, an arbitrary value has to be selected for a day of "low" radiation, and for the purposes of this study, two such values have been taken —100 gm cal/cm²/day and 250 gm cal/cm²/day. Histograms of the frequency of occurrence of periods of successive days of radiation below these two values are shown in figure 3. The height of the histograms indicates the mean number of occurrences each year of the particular length of period. The length of the records and the sources of the data are: Dry Creek, South Australia, 12 years (24); Lisbon, Portugal, 5 years (18); Luanda, Angola, 5 years (18); Lod Airport, Israel, 4 years (28); and Lourenço Marques, Mozambique, 5 years (18). Lisbon and Dry Creek are in similar climates, a "Mediterranean" type climate with strong maritime influences, and the frequencies of occurrence of periods of low radiation are similar.

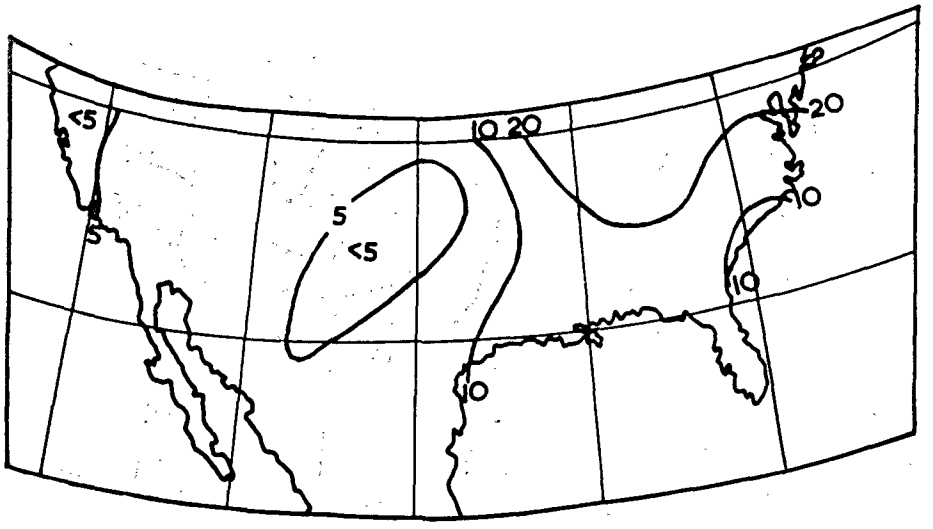


Figure 2. Map of southern United States showing the number of years of observations required for an estimate ± 5 per cent of the true mean, 0.05P. (Based on data for July.)

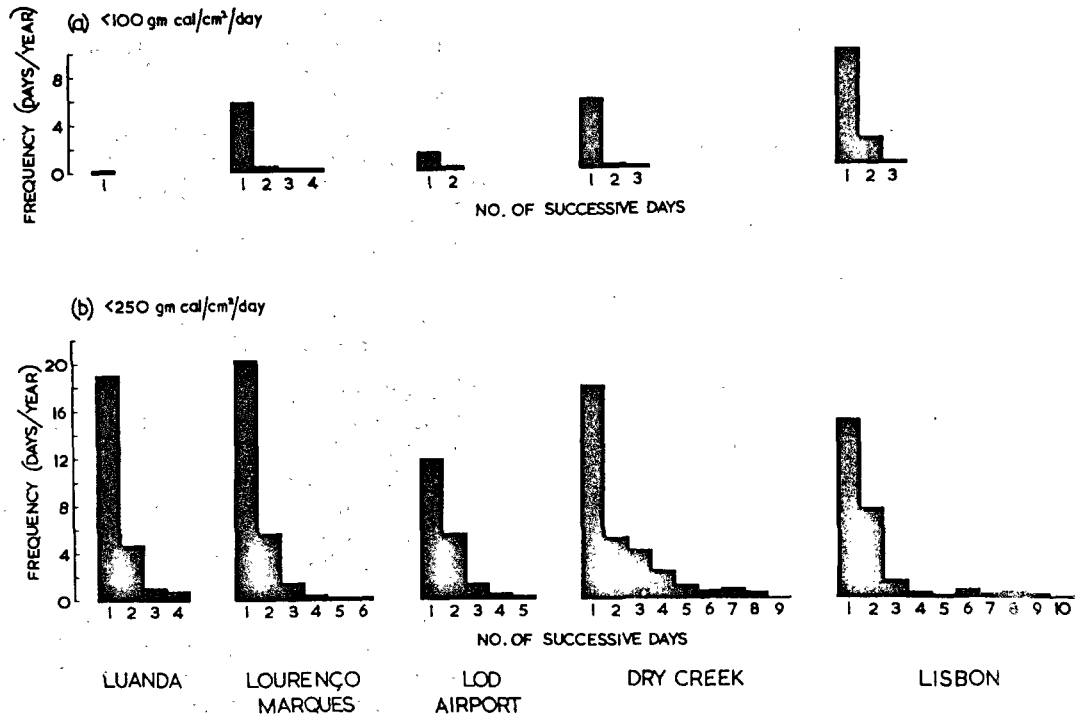


Figure 3. Histograms of the frequencies (occurrences/year) of periods of successive days of low radiation

It is very rare to get two or more consecutive days with radiation below 100 gm cal/cm²/day at either station, but Dry Creek can expect one period of 5 successive days below 250 and Lisbon one period of 3 such days each year. In Luanda, a day with less than 100 gm cal/cm² occurs on the average only once every 5 years, but there are 19 isolated days below 250, four periods of 2 successive days and one of 3 days below 250 gm cal/cm² each year. Lod Airport is of similar latitude to Dry Creek and Lisbon, but in a dry "Mediterranean" type climate. At least one day with radiation below 100 gm cal/cm² occurs each year, and 11 days below 250, with five periods of 2 days and one of 3 days below 250. Lourenço Marques, a subtropical east coast station, has similar characteristics to Dry Creek, but with a lower frequency of periods of successive days below 250 gm cal/cm². It should be noted that for all these stations, the histograms for the periods of radiation below 250 gm cal/cm²/day are not complete, since occasional long periods of very low frequency have not been included (for instance, one period of 37 consecutive days was recorded at Lisbon).

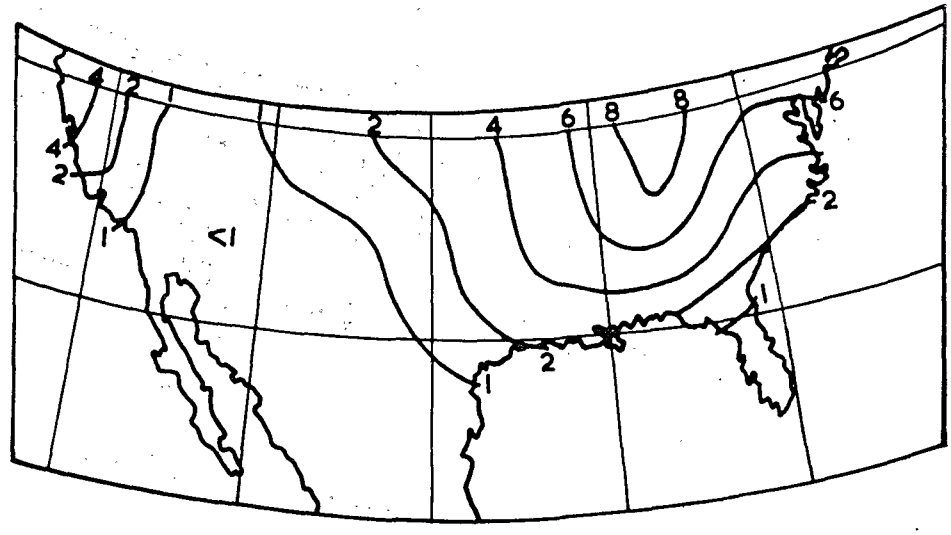


Figure 4. Map of southern United States showing the annual frequencies of occurence of two or more successive days with radiation less than 100 gm cal/cm²

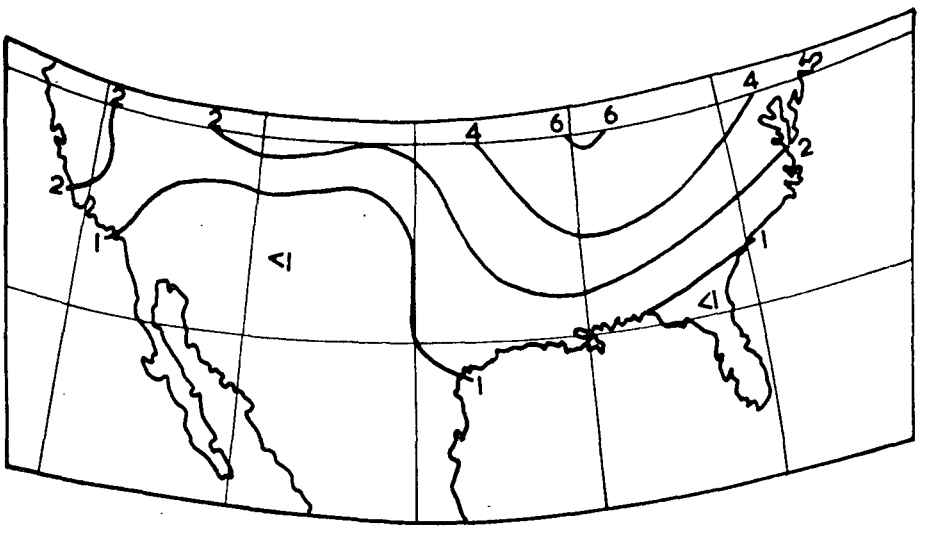


Figure 5. Map of southern United States showing the annual frequencies of occurence of five or more successive days with radiation less than 250 gm cal/cm²

Records of radiation for three years have been published (29) for Ksara, in Lebanon, and over this short period of record reveal rather high frequencies of full days. The annual frequencies of days with radiation less than 100 gm cal/cm² are: 8.7 single days, 0.3 two-day periods and one three-day period; for less than 250 gm cal/cm²: 14.0 single days, 6.7 periods of 2 days, 1.7 of 3 days, 1.3 of 4 days, 1.3 of 5 days and one of 6 days. In comparison with the data for Lod Airport in Israel, there is a markedly higher frequency of periods of dull days in Ksara, probably associated with the higher altitude of Ksara (about 920 m above sea level) than Lod (40 m above sea level).

A short but incomplete record of less than two years was published for Baghdad by Wartena (22). Baghdad has a continental subtropical climate, and of the 572 days for which data are given, there were only 2 isolated days with radiation below 100 gm cal/cm², 25 isolated days with radiation below 250 gm cal/cm², 3 two-day and 2 three-day periods below 250. However, the Baghdad record is short and unfortunately the gaps occur chiefly in the winter months, when the low values are most common. The data are of value in showing that in an environment typical of many less developed countries, periods of several days of low radiation may be expected.

The same frequencies have been calculated for the 32 stations in the United States used in figure 2. Instead of plotting the histograms of the frequency distributions for so many stations, two maps have been drawn: figure 4 shows the frequency of occurrence of periods of 2 or more successive days of radiation below 100 gm cal/cm², and figure 5 shows the frequency of periods of 5 or more days below

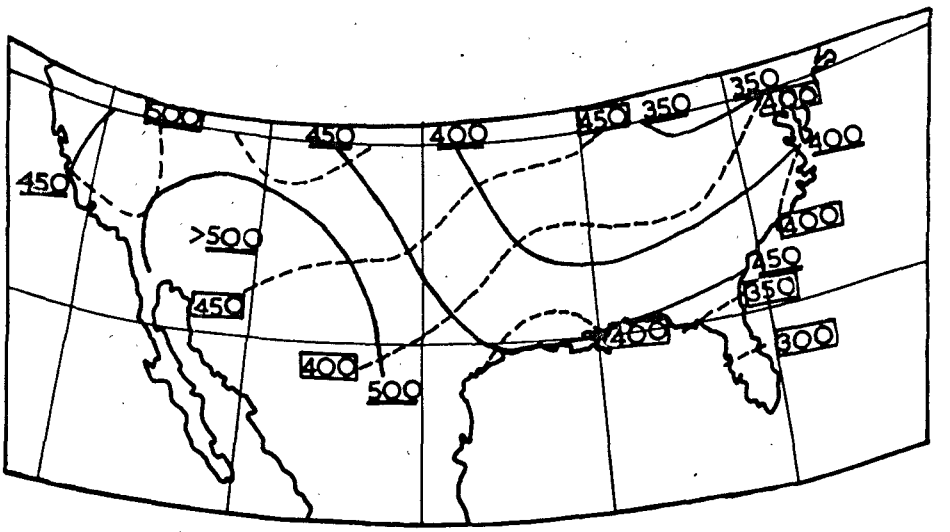


Figure 6. Map of southern United States showing the mean radiation/day (heavy line, reference values underlined) and range (radiation for highest month less that of lowest month; broken line, reference values in "boxes")

250 gm cal/cm². These two maps are generally similar in pattern, and are indeed also similar to the maps of total number of days/year with radiation below 100 and 250 gm cal/cm² respectively. There is in each map the same trend of increasing values from west to east, with an increase in the number of dull days, and of the frequencies of long periods of dull days, at longitudes 85-90°W, as was demonstrated in the map of variability of radiation. For a large part of the southern United States, the chances of having a period of days of low radiation long enough to be of concern in utilizing solar energy are probably small. For instance, in records for 8½ years for El Paso, Texas, only 94 days with radiation less than 250 gm cal/cm² were found; on the average, these occur as 6.6 single days/year, 2.0 periods of 2 days and 0.4 periods of 3 days. Similarly, Inyokern, California, had 81 days with radiation below 250 gm cal/cm² in records for 7 years, 5.7 as single days/year, 1.4 periods of 2 days, 0.6 of 3 days, 0.1 of 3 and 0.1 of 4 days. Taking another station of low latitude but more under maritime influence, Lake Charles, Louisiana, had 438 days of radiation below 250 gm cal/cm² in records for 8½ years, occurring as 17.5 single days/year, 6.4 two-day periods, 2.8 three-day, 1.9 four-day, 0.4 five-day, 0.4 six-day, and 0.7 seven-day periods each year. Some stations, however, have above average frequencies of very long periods: for instance, Fresno, California, had one spell of 34 days below 250 gm cal/cm², and Oak Ridge, Tennessee, one of 36.

In order that greater use can be made of figures 4 and 5, a further map (figure 6) has been prepared. This map shows the distribution over the southern part of the United States of (*a*) the mean radiation per day over the whole year, shown in the heavy black line, with reference values underlined and (*b*) the range of the monthly values (the value for the highest month less that of the lowest), shown in the broken line with the reference values in "boxes".

Conclusion

It is hoped that the various aspects of radiation climatology discussed in this survey may be useful in the application of solar energy. The principal need is obvious: more radiation observations in the less developed parts of the world and intensive studies of the data collected.

References

1. Morse, R. N., The design and construction of solar water heaters. Comm. Sci. Ind. Res. Org. (Australia), Central Experimental Workshops, Report E.D.1 (1954).
2. Lejay, P., Etude de la radiation solaire totale, juillet 1935 - janvier 1937. Zi-ka-wei, *Notes Met. Phys. Fasc.* 6 (1937).
3. Budyko, M. I., *Atlas of heat balance* (Russian). Leningrad, 1-41 (1955).
4. Black, J. N., The distribution of solar radiation over the earth's surface. *Arch. Met. Geoph. Biokl.* B7: 165-189 (1956).
5. Bernhardt, F. and Philipps, H., Die Räumliche und zeitliche Verteilung der Einstrahlung der Ausstrahlung und der Strahlungsbilanz im Meersniveau. *Met. Hydr. Dienst D.D.R. Abh.* 45: 1-227 (1958).
6. Mateer, C. L., A preliminary estimate of the average insolation in Canada. *Can. Journ. Agric. Sci.* 35: 579-94 (1955).
7. Jackson, C. I., Insolation and albedo in Quebec-Labrador. *McGill Sub-arctic Res. Papers* 5: 1-105 (1959).
8. Fritz, S., and MacDonald, T. H., Average solar radiation in the United States. *Heating and Vent.* 46: 61-64 (1949).
9. Auren, T. E., Radiation climate in Scandinavian peninsular. *Ark. Math. Astr. Fys.* 24 (A): 1-50 (1939).
10. Lunelund, H. H., In Finnland eingestrahlte Wärmemenge. *Soc. Sci. Fenn., Comm. Phys. Math.* 11: 1-19 (1941).
11. Berliand, T. G. and Efimova, N. A., Monthly charts of the total solar radiation and the radiation balance over the territory of the Soviet Union (Russian). *Trudy Glav. Geoph. Obs.* 50: 48-82 (1955).
12. Gabites, J. F., A preliminary estimate of the mean daily insolation in New Zealand. *N.Z. Meteor. Service, Circular Note* 71: 1-10 (1951).
13. Dubief, J., La radiation solaire globale, *Le climat du Sahara*, 54-60. Alger, 1959.
14. Black, J. N., A contribution to the radiation climatology of Northern Europe. *Arch. Met. Geoph. Biokl.* B 10: 182-92 (1960).
15. Penman, H. L., Weather problems in agriculture. *Nature* 187: 995-6.
16. Kawabata, V. and Fujito, M., Distribution of total horizontal insolation in Japan and its neighbourhood. *Geoph. Mag.* 22: 143-56 (1950).
17. Drummond, A. J. and Vowinckel, E., The distribution of solar radiation throughout Southern Africa. *J. Meteor.* 14: 343-53 (1957).
18. Portugal, Serviço Meteorológico nacional, *Boletim actinométrico de Portugal.* Mimeo. Lisbon, 1955-1960.
19. De Pasquale, O., La rete attinometrica del Servizio Meteorologico dell'Aeronautica Italiana. Risultati del primo anno di misura della radiazione globale. *Riv. Meteor. Aeron.* 16: 1-18 (1956).
20. Hinzpeter, H., Vergleichende Prüfung von Formeln zur Berechnung von Globalstrahlungssummen. *Arch. Met. Geoph. Biokl.* B 9: 60-72 (1958).
21. Kacvinská, K., Porovanie niektorých vzorcov na výpočet globálneho ziarenia. *Meteor. Zpravy* 12: 101-7 (1959).
22. Wartena, L., Het klimaat en de verdamping van een meer in centraal Irak. *Med. Landb. Wageningen* 59 (9) (1959).
23. Gorczynski, L., *Comparison of the climate of the United States and Europe.* Polish Inst. Arts. Sci. in America. New York, 1945.
24. I.C.I. Alkali (Austr.) Pty. Ltd., Solar radiation measurements at Dry Creek, South Australia. 1947-1958. Mimeo. Adelaide, 1959.
25. United States Weather Bureau, *Climatological Data, National Summaries* (1950-1958).
26. Portugal, Serviço Meteorológico nacional, Insolação e radiação global em Lisboa, Porto e Funchal no periódo de 1939-1954. Mimeo. Lisbon, 1955.
27. Lileev, M. V., Characteristics of the radiation balance and its components in the Sverdlovsk region (Russian). *Trudy Glav. Geoph. Obs.* 50: 88-110 (1955).
28. Israel, Meteorological Service, *Monthly Weather Report.* Hakirya, 1956-1960.
29. Ksara, Observatoire, *Annales climatologiques* (1957-1959).

Summary

A knowledge of the radiation climate is necessary for the design of efficient and economic apparatus for the utilization of solar energy, but in the less-developed parts of the world the information required is not available. This paper surveys the basic radiation data which have been collected, and examines in particular three aspects of radiation climatology important in solar energy utilization : first, the paucity of radiation records in the less developed parts of the world, and the ways in which estimates may be used to supplement observations; secondly, the number of years of observations required to establish reliable estimates of the mean global radiation; and thirdly, the frequencies of periods of radiation low enough to affect efficient utilization.

The construction of charts of radiation income is hindered by the uneven distribution over the earth of the recording stations, although there are now available records for over 400 stations. It has been possible to chart radiation from observed data only for a few small areas, but surveys of a number of countries have been made, using estimates of radiation based on duration of sunshine or cloudiness. A map has been prepared to show the regions covered by published surveys. In addition to these regional surveys, three sets of world-wide charts have been published. The ways in which the accuracy of surveys may be assessed are discussed, and it is shown that a method of estimation satisfactory in one climate may be inappropriate in another.

The between year variability of global radiation for each month has been examined for a number of stations. These variabilities have been used to calculate the number of years for which it is necessary to maintain observations in order to obtain an estimate within 5 per cent of the true mean radiation, at a probability of 0.05. The number of years is generally smaller in summer than in winter, though there are exceptions to this generalization, and the differences between stations are marked. Since the climates of many less-developed areas are paralleled in the United States, similar calculations have been made for July for 32 stations south of latitude 40°N in the United States, and the results are presented on a map. It is shown that for July, the necessary length of record increases from about 5 years on the west coast to over 20 years in the east.

The third aspect studied is the frequency of periods of successive days of radiation less than (*a*) 100 and (*b*) 250 gm cal/cm^2. These frequencies were calculated for a number of stations for which daily observations have been published. Histograms of the annual frequencies of these periods are given for five stations with climates similar to those of many less developed countries, and it is shown that periods of two or more days of radiation less than 100 gm cal/cm^2 are rare, but 4 or 5 periods of two or more successive days of radiation less than 250 gm cal/cm^2 may be expected each year in many climates. These calculations were repeated for the stations in the United States, and charts are presented of the distribution of annual frequencies of (*a*) periods of two more days with radiation less than 100 gm cal/cm^2 and (*b*) periods of five or more days with radiation less than 250 gm cal/cm^2. Both maps show an increase in the frequencies of these periods from west to east across the United States.

In conclusion, attention is drawn to the need for more observations of radiation in the less developed countries.

QUELQUES ASPECTS DE LA CLIMATOLOGIE DU RAYONNEMENT

Résumé

Une connaissance du climat du rayonnement est nécessaire pour la mise au point de matériel efficace et économique en vue de l'utilisation de l'énergie solaire, mais, dans les régions peu développées du globe, ces renseignements font défaut. Dans la présente communication, l'auteur passe en revue les données fondamentales qui ont été recueillies au sujet du rayonnement et examine, en particulier, trois aspects de la climatologie du rayonnement qui sont importants en ce qui concerne l'utilisation de l'énergie solaire : tout d'abord le manque de données sur le rayonnement dans les régions peu développées du globe, et la manière dont les évaluations peuvent être utilisées pour compléter les observations; deuxièmement, le nombre d'années d'observation nécessaire pour mettre au point des évaluations valables sur le rayonnement global moyen; et troisièmement, la fréquence des périodes de rayonnement assez faible pour porter préjudice à une utilisation efficace de ce rayonnement.

L'établissement de tables indiquant les quantités de rayonnement reçues est gêné par les irrégularités de répartition des stations d'enregistrement de par la surface du globe, bien que l'on dispose maintenant de données provenant de plus de 400 postes de ce genre. On n'a réussi à faire des relevés du rayonnement à partir de données d'observation que dans quelques régions restreintes, mais on a exécuté des études dans nombre de pays en se servant d'évaluations du rayonnement basées sur la durée d'ensoleil-

lement ou d'ennuagement. On a préparé une carte pour indiquer les régions sur lesquelles portent les travaux déjà publiés. Outre ces études régionales, on a publié trois jeux de cartes à l'échelle mondiale. L'auteur examine la manière dont l'exactitude des cartes peut être évaluée, et montre qu'une méthode d'évaluation satisfaisante pour un climat donné peut être contre-indiquée pour un autre.

Les variations du rayonnement global d'une année à l'autre ont été étudiées pour chaque mois en un certain nombre de postes. On s'est servi de ces degrés de variabilité pour calculer le nombre d'années pour lesquelles il est nécessaire de procéder à des observations en vue d'obtenir des évaluations exactes à 5 p. 100 près par rapport au rayonnement moyen véritable, avec une probabilité de 0,05. Le nombre de ces années est généralement plus petit en été qu'en hiver, bien que cette généralisation souffre certaines exceptions et que les différences entre postes soient sensibles. Étant donné que le climat de plusieurs régions peu développées se retrouve aux États-Unis, on a fait des calculs analogues, pour le mois de juillet, à 32 postes situés au sud de la latitude 40° Nord aux États-Unis, et les résultats de ces mesures ont été résumés dans une carte. On démontre que, pour juillet, la durée nécessaire des enregistrements passe d'environ 5 ans, sur la côte du Pacifique, à plus de 20 ans sur la côte de l'Atlantique.

Le troisième aspect étudié est la fréquence des périodes de journées consécutives pendant lesquelles le rayonnement reçu est inférieur à (a) 100 et (b) 250 gm cal/cm². Ces fréquences ont été calculées pour un certain nombre de postes pour lesquels on a publié des observations quotidiennes. On donne des histogrammes des fréquences annuelles de ces périodes pour cinq postes ayant des climats analogues à ceux de nombre de pays peu développés, et on démontre que les périodes de deux jours ou davantage pendant lesquels le rayonnement est inférieur à 100 gm cal/cm² sont rares, mais que quatre ou cinq périodes de deux jours consécutifs ou davantage où le rayonnement est inférieur à 250 gm cal/cm² peuvent être prévues chaque année sous nombre de climats. Ces calculs ont été répétés pour les postes des États-Unis, et l'auteur présente des cartes qui donnent la répartition des fréquences annuelles a) des périodes de deux jours consécutifs ou davantage pendant lesquels le rayonnement est inférieur à 100 gm cal/cm², et b) des périodes de cinq jours ou davantage ayant un rayonnement inférieur à 250 gm cal/cm².

Les deux cartes indiquent une augmentation de la fréquence de ces périodes quand on se déplace de l'ouest vers l'est des États-Unis.

En conclusion, l'auteur souligne le besoin d'observations plus abondantes dans les pays sous-développés.

DONNÉES MÉTÉOROLOGIQUES CONCERNANT L'ENSOLEILLEMENT ET L'ÉCLAIREMENT ÉNERGÉTIQUE EN VUE DES APPLICATIONS PRATIQUES

R. Dogniaux *

Grâce à des observations continues et à l'application de formules représentatives des éclairements énergétique et lumineux en relation avec la durée d'insolation, il est possible de connaître avec précision le climat solaire d'une région et d'aborder avec succès des études techniques portant sur l'insolation des façades des îlots bâtis, l'ensoleillement des pentes, l'irradiation des bâtiments.

L'objet de cet exposé, forcément limité, sera de présenter certaines données caractéristiques du climat solaire en Belgique et d'indiquer par quelques exemples pratiques des formes d'utilisation concrète.

* Institut royal météorologique de Belgique, Bruxelles.

Les *composantes du rayonnement énergétique* peuvent se schématiser comme il est indiqué à la figure 1 dans le cas d'un récepteur à surface horizontale situé à un niveau déterminé. Cette nomenclature peut s'étendre à d'autres formes de récepteurs : sphériques, cylindriques ou autres.

Les qualités spectrales de ces différents types de rayonnement dépendent de la nature des sources émettrices. On distingue :

a) Le *rayonnement global* (incident et réfléchi), dont la source première est le soleil et dont les radiations se situent grosso modo entre 2 500 Å et 2,5 μ;

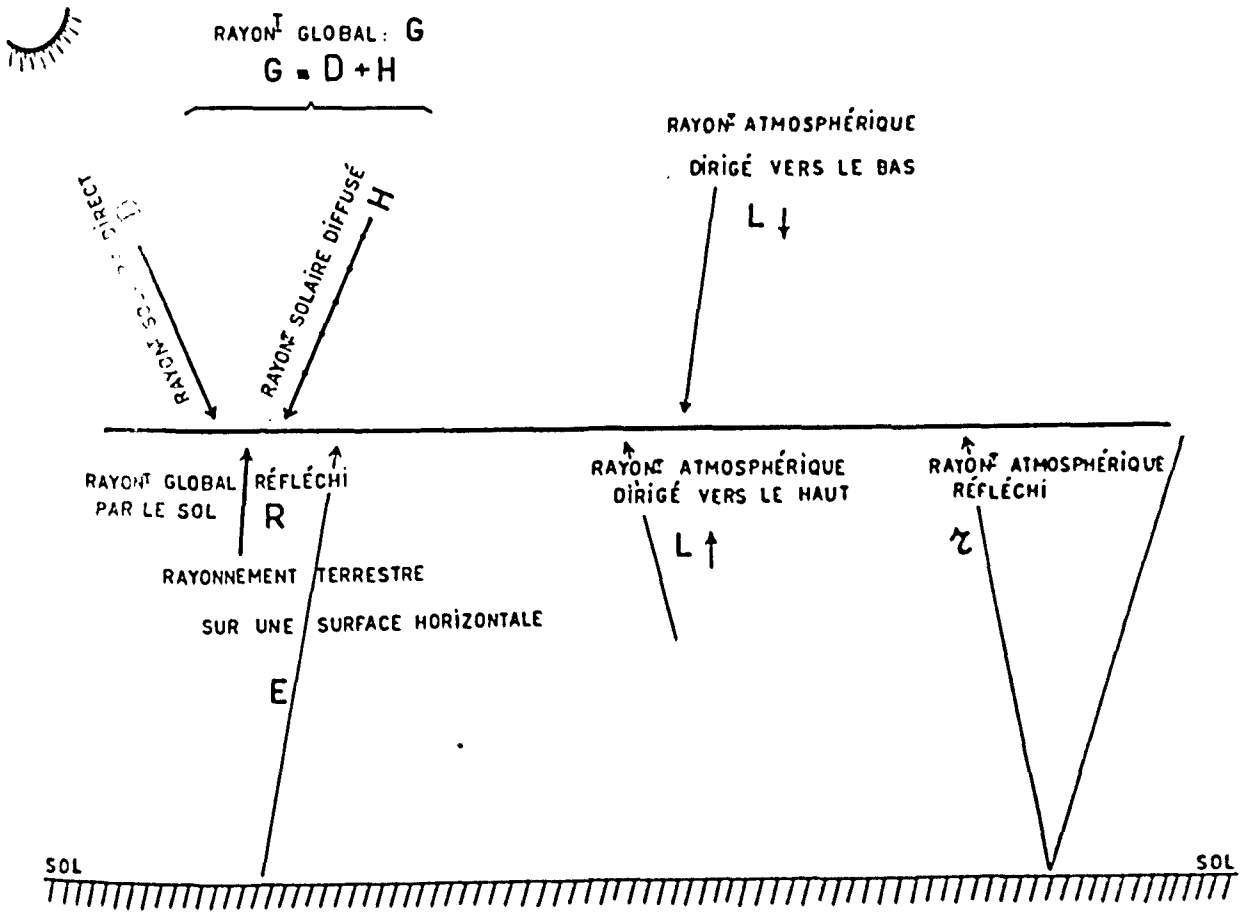


Figure 1. Rayonnements énergétiques au sein de l'atmosphère et au niveau du sol

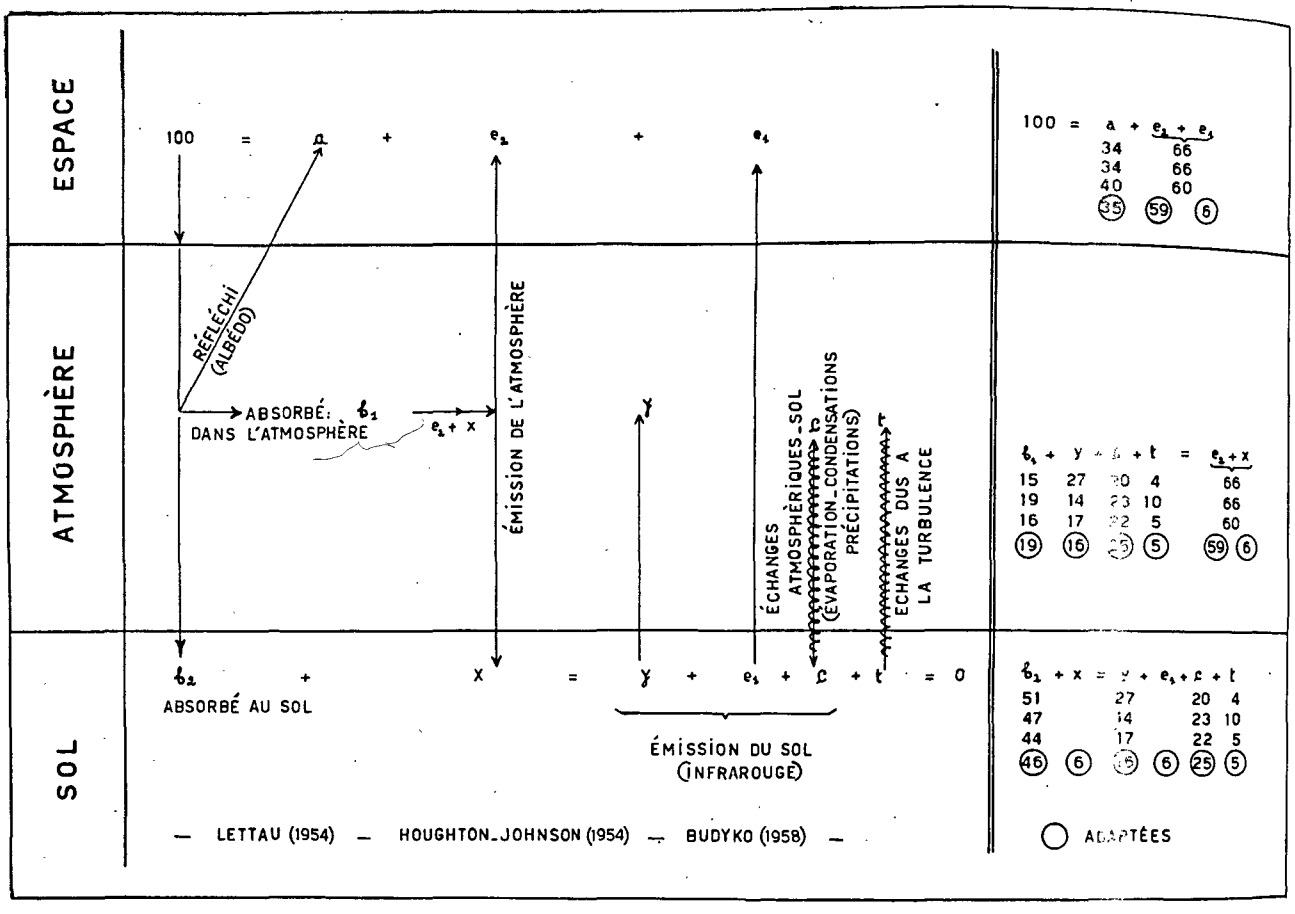


Figure 2. Bilans des rayonnements

b) Le *rayonnement atmosphérique*, correspondant à l'émission de corps à basses températures, de l'ordre de 1 000 °K (haute atmosphère) à 300 °K (troposphère), de longueurs d'onde comprises entre 2 et 16 μ avec un maximum à 2,9 μ pour un corps noir à 1 000 °K;

c) Le *rayonnement terrestre*, dont le spectre d'émission s'étale de 4 μ à 40 μ, avec un maximum voisin de 10 μ.

Tout rayonnement est soumis dans l'atmosphère terrestre à un effet d'*extinction* résultant de divers processus tels que :

a) La *diffusion par les molécules atmosphériques* dans une atmosphère pure et sèche, ne contenant ni poussière, ni vapeur d'eau;

b) L'*absorption sélective par les gaz de l'atmosphère* : azote et oxygène à très haute altitude, ozone et vapeur d'eau, dont le rôle est très important dans les problèmes liés au bilan thermique de l'atmosphère;

c) L'*extinction par les aérosols*, qui se traduit dans l'expression générale du coefficient d'absorption par l'introduction d'un terme faisant intervenir le nombre de particules, leurs dimensions, les rapports entre les dimensions des particules et la longueur d'onde de la radiation incidente.

Enfin, il importe de tenir compte des échanges de rayonnements entre l'atmosphère et le sol. Nous tenterons de donner un schéma du *bilan général des rayonnements* au sommet de l'atmosphère, dans l'atmosphère et au niveau du sol.

a) *Au sommet de l'atmosphère*, il faut admettre un état d'équilibre entre le gain procuré par l'apport de l'énergie solaire provoquant une irradiation journalière de 720 calories par cm², posée comme gain égal à 100 p. 100, et les pertes par rayonnement réfléchi, par l'atmosphère (albédo) et par rayonnements atmosphériques et terrestre renvoyés vers l'espace. Remarquons que l'albédo peut varier de 35 p. 100 (nouvelle valeur) à 42 p. 100 (ancienne valeur) et que l'énergie solaire b_1 absorbée par l'atmosphère est comprise entre 13 et 20 p. 100.

b) *Dans l'atmosphère*, il faut considérer un état d'équilibre entre l'apport d'énergie constitué d'une part par le rayonnement solaire absorbé, b_1, le rayonnement terrestre, y, et la résultante des énergies provenant des divers échanges liés aux processus d'évaporation, de condensation, des précipitations et de la turbulence, C, et d'autre part par les pertes dues à l'émission propre de l'atmosphère vers l'espace, e_2, et vers le sol, x.

c) *Au niveau du sol*, il doit exister de même un état d'équilibre entre le rayonnement solaire absorbé,

b_2, le rayonnement atmosphérique effectif, x, et les émissions totales du sol vers l'atmosphère, y, vers l'espace, e_1, et comme résultante des processus d'échange terre-atmosphère, C et t.

L'examen de la figure 2 donne un ordre de grandeur des divers paramètres énumérés ci-dessus.

Insolation et orientation

De nombreux problèmes de la vie domestique sont liés à l'orientation et à l'insolation. Les urbanistes chargés de plans d'aménagement constatent journellement combien il est difficile de se faire une opinion suffisamment précise sur les points suivants : implantation optimum d'un local isolé, meilleure orientation à donner aux voiries, distances à réserver entre constructions, hauteurs à prescrire à celles-ci.

Les réponses à ces questions découlent immédiatement de la prise en considération d'abaques représentant les trajectoires apparentes du soleil et des conditions climatiques réelles.

L'*insolation possible*, en un lieu à l'horizon parfaitement dégagé est conditionnée par la trajectoire apparente du soleil.

L'*insolation effective*, ou durée réelle de l'ensoleillement observé, est directement liée à la nébulosité et à la topographie du site entourant la station. A titre d'indication, nous donnons au tableau 1 les valeurs moyennes de l'insolation à Uccle, en heures par décade, établies pour la période 1901-1930 pour les quatre cas suivants : P, maximum possible; F, cas favorables; D, cas défavorables; N, cas normaux.

L'*ensoleillement d'un local supposé isolé* de toutes constructions voisines affectant uniquement ses façades verticales (nous n'envisageons pas ici les locaux susceptibles d'être éclairés par le plafond) dépend à la fois de l'orientation de la façade et de la trajectoire apparente du soleil. Il se trouve réalisé pour autant que l'azimut du soleil reste compris entre les valeurs A et $A + 180°$, où A est l'azimut d'une direction parallèle à la façade.

Quelques considérations pratiques découlent immédiatement de l'examen de la figure 3, donnant les insolations maximales possibles en fonction de l'orientation de la façade à trois périodes caractéristiques de l'année (solstices d'hiver et d'été et équinoxes). Les rayons vecteurs des courbes polaires sont proportionnels aux durées d'ensoleillement (la direction de ce rayon étant normale à la façade considérée).

a) La façade nord ne reçoit du soleil que pendant la moitié de l'année (du 21 mars au 21 septembre).

b) Les façades NE et NW présentent une grande variation annuelle (7 heures en été, entre 3 et 4 heures aux équinoxes, et moins d'une heure en hiver).

c) Les façades est et ouest présentent également de grandes variations annuelles (environ 8 heures en été, 6 heures aux équinoxes, et 4 heures en hiver).

d) Les façades SE et SW présentent au cours de l'année le plus d'uniformité dans la durée d'ensoleillement (10 heures en été, 8 heures et demie aux équinoxes, et 7 heures et demie environ en hiver).

Tableau 1: Durées d'ensoleillement (en heures) à Uccle

	Janvier				*Février*				*Mars*				*Avril*			
	P	F	N	D	P	F	N	D	P	F	N	D	P	F	N	D
1re décade	79	32	14	9	93	43	25	13	110	59	35	22	130	77	48	28
2e décade	82	34	19	10	99	45	28	14	117	63	39	23	137	81	55	30
3e décade	96	39	26	11	86	40	26	13	136	73	48	26	142	84	57	30
TOTAL du mois	237	105	60	30	278	128	79	40	363	195	122	71	409	242	160	88
	Mai				*Juin*				*Juillet*				*Août*			
	P	F	N	D	P	F	N	D	P	F	N	D	P	F	N	D
1re décade	148	106	67	48	161	89	67	43	161	111	64	41	149	97	66	39
2e décade	153	109	67	50	162	89	64	44	158	108	72	40	144	93	66	37
3e décade	174	124	86	56	163	90	65	44	170	117	63	43	151	98	66	39
TOTAL du mois	475	339	220	154	486	268	196	131	489	336	199	124	444	288	198	115
	Septembre				*Octobre*				*Novembre*				*Décembre*			
	P	F	N	D	P	F	N	D	P	F	N	D	P	F	N	D
1re décade	131	83	58	40	112	73	42	24	93	41	27	8	80	22	14	5
2e décade	125	79	51	39	106	69	38	24	88	38	22	8	77	22	12	5
3e décade	118	74	52	36	109	71	34	24	83	37	15	7	85	24	15	6
TOTAL du mois	374	236	161	115	327	213	114	72	264	116	64	23	242	68	41	16

P. — Maximum possible (insolation possible)
F. — Maximum relevé (insolation la plus favorable)
D. — Minimum relevé (insolation la plus défavorable)
N. — Moyenne relevée (insolation normale)

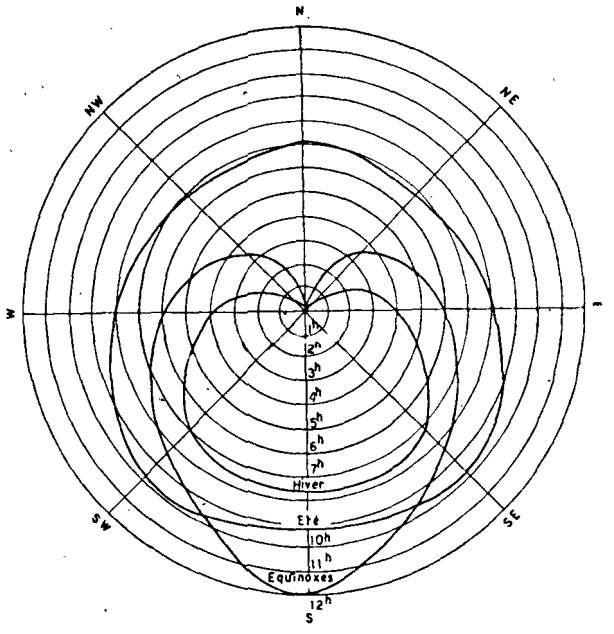


Figure 3. Insolations maximales possibles en fonction de l'orientation des façades

e) La façade sud reçoit une durée d'ensoleillement possible maximum de 12 heures aux équinoxes, réduite à environ 9 heures en été et environ 7 heures et demie en hiver.

Pour obtenir l'insolation effective, ces durées maximales possibles doivent être réduites grosso modo à 40 p. 100 en été, 20 p. 100 en hiver et 40 p. 100 aux équinoxes par suite des conditions météorologiques moyennes prévalant dans l'agglomération bruxelloise. Ainsi se trouvent diminuées d'une manière appréciable les durées d'insolation possibles.

Des conclusions définitives quant à l'orientation optimale et la destination domestique des locaux selon leur orientation ne peuvent toutefois être avancées avant la prise en considération des effets calorifiques du rayonnement incident, car l'importance énergétique d'un rayonnement dépend non seulement de sa durée, mais encore de son incidence par rapport à la surface réceptrice. Ce dernier facteur détermine également la profondeur de pénétration des rayons à l'intérieur du local.

Le problème de la détermination de l'*insolation possible sur les façades d'immeubles groupés en alignements parallèles*, de part et d'autre de voies de circulation, est conditionné par un ensemble de facteurs simultanés intervenant dans la pratique d'une manière souvent contradictoire. En effet, si les exigences de l'insolation imposent la dissémination et la création de larges avenues, les nécessités pratiques ou économiques, résultant de gabarits urbains existants, ont poussé à l'agglomération des habitations.

Les facteurs déterminant les conditions d'ensoleillement des façades sont : la hauteur et l'azimut du soleil, dépendant de la saison et de l'heure de la journée; la distance et la hauteur des bâtiments de vis-à-vis portant ombre sur la façade considérée; l'orientation de la façade ou de la rue.

Les résultats sont représentés par les courbes de la figure 4 donnant la variation des facteurs H/L entre la hauteur des habitations et la largeur des voiries en fonction de l'orientation des façades. On adopte dans chaque cas pour valeur de référence égale à 100 p. 100, le nombre d'heures par jour de soleil sur une surface verticale sud dans le cas

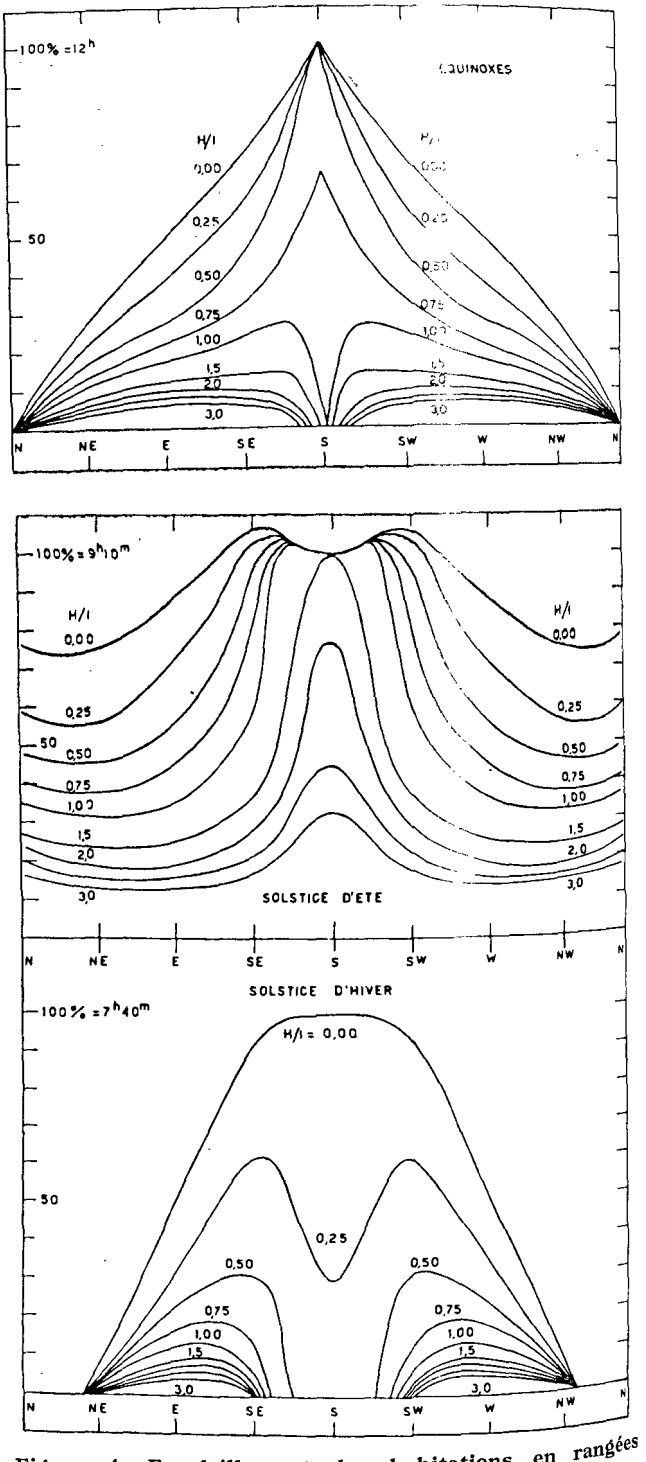


Figure 4. Ensoleillement des habitations en rangées parallèles

d'un horizon complètement dégagé ($H/L = 0$). Ces figures sont suffisamment explicites en elles-mêmes sans qu'il soit nécessaire de les commenter.

Ici s'applique également la même remarque que celle établie à propos des locaux isolés : à savoir la réduction de ces quantités par suite de l'insolation effective.

Éclairement énergétique solaire

Rayonnement solaire direct

Le rayonnement solaire, au niveau du sol, est composé du rayonnement solaire direct et du rayonnement diffusé. Ces deux composantes dérivent d'un même rayonnement extra-terrestre qui subit, lors de la traversée de l'atmosphère, de profondes modifications tant spectrales qu'énergétiques par suite des différents processus de diffusion moléculaire et d'absorption sélective. Il faut aussi considérer l'état de pureté de l'atmosphère qui peut être troublée par les aérosols (diffusion et absorption par les poussières, la brume, le brouillard et les nuages), dont les effets sélectifs dépendent de circonstances locales (différence entre villes et campagnes).

Considéré au point de vue énergétique, l'effet des affaiblissements du rayonnement dans son passage à travers l'atmosphère peut se traduire, en Belgique, par des variations dont la représentation graphique est donnée à la figure 5, qui fournit la variation au cours de l'année de l'énergie du rayonnement solaire direct que recevraient diverses surfaces et façades orientées au cours d'une journée de très beau temps. Ce sont des valeurs maximales.

La courbe supérieure (marquée *n*), qui correspond à une surface constamment normale aux rayons solaires, représente le maximum maximorum. Le maximum absolu pour l'agglomération bruxelloise est égal à environ 8 890 kcal/m² au cours des journées du mois de juin. Aux équinoxes, l'énergie maximum d'une journée est de l'ordre de $\frac{2}{3}$, pour tomber à

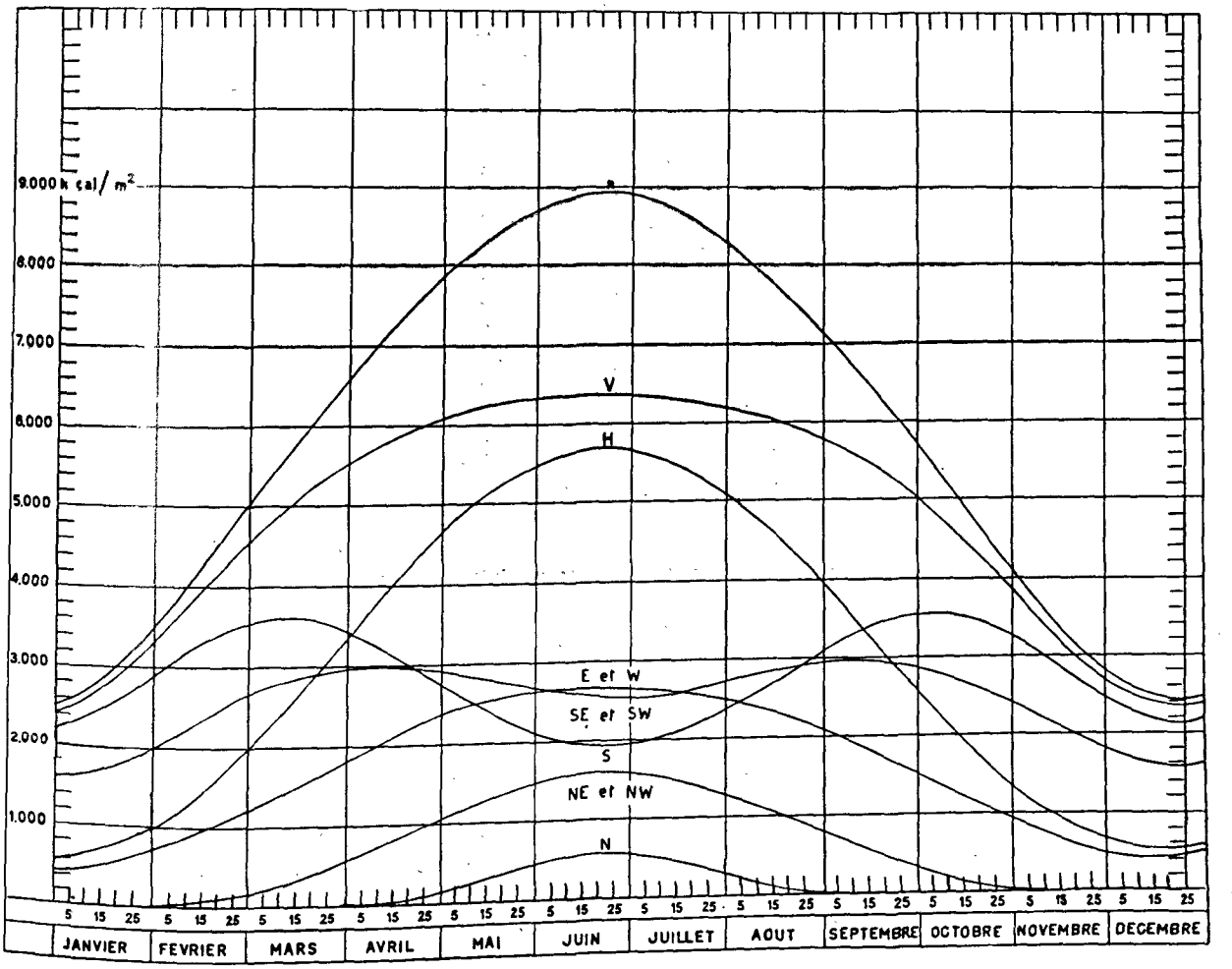


Figure 5. Irradiation journalière directe par ciel serein

n — La surface réceptrice est maintenue constamment normale aux rayons solaires.
V — La surface réceptrice est un plan vertical perpendiculaire au plan d'incidence des rayons solaires.
M — La surface réceptrice est horizontale, H, ou verticale exposée à l'Est ou à l'Ouest, au Sud... (E, W, S, ...).
En abscisse sont portés les différents jours de l'année, en ordonnée l'énergie totale reçue (exprimée en kcal. par mètre carré de surface plane).

Tableau 2. Comparaisons entre la fraction d'insolation et la fraction d'irradiation

Résultats obtenus à Uccle sur une surface normale aux rayons solaires dans des conditions moyennes. Valeurs en pourcentages

Mois	Décades	Fraction d'insolation			Fraction d'irradiation		
		matin	soir	journée	matin	soir	journée
Janvier	I	19	18	18	14	13	14
	II	24	23	24	19	18	18
	III	28	26	27	22	20	21
Février	I	27	27	27	20	20	20
	II	29	29	29	22	21	22
	III	30	30	30	23	23	23
Mars	I	31	31	31	22	22	22
	II	33	33	33	25	24	25
	III	35	36	36	27	27	27
Avril	I	38	36	37	28	26	27
	II	41	39	40	32	30	31
	III	41	39	40	33	31	32
Mai	I	44	45	45	33	34	33
	II	43	44	44	32	33	33
	III	49	50	50	40	41	40
Juin	I	40	44	42	29	32	31
	II	38	42	40	27	29	28
	III	38	42	40	27	29	28
Juillet	I	38	41	40	26	30	28
	II	44	48	46	33	37	35
	III	36	39	37	24	26	25
Août	I	43	46	44	34	35	35
	II	45	47	46	36	37	36
	III	43	44	44	32	33	33
Septembre	I	44	45	45	37	38	37
	II	40	42	41	32	33	33
	III	43	44	44	34	34	34
Octobre	I	37	37	37	29	29	29
	II	36	36	36	27	27	27
	III	31	31	31	22	22	22
Novembre	I	30	28	29	25	23	24
	II	25	24	25	20	18	19
	III	19	18	18	14	12	13
Décembre	I	20	16	18	16	12	14
	II	17	14	15	14	11	12
	III	19	15	17	15	12	14

moins de $\frac{1}{3}$ (2 000 kcal/m² en hiver, décembre-janvier). C'est pendant ces mois que la deuxième courbe (marquée *V*), qui représente la variation annuelle du rayonnement solaire direct sur une surface verticale perpendiculaire au plan d'incidence des rayons, se rapproche de la courbe supérieure, car la hauteur du soleil est très faible (< 20°). Par suite de son orientation privilégiée, la façade sud est la façade pour laquelle les effets calorifiques solaires ont les caractères les plus importants. Cette façade sud est susceptible de recevoir le maximum de rayonnement solaire direct au cours de la période des basses températures de l'année. Les maximums de l'effet calorifique de 3 600 kcal/m² apparaissent vers les 10-15 mars et (légèrement inférieurs) vers les 5-10 octobre, tandis qu'au cours du mois de juin le minimum de la façade sud est tellement prononcé que, par très beau temps, l'énergie, pour toute une journée, est inférieure à 1 780 kcal/m², c'est-à-dire de l'ordre du tiers de l'énergie qui tombe sur une plate-forme ou sur le sol horizontal. En d'autres termes, la façade sud subit le maximum de l'effet calorifique du soleil pendant les saisons froides et le minimum pendant les saisons chaudes. En opposition des résultats obtenus pour la façade sud, il faut placer ceux que l'on obtient pour les façades est et ouest. Celles-ci sont soumises principalement à l'effet calorifique du soleil en été alors que les températures sont les plus élevées. L'effet calorifique de toute une journée de très beau temps en juin-juillet sur les façades est et ouest dépasse celui qui intéresse la façade sud, alors que la durée d'ensoleillement pour la façade sud est plus longue.

Les *conditions atmosphériques* ont pour effet de réduire sensiblement les valeurs énergétiques obtenues par très beau temps. Il a déjà été indiqué,

dans la partie traitant de l'insolation, dans quelle mesure les heures d'insolation théorique possibles se trouvaient en moyenne réduites. Il en est de même pour les éclairements énergétiques. Toutefois, les facteurs de réduction diffèrent de ceux obtenus pour la durée d'ensoleillement.

A titre de comparaison, nous donnons au tableau 2 les pourcentages respectifs de la durée d'ensoleillement et de l'énergie du rayonnement solaire direct sur une surface normale dans les conditions moyennes par rapport aux conditions de très beau temps.

Ces facteurs peuvent d'ailleurs être appliqués sans grands changements aux surfaces orientées.

Conditions climatiques de la radiation solaire directe en Belgique

La rentabilité d'un équipement d'utilisation de l'énergie solaire directe pour des applications de haute pyrométrie (four solaire) est essentiellement fonction des conditions d'insolation au lieu d'installation. Le pouvoir de concentration exige un éclairement énergétique solaire appréciable et, partant, des conditions de ciel serein pendant les heures où ce rayonnement est suffisamment élevé.

Les observations effectuées dans ce domaine à Uccle pendant dix années permettent d'apprécier dans quelles mesures l'exploitation serait rentable. On constate que, en moyenne, 46 journées par an sont des journées à ciel couvert, sans soleil, 48 présentent moins d'une heure de soleil. Si l'on considère les journées pour lesquelles l'insolation atteint au moins 7 heures par jour, on voit que le nombre en est de 120, soit $\frac{1}{3}$ de l'année environ.

Mais ces résultats, pour être significatifs, ne sont pas suffisants. Il importe moins de considérer l'insolation totale journalière que la répartition des journées d'après le nombre de cas pour lesquels le ciel a été serein pendant au moins une heure entière, et de considérer en même temps l'éclairement

Tableau 3. Période 1949-1957 : nombre moyen par décade, au cours de ces neuf années, des journées avec ciel serein pendant les heures indiquées

	Heures solaires	*6-7*	*7-8*	*8-9*	*9-10*	*10-11*	*11-12*	*12-13*	*13-14*	*14-15*	*15-16*	*16-17*	*17-18*
J	I				0,9	1,6	1,6	1,9	1,4	1,2	0,1		
	II			0,2	1,2	1,4	1,6	2,0	1,3	1,8	0,6		
	III			2,2	2,9	3,4	3,3	3,1	3,0	3,0	2,2		
F	I			2,1	2,1	2,6	2,3	2,2	1,8	1,7	1,5		
	II			1,4	2,2	2,1	2,1	2,2	2,2	1,4	1,2	0,1	
	III		1,3	2,5	2,4	3,0	3,0	2,3	2,8	2,8	2,4	1,1	
M	I		2,7	3,3	3,2	3,6	3,7	3,6	3,4	3,6	3,2	2,9	
	II		1,8	2,8	2,8	2,6	2,6	2,7	2,2	2,1	2.6	2,2	
	III	0,6	2,0	2,1	2,3	1,9	1,6	1,7	2,0	2,0	2,2	2,4	0,7
A	I	1,6	1,7	2,1	2,4	1,9	2,1	2,0	2,4	2,2	2,1	2,0	1,6
	II	3,7	3,9	3,6	3,8	3,6	3,7	3,2	2,4	2,2	3,0	3,2	2,7
	III	3,9	4,2	4,2	3,8	4,2	3,7	3,7	3,7	3,4	3,1	3,2	3,3
M	I	3,3	3,0	3,1	2,8	2,8	1,7	1,8	1,8	1,7	1,9	2,2	2,3
	II	2,9	3,3	4,3	3,4	2,9	2,4	1,9	1,8	1,1	1,1	1,1	1,7
	III	2,8	3,1	3,2	3,2	2,7	2,8	2,3	2,5	2,1	2,5	2,4	2,1
J	I	4,2	3,7	3,8	3,2	2,8	2,4	2,1	2,4	2,2	2,0	2,2	2,3
	II	3,4	2,9	3,2	2,6	2,2	1,8	1,8	1,9	1,9	1,7	1,7	2,0
	III	1,9	2,6	2,9	2,7	2,1	1,9	2,0	1,9	1,7	1,9	2,7	2,8
J	I	2,8	2,9	2,7	2,9	3,1	3,2	2,6	2,1	2,1	2,4	2,2	2,6
	II	2,0	2,0	2,2	2,1	1,1	0,3	0,3	0,9	0,4	0,6	1,2	1,4
	III	1,9	2,3	2,3	2,2	1,7	1,6	0,9	1,2	1,2	1,2	1,5	1,9
A	I	3,0	2,9	2,7	2,8	2,4	2,1	2,1	2,0	2,3	2,3	2,9	2,4
	II	2,4	2,6	2,2	2,1	1,8	1,8	1,4	1,2	1,1	1,1	1,1	1,6
	III	1,9	2,8	2,8	2,6	2,3	2,0	1,6	1,2	1,6	1,8	2,3	1,9
S	I	2,2	2,7	3,1	3,0	2,6	2,1	1,4	1,2	1,4	1,0	1,6	0,9
	II	1,2	2,4	2,4	2,5	2,1	1,9	1,3	1,4	1,7	1,7	2,1	1,2
	III		2,0	2,2	2,3	2,4	2,1	1,2	1,4	1,3	1,0	1,2	
O	I		1,6	2,9	3,0	2,7	3,0	2,6	2,3	2,8	3,1	2,4	
	II		1,9	2,8	3,6	3,8	3,3	3,0	3,0	2,9	3,6	1,6	
	III			1,7	2,0	1,6	1,5	1,3	1,5	1,5	1,4		
N	I			2,1	2,7	2,3	2,7	2,3	1,8	1,3	1,3		
	II			0,9	1,0	1,7	1,7	1,4	1,1	1,2	0,8		
	III			0,4	1,2	1,9	1,9	1,9	1,7	1,4	0,3		
D	I				1,3	2,0	1,6	1,6	1,6	1,4			
	II				1,8	2,2	2,1	1,8	1,3	1,1			
	III				0,5	1,0	1,0	1,2	1,2	1,1			

Tableau 4. Période 1949-1957 : éclairement énergétique moyen par décade du rayonnement solaire direct sur une surface normale à Uccle (en cal. cm^{-2}. min^{-1}), pendant les heures de la décade à ciel serein

	Heures solaires :	*6-7*	*7-8*	*8-9*	*9-10*	*10-11*	*11-12*	*12-13*	*13-14*	*14-15*	*15-16*	*16-17*	*17-18*
	I				0,70	0,71	0,71	0,69	0,55	0,46	0,39		
J	II			0,44	0,50	0,70	0,77	0,64	0,72	0,54	0,30		
	III			0,44	0,63	0,69	0,76	0,76	0,68	0,58	0,34		
	I			0,43	0,71	0,79	0,77	0,78	0,73	0,67	0,44		
F	II			0,50	0,70	0,80	0,87	0,85	0,75	0,69	0,54	0,54	
	III		0,41	0,60	0,80	0,82	0,80	0,89	0,89	0,80	0,63	0,40	
	I		0,49	0,77	0,87	0,85	0,87	0,92	0,92	0,81	0,61	0,38	
M	II		0,53	0,66	0,86	0,95	0,89	0,88	0,79	0,72	0,69	0,49	
	III		0,55	0,77	0,81	0,88	0,93	0,96	0,90	0,84	0,69	0,53	
	I	0,46	0,63	0,79	0,88	0,95	0,91	0,95	0,84	0,79	0,76	0,57	0,36
A	II	0,47	0,70	0,86	0,83	0,98	0,95	0,94	0,97	0,94	0,80	0,69	0,45
	III	0,61	0,76	0,85	0,98	0,92	0,97	1,02	0,95	0,97	0,98	0,73	0,46
	I	0,62	0,72	0,88	0,94	0,96	1,00	0,96	0,94	1,02	0,93	0,72	0,55
M	II	0,65	0,75	0,84	0,95	1,00	1,03	0,90	1,11	1,00	0,97	0,64	0,55
	III	0,70	0,80	0,90	0,96	1,00	0,98	1,06	1,11	1,07	0,93	0,79	0,64
	I	0,68	0,82	0,90	0,94	1,06	0,96	0,95	0,92	0,97	1,00	0,86	0,67
J	II	0,78	0,85	0,97	1,03	1,08	1,02	1,12	1,05	1,01	0,91	0,85	0,69
	III	0,75	0,88	0,96	1,05	1,05	1,12	1,04	1,04	1,09	0,94	0,80	0,69
	I	0,68	0,79	0,82	0,89	0,87	0,99	1,03	0,99	0,92	0,92	0,87	0,64
J	II	0,71	0,75	0,89	0,85	0,98	1,15	1,25	0,95	1,07	1,00	0,76	0,66
	III	0,67	0,81	0,89	0,95	0,87	1,01	1,06	1,00	0,90	0,82	0,77	0,57
	I	0,66	0,72	0,88	0,85	0,93	1,00	0,94	0,98	0,86	0,81	0,71	0,57
A	II	0,60	0,83	0,90	0,93	0,95	0,90	0,86	0,92	0,83	0,70	0,54	0,47
	III	0,50	0,59	0,72	0,82	0,83	0,95	0,86	0,91	0,87	0,79	0,76	0,43
	I	0,39	0,65	0,78	0,86	0,80	0,89	1,01	0,97	0,72	0,80	0,63	0,39
S	II	0,39	0,69	0,84	0,86	0,75	1,00	1,04	1,01	0,80	0,97	0,53	0,32
	III		0,50	0,73	0,87	0,98	0,98	0,95	0,87	0,72	0,68	0,46	
	I		0,45	0,72	0,88	0,95	0,92	0,94	0,91	0,77	0,59	0,36	
O	II		0,42	0,63	0,77	0,86	0,91	0,92	0,84	0,68	0,52	0,40	
	III			0,43	0,61	0,79	0,83	0,82	0,71	0,57	0,35		
	I			0,58	0,65	0,75	0,82	0,74	0,71	0,58	0,41		
N	II			0,35	0,61	0,73	0,80	0,87	0,71	0,72	0,42		
	III			0,31	0,52	0,54	0,67	0,69	0,62	0,47	0,50		
	I				0,48	0,65	0,77	0,67	0,57	0,43			
D	II				0,52	0,71	0,73	0,64	0,60	0,40			
	III				0,48	0,61	0,64	0,60	0,49	0,41			

énergétique effectif pendant ces périodes. Les tableaux 3 et 4 donnent respectivement le nombre moyen par décade, pour la période 1949-1957, des journées avec ciel serein pendant les heures indiquées, ainsi que l'éclairement énergétique moyen correspondant reçu sur une surface normale.

La période d'utilisation la plus intéressante semble être celle s'étendant d'avril à septembre, pour laquelle, grosso modo, 2 à 3 jours par décade en moyenne sont favorables aux essais. Les éclairements énergétiques au cours de cette période ont atteint pendant les heures voisines de midi des valeurs moyennes de 1 cal par cm^2 et par minute.

Irradiation des terrains en pente

Un autre problème, dont l'importance est évidente pour l'urbanisme, la pédologie, les stations climatiques, la météorologie agricole, etc., est l'ensoleillement des pentes, c'est-à-dire de surfaces diversement inclinées et orientées. Rappelons d'abord les conditions d'études de ce problème. Le sol, de pente et d'orientation fixées, reçoit, pendant un temps déterminé, le rayonnement solaire direct suivant une incidence donnée. A celui-ci s'ajoute l'apport énergétique dû au rayonnement diffusé par le ciel. En outre, les conditions atmosphériques modifient les résultats obtenus par ciel serein.

Les données numériques présentées au tableau 5 représentent, en pourcentage par rapport à une surface horizontale, les rapports des énergies reçues, abstraction faite des causes accidentelles, par les pentes pour chaque saison et pour l'année.

Ensoleillement et irradiation des façades des îlots bâtis

Le problème de l'ensoleillement des façades des îlots urbains bâtis peut être envisagé à la fois sous l'aspect de la durée d'insolation possible et de l'énergie reçue par les différentes façades de l'îlot, compte tenu de leur orientation, de la largeur de la voirie, de la distance entre îlots et de la hauteur des

immeubles. Cet aspect important en soi (il suffit de songer au pouvoir bactéricide du soleil) n'est pas le seul à retenir.

En effet, l'action calorifique est, à d'autres points de vue, utile à considérer. Car s'il importe parfois de se protéger contre un apport excessif de chaleur sur une façade, particulièrement en été, il est par contre bien intéressant en hiver ou aux périodes équinoxiales de l'année de choisir les conditions optima pour capter au maximum l'énergie solaire naturelle.

Les conditions physiques sont telles que l'efficacité d'une heure d'insolation n'est pas constante, non seulement au cours de la variation journalière, mais même au cours de la variation horaire. C'est pourquoi le problème, pour être résolu utilement, doit être examiné sous ses deux aspects différents : insolation et éclairement énergétique.

Les figures 6, 7 et 8 traduisent le résultat des calculs de l'insolation (en minutes) et de l'éclairement énergétique (en kilocalories par mètre carré) pour une journée complète d'ensoleillement par très beau temps. Ce sont donc des valeurs maxima. Elles sont importantes à considérer pour un examen comparatif des meilleures conditions d'urbanisation d'un quartier à bâtir. On a adopté pour le calcul les paramètres suivants : D = distance entre immeubles; L = largeur de la voirie; H = hauteur des immeubles; orientation de la rue.

Quatre types de disposition ont été retenus :

Type I $L = D = H$
Type II $L = H$; $D = 2H$
Type III $L = 2H$; $D = H$
Type IV $L = D = 2H$

Trois conditions particulières ont été envisagées : solstice d'été; solstice d'hiver; équinoxes.

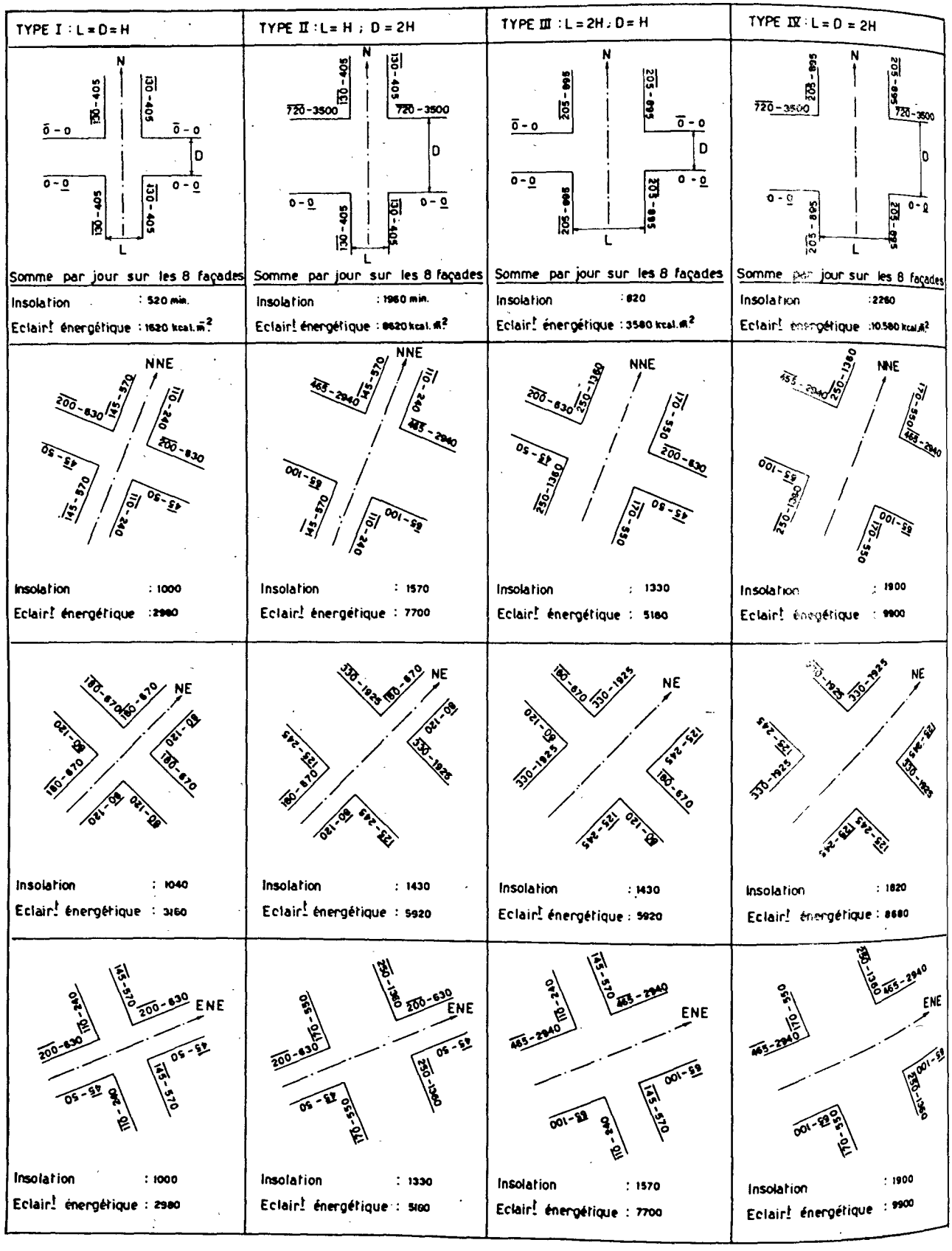
Les valeurs calculées ne tiennent pas compte des effets particuliers aux abords immédiats des carrefours, où l'ensoleillement risque d'être quelque peu

Tableau 5. Rapports en pourcentages des énergies du rayonnement solaire direct reçues au cours des saisons et de l'année par des surfaces inclinées par rapport à une surface horizontale

Pente en pourcentage	*S*	*S-E et S-O*	*E et O*	*N-E et N-O*	*N*
A *Printemps*					
0-1	100	100	100	100	100
1-2,5	102	101	100	99	98
2,5-5	103	102	100	97	96
5-10	105	104	100	93	91
10-15	111	107	99	88	84
B. *Été*					
0-1	100	100	100	100	100
1-2,5	100	100	100	100	99
2,5-5	101	101	100	99	99
5-10	102	101	100	98	97
10-15	103	102	100	97	95
C *Automne*					
0-1	100	100	100	100	100
1-2,5	101	101	100	99	98
2,5-5	103	102	100	97	96
5-10	107	104	99	95	92
10-15	112	108	99	90	87
D. *Hiver*					
0-1	100	100	100	100	100
1-2,5	106	103	100	97	95
2,5-5	114	109	100	92	89
5-10	126	118	100	83	76
10-15	144	130	100	71	59
E. *Année*					
0-1	100	100	100	100	100
1-2,5	102	101	100	99	98
2,5-5	103	102	100	98	96
5-10	106	104	100	95	93
10-15	110	107	99	91	88

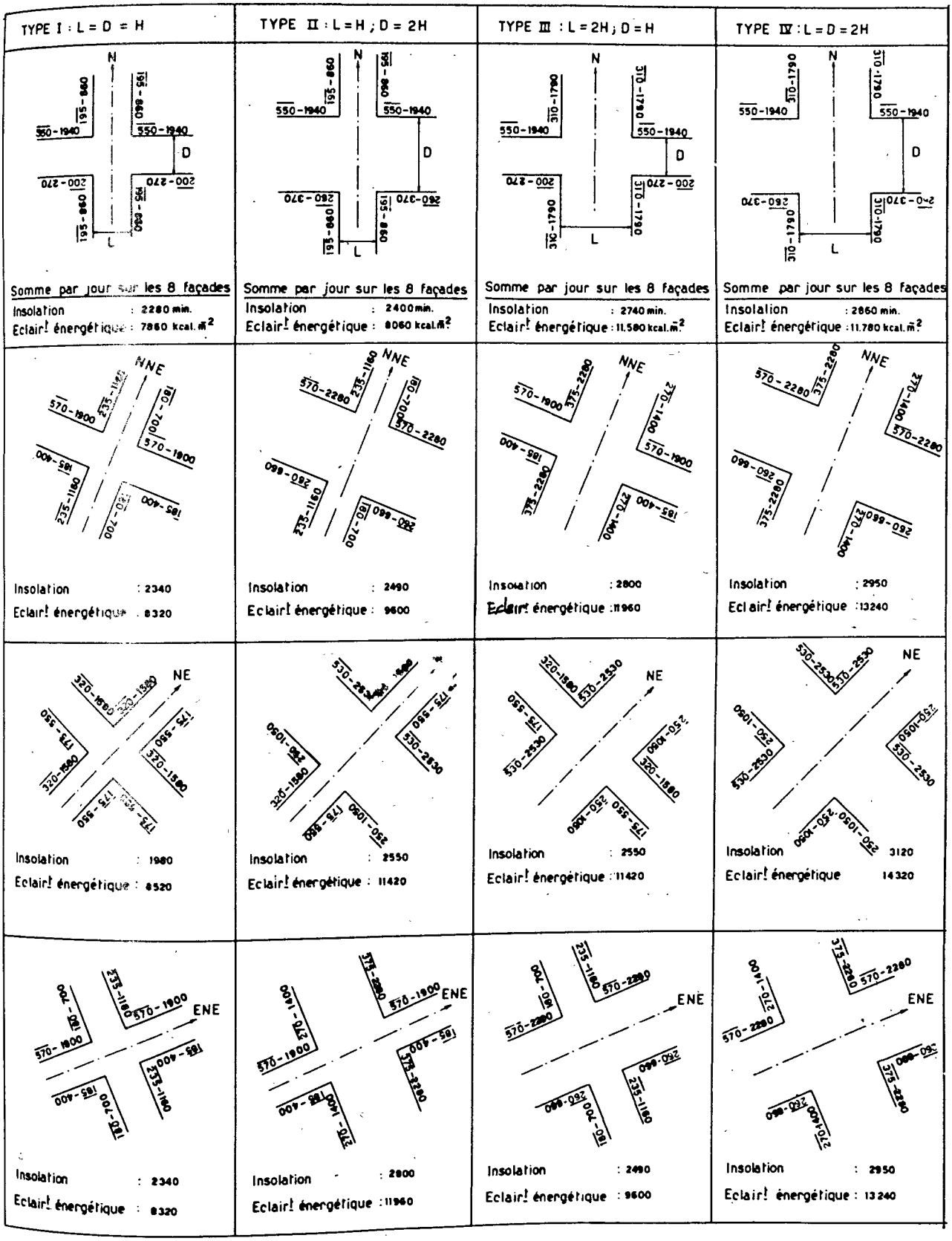
Les valeurs absolues, pour une surface horizontale, sont les suivantes :

Printemps : 244 000 kcal par m² pour la saison
Été : 492 000 kcal par m² pour la saison
Automne : 293 000 kcal par m² pour la saison
Hiver : 66 000 kcal par m² pour la saison
Année : 1 095 000 kcal par m² pour l'année.



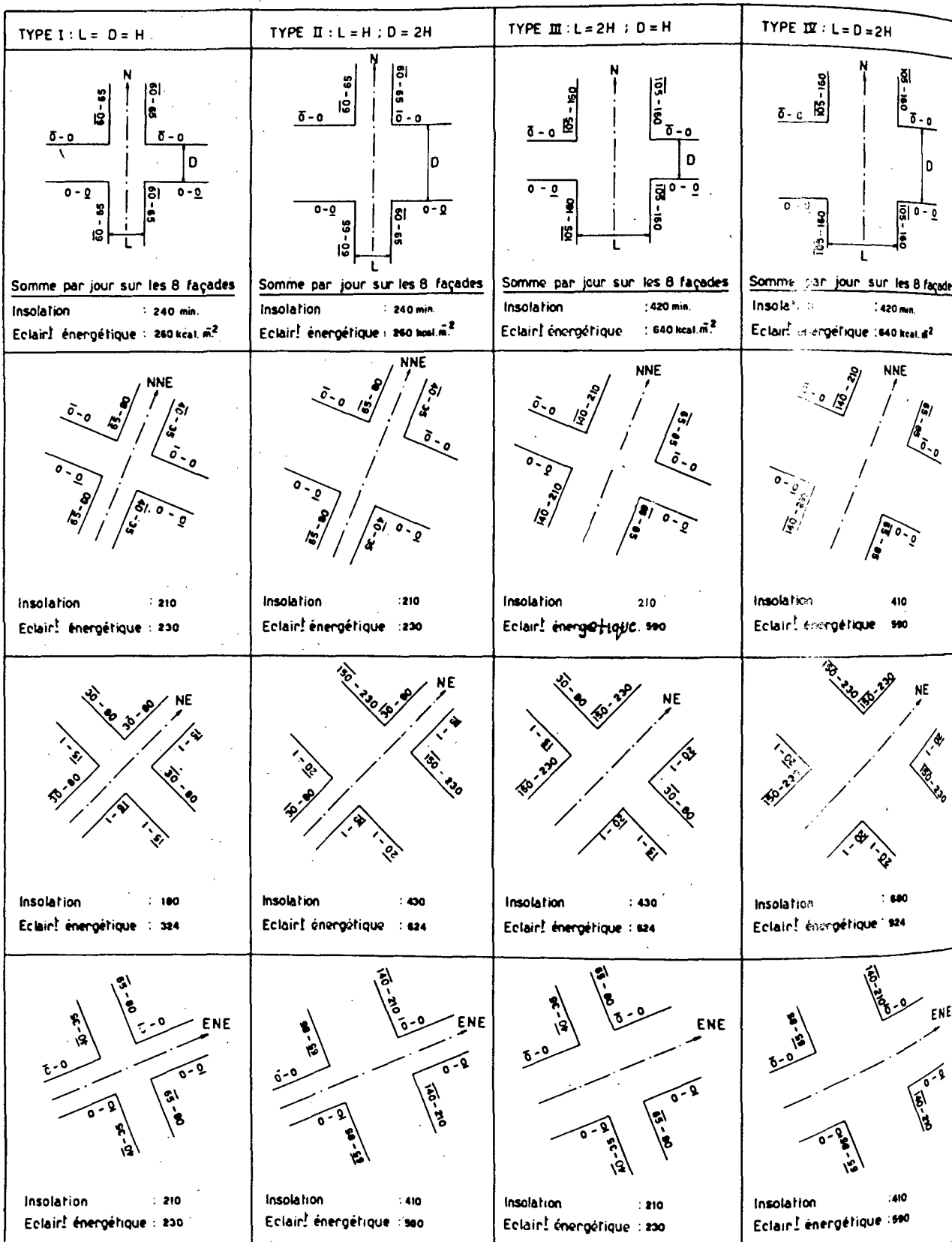
Insolation : valeurs surlignées

Figure 6. Ensoleillement et orientation des façades : équinoxes



Insolation : valeurs surlignées

Figure 7. Ensoleillement et orientation des façades : été



Insolation : valeurs surlignées

Figure 8. Ensoleillement et orientation des façades : hiver

Tableau 6. Pourcentages d'insolation et d'irradiation sur les façades d'îlots bâtis selon le type envisagé

Orientation rue	Insolation			Irradiation		
	Type I	*Type II*	*Type III*	*Type I*	*Type II*	*Type III*
Équinoxe						
N	23	87	*36*	15	81	*34*
NNE	53	83	*70*	30	78	*52*
NE	57	*79*	*79*	36	*68*	*68*
ENE	53	*70*	83	30	*52*	78
E	23	*36*	87	15	*34*	81
Été						
N	80	84	*96*	67	68	*98*
NNE	79	84	*95*	63	72	*90*
NE	63	*82*	*82*	59	*80*	*80*
ENE	79	*95*	84	63	*90*	72
E	80	*96*	84	67	*98*	68
Hiver						
N	57	57	*100*	41	41	*100*
NNE	51	51	*100*	39	39	*100*
NE	26	*63*	*63*	35	*68*	*68*
ENE	51	*100*	51	39	*100*	39
E	57	*100*	57	41	*100*	41

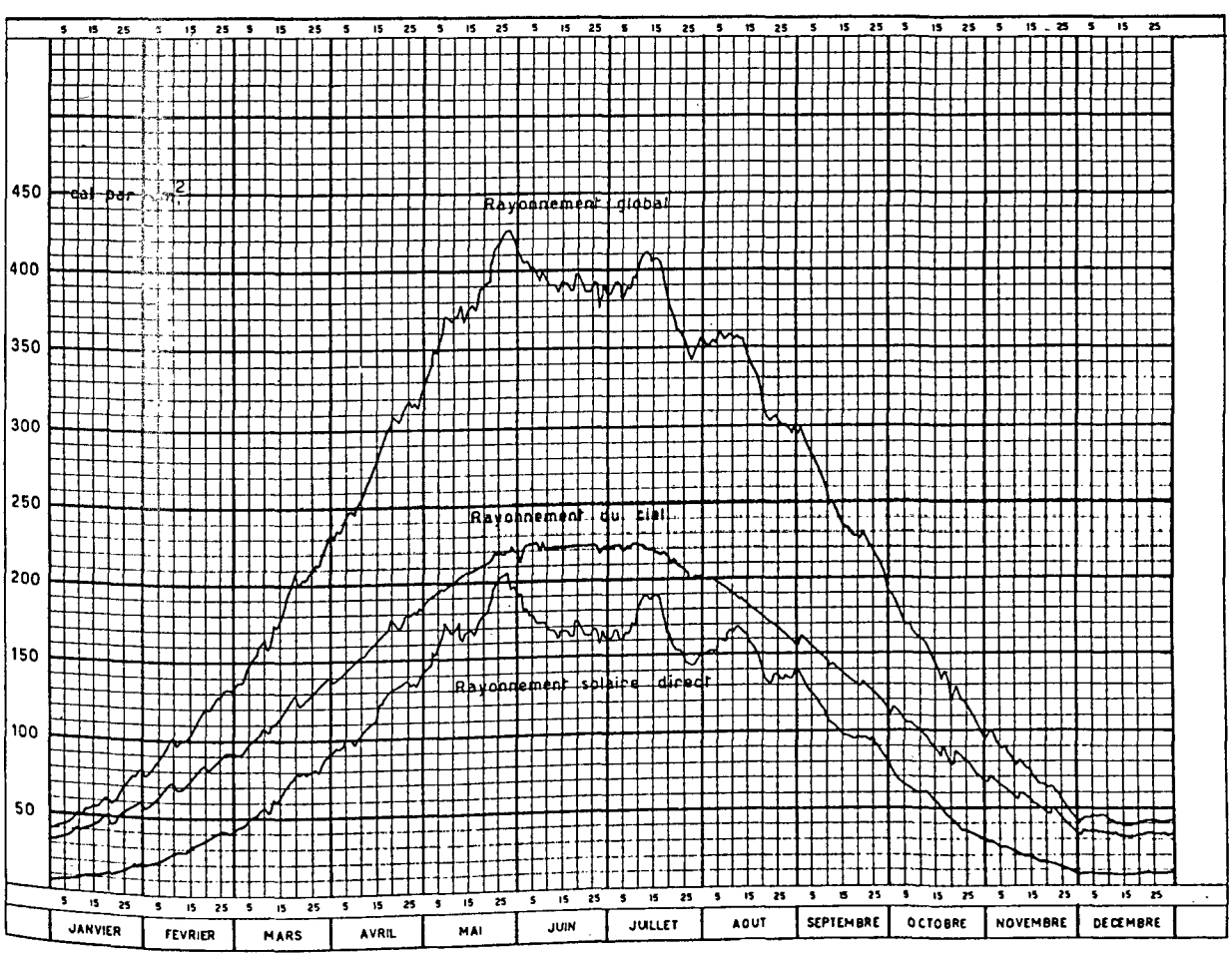


Figure 9. Irradiation globale journalière et ses composantes au cours de l'année. Surface réceptrice horizontale. Conditions moyennes (1901-1930)

supérieur aux valeurs trouvées, par suite de la présence du soleil dans un angle azimutal momentanément dégagé. Le tableau 6 fournit les pourcentages d'insolation et d'irradiation des trois premiers types par rapport au type IV, ce dernier étant indiscutablement le plus intéressant. Car si le rôle bactéricide et assainissant du rayonnement solaire joue très peu à l'intérieur des habitations, par suite de l'absorption des radiations germicides par les vitres des fenêtres, par contre, il contribue largement, par son action directe sur l'air extérieur et les plantations, à l'assainissement d'un quartier. C'est pourquoi il ne faut pas sous-estimer l'importance de la largeur des rues ni le choix d'une orientation susceptible d'admettre au maximum au niveau de la rue les rayons solaires incidents.

Rayonnement global

On entend par rayonnement global atteignant une surface de la somme du rayonnement direct et du rayonnement diffusé par le ciel sur cette surface. Diverses formules classiques se proposent de déterminer le rayonnement global à partir des durées d'ensoleillement. Le degré de précision obtenu dépend du nombre de paramètres contenus dans ces relations.

Afin de se rendre compte de l'importance relative des composantes du rayonnement global au cours de la variation journalière, on donne à la figure 9 une représentation complète des rayonnements pour les conditions moyennes d'ensoleillement. Il convient d'insister sur l'importance du rayonnement du ciel dans le rayonnement global. Au cours de toute l'année, d'une manière générale, on peut affirmer qu'en Belgique le rayonnement du ciel est plus important que le rayonnement solaire direct qui atteint une surface horizontale.

Comme application d'utilisation domestique d'énergie par captation du rayonnement global, nous nous attacherons aux *insolateurs plans*, et particulièrement aux *collecteurs utilisés comme chauffe-eau*. Ces deux types d'appareils ne diffèrent que par le fait que dans le premier le fluide constitue lui-même le collecteur d'énergie, tandis que dans le second le fluide emporte par conduction l'énergie captée par un collecteur constitué en général par un récepteur métallique.

Il conviendrait évidemment de considérer la rentabilité de tels dispositifs relativement aux autres systèmes de chauffe-eau.

Afin de baser ces études sur des données climatiques réelles, nous présentons à la figure 10 les

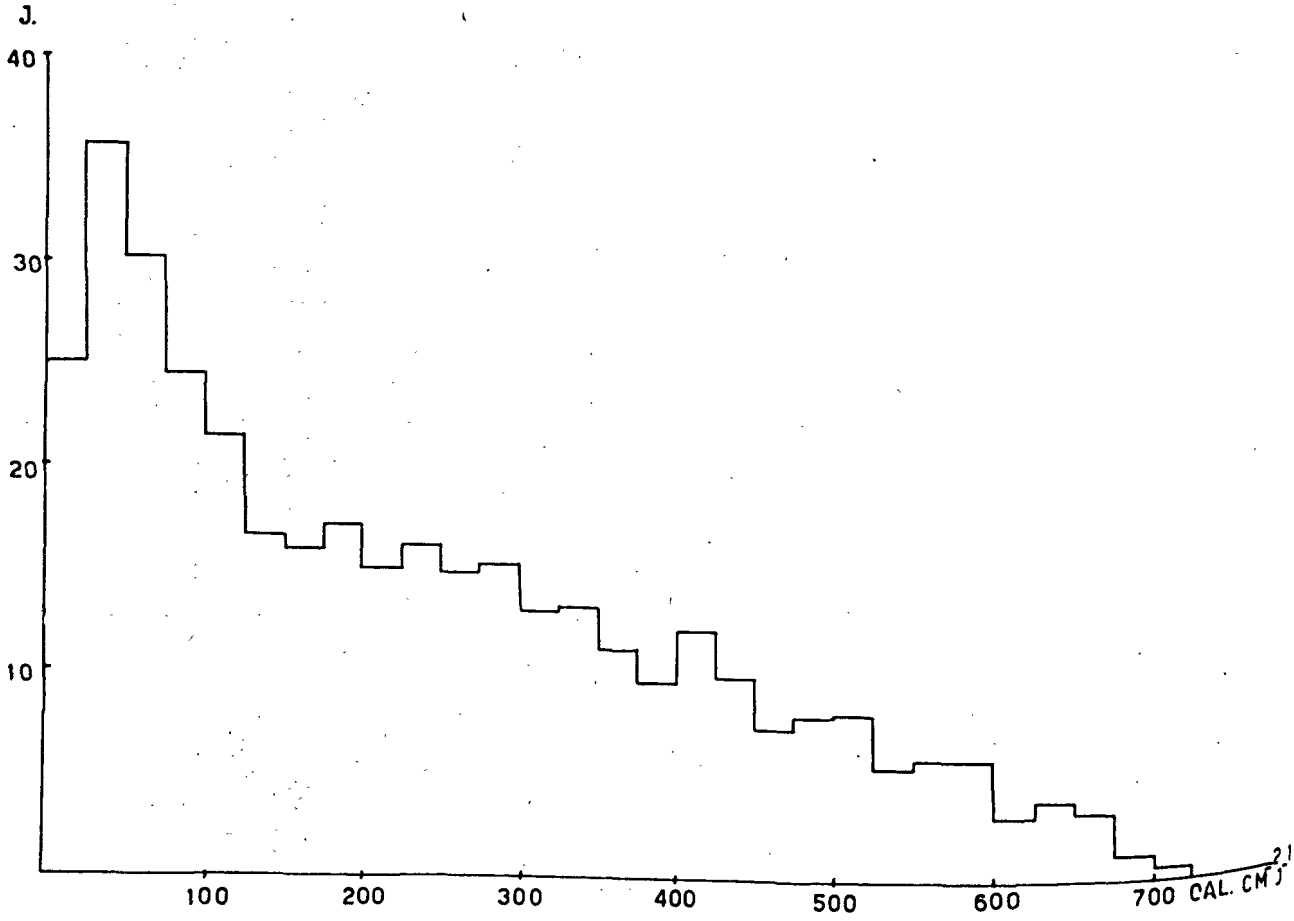


Figure 10. Nombre de jours par an dont l'irradiation journalière a été comprise entre les valeurs indiquées. Moyennes des 10 années : 1950-1959

IRRADIATION GLOBALE MENSUELLE

MOYENNE A UCCLE

JANVIER	15.793	KCAL. M.$^{-2}$
FEVRIER	30.326	
MARS	63.666	
AVRIL	96.894	
MAI	126.562	
JUIN	129.844	
JUILLET	124.260	
AOUT	105.409	
SEPTEMBRE	75.967	
OCTOBRE	47.445	
NOVEMBRE	21.119	
DECEMBRE	13.363	
ANNEE :	850.648	

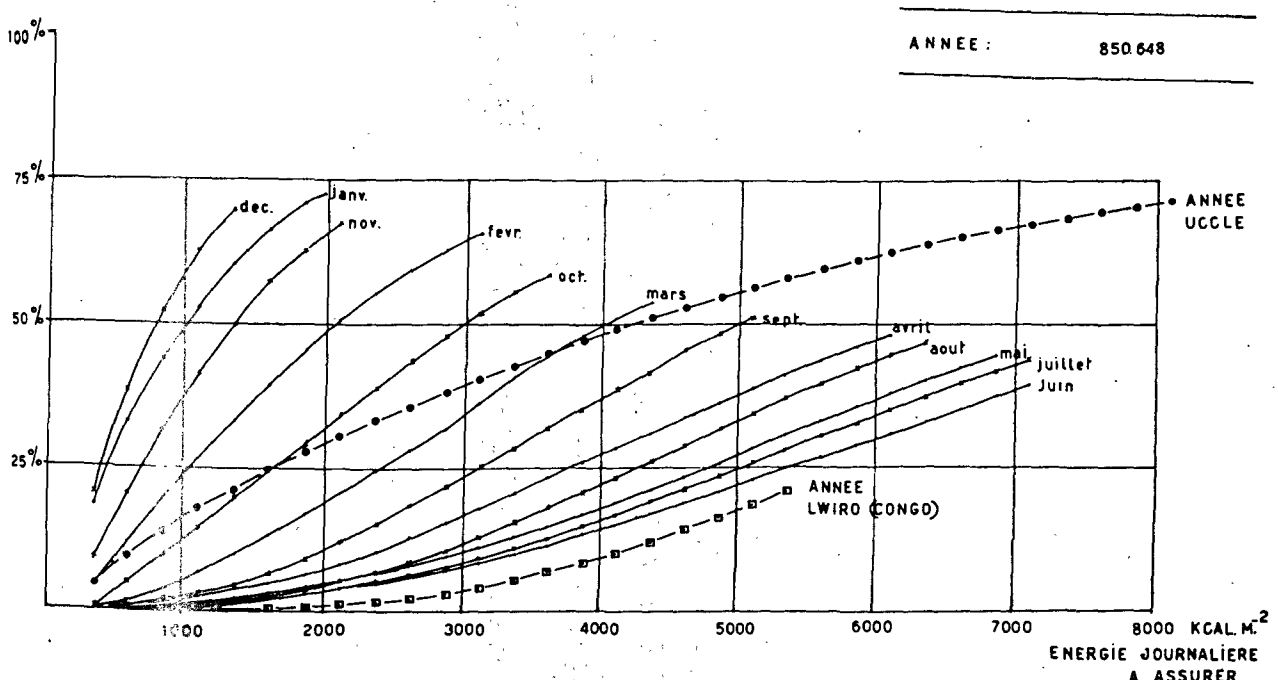


Figure 11. Pourcentage de l'énergie d'appoint nécessaire pour assurer journellement une énergie utile (indiquée en abcisse) dans le cas d'un collecteur d'énergie solaire à surface horizontale de 1 m² et dont le rendement serait égal à 100 p. 100

résultats basés sur les observations du rayonnement global à Uccle depuis 1951, donnant les fréquences des journées à irradiation sur une surface horizontale comprise entre des intervalles de valeurs déterminées.

Ces observations permettent de résoudre le problème suivant : étant donné un chauffe-eau solaire de dimensions fixées, installé horizontalement en permanence en Belgique, quel pourcentage d'énergie solaire peut-on recevoir journellement en vue d'élever d'une température donnée une certaine quantité d'eau? La solution doit tenir compte :

a) De la surface du collecteur;

b) Du débit journalier et de l'accroissement de température imposés;

c) Du nombre de journées par période envisagée (le mois dans ce cas) pendant lequel le chauffage solaire nécessaire est assuré à 100 p. 100;

d) Du nombre de journées par période pendant lequel il faut suppléer à la déficience de l'énergie solaire irradiée.

Les résultats sont présentés à la figure 11, qui indique la variation, au cours des mois et de l'année, du pourcentage d'énergie d'appoint nécessaire pour assurer journellement une énergie utile dans le cas d'utilisation d'un collecteur de 1 m² à surface horizontale dont le rendement serait de 100 p. 100. Cette figure indique également les valeurs de l'irradiation globale moyenne reçue à Uccle sur une surface horizontale.

A titre indicatif, nous avons indiqué le pourcentage à fournir dans le cas d'utilisation d'un tel collecteur dans les régions équatoriales, d'après les éléments calculés par De Bremaecker à Lwiro (République du Congo).

Conclusion

Au cours de cette esquisse, nous nous sommes attachés à montrer comment la connaissance précise des facteurs réels du climat solaire pouvait apporter à bien des problèmes pratiques des solutions concrètes. Des considérations semblables pourraient être développées en ce qui concerne les applications de l'éclairement lumineux.

Sur le plan d'utilisation de l'énergie solaire, les exemples choisis laissent entrevoir des possibilités réelles d'exploitation (même dans les climats peu favorisés du point de vue insolation), tant dans les domaines de la métallurgie des métaux et d'alliages très réfractaires que dans ceux de la céramique et de la verrerie. Les techniques de chauffage urbain et de distribution d'eau chaude pourraient même être repensées à la lueur des données disponibles.

Mais il importe de souligner que, quels qu'ils soient, les problèmes ne recevront de solutions exactes que s'ils tiennent compte des différents éléments du climat, dont aucun paramètre ne peut être négligé sous peine de fausser les données fondamentales du problème envisagé.

Bibliographie

Nicolet, M., *La mesure du rayonnement solaire*, Institut royal météorologique, Miscellanées, fasc. XXI, 1948.

Bossy, L. et Pastiels, R., *Étude des propriétés fondamentales des actinomètres*, Institut royal météorologique, Mémoires, vol. XXIX, 1948.

Nicolet, M., *Ensoleillement et Orientation en Belgique*, IRM, Mémoires, vol. XXXII, 1949.

Nicolet, M. et Bossy, L., *Ensoleillement et Orientation en Belgique, II, Étude pratique des surfaces verticales orientées*, IRM, Mémoires, vol. XXXVI, 1950.

Nicolet, M. et Dogniaux, R., *Ensoleillement et Orientation en Belgique, III, Étude de l'effet des conditions atmosphériques*, IRM, Mémoires, vol. XL, 1950.

Nicolet, M. et Dogniaux, R., *Étude de la radiation globale du Soleil*, IRM, Mémoires, vol. XLVII, 1951.

Nicolet, M. et Dogniaux, R., *Ensoleillement et Orientation en Belgique, IV, Rayonnement reçu sur une surface horizontale*, IRM, Mémoires, vol. XLIX, 1951.

Dogniaux, R., *Étude du climat de la radiation en Belgique*, IRM, Contributions, nº 18, 1954.

Dogniaux, R. et Pastiels, R., *Techniques modernes de mesure de l'éclairement*, IRM, Publications, série B, nº 16, 1955.

Pastiels, R., *Contribution à l'étude des problèmes actinométriques*, IRM, Publications, série A, nº 11, 1959.

Dogniaux, R., *Données météorologiques concernant l'ensoleillement et l'éclairage naturel*, Cahiers du Centre scientifique et technique du bâtiment, nº 44, Paris, 1960.

Résumé

L'objet de ce mémoire est de montrer comment, à partir d'observations climatologiques liées au climat de la radiation, il est possible d'envisager des études portant sur les applications pratiques relevant des diverses techniques de la construction et de l'urbanisme conditionnées en tout ou en partie par les conditions énergétiques réelles du climat.

Les résultats d'observations, présentés sous forme de tableaux numériques, de graphiques ou de figures, sont relatifs aux éléments suivants : ensoleillement ou durée d'insolation; éclairements énergétiques prévalant en Belgique.

Les différents facteurs sont brièvement analysés de manière à préciser nettement les conditions d'obtention de ces grandeurs. Quelques considérations sont développées sous forme de suggestions en vue des applications diverses, notamment : ensoleillement des façades d'un local isolé, des habitations en rangées parallèles; irradiation des terrains en pente; insolation et irradiation des îlots bâtis.

Enfin, des données du climat solaire permettent de fixer les conditions d'utilisation en Belgique de dispositifs tels que four et chauffe-eau solaires.

METEOROLOGICAL DATA ON SUNSHINE DURATION AND INSOLATION FOR PRACTICAL APPLICATIONS

Summary

The purpose of this paper is to show how, starting out from climatological observations of radiation, studies may be envisaged in relation to practical applications concerning the various techniques of construction and town-planning entirely or partially conditioned by the actual energetic conditions of the climate.

The results of the observations, presented in the form of tables, graphs or figures, relate to the following factors: sunshine duration; insolation prevailing in Belgium.

The various factors are briefly analysed to indicate, clearly and definitely, the conditions under which these quantities were found. Several suggestions on various applications are made, especially sunshine duration for the front walls of an islated building and of dwellings in parallel rows; insolation of sloping sites; sunshine duration and insolation of small blocks of buildings.

Finally, data on the solar climate are employed to determine the conditions, for utilisation in Belgium, of devices such as solar furnaces and solar water-heaters.

INSTRUMENTATION FOR THE MEASUREMENT OF SOLAR RADIATION— A SURVEY OF MODERN TECHNIQUES AND RECENT DEVELOPMENTS

A. J. Drummond *

It has long been recognized that a knowledge of the amounts of solar energy reaching the earth's surface is of prime importance in any investigation of the heat exchange at the surface and in the adjacent layer of air. The meteorologist is therefore concerned with the determination of the resulting radiation fluxes to and from the earth's surface with respect to evaluation of the thermal balance, locally and globally, of the terrestrial system. From the general geophysical viewpoint, increasing attention is now being paid to the assembly, on a large scale, of the basic information required to construct cartographical representations, in greater detail than has so far been possible, of the different radiation components with respect to area and also to time. In this connection, perhaps the most significant single requirement for a proper appreciation of physical climatology is an adequate knowledge of the distribution, geographically, of the (short-wave) radiation received, on a horizontal surface, totally from sun and sky. However, such effort is by no means confined to observation at the ground or over the ocean as the divergence aloft, with altitude, of the difference between the incoming and outgoing fluxes of long-wave terrestrial radiation is directly related to the heating or cooling of the atmosphere. This exchange of lower temperature, infra-red radiation results, mainly, from absorption by (and emission from) natural surfaces and atmospheric constituents of the primary solar radiation.

Largely on account of instrumental difficulties, the collection of solar radiation data, on a world scale, is in a markedly inferior state as compared with the other principal meteorological elements. And, unfortunately, in the lesser developed regions of the globe (especially in the permanent anticyclonic belts containing such climatic zones as the Sahara and Kalahari deserts of Africa and the arid central areas of Australia) the observational material presently available is pitifully scanty. This is unfortunate, not only from pure geophysical interests but also from the more immediately practical requirements in the fields of agriculture, engineering and architecture and, certainly, for the successful introduction of economic domestic schemes for the utilization of solar energy in the under-developed countries, which is one of the concerns of this Conference on New Sources of Energy, sponsored by the United Nations. In many instances, large areas of the earth, where the introduction and operation of unconventional power systems at relatively low cost would lead to a better economy of their populations, are characterized by climatic regimes which provide optimum availability of solar radiation. So, the realization of this objective will depend, to no small degree, on the obtaining of a fuller understanding of the truly enormous resources of power which we possess in the ordinary sunshine falling upon these lands.

* The Eppley Laboratory, Inc., Newport, Rhode Island, United States.

Attenuation of the solar beam

The quantity of radiant energy which falls upon a horizontal surface at the outer confines of the terrestrial atmosphere may be evaluated, for any place and on any day of the year, through consideration of the astronomical and trigonometrical principles involved, together with access to the so-called "solar constant of radiation" (now generally accepted to be approximately 1.98 cal cm^{-2} min^{-1} or 138 mw cm^{-2}). Specifically, by this we infer the intensity of the solar beam in energy units per unit of area normal to the beam and at earth's mean distance. In its passage downwards through the atmosphere, a diminution of the strength of the solar rays results chiefly from selective absorption by the constituent gases and by water vapor, from backward scattering by molecules of air and by solid and liquid particulate matter, and from reflection outwards to space by larger particles and by cloud surfaces. Changing conditions of atmospheric absorption and reflection therefore determine the diurnal, monthly and seasonal variations in the energy fluxes at the earth's surface. These optical processes also cause the measured radiation to have a different spectral composition from that expected according to the sun's radiative temperature.

At the higher levels, scattering is almost entirely molecular and is of a diffuse nature. But whether such scattering conforms completely to Rayleigh's law for spherical scattering centers smaller than the wavelength of light is still open to question. For convenience, nevertheless, the depletion is usually regarded as being symmetrical, half of the energy so scattered reaching the surface of the earth, in the absence of cloud cover, as skylight. Such Rayleigh scattering is dependent upon the fourth power of the wavelength, and as the distribution of energy

in the spectrum depends upon the length of the optical path traversed, the amount of scattering is thus a function of the solar altitude. However, overall values of the path lengths and solar altitudes can be derived, practically, from Bouguer's law $I_m = I_o\, q^m$, in which I_m represents the solar intensity at the surface, I_o that outside the atmosphere and m the air mass or path thickness (m is ordinarily specified as unity for a zenith sun at sea level).

At the lower levels, of say 1-2 kilometers, particle scattering predominates. If the particles are large as compared with the wavelength of light and the concentration of suspensions is great, the resulting scattering is mainly into the forward hemisphere. The complication of this mechanism of attenuation is increased by the occurrence of multiple scatter, which is pronounced in mist and clouds. Also, in greatly polluted air (e.g., industrial fogs), the number of very large particles is often increased and energy absorption may then become pronounced. There are good reasons, too, for the belief that dust absorbs as well as scatters solar radiation. The contribution to the diffuse skylight by secondary scatter has been investigated and it has been found that such scattered sunlight is chiefly responsible for the luminance of those portions of the sky which are at great angular distances from the sun.

Whereas the scattering processes operate principally in the short-wave portion of the spectrum, absorption occurs throughout in bands which are well defined and of greatest frequency and strength in the near infra-red region. In the troposphere, water vapor and, to a lesser extent, carbon dioxide, are the most active agencies of depletion. In the stratosphere, the presence of ozone, which is found at heights of between about 15 and 35 kilometers, introduces a controlling influence on the spectral range of the penetrating solar stream, mainly due to its strong absorptive properties at the ultra-violet end.

The components of solar radiation

Any object located near the earth's surface, and freely exposed, is subjected to three components of thermal radiation of immediate solar (short-wavelength emission) origin, i.e., direct sun or solar beam radiation, diffuse or scattered radiation and radiation reflected by the earth's surface. The spectral quality of these radiative fluxes is variable, as indicated above. In the case of the direct radiation, the energy spectrum is usually contained (for all practical purposes) within the limits 0.3-3 microns. The diffuse radiation is generally of wavelength shorter than 1 micron and the reflected radiation is of similar range to the direct component but with, obviously, different energy distribution spectrally. For a high sun (solar elevation $> 30°$), the energy maximum of the direct radiation peaks between 0.5 and 0.7 micron normally; the diffuse radiation, from cloudless skies, is particularly rich in blue light (0.4 micron) and the reflectance of many natural surfaces is greater for energy of wavelength corresponding to red and near infra-red radiation than for shorter wavelengths.

The solar radiation measurement which is generally undertaken within meteorological networks (which provide the bulk of the world's observational series) on a regular routine basis is that of the vertical integral wavelength flux, near the surface, from the sun and sky. To a much lesser extent, intermittent observations are made of the direct solar component received on a surface perpendicular to the solar beam. This type of measurement is generally assembled to serve one or other of the following purposes:

(*a*) Periodic standardization of the horizontal-surface records of total sun and sky radiation (see below).

(*b*) Determination of atmospheric turbidity coefficients, with the aid of colored filters.

In recent years, an effort has been made to increase the distribution of solar radiation stations where there is provision for the measurement, continuously, of the diffuse sky radiation received on a horizontal surface (generally through the employment of a shadow band in conjunction with a radiometer—strictly a pyranometer—intended for the measurement of total incoming solar short-wave radiation). The number of such stations, however, is probably less than one-tenth of the number providing systematic tabular data of total radiation. Very few series of radiation measurements are available for fixed inclinations other than horizontal exposure, and it is only in the last year or so that systematic measurements of spectral radiation from sun and sky, received on a horizontal surface, have been introduced (in the United States).

It is therefore quite clear that, for a first approximation, the meteorological "standard" record of total sun and sky (whole spectrum) radiation has to be employed in solar energy utilization studies, either where the preferred other measurement is not available or where interpolation has to be made, in the absence of radiation data, from information available for other locations. In the former case, where the solar energy collector has to be tilted out of the horizontal plane, particular attention has to be paid to the relative contributions accruing from the diffuse sky and from the ground reflected radiation fluxes. The sky radiation may vary, in intensity, from about 5 per cent of the direct solar component to a maximum approaching the latter, depending upon the transparency and the nature of the cloudiness of the sky. The ground reflectance, for solar radiation (integrated wavelengths), can range from 0.05 to 0.90 according to the terrain. If it is desired to estimate the direct solar radiation, e.g., for the calibration of solar furnaces (which are only energized by parallel beam radiation) then this follows from the relationship $I \sin h = T\text{-}D$, where I is the required direct intensity, h the relevant solar elevation, T the total radiation and D the diffuse radiation (T and D referring to horizontal surface exposure). At locations

where simultaneous measurements or reliable estimates of T and D are not available, it will probably be preferable to attempt evaluation of I from cartographical representations of I_o (i.e., direct radiation intensity outside the earth's atmosphere) combined with local measurements of atmospheric transparency (i.e., derivatives from atmospheric turbidity coefficients) or with estimates from other station data of measured I.

Solar radiation instrumentation

Two types of radiometer are employed generally throughout the countries of the world in observational programs of solar radiation short-wave components. These are:

(*a*) The pyrheliometer, with or without filters, for the measurement of the direct solar radiation at normal incidence.

(*b*) The pyranometer (now also available commercially with filters for sub-division of the solar spectrum) for the measurement, basically, of the total incoming sun and sky radiation received on a horizontal surface.

The second type can be used, with its receiver tilted out of the horizontal plane, for the measurement of the radiation falling upon a specified inclined surface, directly from the sun, diffused from the sky (but, of course, less than the total hemispherical component) and reflected, partially, from the surrounding surfaces (which will include artificial as well as natural ones unless precautions are taken to screen the receiver from local reflections). All models of the other type admit not only the radiation emission of the sun's disc but also that from a specific (but not standard) annulus of circumsolar sky.

Despite the fact that during the first three decades of the 20th century a very large number of radiometer models for the detection of solar short-wave radiation (direct and total sun and sky) and also of terrestrially originated long-wave radiation had been introduced (see below), the measurement position was far from satisfactory at the outbreak of World War II (1). Only in a relatively few instances was the observational accuracy of series of radiation measurements up to the level which can now be expected from the primary and secondary radiometers currently disposed throughout the governmental meteorological networks and at geophysical institutes. Indeed, in many cases, the resulting accuracy obtained from the then higher quality classes of instruments was not much better than can be obtained today with the simpler (and more economical) type presently available. However, this all important matter of accuracy inherent in the assembled records of solar and terrestrial radiation is not only a result of local instrumental performance but, to a large extent, is dependent upon the nature of the personal attention afforded the instrumentation and also, more so perhaps, upon the manner in which the eye observations or automatic recordings are controlled (2).

Prior to the commencement of the Third International Geophysical Year, the mutual existence of two internationally acceptable reference scales of pyrheliometry (3), which diverged considerably, was rather a disturbing factor, especially in comparing different series of measurements where, frequently, the references employed were not stated.

Instrumental requirements and practical possibilities

The principal requirements of radiometers intended for the measurement of short- or long-wavelength natural thermal radiation may be tabulated as follows (not necessarily in order of importance):

(*a*) Long-term stability, with good short-term reproducibility, preferably over several years;

(*b*) Relatively good degree of adherence to the Lambert cosine law (i.e., for pyranometers and total or net long-wave flux radiometers);

(*c*) Relatively good degree of freedom from the effects of ambient temperature;

(*d*) Independence of sensitivity with respect to the wavelength limits of the energy component to which the instrument is exposed;

(*e*) Completely weatherproof conditions;

(*f*) Ease of solar tracking, whether manually or automatically operated (i.e., for pyrheliometers);

(*g*) Reasonably fast response, especially where hourly or shorter period integrals are required;

(*h*) Freedom from asymetry of response during the sunrise-to-sunset period when the true radiation distribution is symmetrical about the median;

(*i*) Ease of calibration;

(*j*) Facility for remote recording, on commercially available equipment, where this is required;

(*k*) Relative robustness in design and construction, to withstand transportation and, as far as practicable, weather elements.

In present-day instrument design, most of the above-listed idealized requirements have been met realistically in the case of the short-wave radiometers; on the other hand, there is still much to be desired with the existing long-wave radiometers.

For many years, the primary working standard instruments have been of two types, i.e., the Ångström electrical compensation pyrheliometer (widely used, first in Europe) and the Abbot silver disk pyrheliometer (widely used, first in North America) (2). In recent reviews, Drummond (1) and Drummond and Greer (4) have indicated that reproduction of radiation intensity of the order of one part in one thousand is possible with either instrument, provided that very transparent atmospheric conditions are present. Agreement between specimens of the two types of two or three parts in one thousand is readily realizable under these conditions. On more

average observing days, these figures could be revised to ±0.5 per cent and ±1 per cent, respectively. As it is believed that the uncertainty of the present radiometric reference (2, 4), i.e., the International Pyrheliometric Scale (1956), may be ±0.5 to 1 per cent as compared with the (undetermined) true absolute scale of radiation, it is obvious that, absolutely, in our best measurements of the direct solar radiation we may easily be in error by ±1 to 2 per cent. Then, there is the question of transferring readings obtained with a so-called primary standard of either type to a working primary or secondary standard instrument, in order to calibrate the field radiometers (which may be other pyrheliometers or, more likely, pyranometers). It will therefore be appreciated that, even with the best quality radiometers, accuracy levels of ±2 per cent, for secondary pyrheliometers, and ±3 per cent for pyranometers (which are secondary instruments) are tolerably good targets at which to aim.

The secondary pyrheliometers recommended by the World Meteorological Organization are thermopile detector types (2), i.e., the Eppley, Linke-Feussner and Gorczynski pyrheliometers. All are capable of a precision in output reading (voltage) of ±1 per cent, provided that proper attention is paid to periodic calibration against a primary working standard. The Michelson bimetallic actinometer is also suitable for this purpose. In each instance, however, the instrument sensitivity is temperature dependent (values of the temperature coefficient of up to —0.2 per cent/1°C rise in ambient temperature are not uncommon) and due allowance has to be made for this effect if the highest accuracy is demanded. Recently, an improved version of the Eppley normal incidence pyrheliometer, and also a new high-precision type pyranometer, were introduced (1, 5) incorporating temperature compensation of the thermopile unit. With this arrangement, reproducibility better than ±0.5 per cent was demonstrated, over a period of continuous instrumental exposure of nearly six months in extent, with ambient temperatures varying between 0 and +25°C (1).

For reasons of convenience (and economy) with regard to the solar tracking device to be employed with pyrheliometers, the magnitude of the opening (i.e., half aperture) angle of pyrheliometers usually varies between about 2.5 and 5°. If the opening angle, so defined, is smaller than 1.0°, serious difficulty may be experienced with the observations. Pastiels has produced a very valuable study in such a connection (6).

For many years, the classical Eppley (Kimball) and Kipp (Moll-Gorczynski) thermoelectric pyranometers have been extensively used for the measurement of total sun and sky radiation, of radiation falling on inclined surfaces and of the reflectance of natural surfaces. Their characteristics have been described, respectively, by MacDonald (7) and Fuquay and Buettner (8), and by Bener (9). A summary of the instrument characteristics of the currently produced model of the Eppley pyranometer (long referred to as the Eppley 180° pyrheliometer) is available, on request, from the Eppley Laboratory, in mimeographed form (10). The main improvements over the older model are better glass envelopes and a better detector blackening; these result in a closer adherence to the cosine law. Temperature compensation of sensitivity (to within approximately ±1 per cent over an ambient temperature range of about 60°C) has just been introduced as an optional item. With these pyranometers, *overall accuracy generally* (e.g., for daily summations) is in the region of ±2 to 3 per cent if systematic control of the instrumental sensitivities is attempted; for hourly values, the error may frequently reach 5 per cent, especially for the lower solar altitudes. However, these figures imply carefully calibrated electrical recorders (e.g., a recording potentiometer with a full-scale error of 0.5 per cent can entail recorder inaccuracy of 1-2 per cent in the lower half of the scale).

To turn to the two extremes of this problem, if we replace the glass envelope(s) of the pyranometer by one(s) more perfectly formed and introduce temperature and cosine error compensations, at the expense of economy, we can achieve an instrumental precision of ±1 per cent (5). At the other end of the scale, use of the simple, direct recording Robitzsch-type pyranographs (11, 12) will only continue to yield reliability to within ±10 per cent, for daily values, if regular control is exercised; this instrument is not suitable for shorter period analyses.

The subject of the measurement of the incoming and outgoing long-wave terrestrial fluxes will not be considered here in detail. It is sufficient to state that the current internationally recommended radiometers suffer markedly from the effects of temperature dependence, poor weather resisting qualities and undesirable transmission characteristics of the protective envelopes (or from the absence of such an envelope during windy and rainy conditions) (2).

Conclusions

The attainment of accuracy levels in the measurement of total sun and sky radiation of 5 per cent or better, repeatedly, has its difficulties. With simpler instruments, reliability of 10 per cent can be accomplished regularly only when there is adequate provision for checking the records.

References

1. Drummond, A. J., Solar Energy, 5, 19, 1961.
2. *IGY Instruction Manual*, vol. 5, part. IV, Pergamon Press, London, 1958.
3. Drummond, A. J., *WMO Bulletin*, 5, 75, 1956.
4. Drummond, A. J. and Greer, H. W., *Sun at Work*, 3, 3, 1958.
5. Marchgraber, R. M. and Drummond, A. J., Contribution to the International Radiation Symposium, Oxford (mimeographed), 1959.
6. Pastiels, R., *Inst. Roy. Met. de Belgique*, Pub., Ser. A, No. 11, 1959.
7. MacDonald, T. H., *Mon. Wea. Rev.*, 69, 146, 1941.
8. Fuquay, D. and Buettner, K., *Trans. Amer. Geophys. Un.*, 38, 38, 1957.
9. Bener, P., *Archiv. für Met., Geophys. und Biokl.*, Serie B, 2, 188, 1950.
10. Eppley Laboratory leaflet, *Performance Characteristics of Eppley 180° 10- and 50-Junction Pyrheliometers (Pyranometers)*, 1960.
11. Blackwell, M. J., Air Ministry Met. Res. Ctee., London, M. R. P., No. 791, 1953.
12. Fowler, J. R., *Bull. Amer. Met. Soc.*, 34, 170, 1953.

Addendum

On the distribution of solar radiation at the earth's surface

It has been pointed out that during the last 10-15 years there has been an intensification of effort within national meteorological services and by governmental, educational and other geophysical institutes to improve our knowledge of the distribution of solar radiation over the earth's surface. A stimulus in this direction was apparent in the planning for the Third International Geophysical Year. However, despite such efforts as those by Canada (1), the Union of South Africa (2) and the United States (3) in the provision of serial publication of daily (and in the case of (1) and (2) hourly where available) data for extensive areas, and Italy (4), Portugal (5) and the United States (3) in issuing monthly mapped data for their networks, much of the information assembled throughout this period is not readily available. It is true that the World Meteorological Organization has made arrangements for the publication of the IGY radiation data and this will certainly be a most welcome addition to what has already been widely disseminated.

In the past, numerous attempts have been made, since the original one of Ångström (6, 6a), to compute daily amounts of total sun and sky radiation from the relative duration of sunshine or from the cloudiness, measurements of the former element and/or estimates of the latter being standard in all weather services. In this connection, the efforts by Fritz and MacDonald (7), Black, Bonython and Prescott (8), Albrecht (9), Hinzpeter (10) and de Boer (11) are typical. Other workers have tackled associated problems such as those of the derivation (from the measured total solar radiation received on a horizontal surface) of the solar radiation available on surfaces with various orientations (12, 13), the diffuse sky component on clear days and under specified conditions of cloudiness (14) and the hourly distribution from daily summations (15).

Another very important contribution to radiation climatology has been the recently published maps for the world showing the (largely estimated) distribution of the total incoming solar radiation for each calendar month (16, 17). Other average cartographical surveys, on a monthly or seasonal basis, have been prepared for specific regions, for example, Canada (18), Japan (19), Southern Africa (20) and the United States (7); the second and third of these sets of maps have been charted practically entirely from measured data.

The principal purpose of including this addendum with the present contribution is to focus attention upon the need for assessing the reliability, in different climatic regimes, with which representative long-period average values, for specific localities, of the total solar radiation may be computed or converted into components of different orientation, with the aid of the observational material presently available and the computational techniques already established. If, for instance, the accuracy desired for a certain project is 10 per cent and it appears possible to derive the required period values, indirectly, within this limitation, then there would be little point in setting up one of the so-called "simpler instruments". On the other hand, if more meaningful information is considered necessary, then the proper recourse is to employ one of the conventional meteorological secondary-type paranometers, with adequate instrumental control facilities. With regard to the question of the assembly of radiation figures, statistically, in the form, for example, of frequency distributions (21, 22, 23), whether this can be achieved reasonably, in an indirect manner, will largely depend upon the detail and accuracy stipulated and upon the nature of the secondary information (e.g., location and type of nearest radiation measurements and other applicable meteorological information).

Another purpose of this addendum is to urge that attention be paid to making available the large mass of solar radiation observational data, currently not generally accessible, either in digest suitable for statistical analysis or in the form of standard frequency distributions.

It has not been the intention to offer a complete bibliography along the lines of the above discussions; the references given are purely for illustration.

References

1. *Monthly Radiation Summary*, Meteorological Dept., Toronto, 1960.
2. *Quarterly Radiation Bulletin (Regional Association I)*, Weather Bureau, Pretoria, 1955.
3. *Climatological Data (National Summary)*, Weather Bureau, Asheville.
4. *La rete attinometrica del Servizio Meteorologico dell'Aeronautica Italiana*. Risultati del primo anno di misura della radiazione globale. Riv. Meteor. Aeron.; Rome, 16, 1-18, 1956.
5. 1955- Servico Meteorologico nacional. *Boletim actinometrico de Portugal*. Mimeo. Lisbon, 1955.
6. Ångström, A. K., *Q. J. Roy. Met. Soc.*, 50, 121, 1924.

6a. Ångström, A. K., *Archiv für Geofysik*, 2, 471, 1956.

7. Fritz, S. and MacDonald, T. H., *Heating and Ventilating*, 46, 61, 1949.
8. Black, J. N., Bonython, C. W. and Prescott, J. A., *Q. J. Roy. Met. Soc.*, 80, 231, 1954.
9. Albrecht, F. H. W., *Geofisica Pura e App.*, 32, 131, 1955.
10. Hinzpeter, H., *Archiv für Met. Geophys. und Biokl.*, Serie B, 9, 60, 1958.
11. de Boer, H. J., *Archiv für Met. Geophys. und Biokl.*, Serie B, 10, 537, 1961.
12. Becker, C. F. and Boyd, J. S., *Solar Energy*, 1, 13, 1957.
13. Schüepp, W., *Archiv für Met. Geophys. und Biokl.*, Serie B, 9, 272, 1958.
14. Liu, B. Y. H. and Jordan, R. C., *Solar Energy*, 4, 1, 1960.
15. Whillier, A., *Archiv für Met. Geophys. und Biokl.*, Serie B, 7, 197, 1956.
16. Budyko, M. I., *Atlas of Heat Balance* (Russian), Leningrad, 1955.
17. Black, J. N., *Archiv für Met. Geophys. und Biokl.*, Serie B, 7, 165, 1956.
18. Mateer, C. L., *Can. J. Agric. Sc.*, 35, 579, 1955.
19. Sekihara, K. and Kano, M., *Papers in Met. and Geophys.*, 8, 144, 1957.
20. Drummond, A. J. and Vowinckel, E., *J. Meteor.*, 14, 343, 1957.
21. de Barry, E., *Solar Energy*, 4, 2, 1960.
22. Hinzpeter, H., *Solar energy*, 4, 8, 1960.
23. Fritz, S. and MacDonald, T. H., *Solar Energy*, 4, 20, 1960.

Summary

A review is presented of the principal objectives of the measurement of the different components of solar radiation, particularly with regard to the applicability of the derived radiation data in the several aspects of the utilization of solar energy. These radiation components of the thermal radiation balance at the ground are the direct solar contribution, the diffuse sky radiation, the reflected solar radiation and the longer wavelength temperature radiation which is exchanged within the terrestrial system. As in the case of the short-wave components, three categories of long-wave radiative transfer are involved, i.e., outgoing infra-red radiation from the earth and its atmosphere, incoming infra-red radiation resulting from downward emission by the atmospheric constituents, and reflected infra-red radiation at the various natural surfaces. With regard to the short-wave radiation fluxes, a further sub-division into well-defined regions of the solar spectrum is increasingly gaining in importance as improved and readily operable techniques for effecting the energy separation become available. A knowledge of the spectral energy distribution of the direct solar or the total sun and sky radiation is highly desirable, for instance, in the evaluation of the efficiency of photoelectric converters which are intended for exposure under natural conditions.

The major problems associated with the design of thermal radiation detectors for such purposes are discussed, as are also the limiting factors, introduced by reasons of economy, which dictate instrumental performance. It is not sufficient to construct the radiometers to comply with certain specifications of precision which is here better expressed, perhaps, as readout repeatability. It has to be demonstrated that the required instrumental tolerances can be realized in climatic regimes other than those where the basic calibrations were undertaken and that there is adequate long-term stability in the functioning of the radiometers (term used generally). Then, there is the question of the reproduction, locally, of the international standard of pyrheliometry in order that comparability of the individual series of radiation measurements may be achieved with the requisite precision, on a global basis.

An outline is given of the precision and accuracy levels obtainable, generally, in the present state of the art, with the main radiometers in use, in improved form, and also introduced since World War II, in measurement programs of integral and spectral wavelength radiation.

INSTRUMENTS DE MESURE DU RAYONNEMENT SOLAIRE : APERÇU DES MÉTHODES NOUVELLES ET DES PROGRÈS RÉCENTS RÉALISÉS

Résumé

Dans le présent mémoire, il est procédé à un examen des objectifs principaux de la mesure des divers composants du rayonnement solaire, particulièrement en ce qui concerne l'applicabilité des données obtenues à l'utilisation de l'énergie solaire sous ses aspects multiples. Ces composants de rayonnement du bilan de radiation thermique au sol comprennent la contribution solaire directe, la radiation céleste diffuse, la radiation solaire réfléchie et la radiation thermique à plus grande longueur d'onde, qui est échangée à l'intérieur du système terrestre. Comme dans le cas de composants à courte longueur d'onde, trois catégories de transferts de radiations à grande longueur d'onde entrent en jeu, à savoir : des radiations infrarouges émises par la terre et son atmosphère, des radiations infrarouges résultant d'une émission vers le bas par les constituants atmosphériques, et des radiations infrarouges réfléchies par diverses surfaces naturelles. En ce qui concerne les flux de radiations à courte longueur d'onde, une nouvelle subdivision dans des régions bien définies du spectre solaire prend une importance croissante, à mesure que des méthodes perfectionnées et d'application facile pour effectuer la séparation d'énergie, deviennent disponibles. Une connaissance de la répartition de l'énergie spectrale, du rayonnement solaire direct ou du rayonnement global du soleil et du ciel est très utile, par exemple, pour l'évaluation du rendement de convertisseurs photoélectriques destinés à être exposés sous des conditions naturelles.

L'auteur examine les principaux problèmes qui se posent lors de l'étude d'un instrument détecteur de radiations thermiques à ces fins, ainsi que des facteurs limitatifs, dictés pour des raisons d'économie, qui commandent le rendement de l'instrument. Il ne suffit pas de construire des radiomètres obéissant à certaines spécifications de précision que l'on pourrait peut-être mieux qualifier, en l'occurrence, de possibilité de répétition de lecture. Il y a lieu de démontrer que les tolérances de mesure requises peuvent être obtenues dans des régimes climatiques autres que ceux sous lesquels l'étalonnage de base a été effectué et que les radiomètres (terme habituellement employé) fassent preuve dans leur fonctionnement, d'une stabilité suffisante à long terme. Puis, il y a la question de la reproduction, localement, de la norme internationale de pyrhéliométrie, afin d'obtenir avec la précision nécessaire, sur une base globale, la comparabilité des séries particulières de mesures de rayonnements.

L'auteur donne un aperçu des niveaux de précision et d'exactitude que l'on peut obtenir, en général, au stade actuel de nos connaissances, avec les principaux radiomètres en usage, sous forme perfectionnée, et présentés depuis la deuxième guerre mondiale, dans des projets de mesure de rayonnements de longueur d'onde intégrale et spectrale.

SOLAR RADIATION AVAILABILITY IN THE UNITED ARAB REPUBLIC

M. K. Elnesr and A. M. Khalil *

The solar radiation which reaches the outer limits of the atmosphere and is received in one minute by an area of 1 square cm placed perpendicular to the sun's rays and at the mean distance between the sun and the earth is known as the solar constant, and is usually denoted by I. Its most accepted value is 1.94 ly/min (1). For practical purposes the spectral distribution of this energy outside the atmosphere lies between the limits of 0.22 and 4 μ.

The solar beam, when penetrating the atmosphere, sustains different losses. At the top of the atmosphere, it is slightly depleted by the absorption characteristics of molecular oxygen and nitrogen. When traversing the ionosphere, most of the energy in the ultraviolet region and in a small portion of the visible part of the solar spectrum is absorbed, so that below 0.29 μ solar energy is cut off. As the remaining energy proceeds through the atmosphere, it undergoes two principal variations: scattering and absorption.

The first is caused by molecules, dust and other atmospheric suspended impurities, while the second is accomplished mainly by water vapour.

A considerable portion of the solar beam which has been scattered and diffusely reflected arrives at the earth unchanged in wave length as diffuse radiation, which must be added to the direct radiation from the sun, to make up the total radiation.

The ratio between the solar constant I_o and the radiation received at normal incidence at the earth's surface I is given by q^m

or

$$\log I = \log I_o - m \log q \qquad [1]$$

where q is the atmospheric transmission coefficient, and m is the thickness of the atmosphere traversed by the solar beam. q integrates transmission over all wave lengths of the solar spectrum and should not be confused with the classical Bouguer transmission coefficient, which refers to monochromatic radiation only.

The thickness of the atmosphere m, known as the air mass, is equal to unity when the sun is in the zenith and the point of observation is at sea level. For other elevations, m is proportional to the secant of the zenith distance z

i.e., $m = \sec z$

or more precisely $m = \sec z\ (1\text{-}0.001 \tan^2 z)$ [2]

when taking the refraction of the atmosphere into consideration.

For any oriented surface at the ground, the irradiation by the sun is the product of the direct normal radiation I_D and the cosine of the angle of incidence i. This angle changes from day to day and from hour to hour owing to the varying position of the earth relative to the sun and to the rotation of the earth about its axis. This position is defined by two angles, the solar altitude h ($h + z = 90°$), and the solar azimuth A, which can be secured directly from the U.S. Hydrographic Office Tables No. 214, for any local hour angle when the latitude of the place and the declination of the sun are known (2).

This paper gives, for clear sky conditions, estimates of the total solar radiation incident on surfaces at various orientations. This information is frequently needed by research scientists interested in solar energy utilization.

Pyrheliometric measurements at Helwan Observatory

Measurements of the total solar radiation at normal incidence had been started at Helwan Observatory (29° 52′ N, 31° 20′ E) in February 1914. An Ångström pyrheliometer No. 110 (constant $k = 1\,408$) was used till August 1916, and followed by the No. 171 (constant $k = 1\,310$) which had just been returned from standardization at Upsala. Pyrheliometer No. 110 was then sent at Upsala and returned in January 1920. It has since been kept as standard. No. 171 has been compared with it twice a year and there has been found a slight increase from year to year in the constant of the pyrheliometer in regular use, owing probably to the decrease of the absorptive power of the blackened strips caused by the deposit of dust. Comparisons gave continuous confidence in the good state of the pyrheliometer No. 171 and in the absolute values of the measured radiations.

Observations were made on nearly every fine day, three times a day, at air masses 3.0, 2.3 and 1.7 in winter and at air masses 3.0, 1.7 and 1.15 in summer. All the observations were made in the morning before 11 o'clock, as after this the transparency of the atmosphere generally becomes unsteady.

Two bulletins were published by Helwan Observatory, giving in particular the daily solar constant determinations during the years 1914-15, 19, 20, 21 (3, 4). In 1927, Kimball gave an excellent summary of the solar radiation intensity measurements at

* University College for Girls, Ain Shams University, Cairo.

Table 1. Hourly rates of total solar radiation intensity (ly/min) for clear sky conditions at Helwan Observatory

Local time	J.	F.	M.	A.	M.	J.	J.	A.	S.	O.	N.	D.
6	—	—	—	.32	.53	.56	.44	.36	.29	—	—	—
7	—	.51	.81	.83	.88	.91	.87	.82	.82	.76	.65	.23
8	1.00	.94	1.17	1.11	1.08	1.09	1.07	1.07	1.09	1.07	1.01	.93
9	1.24	1.18	1.36	1.23	1.20	1.19	1.16	1.20	1.22	1.23	1.20	1.17
10	1.35	1.33	1.45	1.30	1.26	1.25	1.22	1.26	1.28	1.28	1.29	1.30
11	1.40	1.39	1.49	1.33	1.31	1.29	1.25	1.28	1.31	1.31	1.33	1.34
12	1.42	1.42	1.51	1.33	1.31	1.31	1.27	1.29	1.31	1.32	1.34	1.36

most parts of the world (5). He gave the mean monthly values of the total solar radiation, measured at normal incidence at Helwan Observatory, during the period from February 1914 to December 1923, for air masses 1 and 2.

Hourly rates of total solar radiation at normal incidence during cloudless days

The pyrheliometric observations taken at Helwan Observatory were the only possible information in the U.A.R. on solar radiation intensity for clear sky conditions, and we were therefore obliged to make use of them in the study of the availability of solar radiation on surfaces at various orientations. The calculations were carried out, for each month of the year, as follows:

(*a*) Plot log I against m using the values given by Kimball for $m = 1$ and $m = 2$, as well as the values for $m = 1.7$, which we have calculated from detailed observations during the same period 1914-1923, furnished by the permission and through the courtesy of the director of Helwan Observatory.

It is to be noted that the results given by Kimball for $m = 1$ and $m = 2$ were reduced to mean solar distance and expressed in the Smithonian Scale. To convert them to the Ångström Scale, they should be multiplied by 0.9685, and to account for the variations in the distance between the sun and the earth, they should be multiplied by 1.03 for December and January; 1.02 for February and November; 1.01 for March and October; 0.99 for April and September; 0.98 for May and August; and 0.97 for June and July (6).

(*b*) Calculate, for each hour of the month represented by its 15th day, the zenith distance z, the air mass m, and hence, from the (log I — m) curve, the hourly rates of the total solar radiation at normal incidence, as given in table 1.

Total solar radiation on surfaces at various orientations

(*a*) It has already been indicated that the total solar radiation reaching the earth's surface constitutes a diffuse part. It has no fixed direction and does not obey the law of cosine ratios. To predict radiation incident on a certain plane, it is necessary, as a first step, to know the magnitude of this diffuse part. Unfortunately, no separate measurements of diffuse radiation have been undertaken at Helwan Observatory. On the other hand, the amount of data in the literature on diffuse radiation is very limited and mainly concerns horizontal surfaces and clear sky conditions (7, 8). The best information at the time may be that contributed by Parmelee (9), who has measured the diffuse radiation on horizontal and vertical surfaces and plotted his results versus solar altitude and wall solar azimuth,[1] such that it can be estimated for any vertical surface of any orientation. As during cloudless days the diffuse radiation is generally small compared with the direct radiation, and as it depends mainly on the air mass penetrated by the solar beam, Parmelee's data may be considered as representative to other localities (e.g., Helwan Observatory) and has been

[1] The various angles referring to sun and wall positions are described in the Ventilating, Air Conditioning Guide; 275 (1954).

Table 2. Hourly rates of direct solar radiation intensity (ly/min) for clear sky conditions at Helwan Observatory

Local time	J.	F.	M.	A.	M.	J.	J.	A.	S.	O.	N.	D.
6	—	—	—	.28	.47	.49	.36	.31	.27	—	—	—
7	—	.47	.67	.73	.76	.80	.76	.72	.73	.70	.63	.22
8	.92	.84	.95	.98	.94	.95	.93	.93	.96	.96	.92	.84
9	1.11	1.05	1.11	1.08	1.06	1.05	1.02	1.05	1.07	1.09	1.07	1.05
10	1.21	1.17	1.18	1.15	1.12	1.10	1.07	1.12	1.13	1.13	1.14	1.15
11	1.25	1.23	1.21	1.18	1.16	1.14	1.10	1.14	1.16	1.16	1.17	1.18
12	1.27	1.26	1.23	1.18	1.17	1.16	1.12	1.15	1.16	1.17	1.18	1.21

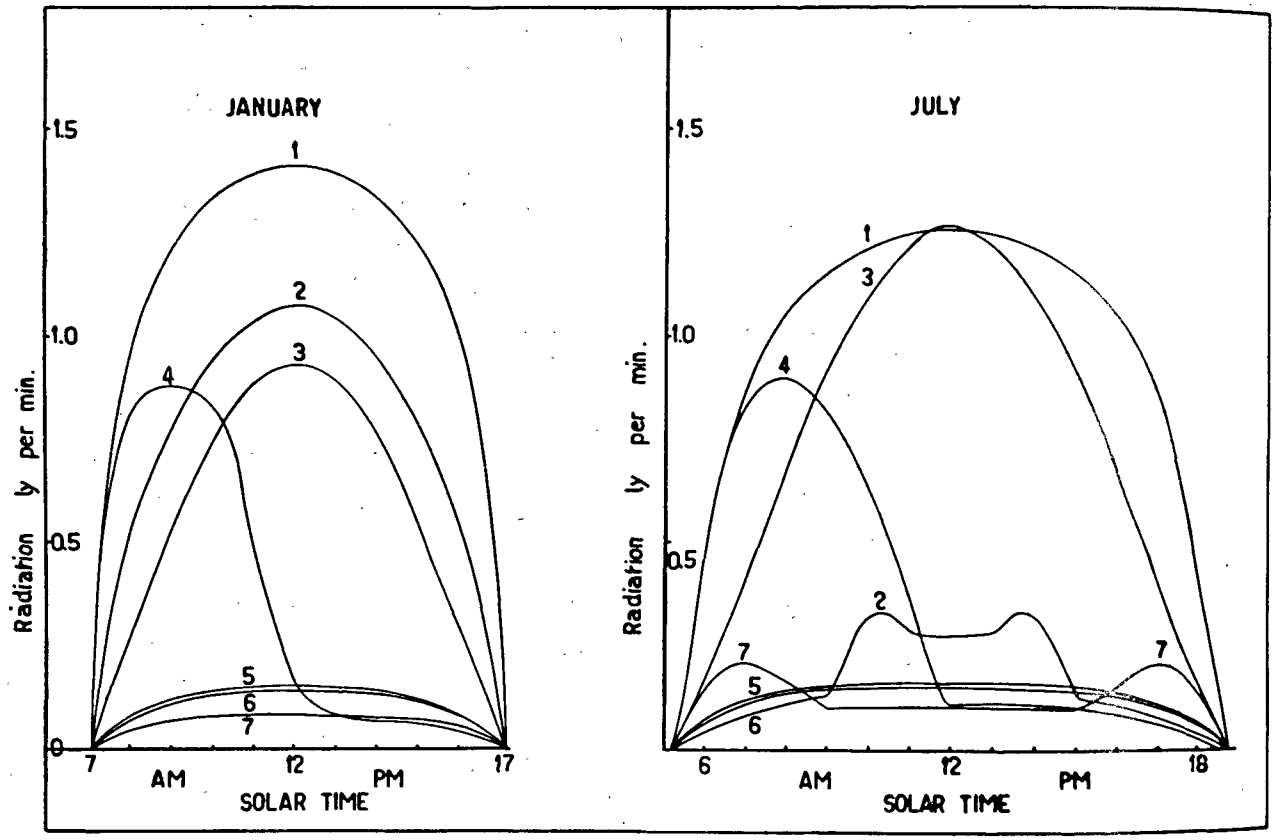


Figure 1. Intensity of total solar radiation on cloudless days at Helwan Observatory

1. Total normal; 2. Total facing south; 3. Total horizontal; 4. Total facing east; 5. Normal diffuse; 6. Horizontal diffuse; 7. Total facing north

used to calculate the hourly rates of diffuse radiation at normal incidence for the latitude of Helwan. This has been done by linear interpolation between the values secured for a horizontal surface H_d and for a vertical surface V_d having a wall solar azimuth angle equal to zero, such that

$$I_d = H_d - (H_d - V_d)\frac{z}{90} \qquad [3]$$

The values obtained were subtracted from the corresponding total solar radiation to obtain table 2. With the hourly rates of the direct radiation at normal incidence I_D.

(*b*) Applying the law of cosine ratios to I_D, the hourly rates of the direct solar radiation, incident on the principal vertical orientations, were calculated, and to account for the corresponding hourly rates of diffuse radiation, Parmelee's data were again used. The sum of the computed direct and diffuse components has been plotted graphically, against the mean local time. Figures 1 and 2 give an example of the curves obtained for the months of January and July, considered representative of the winter and summer periods. From these curves, the daily total radiation received on the principal vertical orientations were calculated and presented in table 3.

(*c*) In the design of solar equipment, such as a solar water heater, the flat plate collector should be erected to receive the maximum possible radiation. It should be facing south and tilted with a certain angle $\varnothing$ to the horizontal. To account for the best tilt, the daily total radiation received when $\varnothing = 15$,

Table 3. Daily total solar radiation received on surfaces of various orientations

Surface	*J.*	*F.*	*M.*	*A.*	*M.*	*J.*	*J.*	*A.*	*S.*	*O.*	*N.*	*D.*
Horizontal. .	360	415	515	595	630	640	620	595	550	450	365	320
Facing S . .	480	420	340	210	140	110	135	215	280	390	450	455
Facing N . .	40	47	55	62	105	125	105	75	60	50	40	40
Facing E . .	220	235	250	290	290	300	280	280	280	260	230	200
Facing W . .	220	235	250	290	290	300	280	280	280	260	230	200

Table 4. Daily total solar radiation received on a south-facing surface with different orientations (ø angle of tilt with the horizontal)

ø	J.	F.	M.	A.	M.	J.	J.	A.	S.	O.	N.	D.
15°	465	505	575	610	620	620	610	600	575	525	465	420
30°	530	548	575	590	575	575	565	565	575	565	525	500
45°	560	565	575	534	500	485	490	515	550	570	560	535
60°	570	555	520	450	395	380	275	420	485	540	550	545
75°	545	500	440	345	275	180	270	310	395	485	520	520

30, 45, 60 and 75 to the horizontal was calculated, and tabulated in table 4, following the same procedure as in (*b*) above.

Pyrheliometric records of total solar radiation on the horizontal

Measurements of the total solar radiation, received on a horizontal surface, and under all sorts of weather conditions, were started at the Agro-meteorological station at Giza (30° 2′ N, 31° 13′ E), in December 1955, by equipping the station with various recording instruments. As it has been planned to develop a network of pyrheliometric stations in the U.A.R., one of these instruments has been a Robitzsch actinograph, which could be generalized for its robustness and simplicity in operation.

When comparing the daily records obtained during a whole year by the Robitzsch with those obtained by a 10-junction calibrated Eppley pyrheliometer, subjected to the same conditions of exposure, it has been found that the Robitzsch gives consistently higher values with an increase in summer (10). This has been found to be due to the seasonal changes in the temperature of the outside air. A correction factor has been evaluated for each month of the year, permitting the measurements to be accurate to within ± 4 per cent.

In January 1958, the sensitive element of this actinograph was destroyed, and a new instrument was used instead. Applying the same test to this actinograph, it has been found that the error lies between 0 & 4 per cent, allowing its use without any correction. The data obtained during the three

Table 5. 5-day means of daily values of total solar radiation (ly/day) received on a horizontal surface at Giza

Month period	Year	J.	F.	M.	A.	M.	J.	J.	A.	S.	O.	N.	D.
1-5	56	287	390	384	550	620	617	618	602	539	467	372	215
	57	309	269	486	591	564	681	638	629	897	505	386	278
	58	257	313	271	578	538	662	649	620	545	470	333	268
	Mean	284	324	447	573	574	653	635	617	500	481	354	254
6-10	56	300	380	516	412	654	643	603	561	545	465	274	232
	57	281	352	476	534	470	674	668	645	571	462	334	313
	58	242	333	495	579	633	652	638	614	534	430	333	193
	Mean	274	355	496	508	585	656	637	607	550	452	314	246
11-15	56	256	368	535	622	641	621	616	566	527	432	336	276
	57	307	448	437	605	634	673	677	642	554	415	360	297
	58	281	358	513	541	643	653	640	607	533	413	296	224
	Mean	281	391	495	589	639	649	644	605	538	420	331	266
16-20	56	305	319	499	624	650	633	622	585	536	416	302	227
	57	318	434	452	583	647	656	657	625	555	344	310	282
	58	291	412	540	500	632	643	636	599	496	403	297	267
	Mean	305	388	497	569	643	644	638	603	529	388	303	259
21-25	56	326	427	612	626	639	648	593	542	502	378	265	264
	57	344	446	517	509	582	676	674	622	492	395	337	293
	58	251	470	545	622	655	667	648	585	506	402	279	256
	Mean	307	448	558	586	625	664	638	583	500	392	294	271
26-31	56	271	363	558	622	656	637	592	546	506	378	284	271
	57	184	458	515	668	669	694	674	621	511	364	294	239
	58	326	461	550	634	629	648	644	572	495	359	244	239
	Mean	260	427	561	641	651	653	637	580	504	367	274	250
1-31	56	290	375	519	576	643	633	607	566	526	421	306	248
	57	287	397	493	502	595	672	665	630	547	415	298	282
	58	276	386	520	576	622	652	643	598	518	411	287	241
	Mean	285	386	511	578	620	653	638	598	530	415	300	257

calender years 1956-1958 are appended in table 5, as 5-day and monthly mean daily values.

Sunshine duration

In addition to the knowledge of solar radiation intensity received at any place, an important factor in the utilization of solar energy is the sunshine duration. It is recorded at most of the meteorological stations in the U.A.R. with a Campbell Stokes sunshine recorder.

A complete analysis of the recorded duration, with a special reference to Helwan Observatory for the period 1923-1953, has been given by one of the authors (11). The same author has also given the sunshine duration measurements at Giza in a form suitable for prospective solar applications (12).

References

1. Johnson, F. S., The Solar Constant, *J. Meteo.*, 11 : 431-439, 1954.
2. U.S. Hydrographic Office, *Tables of Computed Altitude and Azimuth*, Publication No. 214, 1940.
3. Eckersley, T. H., Observations of Solar Radiation, *Helwan Obs. Bulletin No. 14*, 1914.
4. Knox Shaw, H., Observations of Solar Radiation, *Helwan Obs. Bulletin No. 23*, 1921.
5. Kimball, H., Measurements of Solar Radiation Intensity, *Moth. Weath. Rev. 55 :* 155-169, 1927.
6. Smithsonian Institution, *Smithsonian Physical Tables*, 6th Edition, Washington, D.C.
7. Hand, I. F., Insolation on Clear Days for Lat. 42° N., *Heat. and Vent. 47 :* 92-4, 1950.
8. Stagg, J. M., Solar Radiation at Kew Observatory, *Geophys. Memoirs 86*, Met. Off., 1950.
9. Parmelee, G. V., Irradiation of Vertical and Horizontal Surfaces by Diffuse Solar Radiation from Cloudless Days, *Heating, Piping and Air Conditioning*, 129, 1954.
10. Elnesr, M. K. and others, Measurements of Total Solar Radiation at Giza, *Geofisica Pura I Applicata 45 :* 298-302, 1960.
11. Elnesr, M. K. and Firesah, A. M., Contribution à l'Étude de l'Énergie Solaire, *J. Sc. de la Met. 34 :* 85-92, 1957.
12. Hafez, M. M. and Elnesr, M. K., Demineralization of Saline Water by Solar Radiation; *Proceedings of the United Nations Conference on New Sources of Energy*, 1961, included below, paper S/63, agenda item III E.

Summary

Measurements of the total solar radiation at normal incidence, I, was started at Helwan Observatory (29° 52′ N, 31° 20′ E) in February 1914. On every fine day, observations were made with an Ångström pyrheliometer, three times a day at three different air masses. From these observations, we have evaluated for every month of the year:

(*a*) The hourly rates of total solar radiation at normal incidence, by plotting log I against the air mass m (m is a function of the local mean time). We have made use of the mean monthly values of I for $m = 1$ and $m = 2$, measured at Helwan Observatory, during the period between February 1914 and December 1923, and already published. As a third point is needed to plot any linear relation, we have calculated, from individual observations during the same period, the mean monthly values of I for $m = 1.7$.

(*b*) The hourly rates of the direct solar radiation at normal incidence I_D, by subtracting the hourly rates of diffuse radiation at normal incidence I_d, from the corresponding total solar radiation I. As no separate measurements of I_d were made at Helwan Observatory, we have made use of the data available in the literature, as during cloudless days I_d is generally small compared with I_D and depends, mainly, on the air mass penetrated by the solar beam.

(*c*) The daily total radiation available on surfaces with various orientations (the principal vertical orientations and tilted south-facing surfaces. To do this we have proceeded for each surface as follows:

1. Applied the law of cosine ratios to I_D, to get the hourly distribution of the direct radiation;
2. Evaluated the corresponding hourly distribution of the diffuse radiation, as in (*b*);
3. Plotted the hourly distribution of total radiation (direct + diffuse), against the local mean time;
4. Computed the daily total radiation incident on the surface in consideration, from the curve obtained in 3.

Measurements of the total solar radiation received on a horizontal surface under all sorts of weather conditions have been recorded recently at the Agrometeorological station at Giza (30° 2′ N, 31° 13′ E), with a Robitzsch actinograph. For the interest of research scientists in solar energy utilization, the difficulties in obtaining precise measurements have been discussed and the data recorded during the 3 calendar years 1956-1958 have been summarized both as a 5-day and monthly mean daily value.

MESURES DU RAYONNEMENT SOLAIRE EN RÉPUBLIQUE ARABE UNIE

Résumé

On a commencé des mesures du rayonnement solaire total sous une incidence normale, I, à l'Observatoire de Helwan (29° 52′ N-31° 20′ E) en février 1914.

Tous les beaux jours, on procède à des observations avec un pyrhéliomètre de Ångström, trois fois par jour et sur trois masses d'air différentes. En se basant sur ces observations, on a évalué, pour chaque mois de l'année :

a) Le nombre d'heures de rayonnement solaire total à une incidence normale, en établissant un tracé de la valeur log I par rapport à la masse d'air m, (m est une fonction de l'heure locale moyenne). Nous nous sommes servis des moyennes mensuelles de I pour $m = 1$ et $m = 2$, mesurées à l'observatoire de Helwan, pendant la période allant de février 1914 à décembre 1923, valeurs déjà publiées. Un troisième point au moins est nécessaire pour établir un rapport linéaire, et nous avons donc calculé, à partir d'observations individuelles prises sur la même période, les moyennes mensuelles de I pour $m = 1{,}7$;

b) Les quantités horaires de rayonnement solaire direct apportées à l'incidence normale I_D sont obtenues en soustrayant les valeurs horaires de radiation diffuse à l'incidence normale I_d, du rayonnement solaire total correspondant I. Pour autant qu'il n'est pas possible de faire des mesures séparées de I_d à l'observatoire de Helwan, nous nous sommes servis des données fournies par les communications techniques car, pendant les jours sans nuages, I_d est habituellement petit par rapport à I_D et dépend, en gros, de la masse d'air qui est pénétrée par les rayons solaires;

c) Le rayonnement quotidien total disponible sur des surfaces ayant des orientations diverses (principalement verticales ou inclinées et face au sud). Pour ce faire, nous avons procédé comme suit pour chaque surface :

1) Application de la loi des cosinus à I_D, de manière à obtenir la répartition horaire du rayonnement direct;

2) Évaluation de la répartition horaire correspondante du rayonnement diffus, ainsi qu'il a été fait au paragraphe *b*;

3) Tracé de la répartition horaire totale (direct + diffus) en fonction du temps local moyen;

4) Calcul du rayonnement total quotidien incident sur la surface en cause à partir de la courbe obtenue au point 3.

Des mesures du rayonnement solaire total reçu sur une surface horizontale, sous toutes sortes de conditions météorologiques, ont été notées récemment au poste agro-météorologique de Giza (30° 2′ N-31° 13′ E) avec un actinographe de Robitzsch. Dans l'intérêt des chercheurs qui s'intéressent à l'utilisation de l'énergie solaire, les auteurs ont passé en revue les difficultés auxquelles on se heurte pour obtenir des mesures exactes, et les données enregistrées pendant les trois années de calendrier 1956 à 1958 ont été résumées sous forme de valeurs moyennes quotidiennes sur cinq jours et sur un mois.

ASPECTS OF RADIATION CLIMATOLOGY FOR THE UTILIZATION OF APPLIED SOLAR ENERGY

E. Flach and W. Mörikofer *

The natural sources of caloric radiation on the earth and in the atmosphere

Survey of the different meteorological radiation fluxes

In open air different caloric radiation sources are to be distinguished which partly belong to various spectral regions.

Radiations with spectral qualities of solar radiation (290 mμ-3 000 mμ)

The main source of heat radiation for the earth is the emission of the sun; in practice we have to distinguish three fluxes of solar radiation:

Direct solar radiation (290 mμ-3 000 mμ, including the whole visible spectrum, a weak ultraviolet part, and a large part in the near infrared). This directed solar radiation always appears when the sun is above the horizon and not covered by clouds. Its intensity shows considerable variations in the course of the day and of the year and with varying altitude and latitude. This intensity at normal incidence lies in general between 0.5 and 1.5 gcal/cm² min. In general it can be supposed that the intensity of the radiation of the sun having an elevation of 10° or more above the horizon may be sufficient for a technical utilization.

Diffuse sky radiation (290 mμ-1 000 mμ). By the process of diffusion a part of the solar radiation traversing the atmosphere becomes diffused. This diffusion concerns mainly the short-wave part of the solar radiation, so that the diffuse sky radiation contains mainly the visible and the ultraviolet part of sun radiation. The diffuse sky radiation comes from the whole upper hemisphere. It appears in the daytime, with clear as well as with cloudy sky. The intensity of the energy incoming from the whole upper sky hemisphere on a horizontal surface is smaller than that of the sun; it varies in general between 0.1 and 0.8 gcal/cm² min with a maximum for sky covered with bright clouds and a minimum for dark overcast as well as for cloudless blue sky. In spite of these minor intensities the diffuse sky radiation plays practically the same role in the radiation economy of the earth as the direct solar radiation, because it appears always by day and not only with fine weather.

Reflected solar radiation. The radiation incoming from sun and sky is not absorbed totally, but partly reflected by the ground. This reflected part does not contribute to the heat economy of the earth or of any body struck by the radiation. The absorption depends on the reflecting power (albedo) of the soil or of the other bodies concerned. The absorption can vary from 10 to 40 per cent for snow and water and 50 to 90 per cent for different sorts of soil.

Long-wave temperature radiations (3 000 to 50 000 mμ)

Any body with a temperature different from the absolute zero emits an invisible long-wave radiation the energy of which depends on the absorption and emission power and on the actual temperature of the body's surface. Therefore we have to distinguish in nature three long-wave radiation fluxes:

Outgoing infrared radiation from the surface of the earth and from any body. It varies for different temperatures and ground conditions practically between 0.3 and 1.0 ccal/cm² min and in the spectral region between 3 and 50 μ.

Incoming radiation from the atmosphere, caused by the temperature of atmosphere (4.5 to 7.5 and 12.5 to 50 μ). As the clear atmosphere is transparent for radiation between 7.5 and 12.5 μ, it shows no emission in this spectral region; the total atmospheric radiation is therefore in general smaller than the outgoing terrestrial radiation. These two long-wave radiation fluxes are usually not measured separately, but only their difference. This is called the "effective" or "nocturnal radiation" and shows the profit or loss of the earth by long-wave radiation; it is in general a loss of 0.1 to 0.2 gcal/cm² min.

Reflected long-wave radiation. Theoretically the atmospheric radiation can suffer a reflection at the ground and at any surface. But as the different types of ground and of bodies in general show in this spectral region only a very small reflection power, a very high percentage of the atmospheric radiation is absorbed by the ground surface, so that the reflection of long-wave radiation at the ground and at natural substances can practically be neglected.

Practical aspects for the use of radiation data for the application of solar energy

For the selection of instruments for radiation measurements as well as for the practical interpretation

* Physical-Meteorological Observatory, Davos, Switzerland.

of existing observation data, the following points of view have to be considered:

Direction of the radiation flux

Form, mounting and orientation of the instrument receiver surface depend on the direction of the radiation flux to be measured. For measuring the direct solar radiation, the surface of the receiver has to be mounted perpendicularly to the direction of the incoming beam; in order to avoid diffuse sky radiation from being also covered by the measurement, the receiver surface is enclosed in a tube which allows only the radiation of the sun and of the adjacent circum-solar sky to reach the surface of the receiver.

For measuring the diffuse sky radiation from the whole upper hemisphere, the receiver surface must be mounted horizontally and freely exposed without any tube; the influence of cooling by wind and convection has to be eliminated by a glass hemisphere. The direct solar radiation which would also fall on such a free surface has to be kept away by special designs (i.e., a rotating disc or a fixed ring).

For many problems of pure or applied radiation climatology as well as for many constructions for the utilization of solar energy it is just the knowledge of the combined effects of sun and sky radiation that is wanted; both work together in the same sense and practically in the same spectral region. This sum is called "global radiation". In this case the receiver surface can be exposed without any screen, but of course with a glass hemisphere. In general it is in the horizontal position in order to measure the caloric radiation falling on plane earth or a horizontal surface. Various instruments can be inclined to measure the radiation from sun and sky falling on a slope, an oblique roof or an apparatus for collecting solar energy.

For many purposes it is of interest to measure the radiation falling from all directions on a freely exposed point such as a plant, an upright man, or a building as a whole. For such problems a spherical receiver supplies the requested results with the modification that in this case the measurement gives the sum of the radiation of sun and sky and of its reflection at the ground and the surroundings.

Relation with time

For the judgement of radiation values it is important to consider also the relation with time. There is an important distinction between instantaneous values (intensities), records of the diurnal variations and radiation totals for a given time.

A number of radiation measuring instruments give instantaneous values. For many problems such as heat economy of the ground, biological processes and application of radiation energy, recorded or totalized values are indispensable, because otherwise the irregular variations of incoming radiation caused by cloudiness and turbidity would not be grasped. Recording instruments are much more complicated and expensive than those for instantaneous values, and their supervision and evaluation need a well-trained staff. Some totalizing methods are simpler in this respect.

Spectral region

For many reasons it is important to distinguish between the different spectral regions of radiation, e.g., for effects of ultraviolet radiation or of visible illumination. But for all problems dealing with caloric energy as such, these spectral distinctions are of minor importance; this is the case for all heat effects of radiation and for the application of solar energy. It must, however, be considered that for many bodies the optical qualities of absorptivity and reflectivity are different for solar and for long-wave radiation.

Accuracy of radiation values

The accuracy of the various types of instrument is quite different. But if we admit that for the study of the application of solar energy an inaccuracy of 10 per cent is not prohibitive, all radiation measurements obtained with normal precaution may be of practical value.

The radiation balance of the ground and of any body in open air

The *total radiation balance* of the ground or of any body in open air is represented by the sum respectively of the difference of the six radiation fluxes enumerated above. If

I = direct solar radiation
D = diffuse sky radiation
R = reflected sun and sky radiation
E = terrestrial radiation outgoing from the earth and from any body
A = atmospheric radiation
r = atmospheric radiation reflected at the ground and the surroundings,

the following formulae correspond to the different radiation conditions:

(1) In the daytime with sunshine:

$$Q = I + D - R - E + A - r$$

(2) In the daytime without sunshine:

$$Q = D - R - E + A - r$$

(3) At night:

$$Q = -E + A - r$$

In the daytime the radiation profits prevail in general, while at night the losses dominate.

For the sake of judging the effect of the radiation balance on any construction for collecting solar energy, the short-wave radiation fluxes, i.e., the global radiation of sun and sky minus the radiation reflected from the receiver surface, play a predominant role. The long-wave fluxes should not be dis-

Table 1. Tentative statistics on the existing radiation observations (state 1959)

Continent and region	*Number of stations with radiation measurements*			*PP*
	I	*T h/s*	*SS*	
Africa				
Central Africa	4	64	70?	1
South Africa	2	12	20	1
North Africa (incl. arid zone)	3	10	35	1
America				
Canada	—	17	ca. 100	1
United States	10	90	?	1
Central and South America	1	24?	?	—
Asia (without USSR and China)				
Asia Minor, India, Indonesia, Japan	25	35	?	2
Australia				
Commonwealth	7	7	?	—
Europe				
Central Europe (Austria, Czechoslovakia, Germany, Hungary, Switzerland)	37	102	268	ca. 12
Northern Europe (Denmark, Finland, Norway, Sweden)	7	20	?	—
Western Europe (England, Ireland, Iceland, Netherlands, Belgium, France)	7	14	23?	ca. 6
Southern Europe (Portugal, Spain, Italy, Yugoslavia, Greece)	6	35?	33?	ca. 6
Eastern Europe (USSR, Poland, Romania, Bulgaria)	?	?	?	?
Polar regions				
Arctic and Antarctic	Several stations especially during IGY and IGC 1957/59			

The abbreviations in the columns of table 1 are to be interpreted as follows:
I = Intensity of direct solar radiation at normal incidence
T h/s = Daily and monthly totals of global radiation of sun + sky
h = on a horizontal surface
s = on a spherical surface
SS = Daily and monthly duration of bright sunshine
PP = Number of periodical publications of radiation results in extenso (in annual or monthly bulletins)

regarded, however, because it requires certain precautions to save the energy received as short-wave radiation from being lost in the form of long-wave emission from the receiver surface. This target can best be reached with a receiver surface, the absorptivity of which is high for short-wave and low for long-wave radiation.

The radiation elements of importance for the estimation of applied solar energy

For planning the exploitation of solar energy the planning organization should dispose of some basic information, in order to ensure whether some minimum requirements as to the available radiation energy are fulfilled. In climates where such requirements cannot be guaranteed with sufficient probability, it would not be justifiable to prepare expensive constructions for receiving the solar radiation.

The wish to profit by the results of radiation climatology for this purpose meets with some difficulties:

The various designs for radiation receiver constructions show different form and orientation of the receiver surface; it will be difficult to obtain radiation measurements corresponding to all these possibilities.

In general, only for one or a few of the classical radiation elements observational data are available for the region, but not for all desired possibilities.

Often only instantaneous values are available, while for the practical application, totals of the energy and of its duration would be of interest.

For many regions, and especially in countries where the application of solar energy would prove to be profitable, measurements or records of intensities and totals of solar radiation do not exist; for such regions the knowledge of the duration of sunshine (and under certain conditions even of the mean conditions of cloudiness) would represent a quite useful compensation.

For regions where no numerical knowledge of the radiation quantities or of the elements quoted above exists, the application of some knowledge of radiation

climatology may lead to a certain estimate of conditions.

At a first glance it may seem that the complications enumerated above are a serious impediment to good progress in the field in question. But as the numerical accuracy of the data required for this purpose is not very high, it should be possible to overcome most of these difficulties by close co-operation with the radiation climatologist and a study of the basic laws of this field.

After these introductory remarks, a survey shall be given of the various elements of radiation climatology which may be of interest for the estimation of radiation energy for practical use.

The following suggestions are based in principle on the results of the solar radiation expert group (UNESCO/WMO meeting, Geneva, February 25-27, 1959, UNESCO/NS/AU/424) which had to discuss the scientific aspects of applied solar energy. Various steps of completeness are to be considered.

An ideal program for an exhaustive knowledge of the radiation climate of a place for the purpose of practical application would comprise the following elements:

(1) Monthly means of the daily march of the intensity of direct solar radiation;

(2) Monthly means of the daily march and of the daily totals of the global radiation of sun plus sky on a horizontal plane;

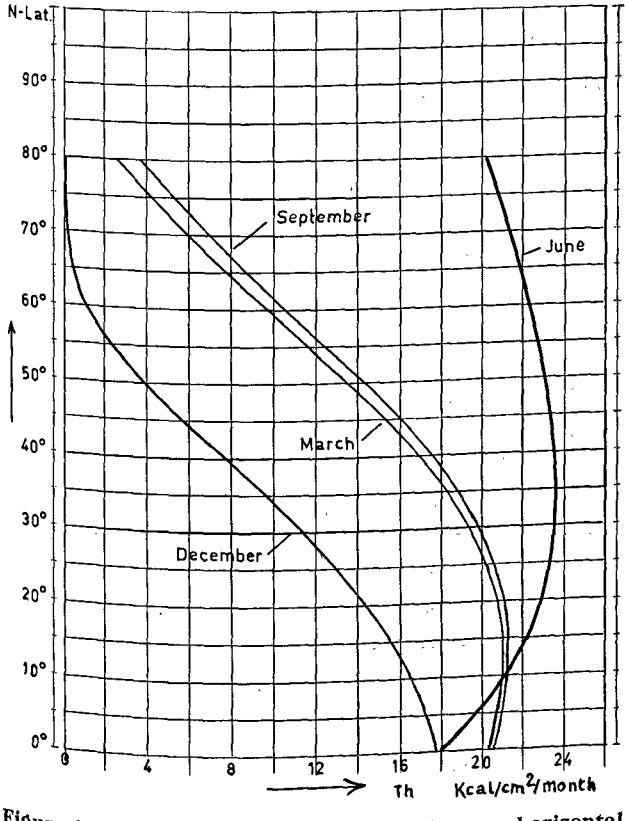


Figure 1. Monthly totals of global radiation on a horizontal surface (Th) for cloudless sky in function of geographical latitude (northern hemisphere), according to M. I. Budyko

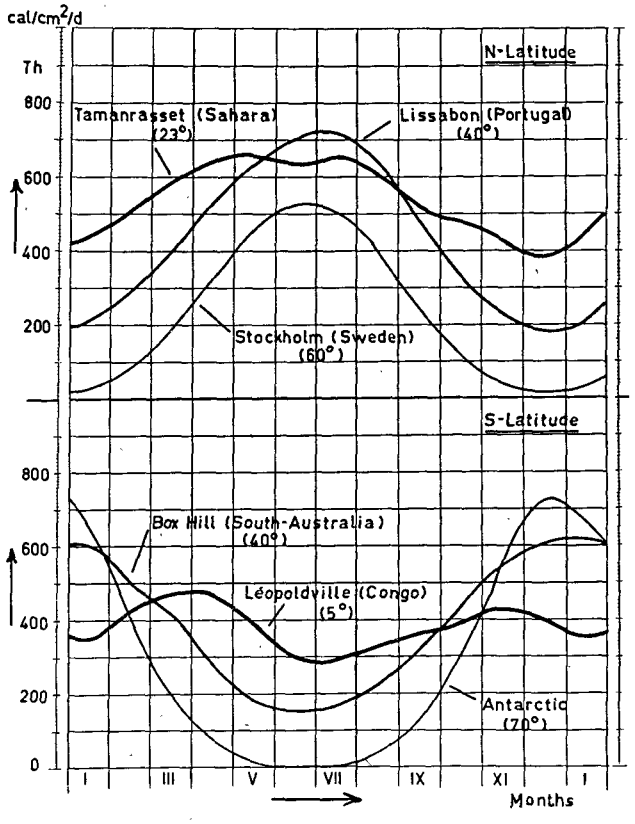


Figure 2. Annual march of the monthly means of daily totals of global radiation on a horizontal surface (Th) under average conditions

(3) Monthly means of the daily march and of the daily totals of diffuse radiation on a horizontal plane;

(4) Daily totals of radiation on a spherical receiver;

(5) Monthly means of the daily march and monthly totals of the duration of bright sunshine;

(6) Statistical data on the frequency of sequences of days reaching certain steps of absolute and relative duration with and without sunshine.

As such an ideal program as given above has only rarely been realized, the following much simpler combinations can be recommended as useful substitutes which give practically sufficient information for technical use:

Reduced but quite difficult program

1. Continuous records of direct solar radiation at normal incidence or on a horizontal plane;

2. Continuous records of diffuse radiation on a horizontal plane.

Simplified program not needing electrical recording instruments

1. Daily totals of solar radiation at normal incidence or on a horizontal plane;

2. Daily totals of diffuse radiation on a horizontal plane;

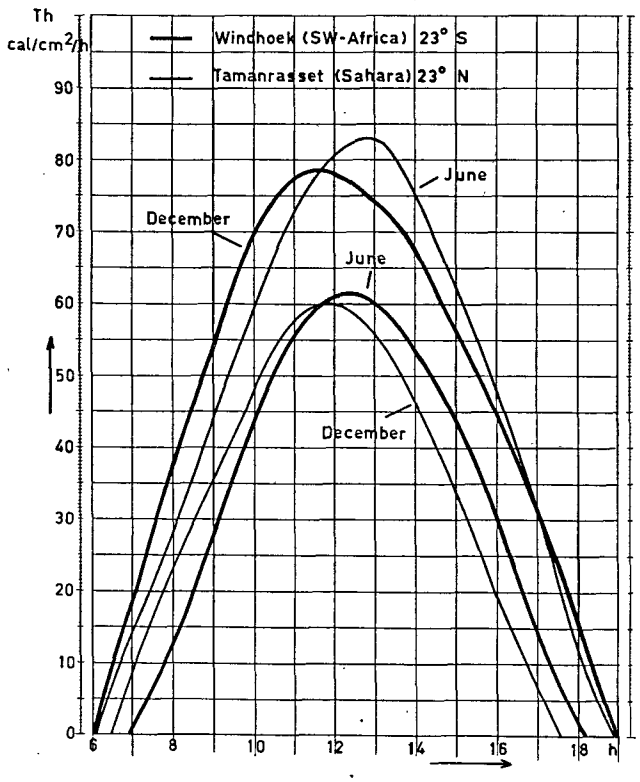


Figure 3. Daily variation of global radiation on a horizontal surface for any weather condition and for two African stations north and south of the Equator

3. Records of duration of sunshine in order to obtain information about the diurnal march of radiation.

The simplest but for most purposes sufficient combination would be represented by

1. Daily totals of incoming radiation from sun and sky totalized by an instrument with a horizontal, tilted or spherical surface;

2. Records of the daily variation of sunshine obtained by a sunshine recorder.

Indications on cloudiness. For regions where data for radiation values and for the duration of sunshine are not available, the following indications on cloudiness, if based on reliable observations, may provide valuable hints on the radiation climate :

1. Mean monthly values of cloudiness, if possible separately for the different parts of the day;

2. Monthly frequency statistics on the occurrence of clear, partly cloudy and overcast days.

Short-wave and long-wave components of the radiation balance. More for basic considerations, but less for application in each country observations of the different short-wave and long-wave components of the radiation balance are of importance for the understanding of the interdependence of incoming short-wave radiation and outgoing long-wave heat losses.

Tentative statistical survey of the data of radiation observations available for the different continents and regions

In order to obtain a scientific basis for the technical application of solar energy, it is of high interest to get sufficient information on the climatological material referring to radiation measurements throughout the world. Table 1 gives a tentative and provisional statistical survey in this sense for the different parts of the earth. This table is primarily based on the results of the inquiry which had been prepared and published in April 1953 by the CIMO (WMO) Working Group on Radiation and has been completed by all further information which has come to our knowledge in the meantime.

According to this tentative statistical table, it may be registered that more than 100 stations make regular measurements of the intensity of direct solar radiation at normal incidence and more than 400 stations are dealing with the total incoming short-wave radiation falling on a horizontal or a spherical surface. The number of stations recording the duration of sunshine may lie between 600 and 1 200.

There is no doubt that because of the widespread co-operation shown during the International Geophysical Year (July 1957 to December 1958, and its extension to 1959), the number of radiation stations

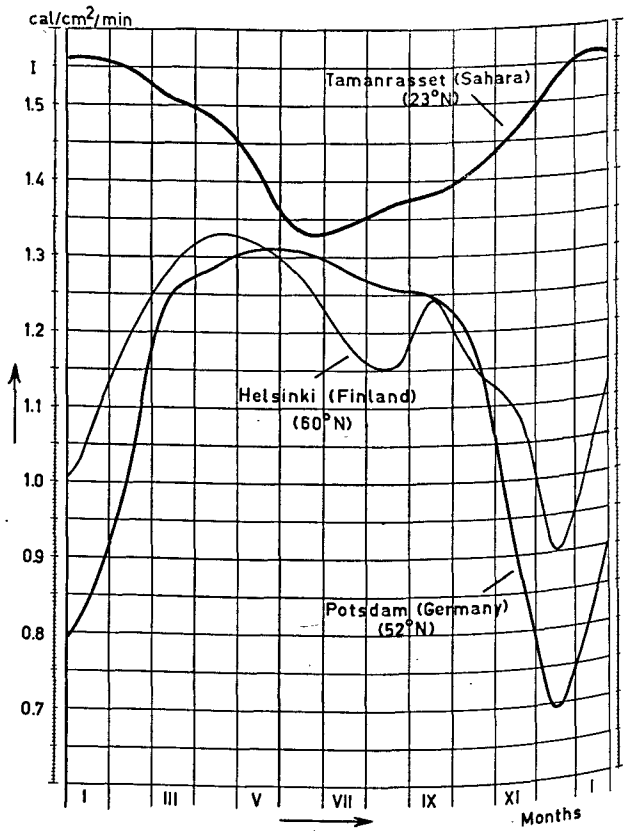


Figure 4. Annual march of the intensity of direct solar radiation (I) at noon (normal incidence)

and the extent of valuable information has been considerably increased. According to the Data Centre of WMO, about 600 stations have undertaken radiation measurements. More exact and detailed information will be available when this material is published by the Data Centre. Some fundamental gaps in table 1 can then perhaps be filled.

The considerable number of radiation stations provides a good perspective for the derivation of a world-wide knowledge of the elements of the radiation climate. It must, however, be considered that not all stations meet the requirements of reliability and comparability of the results. It can, on the other hand, be noted that in the last years some very valuable summarizing publications in this field have appeared.

Some characteristic examples of the results of radiation climatology

Figures 1-6 show some characteristic examples for the annual or the daily variation of the direct solar radiation, the duration of sunshine and the global radiation of sun plus sky in dependence on the geographical situation. All the curves are based on mean values of many years.

The following comments may facilitate the interpretation of the curves.

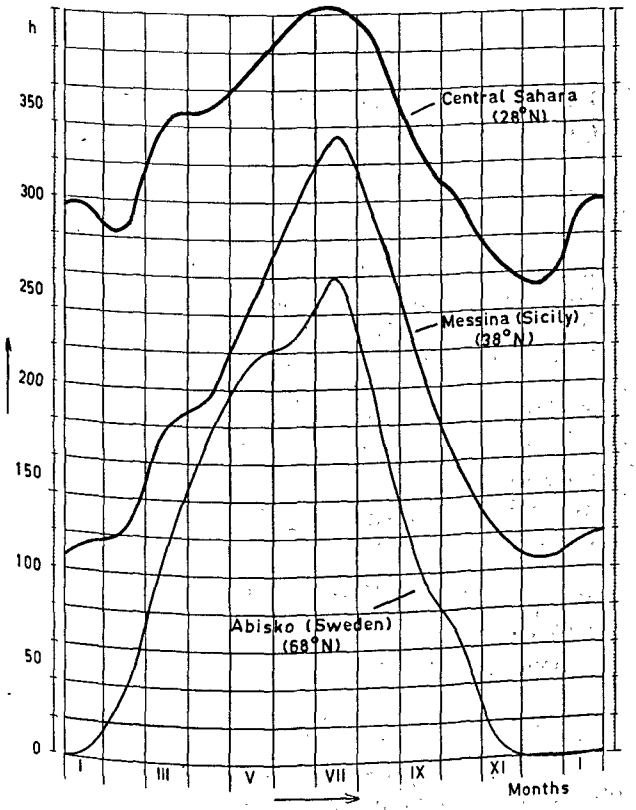


Figure 5. Annual march of the monthly totals of the duration of bright sunshine in hours (h)

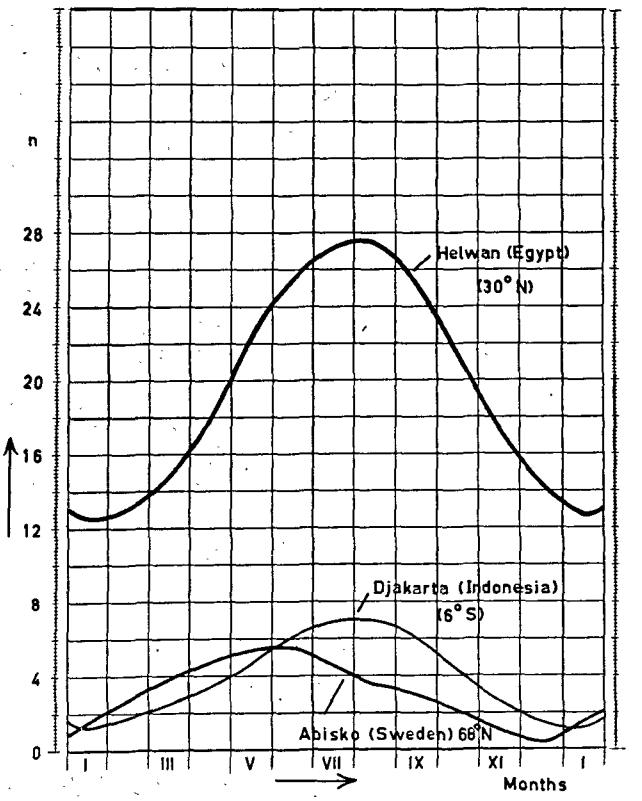


Figure 6. Annual march of the monthly frequency (n) of clear days with 80 per cent possible duration of sunshine

While in summer the quantities of global radiation are quite similar in the various latitudes of the northern hemisphere, the dependence on latitude is very pronounced during the other seasons; the totals diminish then extremely for higher latitudes.

While in tropical and subtropical regions the annual variation of global radiation on a horizontal surface under average conditions of clear, cloudy and overcast weather is not very important, the annual march shows enormous variations for temperate and more polar latitudes, both for the northern and the southern hemisphere.

The daily variation of global radiation on a horizontal surface (for average weather conditions) is very pronounced both for an African station south and north of the equator as well as for the months with minimum and maximum solar elevation.

The annual march of the intensity of direct solar radiation at noon (for cloudless sky) is not very pronounced in the subtropical arid zone compared with the diminution during the winter period in middle and high latitudes.

The annual variation of bright sunshine shows an enormous amplitude in middle and high latitudes while the subtropical arid zone is characterized by favourable conditions of the duration of sunshine also during the winter period.

For regions where observations of radiation and duration of sunshine are missing, observations of cloudiness may offer a certain compensation for information. From a basic study can be concluded that on average days where the clouds have never covered more than half the sky the effective duration of sunshine has been 80 per cent of the possible value. In this sense figure 6, which is based on observations of cloudiness exclusively, gives a good idea of the abundance of sunshine in the desert region in comparison with polar and wet tropical seasons respectively.

Summary

THE NATURAL SOURCES OF CALORIC RADIATION AT THE EARTH AND IN THE ATMOSPHERE

Survey of the six different short-wave and long-wave radiation fluxes incoming or outgoing from sun, sky, atmosphere and ground.

Practical aspects for the use of radiation data for the application of solar energy:

1. Direction of the radiation flux;
2. Relation with time;
3. Spectral region;
4. Accuracy of radiation values.

The radiation balance of the ground and of any body in open air and its components.

The radiation elements of importance for the estimation of applied solar energy. After a discussion of the various difficulties to obtain the necessary practical information from radiation climatology, different possibilities are developed which meet the practical requirements; they extend from an ideal programme for radiation investigations to some reduced combinations which may be useful for most practical purposes.

TENTATIVE STATISTICAL SURVEY OF THE DATA OF RADIATION OBSERVATIONS

According to table 1 observational results may be supposed to be available from the following radiation stations:

For direct solar radiation . . . more than 100
For global short-wave radiation more than 400
For duration of sunshine . . 600 to 1 200

SOME CHARACTERISTIC EXAMPLES

Figures 1-6 show the annual or the daily variation of the direct solar radiation, the global radiation of sun and sky, and the duration of sunshine depending on the geographical situation.

ASPECTS DE LA CLIMATOLOGIE DU RAYONNEMENT POUR L'APPLICATION DE L'ÉNERGIE SOLAIRE

Résumé

LES SOURCES NATURELLES DU RAYONNEMENT CALORIFIQUE A LA TERRE ET DANS L'ATMOSPHÈRE

Aperçu des six différents flux, de courte et de grande longueur d'onde, émis ou incidents, du soleil, du ciel, de l'atmosphère et du sol.

Aspects pratiques de l'emploi des données du rayonnement en vue de l'utilisation de l'énergie solaire :

a) Direction du flux du rayonnement,
b) Relation temporelle,
c) Région spectrale,
d) Précision des valeurs du rayonnement.

Le bilan radiatif du sol et d'un corps quelconque en plein air et les composantes de ce bilan.

Les éléments du rayonnement ayant de l'importance pour l'estimation de l'énergie solaire exploitable. Après avoir discuté des différentes difficultés pour obtenir les informations pratiques nécessaires à partir de la climatologie du rayonnement, les diverses possibilités sont exposées qui correspondent aux exigences pratiques; elles s'étendent d'un programme idéal pour des recherches du rayonnement jusqu'à quelques combinaisons réduites qui peuvent toutefois être suffisantes pour la plupart des besoins pratiques.

ESSAI D'UN APERÇU STATISTIQUE SUR LES DONNÉES DES OBSERVATIONS DU RAYONNEMENT

Suivant le tableau 1, il semble qu'on puisse s'appuyer sur les résultats d'observation des stations suivantes du rayonnement :

Pour le rayonnement solaire direct plus de 100
pour le rayonnement global à ondes courtes . . . . . plus de 400
pour la durée d'insolation . . entre 600 et 1 200

QUELQUES EXEMPLES CARACTÉRISTIQUES

Les figures 1 à 6 montrent la variation annuelle ou diurne du rayonnement solaire direct, du rayonnement global du soleil et du ciel et de la durée d'insolation, qui dépend de la situation géographique.

DISPOSITIFS DE MESURE DU COEFFICIENT DE RAYONNEMENT NOCTURNE DE MATÉRIAUX DIVERS, DANS LEURS CONDITIONS LOCALES D'EMPLOI

M. Gondet *

Si les mesures de rayonnement solaire, notamment dans les zones arides, sont relativement faciles à effectuer avec un appareillage standard, sous réserve de modifications de détail tenant compte des conditions locales d'utilisation, la mesure du coefficient de rayonnement nocturne de matériaux divers ne semble pas avoir donné lieu à des recherches systématiques effectuées au moyen d'un appareillage permettant une étude de longue durée.

Cependant cette mesure du nombre de calories perdues par rayonnement pendant la nuit, à différentes époques de l'année, est extrêmement intéressante si l'on veut réaliser par des moyens aussi simples que possible, avec le minimum d'apport d'énergie électrique ou autre, des conditions de climatisation convenable des habitations dans les régions désertiques et chaudes.

C'est dans ce but que le dispositif décrit ci-dessous a été étudié et réalisé.

Principe de la mesure

Le dispositif faisant l'objet de ce mémoire a été mis au point en partant des travaux déjà anciens d'Ångström et de Boutaric. Bien d'autres études ont été reprises depuis par des chercheurs de divers pays, toutes basées sur le même principe, mais d'une réalisation plus ou moins compliquée.

En principe, on maintient à la même température, celle de l'air ambiant, deux plaques dont l'une est réfléchissante pour une large bande de fréquences dans le visible et l'infrarouge et qui, de ce fait, se maintient automatiquement à la température ambiante, et dont l'autre, recouverte du matériau en essai (noir de fumée, sable, poudres diverses), tend à se refroidir en émettant un rayonnement global qui dépend à la fois de la nature du corps et des conditions atmosphériques, notamment de l'humidité de l'air.

Un apport convenable de calories sous forme d'énergie électrique maintient automatiquement cette plaque émettrice à la température de la plaque réfléchissante.

L'énergie perdue en calories par unité de temps et unité de surface, ou en watts par unité de surface, résulte de la différence entre l'énergie rayonnée par le matériau et celle qu'il reçoit de l'atmosphère.

Les valeurs des différents paramètres (température, degré hygrométrique, énergie rayonnée mesurée en watts) sont inscrites sur un enregistreur par points.

Pratiquement, les plaques utilisées ont des surfaces de 40 × 40 cm de côté, ce qui permet de dissiper un nombre de watts de l'ordre d'une vingtaine.

Sous chacune des plaques, l'une réfléchissante, l'autre émettrice, s'en trouve une autre en cuivre rouge, l'ensemble reposant dans une boîte plate formée d'une matière légère et très peu conductrice de chaleur, en l'espèce des panneaux de klegecel d'une épaisseur de 40 mm.

Entre les plaques de chacun des deux groupes se trouvent logées des résistances de mesure constituées par du fil fin de nickel, bobiné en grecque, réalisant un ensemble très plat genre stain-gages d'environ 800 ohms de résistance.

Enfin, sous la plaque émettrice se trouve logé, couvrant toute sa surface, un élément résistant de chauffage dans lequel on peut faire passer une intensité de courant de 2 ampères sous 24 volts, la durée du passage de ce courant étant enregistrée par un dispositif décrit ci-dessous.

Montage électrique

Les deux résistances de mesures placées l'une sous la plaque émettrice, l'autre sous la plaque réfléchissante, forment les deux bras d'un pont de Wheastone fermé sur deux résistances en manganine, l'ensemble étant alimenté sous une tension de 4 volts.

Le déséquilibre du pont, qui se produit pour une variation de température bien inférieure à 1/10 de degré, provoque le fonctionnement d'un relais galvanométrique optique placé dans la diagonale du pont, commandant l'envoi du courant dans la résistance de réchauffage par l'intermédiaire d'un relais auxiliaire.

Un second contact du même relais électromagnétique actionne le dispositif d'enregistrement combiné comme suit. La résistance de chauffage, en constantan, fonctionnant à intensité constante, le nombre de watts dissipés en moyenne dans un intervalle de temps connu et constant, par exemple 15 minutes, se détermine facilement en totalisant les temps effectifs de passage du courant pendant cet intervalle de temps pris comme base.

* Section de physique du Centre de recherches sahariennes, Beni-Abbès, Algérie.

Dans ce but, un petit moteur fonctionnant en synchronisme avec celui de l'enregistreur à plume peut entraîner par l'intermédiaire d'un réducteur de vitesse le curseur d'un potentiomètre circulaire, en lui faisant effectuer un tour en 15 minutes. Mais ce moteur ne fonctionne que pendant les temps de passage du courant dans les résistances de chauffage.

De plus, entre l'arbre de sortie à faible vitesse et l'axe du potentiomètre est intercalé un embrayage à friction de faibles dimensions qui se trouve normalement au collage, mais décolle pendant un temps très court de l'ordre de 5 secondes au bout de 15 minutes. Pendant cette durée du décollage provoqué par l'enregistreur grâce à un relais, le curseur du potentiomètre est ramené au zéro par un ressort spiral.

Une légère modification de l'enregistreur à plume utilisé pour les trois enregistrements (température, degré hygrométrique, watts dissipés) permet de ramener le potentiomètre au zéro toutes les 15 minutes à un moment où la plume de l'enregistreur n'est pas appliquée sur le papier d'enregistrement.

Connaissant la tension totale, constante, d'alimentation du potentiomètre (4 volts) et la tension maximum correspondant à la position du curseur du potentiomètre au bout des 15 minutes (tension enregistrée par points toutes les 60 secondes), on en déduit par un simple rapport de ces tensions, provenant des temps de fonctionnement, la valeur moyenne du nombre de watts dissipés pendant 15 minutes.

Il est à remarquer que la constante de la vitesse du moteur d'entraînement du potentiomètre n'est pas impérative. Il suffit de réaliser un synchronisme avec le moteur de l'enregistreur et de maintenir constante la tension du courant de chauffage de la plaque rayonnante.

L'énergie dissipée en moyenne pendant une durée fixée par avance est un des trois paramètres normalement enregistrés. Les deux autres se rapportent à la température ambiante et à l'humidité relative de l'atmosphère au voisinage du sol. Connaissant l'humidité relative et la température de l'air grâce à un psychromètre, on en déduit la tension de la vapeur d'eau, ce qui permet de déterminer l'influence de ce facteur sur le rayonnement net du matériau en essai.

Dans le dernier modèle, le réchauffage de la plaque émettrice peut être supprimé pendant un intervalle de temps défini par avance, ce qui permet d'enregistrer la chute de température de cette plaque par émission de rayonnement; ceci n'est, d'ailleurs, valable qu'à condition de ne pas descendre en dessous du point de rosée.

Cette méthode n'est donc applicable que dans les régions et aux époques où l'humidité relative n'est pas trop importante.

Les premiers essais, effectués au Sahara dans la vallée de la Saoura, au mois d'avril, ont montré que même par ciel clair et vent nul ou très faible, le rayonnement global pour une plaque corps noir n'était en moyenne que le tiers du rayonnement théorique; et ceci en dépit de la faible humidité relative (25 p. 100 à 18 °C).

Compléments particuliers des dispositifs de mesure du rayonnement nocturne et diurne

L'équipement est complété par un psychromètre enregistreur à deux thermomètres, l'un sec, l'autre humide, dont les caractéristiques consistent dans une bonne protection des thermomètres contre le rayonnement et dans une alimentation en eau très soignée du thermomètre mouillé.

Ces deux thermomètres sont constitués par deux résistances de 100 ohms en fil de platine enroulé sur un petit cylindre de pyrex. Un ventilateur assure une vitesse convenable d'aspiration de l'air.

L'humidification du thermomètre mouillé est produite par une mousseline trempant dans l'eau distillée enroulée autour du cylindre supportant le fil de platine.

Le montage électrique a comme principe la comparaison des deux résistances thermométriques par rapport à une résistance étalon, au moyen d'un montage logométrique.

Les valeurs des températures des thermomètres sec et humide sont enregistrées par points toutes les 30 secondes.

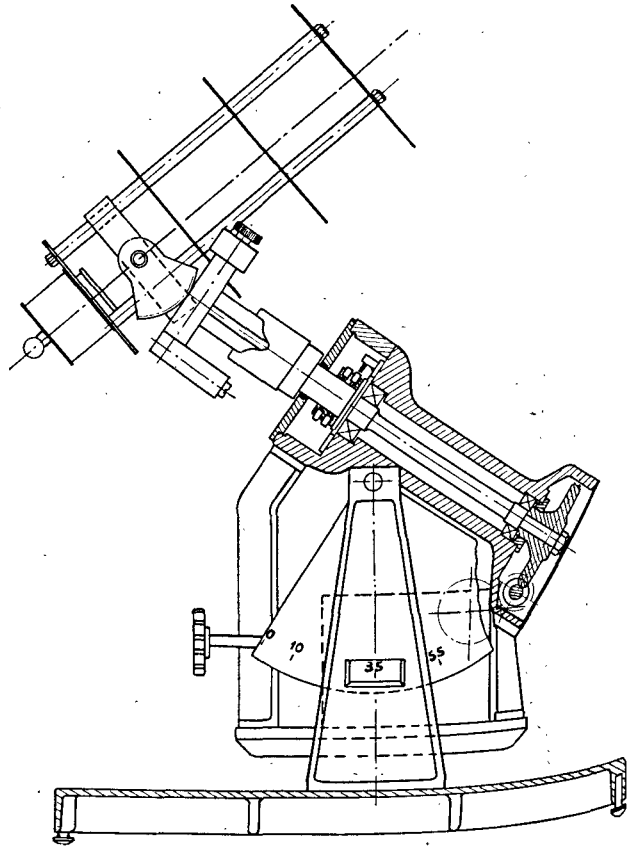


Figure 1. Monture équatoriale de pyrhéliomètre

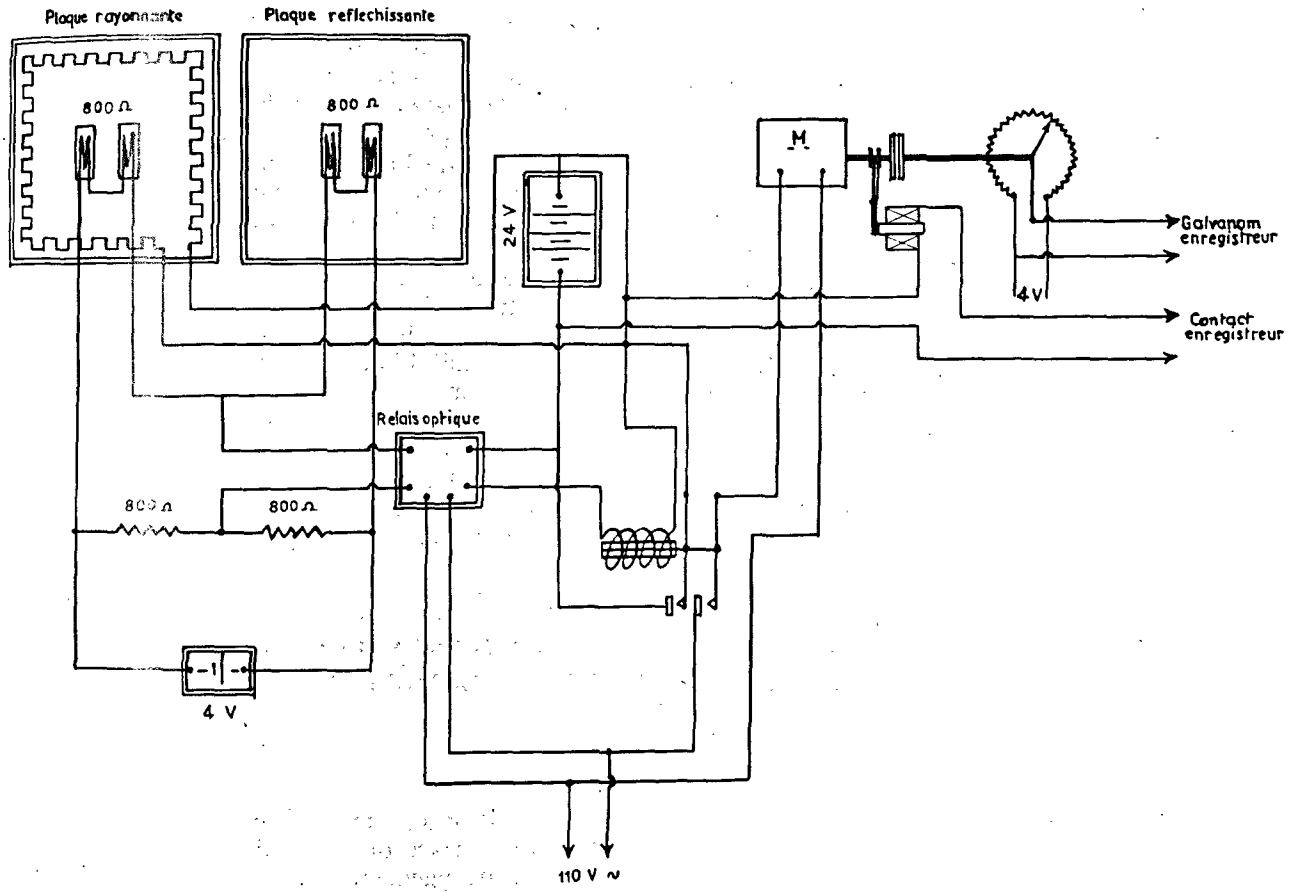


Figure 2. Schéma de montage du dispositif de mesure du coefficient de rayonnement nocturne

L'appareillage de mesure du rayonnement solaire comprend en plus des solarimètres d'un type standard, un pyrhéliomètre dont le statif a été étudié spécialement pour assurer à l'instrument une très bonne stabilité ainsi qu'une protection efficace envers les intempéries, et notamment le vent et la poussière de sable.

Dans ce but, on a repris une monture équatoriale rigide dont l'entraînement peut être commandé soit par un moteur synchrone, lorsque l'on dispose d'un secteur électrique stable, soit d'un mouvement d'horlogerie insensible aux variations de température.

Un réducteur de vitesse convenable impose finalement à l'arbre de la monture équatoriale une vitesse de rotation de un tour par 24 heures.

L'ensemble moteur-arbre principal est monté dans un berceau susceptible de tourner autour d'un axe horizontal permettant l'emploi de l'appareil sous diverses latitudes. Un repère angulaire sur un secteur de grand rayon et une fixation par pince assurent une fixité parfaite de la direction de l'axe du monde.

L'extrémité supérieure de l'arbre porte une fourche réglable en rotation et bloquable, autour de l'axe principal.

Cette fourche sert de support à l'élément détecteur, une pile thermo-électrique en l'occurence, dont la position est réglable par secteur denté et vis tangente autour d'un axe horizontal.

Enfin, les fils de connexion de la thermopile passent dans l'axe de la partie supérieure de l'arbre et sont connectés à deux bagues sur lesquelles s'appliquent deux balais souples assurant la prise de la force électromotrice du détecteur vers un appareil de mesure.

La fourche supérieure, largement dimensionnée, permet de recevoir des détecteurs de types très variés.

Résumé

L'ensemble de l'équipement conduisant à la mesure du coefficient de rayonnement nocturne de matériaux divers dans leurs conditions locales d'emploi comprend : un appareillage de mesure de l'énergie calorifique dissipée sur une plaque de 40 × 40 cm, la mesure de la température de l'air ambiant et celle de l'humidité relative.

Les différentes courbes, au nombre de quatre (nombre de calories dissipées, température sèche, température humide et chute de température de la

plaque rayonnante lorsqu'elle n'est pas réchauffée) sont inscrites sur le même enregistreur par points.

Le système de mesure de l'énergie rayonnée se compose de deux plaques de 40 × 40 cm, l'une réfléchissante dans le spectre visible et l'infrarouge, l'autre constituée par le matériau en poudre en essai.

La chute de température que présenterait la plaque rayonnante est décelée au moyen d'un montage en pont de Wheatstone dont les deux résistances actives en fil de nickel sont placées l'une sous la plaque réfléchissante, l'autre sous la plaque rayonnante. Le déséquilibre résultant d'une baisse de température de 1/10 de degré provoque le fonctionnement d'un relais galvanométrique optique qui actionne un relais auxiliaire assurant l'alimentation en courant électrique d'une résistance chauffante placée sous presque la totalité de la surface de la plaque rayonnante. Un montage électrique spécial permet la mesure de l'énergie électrique dissipée pendant un temps connu pour maintenir la plaque rayonnante à la même température que celle de la plaque réfléchissante, d'où le nombre de calories dissipées par rayonnement.

L'ensemble de l'installation est complété par un psychromètre enregistreur comprenant deux thermomètres constitués par deux résistances en fil de platine. L'une reste sèche, l'autre est continuellement humidifiée par une mousseline trempant dans de l'eau distillée. Un montage logométrique permet l'enregistrement des températures sèche et humide d'où l'on déduit l'humidité relative et la teneur en eau de l'air ambiant.

Enfin, pour la mesure du rayonnement solaire, on utilise en plus de solarimètres d'un type classique, un pyrhéliomètre à monture équatoriale spécialement étudié pour assurer une très bonne stabilité ainsi qu'une protection efficace contre la poussière de sable.

DEVICES FOR MEASURING THE COEFFICIENT OF NOCTURNAL RADIATION OF VARIOUS MATERIALS UNDER LOCAL CONDITIONS OF USE

Summary

The equipment used for measuring the coefficient of nocturnal radiation of various materials under local conditions of use consists of apparatus to measure the thermal energy dissipated by a plate 40 × 40 cm, to measure the atmospheric temperature, and to measure the relative humidity.

The same recording instrument draws the points for four curves: number of calories dissipated, dry temperature, wet temperature, and temperature drop of the radiating plate when it is no longer heated.

The system for measuring the energy radiated consists of two plates, each 40 × 40 cm, one of them reflecting in the visible and infrared regions, the other composed of the powdered test material.

The temperature drop of the radiating plate is found by means of a Wheatstone bridge circuit whose two nickel-wire resistances are placed under the reflecting plate and the radiating plate, respectively. The unbalance resulting from a temperature fall of 1/10°C operates an optical galvanometer relay, which, in turn, operates an auxiliary relay feeding a heater resistor occupying almost the entire space under the surface of the radiating plate. A special electrical arrangement is used to measure the electrical energy dissipated in known time to hold the radiating plate at the same temperature as the reflecting plate, thus giving the number of calories dissipated by radiation.

The measuring equipment is completed by a recording psychrometer consisting of two thermometers, in the form of two platinum-wire resistors. One of them remains dry, while the other is continuously moistened by a piece of muslin soaked with distilled water. A logometric mounting permits the recording of the dry and wet temperatures, from which the relative humidity and the moisture content of the atmosphere are calculated.

Finally, the solar radiation is measured by conventional solarimeters and, in addition, by a pyrheliometer in a specially designed equatorial mounting to ensure very high stability and provide efficient protection against sand dust.

MEASUREMENTS OF TOTAL RADIATION IN NETWORKS

Kurt Gräfe *

General remarks

Solar energy has been used for various purposes, but up to now engineers have not been very interested in radiation data. They regarded the sun merely as a source of energy, without knowing the amount of radiation received at the earth's surface. In recent years, however, it has become clear that the efficiency of apparatus used at present can be improved by considering the radiation data. In discussing the application of solar energy, the knowledge of the direct solar radiation will not be sufficient; it will also be necessary to get information on the diffuse component as well. Therefore in this paper we shall deal with the total (shortwave) radiation of sun and sky which reaches the ground.

* Untersuchungsanstalt—im Hygienischen Institut der Hansestadt Hamburg, Germany.

Instrumental questions

Suggestions for the instrumentation

In measuring the total radiation of sun and sky, several instruments are being used (1, 2, 3). These pyranometers should meet the following demands: (*a*) robustness in design, (*b*) resistance against the corrosive action of damp air (for details see 4), (*c*) efficiency with plane and horizontal surface, (*d*) inclusion of angle of incidence : 2 π, (*e*) ability to follow the Cosine-law, (*f*) reliability, and (*g*) simplicity,

Table 1

Date	July 1955			December 1955		
	Sol.	Rob.	Rob. / Sol.	Sol.	Rob.	Rob. / Sol.
	cal/cm² d			cal/cm² d		
1	467	447	.96	25	31	1.24
2	463	465	1.00	37	44	1.19
3	627	632	1.01	7	6	.86
4	170	169	.99	62	66	1.06
5	89	92	1.03	33	38	1.15
6	362	352	.97	9	9	1.00
7	489	474	.97	8	6	.75
8	571	573	1.00	66	63	.96
9	702	710	1.01	22	28	1.27
10	577	589	1.02	16	16	1.00
11	497	500	1.01	104	95	.91
12	581	572	.98	65	60	.92
13	590	559	1.06	35	38	1.09
14	583	583	1.00	21	25	1.19
15	595	611	1.03	14	13	.93
16	578	580	1.00	12	13	1.08
17	584	622	.94	18	19	1.05
18	425	410	.96	48	51	1.06
19	375	349	.93	66	69	1.05
20	528	528	1.00	37	35	.95
21	596	598	1.00	14	16	1.14
22	624	595	.95	80	69	.86
23	444	416	.94	23	25	1.09
24	479	519	1.08	16	19	1.19
25	427	469	1.10	17	19	1.12
26	514	524	1.02	6	6	1.00
27	344	328	.95	36	35	.97
28	402	389	.97	6	6	1.00
29	416	413	.99	44	44	1.00
30	287	282	.98	50	47	.94
31	416	430	1.03	23	22	.96

Table 2

1955	Solarimeter Robitzsch		Rob.
	cal cm^{-2} d^{-1}		Sol.
January	54	54	1.00
February	131	130	0.99
March	213	213	1.00
April	309	309	1.00
May	392	401	1.02
June	392	396	1.01
July	478	480	1.00
August	393	395	1.00
September	258	265	1.03
October	123	126	1.03
November	73	74	1.01
December	33	33	1.00
MEAN	240	242	1.008

i.e., able to be used by unskilled operators, for networks.

In order to satisfy the above demands, it would be necessary to make a compromise because the pyranometers with the highest reliability need electric current. It is, therefore, suggested that Robitzsch bimetallic actinographs be distributed in large numbers since they do not require electric current; at the same time electrical pyranometers should be operated at selected stations only. These stations are meant to be "radiation-centres" of particular areas. The electrical pyranograph may not only be used for continuous records, but also for standardizing the actinographs by comparison under natural conditions of exposure.

Among several electrical pyranometers, in accordance with several authors (4), and on the basis of our experiences (3, 5), the Moll-Gorcynski solarimeter has been recommended. The solarimeter has proved satisfactory for the purposes mentioned above and, if operated with an electrical recorder, instantaneous values are available. These data are reliable and valuable for special questions.

THE RELIABILITY OF ROBITZSCH BIMETALLIC ACTINOGRAPHS

It is not our aim to repeat the numerous publications[1] about actinographs, and as we have no experience with the different models, the following details about the bimetallic actinograph should be regarded only as a small contribution to this subject (6). It has to be stressed that we evaluated only daily sums of the actinograph-records. Without repeating the criticisms about the actinograph concerning its sensitivity to temperature, solar altitude, azimuth etc., and without mentioning our numerous tests on the calibration factor,[2] it will be discussed which calibration factors we used and how reliable this simple method was.

We standardized the Robitzsch bimetallic actinograph[3] as mentioned above and determined calibration factors which varied only with the size of the recorded area of the radiation curve, receiving, e.g., the factor 0.63 between 0 and 350 mm^2, 0.66 between 350 and 500 mm^2, 0.67 between 500 and 700 mm^2, and 0.67 above 700 mm.[2] Contrary to these results in moderate climate, it is supposed that the calibration factor may be uniform in areas with a large amount of daily radiation.

In order to test the accuracy, the daily sums of the total radiation measured with the Robitzsch actinograph were compared with those measured with the Moll-Gorczynski solarimeter at the same place in 1955. As an example, the results of July and December are given in table 1 of the annex. In table 2 the monthly means are stated; the annual means of actinograph and solarimeter measurements differ by only 0.8 per cent. The frequency of the ratios $G_{Rob.}/G_{Sol.}$[4] is illustrated in figure 1 for all days of one year. Figure 2 shows the corresponding diagrams for July and December 1955. In July the deviation was never larger than ± 10 per cent. On the contrary, in December where the total radiation is small, the distribution of the frequencies is very broad. The investigation shows that

80 per cent of the results of 1955 have a deviation of ± 5.8 per cent,
80 per cent of the results of July 1955 have a deviation of ± 5 per cent, and
80 per cent of the results of December 1955 have a deviation of ± 15 per cent.[5]

[1] Some publications are quoted in references 1, 2, 3 and 4.

[2] Author's investigations during his membership at the Meteorological Observatory of the German Weather Service.

[3] Manufacturer: Fuess, Berlin-Steglitz.

[4] $G_{Rob.}$ = daily sum of total radiation measured with Robitzsch actinograph
$G_{Sol.}$ = daily sum of total radiation measured with solarimeter.

[5] A. I. Drummond, Newport, R.I., stated at the International Radiation Conference in Davos in Sept. 1956 that — considering the lower radiation income in north Germany — these results

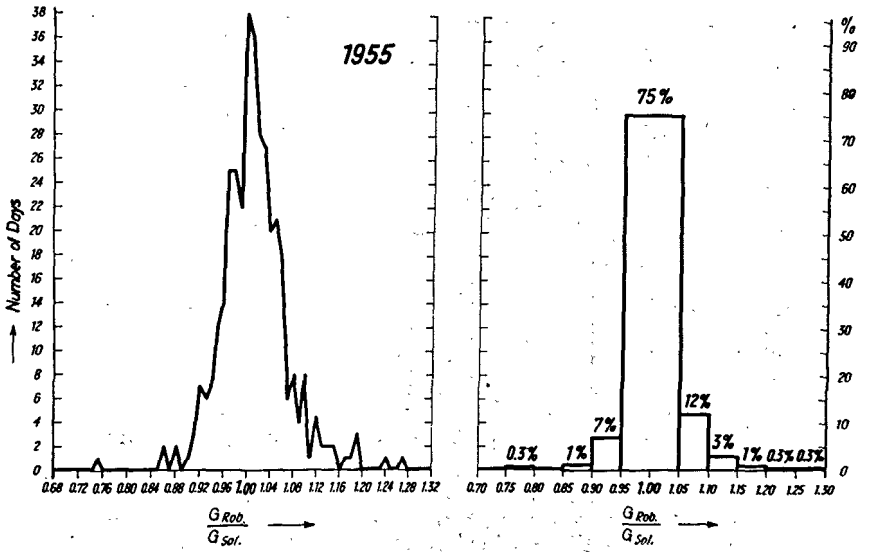


Figure 1. Absolute and relative frequency of the ratios $G_{Rob.}/G_{Sol.}$ of the year 1955

As the calibration factors were carefully determined, the deviations spring from the differences of the electrical and the mechanical systems, especially from the lag in the indication of the actinograph. The better accuracy of the July values compared with the December data is caused by the larger amount of radiation in summer. We may therefore be allowed to form the conclusion that the actinograph will be sufficiently reliable in areas with a large amount of radiation, and only these are of interest for solar energy utilization.

Some results of special measurements

As seen above, it was suggested setting up in each particular area at least one selected station with electrical pyranometers. If skilled operators are available, electrical pyranometers should be used to get special information which will be valuable for solar energy utilisation. Such information, obtained in Hamburg by means of Moll-Gorczinsky solarimeters and Hartmann & Braun recorders, will be demonstrated in the following sub-paragraphs.

Total radiation received by surfaces other than horizontal

Solarimeters were exposed on surfaces other than horizontal to different directions of the sky in order to measure the direct solar radiation (S) *together* with the diffuse radiation from both sky (DS) and ground (DG) continuously (7). Only two of the expositions published in (8) show the value of these records. The daily sums of the records from 1952 to 1954 were compared with the corresponding theoretical maxima of the direct solar radiation (curve 1 in figures 3 and 4) according to Kaempfert and Morgen

agree with his measurements in Pretoria; he observed a deviation of about ± 2 per cent on clear days and of about ± 5 per cent on days with changing clouds.

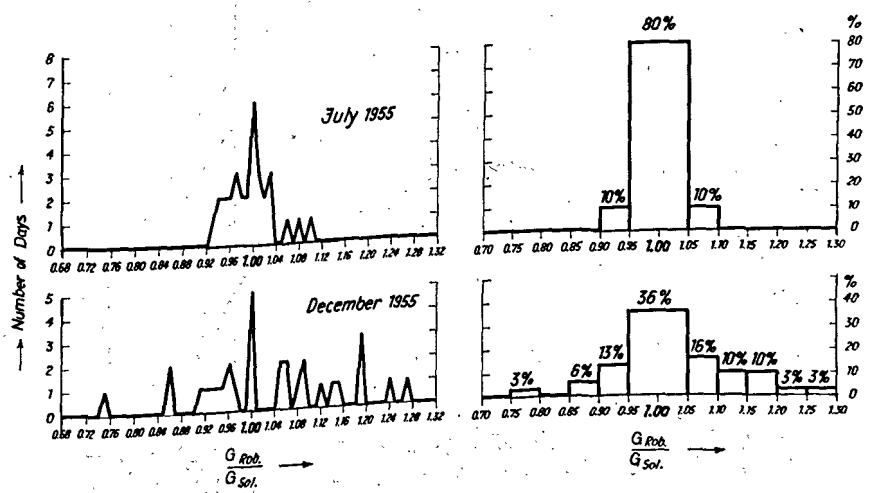


Figure 2. Absolute and relative frequency of the ratios $G_{Rob.}/G_{Sol.}$ of July 1955 and December 1955

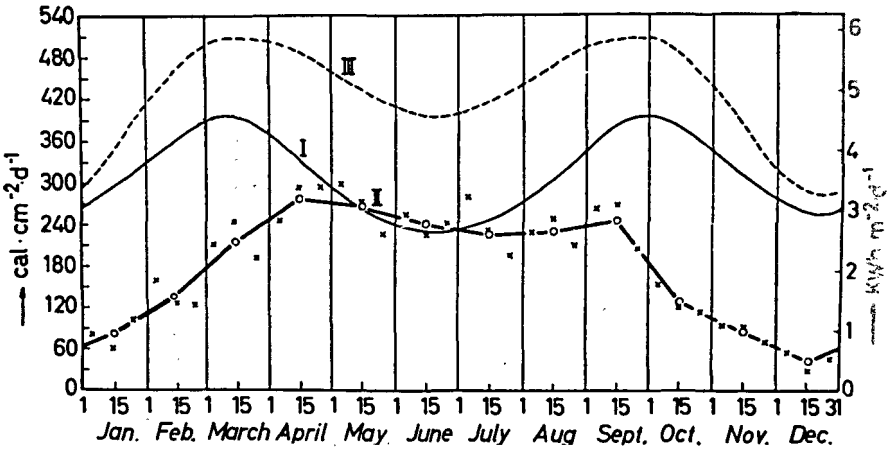


Figure 3. Total radiation received by a vertical surface exposed to the *south* (VS). Curve I : Theoretical maxima of the direct solar radiation (S); curve II : Annual course of the direct solar radiation (S) *together* with the diffuse radiation from both sky (DS) and ground (DG) obtained from monthly (O) means from 1952-1954, means of ten days (X) obtained from the daily radiation of S + DS + DG measured from 1952-1954; curve III : practical maxima of S + DS + DG obtained by circumscribing the maxima from 1952-1954

(9), in order to illustrate by daily sums [6] and means (curve 2 in figures 3 and 4) the energetic contribution of the diffuse radiation.

First is discussed the total radiation received by a vertical surface exposed to the south. The summarized results of the measurements are given in figure 3. The theoretical maxima [7] of the direct solar radiation in Hamburg are lower in summer than in winter. The reason is that the sun reaches its highest point during the winter solstice at an altitude of 13°, whereas during the summer solstice it reaches its highest point at an altitude of 60°. This deficiency in summer is partially compensated for by the double length of the day since the sun reaches the southern wall only when it is in the south of the east-west line. Thus we see, when comparing curves 1 and 3 in figure 3, that the southern wall has a relatively large increase of energy by the diffuse radiation from both sky and ground in summer and a small increase in winter. This is due to the high sun's altitude as well as the shorter length of the day. The means of ten days and the monthly means (curve 2) of S + DS + DG are in general considerably below the theoretical curve 1, because curve 2 contains cloudy as well as overcast days.

Figure 4 gives the corresponding results for a surface with an inclination of 45° to the south; the respective numbers of the curves 1, 2, and 3 correspond with the numbers 1, 2 and 3 in figure 3. The annual course of S + DS + DG (curve 2), which has been obtained from monthly means as well as

[6] The daily sums are not entered here as in (8), but curve 3 in the figures 3 and 4 circumscribes the measured maxima of S + DS + DG.

[7] Theoretical because a cloudless condition was assumed.

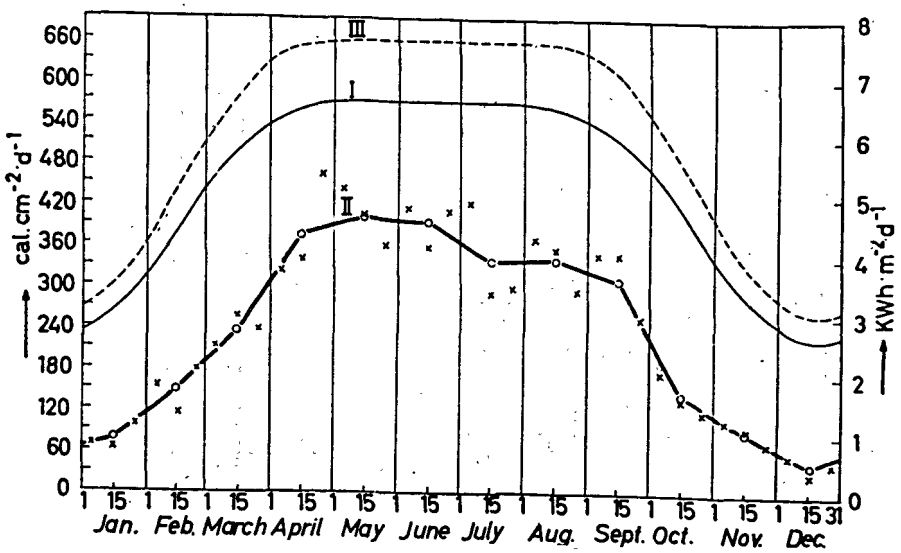


Figure 4. Total radiation received by a surface with an inclination of 45° to the *south* (45°S). Details analogue to figure 3

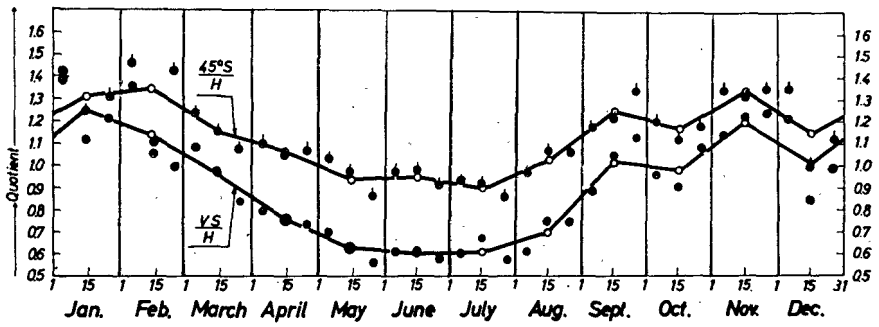


Figure 5. Annual course of VS/H[8] and 45°/H[8] obtained from monthly (O) means. Means of ten days of VS/H (●) and of 45°/H (●)

the means of ten days, never reach the theoretical maxima (curve 1) of the solar radiation because of the inclusion (in curve 2) of cloudy and overcast days. The daily sums, however, may be greater than curve 1 (as illustrated in curve 3), which is 16 per cent greater than the direct solar radiation.

Finally, the total radiation received by inclined surfaces and horizontal surfaces was compared. The ratios VS/H and 45° S/H are shown in figure 5.[8] A vertical surface exposed to the south in Hamburg receives an annual mean of 90 per cent of the radiation which a horizontal surface receives. The ratios of the individual daily sums VS/H, however, vary from 0.33 to 2.87. That is the reason why S + DS + DG cannot be reliably calculated from the total radiation by using the annual mean 0.90 of the ratio VS/H. If the radiation received by a surface directed vertically to the south is to be derived from the total radiation of a horizontal surface, the means of ten days or the monthly means as given in the curve VS/H in figure 5 should be used.

The daily ratios 45° S/H vary between 0.58 in the case of overcast days and 3.08 in the case of clear days, and although the means of 45° S/H (figure 5) vacillate less than those of VS/H, it does not seem advisable to use the annual mean of 1.13 for calculations. The comparison of the radiation received by a surface with an inclination of 45° to the south with that of a horizontal surface illustrates the reason why farmers and winegrowers prefer surfaces inclined to the south for plants which need a great amount of energy.

[8] VS/H and 45°S/H = daily radiation received by the vertical surface (VS) or the surface inclined 45° (45°S) respectively, divided by the daily radiation received by the horizontal surface (H).

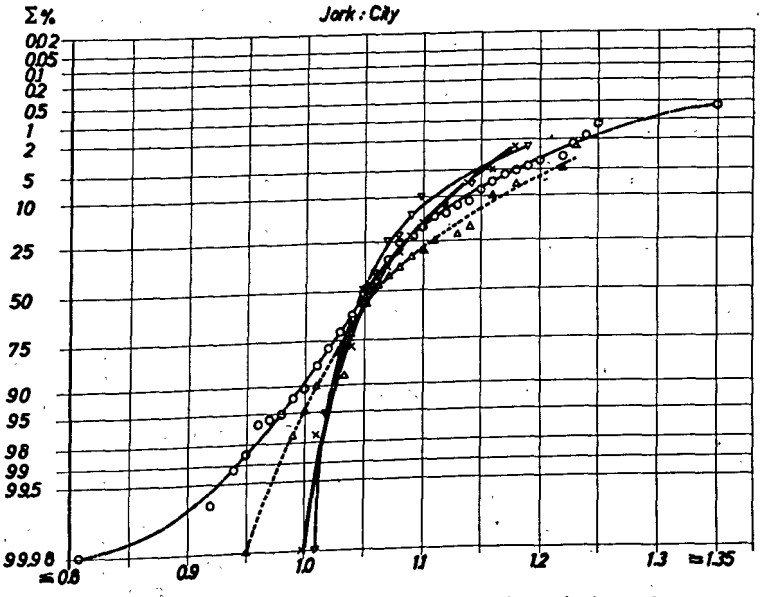


Figure 6. Comparison of Jork with City. Total radiation of clear days measured in Jork divided by the total radiation measured in the City at the same time; presented as accumulated relative frequencies of the ratios

X———X Ratios of the daily values
Δ----------Δ Ratios of the a.m. values
∇— — — —∇ Ratios of the p.m. values
O—·—·—·—O Ratios of the 3-hour values

Variations of total radiation in a small network

The network

Since 1958 the total radiation has been measured with solarimeters at four different places in Hamburg with the main aim to investigate the effect of air pollution on total radiation, as well as the influence of other factors that may determine micro-climatic conditions, such as cloudiness, air mass, wind direction, etc. (10). The measuring places are situated (*a*) in the *City* of Hamburg, (*b*) in the southern industrial district of *Harburg*, (*c*) in the small country town of *Jork* west-south-west of Hamburg, and (*d*) in the eastern suburb of *Bergedorf*. The distances between the three out-stations and the City station are as follow: from Harburg to the City 10 km, from Jork 18 km, and from Bergedorf 19 km. The solarimeters were standardized before their installation and recalibrated in 1960.

Evaluation of the measurements

The total radiation values of the three out-stations are occasionally compared the one with the other. However, they are regularly compared with the values of the City station. Ratios were calculated for three-hour values (3 to 6 hrs, 6 to 9 hrs, etc.), for a.m. and p.m. values, and for the daily sums of total radiation. These ratios show the radiation differences of the various stations—e.g., 1.06 means that one station receives 6 per cent more radiation than the other.

In order to appreciate the full influence which the possible micro-climatic factors may have on the total radiation, it will be necessary to make a series of correlations to separate the different influences which come into play. The ratios obtained on cloudy days show greater variations than on clear days. Correlations on cloudy days are much more complicated.

For this special investigation, however, only records of clear days have been considered as they are of particular interest for the utilization of solar energy. Besides, the structure of micro-climatic conditions may be assumed to be relatively uniform on these days, so that statements of considerable reliability can be made about the radiation variations in large communities without specific correlations to the different climatic factors. Nevertheless, the possible influences of micro-climatic factors other than air pollution (caused by the aerosol emissions of the community), must be borne in mind. The restriction of our investigation to clear days presents one serious difficulty. Clear days are rare in Hamburg, so that our statistical material has not the magnitude that we should wish it to have. In more than two years there were only 40 clear days recorded.

Analysis of the radiation variations from Jork to City on clear days

When the radiation values of the two stations (Jork and City) were compared, it was found that the majority of values obtained fell in close proximity to the mean value of all the ratios (see figure 6), which almost coincides with the 50 per cent point (or median).

The average ratio is 1.06; the 50 per cent point is reached at 1.05. That means that, on the average, Jork has a radiation surplus of about 5 per cent on clear days. The standard deviation σ is ± 0.04. Within the limit of above and below the median we find 80 per cent of the ratios. It may therefore be said that a radiation surplus of 5 per cent of Jork over the City, as represented by the median, is typical for clear days. A certain restriction to this affirmation will be given later with regard to the

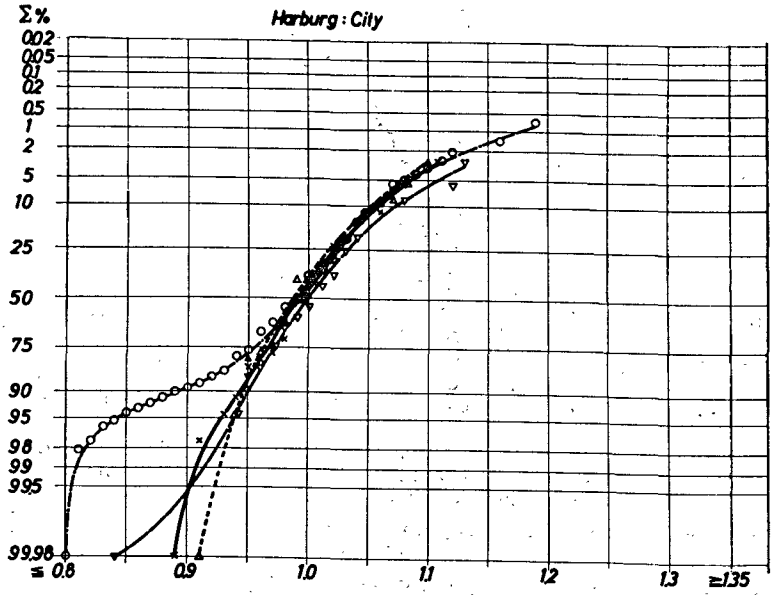


Figure 7. Comparison of Harburg with City. Details similar to figure 6

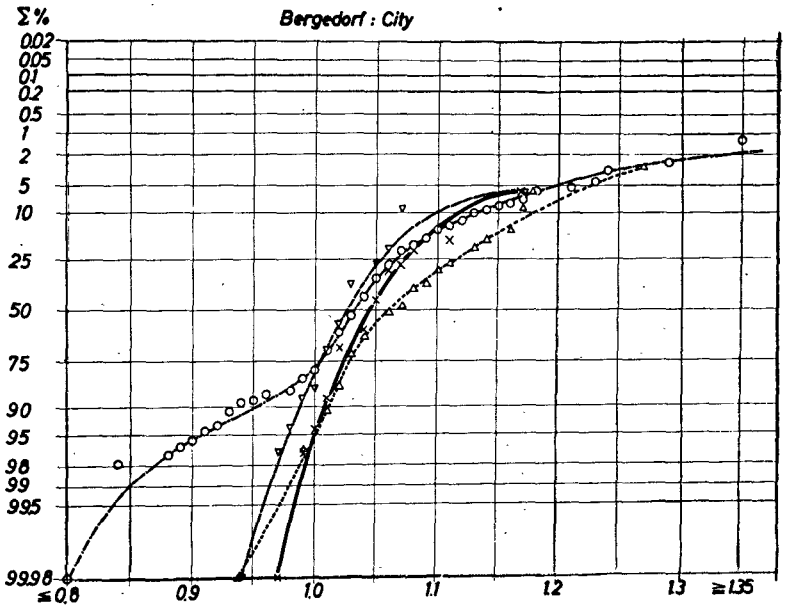


Figure 8. Comparison of Bergedorf with City. Details analogue to figure 6

fact that the distribution is not homogeneous. The extreme value of the distribution amounts to 1.18; it lies just beyond the $\pm 3\ \sigma$ range, which includes 97.5 per cent of the ratios. The fact, however, that quotients occur up to 1.18 is very interesting. It means that even on clear days and within a rather small area, the total radiation may vary considerably, i.e., up to 18 per cent in our case.

Over a shorter period—e.g., the morning or the afternoon only—the factors which are suspected to cause the radiation variations may have a somewhat more effective transitory influence. Thus, the ratios for the morning vary from 0.95 to 1.23 and those of the afternoon from 1.01 to 1.19. Their 50 per cent points coincide with those of the daily ratios, as does the median of the three hour ratios, which as a whole vary from 0.81 to 1.35. Part of the wider dispersion of these values (might) be due to the fact that the three hour radiation values are in some cases rather small,[9] so that small absolute variations turn into high relative variations. It is still remarkable that 75 per cent of the morning ratios, 90 per cent of the afternoon ratios, and 77.8 per cent of the three hour ratios are within the $\pm\ \sigma$ range above and below the median.

A few words may be added about the curves in the accumulated relative frequency (Σ per cent) diagram

[9] Radiation values below 10 cal. have not, however, been taken into consideration.

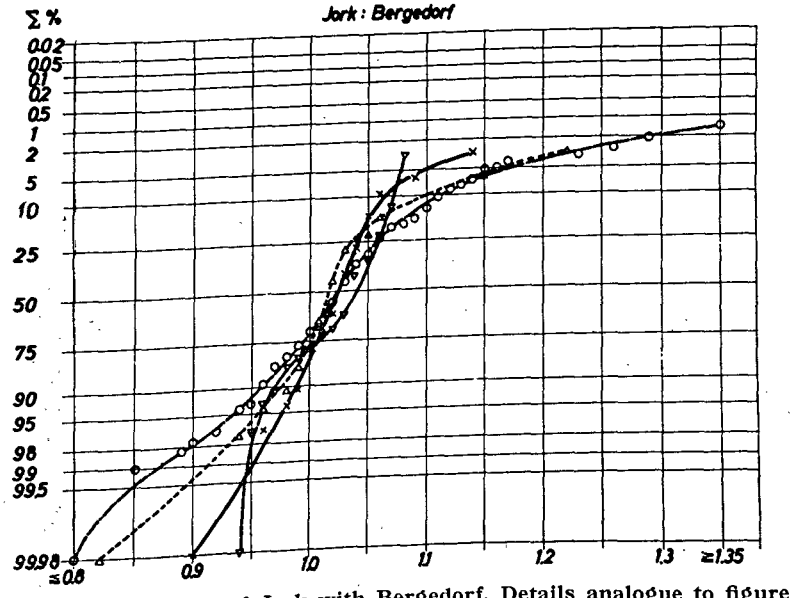


Figure 9. Comparison of Jork with Bergedorf. Details analogue to figure 6

(figure 6). It is easily seen that they do not connect the empiric values of relative frequency but give an abstraction, which may approach the general tendency or trend of the distribution (which, however, was not determined mathematically). If we had a steadily rising and falling distribution of the frequencies of the different ratios with one clear maximum (Gauss distribution), the Σ per cent curve in this diagram should have resulted in a straight line. We have, however, obtained curved lines, one of which even has a turning point. This shows that our distribution is not homogeneous in itself, but that it consists in reality of various distributions. That is perfectly in agreement with our statement that the various micro-climatic factors act in different ways on the variations of the total radiation.

Analysis of the variations on clear days at four stations

From our various comparisons we calculated the following averages for the ratios of the daily sums of total radiation:

Jork	: City	1.06
Harburg	: City	0.99
Bergedorf	: City	1.05
Jork	: Bergedorf	1.02

For the distributions of the ratios, see figures 7, 8, and 9. It seems therefore that on an average, the radiation conditions of Jork and Bergedorf are nearly equal, while on the other hand the radiation conditions of the City differ very little from the industrial district. However, both Bergedorf and Jork receive a greater amount of radiation than the City or the industrial area. We are inclined to suppose that the air pollution over the City and the industrial district may have absorbed some of the incoming radiation.

Conclusions

During the Geophysical Year radiation measurements have been made at various places all over the world, and the differences of radiation measured in different countries or continents have been discussed. The extreme value of our comparisons shows that even over small areas the total radiation may vary considerably. This result is the more remarkable as we have restricted this investigation to radiation records obtained under such comparatively uniform climatic conditions as found on clear days. We think, therefore, that great care should be taken in forming conclusions about radiation variations that have been observed between distant places.

References

1. Kleinschmidt, E., *Handbuch der meteorologischen Instrumente*, Berlin, 1935.
2. Mörikofer, W., Meteorologische Strahlungsmessmethoden, *Abderhaldens Handbuch der biologischen Arbeitsmethoden*, Abt. II, Teil 3, Urban u. Schwarzenberg, Berlin u. Wien, 1939.
3. Gräfe, K., Über Möglichkeiten der Bestimmung, Berechnung und kurzfristigen Vorhersage der Globalstrahlung am Erdboden, *Arch. Met. Geoph. Biokl.*, Serie B, 5, 344-376, 1954.
4. International Union of Geodesy and Geophysics, Radiation Commission, Radiation Instruments and Measurements, *IGY Instruction Manual*, Part VI, Pergamon Press, London, New York, Paris, 1958.
5. Gräfe, K., Zur Prognose des Globalstrahlung, *Meteorol. Abh. Fr. Univ. Berlin*, 2, H.4, 145-151, 1955.
6. Gräfe, K., Comparison of the records of actinographs with those of solarimeters in Hamburg in 1955, presented at the International Radiation Conference in Davos, 1956, not published.
7. Schulze, R., Strahlungsempfang geneigter ebener Flächen, *Arch. Met. Geoph. Biokl.* Serie B, 6, 128-138, 1954.
8. Gräfe, K., Strahlungsempfang vertikaler, ebener Flächen; Globalstrahlung von Hamburg, *Ber. d. Deutschen Wetterdienstes*, Band. 5, No. 29, 1956.
9. Kaempfert, W. and Morgen, A., Die Besonnung, *Zeitschr. f. Meteorologie*, 6, 138-146, 1952.
10. Gräfe, K., Hettche, H. O. and Peters, K H., SO_2-Gehalt der Stadtluft in Beziehung zur Gesundheit und zum Wetter, *Gesundheits-Ingenieur*, 80, 302-308, 1960.

Summary

In order to obtain sufficient knowledge to use solar energy, it is necessary to use instruments which fulfill certain demands, i.e., among others, simplicity and reliability, and which are at the same time so constructed that they can be distributed in large numbers without difficulty. The instrument which approximates these requirements is the Robitzsch bimetallic actinograph, in spite of the fact that it does not quite attain the accuracy of good electrical pyranometers. In order to illustrate the reliability of the Robitzsch bimetallic actinograph, a comparison of the daily sums of total radiation over a period of one year has been made with the Moll-Gorczynski-solarimeter in the same station. The results indicate that the actinograph is more suitable for areas receiving greater amounts of radiation than areas receiving smaller amounts, that is to say, that the actinograph gives data for the utilization of solar energy. However, in order to obtain well balanced and more precise results, it is necessary to establish a compromise between the Robitzsch bimetallic actinograph and the electrical pyranometers like the networks that are being installed in particular areas which have,

in addition to the various actinographs, at least one electrical pyranograph (e.g., a Moll-Gorczynski-solarimeter) which can be used for the standardization of the actinographs and at the same time maintain continuous records, as well as give instantaneous data.

Wherever skilled operators are available, there should be electrical pyranometers so as to obtain data of the total radiation of non-horizontal surfaces exposed to different directions of the sky. Examples of measurements in Hamburg (i.e., daily radiation of surfaces exposed to the south and under angles of 45° and 90°) illustrate the importance of the diffuse radiation. The total radiation received by non-horizontal surfaces is compared with the results of the horizontal surface. The ratios of these comparisons show the different amount of radiation received by each surface. On the basis of the means of these ratios the radiation received by non-horizontal surfaces can be approximately calculated.

Radiation values derived from measurements at four different stations in Hamburg indicate that the total radiation may vary considerably even at distances of only 20 km. These variations are supposed to be due to micro-climatic conditions such as cloudiness, air mass, wind direction, and air pollution. For this investigation only the records of clear days have been considered since they are of particular interest for solar energy utilization. Ratios were worked out from the radiation values of different measuring stations. These ratios showed an average surplus of about 5 per cent of an outstation over the station in the City of Hamburg. But even on clear days in this small network, the total radiation varied up to as much as 18 per cent.

An analysis of the distribution of the ratios illustrates how satisfactory the statistical material really is. About 80 per cent of the values lie within the range of the average deviation. Nevertheless, the curves in the Σ per cent diagram indicate that the distribution is not homogeneous. This is not surprising as the different micro-climatic factors act in different ways on the variations of the total radiation. The results discussed here will illustrate that values of total radiation obtained at selected stations should not be regarded as representative of larger areas.

MESURES DU RAYONNEMENT GLOBAL DANS DES RÉSEAUX DE STATIONS

Résumé

Il est nécessaire, pour acquérir des données suffisantes en vue de l'utilisation de l'énergie solaire, de faire appel à des instruments qui satisfont certaines exigences telles, entre autres, que la simplicité et la sûreté du fonctionnement, tout en étant conçus de telle sorte qu'il soit possible de les distribuer en grand nombre et sans difficulté. L'actinographe bimétallique de Robitzsch remplit sensiblement ces conditions, bien qu'il n'atteigne pas tout à fait la précision des bons pyranomètres électriques. On a procédé à une comparaison entre cet actinographe et le solarimètre de Moll-Gorczynski à un poste donné sur les sommes du rayonnement global quotidien pendant un an. Les résultats ainsi obtenus indiquent que l'actinographe convient mieux aux régions qui reçoivent des quantités appréciables de rayonnement qu'aux autres. Ceci revient à dire que l'actinographe fournit des données utiles pour l'utilisation de l'énergie solaire. Cependant, pour obtenir des résultats bien compensés et plus exacts, il faut réaliser un compromis entre l'actinographe bimétallique de Robitzsch et les pyranomètres électriques en installant des réseaux de postes dans des régions disposant, en plus des divers actinographes, d'un pyranographe électrique au moins (par exemple d'un solarimètre de Moll-Gorczynski) dont on peut se servir pour l'étalonnage des actinographes, sans préjudice des enregistrements continus et de la lecture des données instantanées.

Partout où l'on dispose d'opérateurs bien entraînés, il faut prévoir des pyranomètres électriques susceptibles de fournir des données relatives au rayonnement total sur les surfaces non-horizontales exposées au ciel dans diverses directions. Des exemples de mesures faites à Hambourg (par exemple celle du rayonnement quotidien sur des surfaces exposées au Sud et à des angles de 45 et 90°) illustrent l'importance du rayonnement diffus. On compare le rayonnement total fourni aux surfaces non-horizontales aux résultats applicables à la surface horizontale. Les rapports qui ressortent de ces comparaisons indiquent les doses de rayonnement que reçoit chaque surface. Sur la base des moyennes de ces proportions, on peut calculer, d'une manière approchée, le rayonnement que reçoivent des surfaces non-horizontales.

Les valeurs du rayonnement que donnent des mesures prises à quatre postes à Hambourg indiquent que le rayonnement total peut varier sensiblement, même pour des distances ne dépassant pas 20 km. Ces variations sont censées s'expliquer par des considérations microclimatologiques telles que l'ennuagement, les masses d'air, la direction du vent et les impuretés de l'air. On n'a pris en considération pour les besoins de la présente étude, que les enregistrements relatifs à des jours clairs, pour autant qu'ils présentent un intérêt particulier pour l'utilisation de l'énergie solaire. On a mis au point des proportions à partir des valeurs trouvées pour le rayonnement aux divers postes de mesures. Ces proportions font ressortir un excès de 5 p. 100 en moyenne, pour un poste de banlieue, par rapport à ce qu'on trouve dans la ville de Hambourg. Cependant, pour ce petit réseau, le rayonnement total a varié dans une proportion allant jusqu'à 18 p. 100,

même pour les jours clairs. Une analyse de la répartition de ces proportions illustre combien les données statistiques sont véritablement satisfaisantes. Environ 80 p. 100 des valeurs trouvées s'inscrivent dans le cadre défini par les écarts moyens. Le fait reste que les courbes du diagramme donnant Σ p. 100 indiquent que la répartition n'est pas homogène. Ceci n'est pas surprenant, pour autant que les divers éléments microclimatologiques ont des répercussions différentes sur les variations du rayonnement total. Les résultats passés en revue dans ce mémoire illustrent que les valeurs du rayonnement total obtenues en des postes convenablement choisis ne devraient pas être considérées comme représentatives pour des zones plus grandes.

SIMPLE INSTRUMENTS FOR THE ASSESSMENT OF DAILY SOLAR RADIATION INTENSITY

Harold Heywood *

The number of meteorological stations which possess accurate pyrheliometers and recorders is limited by the cost of such equipment and the need for trained personnel. A much closer network of instrumentation is necessary to assess solar energy availability over the whole of a large country, in which conditions may vary considerably from one location to another. During the last ten years, the author has given much study to the design of simple instruments which would assess the radiation received daily on a flat surface, primarily with the object of predicting the performance of flat-plate types of solar water heater.

Operating principles

The basic operating principles of pyrheliometers in general use are as follows:

(*a*) Equilibrium instruments in which the receiving surface attains an equilibrium temperature at which there is a balance between the energy received by radiation and the heat losses.

(*b*) Capacity instruments in which the heat gained during a period which may vary from a few minutes to the whole day is measured by the rise in temperature of a suitable mass of water or metal.

(*c*) Flow calorimeters with cooling by a known water flow and measurement of the corresponding temperature rise.

(*d*) Evaporation instruments in which the volume of a liquid evaporated at approximately constant temperature is assumed to be proportional to the radiation received.

Conditions of design

The conditions of design which should be fulfilled by a simple instrument for the purpose described above are stated below.

(*a*) Ability to withstand all weather conditions.

(*b*) Minimum cost; hence, the use of a chart recorder is inadmissible.

(*c*) Simplicity of construction containing no fragile parts which cannot be replaced easily.

(*d*) The radiation received during a complete day to be registered as an integrated record.

(*e*) No electrical supply or running water required.

(*f*) Minimum attention required for operation, and not at any fixed times.

(*g*) No scientific training or knowledge required by the operator.

The characteristics of the various types of pyrheliometer listed above are examined below in accordance with the conditions of design set out immediately above.

The Kipp and Eppley pyrheliometers are based on the use of a thermopile and are equilibrium instruments having very small heat capacities, so that the receiving surface attains the equilibrium temperature in a few seconds. The temperature of the receiving surface in these instruments is measured by the electrical output and is normally recorded, but the temperature could be determined in other ways, such as by the use of a bi-metallic strip or even by direct thermometric measurement, though this would increase the thermal capacity of the instrument. Since the integration of a record is inadmissible, none of these designs fulfills the requirements, though it has been found that the temperature of a copper block measuring $7 \times 5 \times 1$ cm with a thermometer inserted follows closely the readings of a thermopile. There is considerable smoothing of rapid fluctuations of radiation, but this is not necessarily a disadvantage for the purpose intended. Further research on such devices is in progress since they could fulfill a useful purpose. They are not suitable, however, for the primary objective.

Capacity instruments

Preliminary experiments were made with copper blocks and small rectangular water vessels having thermal capacities expressed as water equivalents varying from 7 to 50 kg/m^2 of frontal exposed area. These showed that under conditions of steady radiation, the rate of temperature rise of the absorber was constant whilst the temperature did not exceed 10°C above atmospheric temperature, but that heat losses significantly reduced the rate of temperature rise at more than 20°C above atmospheric temperature. Provided that the temperature rise is limited

* Principal, Woolwich Polytechnic, London.

to approximately 15°C, capacity absorbers may be used to assess solar radiation by either of the two following methods of operation:

(*a*) If constructed of copper with a water equivalent of the order of 5 kg/m², the permissible temperature rise is attained in a few minutes and the instantaneous radiation intensity can be calculated. The copper block must be allowed to cool to atmospheric temperature before a further test is made. Hence, although this device does not comply with conditions set out above it could be developed as an inexpensive method of estimating solar radiation by means of a portable instrument.

(*b*) If water is used as the medium for heat storage and the total water equivalent, including the container, is of the order of 200 kg/m², the permissible temperature rise will not be exceeded for a whole day's exposure to continuous radiation. Hence, such a device, if suitably designed, might fulfil all the conditions given above. The solar calorimeter described in the main section of the paper is based on this principle.

Flow calorimeters are in effect minature flat-plate water heaters, and have been found very useful for exploratory experiments on the factors influencing the performance of larger scale heaters of the same type. They are inapplicable as simple instruments for the purpose intended as they do not fulfil conditions stated above.

The usual design of evaporation radiometer consists of a hollow copper sphere with blackened surface to absorb the radiation which is connected through a cooling section to a long graduated glass tube. The outlet tube leaves the sphere at the base but projects inside the sphere to within a short distance of the top interior surface. The sphere is nearly filled with a volatile liquid, which is partially vaporised by the heat derived from radiation, the vapour passing through the cooling section and collected as liquid in the graduated glass tube. The spherical absorber is enclosed within a glass sphere and the space between is evacuated. The spherical type of absorber is non-directional, and a modification has a flat top so that the absorbing surface may be used in a directional manner.[1] Since the evaporation takes place at a constant temperature very little above that of the atmosphere, the heat losses are minimized. The volume of liquid evaporated and condensed in the graduated tube is taken as a measure of the total radiation absorbed during the day, and the instrument is then inverted to return the liquid to the spherical absorber. This device fulfills many of the conditions of design, but its construction involves skilled glass working with difficult glass-to-copper joints. As it is nearly 1 metre in length, it is very fragile.

[1] Trickett, E. S., Moulsky, L. J., Edwards, R. I., Measurement of solar and artificial radiation with particular reference to agriculture and horticulture, *Jl. of Agric. Eng. Res.*: 2: 86, 1957.

Description of the solar calorimeter

As a result of the survey described briefly above, it was decided that a capacity type of instrument would best fulfil the conditions of design that had been postulated. Various models have been constructed and tested during the past three years, and the final model has been reduced to the simplest possible form compatible with a practical degree of accuracy. The essential object is to assess the heat which could be collected by means of a flat-plate water heater. It was not expected that the results obtained would always coincide with the radiation measured by a standard pyrheliometer, taking into consideration the widely varying conditions from brilliant sunshine in a cloudless sky to complete cloud cover.

A cross sectional drawing of the final model is shown in figure 1. The water capacity consists of a standard Thermos flask (1 pint = 570 ml). The radiation absorbing surface is a copper disk 5.08 cm diameter soldered co-axially to a copper tube 2.15 cm external diameter, the end of the tube being spun to a flange so that improved thermal contact with the disk is obtained. The top surface of the disk is blackened and the under surface and part of the tube are chromium plated. The screw cap of the flask is bored to take the tube, and a

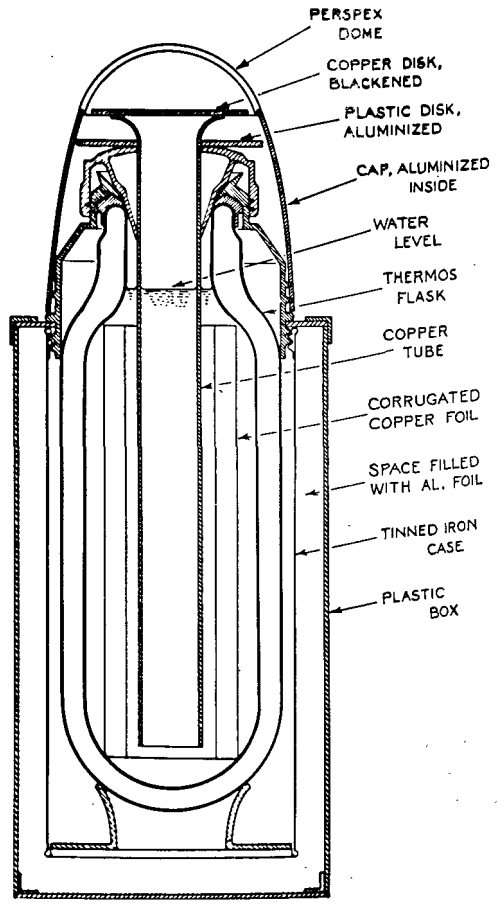


Figure 1. Section of solar calorimeter incorporating Thermos flask as water container

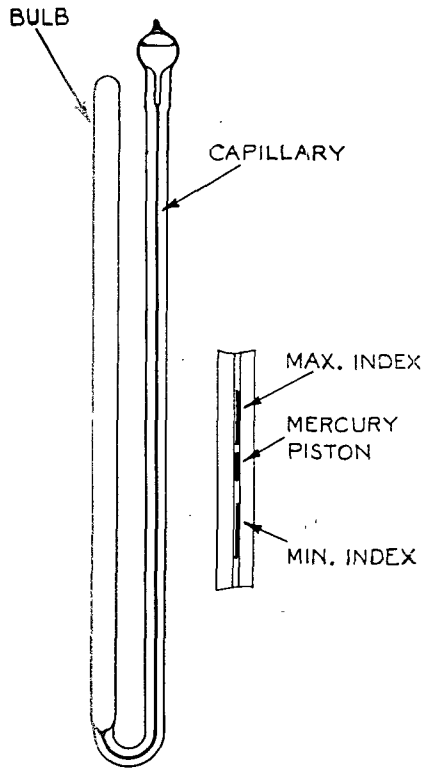


Figure 2. Maximum/minimum thermometer for insertion in tube of solar calorimeter

plastic disk aluminized on both surfaces reduces radiation loss from the underside of the copper disk. A perspex dome replaces the flat top of the flask cup, which is aluminized on the interior surface. A roll of corrugated copper foil between the tube and the inner surface of the flask acts as a heat equalizer. As a further protection against heat flow from or to the atmosphere, the flask is enclosed in a square plastic box with aluminium foil filling the space between. The cost of materials for the solar calorimeter is about U.S. $6; including manufacturing costs, it should be possible to produce the instrument for about $18. A patent has been applied for.

The principle of operation needs little explanation. Radiation impinges on the copper disk and the heat generated is conducted through the walls of the tube to the water in the flask. The temperature rise of the water is a measure of the radiation received during a day, and since the area of the disk and the water capacity are so proportioned that the temperature rise rarely exceeds 15°C, the heat losses are relatively small. The temperature rise is measured by means of a specially designed maximum and minimum thermometer shown in figure 2. The thermometer bulb is long in order to attain the mean temperature of the water, and is filled with creosol. The capillary tube contains the normal indices to indicate the maximum and minimum positions of a mercury piston 3 mm long, which is moved by the change in volume of the liquid in the bulb. This thermometer is placed within the copper tube, which is slotted to enable the indices to be observed.

The thermal parameters for the instrument are as follows:

Frontal area of copper disk	20.25 cm^2
Weight of water in flask	420 g
Water equivalent of copper parts	20 g
Water equivalent of flask	25 g
Total water equivalent	465 g

Ratio of water equivalent to absorbing surface area 23 $g/cm_2 = 230\ kg/m_2$.

Hence 1°C rise in temperature represents 23 cal/m^2 = 26.7 mwh/cm^2 = 267 wh/m^2.

Procedure for observations

The flask may be placed with the axis vertical and the disk in a horizontal plane, or may be mounted so that the disk is at any desired inclination to the horizontal, including a vertical plane. Thus, a number of the instruments may be used simultaneously to assess the heat which could be collected on surfaces with different attitudes, a research which is now in progress. The preferable procedure for taking readings is to read the minimum index in the early morning, 8 to 10 a.m., and then to bring both indices into contact with the mercury piston by means of a magnet. The position of the maximum index is read after sunset, when both indices are again brought into contact with the mercury. The difference between the two readings, less the length of the mercury piston, is proportional to the rise in temperature. Alternatively, the position reached by the maximum index may be read on the following morning, but there is a possibility that the mercury will not have reached the minimum index position for the previous day. However, the most attention needed is on two occasions a day, and under settled weather conditions once a day may be sufficient. A further simplication of procedure would be to use a sliding scale calibrated directly in energy units to measure directly the distance between the two indices. The warmed water in the calorimeter is not changed, but is allowed to cool during the night; the minimum temperature of the flask above minimum night atmospheric temperature is about 35 per cent of the difference between the maximum water temperature for the previous day and the night temperature. The influence of this factor on the readings is discussed above. The calorimeter will withstand short periods with atmospheric temperatures below freezing point, but if such periods are prolonged the water could be replaced by a non-freezing liquid.

Results of tests

Continuous daily readings have been taken on a calorimeter in the outer London area since September 1959. The surface of the disk was in a plane inclined at 40° to the horizontal and facing south. The daily minimum and maximum temperatures for the year 1960 are shown in figure 3. The year has been divided into periods limited by selected solar declinations such that the positive and negative values are nume-

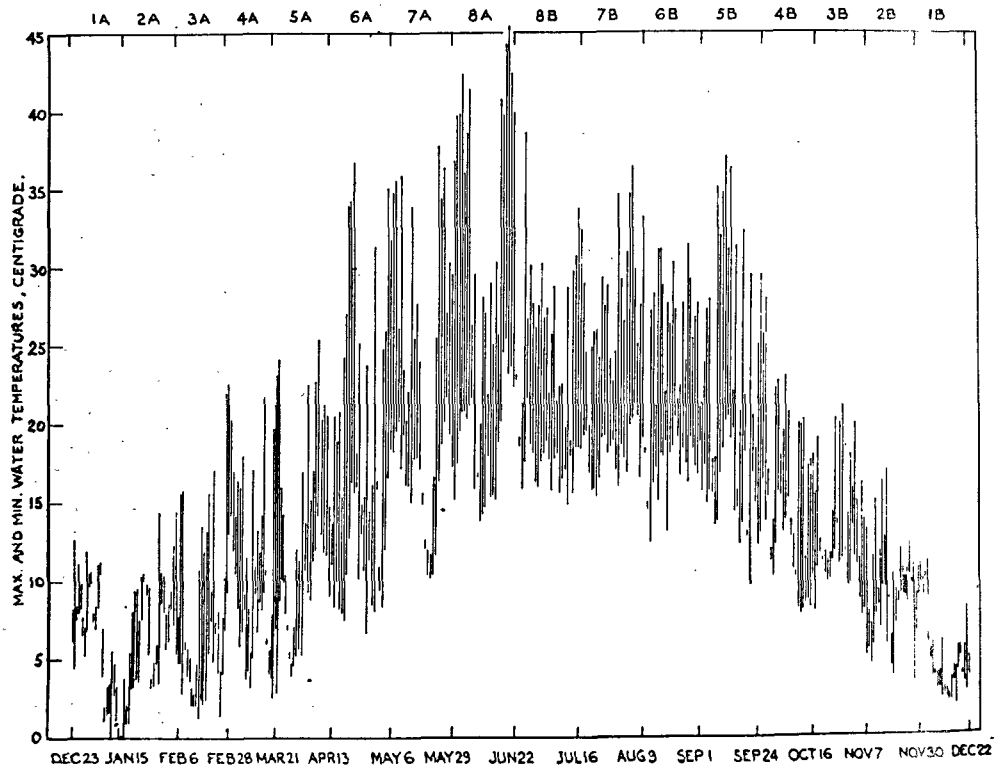


Figure 3. Maximum and minimum temperatures attained by solar calorimeter each day during year 1960. Attitude of receiving surface of disk, south at inclination 40° to horizontal

rically the same. The object is to provide a more rational grouping of days than by calender months and to facilitate computations of angles of solar incidence. Due, however, to the eccentricity of the earth's orbit round the sun, the groupings cannot be symmetrical about the equinox date and vary from 22 to 24 days per group or period; the actual dates also vary slightly from one year to another, and are shown for the year 1960 in table 1. The average heat recovery per day is shown for each period from September 1959 to February 1961 in table 2. The fourth column of the table shows the mean daily recovery on a calorimeter with the attitude stated above. These have been converted

Table 1. Declination periods, epoch 1960

Period No.	*Number of days*	*Limiting dates*	*Declination*	*Limiting dates*	*Number of days*	*Period No.*
1 A	23	Dec. 23[a]	— 23° 27′	Dec. 22	23	1 B
		Jan. 14	— 21° 30′	Nov. 30		
2 A	22	Jan. 15	— 21° 30′	Nov. 29	23	2 B
		Feb. 5	— 16° 12′	Nov. 7		
3 A	22	Feb. 6	— 16° 12′	Nov. 6	22	3 B
		Feb. 27	— 8° 42′	Oct. 16		
4 A	22	Feb. 28	— 8° 42′	Oct. 15	22	4 B
		Mar. 20	0	Sep. 24		
5 A	23	Mar. 21	0	Sep. 23	23	5 B
		Apr. 12	8° 42′	Sep. 1		
6 A	23	Apr. 13	8° 42′	Aug. 31	23	6 B
		May 5	16° 12′	Aug. 9		
7 A	23	May 6	16° 12′	Aug. 8	24	7 B
		May 28	21° 30′	Jul. 16		
8 A	24	May 29	21° 30′	Jul. 15	24	8 B
		Jun. 21	23° 27′	Jun. 22		

[a] Epoch 1959 — total days, 366.

to probable values for a horizontal surface by means of tentative factors which are still the subject of another research, as shown in the fifth column. The final column shows the total of direct and diffuse radiation received on a horizontal surface at Kew Observatory, situated about 40 km from the place of the experiments. These results show that the efficiency of heat collection by the solar calorimeter averages 80 to 90 per cent. More exact comparisons on individual days indicate that the calorimeter is about 90 per cent efficient with direct radiation, decreasing to about 50 per cent efficiency with diffuse radiation. Further comparisons are in progress, using Kipp pyrheliometers at the same site as the calorimeters.

Critical consideration of procedure and results

The procedure for the operation described above is not ideal, and is necessarily somewhat of a compromise in order to retain simplicity. For instance, a stirring device would improve the heat transfer, but could not be introduced without complication or the need for frequent attention. The temperature difference between the disk and the mid-length of the tube is greatest when the rate of heating is a maximum, and amounts to about 0.6°C when the rise is 2.8°C per hour. The difference becomes zero after the water has reached a maximum temperature, and during night cooling at a rate of 1.3°C per hour the disk is 0.5°C below the tube temperature. The temperature difference between the tube and the equalizer is very small, the maximum observed being 0.2°C. These temperature variations are not considered to be significant. One disability that cannot be avoided and which also affects large flat-plate solar water heaters is that before noon the increasing radiation intensity is in phase with the increasing water temperature, whereas after noon these factors oppose each other in phase. Hence the efficiency of the solar calorimeter is less after noon than before; indeed its efficiency towards sunset may be zero even though there is still appreciable radiation. However, if the object is to provide data for heat collection, this effect is no disadvantage. Anomolous results may be obtained because of variations in the minimum temperature attained by the calorimeter during the night, this being dependent upon the energy collected during the previous day and any change in night air temperature. Temperature variations and energies collected have been calculated for a hypothetical case, and the results are shown in figure 4. A constant night air temperature of 15°C has been assumed and four days of continuous solar radiation of equal magnitude. The left hand side diagram shows that equilibrium between the heating and cooling effects is attained on the fourth day. If now the radiation is reduced to half the former intensity, it again takes four days for a new state of equilibrium to be established. The right hand side diagram shows the effect of a 5°C drop in night air temperature, radiation conditions remaining constant. Thus the temperature rise on a particular day is to some extent affected by previous conditions, but statistically these effects should balance since changes of atmospheric and radiation conditions occur in both directions. Anomolous results may be obtained on completely overcast days, especially in mid-winter. Though the calorimeter is normally less sensitive to diffuse radiation than to direct

Table 2. Energies in milliwatt hours per m² (mWh/cm²)

Year	*Period*	*Number of days*	*Solar S40*	*Calorimeter horz.*	*Kew Observatory total horz.*
1959	4 B	23	321	247	250
	3 B	22	162	112	130
	2 B	22	132	82	71
	1 B	23	63	36	35
1960	1 A	23	58	33	41
	2 A	22	93	58	62
	3 A	22	156	107	118
	4 A	22	162	125	144
	5 A	23	200	176	220
	6 A	23	300	290	363
	7 A	23	248	258	378
	8 A	24	386	420	542
	8 B	24	230	250	382
	7 B	24	264	274	412
	6 B	23	239	231	338
	5 B	23	257	226	261
	4 B	22	197	152	194
	3 B	22	126	87	117
	2 B	23	97	60	72
	1 B	23	51	29	38
1961	1 A	22	88	51	59
	2 A	22	82	51	63
	3 A	22	120	83	93

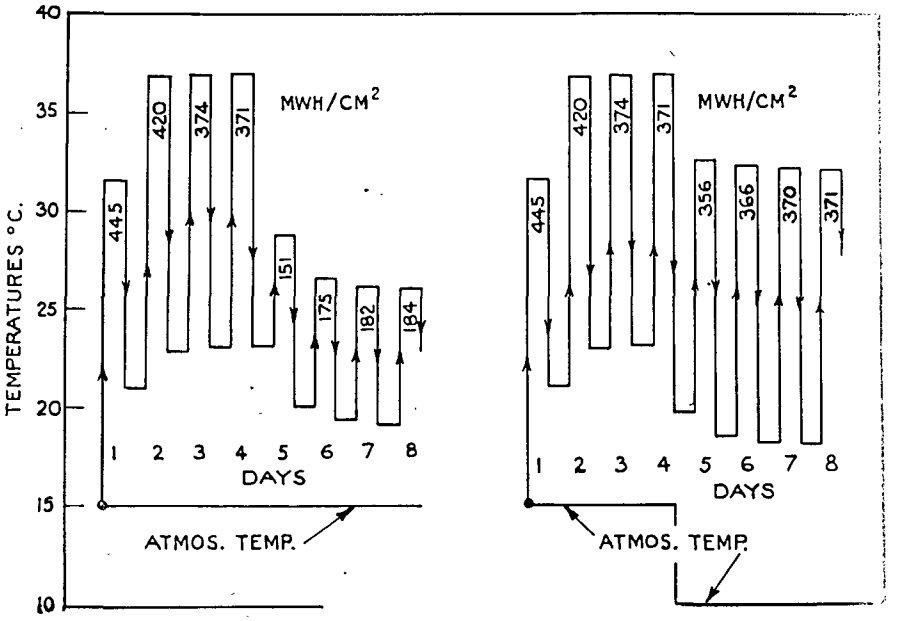


Figure 4. Calculated variation of temperatures due to changes in atmospheric conditions. Left-hand sequence constant atmospheric temperature at night, 1st to 4th days continuous insolation, 5th to 8th days insolation at half previous value. Right-hand sequence continuous insolation at constant value, 5°C decrease in atmospheric temperature at night after 4th day

radiation, if the atmospheric temperature rise is unusually high there may be sufficient heat flow into the flask to cause a temperature rise greater then the equivalent of the incident diffuse radiation. An investigation is in progress to ascertain whether a system of correcting factors for this effect can be devised.

Conclusions

The test results described substantiate the claim that the particular design of solar calorimeter described will assess the availability of solar radiation as regards the operation of flat-plate water heaters. With further experience and possible modifications in procedure, it may be possible to use it for the assessment of solar radiation intensities; research is being continued and results may be available at the Conference.

Acknowledgements

The author wishes to express acknowledgement to the Superintendent of Kew Observatory for permission to use data recorded there and to the staff of the physics and engineering departments at Woolwich Polytechnic for the construction of equipment.

Summary

The number of meteorological stations which possess accurate pyrheliometers and recorders is limited by the cost of such equipment and the need for trained personnel. A much closer network of instrumentation is necessary to assess solar energy availability over the whole of a large country, and the author has given much study to the design of simple instruments which would assess the radiation received daily on a flat surface, primarily with the object of predicting performance of flat-plate types of solar water heater.

The conditions of design which should be fulfilled by a simple instrument for the purpose described above are stated below.

(*a*) Ability to withstand all weather conditions.

(*b*) Minimum cost; hence, the use of a chart recorder is inadmissible.

(*c*) Simplicity of construction containing no fragile parts which cannot be replaced easily.

(*d*) The radiation received during a complete day to be registered as an integrated record.

(*e*) No electrical supply or running water required.

(*f*) Minimum attention required for operation, and not at any fixed times.

(*g*) No scientific training or knowledge required by the operator.

The basic operating principles of pyrheliometers in general use are described briefly and it is explained why existing instruments do not fulfil the conditions

postulated above. The reasons are given for the decision to use a capacity instrument in which the heat gained during a period which may vary from a few minutes to the whole day is measured by the rise in temperature of a suitable mass of water or metal.

Description of the solar calorimeter

Various models have been constructed and tested during the past three years, and the final model has been reduced to simplest possible form compatible with a practical degree of accuracy. The water capacity consists of a standard Thermos flask (1 pint = 570 ml). The radiation absorbing surface is a copper disk 5.08 cm diameter soldered coaxially to a copper tube 2.15 cm external diameter, the end of the tube being spun to a flange so that improved thermal contact with the disk is obtained. The top surface of the disk is blackened and the under surface and part of the tube are chromium plated. The screw cap of the flask is bored to take the tube, and a plastic disk aluminized on both surfaces reduces radiation loss from the underside of the copper disk. A perspex dome replaces the flat top of the flask cup, which is aluminized on the interior surface. A roll of corrugated copper foil between the tube and the inner surface of the flask acts as a heat equalizer. As a further protection against heat flow from or to the atmosphere, the flask is enclosed in a square plastic box with aluminium foil filling the space between. The cost of materials for the solar calorimeter is about U.S. $6; including manufacturing costs, it should be possible to produce the instrument for about $18. A patent has been applied for.

The principle of operation needs little explanation. Radiation impinges on the copper disk and the heat generated is conducted through the walls of the tube to the water in the flask. The temperature rise of the water is a measure of the radiation received during a day, and since the area of the disk and the water capacity are so proportioned that the temperature rise rarely exceeds 15°C, the heat losses are relatively small. The temperature rise is measured by means of a specially designed maximum and minimum thermometer. The capillary tube contains the normal indices to indicate the maximum and minimum positions of a mercury piston 3 mm long, which is moved by the change in volume of the liquid in the bulb. This thermometer is placed within the copper tube, which is slotted to enable the indices to be observed. The use of this thermometer ensures that the periods of attention are limited to twice a day.

Results of tests

Continuous daily readings have been taken on a calorimeter in the outer London area since September 1959. Figure 3 of the paper shows the daily minimum and maximum temperatures attained for the year 1960. The daily heat collection, averaged for periods limited by selected solar declinations as detailed in table 1 of the paper, is compared in table 2 with readings of the total of direct and diffuse radiation received on a horizontal surface at Kew Observatory, situated about 40 km from the place of the experiments. These results show that the efficiency of heat collection by the solar calorimeter averages from 80 to 90 per cent. More exact comparisons on individual days indicate that the calorimeter is about 90 per cent efficient with direct radiation, decreasing to about 50 per cent efficiency with diffuse radiation. Further comparisons are in progress, using Kipp pyrheliometers at the same site as the calorimeters. Anomolous results are sometimes obtained and the readings do not always coincide with the radiation measured by a standard pyrheliometer, taking into consideration the widely varying conditions from brilliant sunshine in a cloudless sky to complete cloud cover. Thus the temperature rise on a particular day is to some extent affected by previous conditions, such as the storage effect of the previous day's heating or a change in night air temperature, statistically these effects should balance since changes of atmospheric and radiation conditions occur in both directions.

Conclusions

The test results described substantiate the claim that the particular design of solar calorimeter described will assess the availability of solar radiation as regards the operation of flat-plate water heaters. Further tests are under consideration, and it is hoped that comparative experiments may be made in other types of climate.

INSTRUMENTS SIMPLES POUR L'ÉVALUATION DE L'INTENSITÉ DU RAYONNEMENT SOLAIRE QUOTIDIEN

Résumé

Le nombre des stations météorologiques dotées de pyrhéliomètres et d'appareils enregistreurs précis est limité par le prix de ce matériel et le besoin de personnel spécialisé. Il faut un réseau d'instruments beaucoup plus serré que celui qui existe actuellement pour évaluer les disponibilités en énergie solaire sur l'ensemble d'un grand pays, et l'auteur de ce mémoire a porté son attention tout spécialement sur la réalisation d'instruments simples qui permettraient de déterminer le rayonnement

reçu chaque jour par une surface plane, au premier chef dans le but de prévoir le rendement des chauffe-eau solaires à plaques plates.

Les caractéristiques que doit présenter un instrument simple, pour réaliser les objectifs passés en revue ci-dessus, sont les suivantes :

a) Résistance à toutes les conditions météorologiques;

b) Coût minimum, ce qui exclut tout enregistreur à bande;

c) Simplicité de construction, présupposant l'absence de toutes pièces fragiles qui ne peuvent pas se remplacer facilement;

d) Possibilité d'enregistrer sous une forme intégrée le rayonnement reçu pendant toute une journée;

e) Indépendance de toute source d'électricité ou d'eau courante;

f) Besoins réduits de surveillance en fonctionnement, sans horaire ou calendrier fixes de surveillance;

g) Possibilité d'être mis entre les mains d'opérateurs sans formation technique ni connaissances scientifiques.

Les principes fondamentaux de fonctionnement des pyrhéliomètres d'emploi généralisé font l'objet d'une brève description, et l'auteur explique pourquoi les instruments actuellement en service ne remplissent pas les conditions indiquées ci-dessus. Il présente les raisons qui militent en faveur de l'emploi d'un instrument à capacité, dans lequel la chaleur acquise pendant une période qui peut durer de quelques minutes à la journée entière, est mesurée par l'entremise de la montée de température d'une masse d'eau ou de métal appropriée.

Description du calorimètre solaire. Divers modèles ont été réalisés et essayés au cours de ces trois dernières années, et le type final a été réduit à la forme la plus simple qui soit compatible avec un degré de précision pratique. La capacité d'eau est constituée par une bouteille thermos standard (1 pinte impériale ou 570 ml). La surface d'absorption du rayonnement est un disque en cuivre de 50,8 mm de diamètre, soudé coaxialement à un tube également en cuivre ayant un diamètre extérieur de 21,5 mm. L'extrémité du tube a été évasée en forme de bride par centrifugeage, pour qu'un meilleur contact thermique soit réalisé avec le disque. La surface supérieure du disque est noircie et sa surface inférieure, ainsi qu'une partie du tube, sont plaquées au chrome. Le chapeau à vis de la bouteille présente un évidement approprié pour recevoir le tube, et un disque en composition plastique traité à l'aluminium sur ses deux faces réduit les pertes par rayonnement de la partie inférieure du disque en cuivre. Un dôme en perspex remplace la surface plate du gobelet habituel de la bouteille thermos, et il est revêtu d'aluminium sur sa surface intérieure. Un rouleau de feuille de cuivre ondulée est prévu entre le tube et la surface intérieure de la bouteille pour égaliser les températures. Comme protection supplémentaire contre les échanges de chaleur avec l'atmosphère dans les deux sens, la bouteille est logée dans une boîte carrée en composition plastique, et une feuille de papier d'aluminium remplit l'espace entre la boîte et la bouteille. Les matériaux nécessaires pour la réalisation du calorimètre solaire coûtent environ 6 dollars. En comptant les frais de fabrication, on doit pouvoir produire l'instrument pour 18 dollars environ. Une demande de brevet a été déposée.

Le principe de fonctionnement de l'appareil est fort simple. Le rayonnement frappe le disque en cuivre, et la chaleur ainsi produite est communiquée par les parois du tube à l'eau qui se trouve dans la bouteille. La montée de température de cette eau constitue une mesure de la quantité de rayonnement reçue au cours d'une journée et, pour autant que le rapport entre la surface du disque et la capacité constituée par l'eau a été choisi de telle façon que cette montée de température dépasse rarement 15 °C, les pertes de chaleur sont relativement faibles. La montée de température se mesure au moyen d'un thermomètre à maximum et à minimum spécialement conçu. Le tube capillaire porte les repères habituels qui indiquent les positions, pour le minimum et le maximum, d'un piston de mercure de 3 mm de long, dont la position change avec les variations de volume du liquide que contient l'ampoule. Ce thermomètre est logé à l'intérieur du tube en cuivre dans lequel sont prévues des fenêtres permettant l'observation des repères. Avec ce thermomètre, les périodes d'observation du matériel se limitent à deux par jour.

Résultats des essais. On a procédé à des lectures quotidiennes continues avec un tel calorimètre dans la grande banlieue de Londres depuis septembre 1959. La figure 3 du présent mémoire indique les maxima et les minima journaliers pour l'année 1960. La quantité de chaleur recueillie chaque jour, ramenée à une moyenne pour des périodes limitées par des déclinaisons solaires choisies et indiquées dans le détail au tableau 1 de la présente communication, est comparée au tableau 2 avec les lectures du rayonnement total, direct et diffus, reçu par une surface horizontale à l'observatoire de Kew, situé à une quarantaine de kilomètres du lieu où se sont effectuées les expériences. Ces résultats montrent que le rendement de l'absorption de la chaleur par le calorimètre solaire se monte en moyenne à une valeur comprise entre 80 et 90 p. 100. Des comparaisons plus précises indiquent que le calorimètre a un rendement d'environ 90 p. 100 pour le rayonnement direct, et d'environ 50 p. 100 pour le rayonnement diffus. On procède actuellement à d'autres comparaisons, en se servant de pyrhéliomètres de Kipp, au même poste que les calorimètres. On obtient parfois des résultats anormaux, et les lectures ne coïncident pas toujours avec le rayonnement mesuré au pyrhéliomètre standard, eu égard aux conditions qui varient largement entre un soleil brillant dans un ciel sans nuage et une couche de nuages couvrant tout le ciel. C'est dire que la montée

de température, pour un jour donné, exprime dans une certaine mesure les conditions régnant avant que l'on procède aux lectures, par exemple l'effet d'emmagasinage de la chaleur de la journée précédente ou le changement de température de l'air nocturne; statistiquement, ces effets doivent se compenser, car les conditions atmosphériques et le rayonnement varient dans les deux sens.

Conclusions. Les résultats des essais dont la description a été donnée confirment l'affirmation que la conception du calorimètre solaire décrit ci-dessus permettra d'évaluer les disponibilités en rayonnement solaire pour les besoins des chauffe-eau à plaques plates. On envisage des essais ultérieurs, et on espère pouvoir exécuter des expériences comparatives dans des climats différents.

THE ESTIMATION OF MONTHLY MEAN VALUES OF DAILY TOTAL SHORT WAVE RADIATION ON VERTICAL AND INCLINED SURFACES FROM SUNSHINE RECORDS FOR LATITUDES 40°N-40°S

John K. Page *

One of the first problems in the design of flat plate collectors is to decide the amount of energy actually available at any locality and the best orientation for optimum efficiency. Techniques for calculating the total radiation on cloudless days on inclined surfaces are well known. In practice, however, the problem is to determine rather the radiation received on surfaces with different orientations under average conditions.

Few observations of radiation intensities have been made in many parts of the tropics, particularly on a long-term climatological basis. Records of sunshine, however, are often available over relatively long periods. It was decided any prediction technique of widespread engineering interest must therefore be based on the use of sunshine data. The order of accuracy sought was of the order ± 10 per cent, and the technique developed below appears to give results somewhat better than this where it has been possible to check it.

The average amount of radiation received can be calculated only for inclined and vertical surfaces, if the diffuse radiation component can be assessed with reasonable accuracy. The paper sets out to provide a rapid method of carrying out such computations which can be used by persons relatively unacquainted with either the complexities of the solar radiation climate at different centres or the detailed movements of the sun. It enables the monthly mean daily values of the direct and diffuse radiation to be estimated separately for certain vertical and inclined surfaces using sunshine data.

Part I

The use of Ångström type formulae for the estimation of mean values of global radiation from sunshine records

Regression equations of the Ångström type have been used for many years for estimating mean values of the total daily radiation falling on horizontal surfaces from sunshine records.

The original Ångström formula $\frac{n}{N}$ was written in the form:

$$Q = Qo' \left(a + b \frac{n}{N}\right) \qquad [1]$$

where Q = mean global daily radiation on the horizontal plane for the period under consideration.

Qo' = the global daily radiation on the horizontal plane on cloudless days for the period under consideration.

n = mean daily amount of bright sunshine hours during period under consideration.

N = maximum possible amount of sunshine hours during period under consideration.

a and b = constants depending on locality and climate of station.

The climatological period adopted varies; usually it is one month or ten days. The value of Qo' at high latitudes, however, changes very rapidly from day to day during the winter and a ten day period is better in such regions.

It was often inferred that $a + b = 1$, because on cloudless days $Q = Qo'$ and $\frac{n}{N} = 1$. Such regression equations are based on climatological means, and they cannot necessarily be expected to apply to extreme values for particular days. Several investigations have, in fact, shown that the relationship between the daily global radiation and the percentage of possible sunshine considered on the basis of individual daily values is not linear (2, 12). Ångström type equations usually give an over estimate of total radiation on cloudless days, and on overcast days. This does not mean, however, that it is not possible to derive satisfactory linear equations for calculating mean monthly values of total radiation. It is, however, necessary to relax the condition $a + b = 1$ first.

There are two important practical difficulties in using the original form of the Ångström equation.

(*a*) The definition of possible bright sunshine is ambiguous. Some investigations have applied corrections to allow for the fact that the sunshine recorder

* Professor of Building Science, University of Sheffield, United Kingdom.

does not turn the card until the sun's rays reach a certain critical intensity, and others do not. It is not in fact possible to assess the correction without detailed knowledge of the radiation climate of a particular area.

(*b*) The precise value of Qo' to adopt cannot be determined in the absence of local radiation measurements.

The use of the modified form of Ångström type formula gets round the second difficulty (1). If the formula is written in the following form:

$$Q = Q_o \left(a + b \frac{n}{N_o}\right) \qquad [2]$$

where Q now represents the total radiation per unit area falling on a horizontal plane *outside the atmosphere*, and where the other symbols have the same meaning as before, Q_o can be determined unambiguously for any particular value of the solar constant. Black, Bonython and Prescott obtained the following over-all regression equation for the stations they studied:

$$Q = Q_o \left(0.23 + 0.48 \frac{n}{N}\right) \qquad [3]$$

It appears however, that no attempt was made to reduce records to a common pyrheliometric scale. In addition, the basis on which the percentage of possible sunshine was calculated is not stated. Attention must be drawn to the fact that results of both American measurements based on the Mervin recorder and results obtained in other parts of the world by the Campbell Stokes recorder are grouped together in their calculations. As corrections for the length of day are always applied in American practice, it is clear that the studies of Black *et al.* are based, as they were aware, on an ambiguous definition of percentage of possible sunshine, as well as on imprecisely defined pyrheliometric scales (1).

In this paper an attempt has been made to avoid some of these criticisms by adopting the following procedure:

(*a*) All observed values of Q were reduced to the International Pyrheliometric Scale involving a correction of —2.0 per cent to all values measured on the Smithsonian (1913) scale, and of +1.5 per cent to all values measured on the Ångström scale.

(*b*) The recorded sunshine was expressed as a percentage of the possible sunshine between sunrise and sunset. No attempt was made to correct for the fact that the trace is not burned until the intensity reaches a given critical value because this correction depends on a number of indeterminable factors like the water and dust content of the air, the humidity content of the card, etc. Such corrections cannot be accurate unless based on extensive local studies. Besides, it seems illogical to give a lot of attention to attempting to correct one limitation of sunshine recorders as a radiation recording instrument while ignoring others like the burning of the card through this high cloud, etc. Attention was confined to records made with the Campbell Stokes type of sunshine recorder.

(*c*) Black, Bonython and Prescott's form of the Ångström formula was adopted so that Q_o would be determined unambiguously.

The relationship between the monthly means of total daily radiation on the horizontal plane and the percentage of possible bright sunshine for a number of centres, mainly in the tropics and subtropics, has been studied and the results given in table 2. The original regression equations published by Black, Bonython and Prescott have also been included together with other recently published values for low latitudes.

A solar constant of 2.00 cals. cm.$^{-2}$ min.$^{-1}$ has been used throughout as a result of Johnson's recommendations for the stations studied by the author (7). In practice, the reduction procedure used by Drummond was adopted (4), the correction (for the Ångström scale being too low) being applied to the computed radiation outside the atmosphere Q_o instead of to the surface data Q recorded on the Ångström scale to cut down the amount of computation. Q_o was determined for latitudes 10° N - 60° N by using the tables of radiation outside the atmosphere for given dates at different latitudes based on the work of Milanovitch given in the Smithsonian Meteorological Tables (15). The original values in the tables were increased by the ratio $\frac{2.00}{1.94}$ to allow for the changed value of the solar constant. These adjusted values for individual days were plotted on an extended scale. A smooth curve was drawn, and the mean monthly values were obtained by planimetry. The values for latitudes 0° - 40°S were taken from Drummond's paper, which followed a procedure essentially similar to that described above for the southern hemisphere. The values adopted based on a solar constant of 2.00 gm. cal. cm.$^{-2}$ min.$^{-1}$ are given in table 1. From the values given in table 1, smoothed curves can be drawn for different months giving the variation of the monthly mean value of Q_o outside the atmosphere with latitude. The values adopted for the possible sunshine were taken from the table given by Brooks (3), and no adjustment was applied for failure to record at low solar altitudes. (Suitable tables may also be found in the Smithsonian Meteorological Tables, 15.)

The regression equations were calculated by the method of least squares as a regression of Q/Q_o on $\frac{n}{N}$. The advantage of adopting the above procedure is that all variations between different climates and latitudes appear in the regression coefficients a and b. It is then possible to explore systematically their variation from place to place. It will be shown in a future paper by the author that it is possible to place the Ångström formula on a reasonably sound climatological basis, by selecting the constants according to latitude and the transmission characteristics of the atmosphere for any particular season of

Table 1. Mean values for calendar months of total daily radiation on a horizontal plane outside the earth's atmosphere, latitudes 40°N-40°S. (Solar constant 2.00 cals. cm^{-2} min.$^{-1}$) Units: cals. cm^{-2}. day^{-1}

Latitude	*40°N.*	*30°N.*	*20°N.*	*10°N.*	*0°*	*10°S.*	*20°S.*	*30°S.*	*40°S.*
January	373	521	659	780	884	967	1 020	1 049	1 049
February	500	632	747	844	915	961	974	964	925
March	674	772	848	899	923	918	884	825	741
April	839	899	924	924	893	839	761	658	536
May	970	977	959	916	846	758	648	520	382
June	1 017	1 003	965	902	817	713	589	456	312
July	996	987	959	905	827	729	614	483	344
August	895	927	934	913	867	801	706	591	465
September	740	822	877	904	905	880	826	748	648
October	564	683	784	860	911	937	931	903	841
November	412	558	687	799	888	958	1 001	1 016	1 001
December	332	487	631	760	869	961	1 026	1 067	1 084

the year in any given locality. The author's work on this subject is not yet ready for publication, but his preliminary investigations show little confidence can be placed on the formula suggested by Glover and McCulloch (6).

$$Q/Q_o = 0.29 \cos. \phi + 0.52 \frac{n}{N} \qquad [4]$$

Where ϕ is the latitude.

The author prefers to use monthly mean values of total radiation and sunshine, for this will be the data normally available for calculating climatological mean values of total radiation. The consequent regression formulae cannot be used for predicting daily values of total radiation from daily sunshine values with accuracy, but they were not derived for this purpose. This paper deals only with climatological mean values.

The mean values of a and b were found to be 0.23 and 0.52 respectively. These values are identical with the mean values suggested by Glover and McCulloch for latitude 32 (6) and differ very little from the mean values of 0.23 and 0.48 found by Black *et al.* (1). In practice it is better, however, to try to select climatologically appropriate values of a and b than to use mean values. These can be best established by study of radiation data and sunshine data from other stations in the same type of climate.

Examination of the results so far computed shows:

(*a*) If low percentage of possible sunshine coincides with the season of high turbidity, the value of a will be low, and the value of b high, for example, Kew and Dakar; also, modified by height, Windhoek.

(*b*) If season of high turbidity falls in period with intermediate amount of possible sunshine, the correlation coefficient falls, for the points in the turbid months fall off the curve, for example, Leopoldville.

(*c*) In places where there is little variation in possible sunshine but turbidity variations due to movement of the Intertropical Convergence Zone, the points will be very scattered, and it may become impossible to find a significant regression equation from monthly mean values.

(*d*) If season of high turbidity coincides with season of greatest percentage of possible sunshine, a tends to be high and b low, for example, Pretoria and Stanleyville. This often occurs when dust is responsible for the increased turbidity during the dry season.

(*e*) In places with high values of possible sunshine a tends to be high and b low; the opposite holds for places of very low possible sunshine, where a tends to be low and b high. This effect results because the actual curve is not strictly linear but has an upward curvature if considered over a wide enough range of values of $\frac{n}{N}$. Hence the slope is greater at low values than at medium values of possible sunshine, and vice versa at high levels of possible sunshine.

(*f*) There appears to be a latitudinal effect but it tends to be swamped by variations in turbidity. It follows that the constants a and b must be selected with considerable meteorological intelligence, in the absence of local records which would enable them to be determined satisfactorily for a particular region. The most important factor to consider is the variation of the transmission characteristics of the atmosphere above the site in question at different times of the year.

Part II

The separation of direct radiation from diffuse radiation

The second step in the problem of calculating the monthly mean total daily radiation incident on inclined surfaces from sunshine data is to separate the diffuse radiation from the direct radiation.

Examination of the records of ten selected stations where observations of both total and diffuse radiation have been made immediately revealed that a linear regression equation could be derived from

Table 2. Values of a and b in regression equation $Q/Q = (a + b\ n/N)$

Station	*Latitude*	*Height above sea level (metres)*	*Period*	*No. of months*	*Value of a*	*Value of b*	*r*	*Range of monthly mean values of n/N*	*Annual mean values*		*Source of regression equation*
									Q/Q	*n/N*	
Stanleyville	0° 31′ N	437	Sept. 1952-Aug. 1953	12	.28	.40	.89	.28 — .55	.47	.47	Page
Nairobi	1° 16′ S	1 959	Jan. 1948-Apr. 1943	66	.24	.56	.97	.34 — .81	.56	.57	Page
Singapore	1° 18′ N	120	Aug. 1952-July 1953	12	.21	.48	.45	.32 — .56	.44	.48	Page
Leopoldville	4° 22′ S	450	Jan. 1951-Dec. 1951	12	.21	.52	.65	.31 — .52	.42	.41	Page
Trinidad	10° 38′ N	Not known	Aug. 1957-Aug. 1958	12	(.27)*	(.49)*	N. K.	Not known	Not known		Smith
Dakar	14° 43′ N	Not known	Jan. 1953-Dec. 1953	12	.10	.70	.86	.54 — .84	.60	.70	Page
Jamaica	18° N	Not known	Not known	12	(.31)*	(.49)*	N. K.	Not known	Not known		Cowan
Tananarive	18° 54′S	1 310	Mar. 1953-Feb. 1954	12	.30	.48	.96	.41 — .75	.57	.56	Page
Windhoek	22° 34′ S	1 728	Aug. 1951-Feb. 1954	31	.23	.55	.98	.61 — .95	.69	.81	Page
Pretoria	25° 45′ S	1 369	Jan. 1951-Feb. 1954	38	.27	.46	.97	.61 — .88	.61	.74	Page
Bloomfontein	29° S	1 422	Not known	24	(.25)*	(.50)*	N. K.	Not known	Not knwon		Glover *et al.*
Durban	29°50′ S	5	July. 1951-Feb. 1954	32	.33	.35	.99	.36 — .81	.52	.56	Page
Capetown	33° 54′ S	17	Sept. 1951-Feb. 1954	30	.20	.59	.99	.60 — .82	.62	.71	Page
Dry Creek	34.8 S	Not known	1947-1950	48	(.30)	(.50)	.95	Not known	.60	.59	Black *et al.*
Mount Stromlo	35.3 S	770	1928-1939	144	(.25)	(.54)	.89	Not known		.63	Black *et al.*
Versailles	48.8 N	Not known	1935-1951	99	(.23)	(.50)	.90	Not known	.44	.42	Black *et al.*
Gembloux	50.6 N	Not known	1939-1950	60	(.15)	(.54)	.83	Not known	.33	.33	Black *et al.*
Kew	51.5 N	19	1947-1951	60	.14	.66	.99	.17 — .46	.35	.33	Page
Rothamsted	51.8 N	Not known	1931-1940	84	(.18)	(.55)	.79	Not known	.37	.36	Black *et al.*

NOTES:

(i) Values in parentheses known not to be corrected to International Pyrhetrometric Scale or to solar constant of 2.00 gm. cals. cm^{-2}. min^{-1}.

(ii) * Values based on daily and not monthly values of n/N.

(iii) The following uncorrected alternative values are given by Glover & McCulloch based on daily values of n/N.

Nairobi . . . . . $a = 0.26$ $b = 0.57$ Windhoek . . . . $a = 0.26$ $b = 0.52$ Pretoria . . . . . $a = 0.25$ $b = 0.50$
Durban . . . . . $a = 0.26$ $b = 0.50$ Capetown . . . . $a = 0.29$ $b = 0.50$ Kew . . . . . $a = 0.17$ $b = 0.52$

Table 3. Value of constants *c* and *d* in regression equation $\frac{D}{Q} = c + d\frac{Q}{Q}$ for ten stations

Station	*Latitude*	*Height above sea level in metres*	*Length of record*	*Period*	*Value of c*	*Value of d*	*Correlation coefficient*	*Range of monthly mean values °/₀*	*Comments*
Stanleyville	0° 31′ N	437	12 months	Sept. 1952-Aug. 1953	1.07	— 1.16	.93	39 — 53	Hot humid climate
Leopoldville	4° 22′ S	450	23 months	Feb. 1951 -Dec. 1952	1.08	— 1.21	.96	32 — 52	Hot humid climate
Windhoek	22° 34′ S	1 728	31 months	Aug. 1951-Feb. 1954	0.88	— 0.95	.95	57 — 78	Hot dry climate — high
Pretoria	25° 45′ S	1 369	38 months	Jan. 1951-Feb. 1954	0.98	— 1.16	.93	55 — 69	Hot dry climate — high
Tananarive	18° 53′ S	1 310	13 months	Feb. 1953-Feb. 1954	1.20	— 1.39	.89	48 — 65	Hot humid climate — high
Durban	29° 50′ S	5	32 months	July 1951-Feb. 1954	1.10	— 1.43	.97	46 — 61	Hot humid climate
Capetown	33° 54′ S	17	30 months	Sept. 1951-Feb. 1954	1.07	— 1.26	.93	56 — 68	Mediterranean type climate
Blee Hill	42° 13′ N	205	48 months	Nov. 1945-Oct. 1949	0.72	— 0.67	.75	37 — 63	Temperate climate. Based on weekly values
Uccle	50° 49′ N	120	24 months	Jan. 1949-Dec. 1950	0.96	— 1.01	Fitted by eye	9 — 68	Temperate climate. Mean value for March, June and September
Kew	51° 28′ N	19	60 months	Jan. 1947-Dec. 1951	.94	— 1.03	.98	24 — 45	Temperate climate

the published observations, linking the ratio of diffuse radiation on a horizontal plane to the total radiation with the atmospheric transmission Q/Q_o. Thus we have the relationship

$$D_H/Q = c + d\,Q/Q_o \qquad [5]$$

where D_H is the monthly mean daily diffuse radiation on a horizontal plane, c and d are constants, climatologically determined. Q and Q_o have the same meaning as before.

This equation, like the typical Ångström formula, does not hold for daily values. It is reasonably valid, however, even under these daily conditions except when the weather is overcast or nearly overcast and on completely clear days when the regression equation leads to an underestimate of the value of D_H/Q. This ratio reaches a value of 1.00 on overcast days for a value of Q/Q_o approximately equal to 0.20. However, this paper is concerned with climatological mean values, and not with daily values.

The regression constants derived for the ten stations so far studied are given in table 3. All values are based on the International Pyrheliometric Scale and a value of the solar constant of 2.00 gm. cals. cm.$^{-2}$ min.$^{-1}$. There is some variation from station to station, but a full climatological explanation of these variations has not been found yet. One difficulty was to discover whether the appropriate correction had been applied for the shading ring, and if the correction was properly determined climatologically. This was known to be the case for the South African stations (5) and for the Congo stations. A correction was applied to the Kew observations but this was based on isotropic distribution of diffuse radiation, and was not climatologically determined.

Clearly low values of D_H/Q are normally associated with regions of great clarity, and high values of D_H/Q with regions of high turbidity. It is therefore possible to select from table 3 values of c and d which appear reasonable for a particular area, by considering the characteristics of the atmosphere in that region. The mean regression equation for the ten stations is

$$D_H/Q = 1.00 - 1.13\,Q/Q_o \qquad [6]$$

Thus the values of D_H can be easily calculated using the values of Q/Q_o previously obtained by use of the Ångström type formula. Calculations for humid tropical regions immediately show that about half the mean daily total radiation on horizontal surfaces is diffuse scattered radiation.

The monthly mean direct radiation on the horizontal plane (i.e., $\Sigma I_D \sin\theta$ where I_D is the direct radiation intensity normal to the sun's rays and θ is the solar altitude) can now be found by difference:

$$\Sigma I_D \sin\theta = Q - D_H \qquad [7]$$

The regression equation for the diffuse radiation is, of course, of parabolical form for, rearranging the equation, we have

$$D_H = cQ + \frac{dQ^2}{Qo} \qquad [8]$$

The maximum value of D_H which is equal to $-\frac{c^2 Q_o}{4d}$ occurs when $Q/Q_o = \frac{c}{2d}$. Since $Q/Qo = a + b\,\frac{n}{N}$, it follows that the corresponding value of $\frac{n}{N}$ is $\left(\frac{-c}{2db} - \frac{a}{b}\right)$. Using the mean values of a, b, c, and d obtained from tables 2 and 3, we have max. = 0.221 Qo. It occurs when $Q/Qo = 0.44$ or $\frac{n}{N} = .40$. The maximum diffuse radiation thus occurs on partly clouded days and not on clear or overcast days.

All the observations confirm the fact that linear interpolation between diffuse radiation on clear days and overcast days gives completely erroneous results, and that this theoretical parabolical relationship does actually represent the observations with reasonable accuracy. Certain European studies have been based on the assumption that D_H is not a function of $\frac{n}{N_o}$ (16, 17). This assumption happens to be approximately true, if one is concerned with that part of the parabolic curve near the maximum which is often the case in European centres where $\frac{n}{N}$ approximates to 35 - 50 per cent. The assumption is certainly not sound in the hot dry arid regions of the world.

Part III

The estimation of direct radiation on inclined surfaces

The third stage in the problem is to convert the climatological mean values obtained for horizontal incidence to appropriate values for inclined planes. The direct and the diffuse radiation must be handled separately at this stage.

The method proposed in this paper to convert the mean daily radiation on the horizontal plane to mean daily direct radiation on inclined planes is based on the use of conversion factors derived in the following way:

(*a*) A standard direct radiation curve representative of tropical conditions was selected. This curve is given in table 4. Values slightly lower than Moon's standard curve (11) were adopted, which it was hoped would be more representative of general tropical conditions at stations reasonably close to sea level. The turbidity of the tropical atmosphere is often high, either because of the high moisture or high dust content of the air.

(*b*) Using the standard astronomical formulae, tables of incidence factors were prepared at hourly

Table 4. Values of the direct intensity of the solar beam on a surface normal to the sun's rays with altitude of the sun used to construct table 5

Units: Cals. cm^{-2} min^{-1}. International Pyrheliometric Scale

Solar altitude	*Direct intensity* I_D
0°	.00
5°	.28
10°	.57
15°	.72
20°	.84
25°	.96
30°	1.04
40°	1.15
50°	1.21
60°	1.25
70°	1.27
80°	1.28
90°	1.28

intervals for latitudes 0 - 60° for declinations 0, ± 10°, ± 20°, ± 23°27′ for vertical north south surfaces, vertical east west surfaces and horizontal surfaces. From these basic tables of incidence factors on three planes at right angles, factors for any other surfaces could be rapidly obtained with little further calculation by simple trignometrical methods.

(*c*) The following surfaces were selected for detailed study:

1. Vertical facing equator.
2. Vertical facing away from equator.
3. Vertical east or west.
4. Inclined at 45° to horizontal facing equator.
5. Inclined at tilt equal to latitude facing the equator.

Using the standard radiation curve given in table 4, calculations were made of the direct radiation intensities at hourly intervals on the above five surfaces. The hourly values were plotted graphically, and the daily totals were found by planimetry, together with the daily totals for the horizontal plane.

(*d*) These daily totals were smoothed by use of difference tables as a check against graphical errors in integration. The ratios of the daily direct radiation on the selected planes to the corresponding daily direct radiation on a horizontal plane was calculated for different latitudes at suitable values of the declination. The conversion factors were plotted against declination, and appropriate values for each month were found from the curves. In this way, a series of conversion factors was obtained to convert daily values of $\Sigma I_D \sin \theta$ to corresponding values for the inclined surfaces in question.

The results of this very extended and tedious series of calculations are given in table 5, which covers latitudes 0°-40°. (Conversion factors are available up to 60°.) The conversion factors are given for each month at suitable intervals of latitude for different surfaces. The computed value of $\Sigma I_D \sin \theta$ is merely multiplied by the appropriate factor obtained from the table to find the monthly mean daily direct radiation on the plane in question.

Factors for surfaces other than those actually given in table 5 may sometimes be derived by simple trigonometrical resolution. The essential condition is whether the direct radiation will reach the collector throughout the day at a particular time of year or not, for radiation falling behind the collector must not be considered as negative, but zero. Thus, if we consider an inclined surface facing the equator, in the winter half of the year, normal trigonometrical resolution can be used, for the sun will always reach the surface and can never be behind. This will not be true in summer when the sun will move on the poleward side of the surface for at least part of the day. For example, the factor for a south facing inclined surface at 40°N. tilted at 60° to the horizontal is equal to (1 × cos. 60 + .93 × sin (60) on March 15. However, on June 15th, the factor is *not* equal to (1 × cos. 60 + 0.19 × sin) because the northwards component has been ignored, and the integration condition makes it impossible to take account of the correction from table 5.

The validity of this method of computation depends on the following assumptions:

(*a*) That the sunshine is evenly distributed throughout the day, and is not markedly asymmetrical about noon. This is not always so.

(*b*) That the standard radiation curves are appropriate for average conditions.

The advantages from the computional point of view in working with ratios of radiation values are:

(*a*) The same values of the ratios are obtained for both hemispheres, and no correction for variations in solar distance are required. All the necessary corrections are already incorporated in table 1.

(*b*) Since the Ångström type formulae suggested can make some allowance in variations of transparency according to local conditions, and the values of the conversion factors being ratios are relatively insensitive to change of turbidity, the computed values obtained for inclined surfaces are likely to be more reliable than might be expected from the conventional use of standard radiation curves.

Part IV

Estimation of the diffuse radiation incident on vertical and inclined planes

The diffuse short wave radiation on inclined planes is made up of two parts, radiation diffusely scattered from the sky and radiation diffusely

Table 5. Ratio of direct radiation on inclined surfaces to direct radiation on a horizontal surface at different times of the year for latitudes 40° N-40° S, based on standard radiation curve given in table 3

Column 1. Vertical surface facing equator: horizontal surface; Column 2. Vertical surface facing pole: horizontal surface; Column 3. Vertical surface facing east or west: horizontal surface; Column 4. Vertical surface facing equator tilted at 45° to horizontal: horizontal surface; Column 5. Vertical surface facing equator tilted at angle to horizontal equal to latitude: horizontal surface

Date		*Approx. declination*	*Latitude 0°*				*Latitude 10°*				*Latitude 20°*				*Latitude 30°*				*Latitude 40°*			
N. Hemi.	*S. Hemi.*		*1*	*2→*	*3→*	*4→*	*1*	*2*	*3*	*4*	*1*	*2→*	*3→*	*4→*	*1*	*2*	*3*	*4*	*1*	*2→*	*3*	*4*
Jan. 15	July 17 . .	— 21.3	.53	—	.39	1.09	.76	—	.40	1.24	1.07	—	.43→	1.47	1.49	—	.49	1.75	2.11	—	.57	2.22
Feb. 15	Aug 19 . .	— 13.0	.31	—	.39	.94	.51	—	.40	1.07	.75	—	.42→	1.23	1.06	—	.46	1.44	1.50	—	.53	1.75
Mar. 15	Sept 18 . .	— 2.5	.04	—	.39	.74	.23		.39	.86	.43	—	.41→	1.00	.64	—	.44	1.16	.93	—	.49	1.36
Apr. 15	Oct. 18 . .	+ 9.5	—	.25	.39	.53	—	.14	.39	.65	.16	.06	.39→	.78	.29	.02	.42	.91	.48	.01	.46	1.04
May 15	Nov. 17 . .	+ 18.7	—	.48	.39	.40	—	.31	.38	.52	.02	.16	.39→	.64	.13	.07	.41	.75	.27	.06	.44	.87
June 15	Dec. 17 . .	+ 23.3	—	.58	.38	.33	—	.39	.38	.45	—	.21	.38	.57	.06	.12	.40	.68	.19	.09	.43	.80
June 21	Dec. 22 . .	+ 23.5	—	.59	.38	.31	—	.40	.38	.45	—	.22	.38	.56	.05	.12	.40	.67	.18	.09	.42	.79
July 15	Jan. 13 . .	+ 21.6	—	.55	.38	.35	—	.37	.38	.47	—	.20	.38	.59	.09	.10	.40	.70	.22	.08	.43	.82
Aug. 15	Feb. 11 . .	+ 14.2	—	.35	.39	.46	—	.22	.38	.58	.09	.10	.39	.71	.21	.04	.41	.82	.37	.03	.45	.95
Sept. 15	Mar. 12 . .	+ 3.4	—	.09	.39	.64	.11	.05	.39	.76	.28	.02	.40	.90	.45	Tr.	.43	1.03	.69	Tr.	.48	1.20
Oct. 15	Apr. 11 . .	— 8.2	.20	—	.39	.86	.40	—	.39	.99	.62	—	.42	1.14	.88	—	.46	1.33	1.24	—	.52	1.57
Nov. 15	May 13 . .	— 18.3	.46	—	.39	1.04	.67	—	.40	1.18	.95	—	.43	1.39	1.33	—	.48	1.63	1.86	—	.56	2.03
Dec. 15	June 13 . .	— 23.2	.58	—	.38	1.12	.81	—	.40	1.27	1.13	—	.44	1.52	1.58	—	.49	1.83	2.28	—	.58	2.34
Dec. 22	June 21 . .	— 23.5	.59	—	.38	1.13	.83	—	.40	1.29	1.16	—	.44	1.53	1.61	—	.49	1.84	2.36	—	.59	2.38

Jan. 15	July 17 . .	— 21.3	.53	—	.39	1.09	1.00	.76	—	.40	1.24	1.12	1.07	—	.43→	1.47	1.31	1.49	—	.49	1.75	1.61	2.11	—	.57	2.22	2.15
Feb. 15	Aug 19 . .	— 13.0	.31	—	.39	.94	1.00	.51	—	.40	1.07	1.07	.75	—	.42→	1.23	1.20	1.06	—	.46	1.44	1.40	1.50	—	.53	1.75	1.72
Mar. 15	Sept 18 . .	— 2.5	.04	—	.39	.74	1.00	.23		.39	.86	1.02	.43	—	.41→	1.00	1.08	.64	—	.44	1.16	1.18	.93	—	.49	1.36	1.35
Apr. 15	Oct. 18 . .	+ 9.5	—	.25	.39	.53	1.00	—	.14	.39	.65	.96	.16	.06	.39→	.78	.97	.29	.02	.42	.91	.99	.48	.01	.46	1.04	1.07
May 15	Nov. 17 . .	+ 18.7	—	.48	.39	.40	1.00	—	.31	.38	.52	.93	.02	.16	.39→	.64	.90	.13	.07	.41	.75	.89	.27	.06	.44	.87	.90
June 15	Dec. 17 . .	+ 23.3	—	.58	.38	.33	1.00	—	.39	.38	.45	.92	—	.21	.38	.57	.87	.06	.12	.40	.68	.84	.19	.09	.43	.80	.84
June 21	Dec. 22 . .	+ 23.5	—	.59	.38	.31	1.00	—	.40	.38	.45	.91	—	.22	.38	.56	.87	.05	.12	.40	.67	.84	.18	.09	.42	.79	.83
July 15	Jan. 13 . .	+ 21.6	—	.55	.38	.35	1.00	—	.37	.38	.47	.92	—	.20	.38	.59	.87	.09	.10	.40	.70	.85	.22	.08	.43	.82	.85
Aug. 15	Feb. 11 . .	+ 14.2	—	.35	.39	.46	1.00	—	.22	.38	.58	.94	.09	.10	.39	.71	.93	.21	.04	.41	.82	.94	.37	.03	.45	.95	.98
Sept. 15	Mar. 12 . .	+ 3.4	—	.09	.39	.64	1.00	.11	.05	.39	.76	.99	.28	.02	.40	.90	1.02	.45	Tr.	.43	1.03	1.09	.69	Tr.	.48	1.20	1.20
Oct. 15	Apr. 11 . .	— 8.2	.20	—	.39	.86	1.00	.40	—	.39	.99	1.05	.62	—	.42	1.14	1.16	.88	—	.46	1.33	1.30	1.24	—	.52	1.57	1.57
Nov. 15	May 13 . .	— 18.3	.46	—	.39	1.04	1.00	.67	—	.40	1.18	1.10	.95	—	.43	1.39	1.27	1.33	—	.48	1.63	1.53	1.86	—	.56	2.03	1.98
Dec. 15	June 13 . .	— 23.2	.58	—	.38	1.12	1.00	.81	—	.40	1.27	1.12	1.13	—	.44	1.52	1.33	1.58	—	.49	1.83	1.65	2.28	—	.58	2.34	2.26
Dec. 22	June 21 . .	— 23.5	.59	—	.38	1.13	1.00	.83	—	.40	1.29	1.13	1.16	—	.44	1.53	1.34	1.61	—	.49	1.84	1.67	2.36	—	.59	2.38	2.30

NOTE: This table is based on graphical interpretations and the order of accuracy is about $\neq \pm 1$ per cent.

reflected from the ground. If we assume that the diffuse radiation is isotropically distributed, the total radiation on a plane S will be given by the formula:

$$\Sigma (I + D + r)_s^0 = \Sigma I_s + \left(\frac{1 + \cos \alpha}{2}\right) D_H + \left(\frac{1 - \cos \alpha}{2}\right) r_H$$

$$= f_s \Sigma I_D \sin \theta + \cos^2 \frac{\alpha}{2} D_H + \sin^2 \frac{\alpha}{2} r_H \qquad [9]$$

where f_s is the slope conversion factor for slope S for a particular month, where ΣI_D sin θ and D_H are the monthly mean daily values of the direct and diffuse radiation on a horizontal plane, where α is the angle of inclination of the slope to the horizontal plane, and where r_H is the diffuse flux reflected from the ground.

The reflected flux will be equal to YQ where Y is the albedo of the surface to short wave radiation and Q is the monthly mean daily total radiation, provided that the ground is not overshadowed. This will normally be the case for the majority of solar energy collectors which are orientated to face the equator for maximum collection efficiency.

Equation [9] gives the incoming monthly mean daily total radiation correctly, provided the isotropic approximation is valid. This assumption must now be examined in detail for it is well known that the diffuse radiation is not isotropic. Unfortunately, average conditions have never been studied in detail, though it is believed that work is going on now in this direction in Russia under the control of Kondratiev. Considerable attention has, however, been given to cloudless conditions, and among the more useful studies in this field may be mentioned the studies of Kondratiev and Manolova in Russia (8) and the work of Parmelee in America (13). Parmelee's work is confined to instantaneous values on vertical surfaces while Kondratiev's work deals with instantaneous values on inclined surfaces as well. Parmelee's work shows the great importance of atmospheric turbidity in determining the diffuse radiation on cloudless days. A decrease in the intensity of the direct beam is accompanied by an appreciable increase in the amount of diffuse radiation available. Kondratiev's work shows that there are certain compensating effects which may make the isotropic approximation more reliable for average conditions than would at first sight appear. An important factor influencing the radiation balance of inclined surfaces is the change of albedo of the ground surface with the angle of incidence. The albedo increases very appreciably at low angles of incidence. Another important factor is that appreciably higher diffuse radiation is received from the quadrant of the sky facing the sun than from the quadrant of the sky facing away from the sun. The isotropic approximation is not satisfactory on cloudless days, overestimating the radiation on surfaces away from the sun, and underestimating the radiation on surfaces facing the sun and on surfaces at right angles to the sun's azimuth as well. On overcast days, on the other hand, Kondratiev shows that the diffuse radiation balance of slopes can be estimated satisfactorily by the isotropic approximation.

There appears to be no published information about partly clouded days, but qualitative observation shows that there are two main factors influencing the diffuse radiation distribution:

(*a*) A tendency to find regions of high brightness of clouds close to the sun.

(*b*) A tendency to find regions of high brightness on clouds which stand opposite the sun giving significant back reflection, particularly to steeply inclined slopes, when the clouds are vertically deep, e.g., cumulus clouds.

The various factors mentioned above are to some degree compensatory. The author has made a preliminary study of the mean diffuse illumination values recorded by quadrants at Kew represented by McDermott and Gordon Smith (10). This study indicates, *for vertical surfaces* ($\alpha = 90°$) empirical correction factors might be applied to the daily diffuse radiation as calculated by the isotropic approximation as follows:

(*a*) Vertical or steeply inclined north-south surfaces facing the predominant direction of the sun, if the sun is reasonably low, i.e. $fs \geqslant 0.4$ multiply D_H by a factor of 1.2 before using in equation [9]. If sun is moderately high $fs \leqslant 0.4$ multiply by 1.1 before using in equation [9].

(*b*) Vertical or steeply inclined surfaces facing east or west. Morning excess tends to balance afternoon deficiency on east side and vice versa on west side. Apply no correction.

(*c*) Vertical or steeply inclined surfaces facing away from predominant direction of sun, multiply D_H by 0.8 before using in equation [9].

These corrections are extremely arbitrary, but it is difficult to see how more reliable corrections could be proposed in the light of existing knowledge. These corrections would not appear to be out of line with diffuse radiation data obtained by Tonne (16) for latitude 53°N by careful consideration of the directional characteristics of the sky hour by hour. Their only justification is that they appear to give acceptable results wherever it has been possible to check theoretical predictions against observed results. There are, of course, remarkably few observations of radiation on vertical and inclined surfaces, and most of these have been made in high latitudes.

For sloping north-south surfaces inclined between 30° and 60°, the same factor of 1.2 might be appropriate for surfaces facing the predominant direction

of the sun (provided $fs \geqslant 0.5$) and no correction be applied otherwise, nor to surfaces facing east or west. The factor for inclined surfaces facing away from the sun is likely on the evidence of Kondratiev and Manolova (8) to be somewhat lower than that for vertical surfaces facing away from the sun. This is a result of the fact that the region of the clear sky of lowest brightness is found at a point opposite the sun such that the angle between the altitude of this point and the sun's altitude is 90°. It might be reasonable to adopt a value of 0.75 D_H for such inclined surfaces in light of present knowledge. The whole matter obviously requires far more detailed exploration, however, than the author has been able to give to it.

For surfaces of low tilt, the isotropic approximation is likely to be satisfactory except for north-south surfaces facing the predominant direction of the sun when it might be reasonable to assume that the monthly mean daily diffuse radiation is invariant for tilts between 0°-30° and equal to D_H. In equatorial regions it should be remembered that the predominant direction of the sun changes from north to south according to the time of the year.

The albedo of the ground surface should, if at all possible, be determined locally in view of the wide variations which occur with different types of ground, covered or not as the case may be, with vegetation of different reflection having characteristics which will vary according to season and rainfall. In making such measurements it is essential that the total albedo should be measured by suitable instruments which record over the whole short wave spectrum. The correlation between the visual albedo and the total albedo is often poor, because most plants have a relatively high reflectivity in the infra-red region, and often a relatively low one in the visible. Typical values by Kondratiev, Mironova, and Daeva (9) show reflectivities for gross of the order of 10-15 per cent in the visible region and 40-50 per cent in the infra-red. A summary of the earlier measurements of albedo may be found in the Smithsonian Meteorological Tables (15). Typical values of the total albedo for green vegetation are 25 per cent, for dark soils 10 per cent, for desert sands 20-25 per cent, for dry grass 30 per cent. If detailed information is not available about ground albedo, it would appear reasonable to adopt values of the order of 20-25 per cent on rural sites covered with vegetation and 10-15 per cent on central urban sites, where building and road surfaces may predominate.

Conclusion

A method of calculating mean values of the total radiation on inclined planes from sunshine records has been given which can be used to calculate the optimum orientation of flat plate solar energy collectors. The technique proposed has been checked against the limited number of available meteorological observations of the mean monthly daily radiation on inclined surfaces and reasonable agreement between prediction and measurement has been achieved. The average error of the estimated radiation appears to be of the order of ± 10 per cent. The technique proposed for calculating the mean daily radiation is thus quite satisfactory for general engineering purposes and has the advantage of giving, with very little computation, the relative amounts of direct or diffuse radiation on the plane in question. In many parts of the humid tropics, diffuse radiation predominates. The optimum orientation of a collecting device is thus influenced very much by this factor. At latitude 40°N, for example, the optimum tilt for a collector to collect maximum energy in December is about 57° if the percentage of possible sunshine is 40 per cent and 64° if the percentage of possible sunshine is 75 per cent. The maximum mean daily total radiation available with 40 per cent possible sunshine is 180 cals. cm^2 day compared with 440 cals. cm^2 with 75 per cent possible sunshine. In the first case 45 per cent of the available energy is diffuse, in the second only 14 per cent is diffuse. Solar collectors must therefore be designed to take proper account of the radiation climate in which they are to be used. Efficient use of diffuse radiation is essential in the humid tropics where much cloud is often found. The author would particularly welcome any available information about measured mean values of short wave radiation on inclined surfaces in order to make a more systematic check on the validity of the method of analysis proposed.

References

1. Black, J. N., Bonython, C. W. and Prescott, J. A., *Quart. J. Roy. Met. Soc.*, 84, p. 231, 1954.
2. Blackwell, M. J., Five years' continuous recording of total and diffuse radiation at Kew Observatory, *M.R.P. 895*, Met. Off., London, 1954.
3. Brooks, C. E. P., Relation between the duration of bright sunshine registered by a Campbell-Stokes sunshine recorder and the estimated amount of cloud, *Met. Off. Prof. Notes No. 53*, H.M.S.O., London, 1929.
4. Drummond, A. J., The atmospheric transmission of solar energy over southern Africa, Notes, 3, pp. 272-286, 1954.
5. Drummond, A. J., On the measurement of sky radiation, *Arch. Met. Geoph.*, Serie B, 7, 413-436, 1956.
6. Glover, J. and McCulloch, J. S. G., *Quart. J. Roy. Met. Soc.*, 84, pp. 172-175, 1958.
7. Johnson, F. S., *J. Met.*, 2 (6), p. 131, 1954.
8. Kondratiev, K. J. and Manolova, M. P., Slopes radiation balance, *Reports at the Symposium on Radiation in Oxford*, Leningrad University, pp. 3-19, 1959.
9. Kondratiev, K. J., Mironova, Z. F. and Dava, L. V., Spectral Albedo of Snow and Vegetation Covers, International Geographical Year, University of Leningrad, 1960.

10. McDermott, L. M. and Gordon-Smith, G. W., Daylight illumination recorded at Teddington, Proc. Building Research Congress, London, 1951, Div. 3, pp. 156-161, 1951.
11. Moon, P., *Journ. Franklin Inst.*, 230, p. 583, 1940.
12. Nicolet, M. and Dogniaux, R., Étude de la radiation globale du soleil, *Inst. Roy. Met. Belg. Memoires*, 47, 50 pp, 1951.
13. Parmelee, G. V., Irradiation of vertical and horizontal surfaces by diffuse solar radiation from cloudless skies, *Heating, Piping and Air Conditioning*, Aug. 1954, pp. 129-135, 1954.
14. Smith, G. W., *Quart. J. Roy. Met. Soc.* 86, p. 415, 1960.
15. *Smithsonian Meteorological Tables*, 6th. Ed., Smithsonian Inst., Washington, 1951.
16. Tonne, F, and Norman, W., Die Berechnung der Sonnenwarmestrahlung auf senkrechte und beliebig geneigte Flachen unter Berücksichtigung. Meteorologischer Messungen, Institut für Tageslicht-technik, Stuttgart, 1956.
17. Pleijel, G., The computation of natural radiation in architecture and town planning, *Statens namnd for byggnadsforskning No. 25*, 1954.

Summary

A technique for calculating monthly mean values of total daily radiation on inclined surfaces from sunshine data has been proposed.

The first part deals with the calculation of mean values of total radiation on horizontal planes, using the conventional type of regression equation.

$$Q/Q_o = a + b\,\frac{n}{N}$$

where Q is the monthly mean daily total radiation, Q_o is the corresponding monthly mean daily radiation outside the atmosphere; a and b are constants which are climatologically determined; $\frac{n}{N}$ is the percentage of possible sunshine.

Values of a and b for various tropical stations are given in table 2, while values of Q_o may be found in table 1. It is suggested that the values of a and b should be selected that are representative of the transmission characteristics of the atmosphere in the locality under study.

The second part deals with the separation of the mean horizontal diffuse radiation from the total radiation, using a regression equation of the form

$$D_H/Q = c + d\,Q/Q_o$$

where D_H is the monthly mean daily diffuse radiation on a horizontal plane, where c and d are climatologically determined constants and where Q and Q_o have the same meaning as before.

The monthly mean value of the daily direct radiation on the horizontal plane $\Sigma I_D \sin\theta$ may be found from the relation

$$\Sigma\, I_D \sin\theta = Q - D_H$$

Values of c and d for various localities may be found in table 3. It is shown that maximum diffuse radiation occurs when $\frac{n}{N} = 40\text{-}50$ per cent.

The third part of this paper deals with the conversion of direct radiation on the horizontal plane to direct radiation on inclined planes. Table 5 contains a series of conversion factors f_s for latitudes 0-40° to convert values of $\Sigma I_D \sin\theta$ into values of I_s, the direct radiation on slope S.

Factors are given for the following surfaces

(1) Vertical facing equator,
(2) Vertical facing pole,
(3) Vertical facing east or west,
(4) Vertical facing equator tilted at 45° to horizon,
(5) Vertical facing equator tilted at angle to horizontal equal to latitude.

These factors are based on radiation curves drawn using standard radiation curve given in table 4.

The fourth part of this paper deals with the estimation of diffuse radiation on inclined surfaces using the isotropic approximation.

The total radiation on slope S is given by:

$$\Sigma\,(I + D + r)_s = \Sigma\, I_s + \left(\frac{1+\cos\alpha}{2}\right) D_H + \left(\frac{1-\cos\alpha}{2}\right) r_H$$

$$= f_s\, \Sigma\, I_D \sin\theta + \cos^2\frac{\alpha}{2}\, D_H + \sin^2\frac{\alpha}{2}\, \pi_H$$

where $f_s\ \Sigma I_D \sin\theta$ is the direct radiation on the slope of inclination

$\cos^2\frac{\alpha}{2}\ D_H$ is the diffuse radiation from the sky on the slope

$\sin^2\frac{\alpha}{2}\ r_H$ is the diffuse radiation from the ground.

The value of r_H will be equal to YQ, if the ground is not overshadowed, where Y is the total short wave albedo (not visual albedo).

The limitations of the isotropic approximation are discussed and certain empirical correction factors are proposed to take account of orientation.

The need for further field observations is stressed as well as the fact that the method of analysis is restricted to monthly mean values of possible

sunshine and so is not applicable to daily values of sunshine. The accuracy of prediction appears to be of the order of ± 5 per cent for monthly means. It is shown that collector orientation for maximum efficiency is influenced very much by the diffuse radiation climate in any locality and it is suggested that attention must be given to the problem of properly utilising this diffuse energy in flat plate collectors, particularly in the humid tropics where half the available energy may be diffuse.

ÉVALUATION DES VALEURS MOYENNES MENSUELLES DU RAYONNEMENT TOTAL A ONDES COURTES SUR LES SURFACES VERTICALES ET INCLINÉES, D'APRÈS LES RELEVÉS D'ENSOLEILLEMENT POUR LES LATITUDES 40° N ET 40° S

Résumé

On a proposé une technique de calcul des valeurs moyennes mensuelles du rayonnement quotidien total pour les surfaces inclinées, à partir des données d'ensoleillement.

La première partie du mémoire porte sur le calcul des valeurs moyennes du rayonnement total sur des plans horizontaux, en se servant de l'équation classique de régression :

$$Q/Q_o = a + b\,\frac{n}{N}$$

dans laquelle Q est la moyenne quotidienne du rayonnement total sur un mois, Q_o la moyenne quotidienne extra-atmosphérique correspondante, et a et b des constantes climatologiques, $\frac{n}{N}$ étant le pourcentage d'ensoleillement possible.

Le tableau 2 donne les valeurs de a et b pour les divers postes tropicaux, et le tableau 1 donne les valeurs de Q_o. L'auteur suggère que les valeurs de a et b soient choisies pour bien représenter les caractéristiques de transmission de l'atmosphère dans la localité à l'étude.

La deuxième partie du mémoire porte sur la séparation du rayonnement moyen horizontal diffus et du rayonnement total, en se servant d'une équation de régression de la forme :

$$D_H/Q = c + d\,Q/Q_o$$

dans laquelle D_H est le rayonnement diffus quotidien moyen sur un plan horizontal, c et d sont des constantes déterminées climatologiquement, et Q et Q_o ont la même signification qu'auparavant.

La valeur moyenne mensuelle du rayonnement quotidien direct sur le plan horizontal, $\Sigma I_D \sin\theta$, peut être tirée du rapport $\Sigma I_D \sin\theta = Q - D_H$.

Le tableau 3 donne les valeurs de c et d pour diverses localités. L'auteur montre que le rayonnement diffus maximum se produit quand $\frac{n}{N} = 40$ à 50 p. 100.

La troisième partie de ce mémoire porte sur la conversion du rayonnement direct sur le plan horizontal en rayonnement indirect sur les plans inclinés. Le tableau 5 contient une série de facteurs de conversion, correspondant aux latitudes 0-40°, pour transformer les valeurs de $\Sigma I_D \sin\theta$ en valeurs de I_s, rayonnement direct sur la pente S.

Le mémoire donne les facteurs pour les surfaces suivantes :

1) Verticale, tournée vers l'équateur;
2) Verticale, tournée vers le pôle;
3) Verticale, faisant face à l'est ou à l'ouest;
4) Verticale, faisant face à l'équateur et inclinée à 45° sur l'horizontale;
5) Verticale, faisant face à l'équateur et inclinée sur l'horizontale d'un angle égal à la latitude.

Ces facteurs sont basés sur des courbes de rayonnement établies en se servant de la courbe de rayonnement standard du tableau 4.

La quatrième partie de la communication porte sur les évaluations du rayonnement diffus sur les surfaces inclinées, en se servant de l'approximation isotropique.

Le rayonnement total sur la pente S est donné par :

$$\Sigma\,(I + D + r)_s = \Sigma\, I_s + \left(\frac{1+\cos\alpha}{2}\right) D_H + \left(\frac{1-\cos\alpha}{2}\right) r_H$$

$$= f_s\, \Sigma\, I_D \sin\theta + \cos^2\frac{\alpha}{2}\, D_H + \sin^2\frac{\alpha}{2}\, r_H$$

expression dans laquelle

$f_s \Sigma I_D \sin\theta$ est le rayonnement direct sur la pente d'inclinaison,

$\cos^2\frac{\alpha}{2}\, D_H$ est le rayonnement diffus du ciel sur la pente,

$\sin^2\frac{\alpha}{2}\, r_H$ est le rayonnement diffus du sol.

La valeur de r_H sera égale à YQ si le sol n'est pas ombragé, Y étant l'albédo total ondes courtes (et non pas l'albédo visuel).

Les limitations de l'approximation isotropique sont passées en revue et certaines corrections empiriques sont proposées pour tenir compte de l'orientation.

L'auteur souligne le besoin d'autres observations sur place, ainsi que le fait que la méthode d'analyse est limitée à des valeurs moyennes mensuelles de

l'ensoleillement possible, et ne peut donc pas s'appliquer à des valeurs quotidiennes. L'exactitude des prédictions semble être de l'ordre de $\pm$ 5 p. 100 pour des moyennes mensuelles. L'auteur montre que l'orientation du collecteur, pour avoir le maximum de rendement, dépend beaucoup du climat de rayonnement diffus en tous lieux, et ce mémoire suggère qu'on doit s'attacher au problème d'utiliser convenablement cette énergie diffuse sur des collecteurs à plaque, particulièrement dans les tropiques humides où la moitié de l'énergie disponible peut être diffuse.

ÉNERGIE SOLAIRE : LES RÉSEAUX ET LES INSTRUMENTS ACTINOMÉTRIQUES

C. Perrin de Brichambaut *

Avant la dernière guerre mondiale de 1940, l'étude du rayonnement solaire était particulièrement à l'honneur en France, et les noms de Maurain, Brazier ou Gorczinsky avaient acquis une réputation internationale, au même titre que le centre actinométrique de Trappes.

Entre 1940 et 1956, après les destructions totales dues à la guerre, seules les mesures spéciales ou épisodiques ont pu être effectuées, en particulier à l'observatoire du Parc Saint Maur. Heureusement, l'A.G.I. a permis l'implantation d'un réseau de mesures dans les anciens territoires français d'Afrique, réseau qui doit s'étendre à la France métropolitaine dès cette année (1961).

Buts poursuivis

L'intérêt d'un réseau de mesures actinométriques est généralement d'abord d'ordre pratique, pour des fins utilitaires immédiates. Il s'agit en effet de caractériser les climats actinologiques de diverses régions, en vue de pouvoir fournir à de nombreux utilisateurs les renseignements qui leur sont nécessaires :

a) L'agriculture, qui cherche à préciser la grandeur des échanges énergétiques naturels en vue de mieux définir le mécanisme d'action du complexe hydrothermique, surtout dans ses recherches concernant l'évapotranspiration;

b) L'architecture et l'urbanisme, qui doivent connaître les possibilités d'utilisation du rayonnement solaire, et surtout les nécessités de protection, selon le lieu et l'époque;

c) Le bureau d'études, qui conçoit et construit les divers appareils (fours, distillateurs, chauffe-eau, réfrigérateurs solaires) adaptés à chaque zone climatologique d'utilisation;

d) La météorologie, à qui la détermination des bilans radiatifs au sol et à divers niveaux permettra enfin de tenir compte de ces facteurs primordiaux pour l'élaboration de ses prévisions.

Éléments à mesurer

Avant tout autre élément, il semble nécessaire de pouvoir mesurer le rayonnement solaire global parvenant sur une surface horizontale : c'est en effet l'origine de tous les échanges radiatifs et énergétiques ultérieurs, et sa détermination reste ainsi un besoin fondamental pour tous les utilisateurs de données actinologiques. En particulier, la simple mesure de la somme quotidienne de ce rayonnement global permet actuellement de satisfaire la plupart des besoins habituels.

Cependant, il s'avère parfois nécessaire de séparer les diverses composantes de ce rayonnement, ou de détailler son évolution au cours d'une journée : cette obligation se traduit pratiquement par l'enregistrement complémentaire des rayonnements directs (provenant uniquement du soleil) ou diffus (provenant du ciel et des nuages), et par la possibilité de calculer les sommes horaires de ces rayonnements.

Enfin, pour améliorer l'exactitude des calculs afin d'apporter toutes les corrections et précisions utiles à l'exploitation complète des données actinométriques, l'étape finale des mesures consiste à enregistrer le bilan radiatif (au sol) de l'ensemble des rayonnements solaires, terrestre et atmosphérique.

Le rayonnement solaire global

Mesuré à l'aide d'instruments officiellement dénommés « pyranomètres », il peut être estimé avec des précisions très variables selon le type d'appareil utilisé et la méthode d'exploitation employée (étalonnage initial, dépouillement, contrôles).

Quelques appareils simples ont souvent été proposés, offrant théoriquement de grandes facilités de maintenance en réseau. Il s'agit en particulier des pyranomètres bimétalliques du type Robitzsch et des pyranomètres (sphériques) à distillation du type Bellani : les uns et les autres ne permettent finalement que la mesure des sommes quotidiennes, et avec une précision ne dépassant pas $\pm$ 10 p. 100. Les premiers donnent un enregistrement continu en fonction du temps, et exigent ainsi un planimétrage de surface pour cette détermination, alors que les seconds donnent uniquement et très simplement la somme quotidienne. Tous ces appareils, assez robustes et pas chers, exigent cependant des contrôles fréquents, sur place, ainsi que l'adoption de plusieurs facteurs d'étalonnage liés au lieu et à la saison. Ce dernier point, ainsi que leur manque habituel de fidélité, les fait encore souvent rejeter pour l'équipement d'un réseau.

En fait, la méthode classique actuelle consiste très généralement à installer des thermopiles à

* Ingénieur de la Météorologie nationale, Observatoire de Trappes, France.

surface réceptrice horizontale, et à enregistrer leurs données à l'aide d'un galvanomètre ou d'un potentiomètre enregistreur. Malgré une certaine fragilité des appareils enregistreurs, cette méthode s'avère sûre et souple, et permet le dépouillement aussi bien en valeurs instantanées qu'en sommes horaires ou quotidiennes. Dans des conditions normales d'exploitation en réseau, il semble qu'une précision finale de ± 5 p. 100 puisse être obtenue, sous réserve d'utiliser des thermopiles de construction correcte.

Afin de permettre le dépouillement immédiat des enregistrements, divers systèmes intégrateurs existent et peuvent être couplés au potentiomètre enregistreur. Malheureusement, il s'agit souvent de solutions coûteuses et parfois délicates. Un totalisateur à compteur, simple, robuste et fonctionnant sur batterie, est actuellement en cours de réalisation en France pour tenter de résoudre ce problème.

Les composantes du rayonnement global

Pour mieux préciser la composition spectrale du rayonnement global et son origine directe ou diffuse, il est nécessaire de se livrer à la mesure séparée de ses composantes (directe ou diffuse), et généralement de les enregistrer pour pouvoir en effectuer une étude détaillée.

Dans ce but, une excellente solution consiste à utiliser un pyrhéliographe, ou plus exactement un pyrhéliomètre équipé d'une monture équatoriale. Cependant, l'entretien du pyrhéliomètre, le réglage de la monture, et l'exploitation difficile des enregistrements réduit l'intérêt de cette solution à son seul usage dans des stations centrales ou des laboratoires de recherches dotés de personnel spécialisé. Pour des besoins courants, il semble d'ailleurs que le simple héliographe soit très suffisant : le paragraphe suivant traitera de cet instrument.

Une autre solution consiste à disposer d'une deuxième thermopile avec enregistreur, et de mesurer uniquement le rayonnement diffus, en abritant la surface réceptrice du rayonnement direct à l'aide d'un disque-écran à monture équatoriale, ou, plus pratiquement, à l'aide d'une bande annulaire pare-soleil. On obtient alors l'enregistrement du rayonnement diffus, et cet appareil est parfois dénommé diffusographe. L'exploitation de ces données reste encore longue et délicate, bien que du plus grand intérêt pour la caractérisation du trouble atmosphérique, et doit être menée en fonction des observations météorologiques courantes.

Faute de bureau d'étude spécialisé procédant systématiquement à leur contrôle, à leur dépouillement et à leur exploitation, ces enregistrements s'avèrent généralement inutilisables et inutiles.

Pratiquement, quelques mesures complètes au pyrhéliomètre (équipé de filtres) lors des tournées de contrôle sont toujours nécessaires et souvent suffisantes. Il est aussi possible de prévoir un disque-écran adaptable à la thermopile mesurant le global, régulièrement employé par l'observateur lors de journées de ciel bleu, et permettant ainsi la mesure du diffus pour certaines masses d'air prédéterminées.

La durée d'insolation

Mesurée par des appareils de principes assez divers, la durée d'insolation est sans conteste l'élément actinologique le mieux connu. Plusieurs modèles d'instruments existent (Pers, Marvin, Jordan), mais le type Campbell actuellement recommandé par l'OMM se révèle nettement le plus simple, sûr et fidèle, sous réserve de l'utiliser avec des bandes d'enregistrement de caractéristiques bien déterminées et de dépouiller les diagrammes selon des méthodes clairement précisées.

Il est effectivement remarquable et assez inattendu de constater les enseignements multiples que peut apporter un héliogramme convenablement exploité, tant sur la répartition diurne de l'insolation que sur le type de nuages présents, la variation du rayonnement direct, et même l'ordre de grandeur du rayonnement global. Dans ce dernier but, de nombreux travaux ont permis de déterminer des relations statistiques simples entre la durée d'insolation et la somme du rayonnement global, permettant une précision de ± 10 p. 100 et parfois mieux sur les moyennes décadaires.

Il suffit de disposer de quelques stations actinométriques correctement équipées de pyranographes et héliographes, et judicieusement réparties pour être représentatives des diverses régions climatiques étudiées. Il est alors possible soit d'étendre dans l'espace l'estimation du rayonnement global par de simples mesures héliographiques (Ångström), soit d'interpoler ou d'extrapoler dans le temps pour ces stations les valeurs du rayonnement global grâce aux seuls relevés d'insolation (Dogniaux, Hinzpeter).

Par ailleurs, un simple héliographe peut ainsi suffire pour contrôler, et même éventuellement compléter, les enregistrements des pyranographes. Pour toutes ces raisons, et selon les conseils de la CIMO, la France procède actuellement à l'extension du réseau d'héliographes Campbell et à des travaux portant sur le choix rationnel de la couleur et des caractéristiques des bandes d'enregistrement à employer.

De nombreuses études sont en cours, au sein des divers Groupes de travail sur le rayonnement de l'OMM, pour préciser les liens statistiques existant entre l'insolation et le rayonnement global, selon le lieu et l'époque : il ne reste qu'à espérer d'ici peu des conclusions précises et encourageantes dans cette voie.

Le bilan radiatif

En admettant que la mesure du rayonnement solaire global sur une surface horizontale soit réalisée par l'une ou l'autre des méthodes retenues précédemment, un autre problème se pose assez rapide-

ment pour des calculs d'échanges énergétiques plus détaillés : c'est celui de la mesure des rayonnements terrestre ou atmosphérique, de longueurs d'onde comprises entre 3 et 100 microns. En particulier, le bilan radiatif total au sol est d'utilisation courante et doit pouvoir être enregistré et étudié.

Il existe dans ce but divers instruments de précisions, de prix et de commodités d'exploitation très variables, mais les bilanmètres utilisables en réseau sont assez peu nombreux. On peut en citer deux types généraux, toujours à couples thermo-électriques : à coupelles protectrices transparentes dans l'infrarouge (Schultze) et à ventilation forcée en surface (Gier et Dunkle). Malheureusement, leur étalonnage et leur contrôle restent difficiles, et leur fidélité est souvent douteuse. De plus, l'exploitation complète des enregistrements, longue et délicate, en restreint l'emploi aux stations centrales dotées de plusieurs spécialistes.

Diverses études sont actuellement en cours, aussi bien pratiques, de manière à trouver un bilanmètre simple et fidèle, que théoriques, afin de découvrir les liens statistiques existant entre le bilan radiatif et les relevés météorologiques courants. Ainsi, l'exploitation des radiosondages en altitude grâce aux divers abaques de rayonnement existants, combinée avec les observations météorologiques normales (températures, tension de vapeur d'eau au sol, nature et nébulosité des nuages) permet actuellement d'approcher assez correctement les valeurs des échanges radiatifs dans l'infrarouge.

Par ailleurs, il semble que l'enregistrement des températures, en surface et dans le sol à diverses profondeurs, puisse donner une bonne appréciation du bilan énergétique total, faisant intervenir tant le rayonnement total que les échanges thermiques par conduction-convection et par évaporation-condensation : c'est là d'ailleurs souvent le but final recherché par plusieurs utilisateurs.

Réseaux actinométriques

En tête d'un réseau actinométrique national doit évidemment se trouver un centre de contrôle possédant tous les étalons pyrhéliométriques et électriques nécessaires pour assurer le maintien de l'échelle (IPS 56) et la comparaison avec les centres nationaux ou internationaux voisins. Ce centre doit également être équipé de toutes les installations nécessaires au réglage et à l'étalonnage des appareils du réseau.

A partir de ce centre, il est alors possible d'établir le réseau de pyranomètres, enregistreurs ou seulement intégrateurs selon les possibilités, mais toujours soigneusement entretenus et régulièrement contrôlés. On aura ainsi les sommes quotidiennes exactes du rayonnement global en quelques stations. Des mesures espacées mais systématiques du rayonnement diffus par ciel bleu permettront de schématiser le trouble atmosphérique correspondant.

Par la suite, des réseaux héliographiques homogènes, de densités choisies en fonction des besoins et rattachés séparément à la station pyranométrique la plus représentative du climat de leur région, permettront d'étendre dans l'espace l'estimation du rayonnement global. C'est également cette méthode, simple et bon marché, qui permettra la caractérisation des microclimatologies locales en liaison avec les données météorologiques habituelles.

Par ailleurs, un réseau de bilanmètres pourra être couplé à celui des pyranomètres, sous réserve de disponibilités suffisantes en matériel et en personnel pour le contrôle et le dépouillement. En premier stade, cependant, la simple mesure régulière des températures dans le sol (20, 50 et 100 cm) et à la surface du sol, avec des sondes bien étudiées, devrait déjà permettre de dégrossir les problèmes de bilans énergétiques.

Il est certain qu'un réseau dense de stations très complètes, toutes équipées d'enregistreurs-intégrateurs potentiométriques, facilite tant les mesures que leur exploitation. Cette solution reste cependant très onéreuse et exige des observateurs spécialisés en actinométrie ou un centre national au personnel nombreux. En tous les cas, il est nécessaire de prévoir, dès l'établissement d'un réseau, tout le personnel compétent et en nombre suffisant pour assurer les dépouillements, les étalonnages, les contrôles et les études; des connaissances météorologiques sérieuses devraient même en être exigées, afin de faciliter les recherches liées aux comparaisons avec les données climatologiques courantes.

Conclusions

L'actinométrie, au même titre que la plupart des autres disciplines concernant la physique du globe ou de l'atmosphère, offre une difficulté fondamentale dès qu'un réseau de mesures s'avère nécessaire; il s'agit en effet d'utiliser des appareils de laboratoires, toujours sensibles et délicats, dans de nombreuses stations, entretenus par du personnel souvent peu spécialisé. La valeur des relevés est ainsi essentiellement liée à des vérifications fréquentes et à des étalonnages périodiques des appareils, à leur entretien soigneux, et à une parfaite conscience professionnelle des observateurs.

Les travaux en cours permettent d'espérer la réalisation prochaine d'appareils robustes et fidèles, d'exploitation commode et de fabrication industrielle. De plus, les recherches théoriques et expérimentales actuelles laissent envisager une simplification des mesures par la réduction des éléments à mesurer. En tous les cas, une liaison étroite avec la météorologie et la climatologie semble non seulement utile, mais presque toujours nécessaire.

C'est d'ailleurs dans un contexte météorologique que la connaissance du climat actinologique peut offrir une valeur certaine, en précisant pour chaque région l'énergie solaire utilisable pratiquement selon le type d'appareillage logiquement choisi. De même, dans le domaine de l'agriculture ou de la prévision météorologique, seule l'exploitation simultanée des

données actinologiques et climatologiques (températures, pluie, etc.) peut entraîner des conclusions valables.

De la sorte, et si l'on admet la nécessité d'un réseau actinométrique, il semble impossible de ne pas développer conjointement l'exploitation des relevés météorologiques, et il reste indispensable de disposer du matériel et du personnel nécessaires non seulement pour la création de ce réseau, mais aussi et surtout pour son entretien courant et pour le contrôle et le dépouillement systématique des relevés.

Résumé

L'établissement d'un réseau actinométrique est d'abord fonction des buts poursuivis, mais les appareils actuellement disponibles en déterminent la réalisation. L'auteur envisage successivement la mesure du rayonnement global et de ses composantes, de la durée d'insolation, et du bilan radiatif au sol. Il en tire finalement les conclusions logiques pour la création d'un tel réseau, ainsi que quelques remarques pratiques concernant son organisation.

SOLAR ENERGY— ACTINOMETRIC NETWORKS AND INSTRUMENTS

Summary

The design of an actinometric network is connected first with the objects in view, but its development is dependent on the actual instruments now available. The author considers successively the measurements of the total radiation and of its components, of the sunshine duration and of the radiative balance at the ground. Then, the logical conclusions for the creation of such a network are drawn, as well as some practical considerations about its organization.

UTILISATION PRATIQUE DES DIAGRAMMES DE RADIATION SOLAIRE EN VUE DE LA DÉTERMINATION DES RENDEMENTS, DES FRAIS D'EXPLOITATION ET DES CHARGES D'AMORTISSEMENT DES INSOLATEURS

M. Perrot * *et M. Touchais* **

Tous les travaux qui ont eu pour objet l'étude du rayonnement solaire se confinent dans des préoccupations purement physiques ou météorologiques. Les renseignements que l'on peut tirer de cette masse considérable de documentation n'intéressent somme toute que la climatologie, la thermodynamique de l'atmosphère, la biogéographie, la physiologie, la technique de l'éclairage diurne; ils sont peu utiles au thermicien ou à l'héliotechnicien.

Pourquoi en est-il ainsi? Parce que les problèmes qui se posent aux différents praticiens ne sont pas les mêmes. Les premiers cherchent surtout à connaître les énergies incidentes dans une période donnée; les seconds s'inquiètent en outre des puissances, car ils portent leur attention sur les réactions de l'appareil qu'ils étudient en fonction du rayonnement reçu.

Les thermiciens sont les premiers qui se sont émus de cette situation, et l'on trouve de temps à autre dans la bibliographie l'indication de travaux exécutés par des ingénieurs du bâtiment, ayant pour but de définir les conditions d'échange thermique entre les locaux habités et le milieu extérieur. Parmi ces conditions, le rayonnement solaire intervient d'une façon notable.

Pour nous héliotechniciens, qui avons pour but, non pas d'étudier les transformations naturelles de l'énergie solaire, ni de lutter contre ses excès ou ses défauts, mais de la convertir sous des formes industrielles utilisables, nous devons aborder le problème avec les moyens qui nous sont propres.

Je me bornerai exclusivement ici au point de vue énergétique, c'est-à-dire que la composition spectrale du rayonnement est hors de mon propos. D'autre part, j'éviterai de faire un exposé trop général; le sujet est très vaste, même réduit aux proportions où je désire le maintenir. Il ne sera donc question, dans ce qui suit, que du rayonnement énergétique.

Je signale ici que l'on pourra trouver des renseignements précis sur la climatologie du rayonnement solaire et sa mesure dans l'ouvrage de Ch. Maurain intitulé « Étude pratique des rayonnements solaire, atmosphérique et terrestre » qui, bien que datant de 1937, est encore en partie d'actualité. C'est un ouvrage d'ensemble élémentaire que l'on consultera avec fruit pour l'étude du rayonnement.

Pour les relevés météorologiques, on se reportera à l'ouvrage de M. Seltzer, « Le climat de l'Algérie », et à celui de M. Dubief, « Le climat du Sahara ».

L'exposé ci-après comprend deux parties :

1) Un aperçu sur la théorie générale des diagrammes de puissance, avec introduction à la notion de rendement des appareils convertisseurs d'énergie;

2) L'application aux diagrammes de la radiation solaire.

Je tâcherai, dans cette dernière partie, de montrer que la présentation actuelle des mesures de rayonnement, qui fait état surtout de moyennes diverses (journalières, mensuelles, etc.), ne répond pas aux besoins nouveaux qui résultent des problèmes particuliers posés par l'utilisation pratique de l'énergie solaire.

Les diagrammes de puissance

Pertes et rendement

Nous croyons utile de faire tout d'abord un rappel succinct de la théorie des diagrammes de puissance qui sont couramment utilisés dans l'exploitation des usines hydro-électriques ou des centrales thermiques. Nous y ajouterons des considérations sur certaines transformations des diagrammes, lesquels, à notre avis, et nous le verrons plus loin, peuvent trouver leur utilité dans l'étude des diagrammes types des radiations solaires.

Pertes

Les échanges ou les transformations industrielles d'énergie se font généralement par l'intermédiaire d'organes échangeurs affectés de pertes d'énergie non récupérables. L'énergie ainsi perdue par le fonctionnement de l'organe retourne généralement au milieu extérieur sous forme de chaleur.

Si l'on désigne par P_e la puissance totale entrante, qui est à échanger ou à transformer, de l'un de ces organes, P_s la puissance totale sortante utile évaluée dans les mêmes unités, et $\bar{\omega}$ la puissance perdue ou *pertes*, on a

$$\bar{\omega} = P_e - P_s \qquad (1)$$

On considère généralement $\bar{\omega}$ comme une fonction de la puissance sortante de P_s; il est commode,

* Directeur de l'Institut de l'énergie solaire, Université d'Alger, Algérie.

** Ingénieur chargé de recherches de l'Institut de l'énergie solaire, Université d'Alger, Algérie.

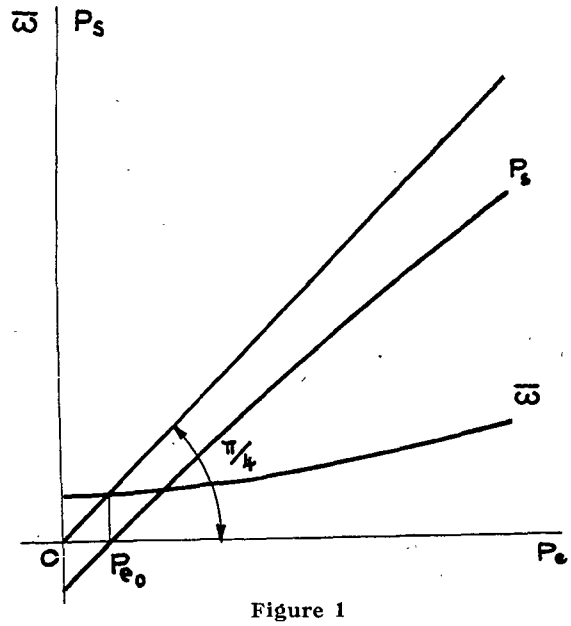


Figure 1

en héliotechnique, de la considérer comme fonction de la puissance entrante

$$\bar{\omega} = \varphi(P_e)$$

On peut écrire en développant en série cette fonction

$$\bar{\omega} = a + b P_e + c P_e^2 + e P_e^3 + f P_e^4 + \ldots,$$

a, b, c, e et f étant des coefficients constants, dont les dimensions sont : pour a, une puissance (par exemple s'il s'agit de la radiation solaire, a s'exprimera en W/m²); pour c, l'inverse d'une puissance; pour e, l'inverse du carré d'une puissance, etc. Par contre, b est sans dimension.

Nous avons aussitôt

$$(2)\quad \begin{aligned} \frac{d\bar{\omega}}{dP_e} &= b + 2cP_e + 3eP_e^2 + 4fP_e^3 + \ldots, \\ \frac{d^2\bar{\omega}}{dP_e^2} &= 2c + 6eP_e + 12fP_e^2 + \ldots \end{aligned}$$

De (1) on tire

$$(3)\quad \begin{aligned} \frac{dP_s}{dP_e} &= 1 - \frac{d\bar{\omega}}{dP_e} \\ \frac{d^2P_s}{dP_e^2} &= -\frac{d^2\omega}{dP_e^2} \end{aligned}$$

On en conclut que les courbes représentatives de la puissance sortante P_s et des pertes $\bar{\omega}$ en fonction de la puissance entrante P_e jouissent des propriétés suivantes :

a) Pour les valeurs positives de $\frac{d\bar{\omega}}{dP_e}$, qui seront les plus fréquentes ainsi que nous le verrons plus loin, l'angle que fait avec l'axe des abscisses une tangente à la courbe $\bar{\omega}$ (figure 1) est inférieur ou au plus égal à 45°.

b) Les courbes P_s et $\bar{\omega}$ ont leurs concavités tournées en sens contraire, et les points d'inflexion ont lieu pour les mêmes valeurs de P_e.

Les courbes représentatives de la fonction $\bar{\omega}$ ont le plus souvent les formes indiquées sur la figure 2. Les pertes à vide $\bar{\omega}_0$, qui correspondent à $P_e = 0$, ont une valeur positive ou nulle, d'où la condition

$$a \geqslant 0$$

A partir d'une certaine puissance P_{e_m} qui peut être nulle, la fonction $\bar{\omega}$ croît en principe indéfiniment. Pratiquement elle croît jusqu'à une valeur limite P_{e_M} de la puissance entrante qui définit la capacité maximum de transformation ou d'échange de l'organe. P_{e_m} est l'abscisse de l'ordonnée minimum de la fonction. Pour toutes les valeurs de P_e satisfaisant à la condition $P_e \geqslant P_{e_m}$, on a

$$(4)\quad \frac{d\bar{\omega}}{dP_e} \geqslant 0$$

La figure 2 donne la forme des courbes que l'on trouve le plus fréquemment dans la pratique.

Les pertes sont souvent d'allure parabolique. On peut alors se contenter d'écrire

$$(5)\quad \begin{cases} \bar{\omega} = a + bP_e + cP_e^2 \\ \dfrac{d\bar{\omega}}{dP_e} = b + 2cP_e \\ \dfrac{d^2\bar{\omega}}{dP_e^2} = 2c \end{cases}$$

Les pertes sont linéaires pour $c = 0$, ce qui entraîne nécessairement

$$b > 0$$

On appelle *puissance entrante initiale* la puissance P_{e_0} définie par la condition $P_s = 0$ ou $P_e = \bar{\omega}$; c'est la puissance entrante minimum nécessaire pour compenser les pertes. Au-dessous de cette puissance, les pertes sont fournies par une source d'énergie auxiliaire. C'est ce qui arrive par exemple pour un insolateur qui rayonne sur un ciel très clair alors qu'un obstacle cache le soleil; c'est le milieu ambiant qui fournit l'énergie ainsi rayonnée.

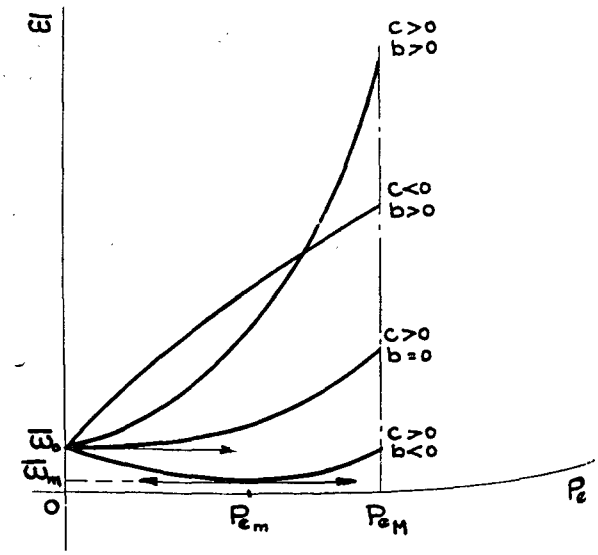


Figure 2

Rendement

On appelle *rendement* de l'organe le rapport

$$\rho = \frac{P_s}{P_e} \tag{6}$$

de par la nature même de la question, ρ n'a de signification que pour les valeurs de P_e satisfaisant à la condition $P_e \geqslant P_{e_s}$; on a alors $\rho \leqslant 1$.

Au voisinage du maximum de ρ, $\frac{d\rho}{dP_e}$ est sensiblement nul; le rayon de courbure est alors donné par l'expression simplifiée

$$R = \frac{1}{\frac{d^2\rho}{dP_e^2}} \frac{\alpha P_e}{\alpha \rho} \tag{7}$$

en désignant par αP_e et $\alpha\rho$ les modules graphiques des abscisses et des ordonnées (α_{P_e}. P_e par exemple, est la longueur, dans l'unité choisie, de la puissance entrante).

On peut écrire en faisant apparaître $\bar{\omega}$

$$\rho = 1 - \frac{\bar{\omega}}{P_e} \tag{8}$$

et en utilisant le développement en série de la fonction $\bar{\omega}$

$$\rho = 1 - \left[\frac{a}{P_e} + b + c P_e + e P_e^2 + f P_e^3 \ldots\right]$$

$$\frac{d\rho}{dP_e} = -\left[\frac{-a}{P_e^2} + c + 2\,e\,P_e + 3 f P_e^2 \ldots\right] \tag{9}$$

$$\frac{d^2\rho}{dP_e^2} = -\left[\frac{2a}{P_e^3} + 2e + 6 f P_e \ldots\right]$$

Pour la puissance initiale P_{e_0}, on a $\bar{\omega} = P_e$ et $\rho = 0$.

Il est intéressant de connaître la forme générale des courbes de rendement suivant la forme de la courbe des pertes. Nous n'examinerons que les deux cas particulièrement importants des pertes de forme linéaire et parabolique.

Dans le cas des pertes paraboliques, le système (9) devient

$$\begin{cases} \rho = 1 - \left[\dfrac{a}{P_e} + b + c P_e\right] \\ \dfrac{d\rho}{dP_e} = \dfrac{a}{P_e^2} - c \\ \dfrac{d^2\rho}{dP_e^2} = -\dfrac{2a}{P_e^3} \end{cases} \tag{10}$$

et pour les pertes linéaires

$$\begin{cases} \rho = (1-b) - \dfrac{a}{P_e} \qquad \text{avec} \qquad P_e \geqslant P_{e_0} \\ \dfrac{d\rho}{dP_e} = \dfrac{a}{P_e^2} \\ \dfrac{d^2\rho}{dP_e^2} = -\dfrac{2a}{P_e^3} \end{cases} \tag{11}$$

Les pertes à vide n'étant jamais négatives, on a donc toujours

$$\frac{d^2\rho}{dP_e^2} < 0$$

ce qui signifie que la courbe de rendement a toujours sa concavité tournée vers le bas.

Le rayon de courbure au voisinage du rendement maximum est sensiblement

$$R = \frac{P_e^3}{2a} \frac{\alpha P_e}{\alpha \rho} \tag{12}$$

Si les pertes à vide $\bar{\omega}_0 = a$ sont relativement faibles devant P_e, R est très grand. La courbe présente de part et d'autre du maximum une région très aplatie pour laquelle le rendement est sensiblement constant.

Dans le cas des pertes paraboliques, le rendement maximum correspond au minimum de l'expression

$$\frac{a}{P_e} + c P_e$$

c'est-à-dire pour

$$a = c P_e^2$$

D'où la règle :

Dans le cas des pertes paraboliques, le rendement est maximum lorsque les pertes à vide sont égales à la fraction des pertes proportionnelles au carré de la puissance entrante.

Diagramme de puissance

Diagramme chronologique

Les puissances en jeu dans un ensemble d'organes varient généralement avec le temps, et le plus souvent d'une manière très irrégulière. On appelle *diagramme chronologique* le diagramme représentatif de la puissance en fonction du temps (figure 3). Si P est la puissance au temps t, on a

$$P = f(t)$$

L'énergie développée depuis le début de la période, prise comme origine des temps, jusqu'au temps t, est

$$W = \int_o^t P\,dt \tag{13}$$

Soient α et β les modules graphiques des abscisses et des ordonnées, et S la surface comprise entre l'axe des temps et les ordonnées au début de la période et au temps t, on a

$$S = \alpha\,\beta\,W \tag{14}$$

L'énergie totale et la surface totale du diagramme au temps T fin de la période sont respectivement :

$$W_T = \int_o^T P\,dt \qquad \text{et} \qquad S_T = \alpha\,\beta\,W_T \tag{15}$$

La puissance moyenne de la période est

$$P_{\text{moy}} = \frac{W_T}{T} \tag{16}$$

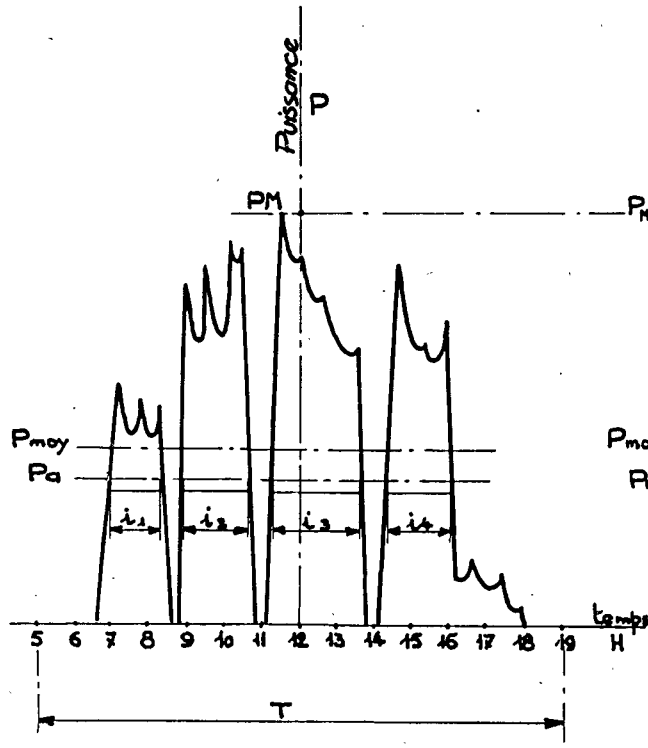


Figure 3

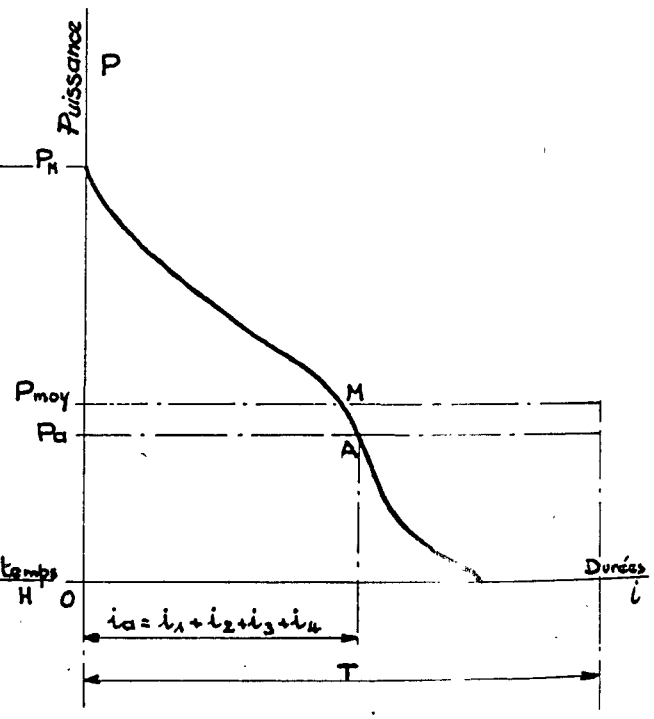


Figure 4

Diagramme monotone

On appelle *diagramme des puissances classées* ou *diagramme de durée* ou encore *diagramme monotone* pendant la période T, le diagramme obtenu en classant par ordre de puissances décroissantes les ordonnées du diagramme chronologique. Le diagramme monotone s'obtient de la manière suivante :

Si $i_a = i_1 + i_2 + i_3 + i_4$ (figure 3) est la durée pendant laquelle la puissance a été égale ou supérieure à P_a, le point A d'abscisse i_a et d'ordonnée P_a appartient par définition à la courbe de durée (figure 4).

La durée de la puissance maximum est le plus souvent infiniment petite; celle de la puissance minimum est la durée T de la période, à moins que cette puissance minimum soit nulle, auquel cas sa durée peut être inférieure à T.

Il existe en général une infinité de diagrammes chronologiques qui correspondent à un même diagramme monotone.

Dans le cas où le diagramme chronologique est formé d'une branche ascendante et d'une branche descendante, il donne immédiatement la durée correspondant à chaque puissance. Le diagramme monotone s'en déduit très facilement. Dans le cas particulier où le diagramme chronologique est aussi symétrique, la branche descendante peut être considérée comme représentant le diagramme monotone. Il suffit de multiplier les abscisses par 2.

La surface du diagramme chronologique peut aussi bien s'obtenir en considérant des variations infiniment petites de la puissance (figure 3).

On a

$$S_T = \alpha\beta \int_o^{P_M} i\, dP$$

Or, cette expression représente également la surface du diagramme tracé avec les mêmes échelles. On peut donc écrire

$$W_T = \int_o^{P_M} i\, dP$$

L'ordonnée moyenne du diagramme monotone est encore P_{moy}.

Le point M d'intersection de la courbe de durée avec la parallèle aux abscisses d'ordonnée P_{moy} détermine deux surfaces égales (hachurées sur la figure 4) dont l'une est définie par toutes les puissances supérieures à P_{moy} et l'autre par toutes les puissances inférieures.

Intégrales caractéristiques

Quelle que soit la fonction $F(P)$, on a toujours

$$\int_o^T F(P)\, dt = \int_o^T F(P)\, di \tag{17}$$

Il en résulte que les ordonnées moyennes, celles des centres de gravité, des diagrammes chronologiques et monotones, sont les mêmes, ainsi que les moments d'inertie de divers ordres pris par rapport aux axes des abscisses. On a en effet, en désignant par P_{moy} l'ordonnée moyenne, G l'ordonnée du centre de gravité, M_1 le moment d'inertie du 1er ordre, ...

$$P_{moy} = \frac{I}{T} \int_o^T P\, dt \tag{18}$$

$$G = \frac{\beta}{2 P_{moy} T} \int_0^T P^2 \, dt \tag{19}$$

$$M_1 = \frac{\alpha \beta^3}{3} \int_0^T P^3 \, dt, \ldots. \tag{20}$$

$$M_2 = \ldots$$

Les puissances moyennes, l'ordonnée du centre de gravité, les moments d'inertie de divers ordres sont dits *intégrales caractéristiques du diagramme* [1].

Ce sont ces intégrales caractéristiques qui interviennent dans le calcul des énergies totales sortantes et du rendement moyen de l'organe étudié.

Cependant, dans le cas particulier du rayonnement solaire on est amené à transformer un diagramme donné établi dans des conditions types pour tenir compte des diverses causes d'absorption atmosphérique. Nous allons examiner maintenant les cas où les transformations se ramènent à de simples proportionnalités.

1) L'ordonnée P est multipliée par un facteur constant k. On a $P' = kp$ et $P'_{moy} = kP_{moy}$, $G' = kG$, $M'_1 = k^3 M_1$, ...

Nous donnerons plus loin un procédé graphique pour passer du diagramme des puissances sortantes au diagramme des puissances entrantes à l'aide de la courbe représentative de rendement ρ.

La nouvelle courbe monotone $P' = f(i)$ transformée par le facteur k de la courbe $P = f(i)$ peut s'obtenir graphiquement à partir d'une construction analogue en utilisant un rendement $\rho = k$ (figure 5).

2) Les abscisses sont multipliées par un facteur constant σ. On a

$$i' = \sigma i \qquad \text{d'où} \qquad T' = \sigma T$$

Désignons par $F'(P)$ la nouvelle courbe et posons

$$\int_0^T F(p) \, di = \int_0^{P_{max}} \varphi(i) \, dp \qquad \text{et} \qquad \int_0^{T'} F'(p) \, di' = \int_0^{P_{max}} \varphi(i') \, dp \tag{21}$$

Relations qui définissent les fonctions correspondantes $\varphi(i)$ et $\varphi(i')$. On a alors

$$P_{moy} = \frac{1}{T} \int_0^T P \, di = \frac{1}{T'} \int_0^{T'} P' \, di' = P'_{moy} \tag{22}$$

$$G = \frac{\beta}{2 P_{moy} T} \int_0^T P^2 \, di = \frac{\beta}{2 P'_{moy} T'} \int_0^{T'} P'^2 \, di' = G' \tag{23}$$

$$M_1 = \frac{\alpha \beta^3}{3} \int_0^T P^3 \, di = \frac{\alpha \beta^3}{3} \frac{1}{\sigma} \int_0^{T'} P'^3 \, di' = \frac{M'_1}{\sigma} \tag{24}$$

$$M_2 = \ldots.$$

La nouvelle courbe peut s'obtenir graphiquement encore ici par le même moyen que précédemment, mais en opérant cette fois sur les abscisses (figure 6).

3) On fait à la fois une déformation proportionnelle par les ordonnées et par les abscisses. On a

$$T'' = \sigma T, \ P''_{max} = k P_{max}, \ P''_{moy} = k P_{moy},$$

$$G'' = k G, \ M''_2 = \sigma k^3 M_1 \ldots$$

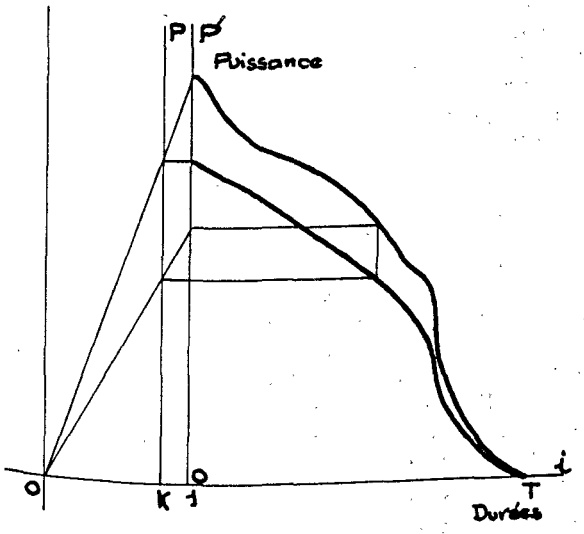


Figure 5

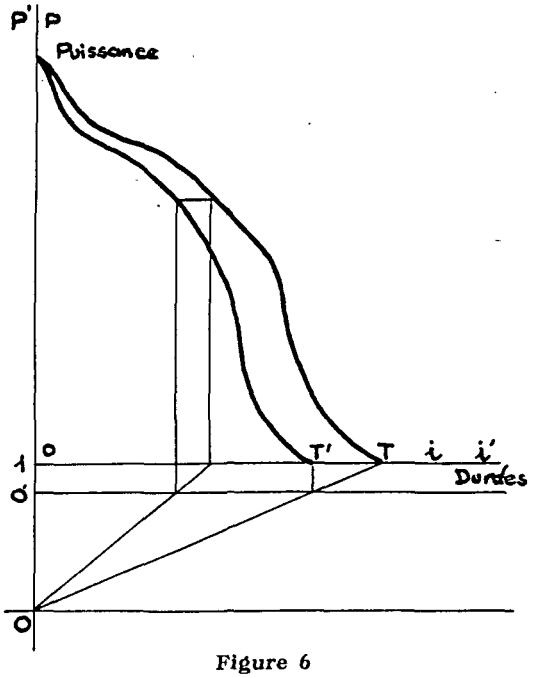


Figure 6

[1] P_{moy} et G s'expriment dans les mêmes unités que P; $\frac{M}{T}$ s'exprime dans les mêmes unités que P^3.

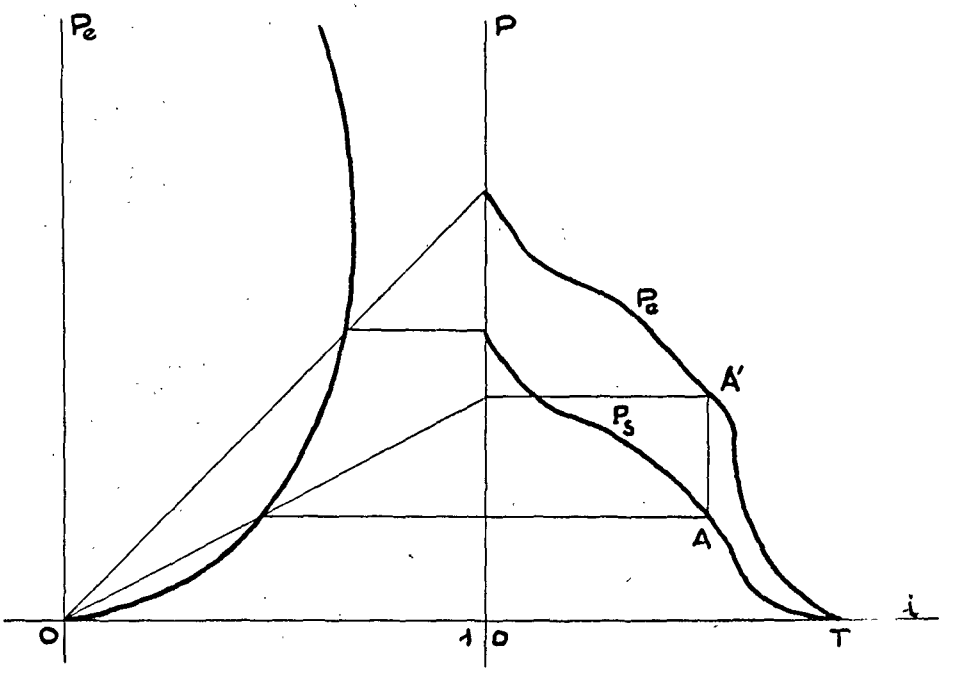


Figure 7

Considérons maintenant le cas d'un diagramme formé de plusieurs périodes : T_1, T_2 ... (par exemple : diagrammes journaliers pour obtenir le diagramme annuel); on montre facilement qu'on a

$$(25)\quad P_{\text{moy}} = \frac{\Sigma_i T_i \cdot P_{i\,\text{moy}}}{\Sigma_i T_i} \qquad \text{avec} \qquad \Sigma_i T_i = T$$

$$(26)\quad G = \frac{\Sigma_i G_i \cdot W_{T_i}}{\Sigma_i W_{T_i}} \qquad \text{avec} \qquad \Sigma_i W_{T_i} = W_T$$

$$(27)\quad M_1 = \Sigma_i M_{1_i}$$
$$M_2 = \ldots.$$

En particulier si le diagramme est symétrique, il suffit de calculer les ordonnées caractéristiques pour une moitié; on a en effet

$$T_1 = T_2,\ W_{T_1} = W_{T_2}$$

et

$$P_{\text{moy}} = P_{1\,\text{moy}} = P_{2\,\text{moy}},\ G = G_1 = G_2,$$
$$M_1 = 2\,M_{1\cdot 2} = 2\,M_{1_i} \ldots$$

Soit n le nombre de périodes qui entrent dans le diagramme total; la période moyenne est

$$(28)\quad T_{\text{moy}} = \frac{T}{n} = \frac{\Sigma_i T_i}{n}$$

Si l'on réduit alors toutes les durées du diagramme total dans le rapport de 1 à n, on a :

$$i = \frac{1}{n} i,\ T' = \frac{T}{n} T_{\text{moy}}$$

et en appliquant les résultats précédemment démontrés

$$P'_{\text{moy}} = P_{\text{moy}},\ G' = G,\ M'_1 = \frac{1}{n} M_1, \ldots$$

D'autre part P'_{max} est le maximum maximorum des $P_{i\,\text{max}}$.

Le nouveau diagramme ainsi obtenu est le diagramme total *ramené à la période moyenne.*

Dans le cas particulier où les périodes T_1, T_2 ..., correspondent à des journées, le diagramme obtenu comme il vient d'être indiqué est le *diagramme journalier équivalent.* La surface du diagramme, qui représente l'énergie $P'_{\text{moy}} \cdot T'_{\text{moy}}$, représente l'énergie moyenne journalière $\frac{P_{\text{moy}}\,T}{n}$.

En résumé, *le diagramme journalier équivalent n'est ni le diagramme moyen, ni un diagramme probable; il résume en quelque sorte tous les diagrammes qui l'ont composé.* Nous verrons ci-après qu'il peut être pris comme base d'étude du fonctionnement d'un appareil transformateur ou échangeur d'énergie.

Rendement moyen

Le diagramme des puissances sortantes s'obtient en réduisant les ordonnées du diagramme des puissances entrantes dans le rapport 1 à ρ. Une construction très simple, indiquée sur la figure 7, permet d'obtenir graphiquement l'un des diagrammes, connaissant l'autre et la courbe de rendement. Cette construction s'applique aussi bien au diagramme de durée qu'au diagramme chronologique...

Désignons respectivement par W_e et W_s les énergies entrantes et sortantes *totales* dans la période T. On a

$$W_e = \int_o^T P_e\,dt = P_{e\,\text{moy}}\,T,\ W_s = \int_o^T \rho\,P_e\,dt$$

Si l'on considère le développement des pertes selon les puissances de P_e, on a

$$\rho = -\frac{a}{P_e} + (-b+1) - c\,P_e - e\,P_e^{2} - \ldots \tag{29}$$

et

$$W_s = -a\int_o^T dt + (-b+1)\int_o^T P_e\,dt - c\int_o^T P_e^2\,dt - e\int_o^T P_e^3\,dt - \ldots \tag{30}$$

Désignons respectivement par G_e et M_{1e}, ... l'ordonnée du centre de gravité du diagramme des puissances entrantes et les moments d'inertie de ce diagramme par rapport à l'axe des abscisses. On a

$$W_s = -a\,T + (-b+1)\,W_e - 2c\,\frac{G_e}{\beta}\,W_e - 3e\,\frac{M_{1e}}{\alpha\beta^3} + \ldots \tag{31}$$

$$= T\left[-a + (-b+1)\,P_{e\,\mathrm{moy}} - 2c\,\frac{G_e}{\beta}\,P_{e\,\mathrm{moy}} - \frac{3_e}{\alpha\beta^3}\,\frac{M_{1e}}{T} - \ldots\right]$$

La deuxième expression montre que ce n'est pas tant la valeur de M_e qui est à retenir dans l'étude des diagrammes que le rapport $\frac{M_e}{I}$, qui a l'avantage de s'exprimer dans les mêmes unités que celles qui sont utilisées pour exprimer la puissance, sans faire intervenir celles utilisées pour exprimer la période, qui peuvent par conséquent rester arbitraires.

Dans le cas des pertes linéaires

$$W_s = T\,[-a + (-b+1)\,P_{e\,\mathrm{moy}}] \tag{32}$$

Dans le cas des pertes paraboliques

$$W_s = T\left[-a + (-b+1) - 2c\,\frac{G_e}{\beta}\,P_{e\,\mathrm{moy}}\right] \tag{33}$$

Le rendement moyen est le rapport

$$\rho_{\mathrm{moy}} = \frac{W_s}{W_e} = \frac{-a}{P_{e\,\mathrm{moy}}} + (-b+1)\,\frac{2c\,G_e}{\beta} - \frac{3_e}{\alpha\beta^3}\,\frac{M_{1e}}{W_e} - \ldots \tag{34}$$

Faisons intervenir le diagramme journalier équivalent; on a

$$W_s = n\,T_{\mathrm{moy}}\left[-a + \left(-b+1-\frac{2c\,G_e}{\alpha}\right)P'_{e\,\mathrm{moy}} - \frac{3e}{\alpha\beta^3}\cdot\frac{M'_{1e}}{T_{\mathrm{moy}}} + \ldots\right. \tag{35}$$

et

$$\frac{W_s}{n} = W'_s$$

On a d'autre part

$$\frac{W_e}{n} = P'_{e\,\mathrm{moy}}\,T_{\mathrm{moy}} = W'_e$$

et

$$\rho_{\mathrm{moy}} = \frac{W_s}{W_e} = \frac{W'_s}{W'_e} \tag{36}$$

Le rendement moyen ne dépend, dans le cas des pertes linéaires, que de l'ordonnée moyenne du diagramme des puissances entrantes; dans le cas des pertes paraboliques, il dépend de cette ordonnée moyenne et de l'ordonnée du centre de gravité. Les coefficients a et $(-b+1)$ étant toujours positifs, le maximum du rendement moyen correspond alors, pour une énergie entrante déterminée, à celui du produit $c\,G_e$; c est le plus souvent positif; la concavité de la courbe des pertes est alors dirigée vers le haut. Le rendement maximum a lieu pour le diagramme dont le centre de gravité est le plus bas; c'est ce qui arrive, on le sait, lorsque la puissance entrante est constante et se confond, en conséquence, avec la puissance moyenne. Dans le cas contraire, le maximum a lieu pour le diagramme dont le centre de gravité est le plus haut. Le diagramme ne doit alors comporter que les puissances extrêmes.

On peut comprendre maintenant pourquoi les diagrammes des météorologistes qui ne sont généralement établis que sur des moyennes et qui leur sont très utiles, ne peuvent cependant pas servir à l'héliotechnicien. C'est que les phénomènes naturels sont provoqués par des différences de température relativement faibles pour lesquelles la courbe des pertes peut être considérée comme linéaire. Les moyennes ont alors une signification, tandis qu'en héliotechnique les courbes des pertes sont au moins paraboliques, et l'on a besoin d'utiliser les intégrales caractéristiques du diagramme.

Puissance maximum et minimum

Nous avons vu que la puissance maximum P_m du diagramme des puissances entrantes ne correspondait, le plus souvent qu'à une durée infiniment petite. Il serait peu économique de construire l'appareil transformateur d'énergie pour cette puissance maximum. On admet alors qu'il vaut mieux le construire pour une puissance plus faible que nous appellerons la *puissance maximum écrêtée.*

Le fonctionnement d'un appareil transformateur d'énergie se fait toujours avec usure ou vieillissement de la matière, et cette usure ou ce vieillissement dépendent de la puissance transformée; ils croissent généralement avec elle; on appelle alors *puissance nominale* d'un appareil, la puissance qui correspond à un amortissement raisonnable. Le technicien

cherche à construire l'appareil de manière que la puissance nominale se trouve dans la zone de bon rendement. Cependant l'appareil peut fonctionner à plus forte puissance au prix d'un amortissement plus rapide; toutefois il ne faut pas dépasser une certaine limite qui correspond à des risques de dégradation. Cette puissance limite dépend surtout du temps pendant lequel elle s'exerce en raison des inerties thermiques. Elle définit ainsi une *puissance de pointe* pour un temps déterminé, par exemple *puissance de pointe semi-horaire.*

Examinons maintenant les zones basses du diagramme. La puissance minimum correspond très souvent à un très mauvais rendement. Parfois il n'est pas possible de l'atteindre sans risquer des défectuosités de fonctionnement. Il faut alors se limiter à un minimum acceptable, et comme rendement, et comme fonctionnement : c'est le *minimum technique.* Les diagrammes de puissance doivent alors être amputés des parties inférieures au minimum technique, ce qui donne de nouveaux diagrammes dont les ordonnées sont $(P - P_m)$ et la durée maximum celle déterminée par l'ordonnée P_m. Il n'est pas de formule simple pour passer des intégrales caractéristiques des anciens diagrammes aux nouveaux.

Il résulte de ces diverses considérations que les *puissances instantanées ne présentent souvent pas d'intérêt dans l'étude de la transformation ou de l'échange;* elles sont résumées dans ce que nous avons appelé les *intégrales caractéristiques* du diagramme, auquel il faut ajouter les valeurs des puissances particulières définies ci-dessus. Ces dernières concernent les possibilités de l'appareil transformateur; les premières son rendement final.

Application aux diagrammes de la radiation solaire

Nous ferons usage des symboles suivants :

Z altitude du lieu, en kilomètres.

φ latitude du lieu, en degrés.

δ déclinaison du soleil, en degrés.

H angle horaire du soleil, en degrés.

H_L, H_c angles horaires du lever et du coucher astronomique du soleil définis par la relation

$$\cos H = -\operatorname{tg}\delta \operatorname{tg}\varphi$$

h hauteur du soleil en degrés. On a

$$\sin h = \sin\delta \sin\varphi + \cos\delta \cos\varphi \cos H$$

h_0 hauteur du soleil à son passage au méridien. On a

$$h_0 = \frac{\pi}{2} - \varphi + \delta$$

pour l'hémisphère boréal.

Q_0 intensité de la radiation solaire moyenne hors atmosphère reçue par l'unité de surface normale, ou *constante solaire,* en W/m²

$$Q_0 = 1\,395 \pm 2 \text{ p. } 100 \text{ (Johnson)}$$

Q_{0_v} composante verticale de Q_0, ou énergie reçue hors atmosphère sur l'unité de surface horizontale, en W/m². On a

$$Q_{0_v} = Q_0 \sin h$$

r facteur de correction de la constante solaire pour tenir compte des variations de distance du soleil à la terre; sans dimension. La radiation normale hors atmosphère, est

$$Q_0 r$$

Affaiblissement selon la loi de Bouguer et dans l'hypothèse des couches planes :

$$Q_n = Q_0 r e^{-km} \qquad \text{et} \qquad Q_v = Q_{0_v} r e^{-km}$$

On néglige les petites erreurs sur l'énergie reçue par une surface et qui sont dues à la sphéricité des couches atmosphériques et à la réfraction atmosphérique. Dans l'hypothèse des couches planes, en effet, la masse atmosphérique m prend une valeur infinie pour $h = 0$; d'autre part du fait de la réfraction, la durée du jour réel est plus grande que la durée du jour astronomique.

Q_n intensité de la radiation normale au sol, en W/m².

Q_v composante verticale de Q_n, en W/m².

K facteur d'absorption. On pose de préférence $e^{-K} = p$.

p facteur de transparence de l'atmosphère. Dans l'hypothèse de l'atmosphère normalisée CINA, on a

$p = 0{,}8425 - 0{,}167\ t$ (J. Dumortier, *Flamme et Thermique,* octobre 1957)

t pression partielle de la vapeur d'eau dans l'atmosphère en mm de Hg.

m épaisseur réduite de l'atmosphère traversée ou *masse atmosphérique,* rapport de la masse atmosphérique rencontrée par un rayon à celle de l'atmosphère à la verticale de la station. Dans l'hypothèse des couches planes, au niveau de la mer, on a

$$m = \frac{1}{\sin h} = \frac{1}{a + b\cos H}$$

avec $a = \sin\delta \sin\varphi$, $b = \cos\delta \cos\varphi$ et la condition $H \leqslant H_c$

ζ rapport de la pression atmosphérique en mm de Hg, à 760. Pour une altitude Z déterminée, il faut remplacer dans la formule de Bouguer m par

$$m\zeta = \frac{\zeta}{\sin h} = \frac{\zeta}{a + b\cos H}$$

$\tau = p^m$ facteur de transmission; sans dimension. On a

$$\tau = \frac{Q_n}{Q_0} = \frac{Q_v}{Q_{0_v}}$$

On peut écrire d'une façon générale

$$Q_n = Q_0 r p^{\frac{\zeta}{a + b\cos H}}$$

et

$$Q_v = Q_0 r (a + b \cos H) p^{\frac{\zeta}{a + bH \cos H}}$$

D_v énergie diffusée par la voûte céleste et reçue par l'unité de surface horizontale, en W/m².

$Q_g = Q_v + D_v$ radiation globale ou éclairement énergétique total d'une surface horizontale, en W/m².

$\tau_d = \frac{D_v}{Q_{0_v}}$ facteur de diffusion; sans dimension.

$\tau_g = \frac{Q_g}{Q_{0_v}}$. On a $Q_g = Q_v \left(1 + \frac{\tau_d}{\tau}\right)$

ou encore

$$\frac{\tau_g}{\tau} = 1 + \frac{\tau_d}{\tau}$$

D'après *Solar Energy* (n° 3, juillet 1960), on aurait *par jour clair*

$$\tau_d = f(\tau)$$

la fonction f serait indépendante de la latitude et de l'altitude, et linéaire dans l'intervalle

$$0{,}4 \leqslant \tau \leqslant 0{,}75$$

On aurait :

$$\tau_d = 0{,}2710 - 0{,}2939\,\tau$$

Par *jour nébuleux*, on aurait une relation

$$K_d = F(K)$$

K_d et K sont des rapports d'énergie journalière reçue par une surface horizontale :

$$K_d = \frac{\int_{H_L}^{H_c} D_v\, dH}{\int_{H_L}^{H_c} Q_{0_v} dH} \qquad K = \frac{\int_{H_L}^{H_c} Q_v\, dH}{\int_{H_L}^{H_c} Q_{0_v} dH}$$

D'après Fournol, Bulletin du CSTB (n° 32 — janvier 1949), on aurait pour la France métropolitaine

$$D_{v\ \mathrm{moy}\ (H)} = 0{,}307^{\frac{1}{a + b \cos H}}$$

la moyenne a été établie sur plusieurs années.

De par sa nature même, le rayonnement solaire réel n'est pas accessible aux calculs. Il faut donc le mesurer et déduire les intégrales caractéristiques journalières et annuelles des diagrammes réels ainsi obtenus. Q_n est mesuré au pyrhéliographe, Q_g au solarigraphe, et on déduit O_v. Malheureusement, ces mesures ne sont effectuées systématiquement que dans un très petit nombre de stations. Plus fréquemment, Q_g est mesuré d'une manière continue et Q_n seulement par ciel clair. Il est évident que, dans ces conditions, il est vain de vouloir tirer des moyennes calculées sur ces mesures la valeur moyenne de O_v.

Il résulte de cet état de choses que l'on ignore à peu près tout pour le Sahara, encore qu'aujourd'hui, des valeurs de D_v. Par ciel clair, il semble que les parties du ciel qui diffusent soient voisines de la direction du soleil et que l'énergie ainsi diffusée soit de l'ordre du dixième de la radiation directe. On peut en tenir compte dans les diagrammes normalisés en affectant la constante solaire d'un coefficient de majoration de 1,1, qui est, il faut le reconnaître, très arbitrairement apprécié.

Par ciel nuageux, c'est toute la voûte céleste qui diffuse plus ou moins, et l'énergie ainsi diffusée dépend de la hauteur du soleil. Selon la distribution et la nature des nuages, les résultats sont très variables; tantôt la radiation globale est supérieure à la composante verticale de la radiation directe, tantôt inférieure, et rien de précis ne peut être donné à ce sujet. Si l'on se contente de moyennes, on peut utiliser les formules données ci-dessus.

Diagrammes réels équivalents

La plupart des stations météorologiques ne possèdent que l'héliographe, appareil qui ne permet que de déterminer le facteur d'ensoleillement, lequel, ainsi qu'on le sait, est le rapport de la durée d'actinisme du soleil à la durée totale du jour. La question se pose de savoir si la simple connaissance du facteur d'ensoleillement suffit à déterminer une forme approximativement suffisante du diagramme d'insolation. Cadiergue et Fournol ont résolu la question pour la métropole, en partant toujours des relevés de l'observatoire de St-Maur et dans l'hypothèse où la connaissance des moyennes est suffisante. Nous allons essayer ci-après de donner le principe d'une méthode plus générale.

Dire que la connaissance du facteur d'ensoleillement suffit pour déterminer les intégrales caractéristiques du diagramme réel, c'est supposer qu'il existe :

1) Un diagramme monotone type;

2) Un procédé de transformation de ce diagramme qui ne dépend que du facteur d'ensoleillement, susceptible de donner après transformation un diagramme monotone possédant les mêmes intégrales caractéristiques que le diagramme réel.

Pratiquement, désignons par d_{j_1} le diagramme monotone réel correspondant au jour j de l'année 1 et σ_{j_1} le facteur d'ensoleillement réel de ce même jour. On considère le diagramme monotone d_j ramené à un jour de l'ensemble des diagrammes d_{j_1}, d_{j_2} ... d_{j_n} relevés pour le même jour calendaire dans un nombre n assez grand d'années. Soit D_j le diagramme monotone établi dans les mêmes conditions à partir de l'atmosphère type. Le facteur d'ensoleillement qui ressort des diagrammes d_j est évidemment

$$\sigma = \frac{\Sigma\, \sigma_j}{n}$$

c'est-à-dire le facteur moyen. Le procédé de transformation à appliquer à D_j pour obtenir d_j peut se concevoir comme une transformation des ordonnées, c'est-à-dire des radiations, suivant une loi déterminée, suivie d'une transformation des abscisses, c'est-à-dire des durées, suivant une loi également déterminée. Or les ordonnées de D_j sont de la forme

$$Q = Q_0\, e^{-Km}$$

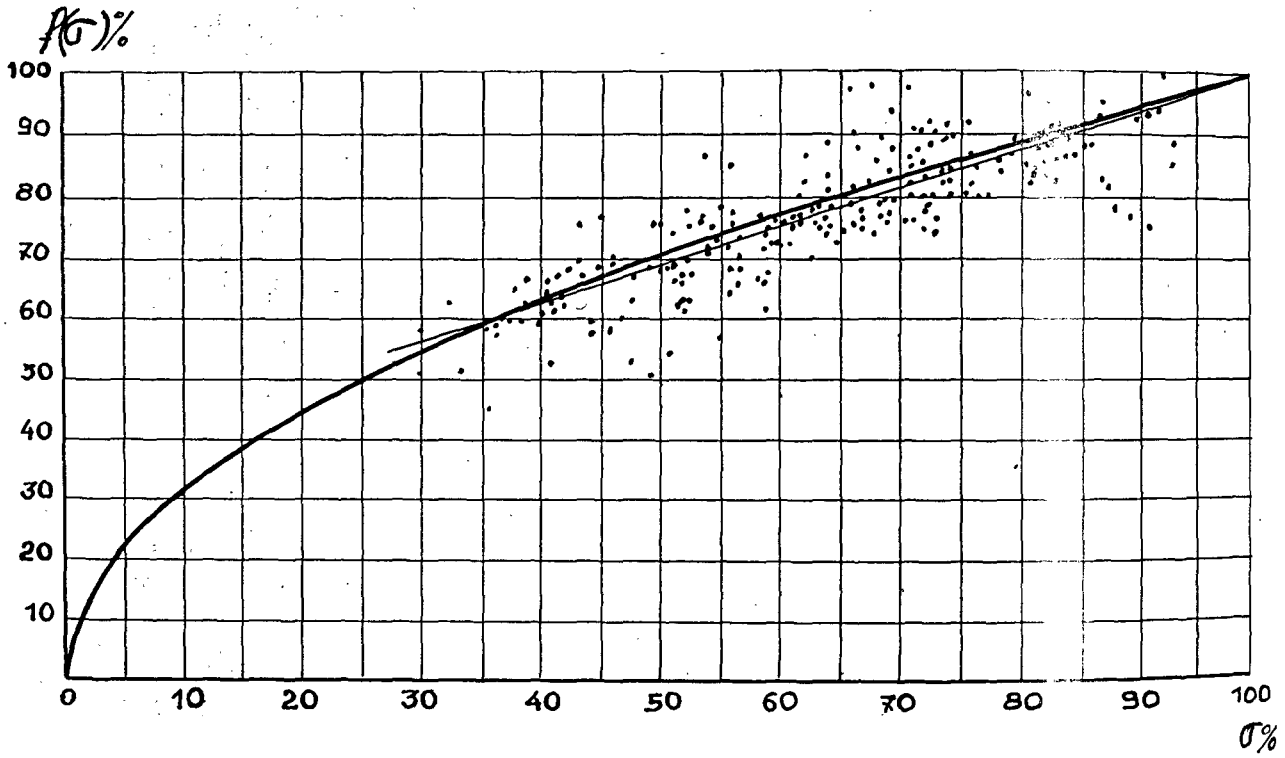


Figure 8

La transformation envisagée sur les ordonnées peut s'écrire, si l'hypothèse était expérimentalement vérifiée,

$$Q' = Q_0 f(\sigma) e^{-K\varphi}(\sigma) m$$

La transformation envisagée sur les abscisses peut s'écrire

$$i' = i \psi(\sigma)$$

La vérification expérimentale consiste à déterminer les fonctions $f(\sigma)$ $\varphi(\sigma)$, $\psi(\sigma)$ et à montrer qu'elles ne dépendent pas de j. Remarquons que $f(\sigma)$ doit satisfaire aux conditions

$$f(0) = 0 \quad ; \quad f(1) = 1$$

Deux simplifications, d'ailleurs très arbitraires, peuvent être essayées :

1) Choisir une atmosphère type moyenne de manière que l'on puisse supposer

$$\varphi(\sigma) = 1$$

2) Admettre, ce que font en définitive les divers auteurs qui se sont occupés de la question, que σ représente une propension générale du diagramme monotone à se rétracter en durée, et poser

$$i' = i\,\sigma$$

D'après les relevés effectués dans les observatoires du Nouveau Mexique [2], il a été proposé pour $f(\sigma)$ une forme linéaire, $0{,}37 + 0{,}622\sigma$, qui n'est valable que pour les valeurs de $\sigma > 0{,}2$. Elle ne satisfait pas en effet à la condition $f(0) = 0$. Nous proposons la forme $\sqrt{\sigma}$ qui résulte des mêmes relevés et qui diffère très peu de la précédente pour les valeurs de σ comprises entre 0,2 et 1. Cette forme a l'avantage de ne posséder aucun coefficient exigeant une détermination expérimentale [3]. La figure 8 donne la comparaison entre les deux formes ainsi que les relevés expérimentaux exécutés dans les stations de Lander et d'Albuquerque, qui sont situées approximativement sous le 35e parallèle.

Les hypothèses faites par Cadiergue et Fournol se ramènent en définitive aux hypothèses précédentes, mais n'ont fait l'objet de vérification qu'en ce qui concerne les moyennes. On peut penser que ces vérifications justifient les hypothèses, et par suite leur application à toutes les intégrales caractéristiques. Toutefois les résultats obtenus pour la métropole ne sauraient être étendus sans vérification préalable au Sahara, d'autant plus que la nébulosité est généralement, dans ces régions, plus élevée l'après-midi que le matin.

Mais tout est à faire dans ce domaine, et des travaux systématiques en liaison avec l'Institut Météorologique et de Physique du Globe d'Alger doivent

[2] Voir *Solar Energy*, janvier 1957, vol. 1 n° 1, "Solar Radiation Availability on Surfaces in the United States as affected by Season, Orientation, Latitude, Altitude and cloudness", par Clarence F. Becker et James S. Boyd, reproduit dans l'article de M. Remeniera.

[3] Il faut bien remarquer que le facteur ne peut être appliqué qu'à la double transformation envisagée. Il faut donc écrire :

$$Q'' = Q_0 \sqrt{\sigma}\, e^{-K/a} + b \cos H'' \qquad \text{avec} \qquad \begin{matrix} a = \sin\delta \sin\varphi \\ b = \cos\delta \cos\varphi \end{matrix}$$

$$H'' = \frac{Hc}{\sigma} \qquad \text{et la condition } H'' \leqslant \frac{Hc}{\sigma}$$

être organisés à cet effet. En particulier, il serait intéressant de pouvoir relier au facteur d'ensoleillement la radiation diffusée par la voûte céleste.

Les intégrales caractéristiques du diagramme réel pour un facteur d'ensoleillement moyen σ se calculent ainsi à partir des intégrales caractéristiques du diagramme type au moyen des formules :

$$\begin{aligned} Q_{max\ réel} &= Q_{max\ type} \\ Q_{moy\ réel} &= f(\sigma)\, Q_{moy\ type} \\ G_{réel} &= f(\sigma)\, G_{type} \\ M_{réel} &= \overline{f(\sigma)^3}\, M_{type} \end{aligned}$$

Dans le cas où l'on adopte

$$f(\sigma) = \sqrt{\sigma}, \text{ on a } \overline{f(\sigma)^3} = \sigma^{5/2}$$

Le facteur d'ensoleillement au Sahara

Les fractions d'ensoleillement horaire sont toujours très élevées au Sahara, avec un minimum de 0,90 en novembre et un maximum de 0,99 en juillet-août; il existe un minimum secondaire de 0,92 en avril et un maximum secondaire de 0,96 en février. En gros, la moyenne des maximums d'insolation oscille entre le 17e parallèle en hiver et le 27e en été.

On peut remarquer que les durées d'insolation sont toujours plus longues le matin que l'après-midi; la dissymétrie du diagramme journalier est un fait général plus accusé en été qu'en hiver.

Les heures du maximum diurne d'insolation varient dans l'année entre 10 et 12 heures l'hiver, entre 8 et 10 heures en juin, entre 9 et 11 heures de juillet à septembre, ce qui montre qu'il y a intérêt à orienter vers l'est, de 15° à 20° environ, les insolateurs fixes.

Le tableau 1 donne le facteur moyen d'ensoleillement annuel de diverses stations sahariennes avec leurs coordonnées géographiques (d'après Dubief), ainsi que les valeurs de $\sqrt{\sigma}$ et $\sigma^{5/2}$.

Critère d'ensoleillement

L'établissement des diagrammes de radiations pour une station donnée fournit les moyens de déterminer l'énergie qui peut être retirée d'un appareil convertisseur du rayonnement solaire, et par conséquent de pouvoir comparer entre eux divers appareils au point de vue du rendement de la transformation, du prix de revient de l'énergie obtenue, etc.

Mais on peut avoir à résoudre un autre problème : celui du choix de la région la plus propice pour l'installation d'un appareil déterminé. Un tel choix fait intervenir non seulement des conditions de radiations, mais aussi des conditions économiques et des sujétions d'exploitation. Aussi n'est-il pas utile de rechercher de critère trop précis. Par contre, il serait intéressant de disposer d'un critère simple. Il est naturel pour cela de comparer les valeurs de la radiation normale pour une heure et un jour caractéristiques, par exemple à midi vrai le jour de l'équinoxe. Or cette radiation normale s'exprime par la formule

$$Q_n = Q_{\Theta\ moy} \sqrt{\sigma}\, p^{\xi/\cos\varphi}$$

Tableau 1

Stations	φ	z	σ	$\sqrt{\sigma}$	$\sigma^{5/2}$
Adrar	27° 52′	258	0,888	0.942	0.742
Aïn-Sefra	32° 45′	1 072	0,754	0,868	0,493
Abulef	26° 58′	290	0,842	0,917	0,649
Beni-Abbès	30° 08′	498	0,795	0,891	0,564
Biskra	34° 51′	124	0,750	0,866	0,552
Colomb-Béchar	31° 36′	770	0,788	0,887	0,552
Djanet	24° 33′	1 079	0,849	0,920	0,664
Djelfa	34° 41′	1 160	0,683	0,826	0,386
El Golea	30° 35′	397	0,849	0,920	0,664
Fort Flatters	28° 06′	381	0,843	0,918	0,651
Fort-de-Polignac	26° 30′	566	0,847	0,919	0,660
Géryville	33° 41′	1 305	0,717	0,846	0,435
Ghardaïa	32° 29′	527	0,777	0,881	0,531
Laghouat	33° 48′	767	0,732	0,855	0,458
Ouallen	24° 36′	347	0,867	0,930	0,698
Ouargla	31° 57′	138	0,802	0,895	0,562
Tamanrasset	22° 48′	1 376	0,830	0,911	0,570
Timimoun	29° 15′	284	0,808	0,898	0,585
Touggourt	33° 07′	69	0,808	0,898	0,585
Cabo Juby	27° 56′	6	0,613	0,784	0,296
Aioun el Atrous			0,740	0,860	0,471
Atar	20° 31′	227	0,720	0,848	0,439
Fort-Gouraud	22° 41′	297	0,745	0,863	0,479
Nema	16° 37′	269	0,707	0,840	0,420
Nouakchott	18° 07′	5	0,741	0,860	0,473
Port-Étienne	20° 56′	8	0,726	0,851	0,449
Tessalit	20° 12′	496	0,754	0,868	0,494

Tableau 2

φ	tg φ	$Z = 0$ Kw tg i	$Z = 0{,}5$ Kw tg i	$Z = 1$ Kw tg i	$Z = 1{,}5$ Kw tg i	$Z = 2$ Kw tg i	$Z = 2{,}5$ Kw tg i	$Z = 3$ Kw tg i
20°	0,364	0,033	0,031	0,029	0,027	0,026	0,024	0,023
21°	0,384	0,034	0,032	0,031	0,029	0,027	0,026	0,024
22°	0,404	0,036	0,034	0,033	0,031	0,029	0,027	0,025
23°	0,424	0,038	0,036	0,034	0,032	0,030	0,029	0,027
24°	0,445	0,040	0,038	0,036	0,034	0,032	0,030	0,028
25°	0,466	0,042	0,040	0,038	0,036	0,033	0,031	0,029
26°	0,488	0,044	0,042	0,040	0,037	0,035	0,033	0,031
27°	0,510	0,046	0,044	0,041	0,039	0,037	0,034	0,032
28°	0,532	0,048	0,045	0,043	0,041	0,038	0,036	0,033
29°	0,554	0,050	0,047	0,045	0,042	0,040	0,037	0,035
30°	0,577	0,052	0,049	0,047	0,044	0,041	0,039	0,036

avec $p \simeq 0{,}8425 - 0{,}0167\,t$, t tension de la vapeur d'eau atmosphérique, en mm de Hg

$$\zeta \simeq 1 - \frac{Z}{10}$$ Z altitude en km

On peut donc prendre comme *critère de l'ensoleillement* en un lieu donné l'expression

$$e = \frac{Q_n}{Q_{\odot\,\text{moy}}} = \sqrt{\sigma}\, p^{\zeta/\cos\varphi}$$

qui ne fait intervenir que les paramètres ayant une incidence sur la radiation : σ, t, ζ et φ.

On peut simplifier les recherches de la région la plus propice, en faisant les observations suivantes : t et σ sont sensiblement constants à l'intérieur de zones assez étendues, d'autre part p et $\sqrt{\sigma}$ sont toujours inférieurs à 1.

Posons $\varepsilon = \dfrac{\cos\varphi}{\zeta}$

On peut prendre ε comme critère local d'ensoleillement. On voit que e croit avec ε.

Si dans la zone considérée, on considère les courbes de niveau, ce sont également les courbes à ζ = cte, par conséquent la valeur de ε sur ces courbes sera d'autant plus élevée que φ sera plus petit. Le point le plus ensoleillé est le point de tangence de la courbe de niveau avec le parallèle le plus au sud, ou à défaut de la tangence, le point d'intersection le plus au sud de la courbe de niveau avec les limites de la zone étudiée. Les points ainsi obtenus s'alignent généralement sur une courbe E qui est la courbe des valeurs maxima de e dans la zone. Il y a lieu de rechercher la plus grande valeur de e sur E. Or il est évident que $\varepsilon = \dfrac{\cos\varphi}{\zeta}$ croît lorsque le terrain s'élève vers le sud. Lorsqu'il s'abaisse, ε croît jusqu'à une certaine pente définie par la condition

$$\frac{\delta\varepsilon}{\delta\zeta}\,d\zeta + \frac{\delta\varepsilon}{\delta\varphi}\,d\varphi = 0$$

Il vient

$$\frac{\cos\varphi}{\zeta^2}\,\frac{d\zeta}{10} + \frac{\sin\varphi}{\zeta}\,d\varphi = 0$$

ou encore

$$\frac{d\zeta}{d\varphi}\,(= 10 - Z)\,\text{tg}\,\varphi$$

La pente du terrain est

$$\text{tg}\,i = \frac{d\zeta}{d\ell}\cos\alpha = \frac{d\zeta}{a\,d\varphi}\cos\alpha$$

a étant la longueur d'un degré sur le méridien, et α l'inclinaison de la courbe E sur le méridien.

$$0 \leqslant \alpha \leqslant 90°$$

Entre le 20e et le 30e parallèle, la moyenne de a est environ 111 km;

d'où $$\text{tg}\,i = \frac{10 - Z}{111}\cos\alpha\,\text{tg}\,\varphi$$

Le tableau 2 donne les valeurs de tg i pour $\alpha = 0$, c'est-à-dire les valeurs les plus élevées de la pente du terrain. Ces valeurs, ainsi qu'on peut le voir, sont encore assez faibles. Entre le 20e et le 30e parallèle, elles varient de 2 à 5 p. 100 pour des stations d'altitude 3 000 m au plus. On en tire cette conclusion, qu'on a le plus souvent intérêt à s'installer en altitude, sauf sur les plateaux ou dans les plaines où la pente est très faible; il y a alors intérêt à s'installer le plus au sud.

Conclusion

Il résulte des considérations qui viennent d'être développées que la seule connaissance des moyennes de la radiation solaire est insuffisante pour les calculs économiques qui concernent les appareils de transformation de l'énergie solaire en une autre forme d'énergie. Or pour établir ces moyennes, il a bien fallu partir des mesures instantanées ou considérées comme telles (moyennes horaires ou semi-horaires). Il eut été alors plus utile d'établir avec ces mesures, poursuivies pendant une assez longue période, les diagrammes journaliers équivalents de la radiation normale (ou radiation directe) et de la radiation globale. Ces diagrammes monotones sont en effet comparables, et comparables également aux diagrammes types; ils éliminent les variations aléatoires

et permettent de rechercher le processus mathématique empirique qui permet de les retrouver approximativement à partir des diagrammes types.

Ces considérations invitent donc à un véritable changement de méthode dans la conception de l'exploitation des relevés météorologiques.

Ainsi, on peut conclure que le rayonnement solaire considéré dans ses applications pratiques est encore fort peu connu. Il importe sans doute, avant de s'aventurer dans des calculs d'exploitation industrielle, de trouver d'abord les procédés pratiques d'utilisation de l'énergie solaire. Les relevés météorologiques actuels, interprétés selon les méthodes que nous venons d'exposer, paraissent être suffisants pour l'instant, à la condition, bien entendu, que ces travaux d'interprétation soient exécutés.

Cela exige le choix définitif d'une atmosphère type adaptée aux différentes régions sahariennes, le calcul des diagrammes journaliers des radiations normales et verticales et la détermination des radiations maxima, des facteurs moyens d'ensoleillement et des intégrales caractéristiques.

Cela exige également les vérifications expérimentales des formules qui permettent l'établissement des diagrammes réels équivalents. Ce sont des travaux assez simples, mais longs et minutieux.

Il ne faut pas oublier cependant que les mesures de rayonnement demandent, pour être utilisables, à être étendues sur de nombreuses années, au moins une dizaine. Or il est certain qu'avant dix ans les appareils d'utilisation de l'énergie solaire auront été mis au point, et les problèmes de prix de revient, de rendement industriel, d'amortissement, ne pourront pas être résolus si l'on ne dispose pas à ce moment de statistiques suffisantes.

Il est donc déjà tard pour commencer ce travail systématique de mesures; il n'y a plus de temps à perdre.

Résumé

Les diagrammes de la radiation solaire établis par les météorologistes ne font habituellement état que de valeurs moyennes; s'ils sont utiles dans l'étude des phénomènes atmosphériques où les transferts de chaleur obéissent généralement à des lois linéaires, ils ne rendent pas à l'héliotechnicien les services dont il a besoin. Ce dernier désire en effet dans certains cas accéder aux puissances instantanées.

D'autre part, on peut observer que le réseau d'observation météorologique du Sahara est assez dilué et que fort peu de stations, pour ne pas dire aucune, se préoccupent de mesures actinométriques continues intéressant simultanément la radiation directe et la radiation diffuse. Par contre, toutes les stations possèdent des héliographes.

Il est donc apparu aux auteurs comme nécessaire de définir d'abord la nature des diagrammes actinométriques utiles à l'héliotechnicien et à rechercher ensuite les moyens d'établir ces diagrammes avec les seuls relevés héliographiques existants.

Le mémoire présenté comporte en conséquence deux parties. La première est un rappel succinct de la théorie des diagrammes, qui est familière aux hydrauliciens et aux thermiciens, mais dont l'application au rayonnement solaire ne semble pas encore avoir été faite. La seconde concerne plus spécialement l'établissement de diagrammes types de la radiation solaire pour un lieu donné.

Les auteurs proposent, en l'absence de toute autre méthode, un moyen de transformer ces diagrammes types à l'aide du facteur moyen d'ensoleillement pour obtenir des diagrammes que l'on peut considérer comme équivalents aux diagrammes réels.

Le mémoire se termine par un exposé d'un critère d'ensoleillement dont la conception dérive des considérations précédentes et qui peut être utilisé dans les espaces sahariens pour la détermination des lieux les plus propices à l'utilisation d'appareils de captation, de transformation et d'utilisation de l'énergie solaire.

Les diagrammes de puissance

Pertes et rendement

Les échanges ou les transformations industrielles d'énergie se font généralement par l'intermédiaire d'organes échangeurs affectés de pertes d'énergie non récupérables. L'énergie ainsi perdue par le fonctionnement de l'organe retourne généralement au milieu extérieur sous forme de chaleur.

Si l'on désigne par P_e la puissance totale entrante, qui est à échanger ou à transformer, de l'un de ces organes, P_s la puissance totale sortante utile évaluée dans les mêmes unités, et $\bar{\omega}$ la puissance perdue ou *pertes*, on a

$$\bar{\omega} = P_e - P_s$$

On considère généralement $\bar{\omega}$ comme une fonction de la puissance sortante P_s; il est commode, en héliotechnique, de la considérer comme fonction de la puissance entrante,

$$\bar{\omega} = \varphi\,(P_e)$$

On peut écrire en développant en série cette fonction

$$\bar{\omega} = a + b\,P_e + c\,P_e^2 + e\,P_e^3 + f\,P_e^4 + \ldots.$$

On appelle puissance entrante initiale la puissance P_{e_o} définie par la condition $P_s = 0$ ou $P_e = \bar{\omega}$; c'est la puissance entrante minimum nécessaire pour compenser les pertes. Au-dessous de cette puissance, les pertes sont fournies par une source d'énergie auxiliaire. C'est ce qui arrive par exemple pour un insolateur qui rayonne sur un ciel très clair

alors qu'un obstacle cache le soleil; c'est le milieu ambiant qui fournit l'énergie ainsi rayonnée.

On appelle rendement de l'organe le rapport

$$\rho = \frac{P_s}{P_e}$$

de par la nature même de la question, ρ n'a de signification que pour les valeurs du $P_e \geqslant P_{e_0}$ et on a alors $\rho \leqslant 1$.

Diagramme de puissance

Les puissances en jeu dans un ensemble d'organes varient généralement avec le temps et le plus souvent d'une manière très irrégulière. On appelle *diagramme chronologique* le diagramme représentatif de la puissance en fonction du temps. Si P est la puissance au temps t, on a

$$P = f(t)$$

On appelle diagramme des puissances classées ou diagramme de durée ou encore diagramme monotone pendant la période T, le diagramme obtenu en classant par ordre de puissances décroissantes les ordonnées du diagramme chronologique.

Si i est la durée, on a aussi bien

$$\int_0^T P\,dt = \int_0^{P_M} i\,dP$$

On montre que les ordonnées moyennes, les ordonnées du centre de gravité, les moments d'inertie de divers ordres par rapport à l'axe des abscisses sont les mêmes pour le diagramme chronologique et le diagramme monotone correspondant.

Les puissances moyennes, l'ordonnée du centre de gravité, les moments d'inertie de divers ordres sont dits *intégrales caractéristiques du diagramme.*

Ce sont ces intégrales caractéristiques qui interviennent dans le calcul des énergies totales sortantes et du rendement moyen de l'organe étudié.

Dans le cas d'un diagramme formé de plusieurs périodes, par exemple diagrammes journaliers pour obtenir le diagramme annuel, on a

$$P_{\text{moy}} = \frac{\Sigma_i T_i P_{i\,\text{moy}}}{\Sigma_i T_i} \qquad \text{avec} \quad \Sigma_i T_i = T$$

$$G = \frac{\Sigma_i G_i W_{T_i}}{\Sigma_i W_{T_i}} \qquad \text{avec} \quad \Sigma_i W_{T_i} = W_T$$

$$M_1 = \Sigma_i M_{1_i}$$

$$M_2 = \ldots\ldots$$

Si n est le nombre de périodes qui entrent dans le diagramme total, la période moyenne est :

$$T_{\text{moy}} = \frac{T}{n} = \frac{\Sigma_i T_i}{n}$$

Si l'on réduit alors toutes les durées du diagramme total dans le rapport de 1 à n, on a

$$i = \frac{1}{n} i \quad , \quad T' = \frac{T}{n} = T_{\text{moy}}$$

et en appliquant les résultats démontrés dans le mémoire,

$$P'_{\text{moy}} = P_{\text{moy}} \quad , \quad G' = G \qquad M'_1 = \frac{1}{n} M'_1, \ldots$$

D'autre part $P'_{\max}$ est le maximum maximorum des $P_{i\,\max}$.

Le nouveau diagramme ainsi obtenu est le diagramme total *ramené à la période moyenne.*

Dans le cas particulier où les périodes T_1, T_2 ..., correspondent à des journées, le diagramme obtenu comme il vient d'être indiqué, est le *diagramme journalier équivalent.* La surface du diagramme, qui représente l'énergie $P'_{\text{moy}} \cdot T'_{\text{moy}}$, représente l'énergie moyenne journalière $\dfrac{P_{\text{moy}} T}{n}$

En résumé, *le diagramme journalier équivalent n'est ni le diagramme moyen, ni un diagramme probable; il résume en quelque sorte tous les diagrammes qui l'ont composé.* Nous verrons ci-après qu'il peut être pris comme base d'étude du fonctionnement d'un appareil transformateur ou échangeur d'énergie.

On montre aisément en effet que l'énergie utile totale dans la période T peut se mettre sous la forme

$$W_s = -aT + (-b+1) W_e - 2c\,G_e W_e - 3_e M_{1_e} + \ldots$$

et on en déduit sans difficulté le rendement moyen dans la même période.

Il est dès lors facile de comprendre pourquoi les diagrammes des météorologistes, qui ne sont établis que sur des moyennes, ne peuvent généralement pas servir à l'héliotechnicien. C'est que les phénomènes naturels sont provoqués par des différences de température relativement faibles, pour lesquelles la courbe des pertes peut être considérée comme linéaire. Les moyennes ont alors une signification, tandis qu'en héliotechnique les courbes des pertes sont au moins paraboliques, et l'on a besoin d'utiliser les intégrales caractéristiques du diagramme.

Application aux diagrammes de la radiation solaire

Établissement des diagrammes types équivalents aux diagrammes réels

Des diagrammes types de la radiation peuvent être obtenus dans un lieu déterminé par application de la loi de Bouguer

$$Q = Q_0\, e^{-km} \qquad \text{avec } m = \frac{\zeta}{a + b\cos H}$$

$$a = \sin\delta \cdot \sin\varphi$$

$$b = \cos\delta \cdot \cos\varphi$$

$$\zeta = 1 - \frac{Z}{10}$$

δ est la déclinaison solaire, φ est la latitude du lieu, H est l'angle horaire du soleil, Z est l'altitude du lieu, en km, m est la masse atmosphérique, et $p = e^{-K}$ est un facteur d'absorption qui en première appro-

ximation dépend de la seule tension de vapeur d'eau dans l'atmosphère.

Les auteurs proposent en se basant sur les travaux de Cadiergue et Fournol à l'observatoire de St. Maur (France) et les relevés expérimentaux des stations de Lander et Albuquerque aux États-Unis de déterminer le diagramme journalier équivalent dans une station donnée en appliquant à Q_0 le facteur $\sqrt{\sigma}$, en désignant par σ le facteur moyen d'ensoleillement de la station, et de réduire la durée du jour dans le rapport σ.

Ce facteur $\sqrt{\sigma}$ peut d'ailleurs fort bien interpréter les relevés effectués aux États-Unis par 35° de latitude (voir figure 8 du mémoire).

Les intégrales caractéristiques du diagramme réel pour un facteur d'ensoleillement moyen σ se calculent ainsi à partir des intégrales caractéristiques du diagramme type au moyen des formules :

$$Q_{max}\ \text{réel} = Q_{max}\ \text{type}$$
$$Q_{moy}\ \text{réel} = f(\sigma)\ Q_{moy}\ \text{type}$$
$$G\ \text{réel} = f(\sigma)\ G_{type}$$
$$M\ \text{réel} = \overline{f(\sigma)^3}\ M_{type}$$

Dans le cas où l'on adopte $f(\sigma) = \sqrt{\sigma}$, on a $f(\sigma)^3 = \sigma^{5/2}$.

Critère d'ensoleillement

L'établissement des diagrammes de radiation pour une station donnée fournit les moyens de déterminer l'énergie qui peut être retirée d'un appareil convertisseur du rayonnement solaire et par conséquent de pouvoir comparer entre eux divers appareils au point de vue du rendement de la transformation, du prix de revient de l'énergie obtenue, etc.

Mais on peut avoir à résoudre un autre problème : celui du choix de la région la plus propice pour l'installation d'un appareil déterminé. Un tel choix fait intervenir non seulement des conditions de radiations, mais aussi des conditions économiques, des sujétions d'exploitation. Aussi n'est-il pas utile de rechercher de critère trop précis. Par contre, il serait intéressant de disposer d'un critère simple; il est naturel pour cela de comparer les valeurs de la radiation normale pour une heure et un jour caractéristiques, par exemple à midi vrai le jour de l'équinoxe.

Les auteurs observent que l'on peut se contenter, pour une région donnée où le facteur moyen d'ensoleillement et l'humidité moyenne sont à peu près constants aux divers points, d'utiliser comme critère l'expression :

$$\varepsilon = \frac{\cos\varphi}{\zeta}$$

dont l'interprétation sur la courbe hypsométrique de la région considérée est facile.

Conclusion

Les considérations ainsi développées semblent inviter à un véritable changement de méthode dans la conception de l'exploitation des relevés météorologiques.

Il ne faut pas oublier cependant que les mesures de rayonnement demandent, pour être utilisables, à être étendues sur de nombreuses années, au moins une dizaine. Or il est certain qu'avant dix ans les appareils d'utilisation de l'énergie solaire auront été mis au point, et les problèmes de prix de revient, de rendement industriel, d'amortissement, ne pourront pas être résolus si l'on ne dispose pas à ce moment de statistiques suffisantes.

PRACTICAL USE OF SOLAR RADIATION DIAGRAMS TO DETERMINE THE EFFICIENCY, OPERATING COSTS AND DEPRECIATION CHARGES OF SOLAR POWER PLANTS

Summary

The actinometric solar radiation diagrams drawn by meteorologists usually take only mean values into account. While they are useful for studying atmospheric phenomena, where heat transfer generally obeys linear laws, they fail to provide the information required by solar engineers, who occasionally need to know the instantaneous power.

Moreover, the meteorological network is rather sparse in the Sahara and very few stations, if any, make continuous actinometric records of both direct and diffuse radiation. All these stations, however, do have heliographs.

The authors therefore wish, first of all, to define the nature of the actinometric diagrams that the solar engineer can use, and then to study the methods of drawing these diagrams from the present heliographic data alone.

This paper consequently consists of two parts. Part I is a brief review of the diagram theory already familiar to hydraulic and heat engineers, though apparently not yet applied to solar radiation. Part II deals more specifically with the technique of drawing typical solar radiation diagrams for a given locality.

In the absence of any other method, the authors propose the transformation of these typical diagrams by means of the mean sunshine factor to obtain diagrams that may be considered equivalent to real diagrams.

In conclusion, the authors give a criterion for the duration of sunshine based on the above considera-

tions, which may be used in the Sahara to determine the most favourable localities for plants to collect, convert and utilize solar energy.

Power diagrams

Losses and efficiency

Energy exchange or conversion is usually accomplished in industry by means of exchangers with non-recoverable energy losses. The energy so lost in the operation of the device usually returns to the external medium in the form of heat.

If P_{in} is the total power input to one of these devices for exchange or conversion, P_{out} the total useful power output, measured in the same units, and $\bar{\omega}$ the power *losses*, then we have:

$$\bar{\omega} = P_{in} - P_{out}$$

$\bar{\omega}$ is usually considered as a function of the power output P_{out}. In solar engineering, however, it is convenient to consider it as a function of the power input instead:

$$\bar{\omega} = \varphi(P_{in})$$

Expanding into series, this function may be written:

$$\bar{\omega} = a + b P_{in} + c P_{in}^2 + e P_{in}^3 + f P_{in}^4 + \ldots$$

The power P_{in_o}, defined by the condition $P_{out} = 0$ or $P_{in} = \bar{\omega}$,

is called the initial power input. This is the minimum power input necessary to compensate the losses. Below this power level, the losses are made up by an auxiliary source of energy. This occurs, for instance, when a solar power plant radiates into a very clear sky whenever the sun is hidden by an obstacle; the source of the energy so radiated is the ambient.

The ratio

$$\rho = \frac{P_{out}}{P_{in}}$$

is called the efficiency of the element. In the very nature of the case ρ has a meaning only for values of $P_{in} \geqslant P_{in_o}$. Then $\rho \leqslant 1$.

Power diagram

The values of the power in an assembly of elements generally vary with time, most often very irregularly. The term *chronological diagram* is applied to a curve representing the power as a function of the time. If P is the power at time t, we have

$$P = f(t)$$

A diagram obtained by arranging the ordinates of a chronological diagram in decreasing order of power is called a power duration curve, duration curve, or monotonic curve, during the period T.

If i is the duration, then :

$$\int_0^T P\,dt = \int_0^{P_M} i\,dP$$

The paper shows the mean ordinates, the ordinatas of the centre of gravity, and the moments of inertie of various orders about the abscissa axis, to be the same for the chronological curve as for the corresponding monotonic curve.

The mean powers, the ordinates of the centre of gravity, and the moments of inertia of various orders are termed the *characteristic integrals of the curve.*

These characteristic integrals enter into the calculation of the total output energies and the mean output of the element under study.

To obtain the annual curve from a curve composed of several periods, for instance daily curves, we have:

$$P_{mean} = \frac{\Sigma_i T_i P_{i\,mean}}{\Sigma_i T_i} \qquad \text{where } \Sigma_i T_i = T$$

$$G = \frac{\Sigma_i G_i W_{T_i}}{\Sigma_i W_{T_i}} \qquad \text{where } \Sigma_i W_{T_i} = W_T$$

$$M_1 = \Sigma_i M^{1_i}$$

$$M_2 = \ldots\ldots$$

If n is the number of periods in the total diagram, then the mean period is:

$$T_{mean} = \frac{T}{n} = \frac{\Sigma_i T_i}{n}$$

If all the durations of the total diagram are reduced in the ratio of 1 to n, then :

$$i = \frac{1}{n} i \qquad T' = \frac{T}{n} = T_{mean}$$

and, applying the results of the paper,

$$P'_{mean} = P_{mean} \qquad G' = G \qquad M'_1 = \frac{1}{n} M_1, \ldots$$

while P'_{max} is the maximum maximorum of the $P_{i\,max}$.

The new diagram so obtained is the total diagram *reduced to the mean period.*

In the special case when the periods $T_1, T_2, \ldots$, correspond to days, the diagram obtained as just indicated is the *equivalent daily diagram.* The surface of the diagram, representing the energy $P'_{mean} T'_{mean}$, represents the mean daily energy $\frac{P_{mean} T}{n}$.

To summarize, *the equivalent daily diagram is neither the mean diagram nor a probable diagram, but, in a sense, a summary of all the diagrams composing it.* We shall see later that it may be taken as the basis for studying the operation of an energy converter or exchanger.

It can be easily shown that the total useful energy during the period T may be put into the form:

$$W_{out} = -aT + (-b + 1) W_{in} - 2c G_{in} W_{in} - 3_{in} M_{1_{in}} + \ldots$$

and the mean efficiency over the same period may be found without difficulty.

It will now be easily understood why the meteorological curves, which are based only on average values, are not as a rule of use to the solar engineer. The point is that meteorological phenomena are produced by relatively small temperature differences, for which the loss curve may be considered linear. In that case the mean values are significant, while in solar engineering the loss curves are at least parabolic, and the characteristic integrals of the diagram must be used instead.

Application to solar radiation diagrams

Drawing of typical diagrams equivalent to real diagrams

Typical diagrams of the direct radiation may be obtained for a given locality by applying Bouguer's law:

$$Q = Q_0 e^{-Km} \qquad \text{where } m = \frac{\zeta}{a + b\cos H}$$

$$a = \sin\delta \cdot \sin\varphi$$

$$b = \cos\delta \cdot \cos\varphi$$

$$\zeta = 1 - \frac{Z}{10}$$

δ is the declination of the sun, φ the latitude of the place, H the hour angle of the sun, Z the altitude of the place in km, m the mass of the atmosphere, and $p = e^{-K}$ an absorption factor depending in first approximation only on the vapour pressure of water in the atmosphere.

Based on the work of Cadiergue and Fournol, of St. Maur observatory (France), and on the experimental data of the Lander and Albuquerque stations (United States), the authors propose to determine the equivalent daily diagram at a given station by applying the factor $\sqrt{\sigma}$ to Q_0, where σ is the mean sunshine factor of the station, and to reduce the duration of the day by the ratio 1 to σ.

This factor $\sqrt{\sigma}$, moreover, gives an excellent interpretation of the United States data for Lat. 35°N (see figure 8).

The characteristic integrals of the real diagram for a mean sunshine factor are calculated from the characteristic integrals of the typical diagram by means of the formulas:

$$Q_{\max\,\text{real}} = Q_{\max\,\text{typical}}$$

$$Q_{\text{mean real}} = f(\sigma)\, Q_{\text{mean typical}}$$

$$G_{\text{real}} = f(\sigma)\, G_{\text{typical}}$$

$$M_{\text{real}} = \overline{f(\sigma)^3}\, M_{\text{typical}}$$

If we take $f(\sigma) = \sqrt{\sigma}$, we have $f(\sigma)^3 = \sigma^{5/2}$.

Sunshine criterion

The radiation diagrams for a given station enable us to determine the energy that can be drawn from a solar radiation converter, and consequently make it possible to compare the conversion efficiencies of various devices, the cost of the energy generated, etc.

The problem, however, may be different: to select the most favourable region for installing a certain plant. Such a choice involves not only radiation conditions, but also economic conditions and the demands and constraints of actual operation, so that there is no point in seeking too precise a criterion. On the other hand, a simple criterion would be desirable. For this purpose one would naturally compare the normal radiation values for a characteristic hour and day, for instance true noon at equinox.

The authors point out that for a given area where the mean sunshine factor and the mean humidity are almost constant at the various points considered, it might be sufficient to use, as the criterion, the expression:

$$\varepsilon = \frac{\cos\varphi}{\zeta}$$

which is easily interpreted from the hypsometric curve of the region.

Conclusion

These considerations seem to call for a complete methodological change in the approach to the utilization of meteorological observations.

We must not forget, however, that any useful series of radiation measurements must cover an extended period—at least ten years. But the industrial development of equipment for utilizing solar energy will surely not take another ten years, and unless adequate statistical data are available at that time, it will be impossible to solve the problems of power cost, industrial efficiency and plant depreciation.

LA MESURE ABSOLUE DE L'ÉNERGIE SOLAIRE

Roger Peyturaux *

Bien que les tentatives pour capter l'énergie du soleil remontent à l'antiquité, ce n'est qu'au siècle dernier que les chercheurs ont essayé de mesurer en valeur absolue l'énergie reçue par la terre du soleil. Les premiers essais sérieux ont été ceux de Pouillet en 1838. Toutefois, les premières mesures dont les résultats ont été réellement utilisables sont celles du Smithsonian Institute, principalement sous la direction d'Abbot, depuis le début de ce siècle.

Évidemment, c'est l'énergie reçue au niveau du sol qui est utilisable; mais si l'on veut des données universelles, il faut déterminer l'énergie solaire au-delà de l'atmosphère, car celle-ci absorbe considérablement les radiations. Elle les absorbe de façon très différente selon les longueurs d'onde. Par exemple, le rayonnement ultraviolet (au-dessous de 3 000 Å) est complètement absorbé. En outre, il y a dans l'infrarouge d'importantes régions spectrales qui sont partiellement ou totalement absorbées, et cela plus ou moins selon l'altitude et la position géographique du lieu d'observation.

Le rayonnement solaire lui-même ramené au-dessus de l'atmosphère terrestre est très complexe. Il se compose d'un rayonnement à spectre continu, un peu analogue à celui d'une source à incandescence, dans lequel diverses radiations sont plus ou moins absorbées par les corps contenus dans l'atmosphère solaire. Ces radiations atténuées constituent les raies de Fraunhofer que l'on voit apparaître en noir sur un spectre du soleil. La figure 1 nous montre quelques aspects du spectre solaire.

Enfin, le rayonnement solaire est variable d'un point à un autre du disque apparent du soleil, même si l'on ne tient pas compte de ses irrégularités locales (taches, facules, granulation). L'observation directe et les mesures longueur d'onde par longueur d'onde ont montré que ce rayonnement diminue du centre vers le bord, et ceci d'autant plus que les longueurs d'onde sont plus courtes. Les raies spectrales ont aussi un comportement très particulier et différent de l'une à l'autre.

Ces considérations nous montrent que pour posséder tous les éléments du rayonnement solaire il faut connaître :

a) Le rayonnement à spectre continu pour toutes les longueurs d'onde et pour tous les points situés entre le centre et le bord du disque apparent du soleil;

b) L'intensité des raies spectrales.

Même pour une détermination globale de l'énergie solaire, ces connaissances sont utiles. En effet, s'il est possible de déterminer l'absorption atmosphérique pour beaucoup de longueurs d'onde, cette détermination n'est possible que si l'absorption n'est pas totale. Si c'est le cas, on doit faire appel à des considérations théoriques. Connaissant à fond tous les aspects du rayonnement solaire, on peut en déduire par des théories en constante amélioration l'état physique interne du soleil. Ainsi on peut calculer le rayonnement émis dans les régions spectrales inaccessibles à nos observations. De cette façon, on peut atteindre avec certitude la constante solaire qui est, rappelons-le, l'énergie reçue de l'ensemble du disque solaire, pour toutes les longueurs d'onde, au-dessus de l'atmosphère.

Mesure directe de la constante solaire

Les mesures directes de la constante solaire effectuées en grande partie par le Smithsonian Institute sont classiques [1]. En attendant les résultats des mesures modernes en cours, c'est la valeur de la constante solaire qui permet de fixer l'échelle des mesures spectrales de l'énergie solaire. Nous rappellerons l'essentiel de ces mesures en insistant un peu plus sur la détermination de l'absorption atmosphérique qui se pratique toujours suivant le même principe.

Pour atteindre la constante solaire, il faut procéder en trois temps :

1) Mesurer l'énergie solaire reçue au sol pour l'ensemble de toutes les longueurs d'onde transmises par l'atmosphère terrestre;

2) Déterminer l'énergie absorbée dans les domaines spectraux où une petite partie de cette énergie subsiste au niveau du sol;

3) Évaluer l'énergie totalement absorbée dans les domaines spectraux où l'atmosphère est complètement opaque.

La première partie des mesures a été effectuée à l'aide d'appareils appelés pyrhéliomètres. C'est Abbot qui a porté ces appareils à un haut degré de perfection. Dans le dernier modèle réalisé, le

* Institut d'astrophysique, Paris. Laboratoire de l'énergie solaire, Mont-Louis.

[1] Les travaux ont été publiés de 1900 à nos jours dans les *Annals of the Astrophysical Observatory of the Smithsonian Institute* et dans la *Smithsonian Miscellaneous Collection*.

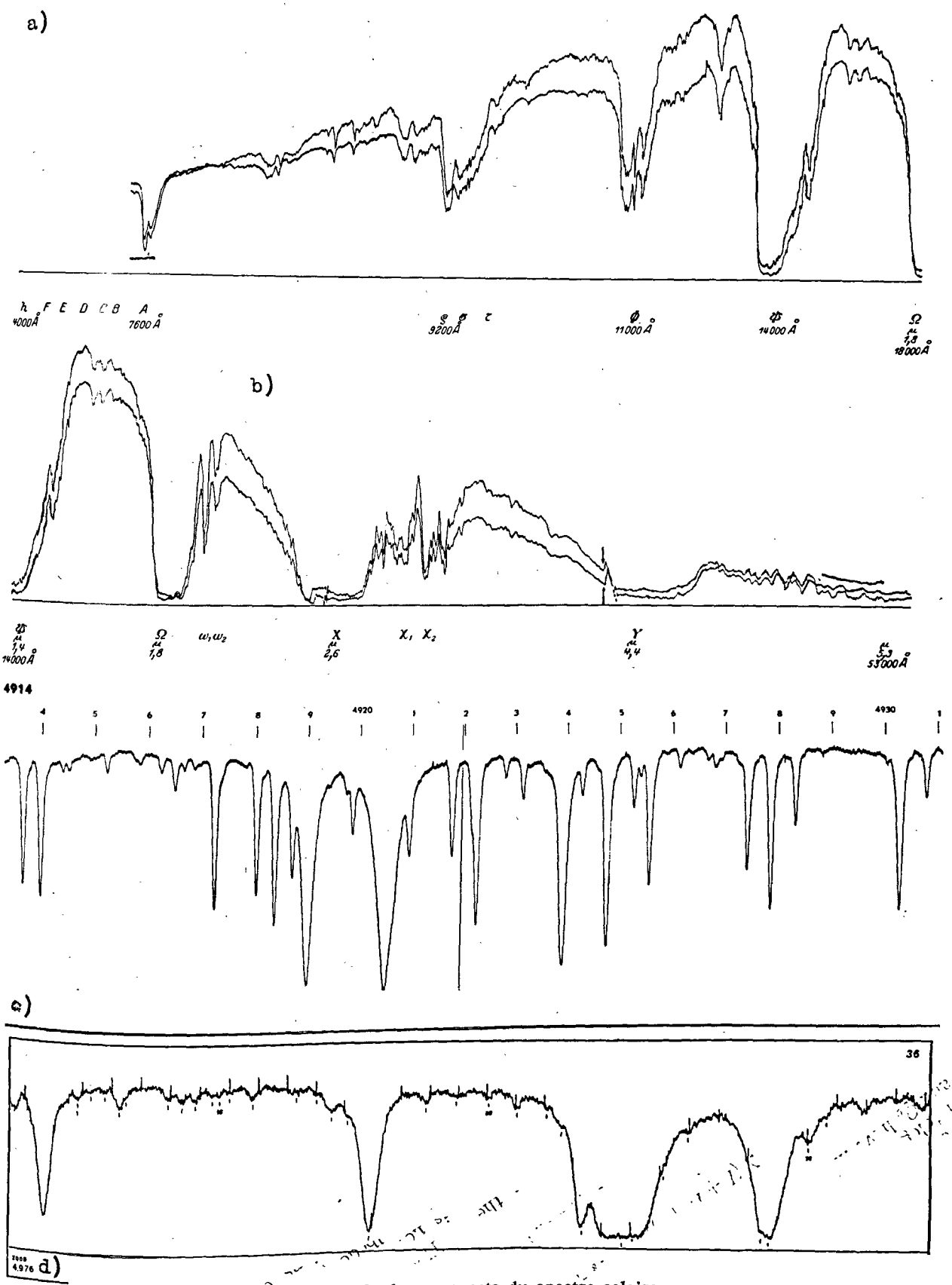


Figure 1. Quelques aspects du spectre solaire

a) A faible dispersion ; *b*) A faible dispersion, selon Abbot ; *c*) A grande dispersion (de 4 914 à 4 931 Å), Atlas d'Utrecht ; *d*) A grande dispersion (de 49 760 à 50 390 Å), selon Migeotte et collaborateurs.

rayonnement solaire était reçu dans une enceinte noircie intérieurement. Cette enceinte était baignée par de l'eau constamment agitée. La mesure consistait essentiellement à déterminer l'élévation de température de l'eau dans un temps déterminé. Afin de rendre la mesure plus relative, donc plus précise dans l'absolu, un deuxième appareil identique était chauffé électriquement et on mesurait la puissance nécessaire pour élever la température de l'eau du deuxième appareil au même niveau que pour le premier. Ensuite, les deux appareils étaient substitués l'un à l'autre afin d'éliminer l'action des différences matérielles.

Pour la deuxième partie, il n'est pas possible de déterminer l'absorption atmosphérique simultanément pour toutes les longueurs d'onde. En effet, la formule de Bouguer

$$I_\lambda = I_{\lambda,0}\, e^{k_\lambda H_\lambda \sec Z}$$

où $I_{\lambda,0}$ est l'énergie reçue au sol,
I_λ l'énergie reçue au-dessus de l'atmosphère,
K_λ le coefficient d'absorption atmosphérique,
H_λ le chemin optique parcouru dans l'atmosphère par le rayon lumineux,
Z la distance angulaire du soleil par rapport au zénith,

n'est valable qu'en rayonnement monochromatique, car tous les éléments autres que Z varient avec λ et indépendamment les uns des autres. Ainsi pour déterminer I_λ il faut mesurer au cours de la journée la variation de $I_{\lambda,0}$ en fonction de Z pour diverses longueurs d'onde. Ensuite on porte sur un graphique $\log I_{\lambda,0}$ en fonction de sec Z. On doit obtenir une droite que l'on extrapole jusqu'à sec $Z = 0$, car sec Z est toujours supérieure à 1 (sec $0 = 1$). L'ordonnée obtenue est proportionnelle à I_λ. Cette méthode est encore celle que l'on emploie à l'heure actuelle en remplaçant H_λ sec Z par la « masse d'air » traversée[2]. De telles masses d'air ont été calculées par Link (1). Pour les longueurs d'onde où l'absorption atmosphérique est fortement sélective, la fonction $\log I_{\lambda,0} = f$ (sec Z) n'est plus une droite et ne peut pas être extrapolée avec certitude, de sorte que l'on ne peut pas déterminer avec précision l'absorption atmosphérique pour ces régions spectrales. On conçoit par conséquent qu'une détermination globale précise de l'absorption atmosphérique est impossible. Ceci nous achemine progressivement vers les méthodes modernes dont il sera question plus loin.

La troisième partie est encore plus délicate, car on peut difficilement évaluer des énergies non mesurables si l'on ne possède pas d'autres informations qui permettent cette évaluation par le calcul. Abbot et ses collaborateurs ont évalué ces rayonnements en admettant que le soleil rayonnait comme un corps noir dans les domaines inobservables. Une légère amélioration a été apportée à ces données par les mesures faites à l'aide des V2 et des ballons. Ces mesures ont permis de préciser la correction ultraviolette.

En faisant une synthèse de tous ces résultats on est arrivé à la valeur 2.00 cal cm^{-2} min^{-1} pour la constante solaire. L'incertitude reste cependant de l'ordre de 5 p. 100.

Les mesures spectrophotométriques du rayonnement solaire

Quand les astronomes ont commencé à étudier la structure de l'atmosphère solaire (d'où nous parvient tout le rayonnement utile), ils ne possédaient comme données d'observation que les résultats du Smithsonian Institute et de quelques travaux partiels. On s'est aperçu alors qu'ils n'étaient pas adaptés à de telles recherches.

Mulders (2) a transformé ces résultats pour les rendre utilisables. En groupant la constante solaire, les données sur la répartition spectrale de l'énergie en fonction de la longueur d'onde et sur la variation de cette énergie entre le centre et le bord du disque solaire, il a obtenu en valeur absolue la répartition spectrale de l'énergie émise par le centre du disque solaire. Cependant ses résultats étaient très incertains du fait de la dispersion spectrale insuffisante des appareils utilisés par les observateurs et du fait de l'incertitude sur l'énergie absolue dans les régions spectrales inobservables.

Il était donc nécessaire d'entreprendre des mesures séparées de différents types :

a) Mesure absolue de la répartition spectrale de l'énergie dans le spectre continu émis par le centre du disque solaire;

b) Mesure de la variation de l'énergie émise entre le centre et le bord du disque solaire, en sélectionnant bien les zones spectrales appartenant au spectre continu et en s'approchant le plus près possible du bord solaire;

c) Mesure de l'absorption dans les raies spectrales d'origine solaire et variation de ces raies entre le centre et le bord du disque solaire.

Les mesures de type (b) et (c) sont des mesures relatives. La mesure (a) est absolue et par conséquent doit être raccordée à des données étalons. Nous décrirons maintenant les travaux récents effectués dans ce sens et nous donnerons des indications sur les recherches en cours.

La mesure absolue de la répartition spectrale de l'énergie dans le spectre continu émis par le centre du disque solaire

Généralités

Pour obtenir des résultats très sûrs dans ce genre de travaux, il faut se ramener à des mesures relatives, c'est-à-dire à la comparaison entre le rayonnement reçu du soleil et le rayonnement reçu d'une source

[2] La masse d'air est proportionnelle à sec Z jusqu'aux environs de $Z = 70°$.

terrestre. En effet, pour des travaux de précision, on ne peut pas compter sur le caractère non sélectif d'un récepteur d'énergie. Il faut en quelque sorte éliminer ce récepteur par une méthode de comparaison. Ainsi on se rend compte que le problème posé est autant un problème de source étalon que d'observation.

La source étalon doit être parfaitement connue au point de vue de la répartition spectrale et de la valeur absolue de son rayonnement. En outre, elle doit être d'une brillance aussi élevée que possible, car il n'est pas encore possible de réaliser une source stable d'une brillance égale à celle du soleil.

Les observations sont délicates, précisément parce que l'on compare des sources de brillance parfois très différentes. En outre, la détermination de l'absorption atmosphérique devant être effectuée avec soin, il faut mettre en œuvre un matériel spécialement étudié et sélectionner les journées d'observation.

Les sources de comparaison

Quelle que soit la source de comparaison employée, il faut qu'elle soit étalonnée d'après un corps noir, car, comme pour les récepteurs, on ne peut pas définir à priori les caractéristiques d'une source étalon. Les observateurs modernes emploient la lampe à ruban de tungstène, l'arc électrique et le corps noir lui-même.

La lampe à ruban

La lampe à ruban de tungstène est d'un emploi très commode. On peut en réaliser avec un ruban vertical assez long (par exemple avec une longueur utile de 20 mm pour une largeur de 2 mm), ce qui permet une utilisation aisée en spectroscopie. En outre, si la température est assez élevée, l'uniformité lumineuse peut être excellente. La température de service peut être sans dommage de l'ordre de 2 800 °K, et elle peut être maintenue constante à une très grosse précision en maintenant le courant constant dans la lampe avec un contrôle au potentiomètre de précision. Toutefois la lampe doit être comparée à un corps noir. En outre la brillance évolue avec une rapidité plus ou moins grande suivant la température de service par usure du ruban qui change la température à courant constant, par cristallisation du ruban, et par noircissement de l'ampoule. Ces variations sont sélectives, de sorte qu'il faut comparer fréquemment la lampe au corps noir. Ces considérations nous montrent que la lampe à ruban ne peut pas constituer un étalon absolu précis. Par contre, c'est une source tare idéale.

L'arc électrique

L'arc électrique au graphite a le gros avantage de pouvoir atteindre une température voisine de 4 000 °K. Cependant pour des travaux de précision on ne peut pas le considérer comme un corps noir parfait. Par contre, on peut dans une certaine mesure (domaine spectral pas trop large) le considérer comme un corps gris. Ainsi quand on a déterminé sa température de couleur par comparaison à un corps noir, on peut considérer celle-ci comme étant constante si l'on maintient stable la température de l'arc avec contrôle au pyromètre optique. Ainsi on se rend compte que l'arc au graphite n'est pas non plus une bonne source absolue. Par contre, il constitue une excellente source pour étudier la répartition spectrale de l'énergie en valeur relative, d'autant plus que du fait de sa grande brillance il facilite les opérations de comparaison avec le soleil.

Les corps noirs

Si l'on veut déterminer avec précision l'énergie en valeur absolue, on se rend compte qu'il est souhaitable d'effectuer la comparaison aussi directement que possible avec un corps noir. Pour cela, il faut réaliser d'abord un corps noir d'un emploi assez commode pour pouvoir être employé directement dans l'observatoire. Depuis longtemps, on a réalisé des corps noirs en métal ou en graphite. Mais à notre connaissance tous les modèles réalisés présentaient un inconvénient pratique, soit une puissance consommée très élevée, soit une durée de chauffe très importante. Ceci nous conduit à réaliser l'appareil dont nous allons donner une description sommaire et que nous employons actuellement.

L'élément rayonnant est constitué par un tube de tantale de 0,1 mm d'épaisseur, 10 mm de diamètre et d'environ 250 mm de longueur totale. A l'intérieur de l'appareil sont disposés des écrans et diaphragmes qui permettent à l'enceinte centrale de rayonner comme un corps noir. Il est fixé verticalement à un support constitué par trois barres de molybdène de 8 mm de diamètre assemblées par des pièces en alumine frittée. La fixation supérieure est rigide, la fixation inférieure est souple afin de permettre la dilatation du tube. Afin de réduire la consommation électrique, tout en ayant une vitesse de chauffe assez grande, le calorifugeage de l'ensemble est assuré par des écrans cylindriques en molybdène et nickel.

L'appareil ainsi réalisé travaille sous vide. La précision est de l'ordre de 10^{-6} mm Hg à froid. Elle s'élève à 10^{-4} mm Hg en chauffe. On atteint couramment une température de 2 600 °K en 15 minutes, et la durée de vie d'un tube semble être du même ordre que celle d'une lampe légèrement poussée.

On voit qu'un tel appareil (ou un appareil analogue, car on peut envisager des variantes suivant les besoins) permet de s'affranchir de tout étalonnage, car la seule donnée de la température permet de connaître avec précision la répartition et la valeur absolue de l'énergie émise. La température peut être mesurée aisément à l'aide d'un pyromètre optique que l'on étalonne à partir d'un corps noir au point de fusion de l'or. Bien entendu, il faut tenir compte de l'absorption de la glace de fermeture et du miroir à 45° qui renvoie la lumière dans une direction horizontale. La figure 2 montre une vue schématique de l'appareil.

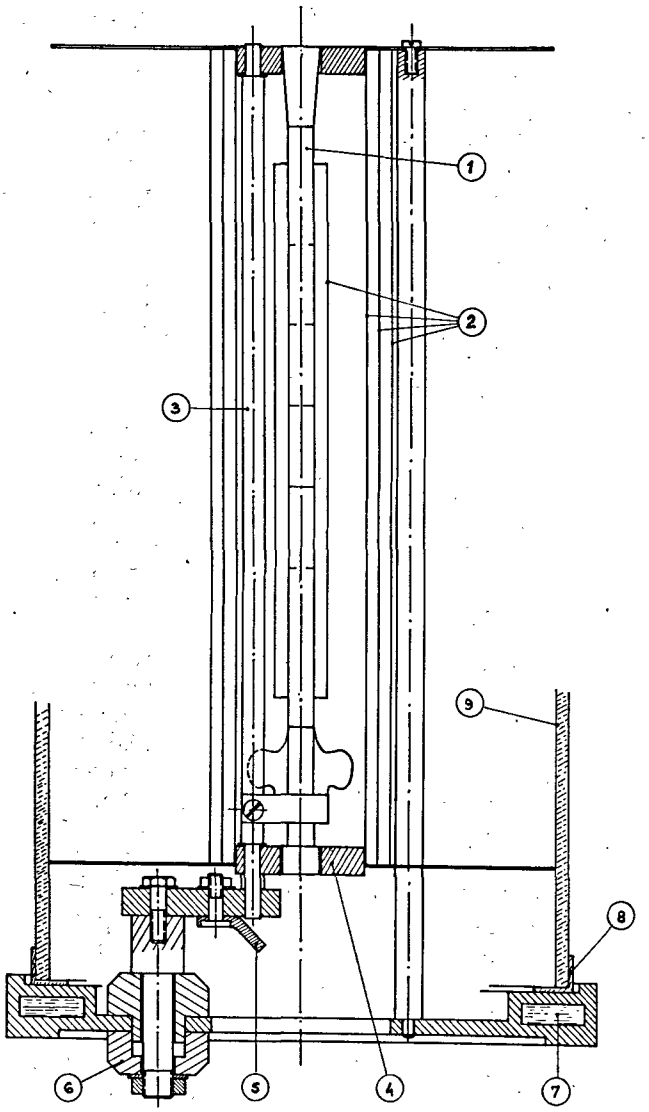


Figure 2. Schéma d'un corps noir dans le vide

1) Élément chauffant — Corps noir.
2) Écrans calorifuges.
3) Barre support — Amenées de courant.
4) Pièces en alumine frittée.
5) Arrivée de courant liée par une tresse au passage air-vide non représenté.
6) Support isolant en stéatite.
7) Eau.
8) Joint de vide.
9) Manchon en Pyrex.

Les observations et les étalonnages

Principes généraux

Pour effectuer la comparaison entre le soleil et une source étalon, on forme tour à tour, sur la fente d'entrée d'un système dispersif, une image du soleil et une image de la source. Pour des mesures absolues précises, le système dispersif est un monochromateur suivi d'une cellule photo-électrique dont le courant est amplifié et enregistré. Il faut ensuite tenir compte : de la présence de l'atmosphère; de la différence d'intensité des deux sources à comparer; de la dissymétrie des deux chemins optiques.

Cela nous conduit à mesurer, outre le rapport de comparaison soleil source :

L'absorption atmosphérique;

La transmission des systèmes optiques destinés à rendre comparables l'énergie solaire et l'énergie de la source;

Les facteurs de réflexion des miroirs qui sont utilisés sur un trajet et non sur l'autre.

L'absorption atmosphérique est généralement mesurée avec un appareil spécial. Les deux dernières mesures sont effectuées au laboratoire.

La comparaison proprement dite soleil source

L'image du soleil est captée à l'aide d'un sidérostat polaire [3] qui renvoie le faisceau sur un miroir concave, lequel forme une image du soleil sur la fente d'entrée du monochromateur. Afin d'éliminer photométriquement les miroirs du sidérostat, il est bon d'utiliser le sidérostat lui même pour capter la lumière de la source de comparaison. Comme le soleil est à l'infini et la source à distance finie, on envoie l'image de cette dernière à l'infini à l'aide d'un miroir collimateur. Bien entendu, afin que la comparaison ait un sens il faut que le miroir concave final soit seul à limiter les faisceaux des deux trajets.

La comparaison peut être faite longueur d'onde par longueur d'onde en sélectionnant des tranches étroites dans le spectre solaire, ou en enregistrant à tour de rôle des bandes spectrales larges du soleil

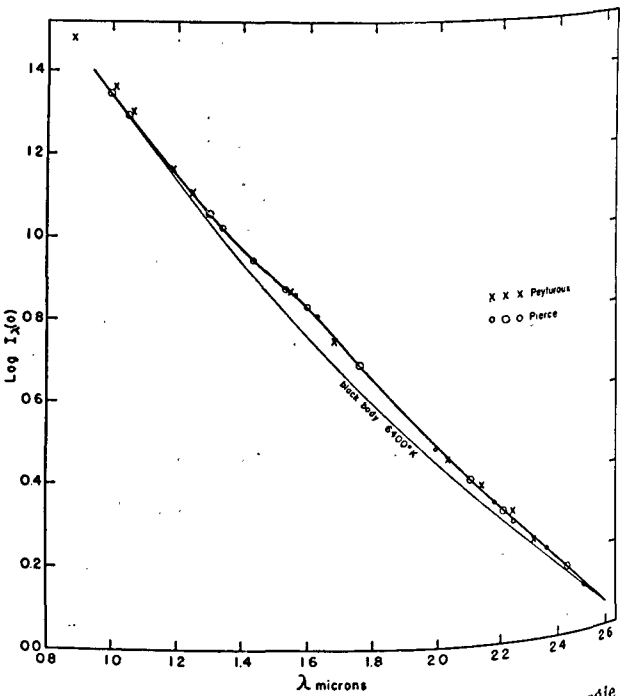


Figure 3 a. Résultats récents sur la mesure de l'énergie au Centre du disque solaire : mesures relatives comparées de Pierce et de Peyturaux dans le proche infrarouge

[3] Le sidérostat polaire est utilisé de préférence aux autres appareils pour le cas particulier actuel, car l'incidence sur les miroirs est indépendante de la position du soleil.

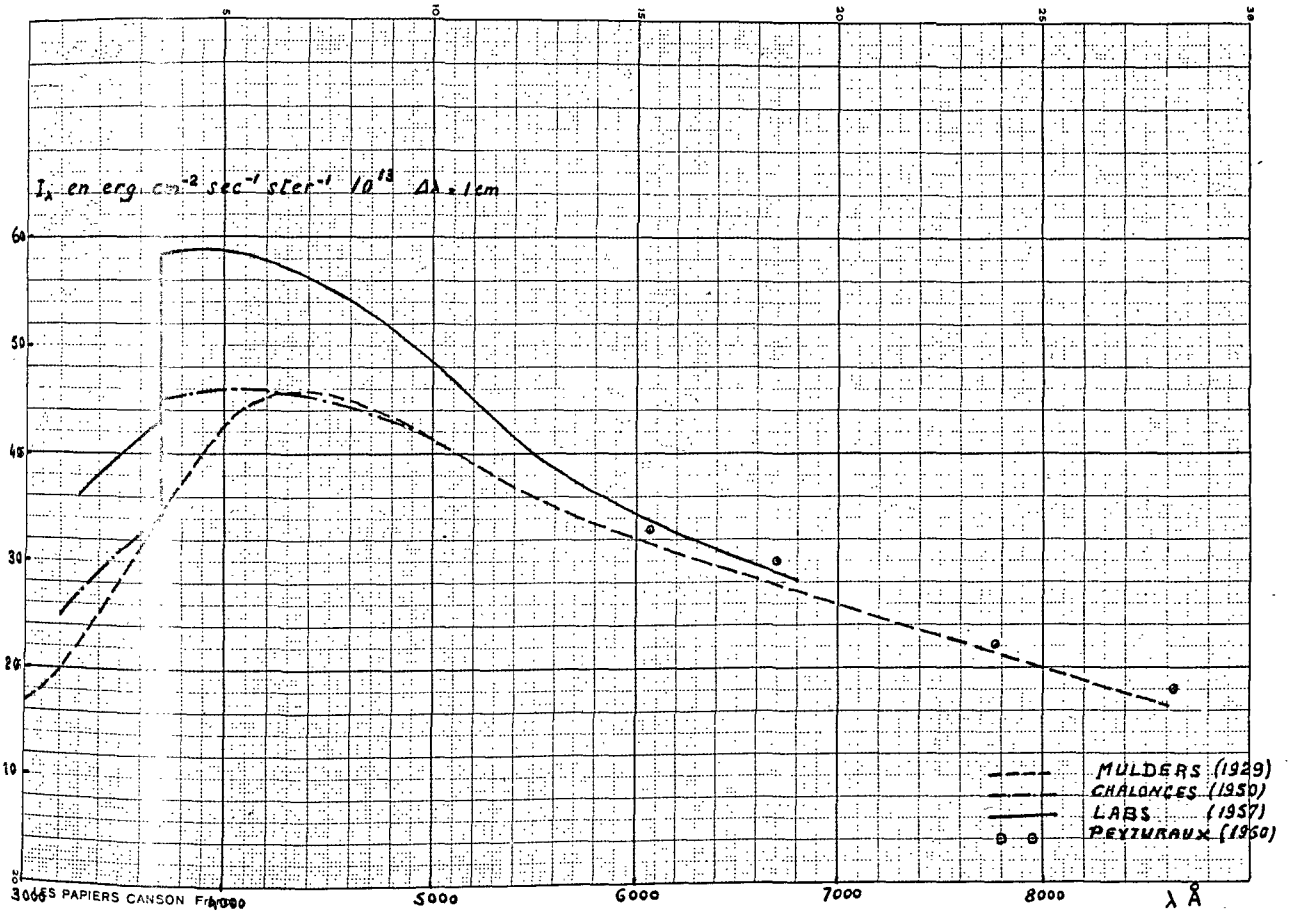


Figure 3 b. Résultats récents sur la mesure de l'énergie au Centre du disque solaire : mesures diverses dans le visible et l'ultraviolet

et de la source. Les deux procédés sont défendables et dépendent surtout du matériel mis en œuvre.

Les récepteurs employés couramment sont :

Pour les régions visible et ultraviolette, les cellules à multiplicateur d'électrons;

Pour les régions du proche infrarouge, les cellules au sulfure de plomb;

Pour les régions d'infrarouge plus lointain, les cellules au tellurure de plomb, les récepteurs thermo-électriques ou les bolomètres.

Mesure de l'absorption atmosphérique

Le principe de la mesure a été indiqué plus haut. Le procédé le plus pratique consiste à enregistrer depuis le lever jusqu'au coucher du soleil l'énergie monochromatique reçue de celui-ci. On peut enregistrer une seule longueur d'onde par jour, ce qui donne un résultat très précis, ou une gamme de longueurs d'onde distinctes, ce qui donne une information plus large. La lumière du soleil est reçue par l'intermédiaire d'un système optique, soit sur la fente d'entrée d'un monochromateur, soit sur un filtre à bande étroite. Elle est reçue ensuite par un récepteur photo-électrique. L'ensemble est fixé sur une monture équatoriale qui suit le soleil. Pour le récepteur, nous donnons la préférence à la pile thermo-électrique suivie d'un galvanomètre sensible. Ce procédé, malgré une certaine incommodité (sensibilité médiocre, vitesse de réponse lente, fragilité du galvanomètre), est le seul qui permette de garantir la stabilité de réponse du récepteur au cours de la journée, et ainsi évite des étalonnages.

Mesures de laboratoire

Le rapport entre le soleil et la source étalon varie de quelques unités à plusieurs centaines selon la longueur d'onde. Il faut donc intercaler un système affaiblisseur sur le trajet du faisceau lumineux solaire. On peut procéder par diaphragmation, mais dans ce cas on ne peut pas atteindre de grands rapports d'affaiblissement sans perturber de façon difficilement calculable l'uniformité du faisceau lumineux. Nous donnons la préférence aux filtres en verre absorbant dans la masse qui, malgré un étalonnage laborieux, offrent toute sécurité.

Enfin, les miroirs tels que le collimateur de la source étalon ou les autres miroirs introduits dans les faisceaux pour des besoins géométriques doivent

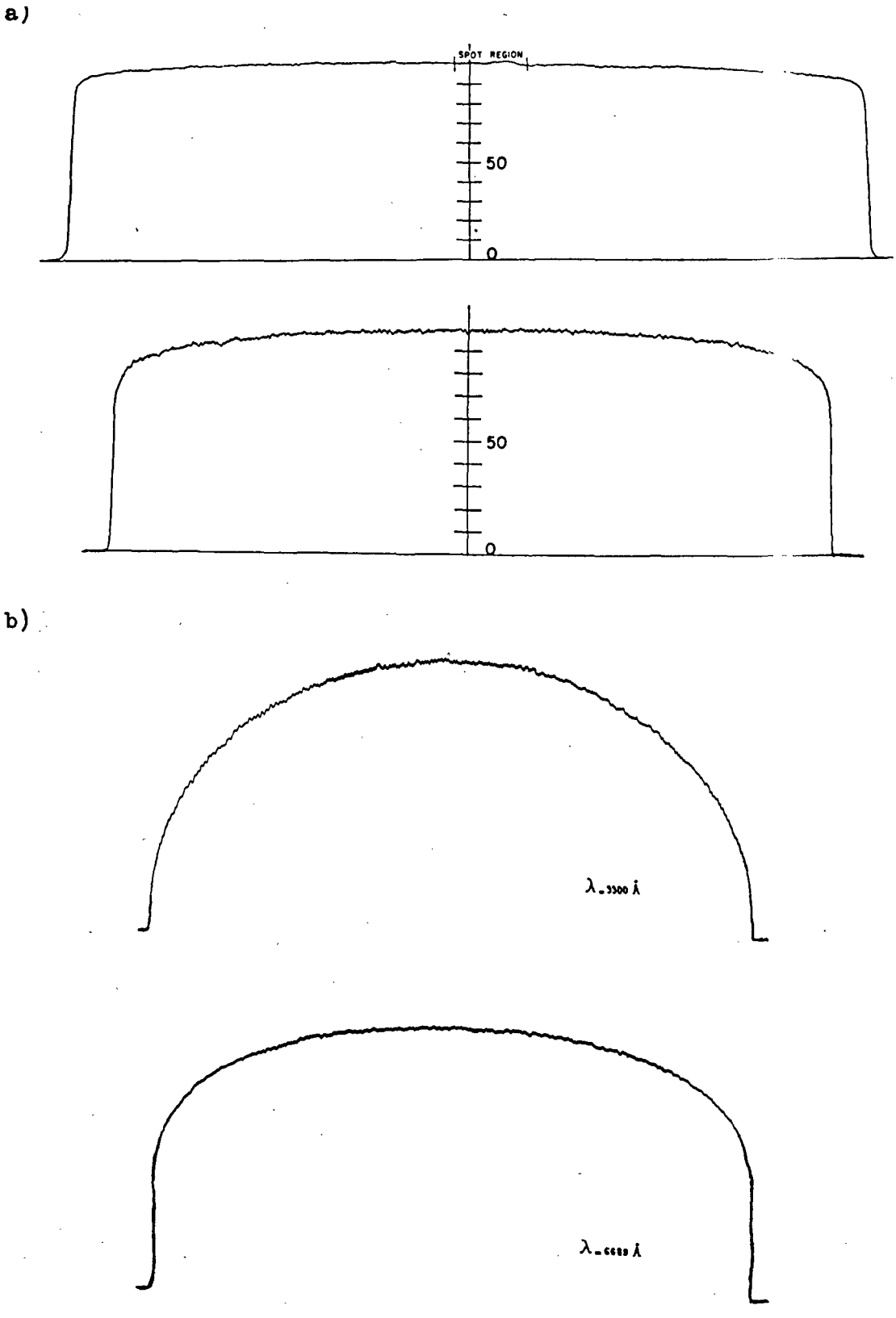


Figure 4. L'assombrissement centre-bord du soleil

a) Selon Pierce, McMath, Goldberg, Mohler : λλ 83 000 Å et 16 932 Å ; *b*) Selon Peyturaux : λλ 6 689 Å et 3 300 Å

être mesurés avec soin par des procédés classiques sur lesquels nous n'insisterons pas.

RÉSULTATS OBTENUS ET PROGRAMMES EN COURS

Les résultats de mesures vraiment absolues sont encore très fragmentaires et provisoires. Par contre, il est bon de faire état de travaux récents qui ont eu pour but de déterminer avec soin la courbe d'énergie du centre du disque solaire en valeurs relatives. L'échelle a été obtenue par raccordement à la courbe de Mulders. Nous citerons les travaux de Chalonge et collaborateurs (3), de Pierce (4) et de l'auteur (5). La courbe de Labs (6) est relative, mais un point a été mesuré de façon absolue, ce qui fixe l'échelle de l'ensemble sans raccordement à des résultats antérieurs. Enfin l'auteur (7) a obtenu à Mont-Louis quatre points absolus qui constituent les premiers résultats d'un programme en cours. Ce programme doit couvrir le plus grand intervalle spectral possible : ultraviolet, visible, infrarouge. De son côté, à notre connaissance, Labs poursuit un programme analogue en Suisse au Jungfraujoch et Sitnik, à Moscou, a aussi entrepris des travaux sur le même sujet. De toutes façons, plusieurs années seront nécessaires avant que nous possédions un ensemble de résultats homogène et précis. Toutefois les données fragmentaires peuvent être utilisées au fur et à mesure de leur parution. La figure 3 montre les courbes obtenues à la suite des travaux récents. On voit que des divergences considérables apparaissent avec les résultats anciens. Ceci nous montre l'importance des mesures en cours pour une connaissance complète et précise du spectre solaire.

La mesure de l'assombrissement centre-bord du soleil

Quand on observe le disque solaire, on constate que le bord est plus sombre que le centre. Cela provient du fait que l'atmosphère solaire ou photosphère est à la fois rayonnante et partiellement transparente. Ainsi le rayonnement qui nous parvient du centre du disque solaire vient en moyenne de couches plus profondes, donc plus chaudes, que celui qui nous parvient du bord.

L'assombrissement centre-bord avait déjà été mesuré par Abbot mais les mesures modernes ont donné un ensemble de résultats homogène et précis. Citons les travaux de Pierce, Mc Math, Goldberg, Mohler (8) et de l'auteur (9).

La méthode de mesure est la même pour tous les auteurs, à quelques variantes près. On forme sur la fente d'entrée d'un monochromateur l'image du soleil et on fait défiler cette image d'un bord à l'autre. On obtient des courbes plus ou moins aplaties suivant les longueurs d'onde, ainsi que le montre la figure 4.

Les résultats de mesures d'assombrissement sont très utiles car ils permettent, jumelés avec les données absolues, de déterminer la structure interne de la photosphère qui est la source du rayonnement que nous recevons.

Les mesures de raies spectrales

On ne peut traiter complètement la question de la mesure absolue du rayonnement solaire sans parler au moins sommairement des mesures de raies spectrales. Les mesures comportent la détermination de l'intensité globale des raies et leur profil. Ce sont là des travaux très complexes qui ont été effectués surtout pour évaluer l'abondance et la répartition en profondeur des éléments responsables de ces raies. Nous donnerons seulement quelques indications sur la physionomie générale du spectre des raies solaires.

On distingue les raies fortes, dues pour la plupart à l'hydrogène, qui est l'élément fondamental de toute atmosphère stellaire. Ce sont les raies de la série de Balmer qui sont situées de 6 563 Å jusqu'à 3 700 Å où le spectre continu montre une forte discontinuité (voir figure 3). Ensuite, on a les raies H et K du calcium dans l'ultraviolet. Les autres raies sont dues à des métaux, surtout le fer. Ensuite on distingue quelques bandes moléculaires dues à CN, à CH, à O, etc.

Ces raies ont fait l'objet d'études approfondies, non seulement du point de vue de leur intensité au centre du disque solaire, mais aussi du point de vue de leur variation centre bord. L'énergie globale absorbée par les raies a été évaluée à plusieurs reprises. D'après les travaux les plus récents (10), elle serait d'environ 12 p. 100.

Conclusion

Les travaux modernes sur la mesure absolue de l'énergie solaire ont été surtout entrepris dans un but purement astrophysique. Cependant, même pour les applications pratiques, les résultats obtenus et à obtenir sont d'une grande importance.

Tout d'abord il est bon de préciser la valeur de la constante solaire. En regroupant :

a) Les résultats de mesures sur la répartition spectrale de l'intensité au centre du disque solaire en valeur absolue,

b) Les résultats de mesures d'assombrissement centre-bord,

c) La détermination de l'énergie absorbée dans les raies spectrales, et

d) L'évaluation par la théorie des énergies émises dans les régions spectrales non observables,

on doit arriver à une valeur de la constante solaire qui peut être très précise, car les calculs comportent surtout des intégrations.

Ensuite, il est bon de connaître la répartition spectrale de l'énergie, car on peut être amené à utiliser le rayonnement de telle ou telle région du spectre.

Enfin, d'une manière générale, une connaissance approfondie des propriétés d'une source d'énergie peut faciliter l'étude d'applications particulières.

Références

1. Link, Nouvelles tables de masses d'air, *Journal des observateurs*, XVII nº 3, p. 41-48 (1934).
2. Mulders, *Zeitschrift für Astrophysik*, 20, p. 239 (1941).
3. Canavaggia, Chalonge, *Annales d'astrophysique*, 9, p. 143 (1946).
   Canavaggia, Chalonge, Oziol-Peltey, Egger-Moreau, *Annales d'astrophysique*, 13, p. 355 (1950).
4. A. K. Pierce, *Astrophysical Journal*, 117, p. 312 (1953).
5. Peyturaux, *Annales d'astrophysique*, 15, p. 302 (1952).
6. Labs, *Zeitschrift für Astrophysik*, 44, p. 37 (1957).
7. Peyturaux, *Comptes rendus de l'Académie des sciences*, 252, p. 668 (1961).
8. A. K. Pierce, R. R. McMath, L. Goldberg, O. C. Mohler, *Astrophysical Journal*, 112, p. 285 (1950).
9. Peyturaux, *Annales d'astrophysique*, 18, p. 32 (1955).
10. Michard, *Bulletin of the Astronomical Institutes of the Netherlands*, XI, nº 416 (1950).

Résumé

Bien que l'énergie reçue du soleil au niveau du sol soit la seule utilisable, il est nécessaire, si l'on veut des données universelles, de connaître l'énergie reçue au-dessus de l'atmosphère. En effet, celle-ci absorbe le rayonnement solaire de façon considérable, et surtout d'une façon très variable selon le domaine spectral (ultraviolet lointain et larges bandes infrarouges totalement absorbées par exemple).

En outre, le rayonnement propre du soleil est lui-même très complexe, du fait de la présence de raies d'absorption très nombreuses.

Par suite, pour avoir une connaissance complète du rayonnement solaire, il faut mesurer l'énergie à spectre continu émise par les différents points du disque solaire et l'énergie absorbée dans les raies spectrales.

Mesure directe de la constante solaire

La constante solaire est, rappelons-le, l'énergie reçue de l'ensemble du disque solaire, pour toutes les longueurs d'onde, au-dessus de l'atmosphère. Cette détermination directe qui ne se pratique plus de nos jours, car on espère obtenir un résultat plus précis par les méthodes indirectes, a été d'une grande utilité et constituait encore il y a quelques années la seule donnée absolue sur l'énergie solaire.

La mesure se faisait en trois temps :

1) Mesure de l'énergie solaire reçue au sol pour toutes les longueurs d'onde transmises par l'atmosphère terrestre; cette mesure était effectuée à l'aide d'un pyrhéliomètre;

2) Mesure de l'absorption atmosphérique par la méthode des droites de Bouguer.

3) Évaluation de l'énergie totalement absorbée dans les domaines spectraux où l'atmosphère est complètement opaque. Cette évaluation était faite en supposant que le rayonnement « invisible » était voisin de celui d'un corps noir. En outre, quelques progrès ont été apportés par les mesures en V_2.

La constante solaire est d'environ 2.00 cal cm^2 min^{-1} avec une incertitude de l'ordre de 5 p. 100.

Mesures spectrophotométriques du rayonnement solaire

Une analyse approfondie des anciennes mesures a montré, il y a quelques années, leur précision insuffisante pour une connaissance certaine de l'émission énergétique du soleil. Les chercheurs modernes ont orienté leurs recherches dans trois voies principales :

a) Mesure absolue de la répartition spectrale de l'énergie émise par le centre du disque solaire;

b) Mesure de la variation de l'énergie entre le centre et le bord du disque solaire;

c) Mesure de l'énergie absorbée dans les raies spectrales.

Mesure absolue de l'énergie au centre du disque solaire

Cette mesure se pratique en comparant le soleil à une source terrestre. Les sources utilisées usuellement sont :

a) La lampe à ruban de tungstène, qui constitue une bonne source tare mais ne peut constituer un étalon absolu du fait de son évolution dans le temps;

b) L'arc électrique, qui permet d'atteindre 4 000 °K, est un bon étalon de répartition spectrale mais ne peut être non plus considéré comme absolument stable dans le temps;

c) Le corps noir, qui est l'étalon absolu parfait. On réalise le corps noir en graphite ou en métal. Celui qui a été construit par l'auteur se compose essentiellement d'un tube de tantale mince chauffé sous vide. On atteint la température de 2 600 °K en 15 minutes, et les conditions de corps noir sont satisfaites à quelques millièmes près.

La comparaison entre la source et le soleil se fait en projetant successivement sur la fente d'un monochromateur l'image du soleil et celle de la source. L'énergie est recueillie par une cellule photo-électrique et enregistrée. On doit en outre mesurer l'absorption atmosphérique par la méthode de Bouguer et étalonner au laboratoire les systèmes optiques qui ont été mis en œuvre pour faire la comparaison.

Des courbes d'énergie relative assez précises ont déjà été obtenues par Chalonge et collaborateurs,

Pierce, Labs et l'auteur. Les mesures absolues ont été faites pour peu de longueurs d'onde par Labs et l'auteur. Les chercheurs qui à notre connaissance traitent le problème sont Labs, Sitnik et l'auteur.

La mesure de l'assombrissement centre-bord du soleil

L'observation montre que le soleil est plus sombre au bord qu'au centre. Les mesures ont montré que cet assombrissement est plus important quand la longueur d'onde diminue. Des mesures très précises ont été faites.

Mesures de raies spectrales

De nombreux chercheurs ont étudié les raies spectrales du soleil, pour diverses raisons. L'absorption totale dans les raies est d'environ 12 p. 100.

Conclusion

Les mesures décrites doivent aboutir à une connaissance précise de :

a) La constante solaire;

b) La nature du rayonnement solaire;

c) La structure interne du soleil.

THE ABSOLUTE MEASUREMENT OF SOLAR ENERGY

Summary

Although the energy received from the sun at ground level is the only solar energy that can be used, the energy received above the atmosphere must be known if universal data are desired. For the atmosphere absorbs solar radiation very substantially and very variably, according to the spectral region (for instance, the far ultraviolet and broad infrared bands are completely absorbed).

Moreover, the sun's own radiation is itself highly complex, owing to the presence of very numerous absorption lines.

Consequently, for complete knowledge of the solar radiation, one must measure both the energy of the continuous spectrum emitted at the various points of the solar disc and the energy absorbed in the spectral lines.

Direct measurement of the solar constant

We recall that the solar constant is the energy received from the entire solar disc, at all wavelengths, above the atmosphere. Its direct determination, which is no longer performed today, since more precise results are expected by indirect methods, was very useful, and only a few years ago it was still the only absolute datum on solar energy.

This measurement was performed in three stages.

(1) Measurement of the solar energy received at the ground for all the wavelengths transmitted by the earth's atmosphere. This measurement was accomplished by means of a pyrheliometer.

(2) Measurement of the atmospheric absorption by the Bouguer method.

(3) Estimation of the energy totally absorbed in the spectral regions where the atmosphere is completely opaque. This estimation was based on the assumption that the "invisible" radiation was near that from a black-body. Moreover, measurements in V2 missiles were responsible for some progress.

The solar constant is about 2.00 cal cm^2 min^{-1}, with an uncertainty of the order of 5 per cent.

Spectrophotometric measurements of solar radiation

A few years of extensive analysis of old measurements showed their inadequate accuracy for a reliable knowledge of the emission of energy from the sun. Modern investigators have directed their research in three main directions:

(*a*) Absolute measurement of the spectral distribution of the energy emitted by the centre of the solar disc;

(*b*) Measurement of the variation of the energy between the centre of the solar disc and the limb;

(*c*) Measurement of the energy absorbed in the spectral lines.

Absolute measurement of the energy at the centre of the solar disc

This measurement is performed by comparing the sun with a terrestrial source. The sources usually employed are:

(*a*) The tungsten ribbon lamp, which is a good calibration source but cannot be an absolute standard, on account of its variation with time.

(*b*) The electric arc, which may reach 4 000°K, is a good standard of spectral distribution, but neither can it be considered absolutely stable with time.

(*c*) The black-body, which is the perfect absolute standard. Black-bodies are made of graphite or metal. The black-body constructed by the author consists essentially of a thin tantalum tube heated in vacuo. The temperature of 2 600°K is reached in fifteen minutes, and the black-body conditions are satisfied within several thousandths.

The source and the sun are compared by successive projection of the image of the sun and that of the source on the slit of a monochromator. The energy is collected by a photocell and recorded. The atmospheric absorption must also be measured by the Bouguer method, and the optical systems used for the comparison must be calibrated at the laboratory.

Rather accurate relative energy curves have already been obtained by Chalonge and associates, Pierce, Labs, and the author. Absolute measures have been made on a few wavelengths by Labs and the author. The investigators dealing with this problem, to our knowledge, are Labs, Sitnik and the author.

Measurement of the darkening between the solar centre and limb

Observation shows the sun to be darker at its limb than at its centre. Measurements have shown that this darkening increases with decreasing wavelength. Very accurate measurements have been made.

Measurements of spectral lines

Numerous investigators have studied the spectral lines of the sun for various reasons. The total absorption in the lines is about 12 per cent.

Conclusion

The measurements described should lead to an accurate knowledge of:

(*a*) The solar constant;

(*b*) The nature of the solar radiation;

(*c*) The internal constitution of the sun.

SOLAR RADIATION AND ITS MEASUREMENT AT A NETWORK OF STATIONS, WITH SPECIAL REFERENCE TO INDIA

L. A. Ramdas *

That the sun sustains life on our earth and is directly or indirectly the ultimate source of most forms of energy available to us has been known from ancient times. It was only in the nineteenth century and thereafter, however, that atmospheric and astro physicists began to study the total intensity as well as the spectral distribution of radiation from the sun. From measurements of the total intensity of solar radiation at different zenith distances from the sun, corresponding to different effective air masses through which radiation has to pass before reaching the earth's surface, the solar constant has been computed. This constant is defined as the amount of solar energy incident per minute per square centimetre of a plane surface held normal to the solar rays, above the earth's atmosphere. Its value is of the order of 2.0 gramme calories per minute, per sq cm, and it is being periodically revised as more and more information regarding the contribution in the ultra-violet and near infrared regions of the solar spectrum becomes available from rocket and satellite records. To the Smithsonian Institute goes the main credit for most of our basic knowledge of solar radiation and the solar constant. Langley, Fowle and Abbot have been the pioneers in this field (1 - 5).

From the point of view of the present symposium, the main interest lies in assessing the intensity and duration of the solar radiation that actually reaches the surface of the ground in different parts of the earth and in different months of the year. It is already known that, while passing through the atmosphere, solar radiation is depleted by the process of (*a*) absorption, mainly by oxygen and ozone, in the upper atmosphere, and water vapour and carbon dioxide in the lower layers of the atmosphere, (*b*) molecular scattering by the gases in the atmosphere and (*c*) scattering by dust and other impurities suspended in the atmosphere.

The distribution of energy in the solar spectrum, particularly in the light of new information in the ultra-violet region, may not conform entirely to the radiation from a black-body at 6 000 Å. However, over most of the visible and infra-red regions, the black-body radiation gives a pretty close approximation to the general energy distribution.

Oxygen in the uppermost layers cuts off the extreme ultra-violet (0.12 to 0.18 μ), while ozone absorbs completely in the region 0.20 to 0.33 μ and to a small extent in the visible region 0.44 to 0.76 μ. Water vapour has a number of absorption bands in the near infra-red centred at 0.93, 1.13, 1.42 and 1.47, while carbon dioxide absorbs in the region of 2.7 μ. These bands cut off a significant percentage of the radiation from the sun in these regions of the spectrum.

As discussed by Moon (6), the transmission coefficients with the sun at zenith (vertical) $T_{a\lambda}$ $T_{w\lambda}$, and $T_{d\lambda}$ associated with atmospheric scattering, water vapour and dust, respectively, at the wavelength λ (expressed in μ) can be represented as

$T_{a\lambda} = 10^{-0.00380/\lambda^4}$ (at pressure of 760 mm of Hg)

$T_{w\lambda} = 10^{-0.0075/\lambda^2}$ (when w, precipitable water, is 20 mm)

and

$T_{d\lambda} = 10^{-0.0353/\lambda^{0.75}}$ (when dust content d is 800 per cubic cm).

The combined transmission T_λ, when the barometric pressure is p, precipitable water w and when the sun's rays are incident at an angle θ, is given by Bouguer's equation,

$$T_\lambda = [(T_{a\lambda})^{p/760} \times (T_{w\lambda})^{w/20} \times (T_{d\lambda})^{d/800}]^m$$

where $m = \sec \theta$.

The above values of T_λ, corrected for ozone absorption, provide a theoretical basis for computing the solar radiation which reaches the earth's surface, provided reasonable values of w, d and ozone contents of the atmosphere are available for different months of the year at different places on the earth's surface. Many excellent review articles containing full discussions of the physical aspects of the problem have already been published. Reference may be made here to the articles by Fritz (8, 9) and Ångström (10). The present writer had occasion to discuss solar energy in relation to the factors controlling the thermal balance at the ground surface in his presidential address to the Physics Section of the Indian Science Congress in 1948. The title of this address was "Physics of the Bottom Layers of the Atmosphere" (7).

In concluding these introductory remarks, it may be pointed out that, though there is general appreciation of the fundamental role of solar radiation as a basic factor in the physics of the atmosphere and as a bountiful source of energy for many practical appli-

* National Physical Laboratory, New Delhi.

cations, there are still many extensive regions of the earth for which practically little or no precise measurements are available. In spite of the enormous strides that were made during the recent International Geophysical Year, the solar radiation network has still many wide gaps. Until these gaps are fully filled, and actual observations begin to be recorded, one can only estimate the likely values of the intensity of solar radiation from knowledge regarding the relationships between this factor and other climatic factors that have already been established from the data accumulated and studied in areas like the United States and western Europe. This aspect of the subject will be discussed very briefly in the next section. Thereafter, in the succeeding sections of the paper, the instrumentation aspects are briefly discussed.

Estimation of "q", "Q_o" and "Q"

This section discusses the estimation of the intensity "q" of solar and sky radiation on a horizontal surface as well as the total daily radiation "Q_o" received from the sun and the sky during cloudless conditions and of "Q", the actual radiation. Relationships between the intensity of the solar radiation and the other controlling factors in the atmosphere have been worked out on the basis of actual systematic measurements carried out over a number of years in the United States at a network of stations. This information is available in the 1951 edition of the *Smithsonian Meteorological Tables* (11). These data may be used to estimate the average values of solar radiation over other regions for which no information is available at present. The present writer and Yegnanarayanan (12) had to adopt this approach in 1954 in a paper, "Solar Energy in India", read before the international symposium on wind and solar energy, held under the auspices of the United Nations Educational, Scientific and Cultural Organization (UNESCO) in New Delhi in 1954. That paper discussed the values of solar radiation computed for a network of twenty-two stations in India. The method followed is briefly as follows.

Table 149 of the *Smithsonian Meteorological Tables* (11) prepared by Fritz (13) gives, in the form of isopleths, the variation in the intensity of radiation from the sun and the sky (i.e., "q") for cloudless skies with the air mass and the amount of precipitable water vapour in the atmosphere. The value of w above the selected twenty-two stations in India for different months of the year was computed from Hann's well-known relation, $w = 0.21\ e$, where e is the normal value of the vapour pressure at the bottom of the atmosphere in mm of Hg, and w is in cm. From the computed zenith distances of the sun, the air masses at different hours of the day were also computed for these stations for different months of the year. With these values of w and the air mass, the values of q for different hours of the day for the twenty-two stations and for the twelve months of the year were obtained from Fritz's isopleths, referred to above. From curves showing the diurnal variation of q it was easy to estimate, by integration, the total mean daily values of Q_o, the total radiation received by a horizontal surface from the sun and the sky under cloudless conditions. These values for the Indian stations are given in table 1.

For many practical purposes one wishes to know the value of q_o, the intensity of the direct solar

Table 1. Total solar and sky radiation, Q_o, during clear days

(gm cal/cm²/day)

Station	Jan.	Feb.	Mar.	Apr.	May	June	July	Aug.	Sept.	Oct.	Nov.	Dec.	Annual
Trivandrum	653	692	749	775	766	749	758	767	752	710	645	628	721
Bangalore	584	650	690	706	703	692	746	704	695	649	631	562	6 668
Madras	649	709	747	764	765	750	749	765	750	709	680	605	720
Dharwar	582	632	701	745	751	732	748	752	717	644	594	562	680
Bombay	553	651	736	789	792	791	795	793	738	661	573	542	701
Poona	554	630	734	756	762	741	755	736	698	632	562	533	675
Sakharnagar	565	648	723	773	785	761	765	762	716	737	576	541	688
Samalkot	580	659	731	771	789	786	783	769	739	662	596	570	703
Ahmedabad	535	618	709	809	811	814	807	785	746	640	558	507	695
Powerkhera	522	602	691	783	783	807	780	768	720	621	547	493	676
Labandhe	550	641	733	779	802	797	781	777	716	647	561	525	693
Karachi	516	591	695	766	786	827	814	795	709	611	531	489	678
Jodhpur	486	574	684	792	810	835	805	770	708	597	507	446	668
Jaipur	471	561	671	777	761	811	793	755	689	594	497	438	652
Allahabad	512	593	699	789	805	827	799	784	698	611	536	470	677
Calcutta	532	617	701	781	784	817	816	800	645	624	557	501	681
Delhi	451	551	662	778	803	827	805	760	693	624	481	421	655
Quetta	384	458	572	671	707	729	707	696	605	544	392	354	568
Lahore	436	539	658	777	847	847	817	768	682	619	453	405	654
Jullundur	430	533	657	774	849	844	812	776	669	617	446	403	651
Peshawar	367	454	612	744	819	835	789	759	636	520	402	336	606
Srinagar	319	402	533	649	711	738	690	660	567	451	356	293	531

Table 2. Hourly values of q_o, the intensity of direct radiation from the sun falling on a surface held perpendicular to the solar rays

(gm cal/cm²/mt)

Station	Latitude	Longitude	January							April						
			6AM 6PM	7AM 5PM	8AM 4PM	9AM 3PM	10AM 2PM	11AM 1PM	12 Noon	6AM 6PM	7AM 5PM	8AM 4PM	9AM 3PM	10AM 2PM	11AM 1PM	12 Noon
Trivandrum	08°-29′	76°-57′	—	0.91	1.28	1.39	1.46	1.46	1.47	0.20	1.10	1.30	1.38	1.42	1.41	1.43
Bangalore	12°-58′	77°-35′	—	0.58	1.17	1.30	1.36	1.38	1.39	0.17	0.99	1.22	1.31	1.31	1.31	1.29
Madras	13°-04′	80°-15′	—	0.84	1.25	1.41	1.48	1.51	1.52	0.21	0.94	1.30	1.42	1.43	1.44	1.40
Dharwar	15°-27′	75°-00′	—	0.77	1.30	1.30	1.38	1.40	1.42	0.24	1.10	1.24	1.37	1.36	1.35	1.35
Bombay	18°-54′	72°-40′	—	0.63	1.26	1.35	1.44	1.49	1.48	0.24	1.15	1.29	1.44	1.45	1.45	1.43
Poona	18°-32′	73°-51′	—	0.67	1.31	1.40	1.50	1.54	1.55	0.28	1.12	1.24	1.37	1.37	1.38	1.39
Shakarnagar	18°-39′	77°-45′	—	0.66	1.24	1.33	1.43	1.49	1.48	0.27	1.15	1.29	1.41	1.41	1.42	1.41
Samalkot	17°-03′	82°-13′	—	0.68	1.24	1.33	1.46	1.50	1.50	0.28	1.12	1.31	1.44	1.43	1.42	1.41
Ahmedabad	23°-02′	72°-35′	—	0.44	1.27	1.38	1.43	1.48	1.50	0.48	1.22	1.37	1.47	1.48	1.50	1.51
Labhandi	21°-20′	81°-45′	—	—	1.22	1.35	1.45	1.48	1.50	0.32	0.97	1.30	1.42	1.44	1.44	1.47
Karachi [a]	24°-53′	67°-07′	—	0.24	1.23	1.43	1.44	1.49	1.49	0.40	1.15	1.29	1.39	1.44	1.42	1.43
Jodhpur	26°-18′	73°-01′	—	0.24	1.18	1.37	1.41	1.49	1.49	0.48	1.22	1.35	1.45	1.45	1.47	1.47
Jaipur	26°-55′	76°-50′	—	0.23	1.15	1.32	1.37	1.45	1.44	0.47	1.17	1.32	1.42	1.43	1.44	1.44
Allahabad	25°-26′	81°-50′	—	0.28	1.23	1.41	1.44	1.49	1.48	0.40	1.20	1.33	1.43	1.44	1.48	1.47
Calcutta	22°-32′	82°-20′	—	0.44	1.22	1.38	1.43	1.48	1.50	0.95	1.12	1.30	1.41	1.43	1.46	1.48
Delhi	28°-35′	77°-12′	—	0.20	1.14	1.33	1.36	1.45	1.45	0.56	1.21	1.33	1.41	1.44	1.45	1.42
Quetta [a]	30°-10′	67°-01′	—	—	0.97	1.13	1.15	1,19	1.25	0.36	1.07	1.13	1.22	1.25	1.26	1.25
Lahore [a]	31°-35′	74°-20′	—	—	1.14	1.34	1.40	1.43	1.46	0.63	1.28	1.36	1.46	1.46	1.47	1.48
Jullundur	31°-25′	75°-35′	—	—	1.14	1.32	1.38	1.42	1.45	0.63	1.26	1.36	1.46	1.46	1.47	1.48
Peshawar [a]	34°-01′	71°-35′	—	—	0.94	1.26	1.32	1.33	1.32	0.56	1.19	1.31	1.40	1.41	1.42	1.42
Srinagar	34°-05′	74°-15′	—	—	0.80	1.09	1.14	1.15	1.16	0.48	1.02	1.15	1.23	1.24	1.27	1.25

Station	Latitude	Longitude	July							October						
			6AM 6PM	7AM 5PM	8AM 4PM	9AM 3PM	10AM 2PM	11AM 1PM	12 Noon	6AM 6PM	7AM 5PM	8AM 4PM	9AM 3PM	10AM 2PM	11AM 1PM	12 Noon
Trivandrum	08°-29′	76°-57′	0.28	1.10	1.27	1.36	1.40	1.41	1.40	—	1.05	1.30	1.39	1.45	1.43	1.44
Bangalore	12°-58′	77°-35′	0.44	1.02	1.15	1.26	1.27	1.30	1.30	—	0.92	1.19	1.29	1.34	1.31	1.32
Madras	13°-04′	80°-15′	0.40	1.07	1.23	1.31	1.39	1.42	1.41	—	0.98	1.30	1.41	1.47	1.44	1.44
Dharwar	15°-27′	75°-00′	0.56	1.12	1.12	1.32	1.34	1.33	1.32	—	0.95	1.21	1.28	1.33	1.35	1.35
Bombay	18°-54′	72°-40′	0.64	1.15	1.17	1.39	1.39	1.38	1.39	—	1.05	1.26	1.34	1.42	1.43	1.41
Poona	18°-32′	73°-51′	0.64	1.15	1.21	1.39	1.42	1.39	1.41	—	0.73	1.28	1.40	1.46	1.48	1.48
Shakarnagar	18°-39′	77°-45′	0.63	1.09	1.16	1.32	1.34	1.32	1.34	—	0.70	1.20	1.33	1.41	1.40	1.40
Samalkot	17°-03′	82°-13′	0.59	1.14	1.30	1.35	1.37	1.38	1.37	—	1.05	1.24	1.37	1.41	1.40	1.42
Ahmedabad	23°-02′	72°-35′	0.81	1.19	1.21	1.38	1.40	1.39	1.37	—	1.23	1.26	1.41	1.46	1.45	1.45
Labhandi	21°-20′	81°-45′	0.68	1.11	1.24	1.34	1.34	1.35	1.36	—	1.12	1.29	1.32	1.37	1.38	1.38
Karachi [a]	24°-53′	67°-07′	0.77	1.12	1.31	1.38	1.39	1.39	1.38	—	1.09	1.21	1.32	1.42	1.45	1.45
Jodhpur	26°-18′	73°-01′	0.91	1.19	1.27	1.34	1.38	1.36	1.36	—	1.09	1.21	1.30	1.41	1.41	1.41
Jaipur	26°-55′	75°-50′	0.90	1.17	1.24	1.32	1.35	1.34	1.32	—	1.08	1.19	1.28	1.39	1.40	1.41
Allahabad	25°-26′	81°-50′	0.77	1.10	1.31	1.36	1.36	1.36	1.35	—	1.09	1.23	1.31	1.44	1.44	1.45
Calcutta	22°-32′	82°-20′	0.81	1.19	1.30	1.39	1.39	1.40	1.39	—	1.16	1.20	1.37	1.39	1.44	1.44
Delhi	28°-35′	77°-12′	0.83	1.12	1.25	1.34	1.35	1.36	1.38	—	1.16	1.26	1.35	1.42	1.45	1.44
Quetta [a]	30°-10′	67°-01′	0.87	1.03	1.09	1.18	1.20	1.19	1.18	—	0.95	1.09	1.17	1.24	1.26	1.25
Lahore [a]	31°-35′	74°-20′	1.02	1.19	1.24	1.34	1.36	1.36	1.35	—	1.20	1.27	1.30	1.41	1.42	1.44
Jullundur	31°-25′	75°-35′	1.02	1.19	1.24	1.34	1.36	1.36	1.35	—	1.20	1.27	1.30	1.41	1.42	1.44
Peshawar [a]	34°-01′	71°-35′	0.95	1.17	1.24	1.31	1.36	1.35	1.36	—	0.87	1.25	1.29	1.35	1.41	1.42
Srinagar	34°-05′	74°-15′	1.85	1.01	1.09	1.16	1.19	1.17	1.21	—	0.79	1.08	1.14	1.18	1.24	1.22

[a] Stations in West Pakistan.

radiation alone on a surface held always perpendicular to the sun's rays.

$$q_o = q^1 \sec\theta$$

where q is the intensity of the vertical component of direct solar radiation alone on a horizontal surface and θ is the zenith distance of the sun. From comparative observations of q^1 and q recorded on clear days, Kimball worked out the ratio "r" of q^1 to q (table 150 on page 439 of *Smithsonian Meteorological Tables*, 1951 edition).

$$\text{Thus } q_o = r\,q.\sec\theta$$

Values of q_o have been worked out for the twenty-two stations from the values of q referred to earlier, using Kimball's factor r; they are given in table 2.

So far, the available solar energy during clear or cloudless conditions has been discussed. Table 3 of the earlier paper mentioned above (12) summarizes the information regarding the duration of bright sunshine collected with Campbell-Stokes sunshine recorders at thirty-three stations in India, for different months of the year. Values of the maximum possible duration of bright sunshine, when there are no clouds, and the actual duration, are also shown clearly in figure 1 of the present paper.

If the actual duration of sunshine is S and the possible duration is S_0, the ratio S/S_0 denotes the fraction of the sunlit hours when the sunshine could reach the sunshine recorder without obstruction by clouds.

Using Ångström's relation:

$$Q = Q_0 \left(0.35 + 0.61 \frac{S}{S_0}\right)$$

the values of Q, the actual solar energy incident per sq cm of a horizontal surface, were computed, using the values of Q_0 already computed for clear days. These values of Q for the twenty-two stations are given in table 3 for different months of the year as well as for the year on an average.

At the time these values of Q_0 and Q were computed, there were only two stations (New Delhi and Poona) for which actual measurements of Q_0 and Q were available from Moll solarigraphs. For the International Geophysical Year and after, data are now available for only two more stations, viz. Calcutta and Madras. This does not represent an adequate network for a large country like India. Nevertheless, it is satisfactory to note that the computations for normal values of Q are in general agreement with the actual measurements, which are only for a few individual years. These measurements, so far as available, have been discussed in detail in the paper by S. P. Venkiteshwaran.[1] Since this paper gives a full discussion of the actual measurements so far recorded in India, they need not be discussed further here.

Instruments for recording solar radiation

In this section the various types of instrument that have been devised for recording solar radiation are mentioned briefly. Fuller details concerning these, together with a critical appraisal of their relative performances, will probably be discussed by other participants at the Conference.

It is not only necessary to use sensitive and efficient equipment, but also to ensure that the records will be reliable on a long-term basis, i.e., over a period of many years. This calls for maintenance of standards in the laboratory for sufficiently frequent comparison with the instruments in continuous use in the open. Among components that may undergo deterioration with use may be mentioned, first, the black paint or deposit on the sensitive face of the thermopile or other receiving surface; then the progressive deterioration in the transparency to visible radiation of the glass cover in the case of instruments provided with such an enclosure.

[1] Distribution of Solar Energy over India, *Proceedings of the United Nations Conference on New Sources of Energy*, 1961; included below, paper S/60.

Table 3. Actual solar and sky radiation Q, all days

(gm cal/cm²/day)

Station	Jan.	Feb.	Mar.	Apr.	May	June	July	Aug.	Sept.	Oct.	Nov.	Dec.	Annual
Trivandrum	561	533	577	504	536	405	402	491	481	440	413	503	487
Bangalore	473	520	580	544	513	408	381	416	431	415	473	450	467
Madras	526	610	643	626	581	495	442	467	510	489	489	473	530
Dharwar	506	544	588	604	541	388	336	398	437	425	497	489	480
Bombay	464	547	596	631	626	459	358	373	457	496	499	477	499
Poona	488	561	631	620	632	489	378	375	475	474	489	464	506
Sakarnagar	491	557	622	626	620	487	390	389	444	465	501	465	505
Samalkot	516	573	636	632	615	478	470	431	429	463	495	496	520
Ahmedabad	476	556	596	696	673	586	452	408	545	557	513	462	543
Powerkhera	470	536	567	681	642	549	413	369	497	521	503	449	516
Labhandi	418	538	572	592	618	486	399	373	465	492	466	457	490
Karachi	444	491	583	643	645	554	423	437	510	513	462	420	511
Jodhpur	418	522	561	657	697	668	523	470	531	513	461	393	534
Jaipur	382	476	570	650	616	560	436	423	489	517	447	381	495
Allahabad	415	480	546	655	644	570	488	485	475	501	467	414	511
Calcutta	442	506	568	617	682	482	416	441	387	431	445	415	486
Delhi	361	441	509	599	610	571	491	486	478	524	442	353	489
Quetta	280	371	440	576	579	627	587	578	551	511	337	283	472
Lahore	319	420	513	630	661	635	539	553	539	532	394	320	505
Jullundur	314	421	473	627	679	641	528	535	509	524	374	323	496
Peshawar	253	318	434	536	622	651	576	570	489	421	329	249	454
Srinagar	185	225	315	435	505	509	490	455	425	357	278	155	361

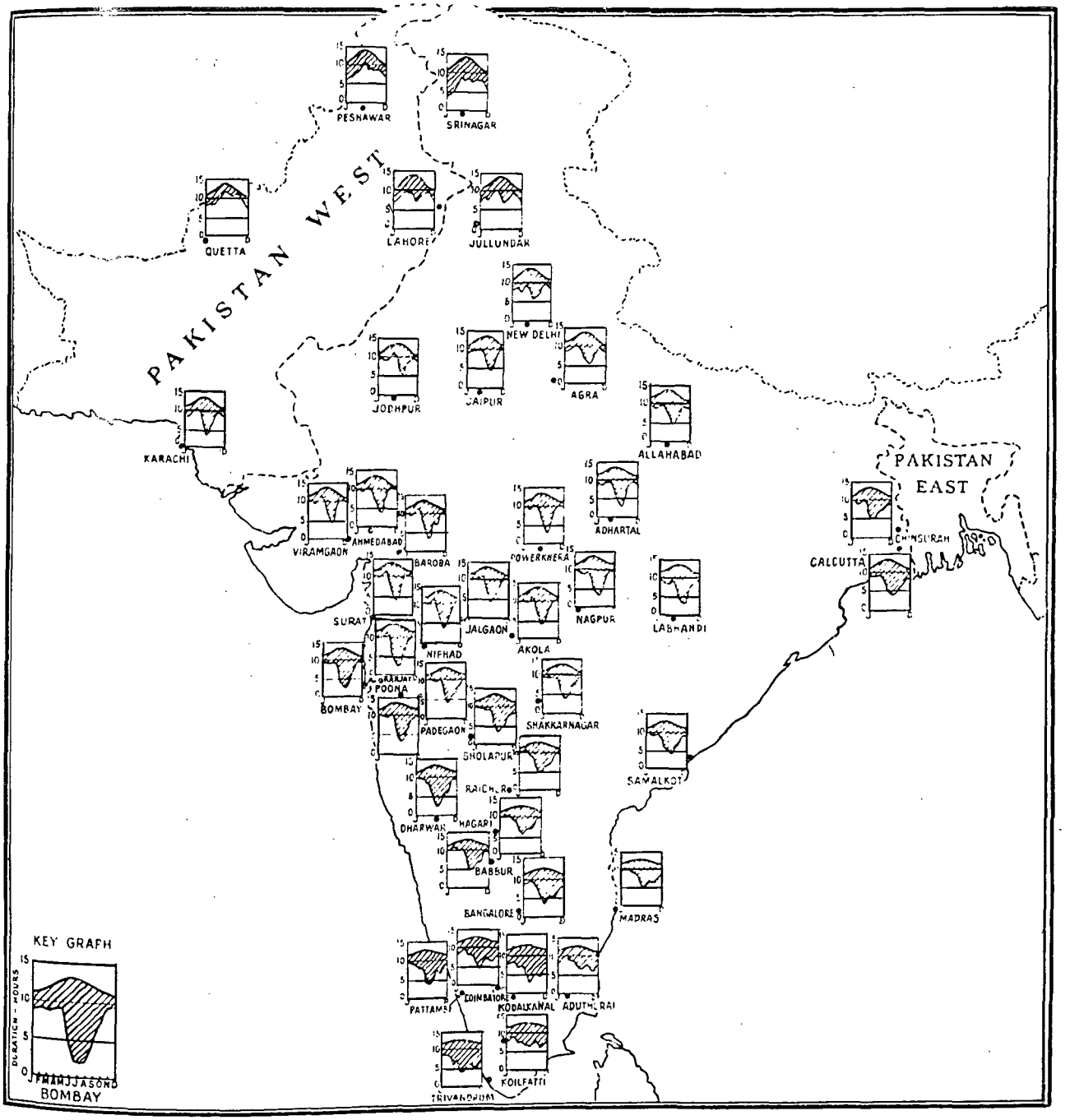


Figure 1. Mean daily duration in hours of "possible" and "actual" bright sunshine at different stations in India (for the different months of the year)

The hatched portions, viz., the difference between the possible and the actual durations, represent the duration of clouds obscuring solar radiation.

Slow changes may also take place in the sensitiveness of thermal junctions. Where recorders are used, these too may undergo progressive deterioration. The maintenance of reliable laboratory standards for different types of instrument and periodical use of these for testing similar equipment in the field require adequate laboratory facilities and a competent physicist to be in charge of the programme.

For measuring the duration of solar radiation or of bright sunshine one uses the well known Campbell-Stokes sunshine recorder with its glass sphere focusing an image of the sun on a blue card. There is a continuous burn on this chart whenever clouds do not obstruct the solar radiation. This instrument is simple and robust; its needs very little attention and maintains itself over many decades. The more

difficult problem is to record the intensity of solar radiation. Here it is necessary to consider methods of measuring:

(*a*) The direct solar radiation, *S*, alone. (This information is also valuable in the design of solar machines and appliances where solar radiation is concentrated by condensing mirrors.)

(*b*) The direct solar radiation from the sun plus the diffuse radiation from the sky.

(*c*) The diffuse sky radiation alone.

Obviously, (*a*) may be measured directly and may also be estimated as the difference between (*b*) and (*c*). Similarly, (*c*) may be estimated by shading (*b*) from direct radiation alone, but otherwise fully exposed to the sky. Equipment that has been devised for measuring (*a*), (*b*) and (*c*) included the following.

(a) *Direct solar radiation*

The Ångström pyrheliometer. This consists of two blackened metallic strips, one of which is shaded from, while the other is exposed to, direct solar radiation. The shaded strip is heated by an electrical current which can be so adjusted that its temperature becomes equal to that of the exposed strip when the galvanometer connected to thermocouples in contact with the strips records zero deflection. The heat losses due to heat radiation and convection are thus equalized so that Ki^2 (where K is the constant of the instrument and K is the electrical current for zero deflection) is an exact measure of the solar radiation. This instrument is an ideal, absolute type, very useful for calibrating or standardizing other types of instrument.

The silver disc pyrheliometer. This has been developed by the Smithsonian Institute. Solar radiation passing through an aperture warms the blackened surface of a silver disc which contains a sensitive thermometer. The intensity of the incident radiation is obtained from the rate of temperature rise after appropriate corrections for heat losses from the sensitive surface. This instrument is not an absolute one like that above, but it is supposed to maintain its constancy over long periods.

Other instruments. The Marvin pyrheliometer and the Michelson pyrheliometer are other instruments in which the rate of heating and cooling of a body, when exposed to direct solar radiation and shaded from it in alternate time intervals, is measured for estimating the radiation intensity. Besides these instruments, there is also the thermopile type exposed to direct radiation alone through an aperture and connected to a millivoltmeter or sensitive galvanometer. In some forms of this instrument there is also provision for measuring radiation in different parts of the spectrum.

(b) *Direct solar radiation plus diffuse radiation from the sun-lit sky incident on a horizontal surface*

The energy received by the unit area of a horizontal surface exposed to the sun and the sky is a fundamental factor controlling the thermal balance at the earth's surface. In solar installations where flat collectors are exposed to the energy from both the sun and the sunlit sky without any concentration by concave or parabolic mirrors, the energy from both the sun and the sunlit sky are utilized. This factor is recorded with one of the following instruments.

The Moll-Gorczynski solarimeter. This has a flat thermopile element covered by a pair of glass hemispheres and connected to a recording millivoltmeter. It is made by Kipp, Delft, Netherlands.

The Eppley pyrheliometer. This has a flat thermopile element enclosed in a spherical glass bulb and connected to a recording milli-voltmeter. It is made by the Eppley Laboratory, Inc., Newport, Rhode Island. This type is now in extensive use in many countries.

The Bellani distillation pyranometer. This has a blackened horizontal surface. The solar heat evaporates very pure alcohol in the container below the sensitive surface. This condenses into a receiver, and the quantity of alcohol so distilled is a measure of the total energy received from the sun and the sunlit sky in a given interval of time. This equipment is reported to be under development at the Davos Observatory in Switzerland.

Bimetallic actinograph of Robitzsch type. Here the blackened bimetallic element which is heated by radiation actuates a recording pen as in a thermograph. It has a large temperature coefficient and is not as accurate as the first two mentioned above.

The integrating solarigraph. Momin (15), working under the present writer at the Meteorological Office, Poona, a few years ago, developed an integrating solarigraph in which the amplified current from a photoelectric cell charges a condenser until it attains the striking potential of a neon lamp, which in turn actuates an electromagnetic counter. For fuller details, see the paper referred to (15). The instrument worked quite satisfactorily for a few years at the Central Agricultural Meteorological Observatory at Poona. Obviously, equipment of this kind needs a physicist to run it successfully, since is more complicated than the simpler types referred to above.

(c) *Diffuse sky radiation alone*

The instruments referred to under (*b*) when shaded just to cut off direct solar radiation give reduced deflections in the millivoltmeter proportional to the diffuse radiation from the sky. Suitable adjuncts for shading the receiver from the direct solar radiation alone, either continuously or at regular intervals, have been devised.

The next section of this paper discusses the problem of time of response and sensitivity of an Eppley thermopile in relation to the pressure of the surrounding air. This problem is of very great interest since instruments of this type are being used at

present in soundings of the upper atmosphere, for recording the changes in solar radiation on approaching the upper limits of the atmosphere.

Response time of the Eppley thermopile

The problem is now examined of the response time of the Eppley thermopile when its enclosure is (*a*) filled with dry air at atmospheric pressure and (*b*) completely evacuated (vacuum). This investigation of the relation of the thermopile to the pressure of the air in its enclosure has been taken up for the entire pressure range from zero to one atmosphere, but for the present conference, is confined to the two extreme cases, viz., one atmosphere and complete vacuum, which have already been examined.

The Eppley thermopile is connected to a very sensitive Moll microgalvanometer of period of 1/5 second. The deflections are proportional to the voltage developed in the thermopile. On switching on the radiation from a 200-watt lamp the galvanometer deflection rises from zero, rapidly at first, then more and more slowly, until the final steady deflection is attained. Similarly, when the radiation is switched off, the deflection, initially at its maximum value, decreases rapidly at first and less and less rapidly later and gradually comes to zero. The times taken for the "growth" and "decay" of the deflection in the "on" and "off" cases mentioned above are equal. It is found that the deflection with the thermopile in vacuum is almost twice the deflection when it is surrounded by air at atmospheric pressure. The time taken for attaining the maximum value is of the order of about 50 seconds in the former case (vacuum) and about 25 seconds in the latter (air-filled). The reason for such a large difference in the response time in these two cases is explained as follow.

Radiation of intensity Q gramme calories per square centimetre per second is incident on, and absorbed by, the blackened area of the flat exposed surface of the thermopile. The temperature of this surface t seconds after switching on the radiation will be $T°_t$ absolute, the initial temperature T_o being equal to the temperature of the enclosing surface which may be assumed to be sensibly constant during the short spell of the experiment. A part of the heat gained by the thermopile surface will be lost by radiative exchange, and another part will be lost by convection within the confined volume, which will be of the cellular type. Since there is no general wind velocity, the convective loss may be put equal to $P.\Delta T_t$, where P is a constant and $\Delta T_t = T_t - T_o$. The radiative loss is assumed to be equal to $4\,\sigma\,T°_3.\,\Delta T_t$ where σ is the Stafan Boltzman constant. It is also assumed that in the infra-red region of the spectrum, at the temperatures concerned, both the glass sphere and the thermopile surface behave like black-bodies. With these assumptions,

$$\frac{dT_t}{dt} = \frac{Q - (4\,\sigma\,T_o^3 + P)\,\Delta T_t}{S} \qquad [1]$$

where S is the thermal capacity of the thermopile element. The equation [1] may be written as:

$$\frac{dT_t}{dt} = \frac{Q - (4\,\sigma\,T_o^3 + P)\,(T_t - T_o)}{S}$$

and

put $$Q^1 = \frac{Q}{S} \text{ and } R = \frac{4\,\sigma\,T_o^3 + P}{S}$$

then $$\frac{dT_t}{dt} = Q^1 - R\,(T_t - T_o)$$

The numerator $dT_t = -\frac{1}{R}\,d\,[Q^1 - R\,(T_t - T_o)]$

since Q^1 and T_o are constant.

$$\frac{1}{R}\cdot\frac{d\,[Q^1 - R\,(T_t - T_o)]}{Q^1 - R\,(T_t - T_o)} = -\,dt$$

Integrating:

$\frac{1}{R}\cdot\log\,[Q^1 - R\,(T_t - T_o)] = -\,t + k$, where k is the constant of integration.

When $t = 0$, then $T_t - T_o = 0$

$$k = \frac{1}{R}\cdot\log Q^1$$

Substituting:

$$\frac{1}{R}\log\left[\frac{Q^1 - R\,(T_t - T_o)}{Q^1}\right] = -\,t$$

or $$\frac{Q^1 - R\,(T_t - T_o)}{Q^1} = e^{-Rt}$$

i.e., $$1 - \frac{R}{Q^1}\,(T_t - T_o) = e^{-Rt}$$

or $$\Delta T_t = \frac{Q^1}{R}\,(1 - e^{-Rt}) \qquad [2]$$

For $t = 0 \qquad \Delta T_t = O$

and

for $t = \infty$

$$\Delta T_\infty = \frac{Q^1}{R} = \frac{Q}{S}\cdot\frac{S}{4\,\sigma\,T_o^3 + P} = \frac{Q}{4\,\sigma\,T_o^3 + P}$$

So, with the thermopile surrounded by air:

$$\Delta T_t\,(\text{air}) = \frac{Q}{4\,\sigma\,T_o^3 + P}\left[1 - e^{\frac{-(4\,T^3 P)}{S}\cdot t}\right] \qquad [3]$$

When the termopile is in vacuum, and P is zero,

$$\Delta T_t\,(\text{vac}) = \frac{Q}{4\,\sigma\,T_o^3}\left[1 - e^{\frac{-(4\,T_o^3)\,t}{S}}\right] \qquad [4]$$

It is easy to see from [3] that when both radiation and convection are controlling factors, the final deflection is smaller and takes less time to attain than in the case of [4], where radiation alone controls the growth of the temperature rise on exposure to the steady radiation source.

On switching off the radiation after the galvanometer connected to the thermopile has already attained a steady maximum deflection, if $t = 0$, when the radiation is switched off:

$$\frac{dT_t}{dt} = -R\,(T_t - T_o)$$

$$\frac{1}{R} \cdot \frac{d\,(T_t - T_o)}{T_t - T_o} = -dt$$

Integrating:

$$\frac{1}{R} \cdot \log\,(T_t - T_o) = -t + k$$

When $t = O$, $T_t = T_x$, the maximum deflection at $t = 0$.

$$k = \frac{1}{R} \log\,(T_x - T_o)$$

Substituting:

$$\log\left(\frac{T_t - T_o}{T_x - T_o}\right) = -Rt$$

$$\Delta T_t = \Delta T_x \cdot e^{-Rt} \qquad [5]$$

$R = \dfrac{4\,\sigma\,T_o^3 + P}{S}$ when the thermopile enclosure contains air at one atmosphere pressure;

and $R = \dfrac{4\,\sigma\,T_o^3}{S}$ when the thermopile is in vacuum.

Here, again, the deflection comes down to zero value, faster in "air" than in "vacuum".

Coming back to equations [3] and [4], the value of the exponential constant R may be found by noting the time taken for the indicating galvanometer to attain a deflection equal to half the final value. This was 4.5 seconds in the case of the air-filled thermopile.

So, $$R_{\text{air}} = \frac{4\,\sigma\,T_o^3 + P}{S}$$

and $$\frac{\Delta T_t}{\Delta T_\infty} = \tfrac{1}{2} = 1 - e^{-Rt}$$

log $$(.5) = -R_{\text{air}} \times 4.5 \times \log_{10}^{e}$$

$$R_{\text{air}} = .1540$$

Similarly, in vacuum, the time to attain the half value of deflection was 7.4 seconds.

$$R_{\text{vac}} = .0937$$

Thus $$\frac{R_{\text{air}}}{R_{\text{vac}}} = \frac{4\sigma T_o^3 + P}{4\,\sigma\,T_o^3} = 1 + \frac{P}{4\,\sigma\,T_o^3} = 1.644$$

$$\frac{P}{4\,\sigma\,T_o^3} = .644 \qquad \text{or } P = .644 \times 4\,\sigma\,T_o^3$$

The value $4\,\sigma\,T_o^3$ can be computed readily, since T_o is known. The value of P can be computed, since $4\,\sigma\,T_o^3$ is known.

Thus, from the galvanometer deflections plotted against time, until the maximum value is attained corresponding to the intensity of the radiation, the values of the radiation and the convection terms in the exponential can be estimated.

Figure 2 shows the "growth" and "decay" curves on putting on and switching off the radiation, in the case of the air-filled (upper curves) and the vacuum (lower curves) thermopile. The smooth curves give the computed theoretical values of deflection, and the points are the actual experimental values. The general agreement is quite satisfactory though simplifying assumptions have been made in the above theory. The experiments at various pressures are completed, it will be possible to see exactly how the convection term P varies with pressure.

In the preliminary experiments, the question whether the "growth" and "decay" curves depend on the actual inclination of the thermopile surface was examined. For this purpose the readings were taken with the thermopile surface horizontal and facing upwards, vertical and horizontal but facing downwards. There are detectable variations in the time of response in "vertical" and "horizontal but facing downward" positions as compared to the usual "horizontal facing upward" position when the thermopile container has air at atmospheric pressure. In the case of the vacuum thermopile, however, no such variations wee found.

It may be mentioned here that when the thermopiles "in vacuum" and "with air" were exposed to actual solar radiation, the ratio of the deflections recorded was 1.8, which is of the same order of magnitude as was noted in the laboratory measurements discussed above.

It may be noted that in recent experiments from aeroplanes and rockets, thermopiles have been used. It is obvious that for such purposes, the vacuum thermopile is superior to the air-filled one in view of its greater sensitivity and constancy of response in different positions.

Concluding remarks

In the present paper some aspects of solar radiation and its measurement on a long-term basis have been discussed. Information regarding the duration of clear sunshine as actually recorded at a network of stations in India is presented. The intensity of radiation from the sun and sunlit sky has been computed for Indian stations from known relationships between this factor and the controlling factors in the atmosphere, as obtained from data recorded in the United States. As will be observed from another paper (S/60), submitted at the Conference by S. P. Venkiteshwaran of India, the actual observations recorded at four stations during the International Geophysical Year are in reasonable agreement with these computed normal values. In the last section of the present paper, the dependence of the sensitiveness and time

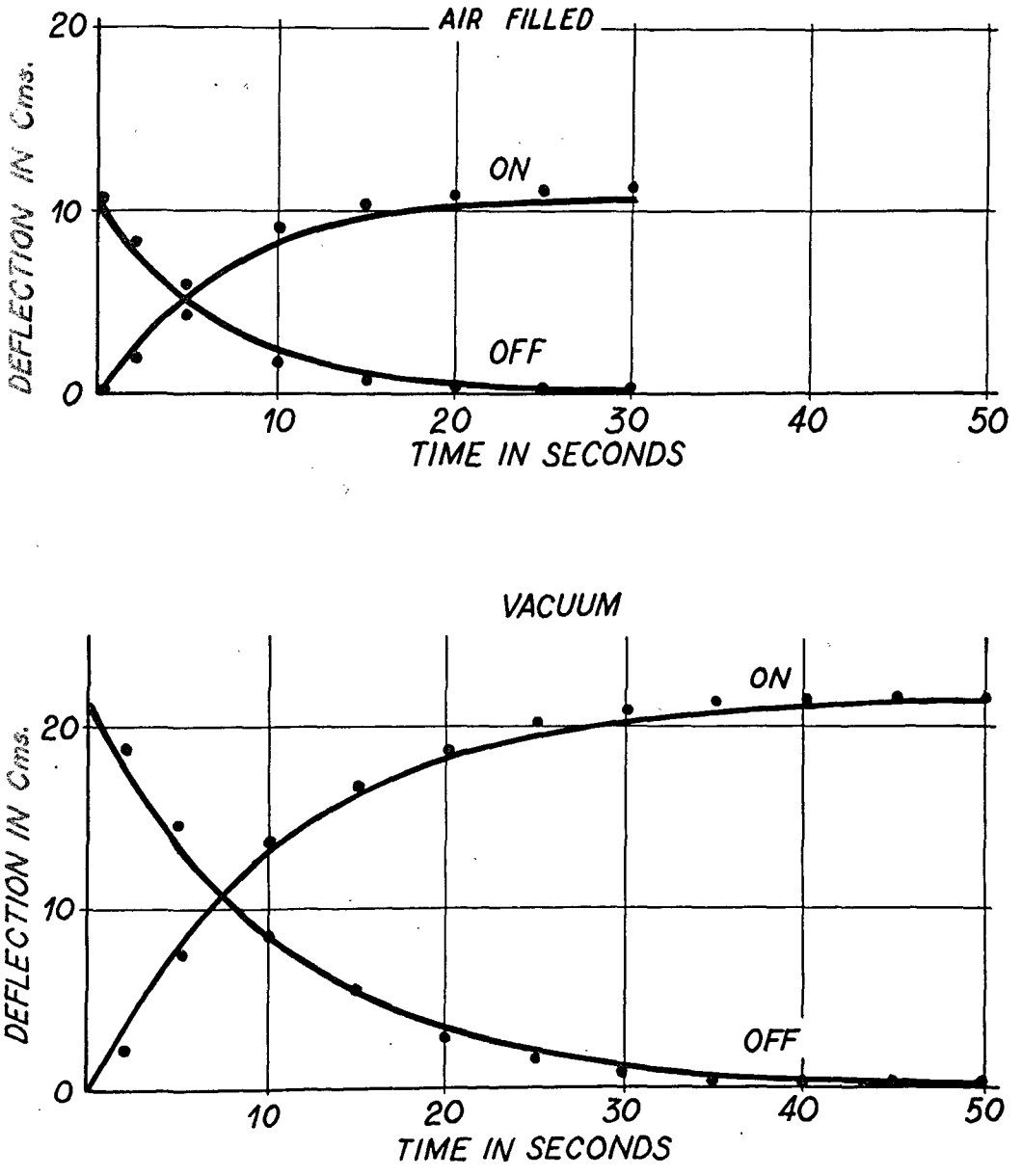


Figure 2. "Growth" and "decay" curves showing deflection against time on putting on and switching off the radiation

Upper curves refer to thermopile "air-filled" and lower curves to thermopile "in vacuum".

of response of an Eppley thermopile on the pressure of the surrounding gas has been examined at some length, and it is shown that though the time of response is greater in vacuum, the sensitiveness is also greatly increased. These times of response are sufficiently small, less than a minute, to ensure accuracy of recording when the equipment is exposed to solar radiation. Further studies on this problem are in progress.

Acknowledgements

The author expresses his thanks to the authorities of the United Nations for inviting him to the Conference, and to the Director of the National Physical Laboratory for the laboratory facilities made available for these investigations. Finally, thanks are due to S. P. Suri for efficient assistance in the experimental work.

References

1. Smithsonian Inst., *Ann. Astrophys. Obs.*, vol. 3, p. 134, 1913.
2. Aldrich, L. B. and Abbot, C. G., *Smithsonian Misc. Collection*, vol. 110, No. 5, 1948.
3. Abbot, C. G., *Smithsonian Misc. Collection*, vol. 94, No. 10, 1935.
4. Fowle, F. E., *Astrophys. Journ.*, vol. 35, p. 149, 1912.
5. Fowle, F. E., *Astrophys. Journ.*, vol. 42, p. 394, 1915; vol. 69, No. 3, p. 12, 1918.
6. Moon, P., *Jour. Franklin Inst.*, vol. 230, p. 583, 1940.
7. Ramdas, L. A., Presidential address to the Physics Section, Indian Science Congress, 1948.
8. Fritz, S., Solar Radiant Energy and its Modification by the Earth and its Atmosphere in *Compendium of Meteorology* edited by Malone, F., American Meteorological Society, 1951.
9. Fritz, S., Transmission of Solar Energy through the Earth's Clear and Cloudy Atmosphere, Trans. Conference on Use of Solar Energy, Tucson, Arizona 1955, vol. 1.
10. Ångström, A., *Geograf Annaler*, vol. 11, pp. 156-166, 1929; vol. 12, pp. 130-159, 1930.
11. *Smithsonian Meteorological Tables*, published by the Smithsonian Institute, Washington, 1951 edition.
12. Ramdas, L. A. and Yegnanarayanan, S., Proceedings of the International Symposium on Wind and Solar Energy, New Delhi, 1954 (UNESCO), pp. 188-196.
13. Fritz, S., *Heating and Ventilating*, vol. 46, p. 69, 1949.
14. Ångström, A., *Medd. Stat. Met. Hydr. Anst.*, vol. 4, No. 3, 1928.
15. Momin, A. U., *Physics Abstracts*, Proc. Indian Sci. Congress, 1946.

SOLAR RADIATION RECORDS IN AUSTRALIA AND THEIR PRESENTATION

C. M. Sapsford *

Australia is particularly well endowed with sunshine, and this fact has undoubtedly contributed to its development as an important primary producing country during its relatively short history. It may at first seem surprising that more data have not been obtained about the quantities of solar radiation received in the country, but the reason is quickly seen when it is realized that the availability of water has been the major controlling factor in settlement and in utilization of the potential of the country. Where sufficient water has been found, there has usually been sufficient solar radiation to provide excellent growing conditions for crops and pasture, while in many cases the solar radiation has been excessive enough to produce uncomfortable living conditions for humans and animals.

With the development of devices to utilize the solar radiation in ways to improve the comfort of settlers, combined with the present intensive studies on the water resources of Australia conducted by the Water Research Foundation, it should now become possible to utilize many parts of the country previously thought to be unsuitable for settlement. It is unfortunate to find in these circumstances that the available solar radiation records are in many cases inadequate to design efficient apparatus to provide some of the comforts desired by settlers, or to assess the practicability of providing distillation plants for purification of salt or brackish water, using solar radiation.

It is the intention in this paper to review the solar radiation data available in Australia and to discuss methods of presenting these data to give maximum information to persons likely to use the data for the design of solar operated devices. Some examples are given of the use of the data for equipment in which the input solar energy is intended to be used to supply energy for heating units with or without "carry-over" storage capacity.

Review of solar radiation records in Australia

Mount Stromlo, 1927 to 1939

The earliest known extensive series of records of solar radiation in Australia was made at the Commonwealth Observatory at Mount Stromlo, Canberra, from 1927 to 1939, and was published by Rimmer and Allen (1). These observations comprised continuous records of total (sun + sky) radiation on a horizontal surface, obtained from an Ångström thermoelectric pyranometer (2) together with daily observations of direct solar radiation at noon on suitable days with an Ångström pyrheliometer (3) and some standardizing checks with an Abbot silver disk pyrheliometer (4). Individual daily values of the total solar radiation are not published by Rimmer and Allen, but these authors do show the monthly mean values for each of the 144 months of records, the average of all monthly means for each of the twelve months of the year, and a comparison between observed and calculated total solar radiation. Study of the relationship between hours of sunshine, as recorded by the Campbell-Stokes sunshine recorder, and total solar radiation resulted in linear curves for each month, from the maximum hours down to approximately one hour of sunshine per day. These curves also showed that for zero hours of bright sunshine approximately 100-150 cal cm^{-2} day^{-1} of solar radiation were observed.

Riverview Observatory, Sydney, 1925 to 1931

A fairly extensive but not continuous series of observations by the Abbot silver disk pyrheliometer and Abbot pyranometer (5) was carried out, mostly on clear days, at the Riverview Observatory, Sydney, during the years 1925 to 1931 (6). The original intention of this work was to study the variations of the solar constant, but the work was discontinued in 1931, partly owing to the unsuitability of the site at 80 ft above sea level and partly because of difficulties in continuing the observations. The main value of these observations to the architect or engineer can be summarized in a figure showing a smooth curve, very closely approximating a sine curve, of seasonal variation of maximum solar radiation on a surface normal to the sun's rays at noon on clear days. The maximum value is 1.54 gm cal/cm^2 min. on 1 January, and the minimum value is 1.32 gm cal/cm^2 min. on 21 June.

Dry Creek, South Australia, 1947 to the present

The longest continuous period of observations of solar radiation in Australia was commenced on 1 January 1947 at the salt fields of Imperial Chemical Industries of Australia and New Zealand (ICIANZ) at Dry Creek, South Australia; these observations are still being continued and published as daily totals of total solar radiation for each day of the period by Bonython (7). Total solar radiation on the horizontal surface is being observed on a

* New South Wales Institute of Technology, Sydney.

Kipp and Zonen solarimeter whose output is recorded on a Kent potentiometric recorder. A Cambridge millivoltmeter recorder was used for the first two years of the records; since 1953 a mechanical integrator has been used in connection with the Kent records. Bright sunshine hours have also been recorded at the site, using a Campbell-Stokes sunshine recorder; and in certain cases where the solarimeter records were not complete, the solar radiation has been estimated, using a well-known relationship between solar radiation and hours of bright sunshine.

CSIRO stations in Australia

Numerous observations have been made at various locations by a number of sections of the Commonwealth Scientific and Industrial Research Organization (CSIRO), but in most cases the solar observations were ancillary to another main research problem which was being studied. In this way some useful data have been obtained, but no long periods of records are as yet available.

CSIRO Division of Meteorological Physics, Aspendale

Solar records at this station were commenced in 1957, and at the present time total solar radiation, diffuse radiation, net radiation and hours of bright sunshine are being observed continuously. For total and diffuse solar radiation, solarimeters manufactured by Kipp and Zonen are used, the diffuse unit being installed in conjunction with a shading ring similar to that described by Drummond (8). The net radiometers were developed by CSIRO, Aspendale, and are described by Funk (9); the Campbell-Stokes sunshine recorder is used to determine hours of bright sunshine. Total radiation records are available from April 1958 to the present, net radiation from August 1958 to the present, and diffuse radiation from September 1958 to the present (10). All three series are obtained on a multi-point electronic recording potentiometer.

CSIRO Division of Plant Industry, Deniliquin

Total solar radiation has been recorded since March 1956, using a Kipp and Zonen solarimeter connected to a two-channel Cambridge thread recorder. The second channel on the recorder has been used since 1960 to record net radiation, using the net radiometer developed by Funk (9). The records of solar radiation have been published by De Vries (11).

CSIRO Irrigation Research Station, Griffith

Total solar radiation has been observed at this station for some years, using first a Kipp and Zonen solarimeter, and later a Fuess bimetallic strip actinograph. Records from these instruments are held at Griffith and used when needed, but the records have not been integrated and published; there is no present intention to publish (12).

CSIRO Division of Land Research and Regional Surveys, Canberra

Various records of total, diffuse and net radiation have been made since 1956 by this division at various places in the Northern Territory and Western Australia. The locations and dates are summarized in table 1, and though none of these has so far been published, it is expected that some data will be ready for publication soon (13).

Radiation network of Commonwealth Bureau of Meteorology

A network of six recording stations in Australia was set up by F.H.W. Albrecht; it commenced continuous recording in 1953. The instruments were

Table 1. Solar radiation records obtained by CSIRO, Division of Land Research and Regional Surveys, Canberra

Location and type of radiation	*Instrument*	*Period of records*
Alice Springs, "17-mile site":		
Global	Kipp and Zonen	Dec. 1958-Apr. 1960
Diffuse	Kipp and Zonen	Jan. 1959-Jan. 1960
Net	Deacon ventilated, Funk	Apr. 1959-Apr. 1960
		May 1959-Apr. 1960
Alice Springs:		
Global	Kipp and Zonen	Aug. 1960-present
Research Institute, Katherine, W.A., research station:		
Global	Kipp and Zonen	Dec. 1959-present
Humpty Doo coastal plains research station:		
Global	Kipp and Zonen	Oct. 1960-present
Kimberley, W.A., research station:		
Global	Kipp and Zonen	Nov. 1956-May 1957

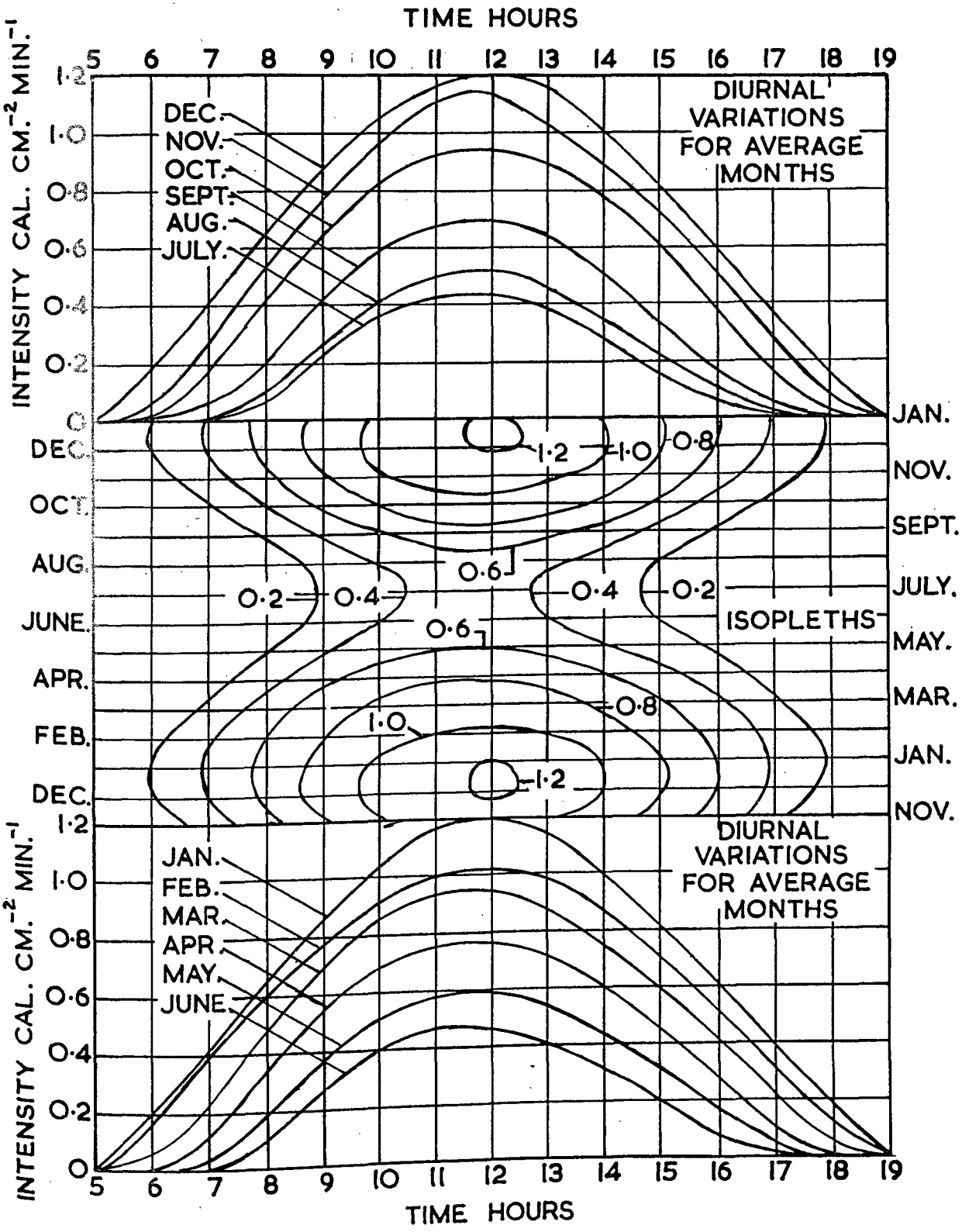


Figure 1. Diurnal and annual variations of total (sun + sky) solar radiation on horizontal surface at Melbourne, Victoria

Lat. 37° 48′ S., Long. 145° 08′ E., Alt. 327 ft.
Mean of years 1953-1956

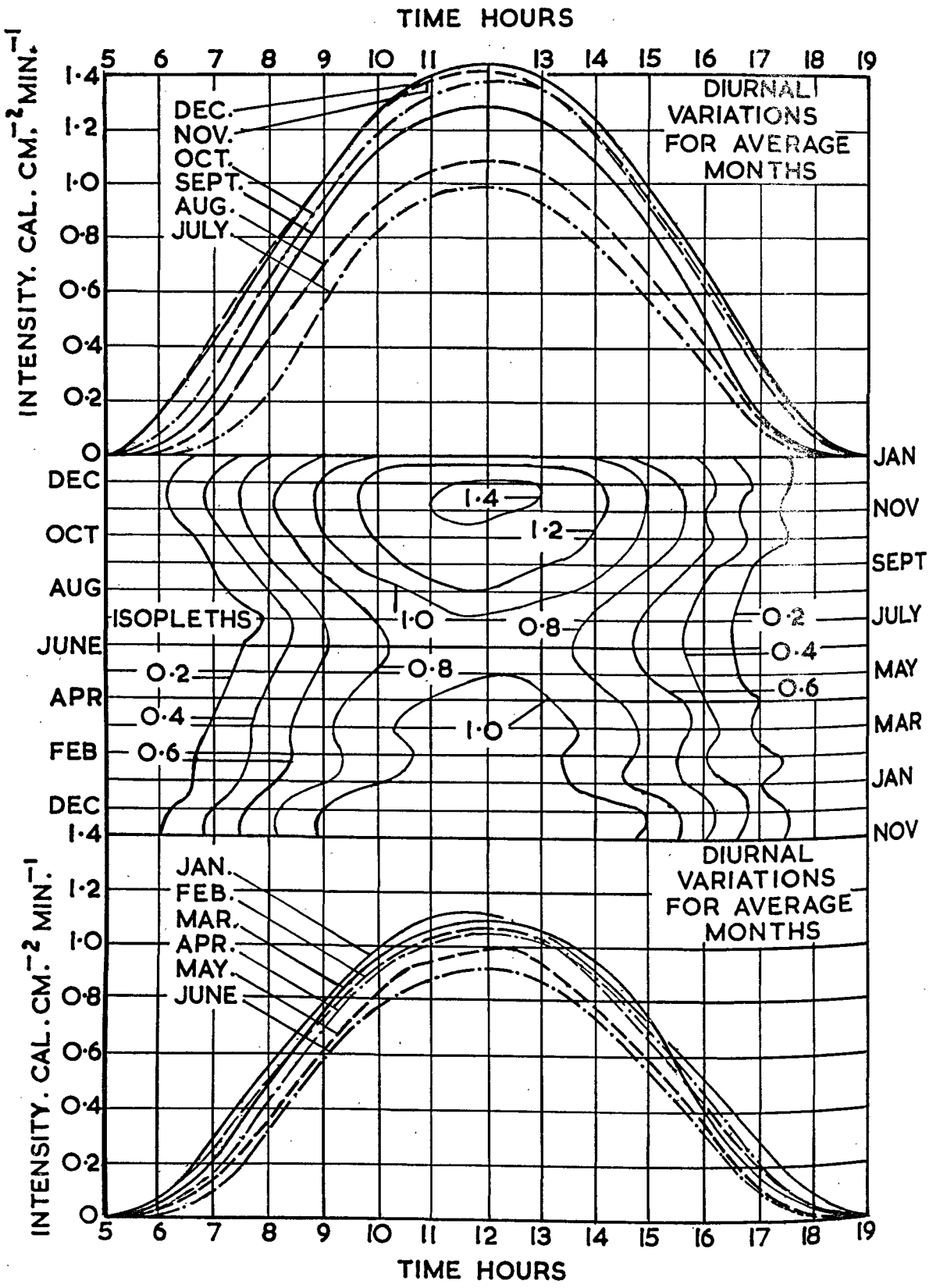


Figure 2. Diurnal and annual variations of total (sun + sky) solar radiation on horizontal surface at Garbutt, Queensland

Lat. 19° 15′ S., Long. 146° 46′ E., Alt. 13 ft.
Mean of years 1953-1956

fully described by Albrecht (14), and some results were published by Albrecht for the Canberra symposium (15). Since 1955 records from two more stations at Rabaul, New Guinea, and Mawson, Australian National Antarctic Research Expeditions (ANARE) base in Antarctica, were included in the radiation network. The observations of all eight stations are being published yearly by the Australian Commonwealth Bureau of Meteorology under the title, *Australian Radiation Records* (16), giving the data detailed below:

1953-1956. Published as hourly means of global radiation, millicalories cm^{-2} min^{-1} for each hour of the day and each month of the year; and, in addition, the average, maximum and minimum daily totals in calories cm^{-2} day^{-1}.

1957. To be published in similar form as the records for 1953-1956.

1958 and subsequently. To be published as daily totals in calories cm^{-2} day^{-1} only.

Observations at University of New South Wales

Solarimeters manufactured by Kipp and Zonen are used in the solar recording stations of the University of New South Wales at Kensington and at Broken Hill, New South Wales. Records of total radiation were started in June 1957 at Kensington, and diffuse radiation was obtained from September 1958, using a Drummond type shading ring (8) over a standard Kipp solarimeter. Total radiation has been measured at Broken Hill since 1959. All three instruments are connected to Kipp and Zonen clockwork driven recording millivoltmeters. Most of the records have been integrated, and it is proposed to publish these in the near future.

Methods of presenting solar radiation data

Various methods of summarizing the solar radiation observations have been devised over the years, and it has been realized that any satisfactory procedure for designing equipment to utilize the solar radiation must take account of (i) the mean value of incident solar radiation, (ii) the random variations from that mean, (iii) the characteristics of the particular equipment as a solar absorber, and (iv) the influence of the environment. Some of these factors have been dealt with recently at the radiation symposium held in Oxford, England, in July 1959, and have been published in papers by de Barry (17), Hinzpeter (18), and Fritz and MacDonald (19). Some Australian radiation data, taken from the Australian radiation records (16), have been summarized here in the form of isopleths for Melbourne, Victoria (Lat. 37° 48′ S) and Garbutt, Queensland (Lat. 19° 15′ S) in figure 1 and figure 2. Frequency distributions of daily totals of solar radiation, based upon the 12-year records for 1947 to 1958 at Dry Creek, South Australia, published by Bonython (7), are also presented here in figure 3 in a form similar to that used by de Barry (17).

The application of solar radiation data to the design of flat plate solar collectors was covered very fully by Hottel and Whillier (20), leading to the definition of a "utilizability" function $\varnothing$, calculated from the solar weather analysis, and this function $\varnothing$ represented "the fraction of the total month's incidence on a horizontal surface, for one particular hour from solar noon, which arrived with sufficient intensity to justify attempted collection".

The function $\varnothing$ defined above certainly makes a distinction between a climate which is variable, on the one hand, and one which is composed of all identical days, on the other, but there are still certain difficulties associated with the occurrence of sequences of above-average or below-average radiation income. These difficulties can be particularly serious when it is not practicable to depend upon standby heating from other energy sources; in these conditions the solar energy collectors must be designed to have a larger collecting surface than would be called for in a design based only upon the average solar radiation income, and it may also be necessary to provide extra energy storage capacity. It has been generally conceded that solar energy collectors cannot be economically justified unless standby heating is provided, but if the analysis detailed below is carried out for suitable localities (mostly tropical), it should be found that collectors

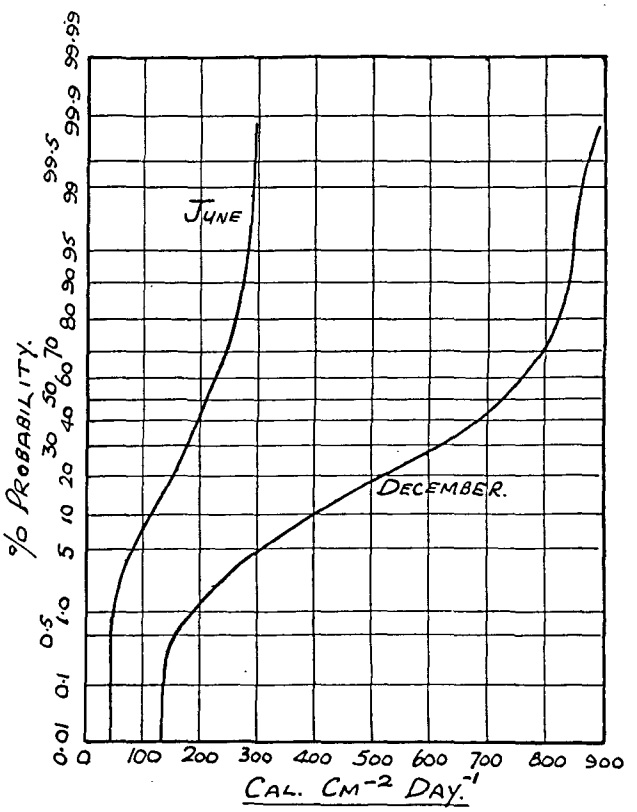


Figure 3. Frequency distribution of daily totals of solar radiation, Dry Creek, S.A., 1947-1958

(December and June)

designed to operate from solar energy alone can compete with alternative means of providing energy in certain cases.

The proposed method of tackling the problem is detailed in the following paragraphs, using the solar radiation data from Dry Creek, South Australia, for the years 1947-1958. Only the records for December (summer) and June (winter) have been used, these representing the extremes of radiation income; this has been considered sufficient to show the working of the proposed method. It would be necessary, however, to study the records for the other months of the year in a similar fashion to obtain a full assessment of the design requirements over the whole year.

Proposed method for study of sequences

The monthly mean values of total solar radiation, for the months of June and December over the 12 years 1947-1958, at Dry Creek, South Australia, were first determined, and their average values over the period computed. The deviations of all daily values, from the 12-year average for the month in question, were then determined and expressed as ratios of the average. These values were defined by the equations [1] and [2] below:

$$D = H - H_a \qquad [1]$$

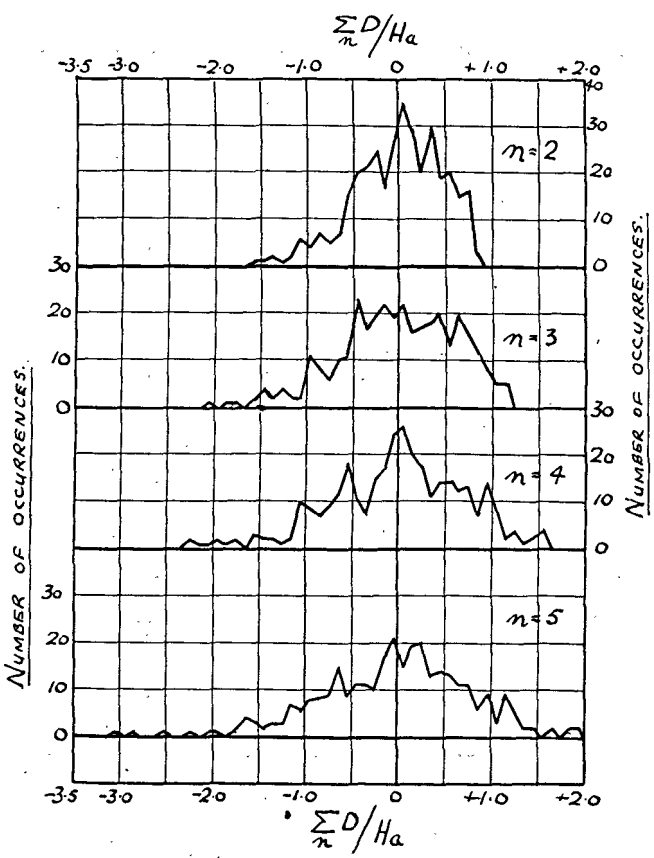


Figure 4. Frequency distribution of $\sum_n D/H_a$ for $n = 2$ to 5 at Dry Creek, S.A., 1947-1958 (June)

where

D = deviation of any one daily value from the average
H = total solar radiation for any one day
H_a = average monthly mean daily total over 12 years.

Dividing by H_a to obtain all values as ratios of the average gives

$$D/H_a = H/H_a - 1 \qquad [2]$$

Obviously D could have positive or negative values, and it was found convenient to define D positive as an excess, and D negative as a deficit. A sequence was defined as any period of days during which D was always positive for a positive sequence, or always negative for a negative sequence. An initial survey of the results for December showed that, in general, negative sequences were rather severe, causing a relatively large cumulative deficit over short sequences, and only one sequence of 5 deficit days was noted over the whole 12 years. Positive sequences were of longer duration; D/H_a never exceeded 0.3 per day, and there were few sequences of more than 5 days, so that it was decided to study the frequency distribution of all groups of 2, 3, 4 and 5 days occurring over the 12 years. The results of these calculations are shown in figures 4 and 5.

When using these frequency plots, one may decide to design in future to meet the worst condition observed over the 12 years. Since, however, this does not of course guarantee that a worse condition may not occur in the future, it seems justifiable to design to cover a certain percentage of the previously noted occurrences, and the values of 95 per cent and 90 per cent have been selected here to give examples of the use of the data.

Application to design of solar energy collectors

With the information detailed above for the place of the proposed equipment, together with knowledge of longer sequences, should this be necessary, the designer is in a position to apply this knowledge to his proposed installation. The method is explained have by means of simple examples illustrating a number of likely installations, and in each case it is assumed that the performance of the installation can be defined by an equation of the type originally used by Hottel and Whillier (20, 21), and described below:

$$Q_u/A = F_R(H R \tau\alpha - Q_L/A) \qquad [3]$$

where

Q_u/A = Useful energy collection per unit area of collector surface
F_R = Heat removal efficiency between collector surface and working fluid
H = Total solar radiation on horizontal surface

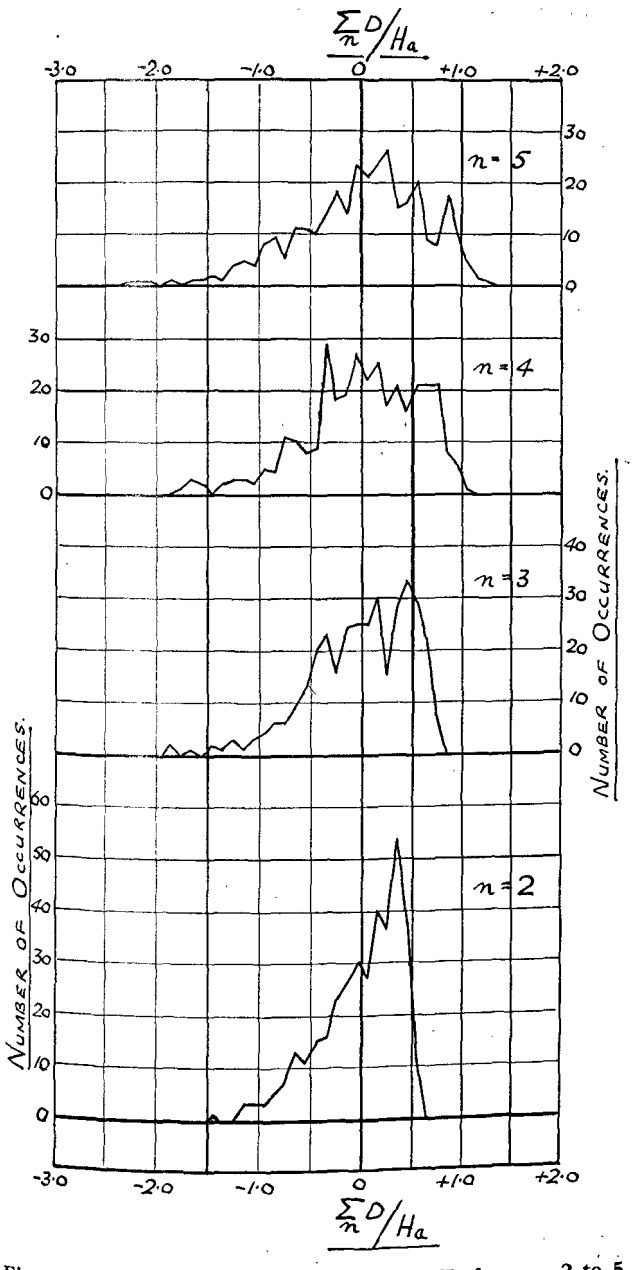


Figure 5. Frequency distribution of $\frac{\Sigma}{n}D/H_a$ for $n = 2$ to 5 at Dry Creek, S.A., 1947-1958 (December)

R = Geometric factor for converting energy per unit horizontal surface to energy per unit collector surface

$\tau\alpha$ = Transmissivity-absorptivity factor for cover material and collector surface

Q_L/A = Energy losses per unit collector surface.

It is further assumed that the solar radiation data for H is in the form of daily totals, and that it is possible to compute values of the factors F_R, R, τ, α and Q_L, representing mean values for the day, suitably weighted to allow for diurnal variations of the angles and intensities involved in these factors. Equation [3] can be simplified to

$$Q_u/A = C_1 H - C_2 Q_L/A \qquad [4]$$

where C_1 and C_2 are constants determined for each month.

The heat balance of the solar collector assembly may now be prepared for the various sequences, making allowance for the fact that it may be necessary to utilize only a proportion (K) of the average incident total radiation (H_a) in order to allow some storage of energy to meet the demands of later days in the sequence.

$$\text{Input energy over } n \text{ days} = C_1 \sum_n H$$
$$= C_1 \left(n H_a + \sum_n D\right)$$
$$= C_1 H_a \left(n + \frac{\sum_n D}{H_a}\right) \qquad [5]$$

$$\text{Output energy over } n \text{ days} = n K H_a + n C_2 Q_L/A \qquad [6]$$

Thus

$$C_1 H_a \left(n + \frac{\sum_n D}{H_a}\right) = n \left(K H_a + \frac{C_2 Q_L}{A}\right)$$

Divide by H_a and bring K to the left:

$$K = \frac{C_1}{n}\left(n + \frac{\sum_n D}{H_a}\right) - \frac{C_2 Q_L}{H_a A} \qquad [7]$$

It will be seen that values of $\left(\frac{\sum_n D}{H_a}\right)$ can be obtained directly from figures 4 and 5, and then $1/n\ (n + \sum_n D/H_a)$ can be computed for all values of n of interest. This represents the extent of handling the solar radiation data and can be carried out independently of the application of the values of C_1, C_2 and Q_L/A, these latter being functions of the collector design.

Examples of the application of the proposed method

Consider the simplest case of a water heater with storage tank capacity equal to one day's energy demand. This would allow no carry-over of energy stored. The values of the constants are assumed to be those detailed in table 2, and the calculations are summarized in table 3. It will be clear from table 3 that the most serious limitation in useful energy

Table 2. Characteristics of projected solar collector at Dry Creek, South Australia

	June	*December*	*Unit*
H_a	201	676	Cal cm^{-2} day^{-1}
R	1.90	0.90	—
$\tau\alpha$	0.70	0.65	—
F_R (C_2)	0.95	0.95	—
Q_L/A	60	50	Cal cm^{-2} day^{-1}
$Q_L/A\ H_a$	0.30	0.074	—
$C_1 = R\ \tau\alpha\ F_R$	1.255	0.554	—
Q_u/A	195	324	Cal cm^{-2} day^{-1}
$Q_u/A\ H_a$	0.97	0.48	—

Table 3. Effect of negative sequences upon performance of projected solar collector at Dry Creek, South Australia

n	$\sum_n D/H_a$		$\frac{C_1}{n}\left(n+\frac{\sum D}{H_a}\right)$		$\frac{C_2 Q_L}{H_a A}$	K		$\frac{K H_a}{Q_u/A}$		$K H_a$ Cal cm^{-2} day^{-1}	
December	*A*	*B*	*A*	*B*		*A*	*B*	*A*	*B*	*A*	*B*
1	−0.525	−0.407	0.262	0.327	0.070	0.192	0.277	0.40	0.57	129	184
2	−0.8	−0.6	0.332	0.387	0.070	0.262	0.317	0.54	0.66	175	213
3	−0.9	−0.6	0.387	0.443	0.070	0.317	0.373	0.66	0.77	213	249
4	−1.0	−0.7	0.415	0.454	0.070	0.345	0.384	0.72	0.80	232	258
5	−1.2	−0.9	0.420	0.454	0.070	0.350	0.384	0.73	0.80	235	258
June											
1	−0.632	−0.480	0.462	0.652	0.285	0.177	0.367	0.241	0.500	36	74
2	−0.9	−0.6	0.690	0.876	0.285	0.405	0.591	0.550	0.805	82	119
3	−1.1	−0.9	0.794	0.879	0.285	0.509	0.594	0.694	0.809	102	120
4	−1.3	−1.0	0.846	0.940	0.285	0.561	0.655	0.763	0.891	113	132
5	−1.4	−1.1	0.904	0.978	0.285	0.619	0.693	0.841	0.944	124	140

collection must be made to satisfy the single expected day of low radiation income, and the provision of even a relatively small amount of extra storage capacity to enable some carry-over of energy should surmount this difficulty.

It is found that on many occasions only one day of excess radiation preceded a sequence of deficit days, and the frequency distribution shows that on 95 per cent of occasions, the excess was > 20 cal cm^{-2} day^{-1} or 0.03 H_a in December and > cal cm^{-2} day^{-1} or 0.045 H_a in June. On 90 per cent of occasions, excess was > 40 cal cm^{-2} day^{-1} or 0.06 H_a in December and > 18 cal cm^{-2} day^{-1} or 0.09 H_a in June. The heat balance then for n days of a negative sequence preceded by one day on which incident energy is $C_3 H_a$ would be:

$$\text{Input energy} = C_1 H_a \left(n + \frac{\sum D}{H_a}\right) + C_3 C_1 H_a$$

$$= C_1 H_a \left(n + C^3 + \frac{\sum D}{H_a}\right) \qquad [8]$$

where

C_3 = 1.03 for 95 per cent of occasions in December
= 1.045 for 95 per cent of occasions in June } [A]

and

C_3 = 1.06 for 90 per cent of occasions in December
= 1.09 for 90 per cent of occasions in June } [B]

$$\text{Output energy} = (n+1)\left(K H_a + \frac{C_2 Q_L}{A}\right) \qquad [9]$$

or $$K = \frac{C_1}{n+1}\left(n + C^3 + \frac{\sum D}{H_a}\right) - \frac{C_2 Q_L}{H_a A} \qquad [10]$$

The results in table 4 show that by providing energy storage capacity of only 1.03 times the expected useful energy collection on the average day in December and using each day only 72 per cent of this average useful energy collection, the installation should meet all design requirements for approximately

Table 4. Effect of negative sequences upon performance of projected solar collector with carry-over storage at Dry Creek, South Australia

n	$\sum_n D/H_a$		$\frac{C_1}{n+1}\left(n + C_3 + \frac{\sum D}{H_a}\right)$		$\frac{C_2 Q_L}{H_a A}$	K		$\frac{K H_a}{Q_u/A}$		$K H_a$ Cal cm^{-2} day^{-1}	
December	C_3 = *1.03 for 95 per cent*					C_3 = *1.06 for 90 per cent*					
	A	*B*	*A*	*B*		*A*	*B*	*A*	*B*	*A*	*B*
1	−0.525	−0.407	0.416	0.457	0.070	0.346	0.387	0.72	0.80	233	259
2	−0.8	−0.6	0.411	0.454	0.070	0.341	0.384	0.71	0.80	230	259
3	−0.9	−0.6	0.431	0.479	0.070	0.361	0.409	0.75	0.85	243	275
4	−1.0	−0.7	0.446	0.483	0.070	0.376	0.413	0.78	0.86	252	278
5	−1.2	−0.9	0.445	0.477	0.070	0.375	0.407	0.78	0.85	252	275
June	C_3 = *1.045 for 95 per cent*					C_3 = *1.09 for 90 per cent*					
1	−0.632	−0.480	0.886	1.010	0.285	0.601	0.725	0.62	0.75	121	146
2	−0.9	−0.6	0.896	1.044	0.285	0.611	0.769	0.63	0.79	123	155
3	−1.1	−0.9	0.922	1.000	0.295	0.637	0.715	0.66	0.74	128	144
4	−1.3	−1.0	0.940	1.026	0.285	0.655	0.751	0.68	0.77	132	151
5	−1.4	−1.1	0.972	1.044	0.285	0.687	0.769	0.71	0.79	138	155

90 per cent of the time (product of the two probabilities). If 81 per cent $\left(\frac{90 \times 90}{100}\right)$ availability is acceptable, then storage capacity of 1.06 times the expected useful energy collection on the average day allows one to use 80 per cent of this average collection. It is clear that greater storage capacity could be provided and could allow somewhat higher values of K to be used if the designer could expect sufficient days of excess radiation to charge the extra storage capacity. Unless long-term storage is being considered, however, the ratio

$$\frac{K H_a}{Q_u/A}$$

cannot exceed unity, and the design analysed in table 4 is already approaching this limit. Decisions on the suitability of providing extra storage capacity would have to be based upon economic considerations, by comparing the cost of extra storage capacity with the saving on collector surface area. This aspect is not discussed here.

Conclusions

The summary of solar radiation observations in Australia shows that the coverage has been exceptionally sparse in the past but is now improving, owing to the efforts of many independent observers. There are still vast areas very poorly covered by solar radiation observations, or even by records of hours of sunshine, so that estimations of solar radiation income have to be made from records of cloudiness by methods similar to those proposed by Black (22), Albrecht (23), De Vries (11) and others.

Some typical techniques of presenting the mean solar radiation data have been shown, and a method of assessing the probability of sequences of above-average and below-average radiation income outlined. This method has shown that it should be possible to design solar operated equipment for heating purposes, without using standby heating, by making suitable provision for short-term storage and by utilizing only a calculated proportion of the useful energy collection expected on an average day. A reasonable period of solar radiation observations must, however, be available to apply the method.

Acknowledgement

The valuable assistance of the computing laboratory of the University of New South Wales, Kensington, is gratefully acknowledged.

References

1. Rimmer, W B. and Allen, C. W., Solar radiation observations at Mount Stromlo, 1927-1939, *Mem. Commw. Solar Obs. Memoir II*, 1st number of vol. III.
2. Ångström, A., A new instrument for measuring sky radiation, *Mon. Weather Review*, 47 : 795, 1919.
3. Ångström, K., *Wied. Ann.*, 67 : 633, 1899.
4. Abbot, C. G., *Smithsonian Misc. Coll. 56 :* No. 19, 1911.
5. Abbot, C. G. and Aldrich, L. B., *Smithsonian Misc. Coll. 66 :* No. 7, 1916.
6. O'Connell, D., *Pyrheliometer and pyranometer observations, 1925-1931*, Riverview College Publications, vol. II : No. 2.
7. Bonython, C. W., *Solar radiation observations at Dry Creek, South Australia, 1947-1958*, ICIANZ, Osborne, S.A., 1959.
8. Drummond, A. J., On the measurement of sky radiation, *Arch. Meteor. Geophys. Biokl. B7 (3/4) :* 413, 1956.
9. Funk, J. P., Improved polythene shielded net radiometer, *Journal Sci. Inst. 36 (6) :* 267, 1959.
10. Anon, *Regular daily radiation records, Aspendale*, World Data Centre, Asheville, 1960.
11. De Vries, D. A., Two years of solar radiation records at Deniliquin, N.S.W., *Aust. Met. Mag. 22 :* 36, 1958.
12. Trickett, E. S., Private communication, 1961.
13. Turner, J. C., Private communication, 1961.
14. Albrecht, F. H. W., Establishment of a radiation network, *Geofisica Pura E Applicata 29 :* 115, 1954.
15. Albrecht, F. H. W., The Australian radiation network, *Climatology and Microclimatology*, UNESCO, 1958.
16. Comm. Bureau of Meteorology, *Australian Radiation Records*, Melbourne (yearly).
17. de Barry, E., Examples of statistical representation of radiation data, *Solar Energy 4 (1) :* 2, 1960.
18. Hinzpeter, H., Frequency distribution of hourly sums of direct solar radiation at Potsdam, *Solar Energy 4 (1) :* 8, 1960.
19. Fritz, S. and MacDonald, T. H., The number of days with solar radiation above and below specific values, *Solar Energy 4 (1) :* 20, 1960.
20. Hottel, H. C. and Whillier, A., Evaluation of flat plate collector performance, *Trans. Conf. on Use of Solar Energy*, Arizona, vol. II, part I, sect. A, p. 74.
21. Anderson, L. B., Hottel, H. C. and Whillier, A., Solar heating design problems, *Solar energy research*, Univ. of Wisconsin, Madison, 1955.
22. Black, J. N., The distribution of solar energy over the earth's surface, *Arch. Met. Geophys. Biokl. B7 (2) :* 165, 1956.
23. Albrecht, F. H. W., Methods of computing global radiation, *Geofisica Pura E Applicata 32 :* 131, 1955/III.

Summary

A review of the solar radiation records available in Australia shows that although Australia has a very high radiation income rate, detailed data are not very plentiful. It is thought that this is mainly due to the fact that the availability of water has been a very much more important criterion for determining which parts of the country could be habitable and arable.

Some long-term records of solar radiation are available from Mount Stromlo, Canberra, for the years 1927-1939 (1), and these include a useful study of the relationship between solar radiation and hours of bright sunshine, from Riverview Observatory, Sydney, for the years 1925-1931 (6) and from Dry Creek, South Australia (7), the latter records being continuous from 1947 to the present. Various sections of the Commonwealth Scientific and Industrial Research Organization (CSIRO) have made observations recently at a number of stations; the University of New South Wales has records from 1957 to the present at Kensington, N.S.W. and from 1959 to the present at Broken Hill, N.S.W.; the Commonwealth Bureau of Meteorology has operated six stations since 1953, increasing this to eight stations since 1955. The setting up of these eight stations of the Commonwealth Bureau of Meteorology has been reported by Albrecht (14, 15), and the standardizing of most of the observing instruments in Australia is carried out by the CSIRO Division of Meteorological Physics at Aspendale, Victoria.

The work of the radiation symposium held in Oxford, England, in July 1959 is noted in the paper; and isopleths and frequency distributions of daily totals at Melbourne, Victoria, at Garbutt, Queensland, and at Dry Creek, South Australia, are shown in figures 1, 2 and 3 in a form similar to those recommended by de Barry (17) at the radiation symposium.

A method of analysing a 12 year period of records at Dry Creek, South Australia, for summer and winter months (December and June) to allow design of heating equipment to operate only from solar energy is outlined. The cumulative divergences from the average monthly mean values for all groups of 2 to 5 days are summarized in figures 4 and 5, and from these it is shown that heat balances (equations [5] to [10] in the text) can be drawn to determine the operating characteristics of the solar heaters over the sequences noted.

Two examples are calculated using the proposed method, one being a solar operated heater with storage capacity equal only to the expected daily demand so that no carry-over storage can be assumed. In the second example, the system is provided with sufficient storage capacity to contain the expected useful energy collection on the one day of above-average radiation to be expected for 90 per cent or 95 per cent of all occasions, and to carry over as stored energy the difference between that collected energy and the useful daily energy utilization permitted by the design. In each case, performance is defined by equation [3], which is similar to that proposed by Hottel and Whillier (20, 21). The calculations carried out in tables 2, 3 and 4 show that in all cases the greatest reduction in permitted useful output must be made to satisfy the one day of low radiation; for the first example only 40 per cent of the expected useful energy collection (Q_u/A) can be permitted in December and only 24 per cent in June. The provision of storage capacity of 1.03 times Q_u/A in December and 1 045 times Q_u/A in June allows the designer to permit utilization of 72 per cent of Q_u/A in December and 62 per cent of Q_u/A in June.

RELEVÉS DU RAYONNEMENT SOLAIRE EN AUSTRALIE

Résumé

L'étude des données dont on dispose sur le rayonnement solaire en Australie révèle que, bien qu'il y soit extrêmement abondant, ces données, tout au moins détaillées, sont rares. On estime que cela s'explique principalement par le fait que les ressources en eau représentaient une considération beaucoup plus importante quand il s'agissait de juger des régions du pays qui seraient habitables et pourraient être mises en culture.

On dispose de relevés complets du rayonnement solaire à l'observatoire de Mount Stromlo, Canberra, pour les années 1927 - 1939 (1), et ces archives comportent une étude utile des rapports entre le rayonnement solaire et les heures de fort ensoleillement, fournie par l'Observatoire de Riverview, Sydney, pour les années 1925 - 1931 (6), ainsi que des données en provenance de Dry Creek, en Australie du Sud (7). Ces dernières sont continues et vont de 1947 à la date actuelle. Plusieurs sections du CSIRO (Commonwealth Scientific and Industrial Research Organization) ont procédé récemment à des observations en nombre de points; l'Université de la Nouvelle-Galles du Sud dispose d'archives allant de 1957 à l'heure actuelle, établies à Kensington, Nouvelle-Galles du Sud. Le Bureau Météorologique du Commonwealth exploite six postes depuis 1953, et huit depuis 1955. L'installation de ces huit postes du Bureau Météorologique du Commonwealth a fait l'objet de rapports d'Albrecht (14, 15) et la normalisation de la majorité des ins-

truments d'observation en Australie est en cours, sous les auspices du CSIRO, Division de la physique météorologique, à Aspendale, Victoria.

Les travaux du colloque du rayonnement, tenu à Oxford, Angleterre, en juillet 1959 ont été pris en considération dans le mémoire, et les isoplèthes et les répartitions de fréquence des totaux quotidiens à Melbourne (Victoria), Garbutt (Queensland) et Dry Creek (Australie du Sud) sont indiqués aux figures 1, 2 et 3, d'une manière analogue à celle qui a été recommandée par de Barry (17) au colloque du rayonnement.

Ce mémoire propose une méthode d'analyse des 12 années sur lesquelles portent les archives de Dry Creek, Australie du Sud, pour les mois d'été et d'hiver (décembre et juin), visant à permettre la réalisation de matériels de chauffage destinés à fonctionner exclusivement au moyen de l'énergie solaire. Les écarts cumulatifs par rapport aux valeurs moyennes mensuelles pour tous les groupes de deux à cinq jours sont résumés aux figures 4 et 5, et il en ressort que des bilans thermiques (équations 5 à 10 incluse) peuvent être établis pour déterminer les caractéristiques de fonctionnement des dispositifs de chauffage solaire pendant les périodes indiquées.

Le mémoire présente les calculs pour deux exemples, en mettant en œuvre la méthode ainsi proposée, dont l'un est relatif à un dispositif de chauffage solaire prévoyant une capacité d'accumulation qui ne dépasse pas les besoins quotidiens prévus, si bien qu'on ne peut pas poser l'hypothèse qu'il y a des réserves à reporter. Dans le deuxième exemple, le système est sensé être doté d'une capacité d'emmagasinage suffisante pour tenir en réserve la quantité utile d'énergie que l'on s'attend à recueillir pendant le jour de rayonnement supérieur à la moyenne à envisager dans 90 à 95 p. 100 de toutes les situations possibles de manière à pouvoir reporter, sous forme d'énergie accumulée, la différence entre le nombre de calories ainsi recueillies et celui qui en sera consommé chaque jour conformément aux plans. Dans chaque cas, le régime de fonctionnement est défini par l'équation 3, analogue à celle que proposent Hottel et Whillier (20, 21). Les calculs qui sont indiqués aux tableaux 2, 3 et 4 révèlent que, dans tous les cas, la plus grande réduction du débit utile autorisé doit être réalisée pour satisfaire les besoins du seul jour où le rayonnement est faible et, pour le premier exemple, on ne peut autoriser que 40 p. 100 du total d'énergie utile que l'on compte récupérer (Q_u/A), avec 24 p. 100 seulement pour juin. Le fait de prévoir une capacité d'emmagasinage égale à 1,03 fois Q_u/A en décembre et 1,045 fois Q_u/A en juin permet à l'ingénieur chargé du projet d'autoriser l'utilisation de 72 p. 100 de Q_u/A en décembre et 62 p. 100 en juin.

INSTRUMENTATION FOR SOLAR RADIATION MEASUREMENTS

P. Schoffer, P. Kuhn * and C. M. Sapsford †*

This paper summarizes the results of several developments in solar radiation instrumentation designed and used for the measurement or integration of incident solar energy. The following instruments are discussed: photovoltaic devices for measurement of radiation intensity; use of photovoltaic devices for high solar flux measurements; a current-sampling integrator for integration of radiation; and an inexpensive radiometer for total or net radiation measurements.

Photovoltaic cells for radiation measurement

Silicon photovoltaic cells are far superior in efficiency to the older selenium photovoltaic cells; mainly because of this they can also be much more accurate and less temperature-dependent in measuring applications. In addition, they are rugged and have been used outdoors in the Wisconsin climate for more than a year without protective covering, with no detectable change in appearance or calibration. Because the silicon cell responds to the high energy part of the solar spectrum it is natural to explore the possibility of its use for measuring solar power. The low series resistance and high reverse resistance furthermore make it possible to measure energy flux up to at least twenty times the normal solar flux.

* University of Wisconsin, Madison, Wisconsin.

† New South Wales Institute of Technology, Sydney.

Principle of operation

A photovoltaic cell behaves as a constant current source with a load having an exponential voltage-current (V-I) relationship, a shunt and a series resistance, as shown in figure 1. The light current, I_L, is proportional to the number of photons striking the cell. In a silicon cell this proportionality holds up to high fluxes. It is customary to measure I_L by measuring the short-circuit current. At high fluxes, however, the voltage drop over the series resistance of the cell cannot be neglected; figure 2 shows experimental high flux current-voltage characteristics of a 1 × 1 cm silicon cell (1). As I_L increases, the curves shift down along the R_s line to the left, and a point is reached at which the I-axis (i.e., the $V = 0$ line) intersects a non-linear part of the curve. Resistance in the external measuring circuit has basically the same effect as increased I_L in limiting the maximum flux which can be measured without non-linearity; a measuring point lies at the intersection of a load line through the origin in the fourth quadrant and the characteristic curve for the particular I_L value.

The series resistance determined by the locus of points at which the I-V curves deviate from near-zero slope is denoted by ρ. Ideally, measurements should be made along a line through the origin parallel to the ρ-line (shown as P_M in figure 2). Because of the high shunt resistance of the silicon cell, however, it is possible to use a constant negative bias of up to 2.5 volts. Because of the small positive slope of the dark-current curve ($I_L = 0$) in the

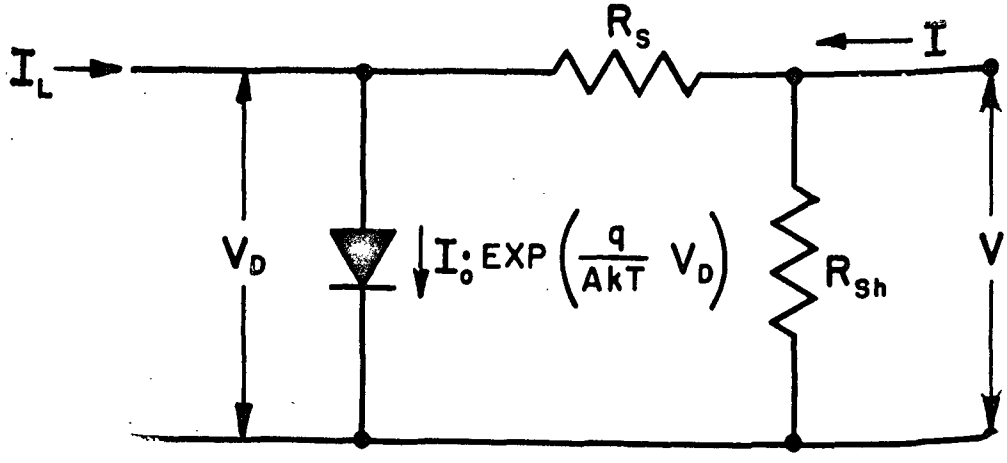


Figure 1. Equivalent circuit for a silicon photovoltaic cell

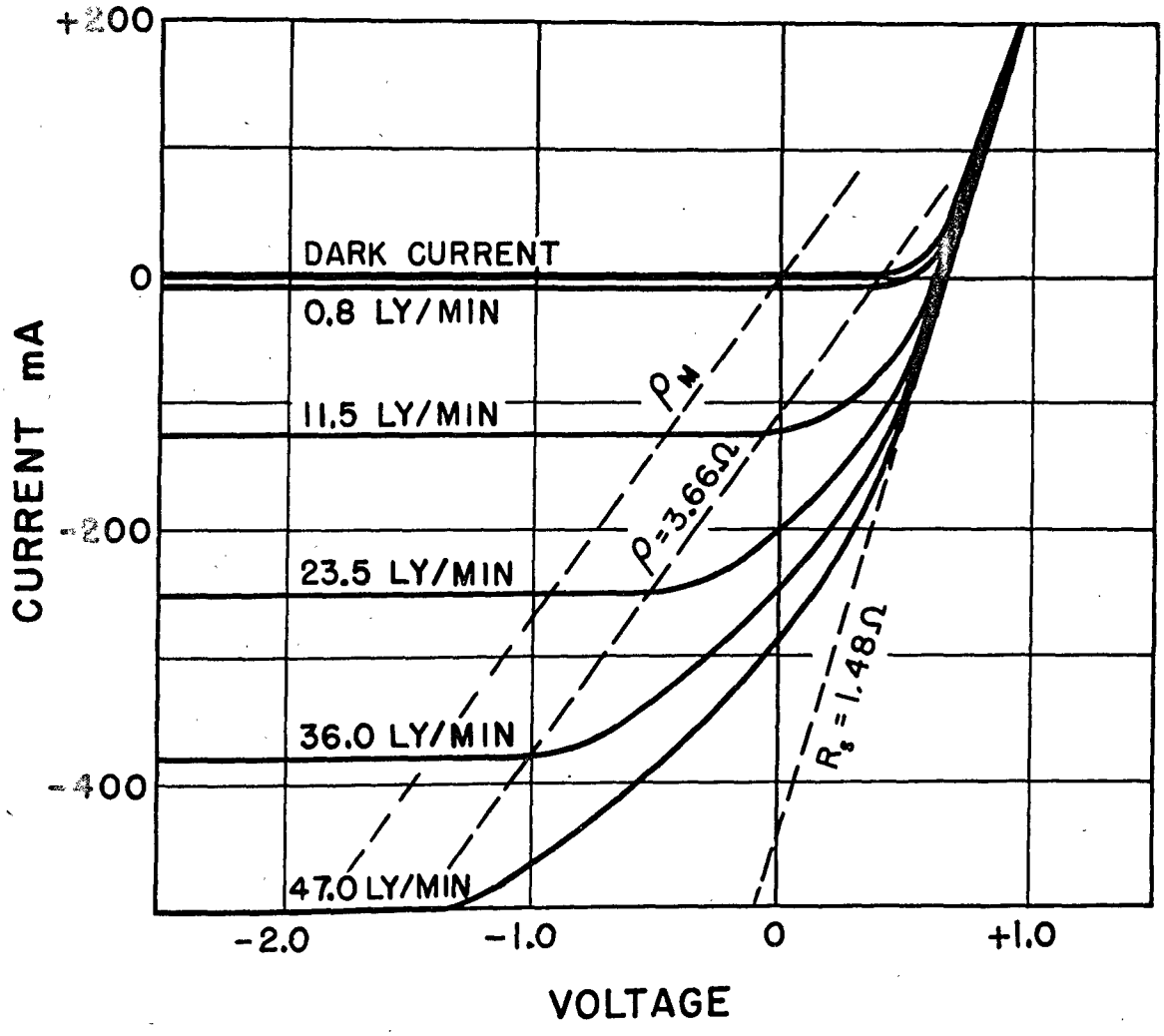


Figure 2. V-I characteristics of a silicon cell at various radiation levels, at a temperature of 77°F

third quadrant (not visible in figure 2 because of the large scale), a small current is obtained with a negatively biased cell when the cell is in the dark. With a bias of 1.5 volts this dark current is equivalent to the current measured at a radiation of about 0.02 Ly/min; this dark current varies with individual cells and increases with temperature.

Insolation measurements

The simplest way to measure the I_L over a range of zero to 2 Ly/min, the normal range of solar radiation intensities, is to use a d'Arsonval type of meter with a low voltage drop. Meters with a 10 mA range and a resistance of about 1.5 ohms are readily available. The scale can then be adjusted to the output of the cell by appropriate shunting. A minimum practical cell size is then 1 × 1 cm; a cell of this size will have an output of about 16 mA/Ly/min. For smaller cells, e.g., a 2.5 x 5 mm cell with an output of about 1.6 mA/Ly/min., it is necessary to use a more sensitive meter, which normally has a full-scale voltage drop of 50-100 mV. A 2.5 × 5 mm cell has an additional internal voltage drop of about 80 mV at 2 Ly/min, and therefore non-linearities are experienced at the high end of the scale. In selenium cells this non-linearity has been taken for granted at a much lower light level; with silicon cells, however, bias can successfully be used. With a bias the voltage drop in the measuring circuit external to the cell is not critical, and sufficient power is available to drive (in addition to a meter) an inexpensive Rustrak recorder having a 1.0 mA movement, and a simple integrating device built around a contact meter. The fixed bias can be provided with a mercury cell with an e.m.f. of 1.35 volts. Disadvantages of this method of providing bias are that a periodic check on the condition of the cell is necessary, and a small dark current exists, as noted above; on the other hand, more than one volt is available to drive instruments. A self-contained system can be obtained by using a larger silicon cell (e.g., 5 × 5 mm) to bias the measuring cell (2.5 × 5 mm). By appropriate loading of the biasing cell, the ideal condition can be approximated where measurements are made on the ρ_m line. Figure 3

shows a circuit for this measurement. Non-linearity of the biasing voltage has an undetectable effect if one stays to the left of the ρ_m line at radiation values below full scale.

Cells used for measuring and bias can be cemented with epoxy resin on an aluminum (or other metal) plate. Because the backs of the cells have to be insulated from each other, a thin layer of epoxy is applied on the plate before the cells are mounted. Heating can be provided by a 3-watt resistor, cemented under the mounting plate, if the cells are to be used in climates where snow and ice removal are necessary.

A large-area cell is being used as the detector in a hemispherical reflectometer where, because of excellent integration over the surface of the cell, stray radiation (i.e., image diffusion) caused by optical imperfections of the hemisphere can be measured. This integration can be demonstrated easily by varying the size of the image of the sun (of fixed total energy) on the cell; the current output of the cell is constant.

Spectral response of silicon photovoltaic cell

Figure 4 shows the spectral response of an average silicon cell (2). Because of a change in effective energy gap, there is a shift in spectral response with temperature; however, this shift is small and has little effect in insolation measurements. Furthermore, heating the cell during winter to an approximate summer temperature is necessary for removal by melting of snow and ice deposited on the cell.

The output of a horizontal silicon cell and an Eppley pyrheliometer (pyranometer) was measured over several winter months (January to March) during clear and overcast days. (During days with scattered clouds, measurements were not taken because of the large difference in time constant between the Eppley and the cell.) The cell was heated to about 60°F to remove snow and ice and to dry it. One typical set of clear day curves for 30 March 1961, for Madison, Wisconsin, is given in figure 5. The cell output was adjusted to an arbitrary value close to the output of the Eppley at noon. Two sets of diffuse radiation values, obtained by shading the detectors from beam radiation, are shown. The cell is seen to have a lower output relative to the Eppley at low solar elevations than at high solar elevations. This can result from a combination of factors, including a shift of spectral distribution of radiation with air mass, and effects of angle of incidence on the relative response of the instruments. For diffuse radiation the cell also reads low, and it is

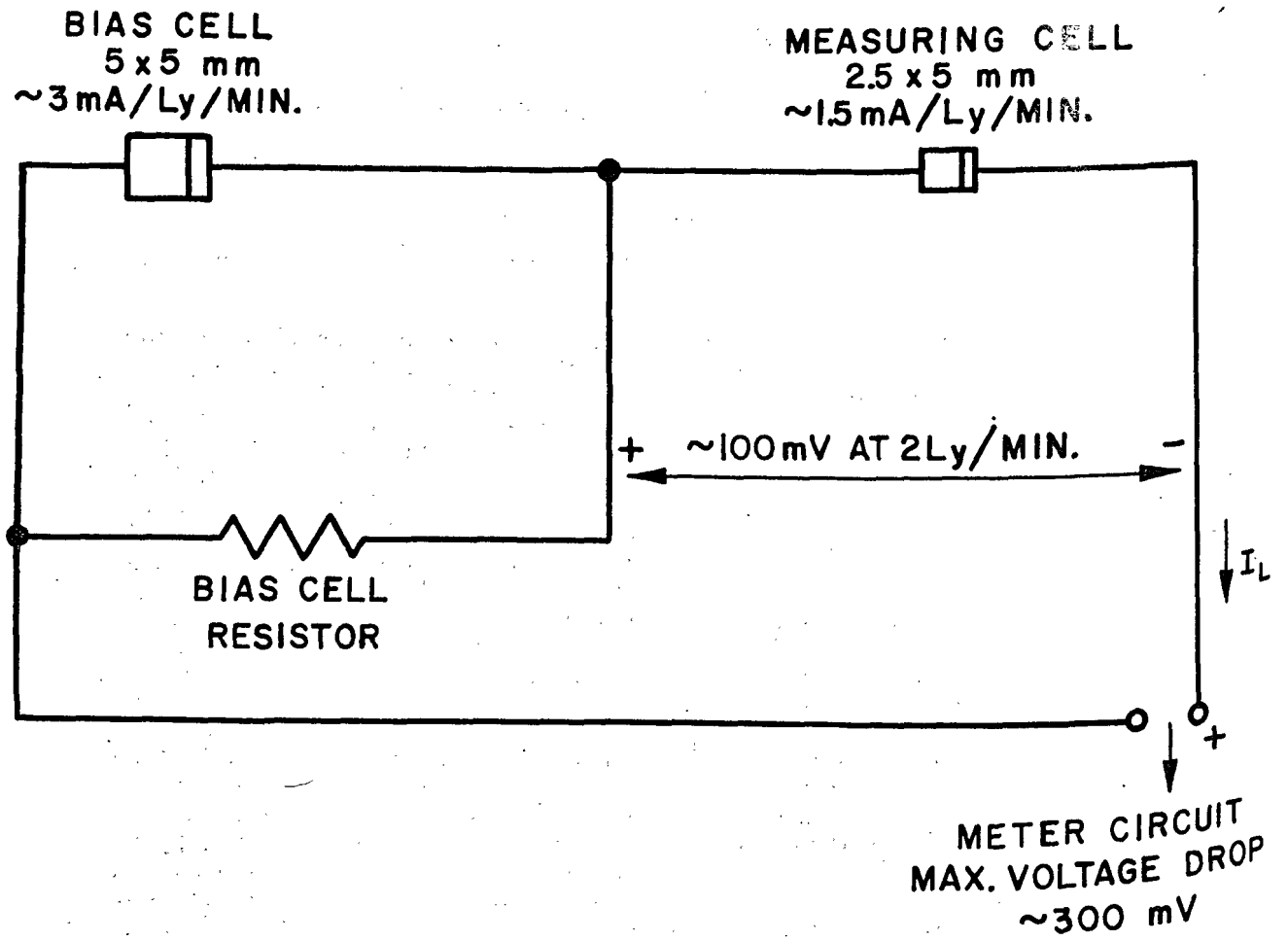


Figure 3. Circuit for light current measurement with biasing cell

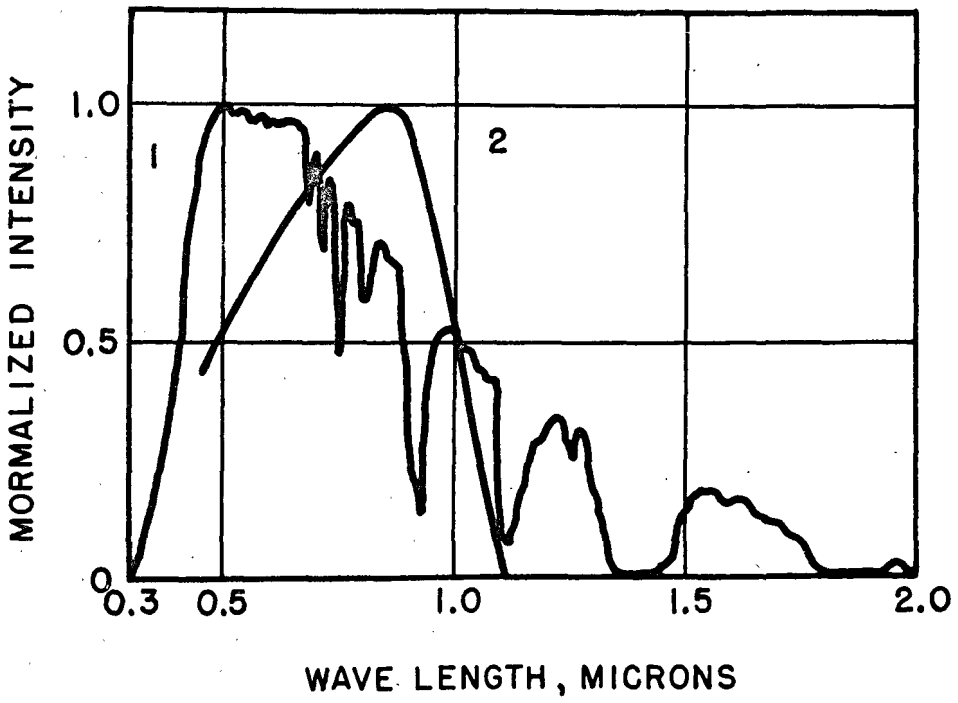


Figure 4. Spectral response of a silicon cell, compared to the spectral distribution of solar radiation for an air mass of 2 (from Moon (11))

therefore necessary to calibrate the cell separately for total horizontal radiation and beam radiation.

The relation between air mass and relative response over a three-month period had the general trend of figure 5 but exhibited a spread, probably due to temperature effects on the Eppley and changes in atmospheric conditions; the deviations were never larger than ± 0.05 Ly/min, overcast days included. Further experimental comparisons are being undertaken with better instrumentation and measurements in several wavelength bands.

High flux measurements

A silicon cell, biased with a mercury cell of 1.35 volts, can be used to measure radiation intensities up to 30 Ly/min. In these measurements, the dark current can be neglected, since it will be a very small percentage of the full-scale radiation values being measured. Because silicon is an excellent heat conductor, the cells can be soldered directly onto a water-cooled heat sink. Since I_L is linear with radiation intensity up to very high flux values (experimentally verified up to 50 Ly/min (1)), it is possible to measure fluxes at least up to that value. A fixed bias, however, would have to be over 2.5 volts for a silicon cell as shown in figure 2, to operate to the left of the ρ-line. Since in the fabrication of solar cells the reverse current properties are not controlled, some individual cells will have a very high dark current at bias voltages of more than 2.5 volts. It is then necessary to adjust the bias during measurements. In addition, cell cooling can become a problem with much higher radiation fluxes.

Silicon cells have been used in mapping the intensity of flux at the focal areas of solar reflectors (3). In this application biasing cannot be provided by silicon cells (as noted above for low flux measurements) because the flux field is not homogeneous; also, because of the necessity for cooling, electrical insulation may become a problem. Measurements in a parabolic collector are now being carried out with the aid of a screen to keep the flux below 30 Ly/min. In measurements of reflected flux distribution, it is advisable to measure the incident radiation as well with a silicon cell, to minimize differences of spectral response.

Radiation integrator

Solar data are more useful for some purposes in integrated form. While recorded insolation values can be hand integrated, the integration is time consuming and generally unsatisfactory. A survey of types of integrator is given in reference 4, which describes an integrator that can be used with low output instruments (i.e., radiation detectors). Because of the high available output voltage of a biased silicon cell, a much simpler integrator can be used; this is built around a meter relay and a synchronous motor, thereby avoiding amplifier systems.

The new integrator is a discontinuous system in the same class with that described by Kassander and Knowles (5). A voltage-divider (potentiometer)

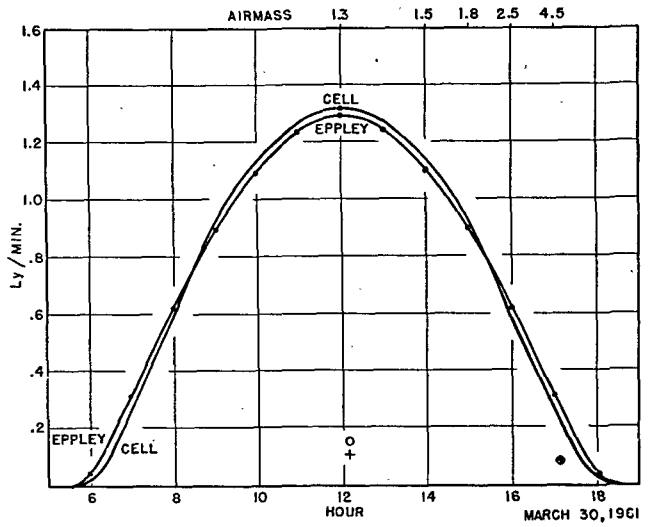


Figure 5. Comparison of total horizontal radiation measurements with a silicon cell and an Eppley pyrheliometer for a clear day

Diffuse radiation measured by shading from beam radiation by the two instruments is also shown by ⊗ for the Eppley, and by ♀ for the silicon cell.

is continuously driven by a synchronous motor. A constant voltage is applied across the voltage divider, and the output voltage is changed at a constant rate during one revolution. At the time this voltage is equal to the voltage to be integrated (obtained from the silicon cell current by means of a voltage-dropping resistor), a second synchronous motor is connected to its power supply for the rest of the cycle. The angular position of the shaft of the second motor is then proportional to the accumulated samples of the input voltage taken during every revolution (cycle) of the first motor. A diagram of this integrator is shown in figure 6. Sampling takes place with a decreasing voltage; thus part of the high range can be used for switching.

The second motor drives a counter which can be a printing type. Alternatively an electrical pulse counter can be driven by a switch and cam on its shaft.

The meter relay is a Weston No. 1092 Sensitrol relay which is reset by a switch and cam on the shaft of the first motor at the point where the potentiometer output is zero. A relay actuated by the meter contact switches the second motor on and off.

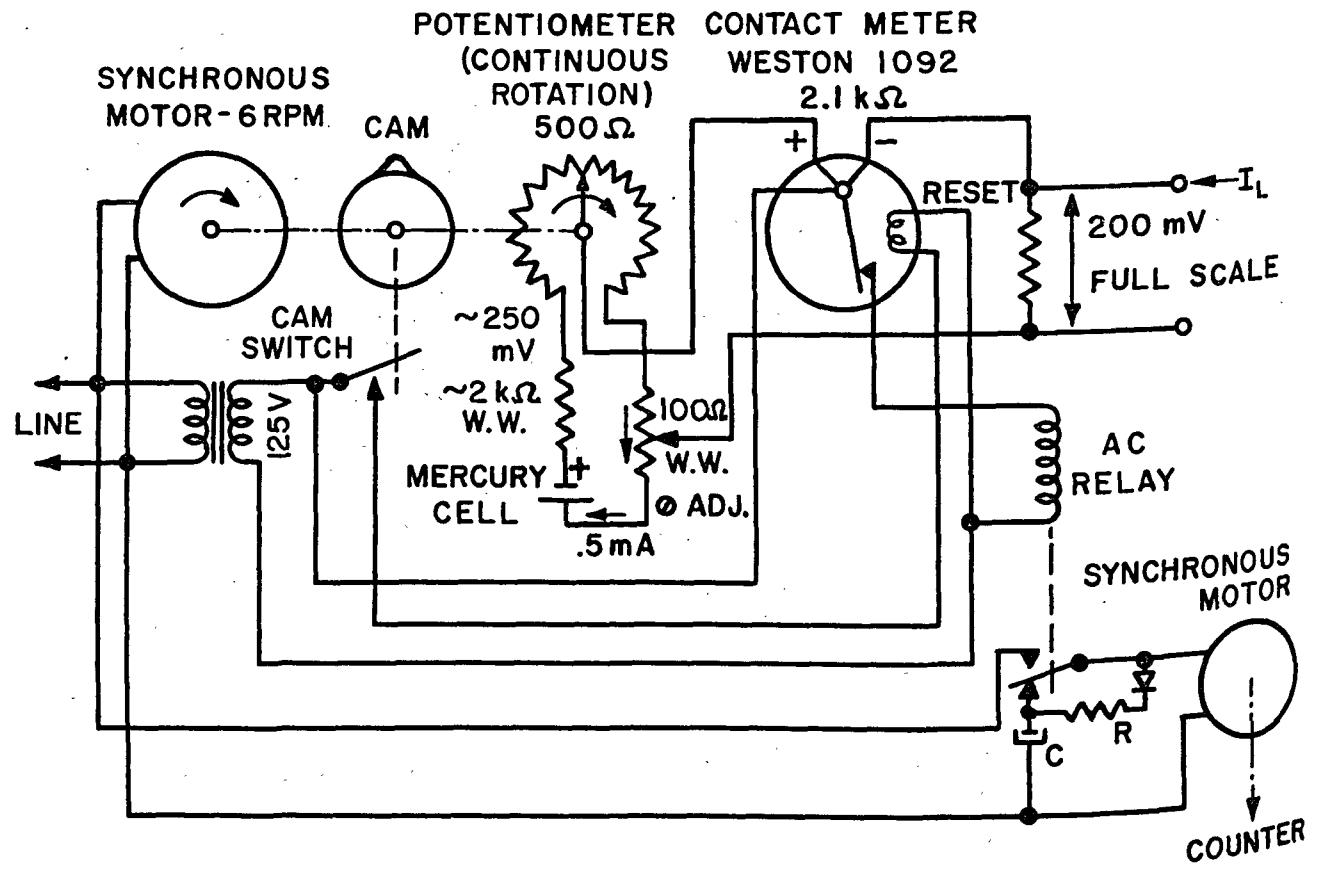


Figure 6. Schematic diagram of the discontinuous radiation integrator

A capacitor is charged while the second motor is running and discharges through the motor windings for fast stopping. The transformer shown in figure 6 is not necessary if the line voltage is 115 V because the contacts of the meter are insulated from the meter movement.

In a battery driven unit, the potentiometer would have to be driven by a clockwork, or a constant speed D.C. motor. It would be necessary to use a secondary shaft connected to the constant speed shaft by a magnetic clutch, instead of a second motor.

The accuracy of this integrating system is determined by:

(a) *Non-linearity of the potentiometer.* Potentiometers with a linearity of 0.1 per cent are reasonably inexpensive, and this error is therefore insignificant.

(b) *Lag of the contact meter.* The meter requires time to reach a full scale value at the beginning of a cycle (typically 0.25 sec); therefore, the whole slide wire cannot be used. The time lag of the meter used in this study is mainly due to the time it takes the moving contact to reach the fixed contact under the influence of the magnetic field of the fixed contact. This time lag is fairly constant and can, therefore, be compensated by adjusting the phasing of the reset switch.

(c) *Accuracy of the meter.* The Weston No. 1092 can switch, according to the manufacturer, with an accuracy of ± 0.5 mV,—i.e., with an accuracy of ± 0.25 per cent, if the full scale voltage is 200 mV. Because of loading of the voltage dividers, the error would be slightly larger than ± 0.25 per cent. (Errors larger than this were found in experimental study of this integrator, and an electrically locking contact meter would result in improved accuracy.)

(d) *Starting and stopping lag of the second motor.* Stopping time is negligible if D.C. braking is used (i.e., it is on the order of 5 milliseconds). However, the starting time lag is in the order of 0.1 second for a motor with a good starting torque and a low inertia rotor (a Hurst synchronous motor was used in this study.) This lag decreases proportionally for running times under 0.2 sec and therefore cannot be completely corrected by phasing. It is possible to compensate for a variable stopping time by increasing the charging time (RC) of the capacitor in the stopping circuit, but this compensation is rather erratic. The minimum useable cycling period is, therefore, limited by the starting lag. At a cycling period of 10 seconds the maximum error caused by slow starting is thus on the order of 1 per cent of the period. This is the most significant source of error in integration, and the use of a magnetic clutch should result in improved accuracy.

(e) *Relay switching time.* This error is small and can be neglected.

(f) *Non-continuous sampling.* The average of two samples is not necessarily the average of the function of the variable. According to the information theory, no information is lost only if samples are taken at intervals 1/2F, where F is the bandwidth of the signal (here effectively the highest frequency component in the signal). However, if the variable has a low correlation with the cycling period, the error tends to average out.

(g) *Sampling intersection error.* This error can be more serious and is caused by the variation of the time of sampling within the cycle. Sampling takes place on the intersection of a sloping line with the curve of the variable (on a time plot). If the sampling line intersects the curve in more than one point, it will end at the topmost one (figure 7), thereby causing high reading. If the variable is a harmonic function of time, the error can occur when $(S/T) < [(2\pi a)/P]$ where a = amplitude of the variable, P = period of the variable, S/T = the speed of sampling. In an extreme case (i.e., for fast moving scattered clouds) it was observed, for the output of a horizontal silicon cell, that $a = 0.15$ of a full-scale value of 2.0 Ly/min, for $P = 10$ seconds. Then, $(2\pi a)/P = 0.095$ full-scale units per second; this is nearly equivalent to a full-scale change in 10 seconds. It therefore appears that a 10-second sampling time is short enough to result in negligible error from this source.

An integrator of the type described above has been built and operated in the laboratory. After adjustments, a maximum error of 2 per cent of full scale was found for constant input voltages between zero and 220 mV.

Economical pyrheliometer (radiometer)

The "economical" radiometer of Suomi and Kuhn (6), with modifications, can be used to measure the incoming and outgoing (reflected) solar radiation flux density, as well as incoming and outgoing long-wave radiation currents. The theory, application and testing of this instrument for solar radiation measurements are briefly discussed here.

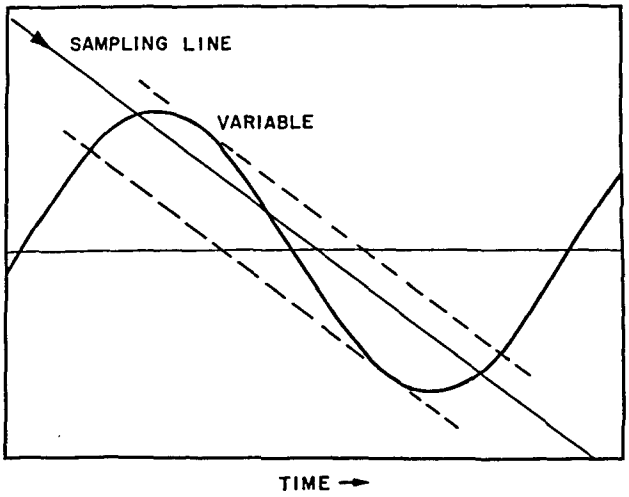


Figure 7. Effect of a varying instant of sampling (example of slow sampling)

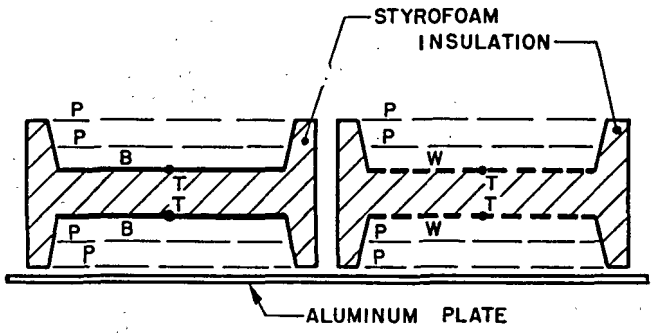


Figure 8. Section diagram of the economical radiometers as used for solar radiation measurements

For net thermal radiation measurements only the left hand unit is used, without the aluminum plate; P denotes polyethylene film, B the black sensing surface, W the white sensing surface, and T the points of surface temperature measurement

The radiometer described by Suomi and Kuhn has been used extensively to measure the upward and downward propagating night-time thermal (long-wave) radiation currents, both as a function of geography and of height in the atmosphere (7). For this purpose, the instrument consists of two blackened sensing surfaces, one facing upward and one facing downward, shielded from ventilation effects by spectrally transparent (one through 50 microns) polyethylene film and separated from one another by an insulating medium such as expanded polystyrene. A section of this radiometer is shown on the left side of figure 8 (for this application, the aluminum plate is not used). The basic energy balance equation for such a radiometer, considering, for example, one of the radiation currents (in this case the downward radiation $R_L\downarrow$), and steady state conditions, is given by:

$$R_L\downarrow = \sigma T_t^4 + K(k_t \Delta T_t + k_t \Delta T_t + f(u) \Delta T_t) \quad [1]$$

The constants and parameters are as follows:

- σ = Stefan-Boltzmann constant, 0.817×10^{-10} cgs units
- T_t = Observed top sensor temperature
- ΔT_t = Difference in top sensor and ambient air (or polyethylene) temperatures
- ΔT_t = Difference in top and bottom sensor (surface) temperatures
- $f(u)$ = Ventilation factor, identically zero in the case of the economical radiometer
- K = A constant measured from the transmissivity of the polyethylene ventilation shield, and absorptivity of the blackened sensor surfaces
- k_t = Thermal conductivity of the insulating medium (expanded polystyrene)
- k_t = Thermal conductivity of upper air cell

Combinations of equations of this type are used to calculate the various currents, as may be appropriate.

Incoming solar and long-wave radiation, and reflected solar and long-wave radiation, can be measured with these instruments, by use of two sets of surfaces (each with an upward and a downward facing surface) having different spectral absorptivities. By use of an opaque plate under the radiometers the instruments can measure only the downward radiation streams; figure 8 shows an assembly of two radiometers, one with "black" and the other with "white" surfaces used for this purpose; this assembly is referred to as the "economical" pyrheliometer. Any temperature sensing elements may be used under the black or white surfaces, to measure the surface temperatures, from which the radiation intensities can be determined.

Calculation of Radiation

From the properties of the polyethylene and black and white surfaces for a pyrheliometer assembly as shown in figure 8, and energy balances of the type of equation [1], an expression for the radiation in terms of the temperatures of the surfaces can be derived. The derivation is discussed in references (8) and (9). The result of this analysis is the expression for incident solar energy on the upward-facing radiometer:

$$R_s\downarrow = A(T_w^4 - T_b^4) + B(C_{iw} + C_{tw}) - B(C_{ib} + C_{tb}) \quad [2]$$

Here

$R_s\downarrow$ = solar radiation (downward).

T_b = temperature of the (upper) black surface.

T_w = temperature of (upper) white the surface.

The system parameters are defined as follows:

$$A = \frac{\sigma}{k-1} \quad [3]$$

$$B = \frac{K}{k-1} \quad [4]$$

$$K = \frac{1}{\alpha(1-\alpha L)} \quad [5]$$

$$k = \frac{\alpha_{sw}(1-\alpha_{sw} L)}{\alpha_{lw}(1-\alpha_{lw} L)} \quad [6]$$

The four terms, C, denote conducted energy, the first subscript denoting conduction across insulation (i) or top air cell (t), and the second denoting the black instrument (b) or the white instrument (w). The same subscripts are used for the temperature differences. Thus

$$C_{ib} = k_t \Delta T_{ib}/2.8 \quad \text{and} \quad C_{iw} = k_t \Delta T_{iw}/2.8 \quad [7]$$

$$C_{tb} = k_t \Delta T_{tb}/1.4 \quad \text{and} \quad C_{tw} = k_t \Delta T_{tw}/1.4. \quad [8]$$

The following additional symbols are used:

- α_{sw} and α_{lw} = short-wave and long-wave absorptivities of the white detector, respectively.
- α = absorptivity of the non-selective black used on the black radiometer.
- L = reflectivity of two layers of polyethylene (= 0.22).

Further, note that in equations [7] and [8], k_t is the thermal conductivity of the air cell, i.e., the

Table 1. Summary of comparisons of Eppley, silicon cell and "economical" pyrheliometer

Date (196) and time	R_s		R_s from economical pyrheliometer at given values of α_{lw} and α_{sw}			Remarks
	Eppley	Cell	$\alpha_{lw} = 0.88$ $\alpha_{sw} = 0.306$	0.70 0.263	0.60 0.238	
Dec 8:						
11:00	1.17	1.14	1.17	1.19	1.17	
11:45	1.21	1.19	1.19	1.19	1.19	
12:30	1.17	1.16	1.15	1.15	1.15	
1:00	1.12	1.12	1.11	1.12	1.12	
1:30	1.03	1.02	1.03	1.04	1.04	
2:00	0.91	0.91	0.92	0.92	0.93	
2:30	0.77	0.77	0.78	0.79	0.80	
Oct. 19:						
9:30	Not in	1.06	1.41	1.43	1.43	No fan
Oct. 16:						
0:38	1.24	1.29	1.37	1.36	1.36	No fan
11:05	1.19	Not in	1.38	1.38	1.38	No fan
Oct. 19:						
2:00	Not in	1.05	1.11	1.12		No fan
Dec. 7:						
11:45	1.16	1.14	1.18	1.18	1.17	
Dec. 10:						
9:45	0.83	0.84	0.84	0.84	0.84	
10:50	1.01	1.00	1.06	1.07	1.07	
Dec. 16:						
4:44	0	0	— 0.02	— 0.01	0	
4:50	0	0	— 0.02	— 0.01	— 0.02	Fan off
4:55	0	0	— 0.02	— 0.01	— 0.01	
Dec. 21:						
1:00	1.06	1.05	1.11	1.11	1.12	
1:30	0.98	0.97	1.02	1.02	1.03	
2:30	0.73	0.72	0.64	0.64	0.64	May be due to shading by cloud
Dec. 18:						
9:10	0.74	0.70	0.74	0.74	0.75	
11:15	1.13	1.09	1.16	1.16	1.16	
11:40	1.14	1.12	1.21	1.21	1.20	Fan off
11:54	1.15	1.13	1.18	1.18	1.18	
2:00	0.89	0.87	0.94	0.95	0.96	

[a] The cell constant was adjusted to indicate approximately the same radiation as the Eppley at noon of a clear day.

thermal conductivity of air at the mean cell temperature. The constants 2.8 and 1.4 are the thicknesses of the styrofoam insulation and air gaps, in centimeters, in the standard instrument configuration.

Though the description of the terms of working equation [2] appears lengthy, the parameters A and B are fixed for instruments with given surfaces and are determined only once. The values for conduction, indicated in equations [7] and [8], depend on the measured temperatures and are readily calculable, or can be found from convenient nomographs. Thus equation [2] is readily solvable for $R_{s\downarrow}$, the solar radiation. In effect, then, a simple and inexpensive pyrheliometer is used, but a calculation is required to determine the incident radiation from the measured temperatures. (A convenient nomogram can also be devised to carry out this calculation.)

Two further observations are made on the economical pyrheliometer. The derivation of the working equation and the energy balance equations of the type of equation [1] are based on the assumption of absence of convection in the air spaces under the polyethylene covers; evaluation of the extremes of Grashof number to be expected for the 0.7 cm thick air layers used in the radiometer shows that the heat transfer is always by conduction alone. Further, it should be noted that the black surface is non-selective, that the white surface has different absorptivities for long-wave and short-wave radiation, and that the long-wave absorptivities of the white and black surfaces are the same; surfaces that meet these requirements are Fullers flat black "Decoret" paint and lead carbonate white.

Standard radiometer

Radiometers for use in thermal radiation measurements as noted above are being manufactured; by changing the surfaces and use in pairs they can provide solar radiation measurements. The production radiometers have the following important dimensions: Thickness of styrofoam insulation, 2.8 cm; width of each air gap, 0.7 cm (or 1.4 cm from outer polyethylene cover to the black (or white) surface). The black and white surfaces have the shape of an equilateral triangle (for convenience of manufacture), 13 cm on a side. The cost of the standard, black radiometer to the United States Weather Bureau is approximately $10 each, including thermistor sensors. (The cost of the pyrheliometer assembly would thus be somewhat more than double this figure.) The plans and specifications of the radiometer are available from the United States Weather Bureau Project, Department of Meteorology, University of Wisconsin, Madison 6, Wisconsin.

Experiments on use of the pyrheliometer

"Black" and "white" economical radiometers as shown in figure 8 were used for solar radiation measurement by the Solar Laboratory of the University of Wisconsin. The assembly was mounted on a flat aluminum sheet carried on a wood frame and mounted on the laboratory roof. The radiometers were taped to the aluminum sheets, and connections were made to four thermocouples in the radiometers and one thermocouple in their shade for measurement of shade ambient temperature. (The black radiometer was modified by the addition of fine threads stretched under the polyethylene covers, to reduce the unsupported span and maintain the air cells between layers. Without this support, the polyethylene softened at high temperature, and sagged to the extent that sections of adjacent layers of it adhered together.) Records obtained from this economical pyrheliometer were compared with records from an Eppley pyrheliometer and from a silicon solar cell (i.e., measurements of short-circuit current from a 1 × 1 cm cell) when all instruments were mounted on the Solar Laboratory roof at 35° to the horizontal, facing south.

Preliminary observations made on these instruments gave rather unsatisfactory results, with the economical pyrheliometer always giving low values when compared with the other instruments, and showing considerable instability. The constants for the white paint were not known, and attempts were made to obtain values of α_{sw} and α_{lw} by treating sets of readings in simultaneous equations. The radiation was measured by the other instruments, but the nature of the solutions gave erratic results of the properties.

The procedure was reviewed, and it was decided to ventilate the outer polyethylene sheets (by blowing air across the top of it with a small fan, to simulate wind) to hold them at temperatures near ambient, and to apply the best available values of absorptivity and emissivity to the white painted polar surface. Thus assuming that α_{lw} was 0.88 and using observations on 8 December at 11:45 a.m., the corresponding value of α_{sw} was 0.306; applying these constants to all other observations when the units were ventilated gave a good agreement between radiation measured by all three instruments in all cases. (Two other assumed values of α_{lw} of 0.70 and 0.60 with corresponding values of α_{sw} of 0.283 and 0.238, respectively, also showed good agreement over the whole range.) Table 1 summarizes these calculations and results.

These results show the importance of ventilation in achieving satisfactory observations, when using the economical radiometer, and they also tend to show that the absorptivity of coated sensing surface is unimportant over a fairly wide range. The second point is being further studied, and more check observations are to be made. Final assessment of these observations should be delayed until that time. More extensive tests recently completed but not yet fully evaluated indicate that the economical pyrheliometer can be used at the 5 per cent accuracy level with encouraging results (10). Continued use of the instrument in remote areas and for maximum areal coverage is indicated to be feasible.

References

1. Pfeiffer, C., Schoffer, P., Spars, B. G. and Duffie, J. A., Performance of Silicon Solar Cells at High Levels of Solar Radiation; paper to be published in *Trans. Am. Soc. Mech. Engrs.*, 1961.
2. Prince, M. B. and Wolf, M., New Developments in Silicon Photovoltaic Devices, *J. British Inst. Radio Engrs., 18,* 583, 1958.
3. Löf, G. O. G., Fester, D. A. and Duffie, J. A., Energy Balances on a Parabolic Cylinder Solar Collector, paper to be published in *Trans. Am. Soc. Mech. Engrs.*, 1961.
4. Schoffer, P. and Suomi, V. E., A Direct-Current Integrator for Radiation Measurements, *Solar Energy, 5,* 29, No. 1, 1961.
5. Kassander, A. R. and Knowles, L. L., An Automatic Printing and Totaling Device for Solar Radiation Measurements, *Trans. Conf. on Use of Solar Energy,* Tucson, *1,* 48, 1955.
6. Suomi, V. E. and Kuhn, P. M., An Economical Net Radiometer, *Tellus, 10,* 160, No. 1, 1958.
7. Kuhn, P. M. and Suomi, V. E., Infrared Radiometer Soundings on a Synoptic Scale, *J. Geophys. Res., 65,* 3669, 1960.
8. U.S. Weather Bureau, *University of Wisconsin, Annual Report* (on University of Wisconsin research project), June 1957.
9. Suomi, V. E., Staley, D. O. and Kuhn, P. M., A Direct Measurement of Infra-red Radiation Divergence to 160 mb, *Quarterly J. Royal Meteorological Soc., 84,* 134, No. 360, April 1958.
10. Tanner, C. B., Businger, J. A. and Kuhn, P. M., The Economical Net Radiometer, *J. Geophys. Res., 65,* 3657, 1960.
11. Moon, P., *Proposed Standard Solar-Radiation Curves for Engineering Use,* J. Franklyn Inst., *230,* 583, 1940.

Summary

This paper summarizes the results of several developments in solar radiation instrumentation. These include silicon photovoltaic cells for solar radiation measurement; use of silicon cells for measurement of high fluxes of solar radiation; a current-sampling integrator for integrating radiation measured with silicon (or other high-output) detectors; an inexpensive radiometer for total or net radiation measurements.

The properties of silicon photovoltaic cells are such that they can be used for solar radiation measurements, the light current, I_L, being proportional to the number of photons (in the proper energy range) striking the cell. The light current can be measured by measuring the short-circuit current of the cell. At high fluxes, however, the voltage drop over the series resistance of the cell cannot be neglected, and the measuring cells can be biased in the negative direction to extend the range of fluxes over which the output of the cells is linear with radiation. In low flux measurements biasing can be used to increase the allowable measuring resistance. The biasing voltage can be provided by a mercury dry cell, or by a second silicon cell of larger area than the measuring cell. For example, a self-contained system can be obtained by using a 5×5 mm cell to bias a measuring cell of 2.5×5 mm; the output can be read with a d'Arsonval-type meter, or recorded with an inexpensive Rustrak recorder.

The silicon cell has a spectrally selective response, and some errors are introduced in radiation measurements made with it by variations in the spectral distribution of incident solar radiation. Comparative measurements were made with a cell and an Eppley pyrheliometer, for clear and overcast days, at Madison, Wisconsin; the deviations of radiation measured by the cell from that of the Eppley were never larger than ± 0.05 Ly/min. Further comparisons are being made. The cells are used unprotected in the Madison climate, but are heated to remove wintertime ice and snow; no detectable change in appearance or output has been noted in over a year.

Silicon cells have been used for experimental purposes for measurements of solar radiation fluxes up to 50 Ly/min. For this purpose, constant voltage bias is used, and the cells must be artificially cooled by immersion in cooling water or by soldering the cell on a cooled heat sink. The application has been in flux mapping of the focal areas of focusing solar exchangers, where the non-homogeneous nature of the flux field makes use of a biasing cell impractical.

For some purposes, solar radiation data are more useful in integrated form. Because of the high available output of a biased silicon cell, a simple integrator can be used to integrate radiation; this is built around a meter relay and synchronous motor and avoids amplifier systems. This integrator is a discontinuous, current-sampling device. A voltage divider is continuously driven by a synchronous motor. A constant voltage is applied across the voltage divider, and the output voltage is changed at a constant rate during one revolution. At the time this voltage is equal to the voltage to be integrated (obtained from the silicon cell current by means of a voltage-dropping resistor), a second synchronous motor is connected to its power supply for the rest of the cycle. The angular position of the shaft of the second motor is then proportional to the accumulated samples of the input voltage taken during every revolution (cycle) of the first motor. A diagram of the integrator is shown in figure 6. Integrated output is obtained by accumulated revolutions of the shaft of the second motor.

An economical radiometer is described which can be used for measurement of incoming and reflected short-wave (solar) radiation and incoming and outgoing long-wave (thermal) radiation. With modifications, pairs of the radiometers can serve as a pyrheliometer for solar radiation measurement. The basic radiometer consists of two blackened sensing surfaces, one facing upwards and one downwards, shielded from ventilation effects by pairs of spectrally transparent polyethylene film, and separated from one another by an insulating medium such as expanded polystyrene. Radiation is determined from air temperature and from the temperatures of the two blackened surfaces, which may be measured with any convenient temperature detectors.

For pyrheliometer use, a pair of radiometers, one with "black" and one with "white" sensing surfaces, are used, over an opaque shield. They constitute an "economical pyrheliometer", and are shown in figure 8. Measurements are made of the temperatures of four surfaces and ambient air temperatures. From the energy balances for the surfaces, an equation can be derived relating the incident solar radiation to the measured temperatures, in terms of the properties of the system; equation [2] of the paper is the working equation:

$$R_s\downarrow = A\,(T_w{}^4 - T_b{}^4) + B\,(C_{iw} + C_{tw}) - B\,(C_{ib} + C_{tb})$$

The terms of the equation are explained above, under the heading, "Calculation of radiation".

The basic radiometers are commercially available, and the estimated cost of a pyrheliometer assembly is under $50, depending on what temperature detectors are used. Comparisons of the output of an Eppley pyrheliometer, a silicon solar cell, and the economical pyrheliometer have been made, and show good agreement when the top layer of polyethylene is near ambient temperature. Further comparisons are being made of these instruments.

INSTRUMENTS DE MESURE DU RAYONNEMENT SOLAIRE

Résumé

Ce mémoire résume les résultats de divers travaux entrepris dans le domaine des instruments servant à la mesure du rayonnement solaire. Les instruments en question comprennent : les cellules photovoltaïques au silicium pour les mesures du rayonnement solaire; les cellules au silicium pour la mesure des flux élevés de rayonnement solaire; un intégrateur d'échantillonnage du courant, qui sert à intégrer le rayonnement mesuré au moyen des appareils au silicium (ou d'autres détecteurs à grand débit); et un radiomètre de prix modique pour les mesures du rayonnement total ou net.

Les propriétés des cellules photovoltaïques au silicium sont telles qu'on peut s'en servir pour des mesures du rayonnement solaire, le courant produit par la lumière, I_L étant proportionnel au nombre de photons (dans la gamme d'énergie qui convient) qui frappent ces cellules. On peut mesurer ce courant en lisant le courant de la cellule en court-circuit. Cependant, quand le flux est élevé, la chute de potentiel dans la résistance en série constituée par la cellule ne peut pas être négligée, et on peut polariser les cellules de mesure dans un sens négatif pour élargir la gamme des flux sur laquelle il est possible d'établir une fonction linéaire du débit des cellules par rapport au rayonnement incident. Dans les mesures portant sur de faibles flux, on peut se servir de la polarisation pour augmenter la résistance de mesure acceptable. La tension de polarisation peut être fournie par une pile sèche au mercure, ou bien par une deuxième cellule au silicium de plus grande surface que la cellule de mesure. On peut réaliser un système autonome, par exemple en se servant d'une cellule de 5×5 mm pour polariser une cellule de mesure de $2{,}5 \times 5$ mm. Le débit peut être lu au moyen d'un appareil du genre d'Arsonval ou enregistré avec un appareil peu coûteux de Rustrak.

La cellule au silicium a une réponse spectrale sélective, et quelques erreurs sont introduites dans les mesures du rayonnement faites au moyen de cette cellule par des variations dans la répartition spectrale du rayonnement solaire incident. On a fait des mesures comparatives avec une cellule et un pyrhéliomètre d'Eppley pour les jours clairs et les jours nuageux à Madison, (Wisconsin), États-Unis; les écarts du rayonnement ainsi mesuré avec la cellule, par rapport aux données d'Eppley, n'ont jamais dépassé $\pm$ 0,05 Ly/min. On procède actuellement à d'autres comparaisons. On utilise les cellules sans protection sous le climat de Madison, mais elles sont chauffées pour éliminer le givrage et la neige de l'hiver. On n'a pas observé de modifications perceptibles d'aspect du matériel ou de son débit sur plus d'un an.

Les cellules au silicium ont été utilisées à des fins expérimentales pour les mesures des flux de rayonnement solaire jusqu'à 50 Ly/min. Dans ce but on se sert d'une polarisation à tension constante, et les cellules doivent être refroidies artificiellement par immersion dans l'eau, ou encore être soudées à un absorbeur de chaleur refroidi. L'application en a été faite pour la détermination des flux dans les zones focales d'échangeurs solaires à concentration, dans lesquels la nature non-homogène du champ de flux rend peu pratique l'utilisation d'une cellule de polarisation.

Dans certaines applications, les données sur le rayonnement solaire sont plus utiles sous leur forme intégrée qu'autrement. Étant donné que la cellule polarisée au silicium a un grand débit, on peut se servir d'un intégrateur simple pour calculer le rayonnement accumulé. Ce dispositif est construit autour d'un relais de mesure et d'un moteur synchrone, ce qui évite le besoin d'amplificateurs. Cet intégrateur est un dispositif de sondage qui prend des lectures discontinues et intermittentes de ce courant. Un répartiteur de tension est continuellement entraîné par un moteur synchrone. On applique une tension constante au répartiteur de tension, et la tension de sortie varie donc à un régime constant sur un cycle. Au moment où cette tension est égale à la tension à intégrer (prélevée sur le courant de la cellule au silicium au moyen d'une résistance de chute de potentiel), un deuxième moteur synchrone est relié à sa source d'énergie pour le reste du cycle. La position angulaire de l'arbre du second moteur correspond alors aux lectures partielles accumulées de la tension d'entrée prise sur chaque tour (cycle) du premier moteur. La figure 6 montre un diagramme de l'intégrateur. Le débit intégré est fourni par le nombre de tours total de l'arbre du deuxième moteur.

Ce mémoire décrit un radiomètre économique dont on peut se servir pour mesurer le rayonnement à ondes courtes (solaire) d'entrée et le rayonnement thermique d'entrée et de sortie. Avec des modifications, des paires de ces radiomètres peuvent servir de pyrhéliomètre pour les mesures du rayonnement solaire. Le radiomètre de base est constitué par deux surfaces de perception noircies, dont l'une est dirigée vers le haut et l'autre vers le bas, protégées contre les effets de ventilation par des paires de pellicules de polyéthylène spectralement transparentes, séparées l'une de l'autre par un produit isolant tel qu'un polystyrène développé. Le rayonnement est calculé à partir de la température de l'air et des températures des deux surfaces noircies sur lesquelles on peut faire des mesures au moyen de tout détecteur de température commode.

Pour l'emploi du pyrhéliomètre, une paire de radiomètres, dont l'un est noir et l'autre blanc, est utilisée avec un écran opaque. Ils constituent un pyrhéliomètre économique et on les voit à la figure 8. Les mesures se font sur les températures des quatre surfaces et de l'air ambiant. D'après les bilans énergétiques des surfaces, on peut écrire une équation qui établit les rapports entre le rayonnement solaire incident et les températures mesurées, en fonction des propriétés du système; l'équation 2 du mémoire est notre équation de travail :

$$R_s\downarrow = A\,(T_w^4 - T_b^4) + B\,(C_{tw} + C_{tw}) - B\,(C_{tb} + C_{tb})$$

Les termes de l'équation sont expliqués dans le mémoire.

Des radiomètres de base sont fournis dans le commerce, et le prix évalué d'un pyrhéliomètre est inférieur à 50 dollars, suivant les détecteurs de température utilisés. Des comparaisons sur les débits d'un pyrhéliomètre d'Eppley, d'une cellule solaire au silicium et du pyrhéliomètre économique ont été faites, et indiquent un bon accord entre la couche supérieure de polyéthylène et la température ambiante. On procède actuellement à d'autres comparaisons sur ces mêmes instruments.

THE AMOUNT AND PROPERTIES OF SOLAR RADIATION IN JAPAN AND THE INSTRUMENTS FOR ITS MEASUREMENT

Kyo Sekihara *

Knowledge of the amount of solar radiation falling on the earth's surface is the most fundamental problem of solar energy utilization. It is strongly affected by the latitudinal location and of the weather conditions at the observing station. As Japan consists of several islands which lie south-to-north from 30°N to 45°N, near the eastern border of the Asian continent, it has a fairly complicated climate, varying from place to place and also from time to time, in spite of the comparatively narrow areas of the territory.

On the other hand, in Japan, where there has been a tradition of meteorological observation for about ten years, there is a well-developed network of

* Meteorological Research Institute, Tokyo.

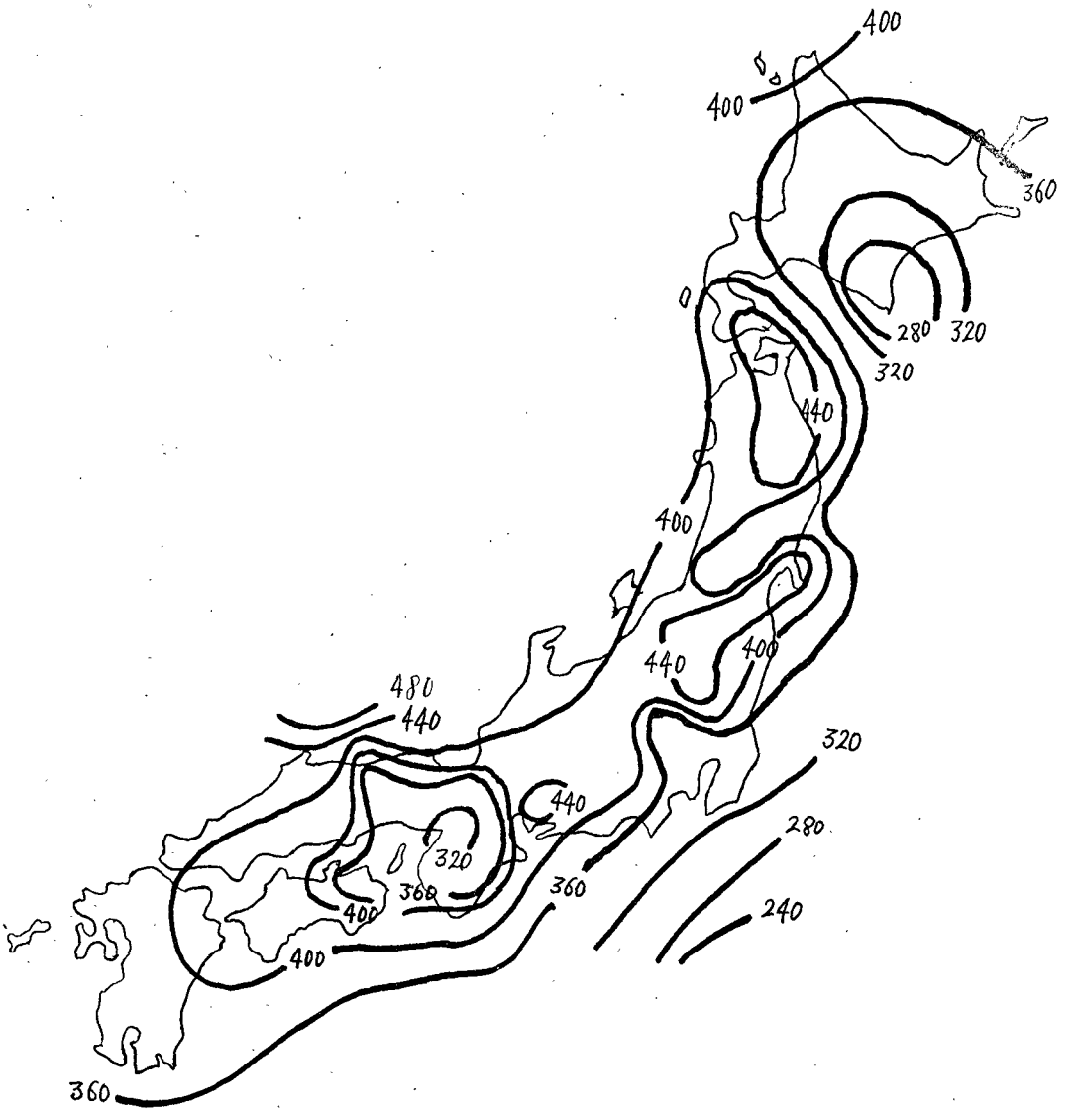


Figure 1. Distribution of solar radiation in Japan: spring (cal/cm²/day, on horizontal surface)

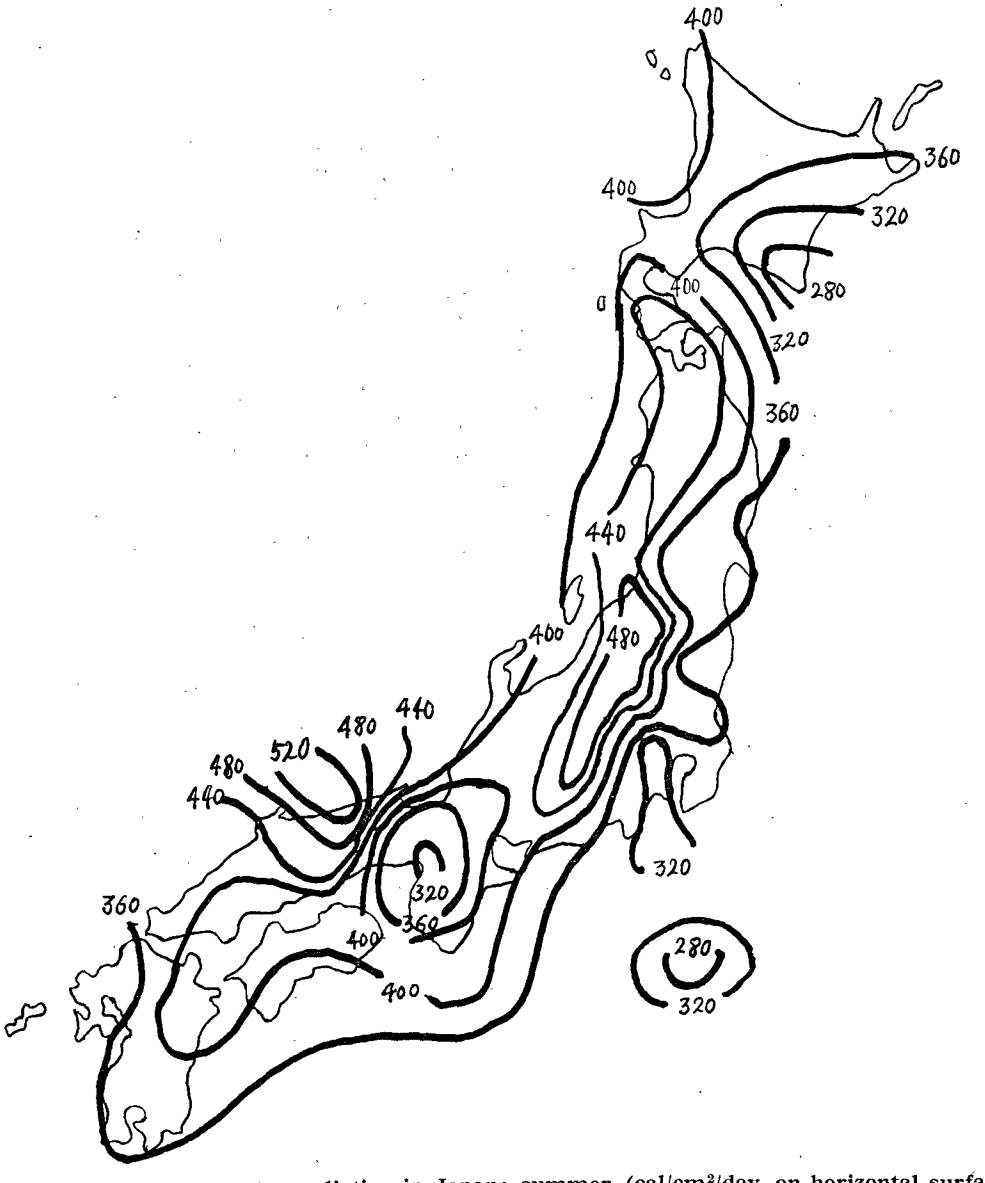


Figure 2. Distribution of solar radiation in Japan: summer (cal/cm²/day, on horizontal surface)

solar radiation measurement, and because of agricultural or industrial requirements, there are many interesting research works of solar radiation for special purposes.

The author intends to describe, first, the present status of usual radiation measurement; secondly, the special variation of solar radiation falling on a horizontal surface; and finally the rather specified measurement of solar radiation for some special purposes.

Networks of usual solar radiation measurement

Since the days before the Second World War, there has been a network of solar radiation measurement of the intensity falling on a horizontal surface and of direct solar radiation of normal incidence, respectively. But this network suffered considerable damage during the war and it was not until several years after the end of the war that recovery was completed. There are now sixty stations of Robitzsch actinograph and twelve stations of silver disc pyrheliometer.

In addition, more accurate measurement using other types of instruments has been planned and carried out since the start of the IGY period, i.e., since the latter half of 1957 or so. The instruments that have been newly equipped are the Eppley 180° pyrheliometer for five stations, the Ångström pyrheliometer for one station and the Gier-Dunkle ventilated pyranometer for five stations. The last-mentioned instrument is that designed for the measurement of atmospheric net radiation.

All these works of solar and atmospheric radiation are administered by the Japan Meteorological Agency, and the results of observation are reported in

the *Actinometric Bulletin* and the *Report of Pyrheliometric Measurement*, both of which are published by the Japan Meteorological Agency, and also in the *Report on IGY Radiation Observation in Japan*, published by the National Committee for the International Geophysical Year, Science Council of Japan, Ueno, Tokyo.

Distribution of solar radiation in Japan (1, 2)

On the basis of the data of Robitzsch actinographs of about thirty stations during the period from 1948 through 1956 which are reported in the *Actinometric Bulletin*, mean values of each station were calculated seasonally or on a year-round basis. From these calculated mean values, contour lines of iso-radiation are drawn to show the general aspect of solar radiation distribution in Japan. These are shown in figures 1-5.

Viewing the distribution diagrams, we can point out the following characteristic tendencies:

(*a*) Solar radiation is generally more intense in the inland area than in the coastal one;

(*b*) The large values of spring and summer seasons are contrasted with the small values of autumn and winter seasons;

(*c*) In autumn and winter, the latitudinal effect is notable, showing remarkably smaller values for the Hokkaido area, the northern-most island of Japan;

(*d*) In winter, the difference between the coastal areas of the western and eastern sides is conspicuous. That is, the lower values of the Japan Sea side are noticeable compared with the values of the Pacific side.

These features can be explained when we consider the geographical or meteorological conditions.

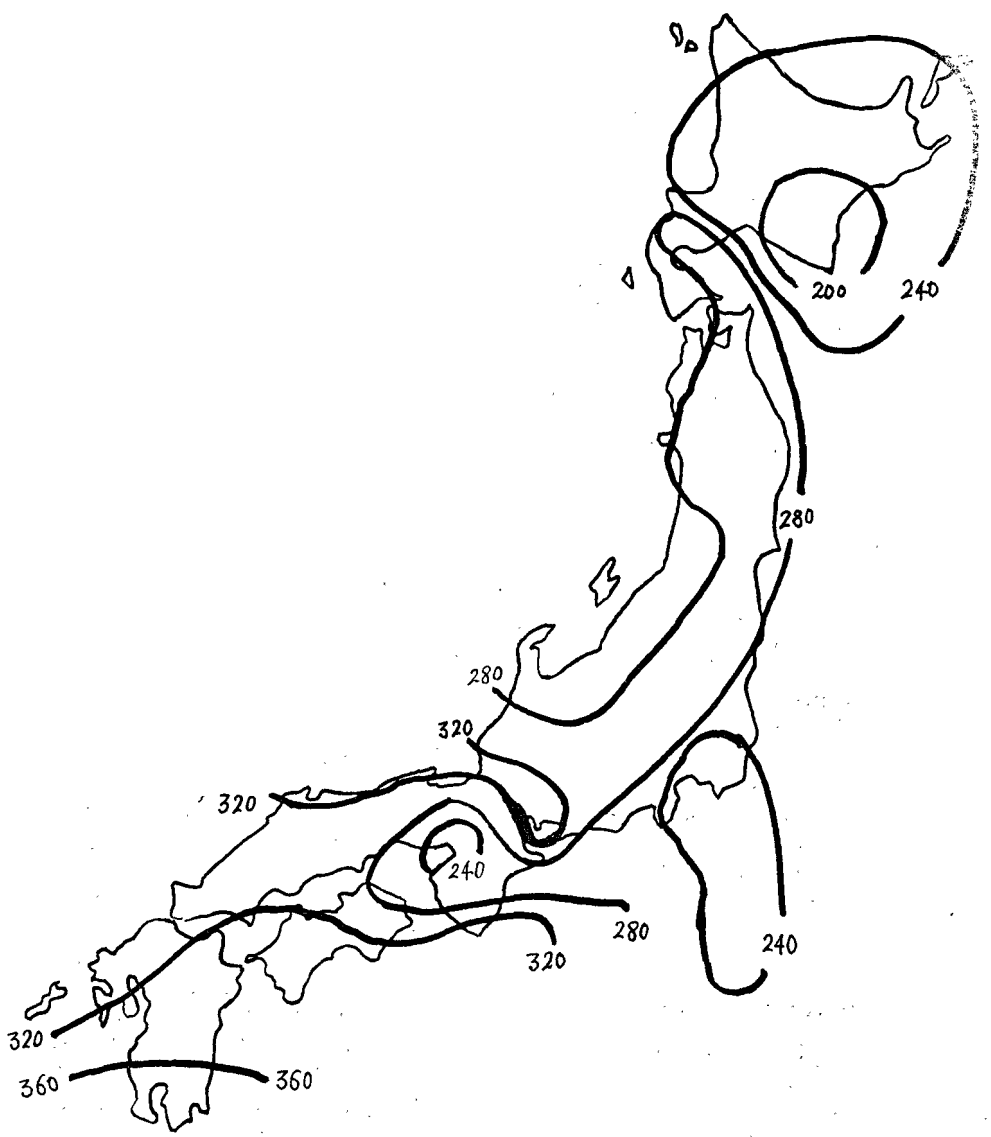


Figure 3. Distribution of solar radiation in Japan: autumn (cal/cm²/day, on horizontal surface)

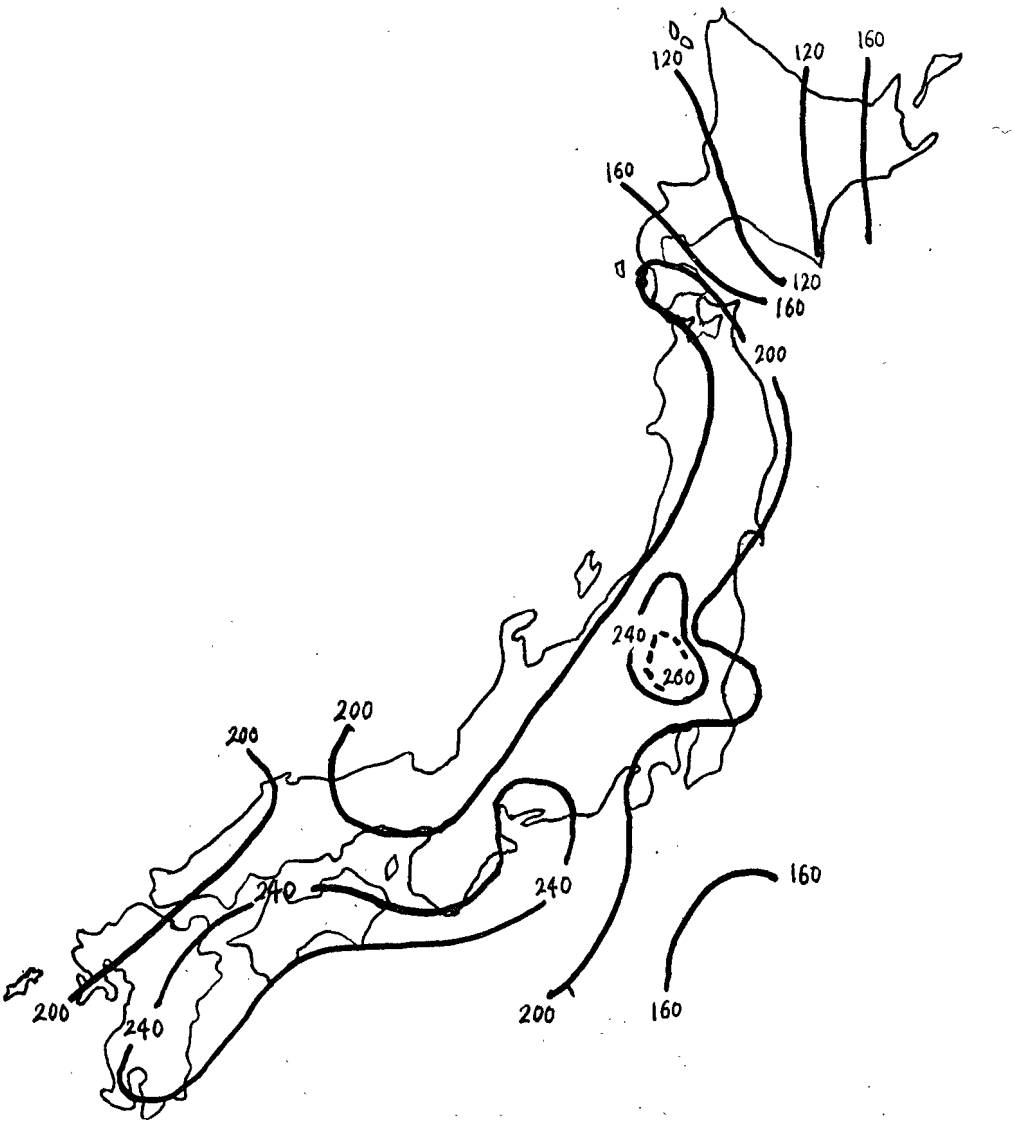


Figure 4. Distribution of solar radiation in Japan: winter (cal/cm²/day, on horizontal surface)

The characteristic noted in (*a*) is partly due to the geographical fact that the inland area is at a higher elevation than the coastal one and partly due to the meteorological fact that the amount of average cloudiness is less in an inland area than in a coastal one.

The characteristics described in (*b*) and (*c*) are the results explainable from a geographical consideration that the elevation of the sun is the chief controlling agent of the amount of solar radiation.

The fact described in (*d*) comes from the climatic characteristic that the continental westerly monsoon prevails in winter and causes steadily cloudy weather in the area of the coast and steadily fine weather on the Pacific side. In summer, on the contrary, there is a steady south-east wind from the Pacific Ocean, but the characteristic feature that comes from this climate is not so remarkable as that of the continental monsoon.

Measurement of solar radiation for special purposes

In addition to the usual network of solar radiation measurement which is chiefly administered by the Japan Meteorological Agency, there are some interesting observations of solar radiation for specific purposes carried out in other organizations, as described below.

Radiation measurement in different spectral regions

Aside from the very rigorous measurement from a purely scientific interest in solar or atmospheric physics, there are many practical requirements of measuring solar radiation in a definite spectral region. One of them is the measurement of ultraviolet solar and sky radiation from the viewpoint of the effect of colour fading or photochemical deterioration of

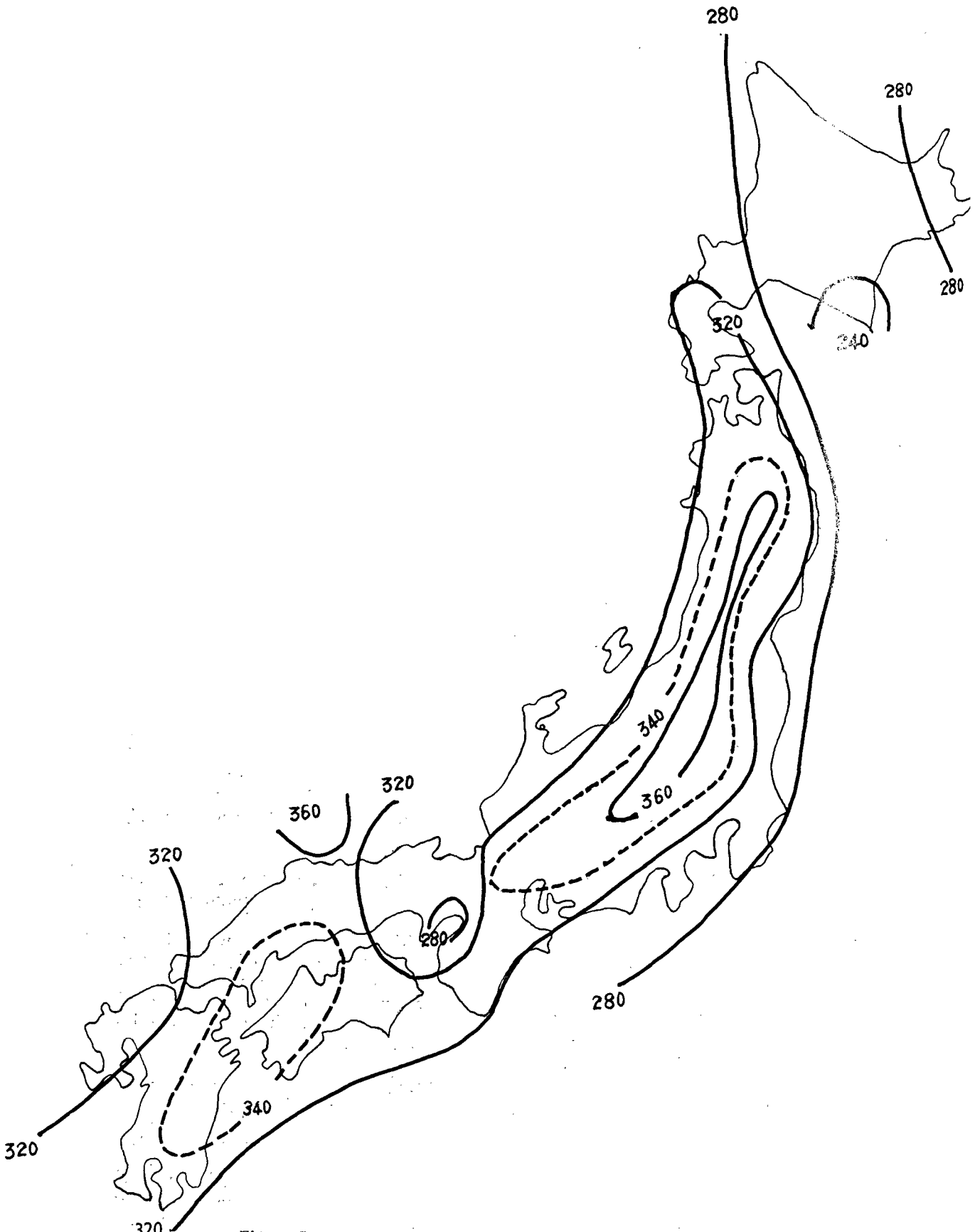


Figure 5. Distribution of solar radiation in Japan: annual mean

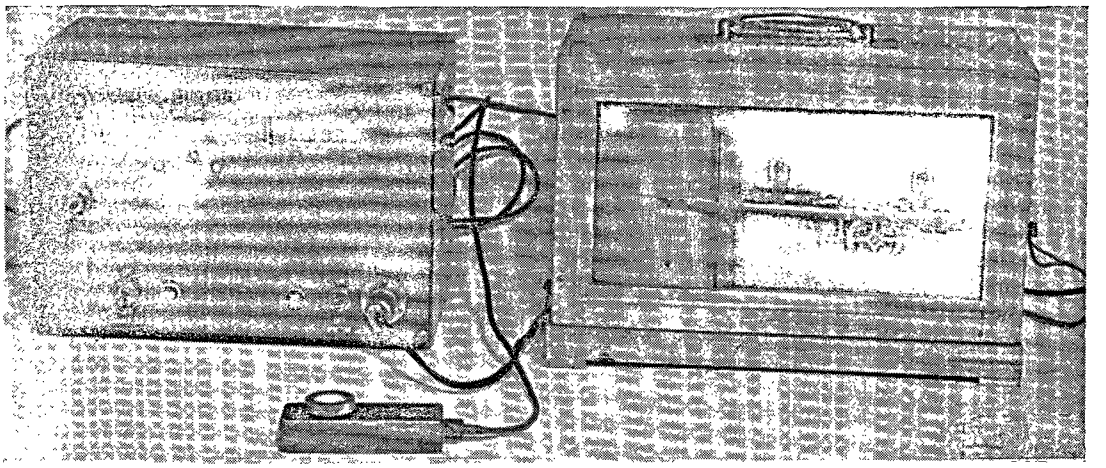


Figure 6. Integrating actinometer: sensing part

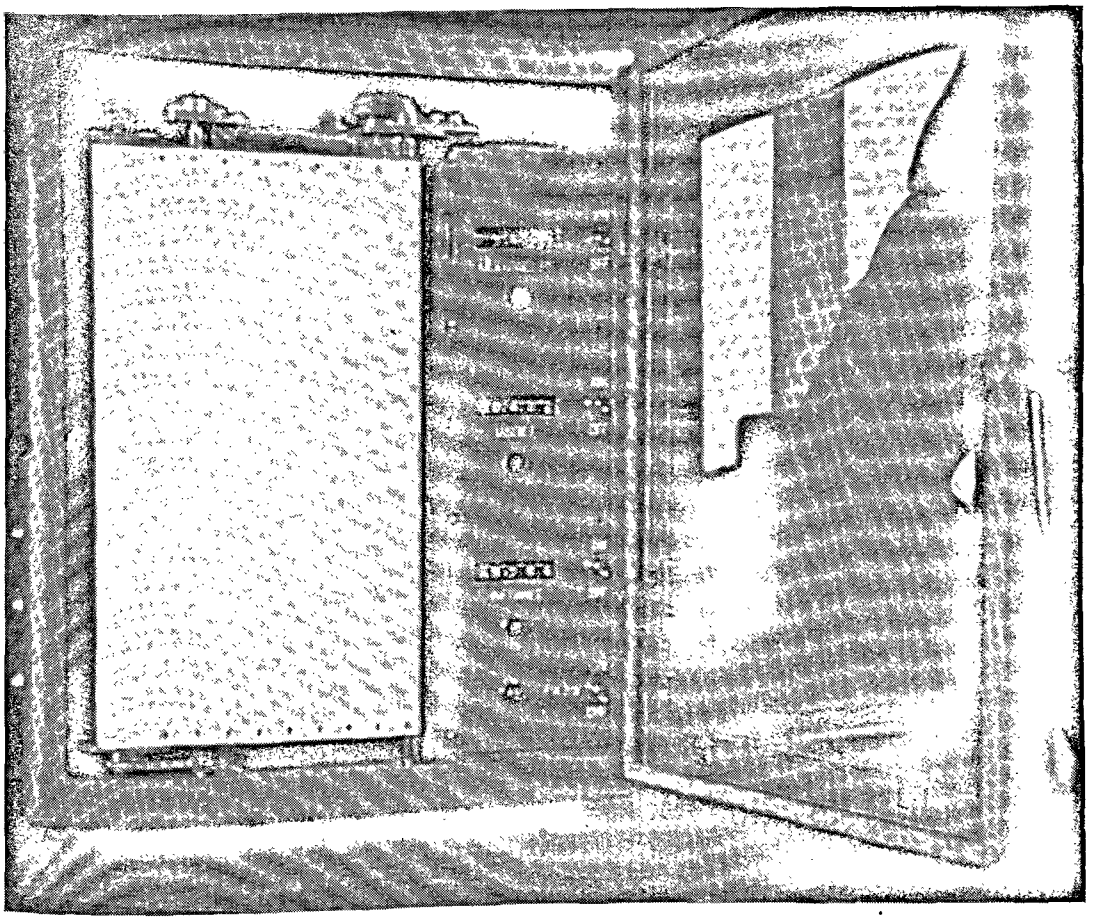


Figure 7. Integrating actinometer: recording part

Table 1. Amount of solar and sky radiation in three different spectral regions

(in mW/day/cm², on a horizontal surface, 5-day means, except when otherwise noted, observed at Toyo-Rika Instruments, Inc., Shinjuku, Tokyo)

Date	Ultraviolet	Visible	Infrared
1959			
Aug.			
1-5	658 (4 days)	4 484 (4 days)	5 650 (4 days)
6-10	582	4 129	6 435
11-15	642	3 711	4 488
16-20	556	4 117	6 248
21-15	426	3 785	4 173
26-30	735	5 485	6 702
Sept.			
31-4	853	5 974	7 687
5-9	548	3 964	4 566
10-14	444	3 305	3 824
15-19	662	5 117	6 006
20-24	472	3 342	4 517
25-29	480	3 094	5 049
Oct.			
30-4	497	3 048 (4 days)	3 585
5-9	548	3 621	4 476
10-14	580	3 750	4 425
15-19	504	3 015	3 383
20-24	153	3 330	4 340
25-29	375	2 223	2 458
Nov.			
30-3	379	2 034	2 390
4-9	441	2 179	2 726
9-13	244	1 223	1 353
14-18	295	2 227 (4 days)	3 459
19-23	328	1 848	2 750
24-28	272	1 659	2 154
Dec.			
29-3	325	1 556 (3 days)	2 504
4-8	313	1 643	2 894
9-13	286	1 630	2 712
14-18	234	1 205	1 928
19-23	228	1 181	2 292
24-29	285	1 365	3 182
1960			
Jan.			
29-2	227 (3 days)	1 124 (1 day)	1 983 (3 days)
3-7	273	1 291	2 789
8-12	218	1 039	1 959
13-17	279	974	2 593
18-22	272	1 217	2 726
23-27	309	1 369	4 181
Feb.			
28-1	324	1 249	4 295
2-6	250 (4 days)	1 027 (4 days)	2 804 (4 days)
7-11	246	1 138	3 533
12-16	284	1 430	4 172
17-21	268	1 581	3 194
22-26	208	810	3 129
Mar.			
27-2	159	624	1 980
3-7	198	789	2 073
8-12	364	1 994	3 032
13-17	586	3 567	5 494
18-22	594	3 389	5 463
23-27	613	3 544	5 300

Table 1. (*continued*)

Date	*Ultraviolet*	*Visible*	*Infrared*
Apr.			
28-1	567	3 279	4 625
2-6	550	2 985	4 007
7-11	782	5 142	6 988
12-16	418	2 478	3 208
17-21	517	3 348	4 612
22-26	529	3 366	4 689
May			
27-1	383	1 993	2 715
2-6	582	3 378	4 635
7-11	410	1 960	2 896
12-16	804	4 727	5 129
17-21	684	4 338	4 927

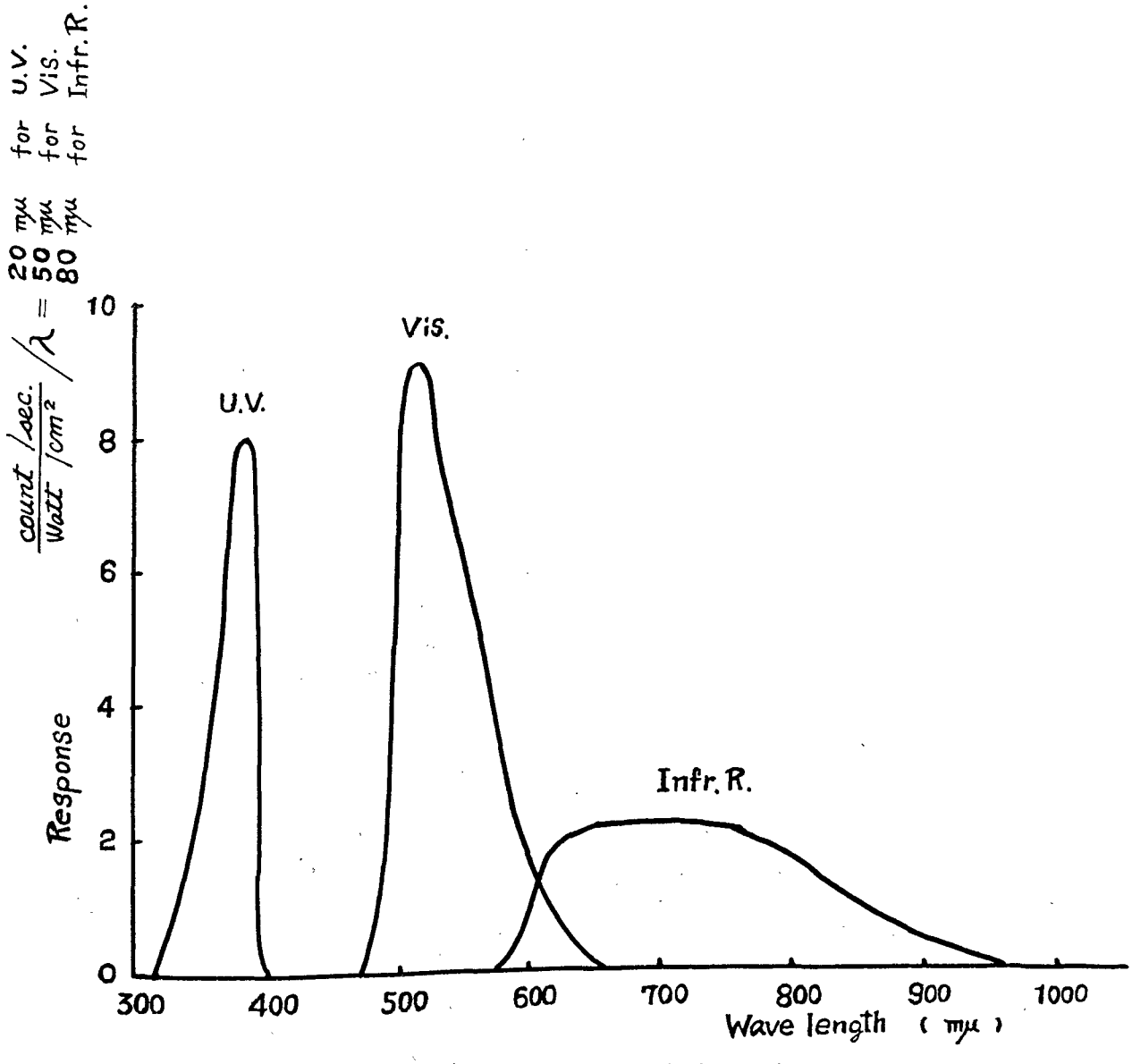


Figure 8. Spectral response curves of the integrating actinometer

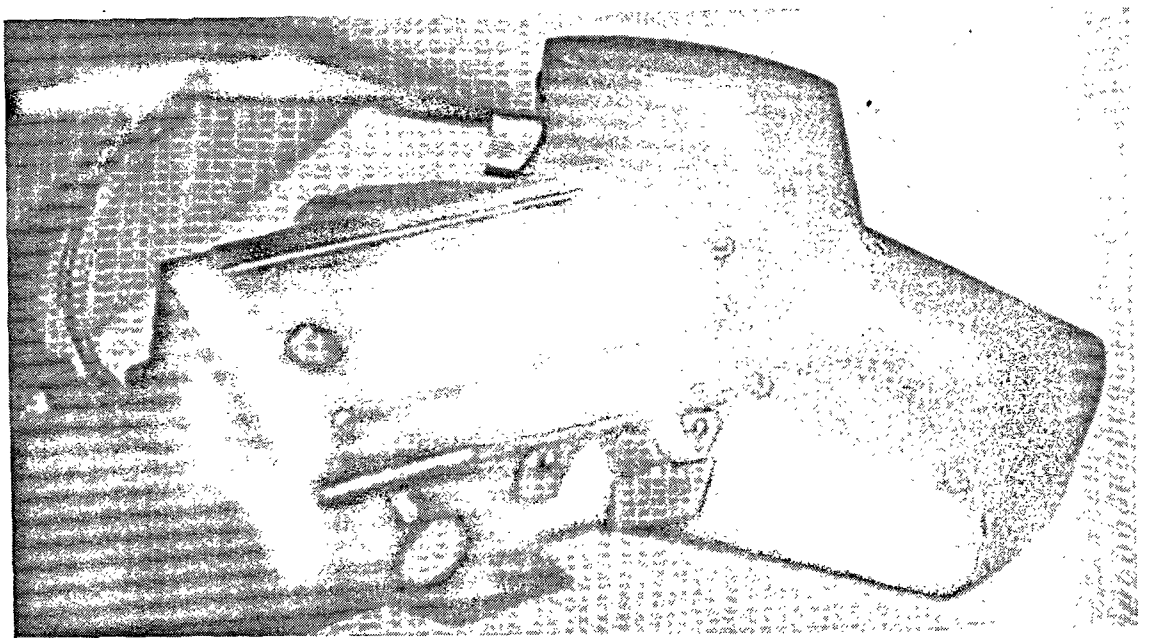


Figure 9. Automatic colour meter for light source: photometric part

plastics, and the other is that of visible radiation to see its illuminating effect for buildings. As regards the usual utilization of solar energy for its heating effect, we are chiefly interested in the total sum of visible and infrared radiation.

Thus the separate measurement of solar radiation in the three regions—i.e., ultraviolet, visible and infrared—is very important for practical use. In Japan an integrating actinometer is designed and manufactured commercially.

The principle of measurement is to use a photoelectric tube and a filter and to measure the accumulated photoelectric current as counted values of a relay counter. Selecting a suitable combination of a filter and a phototube, we can make an observation of a desirable spectral range as mentioned above.

This kind of measurement was carried out at the Meteorological Research Institute, Tokyo (3), as well as at Toyo-Rika Instruments, Inc. Figures 6 and 7 show the sensing part and the counting part of the instrument, respectively. Curves of spectral response of this instrument are shown in figure 8.

Some of the results of observation are given in table 1.

Automatic colour meter for light source

Although this was originally designed for measuring and calculating colour properties of colour

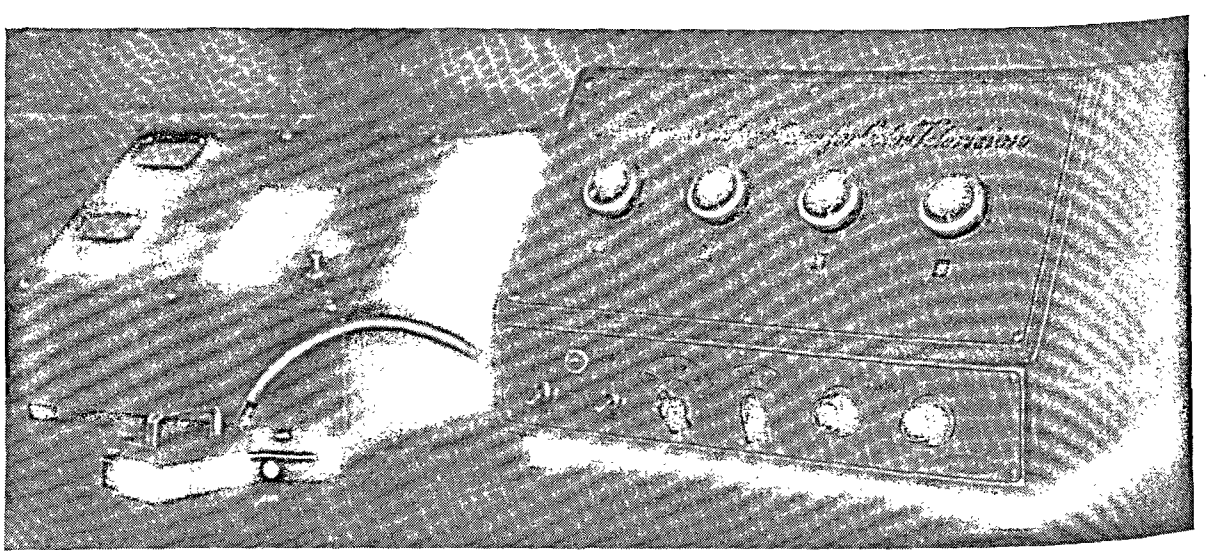


Figure 10. Automatic colour meter for light source: colour calculating part

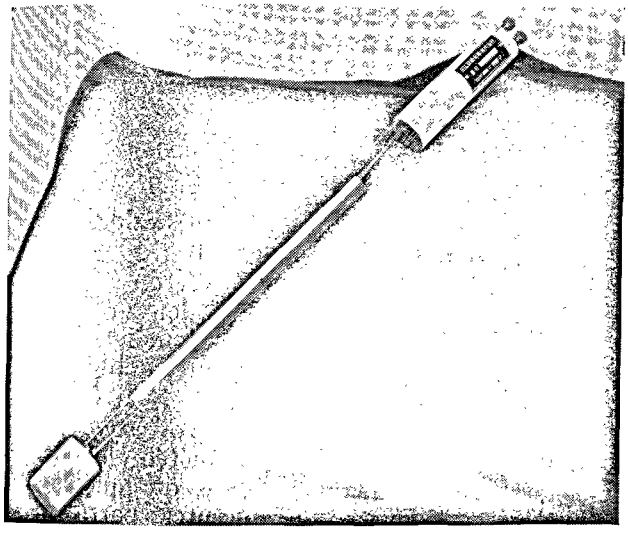


Figure 11. Line-shaped pyrheliometer

television or the illuminating light sources, it can also be used for measuring colour properties of solar or sky radiation. The sensing part consists of a photoconductive cell and of a set of standard colour filters of red, green and blue, as shown in figure 9.

The calculating part consists of a balancing motor and a computing circuit as shown in figure 10.

The merit of this instrument is that the photometric results can be automatically converted to the values of chromaticity of the XYZ system.

Line-shaped pyrheliometer

This is just the same as the Eppley 180° pyrheliometer except for its shape. The sensing element is a black and white strip of rectangular shape, 10 mm × 200 mm in size. It is designed for measuring solar radiation falling on a surface of rectangular shape such as a ridge of a crop field. It can be used for an agricultural or other specific purpose of solar energy utilization. Figure 11 shows the sensing part.

References

1. Sekihara, K. and Kano, M., On the Distribution and Variation of Solar Radiation in Japan, *Met. Geophys. Met. Res. Inst. Tokyo*, vol. VIII, No. 2, pp. 144-149 (1957).
2. Sekihara, K., Amount of Solar Radiation and other Meteorological Data, *Journ. of the D.S.E.*, vol. 34, No. 3, pp. 178-191 (1960). (In Japanese.)
3. Sekihara, K., Murai, K., Kano, M., Ogawa, Y. and Mukai, R., Ultraviolet, Visible and Infrared Solar Radiation and the Meteorological Conditions, *Journ. of Met. Res.* (in Japanese) (to be published).

Summary

In Japan there is a network of solar radiation measurement which is administered by the Japan Meteorological Agency and which contains sixty stations of Robitzsch actinograph for the intensity on a horizontal surface and twelve stations of silver disc pyrheliometer for the intensity of normal incidence.

In addition to this, since the beginning of the IGY period, five stations of Eppley 180° pyrheliometer, one station of Ångström pyrheliometer and five stations of Gier-Dunkle ventilated pyranometer have been added for routine observation.

On the basis of the data of Robitzsch actinographs of thirty stations for eight years from 1948 to 1955, the contour curves of iso-radiation were drawn for each of four seasons and the yearly average, respectively. Concerning these diagrams, the following characteristic features can be pointed out:

(*a*) Solar radiation is generally more intense in the inland district than in the coastal district;

(*b*) The large values of spring and summer seasons are contrasted with the small values of autumn and winter seasons;

(*c*) In autumn and winter, the latitudinal effect is notable, showing remarkable smaller values in Hokkaido, the north-east island in Japan;

(*d*) In winter the difference between the coastal districts of the western and eastern side is conspicuous, that is, the lower values of the Japan Sea side are noticeable compared with the values on the Pacific side. (See figures 1-5.)

In addition to the usual network of solar radiation measurement that is administered by the Japan Meteorological Agency, there are some other instruments for specific purposes.

An integrating actinometer is designed for the measurement of solar radiation in the approximate spectral region of ultraviolet, visible and infrared. Measurement has been carried out at the Meteorological Research Institute, Tokyo, and also at Toyo-Rika Instruments, Inc., Shinjuku, Tokyo, using these instruments. (See figures 6-8 and table 1.)

An automatic colour meter is designed for measuring the chromaticity of a light source. It consists of a spectral photometric (by filter) system and the colour computing system. (See figures 9 and 10.)

A line-shaped pyrheliometer is designed for the measurement of solar radiation falling on a horizontal surface of a rectangular-shaped long area such as a ridge of a crop field. (See figure 11.)

INTENSITÉ ET PROPRIÉTÉS DU RAYONNEMENT SOLAIRE AU JAPON ET INSTRUMENTS UTILISÉS POUR SA MESURE

Résumé

Le Japon est doté d'un réseau de mesure du rayonnement solaire administré par l'Agence météorologique japonaise. Ce réseau comporte 60 stations pourvues d'actinographes de Robitzsch servant à déterminer l'intensité du rayonnement sur le plan horizontal et 12 postes ayant des pyrhéliomètres à disque d'argent servant à mesurer l'intensité du rayonnement dont l'incidence est normale.

Par ailleurs, depuis le début de la période de l'AGI, on a complété ce réseau par cinq stations pourvues de pyrhéliomètres d'Eppley à 180°, une station pourvue d'un pyrhéliomètre d'Ångström et cinq stations pourvues de pyranomètres ventilés de Gier-Dunkle, toutes destinées aux observations courantes.

En se basant sur les données fournies par les actinographes de Robitzsch de 30 stations pour la période de huit ans allant de 1948 à la fin de 1955, on a établi les courbes d'iso-rayonnement pour chacune des quatre saisons, ainsi qu'une moyenne annuelle. En ce qui concerne ces diagrammes, on peut signaler les caractéristiques suivantes :

a) Le rayonnement solaire est généralement plus intense à l'intérieur des terres que sur la côte;

b) Les valeurs considérables notées pour le printemps et l'été sont à opposer aux faibles chiffres de l'automne et de l'hiver;

c) L'effet de la latitude est sensible pendant l'automne et l'hiver, et on observe que les valeurs sont beaucoup plus faibles pour Hokkaido, île située au nord-est de l'archipel japonais;

d) En hiver, la différence observée entre les côtes ouest et est est très marquée. Les valeurs relevées du côté de la mer du Japon sont nettement moindres que celles trouvées sur la côte du Pacifique (voir figures 1 à 5).

Outre le réseau habituel de mesure du rayonnement solaire, administré par l'Agence météorologique du Japon, on trouve, en divers lieux, quelques autres instruments destinés à des mesures particulières.

L'auteur cite un actinomètre intégrateur conçu pour la mesure du rayonnement solaire dans les bandes du spectre correspondant sensiblement à l'ultraviolet, à la lumière visible et à l'infrarouge. Des mesures ont été exécutées à l'Institut de recherches de météorologie de Tokyo, ainsi qu'à la compagnie Toyo-Rika Instrument, Inc., Shinjuku, Tokyo, avec cet instrument. (Voir les figures 6 à 8.)

On a mis au point un colorimètre automatique servant à mesurer la chromaticité des sources de lumière. Il se compose d'un système photométrique spectral (à filtre) et d'un dispositif de calcul de la couleur (voir figures 9 et 10).

Enfin, on a réalisé un pyrhéliomètre linéaire pour la mesure du rayonnement solaire incident sur une surface horizontale d'une plage allongée de forme rectangulaire, telle qu'une butte dans un champ cultivé (voir figure 11).

SOLAR RADIATION MEASUREMENTS IN CANADA

E. H. Truhlar, J. R. Latimer, G. L. Mateer and W. L. Godson *

The network of 30 stations measuring solar radiation in Canada, listed in table 1, is operated on a co-operative basis. Although 17 stations are operated by other governmental agencies or institutes of higher learning, the equipment used at 8 of these stations is owned by the Meteorological Service of Canada.

Measurements of the total daily solar radiation received on a horizontal surface are made at 21 primary stations, equipped with thermoelectric pyranometers of the Eppley pyrheliometer type, and at 9 secondary stations, with bimetallic actinographs.

The radiation record is in graphical form at all locations, but 9 primary stations also are equipped with integrator-printers.

Radiation instruments and recorders

Thermoelectric pyranometer: Eppley 180° pyrheliometer

(*a*) Accuracy: within 2 to 5 per cent when temperature corrections are applied to the observed output and if daily inspections of the instrument are carried out.

(*b*) Maintenance and economy of operation:

(i) The Eppley must be freed of frost or ice under winter conditions. This requires at least one routine early morning inspection.

(ii) The Eppley should be recalibrated and the level of the thermo-pile surface should be checked at least every 2 years.

(iii) With good care, a new Eppley should last about 5 years before need for repair.

Bimetallic actinograph

(*a*) Accuracy: within 5 to 10 per cent.

Most bimetallic actinographs (1) used by the Meteorological Service of Canada are subject to large thermal effects due to convection currents and thermal lag. These seasonal effects are large and must be allowed for in the reduction of the observed data.

(*b*) Dependability: the bimetallic actinograph can be operated with only about 3 to 5 per cent loss of record if routine attention is provided.

(i) Because of severe thermal exposure at some Canadian locations, the clockwork mechanism controlling the chart recorder is inoperative during short periods of extreme cold.

(ii) The instrument chart needs replacement only every 3 days.

(iii) Physical shock from high winds can cause the chart zero to be displaced, resulting in the indication of a false radiation record.

(*c*) Maintenance and economy of operation: the surfaces of the bimetallic strips should be reconditioned every 3 or 4 years at the time of general overhaul.

Recorders

Minneapolis Honeywell electronic self-balancing potentiometer:

(*a*) Accuracy: within $\frac{1}{4}$ of 1 per cent.

(*b*) Dependability: only 1 per cent or less of the radiation record is lost under routine maintenance.

(*c*) Maintenance and economy of operation:

(i) Routine maintenance of motors, slidewires, etc., should be made every 6 months.

(ii) Routine calibration checks should be made every 12 to 18 months.

(iii) A lifetime of nearly 5 years is expected before full overhaul is needed.

Expansion plans

The solar radiation network has grown from one station in 1937 to 5 in 1950, and to 30 in 1960, and by the end of 1963 will include 32 stations.

For the next two years the emphasis in the Canadian expansion plans will be in the direction of greater accuracy of measurement and of more automation of output.

To achieve greater accuracy of measurement: (*a*) all stations will be equipped with thermo-electric pyranometers by the end of 1963; (*b*) the National Radiation Centre at Toronto will provide better control of instrumental calibration than is at present possible.

Graphical output will be replaced by integrator-printout at all but 6 stations within the next 3 years.

National Radiation Centre

The National Radiation Centre serves as the heart of the Canadian radiation network by maintaining the quality control of the radiation instruments, by reducing the radiation charts received

* Meteorological Service of Canada, Toronto.

Table 1. Radiation network in Canada

Station and province	Class*	Lat. °	N ′	Long. °	W ′	Height above msl. (feet)	Start of record	Operating agency
Beaverlodge, Alta.	2a	55	11	119	22	2 500	1960	Dept. of Agriculture
Churchill, Man.	S3a	58	45	94	04	115	1953	Defence Research, Northern Lab.
Dartmouth, N.S.	2aI	44	36	63	28	103	1957	Naval Research Establishment
Departure Bay, B.C.	2a	49	13	123	57	60	1959	Fisheries Research Board
Edmonton, Alta.	2aI	53	34	113	31	2 219	1948	Meteorological Branch
Fredericton, N.B.	2aI	45	55	66	37	130	1960	Dept. of Agriculture
Fort Simpson, N.W.T.	3b	61	52	121	21	422	1954	Meteorological Branch
Goose, Nfld.	3b	53	19	60	25	144	1954	Meteorological Branch
Guelph, Ont.	S3a	43	33	80	16	1 050	1953	Ontario Agricultural College
Inuvik, N.W.T.	2aI	68	18	133	29	198	1948	Meteorological Branch
Kapuskasing, Ont.	3b	49	25	82	28	752	1954	Meteorological Branch
Kentville, N.S.	2aI	45	04	64	29	50	1960	Dept. of Agriculture
Knob Lake, Que.	3b	54	48	66	49	1 681	1957	McGill University
Lethbridge, Alta.	3b	49	38	112	48	3 018	1952	Meteorological Branch
Moncton, N.B.	3b	46	07	64	41	248	1953	Meteorological Branch
Montreal, Que.	3c	45	30	73	37	435	1956	Collège Jean de Brébeuf
Moosonee, Ont.	2a	51	16	80	39	34	1957	Meteorological Branch
Normandin, Que.	2a	48	51	72	32	450	1957	Dept. of Agriculture
Ocean Station P	2a	50	00	145	00	0	1960	Meteorological Branch
Ottawa, Ont.	2aI	45	27	75	37	320	1949	National Research Council
Resolute, N.W.T.	2a	74	43	94	59	209	1957	Meteorological Branch
Saint John's, Nfld.	3b	47	31	52	47	375	1954	Dept. of Agriculture
Saskatoon, Sask.	S3a	52	08	106	38	1 690	1953	National Research Council
Suffield, Alta.	2b	50	16	111	11	2 543	1959	Defence Research Board
Summerland, B.C.	3b	49	34	119	39	1 491	1954	Dept. of Agriculture
Swift Current, Sask.	2aI	50	15	107	45	2 440	1960	Dept. of Agriculture
Toronto, Ont.	2a	43	40	79	24	379	1937	Meteorological Branch
Toronto, Scarborough, Ont.	1I	43	43	79	14	528	1959	Meteorological Branch
Vancouver, B.C.	2a	49	16	123	15	305	1959	University of British Columbia
Winnipeg, Man.	2aI	49	54	97	14	786	1949	Meteorological Branch

* 1 = National Radiation Centre; 2a = station equipped with Eppley 180° pyrheliometer and hourly data are published; 3a = station equipped with Eppley 180° pyrheliometer but only daily totals are published; 3b = station equipped with M.S.C. type actinograph and daily totals are published; 3c = station equipped with Japanese pattern Robitsch actinograph and daily totals are published; S = co-operating station for which record charts are not scaled by the M.S.C. Final radiation data are provided by the co-operating agency for publication; I = station equipped with integrator-output along with the regular graphical output.

from the network and publishing the corrected data, and by providing technical assistance and advice to other agencies.

Quality control

The Toronto standard of radiation is maintained with a group of reference standard pyrheliometers including: 1 silver disc pyrheliometer, 4 Ångström compensation pyrheliometers (Swedish model), 1 Ångström compensation pyrheliometer (Smithsonian model), 1 Abbot pyranometer with tube attachment.

It is planned that one member of the above group will be compared with an accepted international standard of pyrheliometry at least once every five years and preferably every second year.

To facilitate the accurate calibration of field instruments, an integrating sphere (6ft. in diameter) will be in operation by summer 1961. To investigate the instrumental response with respect to ambient air temperature, a cold chamber has been constructed and will be in operation by May 1961; and to investigate other instrumental response characteristics, such as the azimuth and cosine errors, an optical bench is presently under construction. Finally, to study the variation of instrument response when the attitude of operation is different from the attitude of calibration, an optical bar is also under construction.

Processing and publication of data

Hand-scaling of recorder and actinograph charts is the normal procedure. However, the integrator-printout at 9 stations allows about a 75 per cent reduction in the scaling time for each location. The raw scaled or printed data are submitted via transit documents to the Data Processing Section of the Meteorological Service of Canada where the data are punched on cards and then corrected for ambient air temperature. Within 5 years, the hand-scaling procedures will be replaced by integrator-display output or by punched-tape output. Before being stored in the library, the punched card data are tabulated, assembled in logical order and then published once a month in the Meteorological Service's publication entitled *Monthly Radiation Summary*.

Technical assistance

Scientific advice and assistance in regard to radiation problems are provided to research institutes, industry, etc. Calibration services are provided on request. Laboratory and field investigations of the properties and accuracy of existing and newly developed radiation instruments are conducted. Finally, a limited number of radiation instruments, namely, two Linke-Feussner actinometers and one Michelson-Beuttner actinometer, are maintained for temporary loans to scientific expeditions, research institutes and universities engaged in special research projects.

Surveys of solar radiation—past and future

A preliminary survey of the radiation climate of Canada was published by C. L. Mateer (2), who analysed the data which were recorded before 1955. This study utilized Canadian sunshine records in order to extend the loose-knit primary radiation network into sections of Canada where few or no radiation measurements had been made.

A more complete survey of the above-mentioned type will be made over the next two or three years after the primary radiation record at each station extends over more than five years, and after the data observed prior to 1958 have been corrected, chiefly for ambient air temperature and the change in pyrheliometric scale.

Daily totals of the solar radiation received on a horizontal surface at selected Canadian stations have been published in the *Monthly Radiation Summary* since December 1952, and hourly and daily totals since January 1960. Hourly and daily totals of solar radiation observed in Canada during IGY and IGC are in the process of being published by WMO. Monthly means of the total daily solar radiation received on a horizontal surface at selected stations in Canada will appear in 1961 in a compilation of world-wide solar radiation data to be published in the United States.

Solar energy utilization

Table 2 lists the monthly totals (in watt hr cm^{-2}) of the total solar radiation received on a horizontal surface at 17 Canadian stations arranged in order of increasing latitude. The first eleven stations are strung out across Canada near the southern border, while the last six extend northward into the interior. An analysis of the values leads to the following points:

(*a*) In the winter and fall months, September to February, the solar energy has a definite latitudinal variation with maximum values being observed in the southernmost areas. Differences between the totals for southern Canada during this period depend on the geographic location (inland or maritime) as well as the normal climatic regime;

(*b*) In the early spring and mid-summer months, the northern stations receive about the same amounts of radiation as the southern maritime stations (cf. Moncton and St. John's). In the months April to June, the northern stations, because of the longer daylight period, receive radiation amounts equal to or greater than those observed in extreme southern Canada. In particular, Resolute, some 2 200 miles north of the Lower Great Lakes, receives the most solar radiation in Canada during the months of May and June;

(*c*) The maritime nature of the climates of Moncton, St. John's and Vancouver is pointed out by the low yearly totals. Toronto, although the most southerly location listed, shows a low yearly total

Table 2. Monthly totals of solar radiation received on a horizontal surface

(In watt hr cm^{-2})

Station and province	Latitude °	′	Longitude °	′	Height above sea level (feet)	Jan.	Feb.	Mar.	Apr.	May	June	July	Aug.	Sept.	Oct.	Nov.	Dec.	Year
Toronto, Ont.	43	40	79	24	379	4.0	5.9	9.9	12.9	16.0	18.0	18.5	15.8	11.8	8.0	4.0	3.2	128
Ottawa, Ont.	45	27	75	37	320	4.8	6.9	11.8	13.1	17.1	18.3	19.3	16.9	10.3	7.8	4.0	4.3	135
Montreal, Que.	45	30	73	37	435	4.0	6.6	11.5	14.0	16.9	17.1	18.4	15.9	10.8	7.2	3.5	2.9	129
Moncton, N.B.	46	07	64	41	248	3.7	5.9	10.4	13.2	15.8	15.7	16.9	14.7	10.8	7.5	3.9	3.2	122
St. John's, Nfld.	47	31	52	47	375	2.9	5.0	8.6	11.2	14.4	15.0	15.8	12.3	9.8	6.1	2.8	2.5	106
Vancouver, B.C.	49	16	123	15	305	2.7	5.0	9.0	13.2	17.7	18.1	20.1	16.9	11.2	6.5	3.1	2.4	126
Lethbridge, Alta.	49	38	112	48	3 018	4.3	6.9	12.3	14.6	18.7	20.2	22.0	18.7	12.9	8.6	4.8	3.2	147
Winnipeg, Man.	49	54	97	14	786	4.3	7.2	12.1	14.3	17.9	17.8	20.1	16.6	11.0	7.2	3.9	3.1	135
Medecine Hat, Alta.	50	01	110	43	2 365	4.3	7.2	11.5	14.6	19.1	19.5	21.3	18.0	11.5	7.9	4.5	3.7	143
Armstrong, Ont.	50	17	88	54	1 065	4.3	7.5	13.0	15.7	17.7	17.4	19.1	15.8	9.8	6.1	3.3	3.2	133
Regina, Sask.	50	26	104	40	1 884	4.3	7.2	13.0	15.0	19.1	18.5	21.3	17.3	11.5	7.5	3.9	3.7	142
Port Harrison, Que.	58	27	78	08	66	2.2	5.3	10.4	15.4	16.3	16.4	16.6	13.0	7.0	4.3	1.9	1.1	110
Churchill, Man.	58	45	94	04	115	2.4	5.0	11.0	15.5	18.4	18.5	18.2	13.7	7.9	4.2	2.0	1.3	118
Pine Creek, Y.T.	60	45	137	35	2 030	1.1	4.0	8.6	13.6	17.7	18.1	16.6	13.3	7.6	4.3	1.6	0.5	107
Fort Simpson, N.W.T.	61	52	121	21	422	1.1	3.0	8.3	13.6	18.0	18.1	16.6	13.3	7.6	4.0	1.1	0.3	105
Aklavik, N.W.T.	68	14	135	00	198	0.1	1.5	6.4	13.1	17.4	18.4	15.5	10.4	5.4	1.9	0.3	0.02	90
Resolute, N.W.T.	74	43	94	59	209	Nil	0.5	4.5	12.6	19.5	21.6	15.5	9.6	4.0	1.1	0.3	Nil	89

(when compared with non-maritime stations) indicative to some extent of urban pollution and of proximity to the Great Lakes.

(*d*) The sunniest areas over the full year lie in the southern parts of Alberta and Saskatchewan, as well as in south-western Quebec.

The southern sections of Canada show a good potential for solar energy utilization, especially during the spring and summer months. It is important to note that useful applications of solar energy may be possible in the far northern sections of Canada during the long periods of daylight experienced in the spring months, April, May and June.

Simplified instrumentation

In areas of the world where economical utilization of radiation instruments must be made, it appears that bimetallic actinographs would be useful. Although subject to the large errors mentioned in the section on bimetallic actinographs above, which reduce their accuracy by about 10 per cent, actinographs can be easily maintained and operated and the records scaled by unskilled personnel. However, Canadian experience has shown that meaningful results can only be achieved if the data so observed are subject to quality control which is exercised by a competent radiation centre.

References

1. *Bull. Amer. Met. Soc.* 34, 170-174 (1953).
2. Mateer, C. L., A Preliminary Estimate of the Average Insolation in Canada, *Can. J. Agric. Sci.* 35, 579-594 (1955).

Summary

The Canadian network measuring solar radiation is comprised of 30 stations operated jointly by the Meteorological Service of Canada and other governmental agencies or institutes of higher learning.

Measurements of solar radiation are made at 21 primary radiation stations, equipped with thermoelectric pyranometers, and at 9 secondary stations, with bimetallic actinographs. The radiation record is in graphical form at all locations, with integrator printers also being installed at 9 primary stations.

The most accurate radiation measurements are recorded by Eppley pyrheliometers allied with Minneapolis Honeywell electronic recorders. These instruments are easy to operate, and if they are given good care and routine maintenance, their useful life before major overhaul or replacement is approximately five years for the Eppleys and the associated recorders.

By the end of 1963, the network will be expanded to include 32 stations, all equipped with thermoelectric pyranometers. Within 3 years, all but 6 stations will have integrator-printer output.

The National Radiation Centre at Toronto serves the following three main functions:

(a) *Quality control.* A group of reference standards is maintained and compared with recognized international standards of radiation at regular intervals. To further ensure that field instruments will be inspected and correctly calibrated on a routine basis, an integrating sphere, a cold chamber, an optical bar and an optical bench are either under construction or have just been installed at the National Radiation Centre.

(b) *Processing and publication of data.* Most of the current radiation data are hand-scaled from graphs; about 25 per cent is read from integrator-printer tapes. The raw data are then entered on punched cards, corrected for the error due to ambient air temperature and the corrected data are published fn the *Monthly Radiation Summary*. Within the next iew years, hand-scaling will be eliminated and only quality control of the automated output will be necessary.

(c) *Technical assistance.* The National Radiation Centre provides advice to research institutes, industry, etc., in regard to their radiation problems; calibration services on request; loans of radiation instruments to agencies engaged in special research projects; and evaluations, in the laboratory or the field, of existing or newly developed radiation instruments.

A preliminary survey of the radiation climate of Canada, published in 1955 by C. L. Mateer, will be extended within the next few years. Daily totals of solar radiation received at selected Canadian stations have been published in the *Monthly Radiation Summary* since December 1952, and hourly and daily totals since January 1960. Hourly and daily totals of solar radiation recorded during IGY and IGC in Canada are in the process of being published by the WMO. Monthly means of the solar radiation received on a horizontal surface in Canada will be published in 1961 in the United States.

A study of the monthly totals of solar radiation received at 17 selected Canadian stations yields the following results:

(*a*) In the fall and winter months, the solar energy has a latitudinal dependence. Maximum values are observed in southern Canada where geographic location and climatic factors cause minor variations;

(*b*) In the early spring and mid-summer months, northern stations and southern maritime stations

receive comparable amounts of solar energy. For the spring months, April to June, the northern stations receive equal or greater radiation amounts than those observed in southern Canada because of the greater length of day;

(*c*) The maritime nature of certain stations is shown by the low annual totals of radiation. However, Toronto, in the extreme south of Canada, has a low annual total because of urban pollution and proximity to the Great Lakes;

(*d*) The sunniest areas of Canada are in the southern sections of Alberta and Saskatchewan and in south-western Quebec.

Regions which show a good potential for solar energy utilization are southern sections of Canada during the spring and summer months, and far northern areas of Canada during the spring months, when the long periods of daylight occur.

Canadian experience with bimetallic actinographs indicates that these instruments, although only accurate to within 10 per cent, can be operated and maintained (and the records scaled) by unskilled personnel in areas where economical utilization of radiation instruments must be made. However, to achieve meaningful results, the data must undergo quality control exercised by a competent radiation centre.

MESURES DU RAYONNEMENT SOLAIRE AU CANADA

Résumé

Le réseau canadien de mesure du rayonnement solaire est formé de 30 postes qu'exploitent en commun le Service météorologique national et diverses autres institutions gouvernementales ou d'enseignement supérieur.

Les mesures de rayonnement solaire se font à 21 postes principaux dotés de pyranomètres thermo-électriques et à 9 postes secondaires pourvus d'actinographes bimétalliques. Les valeurs enregistrées sont inscrites sous forme de graphiques à tous ces postes. Neuf des stations principales sont dotées d'intégrateurs enregistreurs.

Les mesures les plus exactes du rayonnement se font avec des pyrhéliomètres d'Eppley combinés avec des enregistreurs électroniques Minneapolis Honeywell. Le maniement de ces instruments est facile et, à condition qu'ils soient bien soignés et fassent l'objet de mesures d'entretien appropriées, leur vie utile de service, avant les révisions d'ensemble ou le remplacement, est de l'ordre de cinq ans pour les appareils d'Eppley et les enregistreurs qui les complètent.

Le réseau sera développé d'ici la fin de 1963 et porté à 32 postes uniformément dotés de pyranomètres thermo-électriques. Dans les trois ans, tous les postes, sauf six, seront dotés d'intégrateurs enregistreurs.

Le Centre national du rayonnement, situé à Toronto, a trois fonctions principales :

a) *Contrôle de la qualité.* Le Centre tient à jour un système de normes servant de référence, et les compare aux normes internationales de rayonnement officiellement reconnues à intervalles réguliers. Pour assurer que les instruments en service aux divers postes soient examinés et correctement étalonnés d'une manière systématique, une sphère d'intégration, une chambre froide, une barre optique et un banc optique sont en construction ou viennent d'être installés au Centre national du rayonnement.

b) *Exploitation et publication des données.* On évalue la majeure partie des données communes sur le rayonnement à partir des tracés. On lit une proportion d'environ 25 p. 100 d'entre eux sur les bandes en papier des intégrateurs enregistreurs. On inscrit alors les données brutes sur des cartes perforées, et les données corrigées quant aux erreurs dues à la température de l'air ambiant sont publiées dans le *Sommaire mensuel du rayonnement.* D'ici quelques années, les opérations manuelles seront éliminées, et il suffira aux techniciens de procéder au contrôle de la qualité des données de sortie des instruments automatisés.

c) *Aide technique.* Le Centre national du rayonnement fournit : des conseils aux instituts de recherche, à l'industrie, etc., quant à leurs problèmes ayant trait au rayonnement; des services d'étalonnage sur demande; des prêts d'instruments de rayonnement aux agences qui mènent des projets de recherche spéciaux; et des évaluations, au laboratoire ou à pied d'œuvre, des instruments courants ou récemment mis au point de lecture du rayonnement.

Une étude préliminaire du climat du rayonnement au Canada, publiée en 1955 par C.L. Mateer, sera reprise au cours de ces quelques prochaines années. Les totaux quotidiens de rayonnement solaire reçu en certains postes canadiens spécialement choisis ont été publiés dans le *Sommaire mensuel du rayonnement* depuis décembre 1952, et les totaux horaires et quotidiens depuis janvier 1960. Les totaux horaires et quotidiens du rayonnement solaire enregistré pendant l'AGI et le CGI au Canada sont en cours de publication par l'OMM. Les moyennes mensuelles du rayonnement solaire reçu au Canada sur une surface horizontale seront publiées en 1961 aux États-Unis.

Une étude des totaux mensuels du rayonnement solaire reçu à 17 postes canadiens spécialement choisis donne les résultats suivants :

a) Pendant les mois d'automne et d'hiver, l'énergie solaire dépend de la latitude. On observe les valeurs maxima au sud du Canada, région dans laquelle

la position géographique et les éléments climatologiques provoquent de légères variations.

b) Pendant les mois du début du printemps et du milieu de l'été, les postes septentrionaux et ceux qui sont au sud, mais au bord de la mer, reçoivent des quantités d'énergie solaire comparables. Pour les mois de printemps, d'avril à juin, les postes septentrionaux reçoivent des quantités de rayonnement égales ou supérieures à celles que l'on observe dans le sud du pays, en raison de la plus grande longueur des journées sous ces latitudes.

c) Le régime maritime applicable à certains des postes est indiqué par la modicité des totaux annuels. Néanmoins, Toronto qui est à l'extrême sud du pays, présente un total annuel faible en raison des impuretés de l'air, fréquentes dans de tels centres urbains, et de sa position proche des Grands Lacs.

d) Les parties les plus ensoleillées du Canada se trouvent dans les régions méridionales de l'Alberta et du Saskatchewan, ainsi que dans le sud-ouest de la province de Québec.

Les régions qui se prêtent bien à l'utilisation éventuelle de l'énergie solaire sont les régions méridionales du Canada pendant les mois de printemps et d'été, et le grand nord, pendant les mois de printemps, époque à laquelle les jours sont très longs.

L'expérience acquise au Canada avec les actinographes bimétalliques indique que ces instruments, bien que leur précision ne dépasse pas 10 p. 100, peuvent être maniés et entretenus (et les graphiques interprétés) par un personnel sans spécialisation dans les régions où il faut faire un usage économique des instruments de mesure du rayonnement. Cependant, pour assurer des résultats significatifs, les données doivent faire l'objet du genre de contrôle de la qualité que peut exercer un centre de rayonnement spécialisé.

DISTRIBUTION OF SOLAR ENERGY OVER INDIA

S. P. Venkiteshwaran *

As compared to energy from the wind, solar energy is known to have a greater certainty of occurrence, though it is totally absent at night. In India, while there is a strong annual variation in the wind in many regions, the variation of sunny periods is equally well marked; during the monsoon months, June to September, when the skies are mostly overcast, wind is strongest. This indicates that wind energy can supplement solar energy in many parts of India.

Ramdas and Yegnanarayanan (1) briefly analysed the duration of bright sunshine and calculated the total solar radiation using Ångström's well-known empirical formula correlating hours of sunshine S with the total solar radiation Q. Since then, a few stations have been started by the India Meteorological Department for recording total radiation from sun and sky as a routine. Since a study of the distribution of sunshine over the country and its variations are of interest in a study of the spatial distribution of solar energy over India, the distribution of sunshine and its variation in time and space over the sub-continent are discussed in this paper.

Mean daily duration of bright sunshine

The data of duration of bright sunshine obtained with the Campbell-Stokes sunshine recorder over nearly 30 stations have been studied, and figure 1 shows the distribution, over the Indian peninsula, of the mean daily hours of bright sunshine for each month.

It will be seen that during the cold season, November to February, the duration of sunshine in the Indian peninsula is greatest to the south of the Gangetic plains and to the north of 13°N, the duration exceeding 10 hours in certain places. North of this region, the duration is less, as a result of the passage of winter disturbances from the west and the decrease in the length of the day with latitude. To the south, cloudiness associated with disturbances in the Bay of Bengal or the Arabian Sea and convectional clouds associated with higher humidity as a result of the flow of currents from the adjacent seas are responsible for the reduction in the hours of sunshine.

With the advance of the year, the region of clear skies shifts towards the north-west, till in April the region with hours of sunshine exceeding 10 lies over Gujarat and the adjoining regions of Sind and Rajasthan. This extends further to the north over West Pakistan in May, but the maximum remains over Gujarat.

With the onset of the monsoon in June, the region of maximum sunshine lies over West Pakistan and the adjoining regions of Rajasthan and the Punjab. From July to September the clearest skies are over Quetta and the nearby districts of Pakistan. Skies begin to clear over India by October and the days become shorter over the northern latitudes, till by November the region with clearest skies lies over Gujarat and the adjacent regions.

Considering the whole year, the region with maximum sunshine is Rajasthan and its adjacent areas, with an average distribution of 8 to 9 hours a day. There is also a small area in Mysore and near-by Andhra Pradesh, where the duration of sunshine exceeds 8 hours.

Except in the extreme north, the duration of bright sunshine is least over the whole sub-continent during the monsoon months of July and August, the sunshine received being less than half the possible value. In the west coast of the peninsula and over Bengal and its adjacent districts, the skies remain overcast for days together. At Bombay, for example, more than 20 days in each monsoon month receive, on an average, less than 3 hours of sunshine per day. In the extreme north, on the other hand, the sunshine is less than half its possible value during the months from December to April, the maximum occurring during October and November, just after the retreat of the monsoon, but before the incidence of the western disturbances. The seasonal variation, namely, the monsoon and the rest of the year, is a general feature over India, except on the east coast of the peninsula, which is influenced by the north-east monsoons and its associated cyclones and depressions occurring in the adjacent seas. Even here, less sunshine is received during the south-west than during the north-east monsoon period.

Mean duration of bright sunshine during each hour

Isopleths of duration of bright sunshine in each hour for the different months for fifteen stations distributed from Kashmir in the north to Trivandrum in the extreme south are shown in figure 2. The distribution of bright sunshine has similar characteristics at all the stations in India except in Kashmir.

* National Aeronautical Laboratory, Bangalore, India.

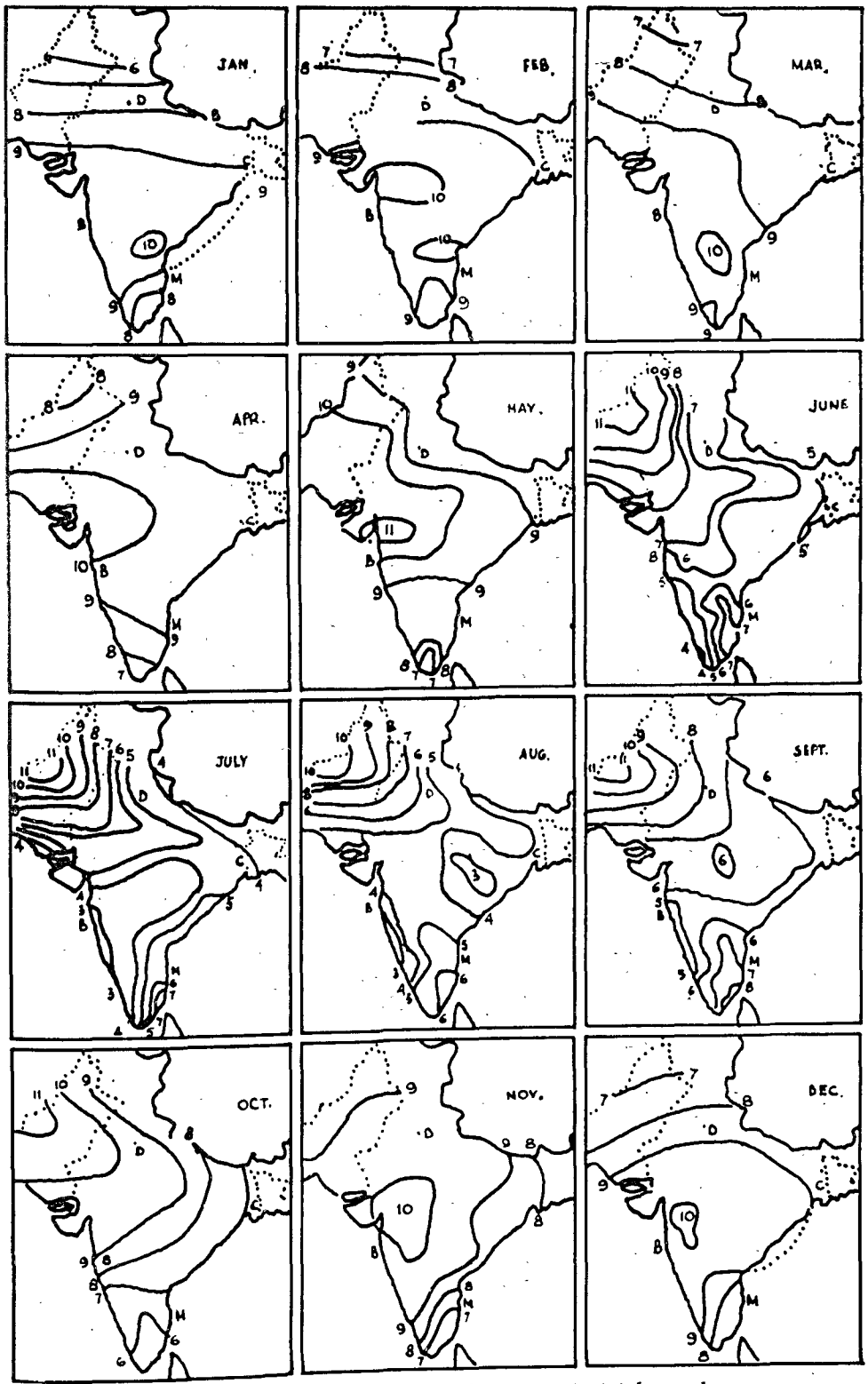


Figure 1. Hours of bright sunshine—average total per day

Frequency distribution of occurrence of bright sunshine of different durations

The important factor in the study of solar energy is the frequency distribution of sunny days during the year, since in addition to large values of hours of bright sunshine, a continuity in the supply is necessary for the proper utilization of solar energy. Table 1 gives the monthly frequencies of occurrence of days with 0.1-3 hrs., 3.1-6 hrs., 6.1-9 hrs. and more than 9 hrs. of bright sunshine for 15 stations in India. It will be seen that sunshine for more than 6 hours

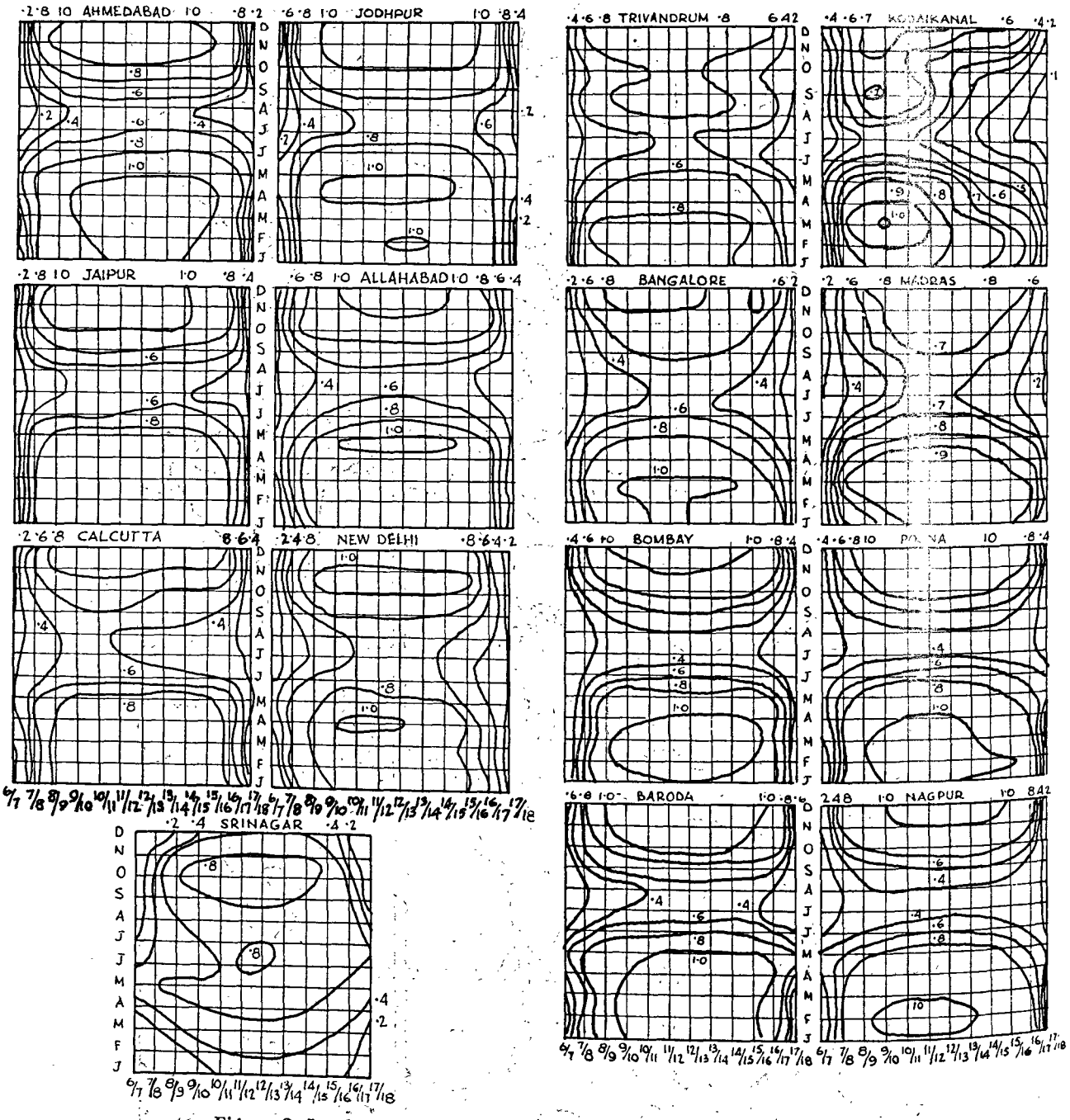


Figure 2. Isopleths of duration of bright sunshine in each hour (lat.)

a day can be expected to occur for more than half the number of days in the months throughout the year only at Jodhpur. During the monsoon, sunshine exceeding 3 hours occurs daily for more than half the month throughout the year at all stations except Kodaikanal, Bangalore, Bombay, Poona and Nagpur.

Figures 3a and 3b show the latitudinal variation of the frequency of occurrence of days with durations of sunshine exceeding 6 hours and less than 3 hours, respectively. For this purpose, the values used are those for Trivandrum, Bombay, Ahmedabad, Jodhpur, Delhi and Srinagar. While the minimum number of days with sunshine exceeding 6 hours occurs at Trivandrum in June, it occurs between July and August in Bombay and in August in higher latitudes. During these months, it is at a maximum at Srinagar. These features are also brought out in figure 3b, which shows the frequency of occurrence of days with duration of sunshine less than 3 hours.

Measurement of the total radiation from sun and sky in India

Measurements of solar radiation have been started regularly at a number of stations in India by the India Meteorological Department since 1957. These

Table 1. Mean monthly frequency of occurrence of bright sunshine of different duration

Station	6.1 to 9 hrs.													Above 9 hrs.											
	J	F	M	A	M	J	Jy	A	S	O	N	D	Year	J	F	M	A	M	J	Jy	A	S	O	N	D	Year
Trivandrum	8	6	9	9	9	7	7	10	10	10	8	7	100	17	18	18	10	10	1	z	5	7	5	10	16	120
Kodaikanal	8	5	10	12	12	7	5	6	8	6	7	7	93	13	17	15	9	8	2	0	2	1	2	6	13	88
Bangalore	12	6	6	10	12	7	5	7	9	10	10	10	104	16	19	23	17	13	5	1	2	4	5	13	15	133
Madras	6	4	3	4	6	9	7	9	10	9	8	9	84	21	23	27	22	18	10	6	6	8	10	13	15	179
Bombay	4	3	13	8	6	7	4	4	11	11	3	4	78	25	24	18	22	23	7	1	1	2	14	25	27	189
Poona	4	2	5	6	5	9	4	4	10	9	6	4	68	25	26	25	22	23	9	1	2	4	15	22	27	201
Baroda	3	2	3	1	1	7	7	7	9	4	1	2	47	28	25	28	28	30	14	4	3	10	26	29	29	254
Nagpur	3	3	5	6	7	7	6	6	8	5	2	3	61	26	25	24	22	23	8	2	2	3	20	26	28	209
Ahmedabad	3	2	6	2	1	6	8	6	10	5	1	3	53	28	25	25	28	30	17	6	3	10	25	29	28	254
Jodhpur	6	4	6	4	3	7	8	9	7	2	2	3	62	23	20	22	25	27	20	13	9	19	29	27	26	260
Jaipur	8	6	7	5	9	7	6	6	7	3	1	4	69	19	20	20	22	19	11	6	5	15	27	28	26	218
Allahabad	8	3	7	5	5	9	7	7	8	4	2	8	73	17	22	21	24	25	12	6	7	12	24	27	22	219
Calcutta	9	7	11	7	8	7	7	7	10	8	6	11	98	19	18	17	20	19	5	3	2	3	11	17	18	152
New Delhi	8	7	13	8	8	7	10	8	10	5	3	11	98	14	17	13	20	17	8	4	9	13	24	26	16	181
Srinagar	3	5	6	7	8	10	9	9	9	9	12	12	99	0	3	3	9	14	10	15	13	16	17	10	0	110

consist of continuous records of the total incoming radiation on a horizontal surface with solarimeters; measurements of total radiation from sun, sky and ground with spherical pyranometers, daily measurements of the direct solar radiation with and without filters and daily measurements of the long wave effective outgoing radiation are also being made. Some observations on the continuous records of the total incoming radiation on a horizontal surface with Moll-Gorczynski solarimeters at a few stations are described below.

Table 2 gives the mean daily total radiation (T) in cal per sq cm for each month during the IGY. (1958) for four stations in India.

Figure 4 gives the isopleths of total radiation T (cal/cm^2/hr.) showing the hourly variation in different months at the above four stations. Figure 4 brings out clearly the chief features in the seasonal and diurnal variation of solar radiation.

Calculation of total radiation Q from values of duration of sunshine S

According to Ångström (2), an approximate estimate of the solar radiation received at the surface of the earth could be obtained from observations of bright sunshine by a relationship between the received solar radiation at the earth's surface and the duration of sunshine. It was expressed in the form

$$Q = Q_o \left[\alpha_1 + (1 - \alpha_2) \frac{S}{S_o}\right]$$

where Q is the radiation actually received, Q_o is the total radiation income on a clear day, S is the number of hours of sunshine measured on a sunshine recorder, and S_o is the maximum possible hours of sunshine; α_1 and α_2 are constants. With an overcast sky, Q/Q_o equals α_1 while with a perfectly clear sky, $Q = Q_o$. It has been pointed by Ångström (3) that

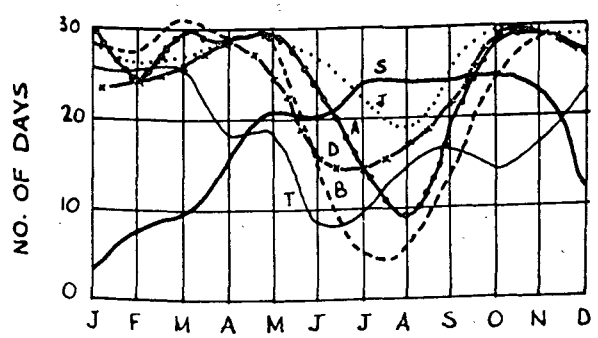


Figure 3 a. Frequency of days with sunshine > 6 hrs

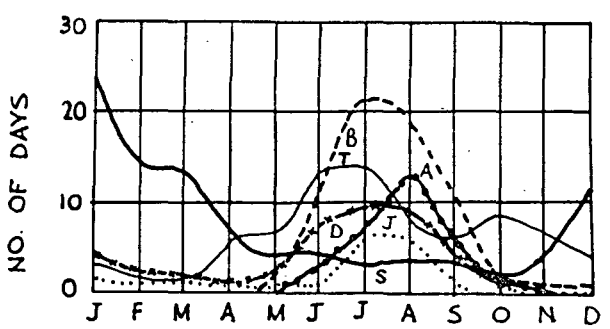


Figure 3 b. Frequency of days with sunshine < 3 hrs

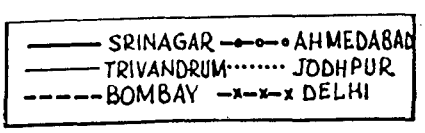


Table 2

	Jan.	*Feb.*	*Mar.*	*Apr.*	*May*	*June*	*July*	*Aug.*	*Sept.*	*Oct.*	*Nov.*	*Dec.*
Madras . . .	472	559	590	591	546	523	423	422	503	369	373	397
Poona. . . .	460	562	598	617	664	588	395	402	496	518	474	417
New Delhi .	350	447	556	606	630	614	245	452	491	501	418	345
Calcutta. . .	339	394	489	506	542	472	454	481	430	396	393	363

α_1 is dependent on the latitude and altitude of the station and on the reflectivity of the ground and the frequency with which higher or low clouds are present when the sky is overcast.

Ångström found α_1 to have a value of 0.25 for Stockholm, and Kimball and Hand (4) obtained a value of 0.22 for Washington. Estimates of the values of α_1 and α_2 using Ångström's formula, obtained from the daily values of the total radiation Q and the duration of sunshine S for the four stations, namely, Poona, Delhi, Calcutta and Madras, on the basis of the IGY data for 1958, are given in table 3. The values estimated by Ramdas and Yegnanarayanan (1) for Q_o and S_o were used; γ represents the correlation coefficient between Q/Q_o and S/S_o.

Table 3

Station	α_1	$1-\alpha_2$	γ
Poona . . .	0.44	0.71	0.93
Delhi	0.38	0.57	0.90
Calcutta . .	0.33	0.48	0.84
Madras . . .	0.37	0.43	0.89

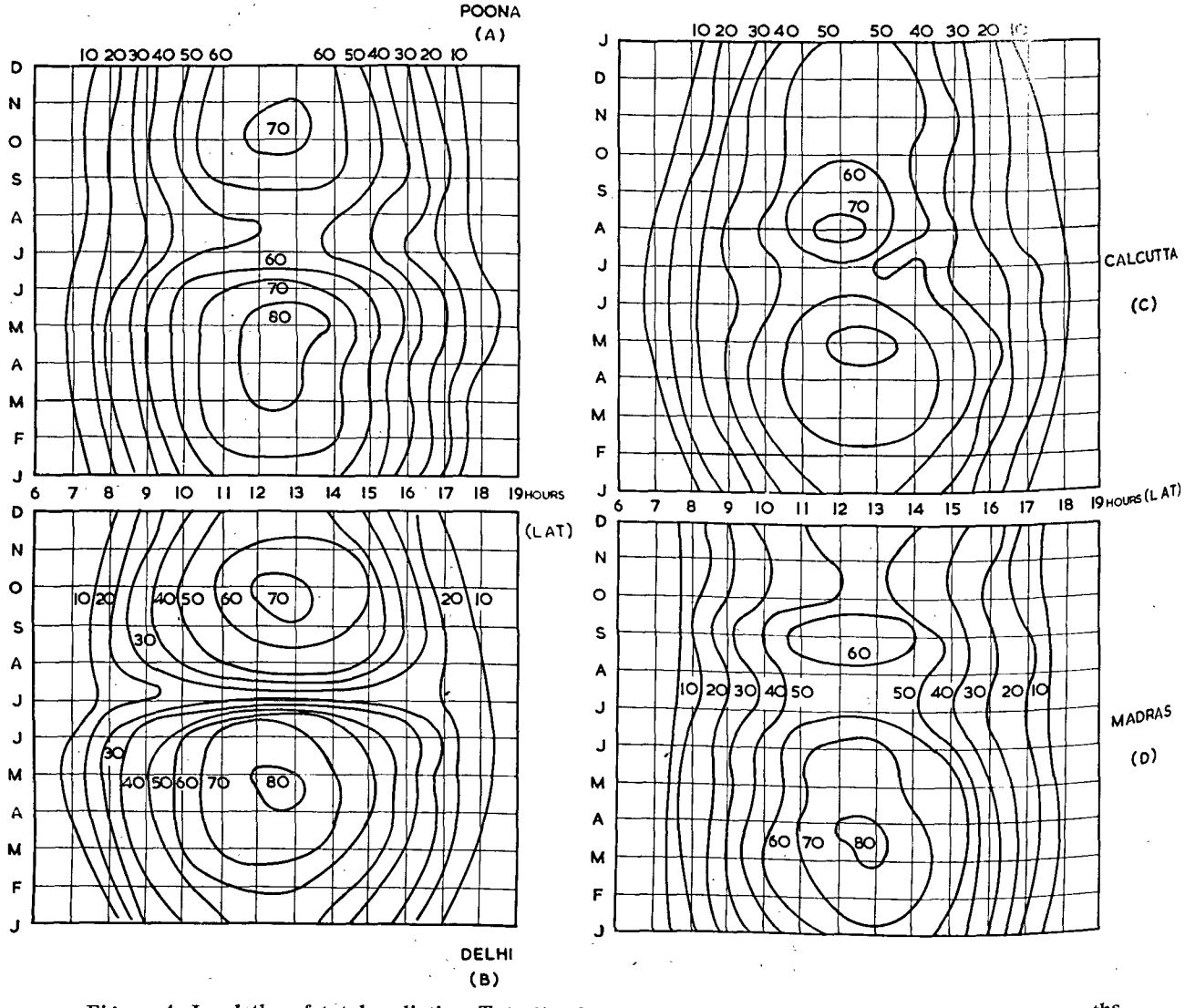


Figure 4. Isopleths of total radiation T (cal/cm²/hour) showing hourly variation in different months

Table 4

	July-September			*Rest of the year*		
	α	$1-\alpha_2$	γ	α_1	$1-\alpha_2$	γ
Poona	0.42	0.61	0.91	0.42	0.52	0.90
Delhi	0.29	0.71	0.95	0.47	0.45	0.85
Calcutta	0.35	0.54	0.88	0.32	0.49	0.86
Madras	0.39	0.49	0.89	0.37	0.49	0.90

Ångström's formula gives only approximate values of Q, the total radiation actually received, for typical average days when cloud cover is nearly normal. In India the variations are very large in the different seasons, during which long spells with skies either perfectly clear, overcast or partly cloudy generally occur. Thus, if using the relation $Q/Q_o = \alpha_1$ on overcast days, one obtains the values of α_1 and the values of α_2 are estimated, the values of Q may be underestimated on partly cloudy days, since the cloud layers on overcast days are much denser than at other times and will give a low figure for the constant α_1. However, the formula can give a fair estimate of the radiation values on clear days, if the values of the constants are known for such days. Estimates of the values of α_1 and α_2 for the four stations for the monsoon months July to September and for the rest of the year have been calculated and are given in table 4.

Ramdas and Yegnanarayanan (1) worked out, on the basis of sunshine data for India, the provisional estimates of the total solar radiation received during the day for different months of the year for a number of stations. For computing the values of q, the amount of radiation from the sun and the sunlit clear sky per sq cm on a horizontal surface per minute at the ground surface, they used isopleths of q computed by Fritz (5) for different values of the precipitable water and air masses corresponding to the different hours of the day at the selected stations for the middle of each of the months of the year. From curves showing the computed diurnal variation of q, the total mean daily radiation Q_o for cloudless skies in different months of the year was estimated by integration. From the data of duration of sunshine, the ratio S/S_o was calculated and they used the formula $Q = 0.35 + 0.61\ S/S_o$ and the computed values of Q_o to obtain Q, the insolation on a horizontal surface for the different months of the year.

Table 5. Sun and sky radiation on a horizontal surface (cal/cm²/day)

	Jan.	*Feb.*	*Mar.*	*Apr.*	*May*	*June*	*July*	*Aug.*	*Sept.*	*Oct.*	*Nov.*	*Dec.*
Poona:												
Computed by Ramdas	488	561	631	620	632	489	378	375	475	474	489	464
Measured during IGY	460	562	598	617	664	589	395	402	496	518	474	447
Delhi:												
Computed by Ramdas	361	441	509	599	610	571	491	486	478	524	442	353
Measured during IGY	350	447	556	606	630	614	245* (485)	452	491	501	413	345
Calcutta:												
Computed by Ramdas	442	506	568	617	682	482	416	441	387	431	445	415
Measured during IGY	339	394	489	506	542	472	454	481	427	396	393	363
Madras:												
Computed by Ramdas	526	610	643	626	581	495	442	467	510	489	489	473
Measured during IGY	472	359	591	595	546	523	423	422	503	369	373	397

* 245 cal/cm²/day were received in July 1958, while 485 cal/cm.²/day were received in July 1957. One may assume that July 1958 was an abnormal month.

The values of Q measured for Poona, Delhi, Calcutta and Madras during 1958 and those obtained by calculation by Ramdas and Yegnanarayanan (1) are given in table 5. It is interesting to note how well the computed values for these four stations agree with the actual observed values of the total radiation from the sun and sky during the IGY.

Acknowledgements

The data used in this paper are those collected by the India Meteorological Department, and the author is grateful to the Department for permission to use them in the present discussion. The author is also grateful to Dr. P. Nilakantan, Director, National Aeronautical Laboratory, for his encouragement in the preparation of this note.

References

1. Ramdas, L. A. and Yegnanarayan, S., Solar energy in India, *Proceedings of the New Delhi Symposium on Wind and Solar Energy*, p. 188, 1956.
2. Ångström, A., *Medd. Stat. Met. Hydr. Anst.* vol. 4, No. 3, 1928.
3. Ångström, A., On the computation of global radiation from records of sunshine, *Arkiv für Geofysik*, vol. 2, No. 22, p. 471, 1956.
4. Kimball, H. H. and Hand, I. V., *Biological effects of radiation*, McGraw Hill, 1936.
5. Fritz, S., *Heating and Ventilating*, vol. 46, p. 69, 1949.

Summary

The paper discusses the hours of bright sunshine over India collected with Campbell-Stokes sunshine recorders. The distribution of the mean daily hours of bright sunshine for each month shows the characteristic large decrease during the monsoon months, June to September, over almost the whole of India; during this period, the average number of hours of bright sunshine is even less than three on many days at some stations. The mean duration of sunshine during each hour in different months is also described for a selected number of stations.

Since the important factor in the study of solar energy is the frequency distribution of bright sunshine of different duration, tables and curves showing the mean monthly frequency of occurrences of bright sunshine of different durations have been given for a representative number of stations.

The paper summarizes also the total radiation from the sun and sky in India measured at a selected number of stations in India during the IGY and shows how these observations agree very well with the values computed by Ramdas and Yegnanarayanan from the values of bright sunshine.

RÉPARTITION DE L'ÉNERGIE SOLAIRE EN INDE

Résumé

Ce mémoire passe en revue les heures, notées au moyen d'un appareil enregistreur de Campbell-Stokes, où l'insolation est brillante sur l'étendue de l'Inde. La répartition du nombre moyen d'heures de soleil brillant par jour et pour chaque mois accuse une réduction caractéristique marquée pendant les mois de mousson, de juin à septembre, sur la presque totalité du pays. Pendant cette période, le nombre moyen des heures d'ensoleillement brillant tombe, au-dessous de trois pendant nombre de jours et à certains postes. La durée moyenne d'insolation pendant chaque heure pour des mois différents est également donnée pour un certain nombre de postes spécialement choisis.

Pour autant que le facteur important, dans toute étude sur l'énergie solaire, est la répartition en fréquence des jours où l'ensoleillement est brillant pour des durées différentes, l'auteur présente des tables et des courbes indiquant la fréquence mensuelle moyenne des manifestations de soleil brillant pendant des durées diverses pour un nombre représentatif de stations.

L'auteur donne également un résumé relatif au rayonnement total fourni en Inde par le soleil et le ciel, mesuré en un certain nombre de postes spécialement choisis, au cours de l'Année géophysique internationale, et il en ressort que ces observations sont en très bon accord avec les valeurs calculées par Ramdas et Yegnanarayanan à partir des valeurs applicables au soleil brillant.

NOCTURNAL HEAT LOSS FROM HORIZONTAL SURFACES IN ARID REGIONS

John Yellott and Panos Kokoropoulos *

Exchange of long wave-length thermal radiation between the earth and the sky has been the subject of several investigations during the past half century, notably by Ångström (1), Brunt (2) and Elsasser (3). Parmelee (4), using a convection-compensated radiometer, measured the long wave-length radiation received during the daytime on vertical and horizontal surfaces at Cleveland, Ohio. He concluded that his results were adequately expressed by an equation developed by Brunt, but with constants determined from his own experimental data.

Yanagimachi (5), in Tokyo, and Bliss (6), in Tucson, Arizona, have successfully used night radiation from bare roof-top flat plate collectors to dissipate heat removed by refrigeration of a residence and a laboratory during summer days.

During the winter of 1960-1961 at the Yellott Solar Energy laboratory in Phoenix (elevation 1 225 feet or 400 meters), measurements were made of nocturnal heat loss from horizontal glass plates to clear desert skies. Analysis of the data showed that a modification of Ångström's procedure led to an equation which is in good agreement with the experimental results. The desert sky apparently radiates as a "gray body", with an emissivity which depends upon its humidity. When the ground level ambient air temperature and vapor pressure are known, the downward radiation from the atmosphere can be calculated. By using conventional methods to evaluate outward radiation and convection exchange between the surface and the atmosphere, the loss or gain of heat can then be calculated for surfaces which face upwards towards the sky.

This paper presents a brief description of the apparatus used in the investigation, and gives typical test results. The experimental data are then correlated by the method suggested by Ångström, and a chart is included by which atmospheric radiation can be determined for night desert conditions.

Experimental apparatus and procedure

The calorimeter used in the present work was an exact duplicate of the apparatus built in 1947 by Parmelee (7) and his colleagues at the Cleveland laboratory of the American Society of Heating and Ventilating Engineers. As shown in figure 1, it consisted of a semi-cylindrical copper heat absorber with a 45-inch (114 cm) square opening. Copper tubing was soldered to the inner surface of the heat absorber, and a dull black paint (emissivity = 0.975 for wavelengths from 3 to 30 μ) was applied. The calorimeter was insulated with glass wool and aluminium foil reflective surfaces. Heat transfer through the insulation was measured by calibrated heat-flow meters.

Nocturnal heat loss from the calorimeter was determined by measuring the temperature drop of water flowing through the tubing at a fixed rate (525 lb or 234 kg per hour). Two 25-junction copper-constantan thermopiles were used for this purpose, while single copper-constantan thermocouples were used to measure the surface temperatures of the calorimeter and the test glasses. The loss of heat by radiation exchange with the sky and the resulting value of the downward atmospheric radiation were calculated from calorimeter heat balances. For this purpose, wind speed and direction, as well as the wet and dry bulb temperatures of the ambient air, were measured in the usual manner.

Both single and double glass samples were used in the test program. All samples were 48 inches

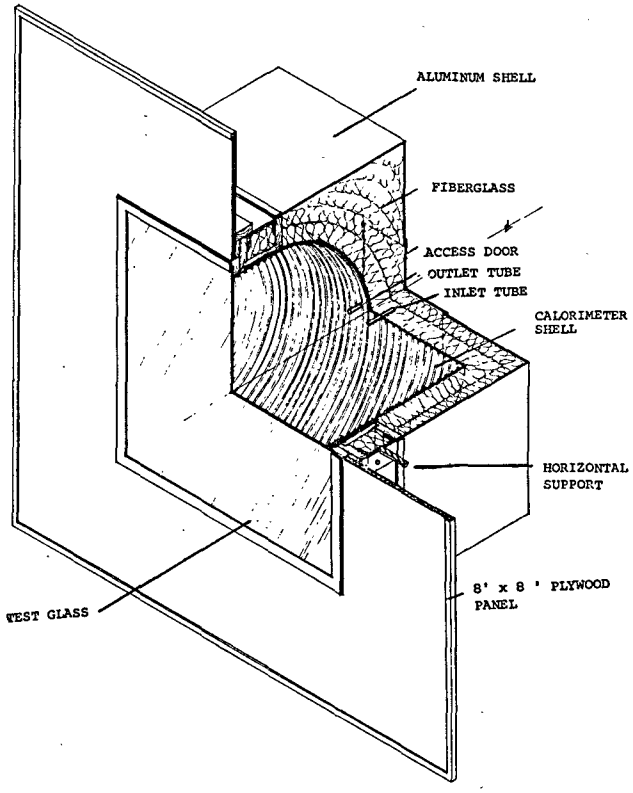


Figure 1. Cut-away isometric of solar calorimeter

* Yellott Solar Energy Laboratory, Phoenix, Arizona.

Table 1. Data and results of test run on 30-31 December 1960

		Observed temperatures and temperature differences								
Time	*AST*	*11*	*12*	*1*	*2*	*3*	*4*	*5*	*6*	*7*
1. Ambient air temperature	t_o	46	42.5	42	41	40.2	38	38	38	37
2. Dew-point temperature	t_{dp}	41	39	38	37	38	37	34	33	33
3. Calorimeter temperature	t_c	71.1	71.3	70.5	69.7	68.7	67.8	67.3	66.8	55.7
4. Indoor glass temperature	t_{gi}	60	59.1	58	57.2	56.4	56	55	54.3	53.9
5. Outdoor glass temperature	t_{go}	47.2	45.5	44.6	43.8	42.8	41.8	41.2	40.5	40.3
6. Calorimeter to indoor glass (3) — (4)	Δt_c	11.7	12.2	12.5	12.5	12.3	11.8	12.3	12.5	11.8
7. Outdoor glass to ambient air (5) — (1)	Δt_o	2	3	2.7	2.8	2.6	3.8	3	2.8	3.5
		Calculated heat flows, Btu/hr/sq ft								
1. Calorimeter to indoor glass by conv. and radiation	q_{RCi}	18.7	19.5	20.1	20.1	19.7	18.8	19.7	20.1	18.8
2. Outdoor glass to ambient air by convection	q_{Co}	4.8	4.8	4.3	4.5	4.2	6.1	3	2.8	3.5
3. Net measured heat loss by radiation = (1) — (2)	q_{Ro}	13.9	15.7	15.8	15.6	15.6	12.7	16.7	17.3	18.3
4. Black-body rad. at outdoor glass temp. = $1\,723 \times T_{go4} \times 10^{-9}$	RF_{go}	114	112	111	111	110	109	109	108	107
5. Calc. atmospheric rad. (4) — $\frac{(3)}{0.892}$	Q_{Rs}	98	95.3	93.3	93.5	92	93.6	90.3	89.6	89.5
6. Atmospheric radiation from chart (figure 7)	q'_{Rs}	98	92.5	91	89	90.5	87.5	84	83	82

Table 2. Data and results of test run on 31 December 1960-1 January 1961

		Observed temperatures and temperature differences								
Time	*AST*	*11*	*12*	*1*	*2*	*3*	*4*	*5*	*6*	*7*
1. Ambient air temperature	t_o	43.5	42	39	38	37	40	36.8	36.8	35.8
2. Dew-point temperature	t_{dp}	34	34	33	31	30	29	28	28	29
3. Calorimeter tempmerature	t_c	68.9	68.3	67.7	67.2	66.8	66	65.2	64.9	69.4
4. Indoor glass temperature	t_{gi}	55.7	55.3	54	53	52.3	52.3	51.2	51.7	50.7
5. Outdoor glass temperature	t_{go}	41	39.5	37	36.4	33.8	36	34	34.8	33.8
6. Calorimeter to indoor glass (3) — (4)	Δtc	13.2	13	13.7	14.2	14.5	13.7	14	13.2	13.7
7. Outdoor glass to ambient air (5) — (1)	Δt_o	— 2.5	— 2.5	— 2	— 1.6	— 3.2	— 4	— 2.8	— 2.0	— 2.0
		Calculated heat flows, Btu/hr/sq ft								
1. Calorimeter to indoor glass by conv. and radiation	q_{Rci}	21.3	21	22.1	22.9	23.4	22.1	22.6	21.3	22.1
2. Outdoor glass to ambient air by convection	q_{co}	— 3.5	—3.3	— 2	— 2.4	— 6	— 8	— 5.6	— 3.2	— 5.0
3. Net measured heat loss by radiation = (1) — (2)	q_{Ro}	24.8	24.3	24.1	25.3	29.4	30.1	28.2	24.5	27.1
4. Black-body rad. at outdoor glass temp. = $1.723 \times Tgo_4 \times 10^{-9}$	RF_{go}	108	107	105	104	102	104	103	103	104
5. Calc. atmospheric rad. (4) — $\frac{3}{0.892}$	q_{Rs}	80.2	79.9	78	75.6	69	70	70.9	75.5	73.6
6. Atmospheric radiation from chart (figure 7)	q'_{Rs}	86	85	82	78	76	76	72.5	72.5	73

(121 cm) square, mounted in wooden frames in such a manner that the outer glass surface was in the same plane as the large wooden panel which surrounded the calorimeter. The calorimeter was supported by an altazimuth mounting, so that is could be turned and tilted to any desired orientation; all tests reported in this paper were run with the glass in the horizontal position, facing upward toward the zenith.

Test data and measured results

The measured quantities consisted primarily of temperatures and temperature differences which were recorded at two-minute intervals on a 24-point potentiometer recorder. Wind speed and cloud cover were determined by direct observation; the results presented below were obtained when the sky above the laboratory was completely clear. Changes of temperature in the glass and the calorimeter were so gradual that there was no appreciable storage of heat in the apparatus.

Results of two of the many tests are presented in tables 1 and 2. These tests were run on a double glass, which consisted of two sheets of 3/16 inch (4.76 mm) thick sodalime plate, separated by a $\frac{1}{4}$ inch (6.35 mm) air space. The glasses were hermetically sealed within a metal frame, so that only the outer surface temperatures could be measured. These tests were run from 11:00 p.m. on 30 December until 7:00 a.m. on 31 December 1960, and during the same hours on 31 December 1960, and 1 January 1961.

The important temperatures are plotted against apparent solar time in figures 2 and 3. On the first night, the outer glass surface temperatures remained slightly higher than the ambient air temperature. During the second night, with considerably lower dew-point temperatures, the glass was consistently colder than the air.

The heat quantities were calculated by the methods outlined in the next section of this paper. The objective of the tests was to find the net loss of heat by radiation from the exposed glass, and then to determine the atmospheric radiation. On the first night, the net loss of heat by outward radiation from the glass ranged from 18.6 to 15.1 Btu/hr/sq ft, while the downward radiation from the sky varied from 95.9 to 90.1 Btu/hr/sq ft. The dew-point temperature range was from 41°F at 11:00 p.m. (solar time) to 33°F at 7:00 a.m. The dry bulb temperature also ranged downward from 48°F to 37°F.

On the second night, 31 December-1 January, the dry bulb temperatures were almost exactly the same as those measured on 30-31 December, ranging from 48°F to 38.5°F. The dew-point temperatures were considerably lower, from 34°F to 28°F. The net loss by radiation was markedly higher, averaging about 27 Btu/hr/sq ft, and the downward radiation from the sky varied from 82.9 at 11:00 p.m., to 71.7 Btu/hr/sq ft at 4:00 a.m. The importance of the dew-point temperature is immediately apparent, since the dry bulb temperatures were essentially the same at comparable hours during both nights.

The results shown in tables 1 and 2 were quite similar to those obtained in a total of twenty tests. Minimum dew-point was 5°F, at a dry bulb temperature of 33°F. Maximum dew-point temperature was 44°F, at a dry bulb temperature of 53°F. Higher dry bulb temperatures were encountered occasionally, but they were accompanied by lower dew-point temperatures.

Study of the test results confirmed the conclusions of earlier workers in this field as to the importance of vapor pressure in determining the magnitude of nocturnal atmospheric radiation. The analysis described in the last section of this paper was carried out to find a generalized relation by which atmospheric radiation could be estimated when the ambient temperature and the dew-point temperature are known.

Calculation of results

The objective of the present test program was to determine the rate at which heat is radiated from the clear night skies. Since this quantity, q_{Rs} (the terminology is explained in annex 1) could not be measured directly, it was calculated by the following analysis.

The heat lost by the water flowing through the calorimeter (corrected for the insulation heat flow) was transferred outward by radiation and convection from the calorimeter shell to the inner glass surface. It was conducted through the glass to the outer surface, where heat exchange took place by radiation to the atmosphere and by forced convection to the ambient air which blew across the glass surface. The following equations express the conditions which must exist when there is no appreciable storage of heat in either glass or calorimeter:

$$q_W - q_I = q_{RCi} = \frac{k}{l}(t_{gi} - t_{go}) = q_{RCo} \qquad [1]$$

$$q_{RCo} = q_{Ro} + q_{Co} = q_{Rgo} - q_{Rs} + q_{Co} \qquad [2]$$

q_{Rs} can be found by using any one of the values for the net heat loss from the calorimeter and substituting it into a revised version of equation [2].

$$q_{Rs} = -[q_{RCi} - q_{Rgo} + q_{Co})] \qquad [3]$$

During many tests, the outer glass surface temperature was below the ambient air temperature, and so the convection heat flow, as found by equation [4], was *negative*, since it was directed *towards* the calorimeter.

$$q_{Co} = f_{Co}(t_{go} - t_o) \qquad [4]$$

The outer surface convection coefficient, f_{Co}, was calculated from the following equation (8), which is believed to be reliable for wind speeds up to 25 miles per hour (42 km per hour):

$$f_{Co} = 1.0 + 0.31 \times v_o \times (530/T_o) \qquad [5]$$

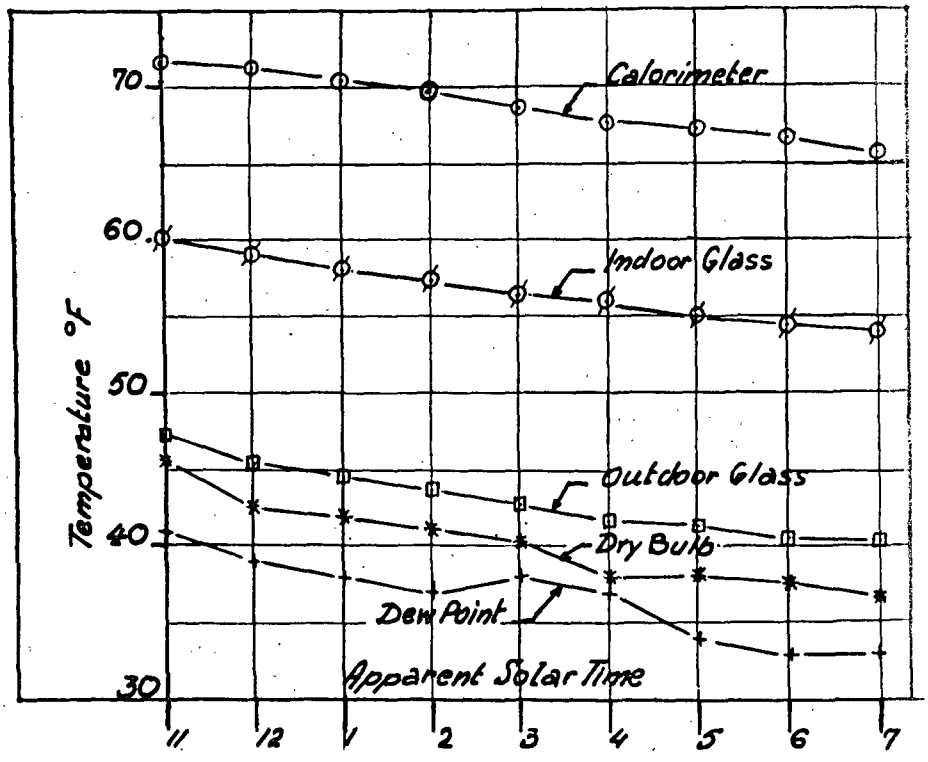


Figure 2. Test data, 30 and 31 December 1960

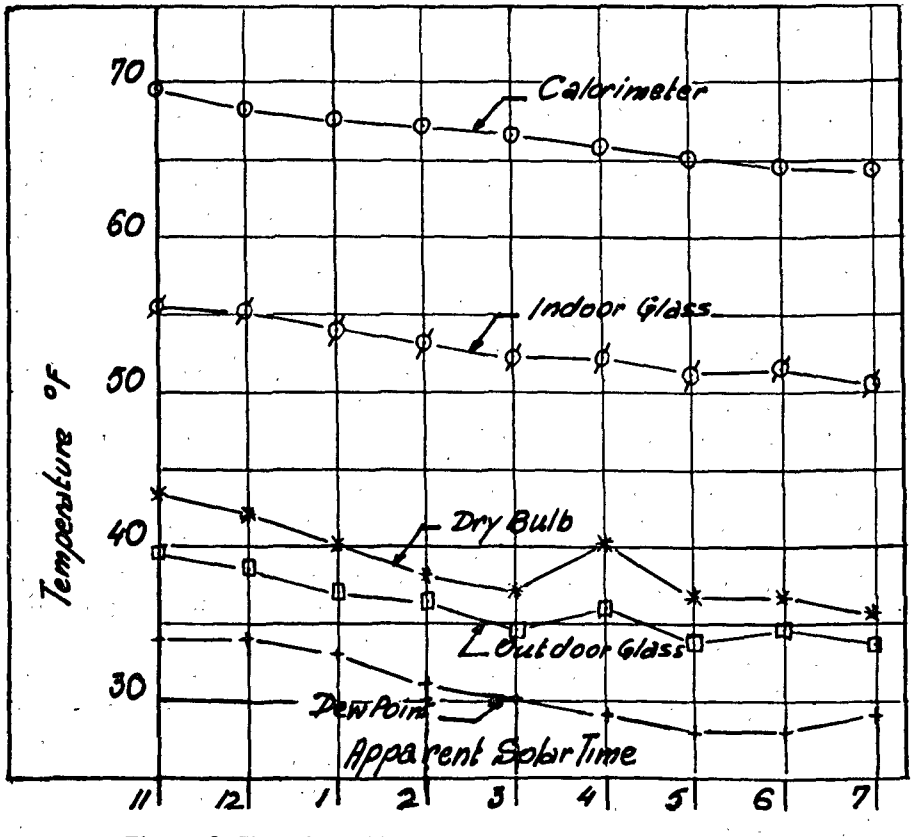


Figure 3. Test data, 31 December 1960 and 1 January 1961

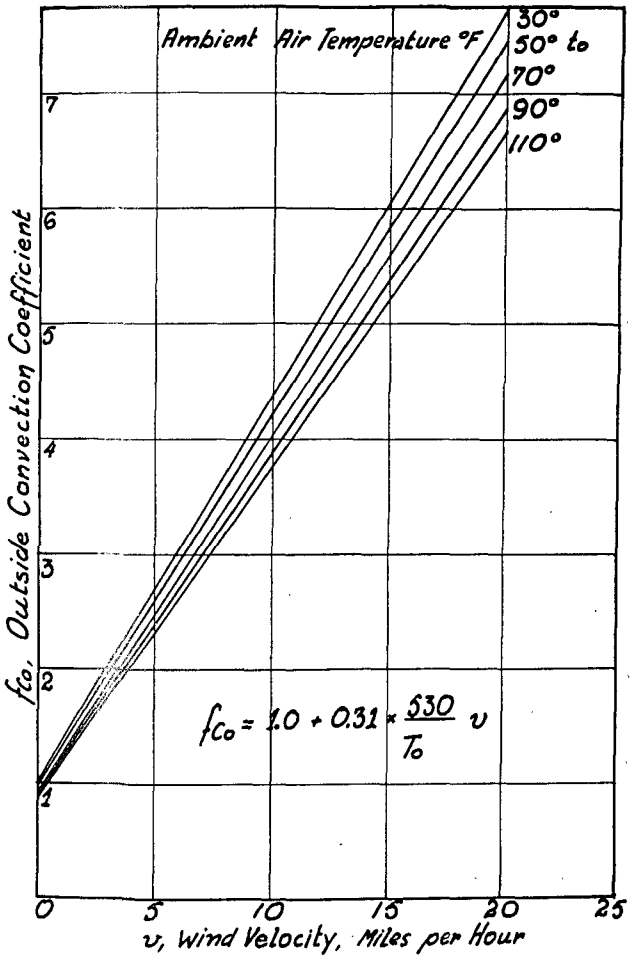


Figure 4. Outside convection coefficient *vs.* wind velocity

Wind direction can be neglected, since all tests reported here were run with the glass in the horizontal position.

Outgoing radiation from the glass is calculated by the usual Stefan-Boltzmann equation:

$$q_{Ro} = e_g \times 1.723 \times 10^{-9} \times T_{go}^4 \qquad [6]$$

The average emissivity of soda lime glass, e_g, at wave-lengths from 3 to 30 microns, is approximately 0.89. The net loss of heat by radiation exchange is:

$$q_{Ro} = e_g (1.723 \times 10^{-9} T_{go}^4 - q_{Rs}) \qquad [7]$$

Analysis of results

The purpose of the analysis was to find a consistent relationship between atmospheric radiation, q_{Rs}, ground level ambient temperature, t_o, and vapor pressure, P_v. The first attempts were made with the following equation, proposed by Brunt (2) as a result of this study of data obtained by Dines (9) in England:

$$q_{Rs}/(T_o^4) = a + b\sqrt{p_v} \qquad [8]$$

The constants a and b have been evaluated by experimenters in various parts of the world. As summarized by Elsasser (3), the average values were 0.50 for a and 0.34 for b; Parmelee (4), used $a = 0.55$ and $b = 0.33$, but this equation did not give consistent correlation for the present work.

Trials were then made with Ångström's equations, developed from data taken *at night* in Algeria and California in 1912 and 1913. The first of these is:

$$q_{Rs} = A\, T_s^4 (B - e^{-Cp_v}) \qquad [9]$$

where T_s is a mean atmospheric temperature.

The second Ångström equation relates the atmospheric radiation at a given dew-point to the ambient air temperature:

$$q_{Rs} = D(p_v) \times T_o^4 \qquad [10]$$

$D(p_v)$ is a function of the vapor pressure of the atmosphere at ground level. For dew-points from 5°F to 35°F, as shown in figure 5, this function was found to be approximately linear.

Ångström's procedure resulted from the fact that his first series of tests (1912) at Bassour, Algeria, extended over a three-month period, during which the ambient air temperatures varied only from 59°F to 80°F, while vapor pressure varied from 0.15 inches (3.8 mm) to 0.42 inches (13.29 mm), corresponding to a dew-point temperature range of 25°F to 55°F. The elevation at Bassour is 3 800 feet (1 160 m).

During his California tests (1913), the humidity varied only from 0.236 in (6 mm) Hg, dew-point 38°F, to 0.35 in (9 mm) Hg, dew-point 54°F, but his temperatures varied from 82°F at Indio (sea level) to 27°F at Mt. Whitney (14 400 feet, 4 420 m).

Ångström's study of his California data led him to conclude that, at *constant humidity*, the atmospheric radiation varied as the *fourth* power of the ambient absolute temperature:

$$(q_{Rs})_1/(q_{Rs})_2 = (T_o)_1/(T_o)_2^4 \qquad [11]$$

In order to evaluate the vapor pressure factor, $D(p_v)$ in equation [10], Ångström reduced his California test data to a common ambient temperature, 68°F. Since this procedure led Ångström to a satisfactory correlation of his results obtained at night under desert skies, it was tried with the data from the present investigation.

Values of atmospheric radiation (q_{Rs}), calculated from observed calorimeter heat loss data, were tabulated for a number of night-long tests under cloudless skies, during which the dew-point temperatures were substantially constant. These data for varying dry bulb temperatures were then reduced by equation [11] to a common value of $t_o = 75$°F. Table 3 gives values of the atmospheric radiation, and the factor $D(p_v)$ for four values of vapor pressure. Within the range of vapor pressure covered during these tests, $D(p_v)$ is essentially linear, as shown by figure 5. The equation for this line is:

$$D(p_v) = (0.674 + 3.33\, p_v) \times 10^{-9} \qquad [12]$$

Consideration of Ångström's equations [9, 10, 11] in the light of the data obtained during the present

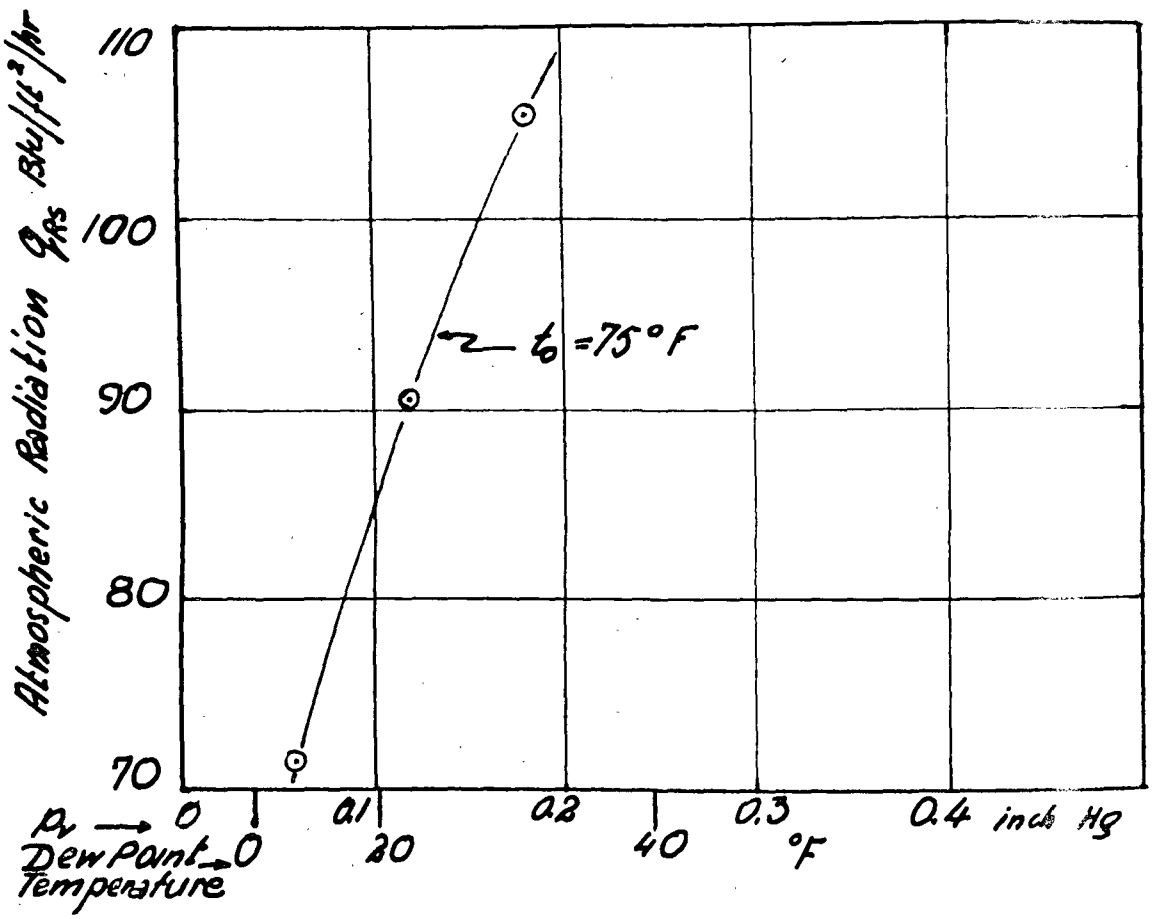


Figure 5. Factor D (p_v) *vs.* water vapor pressure, P_v

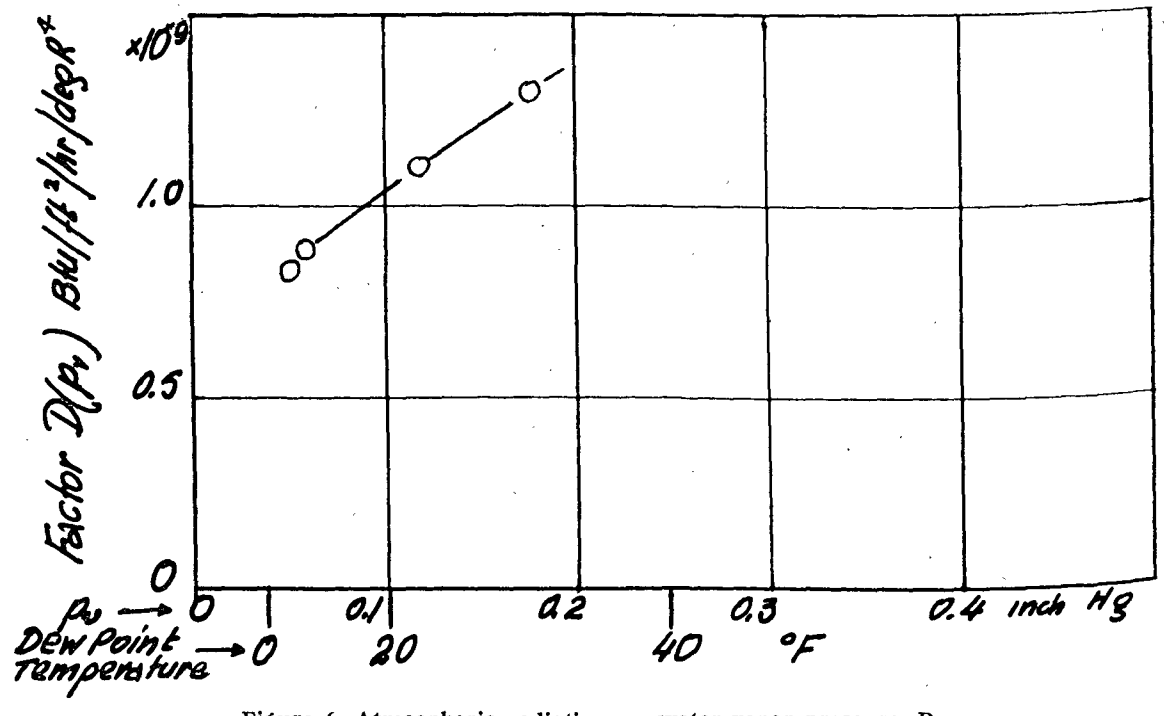


Figure 6. Atmospheric radiation *vs.* water vapor pressure, P_v

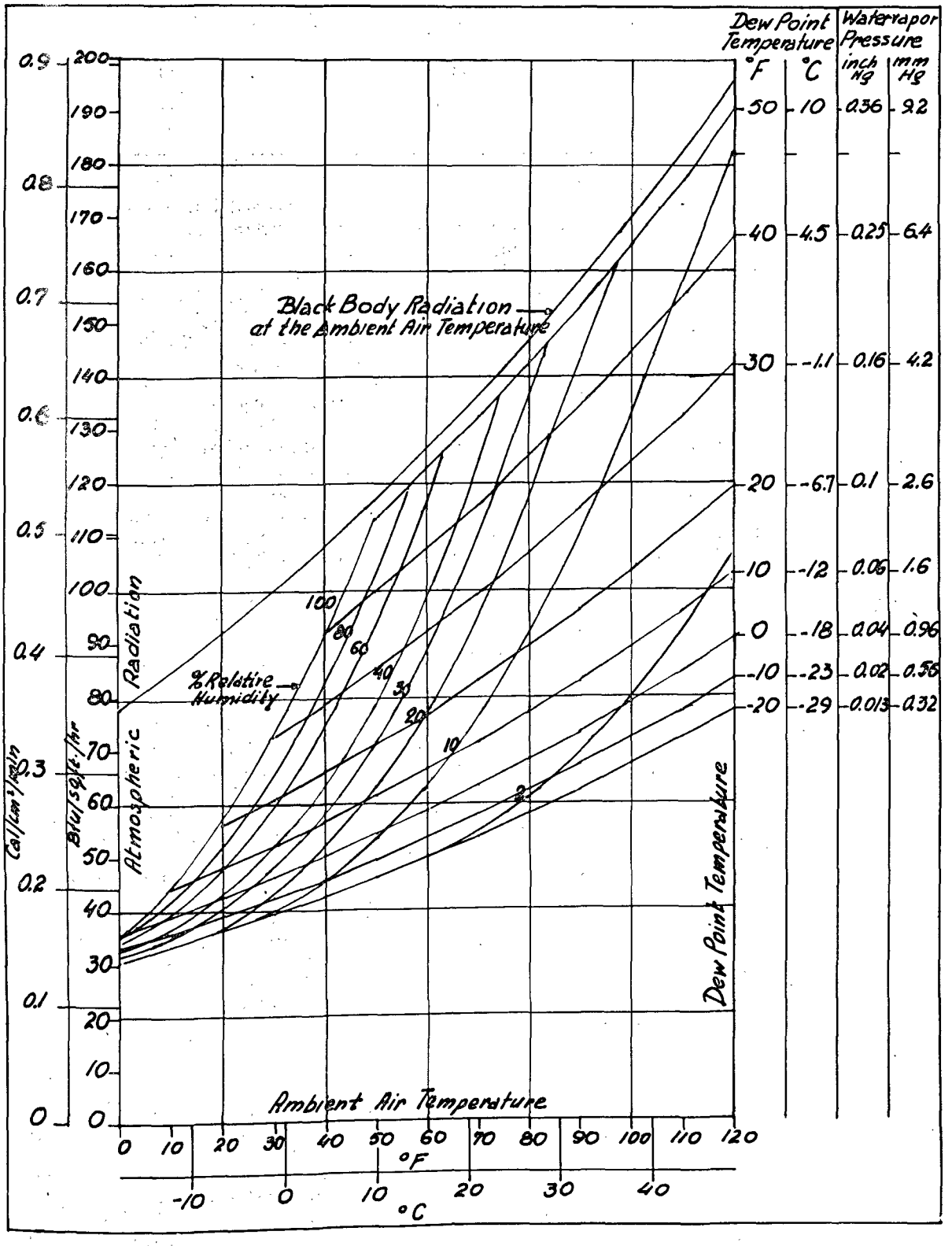

Dew Point Temperature
Water vapor Pressure
°F
°C
inch Hg
mm Hg
50 10 0.36 9.2
40 4.5 0.25 6.4
30 -1.1 0.16 4.2
20 -6.7 0.1 2.6
10 -12 0.06 1.6
0 -18 0.04 0.96
-10 -23 0.02 0.56
-20 -29 0.013 0.32
Black Body Radiation at the Ambient Air Temperature
% Relative Humidity
100
80
60
40
30
20
10
2
Atmospheric Radiation
Cal/cm²/min
Btu/sq ft./hr
Dew Point Temperature
Ambient Air Temperature
0 10 20 30 40 50 60 70 80 90 100 110 120
°F
-10 0 10 20 30 40
°C

Figure 7

Table 3. Values of factor $D\ (p_v)$ and q_{Rs} for night tests at a dry bulb temperature of 75°F

Test date	Water vapour pressure	Dew-point temp. °F	q_{Rs} Btu/ft²/hr	$D\ (p_v) \times 10^{-9}$
12/20-21 1960 . . .	0.048	5-7	69	0.84
12/20-21 1960 . . .	0.06	10	73	0.89
12/22-23 1960 . . .	0.12	23	91	1.11
2/8/1961	0.174	31	106	1.3

work led, by dimensional reasoning, to the conclusion that the mean atmospheric temperature, T_s, proposed by Ångström could be replaced by the existing ambient air temperature, T_o, multiplied by a new constant, A', which has the dimensions of the Stefan-Boltzman constant. Thus:

$$q_{Rs} = A' T_o^4 (B - e^{-Cp_v}) \qquad [13]$$

Thus, by combining equations [10] and [13],

$$D(p_v) = A' (B - e^{-Cp_v}) \qquad [14]$$

which is approximately linear for the limited range of vapor pressures considered here.

To evaluate the constants A', B, and C in equation [14], the data from three of the tests listed in table 3 were inserted into the equation and the following solutions were found:

$$A' = 1.515 \times 10^{-9}$$
$$B = 1.41$$
$$C = 3.33$$

Inserting these values, we obtain:

$$q_{Rs} = 1.515 \times 10^{-9} (1.41 - e^{-3.33 p_v}) \times T_o^4 \qquad [15]$$

A graphical version of equation [15] is presented in figure 7. From this chart, when the ambient air temperature and the relative humidity are known, the atmospheric radiation, q_{Rs}, can be found in both the English and cgs units. From the comparisons given in tables 1 and 2, it is seen that the experimental data agree with the calculated values to within ± 4 per cent.

References

1. Ångström, A., *A Study of the Radiation of the Atmosphere*, Smithsonian Miscl. Collection, vol. 65, No. 3 (Washington, 1915).
2. Brunt, D., Radiation in the Atmosphere, *Quarterly Journal, Royal Met. Soc., Canadian Branch*, vol. 66 (Toronto, 1940).
3. Elsasser, W. M., *Heat Transfer by Infrared Radiation in the Atmosphere*, Harvard Met. Studies No. 6 (Cambridge, Mass., 1942).
4. Parmelee, G. V., Radiant Energy Emission of Atmosphere and Ground, *Trans. Am. Soc. Heat. Vent. Eng.*, vol. 58, p. 85, 1952.
5. Yanagimachi, M., Nocturnal Radiation Cooling in a Year-Round Air-Conditioning System, *Trans. Conf. on Use of Solar Energy*, vol. III, Part II, p. 32 (Tucson, 1958).
6. Bliss, R. W., Solar Energy Research Facility for the Southwest, *Sun at Work*, vol. III, No. 2, p. 8 (June 1957).
7. Parmelee, G. V., Measurements of Solar Heat Transmission through Flat Glass, *Trans. ASHVE*, vol. 54, p. 45 (Cleveland, 1948).
8. McAdams, *Heat Transmission*; 2nd ed. (McGraw-Hill, New York, 1942), p. 207.
9. Dines, W. H., Monthly Mean Values of Radiation from Various Parts of the Sky, *Mem. Roy. Met. Soc.*, vol. 2, No. 11, 1927.

Annex I

Terminology and units

Heat flow rates, symbolized by "q" with appropriate subscripts, are expressed in British thermal units (Btu) per hour per square foot of radiating surface. Heat flow is considered *positive*, when it is directed *away from* the calorimeter, *negative* when it is directed *towards* it.

q_{Rs} = heat radiated downward from the atmosphere
$q_{W'}$ q_I = heat lost by water and through calorimeter insulation
q_{RCi}, q_{RCo} = heat transfer by radiation and convection at glass inner and outer surfaces
kg = thermal conductivity of glass, Btu/hr/sq ft/(°F/inch)
l = thickness of glass, inches
t_cT_c = effective temperature within the calorimeter, °F, °R
q_{Co} = heat transfer by convection alone between outer surface and ambient air
q_{Rgo} = heat radiated outward from glass
q_{Ro} = net heat loss by radiation from outer glass surface
p_v = vapor pressure, inches of mercury
α = Stefan-Boltzman constant, 1.723×10^{-9}, Btu/hr/sq ft/°F⁴

e_g = emissivity of glass surface
t_{go}, T_{go} = temperature of outer glass surface, degrees Fahrenheit and degrees Rankine
t_{gi}, T_{gi} = temperature of inner glass surface, °F and °R
t_o, T_o = temperature of ambient air, °F and °R
f_{Co} = outer surface convection coefficient, Btu/hr/sq ft/°F
v_o = wind speed, miles per hour
A, B, C = constants in the Ångström equation [11]
a, b = constants in Brunt's equation [10]
$D(p_v)$ = factor in Ångström's equation [12] dependent upon vapor pressure
1, 2 = subscripts used in equation [13] to denote data determined during different tests

Summary

Loss of heat by radiation to the night sky has, in the past, been of primary interest to meteorologists concerned with the earth's solar energy balance. The investigations of Brunt and Elsasser in this field are well known, but the earlier experimental work of Ångström, carried out in desert regions during 1912 and 1913, has received less attention.

Recently, night sky radiation has taken on new significance in air-conditioning technology, and particularly in the dissipation of heat removed by refrigeration of buildings. Yanagimachi and Bliss have successfully used bare metallic roof surfaces, both as solar energy collectors during the winter days and as heat radiators during summer nights.

The present paper deals with measurements of nocturnal heat loss to desert skies by radiation from large horizontal glass surfaces. The test glasses were in a calorimeter which is a duplicate of the apparatus originally used by Parmelee at the ASHVE laboratory in Cleveland. By the use of heat balances, the downwards radiation from the atmosphere was calculated, and found to be very strongly influenced by the dew-point temperature of the ambient air.

Results of two eight-hour tests are given in detail, since they were run on consecutive nights when the dry bulb temperatures were virtually identical but the dew-point temperatures were quite different. During the first night, with high dew-point, the glass surface temperature was warmer than the air. During the second night, the loss of heat by radiation to the relatively dry atmosphere was so great that the glass was colder than the ambient air.

In the analysis of twenty similar tests, using both single and double glass, it was found that the procedure originally proposed by Ångström gave a much better correlation of the data than the more familiar equation of Brunt. As a result of his measurements at Bassour, Algeria, and Indio, California, Ångström concluded that, at constant humidity, the downward radiation at night from desert atmosphere varied as to the fourth power of the ambient temperature at ground level. For varying humidity, Ångström proposed the following equation:

$$q_{Rs} = A\,T_s^4\,(B - e^{-Cp_v}) \times 10^{-9}$$

where

q_{Rs} = atmospheric radiation, Btu/hr/sq ft
T_s = mean sky temperature
A, B, C = experimentally determined constants
p_v = vapor pressure at ground level, inches Hg.

In converting the data from the present work by means of Ångström's analysis, his two suggestions were combined into:

$$q_{Rs} = D\,(p_v) \times T_o^4 \times 10^{-9}$$

Where $D(p_v)$ is a function of the vapor pressure of the form:

$$D\,(p_v) = A'\,(B - e^{-Cp_v})$$

The constants were evaluated by solving simultaneous equations in which data were inserted from tests run with widely differing vapor pressures. The resulting equation is:

$$q_{Rs} = 1.515 \times T_o^4\,(1.41 - e^{-3.33\,p_v}) \times 10^{-9}$$

The experimentally determined values of the atmospheric radiation agreed within ± 4 per cent with values calculated by this equation.

The net loss of heat at night from any surface which is exposed to the desert sky can be determined by calculating the convection transfer in the usual manner and adding the radiation exchange which can be found from:

$$q_{Ro} = e_g \times (1.723 \times T_g^4 \times 10^{-9} - q_{Rs})$$

where q_{Ro} = net radiation exchange, surface to atmosphere Btu/hr/sq. ft.
e_g = emissivity of glass or other surface
T_g = temperature of glass or other surface, °R.

PERTES NOCTURNES DE CHALEUR DES SURFACES HORIZONTALES DANS LES RÉGIONS ARIDES

Résumé

Jusqu'à une époque très récente, les pertes de chaleur par rayonnement vers le ciel nocturne intéressaient surtout les météorologistes qui travaillaient à l'établissement de bilans d'énergie solaire pour l'ensemble du globe. Les travaux de Brunt et Elasser dans ce domaine sont bien connus, mais les travaux expérimentaux préliminaires de Ångström, exécutés dans des régions désertiques au cours de 1912 et 1913, ont reçu moins d'attention.

Tout récemment, le rayonnement vers le ciel nocturne a pris une nouvelle importance pour la technologie de la climatisation, en particulier en ce

qui concerne la dissipation de la chaleur évacuée des bâtiments par leur réfrigération. Yanagimachi et Bliss ont fait usage, avec succès, de toitures en métal nu, tant comme collecteurs d'énergie solaire pendant les jours d'hiver que comme radiateurs de chaleur pendant les nuits d'été.

Le présent mémoire discute les mesures des pertes nocturnes de chaleur par rayonnement vers les cieux du désert pour les grandes surfaces horizontales en verre. Les verres essayés se trouvaient dans un calorimètre reproduisant l'appareil utilisé à l'origine par Parmelee au laboratoire de l'ASHVE, à Cleveland. On a calculé le rayonnement de l'atmosphère vers le bas, en ayant recours aux bilans thermiques, et on a pu noter que ce rayonnement subit fortement l'influence de la température du point de rosée de l'air ambiant.

Les auteurs donnent dans le détail le résultat de deux essais de huit heures, exécutés pendant deux nuits consécutives, les températures mesurées au thermomètre à boule sèche étant presque identiques, tandis que celles du point de rosée étaient très différentes. Au cours de la première nuit, le point de rosée étant élevé, la température de la surface de verre était supérieure à celle de l'air. Pendant la deuxième nuit, les pertes de chaleur par rayonnement vers une atmosphère relativement sèche étaient si fortes que le verre était plus froid que l'air ambiant.

Dans l'analyse de vingt essais analogues, en faisant usage de verres simples et doubles, on a trouvé que la technique proposée à l'origine par Ångström permettait une bien meilleure corrélation des données que l'équation plus commune de Brunt. En conséquence des mesures qu'il avait faites à Bassour, Algérie, et Indio, Californie, Ångström avait conclu que, pour un état hygrométrique constant, le rayonnement nocturne vers le bas, en provenance de l'atmosphère d'un désert, variait comme la quatrième puissance de la température ambiante au niveau du sol. Pour un état hygrométrique variable, Ångström a proposé l'équation suivante :

$$q_{Rs} = A\,T_s^4\,(B - e^{-Cp_v}) \times 10^{-9}$$

dans laquelle q_{Rs} = radiation atmosphérique, ne BTU/h/pied carré
T_s = température moyenne du ciel
A, B, C = constantes déterminées par expérience
P_v = tension de vapeur au niveau du sol, en pouces de mercure.

En transformant les données du présent mémoire par l'analyse d'Ångström, on a pu associer ses deux suggestions dans l'équation suivante :

$$q_{Rs} = D\,(p_v) \times T_o^4 \times 10^{-9}$$

dans laquelle $D(p_v)$ est une fonction de la pression ou tension de vapeur de la forme :

$$D\,(p_v) = A'\,(B - e^{-Cp_v})$$

On a évalué les constantes par la résolution d'équations simultanées dans lesquelles des données numériques furent introduites à partir des essais effectués à des tensions de vapeur très différentes. On obtient ainsi l'équation suivante :

$$q_{Rs} = 1{,}515 \times T_o^4\,(1{,}41 - e^{-3{,}37p_v}) \times 10^{-9}$$

Les valeurs du rayonnement atmosphérique déterminées expérimentalement étaient en accord, à $\pm$ 4 p. 100 près, avec les valeurs calculées au moyen de cette équation.

La perte nette de chaleur d'une surface quelconque exposée au ciel du désert pendant la nuit peut être déterminée en calculant la transmission par convection de la manière habituelle et en ajoutant les échanges de rayonnement que donne l'équation :

$$q_{Ro} = e_g \times (1.723 \times T_g^4 \times 10^{-9} - q_{Rs})$$

dans laquelle q_{Ro} = échange net de rayonnement, de la surface vers l'atmosphère, en Btu/h/pied carré.

e_g = émissivité du verre ou d'une autre surface
T_g = température du verre ou d'une autre surface, en degrés R.

Agenda item III.B

NEW MATERIALS IN SOLAR ENERGY UTILIZATION

Point III.B de l'ordre du jour

MATIÈRES NOUVELLES EMPLOYÉES DANS L'UTILISATION DE L'ÉNERGIE SOLAIRE

Chairman — Président

Ibrahim Helmi ABDEL-RAHMAN

Rapporteur

John A. DUFFIE

NEW MATERIALS IN SOLAR ENERGY UTILIZATION

John A. Duffie

This conference deals with the application of energy resources to solve practical problems. In order for these applications to be made, materials must be available that have, in so far as possible, desirable properties and are of reasonable cost. The technology of materials is developing rapidly, and the more basic research on the properties of materials and on solar energy processes improves our understanding of these properties and the uses that can be made of them. It is appropriate to consider new materials as a significant subject area of the Conference.

The designer of solar equipment is limited by and dependent on the materials at his disposal. The development of new materials with desirable sets of properties may reduce limitations and open new possibilities of solar energy applications. Consider, for example, the limitations which have existed on the use of flat-plate solar heat exchangers (collectors). The materials available in the past have limited the usefulness of these exchangers to operation at temperatures no more than 50-75°C above ambient air temperatures. With new materials for covers and for solar energy absorbing surfaces, the temperature range of practical operation is being pushed upward, and the new application of solar energy to such purposes as solar power generation and absorption air-conditioning becomes more promising.

Many aspects of materials and their properties are important in that they substantially affect both the performance of a solar energy device and its cost. An ultimate consideration is the cost of energy or product delivered by the solar device; thus, both performance (output per unit area of solar heat exchanger) and cost (per unit area) must be considered, and thus also the material properties affecting them. There are suggested at least three approaches to materials problems : first, the improvement of performance or raising of temperature limitations by use of materials with superior radiation properties, obtained possibly at additional cost; second, the reduction of cost through the use of very durable materials, or very inexpensive materials which may in fact have a shorter expected useful life; third, the development of unique methods of application of materials of older or more conventional types, to improve the performance of solar devices or decrease their costs. All three of these approaches are well represented in the ten contributions to this agenda item.

* Director, Solar Energy Laboratory, University of Wisconsin, Madison, Wisconsin.

In the following sections, the primary concern will be with new materials as applied to solar heat exchangers. These exchangers are usually items of major cost in solar energy applications, and impose limitations on the other parts of a process. (Materials for other parts of the process, for example, the air-conditioner in a solar cooling application, may be more or less conventional, and some attention is given to them in the appropriate sessions.) Consideration here is given to the effects of materials and their properties on exchanger performance and cost. A statement of the energy balances describing the performance of solar exchangers is presented to aid in understanding the effects of materials' properties on performance. The relationship of cost to performance is noted. In the following sections, desirable goals in materials' properties are noted, and radiation properties of absorbers, transmitters, reflectors and refractors are reviewed. Other means of controlling energy losses through use of unique configurations and fabrication techniques are noted. As is inevitable, the selection of materials for a given application is based on compromises, and the subject of optimum combinations of properties is briefly treated.

The ten papers on this agenda item constitute a substantial review of these many facets of the subject of materials for solar energy applications. They cover a spectrum of topics and describe developments of widely varying nature, all of which are contributing or can contribute to the successful, economical application of solar energy for terrestrial applications. They contain a substantial body of useful data and interpretation thereof which cannot be included in this brief review, and those interested in assessing the utility of solar energy in meeting an energy need are of necessity referred to the complete papers for details.

Materials' properties and their significance—performance

The properties of materials that make them of interest in solar energy applications include radiation properties, i.e., how they absorb, emit, transmit or reflect radiation of various wave-lengths, and physical properties, which determine weight and thickness requirements and resistance to mechanical failures of various types. In solar energy exchanger design, the former properties substantially determine performance, and thus area requirements for a given output; first consideration is thus given to the radiation properties, with subsequent consideration of the physical properties. To aid in understand-

ing the importance of the radiation properties, the energy balance equation which describes the performance of a solar exchanger is briefly reviewed.

A solar exchanger is a unique type of heat exchanger in that energy is transferred from a remote source of radiation to (usually) a fluid in the exchanger. The temperature of the source of radiation (effectively about 6 000°K) is such that the radiation on the exchanger is substantially all in the wave-length range of 0.4μ to 2.5μ, while the radiation emitted by the exchanger (at a temperature no more than a few hundred degrees above ambient) is substantially all of wave-length greater than 2.5μ. Thus there exists a significant difference between the incoming solar radiation and the outgoing long-wave radiation.

The distance of the sun from the earth, and its size, dictate that the flux of energy on the solar exchanger (i.e., the energy per unit time per unit area) is low relative to the fluxes encountered in more conventional exchangers, and at best is about 1.6 cal/cm² min (350 Btu/hr ft²). Flat-plate exchangers use this low flux without concentration; focusing exchangers use optical systems to increase this flux at the energy absorbing surface to levels permitting operation at higher temperatures.

The energy balance

The performance of the solar exchanger is described by an energy balance, which can be written in the following general form:

$$HA_a r \gamma \tau \alpha = [q_u + \Sigma q_{th} + \Sigma q_{hc}] A_x \qquad (1)$$

where H = incident solar radiation on the plane of the exchanger, per unit area;

A_a = effective radiation-intercepting area of the exchanger;

r = specular reflectivity of any reflector between the sun and the energy-absorbing surface, for focusing systems;

γ = an intercept factor, for focusing systems; the fraction of specularly reflected radiation which is intercepted by the energy-absorbing surface;

τ = transmissivity of any optical system covering the energy-absorbing surface for solar radiation;

α = the absorptivity of the energy-absorbing surface for solar radiation (Note: α is the same as a in paper S/42);

A_x = the area of the energy-absorbing surface ($A_x = A_a$ for a flat-plate exchanger);

q_u = useful energy gain from the solar exchanger, per unit area of energy-absorbing surface;

q_{th} = sum of the thermal energy losses from the energy absorbing surface, by conduction, convection and radiation, per unit area of energy absorbing surface (See discussion below);

q_{hc} = sum of heat capacity effects, if the exchanger is not operating at steady temperature, per unit area of energy-absorbing surface.

The left side of the equation represents the amount of energy absorbed by the exchanger, while the right side shows the distribution of this absorbed energy into useful gain and various types of losses. The objective of solar exchanger design is to obtain good performance (with due consideration given to costs) by use of materials with properties which will maximize the absorbed energy and minimize the losses, thus resulting in high useful gain.

Absorbed radiation

Maximizing the absorbed energy is accomplished by maintaining high values of all of the factors in the product $Hr\gamma\tau\alpha$. Radiation is determined by factors external to the exchanger, except that an optimum orientation of the exchanger should be used for the time and purpose of energy collection. The two factors r and γ are included in the product only for focusing systems; r is a property of the material used as the reflecting surface, and γ, the intercept factor, is a function of the shape and position of the reflector (or refractor) and energy-absorbing surface, and thus of the physical properties of the materials and structures supporting and shaping the reflecting surface. Transmissivity, τ, is a function of the refractive index of the cover materials, thickness, and the angle of incidence of the solar radiation; increasing the numbers of transparent covers over an energy-absorbing surface decreases τ. Absorptivity, α, should be as high as possible and is a function of the nature of the absorbing surfaces and angle of incidence of solar radiation; many methods for providing surfaces of high α are available.

Thermal losses

The thermal loss term, q_{th}, is made up principally of radiation and convection losses in the outward direction, i.e., to the atmosphere and sky which the energy-absorbing surface faces. The losses, from an uncovered exchanger, can be written as the sum of radiation and convection as follows:

$$q_{th} = \sigma\varepsilon (T_b^4 - T_a^4) + h_w (T_b - T_a) \qquad (2)$$

where: σ = Stefan-Boltzmann radiation constant;

ε = emissivity for long-wave radiation of the energy-absorbing surface (ε is the same as e in papers S/42 and S/46);

h_w = a convection coefficient, dependent on wind speed;

T_b = energy-absorbing surface temperature;

T_a = air or sky temperature above the exchanger.

These losses, which increase with increasing exchanger temperature, can be controlled or reduced by any one of or a combination of three means.

(*a*) Radiation losses can be reduced by the use of selective surfaces, i.e., surfaces having a low emissivity ε, yet retaining a high absorptivity α for solar (short-wave) radiation. (It should also be noted that for some purposes, e.g. radiative cooling,

surfaces with low short-wave absorptivity and high long-wave emissivity may be desirable.)

(*b*) Radiation and convection can both be reduced by the use, over the energy-absorbing surface, of one or more covers transparent to solar radiation but opaque to long-wave radiation. This reduction of thermal losses is accompanied by an increase in transmission loss (i.e., a decrease in τ in equation (1)) and thus by a decrease in absorbed energy; these two losses must be added to determine an optimum number of covers.

(*c*) Radiation and convection losses can be reduced by use over the absorbing surfaces of structures which suppress convection and effectively reduce emissivity without substantially reducing absorptivity.

Examples of solar exchanger energy balances

The significance of the loss terms in the energy balance and the effect of controlling or reducing the losses are illustrated for flat-plate exchangers by the example of Tabor *et al.* (S/46), which indicates efficiencies improving from zero to 39 per cent for a 200°F exchanger, as covers and selective surfaces are added to control thermal losses. For a focusing system, an example may also be cited: for operation of a cylindrical parabolic system at a temperature of 300°F, at a concentration ratio of 10 and without covers over the non-selective energy-absorbing surface, the optical losses were 34 per cent, the thermal losses were 36 per cent, and the efficiency was 30 per cent; for improved reflectivity and use of a selective surface, the efficiency would be raised to 48 per cent.

Ideal properties

In general, then, the desired properties in an absorbing surface for solar exchanger application are high absorptivity for solar radiation and low emissivity for long-wave radiation. Cover transmissivity for solar radiation should be high, but covers should have low transmissivity for long-wave radiation, i.e., high reflectivity (preferably) or high absorptivity for long-wave radiation. Cover materials must retain useful physical properties and be capable of operation at high temperatures. For reflectors for focusing exchangers, specular reflection must be high throughout the solar spectrum, and the shape and orientation of the reflecting surface must be established and maintained so that the intercept factor γ is high. For refracting concentrators, τ of the refractor must also be high. Low heat capacity is also desirable to reduce heat capacity effects.

All of these desirable properties must be met in greater or less degree in an exchanger when it is new and also must be maintained through the useful life of the exchanger. Durability and weathering may be particularly important where organic (plastic) materials are used. Further, it is not possible to obtain all of these desirable properties in a single exchanger, and it is usually necessary to sacrifice in one property to gain in another; the evaluation of these balances must be made for each solar energy application, and it is not now possible to state in completely general terms which are the most important properties.

It has been noted that the availability of a cover material with 100 per cent transmissivity for solar radiation, opacity for long-wave radiation, and retention of useful physical properties at elevated temperatures would permit use of many covers and thus operation of flat-plate exchangers at temperatures limited (in theory) by the temperature of the sun, or by the temperature limitations of the cover material.

Materials' properties and their significance—costs

As noted, an objective of solar process design is the delivery of energy (or other products of the process, such as distilled water) at minimum total cost. In the broad sense, all process costs should be included, but a completely general treatment of the effects of materials and materials' properties on costs is difficult to formulate. However, several general principles can be set forth by which selection of materials for the solar process can be made.

(*a*) For a specific output of the process, at some predetermined temperature, energy balances of the type of equation (1) can be used to determine the area of exchanger required, when properly integrated to account for variations in solar energy supply and changes in other meteorological variables over the time period of the year in which the process is to be operated. Thus the effects of the properties of materials are two-fold: first, they affect the performance of the exchanger (as shown by the terms of the energy balance) and thus the exchanger area requirements; second, the materials affect and determine the cost per unit area in meeting structural requirements.

(*b*) Changes in materials and their properties can increase the temperature range, or increase the time-fraction of the day over which the solar exchanger can operate. These increases can affect the quantity of energy needed and/or the performance of the rest of the system. For example, increasing the output temperature of an exchanger supplying energy to a heat engine will result in improved heat engine efficiency and thus less energy input to the engine. Ultimately, then, the effects of materials and their properties on the *total process* must be considered in evaluating the costs of output of the process.

(*c*) Selection of materials will be influenced by other than first costs, as maintenance requirements and lifetime will vary with materials. For example, plastic covers (glazing) on an exchanger will cost less but have a shorter lifetime than glass.

(*d*) The properties of materials vary with temperature, time (i.e., ageing), and environmental factors

such as corrosive or erosive atmospheres. In predicting performance and fixing structural requirements, properties of aged or weathered materials should be used, or account should be taken by other means of the possibility of diminished output of the process with time.

Each solar process and application should be studied to determine the best combinations of materials to be used. For example, the incremental cost of a selective black surface over a non-selective black may be less than the value of increased output of a heat engine using energy from the exchanger and available at higher temperature because of the selective surface.

Many of the materials' properties cannot be controlled or fixed independently of other processes. Examples are: the use of multiple cover which decreases convection and radiation loss, but results in decreased τ; the α and ε for the practical selective surfaces now available are not independent of each other, and an increase in α (e.g., by thicker surface coating) is generally accompanied by an increase in ε. The gains in performance on improving one property are offset (more or less) by losses due to changes in the other property. The net gain (or loss) in performance on change of two interrelated properties can only be determined from the integrated energy balance. This question is treated, for the example of the interrelationship of α and ε, by Tabor *et al.* (S/46) and Edwards *et al.* (S/43); an expression is derived (S/46, equation [6]) showing in terms of the radiation exchange the criterion for changes in α and ε which will improve exchanger performance. Similar relationships can be derived for other combinations of interdependent properties; they must, however, be viewed in the light of costs of changes in the materials and properties.

The question can now be asked, "What new materials are available for solar energy applications, and what are their useful properties?" In general terms, the following may be stated:

(*a*) A number of studies of radiation properties have been made which result in surfaces with desirable combinations of radiation properties (particularly α and ε) and in processes for making these surfaces (S/6; S/42; S/43; S/46; S/86);

(*b*) Studies have been made of optical properties of glass and plastic transparent media for solar exchanger covers, with desirable combinations of properties for reduction of thermal losses (S/33; S/91);

(*c*) New materials and methods have been proposed for construction and use of reflectors and refractors in focusing exchanger systems (S/22; S/33; S/91; S/104), and represent promise for solutions of the difficult problems of optical quality in focusing exchanger systems;

(*d*) A new method of construction of flat-plate exchangers (or receivers for focusing exchangers) has been reported (S/71) which reduces both radiation and convection losses and permits operation at substantially higher temperatures.

In the following sections, these materials developments, as described in the papers for this agenda item are reviewed.

Properties of energy-absorbing surfaces

The field of radiation properties of surfaces absorbing solar energy, i.e., of spectral variation of the radiation properties' absorptivity and emissivity, has received much attention in the last few years, with the first papers significant in solar energy applications presented at the 1955 Arizona solar energy conference. More recently, additional impetus has been provided by the needs for solar energy applications in space.

Mechanisms of selectivity

Basic studies of the reasons for spectral variation of absorptivity (and thus emissivity), as noted by Edwards *et al.* (S/43), have suggested several mechanisms of selectivity of energy-absorbing surfaces and thus several methods of their preparation. These mechanisms, or reasons for selectivity, include: variation of the optical constants n (index of refractive) and K (absorptive index) with wave-length for a single surface material, surface roughness of dimensions that are large relative to solar energy wave-lengths but small relative to long-wave reradiation (leading to multiple reflection and increased α for short-wave radiation but having little effect on long-wave emission), layers of small particles of dimensions larger than solar wave-lengths but smaller than long-wave reradiation (with the particles able to absorb radiation of wave-lengths less than their size but transparent to longer-wave radiation), thin anti-reflection films which increase absorptivity, and thick semiconductor films, opaque to short-wave radiation, but transparent to long-wave radiation, over metal substrates which have low emissivity. Also, combinations of these structures and effects act to produce selectivity.

Absorptivity-emissivity data

The materials properties needed for performance calculations are absorptivity for solar radiation and emissivity for long-wave radiation. The spectral distribution of solar energy varies to some extent with solar elevation and atmospheric conditions, but for most practical purposes a single value of α can be used, irrespective of this small variation. Emissivities for long-wave radiation are to some degree a function of surface temperature, with values of ε frequently given for temperatures near usual air temperatures and occasionally for higher temperatures (e.g., of 1 000°K); the data given for near ambient temperatures can be used for most solar exchanger calculations. These data on α and ε are measured by heat balances under known or controlled conditions (where the radiation fluxes can be determined), as by Trombe *et al.* (S/6), Gaumer (S/42) and Tabor *et al.* (S/46), or are calculated from measurements of reflectances at various wave-lengths as determined

with appropriately equipped spectrometers, as by Edwards *et al.* (S/43).

Secondary measurement methods can also be used to get at least qualitative information on absorptivity and emissivity. Vachet and Mercier (S/86) measured equilibrium temperatures of surfaces exposed to solar radiation (where the absorbed energy equals the thermal losses) and made comparative measurements of useful gain from solar exchangers similar except for known and unknown radiation properties. Quantitative data on α and ε from these measurements depend on the availability of sufficient data on other factors in the energy balances.

Table 1 shows α and ε for several surfaces of actual or potential interest in various solar applications. More data on many other surfaces and information on surface preparation are contained in the references.

Selective surface costs

Few cost data are available on surface treatments to produce selective surfaces. Tabor *et al.* (S/46) estimates the cost of the nickel black coating at about 5 per cent of the total collector costs. Other processes of oxidation, plating, chemical treatments, coating and heating are more or less expensive, depending on the complexity of the operations and the scale on which they are carried out. Furthermore, particular materials may be required for the substrate of a selective surface and may add significant increments to solar exchanger costs.

It is of interest to note that there are now two commercial selective surface coating processes. A plant for coating nickel black on galvanized iron is in operation, making absorbers for solar water heaters in Israel (S/46). Ebonol is a commercially available treating compound (S/43), and surfaces are treated with this material for a number of optical applications.

Stability of selective surfaces

Terrestrial application of solar energy absorbers requires operation of the surfaces at more or less elevated temperatures in oxidizing atmospheres for extended periods of time. Other corrosive, or erosive, agents may also be present, and the surfaces must be protected against these agents by a transparent cover, or be stable in their presence, in order that desirable radiation properties are maintained.

Other considerations

For focusing exchanger systems of high ratio of A_a/A_x, termed the "concentration ratio", α becomes the more important property of the surface, and as operation is at a higher temperature, maintenance of the surface becomes more difficult. However, it may be observed that the absorbing surface area per unit of useful energy gain is low, allowing higher investment in obtaining good surfaces. Gaumer (S/42) explores some possibilities of unusual materials, such as thin foils of rare earth metals, which are expensive but which could be used in small quantities in focusing exchanger receivers, to take advantage of chemical stability or desirable radiation properties. Trombe *et al.* (S/6) reports on surface roughening by folding, grooving, or etching to improve α by obtaining multiple reflections; these techniques should also be applicable to receivers for focusing exchangers, possibly in combination with materials proposed by Gaumer.

While radiative cooling itself is not strictly a solar application, the performance of radiative coolers can be treated by the same types of energy balances which describe the performance of solar exchangers. Radiative coolers generally work best with surfaces of low α and high ε; surfaces such as alumina films on aluminium (S/6; S/86) and paints pigmented with materials of high refractive index (S/42) have these desirable properties.

Properties of cover materials

Significant new developments in cover materials for solar energy exchangers have been made in plastics (S/33), with new materials of properties different

Table 1. Some α and ε data for surfaces for solar energy application

Surface	*α, Solar radiation*	*ε, at temp. less than 100°C.*	*Approx. upper temp. range of application*	*References*
CuO on Al.	0.85	0.11	200°C	S/46
Tabor Ni-black treatment 120-20 on galvanized iron	0.89	0.12		S/46; S/43
Ebonol C on copper	0.91	0.16	400°F	S/43, figure 7
Stainless steel, 16 per cent Cr., heated 3 hr. at 600°C	0.75	0.1		S/6; see also S/43, fig. 6
Aluminum treated with $KMnO_4$	0.80	0.35		S/6, figure 5; S/86
Commercial flat black paints	0.93	0.93		S/6, figure 5; S/86
Platinum black	0.95	0.91	900 °C	S/42

from those of glass and having advantages and disadvantages relative to glass. In the field of glass technology, there are possible methods of modifying and controlling the properties of glass, to improve its performance as a cover material (S/6; S/91).

Transparent materials, without practical exception, reflect and absorb some radiation. At a given wave-length, or over a particular range of wave-lengths, the sum of the transmissivity, absorptivity and reflectivity must be unity. Thus, complete data on a cover, or glazing, material should include these properties in appropriate wave-length ranges; the ranges of primary interest are solar, where the transmissivity should be high, and long-wave, where transmissivity should be low.

Plastics

Several newly available plastic films can be considered for covers for solar exchangers and are discussed by Edlin and Willauer (S/33); they include a fluocarbon film, "Teflon", a polyvinyl fluoride film, "Tedlar", and a polyester film, "Mylar" type W. These materials vary in chemical composition, physical and radiation characteristics. They should not, in general, be considered as direct substitutes for glass, as exchanger designs should be modified to account for the different properties of the various plastic films. The properties most unique in these films can be summarized: they are used in thin sections (1 to 5 mils, or 25 to 125 μ), they are generally partially transparent to long-wave radiation, their physical properties are in most cases strong functions of temperature and temperature limitations must be considered in design, and their lifetimes are more or less limited by weathering.

Weatherability, or the ability of a material to retain its properties when exposed to weather, radiation, moisture, flexing due to wind, etc., is a critical property of plastics. It is a combination of optical, physical and chemical properties, and structural factors, that determine the potential lifetime of a material under given conditions of use. An accurate picture of potential life for all films under all conditions is not available; however, the projected lifetimes of three unsupported films exposed to Florida weather are noted (S/33) as: Teflon, 20 + years; Tedlar, 9 years; Mylar type W, 4 years.

Physical properties of films are widely variable, with, for example, the tensile strength of Mylar W being 24 000 psi at 25°C and that of Teflon, 3 000 psi at 25°C. The properties vary with temperature and exposure time; extensive data are presented (S/33) on these properties which serve to assist in the solution of evaluation and design problems.

Of particular concern for solar exchangers is the transmissivity of the film to solar radiation. Teflon and Tedlar have the advantage of relatively low refractive index, with resulting low reflection loss and good transmission. The films being thin, absorption is also low. Data are also presented (S/33) on transmissivities of various numbers and thicknesses of the three types of films. For example, at normal incidence, the transmissivity of a single layer of 1 mil Teflon is indicated as 0.97, and of 1 mil of Tedlar, 0.94.

The transmissivity of plastic films for long-wave radiation is not covered in the papers on this agenda item, and for many plastics it is higher than that of glass. With non-selective energy-absorbing surfaces, the higher transmissivity permits higher radiation loss; with selective surfaces where radiation is a lower fraction of the total thermal losses, the increased long-wave transmissivity is less significant. It is not possible to generalize on these effects at the present time, and new analyses are now being made of exchanger heat balances to assess their importance.

Glass

Glass, in its varying composition, has properties which have long been used to advantage in solar exchangers. Glass of low iron content, having a refractive index of 1.52, will have a transmissivity (typically) of 0.90 for solar radiation at normal incidence. (There are surface treatments which increase the transmissivity of glass by addition of films of refractive index intermediate between glass and air, and transmissivity can be raised to 0.95 with these treatments. However, they are at the present time expensive.) Glass has the advantages of a very long lifetime if properly supported and protected from shock, and low transmissivity for long-wave radiation.

The effects of several variables of glass specifications on the usefulness of glass covers is discussed by Peyches (S/91). Composition can be altered and thus the cut-off wave-length above which the glass becomes essentially opaque. For a cover material for high temperature exchangers, where the wave-lengths of emitted radiation begin to overlap the solar spectrum, borosilicate glasses (Pyrex) are suggested, as their transmissivity cuts off sharply at wave-length below 2.5 μ, thus being opaque for the short-wave end of the emitted radiation from the exchanger. Thickness may also be varied, within limits set by structural requirements and costs. The slope of the transmission curve that separates a region of high transparency from one of lower transparency is steeper at greater thicknesses; for high-temperature operation, an optimum thickness giving best performance may exist.

As previously noted, it would be advantageous to reflect long-wave radiation, rather than absorb it. Trombe *et al.* (S/6, figure 9) point out that glasses have reflection bands in the range of 8 to 10 μ (the range of maximum emission for surfaces at 100°C) with the reflectance varying with the type of glass. Peyches (S/91) suggests that the reflectivity for long-wave radiation of glass can be increased by very light gold films deposited on their inner surface and that by control of the thickness, little additional reflection for short-wave radiation would

be incurred. Data are needed to evaluate the effects of this kind of surface treatment on solar exchanger performance.

Properties of refractors and reflectors

Refractors

Little attention has been given in the past to the use of refractors in practical solar energy applications, on the basis that lenses are substantially more expensive than reflectors. The development of Fresnel lenses (step lenses), and their mass manufacture for use (in small sizes) in cameras, leads to consideration of them for focusing devices for solar exchangers. Oshida (S/22) reports a study of concentration of solar radiation with molded plastic Fresnel lenses and their use in increasing the level of radiation on silicon photovoltaic cells. The present cost of polymethylmethacrylate lenses for view finders for cameras is about U.S. $10 per square foot, with cost reductions expected. The material has high transparency for solar radiation; its weatherability is not specified but should be good, and other materials might be used. These refractors have advantages in that they pack and ship easily, being essentially flat sheets, and are mounted in flat frames. Cylindrical step lenses, and step prisms for use with photovoltaic converters of varying spectral response, are also possible applications of refractors.

Reflecting surfaces

A major problem in applications of focusing exchanger systems for other than laboratory purposes has been to find a material which has and can retain a high specular reflectivity for solar radiation, with reasonable maintenance. Loss of reflectivity may result from degradation of the surface, erosion, dirt accumulation and action of cleaning agents. For some applications, back-silvered glass has served well and has good durability, but its applicability is limited by physical strength and shock resistance, particularly where movable surfaces are concerned.

A new method of making large glass reflectors is suggested by Peyches (S/91). Commercial production of continuous strips of polished plate glass, 2.5 meters wide, is now being started and large mirrors may be fabricated therefrom having the desirable characteristics of glass reflectors but not some of the disadvantages of small segmented reflectors.

Metallized plastic films may also be used, when supported and shaped, for reflecting surfaces. Edlin and Willauer (S/33, figure 19) present some data on initial *total* (specular and diffuse) reflectivity of aluminized Mylar and Tedlar, indicating that reflectivities of 60 to 70 per cent (initial values) might be expected for such films. (Other published data indicate specular reflectivities from 65 to 85 per cent, with variation due to differences in the film substrate and the amount of metal applied to the film.) Weatherability of these films, supported on a rigid structure, would be better than for unsupported films. Data on reflectivity *vs.* time for these films are not now available. They have the advantage of costs generally less than 10 cents per square foot, for the metallized films only, without supporting structure.

Anodized aluminium represents another reflecting material which should be considered for focusing system application.

Reflector support

Materials such as plastic films must be supported and retained in the proper shape. Daniels and Breihan (S/104) note the use of glass-fiber reinforced polyester plastic shells, with metallized Mylar reflecting surfaces adhered to the shells with epoxy resins. The reflectors are formed over molds, are reinforced at the rims, and are mounted on frames constructed on thin-wall tubing. The cost of materials for experimental reflectors of this type is about U.S. $1.00 per square foot.

Many engineering problems must be considered in designing and selecting materials for focusing solar exchangers. In addition to the reflection (and refraction) properties noted, stiffness, distortion in winds, distortion due to thermal stresses, and their effects on the optical quality of the system and thus on its performance, must be evaluated. These factors are particularly important if the concentration ratio, A_a/A_x, is high, as is generally necessary for high-temperature solar energy applications.

Other "energy control" methods

It is possible to affect, within limits, the absorption and emission of radiation by the shape or configuration of the surfaces. A well-known example is the isothermal black-body cavity (large compared to the wave-length of the radiation) which absorbs and emits with unit absorptivity and emissivity. Another example is the increase in absorptivity due to multiple reflections in grooved or corrugated surfaces, with an attendant increase in emissivity, as discussed by Trombe *et al.* (S/6).

Francia (S/71) has proposed an energy-absorbing surface arrangement designed to retain high absorptivity and at the same time reduce the effective emissivity, without the use of a selective surface in the usual sense. In essence, an assembly of thin cylinders, black to long-wave radiation and of high length/diameter ratios (i.e., a "deep" honeycomb) is placed over and perpendicular to the black energy-absorbing surface in such a manner that it limits the field of view of the surface to a small solid angle including the energy source (the sun). The temperature of the walls of the cylinders decreases with distance outward from the energy-absorbing surface; heat transfer outward is by successive reradiation and absorption, with some convection effects, when the

cylinders are constructed of low conductivity material. Thus, in effect, a surface is made having high emissivity in the normal direction but substantially reduced emissivity in directions other than the normal, resulting in reduced hemispherical emissivity. (See S/43 for discussion of directional and hemispherical properties.) The honeycomb must also serve to reduce the usual convection losses.

An analytical study of radiation effects, i.e., of temperature gradients along the length of the honeycomb (cylinders) (S/71), indicates that the temperature should decrease as the fourth root of the distance out along the length. The analysis indicates that radiation losses from deep honeycomb should be a small fraction of that from a plane black emitter (if conduction and convection effects are neglected).

Francia describes experiments with several models of the honeycomb absorber, operating his Collector No. 2 (S/71), a 0.5 m^2 exchanger without optical concentration generating superheated steam at 230°C and operating at a maximum temperature of 320°C, with efficiencies estimated at over 50 per cent. In this system, the honeycomb was made of carbonized paper hexagons with mean diameter of 0.8 cm and length of 12 cm. The system was oriented so that beam radiation was normal to the absorbing surface. In another experiment, with Collector No. 4 (S/71), which uses a conical reflector to concentrate beam radiation by a factor of about 15, steam was generated at about 100 atm and 450°C; in this apparatus, glass tubes were used to make up the honeycomb, meeting the requirement of being black for long-wave radiation but obviating the need for parallel incident radiation.

These temperatures of operation are higher than ordinarily encountered in solar exchanger operation. In contrast, for example, the *equilibrium* temperature of a one (glass) cover exchanger, with a highly selective energy-absorbing surface and without radiation concentration, might typically be 250°C; at this equilibrium temperature, the useful gain is zero.

No cost data are yet available on these new "surfaces", nor are complete data on their performance yet at hand. A number of possible materials may be considered for honeycomb construction, including widely available and inexpensive paper honeycombs, if protection is provided. If the honeycomb is not transparent or highly reflective to solar radiation, the exchanger will operate primarily on beam radiation and must "track" the sun with motion about two axes; if it is transparent, some degree of tracking may still be needed.

Conclusion

The radiation properties of materials determine to a large degree the performance of solar exchangers, while the physical properties determine design variables such as thicknesses of sections. New materials are becoming available, and new modifications of old materials are being developed, which are of immediate and potential importance in reducing the cost of the use of solar energy and increasing the temperature range over which solar exchangers can operate. Notable among these materials are plastics for cover use or for reflecting surfaces, selective surfaces such as nickel black or Ebonol, glasses with particular properties advantageous for cover materials or reflectors, and the honeycomb absorber which limits reradiation and convection.

The field of materials is a rapidly advancing one, anf of necessity, some of the developments discussed in the papers on this agenda item are based on research rather than on experience with practical applications. By the same token, costs of the materials discussed are in many instances not based on quantity production, are projected costs, ore are present costs in times of significant cost changes. Our understanding of the basic problems of solar energy collection is developing to the point where materials, properties can be specified, and the papers indicate promise of additional significant developments to contribute to the progress of practical economical applications of solar energy.

Topics proposed for discussion

In a session covering a broad subject area such as new materials, a wide variety of topics for discussion arises. These topics vary from very practical problems of immediate interest to the builder and user of solar equipment, to more theoretical questions of significance to the designer. It is expected that the authors of several of the papers will have additional data and information to present. The following are also proposed for discussion.

(a) *Reflecting surfaces.* What practical experience is at hand on the use of reflecting surfaces in focusing solar exchangers? What have been the corrosion, erosion and cleaning problems? It is necessary to protect reflecting surfaces with transparent covers?

(b) *Plastic glazing.* What is the best way of mounting and supporting plastic glazing? What relationships are there between method of mounting and lifetime or temperature limitations? Should combinations of glass and plastic glazing be considered, e.g., the use of an outer glass cover to increase the potential lifetime of lower plastic cover?

(c) *Reflector fabrication.* What generalizations can be made on strength, wind resistance, and other design problems of reflectors, which would assist in materials selection? Several methods of reflector construction are noted in the papers; are honeycomb-reinforced structures, or electroformed shapes, or other reflectors of interest in terrestrial applications?

(d) *Use of developments in space applications.* A substantial effort is now going into developments of materials for solar energy applications for space use. What additional or different criteria must be applied for terrestrial applications, to make use of this data and information on materials?

(e) *Selective surfaces.* What data are there available on the long-time thermal stability of various selective surfaces in the atmosphere? What cost projections can be made for applying selective surfaces? What are the criteria for selection of materials for the substrate for selective surface coatings?

(f) *Surface geometry.* What generalizations can be made on the relationships between surface geometry (i.e., cavity or roughness size and shape) and absorptivity and emissivity at various wave-lengths?

(g) *Radiation properties measurement.* Several methods of measurement of radiation properties are noted in the papers. What methods are there available for measuring absorptivity and emissivity *in situ,* i.e., non-destructive methods?

(h) *Honeycomb absorber.* What is the effect of the Francia honeycomb on convection loss from the energy-absorbing surface? What materials and fabrication techniques can be used? What are the effects of a cover, if used to protect honeycomb materials?

MATIÈRES NOUVELLES EMPLOYÉES DANS L'UTILISATION DE L'ÉNERGIE SOLAIRE

(Traduction du rapport précédent)

John A. Duffie *

La présente Conférence traite de l'application des ressources énergétiques à la solution de problèmes pratiques. Pour pouvoir réaliser cette application, il faut pouvoir disposer de matériaux ayant, dans la mesure du possible, les propriétés voulues et un prix de revient raisonnable. La technologie des matériaux se développe rapidement, et les recherches fondamentales sur les propriétés des matériaux et sur le processus de l'énergie solaire améliorent notre connaissance de ces propriétés et les utilisations qu'on peut en faire. L'étude des matières nouvelles constitue donc un sujet important de la Conférence.

Celui qui dresse les plans d'un équipement solaire est limité par les matériaux dont il dispose, et il doit en tenir compte dans ses conceptions. La mise au point de nouveaux matériaux possédant un ensemble de propriétés souhaitables peut diminuer les limitations auxquelles on est soumis et ouvrir de nouvelles possibilités d'application de l'énergie solaire. Étudions, par exemple, les limitations imposées dans le passé à l'utilisation des échangeurs de chaleur solaire à plaque plane (collecteurs). Les matériaux dont on disposait dans le passé ont limité les possibilités d'utilisation des échangeurs au fonctionnement à des températures ne dépassant pas 50 à 75 °C au-dessus de la température de l'air ambiant. Avec les nouveaux matériaux utilisés pour les couvertures et les surfaces absorbant l'énergie solaire, la gamme de température de l'exploitation pratique augmente actuellement, et les nouvelles applications de l'énergie solaire à des fins telles que la production d'énergie hélio-mécanique et la climatisation par absorption deviennent plus prometteuses.

De nombreux aspects des matériaux et de leurs propriétés présentent de l'importance du fait qu'ils influent beaucoup sur les performances des héliomoteurs et leur prix de revient. Ce qui importe en fin de compte, c'est le prix de revient de l'énergie ou du produit fourni par le dispositif solaire; il faut donc étudier la performance (débit par unité de surface de l'échangeur de température solaire) et le coût (par unité de surface) ainsi que, bien entendu, les propriétés du matériau dont ces éléments sont fonction. On a suggéré au moins trois méthodes d'étude des problèmes des matériaux : premièrement, amélioration des performances ou élévation des limitations de température par utilisation de matériaux ayant des propriétés supérieures, en matière de rayonnement, obtenues éventuellement moyennant un supplément de prix; deuxièmement, réduction du prix de revient par utilisation de matériaux très durables ou de matériaux très bon marché qui peuvent de ce fait avoir une durée probable de vie utile plus courte; troisièmement, mise au point de méthodes nouvelles d'application des matériaux des types anciens ou plus traditionnels pour améliorer les performances des dispositifs solaires ou réduire leur prix. Ces trois méthodes sont exposées dans le détail dans les dix mémoires consacrés aux nouveaux matériaux.

Les mémoires en question étudient surtout les nouveaux matériaux tels qu'ils sont appliqués aux échangeurs de chaleur solaire. Ces échangeurs sont généralement les éléments les plus coûteux des applications de l'énergie solaire et imposent des limitations aux autres parties du dispositif. (Les matières premières destinées aux autres parties du processus, par exemple le climatisateur dans une application de réfrigération solaire, peuvent être plus ou moins classiques, et ils sont étudiés au titre des points correspondants de l'ordre du jour). Nous étudions ici les effets des matériaux et de leurs propriétés sur les performances et le prix de revient des échangeurs; nous présentons une étude des bilans énergétiques décrivant les performances des échangeurs solaires, pour aider à comprendre les effets des propriétés des matériaux sur les performances. Nous notons la relation entre le prix de revient et les performances. Dans les sections suivantes, nous notons les propriétés des matériaux dont il serait souhaitable de disposer et nous passons en revue les propriétés relatives au rayonnement des absorbeurs, des transmetteurs, des réflecteurs et des réfracteurs. Nous notons également d'autres moyens d'empêcher les pertes d'énergie en utilisant des configurations et techniques de fabrication uniques. Comme il est inévitable, le choix des matériaux pour une application donnée repose sur des compromis, et nous avons brièvement examiné les combinaisons optimales des propriétés.

Les dix mémoires présentés fournissent un tableau très complet des nombreux aspects du sujet envisagé. Bien des problèmes y sont étudiés et ils décrivent

* Directeur, Solar Energy Laboratory, University of Wisconsin, Madison, Wisconsin.

des progrès très divers qui tous contribuent ou peuvent contribuer au succès économique des applications de l'énergie solaire pour des usages terrestres. Ils fournissent sur ce sujet un ensemble substantiel de données et d'interprétations utiles dont nous ne pouvons faire état dans notre bref exposé; pour les détails, les lecteurs qui voudraient savoir dans quelle mesure l'énergie solaire peut faire face aux besoins d'énergie mécanique doivent obligatoirement se référer aux mémoires complets.

Propriétés des matériaux et leur importance; rendement des matériaux

Les propriétés que doivent avoir les matériaux pour qu'ils puissent présenter de l'intérêt en matière d'applications de l'énergie solaire sont : les propriétés relatives au rayonnement, c'est-à-dire la façon dont ils absorbent, émettent, transmettent ou réfléchissent les radiations de diverses longueurs d'ondes; et les propriétés physiques qui déterminent les impératifs de poids et d'épaisseur et la résistance aux incidents mécaniques de différentes catégories. Dans les plans d'échangeurs d'énergie solaire, les propriétés relatives au rayonnement sont celles qui, dans une large mesure, déterminent le rendement de l'appareil et par conséquent les surfaces nécessaires pour une production donnée; c'est pourquoi nous examinerons d'abord les propriétés relatives au rayonnement, puis les propriétés physiques. Pour aider à comprendre l'importance des propriétés relatives au rayonnement, nous passerons brièvement en revue l'équation du bilan d'énergie qui décrit le fonctionnement d'un échangeur solaire.

L'échangeur solaire est un type unique d'échangeur de chaleur du fait que l'énergie est transférée d'une source de rayonnement éloignée à (généralement) un fluide contenu dans l'échangeur. La température de la source de rayonnement (effectivement aux environs de 6 000 °K) est telle que le rayonnement sur l'échangeur se trouve presque entièrement dans la gamme de longueur d'onde de 0,4 μ à 2,5 μ, alors que le rayonnement émis par l'échangeur (à une température ne dépassant pas quelques centaines de degrés au-dessus de l'ambiante) est presque entièrement composé de longueurs d'ondes supérieures à 2,5 μ. Il existe donc une différence importante entre le rayonnement solaire incident et le rayonnement à ondes longues qui est émis.

La distance qui sépare le soleil de la terre et ses dimensions font que le flux d'énergie sur l'échangeur solaire (c'est-à-dire l'énergie par unité de temps et unité de surface) est faible par rapport aux flux rencontrés dans les échangeurs plus classiques; il est au mieux d'environ 1,6 calories par centimètre carré minute (350 BTU/heure/pied carré). Les échangeurs à plaque plane utilisent ce faible flux sans concentration; les échangeurs convergents utilisent des systèmes optiques pour augmenter ce flux à la surface absorbant l'énergie et permettent le fonctionnement à des températures supérieures.

Le bilan d'énergie

Le fonctionnement de l'échangeur solaire est décrit par un bilan d'énergie qui peut s'écrire sous la forme générale suivante :

$$HA_a r \gamma \tau \alpha = [q_u + \Sigma q_{th} + \Sigma q_{hc} A_x] \qquad (1)$$

les notations étant :

- H = rayonnement solaire incident sur le plan de l'échangeur par unité de surface;
- A_a = surface efficace de l'échangeur interceptant le rayonnement;
- r = réflectance spéculaire d'un réflecteur entre le soleil et la surface absorbant l'énergie pour les systèmes convergents;
- γ = facteur d'interception pour les systèmes convergents, fraction du rayonnement réfléchi spéculairement qui est interceptée par la surface absorbant l'énergie;
- τ = transmittance d'un système optique couvrant la surface absorbant l'énergie pour le rayonnement solaire;
- α = absorbance de la surface absorbant l'énergie pour le rayonnement solaire (Note : α est le même que a dans le mémoire S/42);
- A_x = aire de la surface absorbant l'énergie ($A_x = A_a$ pour un échangeur à plaque plane);
- q_u = gain utile d'énergie réalisé par l'échangeur solaire par unité d'aire de la surface absorbant l'énergie;
- q_{th} = somme des pertes d'énergie thermique par la surface absorbant l'énergie, par conduction, convexion et rayonnement, par unité d'aire de la surface absorbant l'énergie (voir discussion ci-dessous);
- q_{hc} = somme des effets de capacité calorifique, si l'échangeur ne fonctionne pas à température constante, par unité d'aire de la surface absorbant l'énergie.

Le membre gauche de l'équation représente la quantité d'énergie absorbée par l'échangeur, alors que le membre droit représente la répartition de cette énergie absorbée, entre le gain utile et les différents types de pertes. Lorsque l'on fait un projet d'échangeur solaire, le but est d'obtenir un bon fonctionnement (compte tenu, comme il se doit, des prix de revient) grâce à l'utilisation de matériaux ayant des propriétés qui porteront au maximum l'énergie absorbée et réduiront au minimum les pertes, et donneront ainsi un gain très utile.

Rayonnement absorbé

On obtient la valeur maximale de l'énergie absorbée en maintenant à des valeurs élevées les facteurs du produit $Hr\gamma\tau\alpha$. Le rayonnement est déterminé par des facteurs extérieurs à l'échangeur, l'exception étant qu'il faut orienter l'échangeur le mieux possible compte tenu du moment et du but de l'opération. Les deux facteurs r et γ ne sont inclus dans le produit que pour les systèmes convergents; r est une propriété du matériau utilisé comme surface réfléchis-

sante et γ, facteur d'interception, est fonction de la forme et de la position du réflecteur (ou réfracteur) et de la surface absorbant l'énergie, et par conséquent, des propriétés physiques du matériau et des structures qui supportent la surface réfléchissante et lui donnent sa forme. La transmittance τ est fonction de l'indice de réfraction des matériaux de couverture, de leur épaisseur, et de l'angle d'incidence du rayonnement solaire; l'augmentation du nombre de couvertures transparentes au-dessus de la surface absorbant l'énergie, réduit τ. L'absorbance α doit être aussi élevée que possible, et est fonction de la nature des surfaces absorbantes et de l'angle d'incidence du rayonnement solaire; il existe de nombreuses méthodes pour obtenir des surfaces ayant un fort α.

Pertes calorifiques

Le terme des pertes calorifiques, q_{th}, est constitué principalement des pertes par rayonnement et par convection vers l'extérieur, c'est-à-dire vers l'atmosphère et le ciel vers lesquels est dirigée la surface absorbant l'énergie. Les pertes provenant d'un échangeur sans couverture peuvent être écrites sous forme de la somme des pertes par rayonnement et convection comme suit :

$$q_{th} = \sigma \varepsilon (T_b^4 - T_a^4) + h_w (T_b - T_a) \qquad (2)$$

les notations étant les suivantes :

- σ = constante de rayonnement de Stefan-Boltzmann;
- ε = émissivité pour les rayonnements à ondes longues de la surface absorbant l'énergie (ε est le même que e dans les mémoires S/42 et S/46);
- h_w = coefficient de convection dépendant de la vitesse du vent;
- T_b = température de la surface absorbant l'énergie;
- T_a = température de l'air ou du ciel au-dessus de l'échangeur.

Ces pertes, qui augmentent lorsque la température de l'échangeur augmente, peuvent être réglées ou réduites par l'un des trois moyens suivants ou l'une de leurs combinaisons :

a) Les pertes par rayonnement peuvent être réduites par utilisation de surfaces sélectives, c'est-à-dire des surfaces ayant une faible émissivité ε, tout en gardant un fort coefficient d'absorption α pour le rayonnement solaire (à onde courte). (Il faut également noter que pour certains usages, par exemple le refroidissement par rayonnement, des surfaces ayant un faible coefficient d'absorption pour les ondes courtes et une forte émissivité pour les ondes longues peuvent être souhaitables.)

b) Le rayonnement et la convection peuvent être tous deux réduits si l'on place au-dessus de la surface absorbant l'énergie, une ou plusieurs plaques transparentes au rayonnement solaire mais opaques au rayonnement à ondes longues. Cette réduction des pertes thermiques s'accompagne d'une augmentation des pertes de transmission (c'est-à-dire une réduction de τ dans l'équation (1)) et par conséquent d'une réduction de l'énergie absorbée, ces deux pertes doivent être ajoutées pour déterminer le nombre optimal de vitrages.

c) Les pertes par rayonnement et convection peuvent être réduites grâce à l'utilisation, au-dessus de la surface absorbante, de structures qui suppriment la convection et réduisent efficacement l'émissivité sans réduire substantiellement le coefficient d'absorption.

Exemples de bilans d'énergie d'échangeurs solaires

L'importance des termes de pertes dans le bilan de l'énergie et l'effet du réglage ou de la réduction de ces pertes, sont illustrés dans le cas des échangeurs à plaque plane, par l'exemple cité par Tabor et ses collaborateurs (mémoire S/46), qui indiquent des rendements augmentant de 0 jusqu'à 39 p. 100 pour un échangeur à 200 °F lorsque des vitrages et des surfaces sélectives sont ajoutées pour réduire les pertes thermiques. Dans le cas d'un système convergent, on peut aussi citer un exemple : pour le fonctionnement d'un système à cylindre parabolique, à une température de 300 °F et à un taux de concentration de 10 et sans vitrage au-dessus de la surface absorbante non sélective, les pertes optiques étaient de 34 p. 100, les pertes thermiques de 36 p. 100 et le rendement de 30 p. 100; avec une réceptivité améliorée et l'emploi d'une surface sélective, le rendement serait porté à 48 p. 100.

Propriétés idéales

En général, par conséquent, les propriétés demandées à une surface absorbante qui puisse être utilisée dans un échangeur solaire sont un fort coefficient d'absorption du rayonnement solaire et une faible émissivité du rayonnement à ondes longues. La transmittance du vitrage pour le rayonnement solaire devrait être élevée, mais les vitrages devraient avoir une faible transmittance des rayonnements à ondes longues, c'est-à-dire une forte réflectance (de préférence) ou un fort coefficient d'absorption du rayonnement à ondes longues. Les matériaux destinés aux vitrages doivent conserver leurs propriétés physiques utiles et être capables de fonctionner à température élevée. Pour les réflecteurs destinés aux échangeurs convergents, la réflexion spéculaire doit être forte sur tout le spectre solaire, et la forme et l'orientation des surfaces réfléchissantes doivent être fixées et maintenues de façon que le facteur d'interception γ soit élevé. Pour les concentrateurs réfractants, le τ du réfracteur doit également être élevé. Une faible capacité calorifique est également souhaitable afin de réduire les effets de la capacité calorifique.

Toutes ces propriétés souhaitables doivent être présentes à un degré plus ou moins grand dans un échangeur lorsqu'il est neuf, et doivent rester telles quelles tout au cours de sa durée de vie utile. La longévité et la résistance aux intempéries peuvent être particulièrement importantes lorsqu'on utilise

des matériaux organiques (matières plastiques). En outre, il n'est pas possible de trouver toutes les propriétés souhaitables dans un seul échangeur, et il est généralement nécessaire de sacrifier une propriété pour en gagner une autre; l'évaluation de ces bilans doit être faite pour chaque cas d'espèce, et il n'est pas possible actuellement d'indiquer d'une manière absolument générale quelles sont les propriétés les plus importantes.

On a noté que la présence d'un matériau pour vitrage possédant 100 p. 100 de transmittance du rayonnement solaire, d'opacité au rayonnement des ondes longues, et de conservation de ses propriétés physiques utiles aux températures élevées permettrait d'utiliser un vitrage à plusieurs plaques et par conséquent d'exploiter des échangeurs à plaque plane à des températures limitées (théoriquement) par la température du soleil, ou par les limitations de température du matériau de couverture.

Propriétés des matériaux et leur importance; prix de revient

Ainsi qu'on l'a noté, un des objectifs que l'on recherche lors de l'établissement d'un projet de dispositif solaire est la fourniture d'énergie (ou d'autres produits, tels que de l'eau distillée) au prix de revient total minimum. D'une manière générale, il faudrait tenir compte de tous les coûts du processus, mais il est difficile de formuler l'examen absolument complet des effets des matériaux et de leurs propriétés sur le prix de revient. On peut cependant proposer plusieurs principes généraux dont il faut tenir compte lors du choix des matériaux pour les dispositifs solaires.

a) Pour un débit spécifié du dispositif, à une température prédéterminée, on peut utiliser des bilans d'énergie du type de l'équation (1) pour déterminer la surface nécessaire d'échangeur lorsqu'elle est intégrée correctement pour tenir compte des variations de fourniture d'énergie solaire et de celles des autres variables météorologiques au cours de la période de l'année pendant laquelle l'appareil sera exploité. Les effets des propriétés des matériaux sont par conséquent doubles. Premièrement, elles influent sur le rendement de l'échangeur (comme le montrent les termes du bilan d'énergie), et par conséquent sur les impératifs de surface de l'échangeur. Deuxièmement, les matériaux influencent et déterminent le coût par unité de surface par la manière dont ils s'adaptent aux impératifs de structure.

b) Des modifications des matériaux ou de leurs propriétés peuvent augmenter la gamme de températures, ou la période du jour pendant laquelle l'échangeur solaire peut fonctionner. Ces augmentations peuvent influer sur la quantité d'énergie nécessaire et/ou le rendement du reste du système. Par exemple, l'augmentation de la température de sortie d'un échangeur fournissant l'énergie à un moteur thermique donnera une amélioration du rendement de ce dernier, et par conséquent une réduction de sa consommation. Finalement, il faut tenir compte, par conséquent, des effets des matériaux et de leurs propriétés sur le *processus total* lorsqu'on évalue le prix de revient de production de ce dernier.

c) Le choix des matériaux subira d'autres influences que le prix de premier établissement, car les impératifs d'entretien et la durée de vie varieront avec les matériaux. Par exemple, les couvertures plastiques (glaçage) sur un échangeur coûteront moins, mais auront une durée de vie plus courte que le verre.

d) Les propriétés des matériaux varient avec la température, le temps (c'est-à-dire le vieillissement), et les facteurs ambiants tels que les atmosphères corrosives ou érosives. Lorsqu'on prédit le rendement et qu'on fixe les impératifs de structure, on doit calculer en fonction des propriétés des matériaux âgés ou ayant déjà subi l'attaque des intempéries, ou tenir compte d'autres manières des possibilités de réduction de production du processus avec le temps.

Chaque dispositif ou application solaire devrait être étudié pour déterminer les meilleures combinaisons de matériaux à utiliser. Par exemple, le supplément de prix d'une surface noire sélective par rapport à une surface noire non sélective peut être inférieur à la valeur de l'augmentation de production du moteur thermique utilisant l'énergie provenant de l'échangeur et disponible à température plus élevée par suite de la sélectivité de la surface.

De nombreuses propriétés des matériaux ne peuvent être réglées ou fixées indépendamment d'autres processus. En voici des exemples : l'utilisation de vitrages multiples qui réduit les pertes par convection et rayonnement, réduit également τ; l'α et l'ε dans le cas des surfaces sélectives dont on peut disposer actuellement dans la pratique ne sont pas indépendantes l'une de l'autre, et toute augmentation d'α (par exemple, par des revêtements superficiels plus épais) est généralement accompagnée d'une augmentation de ε. Les gains de rendement résultant de l'amélioration d'une propriété sont contrebalancés (plus ou moins) par des pertes dues aux variations d'une autre propriété. Le gain net (ou la perte nette) de rendement par suite de changements de deux propriétés connexes ne peut être déterminé que d'après le bilan d'énergie intégré. Cette question est traitée, dans le cas de l'exemple des relations liant α et ε par Tabor et ses collaborateurs (mémoire S/46) et Edwards et ses collaborateurs (mémoire S/43); une expression a été établie (mémoire S/46, équation (6)) pour montrer, en fonction des échanges de rayonnement, le critère des variations de α et ε qui améliore le rendement de l'échangeur. Des relations semblables peuvent être établies pour d'autres combinaisons de propriétés interdépendantes; toutefois, on doit tenir compte, lorsqu'on les étudie, du coût des modifications des matériaux et des propriétés.

On peut maintenant se demander : « quels sont les nouveaux matériaux disponibles pour les applications de l'énergie solaire, et quelles sont leurs propriétés utiles? » D'une manière générale, on peut indiquer ce qui suit :

a) Un certain nombre d'études des propriétés relatives au rayonnement ont été effectuées et ont permis de mettre au point des surfaces présentant des combinaisons souhaitables de propriétés relatives au rayonnement (en particulier α et ε) et des processus permettant de fabriquer ces surfaces (mémoires S/6, S/42, S/43, S/46, S/86);

b) On a également étudié les propriétés optiques du verre et des milieux transparents plastiques pour les vitrages d'échangeurs solaires, ainsi que les combinaisons souhaitables des propriétés permettant de réduire les pertes thermiques (S/33, S/91);

c) On a proposé, pour la construction et l'utilisation des réflecteurs et réfracteurs dans les systèmes d'échangeurs convergents (S/22, S/33, S/91, S/104), des méthodes et matériaux nouveaux grâce auxquels il est possible d'espérer trouver des solutions aux problèmes difficiles de la qualité optique des systèmes d'échangeurs convergents;

d) On a indiqué une nouvelle méthode de construction des échangeurs à plaque plane (ou des récepteurs pour échangeurs convergents) (S/71) qui réduit à la fois les pertes par rayonnement et convection, et permet un fonctionnement à des températures nettement plus élevées.

Les sections suivantes passent en revue ces perfectionnements des matériaux, tels qu'ils sont décrits dans les divers mémoires.

Propriétés des surfaces absorbant l'énergie

Le domaine des propriétés relatives au rayonnement des surfaces absorbant l'énergie solaire, c'est-à-dire des variations spectrales, des propriétés relatives de rayonnement, telles que le coefficient d'absorption et l'émissivité, ont fait l'objet de nombreuses recherches au cours de ces dernières années, comme en témoignent les premiers mémoires de valeur dans le domaine des applications de l'énergie solaire qui ont été présentés à la Conférence de l'énergie solaire de 1955 en Arizona. Plus récemment, ces recherches ont encore été stimulées par les besoins d'application de l'énergie solaire pour les véhicules interplanétaires.

Mécanismes de sélectivité

Des études fondamentales portant sur les raisons de la variation spectrale du coefficient d'absorption (et donc de l'émissivité), (voir Edwards et ses collaborateurs, mémoire (S/43), ont suggéré plusieurs mécanismes de sélectivité des surfaces absorbant l'énergie, et par conséquent plusieurs méthodes pour les préparer. Ces mécanismes, ou raisons de la sélectivité, comprennent : la variation des constantes optiques n (indice de réfraction) et K (indice d'absorption) en fonction de la longueur d'onde pour un seul matériau superficiel; la présence de rugosités superficielles de dimensions importantes par rapport aux longueurs d'onde de l'énergie solaire mais faibles par rapport au re-rayonnement à ondes longues (qui provoque des réflexions multiples et un accroissement de α pour les rayonnements à ondes courtes, mais a peu d'effets sur l'émission à ondes longues); la présence de couches de petites particules de dimensions plus grandes que les longueurs d'ondes solaires mais plus faibles que le re-rayonnement à ondes longues (ces particules étant susceptibles d'absorber le rayonnement des longueurs d'ondes inférieures à leur propre dimension mais transparentes pour les rayonnements de plus grande longueur d'onde); la présence de fines pellicules anti-réflexion qui augmentent le coefficient d'absorption et de pellicules semi-conductrices épaisses, opaques aux radiations de courtes longueurs d'ondes, mais transparentes pour celles de grandes longueurs d'ondes, recouvrant un substrat métallique ayant une faible émissivité. Des combinaisons de ces structures et de ces effets contribuent également à produire la sélectivité.

Coefficient d'absorption et d'émission

Les propriétés des matériaux nécessaires pour calculer le rendement sont le coefficient d'absorption du rayonnement solaire et le coefficient d'émission de rayonnement à ondes longues. La répartition spectrale de l'énergie solaire varie dans une certaine mesure en fonction de la hauteur du soleil au-dessus de l'horizon, et des conditions atmosphériques, mais en pratique, dans la plupart des cas, on peut utiliser une seule valeur de α, sans tenir compte de cette faible variation. Les coefficients d'émission de rayonnement à ondes longues sont dans une certaine mesure fonction de la température superficielle, les valeurs de ε étant souvent données pour des températures proches de la température ambiante et occasionnellement pour des températures plus élevées (par exemple pour 1 000 °K); les chiffres donnés pour les températures proches de l'ambiante peuvent être utilisés pour les calculs de la plupart des échangeurs solaires. Ces valeurs de α et de ε sont mesurées par des bilans de chaleur dans des conditions connues ou contrôlées (où les flux du rayonnement peuvent être déterminés), comme par Trombe (S/6), Gaumer (S/42) et Tabor et ses collaborateurs (S/46), ou bien elles sont calculées d'après des mesures des réflectances pour diverses longueurs d'ondes déterminées avec des spectromètres équipés en conséquence (voir par exemple Edwards et ses collaborateurs (S/43)).

Des méthodes secondaires de mesure peuvent être également utilisées pour obtenir au moins des informations qualitatives sur les coefficients d'absorption et d'émission. Vachet et Mercier (S/86) ont mesuré les températures d'équilibre des surfaces exposées au rayonnement solaire (l'énergie absorbée étant égale aux pertes thermiques) et ont fait des mesures comparatives du gain utile obtenu par des échangeurs solaires ayant des propriétés semblables, sauf en ce qui concerne les propriétés connues et inconnues relatives au rayonnement. Les données quantitatives sur α et ε obtenues grâce à ces mesures dépendent de la possibilité d'avoir des données suffisantes sur les autres facteurs des bilans d'énergie.

Tableau 1. Quelques valeurs de α et de ε pour les surfaces destinées aux applications de l'énergie solaire

Surface	*α, rayonnement solaire*	*ε pour temp. inf. à 100 °C*	*Temp. supérieure d'applic. (approx.)*	*Références*
CuO sur Al	0,85	0,11	200 °C	S/46
Traitement de Tabor au noir de nickel 120-20 sur fer galv.	0,89	0,12		S/46; S/43
Ebonol C sur cuivre . .	0,91	0,16	400 °F	S/43, figure 7
Acier inoxydable 16 p. 100 Cr., chauffé 3 hres à 600 °C	0,75	0,1		S/6; voir aussi S/43, fig. 6
Aluminium traité au $KMnO_4$	0,80	0,35		S/6, figure 5; S/86
Peinture noire mate commerciale	0,93	0,93		S/6, figure 5; S/86
Noir de platine	0,95	0,91	900 °C	S/42

Le tableau 1 donne α et ε pour plusieurs surfaces qui présentent ou pourraient présenter de l'intérêt pour différentes applications solaires. Les ouvrages cités en référence donnent des renseignements complémentaires sur de nombreuses autres surfaces et sur la préparation des surfaces.

Prix de revient des surfaces sélectives

On dispose de peu de données sur les prix de revient des traitements superficiels destinés à produire des surfaces sélectives. Tabor et ses collaborateurs (S/46) estiment le prix de revient de la couverture de noir de nickel à environ 5 p. 100 du prix de revient total du collecteur. D'autres procédés d'oxydation, de placage, de traitement chimique, de peinture et de chauffage sont plus ou moins coûteux selon la complexité des opérations et l'échelle à laquelle ils sont exécutés. En outre, des matériaux particuliers peuvent être nécessaires comme base d'une surface sélective donnée, et accroissent notablement de ce fait le prix de l'échangeur solaire.

Il est intéressant de noter qu'il existe maintenant deux procédés commerciaux de revêtement sélectif de surface. Une installation pour couvrir de noir de nickel le fer galvanisé est en service et fabrique des absorbeurs pour les chauffe-eau solaires en Israël (S/46). L'ébonol est un composé de traitement que l'on trouve dans le commerce (S/43), et cette matière est utilisée pour traiter les surfaces d'un certain nombre d'applications optiques.

Stabilité des surfaces sélectives

Les applications terrestres des absorbeurs d'énergie solaire nécessitent le fonctionnement des surfaces à des températures plus ou moins élevées en atmosphères oxydantes pendant de longues périodes. D'autres agents corrosifs ou érosifs peuvent également être présents, et les surfaces doivent être protégées contre ces agents par un vitrage transparent, ou être stables en leur présence, afin que les propriétés relatives aux rayonnements restent intactes.

Autres considérations

Pour les systèmes d'échangeurs convergents ayant un rapport A_a/A_x élevé (c'est ce que l'on appelle le « facteur de concentration »), α devient la propriété la plus importante de la surface, et comme la surface fonctionne à haute température, son entretien devient plus difficile. On peut observer, cependant, que l'aire de surface absorbante par unité de gain d'énergie utile est faible, ce qui permet des investissements plus élevés pour obtenir de bonnes surfaces. Gaumer (S/42) étudie les possibilités d'utilisation qu'offrent certains matériaux inhabituels tels que des minces feuilles de métaux de terres rares, qui sont coûteuses mais pourraient être utilisées en faible quantité dans les receveurs-échangeurs convergents pour tirer parti de la stabilité chimique ou des propriétés relatives aux rayonnements. Trombe et ses collaborateurs (S/6) indiquent des méthodes pour rendre rugueuses les surfaces, par pliage, rainurage ou attaque chimique pour améliorer α en obtenant des réflexions multiples; ces techniques pourraient être également applicables aux récepteurs des échangeurs convergents, en combinaison éventuelle avec les matériaux proposés par Gaumer.

Bien que le refroidissement par rayonnement ne soit pas strictement une application solaire, le rendement des réfrigérateurs par rayonnement peut être étudié par le même type de bilan d'énergie que celui qui est utilisé pour les échangeurs solaires. Les réfrigérateurs par rayonnement fonctionnent généralement mieux avec des surfaces à faible α et à ε élevé; ces propriétés peuvent être obtenues par des surfaces telles que des pellicules d'alumine sur aluminium (S/6, S/86) et des peintures pigmentées à l'aide de matériaux ayant un fort indice de réfraction (S/42).

Propriétés des matériaux de couverture

De nouveaux progrès importants ont été faits dans le domaine des matériaux de couverture pour les échangeurs d'énergie solaire grâce aux matières plastiques (S/33), où de nouveaux matériaux ont été

mis au point qui possèdent des propriétés différentes de celles du verre et présentent des avantages et des inconvénients par rapport à ce dernier. Dans le domaine de la technologie du verre, il existe des méthodes permettant de modifier et de contrôler ses propriétés pour améliorer ses performances en tant que matériaux de couverture (S/6, S/91).

Les matériaux transparents, sans exception pratique, reflètent et absorbent certaines radiations. Pour une longueur d'onde donnée ou sur une gamme particulière de longueurs d'onde, la somme des coefficients de transmission, d'absorption et de réflexion doit être égale à N. Parmi les données complètes sur un matériau de couverture ou de glaçage, il faut donc que figurent ces propriétés dans les gammes de longueur d'onde convenables; les gammes d'intérêt principal sont les gammes de rayonnement solaire pour lesquelles le coefficient de transmission doit être élevé et les ondes longues pour lesquelles le coefficient de transmission doit être faible.

Matières plastiques

On peut envisager d'utiliser plusieurs pellicules de matière plastique qui viennent d'être mises au point pour les vitrages des échangeurs solaires et qui sont étudiées par Edlin et Williauer (S/33); citons une pellicule de fluocarbone, le « Teflon », une pellicule de fluorure de polyvinyle, le « Tedlar », et une pellicule de polyester, le « Mylar » type W. Ces matériaux sont différents quant à la composition chimique et aux caractéristiques physiques et relatives au rayonnement. Ils ne doivent pas être, en général, considérés comme des produits de remplacement directs du verre, car la construction des échangeurs doit être modifiée pour tenir compte des différentes propriétés des diverses pellicules de plastique. Les propriétés les plus particulières de ces pellicules peuvent être résumées comme suit : elles sont utilisées en sections minces (1 à 5 mils, ou 25 à 125 μ), elles sont généralement partiellement transparentes aux radiations à ondes longues. leurs propriétés physiques sont dans la majorité des cas fonction directe de la température (il faut donc envisager des limitations de température dans les projets), et leurs durées de vie sont plus ou moins limitées par l'action des intempéries.

La résistance aux intempéries, c'est-à-dire l'aptitude d'un matériau à conserver ses propriétés lorsqu'il est exposé aux intempéries, aux rayonnements, à l'humidité, aux flexions dues au vent, etc. est une propriété critique des matières plastiques. C'est une combinaison de propriétés optiques, physiques et chimiques, et des facteurs structurels qui déterminent la durée de vie possible d'un matériau dans certaines conditions d'utilisation. On ne possède pas de renseignements précis sur toutes les pellicules dans toutes les conditions; on a cependant enregistré, en Floride, les durées de vie possibles de trois pellicules non montées sur des cadres et exposées aux intempéries (S/33). Ce sont : pour le Teflon, 20 ans; pour le Tedlar, 9 ans; et pour le Mylar type W, 4 ans.

Les propriétés physiques des pellicules sont très variables; on note par exemple, une résistance à la traction de 24 000 psi (1 687 kg par cm²) à 25 °C pour le Mylar W et de 3 000 psi (210 kg par cm²) à 25 °C pour le Teflon. Ces propriétés varient avec la température et la durée d'exposition; le mémoire S/33 présente des renseignements nombreux sur ces propriétés, qui contribuent à résoudre les problèmes d'évaluation et de conception.

Le pouvoir de transmission du rayonnement solaire de la pellicule est particulièrement important pour les échangeurs solaires. Le Teflon et le Tedlar présentent l'avantage d'avoir des indices de réfraction relativement faibles, donnant par conséquent des pertes par réflexion faibles et une bonne transmission. Les pellicules étant minces, l'absorption est également faible. On a également présenté des données (S/33) sur le coefficient de transmission de différents nombres et épaisseurs des trois types de pellicules. Par exemple, sous une incidence normale, le coefficient de transmission d'une couche simple de 1 mil de Teflon est de 0,97 et pour 1 mil de Tedlar, 0,94, selon les indications reçues.

Les coefficients de transmission des rayonnements à ondes longues des pellicules de plastique ne sont pas indiqués dans les rapports de cette session, et pour de nombreuses matières plastiques ils sont supérieurs à celui du verre. Avec les surfaces non sélectives absorbant l'énergie, le coefficient de transmission plus élevé permet des pertes par rayonnement plus élevées; avec les surfaces sélectives dans lesquelles le rayonnement constitue une plus faible fraction des pertes thermiques totales, l'augmentation du coefficient de transmission des ondes longues est moins importante. Il n'est pas possible actuellement de généraliser en ce qui concerne ces effets, et de nouvelles analyses des bilans de chaleur des échangeurs sont actuellement en cours pour déterminer leur importance.

Verre

Le verre, dans ses différentes compositions, a des propriétés qui ont longtemps été utilisées avantageusement dans les échangeurs solaires. Le verre à faible teneur en fer, ayant un indice de réfraction de 1,52 aura un coefficient de transmission (typique) de 0,90 pour le rayonnement solaire sous une incidence normale. (Il existe des traitements superficiels qui augmentent le coefficient de transmission du verre par addition de pellicules ayant des indices de réfraction intermédiaires entre celui du verre et celui de l'air, et le coefficient de transmission peut être porté à 0,95 grâce à ces traitements. Ils sont cependant coûteux à l'heure actuelle.) Le verre présente l'avantage d'avoir une très longue durée de vie, s'il est correctement soutenu et protégé contre les chocs, et un faible coefficient de transmission des rayonnements à ondes longues.

Peyches (S/91) a étudié les effets de plusieurs variables des spécifications du verre sur les possibilités d'utilisation des couvertures en verre. La composition peut être modifiée, et donc aussi la

longueur d'onde au-dessus de laquelle le verre devient essentiellement opaque. Comme matériau de couverture pour les échangeurs à haute température, où les longueurs d'onde du rayonnement émis commencent à recouvrir le spectre solaire, Peyches propose le verre au borosilicate (Pyrex), car son coefficient de transmission tombe nettement aux longueurs d'onde inférieures à 2,5 μ, et ce verre devient ainsi opaque pour l'extrémité ondes courtes du rayonnement émis par l'échangeur. L'épaisseur peut également varier entre des limites imposées par les impératifs structurels et le prix de revient. La pente de la courbe de transmission qui sépare une région de grande transparence de celle à transparence inférieure devient plus raide lorsque l'épaisseur augmente; pour le fonctionnement à température élevée, il doit exister une épaisseur optimale donnant les meilleurs rendements.

Comme on l'a noté précédemment, il serait avantageux de réfléchir les rayonnements à ondes longues, plutôt que de les absorber. Trombe et ses collaborateurs (S/6, figure 9) signalent que les verres ont des bandes de réflexion dans la gamme de 8 à 10 μ (gamme d'émission maximale pour les surfaces à 100 °C), le coefficient de réflexion variant avec le type de verre. Peyches (S/91) suggère que le coefficient de réflexion du verre pour les rayonnements à ondes longues peut être augmenté par des pellicules très légères d'or déposées à sa surface interne et, si l'épaisseur est correcte, on ne subira qu'une légère réflexion supplémentaire du rayonnement à ondes courtes. Des données sont nécessaires pour évaluer les effets de cette sorte de traitement superficiel sur les performances des échangeurs solaires.

Propriétés des réfracteurs et réflecteurs

Réfracteurs

On n'a accordé que peu d'attention, dans le passé, à l'utilisation des réfracteurs dans les applications pratiques de l'énergie solaire, parce qu'on a considéré que les lentilles coûtent nettement plus cher que les réflecteurs. La mise au point de lentilles de Fresnel (lentilles à gradins), et leur fabrication en série pour les appareils de photographie (en petites dimensions), ont amené à les envisager pour les dispositifs convergents des échangeurs solaires. Oshida (S/22) signale une étude de concentration du rayonnement solaire à l'aide de lentilles de Fresnel en matière plastique moulée et leur utilisation pour augmenter le niveau de rayonnement sur les cellules photo-voltaïques au silicium. Le prix de revient actuel des lentilles en polyméthyl-méthacrylate pour les viseurs d'appareils de photos est d'environ 10 dollars par pied carré, et l'on envisage des réductions de ce prix. Ce matériau est très transparent au rayonnement solaire; sa sensibilité aux intempéries n'est pas spécifiée, mais doit être bonne, et l'on pourrait utiliser d'autres matériaux. Ces réfracteurs présentent l'avantage de s'emballer et de s'expédier facilement (constituant essentiellement des feuilles planes) et sont montés dans des cadres plats. Les lentilles cylindriques à gradins et les prismes cylindriques pour convertisseurs photovoltaïques ayant des réponses spectrales diverses, constituent également des applications possibles des réfracteurs.

Surfaces réfléchissantes

Un problème majeur rencontré dans les applications des systèmes d'échangeurs convergents à d'autres fins que les essais de laboratoires a consisté à trouver un matériel ayant et pouvant conserver un coefficient de réflexion spéculaire élevé pour le rayonnement solaire, avec un entretien raisonnable. La perte de réflectivité peut résulter de la dégradation de la surface, de l'érosion, de l'accumulation de saletés et de l'action des agents de nettoyage. Pour certaines applications, le verre argenté au dos a rendu de bons services et possède une bonne durabilité, mais ses possibilités d'application sont limitées par sa résistance mécanique et sa résistance aux chocs, particulièrement lorsqu'il s'agit de surfaces mobiles.

Une nouvelle méthode d'exécution de grands réflecteurs en verre est suggérée par Peyches (S/91). La production commerciale de bandes continues de verre plat poli, de 2,5 mètres de large, a maintenant démarré et de grands miroirs peuvent être fabriqués dans ce matériau; ils possèdent les caractéristiques souhaitables des réflecteurs de verre, mais non certains des inconvénients des petits réflecteurs fragmentés.

On peut également utiliser des pellicules plastiques métallisées lorsqu'elles sont soutenues par un cadre et mises en forme, pour constituer des surfaces réfléchissantes. Edlin et Willauer (S/33, figure 19) présentent certaines données sur le coefficient initial de réflexion *totale* (spéculaire et diffuse) du Mylar et du Tedlar aluminisé, et ils indiquent que l'on peut espérer des coefficients de réflexion de 60 à 70 p. 100 (valeurs initiales) avec ces pellicules. (D'autres données publiées indiquent des coefficients de réflexion spéculaire de 65 à 85 p. 100, avec des variations dues aux différences dans la pellicule servant de base et la quantité de métal appliqué sur cette dernière.) La sensibilité aux intempéries des pellicules soutenues sur une structure rigide serait meilleure que celles des pellicules non soutenues par une armature. On ne dispose pas actuellement de données sur les variations du coefficient de réflexion de cette pellicule en fonction du temps. Elle présente l'avantage de coûter généralement moins de 10 cents par pied carré pour les pellicules métallisées seulement, sans structure-support.

L'aluminium ayant subi un traitement anodique représente un autre matériau réfléchissant qui devrait être envisagé pour les applications aux systèmes convergents.

Support de réflecteur

Les matériaux tels que les pellicules plastiques doivent être soutenus par une armature et main-

tenus dans leur forme correcte. Daniels et Breihan (S/104) notent l'utilisation de coques de plastique au polyester armées de fibre de verre avec des surfaces réfléchissantes en Mylar métallisé, collées aux coques à l'aide de résine epoxy. Ces réflecteurs sont formés sur des moules, renforcés sur les bords et montés dans des cadres construits en tubes à mince paroi. Le prix de revient des matériaux pour des réflecteurs expérimentaux de ce type, est d'environ un dollar par pied carré.

Il faut tenir compte de nombreux problèmes techniques lorsqu'on conçoit et qu'on choisit les matériaux pour échangeurs solaires convergents. Outre les propriétés de réflexion (et de réfraction) notées, il faut évaluer la rigidité, la distorsion sous le vent, la distorsion due aux sollicitations thermiques et leurs effets sur les qualités optiques du système et par conséquent sur son fonctionnement. Ces facteurs sont particulièrement importants si le rapport de concentration, A_a/A_x est élevé, comme cela est généralement nécessaire pour les applications de l'énergie solaire à haute température.

Autres méthodes de « contrôle de l'énergie »

Il est possible d'agir, dans certaines limites, sur l'absorption et l'émission des rayonnements par la forme ou la configuration des surfaces. La cavité isothermique en corps noir (grande par comparaison à la longueur d'onde du rayonnement) qui absorbe et émet avec des coefficients d'absorption et d'émission égaux à 1, en est un exemple bien connu. Un autre exemple est constitué par l'augmentation du coefficient d'absorption dû aux réflexions multiples sur les surfaces rainurées ou cannelées, avec une augmentation correspondante du coefficient d'émission, comme l'ont étudié Trombe et ses collaborateurs (S/6).

Francia (S/71) a proposé une disposition de surface absorbant l'énergie, conçue pour conserver un coefficient élevé d'absorption tout en réduisant simultanément le coefficient effectif d'émission, sans utiliser de surface sélective dans le sens habituel. Il s'agit, essentiellement d'un ensemble de cylindres minces, noirs pour le rayonnement à ondes longues et ayant des rapports longueur/diamètre élevés (c'est-à-dire un nid d'abeille « profond ») qui est placé au-dessus de la surface noire absorbant l'énergie et perpendiculairement à cette dernière de manière à limiter le champ visuel de la surface à un petit angle solide comportant la source d'énergie (le soleil). La température des parois des cylindres décroît avec la distance lorsqu'on s'éloigne de la surface absorbant l'énergie; la transmission de chaleur vers l'extérieur s'effectue par re-radiation et absorption successives avec certains effets de convection, lorsque les cylindres sont construits en matériaux de faible conductivité. On obtient ainsi, en effet, une surface ayant un coefficient d'émission élevé dans la direction normale, mais fortement réduit dans les autres directions, ce qui donne un coefficient d'émission hémisphérique réduit. (Voir dans S/43 la section consacrée à l'étude des propriétés directionnelles et hémisphériques.) Le nid d'abeille doit également servir à réduire les pertes habituelles par convection.

Une étude analytique des effets des rayonnements, c'est-à-dire des gradients de température en fonction de la profondeur du nid d'abeille (cylindres), indique que les températures doivent décroître comme la racine quatrième de la distance en profondeur (mémoire S/71). L'analyse indique que les pertes par rayonnement provenant des nids d'abeille profonds devraient être une faible fraction de celle d'un émetteur noir plan (si l'on néglige les effets de la conduction et de la convection).

Francia décrit des expériences sur plusieurs modèles d'absorbeurs en nid d'abeille, l'exploitation de son système n° 2 (S/71), un échangeur de 0,5 m² sans concentration optique, produit de la vapeur surchauffée à 230 °C et fonctionnant à des températures maximales de 320 °C, avec des rendements estimés à plus de 50 p. 100. Dans ce système, le nid d'abeille était constitué d'hexagones de papier carbonisé ayant un diamètre moyen de 0,8 cm et une longueur de 12 cm. Le système était orienté de façon que le rayonnement en faisceau soit normal à la surface absorbante. Dans une autre expérience, avec le système n° 4 (S/71) qui utilisait un réflecteur conique pour concentrer le rayonnement en faisceau d'un facteur d'environ 15, on a produit de la vapeur à environ 100 atm et 450 °C; dans cet appareil, Francia utilisait des tubes de verre pour constituer le nid d'abeille, qui satisfaisait à l'impératif d'être noir pour le rayonnement à ondes longues mais évitant la nécessité de rayonnement incident parallèle.

Ces températures de fonctionnement sont supérieures à celles que l'on rencontre ordinairement dans les échangeurs solaires. Par contraste, par exemple, la température d'*équilibre* d'un échangeur à couverture (de verre), avec des surfaces absorbant l'énergie fortement sélectives et sans concentration du rayonnement, peut atteindre normalement 250 °C; à cette température d'équilibre, le gain utilisable est nul.

On ne dispose pas de données sur le prix de revient de ces nouvelles « surfaces », ni de données complètes sur leur fonctionnement. On peut envisager un certain nombre de matériaux susceptibles de convenir à la construction des nids d'abeille, notamment les nids d'abeille en papier, facilement disponibles et peu coûteux, si on peut les protéger. Si le nid d'abeille n'est pas transparent ou présente un fort pouvoir réfléchissant pour le rayonnement solaire, l'échangeur fonctionnera surtout sur le rayonnement en faisceau et devra être « orienté » vers le soleil suivant un mouvement selon deux axes; s'il est transparent, il peut encore être nécessaire d'assurer une certaine orientation.

Conclusion

Les propriétés relatives au rayonnement des matériaux déterminent dans une grande mesure le rendement des échangeurs solaires, alors que les propriétés physiques déterminent les variables de la construc-

tion telles que l'épaisseur des sections. On commence à disposer de nouveaux matériaux et de nouvelles modifications des vieux matériaux sont en cours; ces progrès présentent une importance immédiate et potentielle puisqu'ils permettent de réduire le coût de l'utilisation de l'énergie solaire et d'accroître la gamme de températures dans laquelle le séchangeurs solaires peuvent opérer. Il faut noter parmi ces matériaux les matières plastiques destinées aux couvertures ou aux surfaces réfléchissantes, les surfaces sélectives telles que le noir de nickel ou l'Ebonol, les verres ayant des propriétés particulières qui peuvent servir utilement pour les matériaux de couverture ou les réflecteurs, et l'absorbeur en nid d'abeille qui limite la re-radiation et la convection.

Le domaine des matériaux fait des progrès rapides, et, nécessairement, certaines des nouveautés étudiées dans les mémoires présentés au titre du point III. B de l'ordre du jour ont fait l'objet de recherches et non pas d'expériences pratiques. De même, le prix de revient des matériaux, dans la majorité des cas, ne correspond pas à une production en série, mais représente un coût calculé ou un coût actuel qui pourra subir d'importantes modifications. Notre connaissance des problèmes fondamentaux que pose le captage de l'énergie solaire a atteint un point où les propriétés des matériaux peuvent être spécifiées, et les mémoires permettent d'envisager de nouveaux progrès qui contribueront au développement des applications économiques pratiques de l'énergie solaire.

Sujets de discussion proposés

Dans une session couvrant un sujet aussi étendu que les nouveaux matériaux, une grande variété de sujets s'offre à la discussion. Cette gamme va des problèmes très pratiques, d'intérêt immédiat pour le constructeur et l'utilisateur d'équipement solaire, aux questions plus théoriques qui présentent de l'importance pour l'inventeur. Il est probable que les auteurs de plusieurs de ces mémoires auront des données et informations complémentaires à présenter. Les points de discussion suivants sont également proposés :

a) *Surfaces réfléchissantes.* De quelle expérience pratique dispose-t-on sur l'utilisation des surfaces réfléchissantes dans les échangeurs solaires convergents? Quels ont été les problèmes de corrosion, d'érosion et de nettoyage? Est-il nécessaire de protéger les surfaces réfléchissantes à l'aide de couvertures transparentes?

b) *Glaçage plastique.* Quel est le meilleur moyen de monter et d'armer les glaçages plastiques? Quels rapports y a-t-il entre les méthodes de montage et les limitations de durée de vie ou de température? Devrait-on envisager des combinaisons de verre et de glaçage plastique, par exemple l'utilisation d'une couverture extérieure en verre pour accroître la durée de vie potentielle de la couverture plastique inférieure?

c) *Fabrication des réflecteurs.* Quelles généralisations peut-on faire sur la résistance mécanique, la résistance au vent et autres problèmes de conception des réflecteurs, susceptibles d'aider au choix des matériaux? Plusieurs méthodes de construction des réflecteurs sont indiquées dans les rapports; les structures renforcées en nid d'abeille ou les formes obtenues électriquement ou d'autres réflecteurs présentent-ils de l'intérêt pour des applications terrestres?

d) *Utilisation de ces nouveaux matériaux dans les applications interplanétaires.* Un grand effort est actuellement en cours en vue de perfectionner les matériaux pour les applications de l'énergie solaire pour les usages interplanétaires. Quel critère complémentaire ou différent doit-on employer si l'on veut utiliser ces données et informations sur les matériaux pour les applications terrestres?

e) *Surfaces sélectives.* De quelles données dispose-t-on sur la stabilité thermique à long terme de différentes surfaces sélectives dans l'atmosphère? Quels sont les coûts que l'on doit prévoir pour l'application des surfaces sélectives? Quels sont les critères à appliquer pour le choix des matériaux destinés aux bases recevant les revêtements superficiels sélectifs?

f) *Géométrie des surfaces.* Quelles généralisations peut-on faire sur les rapports entre la géométrie des surfaces (c'est-à-dire les dimensions des cavités ou aspérités et les formes) et les coefficients d'absorption et d'émission pour différentes longueurs d'ondes?

g) *Mesures des propriétés relatives au rayonnement.* Plusieurs méthodes de mesure des propriétés relatives au rayonnement sont indiquées dans les mémoires. Quelles sont les méthodes disponibles pour mesurer les coefficients d'absorption et d'émission *in situ*, c'est-à-dire les méthodes non destructives?

h) *Absorbeur en nid d'abeille.* Quel est l'effet du nid d'abeille de Francia sur les pertes par convection provenant de la surface absorbant l'énergie? Quels matériaux et quelles techniques de fabrication peut-on utiliser? Quels sont les effets d'une couverture, si on en utilise une pour protéger les matériaux du nid d'abeille?

NEW MATERIALS IN SOLAR ENERGY UTILIZATION

Rapporteur's summation

In contrast to sessions on the applications of solar energy, the session concerned with agenda item III.B, on new materials, dealt with the relatively basic problems of how materials can be used in the construction and operation of solar heat exchangers (collectors). The properties of the materials of construction largely determine the performance of a solar collector (under specified conditions of radiation, orientation, and ambient conditions), its area for a specified output, and thus its cost. It follows that the cost of energy (or other product) delivered from the exchanger is substantially dependent on the materials used, their costs, and their properties. With solar energy being now economically competitive in restricted areas and applications, the use of new materials and new methods of solar exchanger construction noted at this session can in the future substantially enhance the potential breadth of solar energy applications.

The subject matter of the session was diverse, as was to be expected from consideration of the type of properties affecting solar exchanger performance. For convenience in noting the contributions to the session, the subjects have been divided into four categories, and will be dealt with in the following sections. These categories are: (*a*) energy-absorbing surfaces and their properties; (*b*) unique methods for control of radiation and convection losses from exchangers by use of honeycombs; (*c*) properties of transparent materials useful for covers for solar exchangers; and (*d*) properties of reflecting and refracting surfaces and support for them.

It may be noted that there was relatively little mention or discussion at the session of mechanical properties, which are of importance in determining how structural requirements may be met.

The material contained in the papers was not, for the most part, reviewed at the session, and reference must be made to the individual papers and to the General Report[1] for the material therein.

Energy-absorbing surfaces

The continuing interest in, and developments of, surfaces having the desirable properties of high absorptance for solar radiation and low emittance for long-wave radiation were well illustrated at this session. New data, of varying nature and indicative of the selectivity of the surfaces and their durability, were presented, particularly for high-temperature application on receivers for focusing solar exchangers. For example, nickel oxide on a platinum substrate was noted as applicable at temperatures of 800°C, with good selectivity. The effects of grooving or corrugating an energy-absorbing surface on its absorptivity for (beam) solar radiation and on its emissivity were discussed at some length, with the conclusion that grooving to provide multiple reflections, and thus high absorptivity, can result in very high absorptivity but at some sacrifice in increased emissivity. (A grooved surface having two reflections for normally incident radiation may have, for example, about two times the emissivity of the flat surface if the flat surface is highly selective.) The possibilities of development of selective paints, to provide selective surfaces by simpler and presumably less expensive processes, was also noted.

Radiation and convection loss control

Further data and commentary were provided on the use of non-isothermal honeycombs over energy absorbing surfaces to reduce radiation loss and suppress convection. The conical reflector systems using a honeycomb of glass were noted to have good efficiency at high temperatures, with relatively low concentration ratios. The need for orientation of the system, or use of honeycomb materials of high transparency for solar radiation, was noted, particularly if the absorber is to be used with a solar concentrator.

Transparent materials

Radiation and convection losses from solar heated surfaces can also be suppressed by transparent covers over the surface, and further information and commentary came forth at the session particularly on the use of plastic films. A review of a new paper on plastics and solar energy was presented; it dealt with the important problems of the weathering of plastics and its effect on their properties, with the measurement of weatherability by accelerated tests in chambers having severe conditions analogous to unfavourable weather (e.g., high ultraviolet radiation), and with ageing of plastics in various solar energy applications.

The use of plastic covers on solar stills is generally unsatisfactory on account of dropwise condensation occurring when water does not wet the plastics; a possible solution to this problem was noted by roughening the plastic. The maintenance of a con-

[1] Duffie, J. A., *Proceedings of the United Nations Conference on New Sources of Energy*, 1961; included above, paper GR/12 (S).

tinuous film of water between a plastic film and a metal collector plate, by taking advantage of the surface tension of water, may allow easy fabrication of a water heater.

Reflectors and refractors

More attention was given to this area than any other at this session, with interventions dealing with materials and methods of manufacture of reflectors and refractors. A cylindrical reflector (with a triangular receiver) and a concentration ratio of about 3, made of an inflated plastic cylinder clear in its upper portion and aluminised inside on its lower portion, has been shown to operate at 150°C; its developers consider that it can be produced for less than $20/m^2$. A method of construction of light-weight solar reflectors, with aluminium as the reflecting surface, supported on an aluminium "honeycomb sandwich" was described; the process provides duplicates of a master, which can be used repeatedly.

Two methods were proposed for local fabrication of reflectors: a technique for reflector fabrication by construction of a mould by rotation of a shaped knife about a vertical axis to form a plastic mould, with subsequent casting of plastic replicas on the mould; and a design for a coarse Fresnel reflector which would start with a single flat sheet of reflecting material to be cut and formed (without compound curvature) into conical sections. It was suggested that the only material needed for reflector manufacture to be supplied from outside a local area would be the reflecting material itself; aluminium foils and aluminized plastics were considered promising materials.

Conclusions

The discussions of this session dealt with a variety of materials, and the question must be asked: "In the light of the information made available in the formal papers and by interventions, what procedure might be followed in selecting new materials for solar-energy use?"

In a sense, it is unfortunate that we are unable to give a specific answer to this question. Too few cost data are available on most of the materials and techniques noted in the sessions. Furthermore, the effects of the properties of materials on exchanger performance (and thus on costs) are so dependent on the temperature and other characteristics of an application that a single recommendation for most economic energy delivery cannot be set forth. However, the application of sound, ordinary engineering and economic principles, with the unique aspects of solar energy applications taken into account, will provide adequate answers. Among these unique aspects of solar exchangers may be listed:

(*a*) The low energy density of received solar radiation, which dictates very low energy flux in the exchanger compared to usual heat exchanger practice and results in the exchanger's accounting for a major part (usually) of the cost of the total solar apparatus.

(*b*) The energy fluxes being low, performance is highly dependent on the poperties of materials affecting the fraction of incident energy which is absorbed and the thermal losses. Since these radiation properties are usually subject to deterioration for a number of reasons, the long-time value of the properties must be considered.

(*c*) The general observation may be made that low costs will usually be associated with good performance, but that there are many obvious exceptions, and small increments in collector performance may be more expensive than the gain in collected energy will justify.

(*d*) It may also be observed that performance of the exchanger may be interrelated with performance of the rest of a solar energy utilization system; ultimately the performance and costs of the complete system must be considered.

The basic objective of the considerations of materials is to minimize the cost (in whatever terms may be appropriate) of collected and delivered energy, at the desired temperature level. Knowledge of the properties and utility of materials can be described as very good, although we can conceive of ideal materials with better properties. Our knowledge of the costs of these materials, however, as they affect the cost of delivered energy, is in a less satisfactory state.

MATIÈRES NOUVELLES EMPLOYÉES DANS L'UTILISATION DE L'ÉNERGIE SOLAIRE

Résumé du rapporteur

A la différence des séances consacrées aux applications pratiques de l'énergie solaire, la séance consacrée au point III.B de l'ordre du jour, relatif aux matières nouvelles, a traité des problèmes relativement importants de la manière d'employer ces matières pour la construction et le fonctionnement des échangeurs de chaleur solaire (collecteurs). Des propriétés des matières employées dans la construction d'un collecteur solaire dépendent dans une grande mesure ses caractéristiques (dans des conditions données de rayonnement, d'orientation et de milieu ambiant), la surface qu'il doit avoir afin de fournir une quantité d'énergie donnée et, par suite, son coût. Il s'ensuit que le prix de l'électricité (ou de toute autre forme d'énergie produite par le collecteur) fournie par l'échangeur dépend essentiellement des matières utilisées, de leur coût et de leurs propriétés. L'énergie solaire étant déjà compétitive dans certains domaines limités, l'emploi de matières nouvelles et de procédés nouveaux de construction d'échangeurs solaires signalé à la séance peut élargir sensiblement à l'avenir la portée des applications pratiques de l'énergie solaire.

La question à l'ordre du jour de la séance présentait plusieurs aspects, comme il fallait s'y attendre vu le genre de propriétés qui influent sur le fonctionnement d'un échangeur solaire. Pour des raisons de commodité, nous avons divisé les sujets traités dans la séance en quatre catégories : *a*) surfaces qui absorbent l'énergie et leurs propriétés; *b*) élimination des pertes de rayonnement et de transmission de chaleur des échangeurs par l'emploi d'alvéoles; *c*) propriétés des matières transparentes pouvant servir de revêtements pour les échangeurs solaires; *d*) propriétés et support des surfaces réfléchissantes et réfringentes.

On notera que l'on a relativement peu parlé ou discuté en séance des propriétés mécaniques de ces matières, qui ont de l'importance quand il s'agit de déterminer la manière de répondre aux besoins structurels.

La plupart des renseignements contenus dans les mémoires n'ont pas été examinés en séance, et l'on doit se reporter à chaque mémoire et au rapport général [1] pour en connaître la teneur.

Surfaces absorbantes

L'intérêt continu que l'on porte aux surfaces qui ont les propriétés souhaitables de haut pouvoir absorbant pour les rayons solaires et de faible pouvoir émissif des radiations à grande longueur d'onde, ainsi que les progrès réalisés dans ce domaine, ont été bien mis en lumière lors de la séance. Diverses données nouvelles qui illustrent la sélectivité des surfaces et leur durée d'utilisation ont été présentées, en particulier en ce qui concerne le revêtement des collecteurs de concentration de hautes températures des échangeurs solaires. On a noté par exemple que l'oxyde de nickel sur pellicule de platine avait une bonne sélectivité à des températures de 800 °C. On a examiné de manière assez approfondie les effets que le rayage ou le striage d'une surface absorbante peuvent avoir sur son pouvoir absorbant pour un faisceau et sur son pouvoir émissif, et l'on a conclu que le rayage, qui a pour objet de provoquer la polyréflexion, et, par suite, d'élever le pouvoir absorbant, permet en effet de l'élever très fortement, mais il a l'inconvénient d'accroître le pouvoir émissif. (Une surface rayée réfléchissant dans deux directions un rayon perpendiculaire peut avoir, par exemple, un pouvoir émissif à peu près double de celle d'une surface plane si celle-ci est fortement sélective.) On a également noté la possibilité de mettre au point des peintures spéciales permettant d'obtenir des surfaces sélectives par des procédés plus simples et vraisemblablement moins coûteux.

Pertes de rayonnement et de transmission

Des données et des observations nouvelles ont été communiquées au sujet de l'emploi d'alvéoles non isothermes sur des surfaces absorbantes afin de diminuer les pertes de rayonnement et d'éliminer la convection. On a signalé que les systèmes à réflecteur conique utilisant des alvéoles en verre avaient un bon rendement à des températures élevées et un pourcentage de concentration relativement faible. On a noté que le système devait être pointé, ou qu'il fallait utiliser des matières très transparentes aux radiations solaires pour les alvéoles, surtout si l'on veut faire fonctionner l'absorbeur en même temps qu'un concentrateur solaire.

Matières transparentes

On peut également éliminer les pertes de rayonnement et de convection des surfaces chauffées

[1] J. A. Duffie, *Actes de la Conférence des Nations Unies sur les sources nouvelles d'énergie*, 1961; voir ci-dessus document GR/12 (S).

par le soleil en employant des revêtements transparents, et de nouveaux renseignements et observations ont été donnés en séance, notamment sur l'utilisation de revêtements en matière plastique. On a analysé un mémoire nouveau sur les matières plastiques et l'énergie solaire dans lequel l'auteur traite des problèmes importants de l'altération des matières plastiques et de son effet sur leurs propriétés, des moyens de mesurer l'altérabilité par des tests accélérés en chambre où les matières sont soumises à des conditions rigoureuses similaires aux intempéries (par exemple, fort rayonnement ultra-violet), et du vieillissement des matières plastiques dans diverses utilisations pratiques de l'énergie solaire.

L'emploi de revêtements en matière plastique pour les alambics solaires est généralement peu satisfaisant, parce qu'il se produit une condensation sous forme de gouttelettes quand l'eau n'humidifie pas la matière plastique; on a signalé une solution possible de ce problème consistant à utiliser un revêtement rugueux en matière plastique. Le maintien continu d'une pellicule d'eau entre une pellicule de matière plastique et un collecteur plan métallique peut, grâce à la tension superficielle de l'eau, permettre de fabriquer facilement des chauffe-eau.

Réflecteurs et réfracteurs

On s'est intéressé plus à ce domaine qu'à aucun autre au cours de cette séance, et les interventions ont eu pour objet les matières et les méthodes de fabrication des réflecteurs et réfracteurs. On a présenté un réflecteur cylindrique (avec récepteur triangulaire) ayant un taux de concentration de 3 environ, fait d'un cylindre gonflé en matière plastique de teinte claire au sommet et aluminisé à l'intérieur et à la base qui fonctionne à une température de 150 °C; des constructeurs estiment que son prix de revient peut être inférieur à 20 dollars le mètre carré. On a exposé une méthode de construction de réflecteurs solaires légers dont la surface réfléchissante, en aluminium, est montée sur un bâti d'aluminium en « sandwich alvéolé »; on procède par moulage d'une matrice qui peut être utilisée un grand nombre de fois.

On a proposé deux méthodes pour la fabrication locale de réflecteurs : la première consisterait à faire tourner un couteau de forme voulue autour d'un axe vertical de manière à former une matière plastique, à partir de laquelle seraient ensuite faits des moulages en matière plastique; la deuxième méthode concerne la fabrication d'un réflecteur de Fresnel grossier fait essentiellement d'une seule feuille de matière réfléchissante que l'on découpe et à chaque partie de laquelle on donne une forme (sans courbure composée) conique. On a laissé entendre que la seule matière nécessaire pour fabriquer un réflecteur qu'on ne trouverait pas sur place serait la matière réfléchissante elle-même; on a estimé que les feuilles d'aluminium et les matières plastiques aluminisées sont des matières intéressantes.

Conclusions.

Les débats de cette séance ont porté sur des matières diverses et il y a lieu de se demander, compte tenu des renseignements donnés dans les mémoires et au cours des interventions, quelle pourrait être la procédure à suivre pour déterminer quelles sont les matières nouvelles qui pourraient servir dans l'utilisation de l'énergie solaire.

Il est regrettable, en un sens, que nous ne soyons pas en mesure de donner une réponse précise à cette question. Mais on a encore trop peu de données concernant les prix de la plupart des matières et des techniques dont il a été question en séance. De plus, les propriétés des matières et leurs effets sur le rendement des échangeurs (et, par suite, sur les coûts) dépendent tant de la température et d'autres caractéristiques de l'appareil qu'il est impossible de formuler une recommandation unique touchant le moyen le plus économique de produire de l'énergie. Cependant, la mise en œuvre de principes techniques et économiques sûrs et simples, compte tenu des aspects uniques des appareils solaires, fournira les réponses voulues. Parmi ces aspects uniques des échangeurs solaires ont peut citer :

a) La faible densité énergétique du rayonnement solaire capté, qui impose un flux d'énergie très faible dans l'échangeur, à la différence de ce qui se passe généralement dans un échangeur classique, et qui fait que l'échangeur représente (en général) une grande partie du coût de l'ensemble de l'installation solaire;

b) Le flux d'énergie étant faible, le rendement de l'appareil dépend en grande partie des propriétés des matières, qui déterminent la quantité d'énergie incidente absorbée, et des pertes thermiques. Les propriétés relatives au rayonnement tendant généralement à s'altérer pour plusieurs raisons, il faut tenir compte de la longueur de la période pendant laquelle elles demeurent intactes;

c) On peut observer en règle générale que le plus souvent si les coûts sont peu élevés le rendement est bon; mais les exceptions sont évidemment nombreuses et de petits gains de rendement du collecteur peuvent être plus coûteux que le justifie l'augmentation de la quantité d'énergie captée;

d) On peut également observer que le rendement de l'échangeur peut être lié à celui du reste de l'appareil solaire; en fin de compte, il faut prendre en considération le rendement et les coûts de l'installation tout entière.

L'étude des matières a pour objectif essentiel de minimiser le coût (en termes les plus appropriés) de l'énergie captée et fournie à la température souhaitée. On peut dire que la connaissance des propriétés des matières et de la manière de les employer est excellente, mais on peut concevoir des matières idéales ayant des propriétés meilleures. Ce que nous savons des coûts de ces matières, dans la mesure où ils influent sur le coût de l'énergie fournie, laisse toutefois à désirer.

SOLAR FOCUSING COLLECTORS OF PLASTICS

F. Daniels and R. H. Breihan *

Attempts have been made to develop focusing collectors which can be made without highly skilled labor and without electricity or special manufacturing facilities. High optical precision is unnecessary for producing temperatures in the neighborhood of 500°C, which is sufficient for heat engines, refrigerating units and thermoelectric converters. These temperatures can be achieved with reflectors made of aluminized sheet plastics supported on plastic shells made by hand. A simple equatorial mounting for such a collector is described in this paper.

Two types of setting plastic have been used. Epoxy resin and hardener are mixed in the ratio of 4 to 1 and set at room temperature within a few hours. This type of material adheres well to Mylar film and to aluminum surfaces. A polyester resin, mixed with a small amount of accelerator, is useful also. It costs about half as much as the epoxy, but it is less adherent to aluminized surfaces. These liquid plastics are applied to curved surfaces of fibre-glass cloth, or fiber-glass matt, and they set to give hard permanent shapes. (This technique is widely used in the construction of boats, and the materials can be purchased from motorboat supply houses.) Fine and coarse cloth can be used instead of the fiber-glass, but they are weaker and less permanent on long exposure to outdoor weather.

Experimental techniques

The simplest focusing collectors were made by cutting a circular hole 40 inches in diameter in a rectangle of reinforced plywood, and stretching aluminized Mylar one mil thick over the hole. A layer of cloth and of burlap is stretched over the aluminized surface of the Mylar, and a heavy coating of liquid plastic is applied. The frame is then inverted and supported at the edges while fine sand is piled onto the stretched Mylar, causing it to sag like a hammock. After setting overnight the plastic hardens, the sand is poured out, and a reasonably good focusing reflector is obtained. It is not a true parabolic shape, but resembles a catenary. Fairly good, but not sharp, focusing is obtained, sufficient for use with a cooking vessel.

Replicas were made of a searchlight 5 feet in diameter. Here, of course, the shape was excellent. The searchlight was rubbed thoroughly with automobile body wax (as a parting compound), and then fiber-glass matt was packed in and soaked with the liquid plastic. After setting, it was removed from the searchlight reflector, and the convex replica was used as a mold on which to make several concave collectors with stretched aluminized Mylar, fiber-glass matt or cloth, and plastic.

The best reflecting surface with the aluminized Mylar was obtained by inflation techniques. The stretched aluminized surface gives a clearer reflected image and a higher measured reflectivity than when the Mylar is attached to another surface. A large circle of aluminized plastic was sealed at its edge to a flat board, and the space between the plastic and the board was inflated with a hand pump. The curved surface was then covered with plastic and fiber-glass matt. Small leaks led to an imperfect shape while the plastic was hardening. Better results were obtained by making a circular ring of ½ inch thin-walled tubing and attaching layers of aluminized Mylar and clear Mylar to the two sides of the ring with adhesive tape (Scotch tape) and soldering an automobile tire valve through the ring. The space between the two circles of plastic were then inflated with compressed air attached to a small leak arranged so that a constant pressure was maintained while the fiber-glass plastic form was setting.

A good 6-foot parabolic reflector was made by revolving a parabolic knife edge around a central vertical tube. The central tube was surrounded with a pile of sand, which was shaped by the rotating knife. Building plaster was then piled on top of the sand, and while setting it was shaped to a parabolic shape with the rotating knife edge. The paraboloid plaster mold was then used to form the focusing reflector. Pie-shaped sections of aluminized Mylar were laid over the mold and attached together with adhesive Scotch tape. The outer edges of these sections were attached to a ring of steel tubing 6½ feet in diameter with adhesive tape, and the ring was then forced down around the edge of the plaster mold. A slightly smaller ring of tubing 6 feet in diameter was then laid on the stretched Mylar, and the fiber-glass matt and liquid plastic were then applied and allowed to set over night. The extra plastic outside the smaller hoop was then cut away and the focusing reflector removed from the mold, the smaller ring serving as a rim on the finished reflector.

Good focusing was obtained with this reflector, as determined by photographic measurements with moonlight and by calorimetric measurements as

* University of Wisconsin, Madison, Wisconsin.

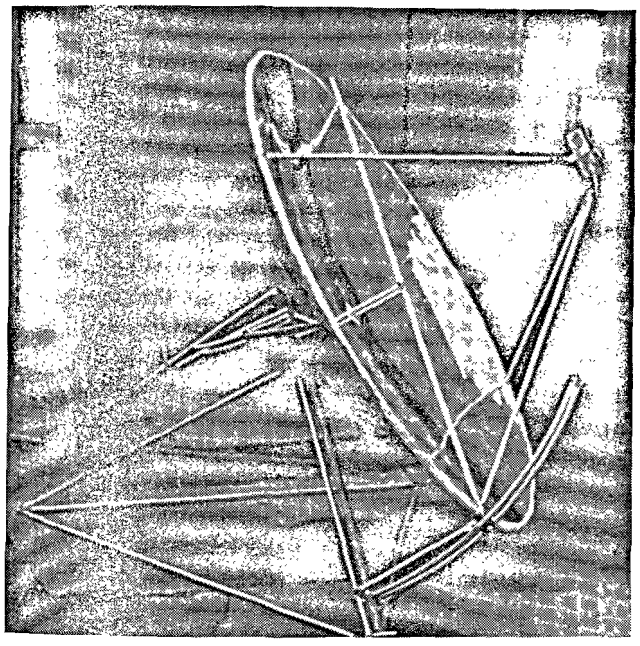


Figure 1. Focusing collector of plastic, six feet in diameter, with metal stand

described in another paper presented at this symposium.[1]

The amount of solar radiation focused onto a given target was determined calorimetrically by holding a heavy, blackened copper target at the focus for short periods of time and immediately plunging it into a calorimeter can holding 500 milliliters of water. The copper block was immersed in the water of the calorimeter for two minutes to achieve the temperature of the calorimeter and quickly dried before exposure to the focused radiation. After exposure, the copper block was immersed immediately in the calorimeter, and the rise in temperature was measured with a 1/10° thermometer. A knowledge of the heat capacity of the water and copper block and copper calorimeter can and the temperature rise permitted calculation of the heat received. The solar radiation intercepted by the reflector was calculated from the area and a solar radiation meter measuring the beam radiation.

[1] Breihan, R. R., Daniels, F., Duffie, J. A., and Löf, G. O. G., Preliminary Tests of a Solar Heated Thermoelectric Unit, *Proceedings of the United Nations Conference on New Sources of Energy*, 1961; included above under agenda item II.C.1 (*b*) (i), paper S/103.

Mounting stand for focusing reflector

The stand is shown in figure 1. It is made by hand from ½ inch thin-walled galvanized steel tubing used for electric conduits. The various parts are cut to length, and the ends flattened in a vise. They are then drilled and held together with bolts. Two thrust ball-bearing mountings permit easy rotation of the central tube one-inch in diameter. It is pointed north and south, and it is adjusted for latitude and season. Each week the axis is changed, depending on the declination. The rotation east and west from 8 am to 4 pm is accomplished with a heavy counterpoise. Each morning the collector is tilted by hand toward the sun and the counterpoise swings it around steadily through the day. The rate of turning from east to west is controlled by leakage of oil through a small valve as it is forced by a tightly fitting piston from one end of a cylinder to the other. Plans are under way for a sun-tracking attachment; without this it was frequently possible to adjust the valve so that the collector turned with the sun and kept the focus on the target for periods of one to three hours.

The cost of the solar collecting unit shown in figure 1, at United States retail prices, and excluding labor and the tracking unit piston and cylinder, is summarized below:

	$
½ in. steel conduit (at 8 cents per foot), circular rim of 6 ft collector and mount, 80.5 ft	6.40
Axis 1″ conduit 5½ ft	.75
2 thrust bearings with ball bearings	2.00
1 door hinge	.40
2 iron plates 6″ × 3″ × 3/16″	.50
Polyester plastic, 2 gallons	12.00
Fiber-glass matt, 28 sq ft (30 cents per sq ft)	2.80
Aluminized Mylar, 28 sq ft (5 cents per sq ft)	1.40
Cradle and support for thermoelectric unit (shown in photograph)	2.00
28 bolts	1.75
TOTAL	30.00

The solar reflector is expected to deliver 1½ kW of heat to a target 5 inches square. The cost per square foot of collecting area is approximately $1.00.

Summary

Several types of plastic focusing reflectors with aluminized Mylar polyester film reflecting surfaces are described in this paper. They include focusing shapes made by replicas from searchlight reflectors, by sagging hammocks, by inflated bubbles and by rotating parabolic knife edges. The efficiency of concentration of radiation is measured calorimetrically.

A satisfactory tripod arrangement with a rotating axis is described; this is easily made from half-inch galvanized steel thin-walled tubing used for electric conduits. Adjustment is made weekly for the season, and a counterpoise and oil leak allow the collector to follow the sun during the day, with occasional hand adjustments. Cost estimates are given in the paper.

COLLECTEURS DE CONCENTRATION SOLAIRE EN COMPOSITION PLASTIQUE

Résumé

Ce mémoire décrit plusieurs types de réflecteurs de concentration en matière plastique recouverts d'une pellicule d'un polyester au Mylar aluminisé, et en particulier des formes de concentration faites en constituant des reproductions de réflecteurs de projecteurs, des hamacs avec flèche au centre, ou des bulles gonflées, ou encore en imprimant un mouvement de rotation aux lames de couteaux paraboliques. Le rendement de la concentration du rayonnement est mesuré par des procédés calorimétriques.

Les auteurs décrivent un dispositif satisfaisant à trépied et à axe rotatif, que l'on peut facilement construire avec du tube de 1/2 pouce (13 mm) à parois minces en acier galvanisé, du type dont il est fait usage pour les conduits électriques. On procède au réglage hebdomadairement pendant la saison; un contre-poids et une fuite d'huile permettent au collecteur de suivre le soleil pendant la journée, avec des réglages manuels occasionnels. Le mémoire donne des évaluations des prix.

PLASTIC FILMS FOR SOLAR ENERGY APPLICATIONS

F. E. Edlin and D. E. Willauer *

In the past, plastic films have been unsuited for solar energy applications because of their short life outdoors, poor mechanical strength, and low melting temperature. New strong, temperature-resistant plastic films are being developed which are quite resistant to outdoor ageing under severe operating conditions. Also, new treatments are improving the requisite properties of older plastic films. As a consequence, successful experiments in the collection of solar energy have utilized these new materials.

Plastic films which are discussed

New types of plastic films which are made from new polymers include a tetrafluoroethylene hexafluoropropylene copolymer hereafter designated "Teflon" [1] FEP-fluorocarbon film; and a polyvinyl fluoride film, hereafter designated "Tedlar" [2] PVF film. New modifications have been developed for polyethylene terephthalate film, hereafter designated Type W "Mylar" [3] polyester film, and for polyethylene film, which extend the outdoor usefulness of these low-cost materials.

1. "Mylar" and "Teldar" are modified physically during manufacture to cause the molecular structure to become oriented, thereby improving the mechanical strength properties. "Teflon" FEP and polyethylene film with little molecular orientation are superior in other physical properties.

2. In general, plastic films are not satisfactorily substituted directly for a vitreous glazing in conventional designs. New structural designs are required to take advantage of the favorable properties and minimize the unfavorable properties of plastic films. Different structures and operating conditions will usually dictate the choice of a specific plastic material. Data and information are presented to exemplify and compare various properties of plastic films for consideration and choice for outdoor and solar energy applications.

3. The data which are presented are intended to serve as a guide to the selection of plastic materials for evaluation. The environmental and structural conditions for specific applications may differ significantly from those of the standard test procedures. Thus, the basic requirements of films for the commercialization of products should be reviewed and critical properties should be checked carefully.

* E. I. du Pont de Nemours and Co., Inc., Wilmington, Delaware, United States.

[1] "Teflon" is Du Pont's registered trademark for its FEP-fluorocarbon film.

[2] "Tedlar" is Du Pont's trademark for its polyvinyl fluoride film.

[3] "Mylar" is Du Pont's registered trademark for its polyester film.

Properties of plastic films

The selection of a plastic film for solar energy application must complement the process design so that the most economical costs are obtained. Due consideration will be given to the initial investment, its rate of amortization, and the production capability. Generally, the service life and replacement costs are major economical factors. Weatherability of plastic film is therefore of commanding interest in evaluating economic practicability.

Weatherability

The weatherability of a plastic film is a complex property which describes its probable useful life outdoors for a variety of applications. Weatherability is stated in arbitrary and relative terms for specific conditions. The property of weatherability is the net result on the optical, physical and chemical properties of a plastic film from its reaction to many environmental and structural factors. Resistance to photodegradation is a major requirement. Resistance to oxidation, thermal ageing, hydrolysis and chemical reaction, and several kinds of mechanical stress may also determine the useful life of a film.

1. One measure of the weatherability of a plastic film is determined by exposing samples at a south-facing angle of 45° in a hot, humid climate of high solar radiation intensity, such as southern Florida, for a period of years. Film life is assumed as the period when the tensile elongation is thereby reduced to 10 per cent. Transparency, color, and surface properties must be relatively unaffected. This test is reliable for estimating the life of non-weatherable films having a life of one year or less. However, this test can be misleading for weatherable films having a longer life. For example, when the tensile elongation of "Tedlar" film has decreased to 10 per cent by exposure for nine years, the tensile strength is 50 per cent of its original value and the clarity is relatively unaffected. Complete embrittlement requires an additional four years' exposure.

2. The Florida test results for weatherability given in table 1 are based on 10 per cent residual tensile elongation. The weatherability life of "Tedlar" (1, 2) and "Teflon" FEP-fluorocarbon film is esti-

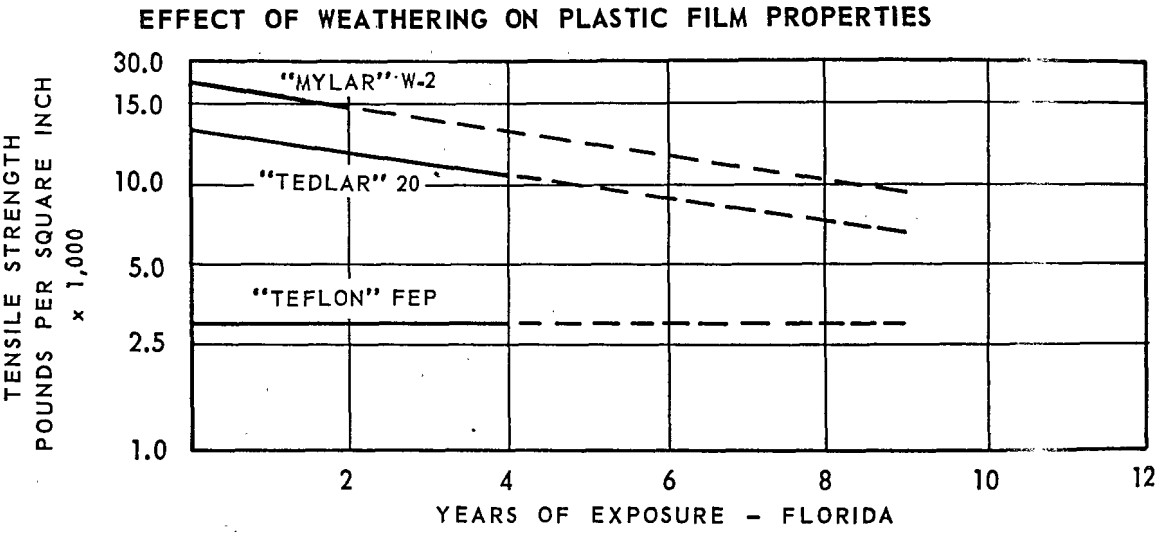


Figure 1. Tensile strength of films and exposure time

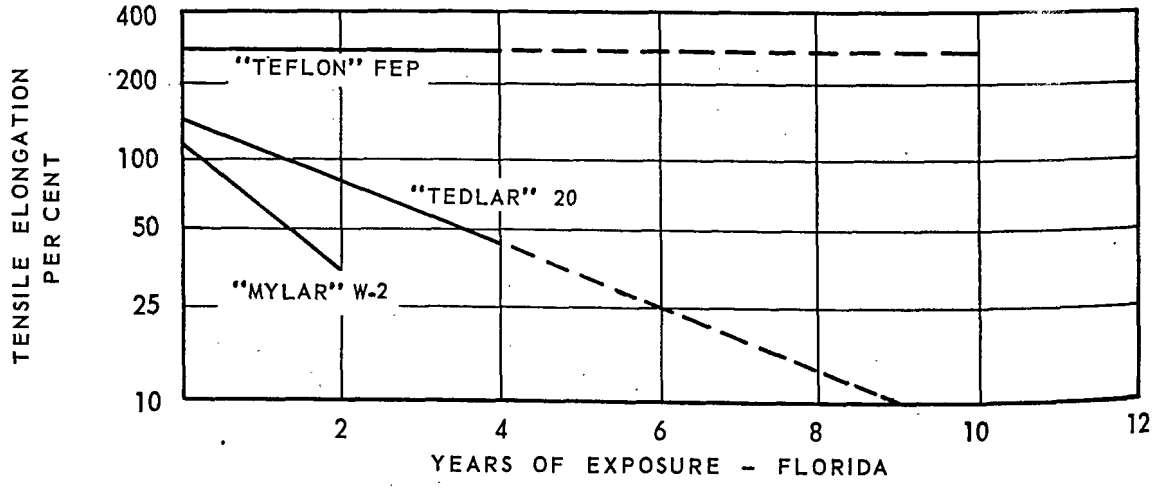


Figure 2. Tensile elongation of films and exposure time

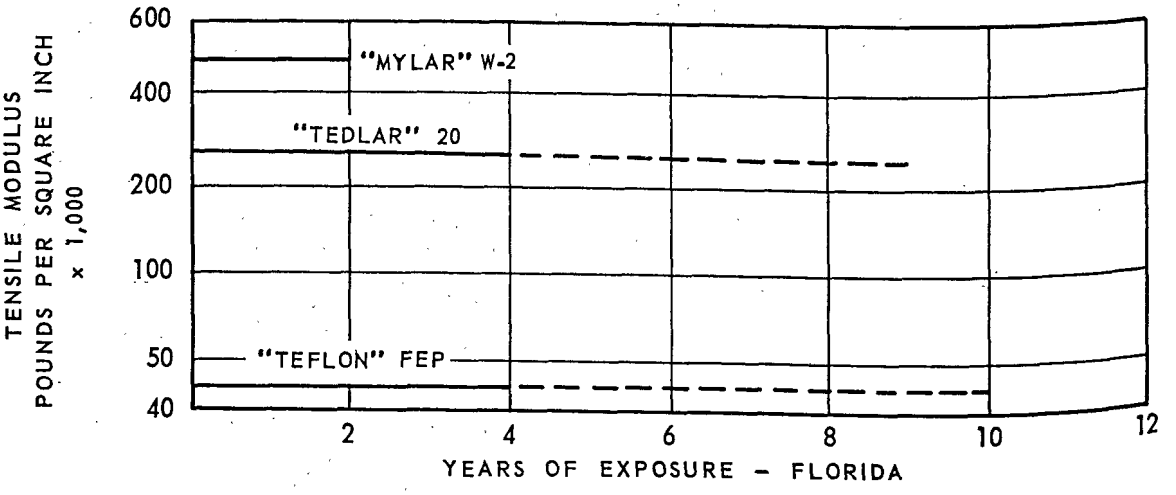


Figure 3. Tensile modulus of films and exposure time

Table 1. Exposure life (weatherability) of plastic films

Film	*Thickness (mils)*	*Life[a] in Florida (test years)*
"Teflon" FEP	2	20+ [b]
"Tedlar"	2	9 [b]
"Mylar", type W	5	4 [b]
"Mylar", type A	5	1/4
Polyethylene	4	1/4
PVC (unplasticized)	5	1/2
Cellulose acetate butyrate	5	1/2

[a] The exposure life is the time required to decrease the tensile elongation to 10 per cent. Exposure samples are mounted, unsupported (attached at edges only) on test racks facing south at an angle of 45°.

[b] Projected life.

mated from accelerated weathering tests, correlated with shorter periods of exposure in Florida. Early, experimental polyvinyl fluoride films, upon exposure in Florida, have retained 50 per cent of their original tensile elongation after ten years (3). Another sample was clear and strong after an outdoor exposure of 16 years. The effect of weathering on the plastic film properties of tensile strength, tensile elongation and tensile modulus is given in figures 1, 2 and 3, respectively.

3. The rate of degradation of "Tedlar", "Mylar", and polyethylene may be increased from 1.5 to 3 for each 10°C rise in temperature. There does not appear to be a similar increase in degradation for "Teflon" FEP-fluorocarbon film. The correlation between degradation rate and weatherable life is not known. Mechanical stress points and wind-flutter severely reduce the life of weatherable films. Minor stress irregularities in large glazings will be minimized after several months from "cold-flow" of the plastic film along stress lines.

4. Transparent plastic films may be adhered to rigid substrates, whereby their weatherable life is increased substantially. "Tedlar" PVF film, with an unsupported normal outdoor life of nine years, may be bonded to a rigid substrate and an outdoor life of as much as 20 years may be obtained. Also, the addition of some pigments to films greatly increases their weatherable life. Transparent polyethylene and polyvinyl chloride films which normally have a weatherable life of less than a year may be compounded with 2 to 3 per cent of carbon black, antioxidants and other chemicals, whereby the life may be increased by a factor of as much as 20.

Physical properties

Molecularly oriented plastic films such as "Tedlar" and "Mylar" W offer the advantages of high tensile impact and burst strengths. Films with lesser degrees of orientation, such as polyethylene, "Tedlar" Type 40, and "Teflon" FEP, are superior with respect to tear strength, elongation, and shrinkage at elevated temperatures. The physical properties of seven plastic films are compared in table 2.

1. The effect of heat ageing on the plastic film properties of tensile strength, tensile elongation, impact strength and flexure is given in figures 4, 5, 6 and 7, respectively. The tensile strength and tensile elongation of "Teflon" FEP film are unchanged after 10 000 hours exposure in air at 200°C. Although "Tedlar" and "Mylar" W films have relatively good ageing properties at 150°C, service temperatures should be kept below 100°C.

2. The effect of temperature on the plastic film properties of tensile strength, tensile elongation and tensile modulus is given in figures 8, 9 and 10, respectively. Molecularly oriented "Tedlar" and "Mylar" films lose some of their orientation at higher temperatures, and consequently their tensile properties approach those of unoriented films.

3. The effect of steam ageing on the plastic film properties of tensile strength, tensile elongation and tensile modulus is given in figures 11, 12 and 13, respectively. The mechanical strength of "Tedlar"

Table 2. Physical properties of plastic films

	"Teflon" FEP	*"Tedlar" 20*	*"Tedlar" 40*	*"Mylar" W*	*Polyethylene*	*Cellulose acetate butyrate*	*PVC (unplasticized)*
Thickness, mils	2.0	2.0	2.0	5.0	4.0	5.0	2.0
Density, g/cc	2.15	1.38	1.38	1.39	0.91	1.19	1.36
Refractive index, n_D	1.34	1.45	1.45	1.64	1.5	1.48	—
Tensile strength, psi, 25°C	3 000	16 000	8 000	24 000	2 000	7 500	7 200
Tensile modulus, psi, 25°C	43 000	260 000	260 000	550 000	40 000	225 000	360 000
Tensile elongation, per cent, 25°C	300	135	250	100	500	50	110
Impact strength, kg cm/mil, 25°C	4	5.7	2	5.8	1.5	2.3	0.3
Mullen burst strength, psi/mil, 25°C	—	40	15	52	—	60	13
Tear strength, g/mil, 25°C	125	18	180	33	300	4	—
Accelerated flex life, cycles, 25°C	90 000	230 000	10 000	5 000	40 000	80	1 300
Coefficient of friction (film to film)	0.09	0.4	0.4	0.4	0.4	0.5	0.4
Zero strength temperature, °C	290	> 300	> 300	250	110	190	180
Thermal conductivity, Btu/hr sq ft	1.35	—	—	1.05	1.6	—	—
Thermal coefficient of linear expansion, inches/inch (°F)	60×10^{-6}	24×10^{-6}	24×10^{-6}	15×10^{-6}	300×10^{-6}	50×10^{-6}	—
Shrinkage at 130°C, per cent	3	3	Neg.	1	Melts	30	40

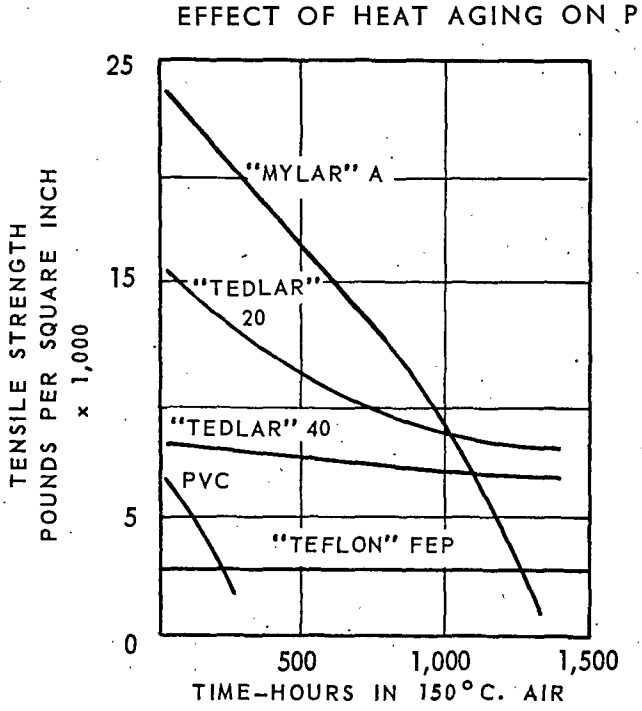


Figure 4. Tensile strength of films exposed to hot air

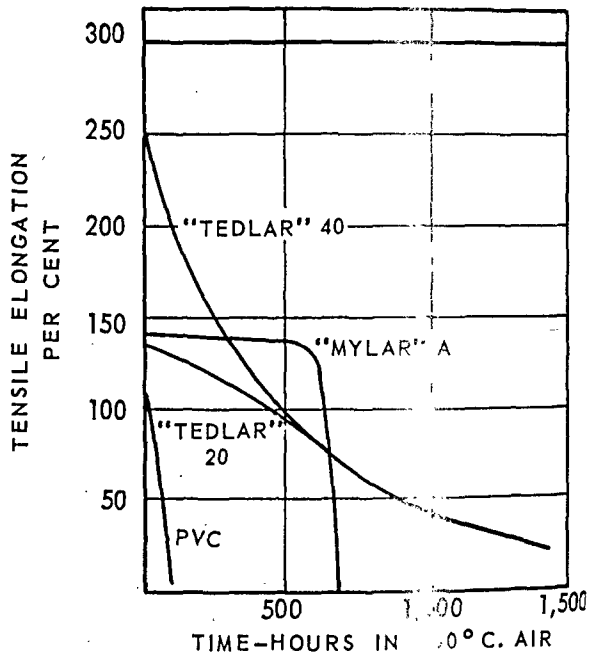


Figure 5. Tensile elongation of films exposed to hot air

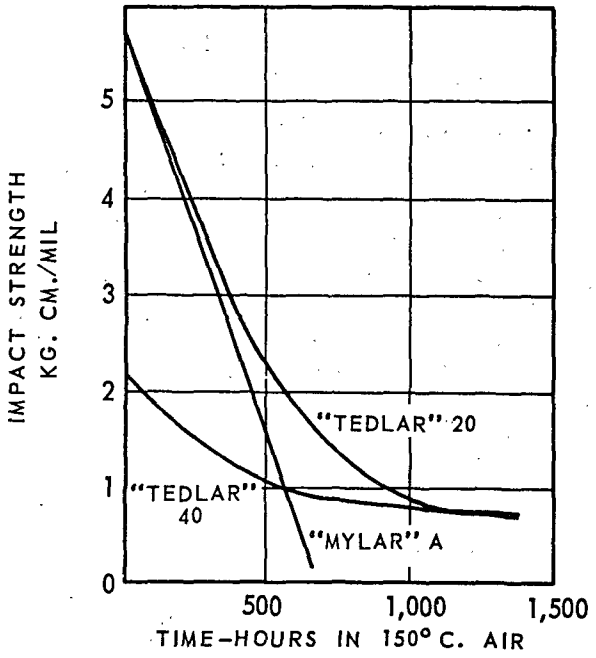


Figure 6. Impact strength of films exposed to hot air

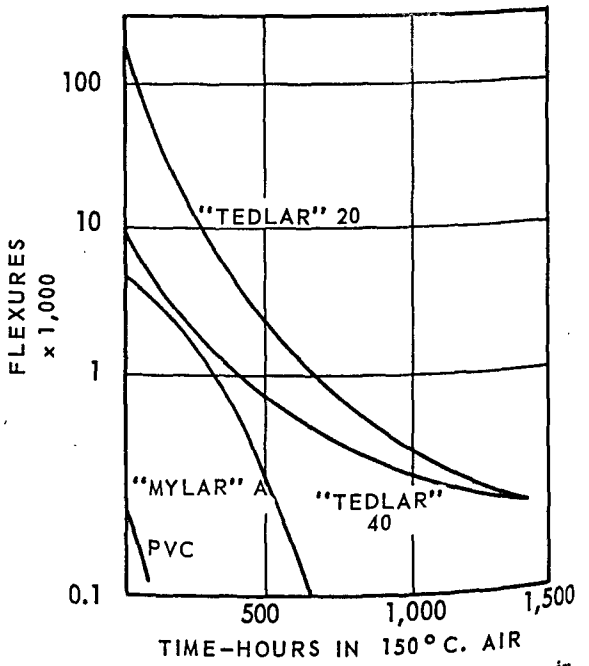


Figure 7. Flexure life of films exposed to hot air

and "Teflon" FEP films is relatively unaffected by steam ageing while the strength of "Mylar" polyester film decreases.

4. Air-supported plastic film structures and taut plastic glazings which are unsupported for several feet are best designed using films of high tensile strength, low tensile elongation and resistance to flexural fatigue. Empirically, design stresses of film systems are usually kept below 10 per cent of the weathered tensile properties. Transient stresses of short duration which are due to gusts of wind, rain, mechanical loading and movement, etc., should not exceed one-fourth of the weathered tensile strength.

Heat-sealing properties

The polyethylene films are readily heat-sealed by bar, rotary band and other commercial units.

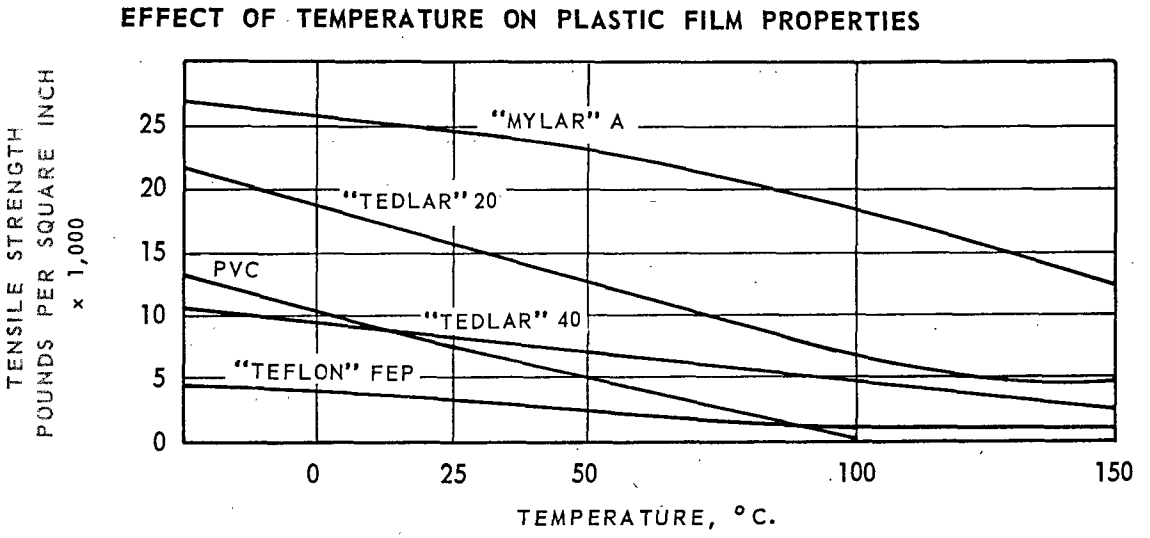


Figure 8. Tensile strength of films and temperature

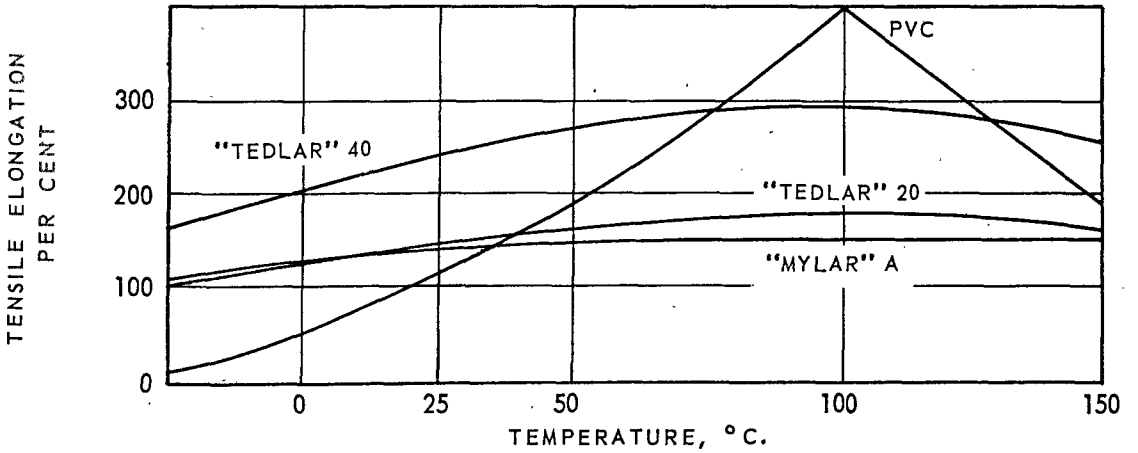


Figure 9. Tensile elongation of films and temperature

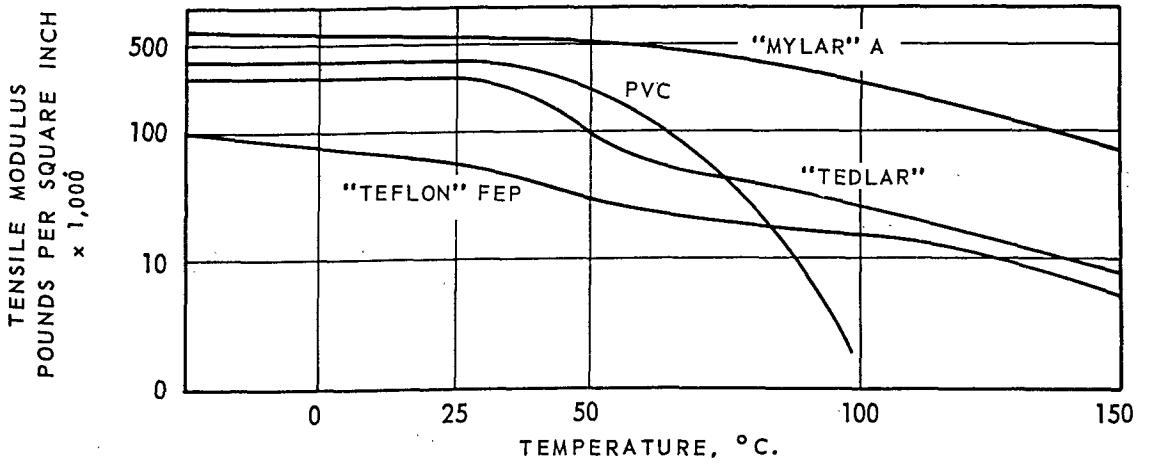


Figure 10. Tensile modulus of films and temperature

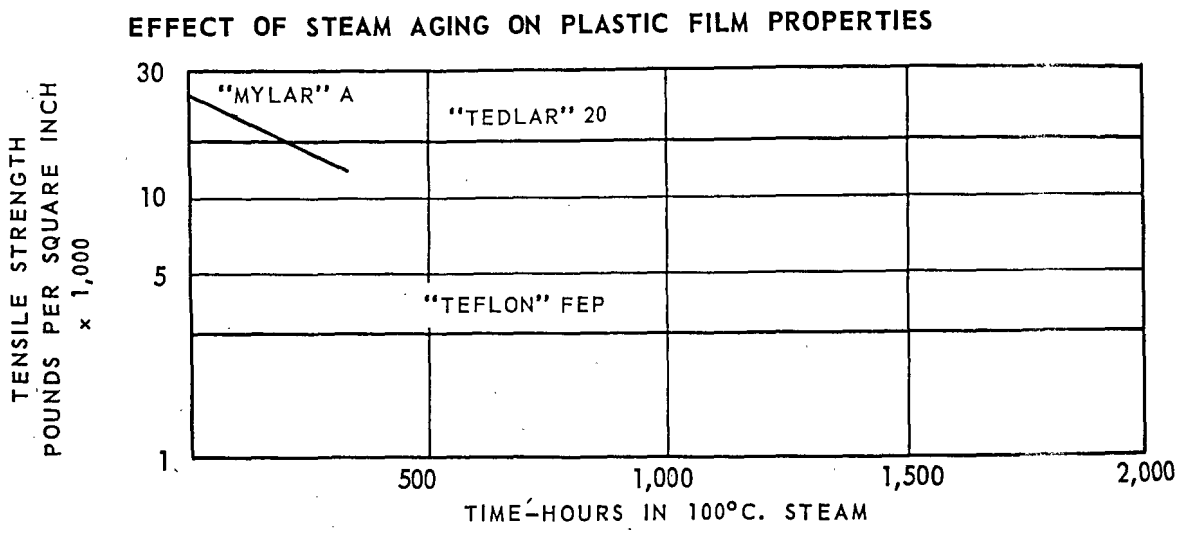


Figure 11. Tensile strength of films exposed to steam

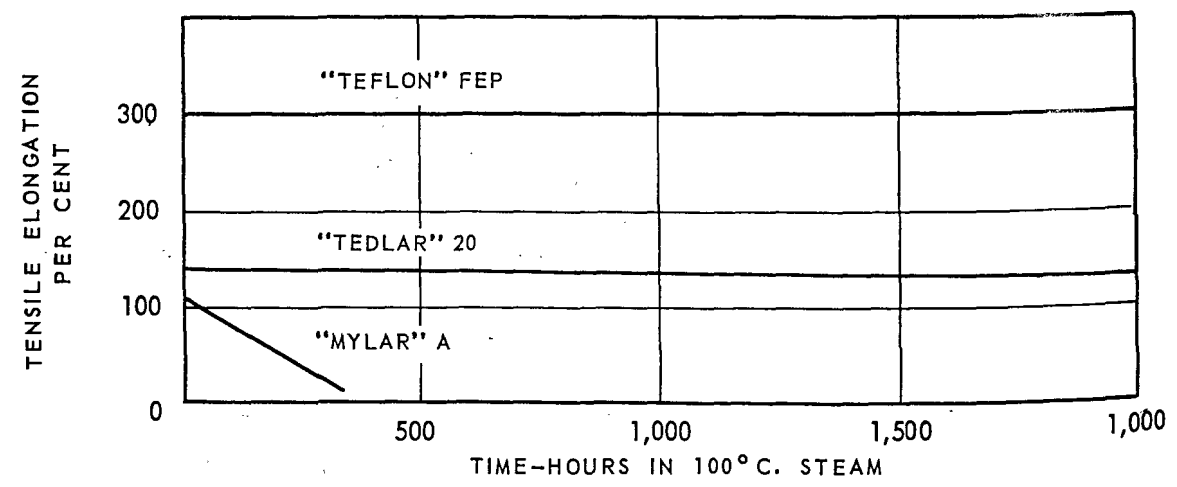


Figure 12. Tensile elongation of films exposed to steam

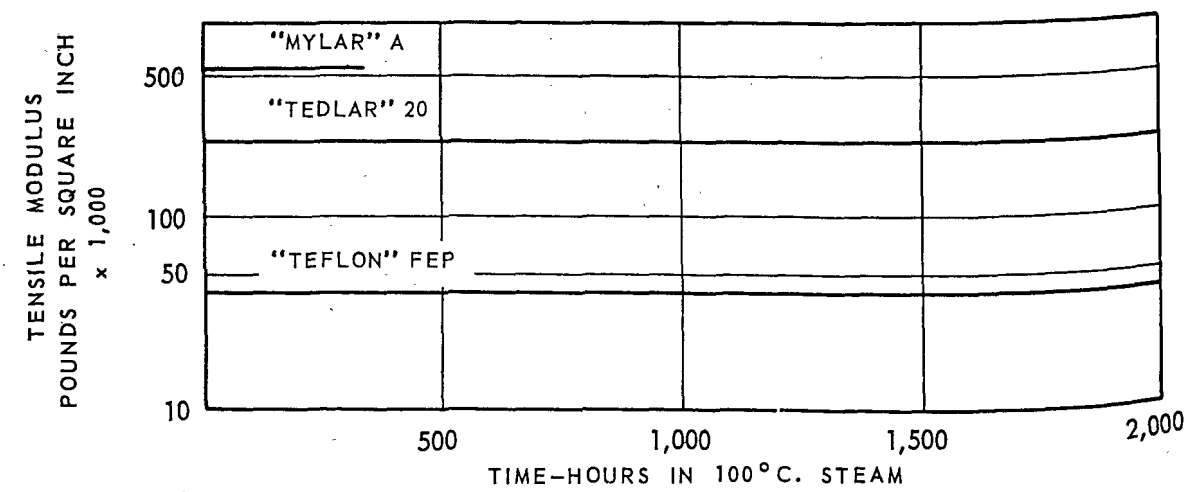


Figure 13. Tensile modulus of films exposed to steam

Table 3. Chemical resistance of plastic films

	"Teflon" FEP	*"Tedlar"*	*"Mylar"*	*Polyethylene*
10 per cent HCl				
1 wk. at 25°C	1	1	1	1
2 hr. at boil	1	1	1	1
10 per cent NaOH				
1 wk. at 25°C	1	1	1	1
2 hr. at boil	1	1	2	—
Acetone				
1 wk. at 25°C	1	1	1	1
2 hr. at boil	1	1	1	1
Benzene				
1 wk. at 25°C	1	1	1	1
2 hr. at boil	1	1	1	2
Carbon tetrachloride				
1 wk. at 25°C	1	1	1	1
2 hr. at boil	1	1	1	2

1 : no change in physical properties.
2 : dissolves.

"Mylar" film is very difficult to heat-seal in substantial lengths, and is generally classed as not heat-sealable. Adhesives are available for sealing "Mylar" film for a variety of applications. "Tedlar" film is available in two modified forms, one that is heat-sealable and one that is receptive to adhesives. Heat-sealing of relatively simple structures of "Tedlar" may be done with the impulse bar or rotary band sealers. Complex structures of "Tedlar" are more readily heat-sealed with dielectric or ultrasonic devices. A seal peel-strength of up to 20 pounds per lineal inch may be obtained on "Tedlar" 3 mil film, although peel-strengths of 12 to 15 pounds are more common at present. Heat-seal shear strengths up to 80 per cent of the film tensile strength may be obtained with "Tedlar". "Teflon" FEP film may be fabricated by both conventional heat-sealing and thermal welding techniques.

Chemical properties

Plastic films such as "Tedlar" and "Teflon" FEP which contain fluorine are generally quite resistant to chemical attack. Weatherable plastic films are generally hydrophobic. Chemical resistance decreases with increased temperature, mechanical stress and often with radiation intensity. There has been no indication that sea water has any greater effect on weatherable plastic films than fresh water at moderate temperatures.

1. The chemical resistance of "Teflon" FEP, "Tedlar", "Mylar" and polyethylene films for a number of chemicals is summarized in table 3. "Teflon" FEP film is compatible with other usual materials of construction. "Tedlar" film is slowly degraded by intimate contact with other materials which contain halogens. Chlorine-containing synthetic rubbers and elastomeric materials, for example, which may be used as adhesives, seals and gaskets, appear to reduce the local weatherability of "Tedlar" film under rigorous weathering conditions due to chemical interaction. "Mylar" film is resistant to neutral chemicals but may be attacked slowly by acidic and alkaline materials such as organic acids and moist lime mortar.

2. Reflective films of aluminum, vapor-deposited in-vacuuo on "Mylar" and "Teflon" FEP films as second surface coatings and protected from the weather are usually quite durable. Aluminum coatings which have been deposited on "Tedlar"

Table 4. Permeability of plastic films to gases

g/100 metres^2, hr, mil of thickness

	"Teflon" FEP	*"Tedlar"*	*"Mylar"*	*Polyethylene*
Oxygen, 25°C	30	0.3	0.35	18
Nitrogen, 25°C	12	0.02	0.04	2.4
Carbon dioxide, 25°C	40	1.4	1.8	97
Water vapour, 40°C.	40	180	160	100
Ethanol, 35°C	4	35	1	—
Ethyl acelate, 35°C	—	1 000	55	9 500
Acetic acid, 35°C	27	45	3	—
Acetone, 35°C	56	20 000	350	4 000

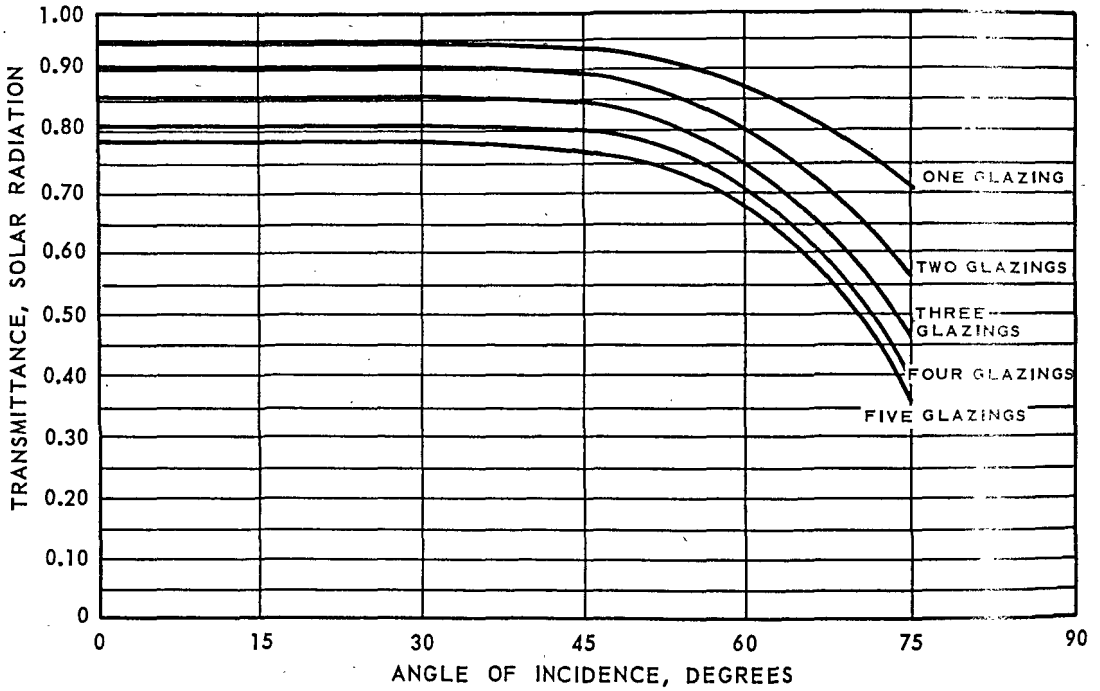


Figure 14. Transmittance of solar radiation through one to five glazings of "Tedlar" film for various angles of incidence

film have lost their relfletivity upon exposure for a year due to chemcai incteraction. New processes now being tested are expected to produce a "Tedlar" film which can be given a more permanent aluminum coating. The reflectance data for aluminized "Tedlar" film which are given in the annex were measured on samples of stabilized material.

3. The permeability of "Teflon" FEP, "Tedlar", "Mylar" W and polyethylene films to eight gases is given in table 4. The permeability of films to gases increases substantially with temperature. The permeability of "Tedlar" film increases the more rapidly. "Tedlar" film has a water vapor permeability of 340 g/100 square meters, hour, mil, at 65°C.

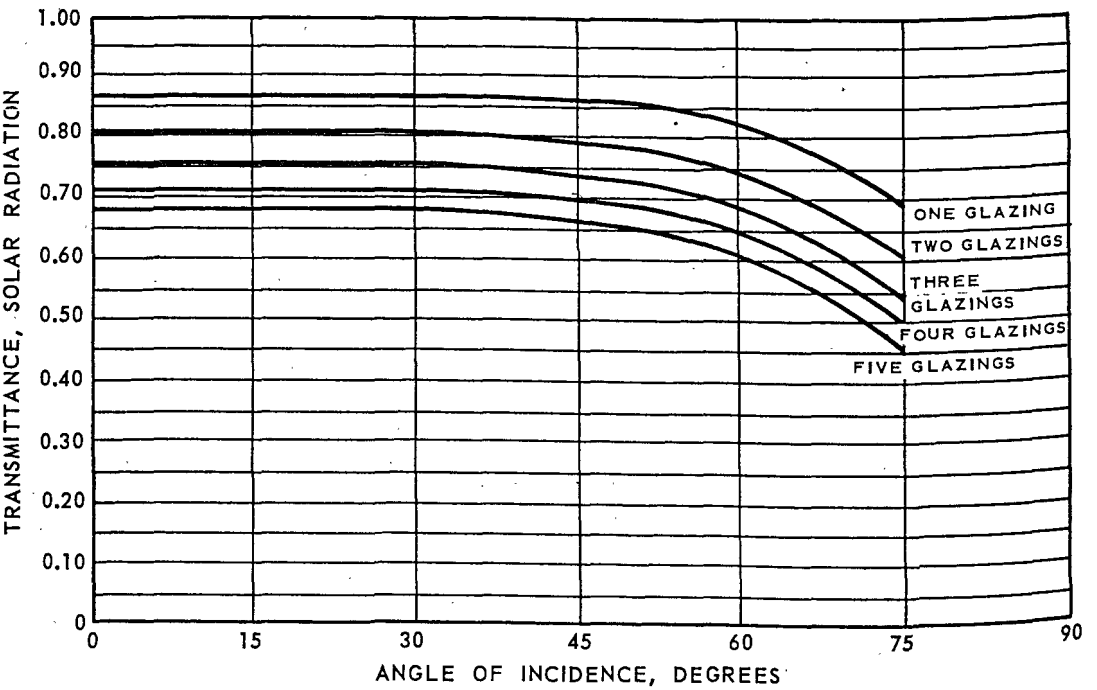


Figure 15. Transmittance of solar radiation through one to five glazings of "Mylar" W film for various angles of incidence

However, the loss of condensate from a plastic solar still from permeability is inconsequential, being 1 to 2 per cent.

Transmittance of radiation

The transmittance, absorbance and reflectance of radiation for diaphanous materials have been examined by theory (4, 5), and measurements have been reported for single and multiple glass panes (6, 7, 8, 9), and early compositions of weatherable plastic films (10, 11). Weatherable plastic films facilitate the study of radiation for they are available as extremely clear surfaces as thin as a few wave lengths of radiation. The precise values from the measurement of the optical geometry of transmittance, absorbance and reflectance are not applicable in many cases to the practical utilization of solar energy for the following reasons:

(*a*) From 15-100 per cent of the total daily solar radiation will be received diffusely from all angles of the sky, varying in intensity and angle of incidence throughout the day.

(*b*) In terms of the wave lengths of the solar spectrum, the surface irregularities and internal crystalline structures of many glazings, and particularly plastic glazings, are heterogeneous.

(*c*) Spectral absorption of solar radiation within polymeric materials is not uniform for various wave lengths. The quality of transmitted radiation will not correspond to that of incident radiation.

(*d*) After first surface reflection, the wave front is not propagated equally in all planes and an undetermined amount of polarization occurs.

(*e*) The photon unit energy level varies widely in nature. The extinction of solar radiation in diaphanous materials appears to vary with the "brightness" of the day.

Values of transmittance, absorbance and reflectance are reported for weatherable plastic films and selected other materials, and these data are compared to theory.

Apparatus

Transmittance and absorbance of solar radiation were measured with a horizontal, facing upward pyroheliometer.[4] A 0.75 meter square plastic film glazing was mounted taut in a frame, centered 2 to 4 cm above the pyroheliometer, and supported in an alta-azimuth mount. Black cloth curtains surround the mount below the frame to eliminate stray radiation. The sun angle of incidence was measured with a shadow gauge on the mount. Radiation was measured with and without the glazing in place. The transmittance τ is the ratio of the radiation through the glazing I_g, to the incident radiation I_s.

$$\tau = \frac{I_g}{I_s} \qquad [1]$$

Data

The transmittance of solar radiation through one to five glazings of "Tedlar" film for various angles of incidence is given in figure 14; for one to five glazings of Type W "Mylar", in figure 15; and

[4] Eppley 50-junction pyroheliometer having U.S. Bureau of Standards calibration.

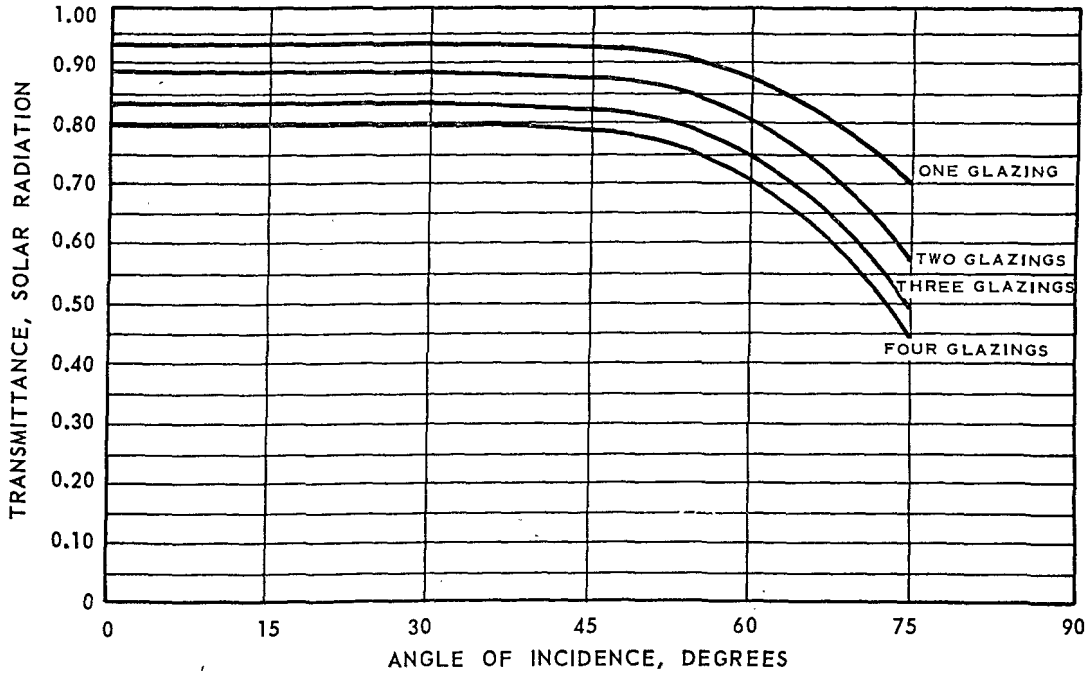


Figure 16. Transmittance of solar radiation through one to four glazings of crystal-clear polyethylene for various angles of incidence

Table 5. Incremental loss of transmittance of solar radiation through multiple glazings of clear plastic films

Angle of incidence, degrees	*0*	*15*	*30*	*45*	*60*	*75*
"Tedlar" film						
First glazing	0.053	0.053	0.053	0.065	0.132	0.290
Second glazing	0.045	0.045	0.045	0.045	0.062	0.145
Third glazing	0.045	0.045	0.045	0.045	0.050	0.104
Fourth glazing	0.043	0.043	0.041	0.045	0.045	0.066
Fifth glazing	0.032	0.032	0.034	0.035	0.035	0.035
Polyethylene, clear						
First glazing	0.064	0.064	0.064	0.075	0.128	0.296
Second glazing	0.053	0.053	0.053	0.054	0.067	0.129
Third glazing	0.045	0.045	0.045	0.047	0.050	0.080
Fourth glazing	0.043	0.043	0.043	0.043	0.044	0.047
"Mylar" W-1						
First glazing	0.132	0.132	0.137	0.143	0.177	0.311
Second glazing	0.063	0.062	0.064	0.075	0.078	0.087
Third glazing	0.050	0.050	0.049	0.053	0.054	0.067
Fourth glazing	0.041	0.040	0.040	0.039	0.040	0.041
Fifth glazing	0.035	0.035	0.036	0.036	0.037	0.038

for one to four glazings of commercial, clear polyethylene film, in figure 16. The incremented loss of radiation which was not transmitted through each glazing is tabulated in table 5. Transmittance of solar radiation through glazings of "Teflon" FEP, polyethylene and glass is given for various angles of incidence in figure 17.

Results

The transmittance of solar radiation through clear, weatherable plastic films is high. Transmittance through single glazings of 2 mil[5] films at normal incidence is: "Teflon" FEP 0.977, "Tedlar" 0.943, "Mylar" W-2 0.874, crystal clear polyethylene 0.923; and single strength window glass 0.921. Fresnel has expressed the reflectance ρ, of non-polarized radiation from a glazing for i angle of incidence and i' angle of refraction as

$$\rho = \frac{\sin^2(i-i')}{2\sin^2(i-i')} + \frac{\tan^2(i-i')}{2\tan^2(i+i')} \qquad [2]$$

[5] One mil in thickness is 1/1000 inch or 1/40 millimeter.

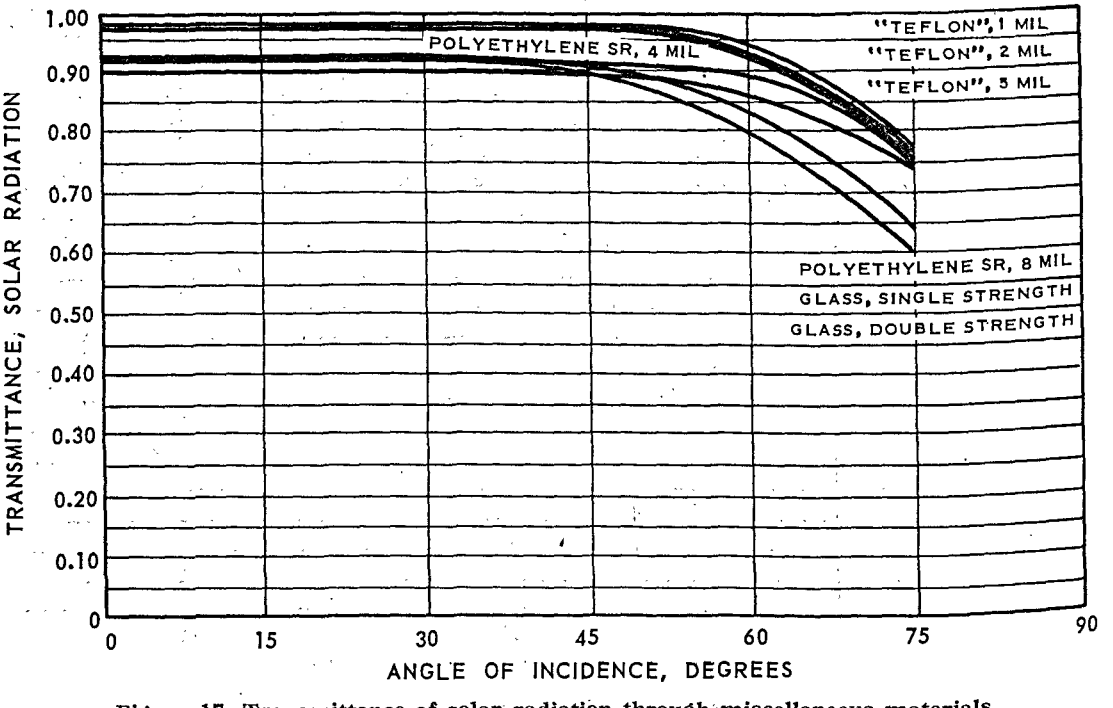


Figure 17. Transmittance of solar radiation through miscellaneous materials for various angles of incidence

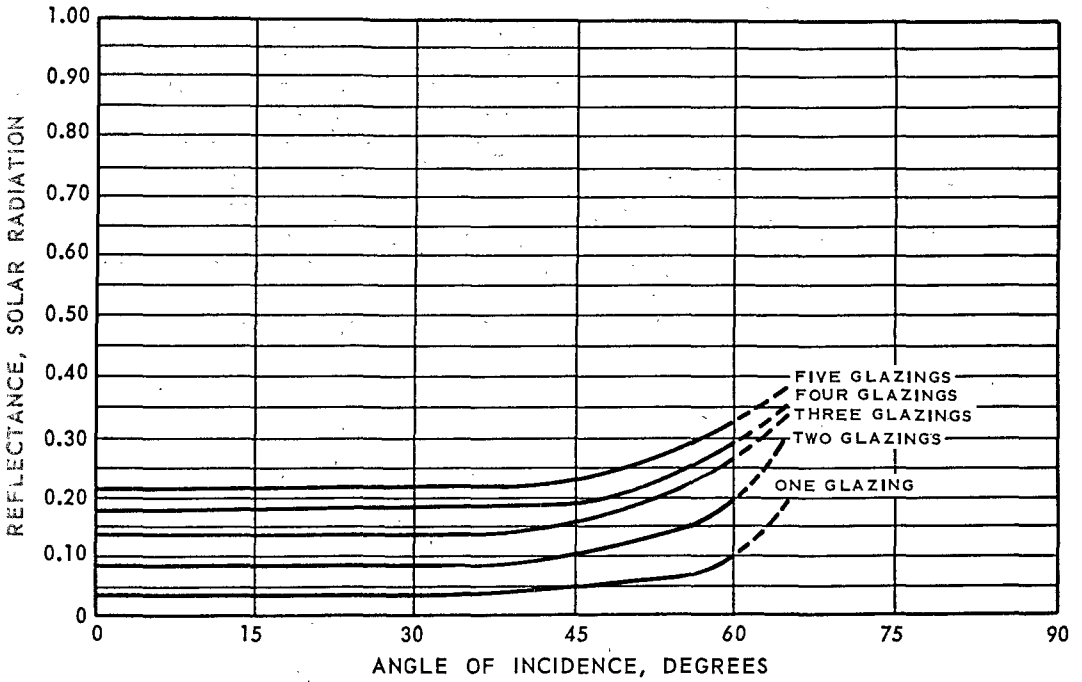


Figure 18. Reflectance of solar radiation from one to five "Tedlar" glazings for various angles of incidence

From Snell's law the angle of refraction i', for a material in air having n' index of refraction, may be evaluated

$$\sin i' = \frac{\sin i}{n'} \qquad [3]$$

The sum of the transmittance τ, absorbance α, and reflectance ρ is unity.

$$\tau + \alpha + \rho = 1 \qquad [4]$$

Neglecting, for the present, the small value of absorbance for thin plastic films, the transmittance may be estimated from the Fresnel expression [2]. The estimated value of transmittance at normal incidence for 5 glazings of "Tedlar", figure 14, of 0.69 compares closely with the measured value of 0.675. Contrarily, the estimated transmittance for 5 glazings at an angle of incidence of 75° of 0.355 is considerably less than the measured value of 0.450. This departure from theory is exemplified further in table 5. The incremental loss in transmittance approaches a constant value for all angles of incidence after the third or fourth glazing, and this loss is nearly independent of the transmissivity for different materials.

Total transmittance throughout the day

One pyroheliometer was mounted below 3 horizontal glazings of "Tedlar", and a second pyroheliometer was mounted nearby and uncovered. The total daily transmittance is shown as a function of the daily radiation level, figure 23, and compared to the mathematical integration of transmittance for the day given for three glazings in figure 14. The correlation is poor, possibly due to the varying types of cloud cover on different days. It would appear that transmittance is related to the clarity of the sky and the altitude of the sun.

Transmittance of thermal radiation

The transmittance of dry and wetted "Tedlar" and "Mylar" type W were measured with a bolometer.[6] Good correlations with these data were obtained under 100°C by placing these films as a radiation shield between two nearly blackbody surfaces which were maintained at different and constant temperatures. The transmittance of thermal radiation for dry and wet "Tedlar" PVF film and type W "Mylar" polyester film is given in figure 22.

Absorbance of solar radiation

The absorbance of solar radiation in plastic films may be estimated conveniently by measuring the transmittance of a series of single films which vary in thickness. The slope of the transmittance curves per unit thickness provides the extinction coefficient as shown in figure 21. The following extinction coefficients were obtained:

	Extinction coefficient	*K/mil*
"Teflon" FEP		0.001
Crystal clear polyethylene		0.001
"Tedlar"		0.003
"Mylar", type W		0.0034

[6] In collaboration with Dr. Maria Telkes, Curtiss-Wright Corporation.

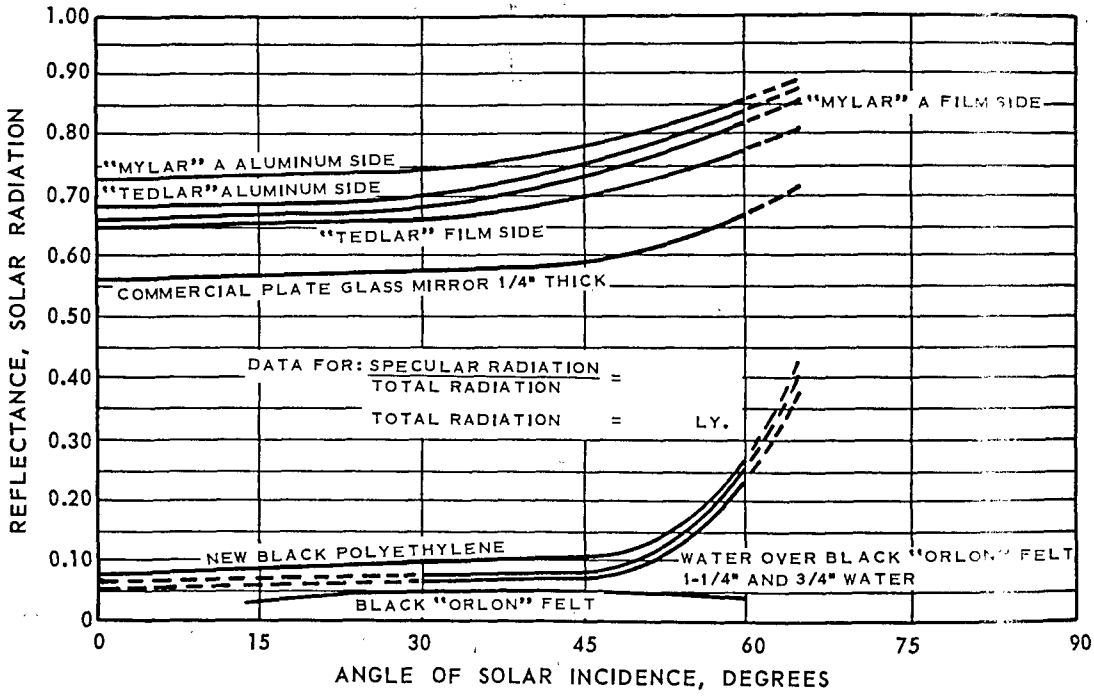


Figure 19. Reflectance of solar radiation from miscellaneous materials for various angles of incidence

From Lambert's law of radiation absorption, the transmittance due to absorption for an intitial radiation intensity I_s, and a transmitted radiation intensity I_t, after passing through a material having an extinction coefficient K, and a length of radiation path L, is:

$$I_t = I_s e^{-KL} \qquad [5]$$

by rearrangement and expansion:

$$\tau\alpha = e^{-KL} = 1 - KL + \frac{(KL)^2}{2!} - \frac{(KL)^3}{3!} + \ldots \frac{(KL)^n}{n!} \qquad [6$$

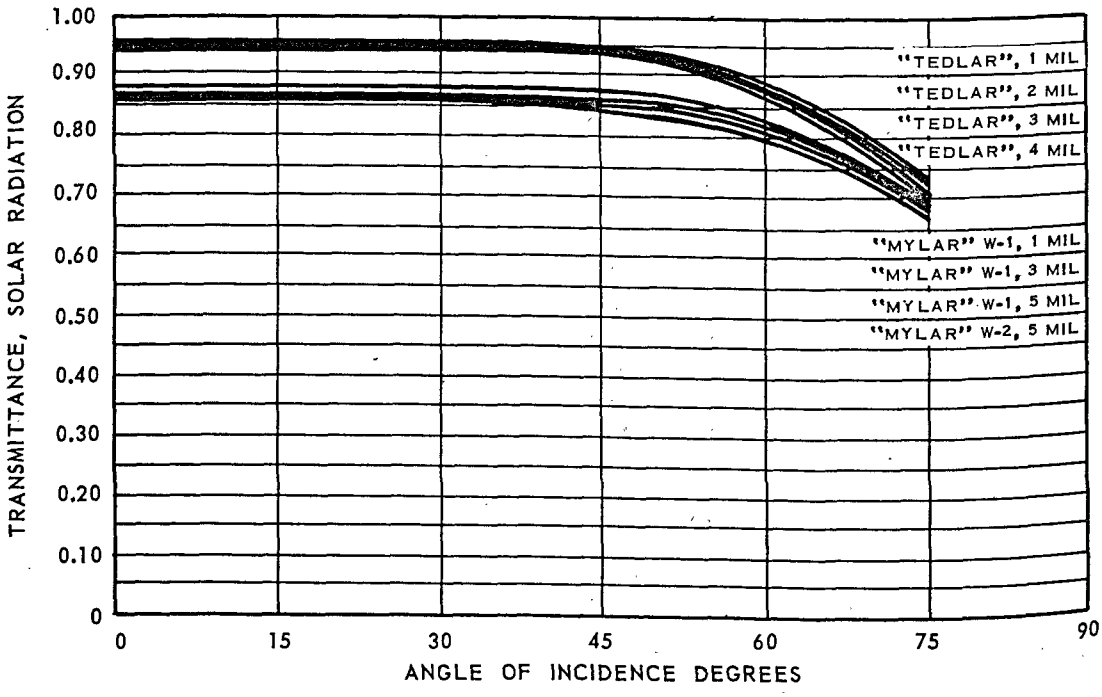


Figure 20. Transmittance of solar radiation through various thicknesses of "Tedlar" and "Mylar" W films for various angles of incidence

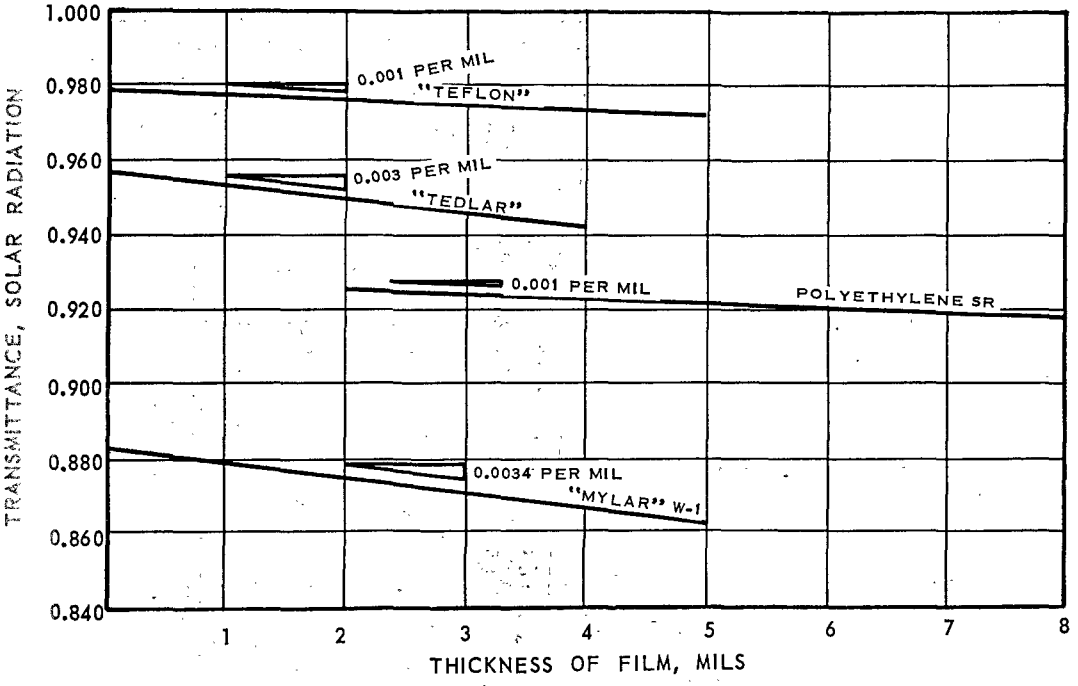


Figure 21. Absorbance at normal incidence of solar radiation in "Teflon", "Tedlar", polyethylene and "Mylar" W films for various thicknesses

For purposes of solar energy applications the expansion may be simplified to:

$$\tau\alpha = 1 - KL \qquad [7]$$

and the absorbance is unity minus the transmittance due to absorption and equivalent to the extinction coefficient multiplied by the radiation path length computed from Snell's law.

$$\alpha = 1 - \tau\alpha = 1 - (1 - KL) = KL \qquad [8]$$

Reflectance of solar radiation

The reflectance of solar radiation from materials involves geeometrical optics of complex systems. A high-quality parabolic reflector will focus an image with a flux which approaches that of the collimated or direct radiation from the source. Instruments having collimated incident and reflected beams are properly used to measure the reflectance. A flat, reflective surface which may—or may not—have minute imperfections will reflect diffuse as well as direct radiation. The radiation which is received at a point near the center of a large, flat reflector will be the sum of the reflectances coming directly from the sun, diffuse sky radiation, and the integrated scatter which may be due to the imperfections of the reflector. For these reasons the spectacular reflectance is important in precise geometrical systems while total reflectance is more important for systems having low concentration ratios. Aluminized plastic films have high total reflectance and moderate specular reflection, and they are most useful in solar collectors of moderate concentration ratio. Also, the measurement of total solar reflectance from transparent glazings provides a value which is additive to the transmittance and absorbence in accordance with equation [4].

Apparatus

The apparatus which was used for transmittance measurements may be modified by providing an axle above the mounting. The pyroheliometer was mounted to the axle so that it could be rotated from a horizontal, upward-facing position to a horizontal downward-facing position, with the pyroheliometer bulb being about 10 cm from the glazing as supported in the mount. A black felt of "Orlon" acrylic fiber,[7] of reflectivity 0.04, was placed beneath the plastic glazing. The mount was made level and the solar altitude was read from the shadow gauge, and then inclined as desired. The pyroheliometer was read facing upward, then downward, then upward to make certain of the constant quality of the solar radiation. The pyroheliometer was calibrated in the downward-facing position by placing a black felt of "Orlon" over the lower hemisphere of the pyroheliometer bulb.

Data

The intensity of the reflected radiation which is measured by the instrument during calibration I_i is the sum of that reflected from the pyroheliometer bulb I_b, and from the black felt I_f.

$$I_i = I_b + I_f \qquad [9]$$

The intensity of the reflected radiation which is measured from a clear glazing sample I_m is the sum

[7] "Orlon" is Du Pont's registered trademark for its acrylic fiber.

of that reflected from the glazing I_r, from the black felt and from the bulb.

$$I_m = I_r + I_f + I_b \qquad [10]$$

by substitution and condensation

$$I_r = I_m - I_t \qquad [11]$$

The intensity of the reflected radiation which is measured from a reflective glazing which is nearly opaque omits reflectance from the black felt beneath it, so the expression must include the reflectance ρ from the felt which is used during calibration.

$$I_r = I_m - I_t + I_f = I_m - I_t + \rho I_s \qquad [12]$$

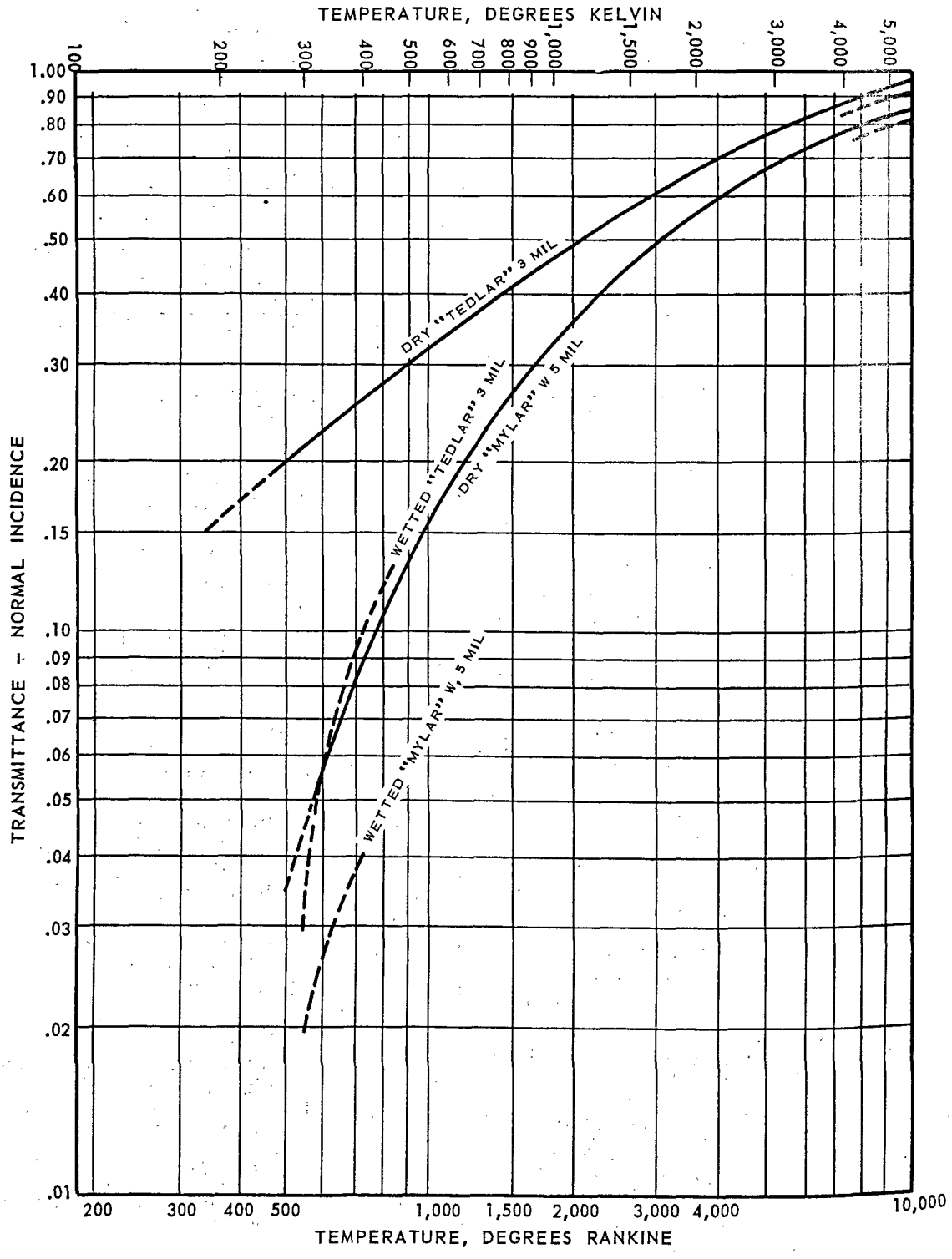


Figure 22. Transmittance of radiation at normal incidence from radiators at various temperatures for "Tedlar" and "Mylar" W film, dry and wetted

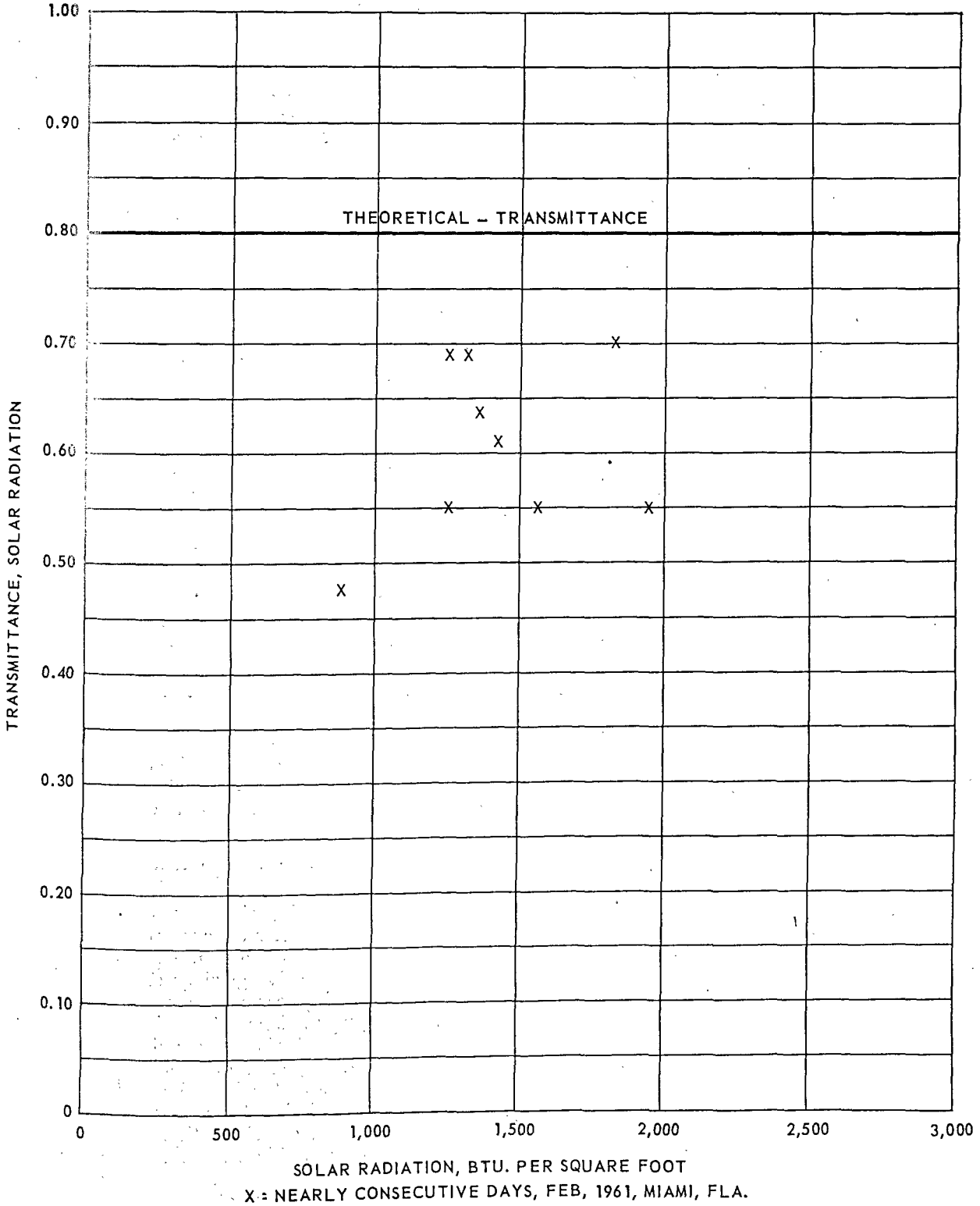


Figure 23. Mean daily transmittance of solar radiation through three "Tedlar" films for various radiation levels

Table 6. The sum of the incremental transmittance, absorbance and reflectance of multiple glazings of "Tedlar" film

Angle of incidence, degrees	*26.5*	*45*	*56.3*
	$(\tau + \rho + \alpha = 1)$		
One glazing of 1 mil			
Transmittance	0.947	0.934	0.868
Reflectance	0.037	0.056	0.076
Absorbance	0.003	0.004	0.005
Total	0.987	0.994	0.949
Two glazings of 1 mil each			
Transmittance	0.902	0.890	0.805
Reflectance	0.085	0.104	0.158
Absorbance	0.006	0.007	0.009
Total	0.993	1.001	0.972
Three glazings, 2-1 mil, 1-2 mil			
Transmittance	0.853	0.837	0.746
Reflectance	0.140	0.157	0.228
Absorbance	0.012	0.014	0.018
Total	1.005	1.008	0.992
Four glazings, 2-1 mil, 1-2 mil, 1-3 mil			
Transmittance	0.810	0.795	0.710
Reflectance	0.180	0.186	0.265
Absorbance	0.021	0.024	0.031
Total	1.011	1.005	1.006
Five glazings, 2-1 mil, 1-2 mil, 1-3 mil, 1-4 mil			
Transmittance	0.774	0.752	0.652
Reflectance	0.219	0.236	0.344
Absorbance	0.033	0.038	0.049
Total	1.026	1.026	1.045

The reflectance of the sample is estimated from the easily derived geometrical expression for the solar altitude h, and the angle of solar incidence on the glazing i,

$$\rho = \frac{I_R}{I_S} \frac{\sin h}{\sin (180° - h - 2i)} \qquad [13]$$

The reflectance of solar radiation from one to five glazings of "Tedlar" is given in figure 18 for various angles of incidence. The reflectance of solar radiation from miscellaneous surfaces is given in figure 19 for various angles of incidence.

Results

The reflectance of solar radiation from one to five glazings of "Tedlar" at normal incidence corresponds to that which is estimated from the Fresnel expression [2]. However, the reflectance at an angle of 60° is less than that which is estimated. The second surface reflectance of solar radiation from aluminized "Tedlar" and "Mylar" at normal incidence is 0.65 and 0.67, respectively, and relates to total sky radiation where direct radiation is 84 per cent. The commercial, quarter-inch plate-glass mirror has excellent specular reflection. Its reflectance of 0.57 of total sky radiation indicates the loss through one-half inch of plate glass and a comparatively poor reflective surface. It has been found that the quality of reflective metal deposit varies widely on both plastic films and glass plates.

Summary of radiation properties

From equation [4] the sum of the measured transmittance, absorbence and reflectance equals unity. Table 6 shows a summary of the values reported for one to five glazings of "Tedlar". Accumulative errors in measurement range up to 5.1 per cent. This energy balance of the intensity of radiation indicates that the measured reflectance from multiple glazing systems does not conform to that which may be estimated from the Fresnel expression for non-polar radiation. This difference may be due to varying degrees of polarization of the transmitted beam or to other unknown factors. The incremental transmittance loss through fourth glazings and lower appears to become almost independent of the angle of incidence and the extinction coefficient of the material.

It is concluded that weatherable plastic films offer a range of materials which could meet many of the basic requirements of solar energy applications.

References

1. Simril, V. L. and Curry, B. A., Polyvinyl Fluoride Film, *Modern Plastics*, July 1959.
2. Simril, V. L. and Curry, B. A., The Properties of Polyvinyl Fluoride Film, *Journal of Applied Polymer Science*, pp. 62-68, vol. 4, issue 10.
3. Kalb, G., Coffman, D. D., Ford, T. A. and Johnston, F. L., Polymers From Vinyl Fluoride, *Journal of Applied Polymer Science*, pp. 55-61, vol. 4, issue 10.
4. Stokes, G. C., The Intensity of Light Reflected from or Transmitted Through a Pile of Plates, Proceedings of the Royal Society of London, vol. II, 1860-62.
5. Hardy, A. C. and Perrin, F. H., *Principles of Optics*, McGraw-Hill Publishing Co., New York, 1932.
6. Hottel, H. C. and Woertz, B. B., The Performance of Flat-Plate Solar Heat Collectors, Transactions of the American Society of Mechanical Engineers, Feb. 1942.
7. Parmelee, G. V., The Transmission of Solar Radiation through Flat Glass under Summer Conditions, Transactions of the American Society of Heating and Ventilating Engineers, vol. 51, pp. 317-344, 1945.
8. Parmelee, G. V. and Aubele, W. A., Solar Energy Transmittance of Figured Rolled Glass, *Heating, Piping and Air Conditioning*, Feb. 1951.
9. Dietz, A. G. H., Diathermanous Materials and Properties of Surfaces, Symposium on "Space Heating with Solar Energy", Massachusetts Institute of Technology, 1954.
10. Edlin, F. E., Plastic Glazings for Solar Energy Absorption Collectors, *The Journal of Solar Energy Science and Engineering*, Association for Applied Solar Energy, Phoenix, Ariz., April 1958.
11. Edlin, F. E., Matériaux Nouveaux pour l'Utilisation de l'Énergie Solaire, Symposium of Solar Energy Applications, CNRS, Mont-Louis, France, 23 June 1958.

Summary

Weather-resistant or "weatherable" plastic films, potentially, are low-cost materials which may be used as transparent, reflective or absorptive surfaces for solar power devices. Pertinent physical, chemical, structural and radiation properties of weatherable plastic films are compared herein. Included are polyester films and films of hydrocarbon and halocarbon polymers. Outdoor and exposure life expectancies of plastic films are predicted as a guide to their choice for specific applications. The radiation properties of transmittance, reflectance and absorbance are given for single and multiple glazings.

PELLICULES EN COMPOSITION PLASTIQUE POUR LES APPLICATIONS DANS LE DOMAINE DE L'ÉNERGIE SOLAIRE

Résumé

Les pellicules en composition plastique résistantes aux intempéries peuvent devenir des matériaux d'un prix modique que l'on pourrait éventuellement utiliser comme surfaces transparentes, réfléchissantes ou absorbantes à l'intention des dispositifs à énergie solaire. Le présent mémoire compare les propriétés physiques, chimiques, structurelles et relatives au rayonnement des pellicules en composition plastique capables de résister aux intempéries. Il s'agit notamment des pellicules constituées par des polyesters et des hydrocarbures et des polymères de ceux-ci. Les durées de service attendues au dehors et dans le cas d'une exposition aux intempéries des pellicules en composition plastique sont prédites pour servir de guide à leur choix en vue d'applications particulières. Les propriétés relatives au rayonnement, telles que la transmittance, la réflectance et l'absorbance, sont indiquées pour les glaçages à couche unique et multiple.

SPECTRAL AND DIRECTIONAL THERMAL RADIATION CHARACTERISTICS OF SELECTIVE SURFACES FOR SOLAR COLLECTORS

D. K. Edwards, J. T. Gier, K. E. Nelson and R. D. Roddick *

A solar heat collector, by definition, serves to convert solar energy into thermal energy by absorption of the incident photons. Thermal energy may be desired for a thermal environment control system, a chemical process system, or a heat-power engine. The purpose of this paper is to present spectral and directional radiation characteristics of materials which may be used in solar collectors.

As a simplification, the absorption and emission processes in the collector itself are considered to be confined to an isothermal layer on the surface at temperature T_C. However, this surface may be only a component of a collector system whose various components would be at different temperatures.

In general, the collector with surface of temperature T_C is irradiated by thermal radiation with intensity $I_\lambda + (\Theta, \Phi)$ where Θ is the polar angle from the surface normal and Φ is the azimuthal angle from some reference, such as a striation, in the plane of the surface. Of the irradiation in solid angle $d\,\Omega$ about the direction Θ, Φ and with wavelengths between λ and $\lambda + d\lambda$, a fraction $\alpha_\lambda\,(\Theta, \Phi)$ is absorbed. The quantity $\alpha_\lambda\,(\Theta, \Phi)$ is termed the directional absorptance. From Kirchhoff's law the intensity of radiation emitted by the collector is then $I^- = \alpha_\lambda\,(\Theta', \Phi')\,I_{b\lambda}\,(T_C)$, where $I_{b\lambda}\,(T_C)$ is the black body intensity given by Planck's law. The total irradiation absorbed is then the

$$\alpha G = \int_0^\infty \int_0^{2\pi} \int_0^{\pi/2} \alpha_\lambda\,(\Theta, \Phi)\, I_\lambda^+\,(\Theta, \Phi) \sin\Theta \cos\Theta\, d\Theta\, d\Phi\, d\lambda \qquad [1]$$

where

$$G = \int_0^\infty \int_0^{2\pi} \int_0^{\pi/2} I_\lambda^+\,(\Theta, \Phi) \sin\Theta \cos\Theta\, d\Theta\, d\Phi\, d\lambda \qquad [2]$$

The total emissive power of the surface is

$$\varepsilon\sigma T_C^4 = \int_0^\infty \int_0^{2\pi} \int_0^{\pi/2} \alpha\lambda\,(\Theta', \Phi')\, I_{b\lambda}\,(T_C) \sin\Theta' \cos\Phi'\, d\Theta'\, d\Phi'\, d\lambda \qquad [3]$$

where

σ is the Stefan-Boltzmann constant

$$\sigma T_C^4 = \int_0^\infty \int_0^{2\pi} \int_0^{\pi/2} I_{b\lambda}\,(T_C) \sin\Theta' \cos\Theta'\, d\Theta, d\Phi'\, d\lambda$$

$$\sigma T_C^4 = \pi \int_0^\infty I_{b\lambda}\,(T_C)\, d\lambda \qquad [4]$$

For an optimum solar collector to operate at temperature T_C, the rate of energy absorbed αG, and hence the absorptance α, should be as large as possible, while that emitted $\varepsilon\sigma T_C^4$, and hence the emittance ε, should be as small as possible. That α is related but not necessarily equal to ε is seen at once from comparison of equations [1] and [3].

The irradiation generally is composed of undeviated solar irradiation, scattered solar irradiation, sky irradiation, and irradiation due to other surrounds. If no concentrator is used, the undeviated solar irradiation is quite directional. Also the bulk of the solar irradiation is confined to the short-wavelength region, about 0.3 to 3.5 μ outside the atmosphere (1) and 0.35 to 2.1 μ inside the atmosphere (2). In order to facilitate reaching some fairly general conclusions concerning what characteristics make a material desirable for use in collectors, the irradiation is considered to be composed of only solar irradiation G_S for which the absorptance is α_S and long-wave irradiation G_L for which the absorptance is taken to be identical with the emittance ε. This procedure is realistic for many materials, as marked changes in $\alpha\lambda$ usually occur in the visible or near-infrared as opposed to the regions beyond 6 or 7 μ.

With the above simplification, a solar absorptance of merit α' can be defined

$$\alpha' = \alpha_S - \varepsilon \frac{\sigma T_C^4 - G_L}{G_S} \qquad [5]$$

The quantity $\alpha' G_S$ represents the net radiant power transferred to a unit area of the surface. The quantities α_S and ε should then be such that α' is as large as possible. It is seen from equation [5]

* University of California, Los Angeles.

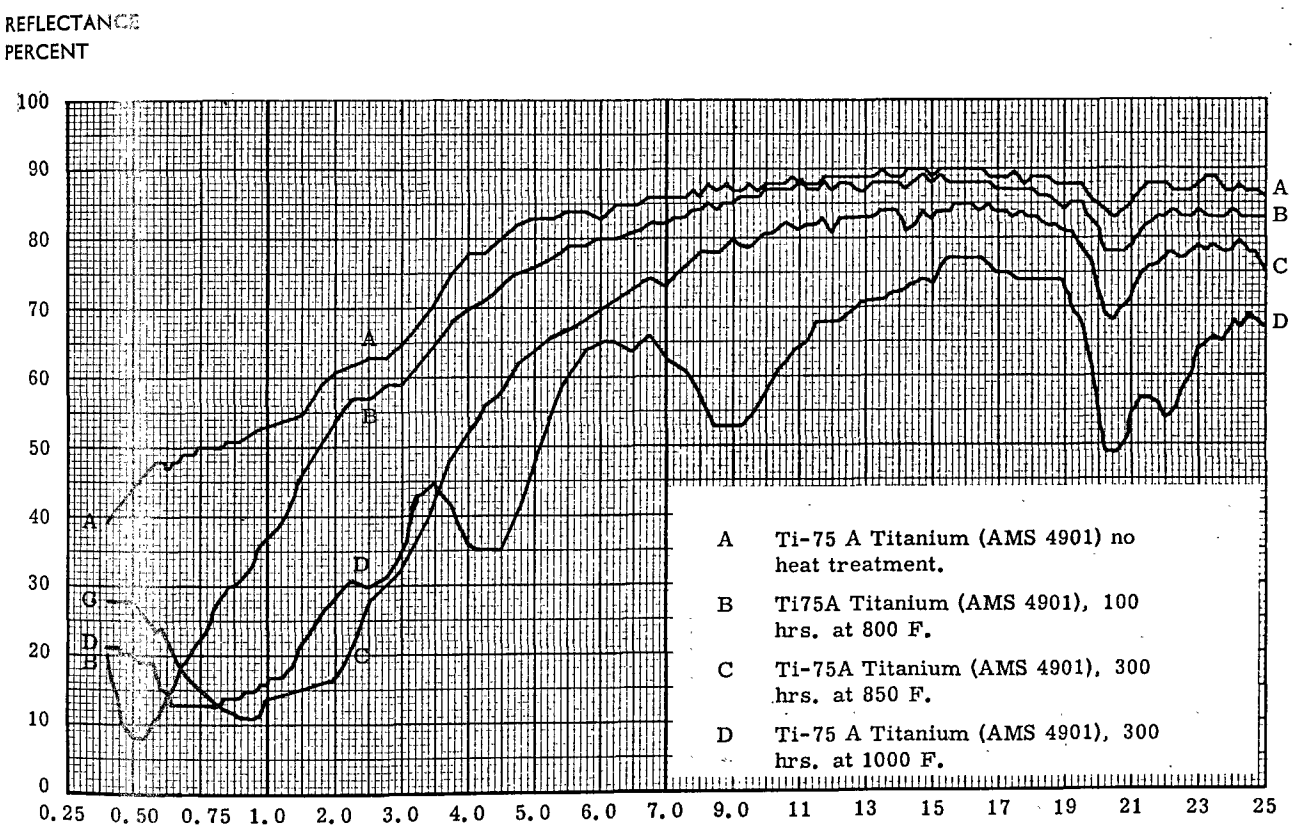


Figure 1. Near-normal spectral reflectance of oxidized titanium (AMS 4901)

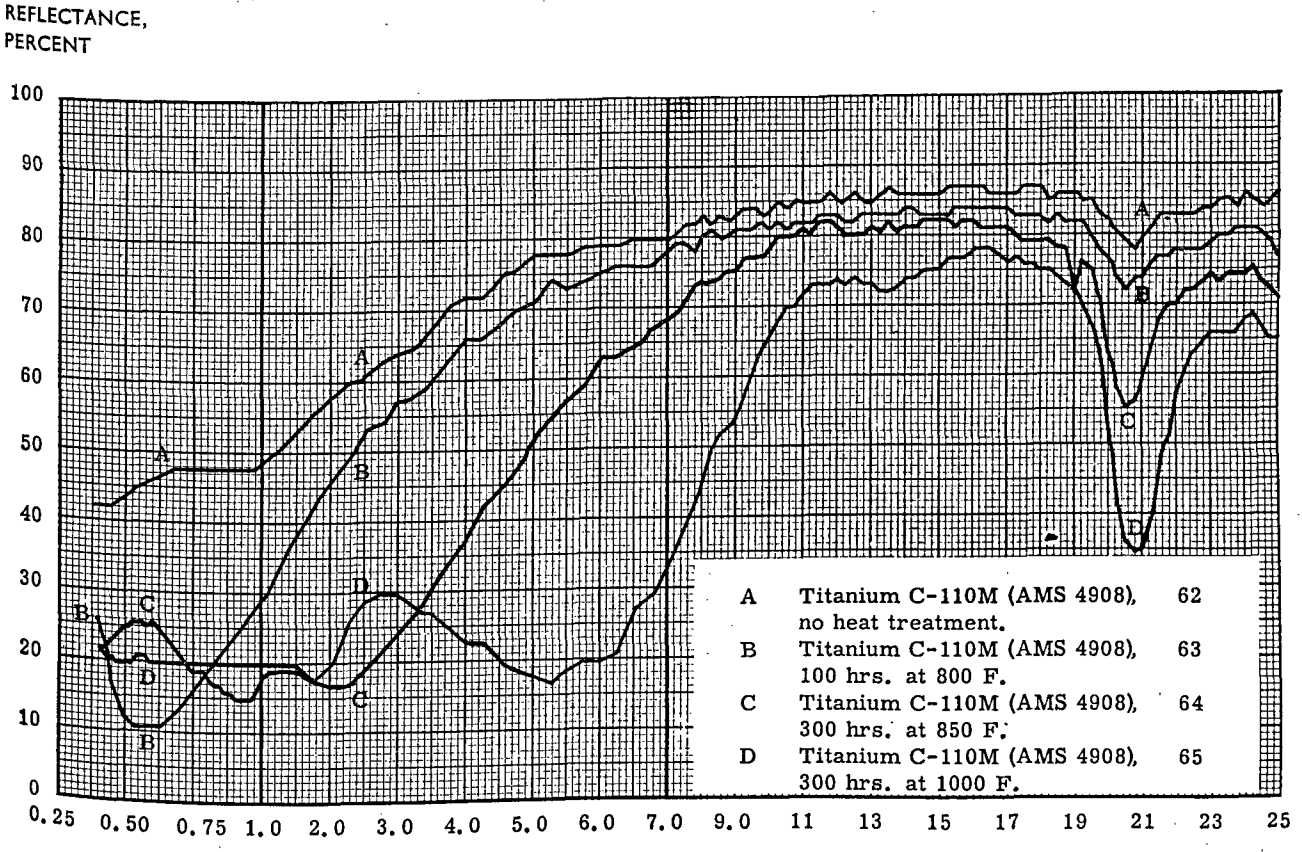


Figure 2. Near-normal spectral reflectance of oxidized titanium (AMS 4908)

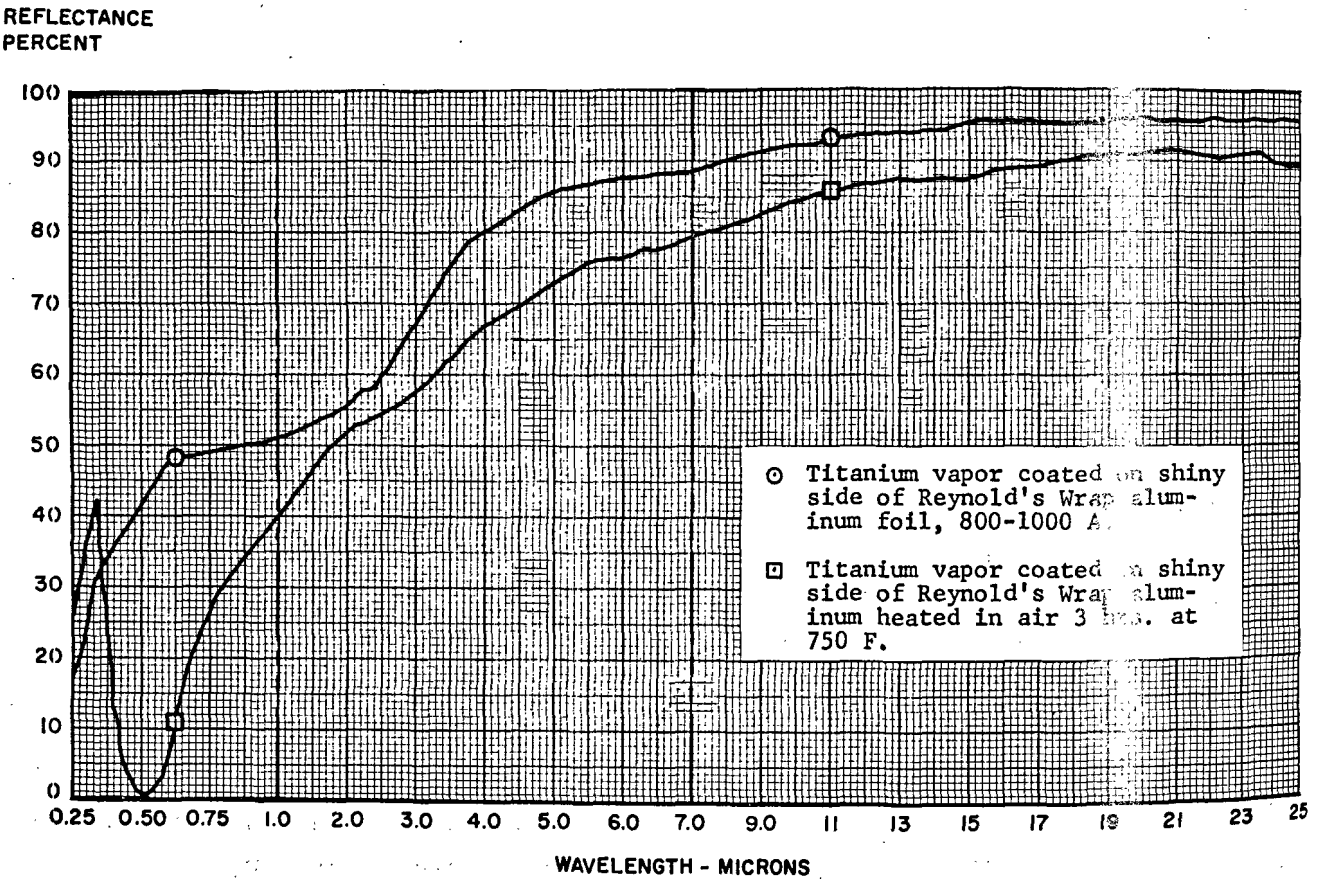


Figure 3. Near-normal spectral reflectance of oxidized titanium on aluminum

that the irradiation, G_S and G_L, and the collector temperature have a profound influence on the choice of α_S and ε. In particular, the α_S/ε ratio alone is not meaningful.

The quantity

$$\beta = \left(\frac{\sigma T_C^4 - G_L}{G_S}\right) \qquad [6]$$

may be termed the α_S-ε trade-off ratio, since it gives the maximum decrease in α_S that a designer would be willing to sacrifice to gain a unit decrease in ε. It may be noted that for lower collector temperatures, an increase of 0.01 in α_S is more desirable than a decrease of 0.01 in ε. This situation is especially true when a concentrator is used.

Equations [1] and [3] may be used to determine the optimum cut-off wavelength λ_{CO} where $\alpha_\lambda(\Theta, \Phi)$ should undergo a step decrease. For example, with a perfectly diffuse collector and in the usual case when I_λ^+ is monatonically decreasing with increasing λ and I_λ^- monatonically increasing with increasing λ, it is seen that λ_{CO} occurs where (3)

$$\int_0^{2\pi}\int_0^{\pi/2} I_\lambda^+(\Theta, \Phi)\sin\Theta\cos\Theta\, d\Theta\, d\Phi = \int_0^{2\pi}\int_0^{\pi/2} I_\lambda^-(\Theta, \Phi)\sin\Theta\cos\Theta\, d\Theta\, d\Phi \qquad [7]$$

Naturally, unless a concentrator is used, or it is desired to collect scattered solar radiation from the entire sky, a perfectly diffuse collector is not optimum. For a low collector temperature and low concentration (low G_S), however, the cut-off wavelength is not critical, and equation [7] is useful to indicate the approximate location of λ_{CO}.

The introductory remarks above serve to indicate what types of spectral and directional characteristics are desirable. In the following sections, simple surface systems exhibiting selective spectral characteristics and their directional characteristics are summarized; measured characteristics of several actual isothermal surface systems are presented; these actual materials are compared and evaluated.

Isothermal surface systems for spectrally selective collectors

Several elementary surface systems may be considered for creation of spectral selectivity. The partial list below contains some of the easily recognized ones. Combinations of such elementary systems would probably yield best results.

Homogeneous plane slab

The simplest system which may be considered is the isotropic, perfectly plane slab. The directional reflectivity of such a system is given by the Fresnel relations (4)

$$\underline{n}_1 = n_1 - \underline{i}k_1 \quad n_0 = 1.00 \qquad [8]$$

$$\underline{r}_{1p} = \frac{\underline{n}_0 \cos\Theta_1 - \underline{n}_1 \cos\Theta_0}{\underline{n}_0 \cos\Theta_1 + \underline{n} \cos\Theta_0}$$

$$\underline{r}_{1s} = \frac{\underline{n}_0 \cos\Theta_0 - \underline{n}_1 \cos\Theta_1}{\underline{n}_0 \cos\Theta_0 + \underline{n} \cos\Theta_1} \qquad [9]$$

$$n_1 \sin\Theta_1 = n_0 \sin\Theta_0 = \sin\Theta_0$$

$$\rho(\Theta_0) = 1/2\,[\underline{r}_p \underline{r}_p^* + \underline{r}_s r_s^*] \qquad [10]$$

where n_1 is the refractive index, k is the absorptive index, $i^2 = -1$, p refers to incident polarization parallel to the plane of incidence, s refers to polarization perpendicular to the plane of incidence, and r^* is the complex conjugate of r.

Spectral selectivity arises from the variation of n and k with wavelength. Metals typically have the proper type of variation of n and k with wavelength to make selective absorbers, but the cut-off wavelength λ_{co} is usually too short. However, in some applications, such as thermal environment control, economic or other considerations may dictate use of this simple surface.

Homogeneous rough slab

Surface roughness may be used to provide another element of spectral selectivity. If the roughness is large compared to the wavelength, the cavities in the surface result in interreflections with consequent increase in absorptance. However, in the long wavelengths, where the roughness is small compared to the wavelength, little effect is present.

Layer of small particles

A coating of small particles may also be used to provide spectral selectivity. When the wavelength is smaller than the particle size, absorption may occur, while at longer wavelengths the layer is transparent (5).

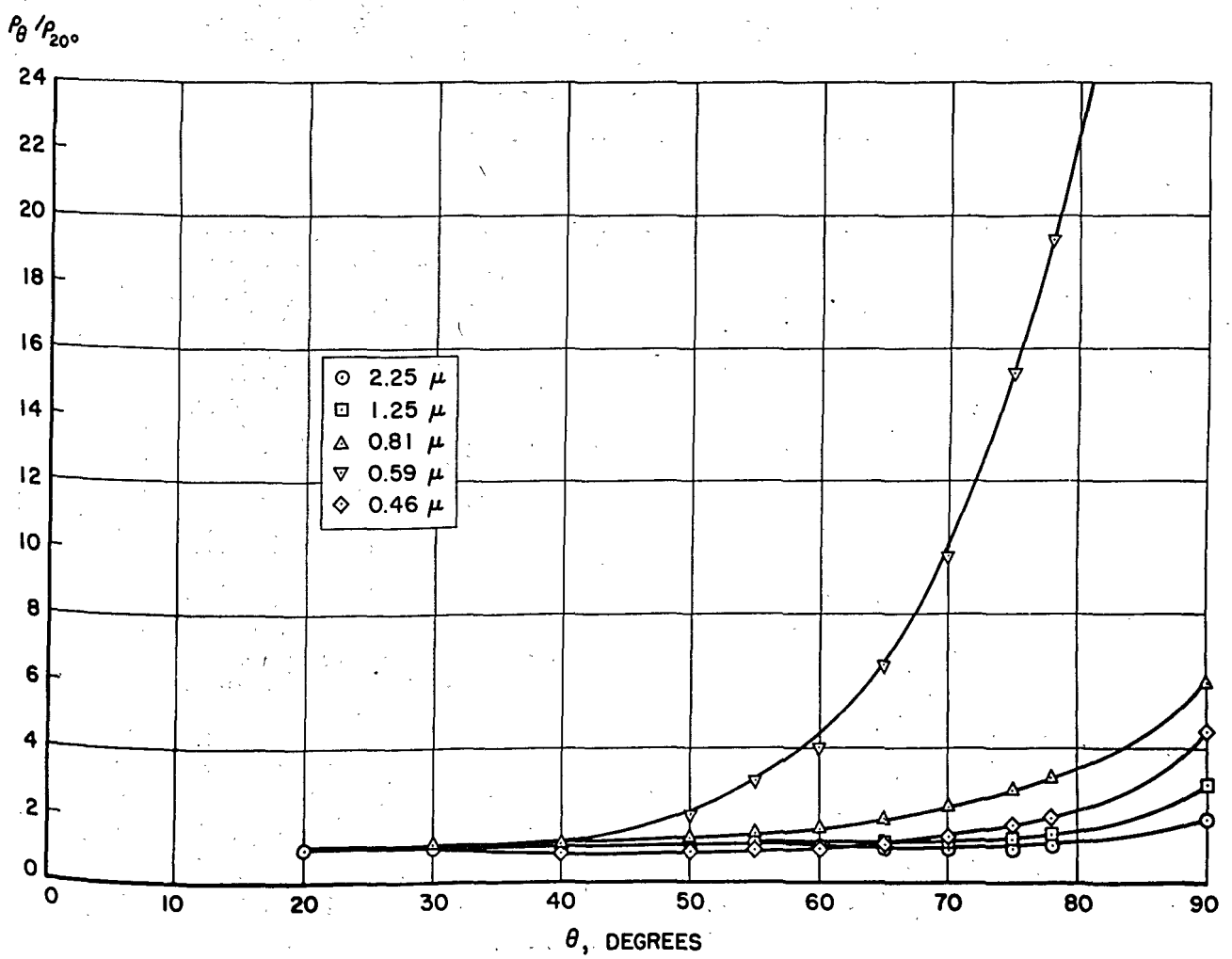


Figure 4. Normalized directional reflectance of oxidized titanium on aluminum

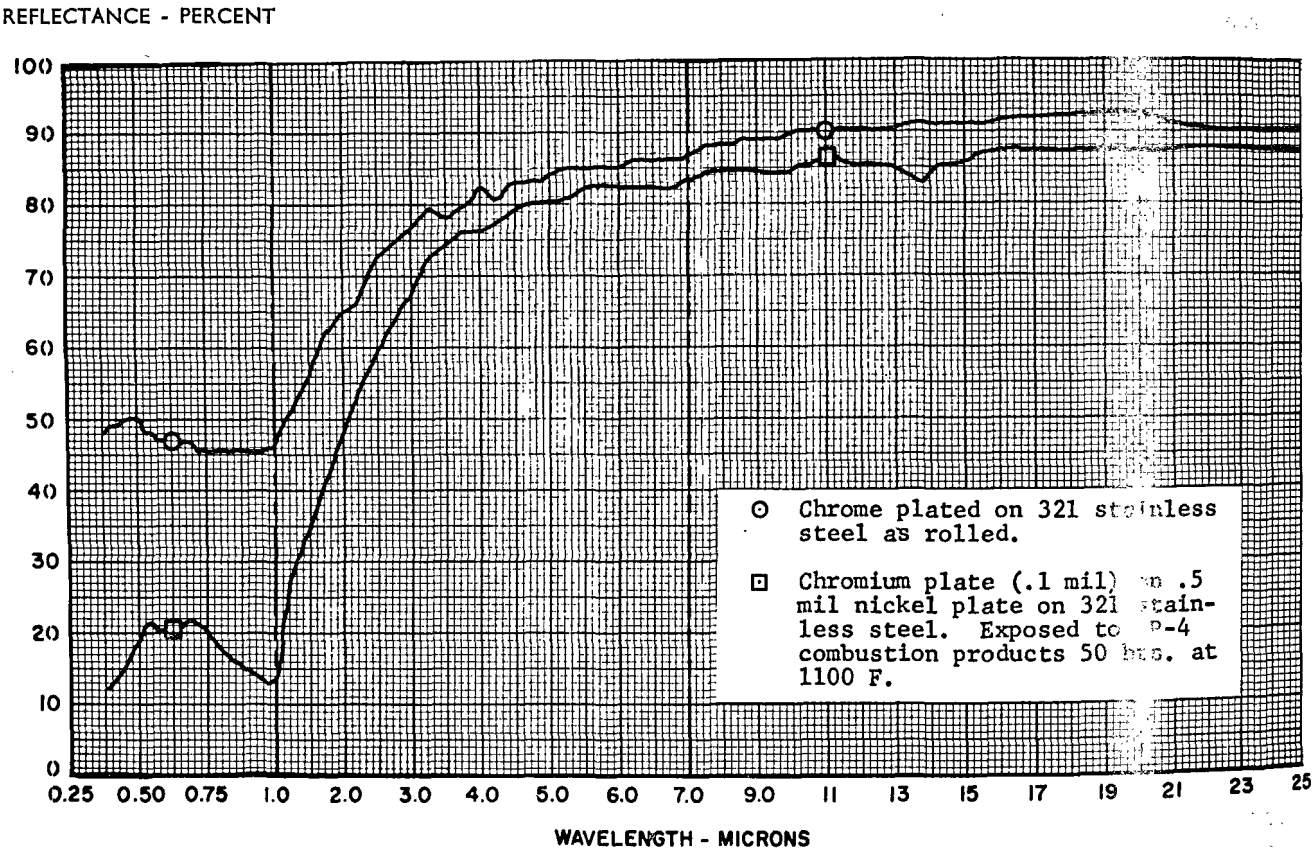


Figure 5. Near-normal spectral reflectance of oxidized chromium

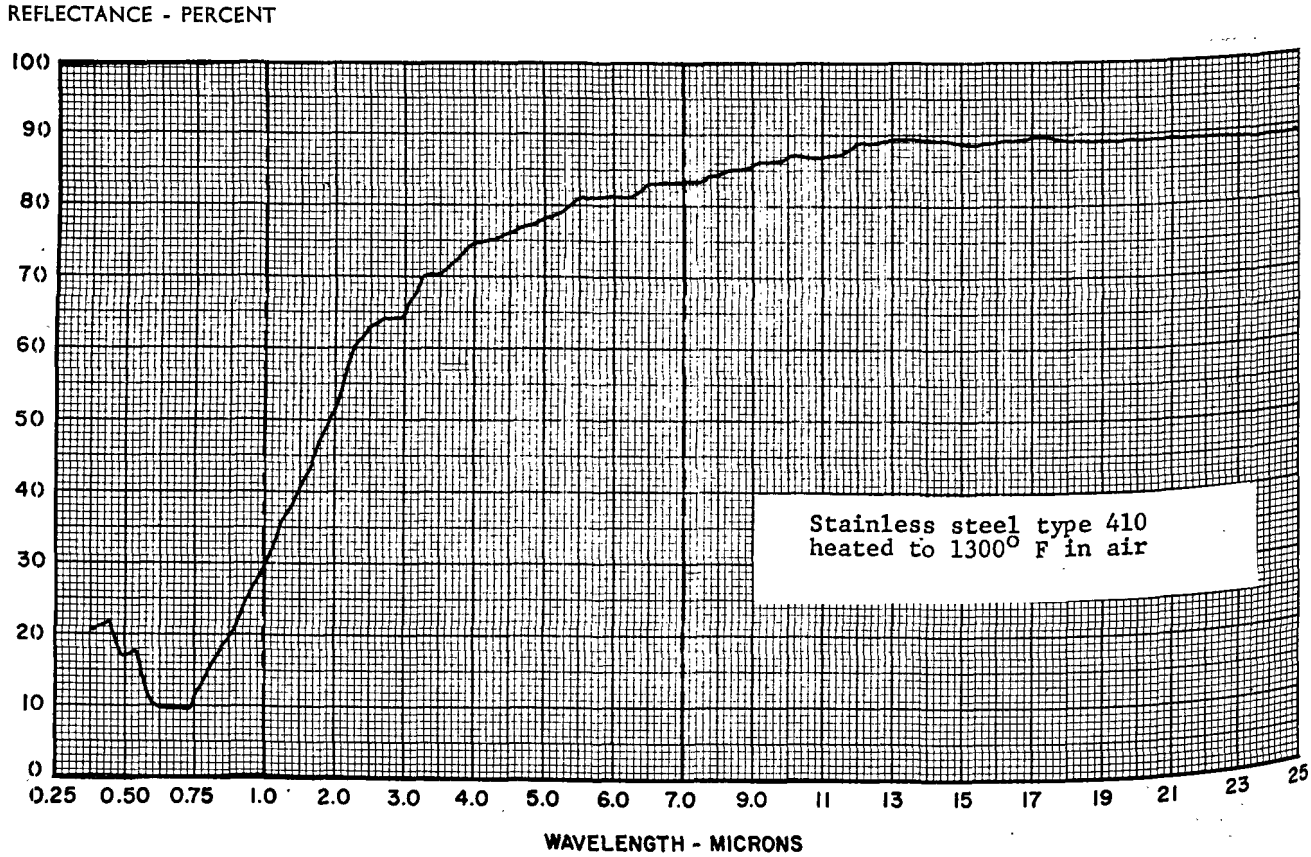


Figure 6. Near-normal spectral reflectance of oxidized stainless steel

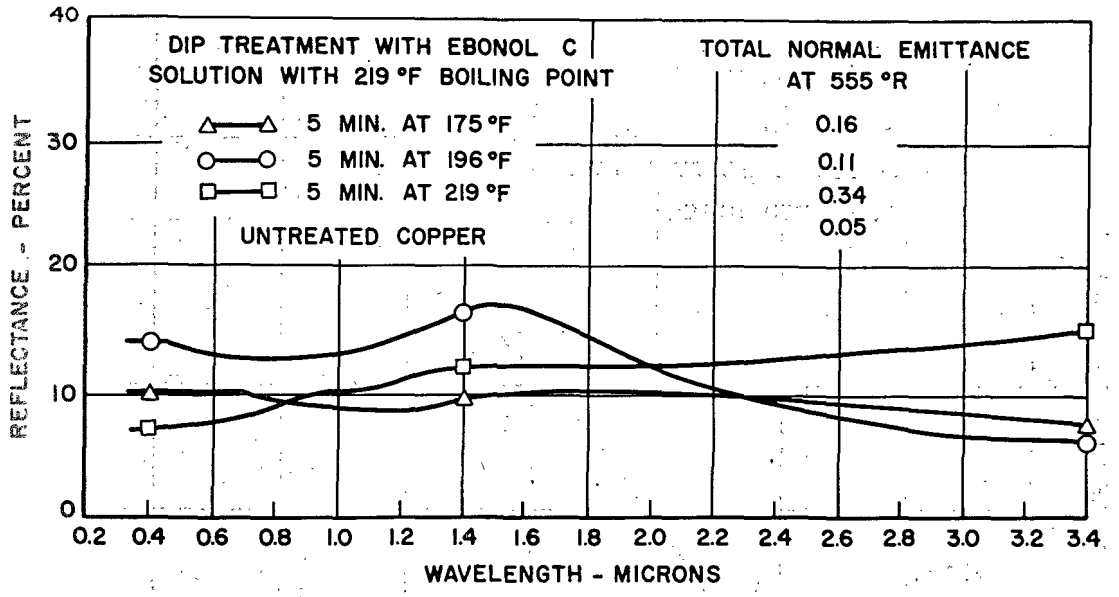


Figure 7. Near-normal spectral reflectance of Ebonol C on copper

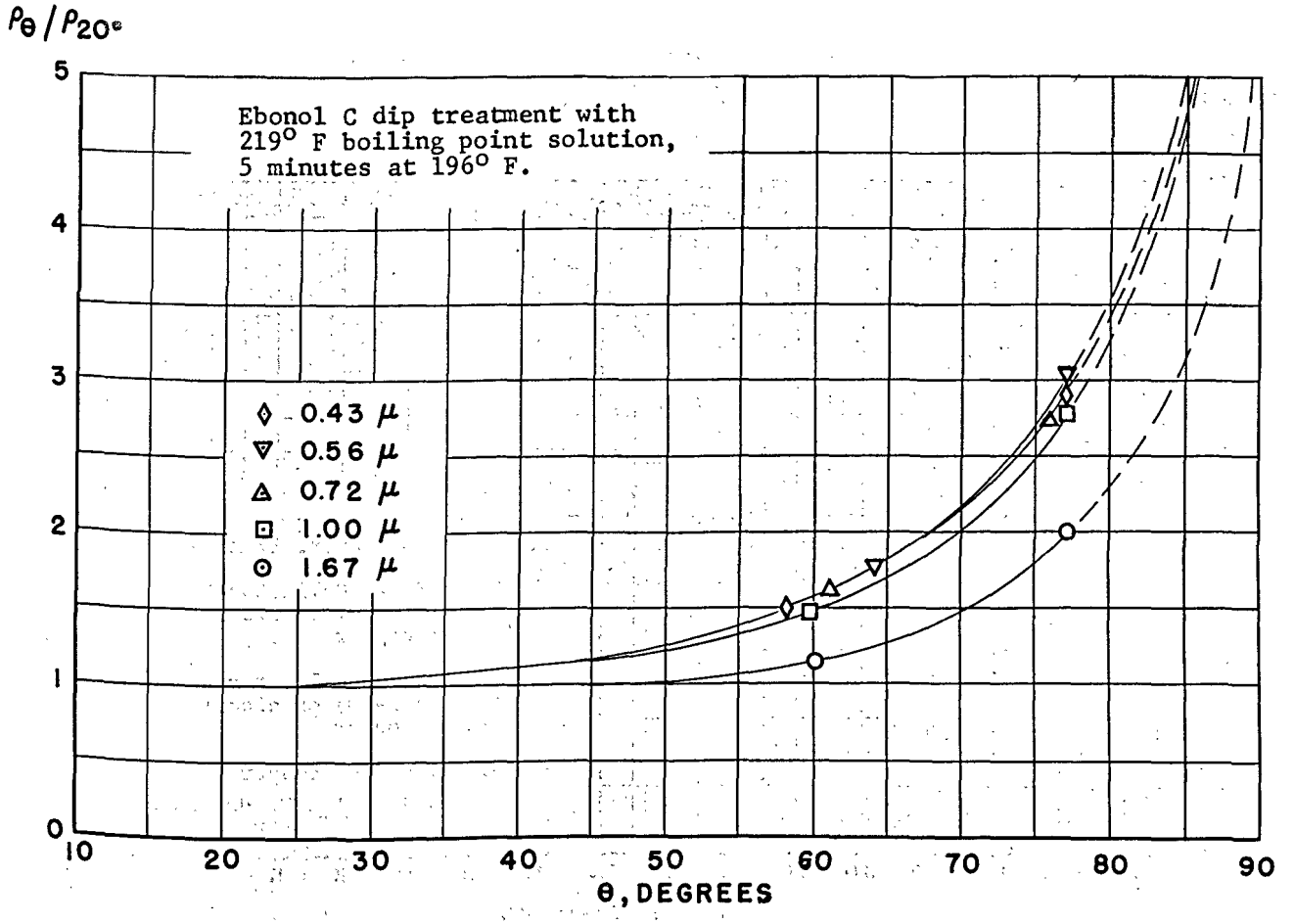


Figure 8. Normalized directional reflectance of Ebonol C on copper

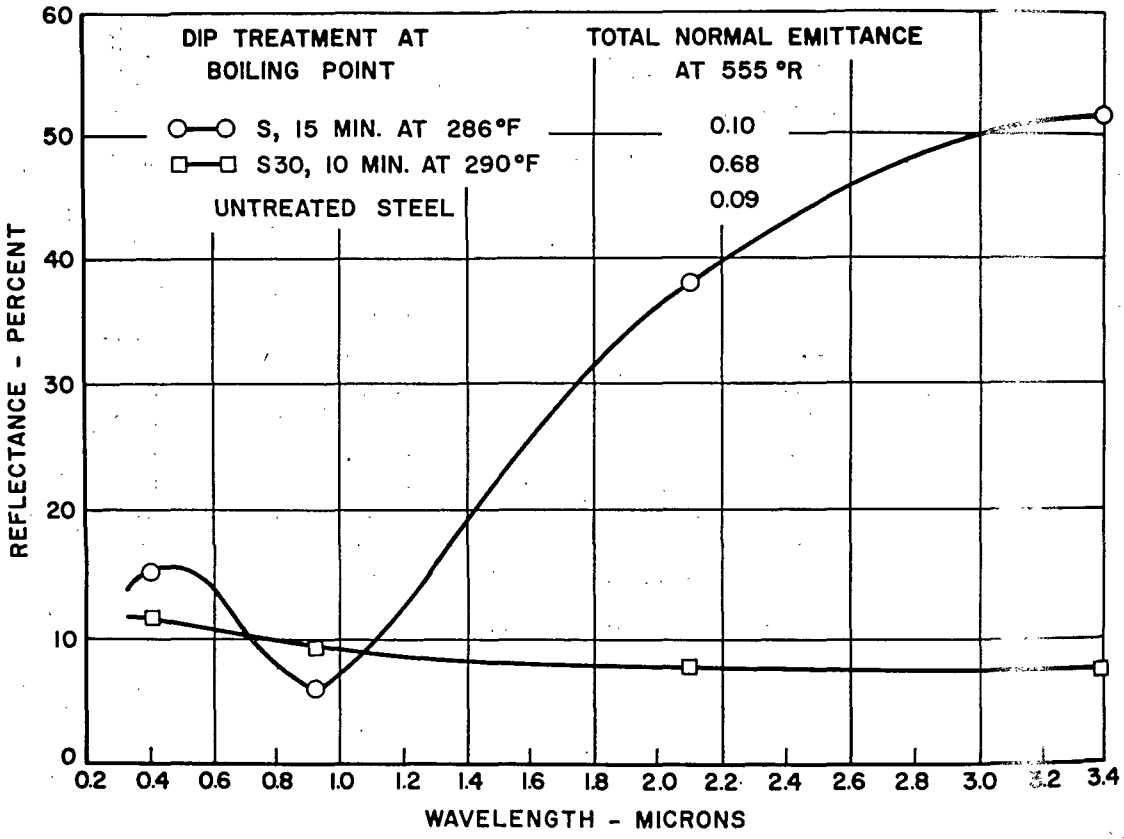


Figure 9. Near-normal spectral reflectance of Ebonol S and S30 on steel

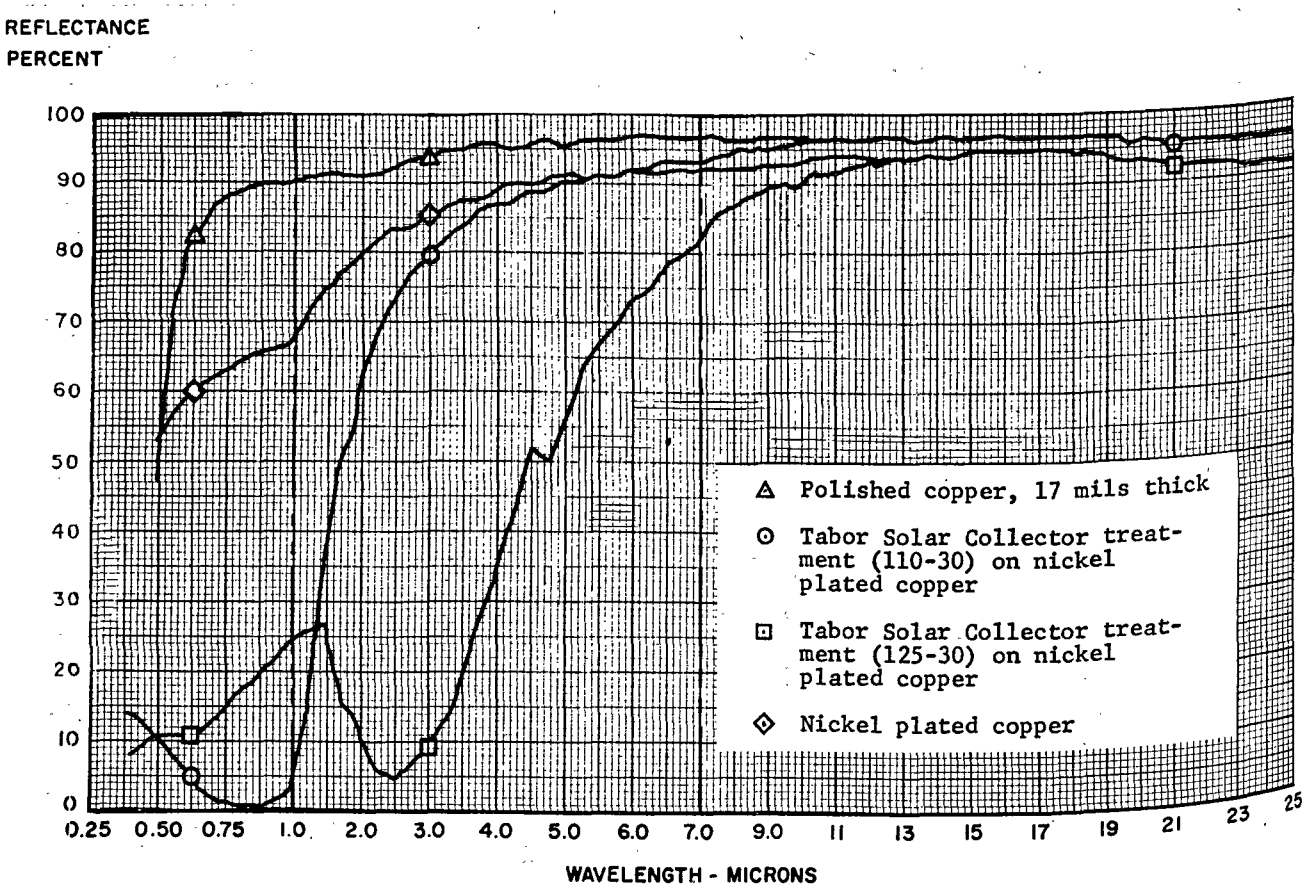


Figure 10. Near-normal spectral reflectance of Tabor treatments on nickel-plated copper

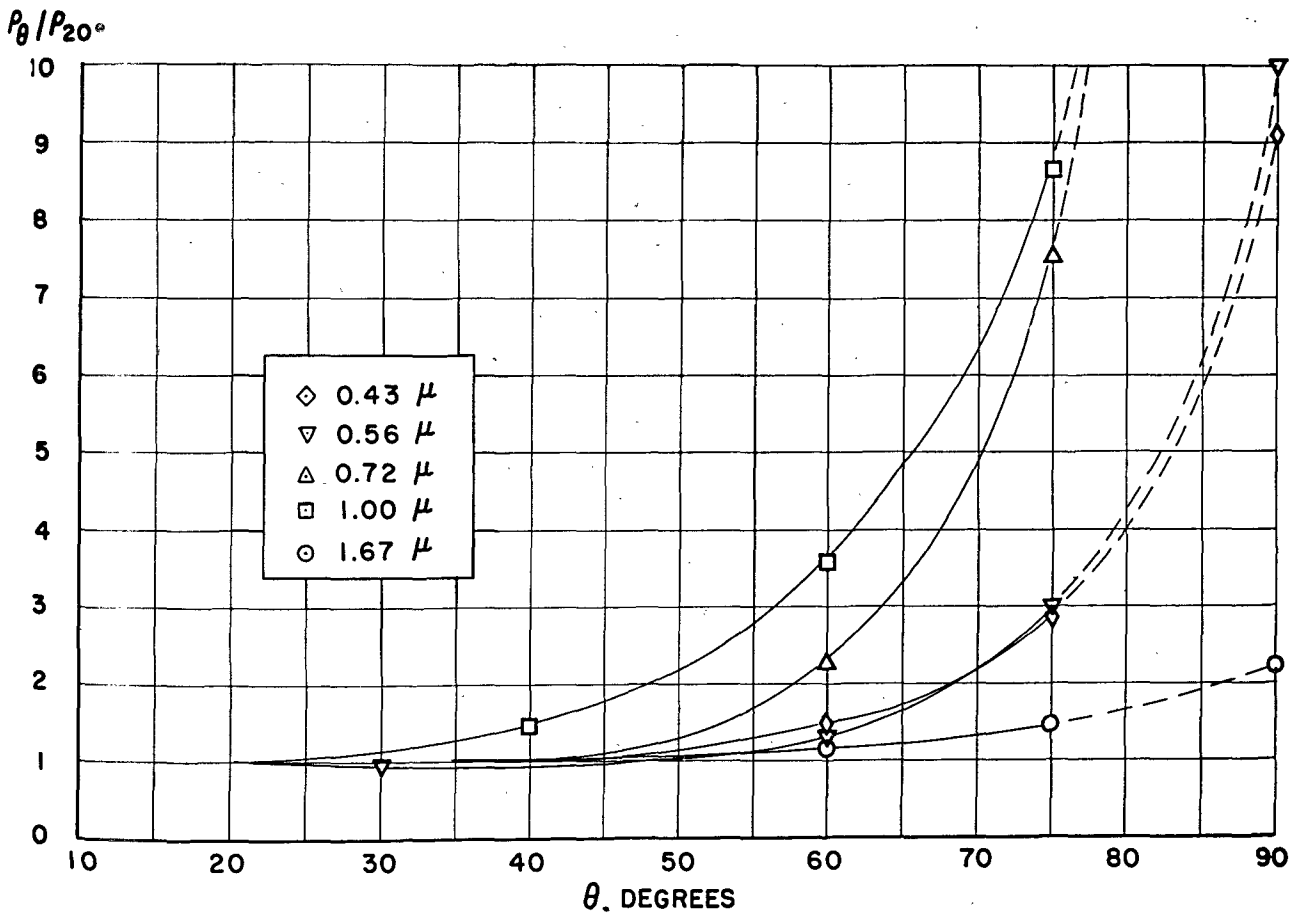


Figure 11. Normalized directional reflectance of Tabor treatment 110-30 on nickel-plated copper

Plane slab with homogeneous antireflection film

The solar absorptance of a metal may be increased without greatly increasing the long-wavelength emittance by a thin non-absorbing homogeneous dielectric surface coating. In this case, the directional reflectance is (4)

$$\rho(\Theta_0) = n_0 \underline{R}\,\underline{R}^* \qquad [11]$$

where

$$\underline{R} = \frac{\underline{r}_1 + \underline{r}_2 e^{-2i\delta_1}}{1 + \underline{r}_1 \underline{r}_2 e^{-2i\delta_1}} \qquad \delta_1 = \frac{2\pi n_1}{\lambda_0} d \cos\Theta_1 \qquad [12]$$

In this case, the subscripts 0, 1, and 2 refer to vacuum (or air), the thin film, and the substrate respectively. The Fresnel coefficients for the substrate-film interface are obtained from equation [8] by replacing subscripts 0 and 1 with 1 and 2 respectively. The spectral range of high absorptance is limited for a single layer but may be extended by use of multiple films (6).

Plane slab with inhomogeneous antireflection film

The effectiveness of a non-absorbing dielectric antireflection film can be increased on the short-wavelength side by contriving a continuous change in the index of refraction from a low value at the surface to that of the absorbing substrate (7). For non-absorbing film and substrate, the normal reflectance of a film with an index of refraction varying exponentially from n_1 to n_1'

$$\rho(\Theta = 0) = \frac{(n_0 n_2 P + n_1 n_1' Q)^2 + (n_0 n_1' T + n_1 n_2 S)^2}{(n_0 n_3 P - n_1 n_1' Q)^2 + (n_0 n_1' T - n_1 n_2 S)^2} \qquad [13]$$

where

$$P = Y_0(\alpha) J_0(\beta) - J_0(\alpha) Y_0(\beta)$$
$$Q = J_1(\alpha) Y_1(\beta) - Y_1(\alpha) J_1(\beta)$$
$$T = Y_0(\alpha) J_1(\beta) - J_0(\alpha) Y_1(\beta)$$
$$S = Y_1(\alpha) J_0(\beta) - J_1(\alpha) Y_0(\beta)$$
$$\alpha = 2\pi n_1 d/\lambda \, Ln\,(n_1'/n_1) \qquad \beta = 2\pi n_1' d/\lambda \, Ln\,(n_1'/n_1)$$

where J and Y are Bessel functions of the first and second kind respectively.

Thick film semiconductor coating

The absorption coefficient of a semiconductor increases greatly with increasing photon energy for energies near the band gap energy, since higher

energy photons free bound electrons into the conduction band (8). The film is then opaque in the short wavelength region and may be transparent in the long wavelength region. If the thick film exists on a metallic substrate, reflection from this substrate occurs where the film is transparent. The effects of phase reinforcement and cancellation given by equations [10] and [11] average to give

$$\rho(\Theta_0, \Phi_0) = \rho_1(\Theta_0, \Phi_0) + \frac{\rho_2(\Theta_1, \Phi_1)\,[1 - \rho_1(\Theta_0, \Phi_0)]^2 \exp[-2Kd]}{1 - \rho_1(\Theta_0, \Phi_0)\,\rho_2(\Theta_1, \Phi_1) \exp[-2Kd]} \quad [14]$$

where ρ_1 and ρ_2 refer to the reflectances of the air-film interface and film substrate interface given by equation [9].

The absorption coefficient K is

$$K = \frac{4\pi nk}{\lambda_0} \quad [15]$$

When λ is larger than λ_{CO}, K is small, and

$$\rho = \rho_1 + \frac{\rho_2(1-\rho_1)^2}{1-\rho_1\rho_2} \quad [16]$$

When λ is smaller than λ_{CO}, K is large and

$$\rho - \rho_1 \quad [17]$$

The cut-off wavelength is related to the band gap energy by Einstein's Photoelectric Law

$$E_g = hv'_{CO} = \frac{hc}{\lambda_{CO}} \quad [18]$$

Directional spectral reflectances of materials for solar absorbers

Spectrally selective materials previously investigated are the Tabor electrochemical treatments (9); oxides of copper (10-12), cobalt (12, 13), and chrome-nickel-vanadium alloy (13); metal blacks (5); and interference film systems (6). To these may be added oxidized or chemically treated metals having a homogeneous or inhomogeneous film perhaps combining interference effects with selective absorption effects. Directional and spectral reflectances of some of these materials are presented.

Directional reflectance measurements in the 0.3 to 3.4 micron region were made with a directional integrating sphere (14) somewhat similar to that of Toporets (15). Near-normal reflectances shown[1]

[1] These near-normal ($\theta = 70$) reflectances were extracted from the compiled data of Professors R. V. Dunkle and J. T. Gier.

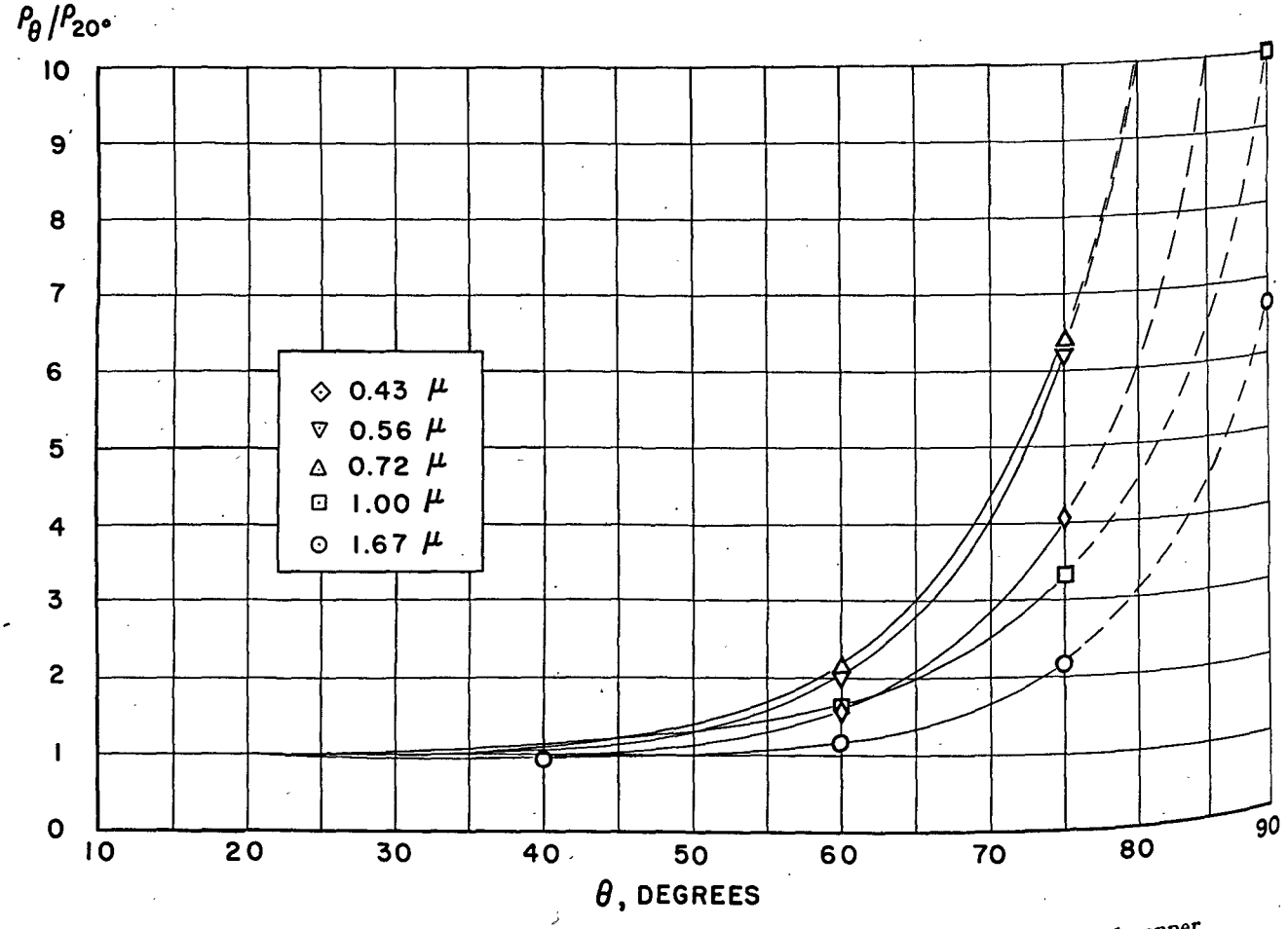


Figure 12. Normalized directional reflectance of Tabor treatment 125-30 on nickel-plated copper

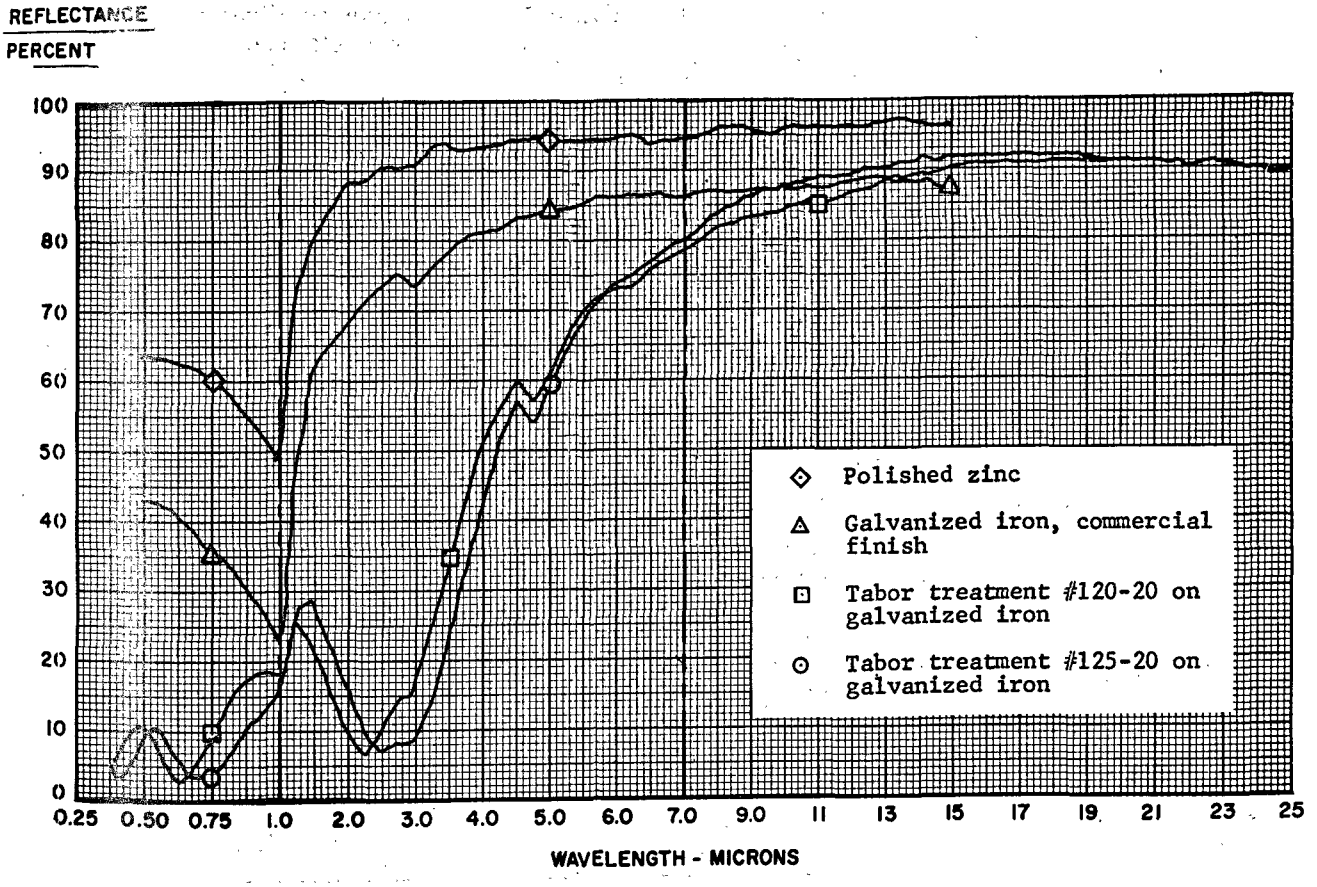


Figure 13. Near-normal spectral reflectance of Tabor treatments on galvanized iron

were obtained with a heated cavity reflectometer for the 1.5 to 25 μ region, a General Electric spectrophotometer for the 0.4 to 1 μ region, and a Beckman DK2 spectro-reflectometer in the 0.25 to 2.5 μ region. The short-wavelength data obtained with these latter two instruments was corrected for error due to direct irradiation of the detector. It is emphasized that the spectral data presented here are valid, independent of whether or not the specimens are diffuse, specular, or have an arbitrary distribution of reflected radiant flux (14). The few normal total emittance measurements shown in figures 7 and 9 were determined with a cooled radiometer (14) similar to the Schmidt type (17).

Metals oxidized by heating give rise to spectrally selective surfaces from the antireflection oxide film. These films may be rough, porous, inhomogeneous, and absorbing as well. However, the spectral and directional characteristics of oxidized titanium in figures 1 to 4 suggest largely an interference effect. Data for oxidized chromium and stainless steel are shown in figures 5 and 6.

Directional spectral reflectances of copper and steel subjected to commercial chemical dip treatments are shown in figures 7 to 9. Ebonol treatments of Enthone, Inc., of New Haven, Connecticut, were used. The Ebonol C commercial process produces a black cupric oxide coating on copper which is very adherent and resistant to atmospheric attack at temperatures up to 400°F. The Ebonol S commercial process produces a black or dark blue oxide film on steel.

Spectral and directional reflectances of several electrochemically treated surfaces prepared by H. Tabor are shown in figures 10-15. It cannot be definitely concluded from the data what mechanism makes these films so selective. Several observations can be made, however. First, the index of refraction of the metallic substrate is decreasing rapidly with decreasing wavelength in the visible. Uncoated zinc itself is fairly selective. Next, the variation of the reflectance with increasing angle from the normal is not as pronounced as for a single homogeneous non-absorbing antireflection film as indicated by equations [10] and [11]. The data for oxidized titanium in figure 4 can be examined for comparison. Finally, the damped oscillations in the reflectance with wavelength in the visible are characteristic of an inhomogeneous film. However, it is probable that the films have selective absorptive properties as do semiconductors. Such absorption, together with the change in optical properties of the substrate, would also damp the oscillations in the visible.

In view of the remarks in the section on thick film semiconductor coating above, a desirable semiconductor for a selective absorber should have the following properties:

(*a*) A band gap energy of approximately 0.5 ev giving a λ_{CO} in the 2 μ region of interest;

(*b*) A sufficiently low absorption coefficient in the infrared K_R and a sufficiently high absorption coefficient in the visible K_V such that a thickness d of about 10 to 100 microns exists such that $K_V d > 4$ and $K_R d < 10^{-2}$;

(*c*) A resistance to atmospheric attack or vaporization in space;

(*d*) A low reflectance.

Un-doped silicon with and without an antireflection coating was chosen for investigation. As shown in figure 16, an extremely sharp cut-off was obtained at the band energy wavelength of 1.1 μ. The directional characteristics are shown in figure 17. Comparison of these characteristics at wavelengths of 0.7 and 0.9 μ shows agreement with the Fresnel relations of equations [10] and [11] within 0.02 at angles up to 75° from the normal. Figure 18 shows the reflectance of a doped silicon solar cell, which has a sintered nickel electrode on the back surface.

Evaluation of measured directional spectral reflectances

Spectral selectivity

As explained in paragraph 7, equation [5] may be used to evaluate selective absorbers. It is seen that the absorptance of merit α' depends on the quantity β defined in equation [6] as well as the solar absorptance and total hemispherical emittance. Two extreme values of β are chosen, one of 0.37 and another of 4.0. The former represents a low temperature collector, such as one at 555 R outside the earth's atmosphere, and the latter represents a fairly high temperature collector, such as one at 1 000 R outside the earth's atmosphere. Solar absorptances were evaluated for irradiation outside the atmosphere (1), and emittances were evaluated at 555 R for $\beta = 0.37$ and 1 000 R for $\beta = 4.0$. Spectral characteristics were assumed to be independent of temperature for the above range.

Table 1 shows the results. Negative values of α' indicate the material will not operate at all. Several materials are attractive for low temperature collectors. Among the best are the Tabor surfaces, the Ebonol treated surfaces, and the solar cell. At the higher value of β, however, only the Tabor surface

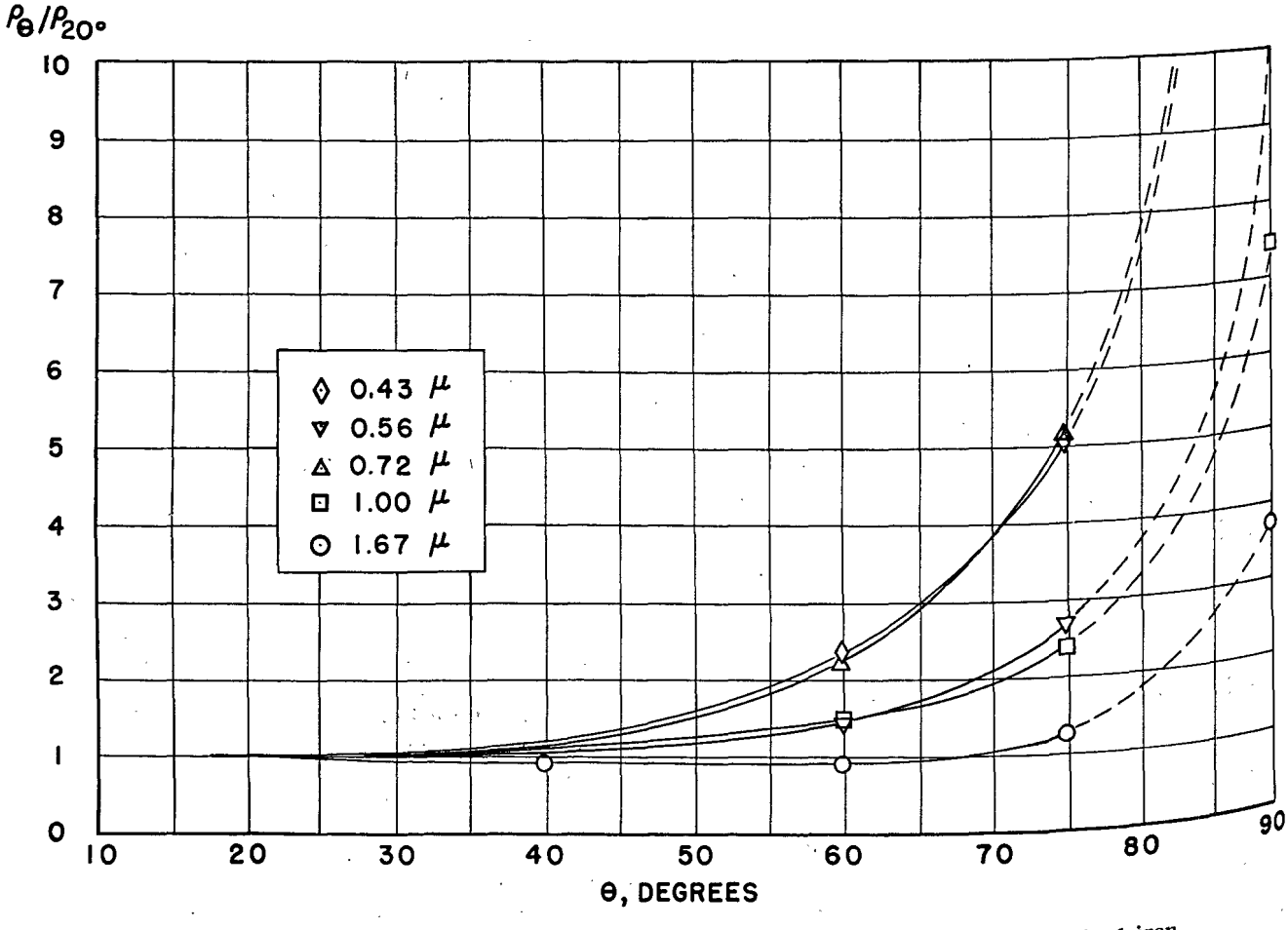


Figure 14. Normalized directional reflectance of Tabor treatment 120-20 on galvanized iron

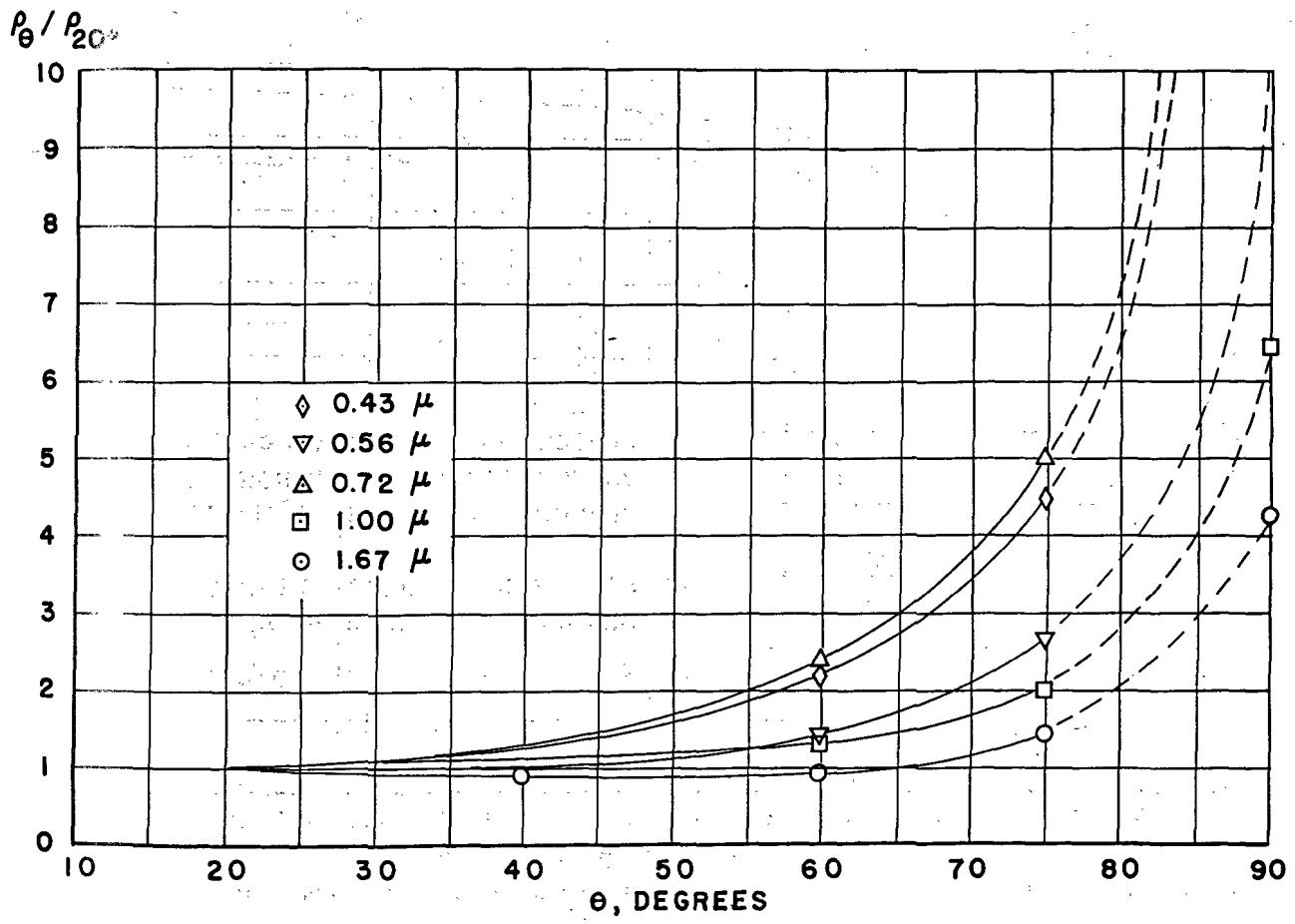


Figure 15. Normalized directional reflectance of Tabor treatment 125-20 on galvanized iron

110-30 and the SiO_2 on Si on Al are outstanding. However, when the former material was heated to 960 R in air, the emittance increased to above 0.11 and the visual color changed from a dark blue-black to a light gold, indicating a decrease of solar absorptance.

Directional selectivity

If a collector is being used together with a concentrator, if collection is desired on overcast days, or if the collector is located on a space vehicle for temperature control purposes, the solar irradiation is not just from the normal direction. It is thus of interest to compare hemispherical with normal solar absorptances. For this purpose hemispherical values were estimated from the directional data, again for solar irradiation outside the atmosphere.

Table 2 shows a comparison of α_S ($\Theta = 20°$) with α_{SH}. It may be noted that the Tabor, Ebonol, and silicon surfaces all have a hemispherical absorptance which is only slightly less than the normal value. The titanium oxide coated aluminum, however, has a hemispherical absorptance appreciably smaller than its normal absorptance.

Conclusion

This paper has considered the following questions:

(*a*) What directional spectral thermal radiation characteristics are desirable for solar collec tors?

(*b*) What surface systems exist for obtaining spectral selectivity?

(*c*) What are the directional spectral characteristics of known solar collector surfaces?

(*d*) Which known surfaces are better?

(*e*) Is directional variation of solar absorptance important for known solar collector surfaces?

Equation [5] gives an approximate answer to the first question. The section on isothermal surface systems for spectrally selective collectors, and the data contained in figures 1-18, give partial answers to the second and third questions respectively. Equation [5], together with the data presented, can answer the fourth question, and table 1 indicates general trends. Table 2 supplies a partial answer to the final question.

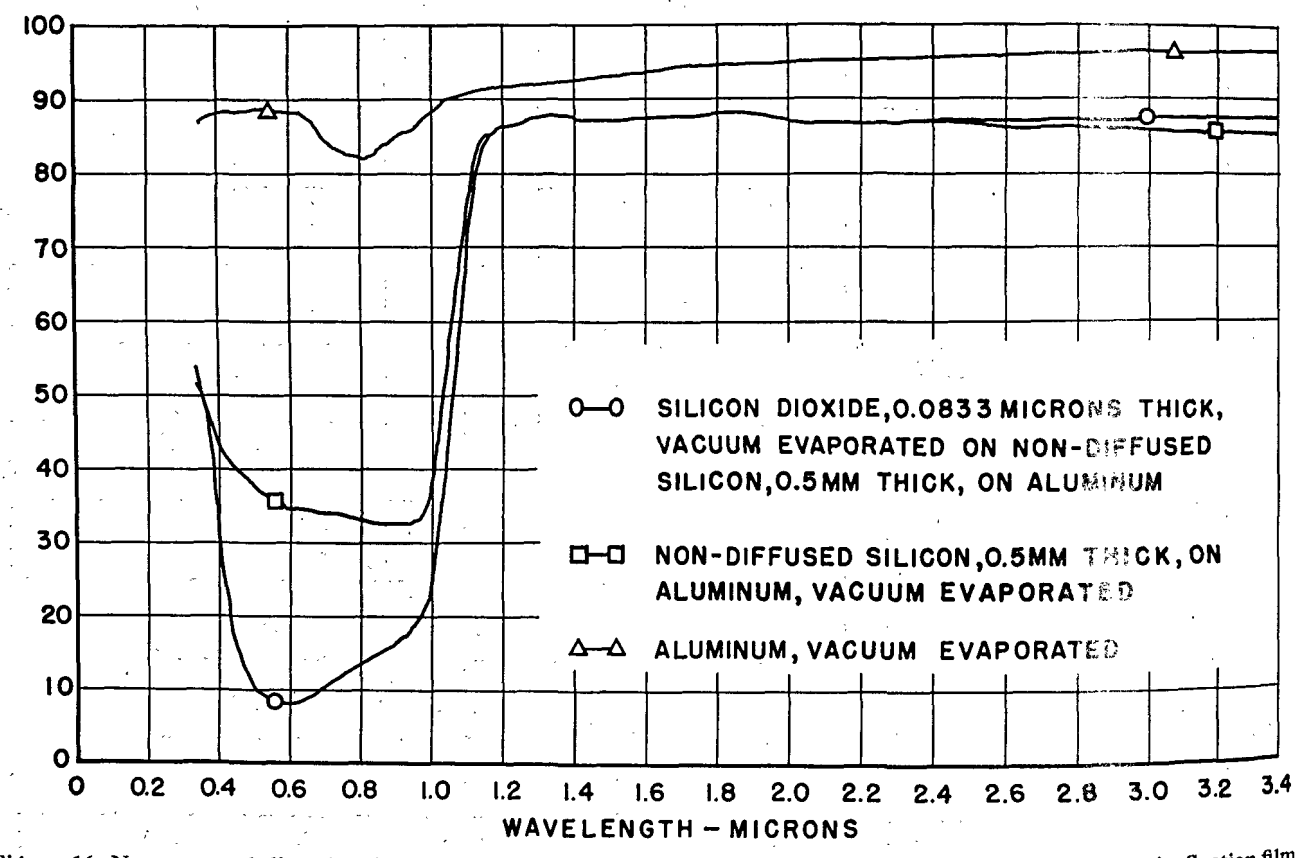


Figure 16. Near-normal directional reflectance of silicon on aluminum with and without silicon dioxide antireflection film

Table 1. Absorptance of merit for collectors in space

($G_S = 442$ Btu/hr ft²; $G_L = 0$)

Figure No.	*Surface*	α_S	$T_C = 555$ R ε	$T_C = 555$ R α'	$T_C = 1\,000$ R ε	$T_C = 1\,000$ R α'
1	Titanium 75A (AMS 4901) heated 300 hr at 850°F in air	0.80	0.21	0.72	0.29	— 0.34
2	Titanium C-110M (AMS 4908) heated 100 hr at 800°F in air	0.52	0.16	0.46	0.20	— 0.26
2	Titanium C-110M (AMS 4908) heated 300 hr at 850°F in air	0.77	0.20	0.70	0.25	— 0.19
3	Titanium vapor coated on bright side of Reynold's Wrap aluminum foil, 80 to 100 microns thick, heated 3 hr at 750°F in air	0.75	0.14	0.70	0.21	— 0.08
5	Chromium plate, 0.1 mil thick, on 0.5 mil nickel plate on 321 stainless steel, exposed to JP4 combustion products 50 hr at 1 100°F	0.78	0.15	0.72	0.18	0.07
6	410 stainless steel heated to 1 300°F in air	0.76	0.13	0.72	0.18	0.06
7	Ebonol C on copper dipped 5 min at 175°F in 219°F boiling point solution	0.91	0.16	0.85	—	—
9	Ebonol S on steel dipped 15 min in a 286°F boiling solution	0.85	0.10	0.81	—	—
10	Tabor solar collector surface treatment 110-30 on nickel-plated copper	0.85	0.05	0.84	0.08	0.55
10	Tabor solar collector surface treatment 125-30 on nickel-plated copper	0.85	0.11	0.81	0.27	— 0.20
13	Tabor solar collector surface treatment 120-20 on galvanized iron.	0.89	0.12	0.84	0.26	— 0.14
16	Crystalline un-doped silicon, 0.5 mm thick, on evaporated aluminum.	0.50	0.12*	0.46	0.12*	0.02
16	Silicon dioxide, 833 Å thick, on crystalline un-doped silicon, 0.5 mm thick, on evaporated aluminum	0.65	0.12*	0.60	0.12*	0.17
18	Silicon Solar Cell, International Rectifier Corp. Boron-doped crystalline silicon on sintered electroless nickel plate substrate.	0.94	0.32	0.82	0.50	— 0.99

* Extrapolated.

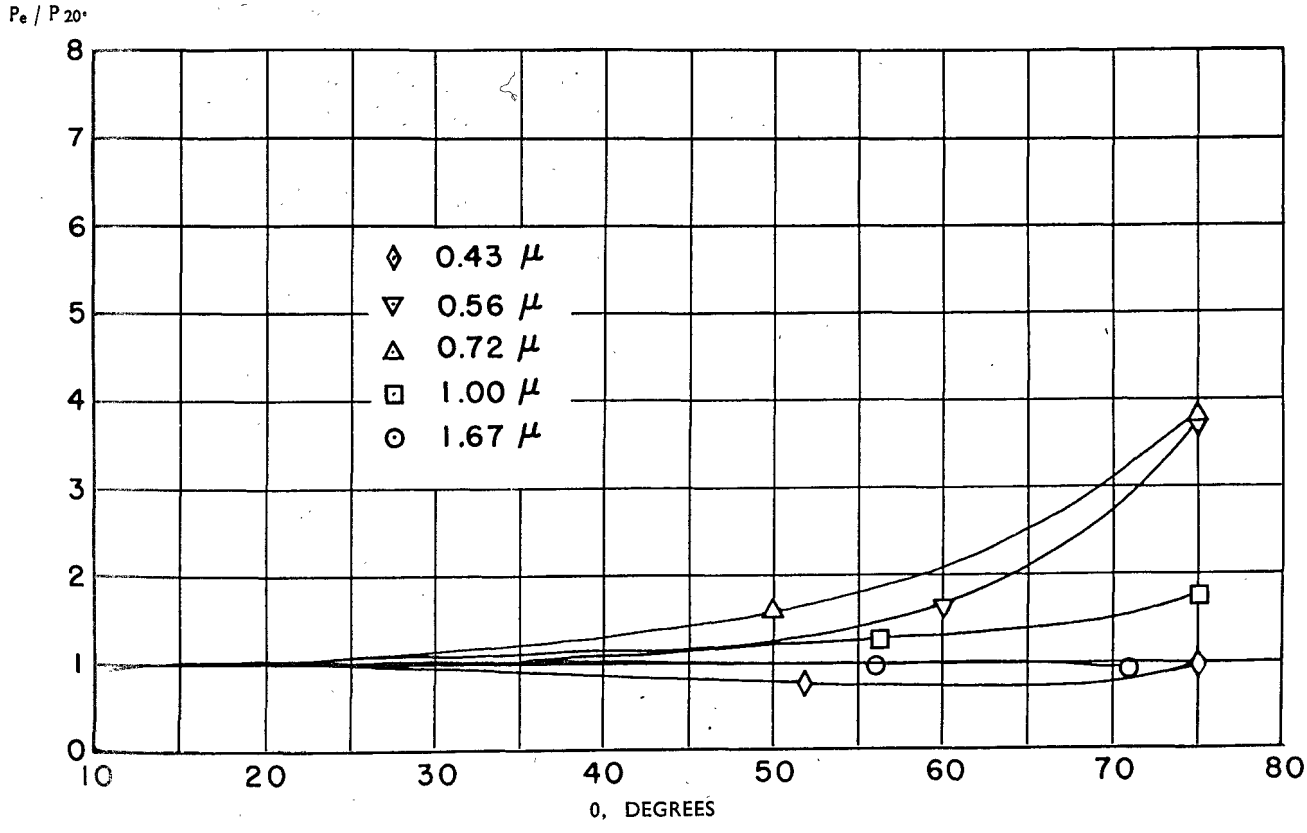


Figure 17. Normalized directional reflectance of silicon dioxide on silicon on aluminum

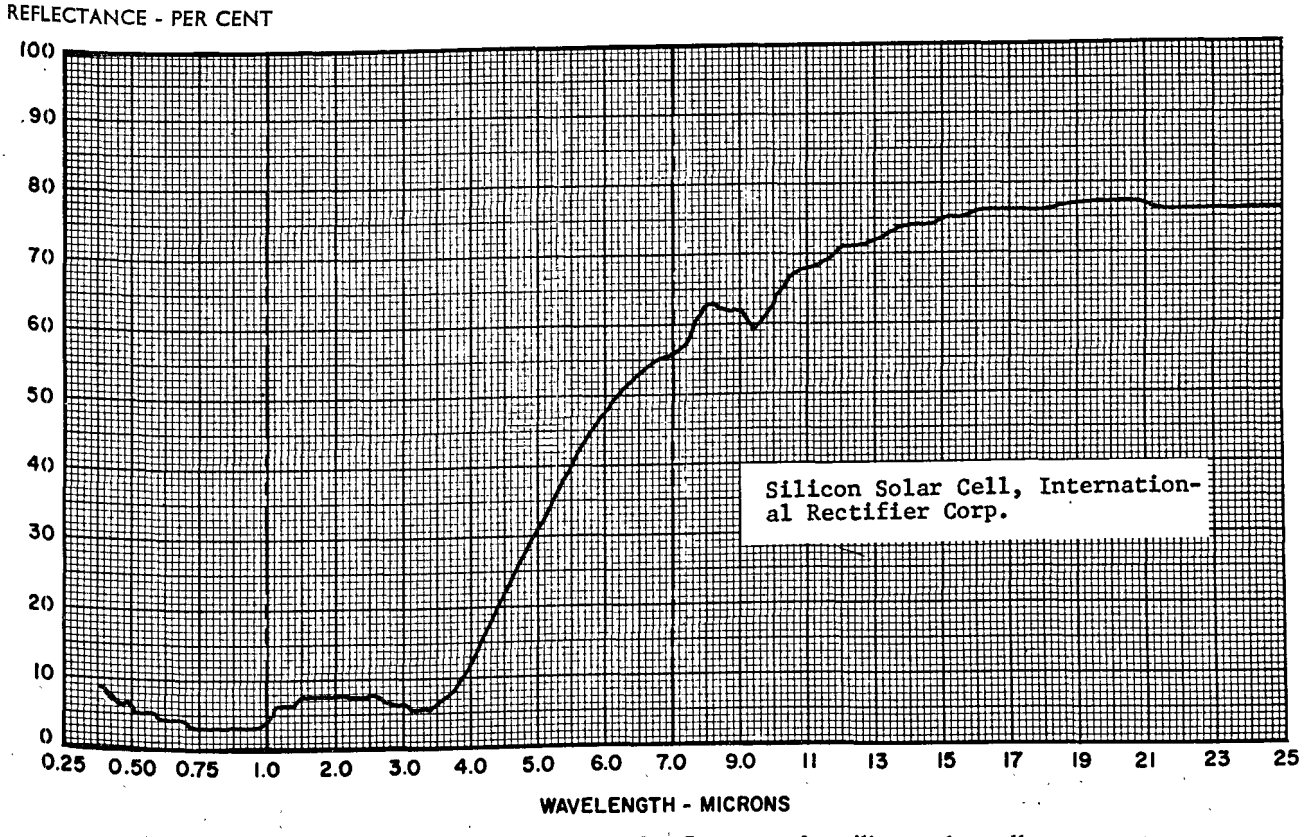


Figure 18. Near-normal spectral reflectance of a silicon solar cell

Table 2. Ratio of hemispherical solar absorptance to near-normal solar absorptance

Surface	*Figure*	α_S (20°)	α_{SH}/α_S (20°)
Titanium vapor coated on bright side of Reynold's Wrap aluminum foil, 80 to 100 microns thick, heated 3 hr at 750°F in air . .	3	0.75	0.68
Ebonol C on copper dipped 5 min. at 196°F in 219°F boiling point solution	8	0.87	0.94
Tabor solar collector surface 110-30 on nickel-plated copper . . .	11	0.85	0.93
Tabor solar collector treatment 120-20 on galvanized iron . .	14	0.89	0.96
Tabor solar collector treatment 125-20 on galvanized iron . .	15	0.90	0.96
Silicon dioxide, 833 Å thick, on un-doped crystalline silicon, 0.5 mm thick, in evaporated aluminum	16	0.65	0.94

The following conclusions are reached.

(*a*) Promising low-temperature collector surfaces appear to be copper or steel treated by the commercial Ebonol processes. These surfaces compare favorably with Tabor surfaces.

(*b*) Stable surfaces for higher temperature collectors appear to be thick film semiconductors such as silicon, with antireflection coatings such as silicon dioxide.

(*c*) Directional variation of solar absorptance of materials investigated to date is of major significance only at angles of incidence above 60° from the surface normal. Hemispherical solar absorptance differs 32 per cent at most from normal solar absorptance for the materials investigated.

Acknowledgement

The authors wish to acknowledge support from National Science Foundation Grant G9505.

References

1. Johnson, F. S., The Solar Constant, *J. Meteorol., 11*, 431, 1954.
2. Moon, P., Proposed Standard Solar Radiation Curves for Engineering Use, *J. Franklin Institute, 230*, 583, 1940.
3. Whitaker, R. O., Methodology for Determination of Performance Characteristics of Spectrally Selective Surfaces, *Solar Energy, IV*, No. 2, p. 40, 1960.
4. Heavens, O. S., *Optical Properties of Thin Solid Films*, Butterworths Scientific Publications, London, 1955.
5. Kozyrev, B. P. and Vershinin, O. E., Determination of Spectral Coefficients of Diffuse Reflection of Infrared Radiation from Blackened Surfaces, *Optics and Spectroscopy, 6*, 345, 1959.
6. Hass, G., Schroeder, H. H. and Turner, A. F., Mirror Coatings for Low Visible and High Infrared Reflectance, *J. Opt. Soc. Am., 46*, 31, 1956.
7. Monaco, S. F., Reflectance of an Inhomogeneous Thin Film, *J. Opt. Soc. Am., 51*, 280, 1961.
8. Moss, T. S., *Optical Properties of Semiconductors*. Butterworths Scientific Publications, London, 1959.
9. Tabor, H., Selective Radiation I. Wavelength Discrimination, *Trans. of the Conference on the Use of Solar Energy*, vol. II, part I, sec. A, p. 24, 1955.
10. Gier, J. T. and Dunkle, R. V., Selective Spectral Characteristics as an Important Factor in the Efficiency of Solar Collectors, *Trans. of the Conference on the Use of Solar Energy*, vol. II, part 1, sec. A, p. 41, 1955.
11. Hottel, H. C. and Unger, T. A., The Properties of a Copper Oxide-Aluminum Selective Black Surface Absorber of Solar Energy, *Solar Energy*, vol. III, No. 3, p. 10, 1959.
12. Kokoropoulos, P., Salam, E. and Daniels, F., Selective Radiation Coatings. Preparation and High Temperature Stability, *Solar Energy*, vol. III, No. 4, p. 19, 1959.
13. Gillette, R. B., Selectively Emissive Materials for Solar Heat Absorbers, *Solar Energy*, vol. IV, No. 4, p. 24, 1960.
14. Edwards, D. K., Nelson, K. E., Roddick, R. D. and Gier, J. T., Basic Studies on the Use and Control of Solar Energy. Univ. of Calif., Los Angeles, Dept. of Engin. Report 60-93, 1960.
15. Toporets, A. S., Study of Diffuse Reflection from Powders under Diffuse Illumination, *Optics and Spectroscopy, 7*, 471, 1959.
16. Gier, J. T., Dunkle, R. V. and Bevans, J. T., Measurement of Absolute Spectral Reflectivity from 1 to 15 Microns, *J. Opt. Soc. Am., 44*, 558, 1954.
17. Jakob, M., *Heat Transfer*, vol. II, chap. 31. John Wiley and Sons, New York, 1959.

Summary

The purpose of the paper is to present spectral and directional characteristics of materials which may be used in solar collectors. Only isothermal surfaces are considered.

The collector surface is considered to be irradiated by intensity $I_\lambda^+ (\Theta, \Phi)$, where Θ is the polar angle from the surface normal and Φ is the azimuthal angle in the plane of the surface. A fraction $\alpha_\lambda (\Theta, \Phi)$ of the incident energy flux in solid angle $d\Omega$ about Θ, Φ is absorbed by the surface. It follows from Kirchoff's law that the intensity emitted by the surface is $I_\lambda^- = \alpha_\lambda (\Theta', \Phi') I_{b\lambda} (T_C)$ where $I_{b\lambda} (T_C)$ is given by Planck's law. The irradiation absorbed αG is then given by equation [1] of the text, and

the radiant flux emitted $\varepsilon\sigma T_C^4$ is given by equation [3] of the text.

For an optimum solar collector αG should be large and $\varepsilon\sigma T_C^4$ small, but α and ε are related as indicated by equations [1] and [3].

In order to make some useful generalizations, the irradiation is considered to be composed spectrally of a solar component G_S and an infrared component G_L. The absorptance for the former is designated α_S and that for the latter is taken as ε.

A solar absorptance of merit α' can now be defined as in equation [5].

The quantity β defined by equation [6] can be designated the α_S—ε trade-off ratio, since it gives the maximum decrease in α_S that a designer would willingly sacrifice to gain a unit decrease in ε. For low collector temperatures, covered collectors and/or concentrators, this ratio is low.

Equations [1] and [3] may be used to determine the optimum cut-off wavelength λ_{CO} for each direction Θ, Φ. For a *perfectly diffuse collector* only, the cut-off wavelength where α_λ should undergo a step decrease is given by equation [7]. For low-temperature collectors and low concentration, the cut-off wavelength is not critical, however.

The introductory remarks above indicate what characteristics are desirable. The sections below give some simple selective systems; present measurements; and show an evaluation of the measured materials.

Isothermal surface systems for spectrally selective collectors

Several elementary surface systems are considered.

Homogeneous plane slab. The simplest is the homogeneous slab whose directional reflectance is given by equation [10]. Spectral selectivity arises from variation of the refractive and absorptive indices with wavelength. However, λ_{CO} is usually too short for known materials.

Homogeneous rough slab. Surface roughness may add to the selectivity.

Layer of small particles. Finely divided particles such as metal blacks (5) are selective.

Plane slab with homogeneous antireflection film. Use of an interference film gives the directional reflectance indicated by equation [11]. The subscripts 0, 1, and 2 refer to vacuum (or air), the film, and the substrate, respectively. Multiple films can be used to extend the spectral range of high absorptance (6).

Plane slab with inhomogeneous antireflection film. An inhomogeneous antireflection film increases absorptance in the short wavelengths. The reflectance of a dielectric film with an expontentially increasing refractive index from n_1 to n_1' in a depth d is given by equation [13] (7).

Thick film semiconductor coating. The absorption coefficient of a semiconductor changes greatly at the wavelength corresponding to the band gap energy (8). Equation [14] gives the directional reflectance of a thick film. Equation [16] gives the reflectance in the long wavelengths where the semiconductor is transparent; and equation [17] gives the reflectance when the film is opaque in the short wavelengths.

Directional spectral reflectances of materials for solar absorbers

Several selective materials have been reported (5, 6, 9-13).

An integrating sphere (14) was used for short-wavelength measurements and a heated cavity reflectometer (16) for long wavelengths. It is emphasized that the measurements are valid for specular, imperfectly diffuse, or perfectly diffuse materials.

Figures 1 to 6 show the reflectance of oxidized metals.

Directional reflectances of copper and steel treated with Ebonol chemical dips are shown in figures 7 to 9.

Reflectances of several Tabor surfaces are shown in figures 10 to 15.

A desirable semiconductor is one with a band gap energy of about 2 ev.

Figures 16 to 18 show the directional reflectances of silicon on aluminum and nickel.

Evaluation of measured directional spectral reflectances

Spectral selectivity. Equation [5] is used to compare the merit of several of the surfaces for two values of β. Table 1 shows the results. High values of α' are best. It is not certain that all of the materials are stable at 1 000 R.

Directional selectivity. Solar irradiation at off-normal angles occurs when the sky is overcast, when the collector is not oriented toward the sun, or when a concentrator is used.

Table 2 shows a comparison of α_S ($\theta = 20°$) and the hemispherical solar absorptance α_{SH}.

Conclusions

The conclusions are as follows:

(*a*) Promising low temperature collector surfaces are copper and steel treated with the Ebonol process;

(*b*) Thick semiconductor films may offer selective surfaces with high-temperature stability;

(*c*) Hemispherical absorptance may differ by 32 per cent from normal absorptance.

CARACTÉRISTIQUES SPECTRALES ET THERMO-DIRECTIONNELLES DE SURFACES SÉLECTIVES POUR LES COLLECTEURS SOLAIRES

Résumé

Cette communication présente les caractéristiques spectrales et directionnelles de matériaux qui peuvent être utilisés à la réalisation de collecteurs solaires. Elle ne considère que les surfaces isothermiques.

Les auteurs admettent que la surface du collecteur est irradiée par une intensité $I_\lambda^+ (\theta, \phi)$ dans laquelle θ est l'angle polaire compté à partir de la normale à la surface et ϕ l'angle azimutal dans le plan de la surface. Une fraction $\alpha_\lambda (\theta, \phi)$ du flux d'énergie incidente dans l'angle solide $d\Omega$ autour de θ, ϕ est absorbée par la surface. Il s'ensuit, de la loi de Kirchoff, que l'intensité émise par la surface est $I_\lambda^- = \alpha_\lambda (\theta', \phi') I_{b\lambda} (T_C)$, expression dans laquelle $I_{b\lambda} (T_C)$ est donné par la loi de Planck. Le rayonnement absorbé αG est donc fourni par l'équation 1 du texte et le flux rayonnant émis $\varepsilon \sigma T_C^4$ est donné par l'équation 3 du texte.

Pour que le collecteur solaire soit idéal, il faut que αG soit grand et $\varepsilon \sigma T_C^4$ petit, mais α et ε sont liés de la manière exprimée par les équations 1 et 3.

Pour faire quelques généralisations utiles, on considère l'irradiation comme étant constituée, spectralement parlant, par une composante solaire G_S et une composante infrarouge G_L. Le coefficient d'absorption pour la première est désigné par α_S et celui de la seconde par ε.

On peut donc maintenant définir, comme dans l'équation 5, un coefficient de mérite pour l'absorption (absorbance) solaire.

La grandeur β définie par l'équation 6 peut être considérée comme étant la proportion α_S—ε acceptable de perte, car elle donne la réduction maximale de α_S qu'un ingénieur serait tout disposé à sacrifier pour gagner une diminution unitaire de ε. Pour les collecteurs à basse température, les collecteurs couverts et/ou les concentrateurs, cette proportion est faible.

On peut se servir des équations 1 et 3 pour déterminer la longueur d'onde de coupure idéale λ_{CO} pour chaque direction θ, ϕ. Pour un *collecteur parfaitement diffus* seulement, la longueur d'onde de coupure pour laquelle α_λ doit faire l'objet d'une réduction marquée est donnée par l'équation 7. Pour les collecteurs à basse température et à faible concentration, cependant, la longueur d'onde de coupure n'est pas critique.

Ces remarques mettent en lumière les caractéristiques souhaitables. Les sections qui suivent mentionnent quelques systèmes sélectifs simples, résument les mesures et donnent une évaluation des matériaux sur lesquels on les a faites.

Systèmes à surface isothermique pour collecteurs à sélection spectrale

Le mémoire examine plusieurs systèmes élémentaires de surface.

Plaque homogène plane. Le plus simple de ces systèmes est la plaque homogène, dont le coefficient directionnel de réflection est donné par l'équation 10. La sélectivité spectrale est due aux variations des indices de réfraction et d'absorption en fonction de la longueur d'onde. Néanmoins, λ_{CO} est habituellement trop court pour les matériaux connus.

Plaque homogène rugueuse. La rugosité de la surface peut améliorer la sélectivité du système ci-dessus.

Couche de petites particules. Les particules finement divisées telles que les noirs métalliques (5) sont sélectives.

Plaque plane avec pellicule homogène contre la réflexion. L'emploi d'une pellicule à interférence donne la réflectance directionnelle indiquée par l'équation 11. Les indices 0, 1 et 2 se rapportent au vide (ou à l'air), à la pellicule et à son support respectivement. On peut se servir de pellicules multiples pour augmenter la largeur de la plage spectrale sur laquelle le coefficient d'absorption est élevé (6).

Plaque plane avec pellicule non homogène contre la réflexion. La pellicule non homogène contre la réflexion augmente le coefficient d'absorption dans les ondes courtes. La réflectance d'une pellicule de diélectrique dont l'indice de réfraction augmente suivant une fonction exponentielle entre n_1 et n_1' sur une épaisseur d est donnée par l'équation 13 (7).

Enduit constitué par une pellicule épaisse de semi-conducteur. Le coefficient d'absorption d'un semi-conducteur change beaucoup à la longueur d'onde qui correspond à l'énergie de la coupure de bande (8). L'équation 14 donne le coefficient directionnel de réflectivité d'une pellicule épaisse. L'équation 16 donne la réflectance dans les ondes longues lorsque le semi-conducteur est transparent, et l'équation 17 donne la réflectance lorsque la pellicule est opaque dans les ondes courtes.

Réflectances spectrales directionnelles des matériaux utilisés dans les absorbeurs solaires

Le mémoire signale plusieurs matériaux sélectifs (5, 6, 9-13).

Une sphère d'intégration (14) a été utilisée pour les mesures sur les ondes courtes et un réflectomètre

à cavité chauffée (16) pour les ondes longues. Ces mesures s'appliquent à des matériaux spéculaires, imparfaitement ou parfaitement diffus.

Les figures 1 à 6 donnent la réflectance des métaux oxydés. La réflectance directionnelle du cuivre et de l'acier traités par immersion dans des produits chimiques Ebonol est donnée aux figures 7 à 9. Les figures 10 à 15 donnent les réflectances de plusieurs surfaces Tabor.

Un semi-conducteur souhaitable présente une énergie de coupure de bande de l'ordre de 2 ev.

Les figures 16 à 18 donnent les réflectances directionnelles du silicium sur aluminium et sur nickel.

Évaluation des réflectances spectrales directionnelles mesurées

Sélectivité spectrale. On se sert de l'équation 5 pour comparer le mérite de plusieurs des surfaces pour deux valeurs de β. Le tableau 1 donne les résultats. Les grandes valeurs de α' sont les meilleures. Il n'est pas sûr que tous les matériaux soient stables à 1 000 *R*.

Sélectivité directionnelle. L'irradiation solaire à des angles différents de la normale se présente lorsque le ciel est couvert, lorsque le collecteur n'est pas orienté vers le soleil, ou quand on se sert d'un concentrateur.

Le tableau 2 donne une comparaison entre α_S ($\theta = 20°$) et l'absorbance solaire hémisphérique α_{SH}.

Conclusions

On aboutit aux conclusions suivantes :

a) Des surfaces pour collecteurs à basse température qui promettent d'être bonnes sont constituées par le cuivre et l'acier traité par le procédé Ebonol.

b) Les pellicules épaisses de matières semi-conductrices peuvent constituer des surfaces sélectives ayant une grande stabilité aux températures élevées.

c) Le coefficient d'absorption hémisphérique peut différer de l'absorbance normale de 32 p. 100.

UN NOUVEAU COLLECTEUR DE L'ÉNERGIE RAYONNANTE SOLAIRE — THÉORIE ET VÉRIFICATION EXPÉRIMENTALES

Giovanni Francia *

La température d'équilibre d'un collecteur classique d'énergie rayonnante, composé par exemple d'un corps noir exposé au soleil, est de loin inférieure à la température du soleil, même quand, comme dans le cas d'un corps noir, toute l'énergie incidente est retenue et transformée en chaleur.

Cela s'explique par exemple par le fait que l'angle solide dans lequel le corps noir ré-émet l'énergie, est d'un demi-espace, c'est-à-dire 2 π, tandis que l'énergie arrivée est contenue dans un angle solide fort petit, qui est l'angle sous lequel on voit le soleil et qui, si la grandeur apparente de celui-ci est de 32', est égal à 0,0000678.

Compte tenu de la règle du cosinus et de la proportionnalité entre l'énergie irradiée et la quatrième puissance de la température absolue, la température du soleil mesurée par la méthode du corps noir étant dénommée T_s, et celle du collecteur T_n, de simples calculs nous donnent la relation d'équilibre :

$$2\pi \int_0^{\frac{\pi}{2}} T_n^4 \cos\varphi \sin\varphi \, d\varphi = 0{,}0000678\, T_S^4 \qquad (1)$$

c'est-à-dire

$$\pi T_n^4 = 0{,}0000678\, T_S^4 \qquad (2)$$

où l'on a supposé la surface du corps noir perpendiculaire aux rayons du soleil et, donc, dans la seconde partie, $\cos\varphi = 1$.

De l'équation (2) il résulte :

$$T_n = 0{,}0682\, T_s \qquad (3)$$

et, avec une assez bonne approximation, $T_s = 6\,000$ °K, sera $T_n = 409$ °K, équivalant à 136 °C.

Cette température, qui doit de toute façon être considérée comme une température limite, est tellement basse que toute utilisation industrielle par ce seul moyen est à écarter.

L'augmentation de la température du collecteur peut être obtenue soit en augmentant l'angle solide de l'énergie à l'arrivée, soit en limitant de quelque façon l'énergie ré-irradiée.

Nous avons à dessein employé la locution « en augmentant l'angle solide de l'énergie à l'arrivée » au lieu de celle plus employée « en concentrant l'énergie à l'arrivée » pour éviter une équivoque qui peut dériver de cette dernière. En effet, il est évident que l'angle solide de l'énergie à l'arrivée ne peut dépasser un demi-espace, mais la limite au-delà de laquelle la concentration de l'énergie devient impossible n'est pas aussi évidente. Cette limite, requise par le deuxième principe de thermodynamique, est en effet liée à des propriétés très générales de toute l'énergie rayonnante qu'il n'y a pas lieu d'exposer ici. Nous voulons dire seulement que de l'étude de ces propriétés l'auteur a déduit la théorie et les applications qui en découlent et qui sont exposées par la suite dans ce mémoire.

L'augmentation jusqu'à quelques milliers de fois de l'angle solide de l'énergie à l'arrivée s'obtient facilement avec des miroirs ou des lentilles et, en accord avec l'exposé ci-dessus, permet d'atteindre des températures assez proches de celle du soleil. Cette méthode, très utile quand on demande des températures très élevées mais avec une modeste quantité d'énergie, est toutefois, à elle seule, trop coûteuse pour l'exploitation industrielle de l'énergie solaire.

La méthode de la limitation de l'énergie ré-irradiée paraît beaucoup plus économique, soit que l'on exploite « l'effet de serre » en protégeant le collecteur avec des surfaces à transparence sélective, soit que l'on utilise les collecteurs sélectifs étudiés par Tabor et son école, soit par les deux moyens combinés.

Le but du présent mémoire est de décrire un appareil de limitation de l'énergie ré-irradiée qui, non seulement permet d'atteindre, en cas de besoin, des températures très élevées, mais encore peut être construit par des méthodes industrielles. Ces méthodes pourraient être si économiques que l'énergie solaire rayonnante en arriverait à concurrencer l'énergie obtenue par les autres sources actuelles.

Soit 1 (figure 1) la surface d'un collecteur classique, par exemple un corps noir ; soit 2 la direction moyenne des rayons solaires qui entrent dans 1. Nous avons déjà dit que, en conditions d'équilibre, la température T_n du collecteur est de beaucoup inférieure à la température T_s du soleil, l'angle solide de l'énergie ré-irradiée par le corps noir réchauffé étant beaucoup plus grand que l'angle solide dans lequel est contenue l'énergie à l'arrivée.

La situation est toutefois radicalement modifiée si on limite l'angle solide de l'énergie à la sortie, sans modifier l'angle solide de l'énergie à l'entrée. Nous démontrerons que ce résultat peut être atteint en appliquant devant le collecteur 1 des écrans appropriés. Dans la figure 2, ces écrans apparaissent schématiquement comme un tronc de cône 3, à parois parfaitement noires et calorifugées, ayant

* Professeur, Università di Genova, Gênes.

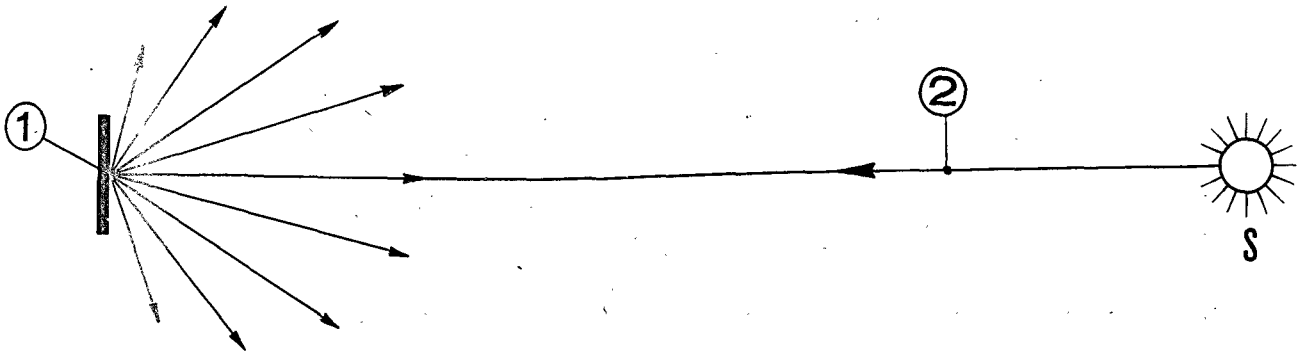


Figure 1

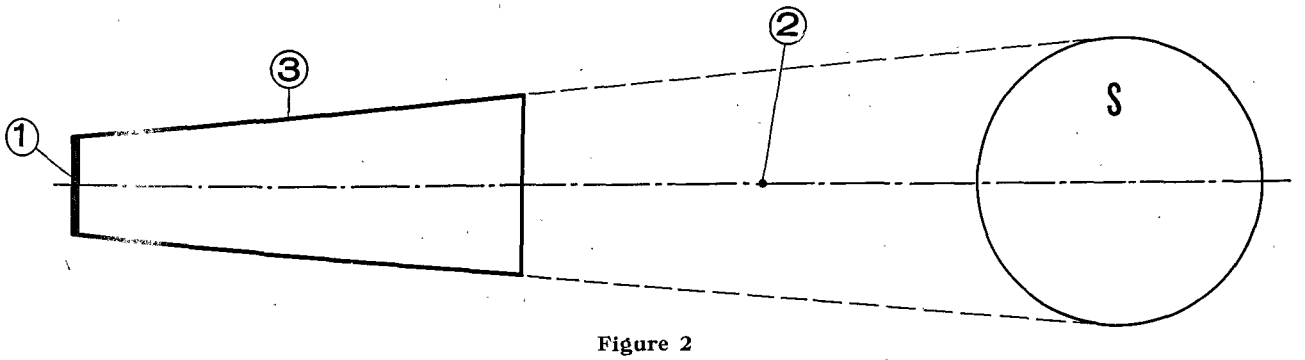


Figure 2

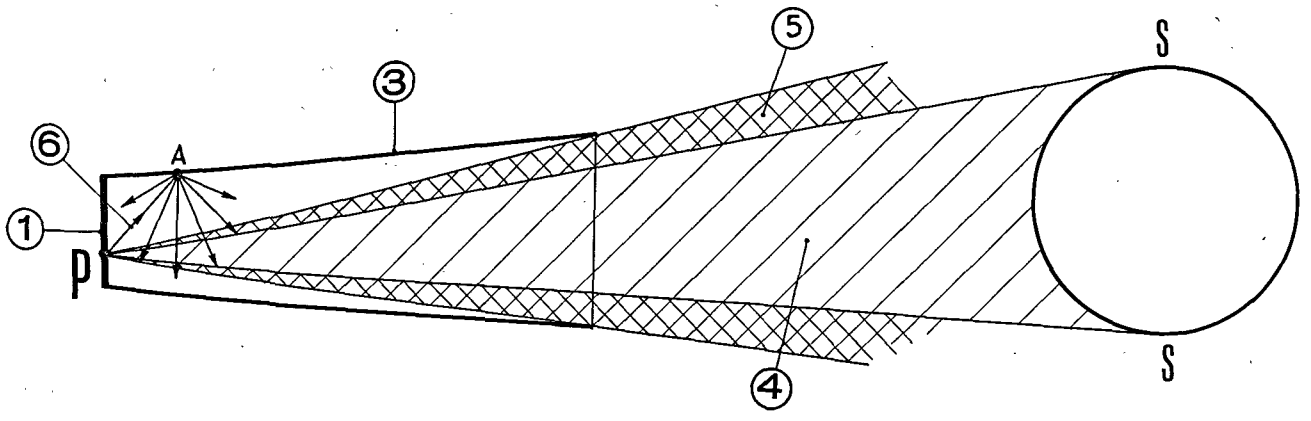


Figure 3

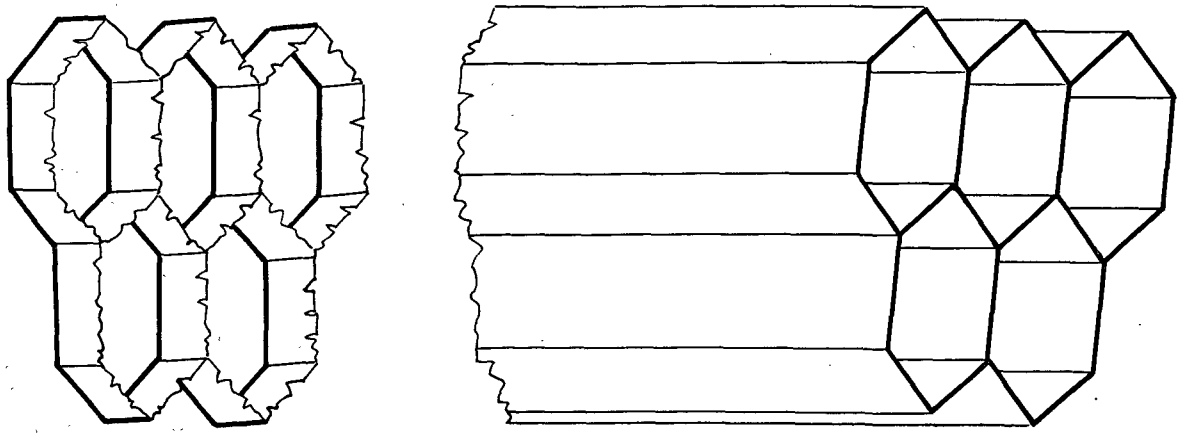


Figure 4

le corps noir classique 1 comme base mineure, l'axe dirigé vers le soleil et une ouverture égale à la grandeur apparente de l'astre.

Avant d'exposer le développement analytique qui, tout en ne présentant aucune difficulté particulière, est toutefois quelque peu complexe, nous pouvons nous rendre compte du phénomène par un raisonnement qualitatif. Sauf un avis contraire explicite, tous les raisonnements qui suivent feront abstraction de toutes les propriétés sélectives des surfaces d'absorption, d'émission, de réflexion ou de transparence.

Examinons (figure 3) les divers rayons sortant d'un point P de la surface du corps noir 1. Ils sont de trois sortes :

1) Les rayons qui, partant de P, arrivent directement au soleil sans toucher les parois du tronc de cône; ils sont contenus dans le cône pointillé 4 de la figure 3. Sans l'aide des propriétés sélectives, on ne peut limiter l'énergie sortant avec ces rayons sans limiter en même temps l'énergie à l'entrée.

2) Les rayons qui, partant de P, sortent du tronc de cône sans en toucher les parois et ne rencontrent pas le soleil; ils sont compris dans la zone 5 quadrillée dans la figure 3 et délimitée par deux cônes sortant du même sommet P. L'énergie qui sort avec ces rayons peut être diminuée en allongeant le tronc de cône 3 jusqu'à l'annuler à la limite.

3) Les rayons qui, partant de P, rencontrent la paroi du cône. Soit 6 un de ces rayons, et A le point de rencontre. En supposant que la paroi du cône soit noire, c'est-à-dire parfaitement absorbante, toute l'énergie du rayon 6 sera absorbée par le point A et, en conditions d'équilibre, ré-irradiée dégradée (puisque, comme nous le démontrerons, la température de A est toujours inférieure à la température de P) dans toutes les directions, avec la règle bien connue du cosinus. Suivons le chemin des rayons ré-irradiés par A.

a) Une partie retourne sur 1 et limite ainsi la perte d'énergie.

b) Une partie sort du tronc de cône et doit être considérée comme perdue.

c) Une partie rencontre encore les parois du tronc de cône : elle est absorbée, et ré-irradiée de la même façon décrite plus haut.

L'examen qualitatif effectué démontre la limitation que le cône 3 apporte à l'énergie ré-irradiée par la surface 1. Le développement analytique, qui sera exposé plus bas, nous donnera la mesure quantitative de cette limitation. Nous verrons ensuite, dans l'exemple numérique que nous baserons sur les données fournies par le collecteur du moteur solaire construit par l'auteur, que la limitation de la perte d'énergie peut facilement permettre à elle seule d'atteindre des températures proches de celle du soleil ou, pour des températures plus basses mais toujours élevées et suffisantes pour une utilisation industrielle, des rendements dépassant 95 p. 100.

Trois observations sont encore nécessaires pour bien apprécier la portée de ce qui précède et du développement analytique qui suivra, en vue d'une utilisation industrielle et économiquement viable de l'énergie solaire.

Première observation. A cause de la petitesse du diamètre apparent du soleil, le cône 3 des figures 2 et 3 peut être remplacé par un cylindre, ou même, pour des raisons pratiques, par un prisme hexagonal ou carré ou de quelque autre forme. En unissant un grand nombre de ces prismes (figure 4), leurs parois ne devront plus nécessairement être calorifugées, étant donné que deux prismes adjacents ont des distributions de températures égales et, de ce fait, aucun passage de chaleur à travers les parois n'a lieu. L'ensemble formé par un grand nombre de ces prismes (disposés, par exemple comme dans la figure 4, en nid d'abeille, avec des parois minces et noires, chaque prisme étant très long par rapport à la corde la plus longue de sa section) pourra être dénommé corps noir absolu parce qu'il absorbe toute l'énergie rayonnante provenant d'une source lointaine sans ré-émettre de l'énergie dans une direction différente de celle de la source même.

Le corps noir absolu peut être considéré, tout compte fait, comme une matérialisation des tubes de flux de l'énergie à l'entrée; comme nous le démontrerons, il peut aussi ordonner et guider l'énergie à la sortie en l'obligeant à parcourir les mêmes tubes de flux de l'énergie à l'entrée.

Cela explique comment un tel collecteur dirigé vers une source, même très lointaine, se trouve en condition d'équilibre thermodynamique avec la source, à la température de cette dernière.

Deuxième observation. Le collecteur que nous avons dénommé corps noir absolu et qui est à la base de toutes les applications qui seront exposées par la suite, est difficilement utilisable comme collecteur d'énergie solaire sur une échelle industrielle, dans la forme schématique que nous avons décrite, surtout à cause de la faible densité de l'énergie solaire. Nous reportons la description des utilisations particulières à la seconde partie de ce mémoire, mais nous remarquerons ici que, si on veut bien se contenter de températures entre 400 et 500 °C, les parois du corps en nid d'abeille peuvent être composées d'un matériau à transparence sélective, et plus précisément noir pour les radiations à grande longueur d'onde et transparent pour les radiations solaires, tel que le verre, le mica, les matières plastiques, etc. Un limitateur de l'énergie ré-irradiée en une de ces matières, s'il a la même géométrie que le corps noir absolu, en diffère substantiellement par les deux caractéristiques suivantes :

a) Il ne peut pas atteindre des températures très élevées auxquelles, si les matières pouvaient y résister, il manquerait la sélectivité de la transparence; et celle-ci est une caractéristique négative.

b) Il ne doit pas nécessairement être pointé en direction du soleil, puisqu'il peut absorber de l'énergie des rayons à n'importe quelle incidence d'angle. Il suffit de noter que la composante de la quantité de mouvement des photons à l'arrivée, selon la

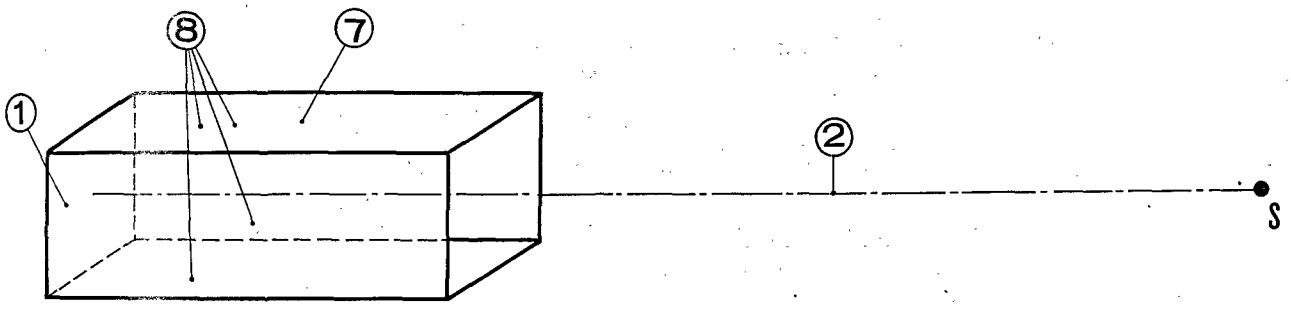


Figure 5

direction des axes des prismes, n'est pas altérée par les réfractions ou réflexions successives provoquées par les parois des prismes mêmes [1].

Cette qualité est extrêmement avantageuse parce qu'elle permet d'utiliser le collecteur sans devoir lui faire suivre le mouvement du soleil ou de l'utiliser en concentrant modérément les rayons solaires. Ces deux caractéristiques qui, au moyen de schémas bien étudiés, peuvent être exploitées en même temps, sont celles qui pourraient permettre à ces collecteurs de concurrencer les autres sources d'énergie dans l'industrie.

Troisième observation. Le limitateur de l'énergie ré-irradiée peut dans certains cas se réduire à un système de plans parallèles entre eux et à la direction des rayons à l'entrée. Un tel partialisateur peut être employé, par exemple quand la direction des rayons à l'entrée se déplace sur un même plan.

Développement des calculs

Soit S une source ponctuelle (figure 5) et 7 un élément du corps noir absolu orienté vers cette source. Plus exactement, soit 7 un prisme que nous supposerons de section rectangulaire, ouvert à l'extrémité tournée vers la source S et fermé par le corps noir 1 du côté opposé. Les quatre parois 8 parallèles à la direction 2 de la source sont noires et calorifugées.

Nous avons donné plus haut une description qualitative du fonctionnement des parois 8 en tant que limitateurs de l'énergie ré-irradiée de 1. Pour étudier le problème du point de vue quantitatif, nous le diviserons en deux parties :

1) Nous supposerons la température du collecteur connue, c'est-à-dire, pratiquement, que nous suppo-

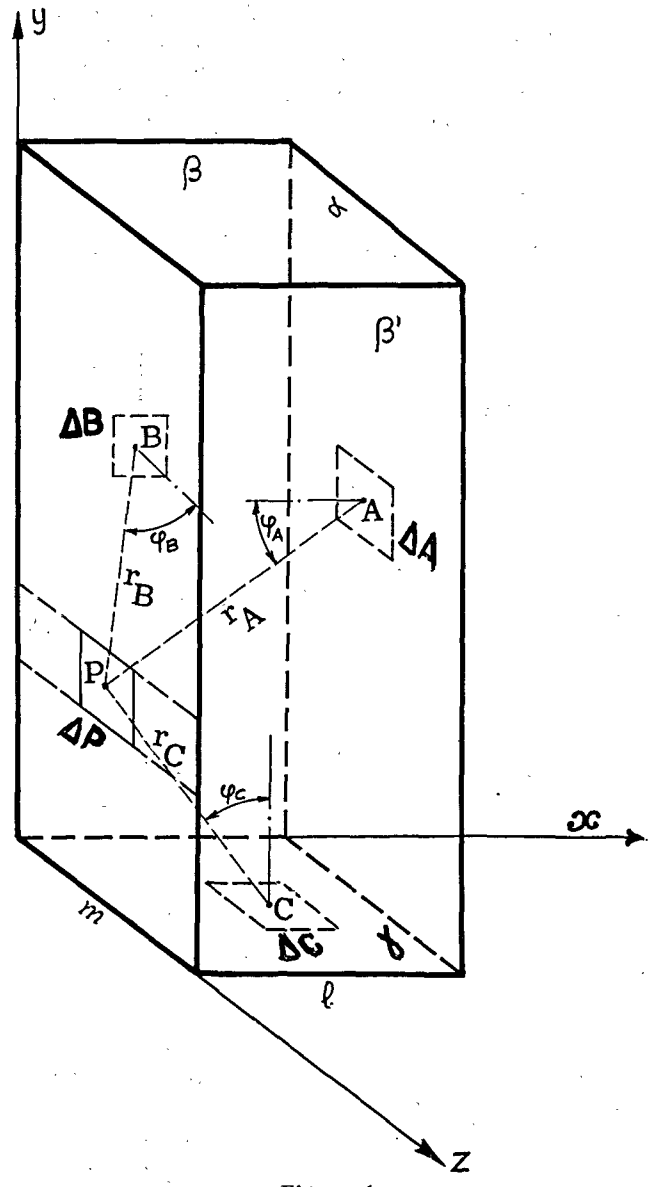


Figure 6

[1] Nous remarquons que cela n'est pas vrai si l'on protège le corps noir avec des plaques de verre ou une autre matière à transparence sélective, comme pour obtenir l'effet de serre. Dans ce cas, les deux réflexions partielles de la lumière sur la face d'entrée et sur celle de sortie de chaque plaque coûtent, dans les conditions d'incidence les plus favorables, à peu près 10 p. 100 de l'énergie incidente, si les surfaces ne sont pas protégées par des traitements spéciaux et jusqu'à présent onéreux, et toujours au moins 1 p. 100 si elles le sont. Cela limite le nombre de couches de protection possibles. Puisque la protection au moyen des matières jusqu'ici employées est vérifiable par absorption et réchauffage subséquent, n couches de protection réduisent l'énergie perdue à $\frac{1}{n+1}$ et le nombre des couches requises pour une réduction suffisante est trop élevé. Ce serait bien différent si la protection était vérifiable par réflexion sélective. Une surface de protection en matière transparente pour la longueur d'onde de l'énergie à l'entrée et en matière réfléchissante pour la longueur d'onde de l'énergie à la sortie serait une parfaite solution du problème.

serons la température de régime établie et nous chercherons la distribution des températures sur les parois 8;

2) La distribution des températures sur les parois du prisme ouvert 7 étant connue, on peut calculer l'énergie qui sort par rayonnement de la façade opposée à 1.

Soit l et m les côtés du rectangle γ formant la base du prisme, que nous supposerons coïncidant avec la surface 1, à la température constante du collecteur; soit h la hauteur; soit x, y, z trois axes cartésiens sortant de sommets de la base γ comme indiqué à la figure 6; x et z coïncident avec deux arêtes sur la façade γ, y est dirigé vers la source S. La température constante de la base γ est T_0, et les quatre faces latérales du prisme ouvert à l'extrémité supérieure sont supposées noires et calorifugées. Nous cherchons la distribution des températures sur ces faces, en conditions d'équilibre.

Soit P un point d'une des faces latérales du prisme, dans le cas de la figure 6, la face qui se trouve sur le plan yz; soit o, y, z les coordonnées de P; soit $\Delta P = \Delta y \Delta z$ près de P. La condition d'équilibre demande que l'énergie irradiée par ΔP soit égale à la somme des énergies qui, sur ΔP, irradient la base γ et les autres faces latérales, α, β, β', du prisme.

Nous supposerons que la température d'un point générique P des parois latérales dépend seulement de la distance y de la base γ : nous appellerons cette température $T(P) = T(y)$ [2].

Par la loi de Stefan-Boltzmann, l'énergie émise par rayonnement par l'élément de surface ΔP est :

$$I_P \Delta P = \pi a T^4(P) \Delta P = k T^4(y) \Delta y \Delta z \qquad (4)$$

Nous calculons séparément l'énergie que chacune des autres faces du prisme envoie sur ΔP.

Énergie irradiée sur ΔP par la face α. Soit A (l, y_A, z_A) un point de α, et $\Delta A = \Delta y_A \Delta z_A$ un autre point près de A; la température de A sera $T(y_A)$. En tenant compte de la loi du cosinus, on trouve facilement que l'énergie envoyée par ΔA sur ΔP est :

$$I_{A,P} \Delta A \, \Delta P = \frac{k l^2 T^4(y_A) \Delta y \Delta z \Delta y_A \Delta z_A}{[l^2 + (y - y_A)^2 + (z - z_A)^2]^2} \qquad (5)$$

L'irradiation totale de la face α sur ΔP sera l'intégrale de $I_{A,P} \Delta A \, \Delta P$ étendue à toute la face α, c'est-à-dire :

$$I_{\alpha,P} \Delta P = k \Delta P \iint_\alpha I_{A,P} \Delta A$$

$$= k \Delta y \Delta z \int_o^h T^4(y_A) \, dy_A \int_o^m \frac{l^2 \, dz_A}{[l^2 + (y - y_A)^2 + (z - z_A)^2]^2}$$

$$= k \Delta y \Delta z \, l^2 \int_o^h \frac{T^4(y_A)}{2[l^2 + (y_A - y)^2]} \left[\frac{\operatorname{arctg} \dfrac{m - z}{\sqrt{l^2 + (y_A - y)^2}} + \operatorname{arctg} \dfrac{z}{\sqrt{l^2 + (y_A - y)^2}}}{\sqrt{l^2 + (y_A - y)^2}} \right. \qquad (6)$$

$$\left. + \frac{m - z}{l^2 + (y_A - y)^2 + (m - z)^2} + \frac{z}{l^2 + (y_A - y)^2 + z^2} \right] dy_A$$

Énergie irradiée sur ΔP de la face β. Avec des calculs semblables aux précédents, on trouve que l'irradiation de toute la paroi β sur ΔP est :

$$I_{\beta,P} \Delta P = \frac{k z \Delta y \Delta z}{2} \int_o^h T^4(y_B) \left[\frac{1}{(y_B - y)^2 + z^2} - \frac{1}{l^2 + (y_B - y)^2 + z^2} \right] dy_B \qquad (7)$$

Énergie irradiée sur ΔP de la face β'. De l'équation (7) on déduit, en substituant $m - z$ à z :

$$I_{\beta,P} \Delta P = \frac{k (m - z) \Delta y \Delta z}{2} \int_o^h T^4(y_B) \left[\frac{1}{(y_B - y)^2 + (m - z)^2} - \frac{1}{l^2 + (y_B - y)^2 + (m - z)^2} \right] dy_B \qquad (8)$$

Énergie irradiée sur ΔP de la face γ. En reprenant les précédents raisonnements, on trouve :

$$I_{\gamma,P} \Delta P = \frac{k y T_o^4 \Delta y \Delta z}{2} \left[\frac{1}{y} \operatorname{arctg} \frac{m - z}{y} + \frac{1}{y} \operatorname{arctg} \frac{z}{y} - \frac{1}{\sqrt{l^2 + y^2}} \operatorname{arctg} \frac{m - z}{\sqrt{l^2 + y^2}} - \frac{1}{\sqrt{l^2 + y^2}} \operatorname{arctg} \frac{z}{\sqrt{l^2 + y^2}} \right] \qquad (9)$$

En imposant la condition que l'énergie totale irradiée par l'élément de surface ΔP et exprimée par le second membre de l'équation (4) soit égale à la somme des énergies irradiées sur ΔP par les parois α, β, β', γ, respectivement exprimées par les seconds membres des équations (6), (7), (8) et (9), on trouve la condition d'équilibre thermodynamique pour l'élément de surface ΔP.

[2] L'hypothèse est vraie quand la base 1 est un cercle ou une bande de plan; l'erreur introduite dans les autres cas qui nous intéressent est absolument négligeable.

Mais en vue de l'hypothèse ci-dessus que la température de P dépend de la seule variable y, hypothèse déjà utilisée pour aboutir aux équations (6), (7), (8), (9), la condition d'équilibre thermodynamique pourra être imposée à l'entière bande horizontale contenant ΔP. Cela équivaut à intégrer, par rapport à z entre o et m, les deux membres des équations (4), (6), (7), (8), (9).

En effectuant ces intégrations, en égalisant et en réduisant, on trouve la condition d'équilibre :

$$m\pi T^4(y) = m l^2 \int_0^h T^4(t)\,[l^2+(y-t)^2]^{-3/2} \operatorname{arctg} \frac{m}{\sqrt{l^2+(y-t)^2}}\,dt$$
$$+ \frac{1}{2}\int_0^h T^4(t) \left[\ln \frac{(y-t)^2+m^2}{(y-t)^2} - \ln \frac{(y-t)^2+m^2+l^2}{(y-t)^2+l^2}\right] dt \qquad (10)$$
$$+ T_o^4 \left[m \operatorname{arctg} \frac{m}{y} - \frac{my}{\sqrt{l^2+y^2}} \operatorname{arctg} \frac{m}{\sqrt{l^2+y^2}} - \frac{y}{2} \ln \frac{m^2+y^2}{y^2} + \frac{y}{2} \ln \frac{m^2+y^2+l^2}{l^2+y^2}\right]$$

L'équation (10) donne la distribution $T(y)$ des températures. C'est une équation intégrale, du type de Fredholm, et elle peut être facilement résolue, même si elle ne remplit pas la condition générale d'intégrabilité pour ces équations.

En effet, dans l'équation (10)

$$T^4(y) = a + by \qquad (11)$$

en effectuant les calculs et posant une fois $y=o$ et une fois $y = h$ (par analogie avec ce qu'on fait dans le principe d'identité des polynômes), on obtient deux équations au moyen desquelles on peut trouver les valeurs inconnues de a et de b. En substituant ces valeurs dans (11), on obtiendra une première approximation de la fonction qu'on recherche.

Comme des considérations physiques, omises pour brièveté, le laissaient prévoir, cette première approximation est déjà très bonne. On en trouve une seconde en substituant la valeur obtenue dans le second membre de l'équation (10), et en calculant le premier membre pour un certain groupe de valeurs de y. Les secondes approximations ainsi obtenues diffèrent de très peu des premières, ce qui confirme la validité de la procédure.

Nous avons déjà dit que, dans certains cas, le limitateur de l'énergie ré-irradiée peut être formé par une série de plans parallèles entre eux et aux rayons en arrivée, comme indiqué à la figure 7.

De tels collecteurs, capables d'absorber de l'énergie rayonnante dans toutes les directions d'un plan plutôt que dans une seule, sont compris dans la théorie émise dans les précédents paragraphes, à la condition qu'un des côtés du rectangle de base du tube devienne infini.

Passant à la limite par $m = \infty$ l'équation (10) devient :

$$T^4(y) = \frac{T_o^4}{2}\left[1 - \frac{y}{\sqrt{y^2+l^2}}\right] + \frac{l^2}{2}\int_0^h \frac{T^4(t)\,dt}{[l^2+(y-t)^2]^{3/2}} \qquad (12)$$

L'équation (12), qui est du même type que (10), donne la distribution des températures aux différents points des parois, en fonction de leur distance du fond.

La solution de (12) est semblable à celle de (10), comme procédure aussi bien que comme résultat. Un collecteur à plans parallèles ne pourra être considéré comme un corps noir absolu que pour une énergie rayonnante distribuée uniformément en toutes les directions d'un plan; nous verrons comment on peut construire des appareils réalisant cette condition, au moins à la première approximation.

La connaissance de la distribution des températures sur les parois et sur le fond du prisme de la figure 6 permet de calculer facilement l'énergie irradiée par celui-ci en chaque direction de l'espace et, par conséquent, l'énergie totale irradiée.

Quand la hauteur h devient très grande par rapport à la corde la plus longue de la base, l'énergie irradiée peut être considérée nulle en toute direction autre que celle commune aux parois latérales des prismes. Le corps noir absolu acquiert ainsi la propriété de renvoyer l'énergie rayonnante irradiée par sa base dans des tubes de flux, les parois desquels coïncident avec les parois de sa structure cellulaire.

La comparaison entre cette géométrie de l'énergie à la sortie et celle de l'énergie sortant d'une source située dans le foyer d'un réflecteur parabolique rend compte de la capacité des deux systèmes d'atteindre des températures élevées quand ils sont touchés par l'énergie rayonnante provenant d'une source lointaine.

Pour des températures du collecteur relativement basses par rapport à celle de la source mais, dans le

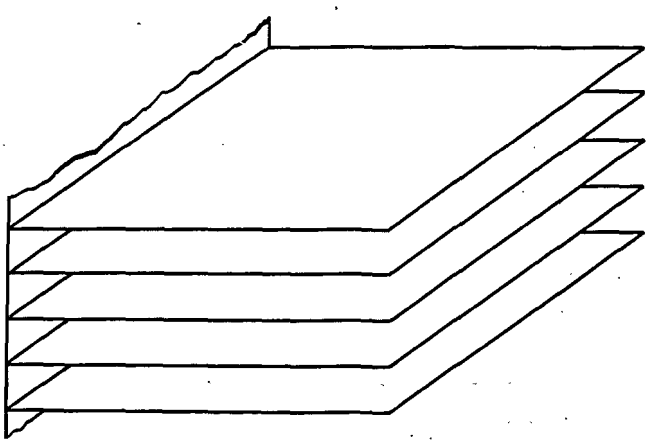


Figure 7

Tableau 1

y	0	2	10	50	100
$0{,}9722 - 0{,}003783\ y$	$0{,}9722\ T_0^4$	$0{,}9646\ T_0^4$	$0{,}9344\ T_0^4$	$0{,}7830\ T_0^4$	$0{,}5939\ T_0^4$
$T^4(y)$	$0{,}9722\ T_0^4$	$0{,}9639\ T_0^4$	$0{,}9339\ T_0^4$	$0{,}7827\ T_0^4$	$0{,}5939\ T_0^4$
$\varepsilon = T^4(y) - [0{,}9722 - 0{,}003783\ y]$	0,0000	$-0{,}0007\ T_0^4$	$-0{,}0005\ T_0^4$	$-0{,}0003\ T_0^4$	0,0000
$T(y)$	$0{,}993\ T_0$	$0{,}991\ T_0$	$0{,}983\ T_0$	$0{,}941\ T_0$	$0{,}878\ T_0$

y	150	200	240	248	250
$0{,}9722 - 0{,}003783\ y$	$0{,}4047\ T_0^4$	$0{,}2156\ T_0^4$	$0{,}0643\ T_0^4$	$0{,}0340\ T_0^4$	$0{,}0264\ T_0^4$
$T^4(y)$	$0{,}4047\ T_0^4$	$0{,}2158\ T_0^4$	$0{,}0653\ T_0^4$	$0{,}0350\ T_0^4$	$0{,}0264\ T_0^4$
$\varepsilon = T^4(y) - [0{,}9722 - 0{,}003783\ y]$	0,0000	$0{,}0002\ T_0^4$	$0{,}0010\ T_0^4$	$0{,}0010\ T_0^4$	0,0000
$T(y)$	$0{,}798\ T_0$	$0{,}682\ T_0$	$0{,}504\ T_0$	$0{,}429\ T_0$	$0{,}403\ T_0$

cas du soleil, encore assez élevées pour une bonne utilisation de l'énergie thermique absorbée, un rapport longueur-corde de l'ordre de 15 à 20 suffit déjà à réduire les pertes d'énergie par rayonnement à des valeurs de l'ordre de 3 p. 100 des pertes qui auraient été subies sans la protection.

La capacité de la structure cellulaire décrite d'absorber toute l'énergie à l'arrivée n'existe que dans le cas limite de rayons parallèles, c'est-à-dire d'une source infiniment lointaine. L'énergie rayonnante solaire est, au contraire, contenue dans un angle solide qui est négligeable seulement au cas où le rapport entre la hauteur h des prismes et la corde la plus longue de la base est assez petit, par exemple inférieur à 25, en d'autres termes, tant que la grandeur apparente du soleil est faible par rapport à la grandeur apparente de l'ouverture du prisme, pour un observateur se trouvant sur la base du prisme même.

Dans ce cas, qui est celui de l'exemple numérique ci-dessous et de toutes les expériences effectuées jusqu'ici, l'équilibre énergétique source-collecteur peut être établi simplement en tenant compte de l'énergie à l'arrivée, de l'énergie ré-irradiée et de celle absorbée et transformée en énergie thermique. Dans les autres cas, il faudrait aussi tenir compte de l'énergie à l'arrivée absorbée par les parois et de la diminution de l'énergie atteignant le fond qui en résulterait, ainsi que de la distribution différente de la température sur les parois. Toutefois, en première approximation les deux choses tendent à se compenser.

Exemple numérique

Dans la plupart des expériences faites jusqu'à présent par l'auteur, la structure cellulaire en nid d'abeille a été constituée par des cylindres, des prismes hexagonaux ou d'autres prismes avec un rapport longueur/corde la plus longue allant de 12 à 18. Dans l'exemple numérique de solution de l'équation (10), nous avons posé $m = l = 14$ et $h = 250$, pour nous rapprocher autant que possible

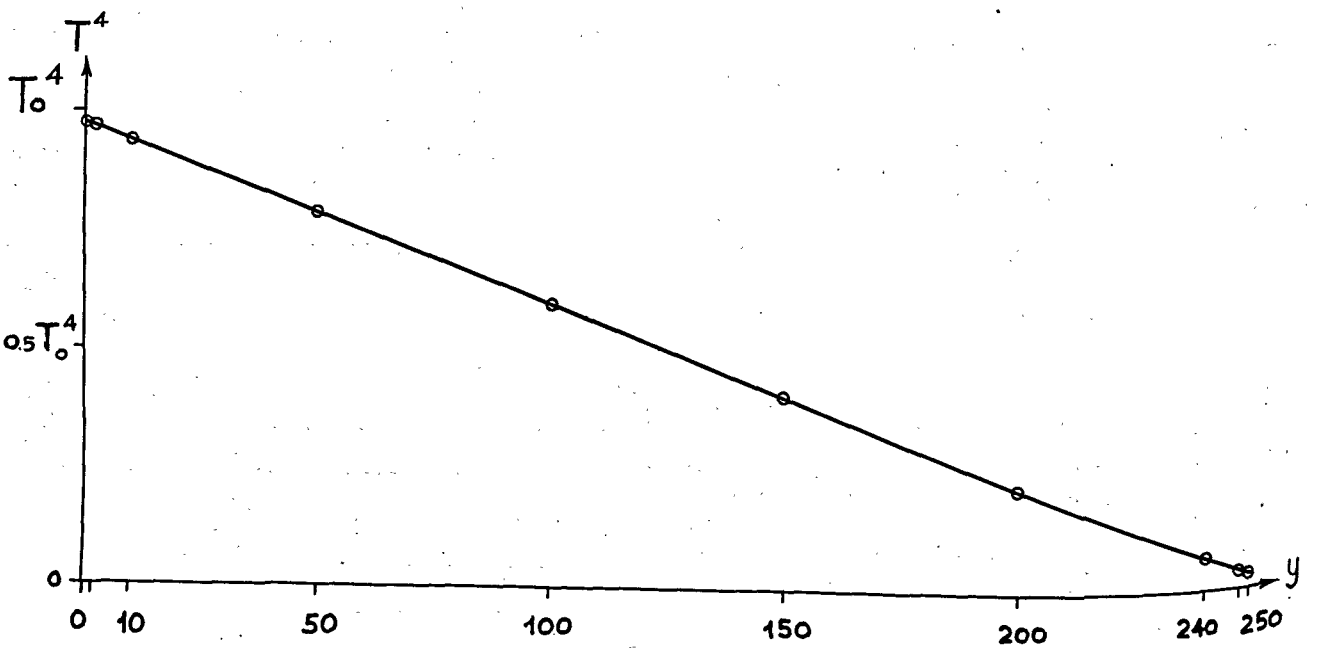


Figure 8

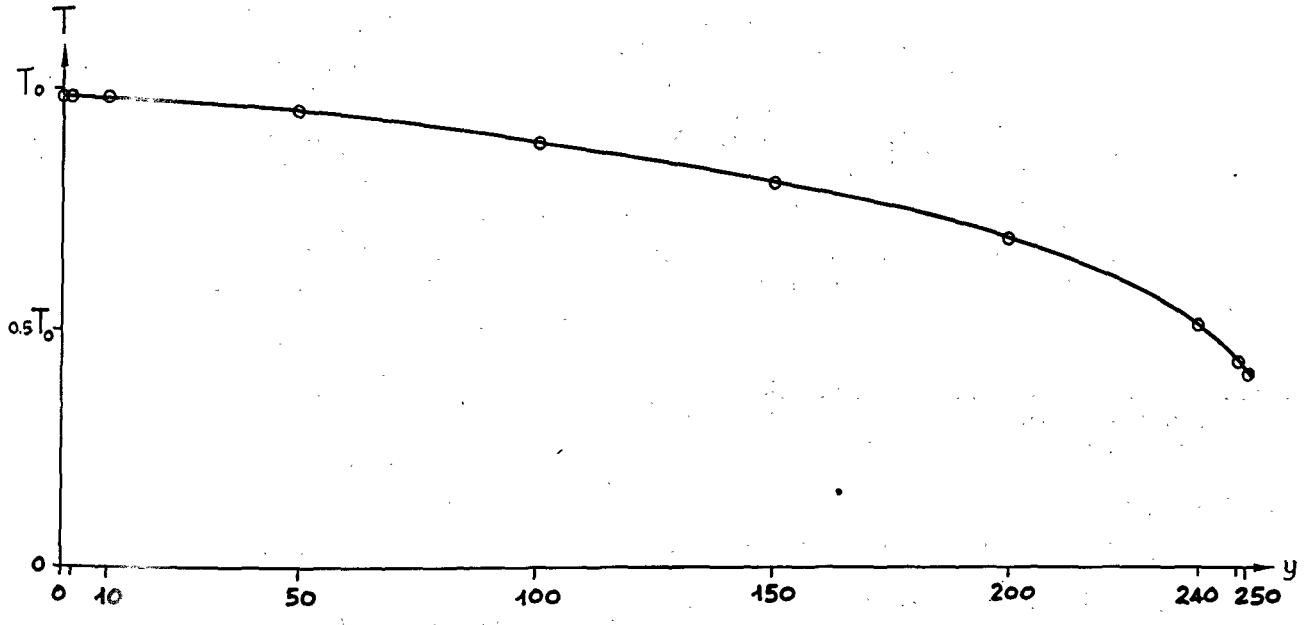


Figure 9

des données du dernier appareil construit, dont la structure cellulaire est en tubes de verre mince d'un diamètre approximatif de 14,5 mm et de 250 mm de longueur. Pour plus de commodité, nous supposerons une température extérieure nulle (en degrés absolus).

Vu que $T^4(y) = a + by$ dans (10), et une fois les calculs avec les valeurs numériques effectués, on obtient une relation entre a, b, y et naturellement T_0. En donnant à y tour à tour la valeur 0 et la valeur 250, on trouve le système d'équations qui nous donne les valeurs de a et b. On obtient :

$$\begin{cases} a = 0{,}9722\, T_0^4 \\ b = -0{,}003783\, T_0^4 \end{cases} \qquad (13)$$

En première approximation, nous trouvons ainsi la solution

$$T(y) = T_0 \sqrt[4]{0{,}9722 - 0{,}003783\, y} \qquad (14)$$

En remplaçant ces valeurs dans le second membre de (10), et en le résolvant pour les valeurs de y indiquées dans le tableau 1, nous trouvons un groupe de valeurs de la fonction inconnue en seconde approximation.

Vu que les valeurs qui nous intéressent réellement sont celles des quatrièmes puissances des températures, le tableau 1 indique :

a) Sur la première ligne, les valeurs de y pour lesquelles le calcul a été effectué;

b) Sur la seconde ligne, les valeurs de $a + by$, c'est-à-dire de la solution en première approximation;

c) Sur la troisième ligne, les valeurs de T calculées en seconde approximation;

d) Sur la quatrième ligne, les différences entre les valeurs en première approximation et celles en seconde approximation.

Les différences entre la première et la seconde approximation des résultats sont minimes, et confirment la validité de la procédure.

La figure 8 représente le graphique des $T^4(y)$: il ne semble pas différer d'un segment de ligne droite. Il est intéressant de noter que la quatrième puissance de la température a une discontinuité entre le fond 1 et le début des parois latérales 8 du prisme. La température décroît le long des parois latérales de façon presque linéaire jusqu'au bord extrême du prisme. Entre la quatrième puissance de sa température et la quatrième puissance de la température extérieure, que nous avons supposée nulle, il y a encore une discontinuité égale à celle

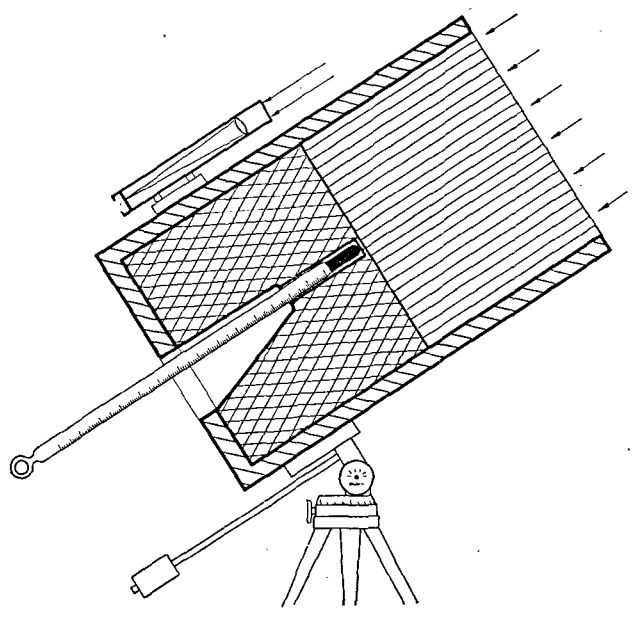


Figure 10

déjà relevée. Toute la courbe, y compris les discontinuités, est symétrique par rapport à son point central.

La figure 9 représente le graphique des températures T (y). Qualitativement, l'expérience confirme assez bien la courbe théorique : il faut tenir compte du fait que, la variation de la température n'étant pas linéaire, la conduction le long de la paroi du tube et la convection due aux mouvements assez limités de l'air à l'intérieur du tube altèrent la courbe théorique.

Vérifications expérimentales. Réalisation d'un collecteur à caractéristiques élevées pour moteur solaire

Appareil n° 1

Dans les premiers mois de 1960, un premier appareil fut construit, dans le seul but de vérifier la théorie. Dans cet appareil, le collecteur en nid d'abeille était réalisé au moyen de prismes hexagonaux d'à peu près 8 mm de diamètre, et de 160 mm de longueur, les parois desquels étaient en papier de 0,03 mm d'épaisseur environ, carbonisé avec une extrême lenteur dans une atmosphère dépourvue d'oxygène. On obtint ainsi une structure très fragile mais extrêmement légère et répondant aux caractéristiques géométriques, optiques et thermiques requises. L'entière structure avait la forme d'un cylindre de 20 cm de diamètre environ.

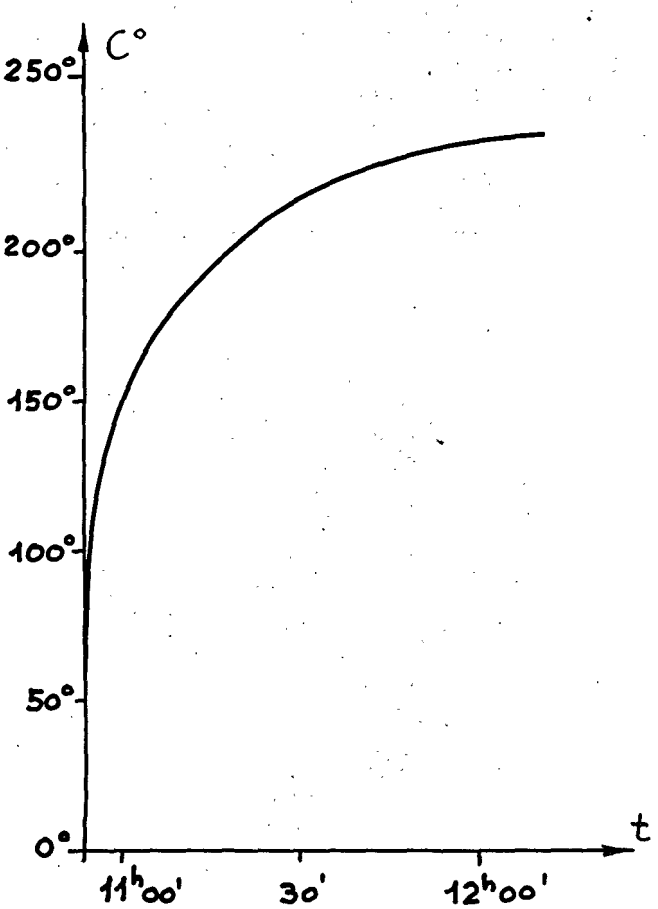


Figure 11

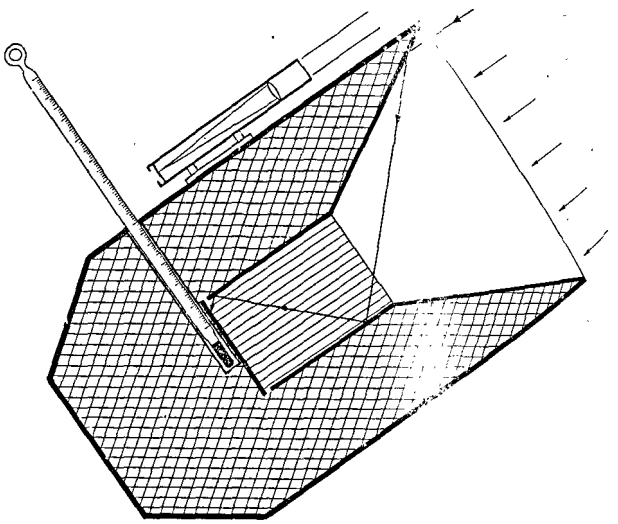


Figure 12

Derrière cette structure en nid d'abeille était placé un corps noir classique, également en cellulose carbonisée; la même cellulose carbonisée servait d'isolant thermique postérieur, d'une épaisseur de 15 cm approximativement. L'emploi de matériel d'un maniement si difficile était imposé par la nécessité d'avoir une masse thermique extrêmement basse, afin d'obtenir un instrument sensible aux faibles quantités d'énergie en jeu, de l'ordre de quelques cal/sec.

Un thermomètre de quartz à l'arrière permettait de mesurer les températures (figure 10); un viseur pour le contrôle de la direction et un trépied à pivot universel complétaient l'équipement. Aucun moyen de recueillir l'énergie thermique n'était prévu; en effet, elle aurait été perdue par conduction à cause de l'isolement insuffisant dû aux petites dimensions de l'appareil.

Le but de ces expériences était de mesurer la température d'équilibre; en se basant sur un calcul approximatif de l'énergie perdue par conduction, on aurait pu déduire la validité de la théorie. Celle-ci a été confirmée, car en plusieurs expériences des températures de l'ordre de 230-240 °C ont été atteintes. La figure 11 rapporte un des graphiques de la température du collecteur par rapport au temps.

Appareil n° 2

Un second appareil, avec le même type de collecteur, en plus grand et muni d'échangeur de chaleur pour une mesure directe de l'énergie absorbée, fut construit après constatation des résultats favorables obtenus par le premier.

Dans ce second appareil (voir figure 12), le corps noir absolu était encore formé par approximativement 10 000 prismes presque hexagonaux, d'un diamètre moyen de 8 mm et d'une longueur de

120 mm, qui formaient dans l'ensemble un cylindre de 80 cm de diamètre. La plaque d'absorption était un disque de cuivre de 0,1 mm d'épaisseur, noir sur sa face antérieure; sur son côté postérieur était soudée une spirale de tube en cuivre d'une longueur totale de 26 m. Une ouverture calibrée à l'entrée du tube pour l'eau, et une autre à la sortie pour la vapeur, permettaient de connaître la portée en fonction des sauts de pression. De la température, qui pouvait facilement être mesurée, découlait la quantité de chaleur fournie.

Les expériences furent effectuées en partie à Sestrère, localité alpestre à 2 018 mètres d'altitude, et en partie à Gênes. En conditions de régime, l'appareil fournissait un maximum de 0,1 gr par seconde de vapeur surchauffée à 230 °C approximativement et à 2 atmosphères à peu près à la sortie; mais, en conditions particulières, on a obtenu jusqu'à 320 °C, avec 0,085 gr de vapeur par seconde. Cela équivaut approximativement à 70 cal/sec dans le premier cas, et à 63 cal/sec dans le second cas. Vu que les expériences étaient faites dans d'excellentes conditions, il y a lieu de penser qu'au moins 125 cal/sec arrivaient sur la plaque; le rendement total de l'appareil dépassait donc de peu les 50 p. 100, ce qui est assez bas étant donné les prévisions théoriques. Toutefois, cela s'explique soit par le parallélisme insuffisant des prismes du collecteur accentué par un petit incendie au cours d'une des premières expériences, soit par l'insuffisance de l'isolement thermique de la plaque.

Il peut être intéressant de noter qu'en ajoutant une plaque en verre devant le collecteur en nid d'abeille, le rendement diminuait de 7 à 8 p. 100. Puisqu'une plaque en verre diminue de presque moitié l'énergie perdue par ré-irradiation, mais cause une perte de 10 p. 100 de l'énergie à l'entrée, la faible valeur de l'énergie ré-irradiée semble confirmée.

Nous avons déjà dit que le corps noir absolu à lui seul ne s'adapte pas à une utilisation industrielle de l'énergie. C'est pourquoi les appareils décrits plus haut doivent être considérés sous le seul point de vue scientifique.

Nous avons aussi mentionné l'avantage d'une concentration modérée de l'énergie. Celle-ci permet, en effet, de remplacer une grande partie de la surface du collecteur (dont le coût, y compris l'échangeur de chaleur et l'isolant, ne peut pas être inférieur à certaines limites) par des miroirs en feuilles minces en aluminium que l'industrie produit à des prix très bas.

Cela demande des matériaux noirs pour les longueurs d'onde de l'énergie ré-irradiée et transparents ou réfléchissants pour l'énergie en arrivée. L'auteur ne connaît pas de matériaux suffisamment sélectifs pour ce qui concerne la réflexion, mais tout le monde connaît les propriétés sélectives de plusieurs matériaux en ce qui concerne la transparence.

De nombreuses expériences ont été faites pour s'assurer que ces matériaux soient non seulement opaques mais « noirs » pour les grandes longueurs d'onde à tous les angles d'incidence. A cet effet, l'énergie rayonnante à grande longueur d'onde était introduite dans des tubes en matériaux à tester, en verre en particulier. On comparait ensuite l'énergie à la sortie avec celle qui, dans les mêmes conditions, sort de tubes à parois également opaques mais pas noires puisqu'elles reflètent ou diffusent. Après le résultat positif de ces expériences, qu'il est inutile de décrire ici, le collecteur n° 3 et le grand collecteur pour moteur solaire n° 4 ont été construits.

Appareil n° 3

Il a été construit dans le seul but de fournir une confirmation qualitative des propriétés d'un collecteur en nid d'abeille en matériel transparent pour l'énergie en arrivée, noir pour l'énergie ré-irradiée. Le collecteur est formé d'environ 150 tubes en verre de 14 à 15 mm de diamètre, de 250 mm de longueur et de 0,2 à 0,3 mm d'épaisseur, disposés de façon à former un cylindre (figure 13) à parois en aluminium réfléchissant, de 200 mm de diamètre et de 250 mm de longueur. Un corps noir classique, formé par une mince feuille de cuivre noirci à la résine de silicone, complète le collecteur; derrière cette plaque est placé un thermomètre en quartz.

Devant le collecteur, un tronc de cône en aluminium spéculaire concentre les rayons lumineux en arrivée sur la bouche d'entrée, dans le rapport théorique d'environ 6 : 1. Le tout est isolé avec de la laine de verre et renfermé dans un cylindre. Puisque la plus grande partie des rayons lumineux

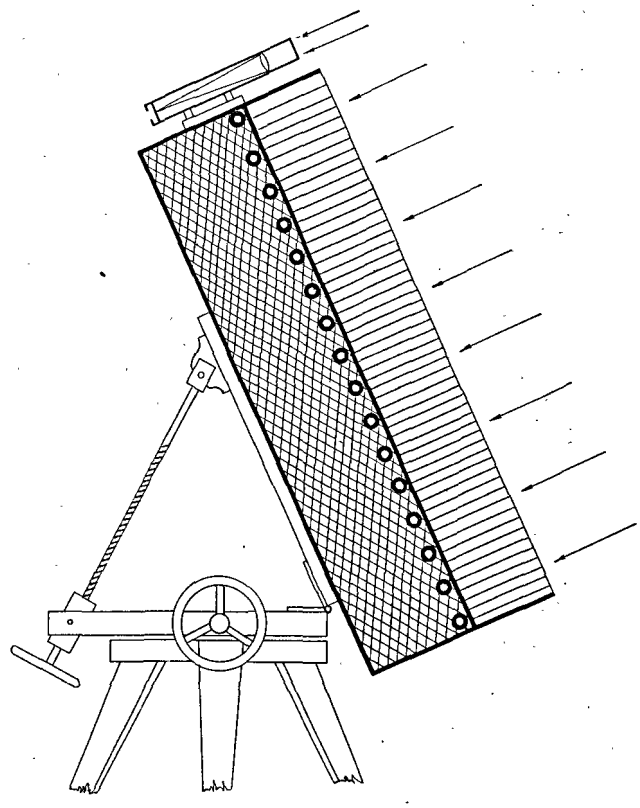


Figure 13

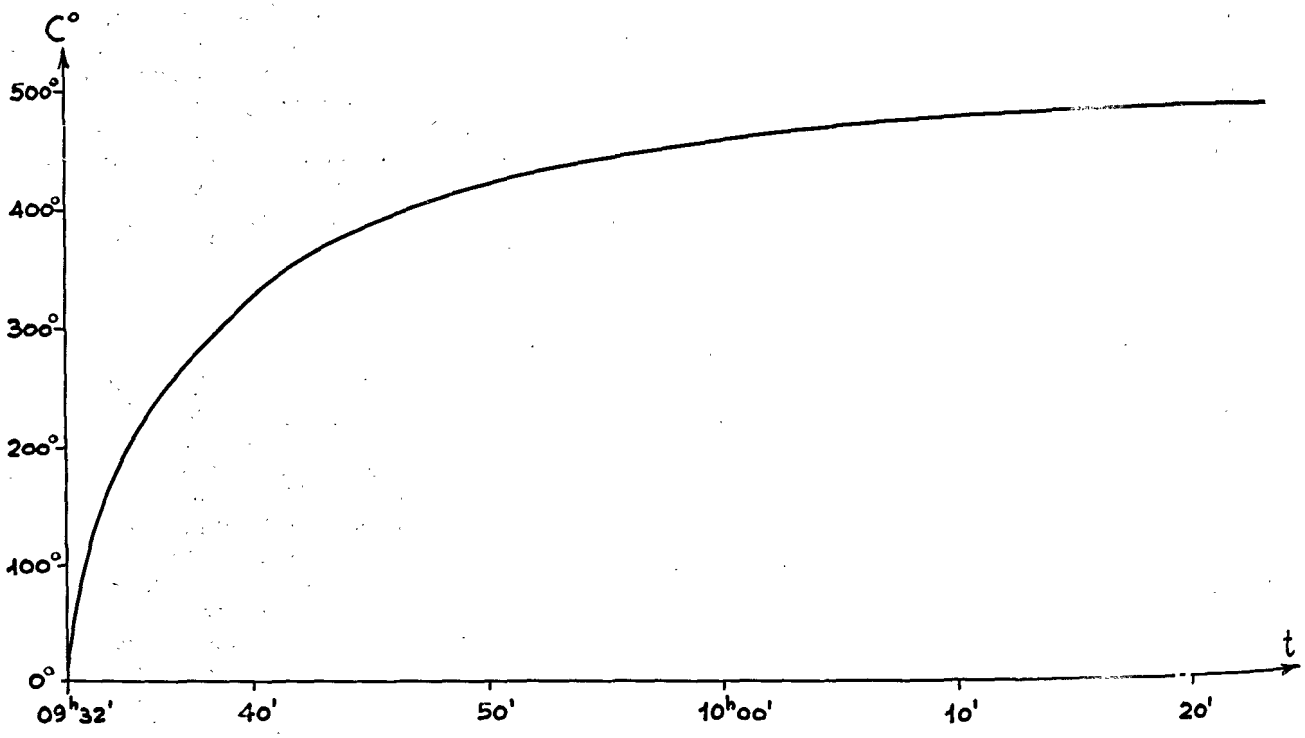


Figure 14

subit plus d'une réflexion sur l'aluminium avant d'être absorbée, la concentration effective de la lumière sur la surface noire est inférieure à 6 : 1, mais encore suffisante pour nous. Le viseur et un robuste trépied non indiqué dans la figure complètent l'appareil.

Dans la figure 14 est indiquée une des courbes de la température par rapport au temps d'exposition.

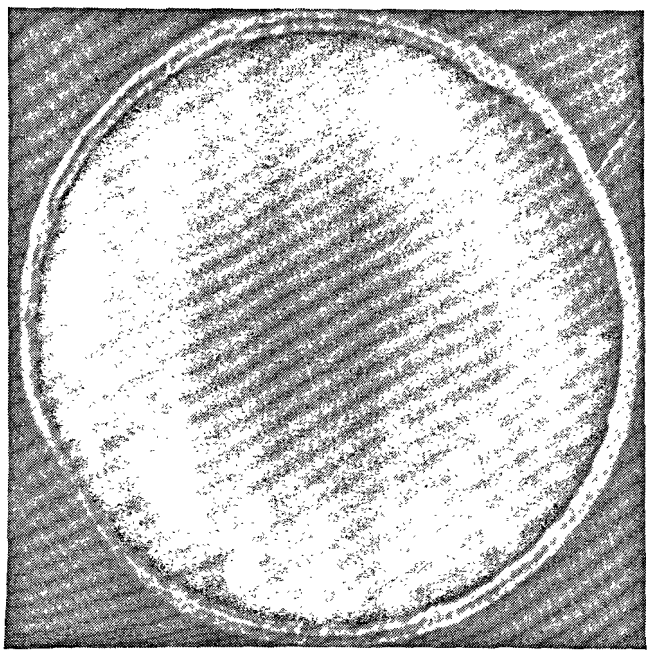


Figure 15

La température finale de 488 °C peut être considérée satisfaisante si l'on tient compte, comme pour l'appareil n° 1, des pertes par conduction dans un appareil aussi petit. La température maximale de la plaque a été de 520 °C, avec un thermomètre placé autrement qu'indiqué dans la figure.

La figure 15 est une photographie du collecteur, à la fin d'une expérience, prise avec une ouverture d'objectif de 1 : 2 et une durée de 2 secondes; l'appareil était protégé contre la lumière extérieure. On peut voir la clarté de la zone centrale due à la couleur rouge naissant du centre de la plaque.

Appareil n° 4

En octobre 1960, on commença la construction d'un collecteur qui pouvait être utilisé comme source d'énergie thermique pour un moteur solaire; il a été terminé et monté vers la fin de mars 1961.

Étant donné les rendements élevés des collecteurs décrits, il a été considéré plus à propos d'adapter les rendements du collecteur aux exigences des machines thermiques modernes, telles que les turbines à vapeur, plutôt que de faire le contraire.

Sur la base de cette considération, les conditions de régime suivantes ont été établies :

a) Pression de la vapeur à la sortie supérieure à 100 atmosphères;

b) Température de la vapeur à la sortie : 450 °C.

On a étudié un système facilement réalisable sur une échelle industrielle et permettant de concentrer économiquement de 10 à 15 fois l'énergie en arrivée sur des collecteurs fixes. Toutefois, comme nous l'avons déjà remarqué pour les appareils 1 et 3

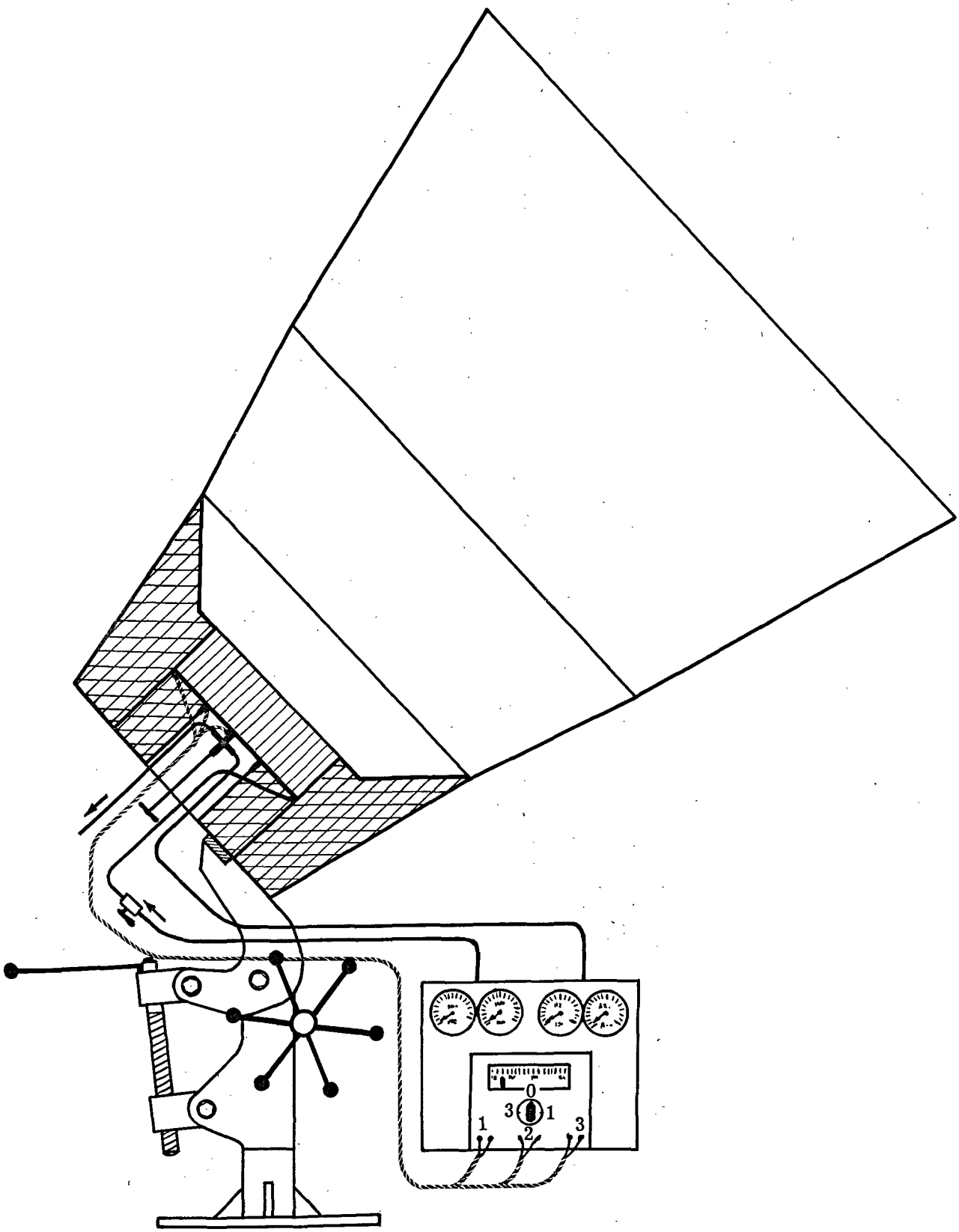


Figure 16

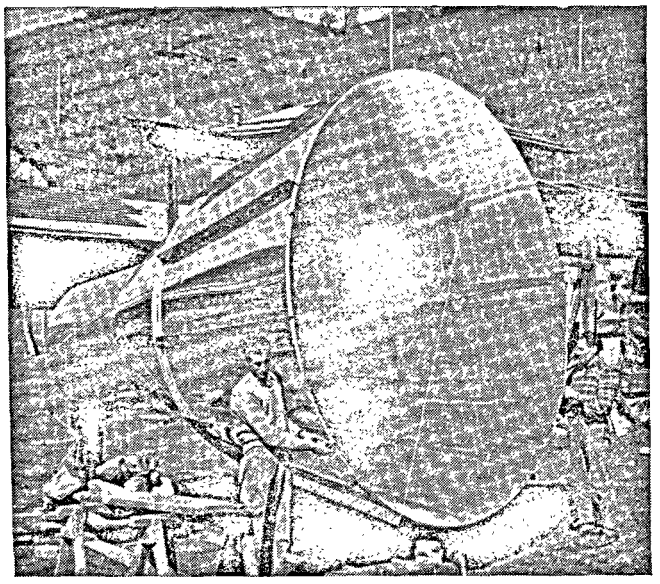


Figure 17

certaines difficultés, comme celle d'assurer un bon isolement thermique, augmentent grandement avec la diminution des dimensions; on a donc préféré obtenir la concentration établie par le système classique des surfaces coaxiales en tronc de cône et en aluminium spéculaire.

L'appareil nº 4 est formé de trois troncs de cône coaxiaux qui, partant d'un diamètre de 3,20 m, concentrent l'énergie rayonnante sur un collecteur en nid d'abeille de 0,80 m de diamètre avec une concentration théorique de 16 : 1 (figures 16, 17, 18).

Le collecteur en nid d'abeille, du type à transparence sélective, se compose de près de 2 000 tubes en verre de 14 à 15 mm de diamètre, de 250 mm de longueur et de 0,2 à 0,3 mm d'épaisseur posés sur la plaque, qui fonctionne en même temps comme récepteur et échangeur de chaleur. Comme dans l'appareil nº 3, les tubes en verre sont enfermés dans un cylindre à parois réfléchissantes.

Pour éviter des pertes dans l'absorption de l'énergie rayonnante, la face de la plaque de verre tournée vers le soleil est entièrement sillonnée d'une incision en spirale semblable à celles des disques de gramophone, qui oblige les rayons de l'énergie incidente à un nombre de réflexions suffisant pour en assurer l'absorption presque totale.

Comme il faut prévoir entre le centre et la périphérie des différences de température qui peuvent être au moins de 400 °C, et comme il faut éviter que les différentes dilatations ne déforment la plaque, celle-ci a été divisée en deux parties concentriques, réunies par un anneau élastique soudé électriquement aux deux parties.

La partie extérieure est une couronne circulaire de 46,5 cm et de 79,5 cm de diamètre; la partie intérieure est un disque de 46 cm de diamètre. L'eau arrive à un point de la circonférence extérieure, parcourt toute la plaque dans un conduit d'à peu près 46 m, se vaporise dans la partie centrale et sort du centre de la plaque par une soupape commandée de l'extérieur.

Comme la capacité de l'eau de retirer de la chaleur est très grande, comme celle du mélange eau-vapeur est moins grande, comme celle de la vapeur surchauffée est minime, et comme le centre de la plaque, à cause de la configuration des rayons en arrivée, reçoit la densité maximale d'énergie, il fallait rapprocher le plus possible les spirales dans la zone centrale et les écarter dans la zone périphérique. Cela a été fait en tirant les vingt-six mètres de spirale de la plaque intérieure, au moyen d'un tour, directement d'une plaque en acier épaisse de 20 mm, et en formant ensuite la canelure ainsi obtenue avec un listel soudé électriquement sur toute la longueur. Dans la partie périphérique, le conduit est constitué d'environ 20 mètres de tube en acier inox soudé à une plaque mince.

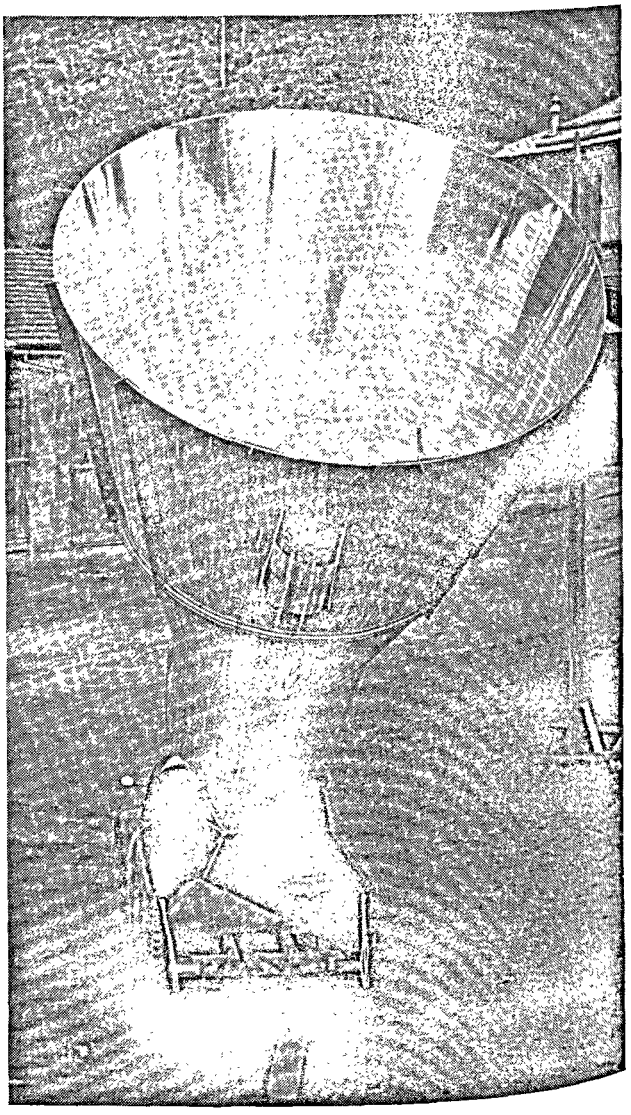


Figure 18

L'isolement postérieur de la plaque est assuré par à peu près 40 cm de laine de verre. Les parois latérales du cylindre contenant la structure en nid d'abeille sont aussi protégées par une épaisseur minimale de 22 cm du même isolant.

L'appareil est soutenu par un robuste support qui lui permet de tourner horizontalement et verticalement, de façon à prendre n'importe quelle position. Le tout est monté sur une camionnette, pour faciliter le transport. A cet effet, le cône majeur peut facilement être démonté en douze pièces.

La température du côté postérieur de la plaque est mesurée en divers points (périphérie, anneau moyen, et centre) par trois thermocouples reliés à un millivoltmètre à trois lectures et calibré en degrés.

Un quatrième thermocouple, placé sur le tube de sortie de la vapeur, peut être relié au millivoltmètre, au lieu de l'un des précédents. On prévoit l'emploi d'un thermomètre de quartz, pour le contrôle.

Quatre manomètres, deux pour les pressions élevées et deux pour les pressions basses, mesurent la pression de l'eau à l'entrée et de la vapeur à la sortie derrière la soupape de réglage placée au centre de la plaque. L'eau comprimée est contenue dans le même tube de support qui sert de réservoir à haute pression; une couche d'air assure l'élasticité nécessaire et la continuité de débit.

Les faibles portées d'eau de 1 à 2 cm^3/sec, et les hautes pressions prévues (l'appareil a été expérimenté pour 350 atmosphères) rendent difficile l'emploi d'appareils pour mesurer la portée.

Le problème a été provisoirement résolu en appliquant à la décharge un ajutage du type Laval, c'est-à-dire, pour plus de clarté, semblable à ceux employés pour les fusées. Des formules connues et très exactes permettent de déduire la portée de ces ajutages par rapport à la pression et à la température à l'amont. Une petite série de tels ajutages a été construite. Un nomogramme à deux entrées permet de déduire immédiatement la portée des mesures indiquées par les autres instruments.

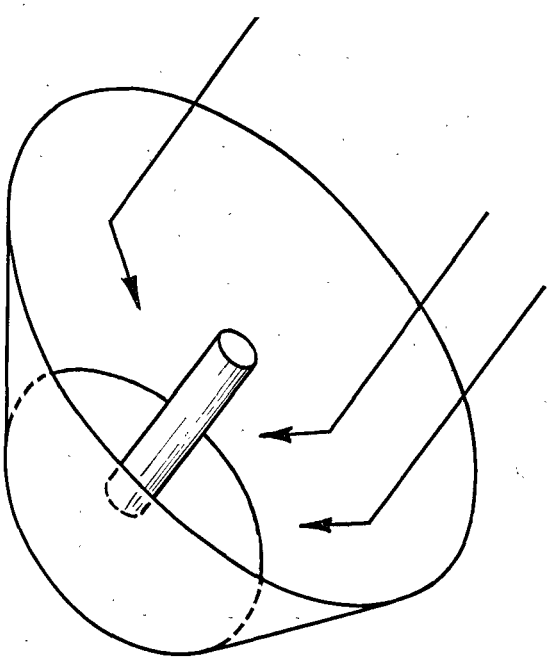


Figure 19

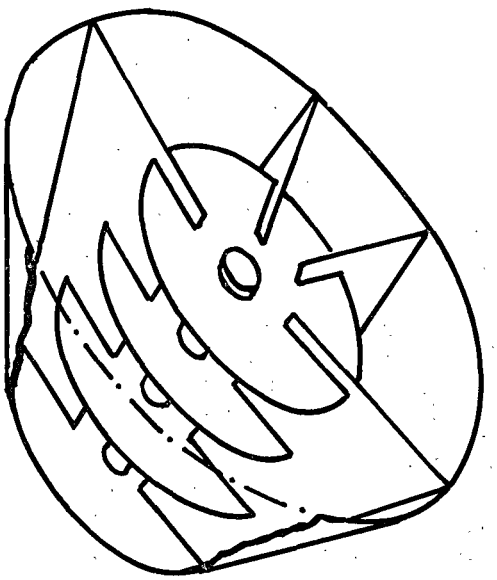


Figure 20

Les expériences effectuées jusqu'ici avec cet appareil confirment très bien les résultats prévus par la théorie. En particulier, des portées de 5,5 kg/h de vapeur surchauffée à 450 °C ont été dépassées, et nous pouvons raisonnablement espérer atteindre, en conditions de régime, 7 kg/h de vapeur à 450 °C et 100 à 150 atmosphères.

Nous avons plusieurs fois parlé de températures d'absorption proches de celles de la source; il devrait sûrement être possible, dans le cas du soleil, d'atteindre des températures de quelques milliers de degrés avec un corps noir absolu du type décrit, et sans concentration de rayons. Un tel résultat ne peut être obtenu que par une technique très raffinée; il serait toutefois d'une très faible utilité pratique à cause de la faible densité de l'énergie solaire; il suffit de mentionner les difficultés de l'isolement d'une grande surface et l'inévitable inertie thermique de cette dernière.

Mais si nous retournons à la première schématisation du corps noir absolu représentée par la figure 2, nous voyons que le parallélisme des rayons en arrivée n'est pas une condition nécessaire à la réalisation d'un corps noir absolu, vu que pour cela il suffit que la surface absorbant les rayons soit protégée de façon à limiter l'angle solide de l'énergie en arrivée. Cela signifie que, même dans le cas d'énergie concentrée par des lentilles ou des miroirs, le collecteur pourra être protégé par des surfaces limitant l'angle solide de l'énergie ré-irradiée par le collecteur même.

Dans le cas de lentilles ou de miroirs paraboliques, l'avantage d'une telle protection est assez limité,

étant donné qu'en général l'angle solide de l'énergie en arrivée est déjà très grand : des concentrations de l'énergie jusqu'à 10 000 fois et plus sont normales dans ces cas. Mais d'autres moyens plus économiques permettent d'obtenir des concentrations de l'énergie allant à quelques centaines de fois. De telles concentrations suffisent pour la densité de l'énergie, mais non pour atteindre des températures élevées sans protections appropriées.

Examinons, en effet, un miroir en forme de tronc de cône d'une semi-ouverture de 45°, et un collecteur d'énergie cylindrique disposé sur son axe (figure 19). De l'énergie concentrée, mais avec un angle solide insuffisant pour atteindre des températures élevées, arrive sur le collecteur. Des surfaces noires en forme de cercles égaux à la base mineure du cône et parallèles à celle-ci, ainsi que des surfaces trapézoïdales sur des plans passant par l'axe du cône (voir figure 20), formeront un limitateur de l'angle de ré-émission possédant les propriétés déjà décrites.

Au point de vue de la réalisation, il peut être important de remarquer que les surfaces du limitateur ne doivent pas nécessairement être continues. Elles peuvent, par exemple, être formées par des fils de tungstène de 10 à 50 microns de diamètre, tendus sur des châssis, éloignés des zones chaudes pour les plans passant par l'axe, et tenus par d'autres fils de tungstène en forme de toile d'araignée pour les plans perpendiculaires à l'axe. Un très faible courant de gaz inerte peut être suffisant pour protéger la structure.

Une dernière application des structures cellulaires décrites mérite d'être brièvement mentionnée. Dans un certain sens, ces structures peuvent être considérées comme des corps froids par rapport à l'énergie rayonnante : elles sont par conséquent utilisables comme isolants thermiques pour les températures très élevées, tout en permettant la vision directe, d'une certaine direction, du corps isolé. En outre, si elles sont, par exemple, en fils de tungstène, elles peuvent être caractérisées par une masse thermique extrêmement basse.

Appendice

Au cours des expériences, on a reconnu la nécessité de munir l'appareil n° 4, qui a déjà été décrit, d'autres moyens de mesure.

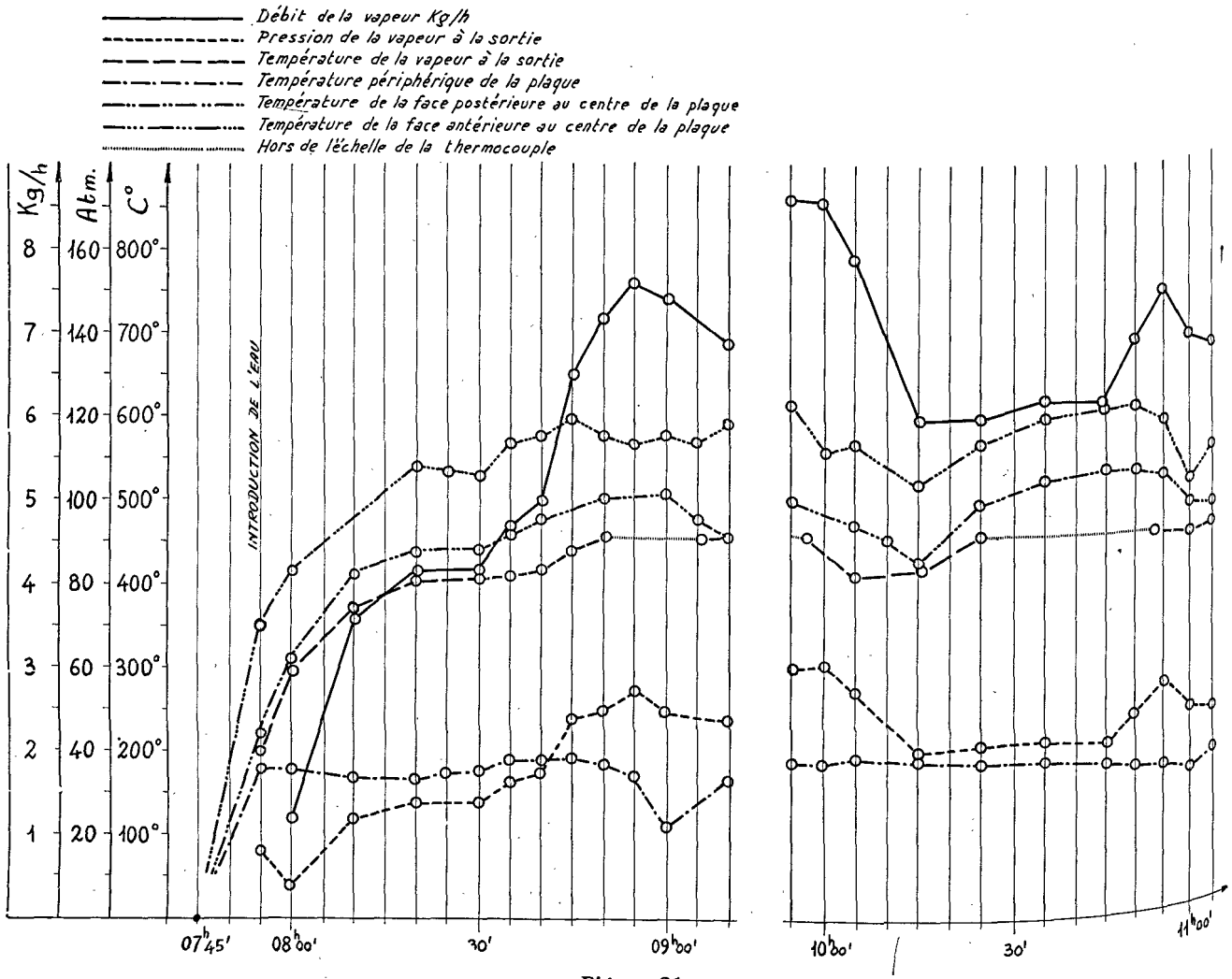


Figure 21

Deux autres thermocouples, reliés à un nouveau millivoltmètre réglé en degrés et pouvant mesurer des températures atteignant 800 °C, ont été mis en contact avec la face antérieure de la plaque. On a trouvé une différence très importante, par rapport aux prévisions, entre les températures de la face antérieure de la plaque et celles de la face postérieure et de la vapeur sortante, respectivement. Cette différence atteint 100 °C dans de bonnes conditions de fonctionnement, mais peut même atteindre 250 °C quand la pression de la vapeur est trop basse.

Pendant les premières expériences, à cause de l'impossibilité de connaître la température sur la face antérieure, des températures de beaucoup supérieures aux prévisions ont été atteintes, températures qu'on peut évaluer à 720-750 °C. Cela a provoqué la fusion des parties en aluminium et verre en contact, ainsi que la destruction partielle du vernis noir au silicone.

Pour mesurer avec plus de précision la production horaire de vapeur, un petit échangeur de chaleur a été construit, qui permet de condenser et récupérer sous forme d'eau froide la vapeur sortante. Cet échangeur est composé d'un serpentin de tube en cuivre, dans lequel circule l'eau de refroidissement, et qui contient à l'intérieur un autre tube en cuivre, plus petit; ce dernier est relié d'un côté à l'ajutage d'où sort la vapeur surchauffée, et de l'autre côté à un récipient gradué qui mesure l'eau condensée. Le tout est bien isolé avec de la laine de verre.

Par cette méthode, les portées théoriques des ajutages ont été contrôlées; elles concordaient parfaitement. Un contrôle facile, et d'ailleurs superflu, de la quantité de chaleur fournie a été obtenu en mesurant la quantité de l'eau de refroidissement, et sa température à la sortie.

Les résultats des expériences ainsi effectuées ont été nettement supérieurs à ceux des expériences précédentes. Cela s'explique facilement en remarquant que, comme on a vu ensuite, les 5,5 kg/h de vapeur avaient été obtenus avec l'appareil endommagé.

La figure 21 rapporte les nouveaux résultats. On voit qu'une portée de 7 kg/h avec des températures de la vapeur oscillant de 450 à 500 °C peut être atteinte et maintenue.

La différence de plus de 100 °C entre les températures de la face antérieure de la plaque et de la vapeur sortante, tout en représentant une confirmation ultérieure du bon rendement du collecteur, dénonce un mauvais rendement de l'échangeur de chaleur. Cela est dû en grande partie à une distribution de l'énergie rayonnante en arrivée sur la plaque non adaptée à des pressions d'exercice inférieures à 100 atm. L'élimination de ce défaut augmentera le rendement total.

Le rendement total de l'appareil dans les conditions actuelles peut être calculé en raison de 70 p. 100 à 75 p. 100 pour une température de la vapeur de 450 à 500 °C.

Toujours à cause des avaries subies, il n'a pas encore été possible de répéter les expériences aux hautes pressions pour lesquelles l'appareil a été conçu. Elles seront reprises après nouvelle révision de la plaque.

Résumé

Les principaux obstacles à l'exploitation industrielle de l'énergie solaire sont la faible densité et l'insuffisante température à laquelle les collecteurs classiques la recueillent. L'auteur entend exposer un nouveau type de collecteur, peut-être assez économique pour une production industrielle, et capable de fonctionner avec des rendements élevés à des températures de 400 à 500 °C. Les expériences effectuées en 1960 avec trois différents modèles de ce collecteur et les premiers résultats d'un collecteur pour moteur solaire à turbine, qui fournit 5 à 7 kg/h de vapeur surchauffée à 450 °C et 150 atmosphères, semblent confirmer la théorie.

La comparaison entre la petitesse de l'angle solide de l'énergie rayonnante qui nous arrive du soleil, mesuré à 0,0000678, par rapport à l'angle solide dans lequel les corps noirs classiques ré-émettent l'énergie (2π), est une des façons d'expliquer leurs basses températures d'absorption.

Les lentilles et les miroirs paraboliques sont les moyens les plus communs pour agrandir l'angle solide des rayons incidents; mais leur coût empêche leur utilisation sur une échelle industrielle.

La solution proposée par l'auteur est plus économique, et peut être schématisée comme suit.

Un tronc de cône ayant l'axe en direction du soleil et une ouverture égale à la grandeur apparente de ce dernier est posé devant un corps noir classique; il ne limite pas l'énergie en arrivée.

Au contraire, s'il a des parois noires et calorifugées, le tronc de cône limite l'énergie ré-irradiée; le développement analytique démontre que, en conditions limites, l'énergie ré-irradiée se réduit à celle contenue dans le même angle solide de l'énergie en arrivée.

En d'autres termes, on peut affirmer que, à l'extrême, un tel limitateur de l'énergie ré-émise oblige cette dernière à parcourir le même tube de flux de l'énergie en arrivée. La source et le collecteur sont ainsi reliés, de telle façon que l'équilibre thermodynamique se fait à des températures égales; pour des températures du collecteur inférieures à celle de la source, le premier absorbe de l'énergie avec un rendement qui augmente très rapidement avec la chute de la température du collecteur.

Vu la petitesse de l'angle solide de l'énergie rayonnante envoyée par le soleil, le collecteur schématisé

plus haut peut être réalisé par un cylindre à parois noires : quand un grand nombre de ces cylindres sont réunis de façon à former une structure en nid d'abeille, la condition que les parois soient calorifugées n'est plus nécessaire, étant donné qu'on peut considérer que deux cylindres contigus ont la même distribution de températures. Cette structure est dénommée ici corps noir absolu, pour sa qualité à la limite d'absorber toute l'énergie en arrivée, sans en ré-émettre dans une direction différente de celle de la source.

L'étude analytique de la distribution des températures aux divers points des surfaces de la structure en nid d'abeille démontre que celle-ci, avec une très bonne approximation, diminue en proportion à la quatrième racine de la distance entre le point et la bouche.

Quantitativement, pour des tubes dont le rapport longueur/diamètre est de 15 à 20, la réduction de l'énergie ré-irradiée est approximativement de 96 à 98 p. 100 de celle qui sortirait si la protection était absente.

Des températures de 400 à 500 °C sont actuellement considérées assez bonnes pour convertir l'énergie thermique en énergie mécanique, au moyen de moteurs à vapeur. D'autre part, des températures même inférieures permettent d'accumuler de l'énergie thermique avec des systèmes qui, sur une vaste échelle, pourraient même être très économiques. Par exemple, un hectomètre cube de terrain pauvre en eau peut être considéré comme un accumulateur complètement gratuit, sauf pour les frais d'installation de l'échangeur de chaleur à l'intérieur : le calcul démontre qu'une telle masse thermique ne nécessite pas d'isolement autre que celui représenté par la terre même ou par la roche à l'entour.

Toutefois, en comparaison avec la température du soleil, 400 à 500 °C sont des températures basses au point de suggérer l'emploi de surfaces à transparence sélective.

Une structure en nid d'abeille composée de matériel transparent par rapport à l'énergie solaire et « noir » par rapport à l'énergie irradiée de 400 à 500 °C aura, jusqu'à concurrence de ces températures, la même efficacité que celui que nous avons dénommé corps noir absolu, sans qu'elle doive nécessairement être pointée vers la source.

On peut en outre étudier des schémas facilement et économiquement réalisables (pas sur une petite échelle) pour concentrer de 10 à 15 fois sur un tel collecteur supposé fixe l'énergie rayonnante solaire, avec des miroirs composés de minces feuilles d'aluminium. Avec ce système, 9/10 à 14/15 de la surface du collecteur, ainsi que l'échangeur de chaleur et l'isolant qui le complètent, sont remplacés par des feuilles d'aluminium, avec un évident avantage économique. Les études conduites par l'auteur, même si elles ne sont pas encore prêtes à être publiées, laissent prévoir le moment où l'énergie solaire pourra concurrencer l'énergie actuellement obtenue d'autres sources.

Une brève description des vérifications expérimentales déjà obtenues permettra de se rendre compte des développements industriels possibles de ce qui a été exposé.

Un des appareils consistait en une structure de près de 10 000 prismes adjacents presque hexagonaux, de 8 mm de diamètre et de 120 mm de hauteur et construite avec des feuilles de cellulose carbonisée par un procédé spécial; elle fut posée devant une mince plaque de cuivre noirci, portant sur le côté postérieur à peu près 26 m de tube en spirale, et elle était protégée par du matériel isolant. Ce collecteur-échangeur de chaleur, d'une surface totale de 0,50 m², pointé vers le soleil, a fourni en conditions de régime près de 0,1 gr/sec de vapeur surchauffée à 230 °C et 2 atmosphères, avec une pointe maximale de 0,085 gr/sec à 320 °C. Cela équivaut à un rendement à peine supérieur à 50 p. 100, et par conséquent nettement inférieur au rendement théorique. Cela s'explique par certaines imperfections dans l'exécution d'une structure aussi complexe.

Un autre appareil consistait en un ensemble d'à peu près 150 tubes en verre de 12 à 15 mm de diamètre, de 250 mm de longueur, de 0,2 à 0,3 mm d'épaisseur, protégé par un cylindre à surface spéculaire et placé devant une plaque noire et calorifugée. Ce fut le premier échantillon de structure en nid d'abeille en une matière à transparence sélective. Aucun échangeur de chaleur ne fut prévu, et la chaleur partit par conduction à travers les parois insuffisamment isolées à cause des petites dimensions. Devant le collecteur, un cône en aluminium concentrait théoriquement à peu près 6 fois l'énergie en arrivée. La plaque atteignit la température limite de 520 °C; on réussit à photographier la couleur rouge naissant de la zone centrale.

Les rendements favorables de ces collecteurs ont permis d'adapter les services du collecteur aux exigences des moteurs thermiques à vapeur, au lieu du contraire. On a ainsi construit un appareil capable de fournir 5 à 7 kg/h de vapeur surchauffée de 400 à 500 °C avec 100 à 150 atmosphères de pression. Il se compose d'un collecteur en nid d'abeille du type à transparence sélective et consiste en environ 2 000 petits tubes en verre, posés sur une plaque en vernis noir qui absorbe la presque totalité de l'énergie incidente. Sur ce collecteur d'à peu près 0,50 m² de surface, des miroirs coniques en aluminium concentrent de l'énergie rayonnante dans le rapport géométrique de 16 à 1. L'appareil, supporté par un robuste trépied, muni des leviers de manœuvre nécessaires, est monté sur un petit camion et facilement déplaçable, après le démontage des parties les plus encombrantes. Un cadre d'instruments (thermomètres à thermocouple, manomètres, etc.) permet la lecture directe des résultats.

Au cours des premières expériences, une portée de 5,5 kg/h de vapeur surchauffée à 450 °C a été obtenue. Nous pouvons raisonnablement espérer atteindre, en conditions de régime, 7 kg/h de vapeur surchauffée à 450 °C et de 100 à 150 atmosphères.

La structure cellulaire du corps noir absolu peut avoir de nombreuses applications : par exemple, ce mémoire décrit un four solaire pour températures

de l'ordre de 3 000 °C, formé par un miroir en tronc de cône qui concentre l'énergie sur un cylindre posé sur son axe et protégé par une structure cellulaire formée, non par une surface continue, mais par des fils de tungstène de 10 à 50 microns de diamètre, tendus sur des châssis et éloignés des parties chaudes.

Par ailleurs, la structure cellulaire qui a la propriété d'être froide et, dans une certaine direction, transparente, peut être mise à profit, dans des conditions particulières, pour des isolants thermiques de masse thermique négligeable à des températures très élevées.

A NEW COLLECTOR OF SOLAR RADIANT ENERGY— THEORY AND EXPERIMENTAL VERIFICATION

(Translation of the foregoing paper)

Giovanni Francia *

The equilibrium temperature of a conventional collector of radiant energy, consisting, for instance, of a black body exposed to the sun, is far lower than the solar temperature, even when all the incident energy is retained and transformed into heat, as it is in the case of a black body.

This may be explained if we note, for instance, that the solid angle through which the black body reradiates the energy is a half space, that is, 2π, while the incident energy is contained in the extremely small solid angle subtended by the sun, and which, assuming the apparent diameter of the sun to be 32′, equals 0.0000678.

Taking the cosine rule into account, as well as the fourth-power law relating the irradiated energy to the absolute temperature, then, if T_S is the solar temperature measured by the black body method, and T_n is that of the collector, simple calculations will give us the equilibrium relation:

$$2\pi \int_0^{\frac{\pi}{2}} T_n^4 \cos\varphi \sin\varphi \, d\varphi = 0.0000678 \, T_S^4 \qquad (1)$$

that is,

$$\pi T_n^4 = 0.0000678 \, T_S^4 \qquad (2)$$

where the surface of the black body is assumed perpendicular to the solar rays, and thus $\cos\varphi = 1$.

It follows from equation (2) that:

$$T_n = 0.0682 \, T_S \qquad (3)$$

and if, in very good approximation, we put $T_S = 6\,000°K$, then we shall have $T_n = 409°K$, equivalent to 136°C.

This temperature, which must in any case be considered a limiting temperature, is so low that any industrial utilization by this means alone would be inadvisable.

The collector temperature may be increased either by increasing the solid angle of the incoming energy or limiting the reradiated energy in some way.

The expression "by increasing the solid angle of the incoming energy" was intentionally used by us instead of the more common expression "by concentrating the incoming energy" to avoid the ambiguity which might result from the latter. While it is, of course, obvious that the solid angle of the incoming energy cannot exceed a half space, the limit beyond which the concentration of the energy becomes impossible is not so obvious. This limit, required by the second law of thermodynamics, is connected with very general properties of all radiant energy, which there is no reason to discuss here. We may say only that, from the study of these properties, the author has deduced the theory and the resulting applications which will be set forth in this paper.

The solid angle of the incoming energy may be easily increased up to a factor of several thousand by means of mirrors or lenses. In accordance with the above exposition, this permits the attainment of temperatures rather close to that of the sun. This method, which is very useful when very high temperatures with only a modest quantity of energy are required, is nevertheless too costly, used by itself, for the industrial utilization of solar energy.

The method of limiting the reradiated energy seems much more economic, whether by exploiting the "hot-house effect", that is, by protecting the collector with selectively transparent surfaces, or employing the selective collectors studied by Tabor and his school, or by a combination of the two.

The purpose of this paper is to present a system of limiting the reradiated energy combining the ability to produce high temperatures, if desired, with suitability for manufacture by industrial methods, perhaps so economic as to make solar radiant energy competitive with the energy currently derived from other sources.

In figure 1, let 1 be the surface of a conventional collector, for instance a black body, and let 2 be the mean direction of the solar rays entering 1. We have already stated that, under equilibrium conditions, the collector temperature T_n is much lower than the temperature T_S of the sun, the solid angle of the energy reradiated by the black body being far greater than the solid angle containing the energy on its arrival.

But this situation is radically modified if the solid angle of the outgoing energy is limited, without changing the solid angle of the incoming energy. We shall demonstrate that this result may be attained by placing appropriate screens in front of the collector 1. In figure 2, these screens are shown schematically as the frustum of cone 3, with perfectly black,

* Professor, Università di Genova, Genoa.

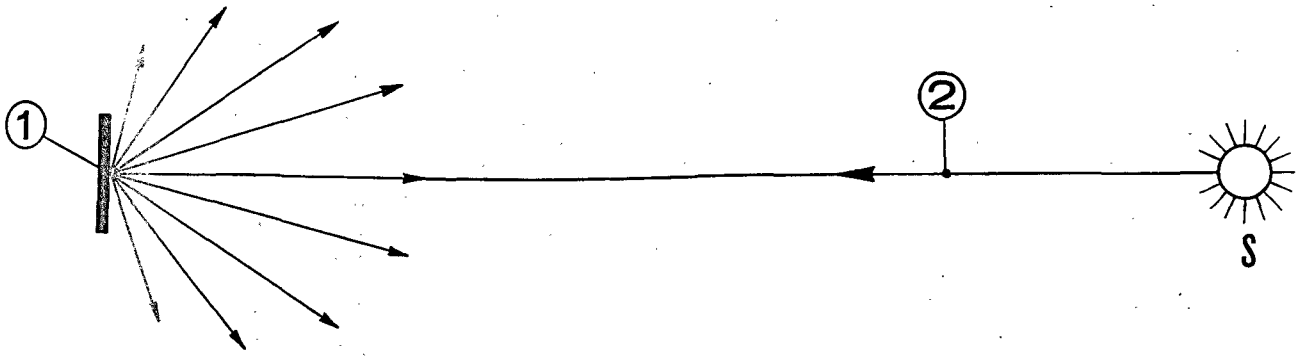


Figure 1

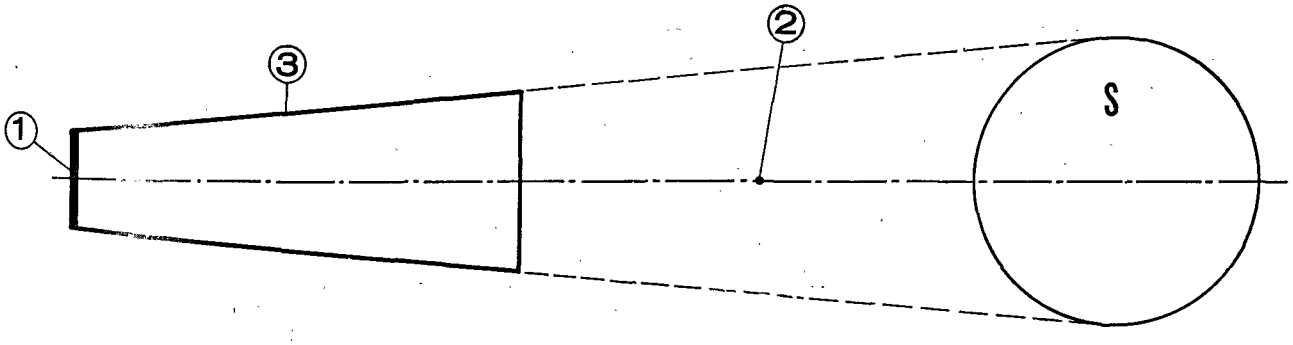


Figure 2

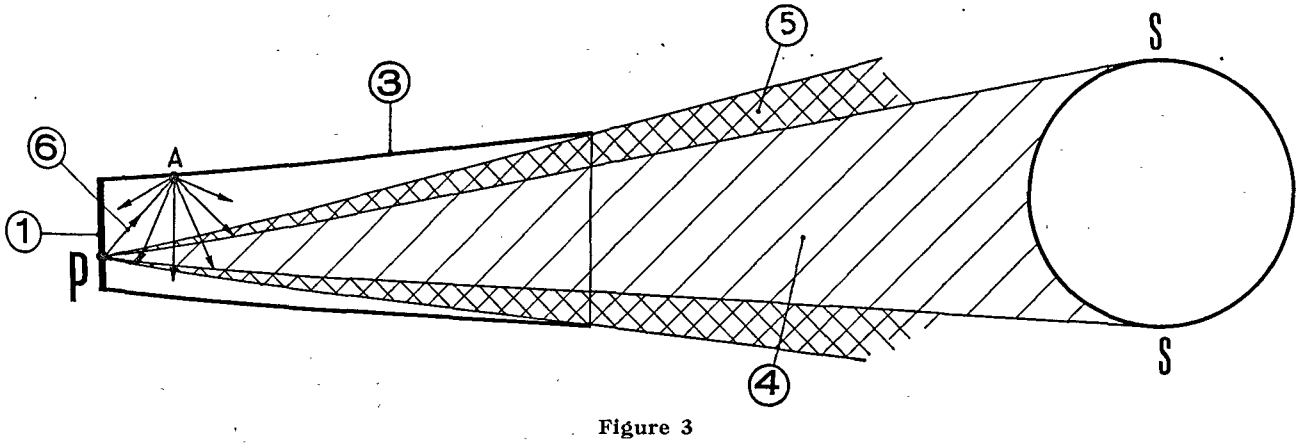


Figure 3

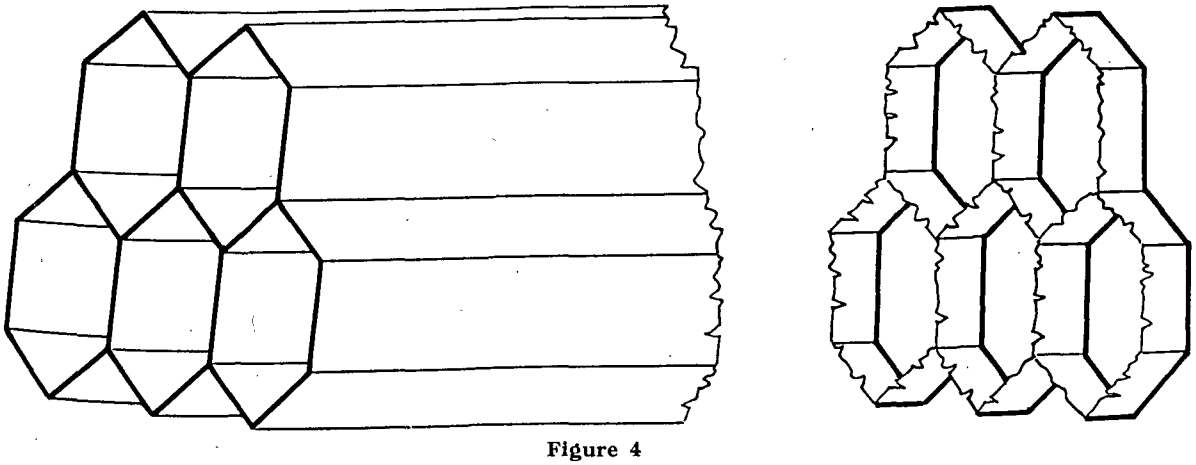


Figure 4

insulated walls, having the conventional black body 1 as its minor base, having its axis directed towards the sun, and having a vertex angle equal to the apparent diameter of the sun.

Before our exposition of the analytic development, which, although it presents no particular difficulty, is still a little complex, we may reach an understanding of the phenomenon by qualitative reasoning. Unless explicitly otherwise stated, all the arguments that follow will omit from consideration all the selective properties of the absorbing, emitting, reflecting or transparent surfaces.

Let us examine (figure 3) the various rays leaving the point P of the black body surface 1. They may be divided into three types:

1) Rays which, on leaving P, arrive directly at the sun without touching the walls of the frustum; they are contained within the inner hatched cone 4 of figure 3. Without the aid of selective properties, the outgoing energy accompanying these rays cannot be limited without at the same time limiting the incoming energy.

2) Rays, which, on leaving P, leave the frustum of the cone without touching the walls, and do not meet the sun; they are contained within the zone 5, cross-hatched in figure 3 and bounded by two cones leaving the same vertex P. The outgoing energy accompanying these rays may be diminished by lengthening the frustum 3 of the cone until the limit is entirely eliminated.

3) Rays which, on leaving P, meet the wall of the cone. Let 6 be one of these rays, and A the point of contact. Since the cone wall has been assumed to be black, that is, perfectly absorbing, all the energy of the ray 6 is absorbed by the point A, and, under equilibrium conditions, it will be reradiated in degraded state (since, as we shall show, the temperature of A is always lower than that of P) in all directions, obeying the well-known cosine rule. Let us trace the path of the rays reradiated by A.

(*a*) One part returns to 1, thus limiting the energy loss.

(*b*) One part leaves the frustum of the cone, and must thus be considered lost.

(*c*) One part meets the walls of the frustum again; it is absorbed, and then reradiated as described above.

This qualitative examination demonstrates the limitation imposed by the frustum 3 on the energy reradiated by the surface 1. The analytic development to be given below will give us the quantitative measure of this limitation. We shall see, still later, in the numerical example that will be based on the data of the collector of the solar motor constructed by the author, that the limitation of the energy loss can by itself easily permit attainment of temperatures close to that of the sun, or, for temperatures that are lower, but still elevated and sufficient for industrial utilization, of efficiencies exceeding 95 per cent.

Three more observations are still necessary to permit us to understand all the implications that the foregoing exposition, and the analytic development to follow, have for the industrial and economically competitive utilization of solar energy.

First observation. Because of the smallness of the apparent diameter of the sun, the frustum 3 of figures 2 and 3 may be replaced by a cylinder, or even, for practical reasons, by a hexagonal or square prism, or one of any other section. When assembling a large number of these prisms (figure 4), their walls need not necessarily be insulated, since, by hypothesis, two adjacent prisms have equal temperature distributions, and, owing to this fact, there will be no heat transfer across the walls. The assembly formed by a large number of these prisms, arranged, for instance, as in figure 4, like a beehive, having thin black walls, and each prism being very long by comparison with the longest chord of its section, might be termed an absolute black body, from its ability, at the limit, to absorb all the radiant energy arriving from a distant source without reradiating energy in a direction different from that of the source itself.

Taking everything in account, the absolute black body may be considered as a materialization of the tubes of incoming energy flux; as we shall show, it is also possible to order and guide the outgoing energy by forcing it, at the limit, to traverse the same tubes of energy flux as on arrival.

This explains how such a collector, directed towards a source, even a very distant one, can be subject to conditions of thermodynamic equilibrium with the source, at the temperature of the source.

Second observation. The collector which we have termed absolute black body, and on which all the applications subsequently to be presented here are based, is difficult to utilize as a solar energy collector on an industrial scale, in the schematic form in which we have described it, primarily on account of the low density of the solar energy. While we must postpone the description of the specific uses to the second part of this paper, we note here that, if temperatures of about 400 to 500°C are sufficient, the walls of the beehive black body may be made of selectively transparent material, or, more precisely, black for the long-wave radiation and transparent for the solar radiation, such as glass, mica, plastics, etc. A reradiated-energy limiter made of such materials, while having the same geometry as an absolute black body, would still differ from it substantially in the following two characteristics:

(*a*) It could not attain very elevated temperatures, at which, even if the materials could resist them, the transparency of such materials would no longer be selective; and this is an unfavourable characteristic;

(*b*) It would not necessarily have to be pointed in the direction of the sun, since it could absorb the energy of rays incident at any angle. It will suffice to note that the component of momentum of the incoming photons, according to the direction of the axes of the prisms, remains unchanged through

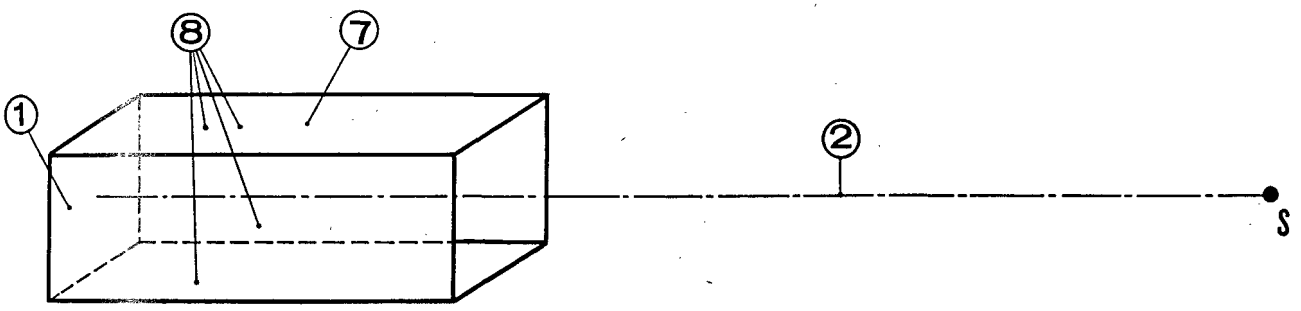


Figure 5

the successive refractions or reflections caused by the walls of the prisms themselves.[1]

This quality is extremely advantageous, for it permits the use of the collector without making it follow the motion of the sun, or its use with a moderate concentration of the solar rays. These two characteristics, which, with systems opportunely studied, can be simultaneously exploited, are those which might authorize the industrial utilization of these collectors in competition with the other sources of energy.

Third observation. The reradiated-energy limiter can in some cases reduce to a system of planes parallel to each other and to the direction of the incoming rays. Such a partializer might be used when, for example, the direction of the incoming rays is displaced while still remaining in a single plane.

Development of the calculations

Let S be a point source (figure 5) and 7 an element of an absolute black body oriented towards that source. More exactly, let 7 be a prism which, for simplicity, we assume to be of rectangular cross section, open at the extremity turned toward the source S, and closed by the black body 1 on the opposite end. The four walls 8, parallel to the direction 2 of the source, are black and insulated.

We have given, above, a qualitative description of the manner in which the walls 8 operate as limiters of the energy reradiated from 1. To examine the problem from the quantitative point of view, we shall divide it into two parts:

(1) Under the assumption that the collector temperature is known, that is, practically, that the

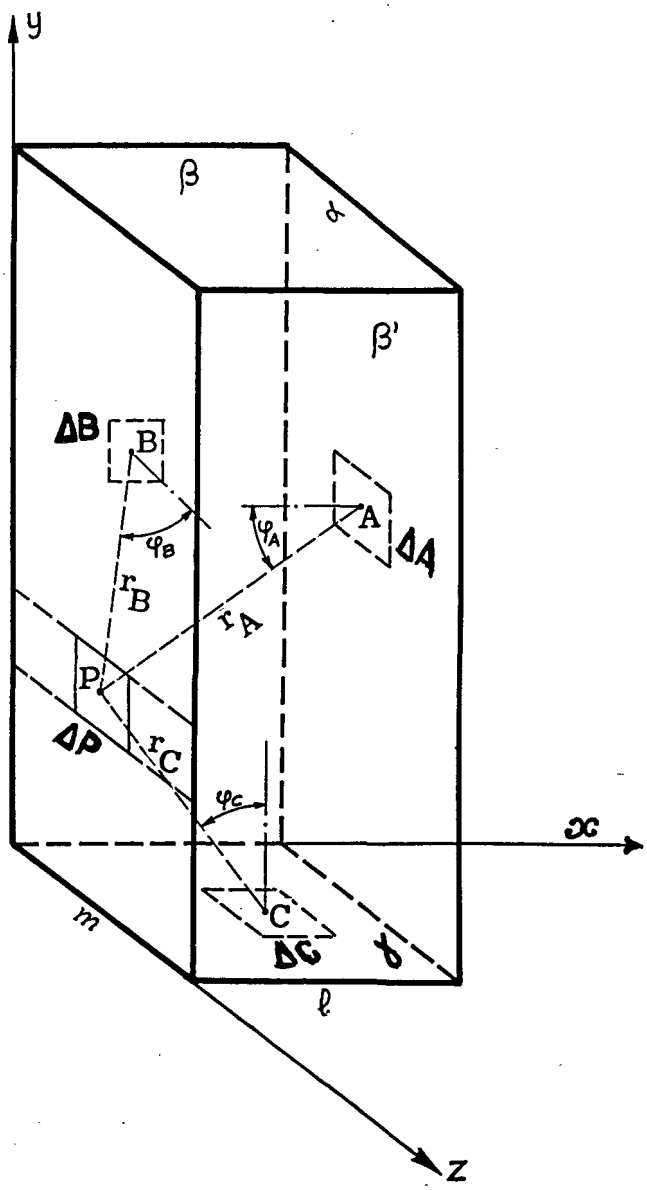


Figure 6

[1] We note that this is not true if the black body is protected with plates of glass or other selectively transparent material, as is done to obtain the hot-house effect. In this case, the two partial reflections to which the light is subjected at the entrance wall and exit wall, respectively, of each plate, will cost about 10 per cent of the incident energy under the most favourable conditions of incidence, unless the surfaces are protected by special treatments, which have been, and still are, costly. Even if this is done, the loss will still be at least 1 per cent. This limits the number of possible protective layers. Since such protection, at least with the materials used up to now, takes place by absorption, with consequent heating, n protective layers will reduce the energy loss to $\frac{1}{n+1}$ and the number of layers required for sufficient protection will be too high. The situation would be very different if the protection were realized by selective reflection instead of selective absorption. A protective surface formed by a material transparent for the wavelength of the incoming energy and reflecting for the wavelength of the outgoing energy would be a perfect solution of the problem.

operating temperature has been established, we shall seek the temperature distribution on the walls 8;

(2) The temperature distribution on the walls of the open prism 7 being known, we may calculate the energy radiated from the front opposite 1.

Let l and m be the sides of the rectangle γ, base of the prism, which we shall assume to coincide with the surface 1, at constant collector temperature; let h be the height; let x, y, z be three Cartesian co-ordinates drawn from a vertex of the base γ, as indicated in figure 6 : x and z coincide with two edges of the base γ, while y is directed towards the source S. The constant temperature of the base γ being denoted by T_0, and the four lateral faces of the open prism being assumed to be black and insulated, let us seek the temperature distribution on these faces under equilibrium conditions.

Let P be a point of one of the lateral faces of the prism — in the case of figure 6, the face located in the plane yz; let o, y, z be the co-ordinates of P; let $\Delta P = \Delta y\, \Delta z$ be near P. The condition of equilibrium requires that the energy radiated by ΔP be equal to the sums of the energies which, on ΔP, irradiate the base γ and the other lateral faces α, β, β' of the prism.

We assume that the temperature of a generic point P of the lateral walls depends only on its distance y from the base γ; let us call this temperature $T(P) = T(y)$.[2]

By the Stefan-Boltzmann law, the energy emitted by radiation from the surface element ΔP is:

$$I_P \Delta P = \pi a\, T^4(P)\, \Delta P = k\, T^4(y)\, \Delta y\, \Delta z \qquad (4)$$

We shall separately calculate the energy radiated on ΔP by each of the other faces of the prism.

Energy radiated on ΔP by the face α. Let A (l, y_A, z_A) be a point of α, and $\Delta A = \Delta y_A\, \Delta z_A$ be another point near A; the temperature of A will be $T(y_A)$. We shall find, by easy calculations, taking account of the cosine law, that the energy radiated by ΔA on ΔP is:

$$I_{A,P} \Delta A\, \Delta P = \frac{k\, l^2\, T^4(y_A)\, \Delta y\, \Delta z\, \Delta y_A\, \Delta z_A}{[l^2 + (y - y_A)^2 + (z - z_A)^2]^2} \qquad (5)$$

The total radiation of the face α on ΔP will be the integral of $I_{A,P} \Delta A\, \Delta P$ taken over the entire face α, that is:

$$\begin{aligned} I_{\alpha,P} \Delta P &= k\, \Delta P \iint_{\alpha} I_{A,P} \Delta A \\ &= k\, \Delta y\, \Delta z \int_0^h T^4(y_A)\, dy_A \int_0^m \frac{l^2\, dz_A}{[l^2 + (y - y_A)^2 + (z - z_A)^2]^2} \\ &= k\, \Delta y\, \Delta z\, l^2 \int_0^h \frac{T^4(y_A)}{2\,[l^2 + (y_A - y)^2]} \left[\frac{\operatorname{arctg} \dfrac{m - z}{\sqrt{l^2 + (y_A - y)^2}} + \operatorname{arctg} \dfrac{z}{\sqrt{l^2 + (y_A - y)^2}}}{\sqrt{l^2 + (y_A - y)^2}} \right. \\ &\qquad \left. + \frac{m - z}{l^2 + (y_A - y)^2 + (m - z)^2} + \frac{z}{l^2 + (y_A - y)^2 + z^2} \right] dy_A \end{aligned} \qquad (6)$$

Energy radiated on ΔP by the face β. By calculations similar to the above, we find the radiation of the entire wall β on ΔP to be:

$$I_{\beta,P} \Delta P = \frac{k\, z\, \Delta y\, \Delta z}{2} \int_0^h T^4(y_B) \left[\frac{1}{(y_B - y)^2 + z^2} - \frac{1}{l^2 + (y_B - y)^2 + z^2} \right] dy_B \qquad (7)$$

Energy radiated on ΔP by the face β'. From equation (7), by substituting m-z for z, we derive:

$$I_{\beta,P} \Delta P = \frac{k\,(m - z)\, \Delta y\, \Delta z}{2} \int_0^h T^4(y_B) \left[\frac{1}{(y_B - y)^2 + (m - z)^2} - \frac{1}{l^2 + (y_B - y)^2 + (m - z)^2} \right] dy_B \qquad (8)$$

Energy radiated on ΔP by the face γ. Repeating the above reasoning, we find:

$$I_{\gamma,P} \Delta P = \frac{k y T_0^4 \Delta y \Delta z}{2} \left[\frac{1}{y} \operatorname{arctg} \frac{m - z}{y} + \frac{1}{y} \operatorname{arctg} \frac{z}{y} - \frac{1}{\sqrt{l^2 + y^2}} \operatorname{arctg} \frac{m - z}{\sqrt{l^2 + y^2}} - \frac{1}{\sqrt{l^2 + y^2}} \operatorname{arctg} \frac{z}{\sqrt{l^2 + y^2}} \right] \qquad (9)$$

Imposing the condition that the total energy radiated by the element of surface ΔP, expressed by the second member of equation (4), shall equal the sum of the energies radiated on ΔP by the walls α, β, β', γ, expressed by the respective right sides of equations (6), (7), (8) and (9), one would find the condition of thermodynamic equilibrium for the element of surface ΔP.

[2] This hypothesis is true when the base 1 is a circle or a plane band; the error introduced, in the other cases of interest to us, is absolutely negligible.

But in view of the hypothesis already adopted, that the temperature of P depends only on the variable y, a hypothesis already used to arrive at equations (6), (7), (8) and (9), the condition of thermodynamic equilibrium could be imposed on the entire horizontal band containing ΔP. This would be equivalent to integrating both sides of equations (4), (6), (7), (8) and (9) with respect to z, between 0 and m.

Performing these integrations, equating and reducing, we find the conditions of equilibrium:

$$m\pi T^4(y) = m l^2 \int_0^h T^4(t)\,[l^2+(y-t)^2]^{-3/2}\,\operatorname{arctg}\frac{m}{\sqrt{l^2+(y-t)^2}}\,dt + \frac{1}{2}\int_0^h T^4(t)\left[\ln\frac{(y-t)^2+m^2}{(y-t)^2} - \ln\frac{(y-t)^2+m^2+l^2}{(y-t)^2+l^2}\right]dt + T_0^4\left[m\operatorname{arctg}\frac{m}{y} - \frac{my}{\sqrt{l^2+y^2}}\operatorname{arctg}\frac{m}{\sqrt{l^2+y^2}} - \frac{y}{2}\ln\frac{m^2+y^2}{y^2} + \frac{y}{2}\ln\frac{m^2+y^2+l^2}{l^2+y^2}\right] \tag{10}$$

Equation (10) gives the temperature distribution $T(y)$. It is a Fredholm-type integral equation, and can be easily solved, even if it does not satisfy the general condition of integrability for these equations.

Now, by setting

$$T^4(y) = a + by \tag{11}$$

in equation (10), performing the calculations and setting, once $y = 0$ and once $y = h$ (as is done in the principle of identity of polynomials), we get two equations, from which the unknown values of a and b may be found. Substituting the values into equation (11), we obtain a first approximation to the function sought.

As would be predicted from physical considerations, which we omit for brevity, this first approximation is already very good. The second approximation is found by substituting the value obtained into the right side of equation (10), and calculating the left side for a certain group of values of y. The second approximations so obtained differ very little from the first approximations, which confirms the validity of the procedure.

We have already stated that, in certain cases, the reradiated-energy limiter may consist of a series of planes parallel to each other and to the incoming rays, as indicated in figure 7.

Such collectors, capable of absorbing the radiant energy in all directions of a plane instead of in only a single direction, are included in the theory treated in the preceding paragraphs, provided that one side of the base rectangle of the tube now becomes infinite.

Passing to the limit, for $m = \infty$, equation (10) becomes:

$$T^4(y) = \frac{T_0^4}{2}\left[1 - \frac{y}{\sqrt{y^2+l^2}}\right] + \frac{l^2}{2}\int_0^h \frac{T^4(t)\,dt}{[l^2+(y-t)^2]^{3/2}} \tag{12}$$

Equation (12), which is of the same type as (10), gives the temperature distribution at the different points of the walls as a function of their distance from the bottom.

The solution of equation (12) formally resembles that of (10), both in procedure and result. A parallel-plane collector could be considered to be an absolute black body only for a radiant energy uniformly distributed in all the directions of a plane. We shall see how devices may be constructed in which this condition can be realized, at least in first approximation.

The knowledge of the temperature distribution on the walls and on the bottom of the prism of figure 6 permits us, by easy calculations, omitted here for brevity, to calculate the energy radiated by it in each direction of space, and, consequently, the total energy radiated.

When the height h becomes very great by comparison with the longest chord of the base, the energy radiated may be considered zero in every direction other than that common to the lateral walls of the prisms. The absolute black body thus takes the characteristic of sending out the radiant energy, radiated by its base, in tubes of flux, the walls of which tubes coincide with the walls of the cellular structure of that black body.

Comparison of this geometry of the outgoing energy with that of the outgoing energy of a source placed in the focus of a parabolic reflector indicates the capability of these two systems for the attainment of high temperatures under the action of radiant energy from a distant source.

For collector temperatures low in comparison to that of the source, but which, in the case of the sun, are still high enough for good utilization

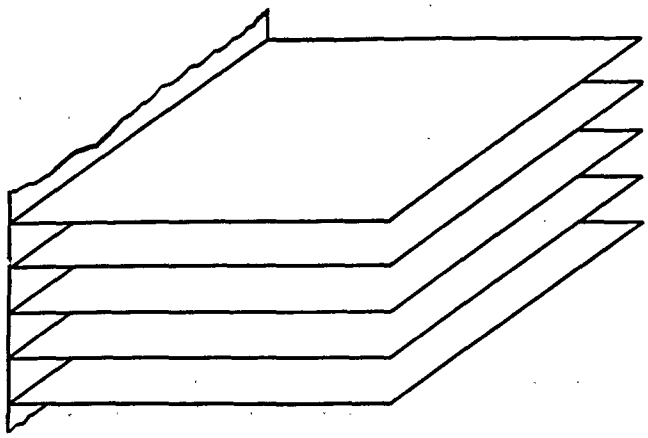


Figure 7

Table 1

y	0	2	10	50	100
$0.9722 - 0\,003783\,y$	$0.9722\,T_0^4$	$0.9646\,T_0^4$	$0.9344\,T_0^4$	$0.7830\,T_0^4$	$0.5939\,T_0^4$
$T^4(y)$	$0.9722\,T_0^4$	$0.9639\,T_0^4$	$0.9339\,T_0^4$	$0.7827\,T_0^4$	$0.5939\,T_0^4$
$\varepsilon = T^4(y) - [0.9722 - 0.003783\,y]$	0.0000	$-0.0007\,T_0^4$	$-0.0005\,T_0^4$	$-0.0003\,T_0^4$	0.0000
$T(y)$	$0.993\,T_0$	$0.991\,T_0$	$0.983\,T_0$	$0.941\,T_0$	$0.878\,T_0$

y	150	200	240	248	250
$0.9722 - 0.003783\,y$	$0.4047\,T_0^4$	$0.2156\,T_0^4$	$0.0643\,T_0^4$	$0.0340\,T_0^4$	$0.0264\,T_0^4$
$T^4(y)$	$0.4047\,T_0^4$	$0.2158\,T_0^4$	$0.0653\,T_0^4$	$0.0350\,T_0^4$	$0.0264\,T_0^4$
$\varepsilon = T^4(y) - [0.9722 - 0.003783\,y]$	0.0000	$0.0002\,T_0^4$	$0.0010\,T_0^4$	$0.0010\,T_0^4$	0.0000
$T(y)$	$0.798\,T_0$	$0.682\,T_0$	$0.504\,T_0$	$0.429\,T_0$	$0.403\,T_0$

of the thermal energy absorbed, a length-chord ratio of the order of 15-20 is already sufficient to reduce the losses of energy by radiation to values of the order of 3 per cent of the losses that such collectors would have sustained without this protection.

The ability of the cellular structure we have described to absorb all the incident energy applies only to the limiting case of parallel incident rays, that is, rays from a source at infinity. The solar radiant energy, on the contrary, is contained within a solid angle that is negligible only in the case where the ratio between the height h of the prism and the longest chord of the base is sufficiently small, for instance less than 25, or, in other words, so small that the apparent diameter of the sun is small by comparison with the apparent diameter of the prism aperture for an observer at the base of the prism itself.

In this case, to which the following numerical example refers, as well as all the experiments performed up to now, energetic equilibrium between source and collector may be established merely by taking account of the incoming energy, the reradiated energy, and the energy absorbed and converted into thermal energy. In the other cases, one must also take account of the incoming energy absorbed by the walls, and the consequent diminution of the energy reaching the bottom, and also of the different temperature distribution on the walls. In first approximation, however, these two factors tend to compensate each other.

Numerical example

In most of the experiments run up to now by the author, the beehive cellular structure was obtained by means of cylinders or prisms, hexagonal or with a different base, with a ratio of length to longest chord ranging from 12 to 18. In the numerical example of the solution of equation (10), we put $m = l = 14$ and $h = 250$, to come as close as possible to the data of the last apparatus built, whose cellular structure is formed by thin glass tubes about 14.5 mm in diameter and 250 mm long.

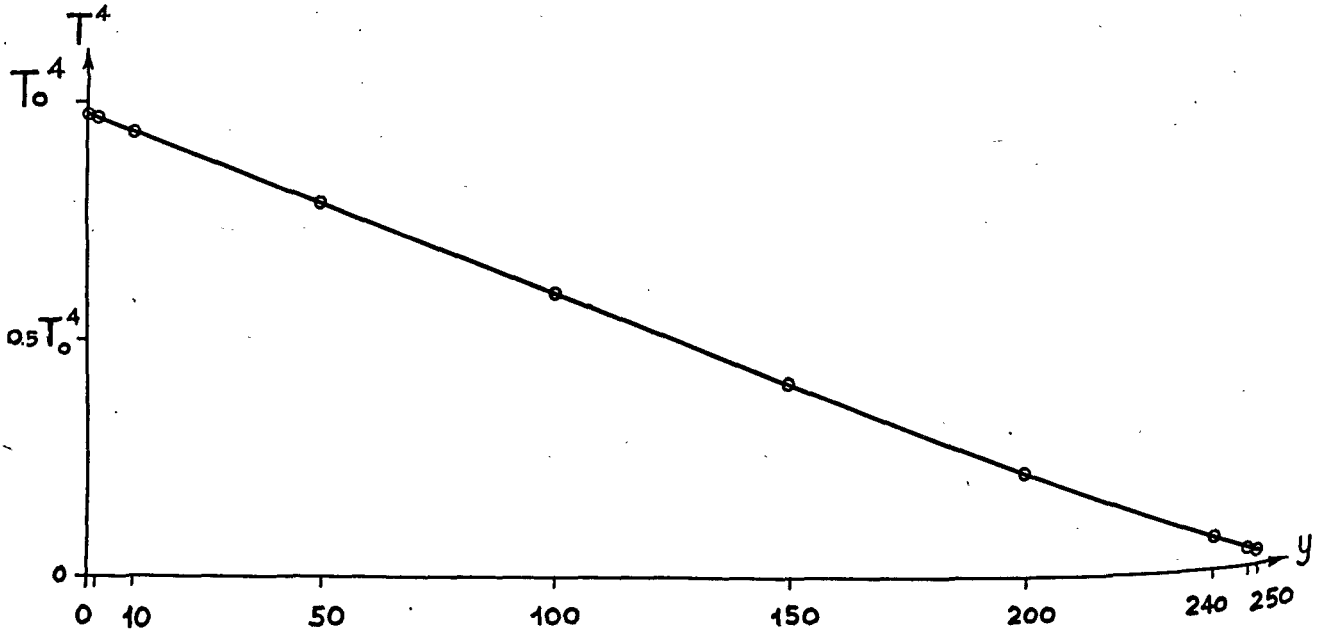


Figure 8

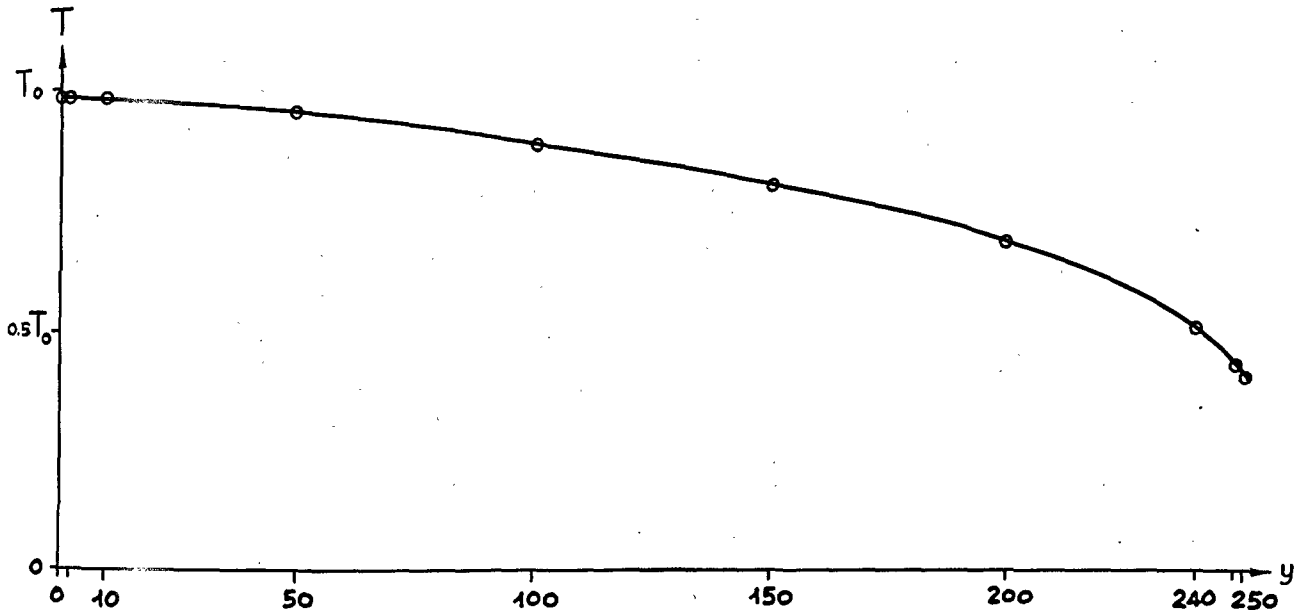


Figure 9

For convenience, the outside temperature is assumed to be 0°K.

Putting $T^4(y) = a + by$, in equation (10), after performing the calculations with the above numerical values, we get a relation between a, b, y, and naturally T_0. Setting, in the latter, once $y = 0$ and once $y = 250$, we find the system of equations that gives us the values of a and b. Performing the calculations, we obtain :

$$\begin{aligned} a &= 0.9722\, T_0^4 \\ b &= 0.003783\, T_0^4 \end{aligned} \qquad (13)$$

In first approximation, we thus find the solution

$$T(y) = T_0^4 \sqrt{0.9722 - 0.003783\, y} \qquad (14)$$

Substituting these values into the right side of (10), and solving for the values of y indicated in table 1, we get a group of values of the unknown function in second approximation.

Since the values of real interest to us are those of the fourth power of the temperature, we give in table 1 :

(*a*) On the first line, the values of y for which the calculations has been performed;

(*b*) On the second line, the values of $a + by$, that is, of the solution in first approximation;

(*c*) On the third line, the values of T, calculated in second approximation;

(*d*) On the fourth line, the differences between the values in first approximation and those in second approximation.

The differences between the first and second approximation of the results are minimum, and confirm the validity of the procedure.

Figure 8 is a graph of $T^4(y)$; it does not appear different from a segment of a straight line. It is interesting to note that the fourth power of the temperature has a discontinuity between the bottom 1 and the beginning of the side walls 8 of the prism. The temperature decreases almost linearly along the side walls to the extreme edge of the prism. There is also a discontinuity, equal to that already noted, between the fourth power of the prism temperature and the fourth power of the outside temperature, which by hypothesis was zero. The entire curve, including the discontinuities, is symmetric about its midpoint.

Figure 9 is a graph of the temperatures $T(y)$. Experiment provides a rather good qualitative confirmation of the theoretical curve: it must be

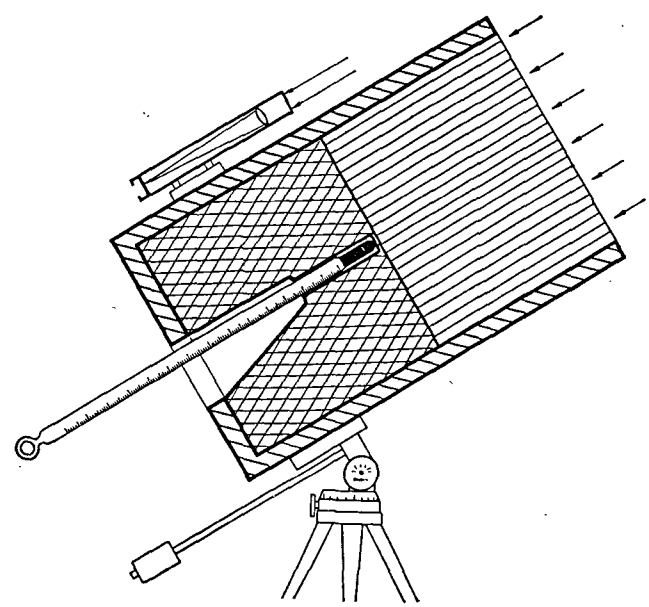


Figure 10

borne in mind that, since the variation of the temperature is not linear, the conduction along the wall of the tube and the convection due to the rather restricted motion of the air inside the tube modify the theoretical curve.

Experimental verifications. Realization of a collector with high characteristics for a solar motor

Collector No. 1

In the early part of 1960, the first system was constructed for the exclusive purpose of verifying the theory. In this system, the beehive collector was built out of hexagonal prisms about 8 mm in diameter, and 180 mm long, with walls of paper about 0.03 mm thick, carbonized at an extremely slow rate in an oxygen-free atmosphere. The structure obtained in this way was very fragile but extremely light, and had the required geometrical, optical and thermal characteristics. The entire structure had the form of a cylinder about 20 cm in diameter.

Behind this beehive structure was a conventional black body, likewise made of carbonized cellulose. The same carbonized cellulose was also used as the rear thermal insulating material, and was about 15 cm thick there. The choice of a material so difficult to handle was imposed by the need to have an extremely low thermal mass, so that the instrument would be sensitive to the very small quantities of energy involved, of the order of a few cal/s.

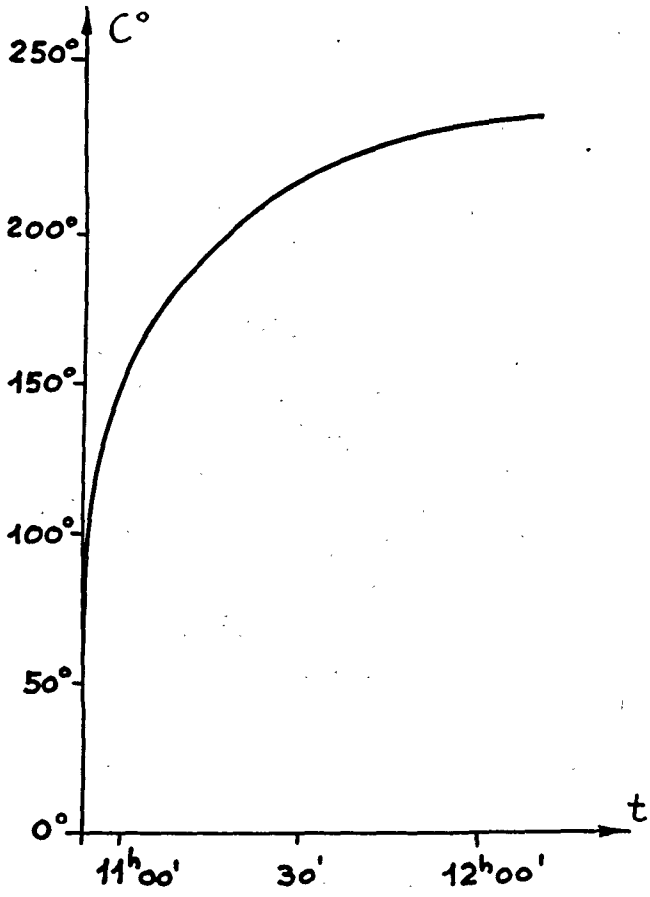


Figure 11

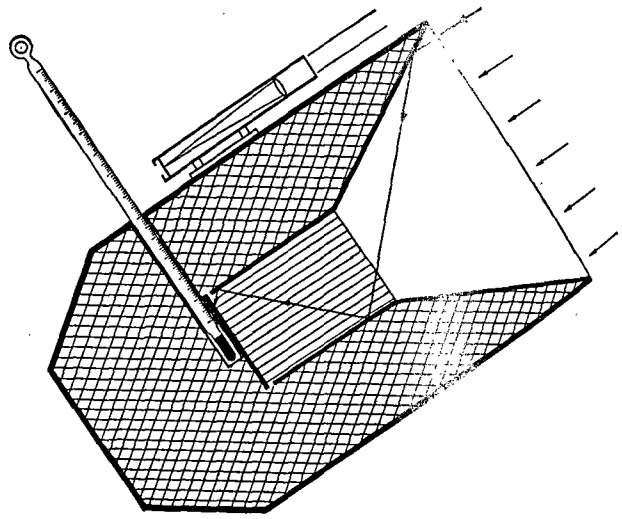


Figure 12

A quartz thermometer suitably located on the back was used to measure the temperatures. Figure 10 is a schematic diagram of the system. The equipment was completed by a sight for determining the orientation and a tripod with a universal joint. No means of collecting the thermal energy was provided, since it would have been lost by conduction, owing to the small scale of the system.

The purpose of these experiments was to measure the equilibrium temperature, from which, on the basis of an approximate calculation of the energy lost by conduction, the validity of the theory might be deduced. This validity was in fact confirmed, for temperatures of the order of 230-240°C were attained in a number of experiments. Figure 11 shows one of the graphs of collector temperature plotted against time.

Collector No. 2

A second system, with the same type of collector, but larger, and provided with a heat exchanger for direct measurement of the absorbed energy, was constructed after the results of the first had been found to be favourable.

In this second system, shown schematically in figure 12, the absolute black body again consisted of almost hexagonal prisms. Their number was about 10 000, their mean diameter was 8 mm, and they were 120 mm long, forming a cylindrical assembly 80 cm in diameter. The absorption plate was a copper disc 0.1 mm thick, blackened in front, with a spiral of copper tubing, 26 m in total length, welded to the back. A calibrated orifice at the inlet of the water pipe and another at the steam outlet allowed determination of the flow rate as a function

of the pressure drop, and, consequently, knowing the temperature, which could easily be measured, the quantity of heat delivered.

Some of the experiments were run at Sestrere, in the mountains at 2 018 m elevation, and some at Genoa. Under normal operating conditions, the device delivered a maximum of 0.1 g/s of superheated steam at about 230°C, at about 2 atm. near the outlet, but under special conditions temperatures up to 320°C were attained, with a flow of 0.085 g/s. These results are equivalent to about 70 cal/s in the former case, and 63 cal/s in the latter. Since, under the excellent conditions of the experiments, one would think that at least 125 cal/s would reach the plate, the global efficiency of the system was little more than 50 per cent, which is rather low by comparison with the theoretical predictions. This may, however, be explained by the insufficiently parallel positioning of the collector prisms, aggravated by a small fire during one of the first experiments, or by the insufficient thermal insulation of the plate.

It may be of interest to note that when a glass plate was placed in front of the beehive collector, the efficiency decreased 7 to 8 per cent. Since a glass plate almost halves the energy loss by reradiation, but also causes a 10 per cent loss of the incoming energy, this seems to confirm the low value of the reradiated energy.

We have already stated that the absolute black body by itself would not be adapted to industrial utilization of solar energy. This is why the models described above must be considered from the purely scientific point of view.

We have also mentioned the economic advisability of a moderate concentration of energy. This would, indeed, permit replacement of a large part of the collector surface, whose cost, including the heat exchanger and the insulating material, could not fall below certain limits, by mirrors made of aluminium foil, which is industrially produced at very low prices.

This requires materials that are black for the wavelengths of reradiated energy and transparent or reflecting for the incoming energy. The author knows of no materials with sufficient selectivity in this sense, with respect to reflection, but everyone knows this type of selectivity of a number of materials, with respect to transparence.

Numerous experiments have been performed to make sure that these materials can be considered not merely opaque, but "black" for long wavelengths at all angles of incidence. These experiments have been performed by introducing long-wave radiant energy into tubes of such materials, with special reference to glass, and comparing the outgoing energy with the energy that, under the same conditions, is emitted from tubes with walls that are likewise opaque but not black in so far as reflection of diffusion is concerned. After the positive result of these experiments, which need not be described here, Collector No. 3 and the large Collector No. 4 for solar motor were constructed.

Collector No. 3

This was constructed for the sole purpose of qualitatively confirming the properties of a beehive collector made of a material transparent to the incoming energy, but black for the reradiated energy. It consists of about 150 glass tubes 14-15 mm in diameter, 250 mm long and 0.2-0.3 mm thick, arranged so as to form a cylinder (figure 13) with walls of reflecting aluminium, 200 mm in diameter and 250 mm long. A conventional black body, formed by blackened copper foil with silicone resin, completes the collector; a quartz thermometer is placed behind this plate.

A frustum of a cone of mirror-finished aluminium in front of the collector concentrates the incoming luminous rays on the entrance aperture in the theoretical ratio of about 6:1. The entire assembly is insulated with glass wool and placed in a cylinder. Since most of the light rays undergo more than one reflection on the aluminium before being absorbed, the effective concentration of the light on the black surface is lower than 6:1, but still sufficient for our purposes. A sight and a sturdy tripod not shown in the figure complete the set.

Figure 14 gives one of the curves of temperature *vs.* exposure time. The final temperature of 488°C may be considered satisfactory if we take account, as with Collector No. 1, of the conduction losses in so small an apparatus. The maximum temperature measured on the plate was 520°C, with a thermo-

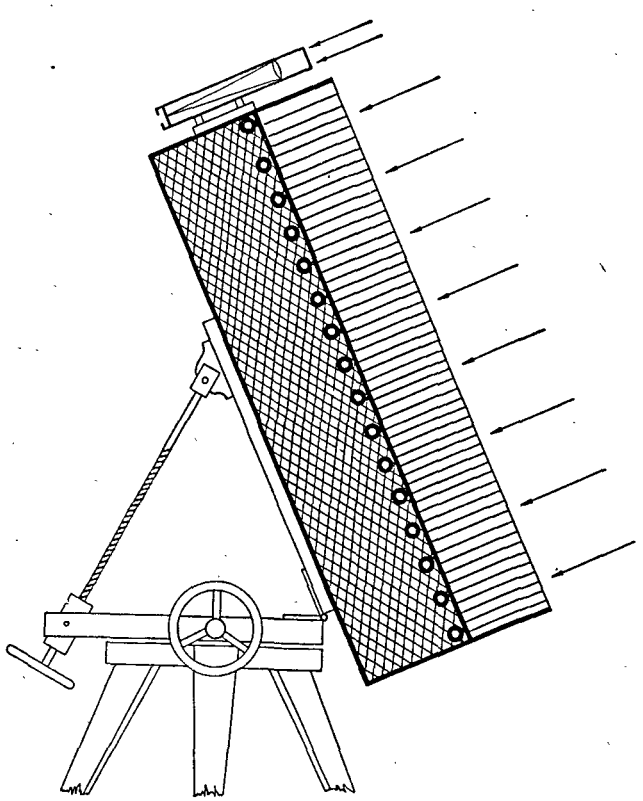


Figure 13

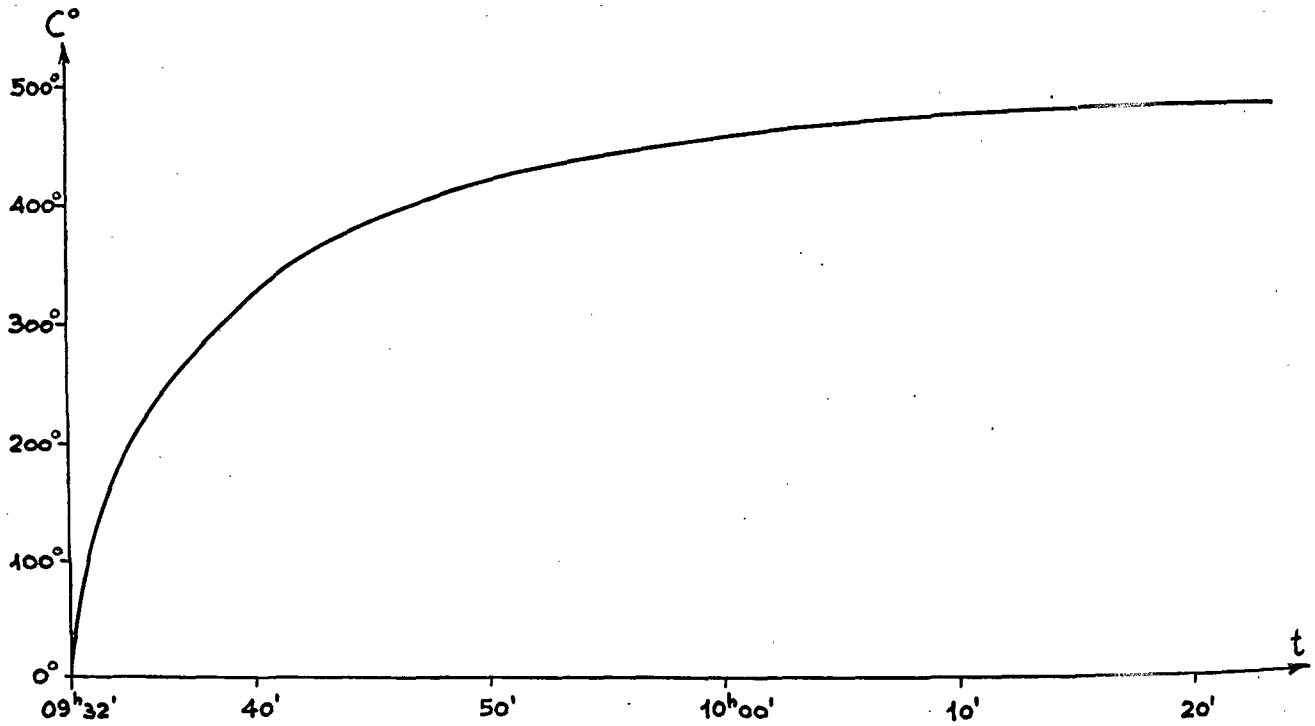


Figure 14

meter in a position different from that shown on the figure.

Figure 15 is a photograph of the collector, at the end of an experiment, taken with a shutter stop of 1:2, time 2 seconds, camera protected against outside light. The brightness of the central zone, due to the incipient redness of the centre of the plate, will be noted.

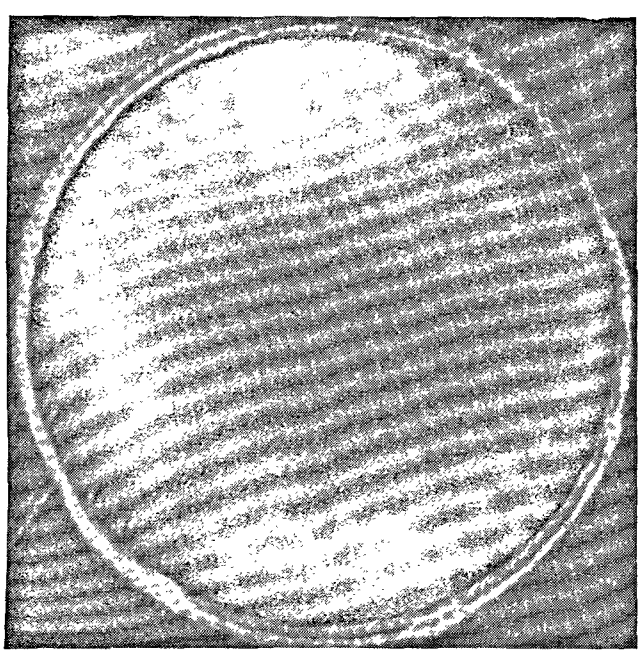


Figure 15

Collector No. 4

In October 1960 we commenced the construction of a collector with characteristics suitable for use as a source of thermal energy for a solar motor. It was completed and assembled towards the end of March 1961.

Taking account of the high efficiencies of the collectors we have described, it was considered more appropriate to adapt the efficiencies of the collector to the demands of modern heat engines, such as steam turbine, rather than the other way around.

On this basis, we established the following normal operating conditions :

(*a*) Steam pressure at outlet: over 100 atm.;

(*b*) Steam temperature at outlet: 450°C.

We studied a system that could easily be developed on an industrial scale, permitting the economic concentration, on fixed collectors, of 10 to 15 times the incoming energy. Since, however, as already noted in describing collectors 1 and 3, certain difficulties, such as that of ensuring good insulation, increase sharply with decreasing size, we preferred to obtain the design concentration by means of the conventional system of coaxial conical frustum surfaces of mirror aluminium.

Collector No. 4 consists of three coaxial conical frustra which, starting at a diameter of 3.20 m, concentrate the radiant energy on a beehive collector 0.80 m in diameter at a theoretical concentration of 16:1 (figures 16 to 18).

The beehive collector, of selective-transparency type, consists of almost 2 000 glass tubes 14-15 mm in diameter, 250 mm long and 0.2-0.3 mm thick,

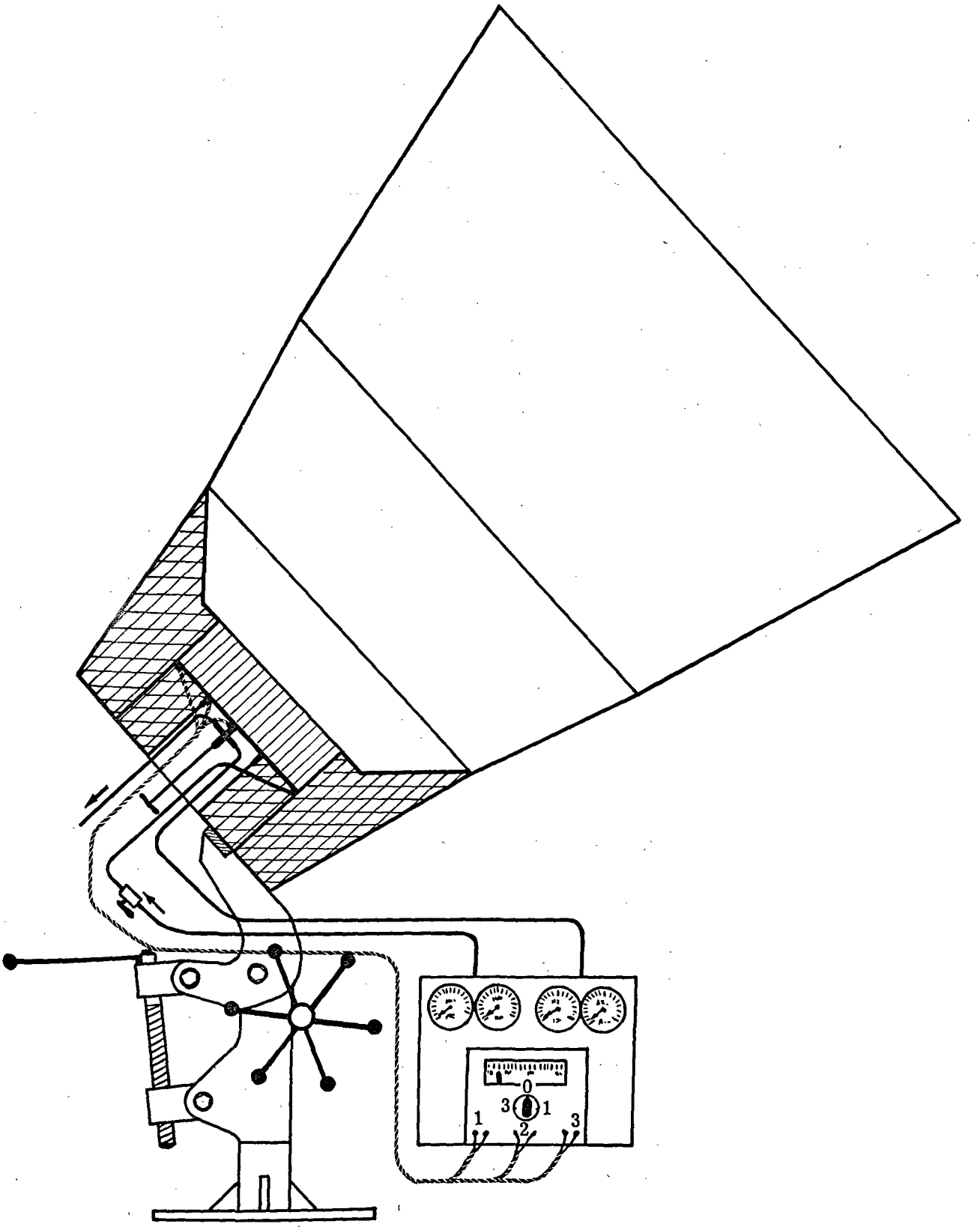


Figure 16

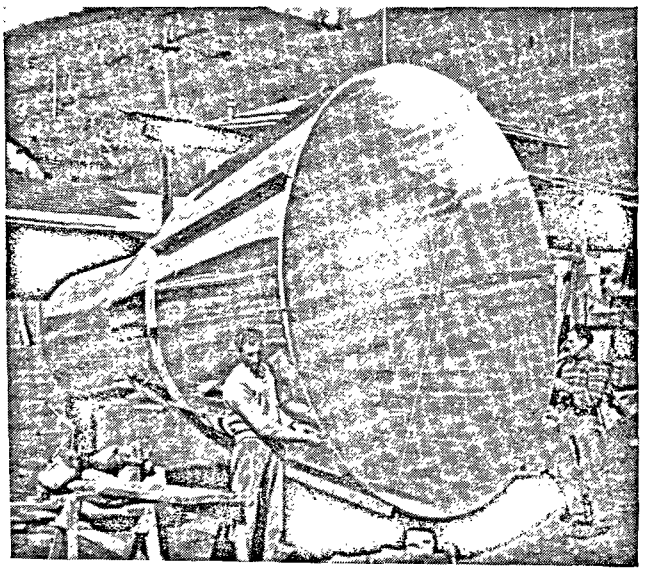


Figure 17

suitably arranged and placed on the plate, which operates at the same time as heat receiver and heat exchanger. As in Collector No. 3, the glass tubes are enclosed in a cylinder with reflecting walls.

To prevent losses in the absorption of radiant energy, the entire face of the glass plate turned towards the sun is spirally grooved, like a phonograph record, in order to force the rays of incident energy to undergo a number of reflections sufficient to ensure almost total absorption.

Temperature differences between the centre and the periphery were to be expected, and were prudently estimated at at least the order of 400°C. Therefore, to avoid deformation of the plate owing to the differences in its expansion, it was divided into two concentric parts joined by an elastic ring electrically welded to both.

The outside portion is a circular annulus with the respective inside and outside diameter of 46.5 and 79.5 cm; the lower part is a disc 46 cm in diameter. The water is admitted at a point on the outer circumference, passes over the entire plate through a duct about 46 m long, is vaporized in the central part, and leaves the centre of the disc through an externally controlled valve.

Since the heat-removing power, which is very great in the case of water, is less for the mixture of water and steam, and becomes minimum for the superheated steam, and since the centre of the plate, on account of the configuration of the incoming rays, receives the maximum density of energy, the spirals had to be brought together as closely as possible in the central zone, and spaced farther apart in the peripheral zone. This was accomplished by drawing the 26 m of spiral of the inner plate by directly turning a steel plate 20 mm thick on a lathe, and then forming the grooving so obtained with a fillet electrically welded along its entire length. In the peripheral portion, the duct is formed by about 20 m of stainless steel tubing welded to a thin plate.

The plate is insulated with about 40 cm of glass wool in the rear. The side walls of the cylinder containing the beehive structure are likewise protected by a minimum thickness of 22 cm of the same insulating material.

The collector is mounted on a sturdy support that allows its horizontal and vertical rotation into any desired position. The entire assembly is mounted on a small truck, which transports it easily from one location to another. For this purpose, the main cone may easily be disassembled into twelve parts.

The temperature of the rear of the plate is measured at various points (periphery, central annulus, and centre) by three thermocouples connected to a three-scale millivoltmeter calibrated in degrees C.

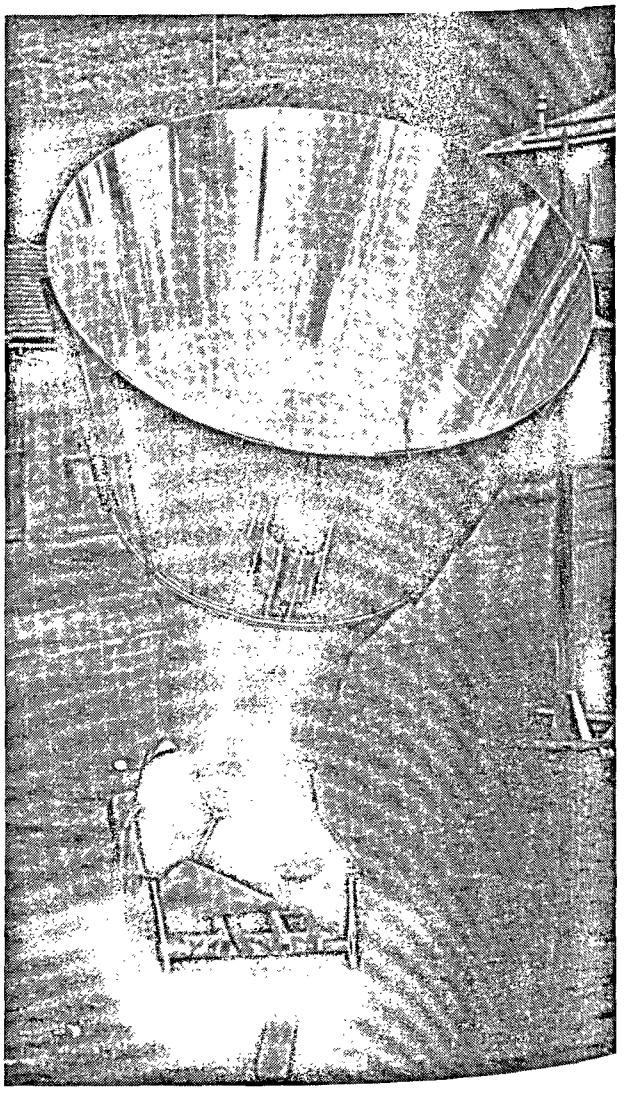


Figure 18

A fourth thermocouple, placed on the steam outlet pipe, may be connected to the millivoltmeter instead of one of the other three. Provision is made for the use of a quartz thermometer as a control.

Four manometers, two for high pressures and two for low, measure the pressure respectively of the water on admission and that of the steam at the outlet behind the expansion valve at the centre of the plate. The pressurized water is contained in the same pipe that supports the system, which serves as the high-pressure reservoir; a layer of air ensures the requisite elasticity and continuity of flow.

The low flow rates of the water, 1-2 cm^3/s, and the high pressures envisaged (the system has been tested at 350 atm.) make the use of flowmeters difficult.

The problem has been solved provisionally by applying a Laval nozzle to the discharge, that is, to put it more clearly, one similar to those used in rockets. Well-known and very exact formulae may be used to estimate the flow rate through these nozzles in relation to the pressure and upstream temperature. A small series of such nozzles has been constructed. A double-entry nomogram is used for immediate estimation of the flow rate from the readings of the other instruments.

The experiments performed on this system up to now are in very good agreement with the results predicted by theory. In particular, flow rates of 5.5 kg/h of steam superheated to 450°C have been exceeded, and we can reasonably expect to attain, under normal operating conditions, 7 kg/h of steam at 450°C and 100-150 atm.

We have spoken several times of absorption temperatures close to those of the source, and it should surely be possible, in the case of the sun,

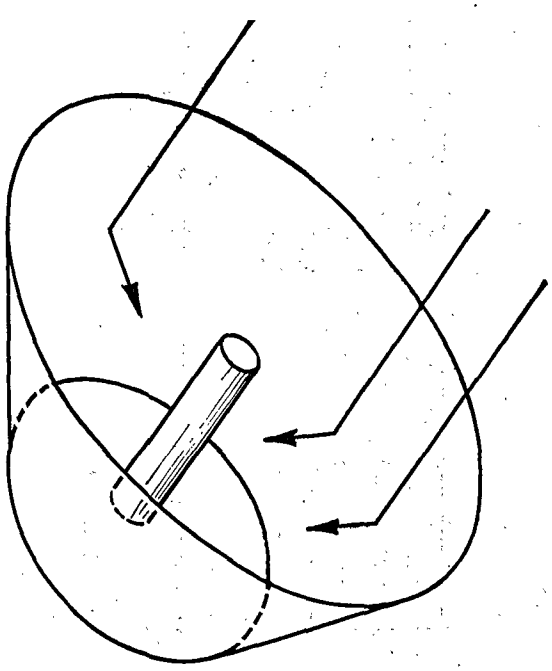


Figure 19

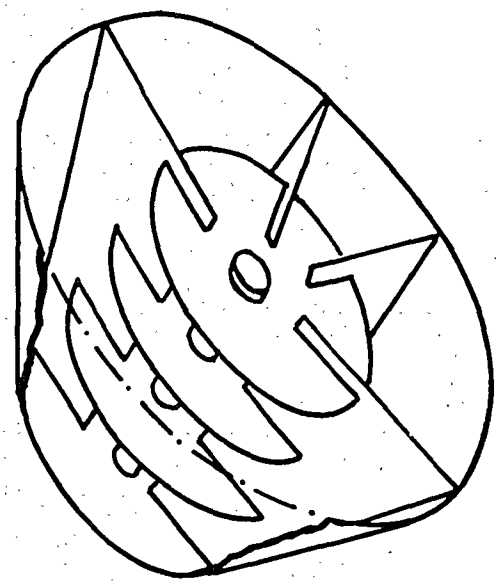


Figure 20

to attain temperatures of several thousand degrees with an absolute black body of the type described, without concentration of the rays. Such a result, which can only be obtained by a very sophisticated technique, would be of very little practical utility, however, on account of the low density of the solar energy. It will suffice if we mention the difficulties of insulating a large surface and the inevitable thermal inertia of that surface.

But if we turn again to the first schematic representation of the absolute black body shown in figure 2, we shall see that the parallel direction of the incoming rays is by no means a necessary condition for the realization of an absolute black body, since for this it is sufficient that the surface absorbing the rays shall be protected in such a way as to limit the solid angle of the entrant energy. This means that even in the case of energy concentrated by lenses or mirrors, the collector could be protected by surfaces limiting the solid angle of the energy reradiated by the collector itself.

In the case of lenses or parabolic mirrors, the advantage of such protection is rather slight, since in general the solid angle of the incoming energy is already very great. Concentrations of the energy up to a factor of 10 000 and more are normal in these cases. But there are other, more economic, means, giving energy concentrations as high as several hundred, sufficient as far as energy density is concerned, but insufficient to attain elevated temperatures without appropriate means of protection.

Let us consider a mirror in the shape of a frustum of a cone with a half-vertex angle of, say, 45°, and a cylindrical energy collector on its axis (figure 19). Energy that is concentrated, but has a solid angle insufficient to allow the attainment of elevated temperatures, arrives on the collector. In this case, a limiter of the angle of reradiation, with the properties already described, will be formed by black

surfaces, consisting of circles equal and parallel to the minor base of the frustum, as well as trapezoidal surfaces lying on planes passing through the axis of the frustum, as indicated by figure 20.

From the viewpoint of realization, it may be important to note that the limiter surfaces need not necessarily be continuous. They may, for instance, be formed of tungsten wires 10-50 microns in diameter, stretched on frames remote from the hot zones, in planes passing through the axis, and help by other tungsten wires in spider-web form on planes perpendicular to the axis. A minimal steam of inert gas might be sufficient to protect the structure.

A final application of the cellular structures we have described is worthy of brief mention. In a certain sense, these structures may be considered cold bodies with respect to the radiant energy. They may consequently be used as thermal insulators for very high temperatures, while still allowing direct view of the insulated body in a certain direction. Moreover, if they are made, for example, of tungsten wire, they may be characterized by an extremely low thermal mass.

Appendix

During the experiments, we found it necessary to provide other measuring equipment for Collector No. 4, described above.

Two other thermocouples, connected to a new millivolmeter calibrated in degrees and capable of measuring temperatures up to 800°C, were placed in contact with the front face of the plate. The temperature difference between the front and rear faces of the plate, and the temperature difference between the front face and the discharged steam were found to be far greater than expected. Under good operating conditions, they reached 100°C, but ran as high as 250°C when the steam pressure was too low.

Since the temperature on the front face could not be determined during the first experiments, temperatures far greater than those expected were reached. They were estimated at 720-750°C. The parts of aluminium and glass in contact were melted, and the black silicone varnish was partially destroyed.

To measure the hourly steam output with greater precision, a small heat exchanger was built, permit-

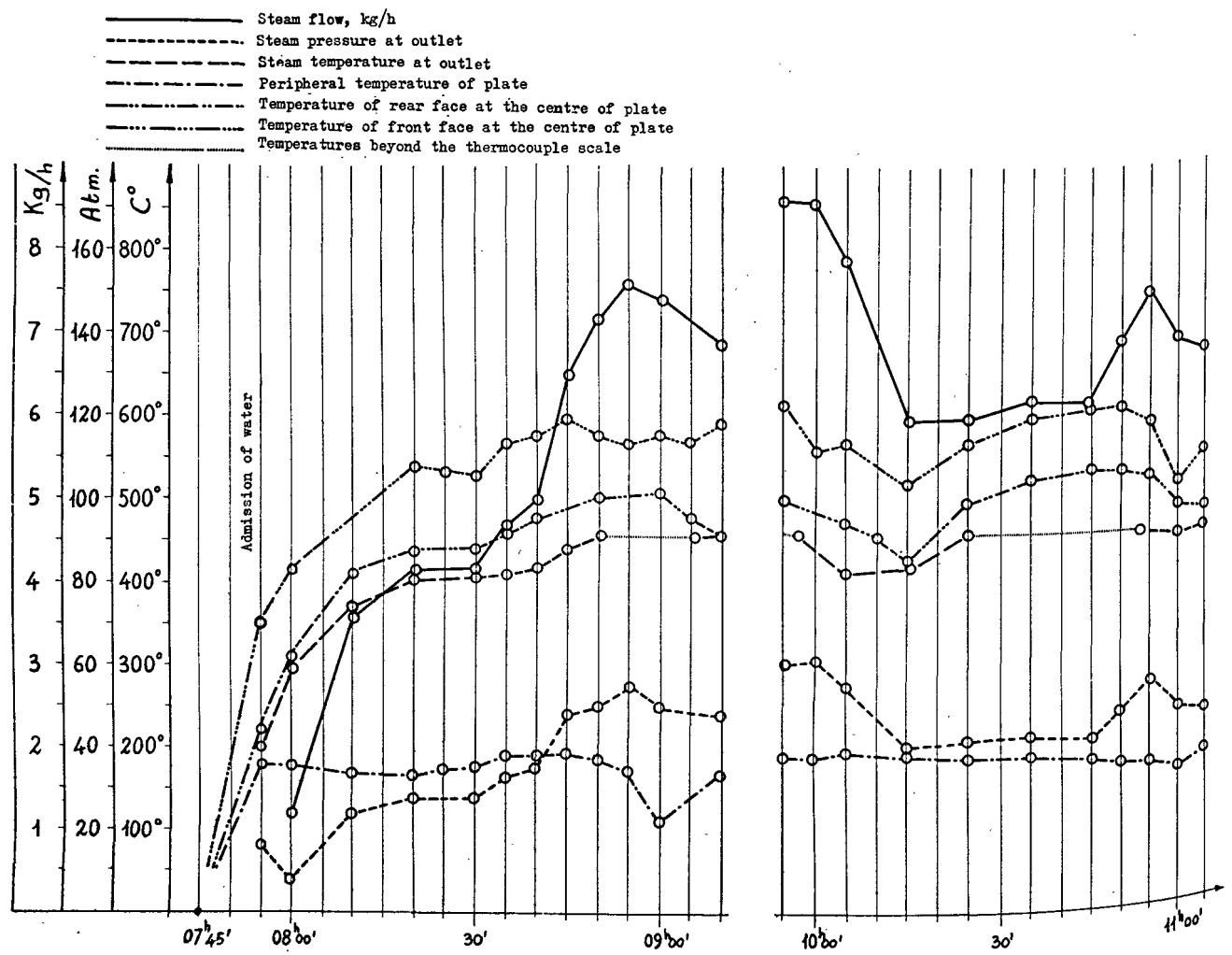


Figure 21

ting the condensation of the discharged steam and its recovery in the form of cold water. This heat exchanger consisted of a copper coil through which cooling water circulated, with another and smaller copper tube inside it. This smaller tube was connected at one end to the nozzle from which the superheated steam issued, and at the other to a graduated receiver to measure the water condensed. The entire assembly was well insulated with glass wool.

By this method, the theoretical flow rates of the nozzles were checked and found to be in perfect agreement. An easy, but also superfluous, check on the quantity of heat delivered was provided by measuring the quantity of cooling water and its temperature at discharge.

The results of the experiments so performed were clearly better than those of the earlier experiments. This is easy to explain if we note that, as was found later, the steam flow of 5.5 kg/h was obtained with damaged apparatus.

Figure 21 gives the new results. It will be seen that a flow of 7 kg/h with steam temperatures ranging from 450° to 500°C can be attained and maintained.

The difference of over 100°C between the temperatures of the front face of the plate and that of the steam being discharged is a confirmation of the high efficiency of the collector, but also indicates the low efficiency of the heat exchanger. This is due largely to the distribution of the radiant energy incident on the plate, which is unsuitable for operating pressures under 100 atm. Elimination of this shortcoming will improve the over-all efficiency.

The over-all efficiency of the apparatus under present conditions may be calculated to be 70 to 75 per cent for a steam temperature of 450° to 500°C.

The damage to the equipment still makes it impossible to repeat the high-pressure experiments for which the apparatus was originally developed. They will be resumed after new modifications have been made to the plate.

Summary

The principal obstacles to the industrial exploitation of solar energy are its low density and the insufficient temperature at which conventional collectors collect it. The author presents a new type of collector, perhaps economical enough for industrial production, and capable of operating at high efficiencies at temperatures of 400-500°C. Experiments in 1960 on three different collectors of this type, and the first results from a collector for a solar turbine engine, which was designed to supply 5-7 kg/h of superheated steam at 450°C and 150 atm., appear to confirm the theory.

Comparison between the small solid angle covered by the incoming radiation from the sun, which is 0.0000678 of the solid angle at which classic black bodies reradiate energy (2π), is one way of explaining the low absorption temperatures of such bodies.

Lenses and parabolic mirrors are the means most commonly used to increase the solid angle of the incoming rays; but their cost precludes their utilization on the industrial scale.

The solution proposed by the author is more economic, and may be schematically described as follows.

A frustum of a cone with its axis pointing in the direction of the sun and a vertex angle equal to the apparent diameter of the sun is placed in front of a classic black body; it does not limit the incoming energy.

On the other hand, provided its walls are black and insulated, the frustum does limit the reradiated energy. The analytic development demonstrates that, under extreme conditions, at the limit, the reradiated energy is reduced to that contained in the solid angle occupied by the incoming energy.

In other words, it may be stated that, at the limit, such a reradiated-energy limiter compels energy to pass through the same flux tube as the incoming energy did. The source and the collector are thus connected in such a way that thermodynamic equilibrium is established at equal temperatures; at collector temperatures lower than those of the source, the collector absorbs energy at an efficiency that increases very rapidly with decreasing collector temperature.

In view of the small solid angle of the radiant energy from the sun, the collector schematically described above may be realized by a black-walled cylinder. When a large number of such cylinders are assembled into a beehive structure, the condition that the walls be insulated is no longer necessary, since the temperature distributions of two adjacent cylinders may be considered the same. This structure will here be termed absolute black body, because of its quality, at the limit, of absorbing all the incoming radiation without reradiating it in a direction different from that of the source.

The analytic study of the temperature distribution at various points of the surfaces of the beehive structure described shows that, in very good approximation, the temperature decreases as the fourth root of the distance between the point and the mouth.

Quantitatively, for tubes with a length-diameter ratio of 15-20, the reduction in the reradiated energy is approximately 96-98 per cent of the energy that would be emitted in the absence of such protection.

Temperatures of 400-500°C are today considered very good for converting thermal energy into mechanical energy in the steam engine. On the other hand,

temperatures even lower than that permit the accumulation of thermal energy with systems which, on an immense scale, might even be highly economic. For instance, a cubic hectometre of soil of low water content might be considered an energy accumulator available entirely without charge, except for the cost of installing a heat exchanger inside it, for calculation demonstrates that such a thermal mass would require no insulator other than that provided by the soil itself, or by the surrounding rock.

In comparison with solar temperatures, however, 400-500°C are so low as to suggest the use of selectively transparent surfaces.

A beehive structure of material transparent to the solar energy but "black" with respect to the energy radiated at 400-500°C, would, outside this latter temperature range, have the same effectiveness as what we have termed an absolute black body, without necessarily having to be pointed towards the source.

One might also study systems that can be easily and economically realized (though not on a small scale) for concentrating radiant solar energy, by a factor of 10 to 15, on such a collector, using mirrors made of aluminium foil. In this system, 9/10 to 14/15 of the collector surface, together with the heat exchanger and insulation complementing it, are replaced by aluminium foil, with an obvious economic advantage. Although the author's studies are not yet ready for publication, they do make it seem possible to use this method to render solar energy competitive with the energy now derived from other sources.

A brief description of the experimental verifications already obtained will give an idea of the possible industrial development of what has just been said.

One of these devices consisted of a structure of about 10 000 almost hexagonal adjacent prisms, 8 mm in diameter and 120 mm high, built out of sheets of cellulose carbonized by a special method. This structure was placed in front of a thin plate of blackened copper with about 26 m of spiral tubing, suitably insulated, placed on its rear. This collector/heat exchanger, with a total surface of 0.50 m², when pointed towards the sun, supplied under standard operating conditions 0.1 g/s of steam superheated to about 230°C at 2 atm., with a maximum of 0.085 g/s at 320°C. This was equivalent to a yield hardly over 50 per cent, and thus distinctly lower than the theoretical yield. This difference is explained by certain imperfections in the construction of so complex a structure.

Another device consisted of an assembly of about 150 glass tubes 14-15 mm in diameter, 250 mm long, and 0.2-0.3 mm thick, protected by a cylinder with a mirror surface, placed in front of a black plate and suitably insulated. This was the first beehive structure made of material having a selective transparency. No heat exchanger was provided, and the heat was allowed to leave by conduction through the walls, which were inadequately insulated on account of the small dimensions. An aluminium cone in front of the collector concentrated the incoming energy at a theoretical factor of about 6. The plate attained a maximum temperature of 520°C, and the red color produced in the central zone could be photographed.

The high yields of these collectors made their application to existing steam engines possible, instead of the reverse situation. Thus a device able to furnish 5-7 kg/h of steam superheated to 400-500°C at 100-150 atm. was designed and constructed. It consists of a beehive collector of selective transparency type, formed by about 2 000 small glass tubes, placed on a plate suitably prepared and varnished black, so as to absorb almost all the incident radiation. On this collector, with a surface of about 0.50 m², the radiant energy from conical aluminium mirrors is concentrated in the geometrical ratio of 16:1. The device, mounted on a sturdy support, provided with the requisite positioning levers, is installed on a small truck and can be easily moved after disassembly of the bulkiest parts. The results can be read directly on an instrument board with thermoelectric thermometers, pressure gauges, etc.

During the first experiments, a flow rate of 5.5 kg/h of superheated steam at 450°C was measured. Under normal operating conditions we may reasonably expect 7 kg/h of superheated steam at 450°C and 100-150 atm.

The cellular structure of the absolute black body may have numerous other applications. As an example, the paper describes a solar furnace for temperatures of the order of 3 000°C, consisting of a cone-frustum mirror concentrating the energy on a cylinder placed on its axis and protected by a cellular structure formed, not by a continuous surface, but by tungsten wires 10-15 microns in diameter, stretched on frames, and remote from the hot portions.

In a different area of application, the property of the cellular structure described has the properties of being cold as well as transparent in one direction. These properties may be usefully applied, under particular conditions, for heat insulators of negligible thermal mass at very high temperatures.

THE SPECTRUM OF MATERIALS AVAILABLE FOR THE UTILIZATION AND CONTROL OF SOLAR ENERGY

Roger E. Gaumer *

The connection between the thermal control of spacecraft and practical systems for solar energy utilization is, perhaps, not obvious. A brief review of the fundamental aspects of these two research areas should suffice to indicate the pronounced similarities which exist. The fundamental physical theory, heat transfer and energy conversion parameters, practical design methods, and optimum materials for thermal control will be found to be virtually identical. The task of designing a satellite surface so that it will maintain an average equilibrium temperature of 20°C in orbit is remarkably similar to that of designing a solar collecting surface to be used in conjunction with a solar still.

There are three sources of radiant energy incident upon a spacecraft. These are direct solar radiation (insolation), solar radiation reflected from a planetary atmosphere (albedo), and direct thermal radiation from nearby planets (earthshine, etc.). Insolation is the predominant energy source for contemporary satellite vehicles. Similarly, insolation is the predominant source of energy for the solar energy conversion apparatus in use today. The only significant difference between terrestrial and extra-terrestrial insolation is that nearly all of the ultraviolet component of the solar energy has been absorbed by the earth's atmosphere prior to reaching the ground. Calculated values for the solar absorptance of various materials show only very slight differences for terrestrial or extra-terrestrial solar spectra (1).

The physical mechanisms by which a material absorbs and radiates electromagnetic energy are common to all surfaces, regardless of the relative position of the surface in space. The law of conservation of energy is fundamental to the development of specialized equations, whether for a satellite solar array or for an industrial solar furnace. The absorption of solar energy by a surface is controlled by the physical condition of the surface and by the optical characteristics of the material. Emission of radiant energy from a surface is similarly controlled.

Spacecraft thermal control is accomplished almost entirely by radiative heat transfer methods. Terrestrial solar energy devices must also consider heat transfer by convective and conductive energy losses in detail, for two reasons. The first reason is that the bulk of the information to be presented has been obtained under simulated space conditions. Secondly, this report is concerned with *materials*, and convective losses from a system are not materials dependent — they are *device* dependent. The thermal conductivity of a material becomes another significant thermophysical property, along with solar absorptance and infrared emittance, for practical solar energy conversion apparatus.

The physical environment for a satellite thermal control surface is much more severe than that for terrestrial devices. In addition to all the terrestrial environmental phenomena, a spacecraft material is exposed to different environmental phenomena while exiting from and re-entering the atmosphere of the earth and is also exposed to the orbital space environment. Operating lifetimes of contemporary spacecraft approximate the anticipated operating period for solar energy conversion apparatus on earth. A partial list of the environmental constituents for a satellite thermal control surface is given below.

Temperatures of 500°C during exit from earth-atmosphere
Aerodynamic shear forces resulting from viscous drag
Amplified oxidation potential during exit
Severe lateral and longitudinal vibratory forces
Extreme high vacuum (10^{-12} mm Hg)
Temperature cycling between, perhaps, 300°C and — 50°C
Exposure to ultraviolet radiation
Sputtering by neutral and charged particles
Micrometeorite erosion
Van Allen belt constituent irradiation
Magnetic storms, solar flares, meteor collisions, etc.
Temperatures up to 1 000°C during re-entry
Very severe aerodynamic shear during re-entry.

A comprehensive discussion of the nature of the environment for materials employed in the radiative thermal control of spacecraft has been given in a brochure of the Defense Metal Information Center (2). A critical assesment of the practical effects of the environment on materials for radiative control has been published by the author (3, 4).

Clearly, if a material will withstand the rigors of the space environment, it should be admirably suited for use in terrestrial solar energy conversion and utilization apparatus. The practical demands of the satellite industry have resulted in a very considerable emphasis upon the development of

* Lockheed Missiles and Space Division, Lockheed Aircraft Corporation, Sunnyvale, California.

new materials for radiative thermal control, which are stable, reliable, durable and reasonably economical. It seems probable that much of the information will be of equal value to the designers of practical terrestrial equipment for solar energy utilization.

The successful operation of any device whose purpose is the practical utilization of solar energy is primarily dependent upon the following two radiation characteristics of material:

(*a*) Solar absorptance, *a*: This is the percentage of radiant energy of solar origin which is absorbed by the surface.

(*b*) Infrared emittance, *e*: This is the percentage of radiant energy emitted by a real surface as compared to the radiant energy emitted by a black body at the same temperature.

The ratio of solar absorptance to infrared emittance — the so-called alpha-over-epsilon ratio — will be shown to be an extremely significant physical materials parameter. This ratio provides an index for the relative amount of energy retained by a surface which is exposed to solar energy, and thus the alpha-over-epsilon ratio is useful in predicting the ultimate equilibrium temperature to which a surface exposed to solar radiation will rise.

Mathematical analysis and the dictates of common sense both lead to the conclusion that the solar absorptance, *a*, is the most important physical characteristic for a material to be used in any device whose function is the utilization of solar energy. For a solar collector of any type, *a* should be as near unity as possible. Materials to be used for the mirror systems of a solar concentrator should have *a* as nearly zero as possible; for an opaque surface the sum of the reflectance and the absorptance must be unity, hence maximum reflectance necessitates minimum absorptance.

The infrared emittance *e* is an important parameter in determining the energy losses by radiation from a solar collector and also in determining the effectiveness with which the boiler of a solar concentrator will absorb incident radiant energy. Kirchoff's law dictates that the emittance of a surface equals its absorptance *when it is in thermal equilibrium with its surroundings:* adequate definition of the radiation characteristics is dependent on an understanding of the spectral distribution of the absorbed and radiated energy. Complete and detailed analyses of optimization or radiation parameters for the various solar energy utilization systems have been performed recently by Edwards *et al.* (5). The conclusion of all investigators has been that the determination of *a*, *e*, and *a/e* is a vital step in assessing the applicability of any material to a solar energy conversion apparatus. In practice it is necessary to determine all these quantities experimentally; existing theory can be used to calculate the radiation parameters of hypothetical substances with hypothetical surfaces; existing theory can be employed to correlate experimental results; but the theory, at present, is not adequate to consider the effect of surface condition upon the radiation characteristics of real materials.

There are basically two different methods by which *a*, *e*, and *a/e* can be determined experimentally. These two methods are the calorimetric determination of emittance and absorptance, and the calculation of the radiation parameters from experimental determinations of reflectance.

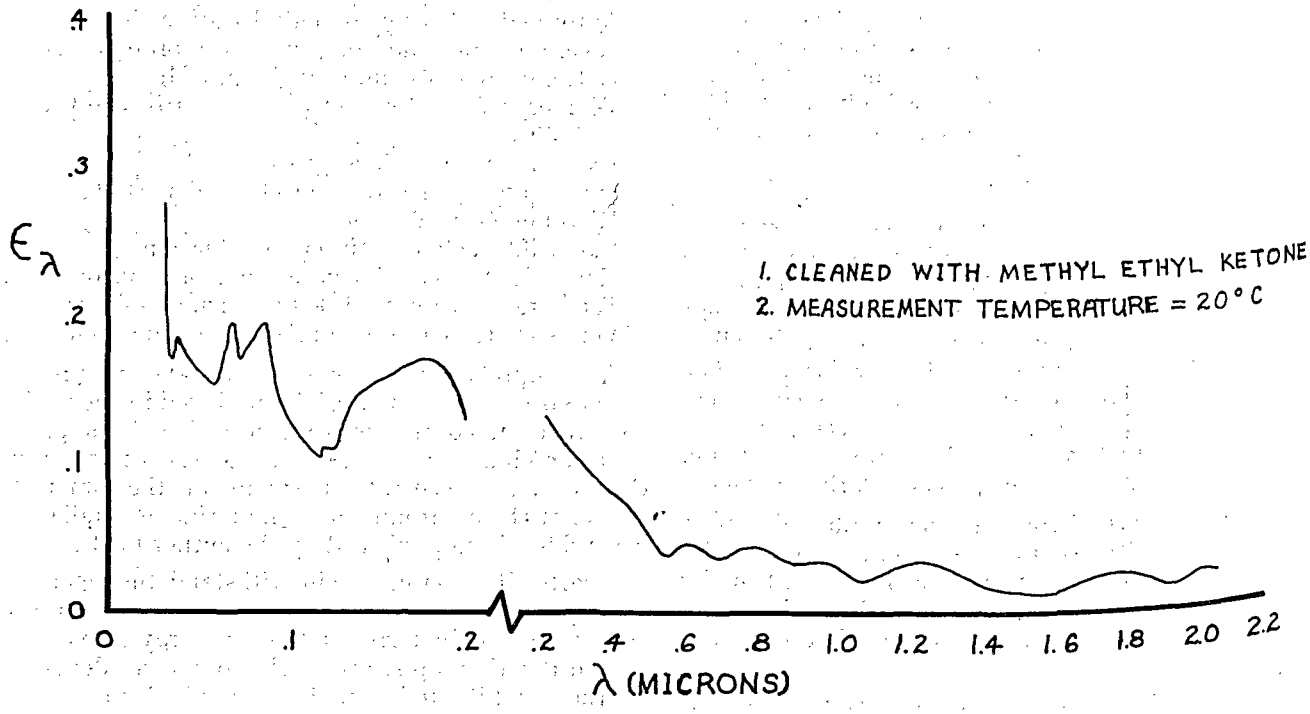


Figure 1. Spectral emittance of aluminum foil

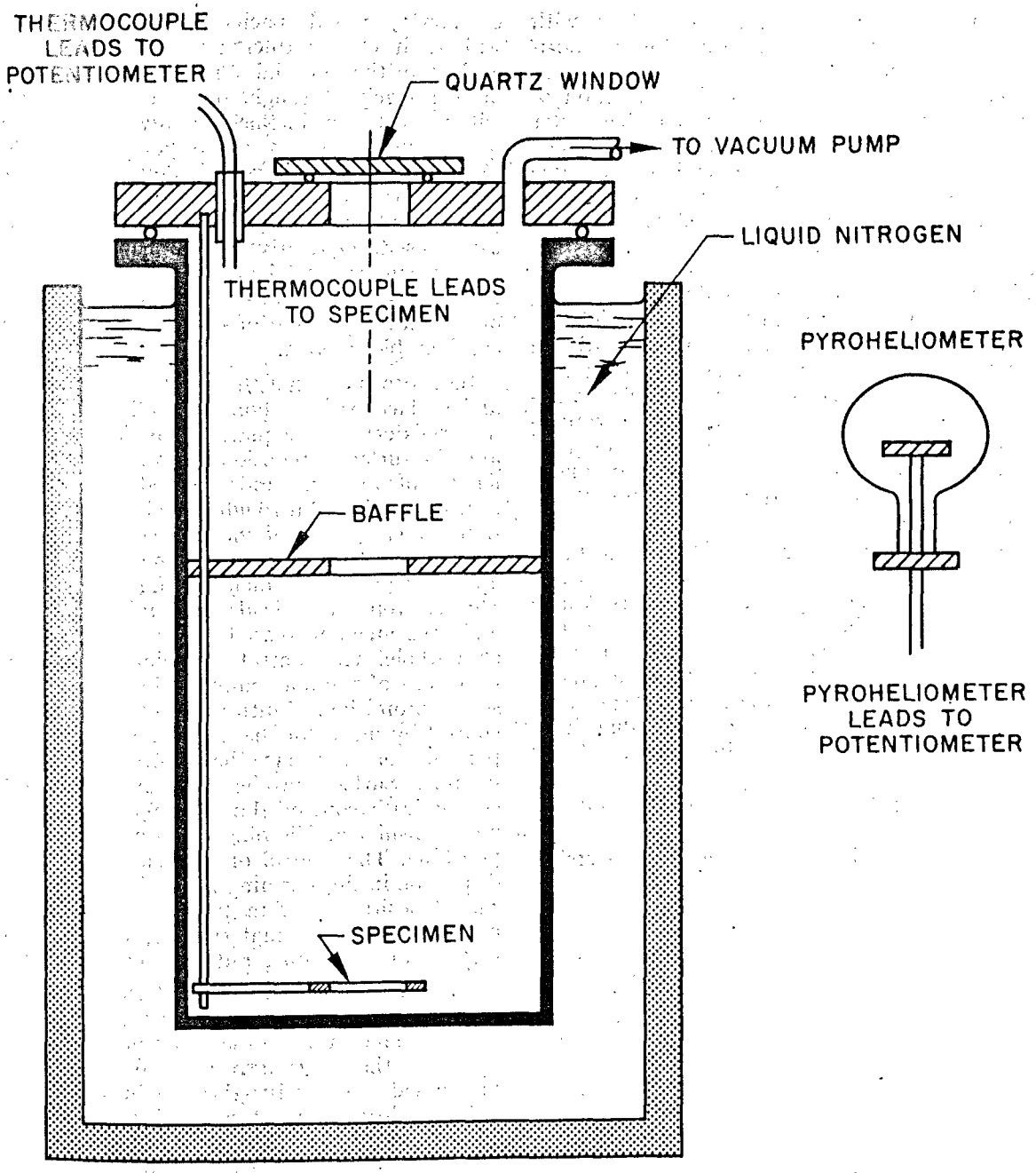


Figure 2. Schematic of apparatus for direct measurement of α_s/ε ratio

Reflectance determinations are the most common, and are particularly useful in providing information as to the spectral nature of the radiation characteristics. A typical plot of reflectance data is given in figure 1. These data, for polished aluminium foil, clearly indicate the different behavior of the radiation characteristics in the solar radiation region (0.2-2.0 microns) and in the 50°C emission region (5.0-25.0 microns). Values of absorptance and emittance are determined from reflectance data by multiplicative integration of the spectral absorption curves and the black body radiation curve for the appropriate temperature. To determine solar absorptance from reflectance data one must know the terrestrial solar spectral distribution curve with adequate precision. The absolute accuracy of radiative characteristics is frequently inadequate; since such determinations involve the subtraction of the reflectance from unity in order to determine emittance, large errors are associated with low emittances.

Calorimetric determinations of a, e, and a/e are based on the fundamental laws of thermodynamics. If a body is absorbing solar energy and emitting radiant energy characteristics of its temperature, the final equilibrium temperature of the body is directly proportional to the ratio a/e. If the source of solar energy is removed, the temperature of the body will approach that of its surroundings at a rate

determined by its emittance, in accordance with the Stefan-Boltzmann law. Figure 2 shows a calorimetric device which is operative at the Lockheed thermophysics laboratory for the determination of the radiation characteristics of materials. The solar energy source can be the sun, a heliostat solar image, or any one of a variety of commercially available solar simulators. Incident radiant intensity is measured with a pyrheliometer. Convective losses are eliminated by the vacuum chamber, and conductive losses minimized by mechanical design. Chamber walls are maintained at the temperature of liquid nitrogen, thereby making radiation from the walls a negligible source of error. Walls are blackened with the platinum black process so that nearly all energy emanating from the sample is absorbed by the walls. The radiative parameters *a*, *e* and *a/e* may be determined for a material in approximately 30 minutes. Adequate engineering accuracy of 5 per cent is easily maintained. A plot of *a/e* versus equilibrium temperature is given in figure 3.

Research projects in progress use both reflectance and calorimetric techniques, to provide a better understanding of the physical parameters which affect the radiative behavior of materials. Parameters which are being investigated include the effect of angle of incidence, the effect of surface roughness, and the relationship of *a* and *e* to the optical constants of materials. Certain conclusions of value have already been drawn from these investigations, and are stated here.

The radiative behavior of materials is entirely characterized by a very thin layer of the exposed surface. For a material which is a good electrical conductor, optical opacity from 0.2 to 25.0 microns will result from a thickness of a few millionths of an inch of the material, and for a dielectric material optical opacity throughout the same spectral range will necessitate a thickness of only a few thousandths of an inch. This is an important consideration for the designers of terrestrial devices for solar energy utilization; it means that very thin coatings or foils can be used for radiative control. Since thin coatings can be used, the relative cost of the material becomes fairly unimportant. The price per pound of a material is not important; considerations such as the cost of vacuum deposition of thin metal foils become of considerable interest.

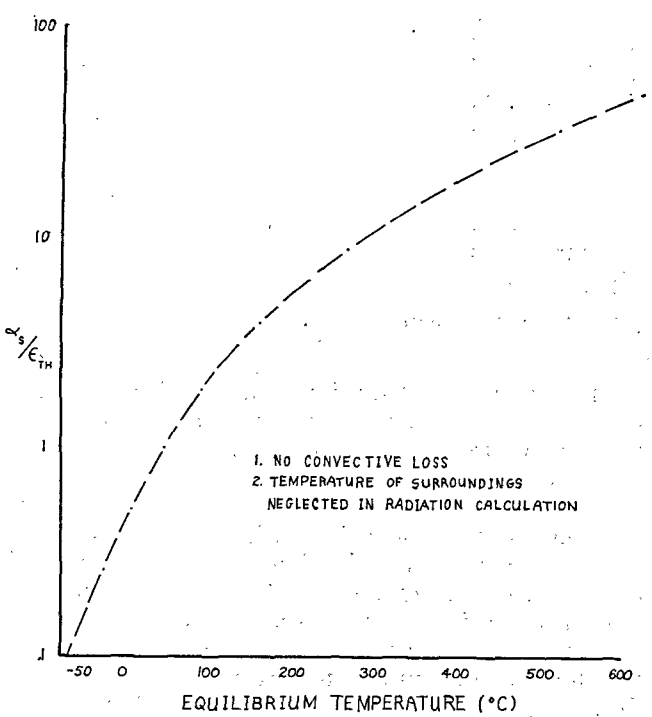


Figure 3. Temperature of flat plate solar collector *vs.* α_S/ϵ_{TH}

Indications are that the effect of surface roughness and surface profile upon the radiative behavior of materials can be adequately explained if one evaluates the surface dimensions with respect to the wave length of incident and emitted radiation. While a surface will appear rough to incident solar radiation if the micro-profile of the surface is of the order of one micron (40 micron-inch) the same surface will appear smooth to incident for infrared energy. Surface roughness leads to multiple reflectances and consequent increased absorption for the surface as a whole. The control of radiative characteristics by means of suitable manipulation of surface profile seems promising. Emittance and solar absorptance control by means of the deposition of finely divided particles on a surface have already been proven feasible. Surface profile may be practically and economically controlled by such techniques as mechanical polishing and lapping, chem-milling, and electropolishing. The control of pigment particle size and dispersion in film-forming paints is another example. The deposition of thin transparent or translucent coatings on the base material is still another practical method of controlling radiative characteristics.

Table 1 contains a list of materials which may be of interest to designers of solar energy utilization devices. The values of solar absorptance tabulated refer to the extra-terrestrial solar spectrum. As mentioned previously, these values usually differ only slightly from terrestrial values. Emittance values listed refer to total hemispherical emittance at 4°C. For solar collector applications a desirable material should possess high solar absorptance, low emittance at equilibrium temperature, high thermal conductivity, etc. Solar concentrators, boilers, and radiators each require a specific set of optimum thermophysical properties. Optimum choice of material for a specific application is usually dependent upon cost, durability, and structural characteristics as well as material thermophysical properties.

It would appear that metallic foils may be strongly recommended for many practical applications. The metallic foils possess all the attributes previously listed and, additionally, are relatively inexpensive and easily bonded to structural frameworks. Aluminum foil is an inexpensive, commercially available material, and usually possesses an *a/e* ratio of about

Table 1. Radiation characteristics of materials

Material and surface condition			
Aluminum: polished and degreased	0.387	0.027	14.35
Gold plated on stainless steel: polished	0.301	0.028	10.77
Gold over titanium with resin undercoat: polished	0.300	0.033	9.10
Gold vacuum deposited on MIL-A-148 slick annealed aluminum foil: polished	0.282	0.034	8.29
Aluminum foil, dull side: crinkle and then smoothed	0.223	0.030	7.43
Beryllium: chemically and mechanically polished	0.444	0.063	7.04
Aluminum foil: cleaned with MEK and alcohol	0.218	0.032	6.81
Vacuum deposited gold on silicone resin base: polished	0.344	0.051	6.75
Aluminum foil tape: as received	0.238	0.043	5.54
Aluminum foil, shiny side: smooth	0.192	0.036	5.33
Inconel X foil: chemically polished	0.624	0.143	4.36
Aluminum: alchemized mill finish	0.218	0.051	4.28
Molybdenum slug: polished	0.480	0.122	3.94
Chrome — aluminized mylar film: as received	0.247	0.085	2.90
Four coats of aquadag on copper: clean	0.782	0.490	1.60
Carbon black pigment K silicate on Dow 17 on magnesium: clean	0.908	0.780	1.16
5 mils of Rokide C (Norton Abrasives Co.) on Rene' 41	0.898	0.789	1.14
Dull black micobond on bare magnesium, thick wet coats: clean	0.936	0.844	1.11
Flame sprayed aluminum oxide on aluminum: mil thickness, clean	0.422	0.765	0.55
Magnesium coated with 5 units of silica: clean	0.349	0.825	0.42
Barium titanate pigmented silicone on Dow 17 on magnesium: clean	0.341	0.836	0.41
Zicron pigmented K silicate on Dow 17 on magnesium: clean	0.195	0.830	0.23
Sodium silicate D and wollastonite: clean	0.141	0.841	0.17

8-10. Precious metal foils are also useful, available, and practical. Foil materials of the refractory metals are becoming available. Titanium, tantalum, and beryllium foils are all being produced in limited quantities. Radiation data for these foil-type refractory materials will be reported soon. Foils of the new, high-nickel-content superalloys are also available, but their atmospheric durability is limited. The use of foils for solar energy purposes is predicated upon the availability of a suitable high-temperature adhesive material with which to bond the foil to the substrate. Research in high-temperature adhesives is progressing. Inorganic adhesive materials of a sodium silicate + aluminium acid phosphate type have exhibited thermal stability up to 500°C. It would seem perfectly possible to use any of the foils listed in table 1 to achieve adequate control of solar energy devices.

For certain purposes, materials with very low a/e ratios are of interest. For example, it is possible, at least in principle, to construct a Carnot engine operating between the highest obtainable temperature (a/e), and the lowest obtainable temperature (a/e). One practical application for low a/e coatings is for tanks used for storage of fluids at reasonably low temperatures.

Many white paints have $a/e = 0.3/0.9 = 0.33$. The relatively high solar reflectance of 70 per cent is achieved by means of pigmentation with a material of characteristically high index of refraction. Still lower ratios of a/e, together with solar reflectances of about 95 per cent, are exhibited by second surface mirrors. The mirror materials investigated have been sapphire, fused silica, and various commercial glasses. Gold, silver, and aluminum opaque coatings are suitable for use in coating the second surface mirrors.

Metallized transparent plastic sheet materials have recently become commercially available. Aluminized mylar is probably the best known of these materials; this product is available in thicknesses of .0005" to .010" and the cost is a few cents per square foot.

The search for a material which varies its a/e ratio as a function of temperature in such a fashion as to maintain an approximately constant temperature even with varying incident flux has led to extensive consideration of the radiative behavior of the rare earth elements. The radiative characteristics of the rare earth metallic element gadolinium is such as to make this metal appear to have distinct promise for use in solar collectors. Measurements of gadolinium indicate an $a = 0.7\text{-}0.8$, nearly twice the solar absorptance of any other metal. This solar absorptance of 0.7-0.8 was for a very highly polished surface; most highly polished metals have solar absorptances of about 0.3. Preliminary measurements

and a calculation based on the Hagen-Rubens relation indicate a room temperature total hemispherical emittance of 0.1. Since the solar absorptance of gadolinium is twice that of other metals, the efficiency of a solar collector made of gadolinium vacuum-deposited on a structural framework would appear to be quite satisfactory. The cost of gadolinium is about $400 per pound, or 25 cents per square foot if a thickness of 10^{-5} inches is assumed. The cost of vacuum deposition is, of course, a factor.

The question of stability, durability, and reproductibility of materials used for solar energy control and conversion apparatus is of primary importance. It would be absurd to make a solar collecting device of copper, even though copper has initially satisfactory properties, owing to the fact that copper is known to oxidize progressively and hence degenerate to a lower solar absorptance as a function of time. Considerations available from the field of solid state physics indicate that there are certain of the metallic elements which form so-called stable oxide coatings. All of the metallic elements oxidize to a greater or lesser degree. Some materials, however, notably aluminum and beryllium, form very thin (approximately equal to 50 Ångströms) coatings of a stable surface material. Furthermore, this thin oxide coating does not significantly affect the radiative properties of the basic material. In broad outline, the conclusions of the research program are that the two most suitable metallic elements are aluminum and beryllium. Data on aluminum have been presented in this paper, and some data on bulk beryllium have also been included. By carefully controlling the surface condition of aluminum foil and beryllium foil, it is possible to achieve a/e ratios of 10. By comparison with figure 3, this will yield an equilibrium temperature for a solar collector of 250°C in a vacuum.

In addition to the effects of atmospheric oxidation, it is also necessary to consider corrosion and tarnishing of some of the metallic materials. None of the elements is free from these effects. However, the so-called superalloys are particularly poor as to their environmental resistance. Such alloys as Rene' 41, Haynes Stellite, and Inconel X, to name but a few, should immediately be eliminated on the basis that they will not stand up under more than one year's practical application. In general, the metallic elements characterized by very high melting temperatures may be considered the most stable at ordinary temperatures of operation. This consideration immediately leads to the refractory metals: titanium, tantalum, beryllium, etc. Some of the other practical aspects that need to be considered are the effects of (*a*) salt spray; (*b*) dust and dirt; (*c*) fingerprint tarnishing; (*d*) ease of cleaning; and (*e*) stability under thermal cycling.

An analysis of all the necessary practical attributes for the optimum solar collector or solar concentrator surface material indicates that, so far as the radiative characteristics are concerned, nearly all metals have rather similar characteristics. Therefore, one should select for the high solar absorptance material one which forms a stable oxide; one which does not continue to oxidize; one which is resistant to corrosion and to atmospheric environmental effects; one which does not tarnish with fingerprints; and one which is easily cleaned. Again, the material which continually suggests itself from every point of view is aluminum, with the possible addition of beryllium as the foil becomes available. The present price of beryllium foil is in dollars per square foot but the price is steadily decreasing.

If paint-type materials are to be utilized, perhaps for low temperature work, the question of ultraviolet stability inevitably arises. The effect of the ultraviolet constituent of even terrestrial solar radiation is known to be very severe, and it is this which causes the "yellowing" of paints. Research efforts have led to the development of inorganic paints of a sodium silicate vehicle plus various refractory oxide pigments. Perhaps the most effective of these pigments is zirconium oxide, which has exhibited relative stability to one year's continuous exposure to extra-terrestrial solar radiation. The a/e value for this paint is 0.25. Such an inorganic paint should be stable for 15 to 20 years of ordinary terrestrial application. As a matter of fact, the paint should be eminently suitable for painting dwellings. Stability of paint-type coatings, particularly spectrally flat absorbers used on boilers, needs to be carefully examined under conditions of repetitive thermal cycling.

Certain practical applications for the materials mentioned in this paper have been commented upon previously. The most obvious applications of high a/e, high a materials are to solar collectors. Metal foils bonded to an inexpensive framework immediately suggest themselves.

Aluminum foil deposited on Mylar or on some other thin, flexible, inexpensive plastic material could be used to construct a solar still which folds like an umbrella, which can be packed away in a small area, and which is light and inexpensive. If set up on four stakes, so that the two loci of suspension are catenaries, an adequate focusing effect for the concentration of solar energy could be realized. Elemental calculations indicate that such a device 3 feet in diameter would achieve a concentrating factor of 2 and would be sufficient to distill about 2 pints of water per hour.

Coatings which have been developed to control the equilibrium temperature of solar cells selectively reflect all the solar energy other than that which is known to be effective in the actual energy conversion mechanism within the solar cells. It is now possible to apply a coating which reflects nearly all the energy between any two wave lengths λ_1 and λ_2 while absorbing outside the range. The emittance of the material is left unchanged because the coating is extremely thin. It is thus possible to control the amount of energy of a certain spectral nature which is absorbed by a material by means of the applica-

tion of a very thin film. Within the last five years, coating techniques have been so extensively developed that it is possible to absorb or reflect selectively nearly any band wave of desirable length; these techniques are relatively inexpensive for single films.

Another practical application for new materials is to solar furnaces. Materials for solar furnaces must have characteristics which differ slightly from those previously discussed. One necessary property is the ability to withstand temperatures of 1 000° to 2 000°C. This, of course, leads to intensive research in the refractory metals area. Aluminum is an optimum choice for solar furnaces up to 200° to 300°C. From there to 700°C, beryllium is an optimum choice. However, at 700°C, beryllium begins to oxidize, and at about this temperature one must use tantalum, titanium, or molybdenum. Data on the refractory metals have been presented in this paper. Molybdenum has a reasonably high thermal conductivity, is quite durable to a temperature of 2 000°C, and is available in electro-deposited coating form.

Various components and devices for solar energy utilization frequently require a coating which has a very high absorptance at elevated temperatures. A few materials have been developed which have broad, high absorptance throughout the entire spectral range from 0.2 to 40 microns. A process called platinum black, which results in leaving platinum metal deposited in very intimately dispersed form on a metallic substrate, is particularly promising. Its value of alpha and epsilon are $a = .95$ and $e_{20°C} = .91$ This material has elevated temperature stability to 900°C, at least, and quite possibly to temperatures in excess of this.

Solar collecting mirrors could be made of sapphire. One of the practical limitations in mirror-type solar concentrators is the temperature of the mirrors. Sapphire is a highly transparent material and optically quite satisfactory for use in collectors. Sapphire, however, has a thermal conductance nearly two orders of magnitude higher than ordinary transparent materials. This, in turn, means that differential thermal expansion and problems of thermal cycling and consequent mirror breakage will be minimized if sapphire-type materials are utilized. The cost of sapphire is not so prohibitive as might be expected. Synthetic sapphire is now commonly made, but the cost is still quite high for quantities of more than one square foot. Investigations indicate that the optimum materials for coating sapphire mirrors are aluminum and silver. Copper can then be electroformed onto the aluminum, and the composite structure may be soldered to a suitable framework.

Some work has been done on metal mirrors. Mirrors have been made of polished beryllium and polished aluminum. Such mirrors should be satisfactory, except that they cannot be ground to as fine a finish as ordinary optical materials, and there is consequent loss of focusing power. For many purposes, however, they are satisfactory, and they do not suffer from any of the mechanical or thermal shortcomings of conventional transparent mirrors.

Intensive research is being conducted in a quest for devices and chemical methods for the conversion of solar energy directly into useable electrical power. The satellite industry uses an enormous number of solar cells for satellite power acquisition. The solar cells are, at this time, standard silicon solar cells. Research is being conducted into solar cells of the cadmium sulfide and gallium arsenide types. Solar cell temperature control is achieved by transparent cover plates, reflective coatings, and controlled emittance from the back face of the cells. Developments in this area may well lead to devices which have significant practical potential for terrestrial conversion of solar energy.

References

1. Olson, O. H. and Morris, J. C., *Determination of Emissivity and Reflectivity Data on Aircraft Structural Materials,* WADC TR 56-222, part II, supplement I, *ASTIA Document No. 202494,* Armour Research Foundation, Published by Wright Air Development Center, Wright-Patterson AF Base, Ohio, October 1958.
2. Allen, J. M., *Environmental Factors Influencing Metals Applications in Space Vehicles, DMIC Report 142,* December 28, 1960.
3. Gaumer, R. E., *Determination of the Effects of Satellite Environment on the Thermal Radiation Characteristics of Surfaces,* SAE National Aeronautic Meeting, New York, *Publ. 339C,* 1961.
4. Gaumer, R. E. and McKellar, L. A., *Thermal Radiative Control Surfaces for Spacecraft, LMSD 704014,* April 1961.
5. Edwards, G. K., Nelson, K. E., Roddick, R. D. and Gier, J. T., *Basic Studies on the Use and Control of Solar Energy,* Department of Engineering, University of California, Los Angeles 24, California, *Report 60-93,* October 1960.

Summary

Basic similarities between the design of spacecraft thermal control surfaces and practical devices for the control and utilization of solar energy are discussed in this paper. The spectral ranges of available radiant energy are reviewed, and the physical principles controlling radiant energy emission and absorption are outlined. It is noted that the total environment for spacecraft materials is very severe. Space environmental constituents are listed and discussed. Since spacecraft environment is quite

severe, any materials employed in the thermal control of spacecraft should be stable for use in terrestrial devices.

The importance of solar absorptance *a*, infrared emittance *e*, and the ratio *a/e* are established, with *a* being the most significant material parameter. The necessity for experimental determination of *a*, *e*, and *a/e* is proven, and the two common methods of such experimental determinations are treated in detail. A comprehensive description of a calorimetric device developed for experimental measurement of radiative characteristics of materials is given, together with a discussion of apparatus shortcomings and assets. Research programs aimed at providing a better understanding of radiation phenomena of basic materials are described, and the principal results to date are stated. Results of particular import to designers of terrestrial solar energy apparatus are given; some results are minimum material thickness for opacity, the effects of surface roughening on *a* and *e*, radiative control by thin film deposition, and effect of angle of incidence.

A lengthy list of useful materials with composition of materials, surface condition, and radiation parameters is included. Values of *a/e* range from 15 to 0.25. Optimum radiation characteristics for collectors, concentrators, boilers, and radiators are discussed generally, and specific recommendations are made. Metallic foils of many types are described, and practical application procedures are considered. New materials for use in concentrators and solar furnaces are mentioned, with emphasis on durability and economics. Practical uses for metalized plastic sheets are conjectured. Gadolinium metal is pointed out to be very promising as a material for solar collector use.

Optimum choices of materials for use in terrestrial systems are described, with a view to system stability, durability, and ease of maintenance. Questions of oxidation, corrosion, tarnishing and similar materials degradation mechanisms are considered. The effects of ultraviolet radiation and thermal cycling are discussed with reference to probable damage of certain systems of materials.

A few practical applications to terrestrial systems for new materials developed by research in satellite thermal control are given. Included are a solar still of metalized mylar, a high thermal conductance solar concentrator, and metal mirror systems. Developments in the temperature control of solar cells are briefly noted.

CHOIX DE MATÉRIAUX DISPONIBLES POUR L'UTILISATION ET LE RÉGLAGE DE L'ÉNERGIE SOLAIRE

Résumé

L'auteur passe en revue les analogies de base entre la conception des surfaces de commande à énergie thermique des astronefs et les dispositifs pratiques servant à régler et à utiliser l'énergie solaire. Il examine également les gammes spectrales d'énergie rayonnante disponible et les principes physiques qui régissent l'émission de cette énergie et son absorption. Il fait observer que le milieu dans lequel se trouvent les matériaux en service dans les astronefs, pris dans son ensemble, est très dur; il donne une liste des éléments qui constituent le milieu interplanétaire et les passe en revue. Étant donné que le milieu dans lequel se trouve l'astronef est très exigeant, tous les matériaux utilisés en vue de leur commande thermique doivent être stables pour les applications à des dispositifs terrestres. Le mémoire établit l'importance du coefficient d'absorption solaire *a*, du coefficient d'émission *e* dans l'infrarouge, et du rapport *a/e*, *a* étant le paramètre matériel le plus important. Il démontre le besoin d'une détermination expérimentale de *a*, *e* et *a/e*, et décrit dans le détail les deux méthodes les plus communes employées pour ces déterminations. Ce mémoire présente aussi une description complète d'un dispositif calorimétrique mis au point en vue de la mesure expérimentale des caractéristiques des matériaux quant au rayonnement, ainsi qu'une revue des insuffisances et des qualités des appareils. Il résume des programmes de recherches visant à assurer une meilleure compréhension des phénomènes de rayonnement intéressant les matériaux fondamentaux, et énumère les principaux résultats obtenus jusqu'à présent. Il indique ceux des résultats qui présentent une importance particulière pour les techniciens mettant au point les matériels destinés à utiliser l'énergie solaire à la surface de la terre, notamment l'épaisseur minimale qui assure l'opacité, les répercussions des rugosités de surface sur *a* et *e*, le réglage du rayonnement par la déposition de pellicules minces, et les effets de l'angle d'incidence.

L'auteur donne une longue liste des matériaux utiles avec leur composition, l'état de leur surface et leurs paramètres de rayonnement. Les valeurs du rapport *a/e* s'échelonnent entre 15 et 0,25. Le mémoire passe en revue d'une manière générale les caractéristiques optimales du rayonnement pour les collecteurs, les concentrateurs, les chaudières et les radiateurs, et formule des recommandations spécifiques. Il décrit des feuilles métalliques de divers types et envisage des techniques pratiques d'application. Il mentionne de nouveaux matériaux destinés à être utilisés dans les concentrateurs et les fours solaires, en soulignant particulièrement leur durabilité et les considérations économiques. Certaines utilisations pratiques pour des feuilles en composition plastique métallisée font l'objet d'un examen

hypothétique. L'auteur souligne que le gadolinium est un métal qui promet beaucoup comme collecteur solaire.

Ce mémoire présente un choix idéal de matériaux destinés à être utilisés dans les systèmes terrestes, dans le but de réaliser une plus grande stabilité, une plus grande durabilité et une plus grande facilité d'entretien des systèmes. Il examine l'oxydation, la corrosion, le ternissement et d'autres mécanismes portant préjudice à l'état des matériaux. Il discute les effets du rayonnement ultraviolet et des cycles thermiques en se rapportant aux avaries qu'ils infligent probablement à certains systèmes de matériaux.

L'auteur signale quelques applications pratiques pour les nouveaux matériaux mis au point par les recherches ayant trait à la commande thermique des satellites dans des systèmes terrestres. Il mentionne un distillateur solaire en mylar métallisé, un concentrateur à haute conductance thermique et un système de miroirs métalliques. Il passe brièvement en revue les réalisations faites dans le domaine du réglage de la température dans les cellules solaires.

STEP LENSES AND STEP PRISMS FOR UTILIZATION OF SOLAR ENERGY

Isao Oshida *

For a solar collector, a concave mirror is used more frequently than a convex lens, chiefly for reasons of economy. In recent years, however, the art has been developed of manufacturing various types of lens, including step lenses such as Fresnel lenses, and other optical surfaces, from synthetic resins. They can be cast with a high degree of accuracy and on mass production lines by using metal patterns, and the cost of production is getting lower and lower. It is of importance to investigate the applicability of these moulded optical surfaces to the utilization of solar energy.

Among others, Fresnel lenses, used as condensers on reflex cameras, are now available commercially at quite low prices. In this paper, the possible applications of Fresnel lenses, as well as of cylindrical step lenses and step prisms, are investigated.

Plastic Fresnel lenses

At present, plastic Fresnel lenses for cameras are produced by a number of manufacturers. Some ingenious methods for making the original metallic patterns have been patented, and the Fresnel lenses thus produced attain a considerable degree of accuracy (1).

In Japan, lenses for use in 12 cm × 10 cm stand cameras, 6 cm × 6 cm twin-lens and 35 mm single-lens reflex cameras are available commercially. The price of a sheet of mass produced, 12 cm × 10 cm Fresnel lens is reduced to about 500 yen ($U.S. 1.40). The cost per square centimetre is about four yen (about one cent), and is far lower than that of a silicon solar battery, at about 350 yen (about $1.00). Of course, larger plastic Fresnel lense are more effective for the utilization of solar energy;[1] the main difficulty in production is in making the large metal pattern. However, a number of Fresnel lenses of moderate size are also sometimes useful. For instance, if solar batteries are combined with an equal number of Fresnel lenses of larger size, more solar radiation can be utilized and at the same time there is a possibility of lowering the initial cost per unit power of electricity.

A test was made with a plastic Fresnel lens, 12 cm × 10 cm in size, supplied by the Nippon Kogaku Jushi Company. It is cast from polymethyl-meta-acrylate, about 1.5 mm thick. Such a thin plate of polymethyl-meta-acrylate is transparent to light of from 0.3 μ to 2 μ, and the transmissive power for solar radiation is very high.

Except for a circular area at the centre, which has a diameter of 2 cm, it has very fine spiral notches, about four per millimetre (figure 1). A flat surface of polymethyl-meta-acrylate with no anti-reflection layer reflects back about 4 per cent of the solar radiation at normal incidence. For carved surfaces the reflection coefficient may be somewhat higher, because of the oblique incidence that necessarily takes place at every part of the notches. Moreover, the scattering of light by the notches and by the lack of homogeneity inside, which is sometimes remarkable for plastic materials, may cause additional losses.

To demonstrate the ability of the Fresnel lens as a collector of light, the following experiment was made. For convenience, artificial sunlight from a 150 watt xenon lamp was used. The lamp was put at the focus of a concave mirror, 9 cm in diameter and 50 cm in focal length, and thus a parallel beam was produced. A silicon solar battery, named SS 301, and 28 mm in diameter (6.15 square centimetres), produced by the Nippon Electric Company, was normally kept in the beam with or without the Fresnel lens in front of it. The photocurrent I generated, as well as the applied bias voltage V, was measured by the zero method. The results are shown in figure 2.

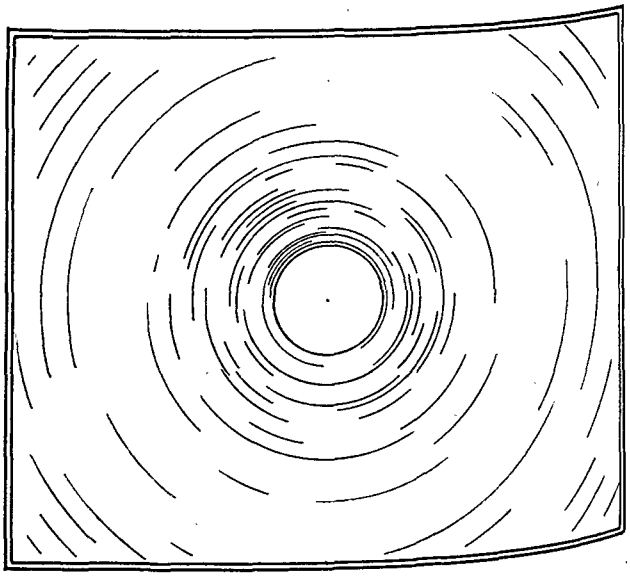


Figure 1

* Kobayasi Institute of Physical Research, Tokyo.

[1] Large Fresnel lenses, or other types of step lens made from hard glass, are used in projectors for stage lighting.

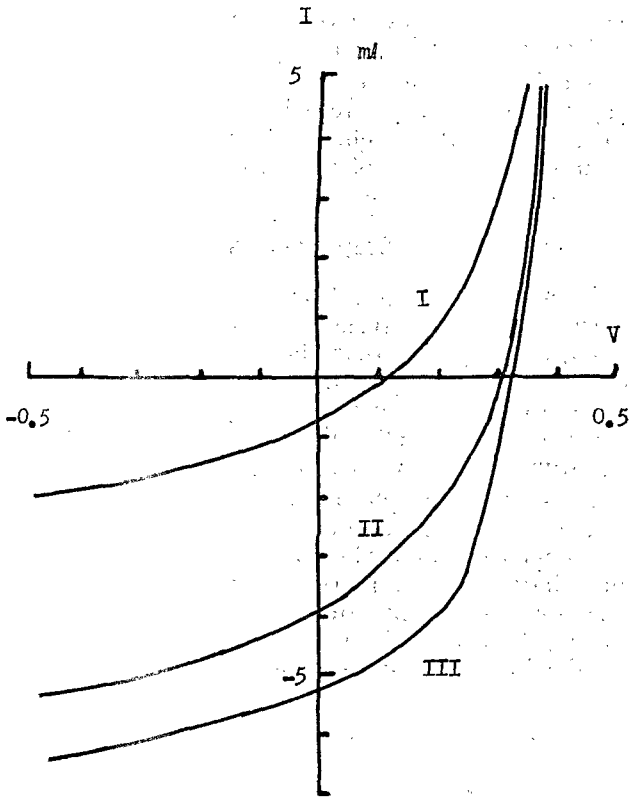


Figure 2

Curve I in figure 2 shows the V-I characteristics without a Fresnel lens. The maximum power output is indicated by the area of the largest inscribed rectangle in the region under the V-I curve in the second quadrant. This is about 0.025 mW.

When the Fresnel lens is put in front of the cell, 10.3 times more radiation is collected in the battery, if loss by reflection and by scattering is eliminated. Curve II shows the V-I characteristics when the Fresnel lens is put in front of the battery, slightly out of the focus so that the surface of the battery is illuminated as uniformly as possible by all of the collected beam. Curve III shows the V-I characteristics when the battery is put just at the focus. Only the centre of the battery is strongly illuminated in this case, and it is interesting to note that larger photocurrents and hence higher efficiencies are obtained in spite of the extraordinarily non-uniform illumination. The maximum power output in these cases is about 0.40 mW, that is, 16 and 32 times larger, respectively, than that without a Fresnel lens.

For such weak radiatio, estimated to be on then order of 0.4 mW/cm, the conversion efficiency of a photovoltaic cell varies with the intensity of radiation. The short circuit photocurrent is nearly proportional to the intensity of the radiation, but the open circuit voltage drops rather rapidly for weak intensities. As a result, the conversion efficiency decreases for low intensities roughly in proportion to the open circuit voltage. Thus the efficiency when using the Fresnel lens is about three times as large as when it is not used. Accordingly, if the lens collects about ten times more radiation, the maximum power output is increased about 30 times. This figure is in agreement in order of magnitude with the results above. At the same time, it implies that the loss of radiation by reflection and scattering in using the Fresnel lens is not serious.

If a lens and a mirror of the same size are available at the same price, the former is generally more advantageous as a solar collector because there is no need for plating and for simplifying the design. Moreover, plastic step lenses have the following advantages:

(*a*) The lesser thickness requires less material and results in a lighter weight, lower absorption and reduced cost.

(*b*) Variety of shape: The lenses can easily be cast in any form desired. For instance, a rectangular lens can be moulded by a process similar to that for producing a circular lens. Rectangular lenses can be arranged so tightly that no area of inefficiency is left, but circular lenses cannot. Thus, if circular solar batteries are combined with rectangular Fresnel lenses, the space factor is much improved.

(*c*) Reproducibility: Lenses of the same size, focal length and quality are readily reproduced by means of the metal pattern.

There remain, however, some difficulties in the practical use of Fresnel lenses as focusing devices for solar energy. The major drawback lies in their vulnerability to high temperatures. Adequate attention to design will virtually overcome this defect.

It is known that the efficiency of silicon solar batteries falls off considerably at very high radiation densities. Duffie *et al.*[2] have shown that at densities as great as 1 000 mW/cm², the efficiency of the silicon cells they used dropped to only 3 per cent or less. This is the normal behaviour of solar batteries. It is very unfortunate but not serious. Assume that a Fresnel lens increases normal solar radiation density 20 times, that is, 100 mW/cm², and that the cost per unit area of the lens is 1/90 that of the silicon solar battery; then, even if the efficiency falls from 8 per cent to 2.5 per cent, six times the electric power is nevertheless obtained, and the cost per unit power of electricity is as low as one-third of that obtained without collectors.

The heat at the focus has unfavourable effects on photovoltaic cells. The temperature coefficient of the power output of a photovoltaic cell is always negative. The power output of the silicon solar battery used here decreases by 0.6 per cent for every 1°C it rises. Moreover, the cell itself is damaged at temperatures above 170°C, and the acrylic capsule at more than 100°C. Cooling by water or an air stream is necessary. This also restricts the size of the lens to be used.

The combination of a thermoelectric element and a Fresnel lens seems to be more promising. If the

[2] Private communication.

original solar radiation density is assumed to be 100 mW/cm², it is intensified by 20 times by a Fresnel lens, giving a radiation density of 2 000 mW/cm², which corresponds to the black body of 500°C.

The last difficulty, which seems to be the most important, is that the use of a solar collector must be accompanied by a proper device, such as a heliostat or an equatorial mounting. The use of a cylindrical step lens, mentioned in the following section, suggests a way to overcome this difficulty.

Cylindrical step lenses

Here a cylindrical lens means a step lens which operates as a convex cylindrical lens, just as a Fresnel lens operates as an ordinary convex lens. If a cylindrical lens is mounted so as to face directly the position of the sun at noon and the axis is horizontal, the position of its focal line is almost unchanged throughout the day, except for movement in the straight line involving itself. When the length of the axis is sufficiently longer than the focal length the relative movement of the focal line is small. This is an excellent feature of the cylindrical lens, and only the inclination requires changing.

A cylindrical step lens can be cast by moulding in the same way as a Fresnel lens and can be applied to a photovoltaic cell, a thermoelectric element, solar steam boilers, solar cookers, etc.

Step prisms

Since the spectrum of solar radiation extends over a wide range of wavelengths, from about 0.3 μ to 2.5 μ, it is expected that higher conversion efficiency could be obtained if the different parts of the spectrum were utilized by different acceptors; for instance, the photovoltaic cells might be of different spectral sensitivities. Thus the use of a prism is suggested.

In a spectrograph, a large prism is preferable because of its high resolving power. Large prisms are expensive and absorb a considerable amount of radiation. In the matter of utilizing solar energy, therefore, a number of very thin prisms, closely arranged, will fit the purpose. This naturally leads to the idea of a step prism, a transparent sheet

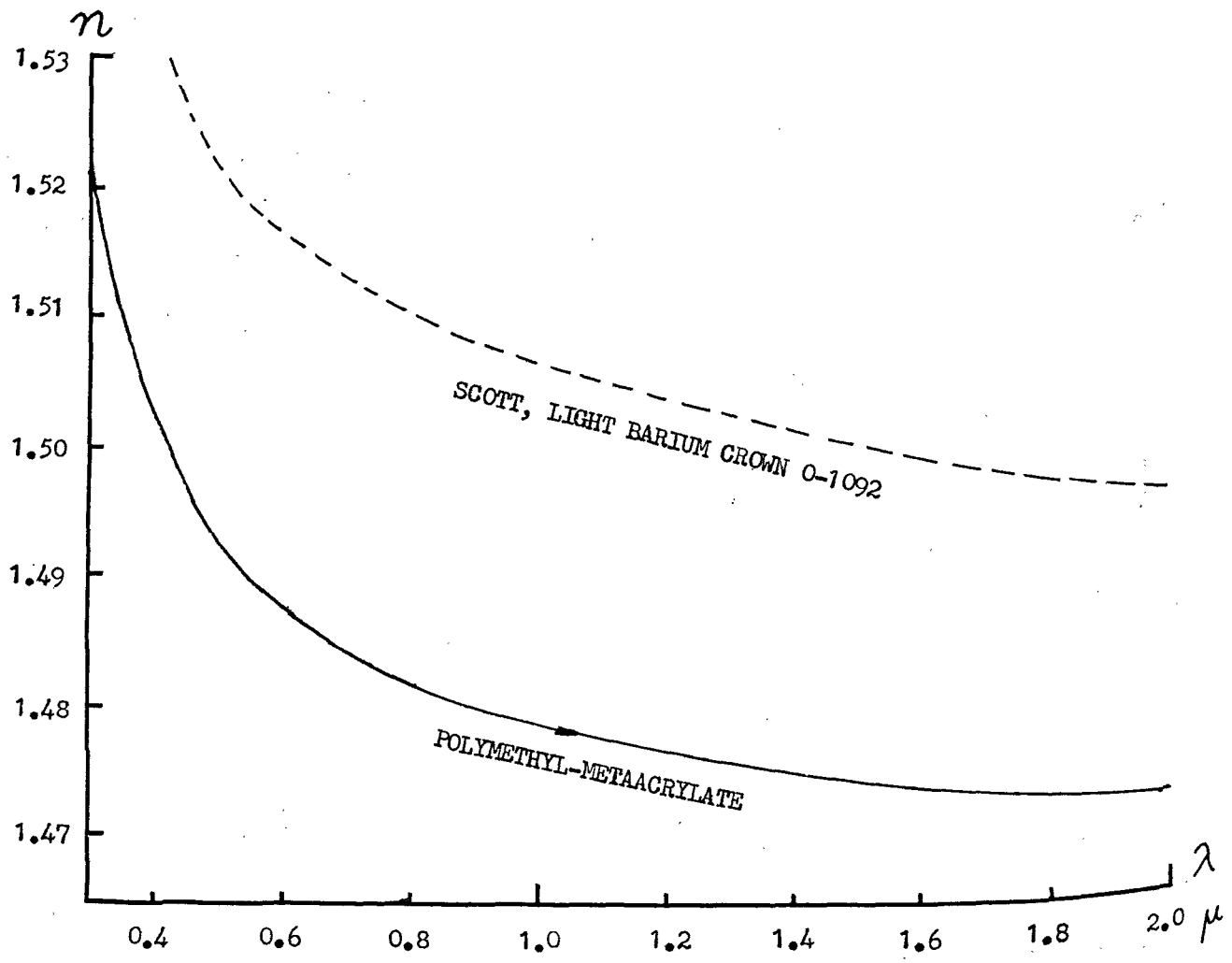


Figure 3

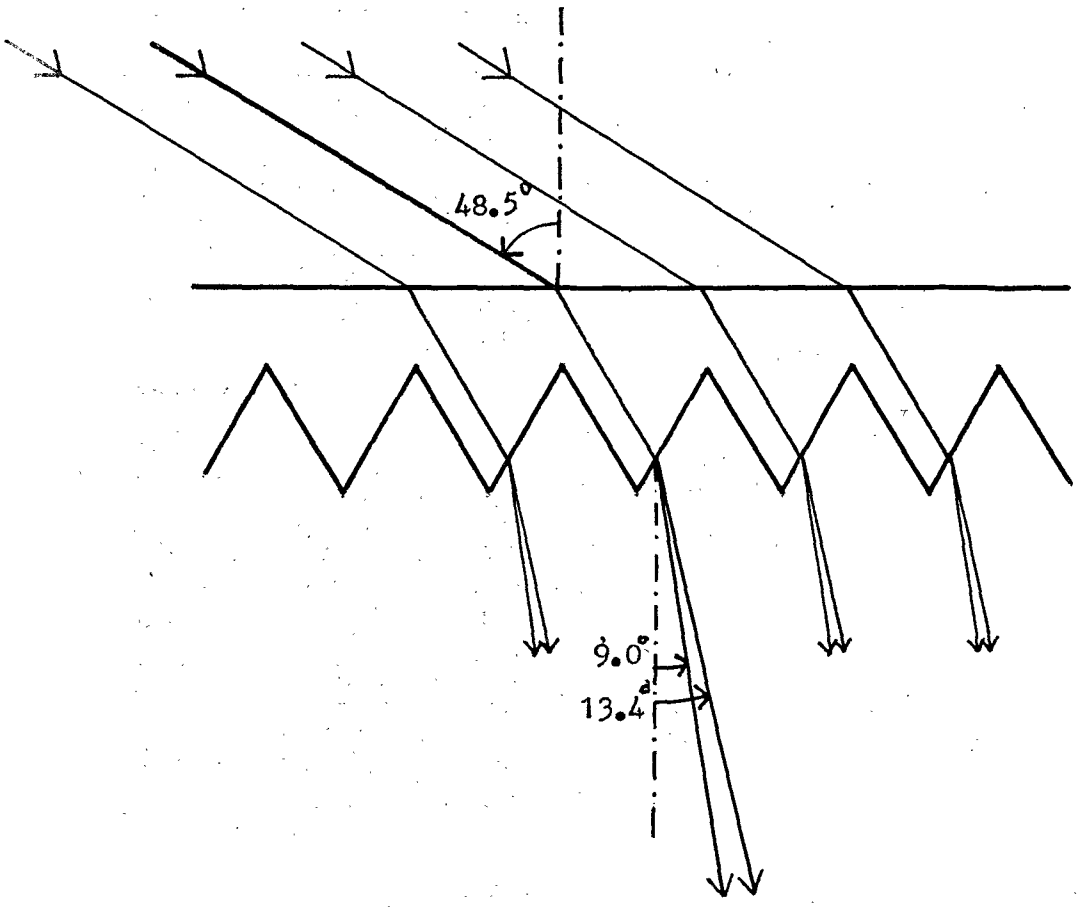


Figure 4

with corrugation capable of prismatic action. Such step prisms could be cast from synthetic resin by a method similar to that used in making a plastic Fresnel lens, and the weight, the light absorption, and the cost can be much reduced by comparison with an ordinary prism.

Johnson (2) reported the refractive indices of polymethyl-meta-acrylate for C, D and F lines of the spectrum. Substituting these data for Hartmann's dispersion formula,

$$n = n_o + \frac{c}{\lambda - \lambda_o}$$

the constants n, λ_o, and C are determined as follows:

$$n = 1.4681 \quad \lambda_o = 1\,235\,A \quad C = 93.42$$

The relation between n and λ is shown in figure 3, as well as that of an optical glass, Scott's light barium crown 0 1092.

If the apex angle of a polymethyl-meta-acrylate prism is 60°C, the incident ray is bent about 37° at the minimum deviation, as shown in figure 4. The change of the angle $\Delta\,\theta$ of deviation with the change $\Delta\,\eta$ of the refractive index is given by

$$\frac{\Delta\,\theta}{\Delta n} = 1.5 \text{ radian}$$

Since the total change of the refractive index from 0.3 μ to 2 μ is about 0.05, as can be observed in figure 3, the angle of deviation has a width of about 0.075 radian, or about 4.5°, as seen in figure 4.

If the step prism is combined with a convex lens or a Fresnel lens, the sun's image at the focus is considerably enlarged, for the rays of different wavelengths focus at different positions. The result is a rather distinguished spectrum, without any slit, because the sun's apparent diameter is only about 0.5°, much smaller than the angle of dispersion.

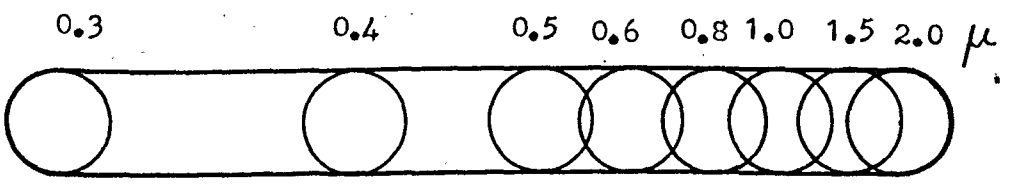


Figure 5

As an example, when a Fresnel lens of 80 cm in focal length is combined with a 60° step prism, the length of the spectrum is about 5.5 cm, while the diameter of the sun's image is about 7 mm. As a result, the spectrum shown in figure 5 will appear. Then if two or three photovoltaic cells of different spectral sensitivities are put in favourable positions to cover the spectrum, the over-all efficiency can be greatly enhanced, compared with the use of a single cell.

Jackson (3) has proposed a multilayer cell to improve efficiency. In the multilayer cell, however, the ineffective absorption of the front layers causes some trouble.

At present, however, photovoltaic cells of high efficiency, other than those made from silicon and from germanium, are not produced. Introduction of binary compound cells, such as those of GaAs, InP and CdTe, seems to be promising. A more promising way is the production of a photovoltaic cell whose surface has continuous different spectral sensitivities at different positions. It is known that if InAs and InP are mixed in varying proportions, alloys having a band-gap of between 0.33 eV and 1.28 eV, corresponding to sensitivity maxima between 0.6 μ and 3 μ, are obtained. Similarly, the mixing of GaAs and GaP will provide sensitivity maxima of between 0.3 μ and 0.6 μ, approximately.

At the present time the conversion efficiency of a silicon solar battery reaches 18 per cent at the highest. This implies that at a sensitivity maximum of about 0.7 μ, the conversion efficiency is as high as about 39 per cent. The latter figure is also the expected over-all efficiency of an ideal solar battery which has varying sensitivity maxima along its surface in accordance with the solar spectrum, although the optical loss is left out of consideration in this case.

Acknowledgements

The author wishes to express his hearty thanks to Koreo Kinoshita of Gakushuin University, and to Mr. Ogawa of the Institute of Physical and Chemical Research for their valuable aid throughout this work, and to Miss Mizuko Yoshida for her help during the course of the experiment.

The author is also indebted to Kazuo Hayashi of Nippon Electric Company, to Yoshio Yatabe of the Nippon Kogaku Jushi Company for supplying samples and reports, and to J. D. Duffie of the University of Wisconsin, Madison, for his kindness in supplying information on unpublished results.

References

1. Miller, O. E., McLeod, J. H. and Sherwood, W. T., *Journ. Opt. Soc. Amer. 41;* 807, 1951. (Japanese patent No. 201621.)
2. Johnson, B. K., Recent Optical Materials and Their Possible Applications, *Proc. Phys. Soc.*, London, 55 310, 1943.
3. Jackson, E. D., Areas for Improvement of the Semiconductor Solar Energy Convertor, *Trans. Conf. on the Use of Solar Energy*, Tucson, 1955; Univ. of Arizona Press, Tucson, vol. 5, 122-126, 1958.

Summary

In recent years the art of manufacturing various types of optical surface from synthetic plastics, using metal patterns, has been developed. Thin plates with corrugated surfaces and acting as lenses, prisms, or other optical elements can now be produced with a high degree of accuracy and on mass production lines. Among others, step lenses such as Fresnel lenses, cylindrical step lenses, and step prisms often serve as elements or parts in a solar plant, as substitutes for ordinary lenses, mirrors, or prisms.

A test with a Fresnel lens, available commercially for use in stand cameras, size 12 cm × 10 cm, showed that it has enough potentiality to be used as a focusing device in place of ordinary lenses or concave mirrors. Its cost, about four yen (one cent) per square centimetre at present, will be lowered still further in the future.

The cost per square centimeter of a silicon solar battery is still far too high and about a hundred times that of a plastic Fresnel lens. The combination of a solar battery and a Fresnel lens lowers the cost per unit power of electricity produced. At high radiation density, however, the efficiency of the photovoltaic cells is lowered, and high temperature at the focus causes unfavourable effects. Upon this point, a combination of a thermoelectric element and a Fresnel lens collector is more promising.

A cylindrical step lens, which has a step profile and acts as a cylindrical lens, is also useful as a solar collector. The main advantage is that it simplifies the mounting for following the movement of the sun.

A step prism, which is a transparent plate with a corrugated surface operating as a prism, can also

be applied to the utilization of solar energy. If it is combined with a Fresnel lens, a spectrum of the sun shows itself. Then if two or three photovoltaic cells of different spectral sensitivities, or a cell having different spectral sensitivities along its surface, are put in the spectrum, higher conversion efficiencies are to be expected than if a single ordinary solar battery is used. In the latter case, if such a cell of a quality equal to that of the silicon solar battery of the highest conversion efficiency now available, 18 per cent, is produced, the efficiency will reach 39 per cent, at least.

LENTILLES ET PRISMES A ÉCHELONS POUR L'UTILISATION DE L'ÉNERGIE SOLAIRE

Résumé

On a mis au point, au cours de ces quelques dernières années, l'art de réaliser des surfaces optiques de divers types à partir de produits plastiques et de gabarits métalliques. Des plaques minces à surface striées agissant comme des lentilles, des prismes ou tous autres éléments optiques peuvent actuellement se produire avec une grande précision et en série. On réalise, en particulier, des lentilles à échelons telles que celles de Fresnel, des lentilles cylindriques à échelons et des prismes à échelons, utilisables comme éléments ou pièces d'une centrale solaire, où ils remplaceront les lentilles, les miroirs et les prismes ordinaires.

Un essai exécuté avec une lentille de Fresnel qu'on trouve dans le commerce en vue de son utilisation dans des appareils photographiques à pied donnant des images de 12 × 10 cm a révélé que ses possibilités autorisaient son emploi comme organe de concentration du rayonnement en lieu et place des lentilles ordinaires ou des miroirs concaves. Son prix de revient actuel de 4 yen environ (1 cent) par centimètre carré sera encore réduit dans l'avenir.

Le coût au centimètre carré d'une batterie solaire au silicium est encore beaucoup trop élevé, environ le centuple de celui d'une lentille de Fresnel en composition plastique. L'emploi combiné d'une telle batterie solaire et d'une lentille de Fresnel réduit le coût unitaire de l'électricité ainsi produite. Aux densités de rayonnement élevées, cependant, le rendement des cellules photovoltaïques s'en trouve réduit et les températures élevées qui règnent au foyer ont des effets défavorables. C'est sur ce point que l'association d'un élément thermo-électrique et d'un collecteur constitué par une lentille de Fresnel est le plus riche en promesses.

Les lentilles plan-convexes à gradins, dont la coupe présente un système d'échelons mais qui agit comme une lentille plan-convexe, présentent également leur utilité comme collecteurs d'énergie solaire. Leur gros avantage est la simplification de l'appareillage nécessaire pour suivre la course du soleil.

Le prisme à gradins, plaque transparente dont la surface en échelons lui permet de se comporter comme un prisme, peut également s'appliquer à l'utilisation de l'énergie solaire. Si on le combine avec une lentille de Fresnel, on obtient un spectre de la lumière solaire. Si donc on installe dans ce spectre, en des points convenablement choisis de la surface en cause, un groupe de deux ou trois cellules photovoltaïques présentant des sensibilités spectrales différentes, on est en droit de s'attendre à des rendements de conversion plus élevés qu'avec un seul élément ordinaire de batterie solaire. En pareil cas, si on réalise de telles cellules avec une qualité égale à celle des batteries solaires au silicium ayant le plus fort rendement de conversion actuellement connu, soit 18 p. 100, le rendement minimal ainsi obtenu sera de 39 p. 100.

VERRES ET MONTAGES SPÉCIAUX POUR L'UTILISATION DE L'ÉNERGIE SOLAIRE

I. Peyches *

Les physiciens et les thermiciens qui se sont penchés jusqu'ici sur les problèmes soulevés par l'utilisation de l'énergie solaire se sont adressés, pour leurs réalisations, aux matériaux disponibles sur le marché et, parmi eux, aux matériaux vitreux (glace et verre à vitres) conçus pour des usages généraux assez éloignés des conditions particulières de ces nouveaux emplois.

La présente étude se propose de dégager les conditions optimales auxquelles devrait satisfaire le verre pour de tels emplois et d'indiquer les possibilités techniques dès maintenant à la disposition des verriers pour y satisfaire.

Nous ne visons ici que les aspects strictement thermiques. Les cas spéciaux n'utilisant qu'une partie du spectre d'émission solaire, comme c'est le cas avec les photopiles, sont ici écartés.

Avec cette restriction, le problème éclate encore en deux cas extrêmes. On peut désirer recueillir un maximum d'énergie de faible concentration et donc de bas potentiel thermique, comme ce sera le cas pour le chauffage domestique, pour la cuisson des aliments, pour l'épuration des eaux, etc., ou au contraire désirer une forte concentration d'énergie pour obtenir des températures élevées tendant vers celle de la source (fours solaires).

Le premier cas fera appel à l'effet de piège que joue le verre par suite de sa forte transparence vis-à-vis du rayonnement solaire et de son opacité élevée vis-à-vis de ce qu'on appelait naguère la chaleur obscure. C'est l'effet de serre bien connu. Le second ne retient que l'effet réflecteur d'un miroir et peut s'adresser à d'autres matériaux que le verre, tels que certains métaux susceptibles d'acquérir un poli superficiel correct. L'effet de concentration dioptrique (effet loupe) n'est pas utilisé pour des raisons techniques évidentes (impossibilité d'obtenir économiquement de grands dioptres).

Lorsqu'on s'adresse au verre en tant que réflecteur, il est le plus généralement métallisé *sur sa face arrière.* Ainsi la couche de métallisation se trouve parfaitement protégée des agressions atmosphériques. Des métallisations face avant ont été utilisées, protégées par des couches minces de monoxyde de silicium, mais cette technique ne s'est pas imposée. Dans l'état actuel, le rayonnement réfléchi traverse donc deux fois la lame de verre. Cette remarque rapproche les deux cas extrêmes précités. Dans tous les cas, il y a traversée de verre et absorption ou réflexion sur une surface en contact ou non avec le verre.

Considérons un rayonnement primitif caractérisé par une certaine distribution spectrale; il s'agit ici du rayonnement solaire et, pour fixer les idées, nous rappelons qu'il s'agit d'un rayonnement assimilable à celui du corps noir à 6 000 °K, modifié par la traversée de l'atmosphère terrestre et ainsi pratiquement limité entre 0,3 μ et 2,5 μ. La diffusion atmosphérique qui défavorise les courtes longueurs d'onde fait glisser d'autre part le maximum que la loi de Wien fixerait à 0,475 μ vers la région jaune du spectre visible. La position du maximum vrai est variable avec la hauteur zénithale du soleil et les conditions géographiques, et se situe vers 0,503 μ pour une hauteur zénithale de 25° et 0,635 μ pour 60°.

De toutes façons, l'aire principale sous la courbe d'émission solaire coïncide avec le trou de transmission maximale de la courbe d'absorption chromatique des verres plats courants : glace et verre à vitres (figure 1).

Dans la figure 1 :

- S courbe du rayonnement solaire utile (unités arbitraires)
- A facteur de transmission globale d'une glace sous 1 cm d'épaisseur
- A' facteur de transmission globale d'un verre à vitre sous 1 cm d'épaisseur
  (on notera vers 1,1 μ la bande d'absorption due à la présence de fer ferreux, au titre d'impureté, dans ces verres)
- N courbe de rayonnement du corps noir à 400 °K
- N' courbe de rayonnement du corps noir à 600 °K

(pour la courbe P, voir plus loin)

Au contraire, les courbes d'émission du corps noir aux basses températures sont tout entières situées dans la région pratiquement opaque de ces verres.

Mais cette apparente simplicité qui conduit à considérer le verre comme parfaitement transparent vis-à-vis du rayonnement solaire et parfaitement opaque pour le rayonnement du récepteur échauffé ne résiste pas à un examen plus profond.

Pour fixer simplement des ordres de grandeur, indiquons les vicissitudes subies par un rayonnement primaire atteignant une lame de verre d'épaisseur « courante » en verre « courant ». L'intensité initiale de ce rayonnement étant prise arbitrairement égale à 100, la réflexion vitreuse sur la première face l'ampute de 4 p. 100 avec un léger effet chromatique

* Directeur du laboratoire de recherches de la Compagnie de Saint-Gobain, Paris.

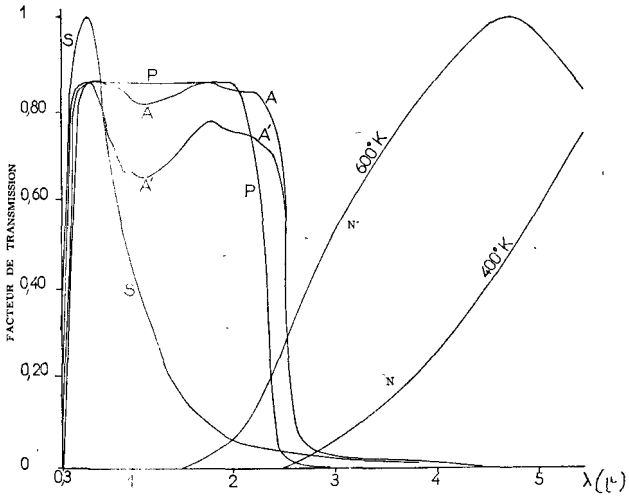


Figure 1

dû à la forme de la règle de Fresnel donnant cette partie réfléchie : $\left(\frac{n-1}{n+1}\right)^2$ Ce rayonnement réfléchi n'est pas perdu dans le cas du réflecteur, mais est perdu pour un capteur. Sur les 96 p. 100 transmis, l'absorption propre du verre va encore sous l'épaisseur considérée (quelques millimètres) enlever 6 p. 100, avec éventuellement un nouvel effet chromatique. A cette phase, deux cas sont à considérer :

a) *Réflecteur* (figure 2)

90 p. 100 du rayonnement incident atteignent la surface arrière que nous supposerons métallique et réfléchissante. Celle-ci absorbe pour son propre compte environ 9 p. 100. Après réflexion et au cours de la nouvelle traversée, 6 p. 100 du reste, soit 5 p. 100 du rayonnement initial, seront encore dispersés dans le verre. Au franchissement de la face avant, la réflexion vitreuse intervient encore, mais, à nouveau réfléchie sur la couche métallique, la fraction principale de ce rayonnement se retrouvera dans le faisceau émergent, qui de ce fait reste de l'ordre de 76 p. 100, à quoi viennent s'ajouter les 4 p. 100 de la première réflexion vitreuse. Au total, le faisceau *utile* réfléchi contient 80 p. 100 de l'énergie initiale. On notera qu'il y a à considérer *deux* surfaces réfléchissantes successives : celle de l'orienteur et celle du concentreur. Au foyer, on disposera donc de 64 p. 100 du rayonnement incident, soit grossièrement 2/3. Pour une densité d'énergie de 1 kWh/m² atteignant l'installation, il restera

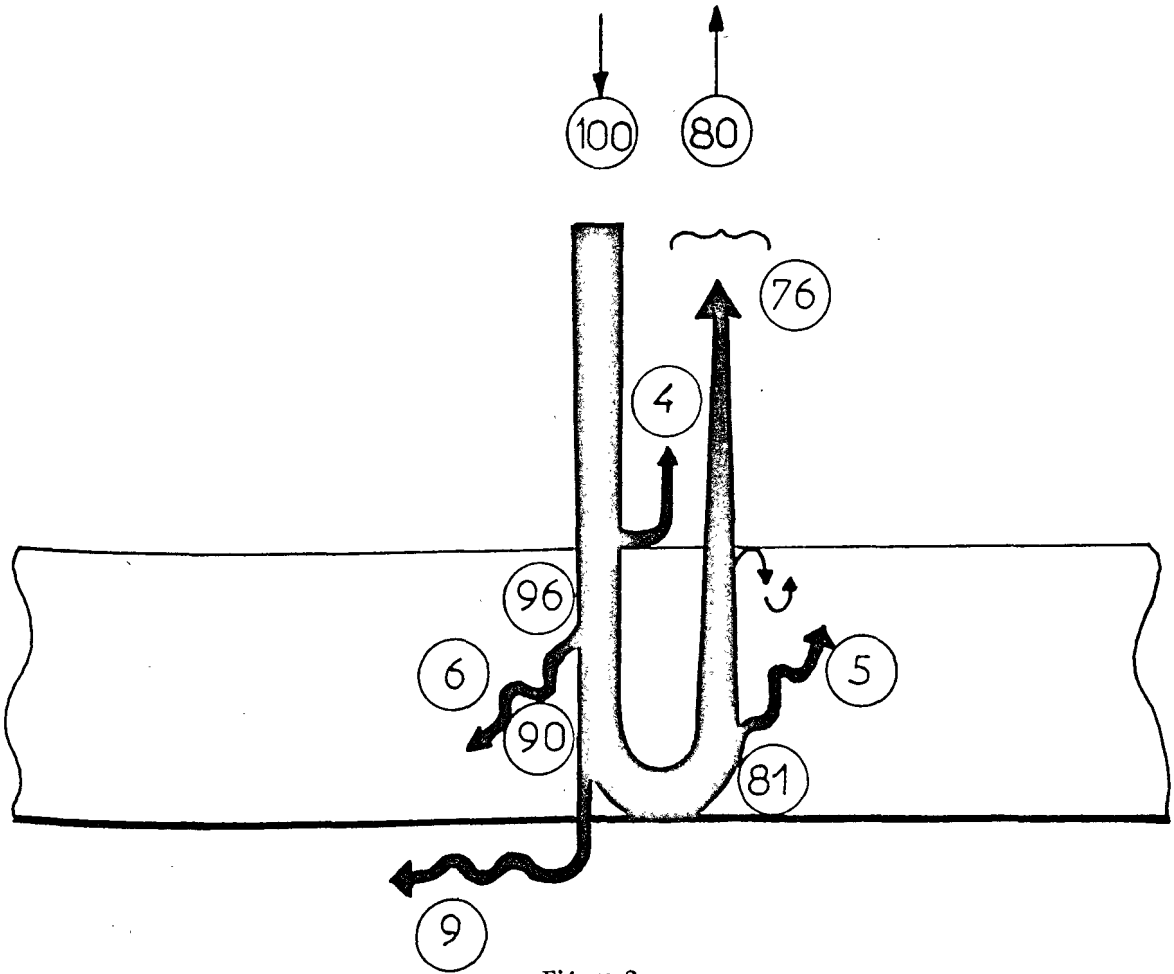


Figure 2

dans l'orienteur 0,2 kWh/m² et dans le concentreur 0,16 kWh.

b) *Capteur* (figure 3)

Ici la seconde face n'est pas métallisée. Sur les 90 p. 100 de l'énergie qui l'atteint, 4 p. 100 subiront encore la réflexion vitreuse et, retraversant la lame de verre, seront presque totalement perdus dans l'espace. 86 p. 100 de l'énergie incidente seront *en principe* utilisables dans l'enceinte de capture. Supposons que celle-ci soit constituée par un corps noir, matériellement séparée de la lame de verre, pour que seuls interviennent les échanges par rayonnement, et pour sa part parfaitement isolée sur sa face arrière. Ce corps noir va s'échauffer et va émettre pour son propre compte. Nous nous retrouvons dans un cas où la source primaire, le soleil, est remplacée par une source secondaire de température beaucoup plus basse, disons, pour fixer les idées, 450 °K. La limitation est évidemment la conséquence des pertes au travers du verre. Or vis-à-vis de ce rayonnement dont le maximum est voisin de 6,4 μ et qui commence vers 2,5 μ, le verre, nous l'avons dit, est pratiquement un corps noir. La partie de ce rayonnement qui pénètre dans le verre après déduction de la partie réfléchie est donc totalement absorbée dans une couche mince qui contribue à la mise en température de l'enceinte, mais qui, par reradiation et conduction vers l'extérieur, provoque les pertes définissant le régime d'équilibre atteint.

Tout cela est intuitif. On conçoit sans calcul que pour le réflecteur le verre doit être seulement le plus

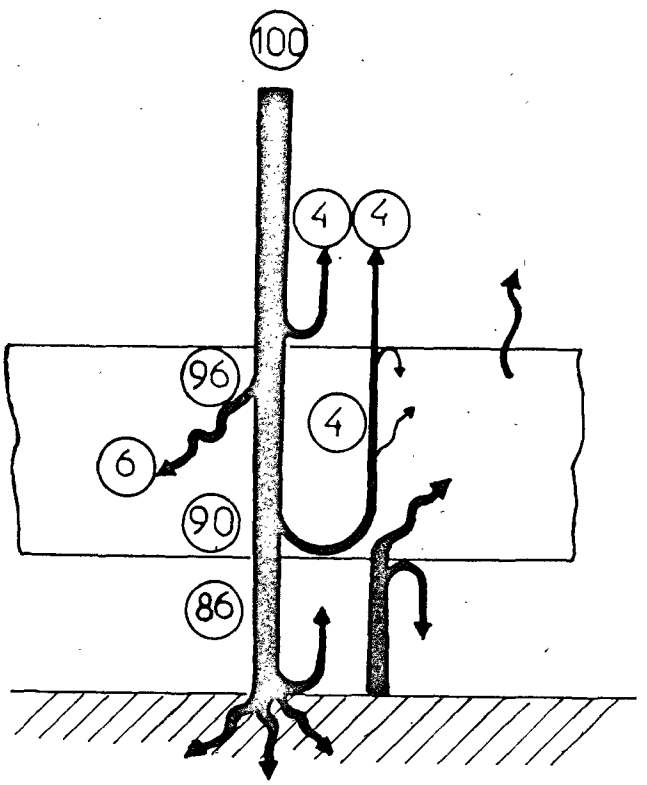


Figure 3

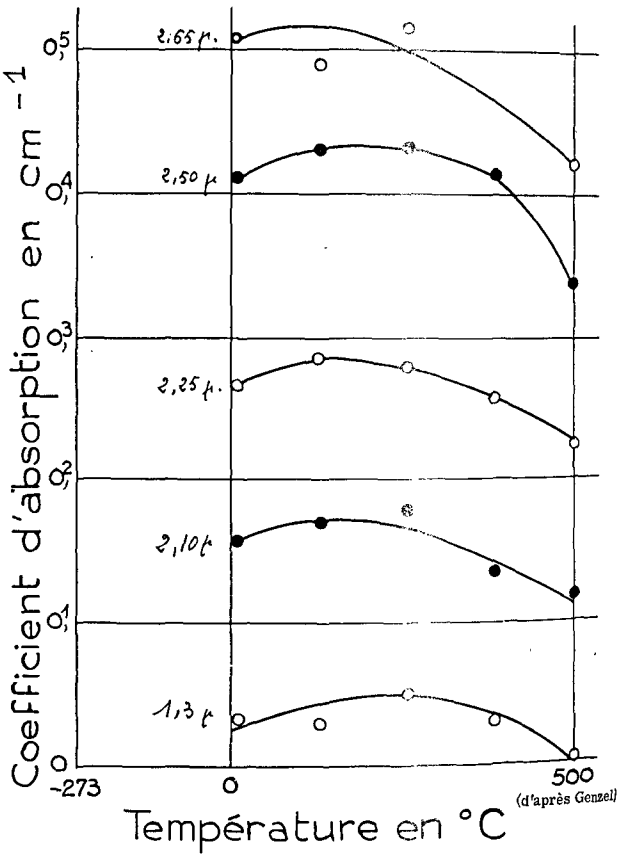


Figure 4

transparent possible pour le rayonnement solaire, alors que pour le capteur il doit satisfaire à la fois à cette condition et être le plus opaque possible vis-à-vis du rayonnement propre du capteur agissant comme source secondaire.

A y réfléchir, les choses sont beaucoup moins simples, et revêtent très vite un aspect inextricable. Prenons cet exemple si simple qu'est l'effet de serre.

Notons en passant que si la loi de Fresnel-Lorentz donnant la fraction atteinte par la réflexion vitreuse $\left(\frac{n-1}{n+1}\right)^2$ s'applique au rayonnement *dirigé* tel qu'il provient du soleil et conduit à la valeur citée de 4 p. 100, elle ne s'applique plus sous cette forme au rayonnement *diffus* provenant de la source secondaire d'un capteur, et c'est sur 9 p. 100 qu'il faut, en fait, compter. Le verre, qui s'échauffe lui-même en absorbant fortement ce rayonnement secondaire, va donner lieu, couche par couche, à tout un processus de reradiation dont une partie émise vers le récepteur sera utilisée et le reste perdu. Gardon a indiqué la démarche mathématique complexe permettant de traiter formellement ce cas et a pu donner des chiffres relatifs à une situation symétrique, mais non à la situation dissymétrique qui caractérise la lame placée entre deux sources de températures différentes.

Si ce problème n'était pas apparu important plus tôt, c'est que l'effet de serre est resté longtemps limité à de basses températures, disons inférieures

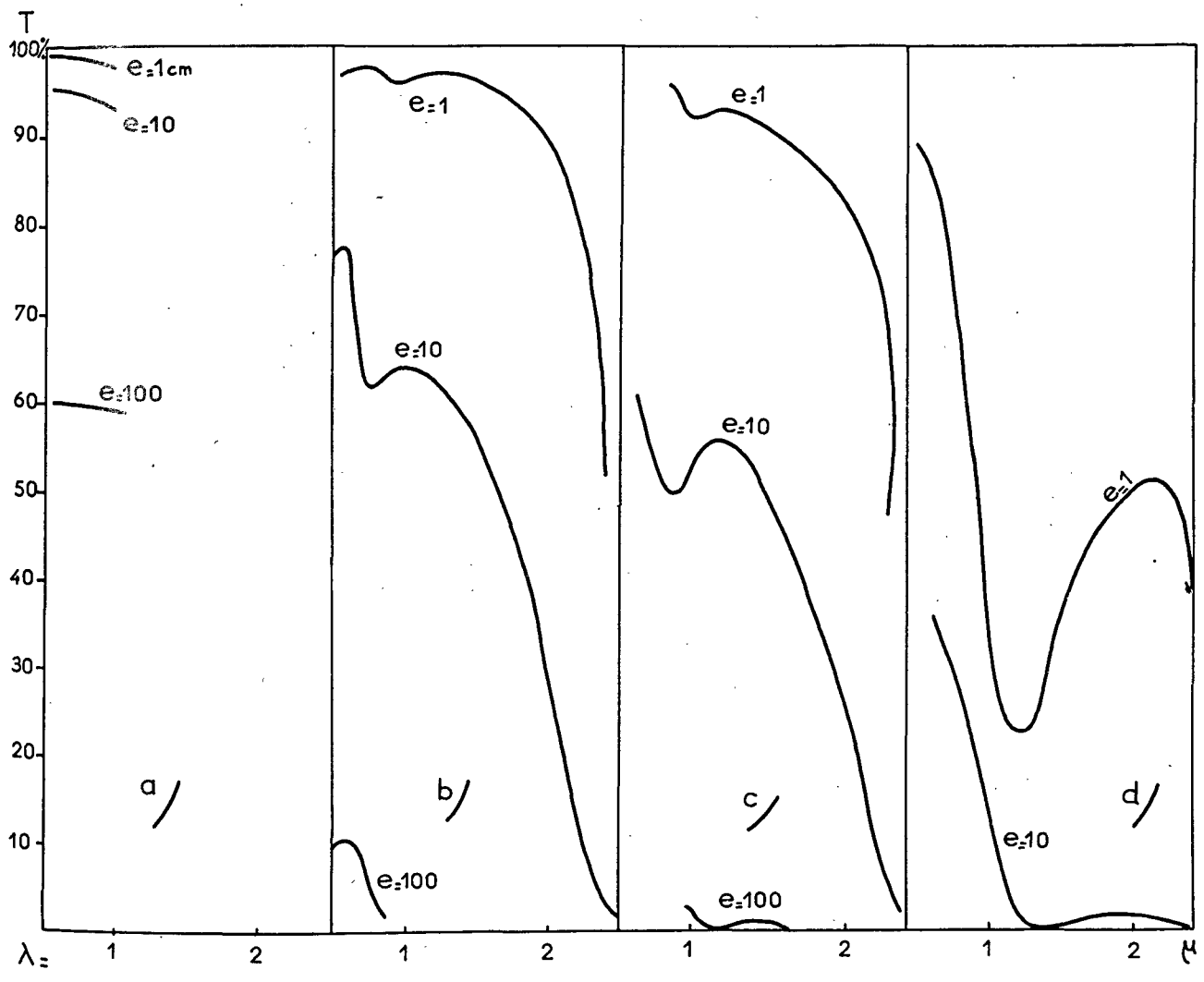


Figure 5

à 100 °C. L'énergie rayonnée à cette température par le récepteur, même assimilé à un corps noir, restait faible, et la température de la lame de verre absorbant cette énergie restait peu différente de la température ambiante.

Or, la tendance est à élever la température de régime du récepteur dans le but d'améliorer le cycle de Carnot dans les applications thermodynamiques. On peut envisager, *avec de faibles concentrations*, d'utiliser comme fluide de transfert des métaux ou alliages fondus, ou de vaporiser des liquides. Dans ce cas, d'une part l'échauffement du verre n'est plus négligeable et il en résulte une diminution de son opacité dans l'infrarouge, comme le montre la figure 4, et d'autre part la courbe d'émission du récepteur se déplaçant vers les courtes longueurs d'onde, commence à filtrer par le trou de transmission du verre.

Autant que le facteur d'absorption du verre restait, pour les grandes longueurs d'onde, très voisin de l'unité, le rôle de l'épaisseur n'apparaissait pas. Mais, aux approches du trou de transmission, la forme exponentielle de la loi de Beer peut distordre totalement l'allure de la courbe de transmission lorsque l'épaisseur varie. La figure 5 représente pour quatre types de verres l'effet de l'épaisseur correspondant à des multiples de 10.

Pour piéger le maximum d'énergie pour une température choisie du récepteur, nous avons à notre disposition plusieurs variables dont nous examinons successivement le rôle ci-dessous.

La *composition* du verre affecte sa transmission; la bande centrée sur 1,1 μ due à la présence de fer ferreux dans le verre est de toute évidence néfaste, puisqu'elle affaiblit le rayonnement solaire transmis, sans retenir mieux pour cela le re-rayonnement de la source secondaire. Dès qu'une énergie notable est rayonnée par cette source secondaire au-dessous de 5 μ, le verre ordinaire ne peut plus être considéré comme totalement opaque. Il y a intérêt à s'adresser alors aux verres du type boro-silicate (Pyrex) qui, sous des épaisseurs de quelques millimètres, arrêtent tout ce qui est supérieur à 3 μ (courbe *P*, figure 1).

Épaisseur : le tableau ci-dessous donne, pour des épaisseurs multiples de 10, les modifications du facteur de transmission.

e = 1	*10*	*100*
1 000	1 000	1 000
0,995	0,951	0,605
0,990	0,904	0,366
0,980	0,817	0,133
0,970	0,737	0,047
0,960	0,665	0,017
0,950	0,599	0,006
0,900	0,348	—
0,800	0,108	—
0,700	0,028	—
0,600	0,006	—
0,500	0,001	—
0,400	0,0001	—

La pente de la partie de la courbe de transmission séparant une région de grande transparence d'une région de moindre transparence est d'autant plus grande que l'épaisseur est plus importante. On peut, en choisissant une épaisseur convenable, *retenir* davantage d'énergie rerayonnée qu'on perdra en énergie primaire.

Le *facteur de transmission* peut être affecté en dehors de ces deux premières causes intrinsèques par des *traitements* superficiels. Un film d'or déposé sur la face interne du verre, si son épaisseur est correcte, réfléchit peu l'infrarouge proche contenu dans le rayonnement solaire, et beaucoup l'infrarouge plus lointain. Des traitements chimiques simples permettent d'obtenir de tels films sur de grandes surfaces.

Le *pouvoir émissif* du capteur lui-même doit être choisi de manière à ce qu'il corresponde au corps noir au-dessous de 2,5 μ, et qu'au contraire il soit faible au-dessus (métaux ternis et non métaux noircis).

Mais c'est surtout le facteur de déperdition globale de l'écran de verre qui a un effet important, et à ce point de vue les vitrages multiples doivent particulièrement retenir l'attention.

Examinons en effet le rôle de piège dû à 1, 2..... n lames de verre.

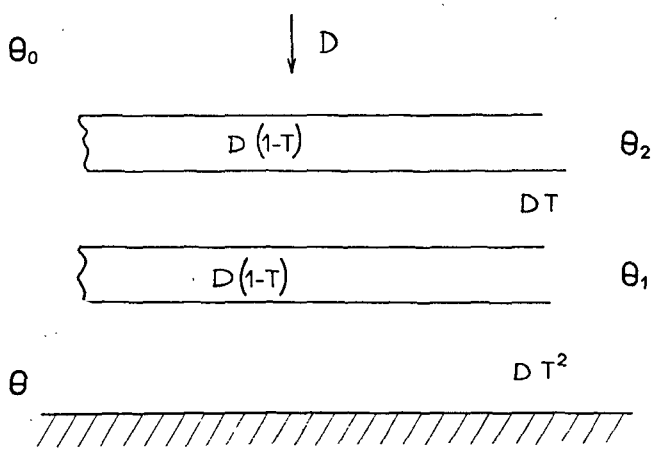


Figure 6

Soit D la densité du flux solaire reçu au niveau de l'installation. θ_0 est la température d'ambiance, θ la température du récepteur supposé constitué par un corps noir, sans perte par sa face arrière. θ_1 la température prise en régime permanent par une lame de verre unique, et T sa transparence globale *vis-à-vis du rayonnement solaire.* T est nul vis-à-vis du rayonnement d'ambiance et en première approximation vis-à-vis du rerayonnement du récepteur.

L'équilibre du récepteur s'exprime par :

$$\sigma \theta^4 = DT + \sigma \theta_1^4$$

L'équilibre de la lame est donné par :

$$l \sigma \theta_1^4 = D(1 - T) + \sigma \theta_0^4 + \sigma \theta^4$$

D'où :

$$\sigma \theta^4 = D(T + 1) + \sigma \theta_0^4$$

Si T est voisin de l'unité (verre très clair et très mince), tout se passe comme si le récepteur recevait le rayonnement de *deux soleils.*

Supposons maintenant que le piège soit constitué par *deux* lames de verre identiques (double vitrage) (figure 6) qui vont prendre respectivement les températures θ_1 et θ_2.

Nous écrivons de même les conditions d'équilibre

Récepteur :

$$\sigma \theta^4 = DT^2 + \sigma \theta_1^4$$

1re lame à partir du récepteur :

$$2 \sigma \theta_1^4 = DT(1 - T) + \sigma \theta^4 + \sigma \theta_2^4$$

2e lame :

$$2 \sigma \theta_2^4 = D(1 - T) + \sigma \theta_1^4 + \sigma \theta_0^4$$

Il vient immédiatement

$$\sigma \theta^4 = D(1 + T + T^2) + \sigma \theta_0^4$$

La généralisation est évidente. Pour n lames on aurait :

$$\sigma \theta^4 = D[1 + T + ... + T^n] + \sigma \theta_0^4$$

Si T est voisin de l'unité

$$\sigma \theta^4 = D(1 + n) + \sigma \theta_0^4$$

Ainsi avec deux lames la température atteinte correspond à celle que fourniraient trois soleils.

La courbe ci-après (figure 7) donne la température atteinte par un corps noir irradié par x soleils (θ_0 = 290 °K = 17 °C).

La valeur $x = 1$ correspond au corps noir nu et dans le vide. Dans l'air, par suite du refroidissement convectif, la température de régime serait 54 °C seulement.

Avec le facteur de transmission globale de 0,86 adopté plus haut, un triple vitrage correspondrait encore à 3,25 soleils.

On voit donc tout l'intérêt des vitrages multiples pour former un capteur d'énergie solaire. L'utilisation d'un verre unique d'épaisseur équivalente ne conduirait pas au même résultat, les interéchanges entre couches s'effectuant alors aussi par conduction.

L'industrie verrière a généralisé depuis quelques années dans le bâtiment les doubles et les triples vitrages de grandes dimensions (surfaces monobloc de plusieurs mètres carrée). Certaines réalisations comportent des assemblages *soudés* qui assurent l'étanchéité totale des espaces intercalaires.

Pour rester dans des limites raisonnables quant au nombre de lames de verre ainsi assemblées, on voit que, sans débit, la température du récepteur ne saurait dépasser 200 °C. Pour monter au-delà, il faut faire tomber sur le capteur un rayonnement au moins partiellement concentré.

Le problème de la concentration pour un simple but énergétique échappe à certaines difficultés qu'on rencontre avec les miroirs destinés à fournir des mages astronomiques. Dans ce dernier cas, et si l'on, iveut bénéficier de la meilleure résolution possible les ondes réfléchies ou diffractées doivent avoir leurs phases cohérentes, et l'on sait que les miroirs-mosaïque sont alors à proscrire. Ce sera au contraire la règle pour les grands orienteurs ou concentreurs. S'il s'agit de faibles taux de concentration, n'importe quel type de réflecteur peut être utilisé, mais s'il s'agit d'obtenir la plus haute température possible, l'image solaire doit être d'une qualité suffisante pour que le maximum d'énergie se répartisse sur la surface utile minimale. Pour les fours solaires de petite puissance, on utilisera des miroirs paraboliques de grande ouverture et de court foyer, mais pour les fours de grande puissance les réalisations sont du type mosaïque, et la focalisation est obtenue par déformation individuelle des éléments constitutifs. Cette sujétion entraîne une grande complexité des supports et des difficultés de réglage. Or, depuis très peu de temps, de nouveaux procédés de fabrication en continu de la glace polie permettent de mettre à la disposition des spécialistes un ruban *indéfini* de glace. Seules les difficultés de transport limitent la longueur de ces rubans, mais des unités de 30 m de longueur ont été déjà transportées sur de très grandes distances. La largeur de ces rubans est de 2,50 m et peut atteindre 3,20 m. Le prix de telles grandes glaces subira certainement dans un proche avenir une évolution tenant compte de la normalisation de ces productions. Il est tentant de penser qu'un réflecteur — préconcentrateur, *en position fixe* — serait constitué par une lame de verre de 3 × 30 m dressée sur sa tranche longue, et déformée de manière à ausculter un segment de cylindre parabolique. Avec des épaisseurs courantes de glace recuite, le foyer peut être de 15 m; il peut encore être réduit avec des glaces durcies par une trempe légère. La ligne focale serait alors reprise par un concentreur de faibles dimensions (3 m × 0,50 m), lié au four, l'ensemble se déplaçant sur une trajectoire asservie à la position du soleil.

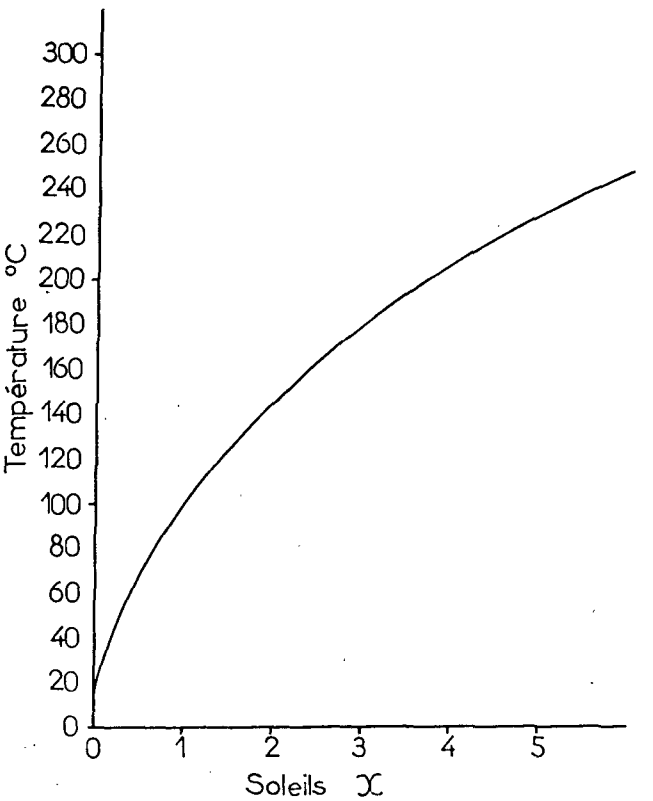


Figure 7

La mise à la disposition des physiciens et des thermiciens de produits verriers très différents en caractéristiques physiques ou en dimensions de ceux auxquels ils pouvaient s'adresser jusqu'ici nous semble de nature à faciliter la résolution du nombre de problèmes auxquels ils s'étaient heurtés.

Bibliographie

Gardon, R., *J. Am. Chem. Soc.*, vol. 41, n° 6, juin 1958, p. 200.

Geffcken, W., *Glas. Ber. 25*, 1952, p. 392 à 396.

Genzel, L., *Glas. Ber. 24*, 1951, p. 55 à 63; *Glas. Ber. 25*, 1952, p. 134 à 139.

Parmelee, G., *A S H V E*, oct.-nov. 1945, p. 562 à 576; *A S H V E*, juin 1948, p. 116 à 126.

V^e^ Internationaler Glaskongress, *Glas. Ber.*, VII, 1959.

Résumé

Les progrès récents réalisés dans différents domaines par les verriers doivent permettre aux physiciens et aux thermiciens de tirer mieux parti des produits verriers pour accroître l'efficacité des capteurs de l'énergie solaire.

Pour les pièges utilisant l'effet de serre, l'auteur attire l'attention sur la forme du front d'absorption situé habituellement vers 2,5 microns, et sur les manières d'agir sur celui-ci : soit par la composition du verre et le contrôle de certaines impuretés, notamment du fer avec sa bande 1,1 μ, soit par l'épaisseur de la lame de verre. L'intervalle qui séparait l'extrémité longue de la courbe du rayonnement solaire de l'extrémité courte de la courbe de rayonnement du récepteur s'amenuise au fur et à mesure que l'on recherche, au besoin par une semi-concentration, à accroître la température de ce dernier; dès lors, les pièges habituels perdent de leur efficacité si le verre n'est pas spécialement adapté à l'effet cherché. L'auteur attire ensuite l'attention sur le rôle prépondérant joué par les vitrages multiples. Un vitrage triple a une efficacité comparable à ce que donneraient 3,25 soleils frappant le récepteur nu. Les vitrages multiples actuellement industrialisés sont soudés d'une manière autogène ou sertis dans des garnitures métalliques ou plastiques parfaitement étanches. L'efficacité du piège peut également être accrue par un très léger dépôt d'or sur la face interne de la dernière lame de verre.

Pour la réalisation de grands concentreurs qui jusqu'ici doivent renoncer aux pièces uniques et sont dès lors constitués par un damier d'éléments plans approximativement parabolisés, l'industrie verrière peut désormais fournir des rubans de glace polie de longueur indéfinie. On peut penser que ces longues glaces permettront de réaliser très simplement des pré-focaliseurs statiques en forme de cylindre parabolique. C'est alors le deuxième focaliseur associé au four qui est asservi au déplacement du soleil.

SPECIAL GLASSES AND MOUNTINGS FOR THE UTILIZATION OF SOLAR ENERGY

(Translation of the foregoing paper)

I. Peyches *

The physicists and heat engineers who have been working on the problems raised by the utilization of solar energy have been using the materials available on the market in developing their designs. The commercial vitreous materials they have thus been employing — plate glass and window glass — were developed, however, for uses that were usually very different from the specialized conditions of these new applications.

This study proposes to determine the optimum conditions that glass for such uses must satisfy, and to indicate the technological opportunities now available to the industry for satisfying them.

We shall here be concerned entirely with the strictly thermal aspects of the problem. We shall not consider the special cases utilizing only part of the solar spectrum, such as photopiles.

With this restriction, the problem now breaks down into two extreme cases. One may wish to collect the maximum quantity of energy at low concentration, and thus also of low thermal potential, as for domestic space heating, cooking, water purification, etc. On the other hand, a high concentration of energy may be desired to produce elevated temperatures, approaching that of the source itself (solar furnaces).

The former case makes use of the trap effect exerted by glass as a result of its high transparency to solar radiation, and of its high opacity to what was once called dark heat. This is the well-known hot-house effect. The latter case utilizes only the reflector effect of a mirror, and may make use of materials other than glass, such as certain metals that take a high superficial polish. The dioptric concentration effect (lens effect) is not utilized, for obvious technical ressons (the impossibility of economic production of large lenses).

When glass is to be used as a reflector, it is usually metal-coated on its *back surface*. The metal film is thus perfectly protected against the corrosive action of the atmosphere. While metal coating on the front face has also been used and protected by a thin film of silicon monoxide, this technique has not been generally adopted. In the present state of the art, the reflected radiation must therefore pass twice through the glass sheet. This is a circumstance common to both the extreme cases mentioned above, and brings them close to each other. In all cases, the radiation passes through the glass and is then absorbed or reflected by a surface that may or may not be in contact with the glass.

Consider an original radiation characterized by a certain spectral distribution. We refer here to the solar radiation. As an approximation, it may be identified with the radiation of a black body at 6 000°K, modified by passage through the earth's atmosphere, and thus, for all practical purposes, confined to the region between 0.3 μ and 2.5 μ. Scattering in the atmosphere, unfavourable to the short wavelengths, shifts the maximum fixed by Wien's law at 0.475 μ towards the yellow region of the visible spectrum. The position of the true maximum varies with the zenith distance of the sun and the geographic conditions, being around 0.503 μ for a solar zenith distance of 25° and around 0.635 μ for a zenith distance of 60°.

In any case, the principal area under the solar emission curve coincides with the gap of maximum transmission of the chromatic absorption curve of commercial flat glass, that is, plate glass or window glass (figure 1).

In figure 1:

S = curve of useful solar radiation (arbitrary units)

A = total transmission factor of mirror glass 1 cm thick

A' = total transmission factor of window glass 1 cm thick
(Note the absorption band towards 1.1 μ due to the presence of ferrous iron in these glasses as an impurity.)

N = radiation curve of black body at 400°K

N' = radiation curve of black body at 600°K

(The curve of P will be explained later on.)

On the other hand, the low-temperature black body emission curves are located entirely in the spectral region where these glasses are practically opaque.

But this apparent simplicity, of considering glass as perfectly transparent to the solar radiation and perfectly opaque to the radiation of the heated receiver, is not adequate on examination.

Merely to indicate the order of magnitude, consider what happens to primary radiation incident on a plate of glass of "commercial" thickness, made of "commercial" glass. Since the initial intensity of the

* Director, Research Laboratory, Compagnie de Saint-Gobain, Paris.

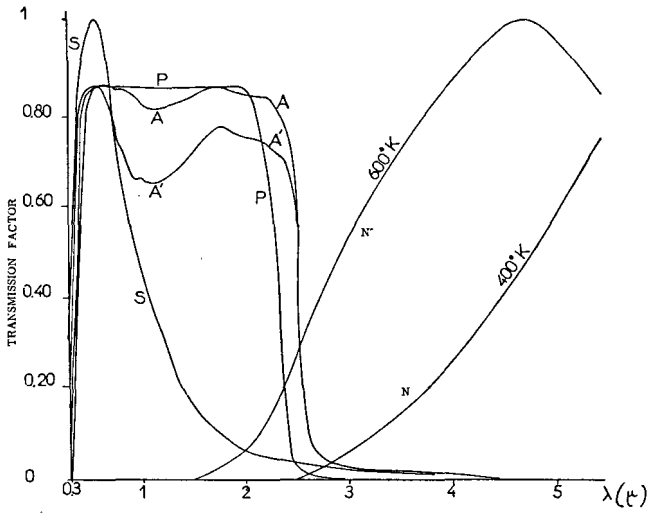


Figure 1

radiation is taken arbitrarily as 100, the reflection on the first face cuts off 4 per cent of this, with a slight chromatic effect due to the form of Fresnel's law giving this reflected part:

$$\left(\frac{n-1}{n+1}\right)^2$$

This reflected radiation is not lost in the case of a reflector, but it is lost with a solar collector. The absorption of the glass itself, for the thickness being considered (several millimetres), will take 6 per cent of the 96 per cent transmitted, with a possible new chromatic effect. In this phase, there are two cases to be considered:

(a) *Reflector* (figure 2)

Ninety per cent of the incident radiation reaches the back surface, which is assumed to be metallic and reflecting. This surface, for its own account, absorbs about 9 per cent. After reflection and in the course of the new passage through the glass, 6 per cent of the remaining radiation, or about 5 per cent of the initial radiation, will also be dispersed in the glass. On passage through the front face, glassy reflection will again take place but, when once again reflected by the metal layer, the main part of this radiation will be in the useful emergent beam, which therefore remains of the order of 76 per cent, to which we must add the 4 per cent from the first reflection. The *useful* beam as a whole contains 80 per cent of the initial energy. It should be noted that *two* successive reflecting surfaces are to be considered: that of the orientator and that of the

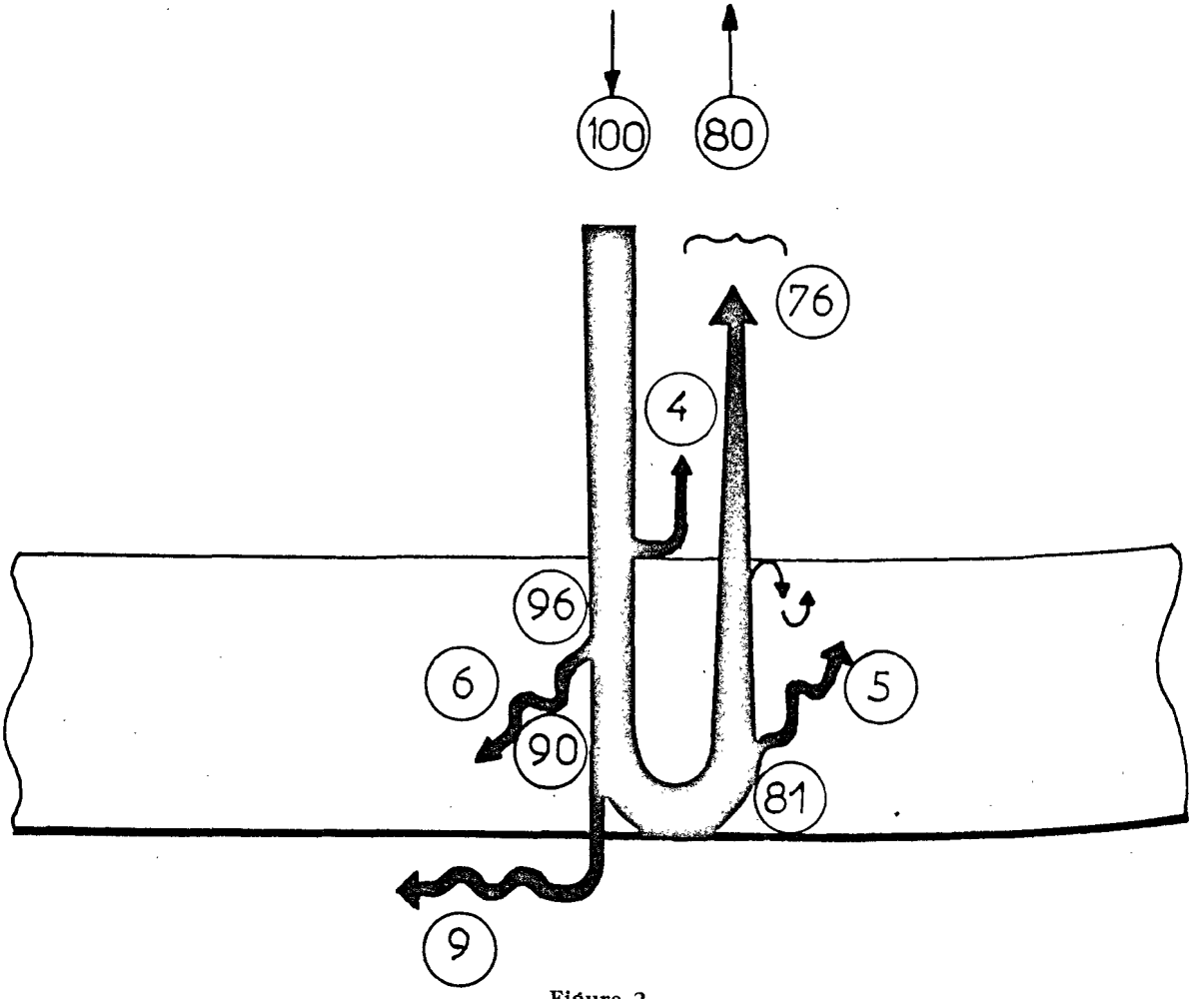


Figure 2

concentrator. At the focus, then, 64 per cent of the incident radiation, or roughly two-thirds, will thus be available. For an energy density of 1 kWh/m² reaching the installation, 0.2 kWh/m² will be absorbed in the orientator, and 0.16 kWh in the concentrator.

(b) *Collector* (figure 3)

Here the second face is not metalized. Of the 90 per cent of the energy reaching it, 4 per cent will again undergo vitreous reflection and return through the glass sheet, to be almost completely lost in space.

Eighty-six per cent of the incident energy will *in principle* be useful in the collection enclosure. Assume that this enclosure is a black body, materially separated from the sheet of glass, so that only radiative exchanges will be involved, and that the black body is perfectly insulated on its back surface. It will become heated, and will itself emit. Thus, in effect, the sun, the primary source, is replaced by a secondary source at a much lower temperature —say, for example, 450°K. The limitation is the obvious result of the losses through the glass. But with respect to this radiation, which has its maximum near 6.4 and which begins at about 2.5, glass, as already stated, is practically a black body. The portion of this radiation penetrating the glass, after allowing for the portion reflected, is therefore totally absorbed in a thin layer that contributes to the heating of the enclosure, but which, by reradiation and conduction towards the outside, causes the losses defining the equilibrium state attained.

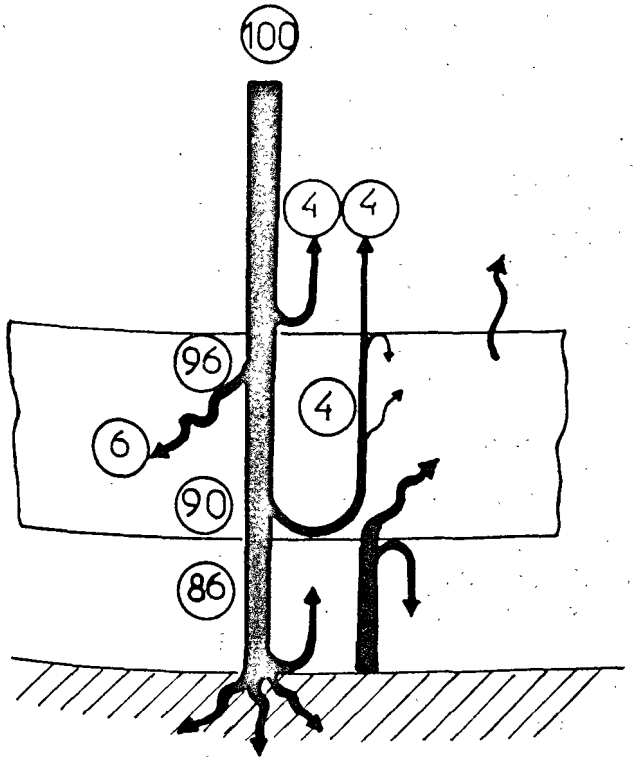


Figure 3. Black body receiver

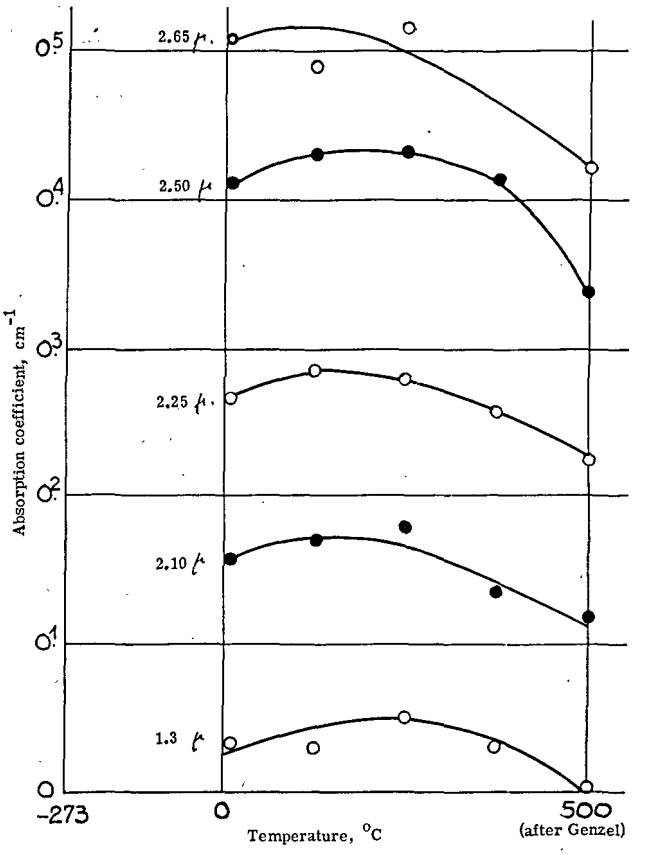


Figure 4

All this is intuitive. It will be realized, without calculation, that for the reflector, the glass need only be as transparent as possible to solar radiation; while for the collector, the glass must satisfy both this condition and be as opaque as possible to the emitted radiation of the collector itself.

On consideration, these problems become more complex. Consider the simple example of the hothouse effect.

We remark, incidentally, that while the Fresnel-Lorentz law giving the fraction of vitreous reflection

$$\left(\frac{n-1}{n+1}\right)^2$$

does apply to *directed* radiation, such as that from the sun, and leads to the value of 4 per cent mentioned above, it does not apply, in this form, to the *diffuse* radiation coming from the secondary source of a collector, and one must, in fact, count on 9 per cent reflection. The glass, which, in strongly absorbing the secondary radiation, itself becomes heated, will then give rise, layer by layer, to a whole process of reradiation, of which one part, emitted in the direction of the receiver, will be utilized, while the remainder will be lost. Gardon has indicated the complex mathematical apparatus for the formal treatment of this case, and has given figures relating to a symmetrical situation, but not the bisymmetric situation that characterizes a sheet of glass placed between two heat sources at different temperatures.

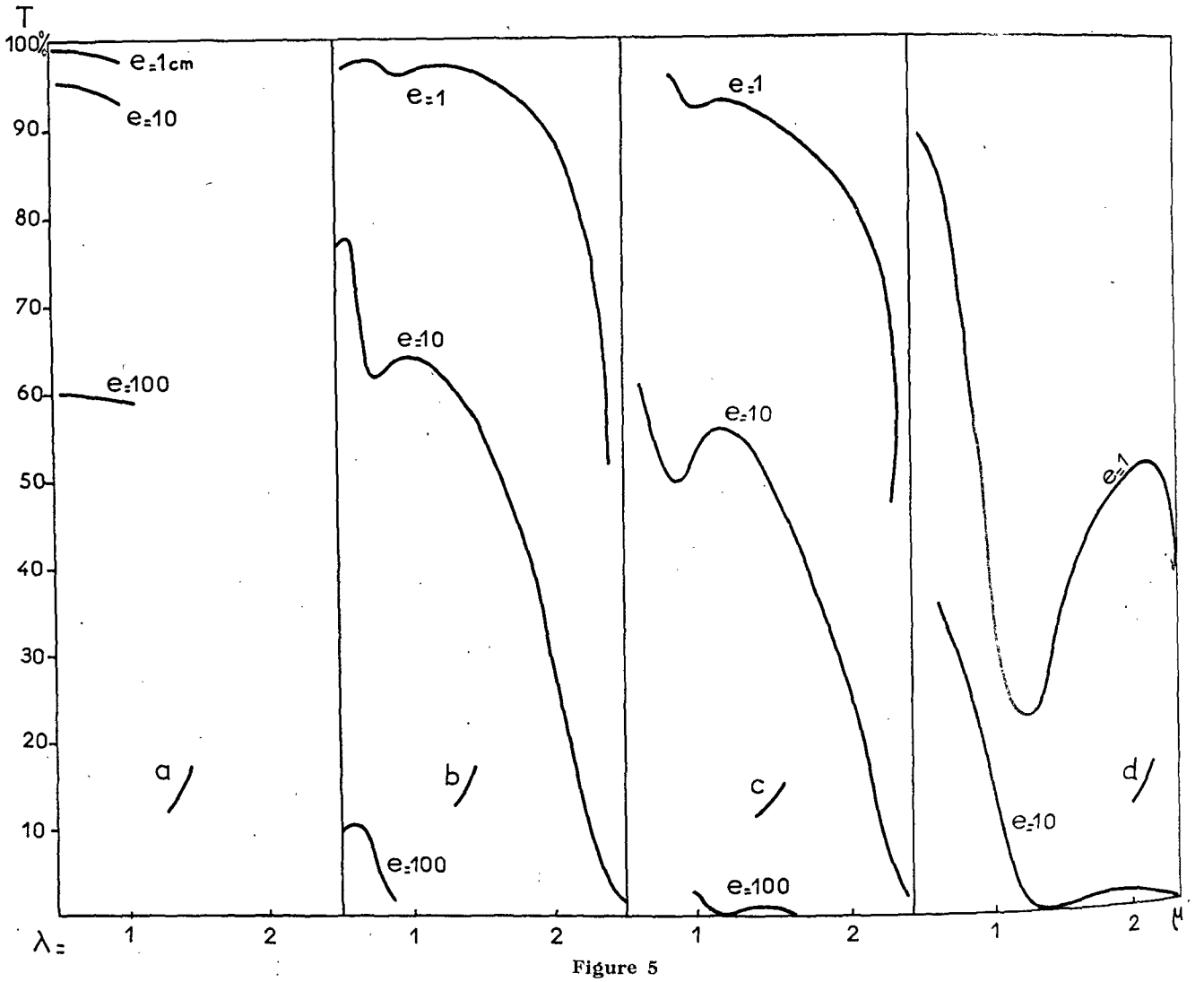


Figure 5

If this problem did not seem important before, it was because the hot-house effect long remained confined to low temperatures, say, below 100°C. The energy radiated at this temperature by the receiver, even one behaving like a black-body, still remained small, and the glass sheet absorbing this energy differed but little in temperature from the ambient.

But the tendency has been to increase the operating temperature of the receiver with the object of improving the Carnot cycle in the thermodynamic applications. *At low concentrations*, one might envisage the utilization of molten metals or alloys as heat-transfer agents, or the vaporization of liquids. In this case, on the one hand, the heating of the glass is not negligible, and its opacity in the infrared decreases in consequence, as shown by figure 4. On the other hand, the emission curve of the receiver shifts towards the short wavelengths, and the receiver emission begins to filter through the transmission gap of the glass.

So long as the absorption factor of glass still remained very close to unity for the long wavelengths, the role of its thickness did not appear. But, on approaching the transmission gap, the exponential form of Beer's law could now totally distort the shape of the transmission curve when the thickness varied. Figure 5 shows, for four types of glass, the effect of thickness (e) varying by multiples of 10.

To trap the maximum energy for a selected receiver temperature, we have several variables at our disposition. Let us examine the role of each.

The *composition* of the glass, which affects its transmission: the presence of the band centered about 1.1 μ and due to the presence of ferrous iron in the glass is determined, according to all evidence, since it attenuates the transmitted solar radiation without making up for it by reducing reradiation of the secondary source.

As soon as a considerable amount of energy is radiated by this secondary source below 5 μ, ordinary glass can no longer be considered totally opaque. It would be of interest in this case to consider the borosilicate type of glasses (Pyrex), for at thicknesses of several millimetres, they stop all radiation longer than 3 μ (curve P, figure 1).

Thickness: the following table gives the transmission factor for thicknesses in multiples of 10.

1	*10*	*100*
1.000	1.000	1.000
0.995	0.951	0.605
0.990	0.904	0.366
0.980	0.817	0.133
0.970	0.737	0.047
0.960	0.665	0.017
0.950	0.599	0.006
0.900	0.348	—
0.800	0.108	—
0.700	0.028	—
0.600	0.006	—
0.500	0.001	—
0.400	0.0001	—

The slope of the part of the transmission curve that separates a region of high transparency from one of lower transparency is steeper, the greater the thickness. By selecting an appropriate thickness, more reradiated energy may be *retained* than is lost in primary energy.

The *transmission factor* may be affected not only by these two intrinsic causes, but by superficial *treatment* as well.

A gold film deposited on the inner surface of the glass, provided its thickness is correct, reflects only a little of the near infrared in the solar radiation, but much of the farther infrared. Such films may be formed on large surfaces by simple chemical treatments.

The emissivity of the collector itself should be so selected as to correspond to a black body below 2.5 μ, but on the other hand to be low above that wavelength.

But it is primarily the factor of over-all loss of the glass screen that produces an important effect, and in this connexion multiple panes are especially deserving of attention.

Let us now examine the role of the trap due to 1, 2 ... n sheets of glass.

Let D be the density of the solar flux received at the level of the installation. θ_0 is the ambient temperature, θ the temperature of the receiver, assumed to be a black-body, without losses on its rear face. θ is the temperature reached under steady state conditions by a single sheet of glass, and T its over-all transparency to the solar radiation. T is zero with respect to the radiation of the surroundings, and, in first approximation, with respect to the reradiation of the receiver as well.

The equilibrium of the receiver is expressed as follows:

$$\sigma \theta^4 = DT + \sigma \theta_1^4$$

The equilibrium of the glass sheet is given by:

$$l \sigma \theta_1^4 = D(1 - T) + \sigma \theta_0^4 + \sigma \theta_4$$

Whence

$$\sigma \theta^4 = D(T + 1) + \sigma \theta_0^4$$

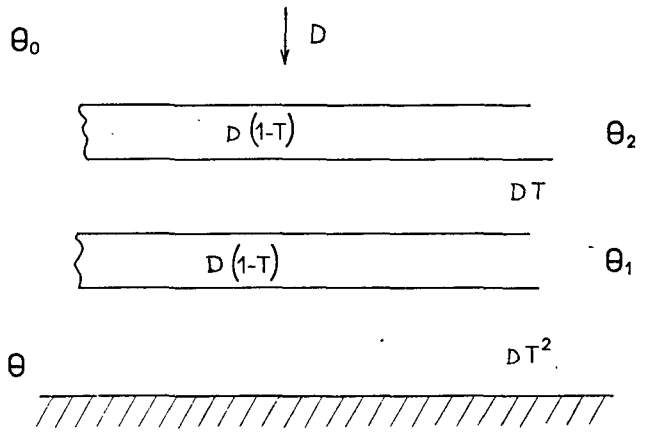


Figure 6

If T is close to unity (very clear and very thin glass), then everything takes place as though the receiver received the radiation of *two suns*.

Assume now that the trap consists of *two* identical sheets of glass (double pane) (figure 6), which will assume the respective temperatures θ_1 and θ_2.

We now write, similarly, the equilibrium conditions:

Receiver:

$$\sigma \theta^4 = DT^2 + \sigma \theta_1^4$$

1st sheet counting from the receiver:

$$2 \sigma \theta_1^4 = DT(1 - T) + \sigma \theta^4 + \sigma \theta_2^4$$

2nd sheet:

$$2 \sigma \theta_2^4 = D(1 - T) + \sigma \theta_1^4 + \sigma \theta_0^4$$

It follows immediately that:

$$\sigma \theta^4 = D(1 + T + T^2) + \sigma \theta_0^4$$

The generalization is obvious. For n sheets we shall have:

$$\sigma \theta^4 = D[1 + T \ldots\ldots + T^n] + \sigma \theta_0^4$$

If T is close to unity:

$$\sigma \theta^4 = D(1 + n) + \sigma \theta_0^4$$

Thus, with two sheets, the temperature attained corresponds to what would be given by three suns.

The curve of figure 7 gives the temperature attained by a black body irradiated by x suns (θ_0 = 290°K or 17°C).

The value $x = 1$ corresponds to the bare black body in a vacuum. In air, owing to convective cooling, the steady temperature will be only 54°C.

With the over-all transmission factor of 0.86 adopted above, a triple pane would correspond to 3.25 suns.

All the interest attaching to multiple panes in designing a solar energy collector will thus be apparent. The use of a single pane of equivalent thickness would not give the same result, since in that case the interchange between the layers would take place by conduction as well.

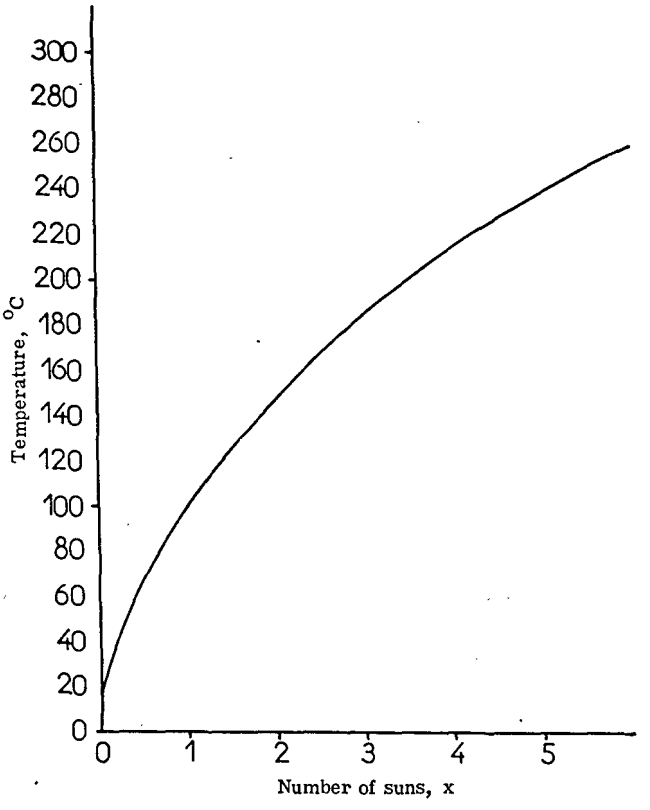


Figure 7

During the last few years, at the initiative of the glass-making industry, the use of double and triple panes of large size (single surfaces of several sq m) has become general in building. Certain of these embodiments are welded assemblies, which ensure total sealing of the intermediate spaces.

To remain within reasonable limits as to the number of glass sheets assembled in this way, it will be seen that without heat outflow, the receiver temperature could not exceed 200°C. To go beyond that level, one would have to have radiation at least partially concentrated falling on the receiver.

The problem of concentration for energy delivery purposes is free of certain difficulties encountered with mirrors used to form astronomical images. In the latter case, if optimum resolution is desired, the reflected or diffracted waves must be in phase, and mirror assemblies cannot be used. It would, on the contrary, be a rule to use mosaic mirrors for large orientators or concentrators. If only low concentration ratios are required, then any reflector type at all may be used, but if the temperature is to be maximized, the solar image must be high-grade enough to have the maximum energy distributed over the minimum useful surface. For low-power solar furnaces, parabolic mirrors of large aperture and short focus are used, but for furnaces of higher power, the embodiments are of mosaic type and the focus is obtained by the individual deformation of the components. This severe condition makes the mountings extremely complicated, and involves great difficulties in adjustment. Very recently, however, new processes of continuous production of polish plate-glass make a plate-glass ribbon of *any desired* length available to the specialists. The length of these ribbons is limited only by transport problems, but units 30 m long have already been shipped very long distances. The width of these ribbons is 2.50 m and may reach 3.20 m. The cost of such large glass plates will certainly undergo modification in the near future, as production becomes standardized. It is interesting to consider that a reflector-preconcentrator, *in fixed position*, will be made of a single sheet of glass 3 × 30 m, on its longitudinal edge and deformed into a segment of parabolic cylinder. With the present thicknesses of annealed plate glass, the focal length could be 15 m, and this could be still further reduced with lightly hardened plate glass. The focal line will then be taken up by a small concentrator (3 × 0.50 m) connected to the furnace, with the whole assembly moving on a trajectory following the position of the sun.

This new availability, to physicists and heat engineers, of glass products varying greatly in physical characteristics or dimensions from those formerly available, appears to be of a nature to facilitate the solution of a number of problems they have encountered.

Bibliography.

For bibliography, see end of French version.

Summary

The recent advances in various fields of glass-making will enable physicists and heat engineers to make better use of glass products to improve the efficiency of solar energy collectors.

For the radiation traps utilizing the hot-house effect, the author calls attention to the shape of the absorption edge, usually located near wavelength 2.5 microns, and to the methods of influencing it by modifying the composition of the glass and controlling certain impurities, especially iron with its band at 1.1 microns, or by modifying the thickness of the glass plate. The interval between the long-wave

end of the solar radiation curve and the short-wave end of the receiver radiation curve diminishes as the receiver temperature is increased, for example, by using semi-concentration techniques. When this is done, the conventional radiation traps lose their effectiveness unless the glass used is specifically adapted to the effect desired. Attention is next called to the importance of multiple panes. A triple pane has an effect comparable to what would be given by 3.25 suns incident on the bare collector. The multiple panes now industrially developed are assembled by gas welding or placed in completely hermetic metal or plastic mountings. The efficiency of the collector may also be improved by an extremely thin film of gold deposited on the inner face of the last glass plate.

To build the large concentrators that could not, up to now, be made in a single piece, and had to be constructed out of a checkerboard assembly of plane elements deformed into approximately parabolic shape, the glass-making industry is now in a position to supply polished plate glass strips of any desired length. Those long pieces of mirror glass should permit the very simple realization of static pre-focus units of cylindro-parabolic shape. In that case, it will be the second focusing element of the furnace that will follow the motion of the sun.

FURTHER STUDIES ON SELECTIVE BLACK COATINGS

H. Tabor, J. Harris, H. Weinberger and B. Doron *

In 1955, at the First World Symposium on Solar Energy, the basic principles of selective radiation applied to solar energy utilisation were laid down (1) and a practical collector using selective surfaces was demonstrated. At the same symposium, Gier and Dunkle (2) discussed the importance of selective spectral characteristics of materials for solar collectors. Subsequently, work on selective surfaces was reported from the Massachusetts Institute of Technology (3) and the University of Wisconsin (4), and several other papers on the subject have appeared. Very recently, Gier and his colleagues have published an excellent report (5) on spectral properties of surfaces, with special reference to their use for solar energy, though the accent is on space applications.

Since 1955 the National Physical Laboratory of Israel has used selective surfaces for experimental work and has set up an industrial plant for the blacking of commercial solar collectors. It is only in the last two years, however, that it has been possible to devote time and energy to a more basic study of what selective surfaces are and how their properties are related to the methods of production. This research is by no means complete, but some observations to date are reported in this paper.

Requirements of a selective black surface

In effect, an ideal selective black surface for a solar heat collector is a band-pass reflection filter; in the solar spectrum reaching the earth, that is, in the range 0.3 to 2.5 microns, the surface should be non-reflecting — a complete absorber — whilst for longer wavelengths it should be a perfect reflector, that is, have negligible thermal emissivity. For terrestrial applications up to about 300°C the transition between absorption and reflection should occur at about 2.5 microns; for higher temperature, the transition point should be at a somewhat shorter wavelength. (Both graphical and mathematical methods are available for determining the optimum transition point.)

Because the real selective surface does not have an ideal spectral distribution, it is usually more convenient to deal with the integrated effects: the integrated absorbtance[1] to solar radiation, α — which means measurement using some standard sun — and the total thermal emittance e, at the temperature of intended use, are also measured. Indeed, it is usually easier to measure the integrated values than the spectral distribution, though a study of the latter is necessary when trying to develop better surfaces.

It turns out in practice that, in general, any attempt to increase α leads also to an increase in e. The significance of changes in α and e may be determined as follows:

The instantaneous efficiency η of a solar heat collector is:

$$\eta = \frac{\alpha \beta PQ - (l_{r\tau} + l_{c\tau})}{PQ} = \alpha\beta - \frac{l_{r\tau} + l_{c\tau}}{PQ} \quad [1]$$

where β = transmission coefficient of the collector system
P = concentration ratio (area of solar collector aperture to area of heated surface)
Q = solar radiation intensity per unit area of solar aperture
$l_{r\tau}$ = heat losses per unit area from heated surface at temperature T, due to thermal radiation
$l_{c\tau}$ = ditto, due to convection and conduction.

Equation [1] is the instantaneous efficiency; as Q varies during the day, the mean efficiency during the day must be computed by graphical or semi-algebraical methods. It will then be found that the average efficiency $\bar{\eta}$ is given approximately by

$$\bar{\eta} = a\left[\alpha\beta - b\left(\frac{l_{c\tau} + l_{r\tau}}{P\bar{Q}}\right)\right] \quad [2]$$

where a and b are constants somewhat less than unity and $\bar{Q}$ is the mean solar intensity during the day.

Assuming that α and $l_{r\tau}$ are variable, by differentiation:

$$d\bar{\eta} = a\left[\beta\, d\alpha - \frac{b}{P\bar{Q}}\, d l_{r\tau}\right] \quad [3]$$

The condition that simultaneous changes of α and $l_{r\tau}$ shall not reduce $\bar{\eta}$ is that

$$d\alpha \geqslant \frac{b}{\beta P\bar{Q}}\, d l_{r\tau} \quad [4]$$

In practice, b is about 0.8 whilst β is of the order of 0.7 to 0.9, dependent upon the number of trans-

* Nationla Physical Laboratory of Israel, Jerusalem.

[1] "Absorbtivity" and "emissivity" refer to properties; "absorbtance" and "emittance" to values (cf. "resistivity" and "resistance").

mission and reflection surfaces. Thus, as a first approximation, equation [4] may be written

$$d\alpha > \frac{1}{P\bar{Q}}\, d l_{r\tau} \qquad [5]$$

Now $l_{r\tau} = e_e \sigma (T^4 - T_0^4)$

where σ = Stephan-Boltzman constant
T = temperature of the heated surface
T_0 = temperature of its surrounding envelope
e_e = effective emittance of the heated body in its surroundings.

Equation [5] becomes:

$$d\alpha > \frac{\sigma (T^4 - T_0^4)}{P\bar{Q}}\, de_e \qquad [6]$$

In any practical design T, T_0, P, $\bar{Q}$ are known, so that equation [6] is readily evaluated. As an example, in a flat plate collector where $P = 1$; $\bar{Q} = 540$ kcals per hr, m² (200 Btu per hr, ft²); $T = 343$°K; $T_0 = 298$°K:

$$d\alpha > 0.6\, de_e \qquad [7]$$

If the surroundings have an emittance approaching unity or the heated body is small compared with its envelope, the effective emittance e_e is almost identical with the actual emittance e.

Thus, for example, if a selective black surface for this application has an absorbtance of 0.90 and an emittance of 0.10, and a modified blackening process will raise the absorbtance to, say, 0.93, the emittance should not rise above 0.15 or no benefit will result from the greater absorbtance.

For a focusing collector with $P = 3$, $\bar{Q} = 460$, $T = 160$°C and $T_0 = 40$°C, equation [7] becomes

$$d\alpha > 0.89\, de_e$$

and the relative importance of α and e are not very different from the flat plate collector case. Only when the concentration ratio is large, and the operating temperature not unduly high does the dominant term become the absorbtance.

In addition to the optical requirements of a selective surface there are some practical considerations: it must be stable against prolonged heating, stable against atmospheric corrosion and, for space applications, not eroded by meteorites, etc.

Because a selective surface *is* a surface — and as will be seen later, is formed by providing an extremely thin coating to a metal base — this coating cannot offer any substantial corrosion protection to the base. Thus the base must itself be a surface stable to the effects of atmospheric corrosion and oxidation. For this reason the first selective surfaces used in this laboratory employed a nickel-plated base metal, but for moderate temperatures, such as in water heaters, other metals such as copper and galvanised iron can be used. Since such metals tarnish in the open air it becomes almost axiomatic that selective surfaces should be protected from rain and dew by a (transparent) window.

Optical and chemical aspects

Methods of measuring absorbtivity (4, 6) and emissivity (4, 5, 7) have already been described.

It has been pointed out (1) that the optical requirements indicated in the previous section can be achieved by one of two mechanisms:

(*a*) By taking a polished metal base, having low emissivity and coating it with a very thin optically dark surface layer which is substantially transparent for wavelengths above about two [2] microns.

(*b*) By taking any base (but preferably dark in colour) and covering it with a layer of finely divided metal, such as gold, where the particle size is such that, for visible light, it is virtually black but at longer wavelengths the true reflecting character of the metal is dominant.

Most of the practical surfaces are of the first class (*a*). As one might expect from theoretical considerations, the thin dark coating is usually a semi-conductor. Some five or six coatings — usually oxides or sulphides — were tried in the laboratory, the most important being copper oxide (on aluminium) and a nickel-zinc-sulphide complex, called "nickel-black", obtained by electrodeposition.

The copper oxide layer is produced by dipping an aluminium plate, whose surface has first been "opened" or provided with a porous very thin oxide layer — by mild anodising, MBV [3] treatment etc. — into a hot acidic solution (90°C) of cupric nitrate and potassium permanganate for ten minutes. This causes a reddish brown deposit which appears to be a mixture of cupric and cuprous oxides. The plate is then dried and heated in air at 350°C for 5 to 10 minutes so as to convert the cuprous oxide to cupric oxide, resulting in a nearly black surface. Emissivities of the order of 0.11 are obtained, but it is difficult to get absorbtances above 0.85. Such surfaces are stable to prolonged heating up to 200°C or more and show very good corrosion resistance. (A collector plate with glass protection window has been exposed on the roof of the laboratory for nearly four years and shows no sign of deterioration.) However, this treatment is not very consistent and appears to depend very greatly on the nature of the aluminium used: every batch needs some modification in the process. For this reason this process has not been pursued further, though copper oxide on aluminium, produced by other means, has been studied by the MIT and Wisconsin groups. The MIT group sprayed weak copper nitrate solution onto a heated aluminium plate and then baked the resultant thin copper nitrate layer in air to yield copper oxide. By careful choice of concentration, drop size, spraying rate, baking cycle, the group was able to obtain good surfaces with $\alpha \sim 0.90$ and $e \sim 0.10$. The Wisconsin group obtained about the same results by oxidising a copper plate in a solution of sodium chlorite and

[2] Terrestrial applications, moderate temperature.

[3] A trade solution comprising 3 per cent sodium carbonate and 1½ per cent sodium chromate, used at 90°C.

sodium hydroxide or by electroplating a thin layer of copper on a base metal and then oxidising in the above solution or by heating.

The "nickel-black" layers have proven to be extremely interesting: in addition to being used for the last two years on commercial solar water heaters they have great scientific interest and have therefore been the subject of special study. Because the number of variables in the process is very large — temperature, pH, buffers, current density, electrode potential — the possibilities of getting specifically desirable results are improved; on the other hand a large number of variables means that special care is required in controlling the process when used industrially.

An important feature of the nickel-black coatings on smooth metal bases is that the resultant layer is smooth (cf. the copper oxide layers which are usually matt) and this leads to the possibility of interference colours. This was noticed quite early and has been used to improve the absorptivity in the solar spectrum by getting an interference zero (or near zero) reflectivity in the middle of the solar spectrum.

An even more fascinating observation was that, if the current density used in the electrodeposition were changed in the middle of the process, better results could be obtained. This at once suggested that:

(*a*) The optical constants of the layer could be changed by changes in conditions;

(*b*) Using a two-layer optical interference phenomenon instead of a single layer clearly gives greater possibilities, in particular in being able to extend the effect of destructive interference over a wider range of wavelengths.

All the deposited layers are extremely thin — from as little as 250 Ångströms to about a thousand Ångströms.[4] Since there was reason to believe that thick electrodeposited layers do not have the same composition as thin layers, the chemical examination involved handling very small quantities of material (about 500 microgrammes) and micro analytical techniques had to be established for the determination of the constituents of the layers. Nickel, zinc and sulphur have been determined, and it is clear that there are small amounts of oxide and possibly hydroxide in the layer. It has been confirmed that, with change in current density, the ratio of nickel, zinc and sulphide in the deposit changes. Thus, for example, the following figures were obtained.

Current density (per cent)	*0.5 ma/cm²*	*1.5 ma/cm²*
Nickel	33.5	15
Zinc	26	56.5
Sulphur	13	12.5
Unaccounted for (probably oxides and hydroxides)	27.5	16
Optical constants, $n - ik$ ($\lambda = 589\ \mu$)	1.85-0.83i	1.68-0.35i

[4] Thicknesses were measured by multiple-beam interferometry.

There is an unstable zone between these current densities so that an infinitely graded range of compositions and optical constants is not obtainable; above and below the unstable zone the composition and optical properties show only slight changes.

A method of measuring the optical constants of these layers was evolved, based upon measuring the intensities of the reflected light polarised parallel and perpendicular to the plane of incidence at a particular angle of incidence. This method is at present used on layers thick enough not to be confused by reflections from the base, but it is shortly expected that this restriction may be removed when the very cumbersome mathematical formulae involved have been put through a computer.

It has been confirmed that the optical constants change with the current density — as one would expect if the chemical composition changes — and this may open up a new area of research: tailor-made thin film optical filters.

A recent mathematical analysis (8) has been carried out; it shows that, whilst to obtain an interference zero (blooming) on a metal base puts severe limitations on the optical properties of the superimposed layer, a double layer gives a double infinity of film combinations that will give blooming.

It is now believed that this explains the very good results obtained with nickel-black. Thus absorbtances of about 0.91-0.94 and emittances of 0.11 or less have been obtained with the double layer. Professor Dunkle has kindly measured some of these surfaces, and the results are given by Gier *et al.* (5). The optical properties of one such layer (index No. 17) on nickel-plated copper show[5] the emittance as 0.049 at 95°F and the absorbtance to a 10 000°R Plankian radiator (sun in outer space) as 0.853. For sunshine at the surface of the earth (air mass = 2) the absorbtance has been computed as 0.901. Another measured layer (nickel-black on galvanised iron, index No. 71) has $e = 0.122$; α (outer space) = 0.885. For air mass = 2 the absorbtance is computed as approximately 0.886. These curves are shown in figure 1 with a standard sun ($m = 2$) superimposed.

Practical coatings and plant

About 2½ years ago a plant was set up in the National Physical Laboratory of Israel — subsequently transferred to the Negev Institute for Arid Zone Research in Beersheba — for coating plates up to 1 × 2 metres in size, using the nickel-black process. The plates are of galvanised iron which, because of its crystalline surface, yields higher emissivities, usually about 0.16-0.18. Galvanised iron, however, suited the local manufacturer, and many thousands of these plates are treated each year and incorporated into water heaters using a single cover glass.

[5] Table 5.2 in reference (5).

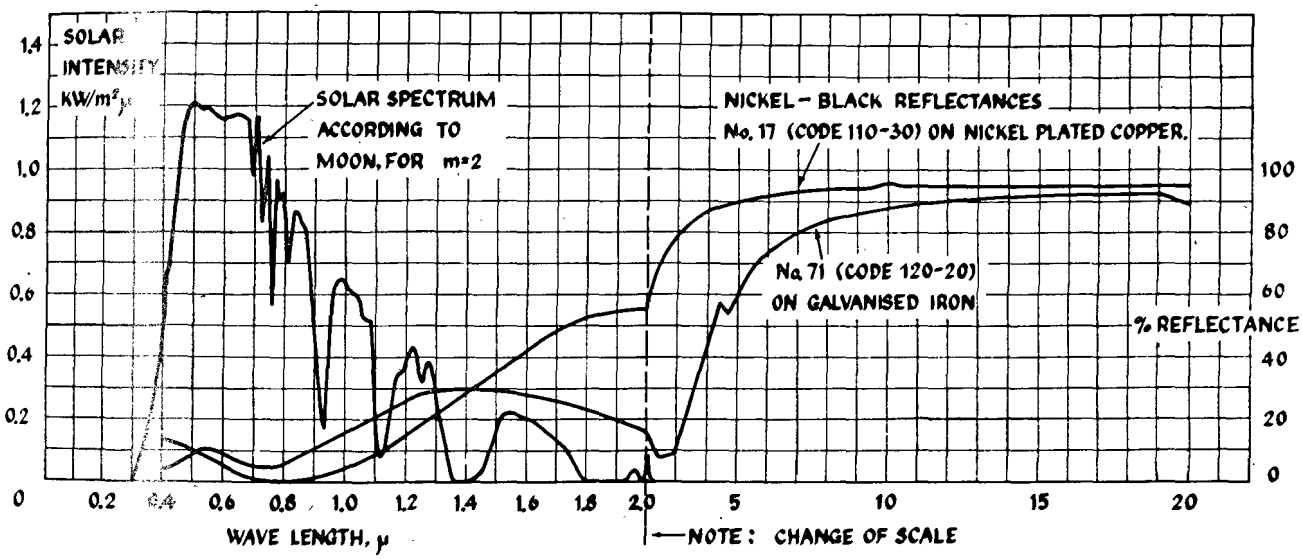


Figure 1

The plant consists of ten tanks containing the usual acid and alkali cleaning solutions, water rinses and the nickel-black solution. Because of the variability of the galvanised iron surface a thin flash of electrodeposited zinc is applied before the nickel-black solution.

Practical benefits

The improvement in performance of a solar heat collector gained by using a selective black coating depends on the operating conditions. Thus in outer space, where convection losses are non-existent, the improvement is very large. For terrestrial applications, convection limits the benefit of selective surfaces, and some designs have contemplated the use of partial vacuum conditions to reduce convection losses.

For the usual flat plate collector it is found that the use of a selective surface ($e \sim 0.1$) together with a single cover glass gives a heat loss slightly less than that of a normal black with two cover glasses; the benefit is thus the economy of the glass saved and the reduction of transmission losses.

For mirror systems of low concentration — such as the stationary cylindrical parabolic mirrors giving a concentration factor of about three (11) — the use of a selective surface can make all the difference in economic viability.

Thus figure 2 shows the computed over-all efficiency for a Carnot engine (sink temperature 40°C) coupled to a parabolic mirror (reflectance 0.85) giving a concentration of three and having a cylindrical receiver about 15 cm diam. surrounded by a 19 cm diam. glass tube. For a day with mean sunshine intensity of 0.59 kW/m² or 187 Btu per hr, ft², the peak performance with a black ($\alpha = 0.95$, $e = 0.95$) is 5.9 per cent conversion, at 100°C. For a selective black ($\alpha = 0.90$, $e = 0.1$) the optimum is 10.7 per cent at 160°C. The power output is thus increased by a factor of 1.81 because of the selective surface (and this ratio will be maintained approximately when real heat engines are used instead of the ideal Carnot). An output of 10.7 per cent could be obtained with the normal black if the concentration ratio of the mirror were raised to about seven, but in this case the mirror would require continuous adjustment of tilt.

It is thus seen that an increase in output of 81 per cent for the cost of the selective surface (about 5 per cent of total collector cost) may make all the difference between a feasible and non-feasible solar power unit.[6]

Another case in which the use of a selective surface may be mandatory is in solar operated absorption air conditioning. An operating temperature of at

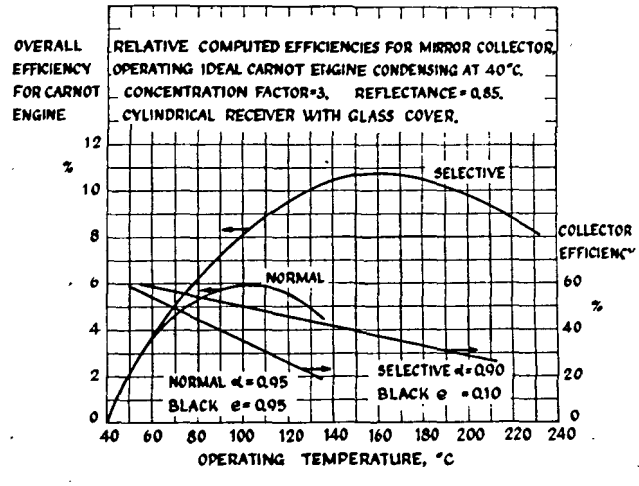


Figure 2

[6] See Tabor, H. and Bronicki, J. L., Small Turbine for Solar Energy Power Package, *Proceedings of the United Nations Conference on New Sources of Energy*, 1961; included above under agenda item II.C.1(*a*), paper S/54.

least 90°C at the collector is required for this application, whereas the ordinary flat plate collector is used for producing hot water at 50-60°C.[7]

From figure 1 of reference (9) the following *relative* clear-day collector efficiencies for large flat collectors at 200°F have been computed.

Case number	*Relative efficiency (per cent)*	*Relative to case 2*
1. Normal black ($e = 0.91$; $\alpha = 0.96$) one cover glass	15	0.49
2. Ditto, two cover glasses . . .	31	1.00
3. Selective black ($e = 0.12$; $\alpha = 0.92$) one coper glass	35.5	1.14
4. Ditto, two cover glasses . . .	39	1.26

This example brings out a well-known point of discussion, namely that the lower losses of a selective black can be obtained with a normal black by use of extra glass covers. Apart from the cost of the covers and their installation, this system of multiple covers will only become attractive when cheap non-reflecting windows have been developed. For focusing collectors multiple covers are usually very difficult to execute technically and the innermost cover operates at an elevated temperature.

New surfaces and outlook

Work is proceeding in the National Physical Laboratory of Israel on two new selective surfaces, one based on nickel-black and one on copper oxide.

The new nickel-black is obtained by electroplating from nickel sulphate (no zinc salts are included) and has emerged from some of the basic studies now being conducted. At first it was thought that this black was a black of the second kind,[8] i.e., a finely divided metal, since the simple electrolysis of nickel sulphate should yield nickel at the cathode, but it was soon discovered that the coating contained nickel oxide and nickel hydroxide and thus is a black of the first kind. This is due to the very strong basic conditions that develop near the cathode. If a trace of a buffer, such as ammonia, is added, a metallic nickel coating is produced. Some good absorbtivity-emissivity ratios have been obtained, but the process is at present very inconsistent, and the layer often not adherent. Much work still has to be done to make this a practical method.

The copper oxide on aluminium system is attractive because it shows a high chemical stability even at temperatures of several hundred degrees. But it is difficult to get very high absorbtivities whilst keeping the emissivity low. Experiments now in progress suggest that certain additives to the copper oxide may increase the absorbtivity which might then make this surface as good as nickel-black.

As understanding of the basic optical phenomena of selective surfaces increases so the ability to produce surfaces that more nearly approach the ideal can be expected to increase; with increased chemical studies the stability of the surfaces will also be improved. Present selective surfaces are not very far from the ideal,[9] but some improvement may be expected in the next few years.

[7] In addition to the higher temperature, it should be noted that the water heater has a "heating" efficiency whereas the collector for an absorption machine has a "boiling" efficiency, which is considerably less; see reference 10.

[8] Mechanism "(*b*)" in the section on Optical and Chemical Aspects, above.

[9] Further reduction of the emissivity below 0.1 has little significance for terrestrial applications where other losses may be dominant; for space applications lower emissivities are exploitable.

References

1. Tabor, H., *Selective Radiation, Bull. Research Council of Israel*, vol. 5A, No. 2, pp. 119-134, 1956, reprinted in *Trans. Conf. Use of Solar Energy*, Tucson, vol. II, part I, section A, pp. 24-39.
2. Gier, J. T. and Dunkle, R. V., Selective Spectral Characteristics as an Important Factor in the Efficiency of Solar Collector, *Trans. Conf. Use of Solar Energy*, Tucson, vol. II, part I, section A, pp. 41-56.
3. Hottel, H. C. and Ungar, T. A., *The Properties of a Copper Oxide Aluminium Selective Black Surface Absorber of Solar Energy*, vol. III, No. 3, pp. 10-15, Oct. 1959; also, D.Sc. thesis, 1958, T. A. Ungar, Massachussets Institute of Technology; and Ungar and Hottel, Contribution to Montlouis Conference, July 1958.
4. Salam, E. and Daniels, F., *Selective Coatings of Copper Oxide*, Dept. of Chem., University of Wisconsin; also, Selective Radiation Coatings for Solar Heating, and Selective Radiation Coatings: Preparation and High Temperature Stability (with P. Kokoropoulus), *Solar Energy*, vol. III, No. 4, pp. 19-23, Dec. 1959.
5. Edwards, D. K., Nelson, K. E., Roddick, R. D. and Gier, J. T., *Basic Studies on the Use and Control of Solar Energy, Report No. 60-93*, Dept. of Eng., Univ. of California, Oct. 1960.
6. Tabor, H. and Steinberger, I. T., An instrument for Measuring Absorbtivities for Solar Radiation, *Journ. Sci. Instr. 33*, pp. 356-358, Sept. 1956.
7. Tingwaldt, C. P., Measurement of Spectral Sensitivity in the Infra-red, *Trans. Conf. Use of Solar Energy*, Tucson, vol. II, part I, section A, pp. 57-61, Oct. 1955.
8. Weinberger, H., *Suppression of Reflection from Metallic Surfaces*, National Physical Laboratory of Israel, *Technical Note No. 1* under contract AF 61 (052)-279.
9. Tabor, H., Solar Collector Developments in Israel, *Solar Energy*, vol. III, No. 3, pp. 8-9, October 1959.
10. Tabor, H., Solar energy Collector Design, *Bull. Research Council of Israel*, vol. 5C, No. 1, pp. 5-27, Nov. 1955; reprinted in *Trans. Conf. Use of Solar Energy*, vol. II, part 1, section A, pp. 1-23.
11. Tabor, H., Stationary Mirror Systems for Solar Collectors, *Solar Energy*, vol. II, No. 3-4, pp. 27-33, July-Oct. 1958.

Summary

The background of selective surfaces for solar collectors is sketched in this paper, and the optical requirements of such surfaces restated: viz., a band-pass filter behaviour with high absorbtance for wavelengths up to about 2.5 microns (the exact value depends upon the temperature of operation and the incident solar spectrum) and low absorbtance — i.e., low thermal emissivity for longer wavelengths. Two types of surface have these properties, the most usual being a polished metal covered by a thin dark layer transparent to long waves. Attempts to improve the absorbtance of a surface tend to increase the emissivity, and it is shown that such an attempt is justified only if

$$d\alpha > \frac{\sigma (T^4 - T_0^4)}{P\bar{Q}}\, de_e$$

where $\sigma (T^4\text{-}T^4_0)$ is the radiation loss from the surface, *if* it were a black body, P the optical concentration factor, $\bar{Q}$ the mean solar intensity, de_e the change in effective emittance and $d\alpha$ the change in absorbtance. For a typical flat plate collector $d\alpha > 0.6\ de_e$ is obtained, whilst for a low concentration collector $d\alpha > 0.89\ de_e$ is obtained.

The substrate must be stable to heating and atmospheric corrosion, and the surface must be protected by a window.

Two of the several surfaces developed in the laboratory are described in some detail, viz., copper oxide produced chemically and "nickel-black" — a complex of nickel and zinc sulphides — produced by electrodeposition. The former has also been studied abroad. Very high absorbtances are difficult to obtain. The nickel-black coatings have been specially studied because absorbtances up to 94 per cent have been obtained by exploiting destructive interference in the coatings which are smooth. Variations of the plating conditions (e.g., current density) cause change in the chemical composition and the optical properties so that multiple layer interference effects can be exploited. A recent mathematical analysis shows the greater ease with which destructive interference (zero reflectivity) can be obtained with double layers than with single. Optical properties of some double layer nickel-blacks, measured by Dunkle, are shown; they indicate absorbtances above 90 per cent and emittances as low as 5 per cent.

A semi-industrial plant has been set up for applying the nickel-black process to galvanised iron solar water heater plates up to 1 × 2 m, of which several thousand are sold commercially every year.

The benefits derived from the use of selective coatings are indicated by several examples, such as for heat engine operation from low concentration mirrors ($P = 3$) where the power output can be increased by 81 per cent because of the higher optimum working temperature, and for flat plate collectors (for absorption refrigerators) where higher efficiency is obtained or fewer glass covers can be used. In outer space, where no convection occurs, very large benefits derive from the use of selective surfaces.

Basic studies on the structure and optical properties of selective surfaces are continuing, with a view to achieving better surfaces ultimately, though the present ones are not far from ideal optically, at least for terrestrial applications, where still lower emissivities bring little extra benefit. There is room for better chemical stability and simpler production techniques. Two new surfaces are being studied: a simpler nickel-black (without zinc being present) and copper oxide with additives.

ÉTUDES SUPPLÉMENTAIRES SUR LES REVÊTEMENTS NOIRS SÉLECTIFS

Résumé

Ce mémoire passe en revue l'ensemble de la question des surfaces sélectives pour collecteurs solaires, et met au point les exigences optiques auxquelles ces surfaces doivent obéir : il faut qu'elles se comportent comme un filtre passe-bande ayant un coefficient d'absorption élevé pour les longueurs d'onde allant jusqu'à environ 2,5 microns (la valeur exacte dépend de la température de fonctionnement et du spectre solaire incident), mais faible, ce qui signifie une émissivité thermique peu élevée, pour les longueurs d'onde plus grandes. Deux types de surface présentent ces qualités, celle que l'on voit le plus souvent étant un métal poli couvert d'une couche sombre mince, transparente pour les grandes longueurs d'onde. Les tentatives visant à améliorer le coefficient d'absorption d'une surface ont tendance à augmenter son émissivité, et on montre qu'une telle tentative n'est justifiée que si

$$d\alpha > \frac{\sigma (T^4 - T_0^4)}{P\bar{Q}}\, de_e$$

expression dans laquelle $\sigma (T^4 - T_0^4)$ est la perte par rayonnement de la surface *si* elle constitue un corps noir, P le facteur de concentration optique, $\bar{Q}$ l'intensité solaire moyenne, de_e la variation utile de l'émittance et $d\alpha$ le changement du coefficient d'absorption ou absorbance. Pour un collecteur type à

plaque plane, on obtient $d\alpha > 0{,}6\ de_e$ tandis que, pour un collecteur à faible concentration, il vient : $d\alpha > 0{,}89\ de_e$.

La base sur laquelle repose le revêtement doit être thermostable et résistante à la corrosion atmosphérique, et la surface doit être protégée par une fenêtre appropriée.

Le mémoire décrit en détail deux des surfaces mises au point en laboratoire, à savoir : l'oxyde du cuivre produit chimiquement et le « noir de nickel », composé de sulfures de nickel et de zinc produit par électro-déposition. La pemière formule a également fait l'objet d'études en dehors d'Israël. Il est difficile de réaliser de très gros coefficients d'absorption. On a prêté beaucoup d'attention aux enduits en noir de nickel, car ils ont permis de réaliser des coefficients d'absorption allant jusqu'à 94 p. 100 par exploitation des interférences destructives au sein de ces revêtements lisses. Les variations dans les conditions de placage (par exemple de la densité de courant) provoquent des modifications dans leur composition chimique et leurs propriétés optiques telles que l'on peut exploiter les phénomènes d'interférence dus à la multiplicité des couches. Une analyse mathématique récente montre que les interférences destructives (réflectivité nulle) se réalisent plus facilement avec des couches doubles qu'avec des couches simples. Ce mémoire donne les propriétés optiques de certains noirs de nickel à double couche, mesurées par Dunkle, qui indiquent des absorbances dépassant 90 p. 100 et des émittances descendant jusqu'à 5 p. 100.

On a organisé une installation semi-industrielle pour appliquer le procédé de préparation du noir de nickel à des plaques de chauffe-eau solaires en fer galvanisé ayant des dimensions pouvant atteindre 1 × 2 m. Plusieurs milliers en sont vendues dans le commerce chaque année.

Les avantages que l'on tire de l'emploi des enduits sélectifs ressortent de plusieurs exemples, tel que l'exploitation d'un moteur thermique au moyen de miroirs à faible concentration ($P = 3$) dans lesquels le débit d'énergie peut être augmenté de 81 p. 100 en raison de l'augmentation de la température idéale de fonctionnement, et la réalisation de collecteurs à plaque plate (pour les réfrigérateurs par absorption), dans lesquels on réalise un plus grand rendement ou on peut réduire le nombre des couvercles en verre. Dans l'espace interplanétaire, où il n'y a pas de convection, l'emploi des surfaces sélectives assure de très gros avantages.

On poursuit des études fondamentales sur la structure et les propriétés optiques des surfaces sélectives en vue de réaliser de meilleures surfaces, en fin de compte, bien que celles dont on dispose actuellement ne soient pas loin d'être idéales optiquement, tout au moins pour les applications terrestres dans lesquelles des émissivités encore plus faibles ne confèrent que peu d'avantages supplémentaires. La stabilité chimique de ces revêtements a besoin d'être améliorée, et les techniques de production aussi. Deux nouvelles surfaces sont à l'étude : un noir de nickel plus simple (dans lequel il n'y aurait pas de zinc) et de l'oxyde de cuivre avec des additifs.

RECHERCHES SUR LES SURFACES SÉLECTIVES UTILISABLES POUR LA CLIMATISATION DES HABITATIONS

F. Trombe, M. Foëx et M. Lê Phat Vinh *

Ces recherches ont pour but la réalisation et l'étude de surfaces chauffantes, refroidissantes ou transparentes servant à l'effet de serre.

Méthodes de mesures

Nous avons procédé à des mesures d'absorption du rayonnement solaire pris dans son ensemble, au moyen d'un dispositif calorimétrique à circulation d'eau, comportant un thermocouple différentiel, donnant l'échauffement d'un courant d'eau dont le débit est déterminé et sous une énergie incidente connue (figure 1). L'énergie totale reçue du soleil est comprise généralement entre 0,1 et 1 kW, la surface éclairée étant de l'ordre de 10 cm². Les tôles métalliques résistent bien à l'action de ce rayonnement, à condition d'être suffisamment réfrigérées (débit d'eau de l'ordre de 50 à 100 cm³/seconde).

La mesure de l'émission globale des tôles à la température ambiante a été estimée par l'abaissement de température qu'elles donnent par rayonnement sur un ciel nocturne très clair. Une surface présentant une très faible émission (aluminium non oxydé) qui reste pratiquement à la température ambiante, et une surface (corps noir) qui se refroidit au maximum, ont servi de points de repère extrêmes. Il a été vérifié qu'il ne se produit pas de rosée ou de gelée blanche pouvant perturber les abaissements de température.

Des mesures d'émission énergétiques en fonction de la longueur d'onde ont été faites par F. Cabannes.

Réalisation de surfaces sélectives chauffantes

Collecteurs a réflexions multiples

Il est possible de réaliser au moyen de tôles métalliques des collecteurs sélectifs absorbant le rayonnement solaire et présentant une faible émission propre. On sait, en effet, que le pouvoir réflecteur des métaux croît généralement d'une façon progressive lorsque la longueur d'onde augmente, pour tendre asymptotiquement vers des valeurs très élevées, souvent comprises entre 95 et 98 p. 100 dans l'infrarouge moyen. Toutefois, le facteur d'absorption des métaux pour le rayonnement solaire étant insuffisant (15 à 40 p. 100 selon le cas), il est nécessaire, pour obtenir une valeur suffisante, de réaliser plusieurs réflexions du rayonnement incident.

Les métaux ainsi utilisés doivent résister aux agents atmosphériques, de façon à ce que leur état de surface n'évolue pas. Ils doivent par ailleurs présenter une absorption beaucoup plus considérable dans le visible et le proche infrarouge que dans l'infrarouge moyen. Nous avons essayé les métaux suivants :

a) L'aluminium brillant absorbe environ 15 p. 100 du rayonnement solaire et ne présente, par contre, qu'une faible émission propre à la température d'utilisation dans les collecteurs (inférieure à 3-5 p. 100 entre la température ordinaire et 100 °C).

b) L'aluminium courant (99 à 99,5 p. 100) pour être brillant doit être à la fois écroui et finement laminé (0,1 mm). Des tôles plus épaisses (1 mm) brillantes peuvent être obtenues par laminage d'aluminium plus pur (99,9 ou même 99,99 p. 100). Par ailleurs, la résistance à la corrosion diffère selon la pureté. Les premiers produits sont meilleur marché; leur prix de revient ne dépasse pas 6 nouveaux francs le kilogramme, soit 22 NF le m² en 1/10 mm. L'aluminium plus pur est sensiblement plus cher (de l'ordre de 20 p. 100 pour le 99,9 p. 100, de 100 p. 100 pour le 99,99 p. 100 au kg). Il faut noter également que, au-dessous de 1/10 mm, le prix au kg de l'aluminium pur est d'autant plus élevé que les tôles sont plus minces. Nous avons aussi commencé à essayer différents alliages d'aluminium, dont le duralumin.

c) Les aciers inoxydables absorbent une plus grande fraction du rayonnement solaire que l'aluminium, par exemple près de 40 p. 100 lorsqu'ils sont laminés, afin d'être glacés autant que possible. Le prix d'un acier inoxydable 18/8, en feuille de 0,1 mm et 150 mm de large, est de l'ordre de 2,4 NF le kg, c'est-à-dire d'environ 19 NF le m². Les feuilles plus fines seraient assez rigides pour être utilisables, mais elles sont actuellement d'un prix plus élevé à surface égale. On doit aussi noter que certains aciers exempts de nickel et contenant par exemple 16 p. 100 de chrome sont sensiblement meilleur marché.

d) Le zinc présente vers un micron un minimum de réflexion assez étroit, mais cependant bien marqué (50 p. 100). Ce métal absorbe donc assez fortement le rayonnement solaire (40 p. 100), alors qu'il est très réflecteur (jusqu'à 97 p. 100) pour le rayonnement infrarouge vers 8 à 10 microns. Ce métal (pur ou

* Laboratoire de l'énergie solaire du Centre national de la recherche scientifique, Mont-Louis, Pyrénées-Orientales, France.

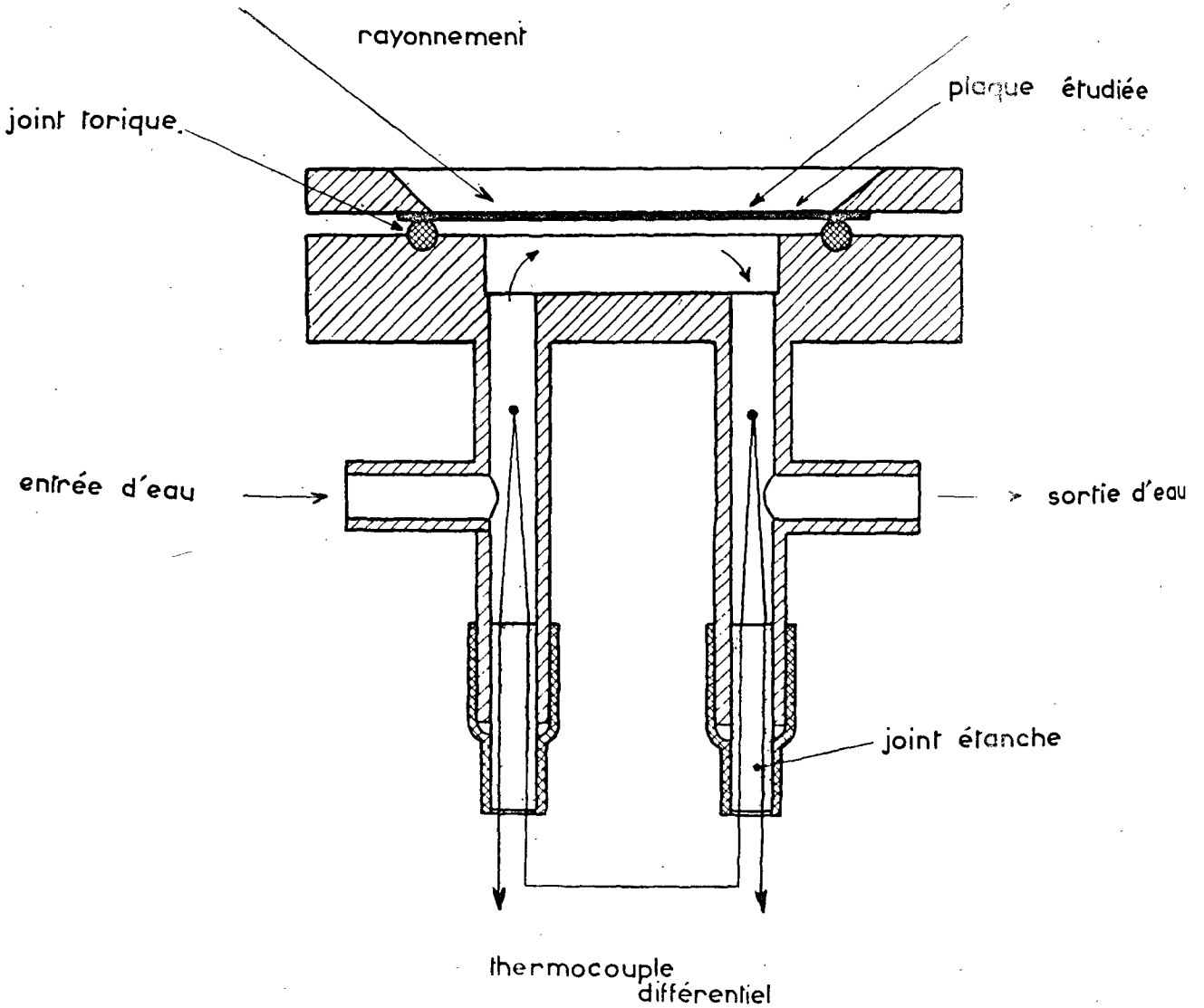


Figure 1. Dispositif calorimétrique pour la mesure de l'absorption de l'énergie solaire pour différentes surfaces métalliques

sous forme de tôles galvanisées) est fortement sélectif, mais il ne présente pas une bonne résistance à la corrosion, sauf, peut-être, en atmosphère très sèche.

Nous avons essayé différents dépôts électrolytiques de métaux susceptibles de recouvrir des tôles de fer ou d'acier.

Différents procédés permettent de réaliser des réflexions multiples. Ce sont essentiellement : les tôles pliées, les tôles parallèles, les tôles striées, rayées ou dépolies, les tôles constituées d'un alliage présentant une fine granulométrie.

Ainsi, par exemple, une tôle pliée à 30° permet de réfléchir six fois le rayonnement incident lorsque celui-ci est dirigé parallèlement à la direction moyenne des plans réflecteurs et trois fois lorsque cette incidence est à 45° (figure 2).

Les tôles parallèles permettent de réaliser un grand nombre de réflexions successives si l'angle d'incidence du rayonnement est convenable (figure 3). Il est nécessaire de prévoir à l'arrière du collecteur une autre tôle qui doit, de préférence, réfléchir le rayonnement d'une façon diffuse.

Afin de ne pas augmenter exagérément le rayonnement propre des tôles, pour les températures d'utilisation (50-120 °C, par exemple), il ne faut pas accroître leur surface totale plus qu'il n'est nécessaire et ne pas dépasser, si possible, quatre à huit fois la surface d'une tôle simple. Le rayonnement augmente en effet à peu près proportionnellement à la surface lorsque le facteur d'émission du métal est très faible.

Les appareils précédents fonctionnent pour le mieux si les tôles métalliques pliées ou parallèles présentent une surface polie aussi peu diffusante que possible. Une méthode apparentée à la précédente permet de s'affranchir de cette sujétion. Elle consiste à réaliser les réflexions multiples sur une surface métallique rayée ou striée. Ces stries doivent être

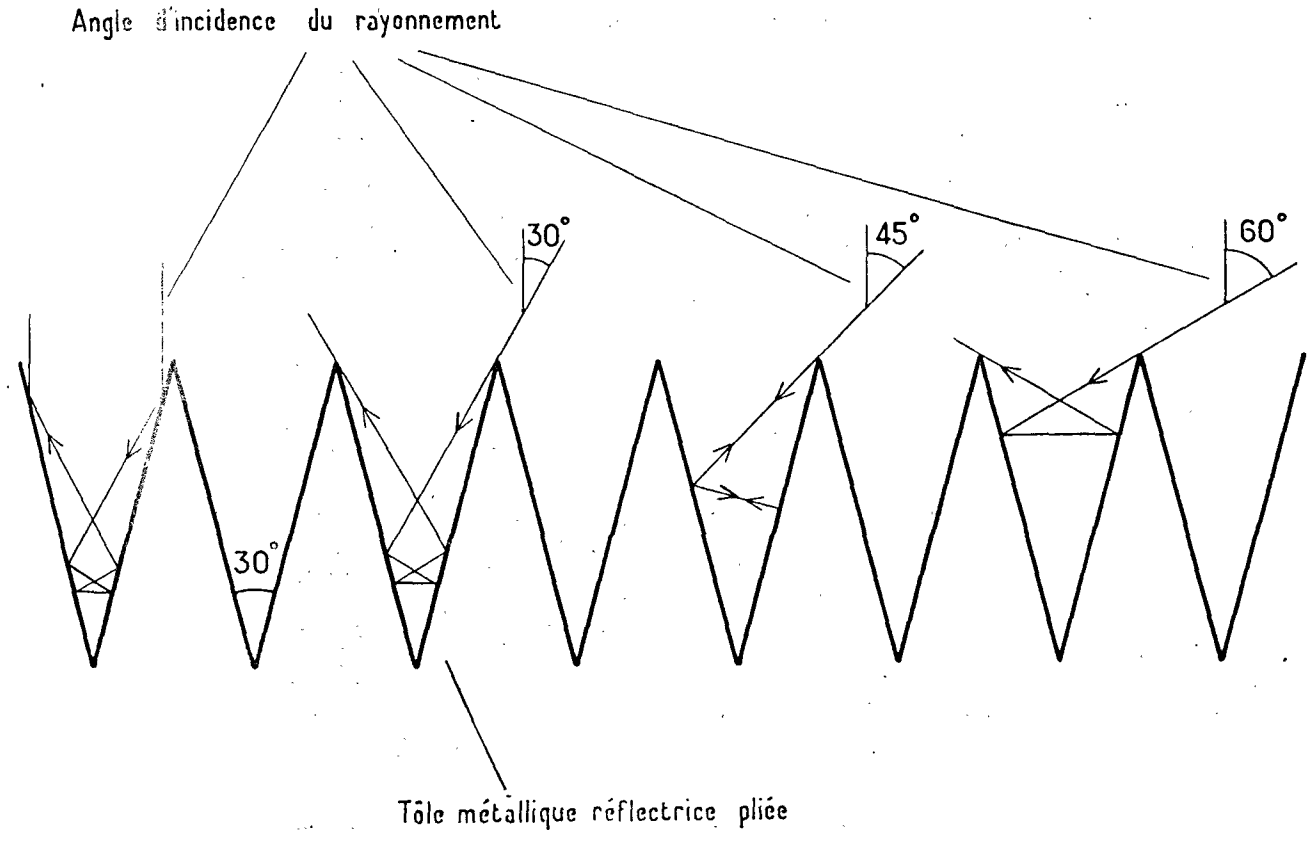


Figure 2. Absorption du rayonnement solaire par réflexions successives sur des tôles pliées

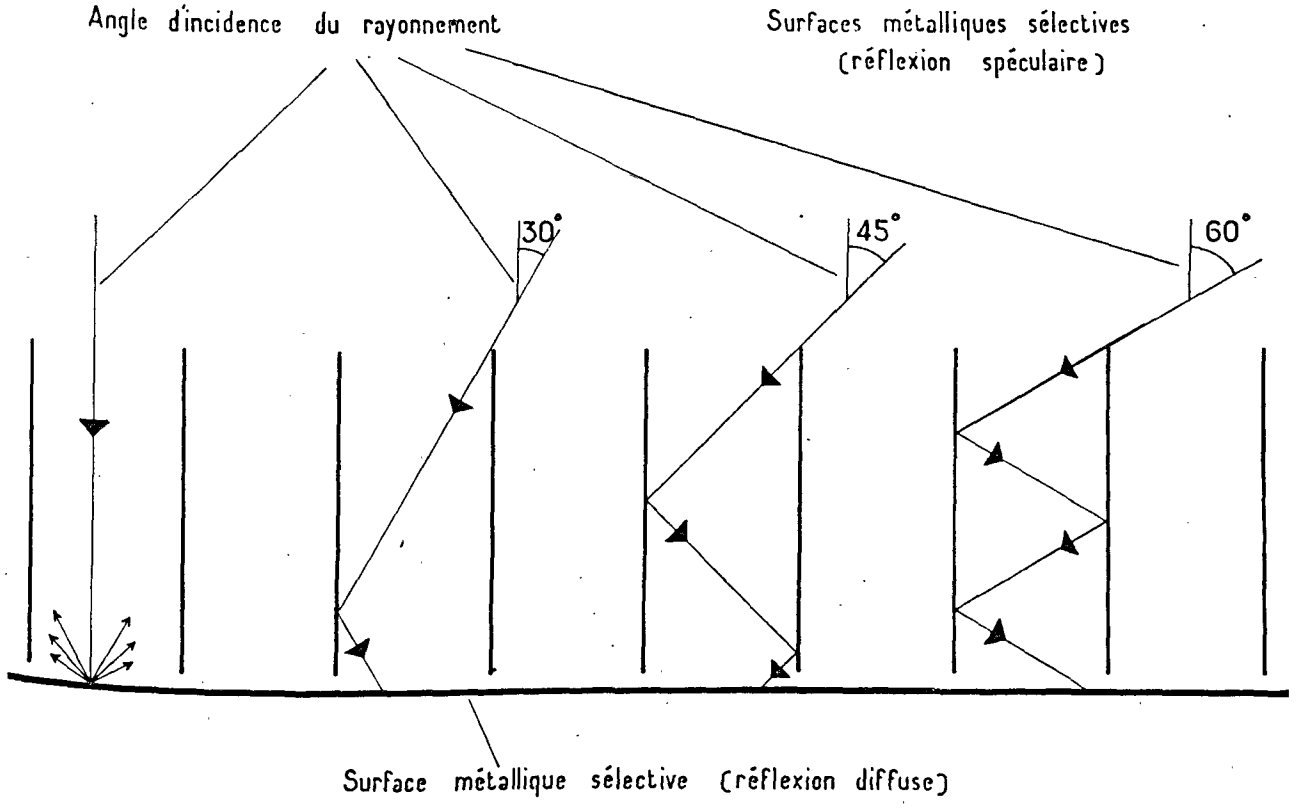


Figure 3. Absorption du rayonnement solaire par réflexions successives sur des tôles parallèles

à la fois aussi rapprochées et aussi profondes que possible; elles peuvent être croisées ou non. De cette façon, on augmente sensiblement l'absorption, cependant que la surface réelle est, par exemple, triplée. Cette augmentation est surtout très importante lorsque l'on compare les résultats obtenus à ceux d'une tôle parfaitement polie; elle est moindre si l'on considère une tôle métallique laminée sans précautions spéciales. Ainsi, dans le cas de l'aluminium, nous avons observé les valeurs suivantes pour l'absorption du rayonnement solaire : 45 p. 100 avec de l'aluminium strié avec des aiguilles de 0,35 mm de diamètre, à pointes effilées, placées côte à côte, dans un support, 25 p. 100 avec de l'aluminium laminé ordinaire. De son côté, l'aluminium bien poli n'absorbe guère plus de 14 p. 100 du rayonnement solaire.

De même, l'absorption pour le soleil d'un acier inoxydable à 16 p. 100 de chrome passe de 40 à 55 p. 100 lorsqu'il est rayé superficiellement. Des valeurs plus élevées peuvent être obtenues avec des rayures profondes.

Le sablage provoque aussi une augmentation de l'absorption de ces différentes tôles, ainsi que du reste les réactifs chimiques, dont l'action corrosive s'exerce en premier lieu au joint des grains. L'attaque chimique aura un effet particulièrement favorable lorsque le produit attaqué est formé de grains fins et, plus encore, s'il s'agit d'un alliage dont un des constituants est dissous de préférence à l'autre. C'est ainsi que certains alliages en proportions eutectiques ou eutectoïdes permettent d'absorber fortement le rayonnement solaire, après corrosion par un réactif chimique.

Dans une récente étude (1), nous avons montré que les dépôts électrolytiques au tampon d'alliages étain-zinc absorbaient mieux l'énergie solaire que les métaux purs. Ces dépôts mats présentent un maximum d'absorption compris entre 70 et 80 p. 100 selon les traitements pour environ 15 p. 100 d'étain en poids dans le zinc. Certains de ces alliages ont une bonne tenue à la corrosion.

Le choix du dispositif à réflexions multiples dépend essentiellement du problème à résoudre. Si l'on désire de larges surfaces d'échanges pour le chauffage de gaz à températures modérées, on utilisera avantageusement les tôles pliées ou les dispositifs à tôles parallèles. Les surfaces de tels collecteurs sont deux à huit fois supérieures à celles d'un collecteur plan ordinaire. L'obtention de températures plus élevées, nécessaires en général pour le chauffage de liquides ou pour des applications

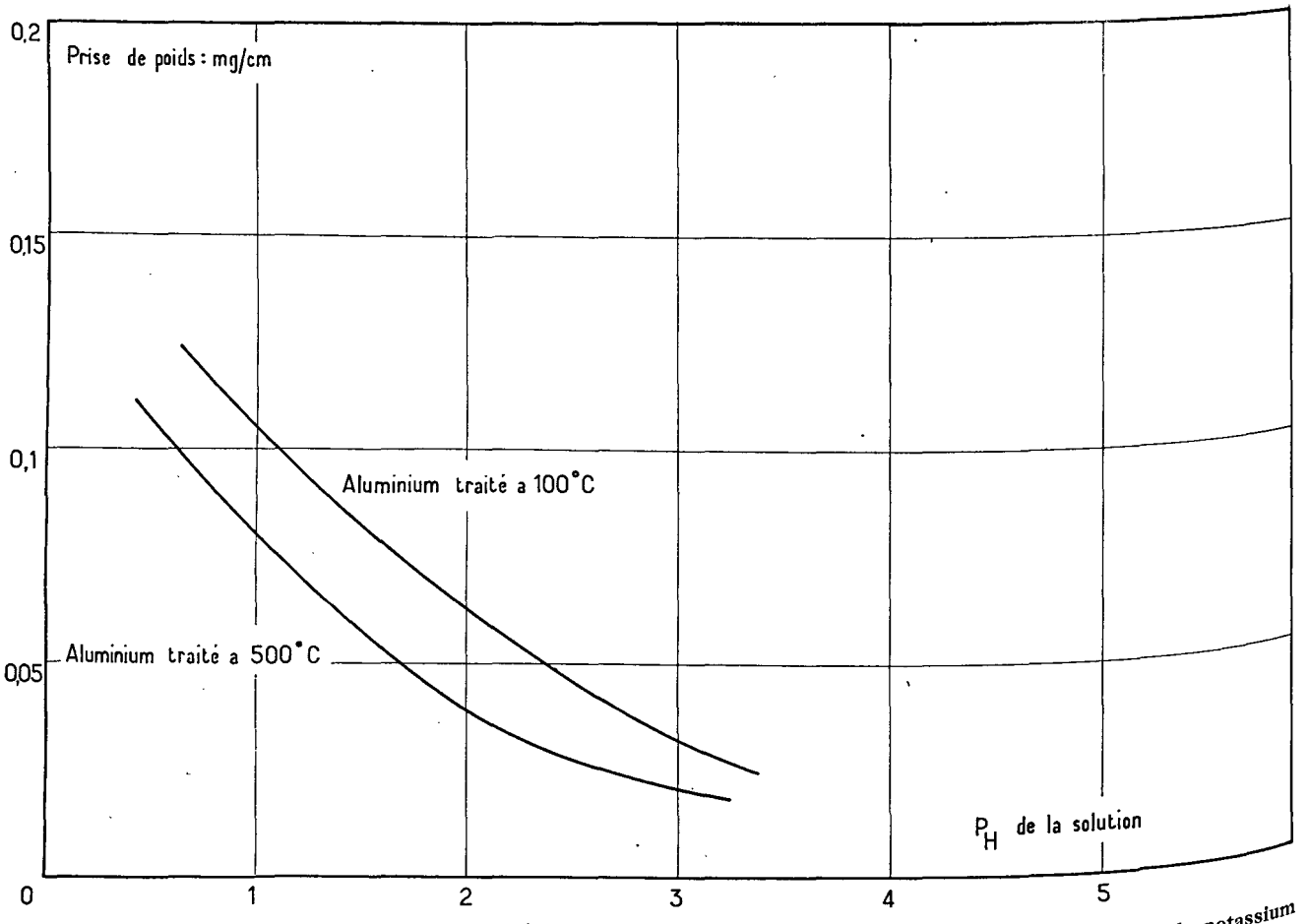


Figure 4. Prise de poids de tôles d'aluminium traitées par des solutions sulfuriques de permanganate de potassium présentant différents pH

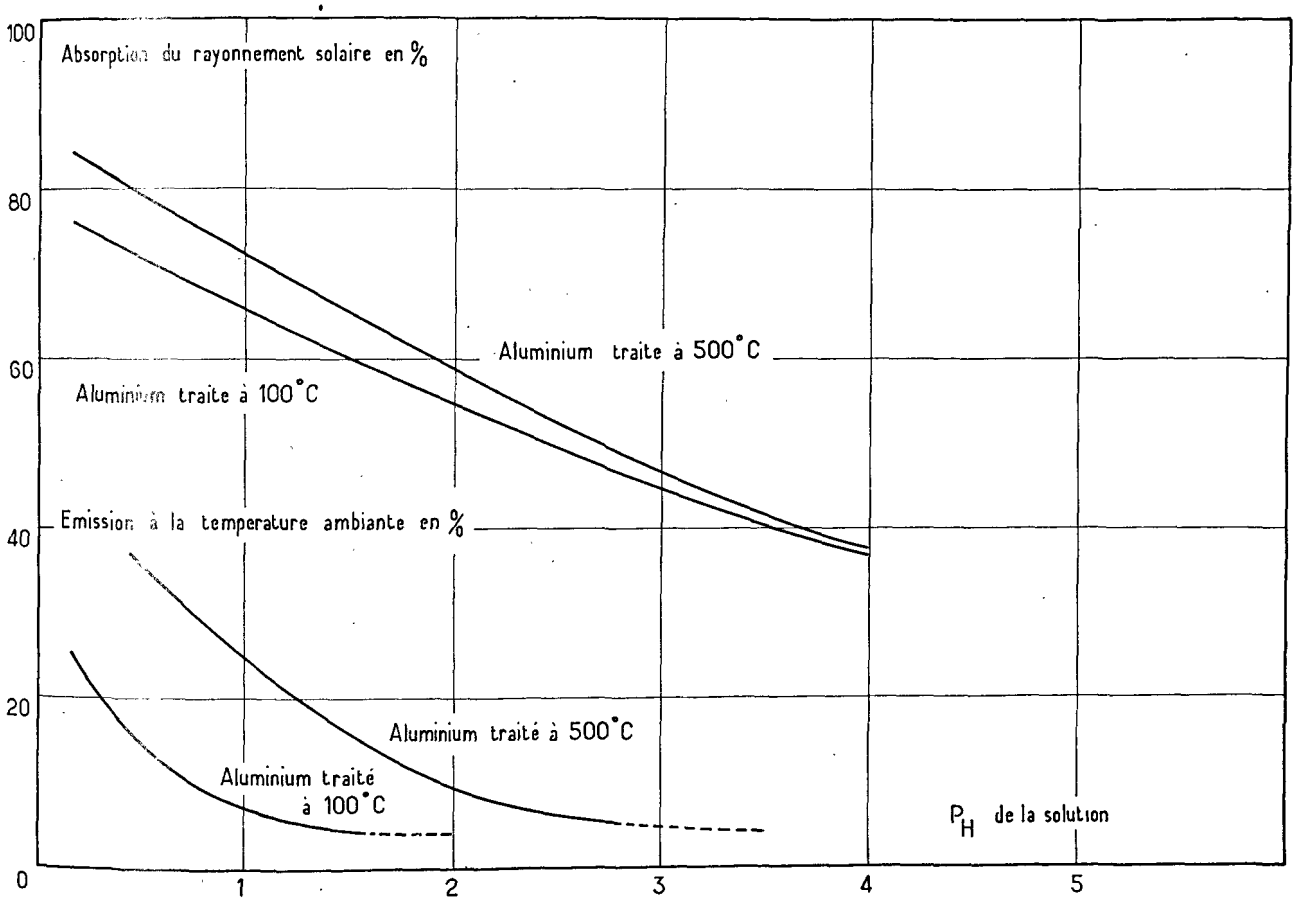


Figure 5. Absorption du rayonnement solaire et émission de tôles d'aluminium traitées par des solutions sulfuriques de permanganate de potassium présentant différents pH

telles que les thermopiles, s'effectuera plus facilement au moyen de tôles striées sur la surface réceptrice du rayonnement. On notera cependant dans ce cas des échanges par convection un peu supérieurs avec la surface striée qu'avec la surface plane.

Réalisation de surfaces sélectives chauffantes par traitement chimique

Nous avons, en particulier, coloré des plaques d'aluminium au moyen de solutions de permanganate de potassium d'une concentration comprise entre 5 et 20 g au litre, avec des additions d'acide sulfurique convenables pour obtenir des pH compris entre 0,5 et 6 (en l'absence d'acide, le pH est un peu supérieur à 6). Les plaques sont préalablement traitées au trichloréthylène afin de dissoudre les dépôts de graisse superficiels, puis sont plongées verticalement dans un bain porté à une température voisine de l'ébullition. On procède ensuite à un lavage poussé, et on recuit à des températures comprises entre 100 et 500 °C.

La coloration obtenue diffère profondément suivant le pH de la solution utilisée, jaune clair pour un pH 6; on obtient des teintes noires avec des solutions plus acides, les pH intermédiaires donnant des colorations bronze ou marron plus ou moins foncées. Le temps de traitement a une influence relativement faible, 10 minutes suffisant généralement. De même, la concentration du permanganate ne semble pas jouer un grand rôle, tout au moins lorsque la concentration dépasse 0,5 p. 100.

On a porté sur les figures 4 et 5 les résultats obtenus pour une série d'essais de ce genre. L'émission propre des plaques à la température ambiante est relativement faible tant que la prise de poids ne dépasse pas 0,1 mg/cm². Cela correspond à une épaisseur des dépôts inférieure au micron.

On peut également utiliser pour constituer les plaques sélectives les aciers « inoxydables ». Une oxydation de ces aciers à des températures comprises entre 250 et 550 °C donne des surfaces d'oxydes colorées extrêmement minces ne présentant pas, après traitement, de prises de poids supérieures à 0,01 mg par cm². Une oxydation plus poussée par un traitement d'une certaine durée vers 500 ou 600 °C conduit à l'apparition par place de petites plaques de particules d'oxyde visibles à l'œil nu.

L'émission dans l'infrarouge moyen reste limitée à 10 p. 100 environ dans les différents cas. Voici

les résultats obtenus pour l'absorption du rayonnement solaire :

Température de traitement (durée : 3 h)	Acier à 16 p. 100 de chrome		Acier à 18 p. 100 de chrome, 8 p. 100 de nickel	
	Absorption du rayonnement solaire %	Couleur	Absorption du rayonnement solaire %	Couleur
Non traité .	45	inaltérée	40	inaltérée
300 °C . . .	52	jaune	48	jaune
400 °C . . .	60	rouge	55	orange
500 °C . . .	70	violet	66	violet
600 °C . . .	75	bleu	70	bleu

Les tôles gardent leur aspect brillant malgré la légère oxydation. La résistance aux agents chimiques est excellente et le prix de revient de tels traitements reste très bas.

Réflexions multiples sur tôles ayant subi des traitements chimiques

Aussi bien dans le cas de l'aluminium que dans celui des aciers, les traitements chimiques précédents peuvent être combinés avec les effets de réflexions multiples (tôles pliées, parallèles ou striées), mais il convient dans tous les cas de réaliser un équilibre judicieux, de façon à ce que l'absorption finale du rayonnement solaire soit importante, cependant que l'émission propre de l'ensemble reste suffisamment faible.

Dans le cas des tôles pliées ou parallèles, il suffira généralement d'utiliser des tôles présentant un facteur d'absorption pour le rayonnement solaire limité à 50 p. 100 de façon à avoir des tôles recouvertes de couches colorées très minces gardant une bonne réflexion spéculaire et aussi une faible émission propre.

Avec des tôles striées, le problème est quelque peu différent, le nombre de réflexions ainsi réalisées étant sensiblement moindre. Lorsque ces tôles sont utilisées seules, sans adjonction de tôles réflectrices auxiliaires, on aura intérêt à utiliser des revêtements plus absorbants. Par exemple, l'aluminium brillant non rayé et traité dans une solution à pH 3 de permanganate de potassium à 5 p. 100 absorbe 60 p. 100 du rayonnement solaire, cependant que la même tôle préalablement rayée absorbe 75 p. 100 de ce rayonnement. L'émission propre de la tôle à la température ambiante est assez limitée (10-15 p. 100) dans le premier cas; elle est de l'ordre de 30 p. 100 dans le deuxième.

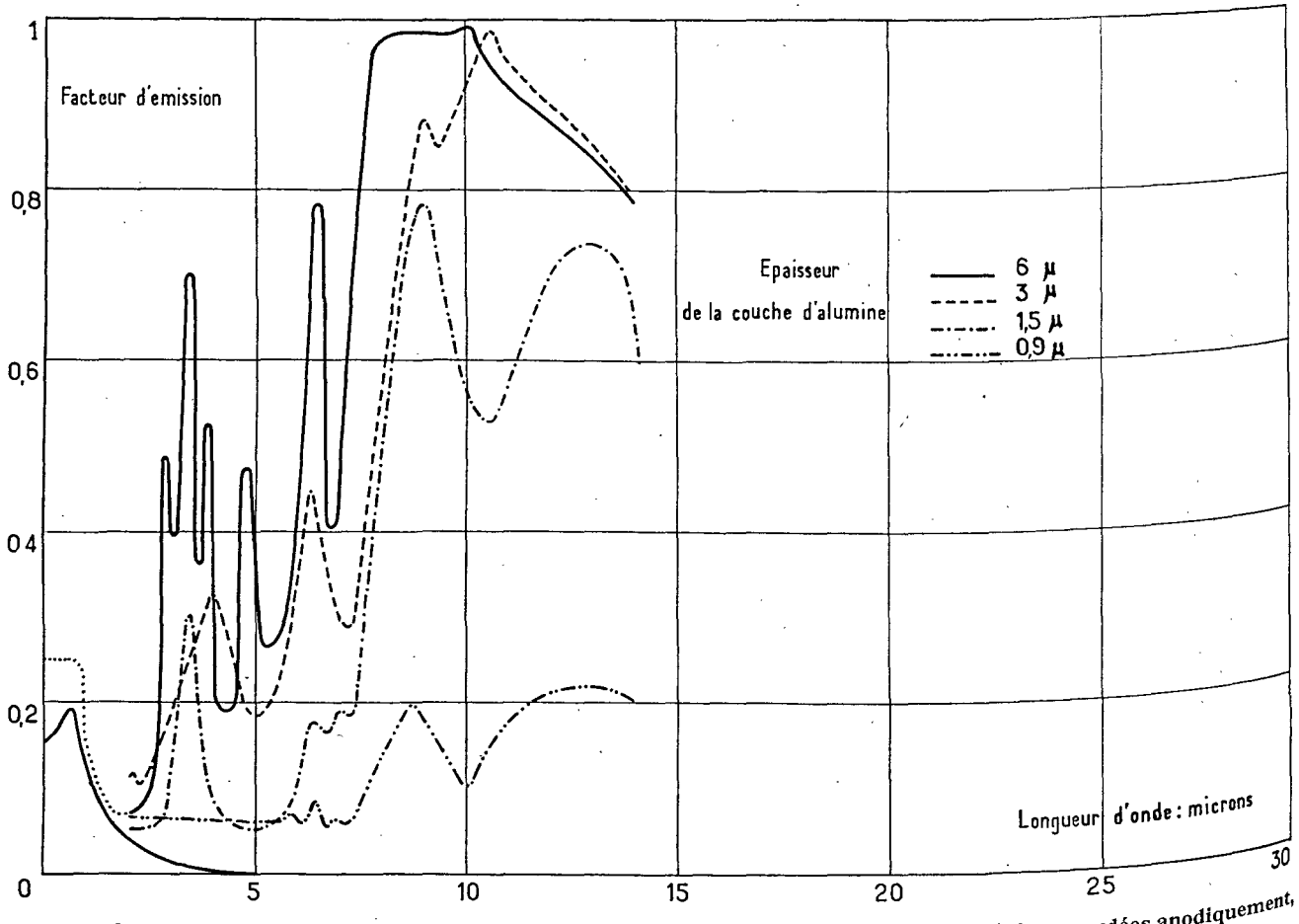


Figure 6. Évolution en fonction de la longueur d'onde du facteur d'émission de tôles d'aluminium oxydées anodiquement, pour différentes épaisseurs d'alumine

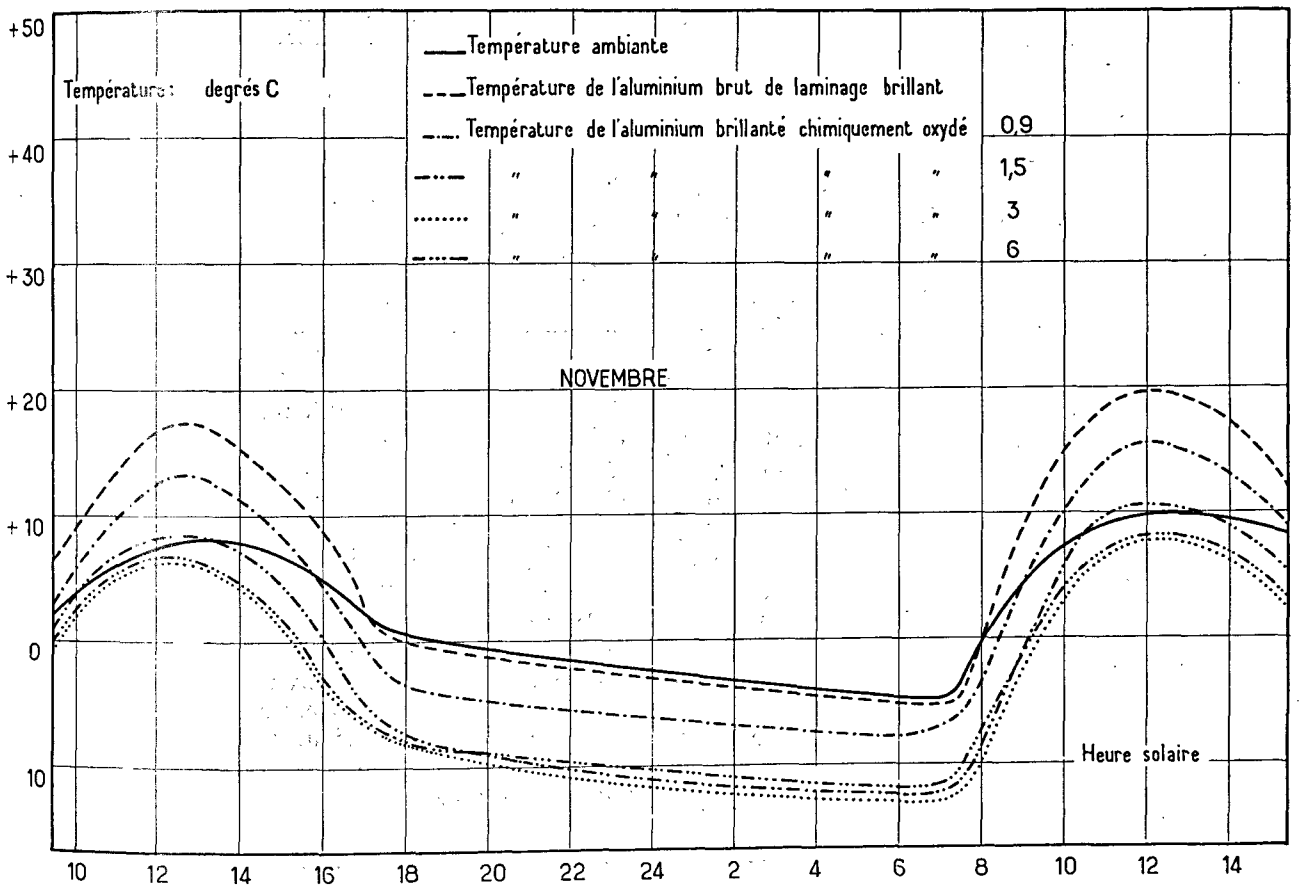


Figure 7. Évolution diurne et nocturne de la température de différentes tôles d'aluminium

Les tôles d'acier « inoxydable » sont susceptibles d'être à la fois striées et oxydées comme il a été indiqué ci-dessus. Dans ces conditions, l'absorption du rayonnement solaire peut atteindre ou même dépasser 85 p. 100, cependant que l'émission de la tôle reste faible (10 à 15 p. 100).

Étude de surfaces sélectives « froides » réfléchissantes pour le rayonnement solaire et présentant une forte émission propre

On a étudié l'émission dans l'infrarouge (figure 6) de feuilles d'aluminium A_9 (99,9-99,98 p. 100)

Tableau 1. Aluminium A_9 (99,99 p. 100 minimum)

Épaisseur de la couche d'alumine formée électrolytiquement	*Absorption du rayonnement solaire* %	*Émission propre vers la température ambiante* %
0 (non traité) [a] . .	14	< 10
0 (brillanté)	14	< 10
0,9 µ	15	environ 40
1,5 µ	15	environ 60
3 µ	15	environ 75
6 µ	15	> 90

[a] La couche protectrice d'alumine qui se forme habituellement sur l'aluminium a le plus souvent une épaisseur inférieure à 0,02 micron.

oxydées anodiquement, fournies par les Tréfileries du Havre et l'Aluminium Français. On constate que cette émission devient importante à partir d'une épaisseur d'alumine de 1 micron et que l'on se rapproche des conditions du corps noir à partir de 3 microns. On note cependant une forte augmentation de l'absorption dans la zone comprise entre 3 et 8 microns lorsque l'épaisseur croît. La figure 7

Tableau 2

Oxydation		*Épaisseur de la couche d'oxyde*	*Absorption du rayonnement solaire* %	*Émission propre vers 10 °C* %
Décapage	*Bain*			
Aluminium A_5 (99,7-99,79 p. 100 Al)				
Non traité	Non traité	0 µ	15	< 10
Décapage électrolytique alcalin . .	SO_4H_2 ord.	10 µ	23	> 90
Brillanté chimiquement	SO_4H_2 ord.	10 µ	23	> 90
Décapage à la soude	SO_4H_2 ord.	10 µ	26	> 90
Décapage électrolytique alcalin . .	SO_4H_2	60 µ	65	> 95
Alliage d'aluminium à 5 p. 100 de silicium : AS_5				
Décapage à la soude	SO_4H_2 ord.	10 µ	60	< 90

donne l'évolution diurne et nocturne de la température des tôles d'aluminium précédentes placées horizontalement sur un calorifuge, la face supérieure libre, ne recevant de rayonnement que du soleil ou du ciel. Le tableau 1 donne les résultats qui ont été observés.

Nous avons également effectué des essais avec des tôles d'alliages aluminium-magnésium à 3 p. 100 de magnésium polies (brillalumag), oxydées anodiquement de la même façon que les tôles d'aluminium. On note qu'à épaisseur égale l'émission est sensiblement plus forte avec les alliages qu'avec l'aluminium pur; des résultats à peu près semblables sont obtenus avec des couches d'oxydes deux fois plus faibles environ.

Le tableau 2 concerne un aluminium ordinaire A_5 (99,7-99,79 p. 100) traité par la Société Péchiney. On note une forte émission propre de ces produits, dont certains réfléchissent bien le rayonnement solaire.

A titre indicatif, donnons les cours de différentes variétés d'aluminium :

	Pourcentage	*Nouveaux francs par tonne*
A_4	99,5 à 99,69	2 435
A_5	99,7 à 99,79	2 485
A_6	99,8 à 99,85	2 580
A_7	99,85 à 99,89	2 730
A_8	99,9 à 99,98	3 500
A_9	99,9 (minimum)	4 300

Tableau 3. Dépôts d'aluminium sur aluminium A_5

Vernis aluminium		*Émission propre vers 20 °C*	*Absorption du rayonnement solaire*
Nature	*Application*	%	%
Non traité . . .		5	15
Cellulosique . . .	Pistolet	90	40
Synthétique . . .	Pistolet	80	46
Synthétique . . .	Brosse	60	39
Gras extérieur . .	Pistolet	65	36
Gras intérieur . .	Pistolet	40	34

La Société Péchiney nous a également confié des plaques recouvertes par différents procédés de dépôts d'aluminium. Certains de ces produits bon marché présentant une excellente émission propre, leur absorption pour le rayonnement solaire est, dans tous les cas, relativement élevée. Les meilleurs résultats ont été obtenus avec les vernis cellulosiques à l'aluminium déposés au pistolet.

Revêtements à base d'étain : l'étain brillanté réfléchit fortement le rayonnement solaire (87 p. 100)-par contre, les produits oxydés anodiquement sont colorés par suite de la formation d'oxydes inférieurs, et ne peuvent être ainsi utilisés pour la confection de collecteurs réfrigérants, malgré leur forte émission dans l'infrarouge.

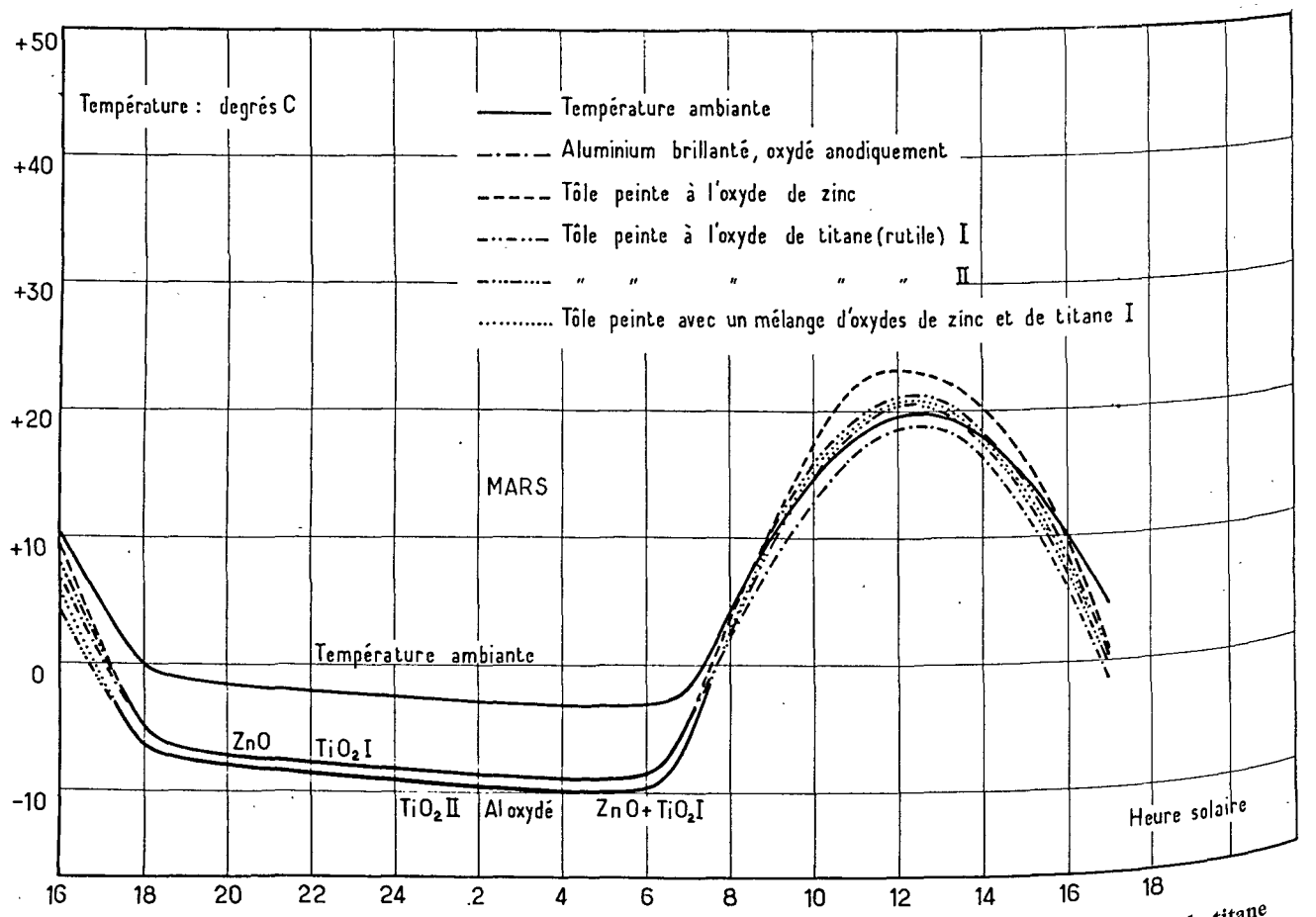


Figure 8. Évolution diurne et nocturne de tôles recouvertes de peintures à l'oxyde de zinc et à l'oxyde de titane

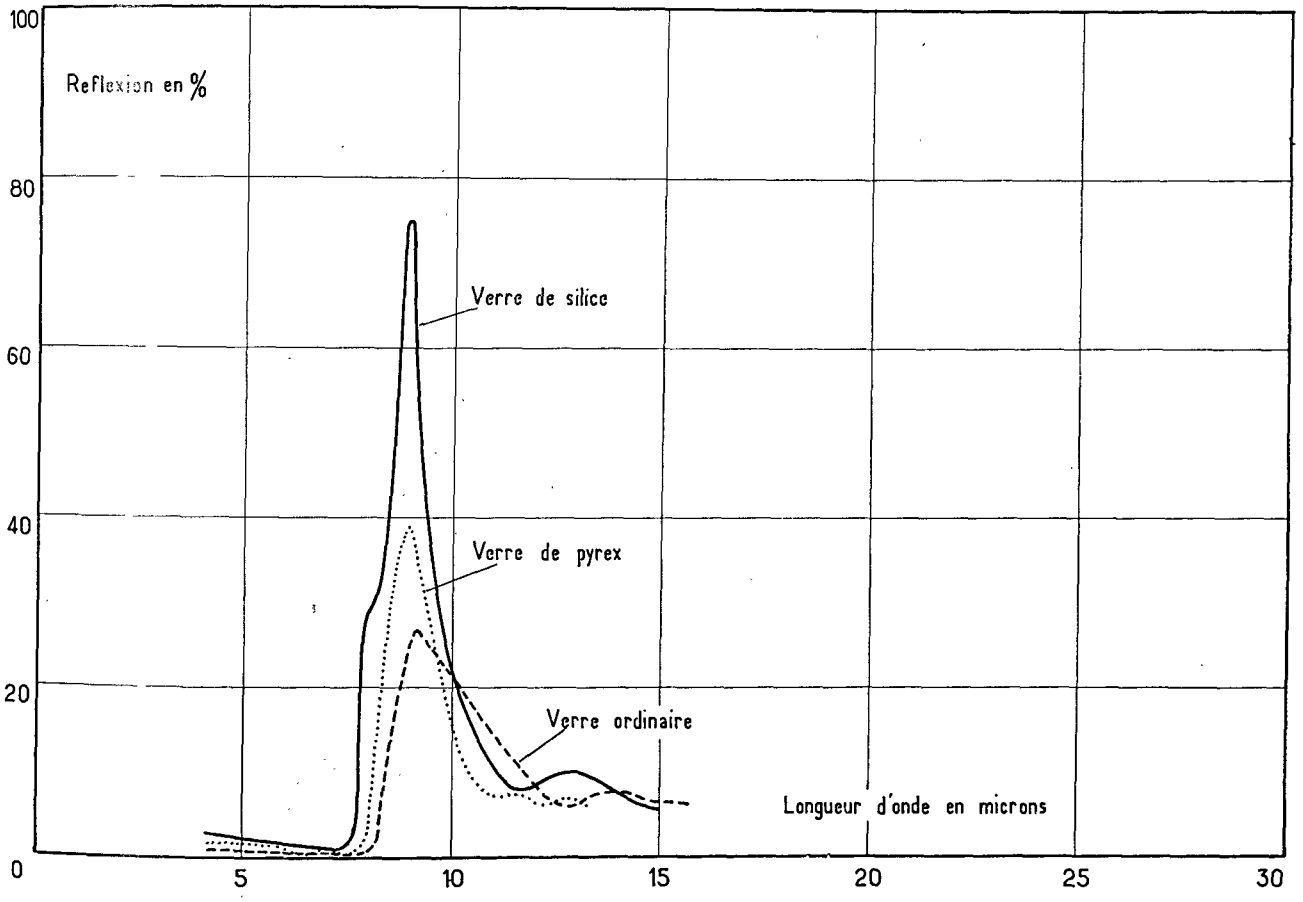


Figure 9. Réflexion dans l'infrarouge du verre ordinaire, du verre pyrex et du verre de silice, d'après Jellyman et Procter (3)

Tableau 4. Revêtements à base d'étain

Nature du métal et de son revêtement	*Traitement*	*Absorption du rayonnement solaire*	*Émission propre vers la température ambiante*
		%	%
Fer blanc étamé à chaud	Non traité	25	Environ 10
Fer blanc étamé à chaud	Traité 30 min à 80 °C dans l'acide chromique à 1 p. 100	17	Environ 75
Fer blanc étamé à chaud	Oxydé anodiquement	78	75
Fer blanc étamé à chaud	Chauffé à l'air à 210 °C (film coloré)	30	Environ 10
Acier avec revêtement électrolytique brillant d'étain (épaisseur 250 microns)	Oxydé anodiquement [a]	56	90
Acier revêtu d'un dépôt électrolytique de cuivre (13 microns) et d'un alliage étain-nickel (40 microns) . .	Non traité	35	Environ 10
Acier revêtu d'un dépôt électrolytique de cuivre (13 microns) et d'un alliage étain-cuivre (7,5 microns) . .	Non traité	28	Environ 10

[a] Solution de traitement 40 g/l Na_2HPO_4 et 20 g/l H_3PO_4 à 75°, pendant 5 minutes, densité de courant 0,04 ampère/cm.

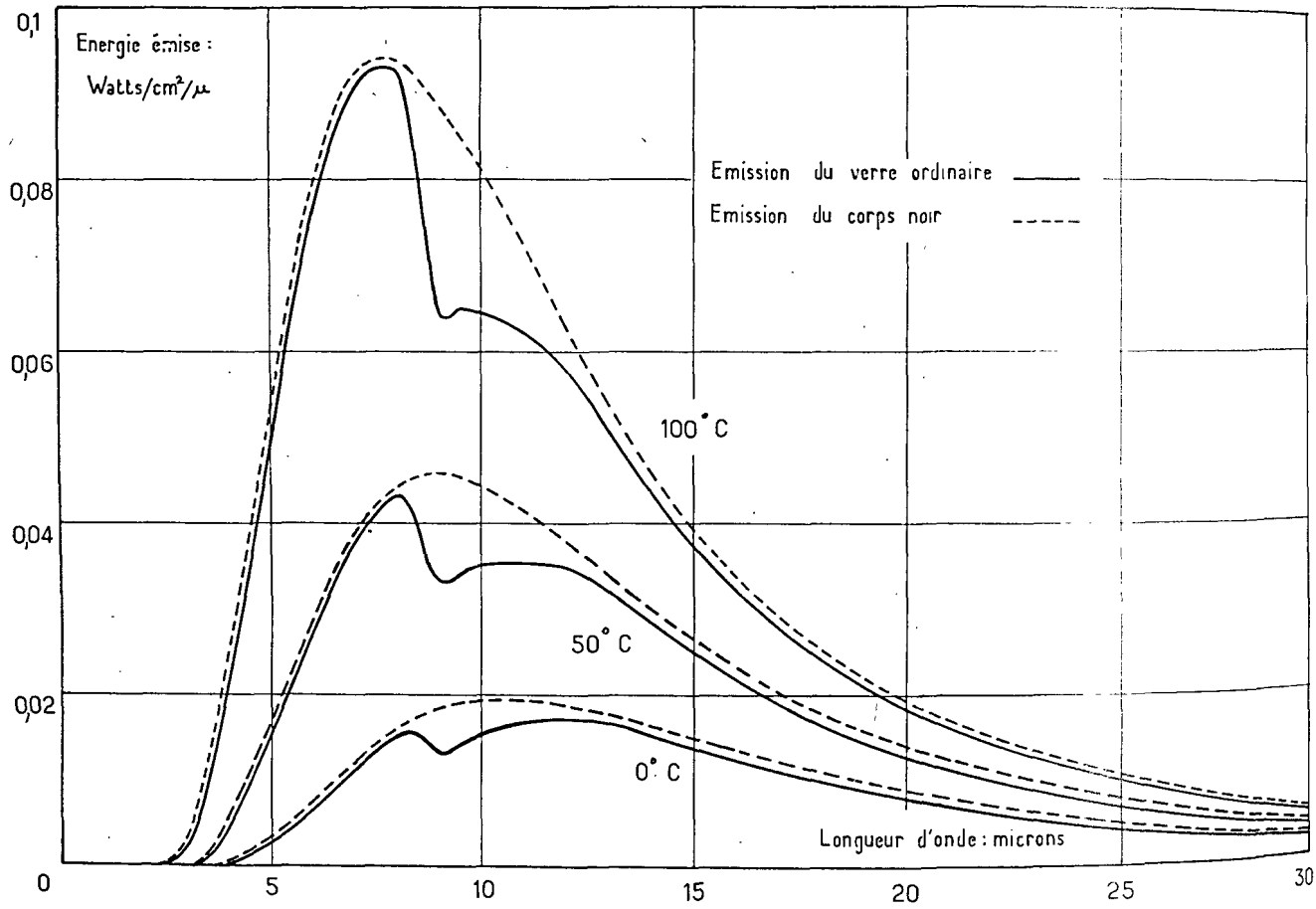


Figure 10. Émission du verre ordinaire à différentes températures, comparée à celle du corps noir

Peintures sélectives : la plupart des oxydes blancs constituent d'excellents pigments pour la confection de peintures sélectives. On note que les peintures à base de titane (rutile) réfléchissent 75 à 80 p. 100 du rayonnement solaire au lieu d'environ 70 p. 100 pour celles à base d'oxyde de zinc, les indices de réfraction du rutile (2,616 et 2,903 produit quadratique) étant plus élevés que ceux de l'oxyde de zinc (2,008 et 2,029 produit hexagonal). L'émission propre des peintures est, à la température ambiante, supérieure à 90 p. 100 ou même 95 p. 100. De tels produits à base de résine glycérophtalique donnent des résultats à peu près aussi bons que l'aluminium oxydé anodiquement, ainsi que le montrent les courbes de températures diurnes et nocturnes de tôles peintes de cette manière (figure 8) [1].

Remarques sur les parois transparentes utilisables dans les collecteurs faisant appel à « l'effet de serre »

Deux solutions sont ordinairement adoptées : les plastiques transparents et les verres. Les premiers sont plus économiques, mais présentent l'inconvénient, pour certains montages, d'être partiellement transparents au rayonnement infrarouge lorsqu'ils se présentent en feuille mince.

Dans l'avenir immédiat, il est difficile de songer à utiliser d'autres verres que les verres à vitres ordinaires. En général, lorsqu'on considère le rôle des verres dans l'effet de serre, on ne tient compte que de leurs propriétés absorbantes pour le rayonnement infrarouge plus long que 3 ou 4 microns. Il n'est pas sans intérêt, cependant, de considérer aussi leur pouvoir réflecteur, qui est important vers 9 microns (figure 9), pour une longueur d'onde très voisine de celle du maximum d'émission de ces verres chauffés entre 0 °C et 100 °C (figure 10). Cette réflexion, assez semblable dans ses effets à celle des métaux (le rayonnement non réfléchi est absorbé sous très faible épaisseur), se place précisément dans la principale fenêtre du rayonnement terrestre situé vers 8-12 microns entre des bandes d'absorption de la vapeur d'eau (figure 11). Elle a donc pour effet, d'une part, de réfléchir vers l'intérieur du collecteur le rayonnement émis par la tôle absorbante et, d'autre part, de limiter le rayonnement propre du verre dans une zone où ce dernier ne reçoit aucune énergie du ciel.

Le verre ordinaire n'est pas le meilleur verre qui puisse se concevoir à cet égard. En effet, le verre

[1] En réalisant des peintures plus riches encore en pigment ou en saupoudrant les peintures avec les pigments précédents, on pouvait obtenir des réflexions du rayonnement solaire supérieures à 90 p. 100, mais les revêtements ainsi obtenus sont rugueux et présentent des grains apparents.

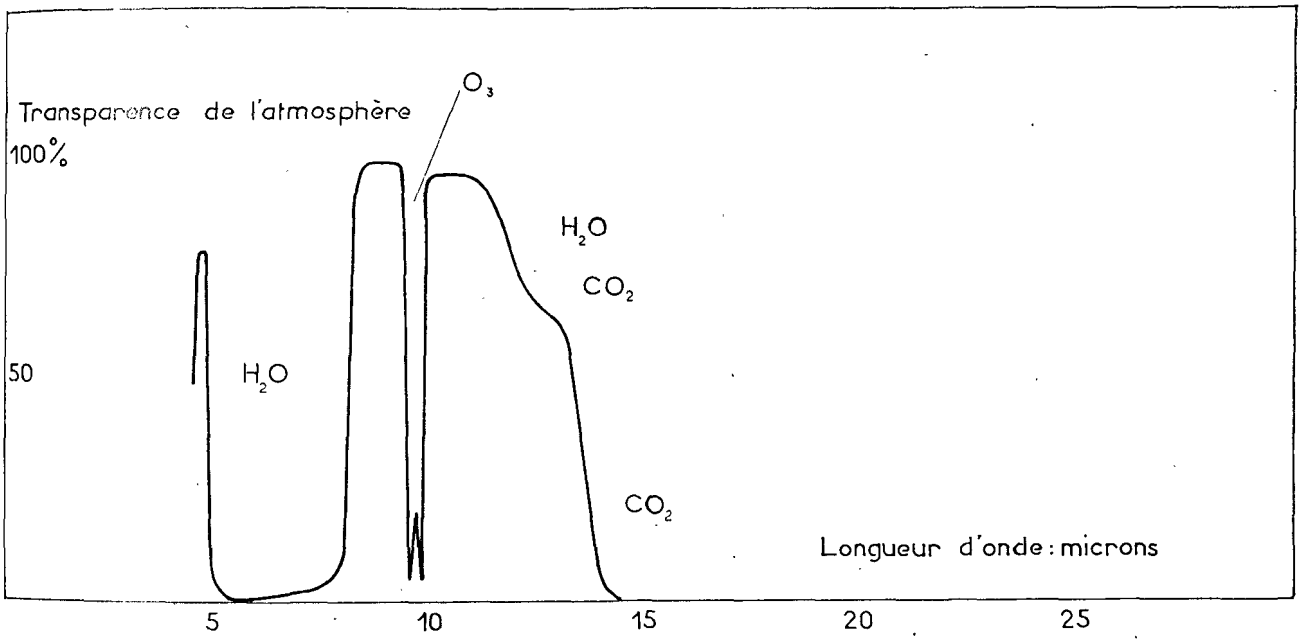


Figure 11. Transparence de l'atmosphère dans l'infrarouge (4)

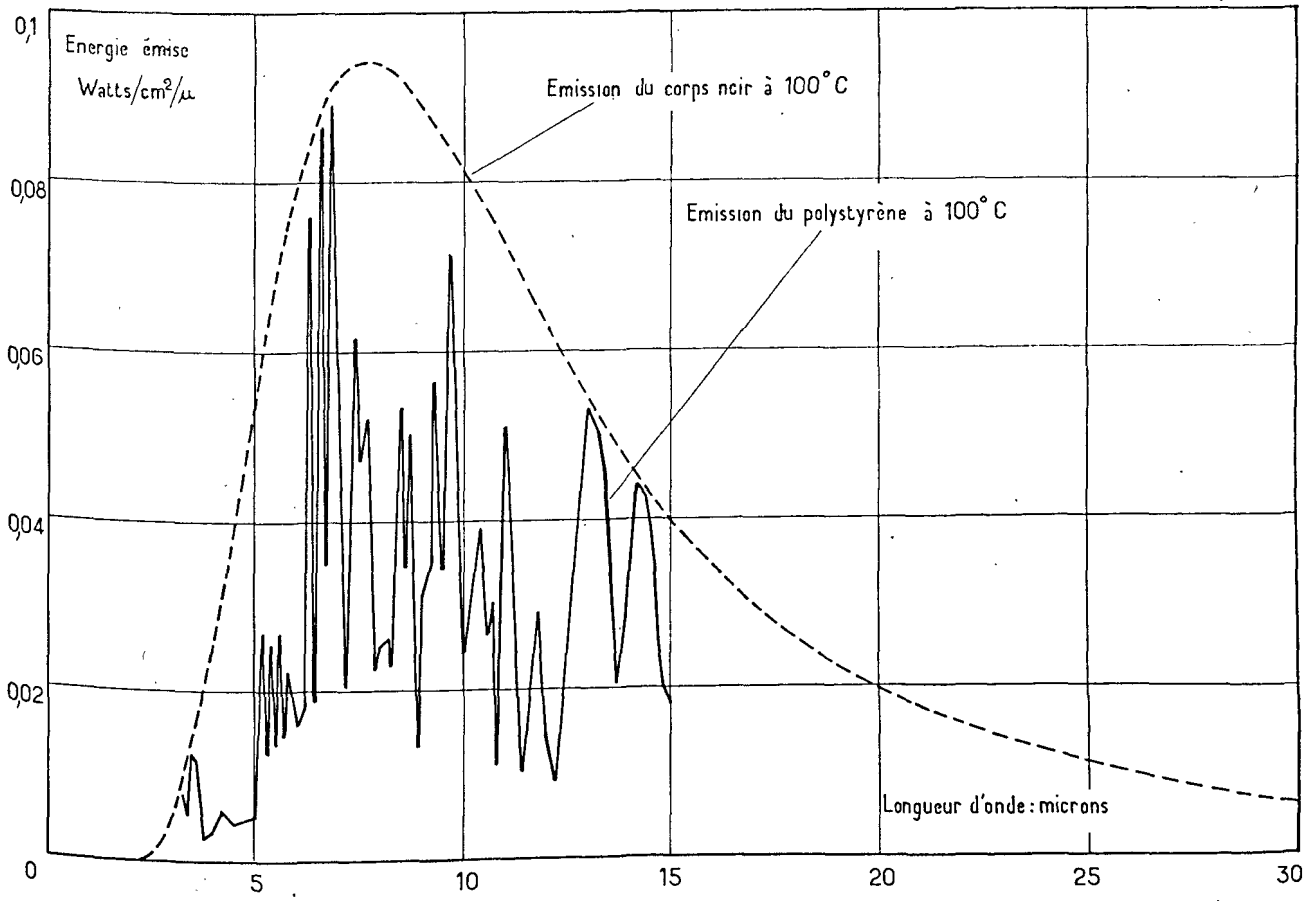


Figure 12. Émission d'une feuille de polystyrène de 70 microns d'épaisseur à 100 °C, comparée à celle du corps noir

pyrex et le verre de silice présentent, dans la même zone, une bande de réflexion plus intense encore. Ces deux derniers verres sont naturellement beaucoup plus chers, mais il serait intéressant de procéder à des recherches de base en vue de trouver un verre d'un prix abordable, présentant des propriétés réflectrices plus accentuées. Les verres étant susceptibles de dissoudre la plupart des oxydes métalliques, le domaine d'investigation semble assez large.

Les plastiques, lorsqu'ils ne sont pas trop épais (1/50 mm par exemple), laissent passer une partie du rayonnement infrarouge et présentent des courbes d'émission caractéristiques (figure 12) (sélectives au polystyrène).

Un autre aspect de cette question est l'utilisation de verres à indices de réfraction élevés, dont l'emploi pourrait être intéressant dans le cas où la surface réceptrice ne capterait pas la totalité du rayonnement solaire (cas général des surfaces sélectives) et serait diffusante. Cela permettrait de recueillir, par réflexion sur le verre, une grande partie du rayonnement diffusé sous de grands angles. Mais le procédé n'est guère applicable qu'aux collecteurs n'utilisant le soleil qu'un petit nombre d'heures par jour, pendant le temps où le rayonnement solaire arrive lui-même normalement à la surface du vitrage ou sous des angles relativement voisins.

Références

1. Trombe, F., et Föex, M. Études sur les collecteurs plats sans concentration d'énergie, Colloque sur les applications thermiques de l'énergie solaire, C.N.R.S., Mont-Louis, 1958.
2. Trombe, F., Föex, M., et Calvet-Le Phat Vinh, M., Sur la climatisation des habitations, *b*) Exploitations des résultats obtenus par le rayonnement des corps sur l'espace, Colloque sur les applications thermiques de l'énergie solaire, C.N.R.S., Mont-Louis, 1958.
3. Jellyman, P. E., et Procter, P. J. Infrared reflexion of glasses — *J. Soc. Glass. Technol.*, 39, 173 T/192 T, 1955.
4. *Handbook of Geophysics*, Revised Edition, MacMillan Co., New York, 1960.

Résumé

Surfaces sélectives « chaudes » absorbant le rayonnement solaire

On sait que les métaux absorbent généralement beaucoup plus fortement le rayonnement visible et le proche infrarouge que les radiations de plus grande longueur d'onde. Les surfaces métalliques permettent donc d'obtenir des collecteurs sélectifs présentant une faible émission propre, l'absorption du rayonnement solaire pouvant être considérablement accrue en réalisant plusieurs réflexions successives du rayonnement incident. Les réflexions multiples s'obtiennent à l'aide de tôles pliées ou parallèles, de tôles striées, rayées ou dépolies, par traitement mécanique, physique ou chimique. La plupart de ces procédés permettent d'obtenir de grandes surfaces d'échanges favorables surtout au chauffage des gaz.

On a également réalisé des surfaces chauffantes en colorant des surfaces métalliques par des moyens chimiques. L'aluminium traité par des solutions sulfuriques de permanganate de potassium donne de bons résultats, les colorations obtenues étant d'autant plus accentuées que le pH est plus faible. On peut également oxyder superficiellement les aciers « inoxydables » de façon à leur donner une teinte rouge ou bleue. Aussi bien dans le cas de l'aluminium que dans celui des aciers, les traitements chimiques précédents peuvent être combinés avec les effets de réflexions multiples (tôles pliées, parallèles ou striées), mais il convient dans tous les cas de réaliser un équilibre entre ces diverses opérations de façon à obtenir un effet sélectif maximal. Des tôles d'aciers « inoxydables » striées et oxydées superficiellement sont susceptibles d'absorber 85 p. 100 du rayonnement solaire, cependant que l'émission de la tôle reste faible (10 à 15 p. 100).

Surfaces sélectives « froides » réfléchissant le rayonnement solaire

On a par ailleurs mis au point, au Laboratoire de l'énergie solaire de Mont-Louis, des surfaces sélectives « froides » réfléchissantes pour le rayonnement solaire et présentant une forte émission propre.

De bons résultats, dans ce domaine, ont été obtenus avec des feuilles d'aluminium pur (99,9-99,98 p. 100) oxydé anodiquement. L'émission à la température ambiante se rapproche de celle d'un corps noir lorsque l'épaisseur de la couche d'alumine formée dépasse 3 microns. Différents dépôts et peintures à base d'aluminium ont été également étudiés, en particulier des vernis cellulosiques à l'aluminium déposés au pistolet. On a étudié aussi des revêtements à base d'étain métallique. Ces derniers sont susceptibles d'être oxydés anodique-

ment, mais deviennent alors beaucoup moins réflecteurs pour le rayonnement solaire.

Parmi les peintures blanches sélectives, celles à base d'oxyde de titane donnent les meilleurs résultats, l'émission propre à la température ambiante dépassant 90 p. 100 ou même 95 p. 100, cependant que la réflexion du rayonnement solaire est de l'ordre de 70 à 80 p. 100, ou même plus lorsqu'on réalise des revêtements avec pigments apparents.

Parois transparentes utilisables dans les collecteurs faisant appel à « l'effet de serre »

Les auteurs examinent, en particulier, le rôle des bandes de réflexion présentées par des verres dans l'infrarouge moyen pour des longueurs d'onde très voisines de celles du maximum d'émission des corps chauffés entre 0 et 100 °C. Des verres complexes, autres que le verre ordinaire, pourraient donner de meilleurs résultats encore dans ce domaine.

STUDIES ON SELECTIVE SURFACES FOR AIR-CONDITIONING DWELLINGS

(Translation of the foregoing paper)

F. Trombe, M. Foëx, and M. Lê Phat Vinh *

The object of these studies is to develop and investigate heating and cooling of transparent surfaces exhibiting the hot-house effect.

Methods of measurement

We measured the absorption of total solar radiation by means of a calorimetric set-up with circulating water, comprising a differential thermocouple indicating the heating of a stream of water of definite flow rate and under a known incident energy (figure 1). The total energy received from the sun generally ranged from 0.1 to 1 kW on the illuminated surface of the order of 10 cm². Sheet metal has a good resistance to the action of this radiation, provided it is sufficiently cooled (water flow of the order of 50-100 cc/s).

The over-all emission of the metal sheets at the ambient temperatures was estimated from their fall in temperature due to their radiation into a very clear night sky. The extreme reference points used were a surface with very low emission (unoxidized aluminium) which remains practically at ambient temperature, and a surface (black body) which shows the maximum degree of cooling. We made sure that there was no dew or frost that could have interfered with the temperature drop.

Measurements of the energy emitted as a function of wavelength were performed by F. Cabannes.

Development of selective heating surfaces

Multiple-reflection collectors

Selective collectors which absorb the solar radiation and themselves have only a slight emission may be realized by means of metal sheets. It is well known that the reflective power of metals generally increases progressively with the wavelength, tending asymptotically towards very high values, often ranging from 95 to 98 per cent in the middle infrared. But since the absorption factor of metals for solar radiation is insufficient (15 to 40 per cent), several reflections of the incident radiation are necessary if a sufficient value is to be obtained.

The metals used for this purpose must resist the atmospheric aggressive agents, so that their surface state undergoes no change. They must also have a much greater absorption in the visible and near infrared regions than in the middle infrared. We tested the following metals.

(*a*) Brilliant aluminium absorbs about 15 per cent of the solar radiation, yet it has only a low emission at the operating temperatures of solar collectors (less than 3-5 per cent between room temperature and 100°C).

(*b*) Commercial aluminium (99 to 99.5 per cent) must be both cold-worked and rolled very thin (0.1 mm) if it is to be brilliant. Thicker sheets (1 mm) may be obtained by rolling purer aluminium (99.9 or even 99.99 per cent). Moreover, the corrosion resistance varies with the purity. The former products are cheaper, costing no more than 6 new francs (NF) per kg, or 22 NF per kg in foil 0.1 mm thick. Purer aluminium is considerably higher in price per kg (about 20 per cent higher for the 99.9 per cent product, and about 100 per cent higher for the 99.99 per cent metal). It should also be noted that in foil thinner than 0.1 mm, the price of pure aluminium per kg increases with decreasing thickness. We have also initiated tests on various aluminium alloys, including duralumin.

(*c*) Stainless steels absorb a larger fraction of the solar radiation than aluminium, for example about 40 per cent when they are rolled, in order to take the highest polish possible. An 18/8 stainless steel, in foil 0.1 mm thick and 150 mm wide, costs about 2.4 NF per kg, that is, about 19 NF/m². Thinner foil than this would still be rigid enough for use, but its present price for equal surface area is higher. We should also note that certain nickel-free steels, with 16 per cent chromium, for instance, are appreciably cheaper.

(*d*) In the neighborhood of 1 μ wavelength, zinc has a rather narrow but marked reflection minimum (50 per cent). This metal thus rather strongly absorbs solar radiation (40 per cent), while it is highly reflective (up to 97 per cent) in the infrared at about 8 to 10 μ. This metal (pure or in the form of galvanized iron sheet) is highly selective, but its resistance to corrosion is not good, except, perhaps, in a very dry atmosphere.

We tested various electrolytic deposits of metals that could be used to coat sheet iron or sheet steel.

* Laboratoire de l'énergie solaire du Centre national de la recherche scientifique, Mont-Louis, Pyrénées-Orientales, France.

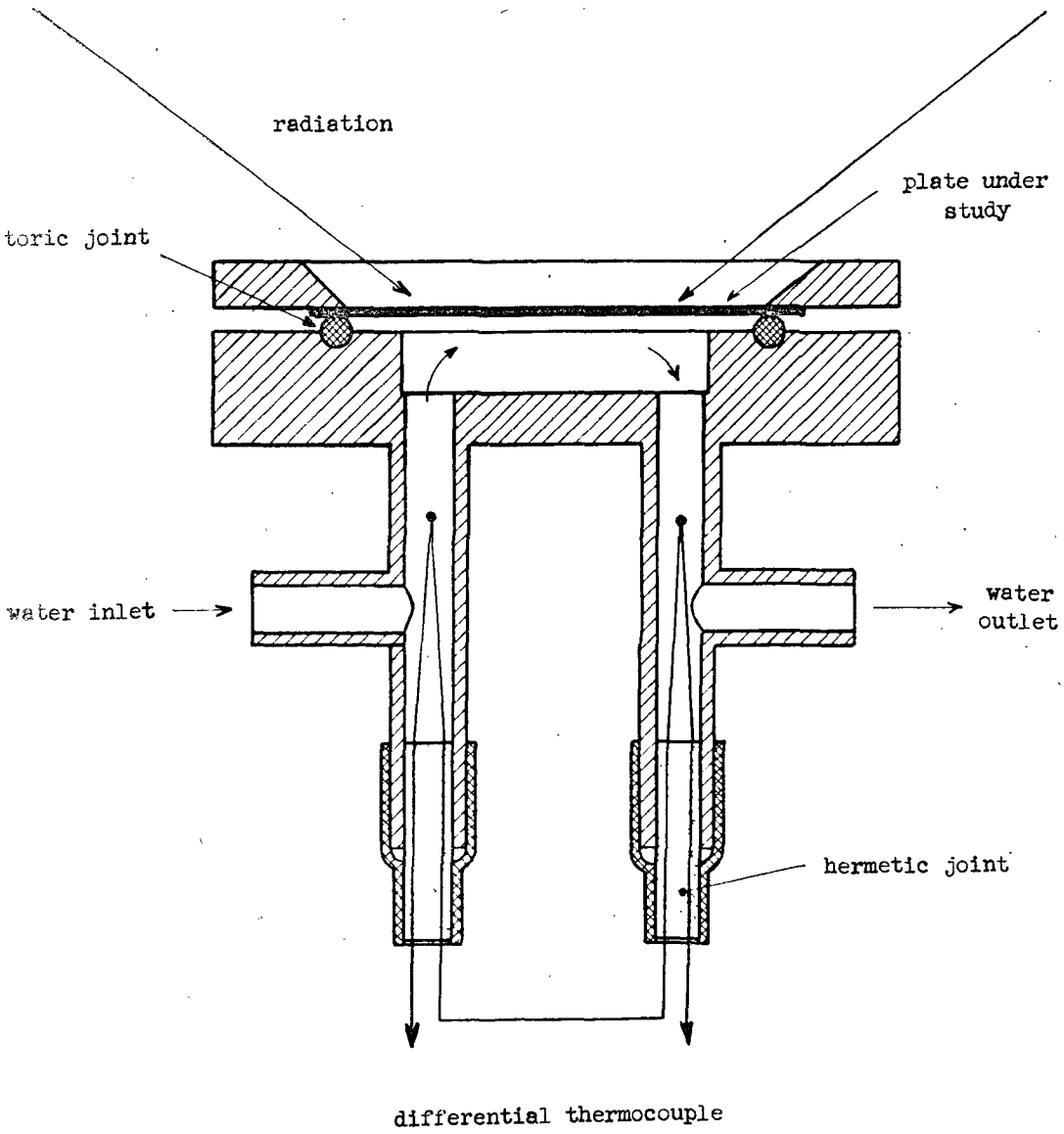


Figure 1. Calorimetric set-up for measuring the absorption of solar energy by various metallic surfaces

Various methods may be used to obtain multiple reflections. They are essentially folded metal sheets, parallel metal sheets, ruled on roughed metal sheets, and sheets of an alloy with a fine grain structure.

Thus, for example, metal sheet folded at a 30° angle gives six reflections of incident radiation in a direction parallel to the mean direction of the reflecting planes and three reflections for incidence at 45° (figure 2).

Parallel metal sheets give a large number of successive reflections if the angle of incidence of the radiation is appropriate (figure 3). Another metal sheet, preferably one giving a diffuse reflection of the radiation, must be placed at the back of the collector.

To prevent excessive increase of the radiation from the metal sheets at the operating temperatures (50 to 120°C, for instance), their total area must not be more than necessary, and should not exceed 4 to 8 times the surface area of a single sheet. The radiation increases about proportionally to the surface when the emission factor of the metal is very low.

These devices operate best if the folded or parallel metal sheets present a polished surface causing the least possible diffusion. A method related to the above makes it possible to escape this condition. It consists in effecting the multiple reflections on a ruled or grooved metal surface. These grooves must be both as closely spaced and as deep as possible. This appreciably increases the absorption, for the real surface is, say, tripled. This increase is very important if we compare these results with those from a perfectly polished metal sheet; but is less significant if we consider a metal plate rolled without special precautions. Thus, in the case of aluminium

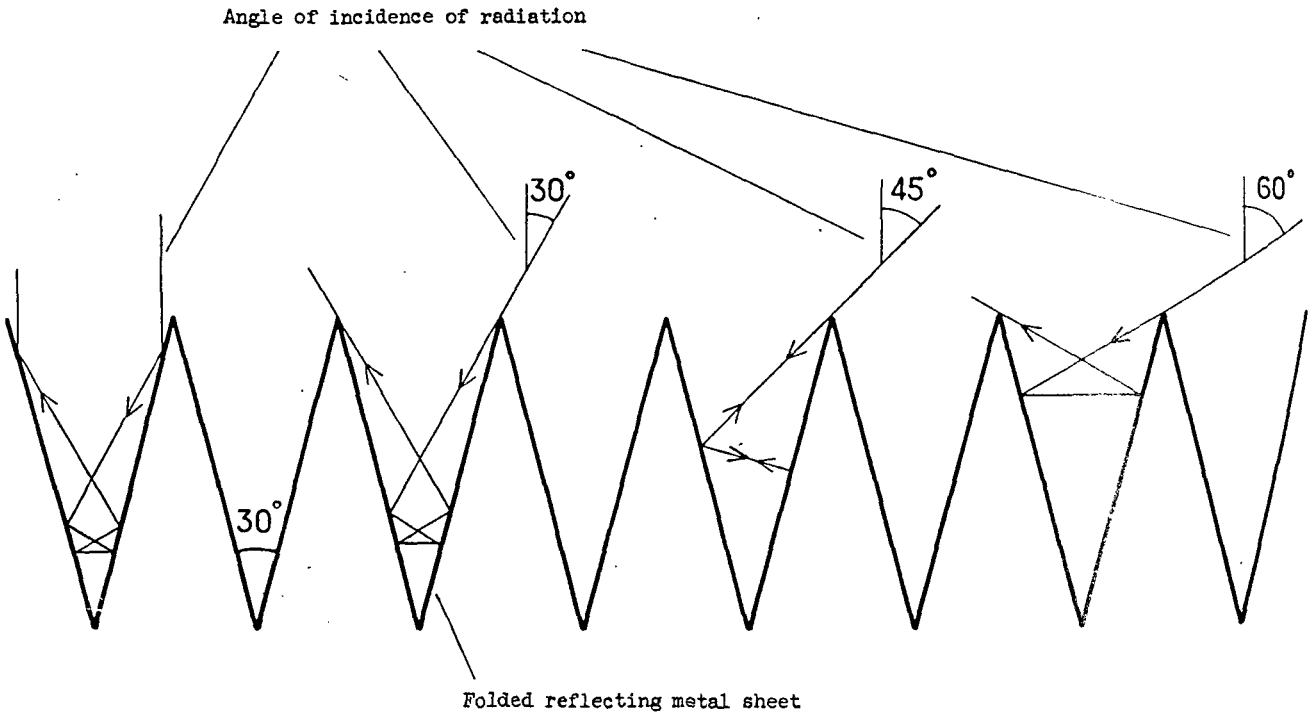


Figure 2. Absorption of solar radiation by successive reflections on folded metal sheets

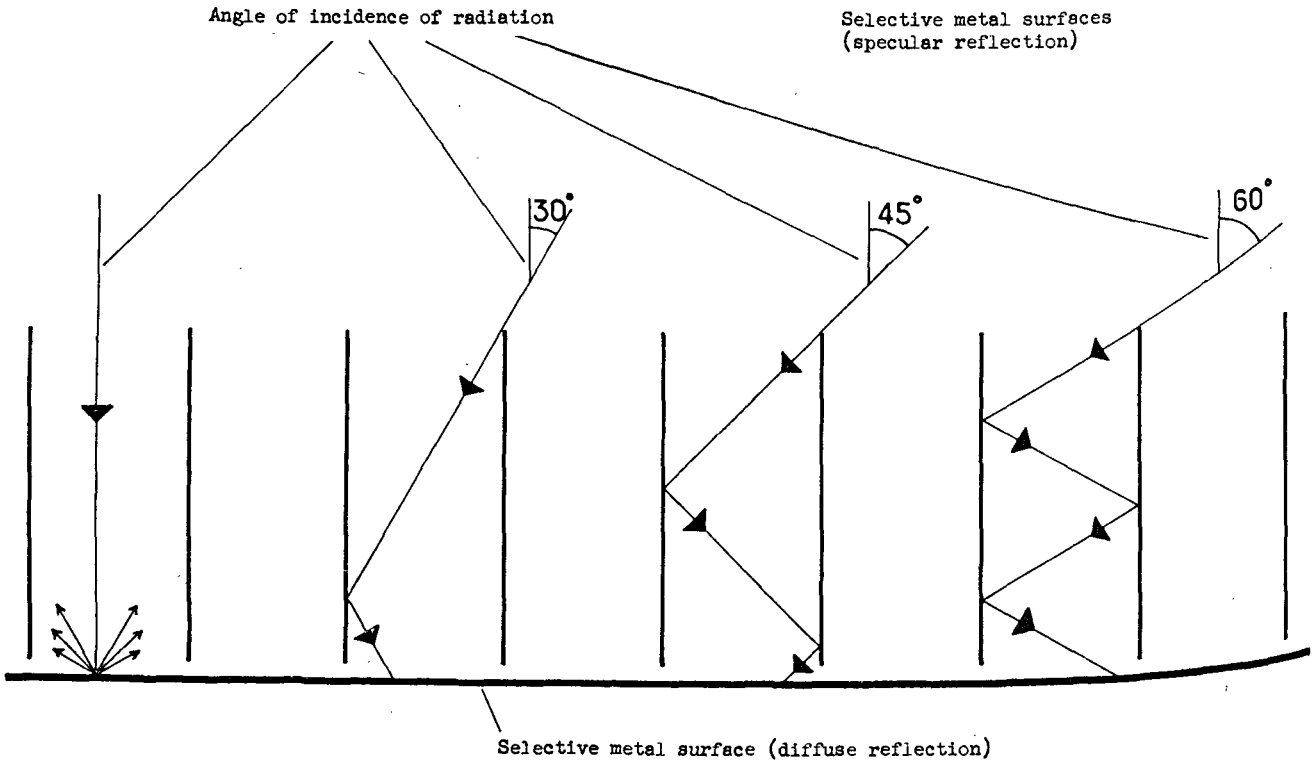


Figure 3. Absorption of solar radiation by successive reflections on parallel metal sheets

we observed the following values for the absorption of solar radiation : 45 per cent for aluminium grooved with needles 0.35 mm in diameter, with tapered points, placed side by side in a support, and 25 per cent with ordinary rolled aluminium. And well-polished aluminium absorbs no more than 14 per cent of the solar radiation.

Similarly, the absorption of solar radiation by a stainless steel with 16 per cent chromium increases from 40 to 55 per cent when it is superficially ruled. Higher values may be obtained with deep rulings.

Sand blasting also increases the absorption of these sheet-metal materials, as do chemical reagents, whose corrosive action is primarily directed against the grain boundaries. Chemical attack will have a particularly favourable effect when the product under attack consists of fine grains, and still more, if it is an alloy, one of whose components is preferentially dissolved as compared with the other. Thus certain alloys in eutectic or eutectoid proportions strongly absorb solar radiation after corrosion by a chemical reagent.

In a recent study (1), we have shown that electrolytic deposits on a tin-zinc base were better absorbers of solar energy than the pure metals. These matte deposits have a maximum absorption between 70 and 80 per cent, according to the treatment, at a tin content of about 15 per cent by weight. Some of these alloys have a good resistance to corrosion.

The choice of the arrangement for producing the multiple reflections depends essentially on the problem under attack. If large heat-exchange surfaces are desired, to heat gas to moderate temperatures, folded metal sheets or arrangements with parallel metal sheets may be used to advantage. The surface area of such collectors is from 2 to 8 times as great as that of an ordinary plane collector. The higher temperatures generally necessary for heating liquids or for applications such as thermocouples are obtained more easily by means of metal sheets ruled on the surface receiving the radiation. In this case, however, it will be noted that the convectional heat transfer is a little greater with the grooved surface than with the plane surface.

Realization of selective heating surfaces by chemical treatment

In particular, we have coloured aluminium plates by means of a solution of potassium permanganate of concentration ranging from 5 to 20 g/l, with enough sulfuric acid added to adjust the pH to a level between 0.5 and 6 (in the absence of acid,

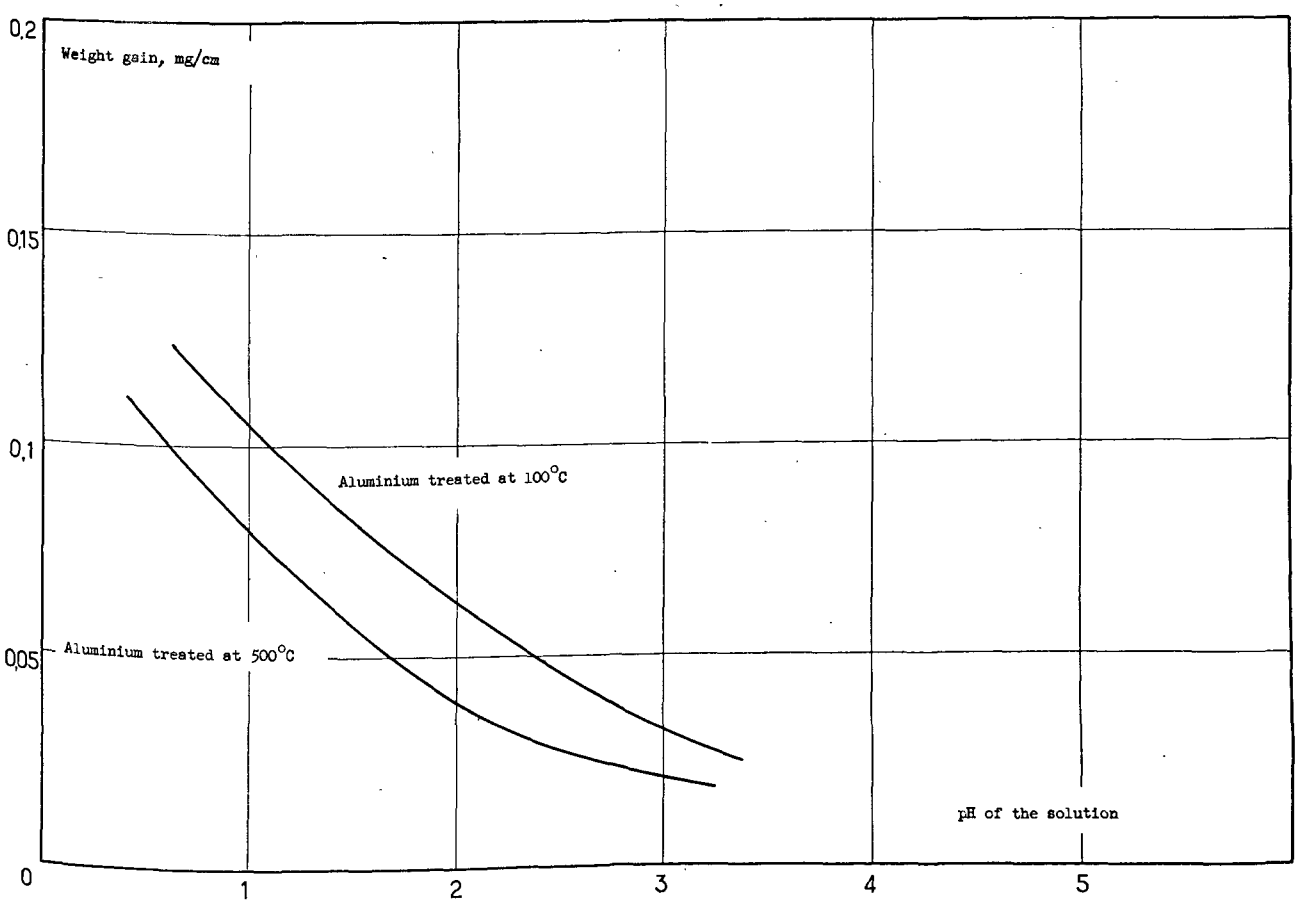


Figure 4. Weight gain of aluminium sheets treated with sulfuric acid solutions of potassium permanganate of various pH values

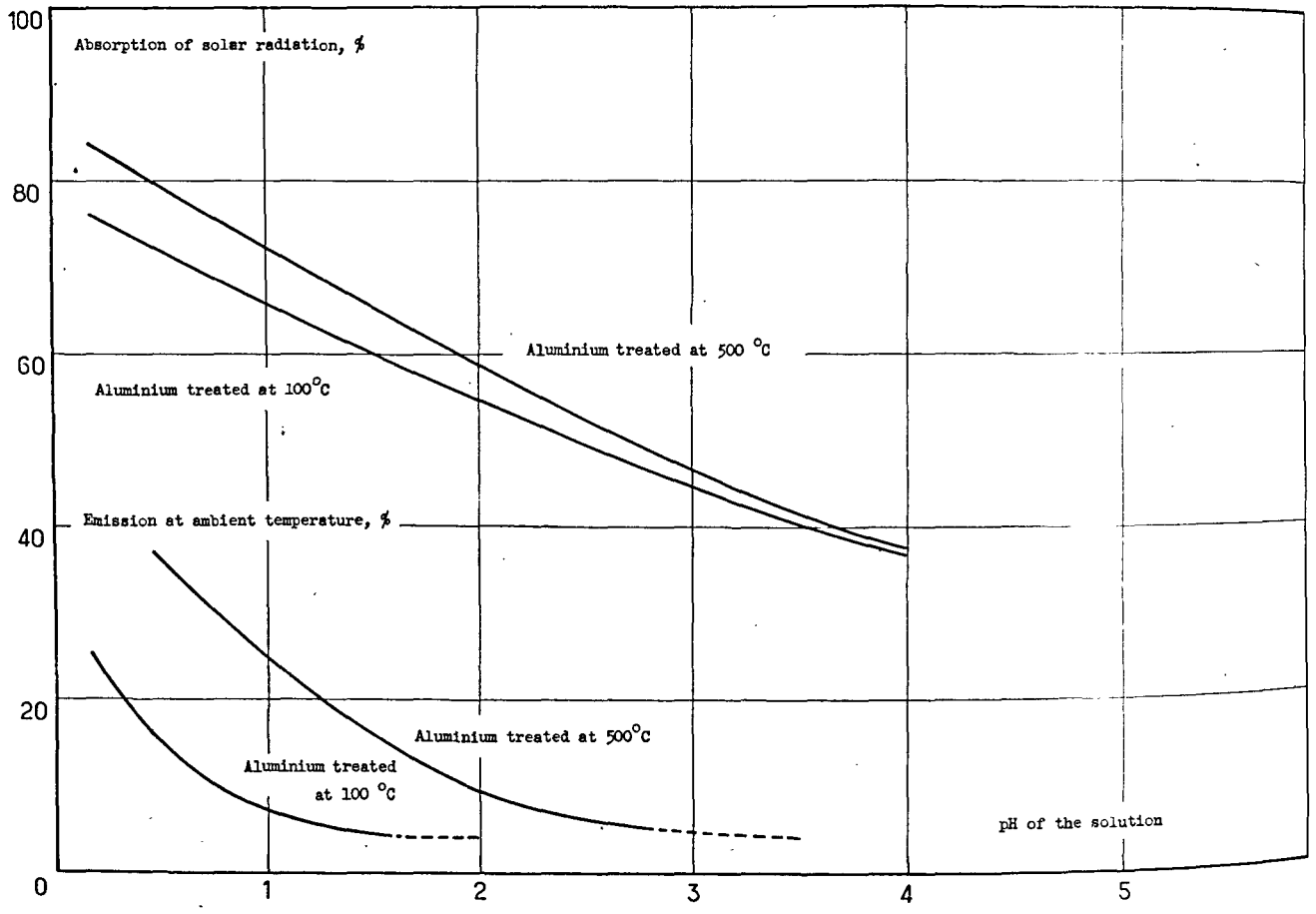


Figure 5. Absorption of solar radiation and emission by aluminium sheets treated with sulfuric acid solutions of potassium permanganate of various pH values

the pH is slightly higher than 6). The plates are first treated with trichloroethylene to dissolve the superficial grease deposits, and then plunged vertically into a bath brought near the boiling point. The plates are then thoroughly washed, followed by annealing at temperatures between 100 and 500°C.

The color obtained varies greatly with the pH of the solution used. At pH 6 it is light yellow; blackish tints are obtained with solutions more acid than that. The intermediate pH values give a more or less dark bronze or chestnut color. The treatment time has relatively little influence. Ten minutes is generally sufficient. The permanganate concentration likewise does not appear to play an important part, at least at concentrations over 0.5 per cent.

Figures 4 and 5 are plots of the results of a series of experiments of this nature. The emission of the plates themselves, at the ambient temperature, is relatively low so long as the weight gain does not exceed 0.1 mg/cm², corresponding to a coating less than a micron thick.

The "stainless" steels may likewise be used for selective plates. Oxidation of these steels at temperatures between 250 and 550°C gives extremely thin surfaces of colored oxides, with a weight gain not exceeding 0.01 mg/cm². More vigorous oxidation, by treatment for a certain length of time, at around 500 or 600°C, leads to the appearance of small plates of oxide particles that can be seen with the naked eye.

Emission in the medium infrared remains limited to about 10 per cent in the various cases. The following results were obtained for the absorption of solar radiation:

Treatment temperature (duration : 3 h)	*Steel with 16 per cent chromium*		*Steel with 18 per cent chromium 8 per cent nickel*	
	Absorption of solar radiation %	*Color*	*Absorption of solar radiation* %	*Color*
Untreated .	45	Unchanged	40	Unchanged
300°C . . .	52	Yellow	48	Yellow
400°C. . . .	60	Red	55	Orange
500°C. . . .	70	Violet	66	Violet
600°C. . . .	75	Blue	70	Blue

The metal sheets still retain their brightness in spite of the light oxidation. Their resistance to chemical agents is excellent and the cost of such treatment remains very low.

Multiple reflection on chemically treated metal sheets

In the case of aluminium, just as in the case of the steels, the preliminary chemical treatments may be combined with multiple reflection effects (folded, grooved or parallel sheets). In all cases, however, a judicious equilibrium should be realized, so that the ultimate absorption of solar radiation will be high, while the over-all emission still remains low enough.

In the case of folded or parallel metal sheets, it will generally suffice to use sheets with an absorption factor of only 50 per cent for the solar radiation, so that one has metal sheets covered with extremely thin colored layers maintaining good specular reflection as well as low emission.

With grooved metal sheets, the problem is somewhat different, since the number of reflections so realized is appreciably smaller. When these metal sheets are used by themselves, without adding auxiliary reflecting sheets, it will be advisable to use the most absorbent coatings. For example, unruled bright aluminium, treated at pH 3 in a 5 per cent solution of potassium permanganate, absorbs 60 per cent of the solar radiation, while the same metal sheet, first ruled, absorbs 75 per cent of the same radiation. The emission of the metal sheet itself at the ambient temperature is rather low (10-15 per cent) in the former case, and of the order of 30 per cent in the latter.

"Stainless" steel sheets may be both grooved and oxidized, as already stated. Under these conditions, the absorption of solar radiation may reach, or even exceed, 85 per cent, while the emission from the sheet still remains low.

Study of selective "cold" surfaces which reflect solar radiation and themselves have a strong emission

The infrared emission of A_9 aluminium foil (99.9-99.98 per cent), supplied by Tréfileries of Le Havre and by Aluminium français, was studied. This emission was found to become great when the thickness of the alumina film reached one micron, and it was found further to approach black body conditions at a film thickness of 3 microns or more. A great increase of absorption, however, is also noted, in the zone between 3 and 8 microns, with increasing thickness. Figure 7 gives the daily course of the temperature of aluminium sheets placed horizontally on thermal insulation, the upper face free, and receiving no radiation except from the

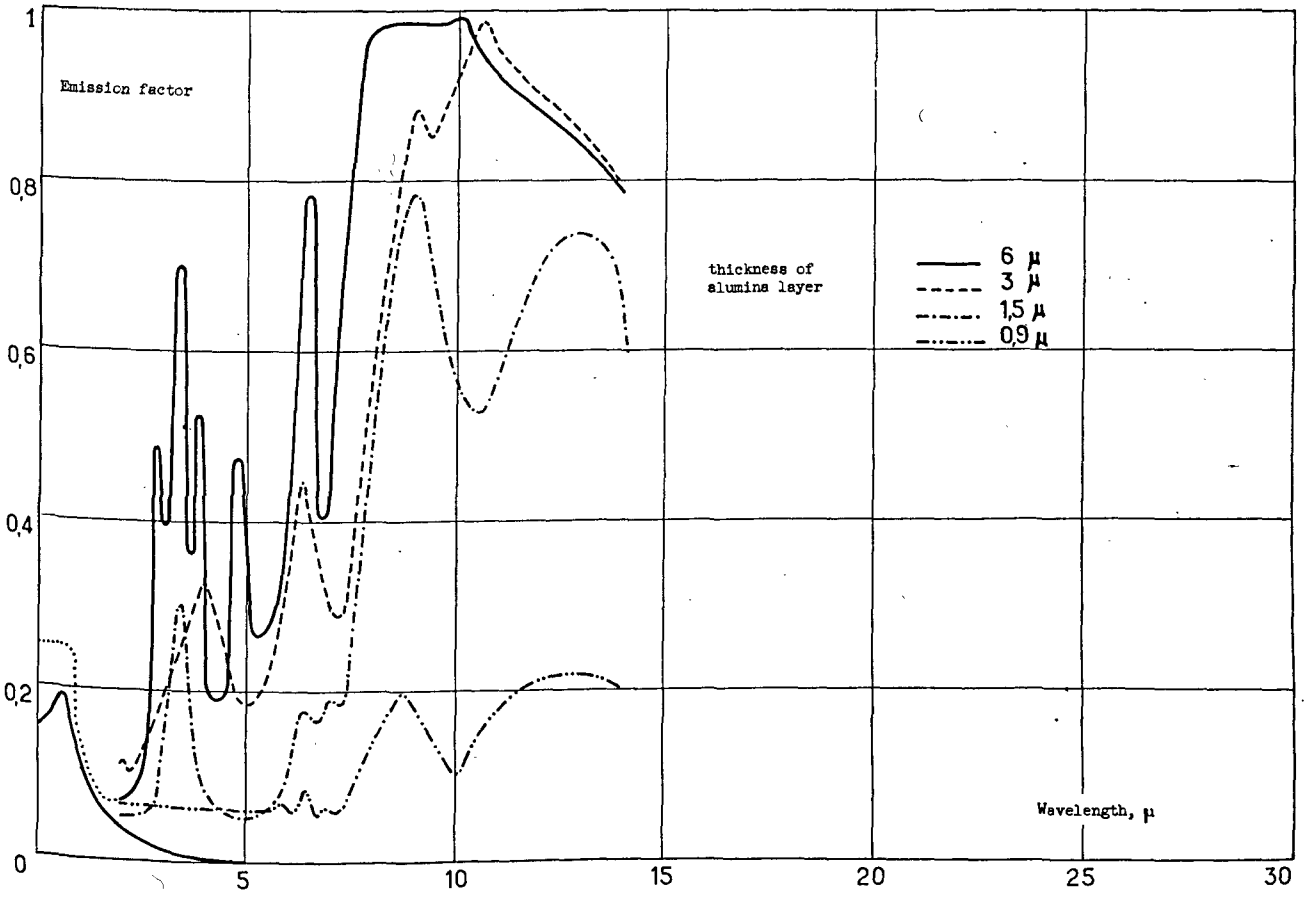


Figure 6. Variation, with the wavelength, of the emission factor of anodically oxidized aluminium sheets for various thicknesses of the alumina film

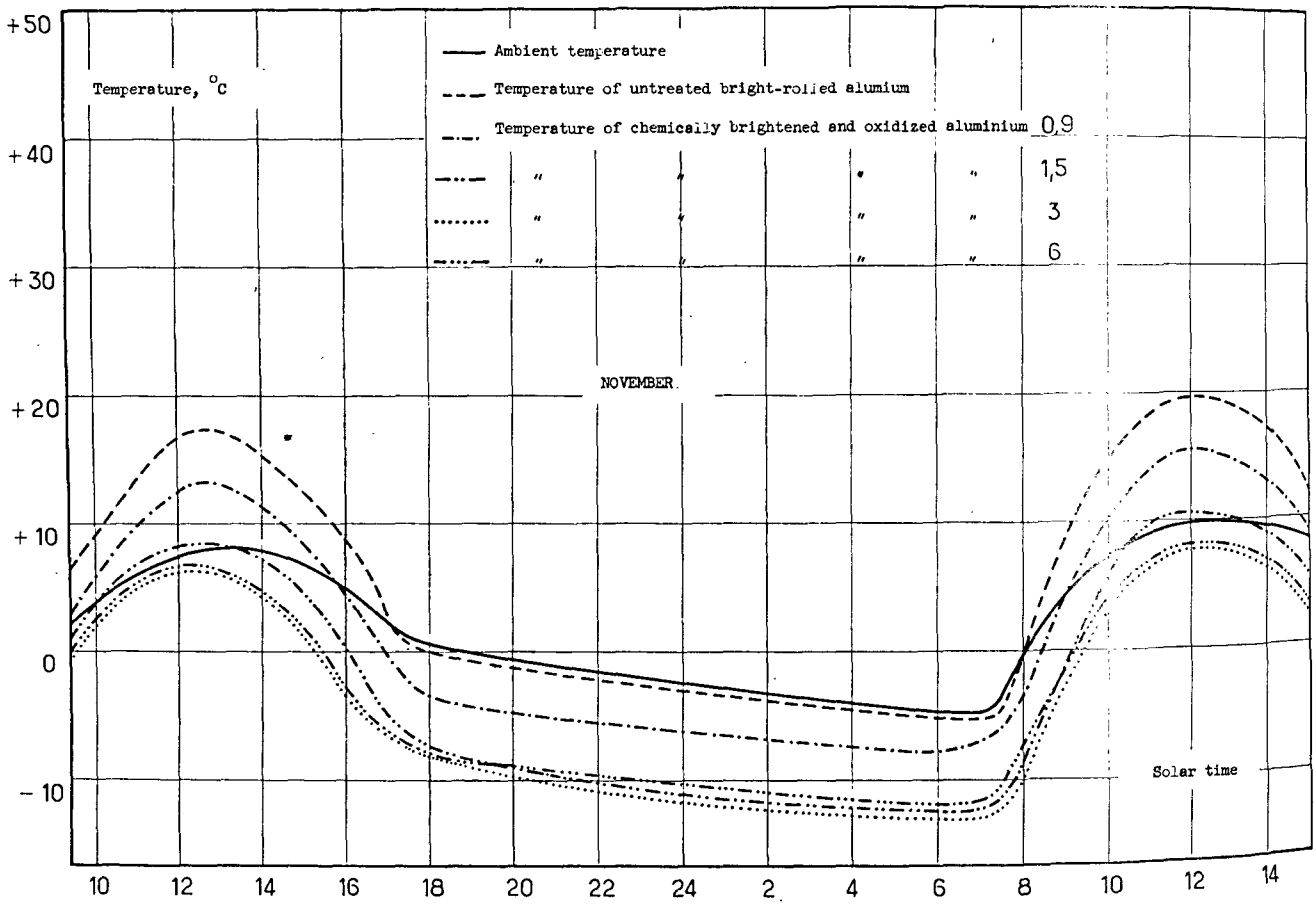


Figure 7. Day and night variation of temperature of various aluminium sheets

sun and the sky. Table 1 shows the results that were observed.

We have also run experiments on sheets of aluminium-magnesium alloys with 3 per cent magnesium, polished (brillalumag), and anodically oxidized in the same way as the aluminium sheets. We noted that at equal thickness, the emission was appreciably less from the alloys than from the pure aluminium. Almost the same results were obtained with oxide films about half as thick.

Table 2 relates to an ordinary aluminium A_5 (99.7-99.79 per cent) treated by the Pechiney Company. We noted a strong emission from these products; some of them are good reflectors of the solar radiation.

Table 1. Aluminium A_9 (minimum 99.99 per cent)

Thickness of film of electrolytically formed alumina	*Absorption of solar radiation (per cent)*	*Emission at ambient temperature (per cent)*
0 (not treated) [a]	14	< 10
0 (brightened)	14	< 10
0.9 μ	15	about 40
1.5 μ	15	about 60
3 μ	15	about 75
6 μ	15	> 90

[a] The protective layer of alumina usually formed on aluminium is less than 0.02 μ in most cases.

We give for information the market prices of the varieties of aluminium:

Percentage	*NF per metric ton*
A_4 . . . . . 99.5 to 99.69	2 435
A_5 . . . . . 99.7 to 99.79	2 485
A_6 . . . . . 99.8 to 99.85	2 580
A_7 . . . . . 99.85 to 99.89	2 730
A_8 . . . . . 99.9 to 99.98	3 500
A_9 . . . . . 99.9 (minimum)	4 300

Table 2

Oxidation		*Thickness of oxide film*	*Absorption of solar radiation %*	*Emission at about 10°C %*
Degreasing	*Bath*			
Aluminium A_5 (99.7-99.79 per cent Al)				
Not treated	Not treated	0 μ	15	< 10
Electrolytic alkaline degreasing . . .	H_2SO_4 ordinary	10 μ	23	> 90
Chemically brightened	H_2SO_4 ordinary	10 μ	23	> 90
Degreased with soda	H_2SO_4 ordinary	10 μ	26	> 90
Electrolytic alkaline degreasing . . .	H_2SO_4	60 μ	65	> 95
Alloy of aluminium with 5 per cent silicon : AS_5				
Degreased with soda	H_2SO_4 ordinary	10 μ	60	> 90

Table 3. Deposits of aluminium on aluminium A_5

Aluminium varnish		*Emission at about 10°C (per cent)*	*Absorption of solar radiation (per cent)*
Nature	*Application*		
Untreated		5	15
Cellulose	Spray gun	90	40
Synthetic	Spray gun	80	46
Synthetic	Brush	60	39
Outside grease	Spray gun	65	36
Inside grease	Spray gun	40	34

The Péchiney Company has also placed at our disposal plates coated by various methods with aluminium deposits. Certain of these inexpensive products have an excellent emission, and their absorption for solar radiation is in any case relatively high. The best results have been obtained with aluminium-base cellulose varnishes, applied with a spray gun.

Tin-base coatings. Brightened tin strongly reflects the solar radiation (87 per cent). On the other hand, anodically oxidized products are coloured owing to the formation of lower oxides and cannot be used for the fabrication of cooling collectors, in spite of the strong emission in the infrared.

Selective paints. Most white oxides are excellent pigments for compounding selective paints. It is noted that paints with a titanium (rutile) base reflect 75 to 80 per cent of the solar radiation, as compared to about 70 per cent for zinc-oxide base paints, the refractive indices of rutile (2.616 and 2.903 square product) being higher than those of zinc oxide (2.008 and 2.903 hexagonal product). The emission of the paints at ambient temperature is over 90 per cent or even 95 per cent. Such products, with a glycerophthalic resin base, give almost as good results as anodically oxidized aluminium, as will be seen from the day and night temperature curves for metal sheets painted with them (figure 8).[1]

Remarks on the transparent walls that can be used in solar collectors utilizing the hothouse effect

Two solutions are usually adopted: transparent plastic or glass. The former is more economical, but has the disadvantage, for certain arrangements, of

[1] If paints still richer in pigment are compounded, or if the wet paint is strewn with the powder of these pigments, solar radiation reflection over 90 per cent may be obtained, but the coats so produced are rough and show apparent grains.

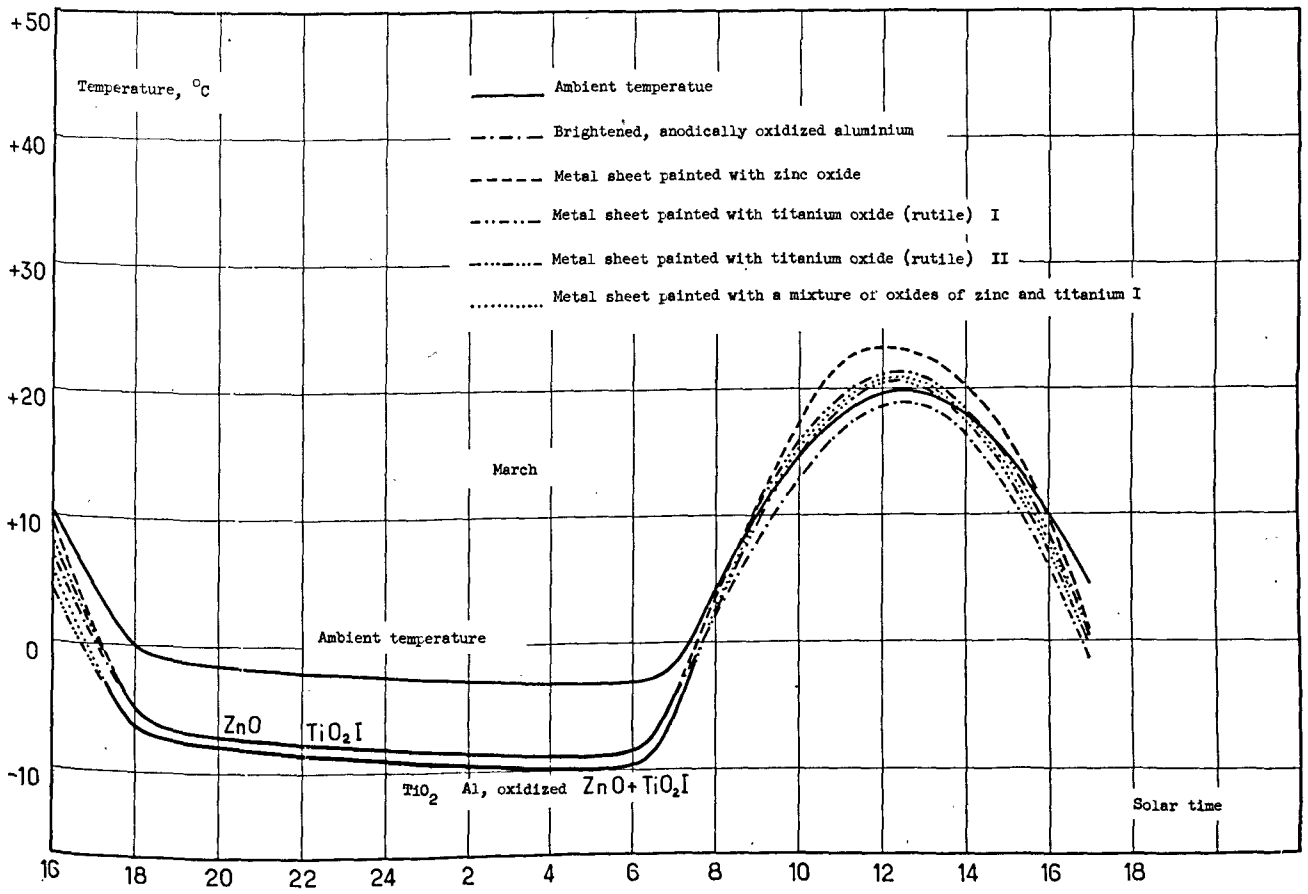


Figure 8. Day and night variation of temperature of metal sheets painted with zinc oxide and with titanium oxide

Table 4. Tin-base coatings

Nature of metal and of its coating	*Treatment*	*Absorption of solar radiation (per cent)*	*Emission at ambient temperature (per cent)*
Hot-tinned tinplate	Not treated	25	about 10
Hot-tinned tinplate	Treated 30 min at 80°C in 1 per cent chromic acid	17	about 75
Hot-tinned tinplate	Anodically oxidized	78	75
Hot-tinned tinplate	Heated in air at 210°C (colored film)	30	about 10
Steel with brilliant electrolytic tin coating (250 μ thick)	Anodically oxidized [a]	56	90
Steel coated with electrolytic deposit of copper (13 μ) and of a tin-copper alloy (40 μ)	Not treated	35	about 10
Steel coated with electrolytic deposit of copper (13 μ) and of a tin-copper alloy (7.5 μ)	Not treated	28	about 10

[a] Treatment solution 40 g/l of Na_2HPO_4 and 20 g/l of H_3PO_4 at 75° for 5 min, current density 0.04 amp/cm.

being partially transparent in the infrared when present in film form.

In the immediate future, it is difficult to think of using other types of glass than ordinary window glass. In general, when we consider the role of the glass panes in the hot-house effect, we take account only of their absorbing properties for infrared radiation of wavelengths longer than 3 or 4 microns. But it is not without interest to consider their reflecting power as well, which is important at

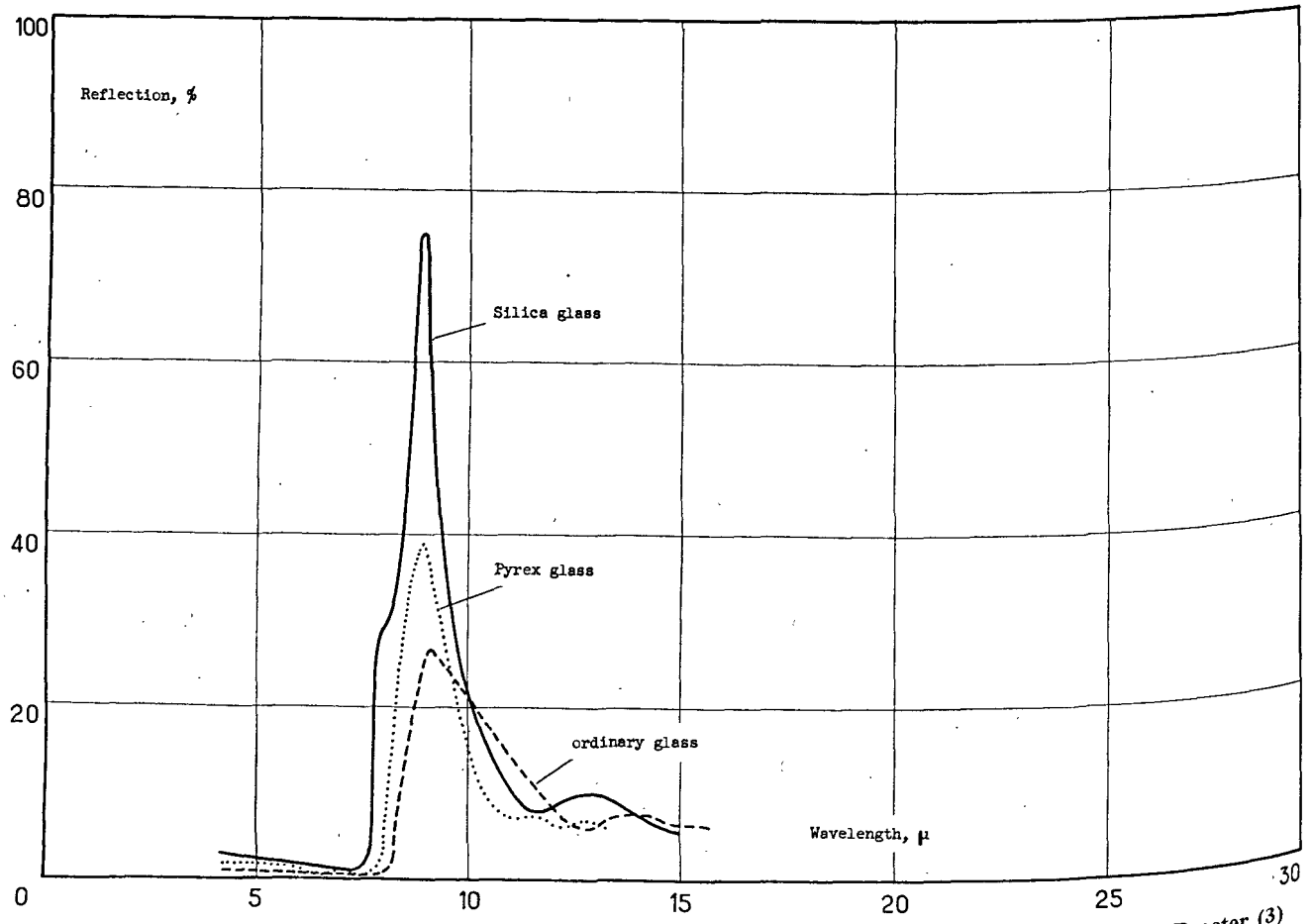


Figure 9. Infrared reflection of ordinary glass, of Pyrex glass, and of silica glass, after Jellyman and Procter (3)

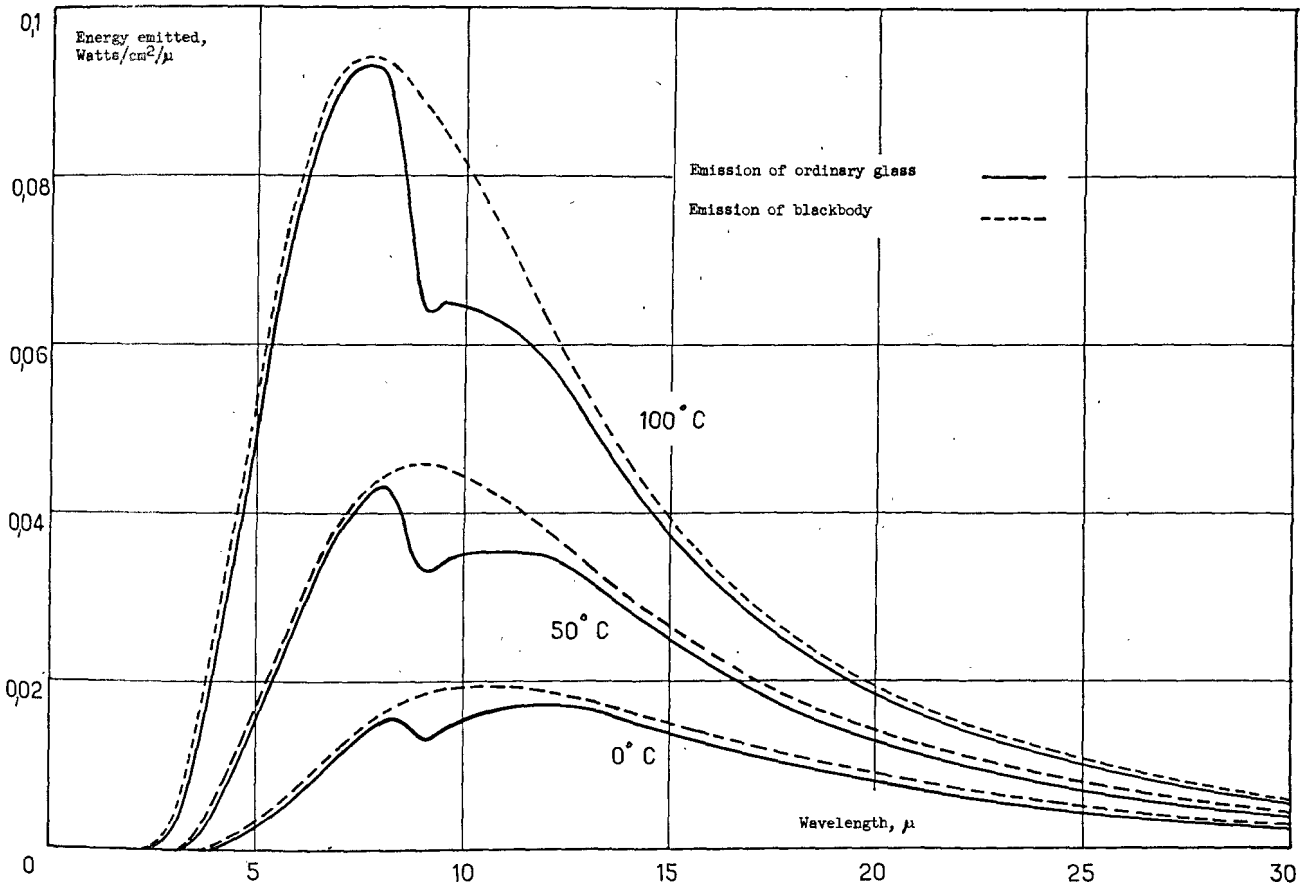


Figure 10. Emission of ordinary glass at various temperatures, compared with black body emission

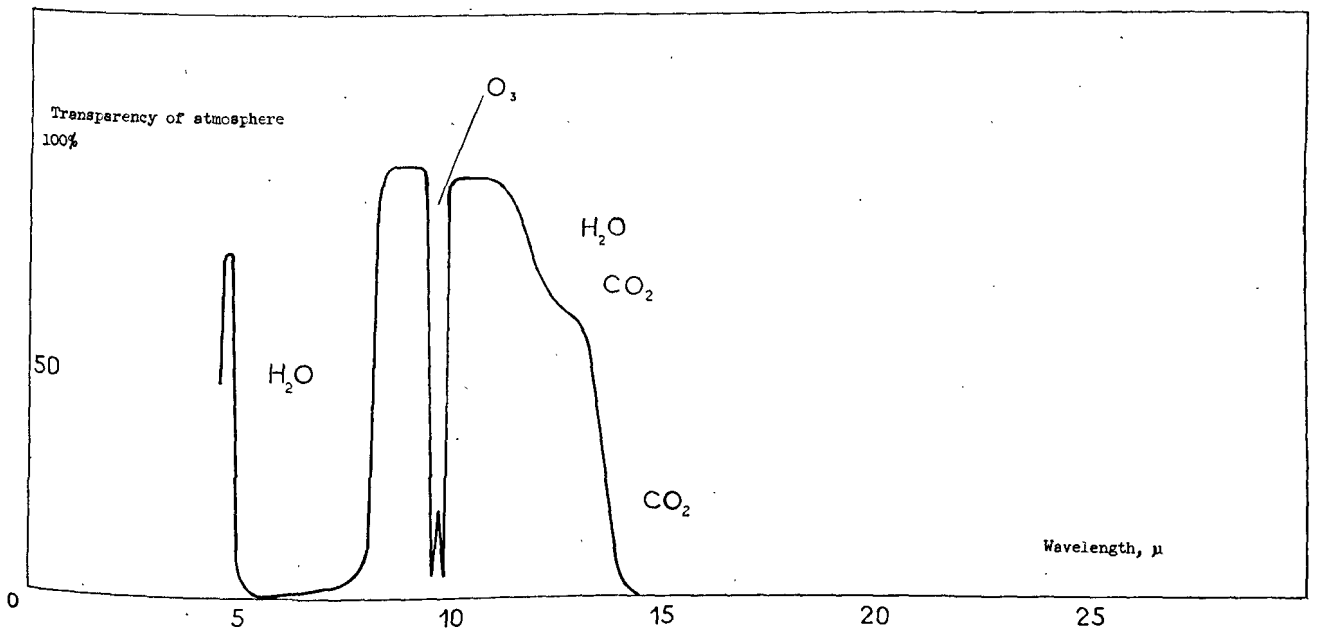


Figure 11. Transparency of the atmosphere in the infrared (4)

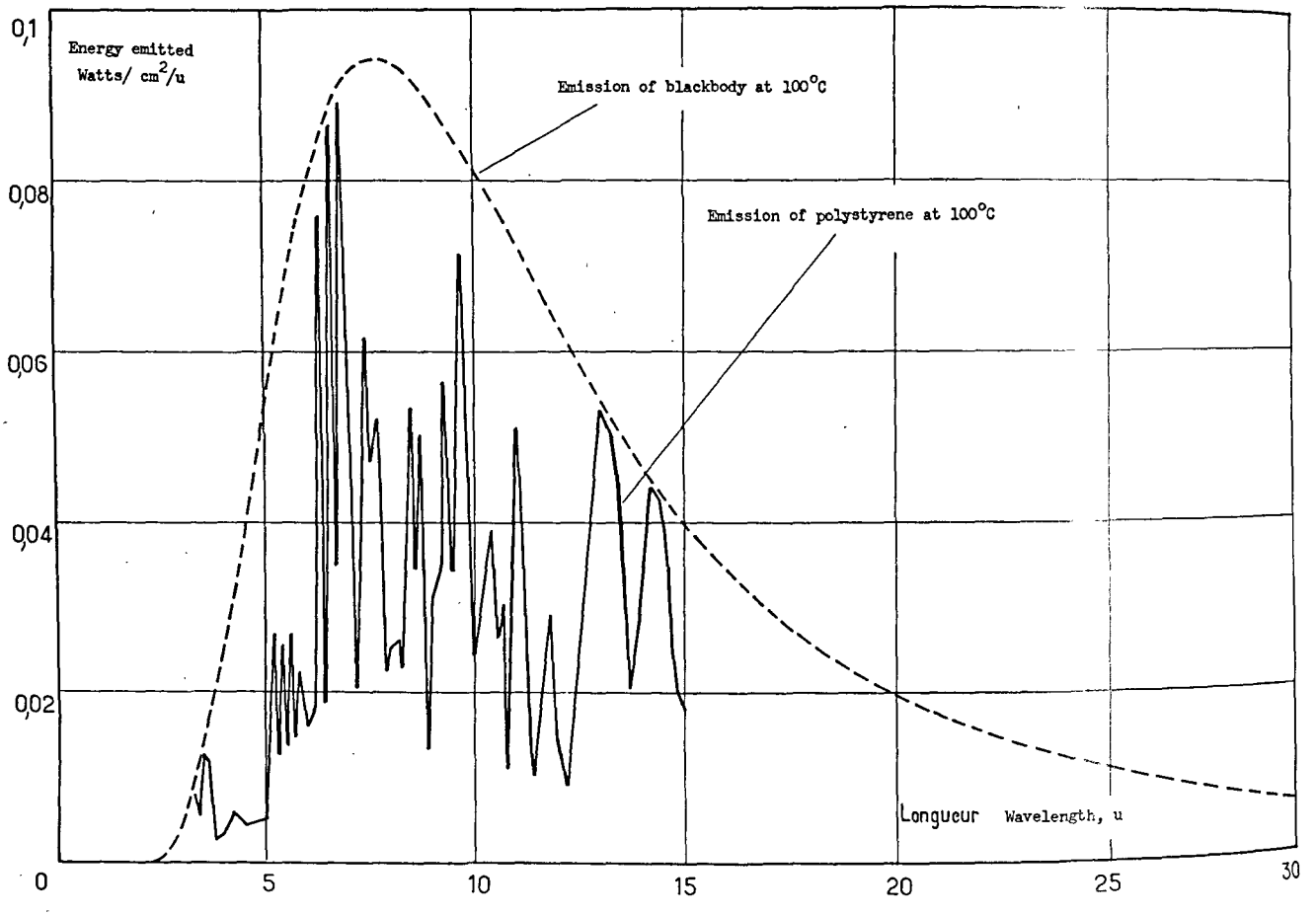


Figure 12. Emission of a polystyrene film 70 microns thick at 100°C, compared with black body emission

around 9 μ (figure 9), for a wavelength very close to that of the emission maximum of these glasses when heated between 0 and 100°C (figure 10). This reflection, rather similar in its effects to that of metals (the unreflected radiation is absorbed at a very shallow depth), is located precisely in the principal opening for terrestrial radiation, situated around 8-12 microns between absorption bands of water vapour (figure 11). Thus its effect, on the one hand, is to reflect towards the interior of the collector the radiation emitted by the absorbing metal sheet, and, on the other hand, to limit the radiation emitted by glass in a spectral zone where the glass receives no energy at all from the sky.

Ordinary glass is not the best glass that could be imagined in this respect. Pyrex glass and silica glass, indeed, have an even more intense reflection band in the same spectral zone. These two glasses are naturally much more expensive, but it would be interesting to stage basic research with a view to finding a glass with more accentuated reflecting properties, and at a cost selling for a bearable price. Since glasses are able to dissolve most metallic oxides, the field for investigation would seem to be rather broad.

The plastics, when not too thick (say, 1/50 mm) transmit part of the infrared radiation and have characteristic emission curves (figure 12) (selectives with polystyrene).

Another aspect of this question is the utilization of glasses with high refractive indices, the use of which might be of interest in cases where the receiving surface does not capture the entire solar radiation (general case of selective surfaces) and would be diffusing. This would permit the collection, by reflection on the glass, of a large part of the radiation diffused at great angles. But this method would be applicable exclusively to collectors utilizing the sun only a few hours a day, during the period of the normal and close-to-normal incidence of the solar radiation on the surface of the collector pane.

References

For references, see end of French version.

Summary

"Hot" selective surfaces absorbing solar radiation

It is well known that metals generally absorb radiation much more strongly in the visible and near infrared regions than in the regions of longer wavelength. Metallic surfaces may therefore be used for selective collectors with low emission, which may absorb considerably more solar radiation if designed to have the incident radiation reflected several times in succession. These multiple reflections are obtained by means of folded or parallel metal sheets, striated, ruled or dulled by mechanical, physical or chemical treatment. Most of these procedures give large heat-exchange surfaces favourable primarily to the heating of gases.

Heating surfaces have likewise been prepared by chemical colouring of metal surfaces. Aluminium treated with sulfuric-acid solutions of potassium permanganate gives good results. The colouration is more marked, the lower the pH. Stainless steels may likewise be superficially oxidized to give them a red or blue tinge. With aluminium, as with steel, these chemical treatments may be combined with the multiple-reflection effects (sheet metal, folded, parallel or striated), but in all cases equilibrium should be established between these different operations in such fashion as will yield the maximum selective effect. Sheets of "stainless" steels, striated and superficially oxidized, are able to absorb 85 per cent of the solar radiation, while the emission from the sheet remains low (10 to 15 per cent).

"Cold" selective surfaces reflecting the solar radiation

The Solar Energy Laboratory at Mont-Louis has also developed "cold" selective surfaces that reflect solar radiation and themselves have a strong emission.

Good results have been obtained in this field with pure aluminium foil (99.9-99.98 per cent), anodically oxidized. The emission at ambient temperatures approaches that of a black body when the thickness of the aluminium oxide film formed exceeds 3 microns. Various aluminium-base coatings and painting procedures have been studied, especially cellulose varnishes deposited with a spray-gun. Coatings based on metallic tin have also been studied. They can be anodically oxidized, but in that case they become much less reflective for solar radiation.

Among the selective white paints, those with a titanium-oxide base give the best results. Their own long-wave emission at ambient temperature exceeds 90 or even 95 per cent, while their reflection of solar radiation is of the order of 75 to 80 per cent, or even more when coated with more conspicuous pigments.

Transparent walls utilizing the "hot-house effect" and available for use in collectors

The authors examine in particular the role of the reflection bands shown by glasses in the medium infrared for wavelengths very close to those of the emission maximum of bodies heated to between 0 and 100°C. Complex glasses, other than ordinary glass, might give still better results in this field.

EMPLOI DE CERTAINS ALLIAGES D'ALUMINIUM POUR L'UTILISATION DE L'ÉNERGIE SOLAIRE

Pierre Vachet * *et Jean Mercier* **

Depuis quelques années, l'industrie du bâtiment utilise pour des buts décoratifs des panneaux de tôles ou des profilés d'alliages d'aluminium renfermant 4 à 5 p. 100 de silicium (connus sous le nom d'A-S4 ou d'A-S5 dans la symbolisation française) que l'on oxyde anodiquement en vue d'obtenir une teinte gris foncé, presque noire.

Ces couches d'oxyde doivent cette teinte à des inclusions de silicium ou de silice. Il était logique de penser qu'elles constituent d'excellents pièges à rayonnement solaire.

C'est ce que nous nous sommes proposé de vérifier. Certains panneaux de tôles furent remis à cet effet au professeur F. Trombe, qui les compara à d'autres échantillons, de tôle d'aluminium non allié cette fois, soit nue soit revêtue d'une couche d'oxydation anodique après différents traitements de surface. Il n'est point question de revenir sur les résultats obtenus.

De notre côté, utilisant un dispositif expérimental employé par le professeur Trombe, nous cherchâmes à nous rendre compte de la façon dont variait la température de tôles d'A-S4 exposées horizontalement au rayonnement solaire sur une table revêtue de 100 mm de laine de verre.

Ces tôles d'une épaisseur de 3 mm avaient un format de 250 × 250 mm. En leur centre, sur leur face inférieure, était rivée une plaquette de cuivre, au moyen de huit rivets. Au centre de cette plaque était brasé un couple thermo-électrique (figure 1). Les températures étaient relevées toutes les heures durant 24 heures d'exposition à un ciel clair, à Chambéry. La température ambiante était relevée sous abri.

Sept échantillons furent ainsi simultanément testés :

1. Aluminium A5 (99,5 p. 100) Brillant, nu.
2. Aluminium A5. Tôle rendue mate par cinq ans d'exposition en atmosphère industrielle particulièrement corrosive (proximité d'une fonderie et d'une cheminée d'évacuation d'un laboratoire d'analyse chimique).
3. Aluminium A5. Oxydée anodiquement sur la face externe, sans décapage préalable (épaisseur de la couche d'oxyde : 15 microns).
4. Aluminium A5. Non décapée au préalable : simplement revêtue d'une couche mince de MnO_2 par immersion dans une solution sulfurique de permanganate de potassium, sur sa face externe.
5. Aluminium-silicium A-S4. Oxydée anodiquement sur la face externe (épaisseur de la couche d'oxyde : 15 microns).
6. Aluminium-silicium A-S4. Oxydée anodiquement sur sa face externe, mais à une épaisseur de 25 microns.
7. Fer. Tôle noire brute.

Les couches obtenues sont reproduites dans la figure 2. On a tracé dans les figures 3 et 4, à des échelles différentes, les courbes donnant les températures diurnes et nocturnes.

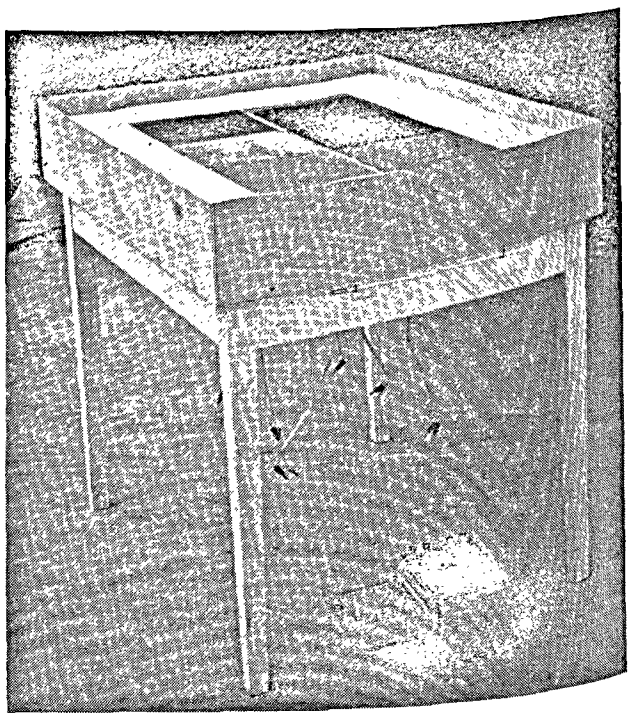


Figure 1

* Chef du service des recherches métallurgiques, Compagnie Péchiney, Paris.

** Ingénieur, service des recherches métallurgiques, Compagnie Péchiney, Paris.

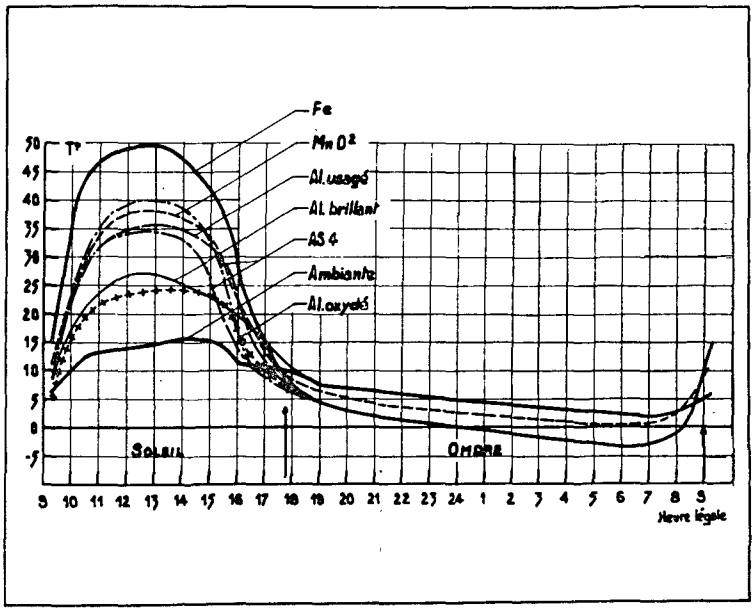


Figure 2

Ces courbes peuvent être résumées comme suit :

Températures diurnes maximales	*Degrés centésimaux*	*Températures nocturnes minimales*	*Degrés centésimaux*
Échantillon 7	50	Température ambiante	3
Échantillon 6	44,5	Échantillon 1	2
Échantillon 4	39,0	Échantillon 4	0,5
Échantillon 2	36,0	Échantillon 2	— 1,5
Échantillon 5	34,5	Échantillon 3	— 2,0
Échantillon 1	27,0	Échantillon 5	— 2,5
Échantillon 3	24,0	Échantillon 7	— 3
Température ambiante	15,0	Échantillon 6	— 4

On constate bien, comme prévu, que la surface d'aluminium nu brillante s'est comportée comme un réflecteur remarquable, absorbant peu de rayonnement solaire de jour et émettant peu la nuit.

Il n'en est plus de même lorsqu'un milieu agressif — que l'on ne trouve heureusement pas dans les expositions habituellement rencontrées en pays à ciel clair — lui a fait perdre son aspect brillant (échantillon 2).

L'oxydation anodique a procuré une surface sélective froide (échantillon 3) et la couche de MnO_2 une surface sélective chaude (échantillon 4), ainsi que le professeur Trombe l'avait mis en évidence.

Quant aux surfaces 5 et 6, obtenues par oxydation anodique de tôles d'A-S4, leurs propriétés se sont d'autant plus rapprochées de celles du corps noir que la couche d'oxyde était plus épaisse.

Grâce à l'aluminium et à l'alliage A-S4, on peut donc obtenir l'éventail complet des propriétés optiques que l'on peut demander à une surface vis-à-vis du rayonnement solaire et du rayonnement propre.

Nous étions donc en droit d'espérer que nous pourrions, grâce à ces surfaces d'A-S4 oxydées, les utiliser pour chauffer de l'eau.

A cet effet, nous avons réalisé des insolateurs de la manière suivante. La surface absorbante est constituée par des Roll-Bond ou tôles à circuit intégrés. On connaît ce type d'échangeur de températures. Il est normalement obtenu en laminant

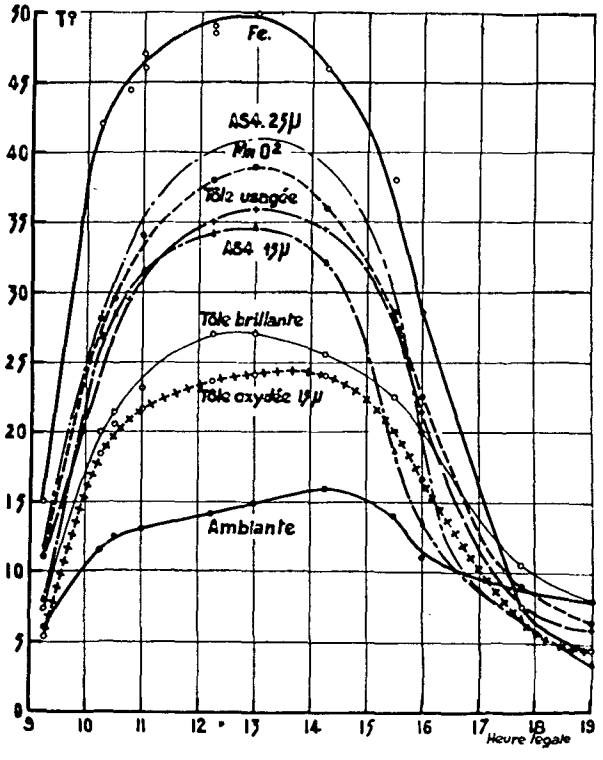


Figure 3

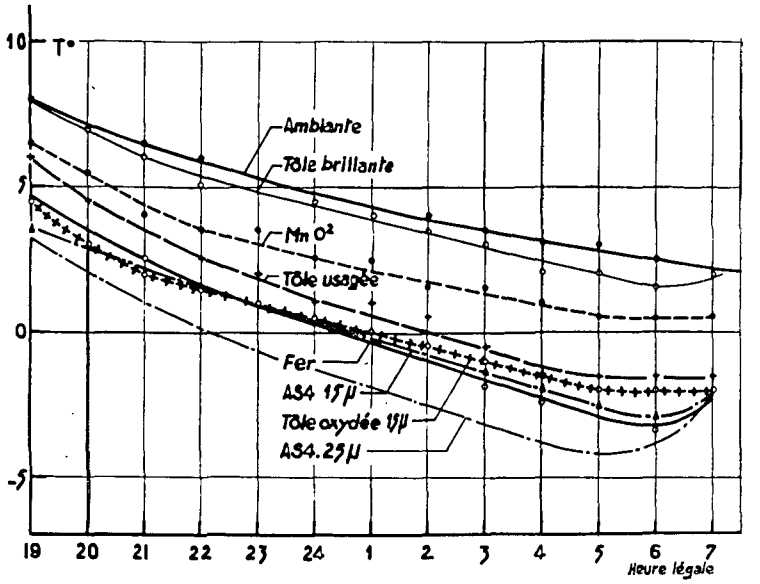


Figure 4

ensemble à chaud deux tôles d'aluminium parfaitement propres et brossées, sur la face interne de l'une desquelles on a dessiné au moyen d'une encre spéciale le schéma d'un circuit de fluide. Lors du laminage à chaud, les deux tôles se soudent sauf sur les surfaces protégées par l'encre. Une des extrémités du circuit étant dégagée, on applique dans cet orifice une pression hydraulique qui fait gonfler le circuit. On dispose ainsi d'un tube plus ou moins replié sur lui-même, en contact intime avec les surfaces planes servant à l'échange de températures.

Dans le cas actuel, l'une des deux tôles était constituée non par de l'aluminium, mais de l'A-S4. Le soudage des deux métaux s'est parfaitement effectué. La surface utile était de 245 × 245 mm,

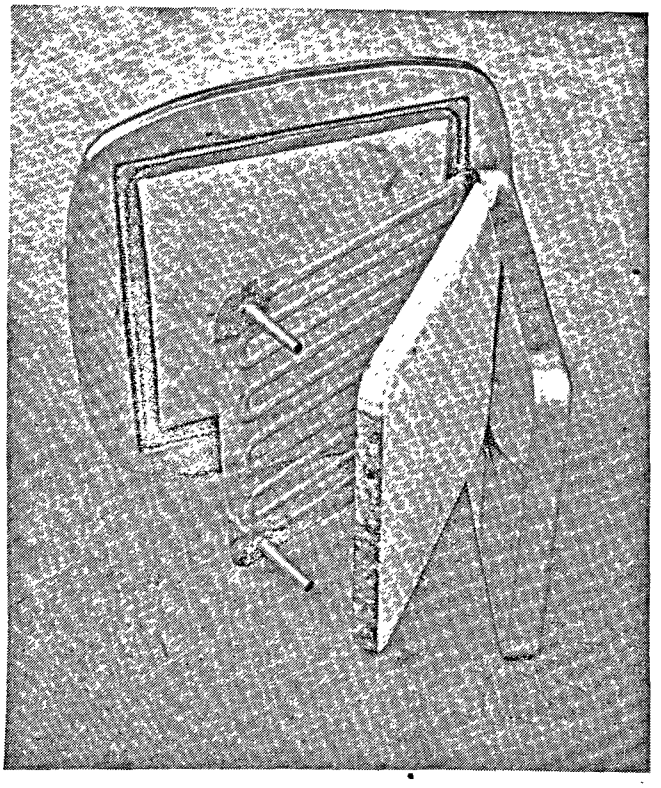


Figure 5

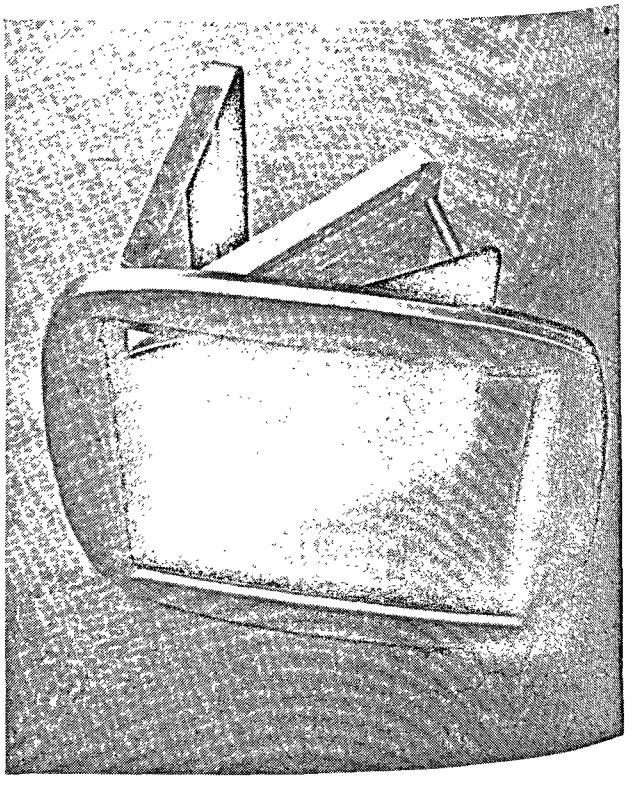


Figure 6

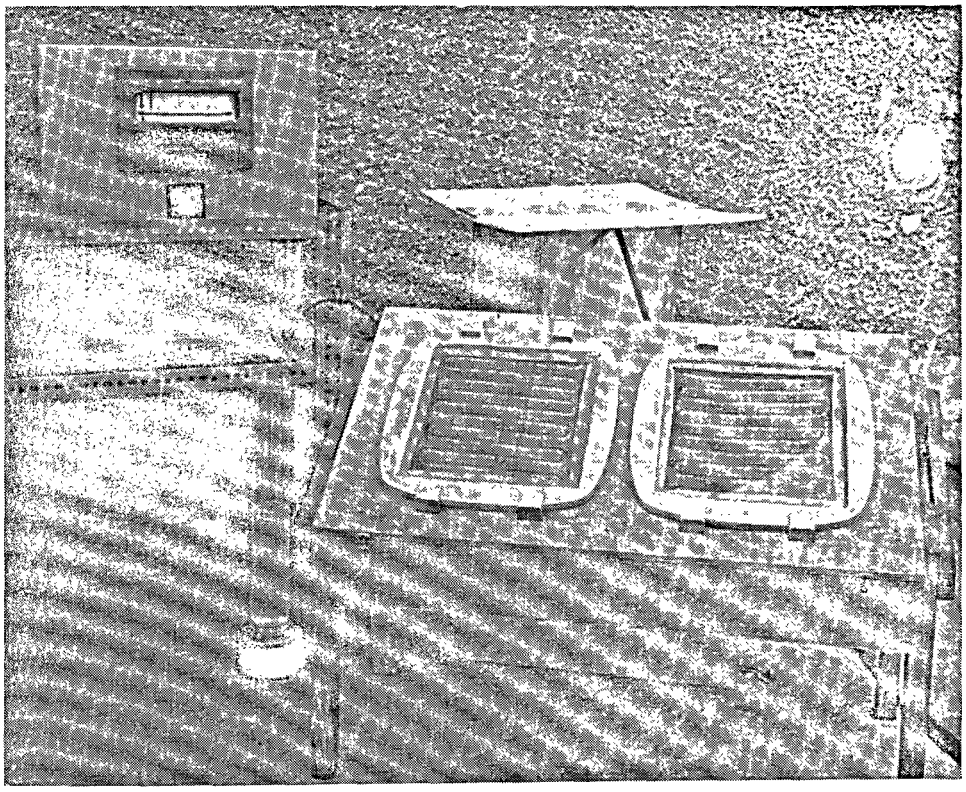


Figure 7

soit 0,06 m², et le serpentin avait une longueur de 2,5 m. La section du canal était de 30 mm².

L'oxydation anodique fut réalisée en bain sulfurique de concentration 20 p. 100 à 20 °C pendant 45 minutes; elle fut suivie de colmatage à l'eau bouillante. Seule la face active en A-S5 était oxydée, l'autre face ayant été protégée pendant cette opération de manière à lui conserver son état de surface naturel brillant, afin de limiter les pertes par rayonnement de ce côté.

Afin de limiter les pertes par convection, cet élément était enfermé dans un capotage métallique dont la face antérieure est constituée par un hublot de verre qui joue un double rôle. D'une part il constitue une protection contre les dépôts de poussières susceptibles de modifier l'état de surface de

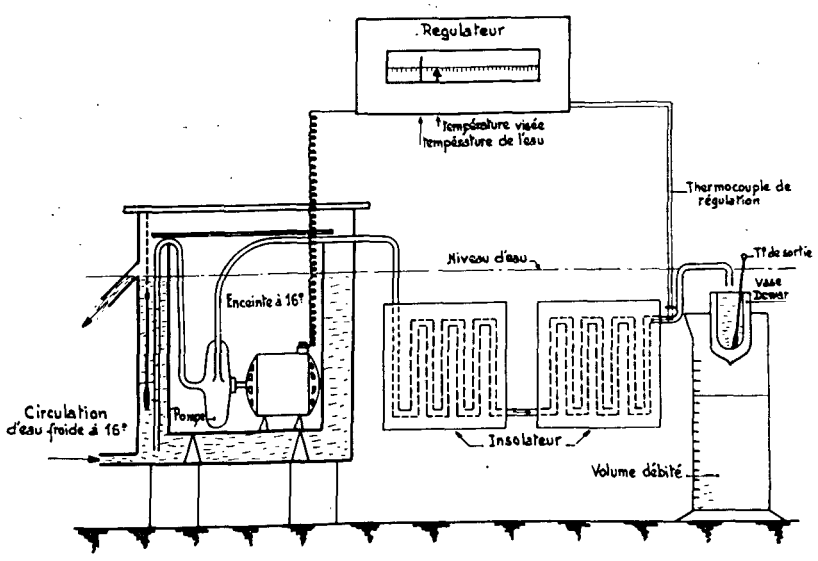


Figure 8. Schéma de l'installation de récupération de l'énergie solaire

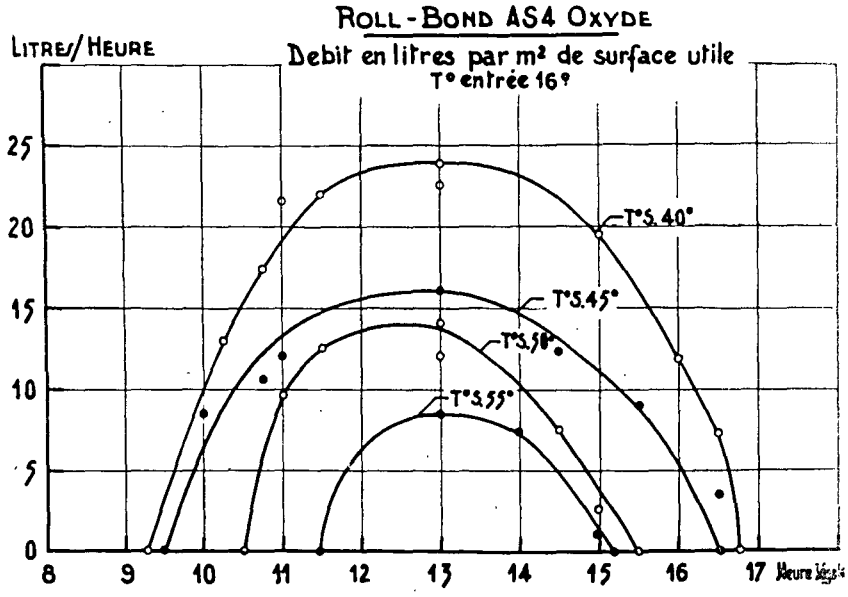


Figure 9

l'élément absorbant et, d'autre part, il sert de piège pour le rayonnement de grande longueur d'onde émis vers l'espace par l'élément.

Ce type de hublot a ceci de particulier qu'il est parfaitement étanche, son cadre en alliage d'aluminium à 5 p. 100 de silicium ayant été directement coulé sur la glace de 4,75 mm suivant un procédé étudié par Saint-Gobain et Péchiney. Il en résulte d'une part une parfaite étanchéité, et d'autre part un effet de frettage de la glace qui augmente d'une manière considérable sa résistance au choc (figures 5 et 6). L'isolement thermique était obtenu entre l'élément métallique et l'ensemble capot-hublot au moyen de joints de caoutchouc mousse, et à l'arrière par une plaque de polyéthylène expansé de 35 mm d'épaisseur.

Ce type d'insolateur fut comparé à un type similaire dans lequel la surface active fut constituée par un Roll-Bond, entièrement en aluminium cette fois, mais dont la surface exposée au rayonnement était recouverte d'une couche très mince de graphite obtenue par pulvérisation fine de graphite colloïdal.

L'insolateur en A-S5 et l'insolateur de référence graphité furent enchassés sur un pupitre en bois incliné à 30° sur l'horizontale et orienté vers le sud (figure 7).

Les mesures furent effectuées non à débit constant, mais à température constante, en mesurant le débit obtenu. Pour obtenir ce résultat, l'eau est puisée au moyen d'une petite pompe mue par un moteur électrique dans un réservoir où circule l'eau de la ville dont la température était constante et égale

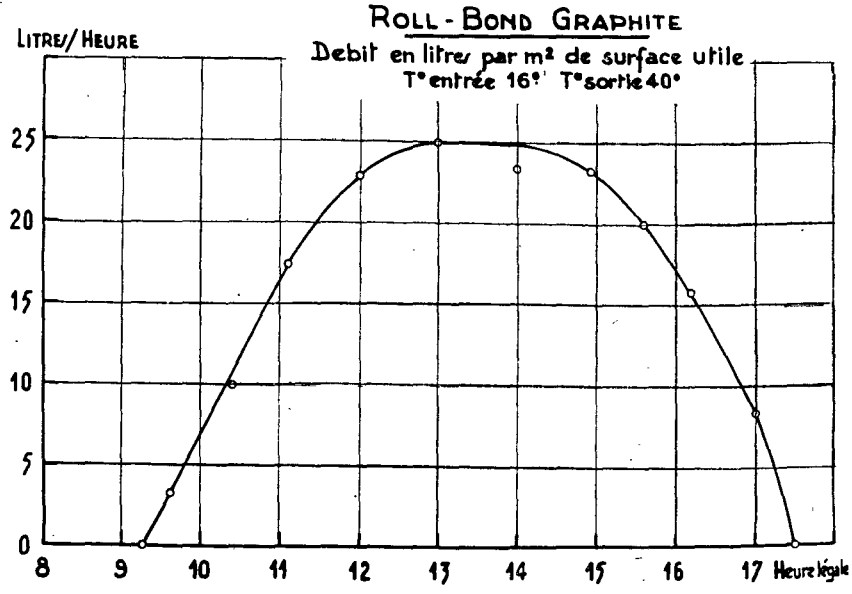


Figure 10

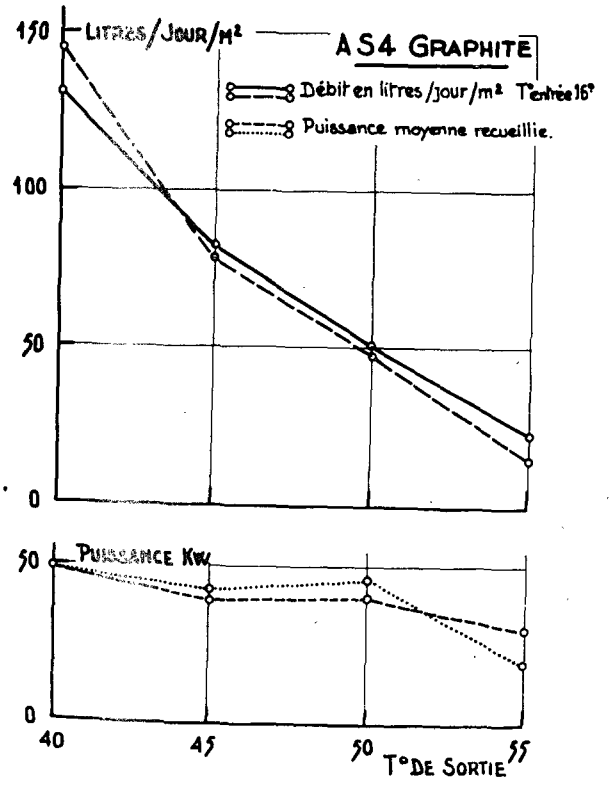


Figure 11

à 16 °C. La pompe et son moteur sont eux-mêmes immergés dans ce réservoir de manière à maintenir leur température constante (figure 8).

Le fonctionnement de cette pompe est commandé par un pyromètre régulateur relié à un thermocouple mesurant la température de l'eau à la sortie de l'élément chauffant. Ce régulateur assure la mise en route de la pompe lorsque la température de l'eau dépasse la valeur désirée et son arrêt au-dessous de cette température. On évite ainsi les ennuis que nous avons rencontrés dans les systèmes à débit constant où des variations appréciables de débit étaient dues à la formation de fines bulles gazeuses accrochées à la paroi des canaux et qui augmentent dans une large mesure les pertes de charge à l'intérieur de ceux-ci.

L'eau est recueillie dans un vase de Dewar de 250 cc dans lequel la température peut être mesurée avec exactitude, puis transvasée dans un récipient gradué permettant de mesurer le débit.

La pompe et l'insolateur sont en charge par rapport au niveau du réservoir de manière à éviter tout incident dû aux bulles qui se dégagent pendant l'échauffement du circuit.

Nous avons fait deux sortes de mesures : mesure du débit à température constante, et mesure de la température maximale à débit nul.

Dans les mesures du débit à température constante, nous avons mesuré le débit à chaque heure de la journée pour des températures de sortie de l'eau de 40, 45, 50 et 55 °C. Nous avons tracé les courbes donnant les valeurs du débit en litres par heure et par m² de surface utile exposée en fonction de l'heure de la journée (figures 9 et 10).

Ces résultats, que résume le tableau ci-dessous, sont obtenus par l'intégration des courbes précédentes, où figurent le débit par jour en litres par m² de surface utile, le débit en calories par jour et par m² ainsi que la puissance moyenne récupérée en kW.

Les courbes correspondantes ont été tracées (figure 11). Il apparaît que si, pour les températures dépassant peu la température ambiante, la surface graphitée est supérieure à celle de l'A-S4 oxydée, par contre, pour les températures plus élevées c'est l'inverse qui se produit, ce qui tend à montrer que pour le rayonnement de grande longueur d'onde émis par la plaque chauffée à des températures supérieures à 50 °C, le pouvoir émissif de la tôle d'aluminium graphitée est supérieur à celui de l'A-S4 oxydé.

Une conclusion analogue découle de la mesure de la température maximale à débit nul. Nous avons reproduit les courbes donnant les températures atteintes à chaque heure du jour par l'un et l'autre des deux dispositifs insolateurs (figures 12 et 13). On voit que la surface en A-S4 oxydé atteint une température supérieure à celle de l'aluminium graphité : 70 °C dans un cas, 68 °C dans l'autre.

En conclusion, il semble donc bien que l'A-S4 oxydé offre de grandes possibilités pour la réalisation de surfaces aptes à capter le rayonnement solaire. Toutefois, il est probable que les métaux légers

	Température de sortie							
	40 °C		*45 °C*		*50 °C*		*55 °C*	
	A-S4	*Graphite*	*A-S4*	*Graphite*	*A-S4*	*Graphite*	*A-S4*	*Graphite*
Débit par jour en litres par m² de surface utile [a]	131,5	145	82	79	50,6	47,5	23	15
Durée de fonctionnement .	7 h 1/2	8 h 1/4	7 h	6 h 1/4	5 h	4 h	3 h 1/2	3 h 1/4
Débit en calories par jour et par m²	3 156	3 480	2 380	2 290	1 720	1 615	897	525
Puissance moyenne récupérée en kW.	0,487	0,487	0,395	0,426	0,400	0,465	0,297	0,185

[a] Pour une température d'entrée de l'eau de 16 °C.

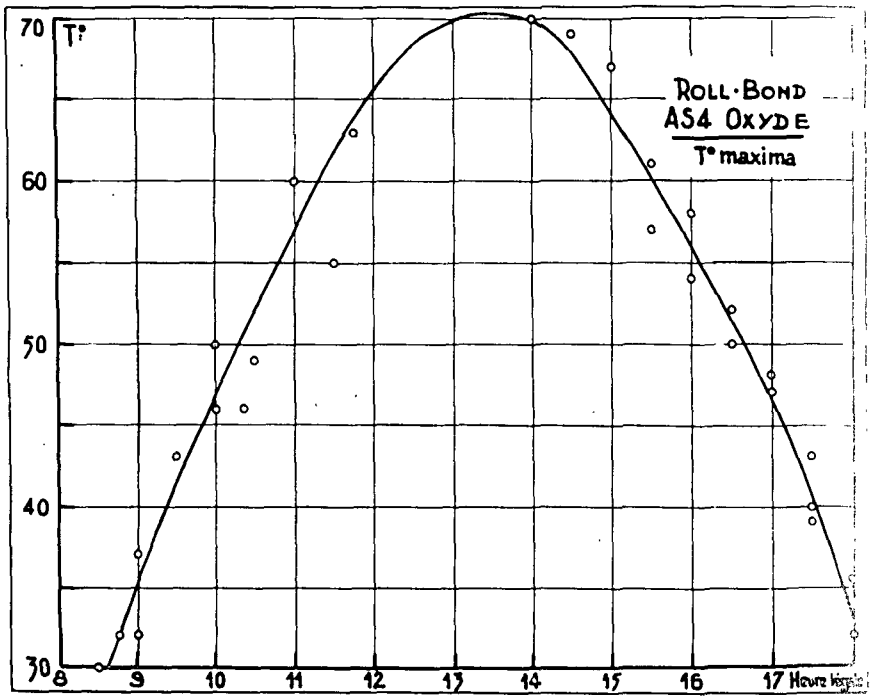


Figure 12

peuvent nous offrir d'autres surfaces inaltérables parfaitement adaptées à cet usage. Nous citerons par exemple :

L'aluminium oxydé anodiquement à basse température pour obtenir des couches dures de 60 à 100 microns;

L'aluminium-manganèse (A-M) oxydé en bain sulfosalicylique (procédé Kalcolor);

L'aluminium-silicium (A-SG) oxydé en bain oxalique, etc.

Cette classe de métaux dérivant de l'aluminium mérite donc de retenir l'attention de ceux qui se livrent à la récupération de l'énergie solaire, bien que leurs propriétés optiques souvent paradoxales déroutent parfois celui qui les utilise sans discernement.

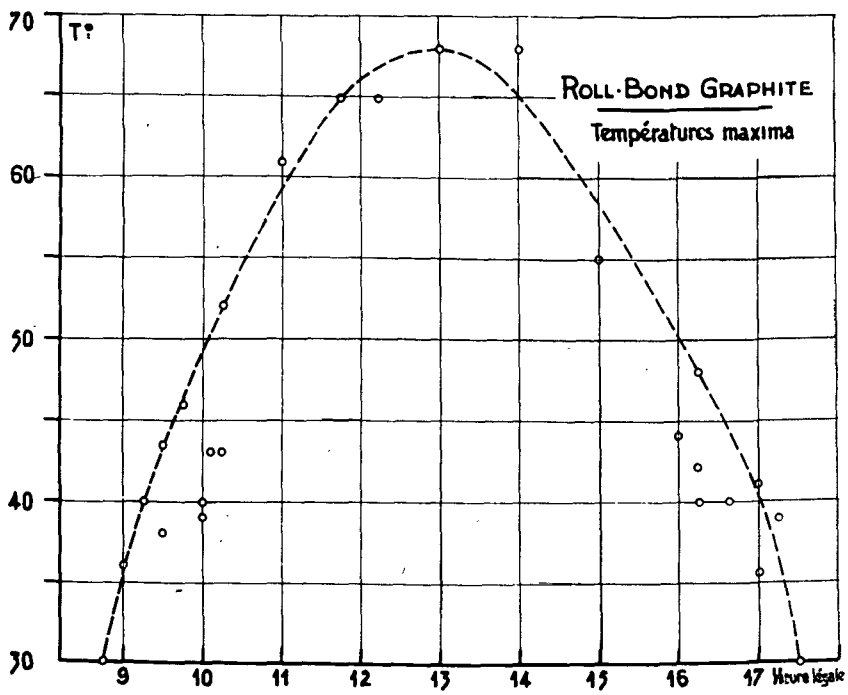


Figure 13

Résumé

L'aluminium est employé pour l'utilisation de l'énergie solaire. Il est très facile de modifier son pouvoir absorbant vis-à-vis du rayonnement solaire et son pouvoir émissif dans la zone de longueurs d'onde correspondant à son rayonnement propre en utilisant l'oxydation anodique. L'utilisation d'alliages, et en particulier d'alliages à 4 p. 100 de silicium, augmente encore les possibilités du métal.

Des mesures d'échauffement diurne et de refroidissement nocturne ont été effectuées sur divers échantillons, montrant que de jour on peut atteindre des températures maximales de 44,5 °C sur alliage au silicium oxydé, pour une température ambiante de 15 °C. La nuit la température s'abaisse à — 4 °C pour une température ambiante de + 3 °C.

Des tôles à circuit intégré dont la couche externe est en alliage à 4 p. 100 de silicium oxydé ont été utilisées pour constituer des insolateurs, et l'on a mesuré le débit pour une température donnée. A 50 °C il est de 51 l/m² de surface utile par jour, ce qui correspond à 1 720 cal/j/m².

USE OF CERTAIN ALUMINIUM ALLOYS IN THE UTILIZATION OF SOLAR ENERGY

(Translation of the foregoing paper)

Pierre Vachet * *and Jean Mercier* **

For the last few years the building industry has been using decorative panels of sheet or shapes of aluminium containing 4 to 5 per cent of silicon (known in the French nomenclature as A-S4 or A-S5) anodized to a deep gray, almost black.

The colour of these oxide layers is due to silicon or silica inclusions. They could logically be expected to be excellent material for solar radiation traps.

It is this proposition that we will discuss. Some panels made of sheet were delivered to Prof. Trombe in this connexion. He was kind enough to compare them with other specimens, this time of unalloyed aluminium sheet, either bare or with an anodic oxide layer after various surface treatments. We do not intend here to revert to his results.

The present authors used an experimental set-up adopted by Prof. Trombe in our attempt to gain an understanding of the variation of the temperature of A-S4 sheet exposed horizontally to solar radiation on a table lined with 100 mm of glasswool.

These sheets were 3 mm thick, and had a surface 250 × 250 mm. At their centre a copper plate was riveted to their lower face by means of eight rivets. A thermo-electric couple was brazed onto the centre of this plate (figure 1). The temperatures were read at hourly intervals during 24 h of exposure to a clear sky, at Chambéry. The ambient temperature was taken under cover.

Seven specimens were simultaneously tested in this way:

1. Aluminium A5 (99.t per cent) . . . . . Bright, bare surface
2. Aluminium A5 . . . . Sheet dulled by five years of exposure to a particularly corrosive industrial atmosphere (near a foundry and the exhaust chimney of an analytical chemistry laboratory)
3. Aluminium A5 . . . . Anodically oxidized on the outer face, without first being degreased (thickness of the oxide layer, 15 microns)
4. Aluminium A5 . . . . Without first being degreased, simply coated on its outer face with a thin layer of MnO_2 by immersion in a sulfuric acid solution of potassium permanganate
5. Aluminium-silicon A-S4 . Anodically oxidized on the outer face (thickness of the oxide layer 15 microns)
6. Aluminium-silicon A-S4 . Anodically oxidized on the outer face and to a depth of 25 microns
7. Iron . . . . . Black paint

The coatings are shown in figure 2. Figures 3 and 4 are curves of the day and night temperatures on different scales:

These curves may be summarized as follows:

Maximum day temperature		*Minimum night temperature*	
Specimen 7	50°C	Ambient temperature	3°C
Specimen 6	44.5	Specimen 1	2
Specimen 4	39.0	Specimen 4	0.5
Specimen 2	36.0	Specimen 2	—1.5
Specimen 5	34.5	Specimen 3	—2.0
Specimen 1	27.0	Specimen 5	—2.5
Specimen 3	24.0	Specimen 7	—3
Ambient temperature . .	15.0	Specimen 6	—4

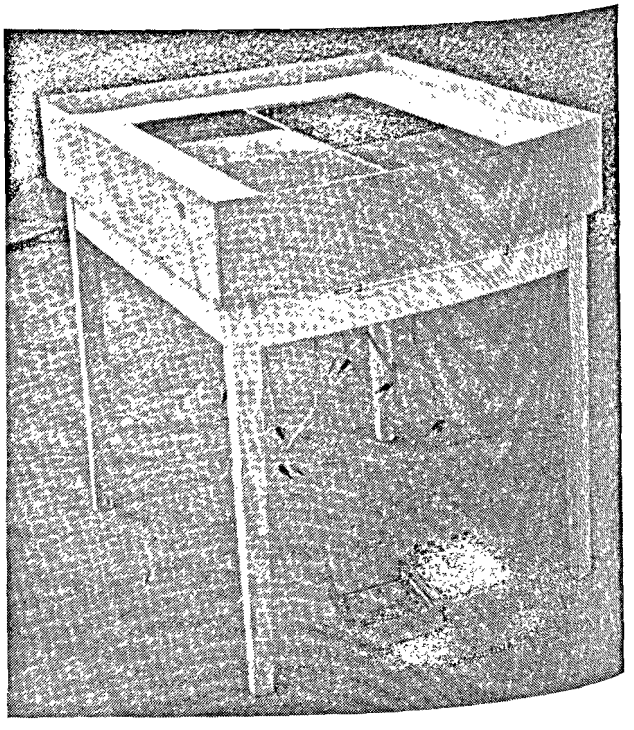


Figure 1

* Chief, Service des recherches métallurgiques, Compagnie Péchiney, Paris.

** Research Engineer, Compagnie Péchiney, Paris.

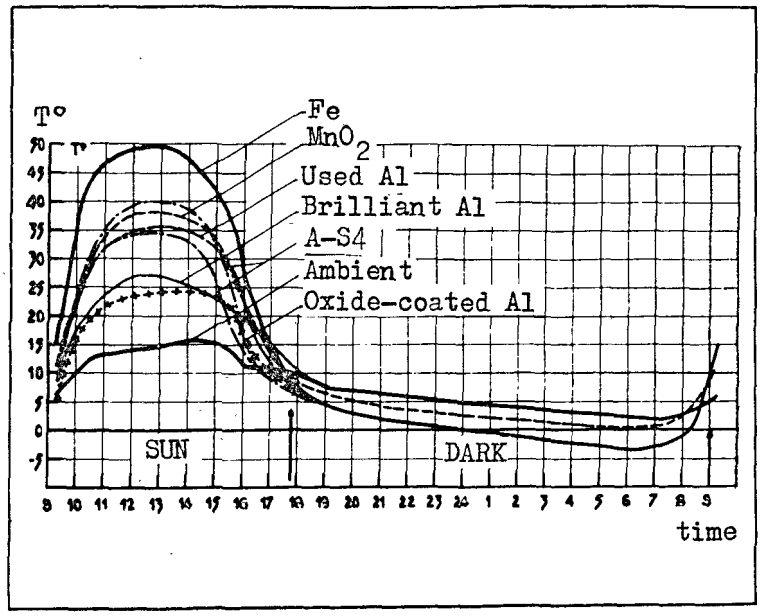
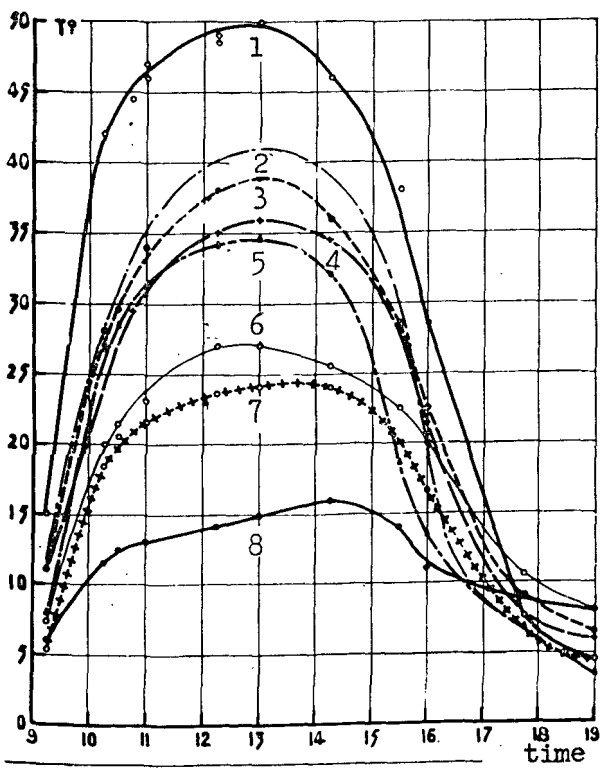


Figure 2

It was found, as foreseen, that the bare brightened aluminium surface behaved as a remarkable reflector, absorbing little solar radiation by day and emitting little by night.

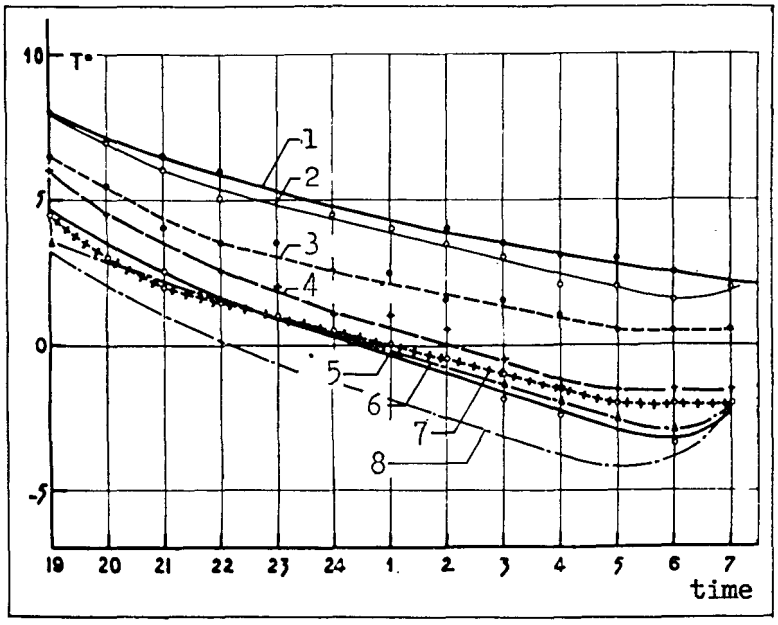
It no longer does so when deprived of its shining appearance by an aggressive agent (specimen 2); but such agents are fortunately not found in the usual exposures in countries with a clear sky.

Anodic oxidation produces a selective cold surface (specimen 3) and a coating of MnO_2 a selective hot surface (specimen 4), as previously shown by Prof. Trombe.



1. Fe
2. A-S4, 25 μ
3. MnO_2
4. Used Al sheet
5. A-S4, 15 μ
6. Brilliant Al sheet
7. Oxide-coated sheet, 15 μ
8. Ambient

Figure 3



1. Ambient
2. Brilliant Al sheet
3. MnO_2
4. Used Al sheet
5. Fe
6. A-S4, 15μ
7. Oxide-coated sheet, 15μ
8. A-S4, 25μ

Figure 4

The properties of surfaces 5 and 6, obtained by anodic oxidation of A-S4 sheet, are closer to those of a blackbody, the thicker the oxide layer is.

Aluminium and A-S4, then, yielded the complete range of the optical properties that could be required of a surface, with respect to the solar radiation and to its own emission.

We thus had the right to expect that these oxidized A-S4 surfaces could be utilized for heating water.

To this end we designed and built solar collectors as follows. The absorbing surface was formed of Roll-Bond or integral-circuit sheet. This type of heat exchanger is well known, and is usually prepared by diffusion bonding of two perfectly clean alu-

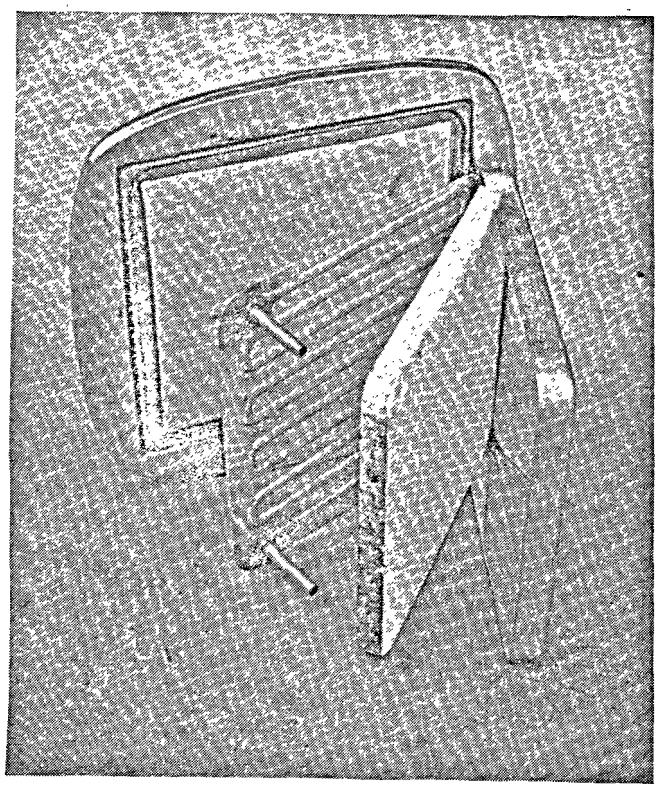


Figure 5

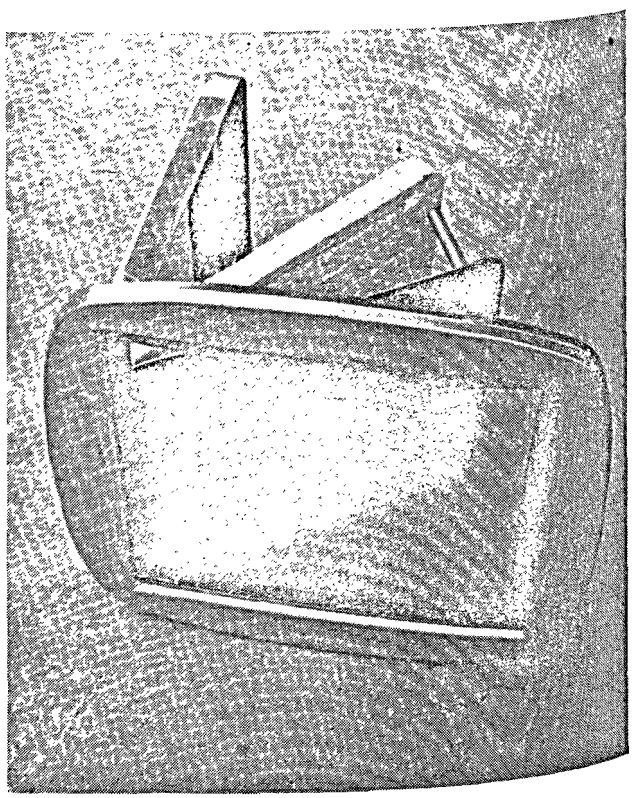


Figure 6

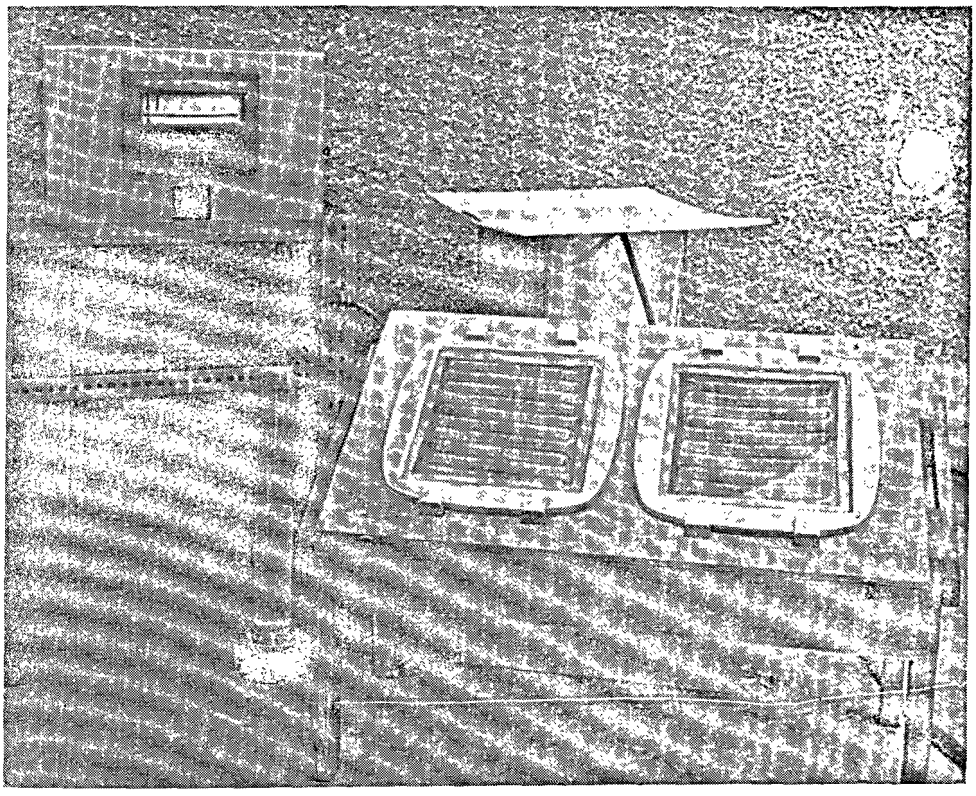
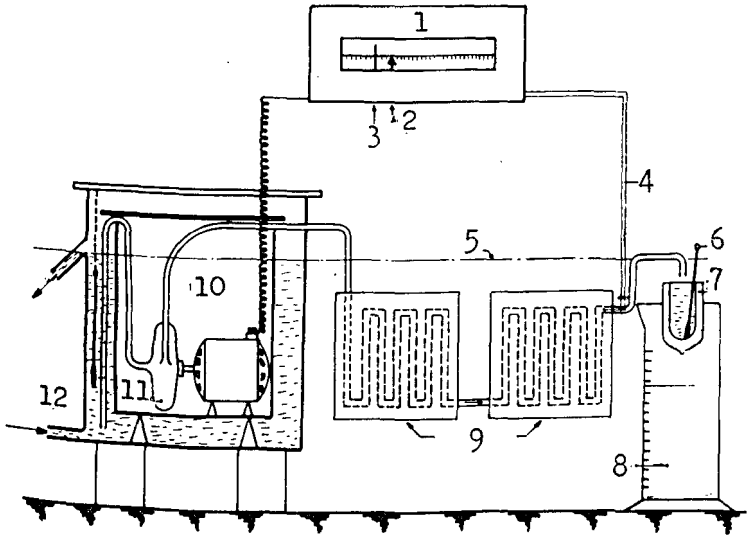


Figure 7

minium sheets, scratch-brushed on the inner faces, with the diagram of a fluid circuit traced on one of them in special ink. During diffusion bonding the two sheets form a bond at all points except those protected by the ink. One of the ends of the circuit being open, hydraulic pressure is then applied to this orifice, thus causing the circuit to distend. This makes available a tube more or less convoluted and in intimate contact with the plane surfaces serving to exchange the heat.

In the present case, one of the two sheets was not of aluminium but A-S4 alloy. The two sheets had been perfectly bonded. The useful surface was 245 × 245 mm, or 0.06 m², and the coil was 2.5 m long, with a channel 30 mm² in cross section.

Anodic oxidation was accomplished in a sulfuric



1. Regulator
2. Desired temperature
3. Ambient temperature
4. Control thermocouple
5. Water level
6. Outlet temperature
7. Dewar vessel
8. Volume delivered
9. Solar collector
10. Enclosure at 16°
11. Pump
12. Cold water circulation (16°)

Figure 8. Schematic diagram of Solar Energy Collector Installation

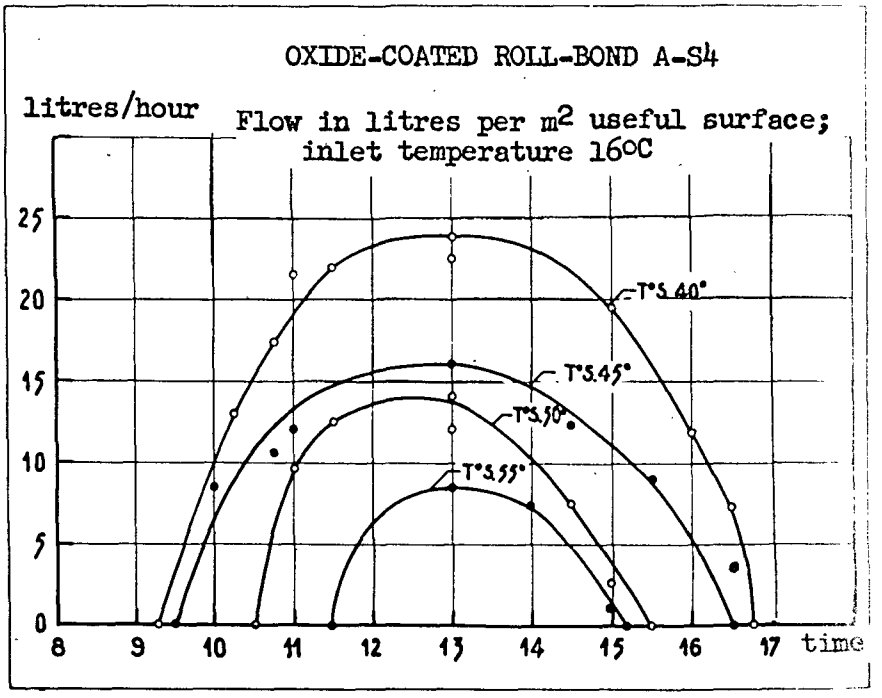


Figure 9

acid bath at 20 per cent concentration for 45 min, and was followed by sealing with boiling water. Only the active A-S5 was oxidized, the other face having been protected during this operation so as to preserve its natural brillant high finish in order to limit the radiation losses on that side.

To limit the convection losses, this element was enclosed in a metal casing whose front face consisted of a glass porthole, which played a dual role. On the one hand it provided protection against deposition of dust that might change the state of the surface of the absorbing element, and on the other, it served as a trap to check longwave emission into space by the element.

This type of porthole has the peculiarity of being perfectly hermetic, since its 5 per cent silicon-

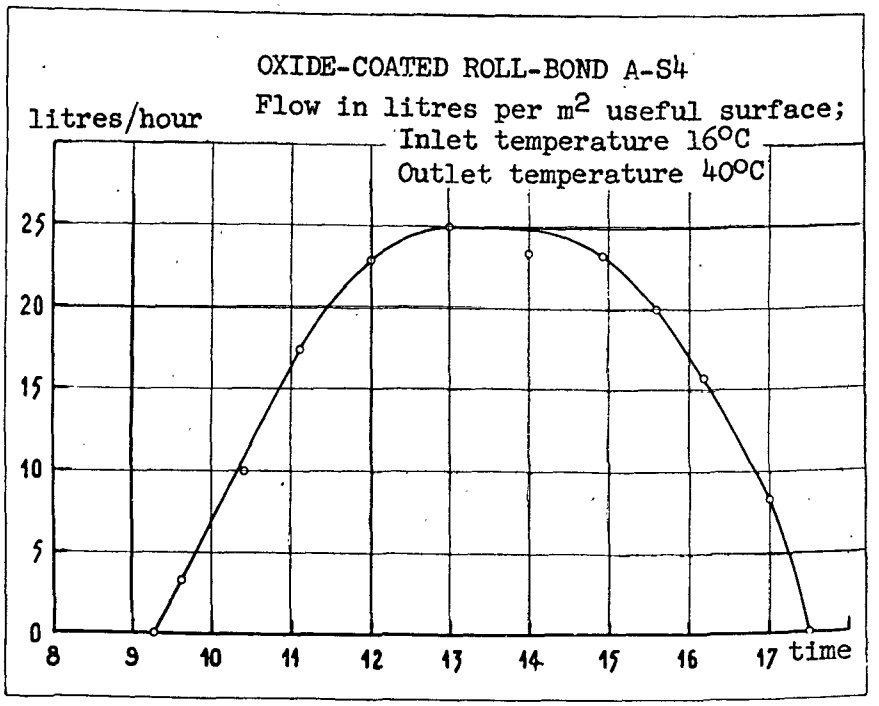


Figure 10

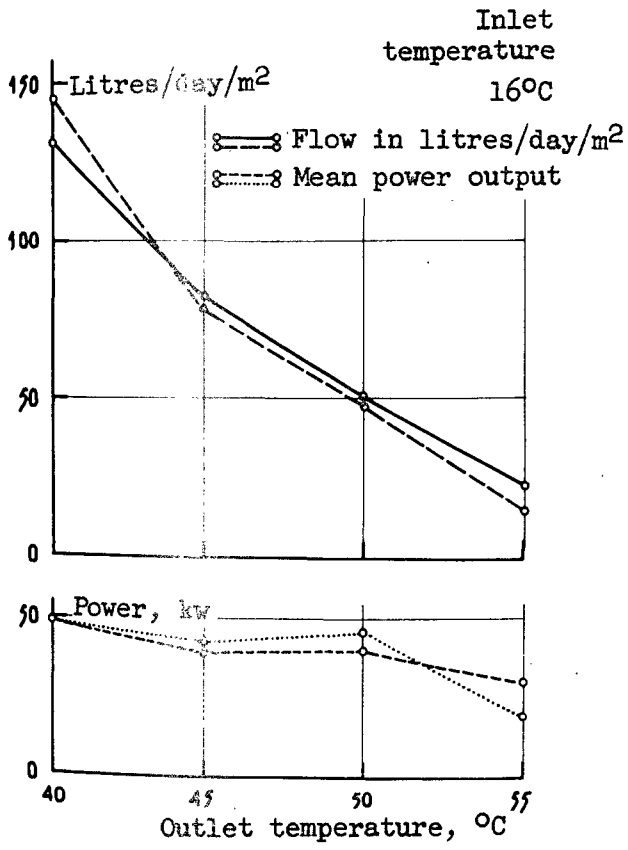


Figure 11. Graphitized A-34

aluminium alloy frame is directly bonded to the 4.75 mm glass by a process studied by Saint-Gobain and Pechiney. The result is both complete hermeticity and an effect of binding the glass, considerably increasing its shock resistance (figures 5 and 6). The metal element was thermally insulated from the casing-porthole assembly by means of sponge rubber joints, with a plate of polyethylene foam 35 mm thick in the back.

This type of solar collector was compared to a similar type whose active surface was made up of a Roll-Bond, entirely of aluminium this time, but with a very thin film of graphite, obtained by fine spraying of colloidal graphite, covering the surface exposed to radiation.

The A-S5 collector and the reference graphite collector were mounted on a wooden desk tilted 30° and oriented to the south (figure 7).

The measurements were made, not at constant rate of flow, but at constant temperature, measuring the rate of flow obtained. To get this result, a small pump driven by an electric motor was used to fill a tank in which city water at the constant temperature of 16°C was circulated. The pump and its motor were both submerged in this tank so as to hold them, too, at constant temperature (figure 8).

The operation of the pump was controlled by a regulating pyrometer connected to a thermocouple measuring the water temperature at the outlet from the heating element. The pump was started when the water temperature exceeded the desired level and stopped when it fell below this level. This avoided the trouble that we had experienced with constant-flow systems in which appreciable variations in flow were due to the formation of minute gas bubbles adhering to the duct walls, considerably increasing the losses of head in the interior of the ducts.

The water was collected in a 250 cc Dewar vessel, in which the temperature could be precisely measured, and then transferred to a graduated receiver to measure the flow.

The pump and the solar collector had a head with respect to the tank level, so as to avoid all trouble due to bubbles disengaged during the heating.

Measurements of two kinds were made: flow rate at constant temperature and maximum temperature at zero flow.

In the measurements of flow rate at constant temperature, the flow was measured hourly at water outlet temperatures 40, 45, 50 and 55°C. The flow in litres per hour and per m² of useful exposed surface was plotted against time (figures 9 and 10).

These results are summarized in the table below, obtained by integration of these curves relating flow per day in litres per m² of useful surface, flow in calories per day and per m², and mean power output in kW.

Figure 11 shows the corresponding curves. It will be seen that while the graphitized surface is better than that of the anodized A-S4 at tempera-

	Discharge temperature							
	40°C		*45°C*		*50°C*		*55°C*	
	A-S4	*Graphite*	*A-S4*	*Graphite*	*A-S4*	*Graphite*	*A-S4*	*Graphite*
Flow per day in litres per m² of useful surface [a]	131.5	145	82	79	50.6	47.5	23	15
Duration of operation, h	7½	8¼	7	6¼	5	4	3½	3¼
Flow in calories per day and per m²	3 156	3 480	2 380	2 290	1 720	1 615	897	525
Mean power output, kW	0.487	0.487	0.395	0.426	0.400	0.465	0.297	0.185

[a] For a water inlet temperature of 16°C.

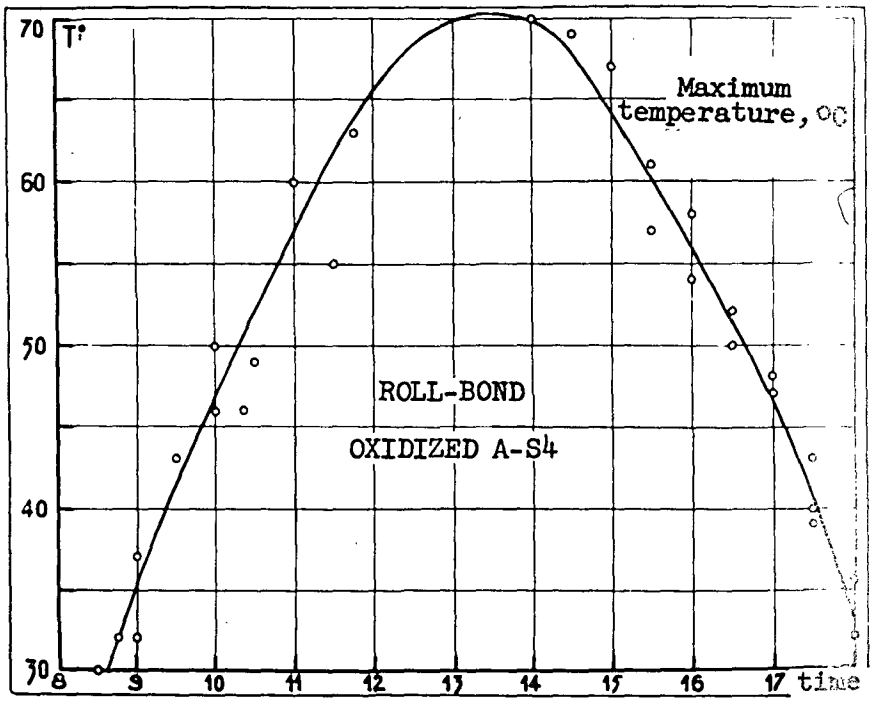


Figure 12

tures little higher than ambient, the reverse is true at higher temperatures, tending to show that for the longwave radiation emitted by the plate heated to over 50°C the emissivity of the graphitized aluminium sheet is higher than that of the anodized A-S4.

A similar conclusion results from the maximum temperatures measured at zero flow. Figures 12 and 13 give the curves of the hourly temperature for both these solar collector arrangements. It will be seen that anodized A-S4 surface reaches a higher temperature than the graphitized aluminium surface: 70°C for the former against 69°C for the latter.

In conclusion, the anodized A-S4 does appear to offer great prospects for the development of surfaces for collecting solar radiation. The light

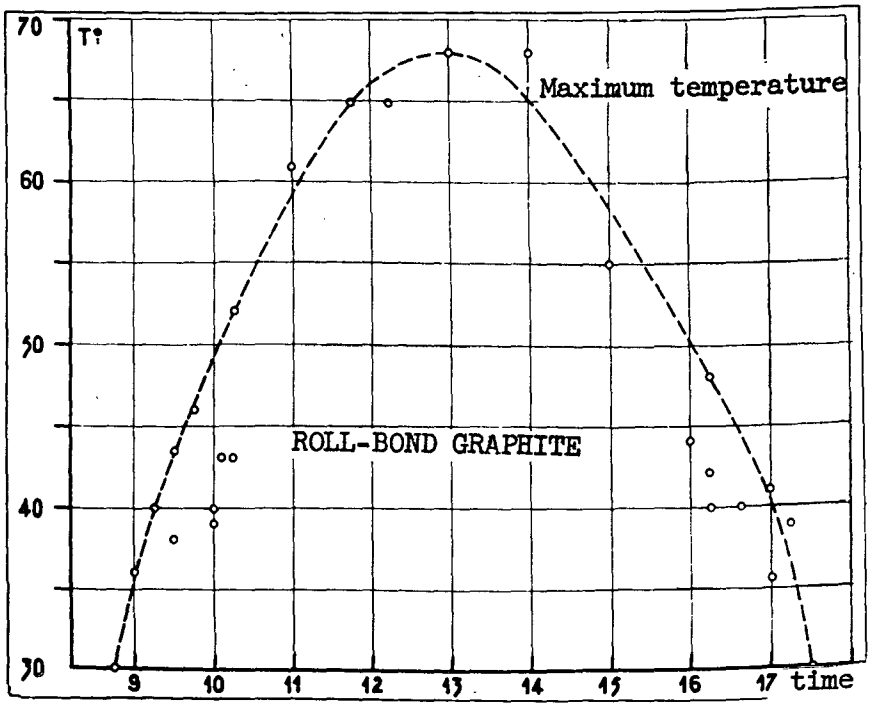


Figure 13

metals, however, will probably offer us other inalterable surfaces that are likewise perfectly suitable for this use. We might mention, for example:

Aluminium anodically oxidized at low temperature to give hard films 60 to 100 microns thick.

Aluminium-manganese alloy (A-M) oxidized in a sulfosalicylic bath (Kalcolor process);

Aluminium-silicon alloy (A-SG) oxidized in an oxalic acid bath; etc.

This class of aluminium alloy thus deserves the attention of those working on the harnessing of solar energy, although their frequently paradoxical optical properties sometimes confuse those who use them indiscriminately.

Summary

Aluminium is employed for the utilization of solar energy. Its absorbing power for solar radiation and its longwave emissivity, corresponding to its own radiation, may both very easily be modified by anodic oxidation. The use of alloys, especially the alloy with 4 per cent of silicon, still further improves the possibilities of aluminium in this respect.

The daytime heating and night-time cooling have been measured on various specimens, showing that maximum temperatures of 44.5°C may be attained on an oxide-coated aluminium-silicon alloy, at an ambient temperature of 15°C. At night the temperature drops to —4°C for an ambient temperature of + 3°C.

Integral-circuit sheets with the external layer consisting of an oxide-coated alloy with 4 per cent of Si were used to build solar collectors, and the flow rate at a given temperature was measured. At a water temperature of 50°C it was 51 l/m² useful surface per day, corresponding to 1 720 cal/day/m².